

CESDOC 2016

Civil Engineering for Sustainable Development - Opportunities and Challenges

19th to 21st December 2016

Conference Proceeding



Department of Civil Engineering
Assam Engineering College
Guwahati, Assam, India

CESDOC 2016

1st International Conference
on
**Civil Engineering for Sustainable Development –
Opportunities and Challenges**

19-21 December 2016

Conference Proceeding



**Civil Engineering Department
Assam Engineering College
Guwahati, Assam, India**

Publication of Civil Engineering Department
Assam Engineering College, Guwahati-781013

Extended Abstracts of the 1st International Conference on
Civil Engineering for Sustainable Development -
Opportunities and Challenges

Guwahati, Assam, India
19 - 21 December, 2016

Editors

- Dr. Binu Sharma
 - Dr. B. Talukdar
 - Dr. M. K. Borah
 - Dr. J. Pathak
 - Dr. D. Goswami
 - Dr. Malaya Chetia
 - Dr. Triptimoni Borah
 - Dr. U. K. Nath
-

Communication Address

Civil Engineering Department
Assam Engineering College, Guwahati-781013, Assam, India
Website : www.aec.ac.in

Disclaimer

Although this book of abstracts and the accompanying full-length manuscript's files have been compiled with utmost care, the Editors cannot be held responsible for any misprints and / or omissions.

© All rights reserved.

Printed at

Brahmaputra Offset
M.C. Road, Guwahati-781003

ADVISORY COMMITTEE

PROF. NAYAN SARMA	(IIT Roorkee)
PROF. NITIN KUMAR TRIPATHI	(AIT Bangkok)
PROF. D.K. PAUL	(IIT Roorkee)
DR. ACHINTYAN. BEZBARUAH	(NDSU USA)
PROF. ARUP KUMAR SARMA	(IIT Guwahati)
DR. DOMINIK H. LANG	(NORSAR Norway)
PROF. NARENDRA KUMAR SAMADHIYA	(IIT Roorkee)
DR. DIGANTA SARMA	(Auckland New Zealand)
PROF. HEMANTA HAZARIKA	(Kyushu University Japan)
PROF. DEEPANKAR CHOUDHURY	(IIT Bombay)
DR. GUNAN. PAUDYAL	(Nepal)
PROF. P.K. SIKDAR	(CRRRI New Delhi)

ORGANISING COMMITTEE

President	:	DR. ATUL BORA
Working President	:	DR. PALASH JYOTI HAZARIKA
Organising Secretary	:	DR. BINU SHARMA
Jt. Org. Secretaries	:	DR. JAYANTAPATHAK DR. DIGANTA GOSWAMI DR. BIPUL TALUKDAR

TECHNICAL COMMITTEE

:	DR. MRINAL BORA
	DR. TRIPTIMONI BORAH
	DR. MALAYA CHETIA
	DR. UTPAL KUMAR NATH

JOINT

TREASURER

:	DR. BIBHASH SARMA
	DR. UTPAL MISRA

TRAVEL & ACCOMMODATION COMMITTEE

: DR. PANKAJ GOSWAMI
MR. SASANKA BORAH

RECEPTION & VENUE COMMITTEE

: DR. BIBHASH SARMA
MS. BHARATI MEDHI
MS. RUPJYOTI BORDOLOI
MS. PUSHPANJALI SONOWAL

CULTURAL COMMITTEE

: PROF. SUNIT KUMAR BHAGABATI
DR. DIGANTA GOSWAMI

LOGISTICS & FOOD COMMITTEE

: MR. BHASKAR JYOTI DAS

Preface

The "1st International Conference on Civil Engineering for Sustainable Development-Opportunities and Challenges" is being organised by the Civil Engineering Department, Assam Engineering College from 19th December to 21st December, 2016. This conference is organised to commemorate 60 years of glorious existence of the Civil Engineering Department of the college. The Assam Engineering College started as the Assam Civil Engineering College in the year 1955. This was the first engineering college in the entire North East India to impart technical education for bachelor degree in Engineering. Later in the year 1957 with the opening of two new departments viz. Mechanical Engg. and Electrical Engineering, the College was renamed as Assam Engineering College. Civil Engineering Department, the oldest department of the College, focuses mainly on student centric programs and it has evolved into a higher learning centre with masters programme and Ph.D. programme. The first masters course in Engineering in the entire North Eastern region started in this premier institute in 1971 on Watershed Manage and Flood Control. With the help of a substantial financial assistance received from the Ministry of Human resource Development, Government of India, the laboratories of the department were modernised and upgraded. This resulted in getting a second PG course on Soil Mechanics and Foundation Engineering in 1988. A total of 20 students till date have obtained their Ph.D. degree in Civil Engineering from Assam Engineering college.

The Department has also carried out many projects funded by the Ministry of Human Resource Development (MHRD), Department of Science and Technology (DST) and All India Council for Technical Education (AICTE). The Civil Engineering Department has also been carrying out various consultancy projects sponsored by different agencies and the department is actively engaged in Research and Development (R & D) projects.

From its humble beginning as a department imparting only the bachelors degree, the Civil Engineering Department has completed 60 glorious year of its academic life of quality and excellence dedicated to the cause of education. Time has come for formal commemoration and introspection of the department standing for the last 60 years. A conference highlighting sustainable development is thought to be an important aspect of celebration. This conference is thus organised to commemorate the 60 years of successful journey of the department.

The aim of this conference is to bring to light a very relevant topic which is sustainable development. At the Sustainable Development Summit on 25 September

2015, UN Member States adopted the 2030 Agenda for Sustainable Development, which includes a set of 17 Sustainable Development Goals (SDGs) to end poverty, fight inequality and injustice, and tackle climate change by 2030. This conference will provide a platform to technocrats to champion the effort towards building capacity for sustainable development. Engineering for Sustainable Development will not happen of its own volition - it needs action by everyone involved in engineering education. Academia has a responsibility to bring up world graduates and qualified engineers who understand sustainable development and can deliver significantly more-sustainable solutions for society.

With sustainable development as the main goal, this conference will cover five major themes as sustainable infrastructure development, sustainable urban development, sustainable rural development, sustainable development by disaster risk management, sustainable development of water system.

This international conference will bring under one roof the specialists from the academia, industry, government and non-government organisations. The conference aims at congregation of policy makers, stakeholders, engineers, architects and planners to brain-storm on various issues to strengthen the internationally mandated approach for sustainable development and discuss the roles of civil engineers in various interdisciplinary core areas of sustainable development.

Prof. Binu Sharma
Organising Secretary, CESDOC 2016

CONTENTS

Invited Lectures

Low Cost and Resilient Solution against Geodisaster - Case History based Adaptation –	1
<i>Dr Hemanta Hazarika</i>	
Innovation in concrete performance for output and performance based contracts	10
<i>Dr Diganta Sarma</i>	

Theme: Sustainable Development by Disaster Risk Management (DM)

DM 01	Static & dynamic analysis of a tailings dam	15
	<i>Ritu Raj Nath, Ashok D. Pandey, Mukat L. Sharma</i>	
DM 02	Site response analysis : A case study of Guwahati city	22
	<i>Nayan Jyoti Das, Mousumi Deori and Sasanka Bora</i>	
DM 03	3- Dimensional Slope Stability Analysis	28
	<i>Mousumi Bania and Diganta Goswami</i>	
DM 04	Seismic strengthening of existing school buildings in Meghalaya, India	34
	<i>Pratim P. Kalita, Jayanta Talukdar, Himanshu S.B.Gohain, Ritukesh Bharali, Bhargob Deka, Jayanta Pathak</i>	
DM 05	Shear wave velocity profile at NITW stadium using MASW	40
	<i>Muzaffar Khan, Akshay Sakhare, Ravi Kr and Kalyan Kumar</i>	
DM 06	Vulnerability analysis of embankment reach: A remote sensing and GIS based study in Nona river in Assam, India	44
	<i>Anjil Baid, B. Talukdar and Ranjit Das</i>	
DM 07	Stability analysis of an ash pond dyke understatic, pseudostatic and seismic conditions	49
	<i>Priyanka Talukdar, Ruplekha Bora and Arindam Dey</i>	

DM 08	Optimum earthquake resistant design based on the lowest rocking response of a system to a particular earthquake excitation using MATLAB <i>Gitartha Kalita</i>	54
DM 09	Seismic response of RCC storage tanks in high-risk seismic zones <i>Pratim P. Kalita, Jayanta Talukdar, Rimjhim Kashyap, Ritukesh Bharali, Bhargob Deka, Jayanta Pathak, Palash J. Hazarika</i>	57
DM 10	Site Response Evaluation Procedures for Earthquake Risk Management A State of the Art Review <i>Jyotisman Saikia, Jayanta Pathak, Diganta Goswami</i>	64
DM 11	Site specific ground response analysis of Jorhat city <i>P. Bhowmick and A. Bhattacharjee</i>	69
DM 12	Slope stability analysis with special reference to Panikhaiti hill area: A case study <i>Parikhit Baruah and Dr. U C Kalita</i>	74
DM 13	Soil-pile interaction under dynamic load : state-of-the-art <i>Nabanita Sharma, JayantaPathak, Diganta Goswami</i>	79
DM 14	Site response studies for sustainable urban planning - A case study of the western Guwahati region <i>Sasanka Borah, Diganta Goswami and Jayanta Pathak</i>	84
DM15	Recent techniques of seismic liquefaction mitigation <i>Bibha Das Saikia</i>	89
DM16	Comparison of liquefaction potential of Guwahati city by two deterministic methods <i>Binu Sharma, Noorjahan Begum and Kewal Aggarwal</i>	94
DM17	Rock slope stabilization along the trek route to Mata Vaishno Devi Shrine - A case study <i>Gourango Singha and Lopamudra Dutta</i>	101
Theme: Sustainable Infrastructure Development (ID)		
ID 01	Comparison of methods for estimating microbial biomass in soil <i>Monikongkona Boruah, Rojumul Hussain and Ankit Garg</i>	107

ID 02	An experimental study on the effectiveness of an optimized pendulum type tuned mass damper in reducing the response of a building structure <i>Dhruba J. Borthakur and Nayanmoni Chetia</i>	112
ID 03	Effects of silica fume on the strength and durability properties of concrete <i>Salim Barbhuiya and Muneeb Qureshi</i>	117
ID 04	Development of analytic model for determining the mechanical factor of coir fiber reinforced soil using genetic programming <i>Prashant K. Sharma, Harsha Vardhan and Ankit Garg</i>	121
ID 05	Pile cap lateral resistance-statistical analysis <i>Utpal K. Nath</i>	126
ID 06	Prediction of pile load capacity using artificial neural network <i>Bhaba J. Das and Utpal K. Nath</i>	130
ID 07	Verifications of pile load capacity using static pile load test <i>Ningombam T. Singh</i>	136
ID 08	A study of modal behaviour of an intz type water tank under seismicloading <i>Pranjal Konwar, Dhurba J. Borthakur and Nayanmoni Chetia</i>	141
ID 09	Experimental evaluation of load-displacement behavior of skirted foundation on sand <i>Kangkan Sarma and Nayanmoni Chetia</i>	149
ID 10	Ductility factor of fibre reinforced soil using evolutionary genetic programming model <i>Shubham Tripathi, Vishal Kashyap, Sanadam Bordoloi</i>	157
ID 11	The effect of a plant based polymeric material on the fresh and hardened states properties of cement mortar <i>Amrita Hazarika, Indranuj Hazarika, Nabajyoti Saikia</i>	162
ID12	Use of a locally available biopolymeric admixture for production of sustainable cement composites: durability behaviour of cement mortar <i>Indranuj Hazarika, Amrita Hazarika, Nabajyoti Saikia</i>	167

ID13	Factors influencing shear strength of sand-tyre waste mixtures <i>Prasanty Borah, Malaya Chetia and Asuri Sridharan</i>	172
ID14	Improvement of engineering properties of clayey soil with addition of different admixtures <i>P. K. Khaundand Pooja Kakati</i>	177
ID15	Sustainable developments and challenges for structural engineers <i>Sukumar S. Ningthoukhongjam</i>	182
ID16	Dynamic analysis of RC shear wall in performance based seismic design of buildings <i>Partha P. Debnath and S. Choudhury</i>	186
ID17	Behaviour of multi-tiered wall: A numerical model study <i>Arup Bhattacharjee and Nayan J. Sarma</i>	192
ID 18	Synthesis and microstructural characterization of geopolymer from rice husk ash and sodium aluminate <i>N Shyamananda Singh, Suresh Thokchom, Rama Debbarma</i>	198
ID 19	Effect of rice husk ash (RHA) on shear parameters and California Bearing Ratio (CBR) of soil <i>N. Daimary and A. Bhattacharjee</i>	202
ID20	Optimization of roller tuned mass damper and its practical validation <i>Nayanmoni Chetia</i>	207
ID21	Application of micropiles for underpinning and seismic retrofitting of structures <i>Binu Sarma</i>	212
ID22	Performance evaluation of reinforced concrete framed structure with steel bracing and supplemental energy dissipation <i>Swanand Patil</i>	218
ID23	Seismic behaviour of bi-symmetric buildings <i>Mayurand Yogendra Singh</i>	223
ID24	Influence of sand and rock quarry dust addition on compaction properties of clay <i>Manash P. Baruah, Malaya Chetia, Asuri Sridharan</i>	228

Theme: Sustainable Development of Water System (WS)

WS 01	Hydrological modelling of Krishnai river basin <i>Sazidur Rahman and Bipul Talukdar</i>	233
WS 02	Development of rainfall-runoff modelling using ArcSWAT and artificial neural network in the Subansiri Basin, Assam <i>Susheta Chanda and Triptimoni Borah</i>	238
WS 03	Morphometric analysis and prioritization of Kushi Basin using remote sensing and GIS <i>Kulendu K. Gogoi, Gulshan Tirkey, Sanjay K. Sharma, C.K. Jain and Mrinal K. Borah</i>	243
WS 04	Development of synthetic unit hydrographs for Kushi River Basin using remote sensing and GIS <i>Ranjan Das, Sanjay K. Sharma, Gulshan Tirkey, C.K. Jain and Mrinal K. Borah</i>	256
WS 05	Infiltration rate of fiber reinforced soil using mini disk infiltrometer <i>Rojimul Hussain, Vikram Agarwal and Soutreya Kundu</i>	261
WS 06	Simulation of aerobic degradation of BTEX compounds by using GMS and RT3D <i>Gyanashree Bora and Triptimoni Borah</i>	267
WS 07	Potential impact of climate change on rainfall intensity-duration-frequency curves of Guwahati City <i>Sagarika Patowary, Jayshree Hazarika and Arup K. Sarma</i>	272
WS 08	A study on hydroelectric and irrigation potential of Bhogdoi River, Assam <i>Mrinal K. Dutta and Mriganka Mazumdar</i>	278
WS 09	Potential of river bank filtration system for augmentation in drinking water supply at lower Brahmaputra Basin <i>Medalson Ronghang, Suchandra Roy, Shatadeepa Das, Nayan J. Konwar, Biswa K. Khakhlari, Nilim Kalita, Fwilao Basumatary, Evangeli Basumatary, Nomita Narzary, Pranjal Barman, Hemantajeet Medh, Kamal K. Brahma</i>	283

WS 10	Investigation of hydraulic conductivity for red soil vegetated with transgenic cowpea in the absence of nutrients <i>Ankit Soni, Bhushan S. Wagh, Sunil K. Sihag, Suraj Kumar and Ankit Garg</i>	291
WS 11	Performance analysis of drought resistant cowpea in red soil under the absence of nutrients <i>Bhushan S. Wagh, Ankit Soni, Sunil K. Praksh, Arka Das and Ankit Garg</i>	297
WS 12	Short term river flow forecasting by group method of data handling method <i>Kukil Kashyap and Md Altafuddin</i>	302
WS 13	Stability analysis of geobag revetment for riverbank protection <i>Rhitwika Barman and Bipul Talukdar</i>	309
WS 14	A study on artificial flood of Guwahati City and its mitigation <i>Bhaskar J. Haloi, Abhinav Bora and Nairita Sarma</i>	314
WS 15	Improvement of water use efficiency: A case study of Sukla Irrigation Project, Assam <i>Syeda N. Sultana, Utpal K. Misra, Uzzal M. Hazarika</i>	319
WS 16	A study of the ground water and drinking water characteristics of Jayanagar and Survey in Guwahati, Assam <i>Archita Borah, Khyati M. Chaudhury and Debangana Sharmah</i>	324
WS 17	Feasibility study of sustainable green irrigation by spiral tube water wheel pump in Assam <i>Dhrupad Sarma, Parimal B. Barua, Biju Gogoi, Khiren Kachari, Kailash J. Saikia and Prakash Mili</i>	328
WS 18	Precision irrigation - A tool for sustainable management of irrigation water <i>Arnab Sarma</i>	334
WS 19	Flow characteristics around bridge pier <i>Souryadeep Chaki and Prasanna K. Khaund</i>	339
WS 20	An experimental study of variation in flow parameters due to the effect of spur <i>Nishimon Konwar and Prasanna K. Khaund</i>	344

WS 21	Development of rubber modified asphalt as sealing material <i>Jyotishmoy Borah</i>	349
WS 22	Competition for water resource in the Brahmaputra River Basin - Issues of concern <i>Arnab Sarma</i>	353
WS 23	Simulation study of Subansiri lower reservoir <i>Dipsikha Devi and Bibhash Sarma</i>	358
WS 24	Application of simulation-optimization model in reservoir planning <i>Krishna K. Das and Bibhash Sarma</i>	363

Theme: Sustainable Urban Development (UD)

UD 01	Assessing applicability of ecological management practices (EMPS) in hilly urban watershed management <i>Banasri Sarma and Arup K. Sarma</i>	368
UD 02	A case study on performance analysis of un-controlled intersection in Silchar, Assam <i>Debasish Das, Mokaddesh A. Ahmed and Saikat Deb</i>	373
UD 03	Prediction of shear parameters of soil using artificial neural network <i>Arunav Chakraborty, Ankurjyoti Bhattacharya, Aditya P. Sarma, Lakhyajit Sarmah, Arnab J. Das and Aminul Islam</i>	378
UD 04	An urban heat island magnitude study over the city of Guwahati - An integration of remote sensing and ground based approach <i>Ajanta Goswami, Pir Mohammad, Ashim Sattar, Rahul Mahanta and Stefania Bonafoni</i>	383
UD 05	A remote sensing approach to study the temporal growth of the urban limits for the city of Hyderabad from 2001-2015 <i>Pir Mohammad, Ajanta Goswami, Ashim Sattar and Stefania Bonafoni</i>	388
UD 06	Source segregation of municipal solid waste <i>Pradip Baishya and Dimbendra K. Mahanta</i>	392

UD 07	Laboratory experimental techniques for determination of diffusion coefficients for landfill liner facilities - A review <i>Partha Das and T.V. Bharat</i>	397
UD 08	Conceptual design for community participation in devolution of sustainable smart city system management <i>Bhabesh Mahanta</i>	401
UD 09	Sustainable interventions in Guwahati city for improving mobility, drainage and infrastructure <i>Rittick Hazarika</i>	410
UD 10	Biomedical waste management of Guwahati - A case study of Gauhati Medical College and Hospital <i>Rupanjan Chakraborty, Rakesh Barman, Kuntal Das and Mrinal Roy</i>	414

Theme: Sustainable Rural Development (RD)

RD 01	Geo-spatial land records database with Bhunaksha as sustainable planning and framework for rural development <i>Dibyojit Dutta, D.S. Venkatesh, Sunish Kumar, Kanika Bansal, Seemantinee Sengupta, Deepak C. Misra</i>	419
RD 02	Effect of polypropylene fiber on strength characteristics of soil at varying compaction states <i>Gaurav K. Das, Akangsha Gogoi and Himashree H. Kashyap</i>	428
RD 03	A laboratory study on CBR and permeability properties of sub-base materials in a road structure using polypropylene fibre as additive <i>Tinku Kalita and Bhaskarjyoti Das</i>	432
RD 04	Investigation of infiltration temporal variation in different soils vegetated with drought sensitive cowpea <i>Shiv Prakash, Sunil K. Sihag, Ankit Soni, Vinay K. Gadi and Ankit Garg</i>	436

Low Cost and Resilient Solution against Geodisaster - Case History based Adaptation -

H. Hazarikaⁱ⁾, K. Yasuharaⁱⁱ⁾, T. Ohsumiⁱⁱⁱ⁾ and M. Yamanaka^{iv)}

i) Professor, Department of Civil Engineering, Kyushu University, 744 Motoooka, Fukuoka 819-0395, Japan.

ii) Professor, Institute for Global Change Adaptation Science, Ibaraki University, 2-1-1 Bunkyo, Mito, Ibaraki, 310-8512, Japan.

iii) Principal Research Fellow, Department of Disaster Mitigation Research, National Research Institute for Earth Science and Disaster Resilience, 3-1 Tennodai, Tsukuba, Ibaraki 305-0006, Japan.

iv) Professor, Department of Safety Systems Construction Engineering, Kagawa University, 1-1 Saiwaicho, Takamatsu, Kagawa 760-8521, Japan.

ABSTRACT

This paper first describes the forensic study conducted on a tire retaining wall that miraculously survived the 2011 Great East Japan Disaster. The earthquake and tsunami resistant characteristics of the retaining wall were evaluated by performing various field tests. The paper then proposes a new concept of using waste tires to prevent coastal erosion based on the lessons learned from the undamaged retaining wall. An eco-friendly adaptive technique using locally available materials and industrial by-products is proposed. Used automobile tires were combined with palm fibers to construct a reinforced dike system as a multiple protective measure. The tires, with mangrove plantation inside, can work well in protecting the dikes against impacts from severe climatic events such as storm surges. Addition of the palm fibers in soils increases the dike stability, particularly when mixed with cement.

Keywords: Cost reduction, Disaster mitigation, Erosion, Scouring, Waste tires

1. INTRODUCTION

The 2011 off the Pacific Coast of Tohoku Earthquake and the record breaking tsunami that easily overtopped the coastal structures, brought devastating damage to many geotechnical structures in the eastern coast of Tohoku area, Japan (Hazarika, 2011; Hazarika et al. 2012b; Hazarika et al. 2012c). While surveying the tsunami disaster areas immediately after the disaster, the authors were amazed to discover a retaining wall (made of recycled tires) that miraculously survived the disaster in Okirai area, Iwate prefecture, Japan (Fig. 1a). Ironically, this tire retaining wall is located just about 150 m away (towards the land) from a completely collapsed sea wall (Fig. 1b). A factory building situated on the backfill ground of the retaining wall was damaged by the tsunami, and a natural slope nearby the tire retaining wall was eroded by the tsunami. Why this tire retaining wall was neither damaged by the earthquake nor by the inundation and scouring due to the tsunami was the source of inspiration of research presented in this paper.

A Japanese government panel is estimating that a 9.0 magnitude earthquake in the Nankai Trough region will bring damage worth \$2.2 billion, a figure that is much higher than the \$177 million damage by the 2011 Great East Japan Disaster. Scientists are predicting that the earthquake is due “in the not-too-distant future”, based on historical rough calculations. The report of central disaster mitigation council of the ministry of Japan (Central Disaster Mitigation Council, 2003),

states that about 2m of tectonic subsidence is expected in the Kochi area of Shikoku island of Japan, by that earthquake. In order to mitigate the damage from such future devastating earthquakes, it is necessary to take appropriate measures that can protect the infrastructures from the compound disasters instigated by the combined effect of events such as an earthquake, liquefaction, tsunami, heavy rainfalls and other extreme events resulting from climate change. To realize that, what is needed most at this moment is to how to make use of the lessons that we civil engineers learned from the 2011 Great East Japan Disaster.

This paper first reports on the site investigations of the non-damaged retaining wall made of tires shown in Fig. 1a, focusing on the structural and geotechnical aspects. The investigations includes seismological, geotechnical and structural aspects of the retaining wall due to the tsunami using both the field survey and laboratory testing. As a part of the field survey, in-situ density test, dynamic cone penetration test, micro tremor measurement and surface wave exploration were conducted.

Secondly, based on the lessons learned from the case history of the tire retaining wall, this paper proposes an eco-friendly multiple adaptive measure for protecting water fronts under severe external forces induced in the context of climate change. The adaptive measures include (i) stabilization of dikes using the techniques of soil improvement and earth reinforcement, (ii) protection of dikes using the units of used tires

placed along the coastal line as a seawall, and (iii) protection of mangroves using a sand mattress placed in front of the mangroves surrounded by used tires.



(a) Undamaged tire retaining wall



(b) Completely damaged concrete sea wall

Fig. 1. Tire retaining wall and concrete sea wall.

2 CASE HISTORY OF TIRE RETAINING WALL

2.1 Overview of the Damage and the Investigations

The whole of Okirai area of Iwate Prefecture, where the tire retaining wall is located, was completely inundated by the tsunami during the 2011 Great East Japan Disaster. The casualties in this area include 66 deaths and 30 missing people. As seen in Fig. 1b, the concrete sea wall along the coastal line completely collapsed. As a result, the tsunami run-up washed away most of the wooden buildings in the area. The tsunami run-up was up to the third floor of the Okirai elementary school, which is located 200 m from the coastline. The tsunami run-up height in this location was found to be 16 m by the RTK-GPS survey conducted by the Hazarika et al. (2012a). According to previous records, the tsunami run-up height in Sugishita area of Okirai was 11.6 m during the Showa Sanriku tsunami in 1933, and was 7.8 m during the Meiji

Sanriku tsunami in 1896 (Shuto, 2011). Based on our surveying data using the total station, the tsunami run-up height this time was estimated to be 16.79 m, which is much higher than past tsunamis that inundated this area.

As a part of the site investigation, GPS surveying, portable dynamic cone penetration test (PDCP), surface wave exploration and micro tremor measurement were conducted.

Fig. 2 shows the plane view of the tire retaining wall in Okirai. The figure also shows the locations of the various field surveys (in-situ density, PDCP test, surface wave exploration, and micro tremor measurement) that were conducted. Disturbed soil samples were also collected from the three locations (No.1, No.2, soil within tire) and laboratory investigations were carried out.

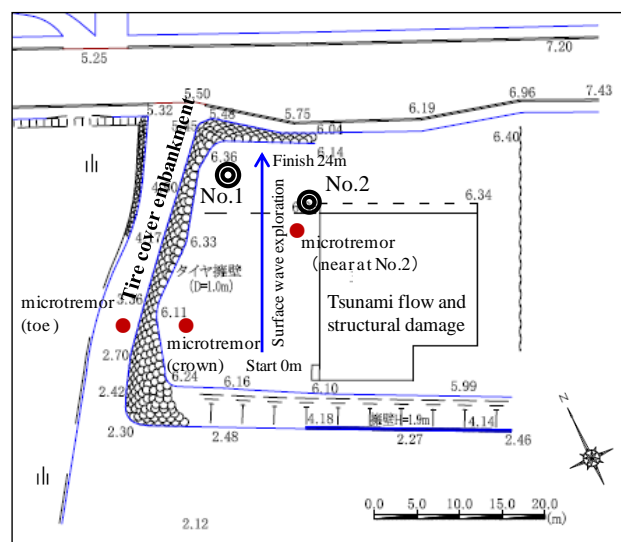


Fig. 2. Plan view of the wall and survey locations.

PDCP is recognized widely as a standard method for obtaining dynamic characteristics of soils at the site by the Japanese Geotechnical Society (JGS 1433). In PDCP, a drop hammer weighing 5 kg is allowed to fall through a rod from 50 cm height, which enables the cone attached at the toe of the rod to penetrate into the ground. The number of blows (N_d) to penetrate every 10 cm of the ground measured. N_d is related to the N-value of the standard penetration test. In this study, using the relationship proposed by Okada et al. (1992) for sandy soils, N_d values were converted to N-values. The location of the ground water table was judged from the wet condition of the rod immediately after termination of the test.

The surface wave exploration is a convenient method to obtain the shear wave velocity distribution (within the ground up to a depth of 10 m), which can measure and analyze the transmission of the surface

wave (Rayleigh wave) that transmits near the ground surface. In this method, a wave is generated by striking the ground surface with a hammer. The generated wave propagates according to the surface and subsurface material conditions. During our investigation, in order to obtain the characteristics of the ground layer indirectly from the surface, the surface wave exploration was carried out together with the PDCP.

Micro tremor measurement has become a powerful tool to estimate the ground motion characteristics, amplification of ground motion in the soil deposits, microzonation and dynamic behavior of existing service structures. The micro tremor observations described in this study were carried out by portable micro tremor equipment (type New PIC). Measurements (2 horizontal and 1 vertical components) were conducted in velocity mode, which were recorded by the sensors. H/V Ratio is then calculated based on the smoothed ratio of horizontal to vertical Fourier spectra of the micro tremor data. The amplitude ratio calculated in this study was based on the method proposed by Nakamura (1989). The value corresponding to the peak represents the predominant frequency of the motion.

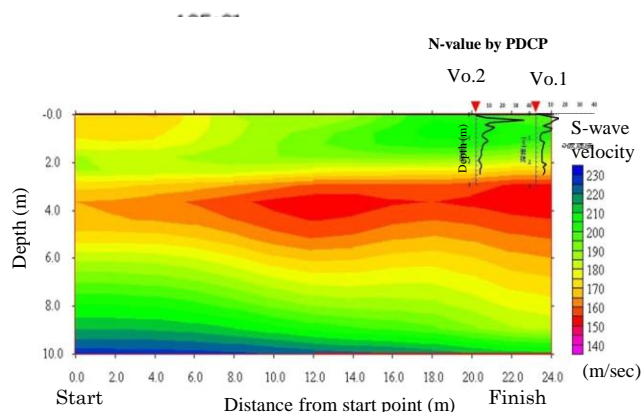
2.2 Results of Field Investigations

The distribution of shear wave velocity by surface wave exploration method conducted on the backfill soils is shown in Fig. 3. As seen in the figure, beyond the depth of 10 m, S-wave velocity is greater than 220 m/s implying a hard stratum near the sloping side. Within the depth of less than 10 m, stratum with 150~200 m/s of S-wave velocity exists. Since the average height of the retaining wall was 3.2 m with a maximum height of about 4 m, it can be said that as a whole, the backfill soil was in the loose state. Fig. 3 also shows converted N-value obtained from the PDCP test. Converted N-value and S-wave velocity in general are showing the similar trend. The converted N-values within the depth of 0~70 cm are high. Therefore, it can be inferred that near the surface the backfill soil has a very high density. The higher density near the surface may be the result of influence of cyclic load experienced by the backfill soils due to parked cars, since the yard was used as a parking lot. On the other hand, converted N-value within the depth of 1~1.5 m is about 5. Therefore, if we consider that the backfill consists only of sandy soil, it can be said that in general the backfill soil was in loose state.

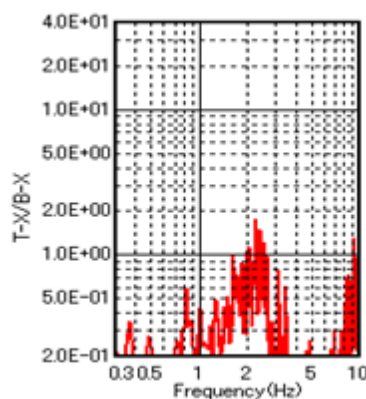
Fig. 4 shows the results of the micro tremor measurements conducted at the top as well as at the bottom of the wall. At location No. 2, the predominant frequency of H/V ratio of the soil deposits is 3.1 Hz (Fig. 4a). Spectral ratio between the top and the bottom of the sloping side was found to be 2.1 Hz (shown in Fig. 4b). The shear wave velocity from Fig. 3 was found to be approximately 200 m/sec beyond 10 m

depth. The predominant frequency of the site is 3.8 Hz. Therefore, it can be said that the results of the micro tremor measurements and the surface wave exploration are in good agreement.

Fig. 3. Distribution of shear wave velocity.



(a) H/V-ratio at the surface



(b) Transfer function

Fig. 4. Results from micro tremor observations.

2.3 Results of Laboratory Investigations

Laboratory tests were conducted for soils samples that were collected at the sites. The in-situ density of the backfill soil was measured using the core-cut

method (JGS1613-2003). The values of in-situ wet density ρ_t at the two locations (No. 1 and No. 2 in Fig. 2) are almost the same (a little more than 1.5 g/cm^3). From the laboratory testing the void ratio of the soil was found to be less than 1.1. The grain size distribution showed that the soils were well-grained (Fig. 5). It can also be said that the soils are well compacted. On the other hand, filled soils inside the tires were found to be of higher density, and thus can be said that they were well compacted. The angle of internal friction of the sample soil (collected within 30 cm from the surface) of the backfill ground is 45.7° , while it is 48.2° for the soil within the tires. Therefore, it can be said that near the surface both soils have high value of internal friction, because the wet density ρ_t is quite high.

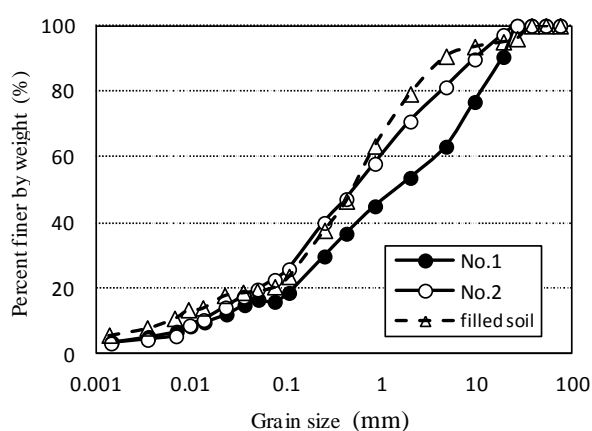


Fig. 5. Grain size distribution of soil samples.

2.4 Damage Analysis

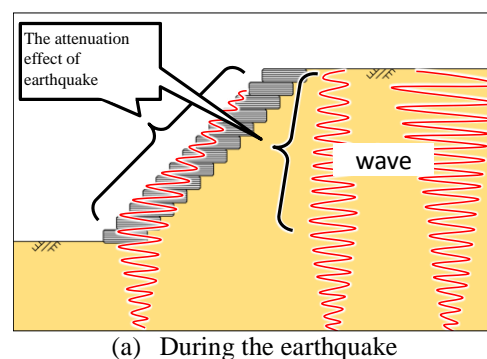
Fig. 6 shows the state of the tire retaining wall at the time of earthquake (Fig. 6a) and tsunami (Fig. 6b). The tire retaining provides the confinement, which can make the wall strong against earthquake, and thus, could prevent any sliding failure or surface failure of the backfill soils. On the other hand, permeable and flexible structures like the tire retaining wall can reduce the earth pressures and water pressures during earthquakes and tsunamis. In addition, the earthquake motion could be attenuated because of the seismic isolation characteristics of the tire and that prevented the failure of the backfill ground.

On the other hand, while tsunami entering from the backfill side damaged the building situated on the backfill ground and also eroded the natural slope opposite to the road parallel to the building, the presence of the tire wall could prevent damage to the backfill as well as the sloping side of the backfill from erosion. The flexible nature of tires could not only reduce the force of impact due to tsunami, but also could prevent any scouring of the wall at the bottom (Fig. 6b), a phenomenon which was prevalent in almost any sea walls, sea dikes, breakwaters and quay walls in

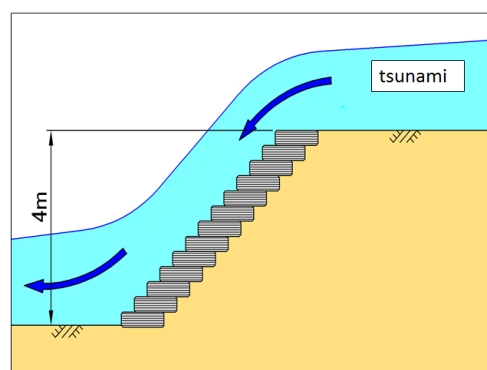
many parts of Tohoku area due to the tsunami this time (Hazarika et al., 2012b).

Based on the D_{20} of Fig. 5, the coefficient of permeability, k was calculated using the relationship proposed by Creager et al. (1945). The permeability of the No. 1 and No. 2 samples was found to be $k = 1 \times 10^{-5} \sim 10^{-6} \text{ m/s}$, which is rather small. The fine contents F_c of the two samples (16% for No.1 and 23% for No. 2) are rather high. Therefore, it is very unlikely that the water level inside the embankment could increase or decrease due to the tsunami run-up.

The fact that tires are strong against scouring is evident from the fact that even during the backrush, the tsunami could not do any damage to the retaining wall. The hoop tension due to confinement, isolation effect and the anti-scouring effect is due to the high strength attributable to the hoop stress in each individual tire, and the resiliency of the tire retaining wall (Fukutake and Horiuchi, 2007; Yasuhara et al., 2006). However, to arrive at a very definite conclusion, detailed study was anticipated. Suzuki et al. (2016) have performed some study in this regard using model tires inside a large-scale direct shear testing apparatus, which revealed that the friction between the individual tires provided good strength to the whole structure.



(a) During the earthquake



(b) During the tsunami

Fig. 6. Behavior of the retaining wall during earthquake and tsunami.

3 MULTIPLE PROTECTION AGAINST COASTAL EROSION USING WASTE TIRES

The case study described above led us to believe

that flexible structures like tires can be very strong against water impact force, and therefore, can be used as a protective layer against wave induced erosion in river and sea coasts. In this section, an adaptation for climate change induced geodisaster is proposed.

3.1 Adaptation to Climate Change Induced Geohazards

The Mekong Delta in the lower part of Mekong River (Vietnam) is the largest granary of Asia, but is nevertheless a region that is vulnerable to climate change. That vulnerability is likely to affect residents' lives and natural environments in numerous ways related to infrastructure, industries (agriculture and fisheries), and ecology. Those impacts are not mutually independent, but rather are expected to share strong mutual correlation. Regarding disasters particularly, difficult situations arise. The so-called "compound disasters" that occur as a consequence of combinations of multiple causes are classifiable as climate change-associated events or climate change-independent events. Unfortunately, however, it seems that many projects related to adaptation to climate change inside and outside of countries associated with the Mekong Delta have been conducted individually. Few achievements have been integrated internally and internationally to proceed to the next stage. To overcome these difficulties, it is necessary to confront obstacles against proper solutions not only from inter-disciplinary aspects, but also from trans-disciplinary aspects, in which many stakeholders such as local residents, governments, researchers, and industries are involved. The second important feature of the Mekong Delta is the proposal of a concrete adaptation, which is able to endow the resilience of stakeholders to climate change by considering the natural as well as the social backgrounds. This adaptation is also necessary to maintain good harmony with industries (mainly agriculture and fisheries) and ecologies in the objective region (Fig. 7).

Given this background, we first proposed a "smart adaptation," which is highly resilient and which constitutes multiple protective dikes as depicted in Fig. 8. This protection is characterized by: (1) resilient dikes improved and reinforced with a mixture of natural fibers and cement, as previously proposed by Sato et al. (2013); (2) locally available and cost-saving soil bags for protecting dikes proposed by Institute of Innovate Water Resources (IIWR) in Vietnam (Van, 2010); (3) mangrove protection using used tires, based on the concept of sea wall protection measure proposed by Hazarika and Fukumoto (2016); and (4) cost-saving sand mattresses used for reducing erosion and increasing accumulation in the river and sea beds proposed by IIWR, Vietnam.

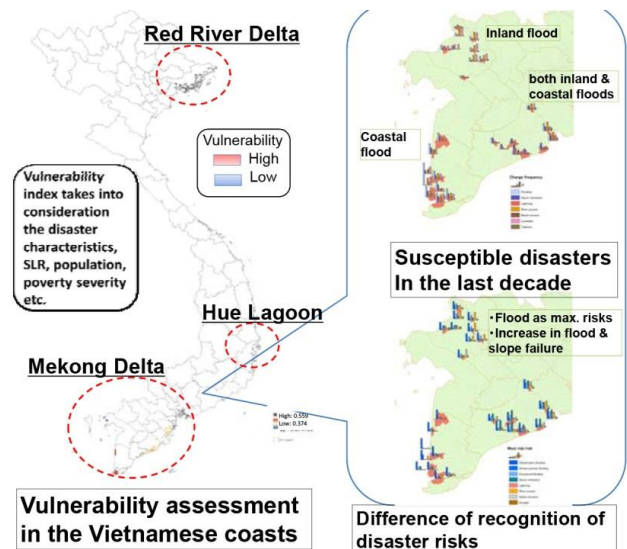
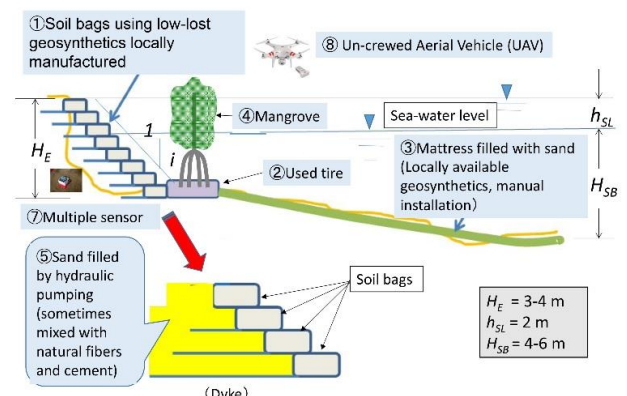


Fig. 7. Objective areas for adaptation to disasters caused by climate change.



(a) Existing adaptation (Van, 2010)



(b) Proposed eco-friendly adaptation

Fig. 8. A comparison between present and proposed adaptation in Mekong delta.

This kind of adaptation using multiple protection system includes not only the disaster prevention aspects, but also the ecological and environmental aspects of

geotechnical engineering. This paper outlines the knowledge of environmental geotechnical engineering that is necessary for the multiple protection proposed herein, although application of this multiple protection technique has just started, and still in its initial stages.

3.2 Stabilization of Dikes

Amongst the impacts of global warming, sea-level rise (SLR) poses the greatest threat to the human settlements along coastlines, particularly in vulnerable areas in Asia–Pacific regions. Areas along coasts and rivers have been affected recently by SLR, underscoring the need to assess the vulnerability of coasts and riverbanks. It is, therefore, necessary to develop countermeasures to mitigate the influences of strong and persistent SLR for coasts and river levees. Among the alternatives available for countering these threats, applying earth reinforcement and soil improvement are promising strategies, not only for coastal structures, but also for river levees that must sustain wave action that is sometimes so severe that it produces storm surges. Furthermore, combinations of conventionally used techniques are anticipated for reducing climate change-induced disasters, as presented in Table 1.

Table 1. Stabilization of dikes through geotechnical measures

Improvement/Reinforcement	Examples of Technique	Remarks
Mechanical improvement/Reinforcement	<ul style="list-style-type: none"> Well-graded soils Well-compacted soils Inclusion of fiber materials 	<ul style="list-style-type: none"> Inexpensive Durable Locally available material or traditionally used material
Chemical improvement/reinforcement	<ul style="list-style-type: none"> Mixture of cement, quicklime and adhesive materials 	<ul style="list-style-type: none"> Attention to contamination
Mechano-chemical improvement/reinforcement	<ul style="list-style-type: none"> Admixture of fiber materials with cement Sandwiched-structure using Non-woven fabrics with quicklime Placement of geosynthetics with soils stabilized by cement 	<ul style="list-style-type: none"> Hybrid Cost/benefit analysis

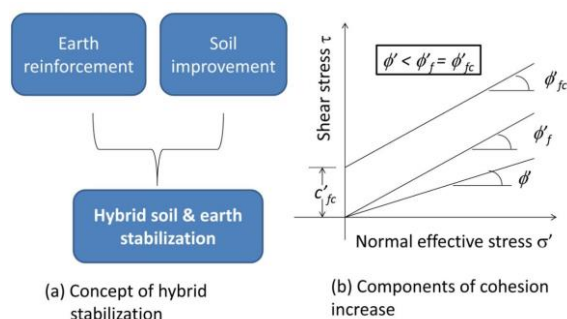


Fig. 9. Soil and earth stabilization using palm fibers and additive cement.

Important issues, however, are: how to reduce the costs for construction practices intended to mitigate disasters, and to reduce the environmental impacts.

Therefore, developing techniques that satisfy engineering effectiveness, eco-friendliness, and cost savings simultaneously is a challenging task. This sub-section, therefore, starts with outline of the past technique, followed by presenting the current circumstances, and finally outlining the future prospects from geotechnical engineering perspectives for protecting coastal riverine dikes.

Fundamentals in geotechnical engineering require that dikes and levees must typically have: (1) well-graded distribution of soil particles, (2) adequate compaction, (3) protective measures against water seepage, and (4) sufficient drainage system. Soil improvement and earth reinforcement can further be adopted to stabilize the river banks, which are endangered due to impact of the excessive external forces in the context of climate change.

As one of the options for increasing the stability of river banks, which enables application of the technique at an actual site in Vietnam, addition of palm fibers (mechanical stabilization), a locally available natural material in Vietnam, is suggested here. Addition of palm fibers to sandy soils increases the frictional force. Addition of cement to soils increases the cohesion force (chemical stabilization) as illustrated schematically in Fig. 9. Both the additions can increase bank stability. Furthermore, combined usage of palm fiber and added cement to sandy soils is expected to increase stability more than in the case of adding palm or cement individually or separately.

Sato et al. (2013) conducted laboratory tests of both seepage failure and permeability tests on sandy soils with and without a mixture of palm fibers. Results show that utilization of soil and palm fiber mixtures in river banks improves both the seepage and the drainage characteristics, particularly for the river banks that constitute sand-rich and coarser soils. Whether increased friction and cohesion contribute to the river bank stability remains an open question.

3.3 Protection of Dikes

Along with conventional countermeasures, such as construction of wall structures and placements of concrete blocks, to protect water-frontal dikes against wave actions, plantation of mangroves is often adopted as a typical measure in Asia–Pacific regions. Measures of this kind are called the “Green Infrastructure.” However, because impacts of climate change have recently been worsened, it is becoming increasingly necessary to protect mangrove forests, which are extremely important from viewpoints of both ecological maintenance and disaster mitigation. To attain this purpose, the current paper presents a proposal for use of waste tires based on the achievements of Hazarika and Fukumoto (2016) who attempted to grow various plants inside of discarded tires, shown in Fig. 10. Some of those plants were found to have a robust growth even in

saline geotechnical environment near sea coast (Hazarika and Yasuhara, 2015). In the present paper, instead of those plants used by Hazarika and Yasuhara (2015) plantation of mangroves is proposed as depicted in Fig. 11. The system of used tires with mangroves described above is regarded as a hybrid structure from the viewpoint that the used tire structure functions both for the protection of dikes and for the growth and maintenance of mangroves.



(a) Hedera



(b) Rubus classic

Fig. 10. Growth of plants inside tires filled with soils

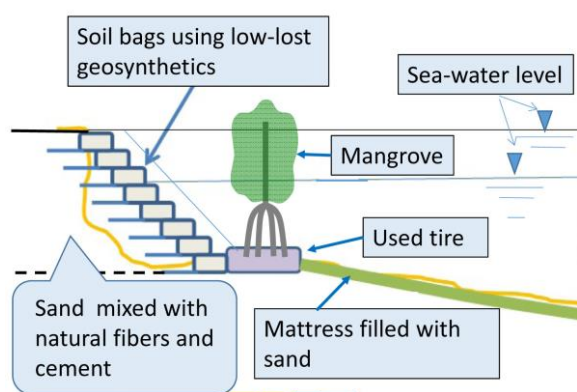


Fig. 11. Protection of mangrove by sand mattress and used tires.

3.4 Extension of a Pilot Project towards Protection of Mangroves

The river bank composition in the Mekong Delta

region is mostly young alluvium with low erosion resistance (critical velocity of 0.5–0.8 m/s). As a result, erosion occurs mostly on canal and river systems even though the flow velocity in this region is not high. Sand mattresses have been developed (Van, 2010) and tested on the Saigon River (Yasuhara et al., 2012; Yasuhara et al., 2013). The sand mattress size can be determined based on the hydraulic condition of the rivers. In small and medium rivers, mattresses of 30–50 cm diameter are applicable. Sand mattresses can also be installed through simple construction through involvement of local residents.

The sand mattress used in the pilot project in Saigon River is shown in Fig. 12. This can be applied for river erosion protection as a low-cost solution by utilizing the techniques presented in Fig. 8a, and explained in Fig. 13. The multiple adaptive system depicted in Fig. 8a comprises two measures for protecting mangroves against severe climate: used tires with mangrove plantation inside and sand mattresses. This system of used tires and sand mattresses is placed along the coast perpendicular to the direction of incident waves.

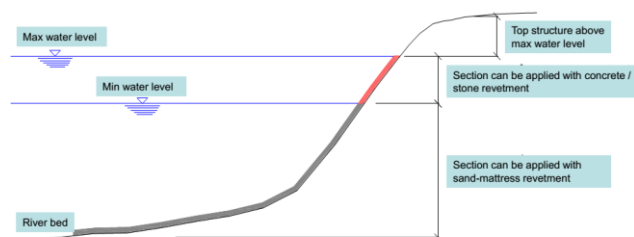


(a) Sand mattresses installation

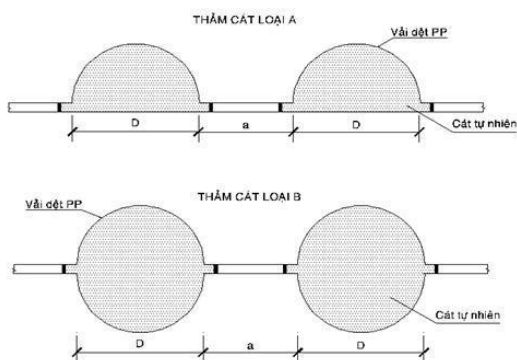


(b) 18 months after installation

Fig. 12. Sand mattresses (Van, 2010).



(a) Bank protection design



(b) Cross-section of mattresses

Fig. 13. River bank protection design using sand mattress.

3.5 Geo-environmental aspects of the proposed adaptation

The following are some of the geo-environmental aspects of the proposed adaptation: (1) The locally available and natural material is used for reinforcement of dikes; (2) Protection of mangroves is emphasized to maintain ecological balance, along with the adaptation of locally available sand mattress technique and utilizing the used passenger car tires; (3) Such approaches lead to the development of cost saving geo-techniques based on the philosophy that environmental impact reduction by successful utilization of waste materials be co-existed with disaster mitigation (Yasuhara, 2010).

4 CONCLUSIONS

The following are the some of the main conclusions derived from this research.

1. The tire retaining wall in Okirai area of Iwate prefecture was not damaged in spite of the loose state of the backfill. Damage to the tire retaining wall could be prevented during the earthquake due to confining effect of each individual tire.
2. The flexibility inherent in tires made the earth pressure and water pressure reduce during the earthquake and the tsunami. The seismic isolation effect was the reason behind such good performance.
3. The flexibilities imparted by the tires could also

prevent any scour and erosion to the slope toe during the leading wave and backrush of the tsunami.

4. The erosion prevention technique proposed here is characterized by eco-friendliness and cost-saving, as the attempts are made to take into the account not only the engineering aspects, but also the ecological aspects.
5. Use of the locally available materials and industrial waste materials for dike stabilization contributes towards the green infrastructure.
6. Last but not least, the technique will work well in vulnerable waterfront areas in Asia and the Asia-Pacific regions, although it was tested only in the Vietnamese waterfronts.

ACKNOWLEDGEMENTS

The financial assistance for the research on forensic investigation on tire retaining wall was provided by Kyushu University under university's P & P research grant for Education and Research in Asian Region. The pilot study in Vietnam was carried out under the supports by the strategic project of Ministry of Environment, Japan, (FY2010-FY2014), and the Grant-in-Aid from Ministry of Education, Sport, Science and Tourism (MEXT) (FY2015-FY2018). The authors gratefully acknowledge this support. The authors are also grateful to Prof. Tadashi Hara of Kochi University, Kochi, Japan and Mr. Hideo Furuichi of Giken Corporation, Tokyo, Japan for their valuable guidance and suggestions during the research. Last but not the least, the authors would like to extend their heartfelt thanks and gratitude to Mr. Kenichiro Yagi, manager of the land on which the tire retaining wall is located, for generously allowing us to use the area during our field survey.

REFERENCES

- 1) Central Disaster Mitigation Council. (2003). Report of the 16th committee meeting, Investigation committee on Tonankai earthquake and Nankai earthquake, *Cabinet Office, Government of Japan* (in Japanese).
- 2) Creager, W.P., Justin, J.D. and Hinds, J. (1945). Engineer for dams, *Earth, Rock-fill, Steel and Timber Dams*, Vol.3: 645-650.
- 3) Fukutake, K., and Horiuchi, S. (2007). Stacks of tires for earth reinforcement using their resistance to hoop tension and land reclamation methods, *Scrap Tire Derived Geomaterials, Hazarika & Yasuhara (Eds)*, Taylor and Francis, London: 205-214.
- 4) Hazarika, H. (2011). Historic tsunami and associated compound disaster triggered by the 2011 great east Japan earthquake - A reconnaissance report, *Keynote Paper, Geosynthetics India' 2011*, Chennai, India: KN57 - KN75.
- 5) Hazarika, H. and Fukumoto, Y. (2016). Sustainable solution for seawall protection against tsunami-induced damage, *International Journal of Geomechanics, ASCE*, doi:

- 10.1061/(ASCE)GM.1943-5622.0000687.
- 6) Hazarika, H., Okada, H., Hara, T., Ueno, M., Ohsumi, T., Yamanaka, M., Yamazaki, T., Kosaka, N, Minowa, H., and Furuichi, H. (2012a). Case studies of geotechnical damage by the 2011 off the Pacific Coast of Tohoku Earthquake and tsunami in Japan, *Proc. of the 15th World Conference on Earthquake Engineering*, Lisbon, Portugal, Paper No 4796.
 - 7) Hazarika, H., Kasama, K., Suetsugu, D, Kataoka, S., and Yasufuku, N. (2012b). Damage to geotechnical structures in waterfront areas of northern Tohoku due to the March 11, 2011 tsunami disaster, *Indian Geotechnical Journal*, Indian Geotechnical Society, Vol. 43(2): 137-152.
 - 8) Hazarika, H., Kataoka, S., Kasama, K., Kaneko, K., and Suetsugu, D. (2012c). Compound geotechnical disaster in Aomori prefecture and northern Iwate prefecture due to the earthquake and tsunami, *Japanese Geotechnical Journal*, Japanese Geotechnical Society, Vol. 7(11): 13-23 (in Japanese).
 - 9) Hazarika, H. and Yasuhara, K. (2015). Sustainable and smart materials in geotechnical constructions, *Proc. Intl. Conf. on Geo-Engineering and Climate Change Technologies for Sustainable Environmental Management*, Allahabad, India, CD-ROM.
 - 10) Nakamura, Y. (1989). A method for dynamic characteristics estimation of subsurface using micro tremor on the ground surface, *Quarterly Report of RTRI*, Vol. 30(1): 25-33.
 - 11) Okada, K., Sugiyama, T., Noguchi, T., and Muraishi, N. (1992). A correlation of soil strength between sounding tests on embankment surface, *Tsuchi to kiso*, Japanese Geotechnical Society, Vol. 40(4): 11-16 (in Japanese).
 - 12) Sato, K., Komine, H., Murakami, S. and Yasuhara, K. (2013). An experimental evaluation on effects on seepage failure using a natural fiber mixed with soils for river dikes, *Proc. International Conf. on Geotechnics for Sustainable Development – Geotech Hanoi*, CD-ROM.
 - 13) Shuto, N. (2011). History of tsunami in Sanriku area (Part 1): Information on tsunami due to 2011 off the Pacific Coast of Tohoku Earthquake, *Joint Investigation Report of the 2011 off the Pacific Coast of Tohoku Earthquake*, <http://www.coastal.jp/tjt/index.php> (in Japanese).
 - 14) Suzuki, M., Hazarika, H., Hara, T., Kuroda, S., Kuribayashi, K., Furuichi, H., Takezawa, K., and Ohsumi, T. (2016). Shear strength characteristics of an undamaged tire retaining wall in Iwate prefecture during the 2011 off the pacific coast of Tohoku earthquake, *Proc. of the 7th Japan-Taiwan Joint Workshop on Geotechnical Hazards from Large Earthquakes and Heavy Rainfalls*, PingTung, Taiwan, CD-ROM.
 - 15) Van, T.C. (2010). Shore erosion in the south of Vietnam, *Workshop on applied protection measures and study needs*, Ibaraki University, Mito, Japan.
 - 16) Yasuhara, K. (2010). Global warming induced climate change adaptation measures from geotechnical perspectives, *Proceedings of the 65th National Conference of Japan Society of Civil Engineers*: 953-954 (In Japanese).
 - 17) Yasuhara, K., Hazarika, H., and Fukutake, K. (2006). Technology for applications of waste tires in geotechnical structures, *Doboku Gijutsu*, Vol. 61(10): 83-85 (in Japanese).
 - 18) Yasuhara, K., Komine, H., Satoh, K. and Duc, D.M. (2013). Geotechnical response to climate change-induced disasters in the Vietnamese coasts and river dikes: A Perspective, *Proc. Second International Conf. Geotechnics for Sustainable Development, Geotech – Hanoi*, Vietnam, 3-21.
 - 19) Yasuhara, K., Van, T.C. and Duc, D.M. (2012). Geosynthetics-aided adaptation against coastal instability caused by sea-level rise, *Proc. Geosynthetics Asia 2012, Bangkok, Thailand*, CD-ROM.

Back to table of contents

Innovation in concrete performance for output and performance based contracts

Dr Diganta Sarma

Contract Management Adviser, Botswana Integrated Transportation Project, World Bank & OFID | International Consultant, Auckland, New Zealand | Dean International Affairs & Visiting Professor, Assam Down Town University, India | Email: dr.d.sarma@gmail.com

ABSTRACT

Output and performance based contracts with rigid pavements and bridges need performance assertion of concrete, where coarse aggregate is generally the major constituent in terms of volume and weight, and naturally it influences the performance of concrete considerably. Although in the available literatures there are indications about the effects of mineralogical compositions of coarse aggregates on strength of concrete, information on failure mechanism for such effects are inadequate. In this paper, a Rapid Quality Identification Technique (RQIT) for characterising variation of constituent deleterious minerals and their influences on coarse aggregates are presented in terms of Aggregate Deterioration Factor (ADF) designated by ADF-templates and ADF-charts developed for the purpose. Supported by petrographic studies, influences of mineralogical compositions on engineering properties are presented for decisively selected coarse aggregates. Further, influence of mineralogical compositions of coarse aggregates on the strength of concrete are experimentally perceived indicating critical aspects of the failure mechanism for common grades of concrete. Subsequent to field applications, research areas for modelling concrete characteristics through the application of RQIT have also been identified.

Keywords: Output and performance based contract, geotechnical innovation, quality surveillance, concrete performance, coarse aggregate, petrographic studies, deleterious minerals, Rapid Quality Identification Technique, Aggregate Deterioration Factor

1. INTRODUCTION

Output and Performance Based Road Contract (OPRC) is a practising model for implementation of major road projects of various government agencies in New Zealand. OPRC is also a recent trend for implementing major road projects funded by the World Bank and several pilot projects are ongoing in Botswana. Although OPRC has considerable advantages over traditional project implementation models, its obligatory requirement for ensured performance for long duration is a great challenge for the contracting entities and project owners in terms of sustainability within and beyond such long defect liability period.

Concrete as one of the costliest and sensitive items in OPRC for construction of rigid pavements and bridges, its performance assertion through quality surveillance needs geotechnical innovation as one of the important requirements.

In this paper, a geotechnical approach of risk Mitigation and sustainability in concrete is presented for heavy and important structures using a Rapid Quality Identification Technique (RQIT) and applied in practice based on the first phase R&D undertaken in Northeast India under the guidance of the author. Subsequently prediction modelling has been developed and presented for sustainable concrete performance.

Strength of concrete depends on the quantity and properties of its ingredients. Constituting up to 80% of volume, coarse aggregates' characteristics significantly affect the performance, quality, and cost effectiveness of concrete [1a], [2a].

Although, wide extent of quality control tests including petrographic tests are specified for the choice of quality coarse aggregates, yet results cannot always provide confidence for bulk concrete production. Moreover, effect of varying mineralogical compositions on quality of coarse aggregates vis-à-vis concrete is an area not yet explored adequately in prevailing literature.

2 BACKGROUND

Variations of constituent minerals were found to be prominent in the coarse aggregates of two nearby quarries 900 m apart, as evident in Research Area -I (RA-I) in the Northeast India (Earthquake designated zone-V). Previous geological studies in RA-I indicated the quarry area as an integral part of the Precambrian basement of Assam (India). In both the quarries of RA-I, granitic and schistose type of rocks were found to be developed [3] and generally of rock type porphyritic granite and hornblende-biotite schist of Q-1 (Ktb) and Q-2 (Mnp) quarries respectively.

Out of several reasons attributable to failure of structures, constructed with the coarse aggregates of

these quarries, variation of constituent-deleterious-minerals was considered as one of the possible reasons and accordingly, as first step, a research [4] was undertaken under the guidance of the author aiming at correlative study.

3 QUALITY CONTROL LIMITATIONS

Collection of representative samples of coarse aggregates for ascertaining typical properties is difficult for varied characteristics of constituent minerals. Notwithstanding that the properties of collected samples of coarse aggregates are adopted without adequate interpretations at each or all stages namely: during approval for opening a quarry, during investigations at the design stage of projects, and during construction quality control and surveillance. Further, assessment of the characteristic of entire stock-piles based on such samples is difficult since guideline for comprehensive interpretations is not available.

Further, observations at the quarry sites indicated considerable variations in constituent minerals with the progress of quarry besides encounter of different types of rocks and effect of such variations in the performance of concrete remains unknown.

4 INVESTIGATION OF COARSE-AGGREGATES

The general approach of sampling for quality control of coarse aggregates is at random from the stockpile. For acceptance of aggregates for usual concrete routine tests are commonly conducted, results of which determine the choice of the stockpile.

Review of Indian Roads Congress [7a], British Standard [8], and Technical Recommendations for Highways of South Africa [9 a & b], it can be construed that the recommendations in the respective codes are inadequate for selection of coarse aggregates. Moreover, prevailing quality control processes do not provide any quality-profile of coarse aggregates for varied constituent minerals within the mass of quarried rock or with the progress of quarry. From the observed variations of coarse aggregates' characteristics it is either way difficult to comment on adequacy or inadequacy of the test frequency, specified in the guidelines, unless some qualitative parameters are available ensuring at least the relative characteristics and quality-profile.

5 QUICK IDENTIFICATION TECHNIQUE (QIT)

5.1 Developments

A typical rock-profile of the study sites is shown in the Figure-1 testifying variation of coarse aggregates' quality with progress of quarry due to wide variation of constituent minerals. In order to characterise variation of constituent deleterious minerals and their impacts on coarse aggregates vis-à-vis concrete, a 'Rapid Quality

Identification Technique (RQIT)' ① was developed for qualitative diagnosis of randomly or gradually variable characteristics of coarse aggregates within the stockpiles or with the progress of quarry. The RQIT is a diagnostic approach to derive deterioration potential of coarse aggregates at any stage. The outcome of RQIT is 'Aggregate Deterioration Factor (ADF)' ①, values of which indicate qualitative comparison of coarse aggregates. This qualitative-based method was developed and used for construction of a multi-storey building in Assam and for quality surveillance of a 40 Km heavy haul mine road project in Orissa of Eastern India. Furthermore, quality surveillance using RQIT was also been outlined in various bid proposals in Mauritius and other parts of Southern Africa. ① - Author's Intellectual Property Right.

5.2 Sampling for RQIT

RQIT is based on the principle that the quantity and the manners of distribution of constituent deleterious minerals have varying influences on the performance of coarse aggregates. In this study coarse aggregates of similar appearance were stacked separately using a secondary chute at the end of crusher-conveyor and sampled for determination of ADF.

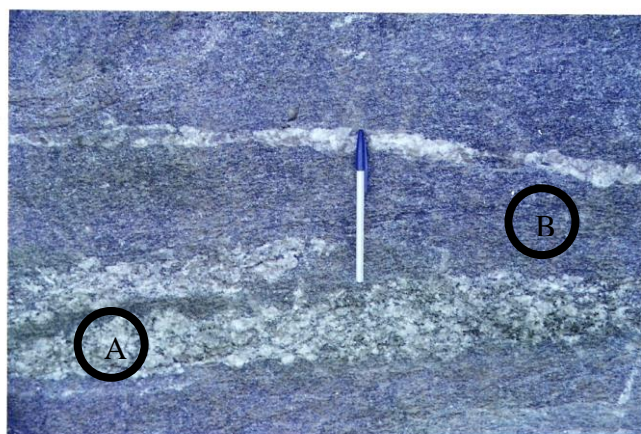


Fig.1. Typical irregular matrix of rock mass, constituent ingredients vary from Quartzo feldspathic (A) to flaky minerals (B).

5.3 ADF Methodology

In RQIT flaky and soft minerals like biotite, muscovite, etc., are designated as deleterious and are considered responsible for performance of coarse aggregates. Once deleterious minerals are identified by 'RQIT-needle' ① of specific hardness, their texture patterns are compared with selected template of total 20 standard 'ADF templates' ①, each designates a specific value in the 'ADF-charts' ① to evaluate 'Aggregate Deterioration Factor' (f_{ad}) that are varying randomly from minimum '6' to maximum '100' and can be evaluated by the equation:

$$f_{ad} = f_a \times \frac{\alpha \cdot \sum_{i=1}^{i=n} f_m + \beta \cdot \sum_{i=1}^{i=n} f_v}{n} \quad (1)$$

Where in (1), n is the number of observations undertaken, f_v is the component of ADF representing effect of veins, f_m is the component of ADF representing effect of matrix, α and β are two importance factors depend on the purpose for which coarse aggregates is used, and f_a is a factor depends on the relative hardness of deleterious minerals.

5.4 ADF of the Coarse Aggregate Stacks

In this study with the aggregates of selected geological features, RQIT was applied to the stacks of coarse aggregates separated taking into consideration their appearance. The stacks of highest ADF of respective quarry materials were selected for study on the strength of concrete supported by petrographic studies, engineering properties, and compressive strengths of concrete cubes. The highest ADF of the selected lots of porphyritic granite (Ktb quarry) and hornblende-biotite schist (Mnp quarry) were found to be 62 and 55 respectively.

6 PETROGRAPHIC MODAL ANALYSES

In order to know the characteristics of the soft minerals those have been designated as deleterious in RQIT and characteristics of other constituent minerals, petrographic study was carried out following standard procedure of preparation of thin rock section [10].

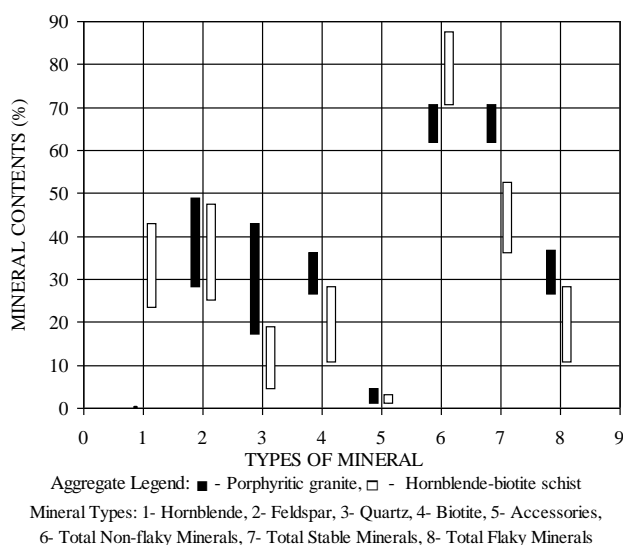


Fig. 2. General variations of mineral constituents in coarse aggregates.

The modal analysis [11] of porphyritic granite indicated average percentages of mineral contents, namely, feldspar (microcline & plagioclase), quartz, biotite, and accessories minerals as 40.16, 26.87, 30.20, and 2.63 respectively. The modal analysis of hornblende-biotite schist indicated average percentages of mineral contents, namely, hornblende, biotite, feldspar (plagioclase), quartz, and accessories minerals as 33.53, 19.40, 33.87, 11.40, and 1.60 respectively [4].

The average percentage contents of porphyritic

granite in terms of flaky and non-flaky/stable minerals were 30.2 and 67.03 respectively. The average percentage contents of hornblende-biotite schist in terms of non-flaky, stable, and flaky minerals were 78.80, 45.27, and 19.40 respectively. Schematic presentations of the variation of different mineralogical constituents of two quarries, in general, are presented in Figure 2.

7 ENGINEERING PROPERTIES OF COARSE AGGREGATES

The strengths of coarse aggregates from the stacks of highest ADF, assessed by the average Aggregate Crushing Strength Value (ACSV) [2c] for porphyritic granite (Ktb quarry) and hornblende-biotite schist (Mnp quarry), were found to be 29.6 and 30.1 respectively. The strengths of coarse aggregates towards sudden shocks and impact were assessed by the aggregate impact tests [2d]. The average Aggregate Impact Value (AIV) for porphyritic granite (Ktb quarry) and hornblende-biotite schist (Mnp quarry) were found to be 35.62 and 33.94 respectively.

The index properties of coarse aggregates were assessed by the specific gravity and water absorption tests [2e]. The average specific gravity (G_s) for porphyritic granite (Ktb quarry) and hornblende-biotite schist (Mnp quarry) were found to be 2.72 and 2.90 respectively. The average apparent specific gravity (G_a) for porphyritic granite (Ktb quarry) and horn-blende-biotite schist (Mnp quarry) were found to be 2.76 and 2.92 respectively. The average water absorptions (w) for porphyritic granite (Ktb quarry) and hornblende-biotite schist (Mnp quarry) were found to be 0.5 and 0.83% respectively. The flakiness of coarse aggregates was assessed by evaluating the percentage weight of flaky particles having least dimension less than three-fifth of its mean dimensions [2f]. The average Flakiness Index (FI) for porphyritic granite (Ktb quarry) and hornblende-biotite schist (Mnp quarry) were found to be 5.53 and 11.93% respectively.

8 MINERALOGICAL COMPOSITIONS' EFFECT ON ENGINEERING PROPERTIES

No noticeable relationships could be identified for ACSV and FI with percentage of flaky minerals, rather with stable minerals. However, results of AIV had propensity towards the percentage of flaky minerals. Although gain in AIV were observed with the gain in percentages of flaky minerals or vice versa, variations of AIV were not so significant unless relatively wide variations of flaky minerals observed.

This was particularly noticed for the samples of higher f_v values possibly due to less damage to randomly orientated coarse aggregates, veins at or near perpendicular to the direction of impact transferred. However, for the samples of higher f_m values comparable variations of AIV were noticed with that of

flaky minerals possibly due to damage of coarse aggregates regardless of their orientations.

Above discussions indicate that only AIV has propensity towards flaky minerals' presence and sensitivity of propensity depends upon vein and matrix factors, which can be evaluated through QIT. Since flaky minerals' contents can be simulated in terms of ADF, it is possible to develop / monitor trends between AIV and ADF at all the stages of investigations, as both AIV and QIT can easily be performed at site without much time and cost.

9 CONCRETE TESTS AND DISCUSSION

Concrete the cubes of most common grades were prepared [12] and tested [13]. Coarse aggregates from the stacks of highest Aggregate Deterioration Factors (ADF) of 62 and 55 respectively were used.

The 7-day average compressive strengths were found to be 2.04 and 2.31 N/mm² for volumetric mixes 1:2:4 and 1:1½:3 respectively for concrete cubes consisting coarse aggregates of hornblende-biotite schist (Mnp quarry). On the other hand, 7-day average compressive strengths were found to be 2.31 and 2.13 N/mm² for respective volumetric mixes for concrete cubes consisting coarse aggregate of porphyritic granite (Ktb quarry) [4].

Relatively less average compressive strengths of the cubes were noticed in comparison to 7-day standard strength of usual concrete for similar volumetric mixes. Further, rate of gain of compressive strengths with increased concrete grade were less than that of typical-usual-concrete. Furthermore, decrease in compressive strengths with increased grade for concrete of porphyritic granite aggregates was an uncommon trend. Cubes of failed concrete were closely observed for the effect of mineralogical compositions.

10 EFFECT OF MINERALOGICAL COMPOSITIONS ON CONCRETE STRENGTH

In this study failure planes were noticed predominantly through coarse aggregates of concrete, despite weak interface and transition zone due to higher water/cement ratio of 0.64 and 7-day concrete strength where the mechanical, geometric and index properties of aggregates were within acceptable limits.

The drop in compressive strengths with increased grade of concrete consisting coarse aggregate of porphyritic granite (Ktb quarry) may be attributable to failure of more aggregates than that of the other type apparently due to relatively higher Aggregate Deterioration Factor (ADF). It was also found that both AIV and flaky minerals' contents of porphyritic granite were higher than the other.

Interpretation of engineering properties, mineralogical compositions and ADF of these coarse aggregates indicated a possible critical limit of concrete for AIV of 35%, flaky minerals' content 25%, and ADF

of 60, beyond which compressive strengths might reduce with improved grades. The flaky minerals' contents can be simulated in terms of ADF, an outcome of RQIT, which together with Aggregate Impact Test can easily be performed at site without much time and cost. Therefore, it is possible to develop/ monitor trends among compressive strength of concrete, ADF and AIV at all the stages of investigations.

11 CONCLUSION

Following conclusions are drawn based on the scope of the study presented in the forgoing chapters:

1. Irregular matrices of constituent minerals remain in different proportions in visually distinguishable rock-profiles. Moreover, in separated stacks of coarse aggregates, based on visual similitude, the variations of major minerals range between 10 to 25% with high content of flaky minerals up to average 30.2%.
2. Variations of deleterious minerals have varying influences on the performance of coarse aggregates and such variations in context to matrix and vein are found responsible for virtually distinguishable texture and shape.
3. A comparison among engineering properties, mineralogical composition and ADF of coarse aggregates indicate possible critical limits of concrete for AIV of 35%, flaky minerals' content 25%, and ADF of 60, beyond which compressive strengths may reduce with improved grade of concrete.
4. With increasing demand of high-strength and high-performance concrete, emphasising durability, investigation of coarse aggregate through RQIT is found suitable for improvement of reliability through performance modelling of concrete and found suitable for OPRC contracts.

REFERENCES

1. QUIROGA, P. N. AND FOWLER, D. W. The Effects of Aggregates Characteristics on the Performance of Portland Cement Concrete, Report No ICAR 104-1F, International Center for Aggregate Research, The University of Texas at Austin, August 2004, (a- pp 1, b- pp 86).
2. INDIAN STANDARD, IS: 2386, Method of Tests for Aggregates for concrete, 1963, (a- Part I pp 3, b- Part VIII pp 11-12, c- Part IV pp 4, d- Part IV pp 10, e- Part III pp 4, & f- Part I pp 11).
3. DEKA, G. A geotechnical study of granitic rock occurring in and around Guwahati of Kamrup District, Assam, with special reference to their utility as road material, PhD thesis, Gauhati University, 1994.
4. DAS, N. A correlative study between engineering and geological properties of rock aggregates with reference to cement concrete, Postgraduate Dissertation on Engineering Geology under Gauhati University, Cotton College, Guwahati -1, India, 1996.
6. AITCIN, P. C. High-performance concrete, E & EN Spon, London 1998, (a- pp 201, b- pp 85).
7. Specifications for road and bridge works, Ministry of Road

Transport and Highways, Fourth edition, Indian Roads Congress, New Delhi, 2001, (a- pp 367, b- pp 206).

8. BS 5400: Part 8: 1978, Recommendations for materials and workmanship, concrete, reinforcement and prestressing tendons, British Standard Institution, pp-3.

9. TRH 14: 1985, Guidelines for road construction materials, Technical Recommendations for Highways, Department of Transport, South Africa, (a- pp 28, b- pp 49).

10. HUTCHISON, C. S. Laboratory handbook of petrographic techniques, First edition, Wiley Interscience publication, New

York, 1974.

11. JOHANNSEN, A. A descriptive petrography of the igneous rocks, Vol: 1, Introduction, Textures, Classification and Glossary, University of Chicago Press, Chicago, 1931, pp 267

12. INDIAN STANDARD IS: 1199, Methods of sampling and analysis of concrete, 1959.

13. INDIAN STANDARD IS: 516, Method of test for strength of concrete, 1959

14. NEVILLE, A M. Properties of Concrete, Third edition, ELBS, London, 1983.

Back to table of contents

Static & dynamic analysis of a tailings dam

Ritu Raj Nathⁱ⁾, Ashok D. Pandeyⁱⁱ⁾ and Mukat L. Sharmaⁱⁱⁱ⁾

i) Ph.d Student, Department of Earthquake Engineering, Indian Institute of Technology Roorkee, Roorkee 247667, India.

ii) Asst.Professor, Department of Earthquake Engineering, Indian Institute of Technology Roorkee, Roorkee 247667, India.

iii) Professor, Department of Earthquake Engineering, Indian Institute of Technology Roorkee, Roorkee 247667, India.

ABSTRACT

The progress of mankind had been propelled by the discovery and subsequent utilization of metals. The process of obtaining metals and other minerals requires mining and crushing of large quantities of rock. They are pulverized and processed to recover metal and other minerals. A fine grind is often necessary to release metals and minerals, so the mining produces enormous quantities of fine rock particles, in size ranging from sand-sized down to as low as a few microns, known as tailings. The disposal of tailings has always been a great challenge to the engineering fraternity which possesses severe threat to the environment. In the past, tailings were disposed of at a site of convenience and naturally the most cost-effective sites were often identified as the flowing water or sometimes directly into drainages. However as local concerns had arisen about sedimentation in downstream watercourses, water use, and other issues, mining operations began impounding tailings behind earthen dams, which were often constructed of tailings and other waste materials. At some projects, tailings embankments reach several hundred feet in height and the impoundments cover several square miles. Hence the safety analysis of this tailings dam under both static and dynamic loading has gained significant importance in the field of engineering as its failure may trigger uncontrolled spills of tailings and other materials, a potential hazard associated with environmental catastrophes, life and property losses and negative company image. Past experiences have shown that due to various reasons, the failures of tailings dam are considerably higher than other retaining structures (e.g. water retention dams). The various factors that have made tailings dam more vulnerable may be categorized as (i) embankments formed by locally collected fills, (ii) subsequent increase in dam height coupled with severe increase in effluent, (iii) lack of regulations on specific design criteria, (iv) lack of dam stability requirements and (v) high cost of maintenance works after closure of mining activities. Again, due to continuous generation of large quantity of tailings, raising the height of an existing dam is the only option by which the tailing material can be confined to a limited area. However this becomes tricky sometimes as it comes across some existing infrastructure and that may obstruct the construction of a stable tailings dam beyond a specific height. In that scenario, to meet the confinement obligations the tailings dam may need to be truncated at some locations by means of appropriate retaining wall configuration. The analysis of the complex assemblage of the fully saturated tailing material, the material of which dam is constructed and the retaining are beyond the scope of conventional linear analysis. An attempt has been made in this study to perform the safety analysis of a tailings dam, situated in India under both static and dynamic conditions using finite element method. The critical state of stresses should be examined with the perspective of 2-D analysis. The study also incorporates a site specific response spectrum compatible time history analysis of such a complex truncated dam-retaining wall assembly. Linear static and Mohr-Coulomb soil constitutive models are used for performing linear and nonlinear analysis. The results are shown in terms of both displacements and stress conditions. It is observed that maximum horizontal displacement occurs at the slope of the dam (fill materials). Seismic loading induces higher displacement in both vertical and horizontal directions. After the insertion of the retaining wall, a steep increase in the stresses has been noticed

Keywords: Tailings dam, 2-D Finite element analysis, response spectrum compatible time history, maximum horizontal displacements

1. INTRODUCTION

The process of obtaining metals and other minerals requires mining and crushing of large quantities of rock. They are pulverized and processed to recover metal and other minerals. A fine grind is often necessary to release metals and minerals, so the mining produces enormous quantities of fine rock particles, in size ranging from sand-sized down to as low as a few microns. These fine-grained wastes are known as tailings. In the past, the majority of mines were small underground operations with correspondingly modest requirements

for tailing disposal. But due to increasing demand, it has become economical to mine large lower-grade deposits. This has greatly increased the amount of tailings. In the gold industry for example, the extraction of only a few grams of gold may result into the generation of tons of dry tailings. Thus, tailings disposal is a significant part of the overall mining and milling operations projects. The disposal of tailings has always been a great challenge to the engineering fraternity which possesses severe threat to the environment. In the past, tailings were disposed of at a site of convenience and naturally the most

cost-effective sites were often identified as the flowing water or sometimes directly into drainages. However as local concerns had arisen about sedimentation in downstream watercourses, water use, and other issues, mining operations began impounding tailings behind earthen dams, which were often constructed of tailings and other waste materials. At some projects, tailings embankments reach several hundred feet in height and the impoundments cover several square miles. Hence the safety analysis of this tailings dam under both static and dynamic loading has gained significant importance in the field of engineering as its failure may trigger uncontrolled spills of tailings and other materials, a potential hazard associated with environmental catastrophes, life and property losses and negative company image. Ideally the intended life span of a tailings dam is more than 100 years but past experiences show that due to various reasons, the failures of tailings dam are considerably higher than other retaining structures (e.g. water retention dams). The various factors that have made tailings dam more vulnerable may be categorized as (i) embankments formed by locally collected fills, (ii) subsequent increase in dam height coupled with severe increase in effluent, (iii) lack of regulations on specific design criteria, (iv) lack of dam stability requirements and (v) high cost of maintenance works after closure of mining activities. An attempt has been made in this study to perform the safety analysis of a tailings dam under both static and dynamic conditions using finite element method. The critical state of stresses should be examined with the perspective of 2-D analysis. Again due to continuous generation of large quantity of tailings, raising the height of an existing dam is the only option by which the tailing material can be confined to a limited area. However this becomes tricky sometimes as it comes across some existing infrastructure and that may obstruct the construction of a stable tailings dam beyond a specific a height. In that scenario, to meet the confinement obligations the tailings dam may need to be truncated at some locations by means of appropriate retaining wall configuration. The analysis of the complex assemblage of the fully saturated tailing material, the material of which dam is constructed and the retaining are beyond the scope of conventional linear analysis. The paper also incorporates a study on the nonlinear finite element analysis of the truncated dam and retaining wall assembly under both static and seismic loading.

Several investigations have attempted to summarize the causes of major tailings dam failures throughout the world. The most recent and comprehensive synthesis was performed by the International Commission on Large Dams (ICOLD) (221 tailings dam incidents) for a period 1917-1989. The analysis of tailings dam performance provides important information on key design factors of dam stability, including in situ

characteristics viz. geology, seismicity, climate, upstream catchment area; selection of embankment and construction sequence types, as well as hazard factors identification (heavy rain, flooding, earthquake vulnerability). The study by Azam and Li reviewed the causes of failures of tailings dam in the last century and concluded that *“The main reasons for dam failures are unusual rain and poor management and these causes have a profound effect on failure mechanisms. The inclusion of climate change effects in the initial design and of the observational method during construction, maintenance, and monitoring are highly desirable.”* The study revealed that from 1910 to 1999, almost 7% of total dam failures were attributed to instability of slopes whereas this value has significantly reduced to 2% in the proceeding decade i.e. 2000- 2010. A different study by Rico and Benito et al. also stated that almost 9% of total tailings dam failures are caused unstable slopes. From these studies it is very evident that stability analysis of tailings dam is a very important aspect of geotechnical engineering. Finite Element Method (FEM) of analysis is widely used for this purpose. Chakraborty and Choudhury tried to find a detail method of seismic analysis which can be used reliably for the design and construction. They performed both static and seismic analysis. They used FLAC, TALREN 4, SEEP/W and SLOPE/W. The static and seismic analysis of a typical section of water retention type tailings earthen dam of 44 m height and with a central core of 4 m is performed in this study. In case of seismic analysis they have used time history of Taft earthquake (21st July, 1952) having magnitude of 7.7. The maximum displacement magnitude obtained by FLAC analysis is compared with the maximum displacement obtained by the Makdisi and Seed method. It has been observed that seismic loading has severe effect on the deformation of the dam. The maximum displacement in the crest region obtained in seismic analysis is about 19 times higher than that in static analysis. This value is also slightly higher than the value obtained by Makdisi and Seed. The base level input acceleration gets amplified with height of the dam and at the crest level the amplification is about three times. Finally they have concluded that earthen dam is not safe under the condition of seismic loading.

2 FINITE ELEMENT MODELLING & INPUT PARAMETERS

The 2D FEM analysis of earth-fill dam is carried out by assuming plane strain condition. This assumption is valid only if the third direction (length) is very large compared to the other two dimensions of the dam body. This implies that the strain in the third direction is almost zero. Several researchers have studied the effect of this assumption on the results for different loading conditions. In most of cases the results were almost in the same range having a small difference. Prevost. Jean

H *et al.* has investigated the results of 2D nonlinear and 3D nonlinear dynamic finite element analyses of an earth dam subjected to two very different input ground motions. The dam they have used in the study is relatively long dam and is not likely to be susceptible to the effects of three-dimensionality. There were only slight differences are found between results of 2D and 3D nonlinear analyses. George Gazetas has studied the recent developments in the estimation of seismic response of earth dams. The response of the earth dams to seismic shaking is dictated by the properties of constituent materials, the geometry, and the nature of the base motion. From their study they have concluded that to make a realistic prediction of an earth dam to seismic loading, careful consideration must be given to the following factors:

- (a) Nonlinear-inelastic soil behaviour
- (b) Dependence of soil stiffness on confining pressure
- (c) Narrow geometry
- (d) Dam – valley interaction

They also concluded that magnitude of nonlinearities is the single major factor in deciding which phenomena to attempt to simulate in the analysis and with what degree of sophistication. In case of seismic loading where the ground shaking is less than 0.2g or less the nonlinearities are unimportant and the other factors are to be modelled properly. They also found that the simplifying assumption of identical and synchronous excitation, mainly for mathematical convenience may be reasonable only for the relatively low frequencies associated with the first one or two fundamental modes of the dam. At high frequencies, when the wavelengths of the incident seismic waves become equal to or smaller than a characteristic dimension of the dam, substantial difference is expected to arise in both magnitude and phase angles of the motions at various points of the base.

2.1 Geometrical Description

A 2D model is considered for both static and dynamic analysis. The length of rock-fill dam is 150m and maximum height is 34m. Foundation width is taken as twice the length of the dam which makes it to 300 m and the depth of the foundation is 150 m.

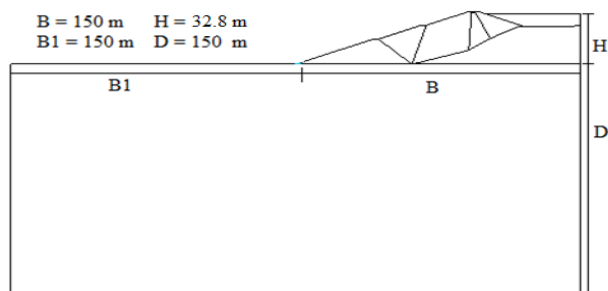


Fig. 1. Physical Dimensions of the Tailings Dam model

The height of the retaining wall is 18.7m and width

is 13.39 m. The triangular portion is filled with stone masonry. The tailings dam is truncated at the downstream end and a retaining wall is constructed. The geometry of the retaining wall and the truncated dam are shown below in fig. 3 and fig. 4 respectively.

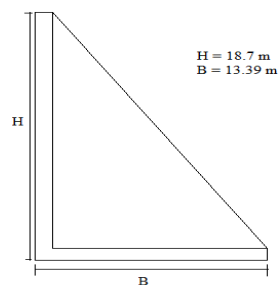


Fig. 2. Physical Dimensions of the Retaining Wall

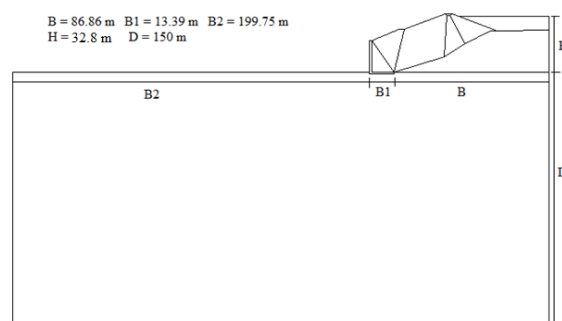


Fig. 3. Physical Dimensions of the Truncated Dam-Retaining wall assembly

2.2 Material properties & soil constitutive models

The representative material properties are as shown in table 1. For both static and dynamic analysis of the dam two different constitutive models i.e. linear elastic and Mohr- Coulomb models are chosen to represent the material behaviours. The linear elastic model is an approximation to figure out the state of stresses in the dam. However, the Mohr- Coulomb model, in which material non linearity is taken into account, represents more realistic in-situ behaviour. For the truncated dam-retaining wall assembly, only Mohr- Coulomb model is chosen. The linear elastic model involves only two input parameters i.e. E (Young’s modulus) and ν (Poisson’s ratio) for soil elasticity. The Mohr-Coulomb model represents a “first order” approximation of soil or rock behaviour. This elastic –plastic model involves five input parameters: i.e. E and ν for soil elasticity; ϕ and c for soil plasticity and ψ as an angle of dilatancy. For each layer a constant average stiffness is calculated. Due to this constant stiffness, computations tend to be relatively fast and one gets the initial approximation of deformations. Besides these five model parameters mentioned above, initial soil conditions play an important role in soil deformations.

Table 1. Representative material properties

Material	Elastic modulus (kPa)	Density ((t/m ³)	Cohesion(kPa)
Pond tailings	1.20E05	1.92	0.001
Compacted tailings	2.52E05	1.92	0.001
Clay	1.47E05	1.96	14.71
Fill material	4.85E05	2.11	0.001
Concrete	2.23E07	2.54	-
Foundation rock	5.11E05	0.001	-
Stone masonry	3.1E07	2.75	-

2.3 Boundary conditions

In the analysis vertical rollers are provided along the edges of the foundation and the bottom of the foundation is restrained in all directions.

2.4 Loadings

The dam under static condition is analyzed for gravity loads and has been subjected to ground motion which is compatible with the site specific response spectrum. A damping of 10% is assumed. However, the expected damping due to the presence of tailings material is much higher than 10%. Fig 5 has illustrated the time history used in the study.

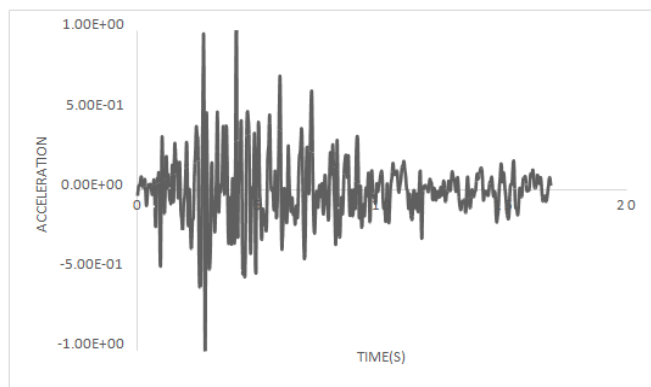


Fig. 4. Response spectra compatible acceleration time history (input motion)

3 RESULTS AND DISCUSSION

In this project work, 2D FEM analysis are performed for five cases viz. nonlinear static lading, linear and nonlinear seismic loading for the complete dam and nonlinear static and seismic loading of the truncated dam. The graphical representation of total displacement and extreme total vertical stress are shown in the paper. Along with the deformation patterns of the structure under various loadings are also illustrated in the following figures. Due to the paper length constraint, the results of only non linear analysis are shown here.

3.1 Analysis of the complete dam

Nonlinear Model under Static Loading

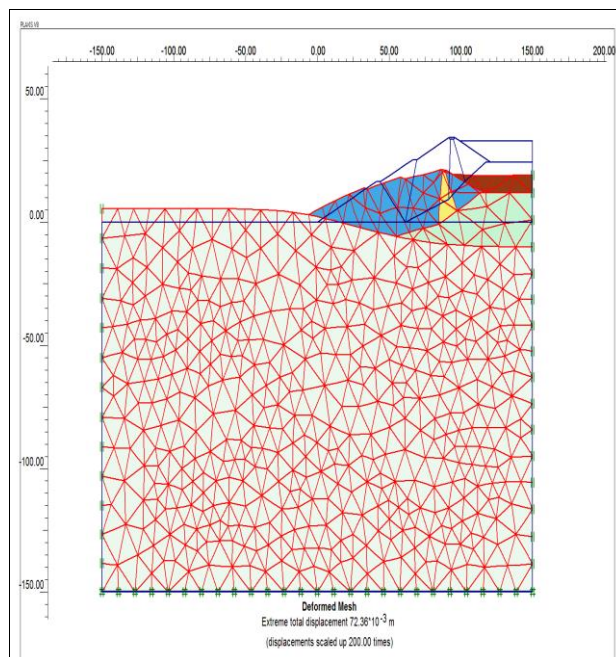


Fig. 5. Deformed Mesh

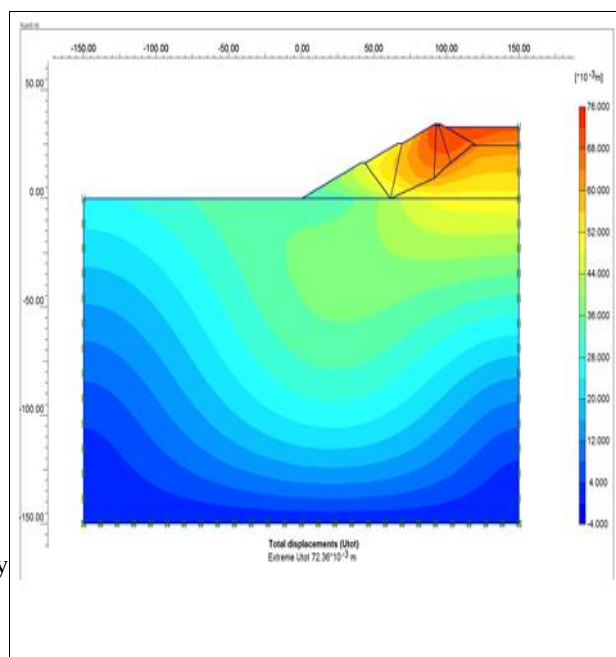


Fig. 6. Extreme Total Displacement (72.36 mm)

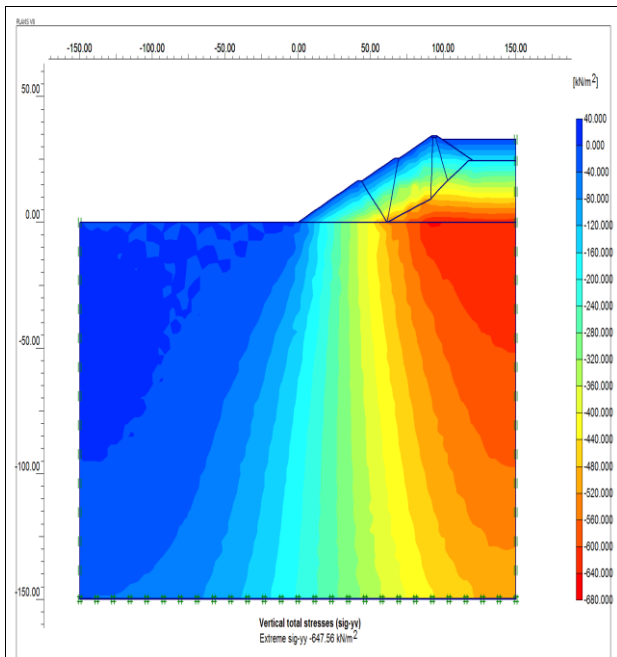


Fig. 7. Extreme vertical total stress (-648 kN/m^2)

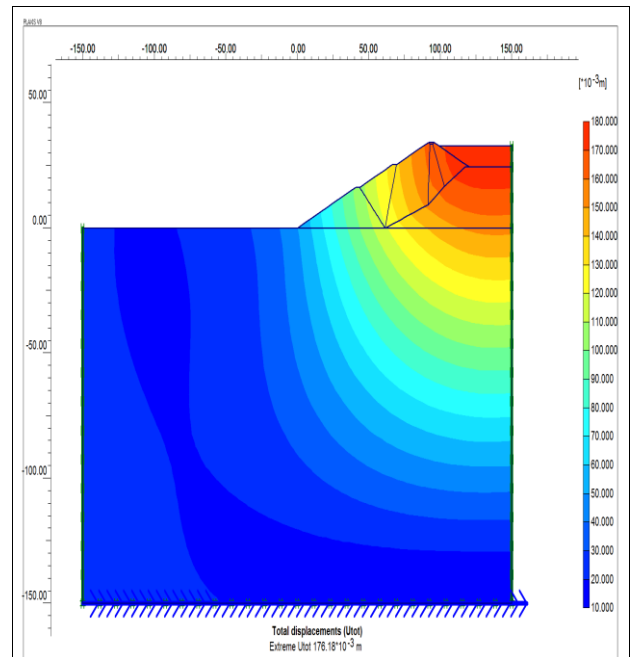


Fig. 9. Extreme Total Displacement (176.18 mm)

Nonlinear Model under Seismic Loading

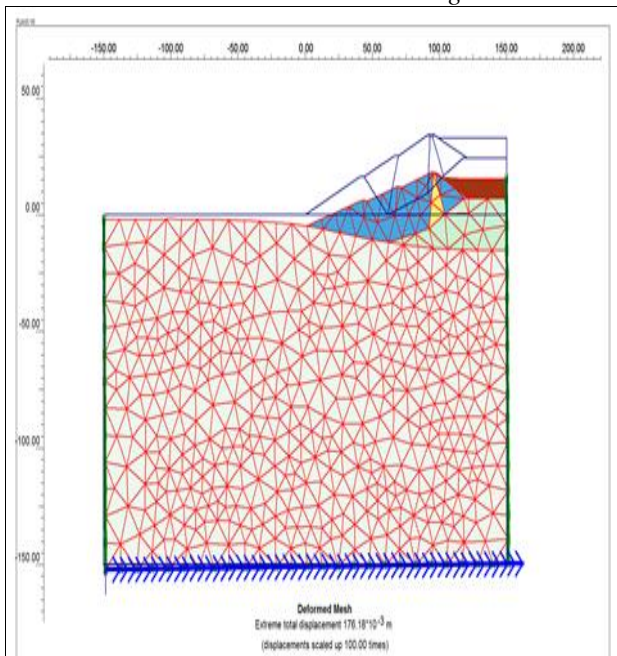


Fig. 8. Deformed Mesh

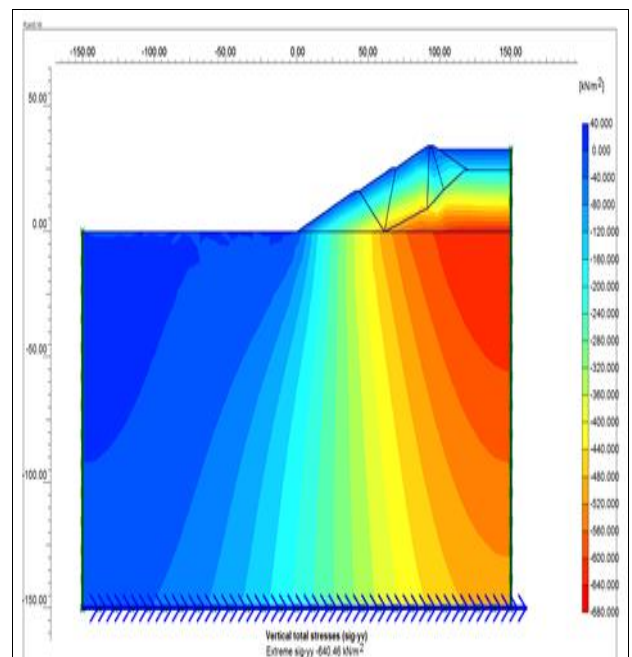


Fig. 10. Extreme vertical total stress (-640 kN/m^2)

3.2 Analysis of the truncated dam
Nonlinear Model under Static Loading

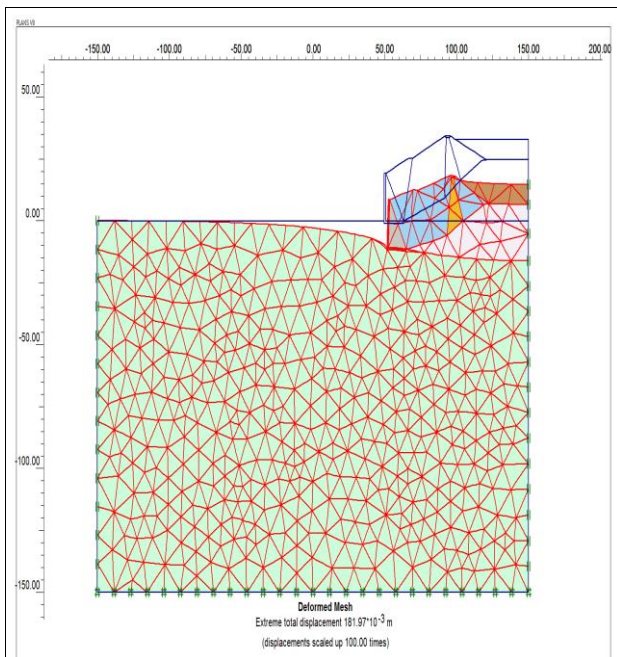


Fig. 11. Deformed Mess

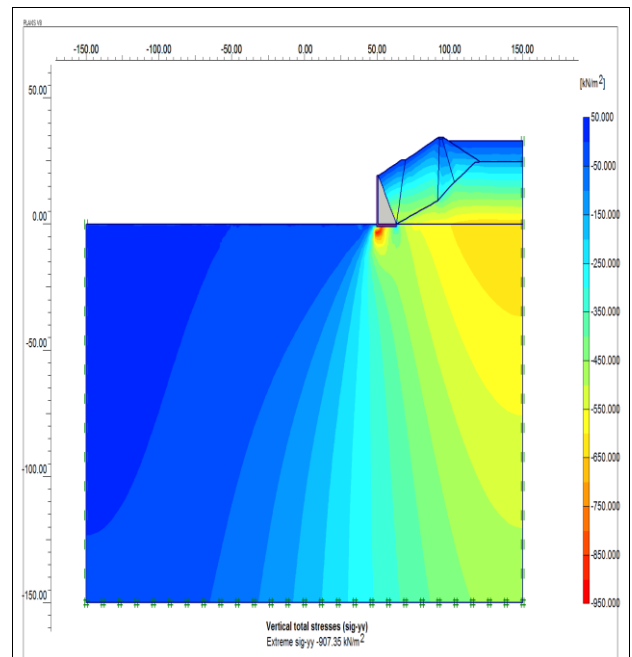


Fig. 13. Extreme vertical total stress (-907 kN/m²)

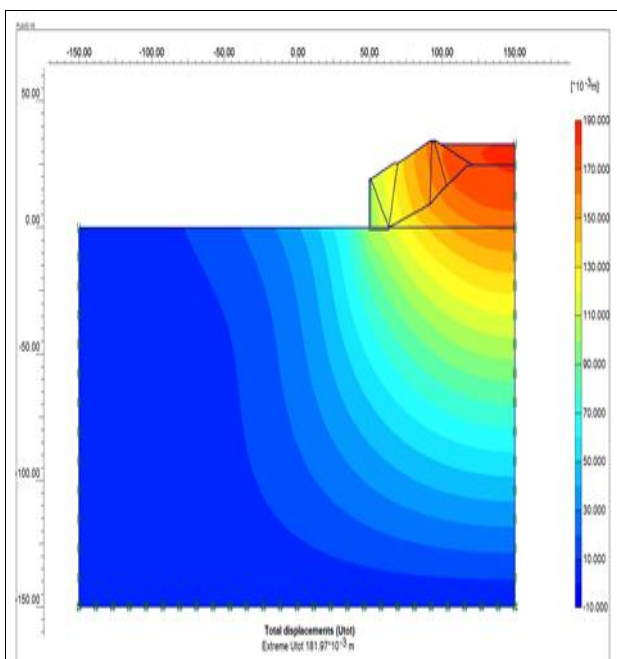


Fig. 12. Extreme Total Displacement (181.97 mm)

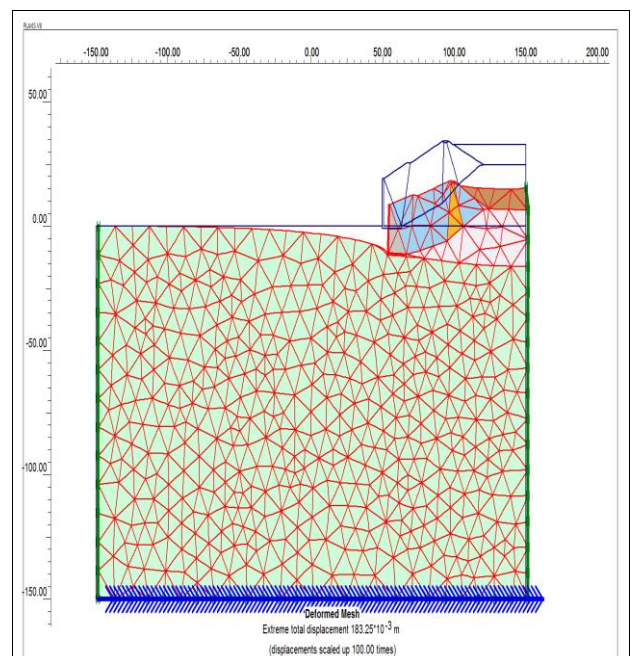


Fig. 14. Deformed Mess

Nonlinear Model under Seismic Loading

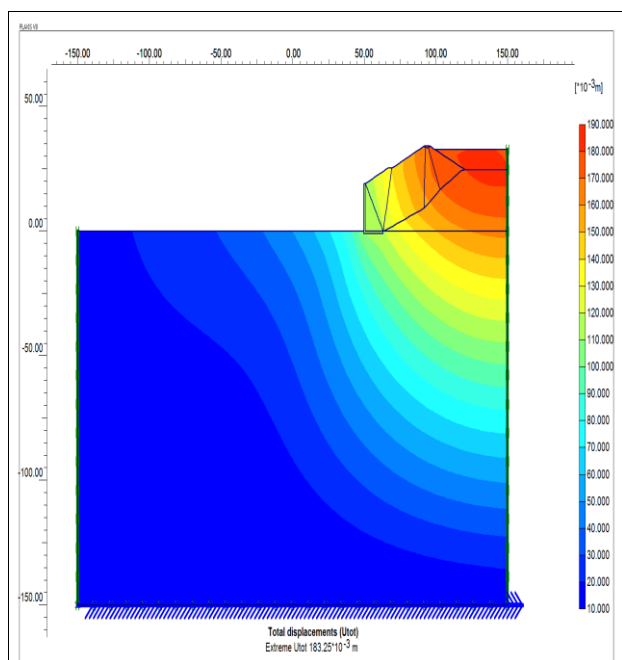


Fig. 15. Extreme Total Displacement (183.25 mm)

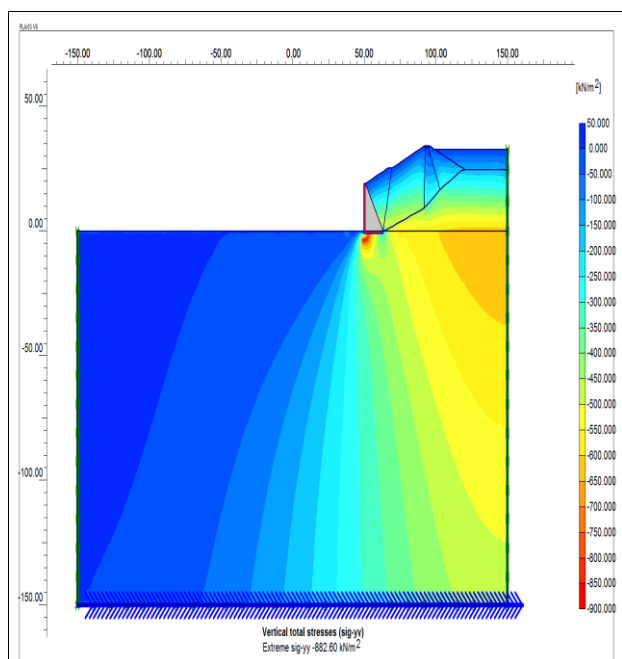


Fig. 16. Extreme vertical total stress (-883 kN/m²)

3.3 Discussions

In both the complete and truncated dams, the maximum displacement occurs at the pond tailings under both static and seismic loadings. Similarly, it is observed that maximum horizontal displacement occurs at the slope of the dam (fill materials). Seismic loading induces higher displacement in both vertical and horizontal directions. After the insertion of the retaining wall, a steep increase in the stresses has been noticed. Table 2 shows the results of all analysis for comparison.

Table 2. A comparison of different parameters of various models

Model/Parameter	Extreme Total Displacement (mm)	Extreme Horizontal Displacement (mm)	Extreme vertical total stress (kN/m ²)
Nonlinear model under static load for complete dam	72.36	46.83	-648
Linear elastic model under static load for complete dam	178.88	26.84	-637
Nonlinear model under seismic load for complete dam	176.18	25.45	-640
Nonlinear model under static load for truncated dam	181.37	35.38	-907
Nonlinear model under seismic load for truncated dam	183.25	51.97	-883

4 CONCLUSION

From the present study, we can observe that insertion of the retaining wall actually decreases the overall stability of the dam slope. Slope stability measurements are recommended after the insertion of the retaining wall. It may also be concluded that linear elastic model yields conservative results. The nonlinear model which takes into account the stiffness degradation gives more realistic values.

REFERENCES

- 1) Akhlaghi, T. and Ali, N. (2014): Evaluation of the Pseudostatic Analysis of Earth Dams Using FE Simulation and Observed Earthquake-Induced Deformations: Case Studies of Upper San Fernando and Kitayama Dams, *Scientific World Journal*, 1-12.
- 2) Azam, S. and Li, Q. (2010): Tailings Dam Failures: A Review of the Last One Hundred Years, *Geotechnical News*, 50-53.
- 3) Brinkgreve, R.B.J. *et al.* (2008): Plaxis 2D Version 8 User's Manual, *Delft University of Technology and PLAXIS the Netherlands*.
- 4) Chakraborty, D and Choudhury, D. (2009): Investigation of the Behaviour of Tailings Earthen Dams under Seismic Condition, *American Journal of Engineering and Applied Sciences*, 2 (3), 559-564.
- 5) Kramer, S. L. (1996): "Geotechnical Earthquake Engineering", *Pearson Publication*.
- 6) Liang, J. and Elias, D. (2010): Seismic Evaluation of Tailing Storage Facility, Proceedings of *Australian Earthquake Engineering Society 2010 Conference, Perth, Western Australia*.
- 7) Zardari, M.A. (2013): Numerical Analyses of Gradually Rising Tailings Dam, *Doctoral Thesis*, Luleå University of Technology, Sweden.

[Back to table of contents](#)

Site response analysis: A case study of Guwahati city

Nayan Jyoti Dasⁱ⁾, Mousumi Deoriⁱⁱ⁾ and Sasanka Boraⁱⁱⁱ⁾

i) M.E. Student, Department of Civil Engineering, Assam Engineering College, Gauhati University

ii) M.E. Student, Department of Civil Engineering, Assam Engineering College, Gauhati University

iii) Assistant Professor, Department of Civil Engineering, Assam Engineering College, Gauhati University

ABSTRACT

Risks to manmade structures due to seismically induced ground deformation have been evident from past earthquakes. Influence of site effects on strong ground motions has been ascertained by many seismologists and earthquake engineers. Guwahati city, considered one of the most seismically active zone in the country, is situated on the bank of the mighty Brahmaputra. It is mainly based on filled alluvium deposits overlying the hard rock, surrounded by hills from the southern and eastern sides of the city. The influence of these loose soil deposits on propagation of seismic waves demands site response analysis in the region. In this paper, an attempt has been made to study the site amplification potential of Panbazar and Khanapara area of Guwahati city by the one-dimensional equivalent linear method using the DEEPSOIL program to estimate the local site effects. Borehole data from available bore-logs have been obtained to define the geotechnical properties of the sites and recorded motions from past earthquakes have been used as input motions for the analysis. Very high amplifications have been observed at both the sites. Also, soft soils have been found to amplify seismic motions much more strongly and at lower frequencies than medium/ hard soils. Additionally, a parametric study, on how the site amplification potential of a site for hypothetic cases, varies with layering of soils as well as depth of bedrock is investigated and presented. The results provided in the seismic response analysis of Guwahati city could be used as guideline for risk assessment and management of future probable events in this region, especially in the absence of site specific data.

Keywords: SPT N-value, shear wave velocity, PGA, amplification factor, fundamental frequency.

1 INTRODUCTION

Seismic site response analysis has been carried out to estimate the stratified soil response (in term of acceleration, PGA profile, amplification spectra, etc.) subjected to a considered bed rock motion. The commonly applied analysis methods are: Linear, Equivalent linear and Non-linear (Kramer, 1996). The present study utilizes the one-dimensional equivalent linear method due to its simplicity, ease of use and low computational cost. The study region, Guwahati is one of the listed cities under the Urban Vulnerability Reduction project. The city which falls in zone V of the Indian seismic code (IS 1893:2002) is most vulnerable against earthquakes. The concentration of soft alluvial deposits in the city greatly influences the site response during shaking. Due to rapid urbanization of the city in the past few decades and the recent decision of transforming Guwahati into a smart city, a detailed site response analysis has become necessary in order to reduce the vulnerability of the existing and upcoming structures against any future seismic event. 1D equivalent linear analysis has been conducted on selected soil profiles using DEEPSOIL v6.0, to study the local site effects. Further the effects of soil type (hard, medium and soft) and bedrock depth on site

response have been studied with the help of a few hypothetical analyses.

2 STUDY REGION

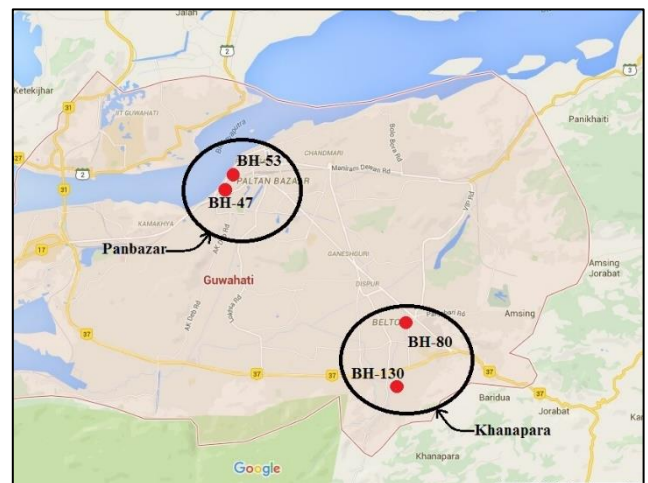


Fig. 1. Location of boreholes in the study region.

The Guwahati city, also known as the gateway of northeast India, is situated on the bank of the river Brahmaputra of over an area of about 600 square kilometers (latitude 26.08°–26.25°N, longitude 91.58°–

91.92°E). The city is mainly based on filled alluvium deposits overlying the hard rock and surrounded by hills from the southern and eastern sides. The city has experienced several devastating earthquakes of different magnitudes ranging from 5 to 8.7 (Nath *et al.*, 2008). Thus, guided by the seismicity level of this region, the city has been considered for site response analysis. Two significant sites viz. Panbazar and Khanapara have been selected for analysis (Fig. 1). Available borehole data from the Microzonation report of Guwahati, 2007 have been collected and two boreholes from each site have been selected for analysis.

3 METHODOLOGY

Site response analysis has been carried out at specific sites of Guwahati city by the equivalent linear method using the DEEPSOIL program. For the response analysis, the input parameters required are input ground motions, shear wave velocity profile and dynamic soil characteristics (strain dependent modulus reduction and damping behaviour and cyclic strength curves). The general methodology adopted in the present study involves:

- Collection of geotechnical and seismic data from the study region,
- Data processing to obtain important geotechnical and seismic parameters,
- Evaluation of site response by one-dimensional equivalent linear method.

3.1 Geotechnical data of the study region

The geotechnical data for the present study have been obtained from available bore-logs for the study region, collected from the Microzonation report of Guwahati region, 2007. A total of four boreholes, two each from Panbazar (BH-47, 53) and Khanapara (BH-80, 130) area have been considered for analysis (Fig. 1). The soil profile in both the sites has been found to consist of mainly silt, clay and sand. The shear wave velocity (V_s) has been obtained by using the empirical correlation between SPT N-value and V_s (m/s), valid for all type of soils by Imai and Tonouchi (1982),

$$V_s = 97 \times N^{0.314} \tag{1}$$

3.2 Input motion

Three earthquake motions recorded at Nongstoin station have been chosen as input motion (Table 1). Nongstoin, which is a site class A station (Mittal. et. al., 2012) has been chosen to simulate rock outcrop motion. The motion database has been collected from the website www.pesmos.in.

Table 1. Details of seismic motions considered in the present study.

Motion No.	Motion	Date	(M_w)	PGA (g)	Duration (sec)
------------	--------	------	-----------	---------	----------------

1	Myanmar India border	11/08/09	5.6	0.0150	79.040
2	Bhutan	21/09/09	6.2	0.0280	106.340
3	Kokrajhar	29/10/09	4.2	0.0106	65.985

3.3 Evaluation of site response by 1D equivalent linear method

The present study utilizes the equivalent linear method of analysis through DEEPSOIL (Hashash *et al.*, 2011) to observe the soil response under earthquake loading and perform a detailed analysis of its outcome. The shear wave velocity has been used as an input to define the shear property of the soil. Standard modulus reduction and damping ratio curves proposed by Vucetic and Dobry (1991) and Seed and Idriss (1991) have been used to define the dynamic behaviour of clayey and sandy soils respectively. An elastic bedrock with a shear wave velocity ($V_s=1500\text{m/s}$), unit weight ($\gamma=25 \text{ kN/m}^3$) and damping ($\xi=5\%$) has been considered at the bottom of each borehole. The shear strain ratio (SSR) has been estimated from the earthquake magnitude (M) from the following relation by Idriss and Sun, (1992):

$$SSR = \frac{M-1}{10} \tag{2}$$

4 RESULTS AND DISCUSSIONS

The results of the site response analysis have been obtained for all the boreholes. The shear wave velocity profile of the four boreholes are shown in Fig. 2.

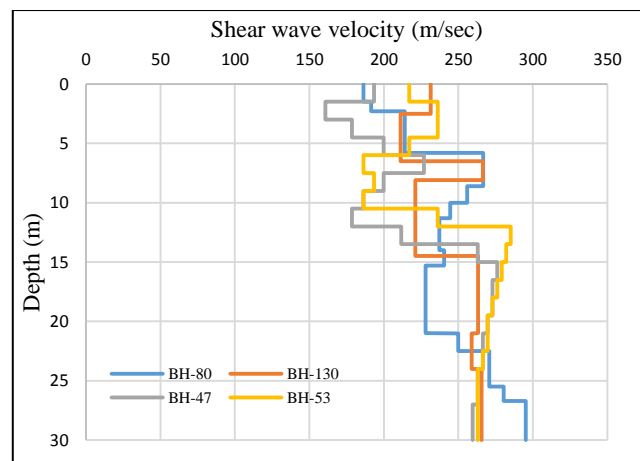


Fig. 2. Shear wave velocity profile of the study boreholes.

The average shear-wave velocity between 0 and 30-metres depth (V_{s30}) for the four boreholes are shown in Table 2.

Table 2. Summary of V_{s30} for the study region.

BH-No.	80	130	47	53
V_{s30} (m/s)	243.19	245.48	233.50	248.14

The V_{s30} has been observed to be in the range of 200 m/s to 250 m/s. Hence, according to the site classification by PESMOS, the study region falls in site class C (soil site).

4.1 Effects of local soil deposits

Significant amplification of PGA of the input motions have been observed at the ground surface for all the four soil columns (Fig. 3 to 5). Softer layers characterized by low shear wave velocity (usually the top layers) displayed higher amplification as compared to the lower, more stiffer soil layers (higher shear wave velocity). The notable deviations in the PGA and surface amplification exhibit the vivid effect of local site geology on the acceleration response recorded at the surface.

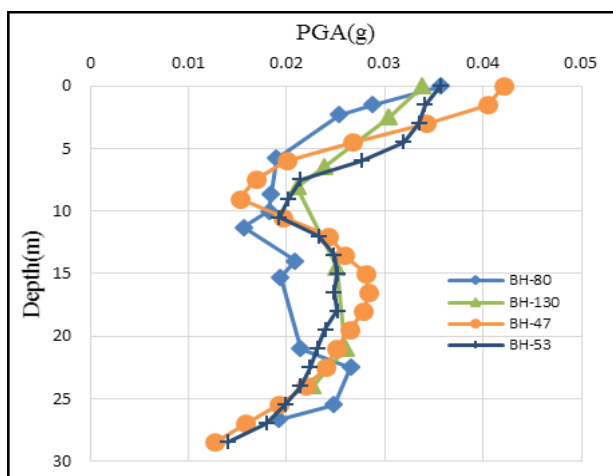


Fig. 3. Peak ground acceleration profile for motion 1.

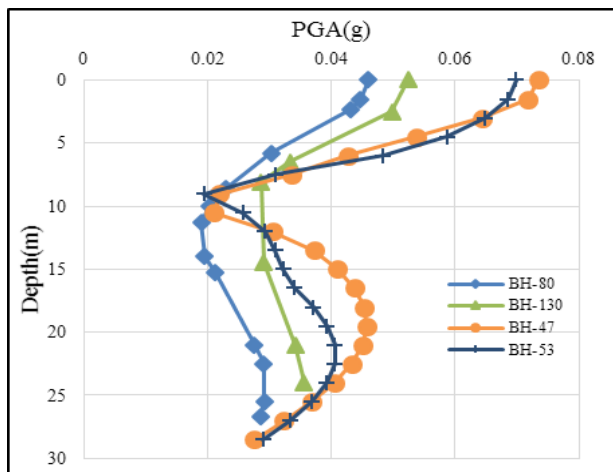


Fig. 4. Peak ground acceleration profile for motion 2.

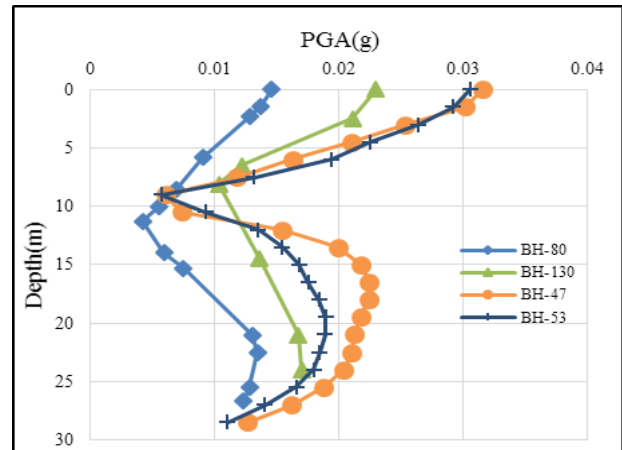


Fig. 5. Peak ground acceleration profile for motion 3.

Site amplification factor is often used as one of the parameters for estimation of site response. It is the ratio of peak ground acceleration at the surface to that of acceleration at the top of bed rock.

$$Amplification\ factor = \frac{PGA\ recorded\ at\ the\ surface}{PGA\ at\ the\ top\ of\ bedrock} \quad (3)$$

The amplification factor in the study region has been found to be in the range of 1.458 to 3.230 which is quite alarming (Table 3).

Table 3. Summary of PGA amplification (surface/input).

BH No	80		
Motion	1	2	3
PGA at top of bedrock (g)	0.014	0.026	0.010
PGA at surface (g)	0.036	0.046	0.015
Amplification Factor	2.550	1.770	1.458
BH No	130		
Motion	1	2	3
PGA at top of bedrock (g)	0.014	0.026	0.010
PGA at surface (g)	0.034	0.052	0.023
Amplification Factor	2.417	2.015	2.295
BH No	47		
Motion	1	2	3
PGA at top of bedrock (g)	0.013	0.028	0.013
PGA at surface (g)	0.042	0.073	0.031
Amplification Factor	3.230	2.600	2.380
BH No	53		
Motion	1	2	3
PGA at top of bedrock (g)	0.014	0.029	0.011
PGA at surface (g)	0.036	0.070	0.031
Amplification Factor	2.570	2.410	2.820

The variation of Fourier amplification ratio (FAR) versus frequency at the surface for the three input motions at the four boreholes have been shown in Fig. 6 to 8. A summary of the above parameters are shown in Table 4.

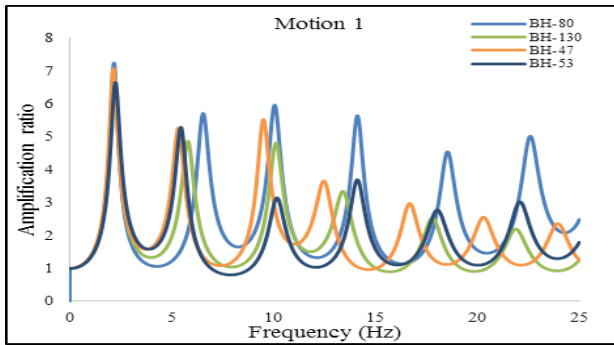


Fig. 6. Amplification spectra for motion 1.

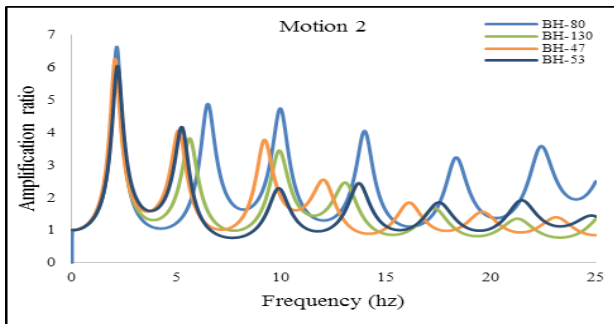


Fig. 7. Amplification spectra for motion 2.

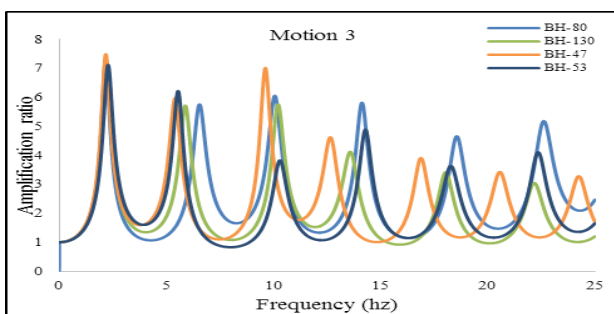


Fig. 8. Amplification spectra for motion 3.

Table 4. Variation of amplification ratio and fundamental frequency.

Motion	Parameter	BH 80	BH 130	BH-47	BH-53
1	FAR	3.01	2.60	7.10	6.61
	Fundamental freq (Hz)	0.90	0.65	2.15	2.25
2	FAR	4.45	3.32	6.22	6.00
	Fundamental freq (Hz)	1.59	1.23	2.10	2.18
3	FAR	7.28	7.11	7.50	7.10
	Fundamental freq (Hz)	2.16	2.22	2.20	2.30

FAR at the surface level has been observed to be in the range of 2.60-7.50 with fundamental frequency range from 0.65 Hz to 2.30 Hz.

4.2 Effects of Sub-surface layering

To understand the effect of sub-surface layers on site response, two boreholes (BH-47 & BH-53) have been analysed using two different subsurface layers for

a particular input motion (motion 1). It has been observed that as the number of sub-layers increases, the natural frequency remains same or slightly shifts towards left (Table 5). This can be attributed to the fact that increase in subsurface layers decreases the soil stiffness which amplifies low frequency motions.

Table 5. Summary of FAR and fundamental frequency.

BH No.	No. of Layers	Fundamental freq. (Hz)	FAR
BH 47	20 Layers	2.15	7.10
	12 Layers	2.15	7.10
BH 53	20 Layers	2.23	6.61
	9 Layers	2.25	6.61

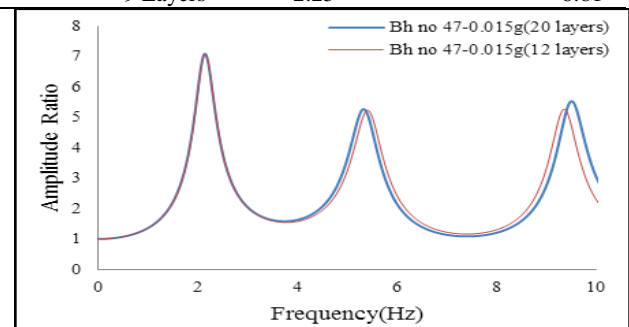


Fig. 9. Amplification spectra of BH-47.

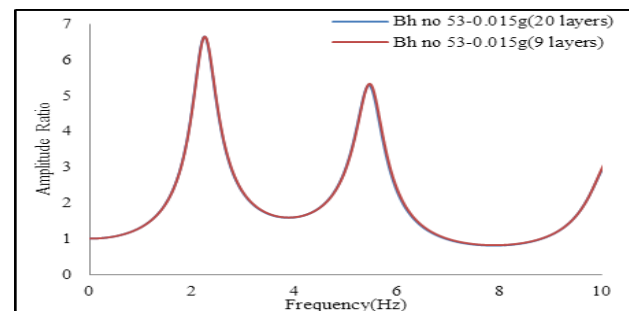


Fig. 10. Amplification spectra of BH-53.

4.3 Hypothetical analysis

4.3.1 Effects of soil type

To understand the effect of soil type on strong ground motion, three hypothetical cases have been assumed with hard, medium and soft soils. The classification is based on shear wave velocity as per IS 1893(Part I): 2002. The bed rock depth in all the cases is 30 metres from the ground surface. Motion 1, with a PGA of 0.015g has been considered as the input ground motion for the analysis. Table 6 shows the values of unit weight and shear wave velocity considered for the three soil types as per IS 1893(Part I): 2002. Amplification spectra for the three soil types have been obtained by performing 1-D equivalent linear analysis (Fig. 11). Table 7 shows the results in tabular form.

Table 6. : Unit weight and shear wave velocity for different type of soils (as per IS 1893(Part I): 2002).

Soil type	Unit weight	Shear wave velocity
-----------	-------------	---------------------

	(KN/m ³)	(m/s)
Soft	12	150
Medium	16	300
Hard	19	500

Table 7. Fourier amplification ratio (FAR) & corresponding fundamental frequencies for all the three soil types.

Soil type	Fundamental frequency (Hz)	FAR
Hard	4.42	3.75
Medium	2.46	6.44
Soft	1.16	8.36

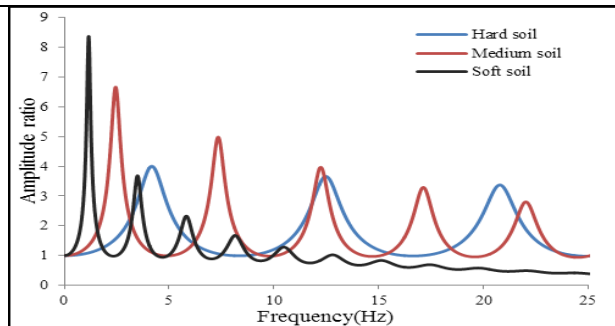


Fig. 11. Amplification spectra for hard, medium and soft soil.

So it has been observed that natural frequency shifts towards left as the soil stiffness decreases i.e., natural frequency is directly proportional to shear wave velocity. Also softer soil caused higher amplification (high FAR) as compared to medium/ hard soils.

4.3.2 Effects of bed rock depth

To understand the effects of bed rock depth on site response, five hypothetical cases have been assumed where bedrock depth from the surface increases from 10m to 30m at 5m interval. For each soil type i.e. hard, medium and soft, same exercise is repeated. Table 8 shows the summary of the amplitude ratios (FAR) and their corresponding natural frequencies for all the cases.

Table 8. Fourier amplification ratio (FAR) & corresponding fundamental frequencies at different bedrock depths.

Soil type	Parameter	Depth of bedrock				
		10m	15m	20m	25m	30m
Hard soil	Natural frequency (Hz)	12.3	8.3	6.5	5.96	4.19
	FAR	3.83	4.04	3.9	3.69	3.85
Medium soil	Natural frequency (Hz)	7.54	4.75	3.53	2.99	2.36
	FAR	6.54	5.78	5.93	6	6.3
Soft soil	Natural frequency (Hz)	3.45	2.37	1.78	1.43	1.27
	FAR	7.09	7.97	8.38	8.45	8.33

It has been observed that as the bed rock depth increases, natural frequency shows a decreasing trend for all the three soil types (Table 8). In other words, as bedrock depth increases, the stiffness of the whole system decreases in totality (thickness of overlying soil layer increases) and amplification takes place at much lower frequencies. A reverse pattern is observed with a decrease in bedrock depth.

5 CONSLUSIONS

One-dimensional equivalent linear site response analysis has been carried out at four typical locations at Panbazar and Khanapara area of the Guwahati city using three different input motions. It has been observed that the response is strongly influenced not only by the local site geology, but also by the strong motion characteristics itself. The PGA at the surface has been found to vary from 0.015g to 0.073g against a bedrock level PGA of 0.010g to 0.029g. Also, with the FAR varying from 2.60 to 7.50 and fundamental frequency in the range of 0.65 Hz to 2.30 Hz, the seismic scenario of the city is found to be highly alarming. The shear wave velocity (Vs30) has been found to be in the range of 200 m/s to 250 m/s, indicating soft soil site according to site classification by PESMOS (site class C).

Further, an attempt has been made to study the effects of soil type (hard, medium and soft) and bedrock depth on site response. Soft soils caused higher amplification and at a lower frequency as compared to stiff soils. Also, with the increase in bed rock depth from ground surface, amplification in all the three soils (hard, medium and soft) occur at low frequencies while a decrease in bed rock depth displayed a reverse trend.

REFERENCES

- 1) Boominathan, A., Dodagoudar, G.R., Suganthi, A. and Maheswari, R.U. (2016). "Seismic hazard assessment of Chennai city considering local site effects." Journal of Earth Science, DOI: 10.1007/s12040-008-0072-4.
- 2) Chatterjee, K. and Choudhury, D. (2016). "Influences of local soil conditions for ground response in Kolkata city during earthquakes." Natl. Acad. Sci., DOI 10.1007/s40010-016 0265-1.
- 3) Hashash, Y.M.A., Groholski, D.R., Phillips, C.A., Park, D. and Musgrove, M. (2011). DEEPSOIL version 4.0, Tutorial and user Manual. 98p.
- 4) Imai, T. and Tonouchi, K. (1982), "Correlation of N-value with S-wave velocity and shear modulus." Proceedings of the 2nd European symposium of penetration testing, Amsterdam, 67-72.
- 5) IS (1893-2002) Indian standard criteria for earthquake resistant design of structures, part 1 general provisions and buildings, 5th edn. Bureau of Indian Standards, New Delhi.
- 6) Kramer, S.L. (1996). "Geotechnical Earthquake Engineering". Prentice Hall, New Jersey (NJ), 653.
- 7) Kumar, S.S. and Krishna, A. M. (2013). "Seismic ground response analysis of some typical sites of Guwahati City", International journal of Geotechnical Earthquake Engineering, Vol. 4(1), 83-101

- 8) Mittal, H., Kumar, A. and Ramhmachhuani, R. (2012). "Indian strong motion instrumentation network and its site characterization." *Int J Geosci* 3(6):1151–1167.
- 9) Raghukanth, S.T.G., Dixit, J. and Dash, S.K. (2011). "Ground motion for scenario earthquakes at Guwahati city." *Acta Geodaetica et Geophysica Hungarica*, DOI: 10.1556/AGeod.46.2011.3.5.
- 10) Rajan, R. (2005). "Seismic Response Analysis of Dehradun city, India." M.Sc. Thesis, International Institute of Geoinformation Science and Earth Observation.
- 11) Seed, H. B., and Idriss, M. (1970). "Soil Moduli and Damping Factors for Dynamic Response Analysis." Earthquake Engineering Research Center, University of California, Berkeley, California.
- 12) Seismic Microzonation Atlas of Guwahati region, 2007.
- 13) Vucetic, M. and Dobry, R. (1991). "Effect of Soil Plasticity on Cyclic Response, *Journal of the Geotechnical Engineering Division*", ASCE, Vol. 111, No. 1, January, pp. 89-107.

[Back to table of contents](#)

3-Dimensional slope stability analysis

Mousumi Bania

i) M.E Student, Department of Civil Engineering, Guwahati University, Jalukbari, Guwahati ,Assam.

ABSTRACT

Soil slopes are required in the construction of highway and railway embankments, earth dams, levees, canals etc. In order to minimize the occurrence of slope failures and landslides, analysis of slope stability is very necessary. Slopes along newly constructed highway are highly susceptible to slope failure and thus landslides and failure of natural slopes and man-made slopes have resulted in human death and destruction. Landslide is one of the most important problem in North Eastern region. The region is full of hilly terrains. The region is also receives significant amount of rainfall throughout the year which makes it more vulnerable to landslides. Hence, slope stability analysis is very necessary for the safe service of the road and livelihood. This paper concentrates on analysing slopes both two-dimensionally and three-dimensionally. For two dimensional analysis an arbitrary slope has been taken and analysed graphically taking into concern Fellenius method and Bishop's method of slope stability analysis. The results obtained have been compared with that from finite element code Slope/W. Graphical calculation using two dimensional methods for slope stability requires lots of time and human labour and is repetitive in nature. Hence a C-program based on the specified methods has been developed. The results are found to be comparable with that from the C-program which validates the C-program. Practically, all slopes are three-dimensional. For three dimensional analysis two real sites, showing soil slope instability has been analyzed using PLAXIS 3-D. Finally, soil nailing with appropriate nail properties has been analysed as a remedy to an otherwise unstable slope. The efficacy of soil nails for soil slope stabilisation is highlighted in this paper.

Keywords: slopes, two-dimensional, three-dimensional, slope/w, PLAXIS 3-D, soil nailing.

1. INTRODUCTION

SLOPES may be manmade or natural. The forces acting on every slopes tends to disturb its stability. The self-weight of soil mass forming the slope is the main force but seismic activity, seepage, and external loads are also disturbing forces. In a stable slope, resisting force due to shear strength are larger than disturbing force (Huat, Ali, Rajoo, 2006). Slope failure is related to the following reasons: type of soil slope or soil properties, weight, geometry of slope, water content, tension cracks and vibrations due to earthquakes. The analysis of slope stability is an important aspect of research in disaster reduction engineering. In the analysis of slope stability, the primary task is to calculate the safety factor of the slope.

1.1 Purpose

Northeast region is situated in zone V which is depicted as one of the foremost region vulnerable to earthquake. Moreover the region is highly susceptible to landslides which is a very important issue to be taken into concern. Thus slope stability analysis is very necessary. As such firstly to understand two dimensional analysis of slope a case of homogeneous slope has been taken for analysis. Two methods of limit

equilibrium mainly the Fellenius method and Bishop's method of slope stability were used for the analysis. Seepage analysis and stability investigation are very important issues that should be considered for analysing slopes. This paper focuses on steady state analysis both by graphical method and using Slope/w software. For ease of calculation and to understand the principle behind the software a two dimensional c- program has been developed. Analysis has been also done using the c-program and results were compared with software obtained results to understand the accuracy of the generalized program.

Practically slopes are three dimensional. Hence analysing slope three dimensionally to get practical results is very necessary. As such in this study two cases of slopes from practical site were taken for analysis having different soil properties. In order to understand the variation of results and to obtain accurate results with practical results analyzing slopes both by two dimension and three dimension is necessary. As such analysis has been done using Plaxis-3d software for three dimension and slope/w software for two dimension and results were compared.

1.2 Study area

The Jorabat-Shillong Expressway Limited, Guwahati has been entrusted four-laning and

development of Jorabat-Barapani section of NH-40 by National Highway is necessary. The proposed road passes through the hilly terrain in the state of Meghalaya which is considerably unstable and therefore needs the assessment for the stability and slope protection measures. Due to catastrophic precipitation and wide variety of rock and sediments, slope failures are extreme in the highway. The region is also prone to earthquake. The problem and sites which have been chosen for the purpose of study consists of the following soil type.

An arbitrary homogeneous slope of height 20m and slope angle 60 degree is taken for two dimensional analysis consisting of varying water table from 5m to 8m. The soil present in the slope consists of cohesion of 4 Kpa, angle of internal friction of 20 degree and unit weight of 15kN/m³. For three dimensional analysis two sites situated near highway connecting Guwahati to Meghalaya is taken for analysis. The soil type present in the slope of site-1 mainly consists of coarse sand and water table is upto 4 m from ground level. The c and ϕ parameters of 1 kN/m² and 43.5 degree are present in the soil. The soil type present in site-2 mainly consists of fine sand and water table is upto 3 m from ground level. The c and ϕ parameters of 39 KN/m² and 30 degree are present in the soil.

2 ANALYSIS

The analysis is done for the static case taking into account steady state condition. SLOPE/W programs of GEOSTUDIO software and PLAXIS 3-d software are used for this purpose.

2.1 Software Used for Analysis

SLOPE/W is a powerful commercially available tool for analyzing the stability of slopes. It is a component in the entire tool kit of GEOSTUDIO 2007. This software works on a limit equilibrium framework and includes methods such as the Morgenstern-Price, Spencer's method, Bishop's simplified method, Janbu's generalized method and Ordinary method of slices etc. Factor of safety for different shapes of slip surfaces – Circular, noncircular and wedged surfaces can be determined. The soil models such as Mohr-Coulomb model, anisotropic strength model, SHANSEP model, etc. are available for modeling the material properties of the different layers of the soil. The main advantage of this program is its ability to be coupled with other programs such as SIGMA/W, SEEP/W, etc.

PLAXIS 3-D is a finite element package intended for 3-dimensional analysis of deformation and stability in geotechnical engineering. It is equipped with features to deal with various aspects of complex geotechnical structures and construction processes using robust and theoretically sound computational procedures. FEM is a general purpose method which can be used to calculate stresses, movements, pore pressure and other

characteristic of earth mass during construction. The most remarkable advantage of this method is using stress-strain behaviour of the soil and removing the assumptions applied in LEM to change static-indeterminate problem to a statically determinate one.

2.2 Material properties

For two dimensional analysis an arbitrary homogeneous slope having bulk unit weight of 15 kN/m³, cohesion 4kN/m² and angle of internal friction of 20 degree is taken.

For three dimensional analysis two sites consisting of different soil parameters are taken for analysis. Site-1 consists of soil of coarse sand type, model used is drained type mohr coulomb model having bulk unit weight of 17kN/m³, saturated unit weight of 20 kN/m³, value of E as 3×10^4 KN/m², Poisson's ratio μ of 0.32, Cohesion 1kN/m², and Friction angle of 43.5 degree is used for analysis. Site-2 consists of soil of fine sand type, model used is drained type mohr coulomb model having bulk unit weight of 17.3kN/m³, saturated unit weight of 20 kN/m³, value of E as 3×10^4 kN/m², Poisson's ratio μ of 0.30, Cohesion 39kN/m², and Friction angle of 30 degree is used for analysis.

2.3 Analysis of slopes

1. Limit Equilibrium Methods

The various limit equilibrium methods used for the analysis are: a. Fellenius method and b. Bishop's method.

a. Fellenius method

The method assumes that the resultant of the interslice forces acting on any slice is parallel to its base; therefore the interslice forces are neglected (Fellenius, 1936). Only moment equilibrium is satisfied. The factor of safety is calculated by the equation

$$F = \frac{\sum (c'l + (W \cos \alpha - \mu l) \tan \phi')}{\sum W \sin \alpha} \quad (1)$$

b. Bishop's Method

In this method, the failure section is divided into a series of vertical slices. The forces on the sides of the slice are assumed to be horizontal and thus there are no shear stresses between slices (Bishop, 1955). It is assumed that the slice weight W acts through the midpoint of the area. The factor of safety is calculated as

$$F = \frac{\sum \left(\frac{c'l \cos \alpha + (W - \mu l \cos \alpha) \tan \phi'}{\cos \alpha + (\sin \alpha \tan \phi') / F} \right)}{\sum W \sin \alpha} \quad (2)$$

Where,

F = Factor of safety

w = weight of slice

c = cohesion

b = width of slice
 Φ = angle of internal friction
 U = pore pressure at each slice

As this equation contains F on both sides, it has to be solved iteratively.

2. Analysis of a homogeneous slope

An arbitrary slope of height 20m and slope angle 60 degree is drawn using Slope/w software. The water table taken varies from 5m to 8m.

Table 1 Parameters used for the homogeneous slope analysis

Material	Cohesion (kpa)	Φ (degree)	γ (kN/m ³)	Height(m)
1	4	20	15	20

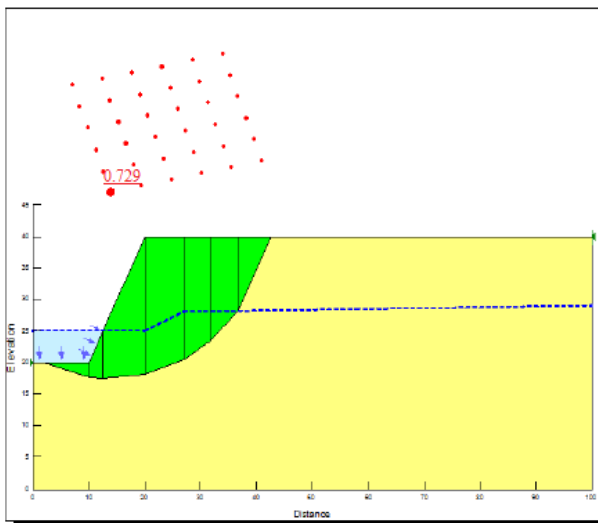


Fig. 1. Eschematic diagram of an arbitrary slope using slope/w software

The factor of safety obtained using ordinary method of slices by slope/w software is further analysed graphically using ordinary method of slices and bishop’s method.

3. Graphical Analysis

Taking the centre of the slip circle from slope/w analysis the slip surface is drawn graphically to some scale. By varying the radius slip circles are drawn. Considerably the soil mass above the assumed slip circle is divided into a number of vertical slices of equal width as shown in fig. 2. A number of slices of 7 is taken into consideration. The mid height of slices and angle of inclination of the base of each slice is measured graphically. The weight of the slice W is calculated and is plotted and then resolved into its normal and tangential components N and τ respectively. A diagram showing the forces and the slip circle is shown in fig. 2.

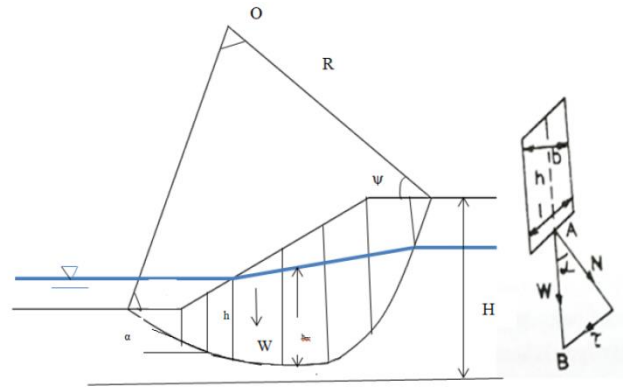


Fig. 2. Division of a slip circle for $c-\phi$ analysis and forces acting on it.

4.C-Programming

C is a particularly popular language for personal computer programmers because it is relatively small and requires less memory than other languages. In order to understand the principle behind the software a c-program is developed. A diagram used for analysis by c-program is shown in fig.3. In C-program the following input parameters were used to find the minimum factor of safety :

1. Co-ordinates of points.
2. Assumed value of x_0 and y_0 (x and y-coordinate of center of slip circle)
3. No. of slices, n
4. Bulk density of the soil
5. Value of cohesion of the soil, c
6. Angle of internal friction, ϕ
7. Variation in pore pressure in slices, U
8. Assumed value of FOS, F
9. Maximum number of iterations.

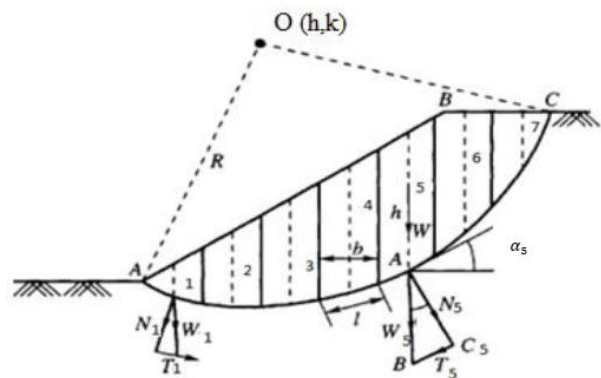


Fig. 3. Slope diagram indicating the center of the slip circle

Since, in this study pore pressure variations were not included therefore water table variation has been input as zero in programming analysis.

The same slope has been analysed using slope/w software under dry condition as shown in fig.4 and 5 and results were compared with the prepared c-program in order to understand the accuracy of the c-program.

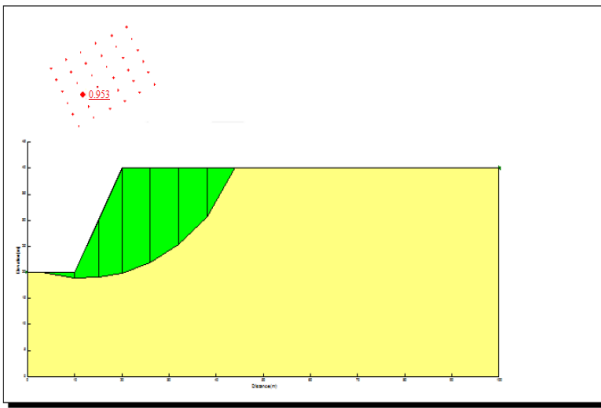


Fig. 4. Calculated Factor of safety value for dry slope by Ordinary method using slope/w.

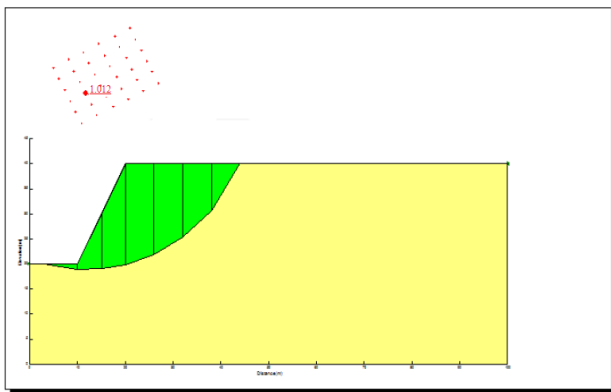


Fig. 5. Calculated Factor of safety value for dry slope by Bishop's method using slope/w.

In reality slopes are in three dimensional space. So in order to get practical results three dimensional analysis is very necessary. As such two sites were taken for three dimensional analysis by Plaxis-3d software. Site – 1 A slope of height 32 m and slope angle 68 degree is taken for analysis. The top width of the slope is 10m and bottom width is 53m. The soil type present in the slope mainly consists of coarse sand and water table is upto 4 m from ground level. Slope is drawn with the above given properties and mesh is generated. The schematic diagram generated using PLAXIS 3-D is shown in fig.6.

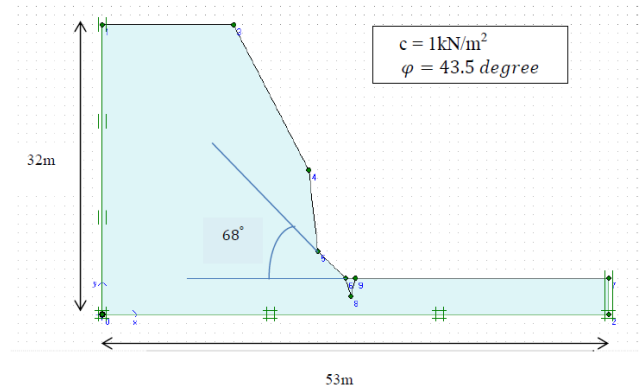


Fig. 6. Eschematic diagram of site-1

The safety factor value obtained using PLAXIS 3-D is shown in fig.7.

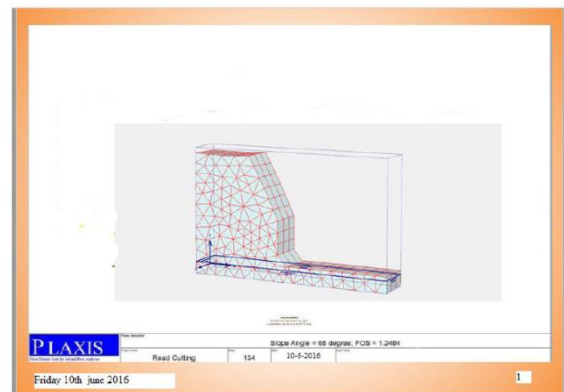


Fig. 7. Calculated Factor of Safety of site-1 by PLAXIS 3-D.

The site 1 slope analysed using PLAXIS 3-D was found to be unstable since FOS < 1.5. Hence it has been tried to made stable by soil nailing. The schematic diagram with soil nailing generated using PLAXIS 3-D is shown in fig.8. Soil nails each of 7m length consisting of modulus of elasticity of $2 \times 10^4 \text{ kN/m}^2$ and spacing of 2m is used for analysis.

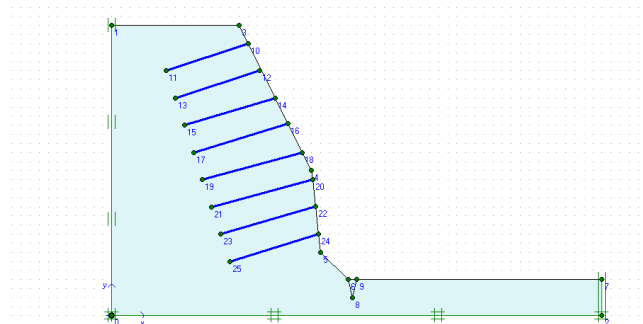


Fig. 8. Site 1 slope stabilisation using soil nailing.

The safety factor value for the corresponding slope obtained using soil nailing is shown in fig.9.

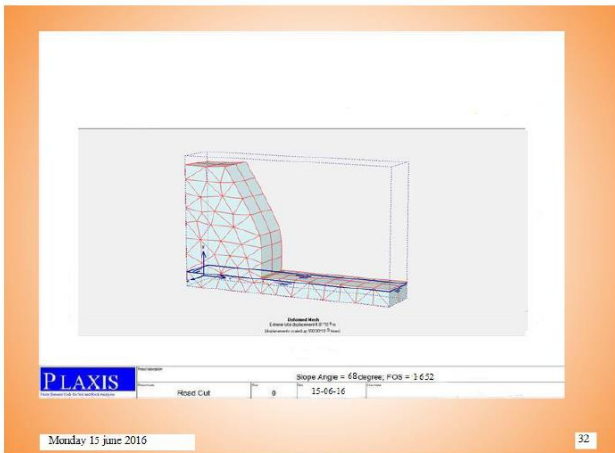


Fig. 9. FOS for site 1 slope using soil nailing

An increase in safety factor value is obtained after soil nailing. Previously we have used rigid interface. The same section was analysed by changing the interface and safety factor obtained is shown in fig.10.

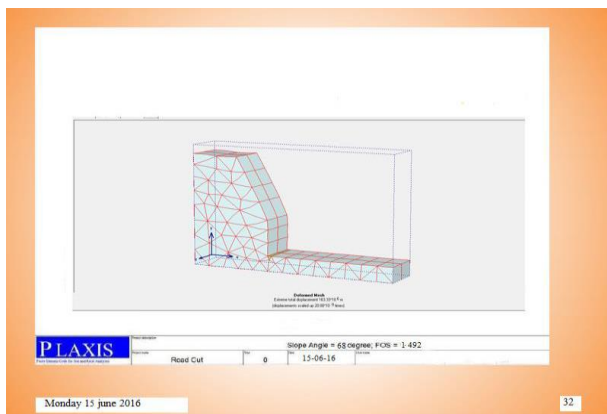


Fig. 10. Calculated Factor of safety of site1 with 0.85 interface

Site – 2 A slope of height 22 m and slope angle 60 degree was taken for analysis. The top width of the slope is 10m and bottom width is 53m. The soil type present in the slope mainly consists of fine sand and water table is upto 3 m from ground level. An schematic diagram of slope with the above data generated using PLAXIS 3-D is shown in fig.11.

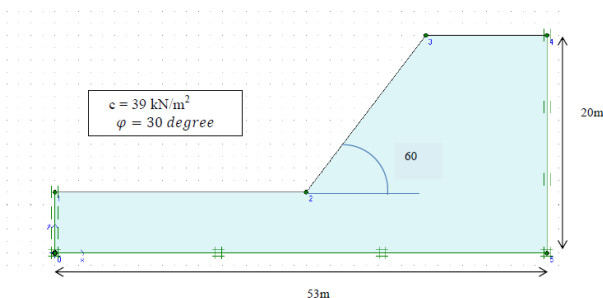


Fig. 11. Eschematic diagram of site 2.

The safety factor value obtained after analysis using PLAXIS 3-D is shown in fig.12.

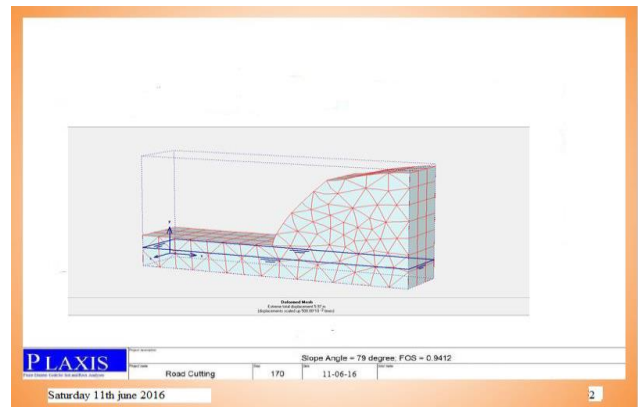


Fig. 12. Calculated safety factor for site 2 using Plaxis 3-d
The site 2 slope analysed using PLAXIS 3-D was found to be unstable since FOS < 1.5. Hence it was tried to made stable by soil nailing. An schematic diagram of the same slope using soil nailing is shown in fig.13.

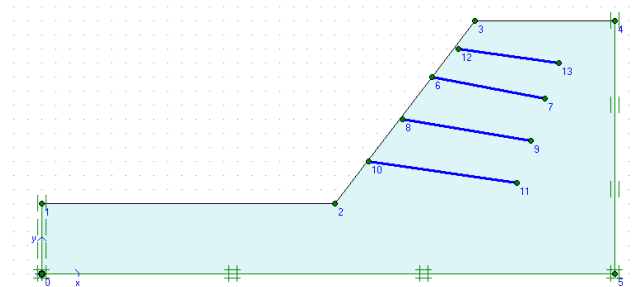


Fig. 13. Slope stabilisation using soil nailing with rigid interface.

A schematic diagram showing safety factor obtained after analysis with soil nailing is shown in fig. 14.

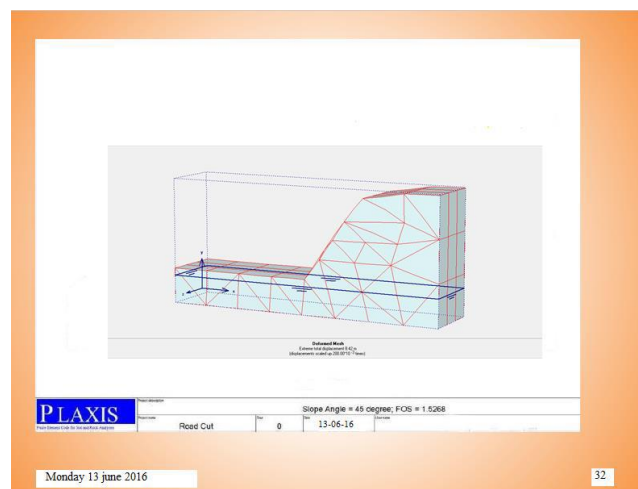


Fig.14 Calculated safety factor of site-2 using soil nailing

Previously we have used rigid interface. In this section we have done the analysis by lowering the value

of interface. An schematic diagram with changed interface using PLAXIS 3-D is shown in fig.15.

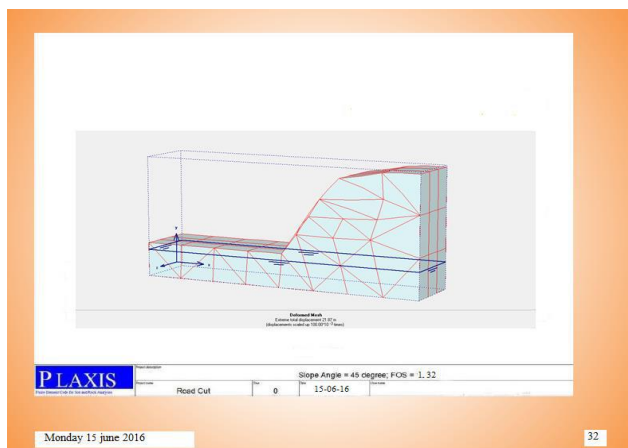


Fig. 15. Calculated Factor of safety for site 2 with changed interface

3. RESULTS AND DISCUSSION

Initially a homogeneous slope has been analysed two dimensionally and the following results were obtained as given in table.2

Table.2 Comparison between different FOS value

Methods	Graphical Method		Software
	Ordinary method of slices	Bishop's method	
FOS	0.718	0.789	0.729

By analysing the arbitrary homogeneous slope using GEOSLOPE software a critical slip circle has been generated and certain safety factor value was found. Taking the center of the critical slip circle analysis for the same slope has been done by graphical. A comparison between Ordinary method and Bishop's method was done and found that the FOS value obtained by Bishop's method has been greater than the Ordinary method. Moreover the results obtained by analyzing the slope tally's with slope/w results. But graphically analysing slope stability by 2-D methods took lot of human labour and time hence a C-program has been developed to ease its calculation and to understand the methodology behind the software. A comparison between safety factor value has been done using slope/w methods and c-program for dry slope is shown in tabulated form in table 3.

Table 3 Safety factor comparison by various methods between slope/w and c-program.

Meth ods	Ordinary method of slices (slope/w)	Bishop's method (slope/w)	Ordinary method of slices (c-program)	Bishop's method (c-program)
FOS	0.953	1.012	0.933	1.007

The factor of safety values obtained by slope/w analysis that from the developed software code using c-language have been found to agree well.

4. CONCLUSION

1. Ordinary method of slope stability analysis has been compared with Bishop's method of slices. Bishop's method of slices is found to yield lower factor of safety and is more rigorous compared to ordinary method of slices.
2. The results obtained through graphical calculation have been found to agree with that from slope/w analysis results, considering a 2-dimensional slope.
3. Real time soil slopes have spacial variation and cannot be approximated to be a plane strain problem. Thus, a real time slope has been analysed using the finite element code PLAXIS 3-D. It has been shown that soil nails can be very effective in stabilising an otherwise unstable soil slope.
4. Various soil nail materials viz. concrete, steel etc. including various hydrological condition may have varying soil-nail interface friction. Effect of this parameter on the factor of safety of a given soil slope stabilised by soil nails have been highlighted.

REFERENCES.

1. Bishop, A. W. (1955). "The use of the slip circle in the stability analysis of slopes." Geotechnique, London, Vol. 5, No.1, pp. 7-17.
2. Fellenius, W. (1936). "Calculation of the Stability of Earth Dams." Transactions, 2nd International Congress on Large Dams, International Commission on Large Dams, Washington, DC, pp 445-459.
3. Huat, Ali, Rajoo (2006), "Stability Analysis and Stability Chart for Unsaturated Residual Soil Slope", American Journal of Environmental Sciences 2 (4): 154-160.
4. Plaxis 3-d tunnel "Introductory version".
5. Stability modeling with SLOPE/W 2007 Version, March (2008), Third edition, Geo-slope International limited, Calgary, Alberta, Canada.

[Back to table of contents](#)

Seismic Strengthening of Existing School Buildings in Meghalaya, India

Pratim P. Kalita ⁱ⁾, Jayanta Talukdar ⁱ⁾, Himanshu S.B.Gohain ⁱ⁾, Ritukesh Bharali ⁱⁱ⁾, Bhargob Deka ⁱⁱⁱ⁾, Jayanta Pathak ^{iv)}

i) Project Assistant, Department of Civil Engineering, Assam Engineering College, India.

ii) Graduate Student, Department of Civil Engineering, Delft University of Technology, Netherlands

iii) Graduate Student, Department of Civil Engineering, McGill University, Canada

iv) Professor, Department of Civil Engineering, Assam Engineering College, India.

ABSTRACT

In this work, an attempt has been made to understand the seismic behavior of existing school buildings in the seismically active Meghalaya state of India. Over 100 schools have been classified into typologies based on the geometrical configuration, construction practice and construction materials. The masonry infill, wherever present, were modeled as equivalent concentric diagonal pin jointed struts, as per FEMA 273, imparting lateral stiffness to the structure. However, struts were placed only at panel locations where there are no openings or openings if present, are less than 50%. The modeling of the buildings was in twofold: the ductile models and the non-ductile models. In case of the ductile models, the buildings were modeled, in conformation to IS 13920 (1993), considering ductile detailing of the beam columns joints. The beam and column sections were modeled as Mander's confined model. The non-ductile models were implemented addressing the possibility improper confinement. The non-ductile models may provide a more realistic result and the beam and columns in this case were modeled as Mander's unconfined model. The lateral force was evaluated and applied as per IS 1893 (2002) in incremental steps and formation of plastic hinges was studied in the representative models. The hinge properties were earlier defined in RC members according to FEMA 356 methodology. The nonlinear static pushover analysis showed a clear picture of the seismic capacity of the existing school buildings under considerations. Depending on the damage levels observed on the structural elements of various buildings in the study, changes in cross-sectional area with provision of additional reinforcements were incorporated as retrofitting measures. Depending on the failure mechanisms, three retrofitting measures - (a) Dwarf Wall below the tie-beam level; (b) Column jacketing with increased column size below the tie-beams (c) Column jacketing with increased column size in upper storey levels were incorporated in the models and re-assessed for lateral load capacity.

Key Words: *Seismic behavior, SAP2000, Infill, Nonlinear static pushover, Lateral load bearing capacity.*

1. INTRODUCTION

The project involves determining the Seismic vulnerability of Schools in the state of Meghalaya, India, which is situated in a highly seismically active zone. Over 100 existing school building have been classified into topologies based on the geometrical configuration, construction materials, construction practice. All the existing schools are modeled and nonlinear static pushover analysis was carried out to study its seismic demand and capacity. The lateral force was applied as per IS 1893 (BIS, 2002) in incremental steps and formation of plastic hinges was studied. Hinge properties were assigned as per FEMA 356 methodology (FEMA, 1999, 2000).

2. MODELLING OF SCHOOL BUILDING:

The school buildings have been modeled in CSI SAP2000 to understand its seismic capacity. The grade of concrete was considered as M15 and Fe415 HYSD for reinforcement bars. The slab thickness was taken 125mm and live load of 3KN/m², conforming to IS875 (Part 2). Masonry infill was modeled as equivalent concentric diagonal pin jointed struts (Fig. 1), imparting lateral stiffness to the structure. However, struts were placed only at the locations where openings were found to be less than 50%.

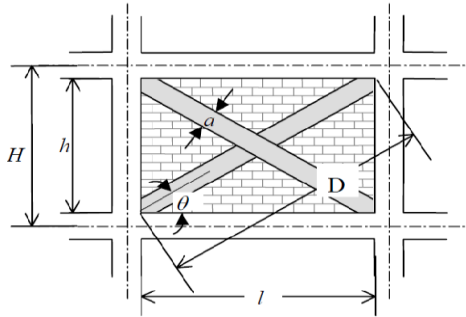


Fig. 1: FEMA 273 Method Designing Equivalent Strut (Ghassan A- Chaar, 2002, FEMA, 1997)

Table 1: Properties of Infill Walls

INFILL MATERIAL PROPERTIES	VALUES
Compressive Strength	4.63 MPa
Modulus of Elasticity	2200 MPa
Shear Modulus	1018 MPa
Thermal Coefficient	0.0000081/C
Poisson's Ratio	0.2

The modeling of the buildings were of two types - the Ductile Model and the Non-ductile Model. In case of the Ductile Model, the buildings were modeled, in conformation to IS 13920 (BIS, 1993), considering ductile detailing of the beam column joints. The beam and column sections were modeled as Mander's confined model (Mander,1988), addressing the possibility of an existing damage and improper confinement ties. A non-ductile model may provide a much realistic result. Hence, the beam and columns in this case were modeled as Mander's unconfined model (Mander,1988). A total of 8 numbers of School building samples are considered here to capture the process of the analysis carried out during the project. The school buildings considered here can be broadly assumed to represent the wide range of topologies that the 100 buildings are categorized for analysis.

Table 2: Material and Geometric Properties of Schools

Name of School	Type	Properties	
ITI Sohra	G+0	Grade of Conc.	M15
		Grade of Steel	Fe415
		Column Size	250x300mm
		Beam Size	300x350mm
		Wall Thickness	127mm
		Slab Thickness	150mm
ITI Jowai	G+1	Grade of Conc.	M15
		Grade of Steel	Fe415

		Column Size	350x250mm
		Beam Size	250x400mm
		Wall Thickness	127mm
		Slab Thickness	150mm
Selsella Higher Secondary School	G+1	Grade of Conc.	M20
		Grade of Steel	Fe415
		Column Size	250mm
		Beam Size	350x250mm
		Wall Thickness	127mm
		Slab Thickness	150mm
Mawsynram Higher Secondary School	G+1	Grade of Conc.	M15
		Grade of Steel	Fe415
		Column Size	450x250mm
		Beam Size	250mm
		Wall Thickness	127mm
		Slab Thickness	150mm
Good Shephard School	G+2	Grade of Conc.	M20, M15
		Grade of Steel	Fe415
		Column Size	350mm
		Beam Size	400x300mm
		Wall Thickness	127mm
		Slab Thickness	150mm
Laishlong School	G+2	Grade of Conc.	M15
		Grade of Steel	Fe415
		Column Size	250mm
		Beam Size	350x250mm
		Wall Thickness	127mm
		Slab Thickness	150mm
Mawrykneng School	G+2	Grade of Conc.	M15
		Grade of Steel	Fe415
		Column Size	300mm
		Beam Size	350x300mm
		Wall Thickness	127mm
		Slab Thickness	150mm
Green Yard Secondary School	G+3	Grade of Conc.	M15
		Grade of Steel	Fe415
		Column Size	350mm
		Beam Size	300mm
		Wall Thickness	127mm
		Slab Thickness	150mm

3. NONLINEAR STATIC PUSHOVER ANALYSIS:

A nonlinear static pushover analysis was carried out in CSI SAP2000, addressing all major potential state of deformations of the buildings, to study their seismic demand and capacity. The lateral force was applied as per IS 1893 (BIS, 2002) in incremental steps and formation of plastic hinges was studied. The hinge properties were earlier defined in RC members per FEMA 356 methodology. (Fig. 2).

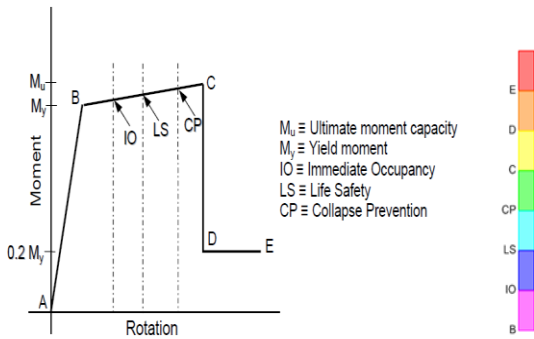


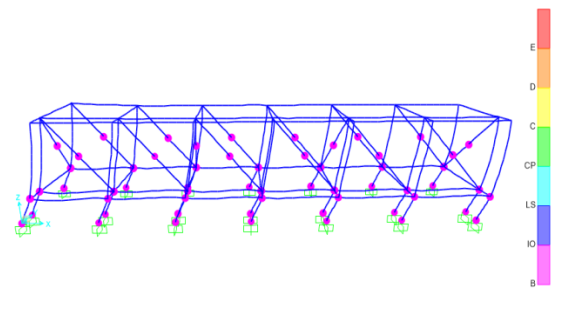
Fig2: Ideal Moment-Rotation Curve

When the demand increases over the yield capacity (B), the corresponding member enters the nonlinear domain and cracks begin to develop. As cracks widen with increase in demand, higher hinge levels are reached until collapse (C) occurs (FEMA 356, 2000).

4. ANALYSIS RESULTS:

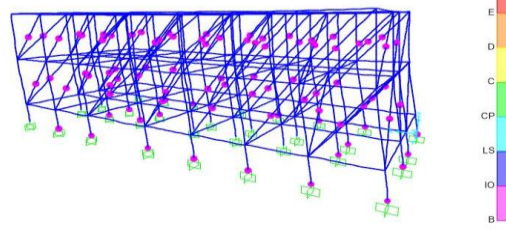
The nonlinear pushover analysis showed a clear picture of the seismic capacity of the school buildings. The hinges of higher level were formed, when demand exceed the yield capacity. The results of the analysis are tabulated in Table 3.1 to 3.3. It was observed that Selsella Secondary School, Good Shepherd school, Laishlong school, Mawrynkneng School and Green Yard Secondary School buildings, wherein the walls were modeled as equivalent struts, showed a very high level of formation of hinges leading to collapse. This is due to the vertical irregularities of wall locations and resulting variations in participation of walls as lateral resisting systems. The irregularities caused torsion, leading to a higher damage level. Retrofitting measures are necessary to counter the torsion. On the other hand, bare frame models, ignoring the presence of the walls, were deceptively safer, with hinge levels at Immediate Occupancy (IO) level.

Table 3.1: Analysis Results of the Schools and hinge levels.

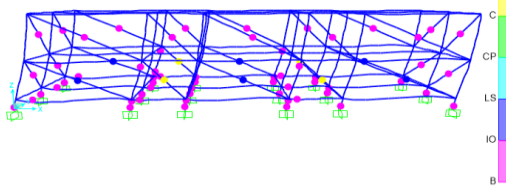


School	Ductility	Wall model	Hinge Level
ITI Sohra	Ductile	Equiv. Struts	IO
	Ductile	Bare Frame,	IO

	Non-ductile	Equiv. Struts	IO
		Non-ductile	Bare Frame

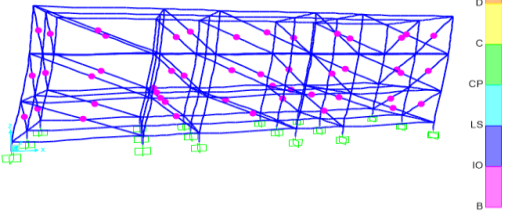


School	Ductility	Wall model	Hinge Level
ITI Jowai	Ductile	Equiv. Struts	IO
	Ductile	Bare Frame,	IO
	Non-ductile	Equiv. Struts	IO
	Non-ductile	Bare Frame	IO

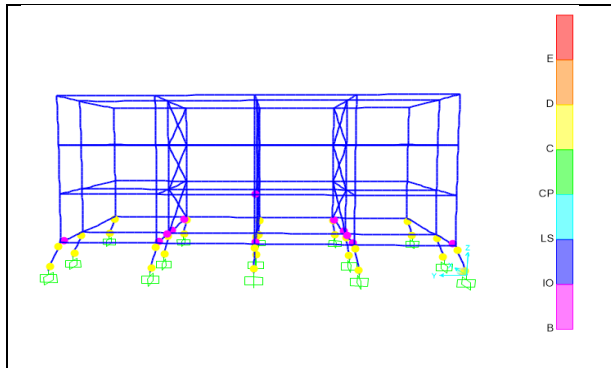


School	Ductility	Wall model	Hinge Level
Selsella Higher Secondary School	Ductile	Equiv. Struts	Collapse
	Ductile	Bare Frame,	IO
	Non-ductile	Equiv. Struts	Collapse
	Non-ductile	Bare Frame	IO

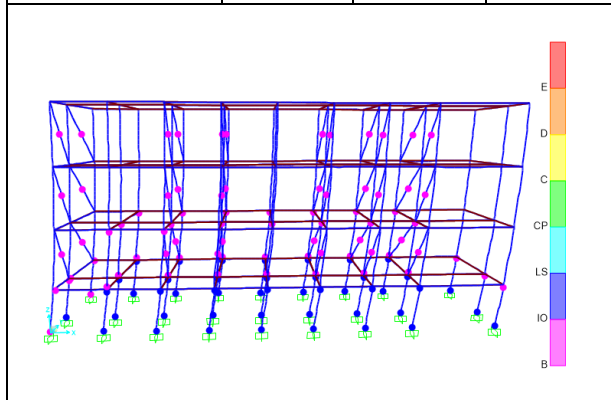
Table 3.2: Analysis Results of the Schools and hinge levels.



School	Ductility	Wall model	Hinge Level
Mawsynram Higher Secondary School	Ductile	Equiv. Struts	IO
	Ductile	Bare Frame,	IO
	Non-ductile	Equiv. Struts	IO
	Non-ductile	Bare Frame	IO
	Non-ductile	Bare Frame	IO

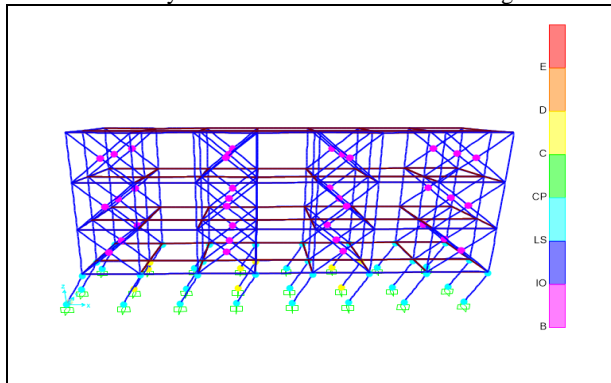


School	Ductility	Wall model	Hinge Level
Good Shepherd School	Ductile	Equiv. Struts	Collapse
	Ductile	Bare Frame,	IO
	Non-ductile	Equiv. Struts	Collapse
	Non-ductile	Bare Frame	IO



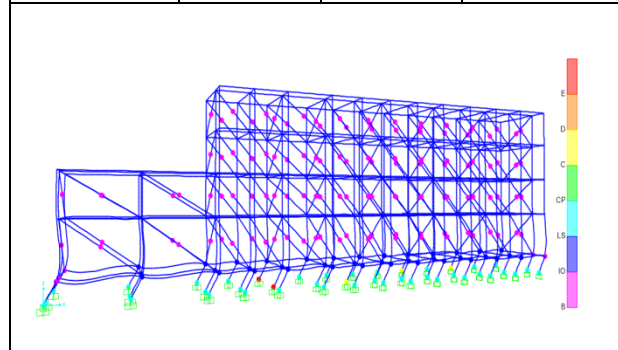
School	Ductility	Wall model	Hinge Level
Laishlong School	Ductile	Equiv. Struts	LS
	Ductile	Bare Frame,	IO
	Non-ductile	Equiv. Struts	LS
	Non-ductile	Bare Frame	IO

Table 3.3: Analysis Results of the Schools and hinge levels.



School	Ductility	Wall model	Hinge Level
Mawrykneng	Ductile	Equiv. Struts	Collapse
	Ductile	Bare Frame,	IO

School	Non-ductile	Equiv. Struts	Collapse
--------	-------------	---------------	----------



School	Ductility	Wall model	Hinge Level
Green Yard Secondary School	Ductile	Equiv. Struts	Total Failure
	Ductile	Bare Frame,	Total Failure
	Non-ductile	Equiv. Struts	Total Failure
	Non-ductile	Bare Frame	Total Failure

The hinge levels defined in the analysis represents the following: IO- Immediate Occupancy, LS – Life Safety, CP- Collapse Prevention, C- Collapse, D/E – Total Failure.

5. RETROFITTING MEASURES:

Three retrofitting measures are proposed. the buildings were modeled and analyzed with the retrofitted frames as follows:

- a. Dwarf wall below tie beam level.
- b. Increase in column size below tie beam and ground Level.
- c. Increase in column size at all levels.

6. ANALYSIS RESULTS-FOR RETROFITTING MEASURES

The retrofitting measures has been incorporated in the structure and same analysis was run again to observe the changes in their dynamic responses.

Table 4.1: Analysis Results of the Schools after retrofit.

SCHOOL:	ITI Sohra	
DUCTILITY:	Ductile/Non-Ductile	
WALL MODEL:	Equivalent Strut Model/Bare Frame	
Hinge Level before Retrofit	Retrofit measure	Hinge level after Retrofit
IO	Dwarf Wall below Tie Beam level	-
IO	Increase column size below Tie beam and Ground Level.	-
IO	Increase column size at all levels.	-
SCHOOL:	ITI Jowai	

DUCTILITY:	Ductile/Non-Ductile	
WALL MODEL:	Equivalent Strut Model/Bare Frame	
Hinge Level before Retrofit	Retrofit measure	Hinge level after Retrofit
IO	Dwarf Wall below Tie Beam level	-
IO	Increase column size below Tie beam and Ground Level.	-
IO	Increase column size at all levels.	-
SCHOOL:	Selsella Higher Secondary School	
DUCTILITY:	Ductile/Non-Ductile	
WALL MODEL:	Equivalent Strut Model/Bare Frame	
Hinge Level before Retrofit	Retrofit measure	Hinge level after Retrofit
Collapse	Dwarf Wall below Tie Beam level	IO
-	Increase column size below Tie beam and Ground Level.	IO
-	Increase column size at all levels.	IO
SCHOOL:	Mawsynram Higher Secondary School	
DUCTILITY:	Ductile/Non-Ductile	
WALL MODEL:	Equivalent Strut Model/Bare Frame	
Hinge Level before Retrofit	Retrofit measure	Hinge level after Retrofit
IO	Dwarf Wall below Tie Beam level	-
IO	Increase column size below Tie beam and Ground Level.	-
IO	Increase column size at all levels.	-
SCHOOL:	Mawrykneng School	
DUCTILITY:	Ductile/Non-Ductile	
WALL MODEL:	Equivalent Strut Model/Bare Frame	
Hinge Level before Retrofit	Retrofit measure	Hinge level after Retrofit
Collapse	Dwarf Wall below Tie Beam level	IO
-	Increase column size below Tie beam and Ground Level.	IO
-	Increase column size at all levels.	IO
SCHOOL:	Green Yard Secondary School	
DUCTILITY:	Ductile/Non-Ductile	
WALL MODEL:	Equivalent Strut Model/Bare Frame	
Hinge Level before Retrofit	Retrofit measure	Hinge level after Retrofit
Total Failure	Dwarf Wall below Tie Beam level	IO
-	Increase column size below Tie beam and Ground Level.	-
-	Increase column size at all levels.	-

Table 4.2: Analysis Results of the Schools after retrofit.

SCHOOL:	Good Shepherd School	
DUCTILITY:	Ductile/Non-Ductile	
WALL MODEL:	Equivalent Strut Model/Bare Frame	
Hinge Level before Retrofit	Retrofit measure	Hinge level after Retrofit
Collapse	Dwarf Wall below Tie Beam level	IO
-	Increase column size below Tie beam and Ground Level.	IO
-	Increase column size at all levels.	IO
SCHOOL:	Laishlong School	

7. CONCLUSION:

It has been observed that, the models in which walls were modeled as equivalent struts, showed higher levels of hinge formation due to torsion arising out of vertical irregularity in stiffness distribution. However, addition dwarf wall infill works as one of the cost-effective option as a retrofitting measure as it reduces the hinge level formation from collapse (C) to Immediate Occupancy (IO) in most cases. Dwarf walls at the end panels along the shorter side in first and second bay are found to be sufficient as a retrofitting measure, compared to other options (Table 4). In case of bare frame model where provision of infill walls are limited, increasing the column size found to enhance the performance of the structure (Table 4).

ACKNOWLEDGEMENT

The authors gratefully acknowledge the support received from PWD (Meghalaya) and LEA Associates South Asia Pvt. Ltd.(LASA), Delhi.

[Back to table of contents](#)

REFERENCES

1. Bureau of Indian Standards (2002), “Indian Standard Criteria for Earthquake Resistant Design of Structures”, BIS, New Delhi, India.
2. Bureau of Indian Standards (BIS), 1993, IS:13920 Ductile Detailing of Reinforced Concrete Structures Subjected to Seismic Forces— Code of Practice. New Delhi, India.
3. FEMA 273 (1997), “NEHRP Guidelines for the seismic rehabilitation of buildings,” Federal Emergency Management Agency, Washington, D.C.
4. FEMA 306 (1999), “Evaluation of Earthquake damaged concrete and masonry wall buildings – Basic Procedures manual,” Federal Emergency Management Agency, Washington, D.C.
5. FEMA 356 (2000), Prestandard and Commentary for the Seismic Rehabilitation of Buildings, Federal Emergency Management Agency, Washington, D.C.
6. Ghassan A- Char (January 2002), “Evaluating Strength and Stiffness of Unreinforced Masonry Infill Structures,” ERDC/CERL TR-02-1, US Army Corps of Engineers.
7. Mander JB, Priestley MJN, Park R., 1988 “Theoretical stress-strain model for confined concrete.” Journal of Structural Engineering 1988; 114(8): 1804-1826.

Shear wave velocity profile at NITW stadium using MASW

Muzzaffar Khanⁱ⁾, Akshay Sakhareⁱⁱ⁾, Ravi Kumarⁱⁱⁱ⁾ and Kalyan Kumar^{iv)}

i) Ph.D Student, Department of Civil Engineering, NIT Warangal, Telangana, 506004, India.

ii) Ph.D Student, Department of Civil Engineering, IIT Madras, Chennai, 600 036, India.

iii) M.Tech Student, Department of Civil Engineering, NIT Warangal, Telangana, 506004, India.

iv) Assistant Professor, Department of Civil Engineering, NIT Warangal, Telangana, 506004, India.

ABSTRACT

The local site assessment for seismic ground motion is a prerequisite for seismic hazard analysis. The site response studies are the first step toward the study of seismic hazard analysis. In this study, the site characterization was carried out by using the active source Multi-Channel Analysis of Surface Wave (MASW) i.e. non-invasive geophysical method to understand the shear-wave velocity profile below stadium at National Institute of Technology Warangal (NITW). Shear wave velocity (V_s) is used to find the dynamic properties of soil (i.e. G_{max}). Unlike traditional shear-wave velocity measurements made in boreholes, the MASW method is based on Rayleigh wave propagation and is performed on the ground surface. MASW utilizes dispersion of Rayleigh waves that usually take more than two-thirds of total seismic energy generated by an impact seismic source at the surface (Park *et al.*, 1999). The three main steps of MASW testing are (i) Data acquisition, (ii) Dispersion analysis and (iii) Inversion analysis. The picking of the fundamental mode of Rayleigh wave is very important for the construction of dispersion curve else it may lead to wrong interpretation of shear wave velocity profile.

The MASW test was carried out using a Geometrics make, 24 channel seismograph with 4.5 Hz geophones. SeisImager/SW software was used for the analysis of the data obtained from MASW test. The test was conducted at NIT Warangal stadium situated at coordinates 17°59'03"N 79°31'51"E, which comes under seismic zone III as per seismic zonation map of India (BIS, 2002). The average shear-wave velocity for the top 30 m of ground (V_{s30}), which is a good indicator for ground amplification factor, is used to classify the soil as per National Earthquake Hazard Reduction Program (BSSC, 2001). The shear wave velocity at NITW stadium is varying from 195 m/s at the ground surface to 1583 m/s at 30 m below ground surface. The average shear-wave velocity (V_{s30}) was 600 m/s and is classified as Class C as per NEHRP (2003) classification system. Being classified as a very dense soil/soft rock, the site can withstand large static vertical loads and weak to moderate earthquake loads. New structures can be planned based on this site characterization. These values can further be used in the microzonation studies of the region.

Keywords: MASW, Shear-wave velocity, NITW, NEHRP classification

1. INTRODUCTION

The seismic site characterization of subsurface soil profiles of a particular site is an important task for the evaluation of site response at the soil surface. The shear wave velocity is an important parameter for site characterization and seismic site response analysis. By conducting one dimensional ground response analysis, the ground motion parameters at the ground surface are analysed. The shear wave velocity is directly related to the damping ratio, density and shear modulus (Karl *et al.*, 2006) of the soil profile. The high shear wave velocity indicates the high shear modulus and a lower shear wave velocity indicates higher damping ratio.

2 STUDY AREA

India has very diversified climate, topography, types

of rocks with different level of weathering, forming very young to matured soils. The soil properties are determined by nature of parent materials, climatic factor and nature of weathering process. Warangal district lies between 17°19' & 18°36' N latitude and 78°49' & 80°43' E longitude in the state of Telangana. It comes under seismic zone III (BIS, 2002). Warangal is situated at an average altitude of around 381 m above mean sea level (MSL). Warangal is one among the 12 heritage cities chosen for Scheme HRIDAY – Heritage City Development and Augmentation Yojana by Government of India. It is settled in the eastern part of Deccan Plateau made up of granite rocks and hill formations which left the region barren making the cultivation depend on seasonal rainfalls. There are no river flows nearby Warangal, which makes it to rely on Kakatiya Canal which originates from Sriram Sagar

Project to meet the drinking water requirements and the topography of the district consists of isolated hills, rain fed tanks, lakes and shrubby forests. The geological formation of the district mainly developed from the granite and genesis of Archean period and dharwars of Precambrian period. NIT Warangal is situated at coordinates 17°59'03"N 79°31'51"E and 137 km from Hyderabad. It was established in 1959.

3 MASW TEST

Seismic site characterization can be performed by various noninvasive methods which include multichannel analysis of surface waves – MASW, (Park *et al.*, 1999; Xia *et al.*, 1999), spectral analysis of surface waves – SASW, (Nazarian *et al.*, 1983), frequency-wave number (Capon, 1969), spatial autocorrelation (Aki, 1957), refraction microtremor (Louie, 2001), horizontal to vertical spectral ratio (Theodulidis *et al.*, 1996) and microtremor array methods (Horike, 1996). Noninvasive methods are becoming more common for measuring V_{S30} . In the present study, the multichannel analysis of surface wave approach has been used to determine the shear wave velocity and the average shear wave velocity for the top 30 meters of soils. The test is based on measurement of Rayleigh waves and the shear wave velocity profiles are obtained by Rayleigh wave dispersion curves. Both the dispersion curve and the ellipticity of Rayleigh waves are controlled by the subsurface velocity structure. To determine the velocity depth profile of the subsurface, measurements of phase velocity of Rayleigh waves of different frequencies have been done as shown in figure 2.

3.1 Field test setup and data acquisition procedure

Multichannel analysis of surface waves (MASW) tests has been carried out using Geometrics make 24 channels Geode seismic recorder. It is a single geode operating software. 24 vertical geophones of natural frequency 4.5 Hz were used to receive the surface wave generated by the active source. To generate the active source, an 8 kg sledgehammer was hit to an iron plate of dimension 30 x 30 x 2.5 cm. The geophones were deployed in a linear pattern with equal receiver spacing of 1m interval with the nearest source to geophone offset of 5m (Xu *et al.*, 2006). All the geophones and the active source generator are connected to an individual recording channel (geode) as shown in figure 1. The hammer was shot at 5 different points along the survey line. One shot at 5 m before the first geophone. Second shot at 5 m after the last geophone. One shot at the middle of the survey line. Two shots at two-third distance of the survey line. A total of 3 stacks of shots were taken so as to increase the signal-to-noise ratio.

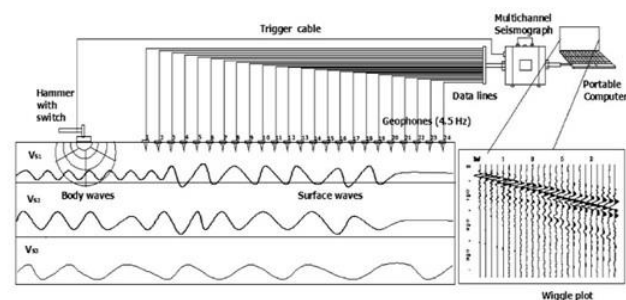


Fig. 1. Field configuration of MASW test

4 METHODOLOGY

4.1 One-dimensional (1D) shear wave velocity profile

The data acquired were processed using the SeisImagerTM software. SeisImagerTM is the master program that consists of four modules such as PickwinTM, PlotrefaTM, WaveEqTM and GeoPlotTM for surface wave and refraction data analysis. Raw data in SEG-2 format obtained from MASW test is fed into the software. The raw data is converted to frequency-phase velocity domain. The phase velocity range of 0 to 2000 m/sec and frequency variation range of 5 to 70 Hz is selected. Phase velocity versus frequency variation at NIT Warangal is as shown in figure 2. Surface wave propagates through several modes, which means that the dispersion property may be represented by several curves of different modes. The fundamental mode of Rayleigh wave is the one with lowest velocity range with frequency which is as displayed by blue shade region in figure 2.

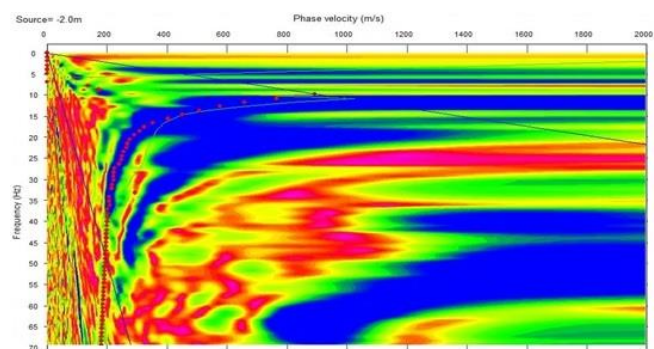


Fig. 2. Phase velocity - frequency domain

The blue shade in phase velocity versus frequency domain other than lowest velocity range is higher mode which will give higher estimation values of shear wave velocity. The chosen lowest velocity range with frequency region in phase velocity frequency domain is inverted to obtain the dispersion curve with high signal to noise ratio. The Pickwin module is used to develop the dispersion curve as shown in figure 3.

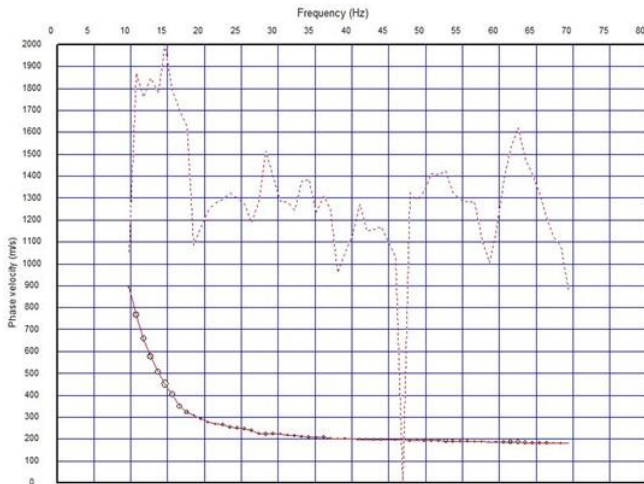


Fig. 3. Dispersion curve with high signal to noise ratio.

Usually the decrease trend of dispersion curve indicates that density of material (Hardness) increase with depth. The dispersion curve shows the variation of phase velocity with frequency in the fundamental mode. To develop the shear wave velocity profile, the dispersion data is used as input. An iterative inversion process is used. The inversion is a mathematical process based on the Least-Squares method, which iteratively modifies the initial model to minimize the difference from the observed data. Iteration is the number of times the initial model will be compared and modified to converge on the best match with the observed data. The dispersion curve was subjected to inversion analysis using the WaveEq module to develop one-dimensional (1D) shear wave velocity profiles as shown in figure 4.

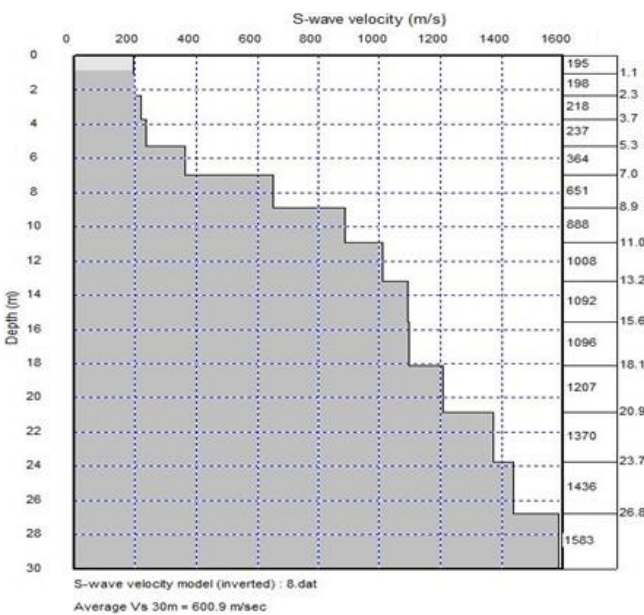


Fig. 4. Shear wave velocity profile at NITW

5 SEISMIC SITE CLASSIFICATION

Seismic design procedure suggested by NEHRP divided the site into five classes based on the average shear wave velocity of subsurface soil profiles. The soil properties within 30 m depth are used for seismic site classification. The IBC (2000) and NEHRP classification systems have been used to classify the sites by many researcher around the world based on the seismic design manuals (BSSC, 2001; Kanli *et al.*, 2006; Dobry *et al.*, 2000) as shown in table 1. The seismic site classification system is based on the average shear wave velocity on the top of a 30 m depth of subsurface soil profiles (Borcherdt, 1994), which is defined by equation 1.

$$V_{S30} = \frac{30}{\sum_{i=1}^N \frac{h_i}{V_{si}}} \tag{1}$$

Where, N is the number of soil layers till 30m depth, h_i is the thickness of the i^{th} layer, V_{si} is the shear wave velocity of the respective layers.

Table 1. Site classification as per NEHRP and IBC (2000)

Site class	Soil profile	V_{S30} (m/s)
A	Hard rock	$V_s > 1500$
B	Rock	$760 < V_s \leq 1500$
C	Very dense soil and soft rock	$360 < V_s \leq 760$
D	Stiff soil profile	$180 < V_s \leq 360$
E	Soft soil profile	$V_s < 180$

6 RESULTS AND DISCUSSION

Surface wave profiling using the multichannel analysis of surface wave method will provide a non-destructive, accurate and quick shallow subsurface image of the shear wave velocities. Here the velocity model with varying soil thickness at NITW stadium is shown in table 2 and the shear wave velocity variation with depth is shown in figure 5. Based on average shear wave velocity (V_{S30}), the site classification as per NEHRP and IBC (2000) is shown in table 1. The study area/site is classified as very dense soil and soft rock as class C, with V_{S30} value as 600 m/sec.

Table 2 Soil profile variation with depth at NITW

Depth (m)	Shear wave velocity classes	Soil profile name
1 – 5.3	$180 < V_s < 360$	Stiff soil profile
5.3 - 11	$360 < V_s < 760$	Very dense soil and soft rock
11- 30	$760 < V_s < 1500$	Rock

7 CONCLUSION

Characterizing the site will give an idea regarding the stiffness of the soil. Based on which the buildings in

the surrounding areas can be planned out in near future. The values can also be used for microzonation studies. Being a very dense soil/soft rock as classified, can withstand large static vertical loads and weak to moderate earthquake loads.

[Back to table of contents](#)

REFERENCES

- 1) Aki, K. (1957): Space and time spectra of stationary stochastic waves, with special reference to microtremors, *Bulletin of Earthquake Research Institute*, 35, 415-456.
- 2) BIS, I. S. (2002). IS 1893 (Part 1): General provisions and buildings: Criteria for earthquake resistant design of structures. *Bureau of Indian Standards*, New Delhi, India.
- 3) Borcherdt, R.D. (1994): Estimates of Site Depending Response Spectra for Design (Methodology and Justifications), *Earthquake Spectra*, 10(4), 617–654.
- 4) Capon, J. (1969): High-resolution frequency-wavenumber spectrum analysis. *Proceedings of the IEEE*, 57(8), 1408-1418.
- 5) Council, Building Seismic Safety. BSSC, (2001): *NEHRP Recommended Provisions for Seismic Regulations for New Buildings and Other Structures*, Part 1.
- 6) Dobry, R., Borcherdt, R.D., Crouse, C.B., Idriss, I.M., Joyner, W.B., Martin, G.R., Power, M.S., Rinne, E.E., Seed, R.B. (2000): New site coefficients and site classification system used in recent building seismic code provisions, *Earthquake Spectra*, 16, 41–67.
- 7) Horike, M. (1996). Geophysical exploration using microtremor measurements. *Xth WCEE, Acapulco*.
- 8) International Code Council, Building Officials, Code Administrators International, International Conference of Building Officials, & Southern Building Code Congress International. (2000): *International building code*. International Code Council.
- 9) Kanli, A.I., Tildy, P., Pronay, Z., Pinar, A., Hemann, L. (2006): Vs30 mapping and soil classification for seismic site effect evaluation in Dinar region. SW Turkey, *Geophysical Journal International*, 165, 223–235.
- 10) Karl, L., Haegeman, W., and Degrande, G. (2006): Determination of the Material Damping Ratio and the Shear Wave Velocity with the Seismic Cone Penetration Test, *Soil Dynamics and Earthquake Engineering*, 26, 1111–1126.
- 11) Louie, J. N. (2001): Faster, better: shear-wave velocity to 100 meters depth from refraction microtremor arrays, *Bulletin of the Seismological Society of America*, 91(2), 347-364.
- 12) Nazarian, S., Stokoe, I. I., Kenneth, H., & Hudson, W. R. (1983): Use of spectral analysis of surface waves method for determination of moduli and thicknesses of pavement systems (No. 930).
- 13) Park, C.B., Miller, R.D., and Xia, J. (1999): Multichannel analysis of surface waves, *Geophysics*, v. 64, n. 3, p. 800-808.
- 14) Theodulidis, N., Bard, P. Y., Archuleta, R., & Bouchon, M. (1996): Horizontal-to-vertical spectral ratio and geological conditions: The case of Garner Valley Downhole Array in southern California, *Bulletin of the Seismological Society of America*, 86(2), 306-319.
- 15) Xia, J., Miller, R.D., and Park, C.B. (1999): Estimation of near surface shear-wave velocity by inversion of Rayleigh wave, *Geophysics*, 64(3) 691–700.
- 16) Xu, Y., Xia, J., and Miller, R.D. (2006): Quantitative estimation of minimum offset for multichannel surface-wave survey with actively exciting source, *Journal of Applied Geophysics*, 59(2) 117–125.

Vulnerability Analysis of Embankment Reach: A Remote Sensing and GIS Based Study in Nona River in Assam, India

Anjil Baid^I, B. Talukdar^{II}, Ranjit Das^{III}

- I) ¹M.E. Student, Civil Engineering Department, Assam Engineering College, Guwahati, Assam, India. Ph.No. - +91 9957353676, Email – anjilbaid@rediffmail.com
 II) ²Associate Professor, Civil Engineering Department, Assam Engineering College, Guwahati, Assam, India. Ph.No. - +91 9859944733, E-mail: bipulaec@gmail.com
 III) ³Research Scholar, Civil Engineering Department, Assam Engineering College, Guwahati, Assam, India. Ph.No. - +91 9436164287, E-mail: ranjit1_das@rediffmail.com

ABSTRACT

Floods of high magnitude are one of the major problems in the north-eastern region of India. Approximately 4464 km of embankments are being constructed in the Brahmaputra basin itself. The embankments are highly vulnerable to flood and flood disaster for embankment breaching is frequent in Assam. Remote Sensing data of a river system of highly unstable bank can be analyzed in GIS environment for identification of river bank erosion as well as reaches of embankment vulnerable to breaching.⁶

A case study was carried out in the Nona River, a north tributary of river Brahmaputra of Assam, to identify reaches of embankment vulnerable to breaching during the flood time. Temporal dataset of satellite imagery for several years along with the topographical maps from Survey of India (SOI) were used for mapping the flow channel of river Nona.

Based on the degree of convergence and narrowness between the flow channel and embankment observed from the digitized images of Nona River from 1999 to 2014, some reaches of embankment which are vulnerable to breaching were selected for the study.

From those vulnerable reaches, a part of river channel was selected for the hydrodynamic analysis by MIKE 21C –Curvilinear Flow Model in order to validate whether the embankment is going to breach due to change of flow pattern of the river observed from the digitized images of the river.

Results obtained from Remote Sensing Data and Flow Velocity Profile from MIKE 21C were split into different categories ranging from 0 to 10 which indicate the vulnerability of embankment.

Floods of high magnitude are one of the major problems in the north-eastern region of India. Heavy flooding causes abrupt changes in the flow pattern of the rivers. The river Brahmaputra shows significant amount of erosion and deposition in the basin. Erosion is mainly caused by the rapid flow of water through soft, disintegrated rocks. Sporadic heavy downpours cause flash floods which also contribute towards erosion.⁷

The study area i.e. the *Nona River Basin* is a major tributary basin of the Baralia River catchment. In the upper part of the basin there lies the Mutunga River while the Nona River uses to follow in the lower part. The master stream of the drainage system oozes at an altitude of about 1068m on the Kurmed district of the Himalayan Kingdom of Bhutan. The river flows for about 71km towards south from its source to its confluence with the Baralia at an elevation of 48m above mean sea level.³

Embankments are the structures constructed parallel to the river utilizing mostly the materials in situ. Due to the meandering nature of the river, the geometry between the flow channel of the river and the embankment does not remain parallel to each other. More the angle between these two more the thrust of water flow on the embankment resulting high probability of embankment breaching.⁷

Remote sensing (RS) Satellite data have the ability to provide comprehensive, synoptic view of fairly large area at regular interval. Integration of Geographic Information System (GIS) to RS, make it appropriate and ideal for studying and monitoring of river bank erosion, changes of channel configuration and the orientations between the river channel and its embankments. Various studies in this regards have been carried for some major rivers. Several investigators have been used RS data for mapping and ascertaining the channel changes of different rivers in the world.

1. INTRODUCTION

The basic data used in this study were as follows:

1.1 Google Satellite Imagery :

In Google Satellite Imagery, most land areas are covered in satellite imagery with a resolution of about 15 m per pixel. This base imagery is 30 m multispectral Landsat which is pan sharpened with the 15 m [Panchromatic] Landsat imagery. The satellite imagery has been used for the digitization of embankment.

1.2 Collateral Data :

Surveys of India (SOI) Topographical Maps were used. i.e.

Table 1. Toposheet Number

State	District	Toposheet No.
Assam	Nalbari	78-N-10 & 78-N-11

1.3 Resourcesat – 1- IRS-1D LISS III Imagery:

The Resourcesat – 1 is an advanced remote sensing satellite built by Indian Space Research Organization. The sensor Linear Imaging Self Scanner (LISS) – 3, which is a part of the payload of Resourcesat – 1, operates in three spectral bands in visible and near infrared (VNIR) and one in shortwave infrared (SWIR) band with 23.5 metre spatial resolution.

To study the changes in the flow pattern of the Nona River, Five Different Year Data over a span of seven years (1999 - 2006), six years (2006-2012), one year (2012-2013-2014) have been considered so that we can see short as well as long term flow pattern change in the Nona River.

Table 2. Details of IRS-1D LISS III Images

River	Path	Row	Date
Nona River	110	53	16-December-1999
	110	53	17-May-2006
	110	53	05-November-2012
	110	53	24-November-2013
	110	53	12-March-2014

The Dataset has been obtained from North Eastern Space Application Centre, Shillong, Meghalaya.

The software used in this analysis are as follows:

- a) ArcGIS 10.2
- b) ERDAS 9.2 Image Processing Software.
- c) QGIS 2.8.1

First of all, **Geo- Referencing** of all the LISS III images was carried out with reference to the ground-co-ordinates of SOI topographical maps

(Toposheet) in ERDAS Image Processing Software.

After geo-referencing, digitization of Nona River for each LISS III images was carried out using ArcGIS in scale of around 8000-10000 and considering standard RGB Composite as 3-2-1 and geographic coordinate system of WGS 1984. Using the Google Satellite Image, latest outline of Embankment of Nona River has been digitized.

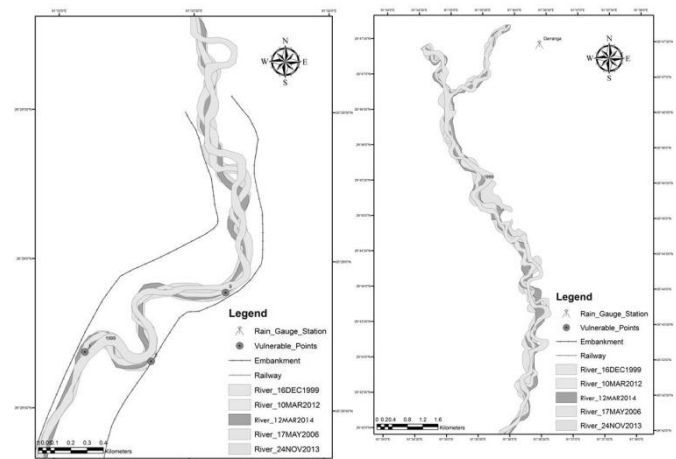


Figure 1. Digitized Images of Nona River & Vulnerable Points.

2. IDENTIFICATION OF VULNERABLE EMBANKMENT REACHES

Identification of Embankment Reaches which are vulnerable to breaching due to Bank Erosion is carried out based upon the change of flow pattern of river towards the embankment observed from the digitized images of Nona River from 1999 to 2014.

From the digitized images of river, **Fourteen Vulnerable Points** were selected and from each points distance were measured from the bank line to the embankment for all selected years i.e. 1999, 2006, 2012, 2013 and 2014.

The distance was calculated using “Measure” Tool in ArcGIS. Based upon the analysis of distances of the river bank line towards the embankment some points has shown highly vulnerable and some low vulnerable to breach.

Table 3. Channel Distance from the Embankment

YEAR	DISTANCE FROM THE EMBANKMENT (in metre)													
	VULNERABLE POINTS													
	1	2	3	4	5	6	7	8	9	10	11	12	13	14
16-Dec-99	44.1506	20.3558	32.7602	81.2131	42.17193	106.6925	16.6324	55.2047	56.0192	58.7849	32.57	70.0915	129.3977	8.1374
10-May-06	35.0344	11.5933	21.2084	50.3841	80.1303	80.9491	30.2369	81.3773	22.2603	35	1.7319	95.3124	142.43	22.9828
10-Mar-12	35.5933	45.5792	16.8415	72.9811	51.5646	68.2378	35.7868	58.5357	29.0261	36.9413	4.3061	77.7066	87.815	27.8415
24-Nov-13	14.9755	27.8355	23.8637	39.2814	40.5392	65.1371	26.2149	73.3249	9.7487	30.5639	64.0781	87.3062	54.3275	31.51624
13-Mar-14	14.3141	10.3845	10.6547	20.0563	39.8443	55.4613	24.7652	42.4196	30.8302	22.6116	27.9931	59.7736	56.0845	46.8441

2.1 Validation Of Vulnerable Points Using Dhi Mike 21-C

From those vulnerable reaches, a part of river channel was selected for the Simulation in MIKE 21C –Curvilinear Flow Model containing three vulnerable points i.e. 1, 2, & 9 in order to validate the remote sensing data observed from the digitized images of the river.²

The effective area under consideration is 1100m x 650m. The individual cells and grid points (a cell being what is defined by four grid points in the corners of the cell) are addressed by indices j and k. The whole study area is covered by the grid, having 100 × 60 cells, so j = 0-98 and k = 0-58, j being used in the direction of the rivers and k is across the river. Thus each cell dimension being 10m x 12 m. A view of the generated grid in MIKE 21C is shown in Figure 5.9. For making bathymetry, depth value, from

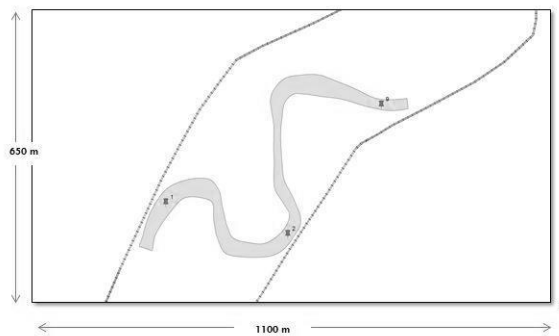


Figure 2. Vulnerable Section used in MIKE 21 & Satellite Image of the Site

Table 2. Calibrated Model Parameters.

CALIBRATED MODEL PARAMETERS	
Parameter	Value
Simulation time step	2 [s]
Flooding depth	0.03 [m]
Drying depth	0.02 [m]
Initial surface elevation	94 [m]

Eddy viscosity (Smagorinsky Formula)	0.75 [velocity based constant]
Manning’s M (1/n)	28 [m ^{0.33} /s]
HD Integration	Fully Dynamic
Morphological Time-step frequency	20
Morphological Time-step	40 [s]

Hydrodynamic calibration is done and model validation is done by first simulating the present condition and then by comparing discharge values at upstream inlet section 1-1 and at downstream outlet section 2-2, which shows good agreement with each other. This indicates that the model is stable and continuity is maintained. This indicates that the model is stable and continuity is maintained. Next the velocity profile around the vulnerable area near upstream side is observed and is found to be near the range of observed maximum velocity of 1.7 m/s at vulnerable points.

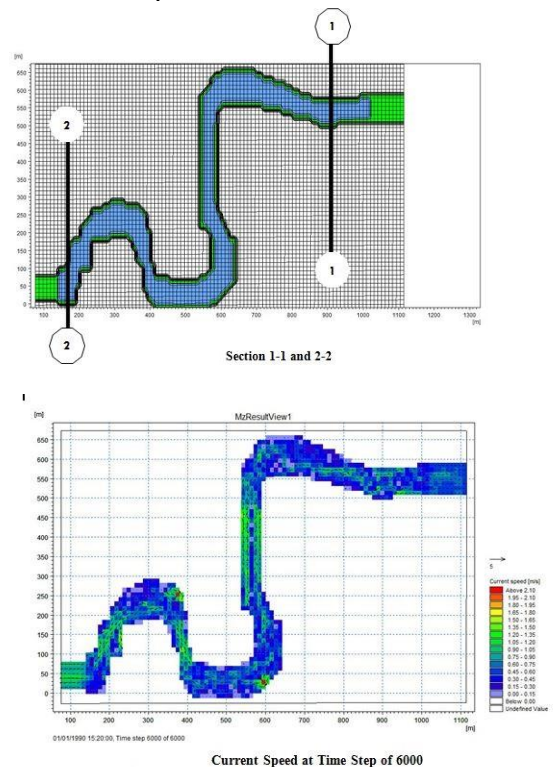


Figure 3. Simulation of Vulnerable Section in MIKE 21

3. RESULTS

The digitized images of Multi Date Satellite Images showed variation in the fluvial features. From this data it was very clear that both the banks have simultaneously undergone erosion and deposition which is shown in the figure-1. The flow of the river is from north to south and meets the Pagladiya River for few kilometers downward, which ultimately meets the Brahmaputra River in the south. The river shows meandering nature. The river bank line changes were mainly observed in the upper-

middle as well as around the embankment reaches of the river.

From MIKE 21-C it was observed that around Point 1 & 2, the velocity of the river is around 1.5 to 2.0 m/s having a discharge of 160 m³/s whereas at point 9 it varies from 0.45-1.2 m/s.

Results obtain from Remote Sensing Data and Flow Velocity Profile from MIKE 21C, the vulnerable points can be split into different categories ranging from 0 to 10 which will indicate the vulnerability of embankment breach based on the degree of convergence and narrowness between the flow channel and embankment observed from the digitized images of Nona River.

Table 4. Calibrated Model Parameters.

Vulnerable Points	Distance from the Embankment	Vulnerability	Range 0 to 10
2	10.3845	Very Highly Vulnerable*	10
3	10.6547	Very Highly Vulnerable	10
1	14.3141	Highly Vulnerable*	9.5
4	20.0563	Vulnerable	8
10	22.6116	Vulnerable	8
7	24.7652	Vulnerable	7.5
11	27.9931	Moderate Vulnerable	7
9	30.8302	Moderate Vulnerable*	7
5	39.8443	Low Vulnerable	6
8	42.4196	Low Vulnerable	5.5
14	46.8441	Low Vulnerable	5
6	55.4613	Low Vulnerable	4
13	56.0845	Low Vulnerable	4
12	59.7736	Low Vulnerable	3.5

From the result, it was found that Nona River Basin has significant geomorphic features like alluvial fans, cones and fan-heads in the upper parts. Ox-bow lakes, meander cut-offs, paleo-channels, sand bars and points bars in the middles and beels, swamps and active flood plains in the lowest section of the basin.

It is a chronic source of trouble due to its frequent changing of flow course and flooding. The river basin is a chronically flood affected area. The flood problem due to inundation may

be attributed to spilling of banks, occurrences of breaches, cuts etc. in embankments and backflow from the river Baralia

The shape of the Nona River Basin is elongated. Actually it is a very narrow basin with a comparatively steep slope up to about upper half of its area. Heavy flooding causes abrupt changes in the flow pattern of the rivers. Erosion is mainly caused by the rapid flow of water through soft, disintegrated rocks. A sporadic heavy downpour causes flash flood which also contributes towards erosion. Apart from all these, factors such as deforestation also contribute towards erosion. When the river enters the plain region with very gentle slope the velocity of water flow greatly decreases and the suspended load which is carried by the river gets deposited. This phenomenon of deposition also contributes towards the change in the flow pattern and meandering of the river channel.

Transportation of heavy amount of silt and aggradation of river bed has been observed to be very prominent phenomenon in the Nona River. Gradual increase of bed and berm level has been observed in the river. The distance between the embankments at some places being narrow, causes afflux and lead to overtopping.

Based on the degree of convergence and narrowness between the flow channel and embankment observed from the digitized images of Nona River, Point 1 & 2 are Highly Vulnerable as there distance from of bank line is less than 10m and if the velocity of the river is around 1.5 to 2.0 m/s during Monsoon Season based upon the simulation of MIKE 21-C, there is a chances that embankment near to the point 1 & 2 may get breached.

4. CONCLUSION

The method may be a good tool for predicting embankment vulnerability to breaching as well as understanding the problems caused by continuous change in the fluvial patterns of the river channels, amount of bank erosion, rate of sedimentation which can be implemented for planning of river bank protection work and preparedness in flood prone state like Assam.

5. REFERENCE

1. Deka M. (2014) “*Mathematical Modeling of an Erosion Affected Reach of River Beki*” M.E. Dissertation, Assam Engineering College, Gauhati University, Assam.

2. DHI Group, “*User Manual Mike 21C*”, Hydrodynamic Modeling Part, Delhi
3. National Disaster Management Authority of India, “*Study of Brahmaputra River Erosion and its control*”, Guwahati, Assam.
4. Purkayastha P. (2014) “*Mathematical Modeling of an Erosion Affected Reach of River Brahmaputra*” M.E. Dissertation, Assam Engineering College, Gauhati University, Assam.
5. Talukdar, A.K. (1999) “*Fluvio-morphological characteristics of the Mutunga-Nona River Basin, Assam*”, M.Phil. Thesis, Gauhati University, Assam.
6. Talukdar B. & Das R. (2015) “*Assessment of River Bank Erosion and Vulnerability of Embankment to Breaching: A RS and GIS Based Study in Subansiri River in Assam, India*” THA 2015 International Conference, Bangkok, Thailand.
7. Talukdar, B., Sarma, B. and Misra, U.K. (2011), “*Evaluation Study of R/S to Nona Embankment, B/B of River Nona from ‘0’ Point of Existing Embankment to Its Outfall*” Evaluation report submitted to Water Resources Department, Nalbari Division and Guwahati West Division, Govt. of Assam, India.

[Back to table of contents](#)

STABILITY ANALYSIS OF AN ASH POND DYKE UNDER STATIC, PSEUDOSTATIC AND SEISMIC CONDITIONS

Priyanka Talukdarⁱ⁾, Ruplekha Boraⁱⁱ⁾ and Arindam Deyⁱⁱⁱ⁾

i) Research Scholar, Dept of Civil Engineering, IIT GUWAHATI, email- priyanka.talukdar@iitg.ernet.in

ii) Trainee Engineer, GAMMON INDIA LTD., Bombay,, email- ruplekhabora888@gmail.com

iii) Assistant Professor, Department of Civil Engineering, IIT GUWAHATI, email- arindamdeyitk@gmail.com

ABSTRACT

With the progressive increase in the number of coal-based thermal power plants, generation of fly-ash have increased manifold. Only 40-50% of the produced fly-ash being re-used for engineering purposes, the storage of fly-ash is a concern. Generally, fly-ash is stored in slurry form in reservoirs termed as ash-ponds. These reserves are built with specific capacity and needs to be further expanded when the fly-ash slurry nearly reaches the brim. This paper highlights on the stability aspects during the stage wise construction of an ash-dyke with raising. Limit equilibrium (LE) and Finite Element (FE) techniques are adopted to explore the aspects of stability for static and pseudo-static conditions. An equivalent linear seismic analysis is also carried out to illustrate the stability aspects of the ash dyke during the seismic condition. The performance of these dykes has been computed using the SEEP/W, SIGMA/W, SLOPE/W and QUAKE/W modules in GEOSTUDIO 2007. The limit equilibrium and finite element methods have been used to study the stability of these dykes in SIGMA/W and SLOPE/W modules whereas the dynamic behavior of these ash dykes has been studied in QUAKE/W to analyze its stability in the seismic conditions. Stability of the ash dyke has been defined in terms of safety factors obtained from the analyses. A comparative note is provided to highlight the aspects of various types of analysis on the stability assessment of ash dykes.

Keywords: Fly ash dyke, Stability analysis, Static, Pseudo-static, Equivalent Linear Dynamic, SEEP/W, SLOPE/W, SIGMA/W, QUAKE/W

1 INTRODUCTION

Only a small quantity of the fly ash generated every year from the thermal power plants and cement plants have been used in alternative applications such as concrete and brick making, soil stabilization and treatment, and construction of ash dykes and earth fills. A large part of the generated fly ash remains unutilized and is generally disposed in its slurry form to the onsite storage ponds bound by dykes. These reserves are generally expanded once the specific capacity is reached and further storage is required. Generally, the initial (or starter) dykes are made up of earthen materials, while the required vertical expansions (or raisings) are either made up of the same earthen material (as an expansion of the starter dyke) or by the hardened fly-ash itself. Such vertical expansions can be inward, outward or centrally raised, depending upon the shift of the line of symmetry of the raising with respect to the line of symmetry of the starter dyke. The inward raising is mostly preferred for the ash impoundment due to constraints of land acquisition on the exterior of the ash pond. The raising, however, rests on the deposited ash which is a weak geomaterial, thus providing an inadequate bearing capacity for the support of the new dykes and thereby making it vulnerable and prone to stability and seepage concerns. Stability of these ash dykes are of utmost importance for the proper functioning of the ash-pond during its operational period. This paper highlights the stability

analysis of one such fly-ash dyke with a single-stage raising (expansion of the starter dyke). The dyke located at Wanakbori, Gujarat, has been studied for its behavior under the static, pseudo-static and dynamic conditions. The formulations have been carried out in LE and FE methods to study the stability aspects.

Many established methods based on limit equilibrium approach are available, namely, Bishop's method (1955), Janbu's method (1957), Morgenstern-Price method (1965) and Spencer's method (1967). However, it is not always possible to obtain realistic stress distributions along the slip surface and localized shear stress concentrations are, of course, not captured in a limit equilibrium formulation. The finite element formulations, therefore, have to be carried out to establish the stress distributions for their subsequent usage in a stability analysis. Geostudio 2007 is capable of considering the above-mentioned aspects in the analyses; the ground stresses can be computed using SIGMA/W has been used in SLOPE/W to compute the actual safety factors. Seepage through the dyke is simulated with the aid of SEEP/W, while the response under seismic behavior is studied with the aid of QUAKE/W module of GEOSTUDIO 2007. It is also possible to combine multiple analyses using different modules into a single modeling project to analyze the coupled stability, deformations, stress, and pore-pressure conditions.

2 PROBLEM STATEMENT AND ANALYSIS METHODOLOGIES

For the present study, the stage-wise construction of the Wanakbori Ash Dyke is taken into consideration. Fig. 1a to Fig. 1d represents the sequential construction stages of the ash dyke, namely (i) Stage I: Construction of the starter dyke, (ii) Stage II: Filling of the ash pond up to the high flood level (HFL), (iii) Enhancement of the starter dyke through vertical raising, and (iv) Filling up of the next level of ash pond up to the HFL of the enhanced dyke.

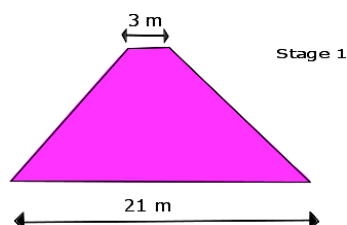


Fig. 1a. Stage1: Starter dyke

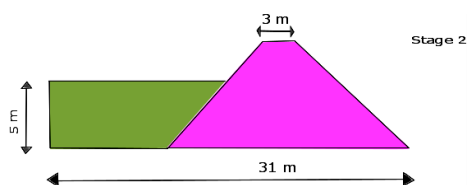


Fig. 1b. Stage2: Starter dyke + pond ash slurry

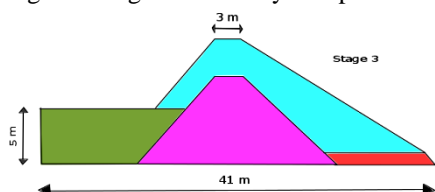


Fig. 1c. Stage3: Raised dyke (material used to raise the dyke is same as the starter dyke)

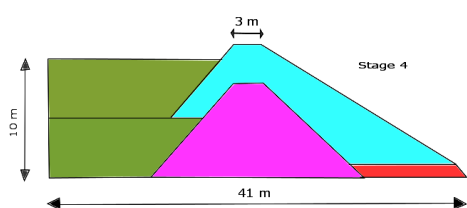


Fig. 1d. Stage4: Raised dyke + raised pond ash slurry

The relevant parameters used for the analysis of the ash dyke are:

Embankment soil: $c = 18 \text{ kPa}$, $\phi = 22^\circ$, $\gamma = 18.5 \text{ kN/m}^3$

Pond ash slurry: $c = 5 \text{ kPa}$, $\phi = 5^\circ$, $\gamma = 10 \text{ kN/m}^3$

Fill soil at the toe of the raised dyke: $c = 20 \text{ kPa}$, $\phi = 24^\circ$, $\gamma = 18.5 \text{ kN/m}^3$

The stage wise stability analysis of the ash dyke had been carried out for the static, pseudostatic and dynamic conditions. Among the various limit equilibrium methods available in SLOPE/W 2007, Morgenstern-Price method was used for static and pseudo-static analysis and the entry exit specification

had been used to define the slip surfaces in the upstream and downstream sections of the dyke. The pseudostatic stability analysis had been carried out considering the zone factors of the four seismic zones of India (IS 1893-I: 2002) as the horizontal seismic coefficient (k_h) and the vertical seismic coefficient (k_v) was taken as 0.075. Maximum possible earthquake scenarios have been used for the present study. For the dynamic analysis, the initial stresses had been obtained from the in-situ analysis (conducted using SIGMA/W) for the first stage of construction; for the subsequent stages of construction, the stresses have been generated by the load/deformation analysis. Thereafter, for each stage, an equivalent linear dynamic analysis had been performed in QUAKE/W. By this way, finite element stability values before and after the earthquake were obtained for all the stages.

For the equivalent linear dynamic analysis, QUAKE/W steps through the entire earthquake record and identifies the peak shear strains at each Gauss numerical integration point in each element. The shear modulus (G) is then modified according to a specified modulus reduction function. This iterative procedure continues until the strain-compatible G -values are obtained within a specified tolerance. The cyclic shear strain is obtained from the finite element analysis. The computed shear strain together with the function and the specified G_{max} are used to compute new G values for each of the iterations. As with G_{max} , the damping ratio in QUAKE/W can be specified as a constant, or as a function. The damping ratio is a function of the cyclic shear strain, similar to the G -reduction function. Damping ratio was considered to be constant for this analysis.

The ash dyke used in this study is located in seismic Zone III; however, this analysis had been carried out by adopting maximum considered earthquake (MCE) with a PGA of 0.35g to check its stability conditions in the worst-case scenario. The initial stress conditions in the dynamic analysis had been incorporated from the SIGMA/W analysis. In the dynamic analysis, a Poisson's ratio and a damping factor of 0.35 and 0.1 respectively, and were considered to be same for the embankment soil, pond ash and the fill soil. The value of G_{max} for pond ash was 18 MPa and that for the other two materials was considered to be 7 MPa. The G -reduction function, which gives the response of the soil to cyclic shear strains when subjected to dynamic stresses, was computed considering a confining pressure of 100kPa for all the three materials. The effect of water due to the pond ash slurry had been included in the study by a steady state seepage analysis in SEEP/W using 'saturated/unsaturated only' model for the embankment soil and 'saturated only' model for the other two materials. The PWP conditions in all the other analysis had been derived from the corresponding SEEP/W analysis.

3 RESULTS AND DISCUSSIONS

3.1 Static Analysis using LE method

The results from the static stability analysis using Morgenstern-Price method based on LE formulation has been presented in Table 1. The analysis had been carried out for two different stages of construction.

Table 1: Stability values from static analysis using LE method

Stages	FoS Values	
	Upstream side	Downstream side
Stage 2: Starter dyke + pond ash slurry	2.426	1.258
Stage 4 : Raised dyke+ raised pond ash slurry	4.059	1.473

From the static analysis, it can be observed that the upstream side of the dykes provides higher stability values as compared to the downstream side for both the analyses cases. Moreover, Stage 4 resulted in higher FoS values as compared to Stage 2. A typical slip surface for the upstream side of the ash dyke from static analysis using LE method is shown in Fig. 2.

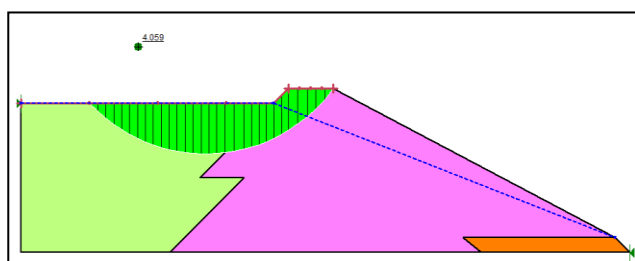


Fig. 2. Typical upstream slip surface static analysis using LE method

3.2 Pseudostatic Analysis

A pseudostatic analysis represents the effects of earthquake shaking by accelerations that create inertial forces, thereby reducing the FoS value. The variation of FoS values corresponding to different horizontal seismic coefficients applicable to different zones is shown in Fig. 3.

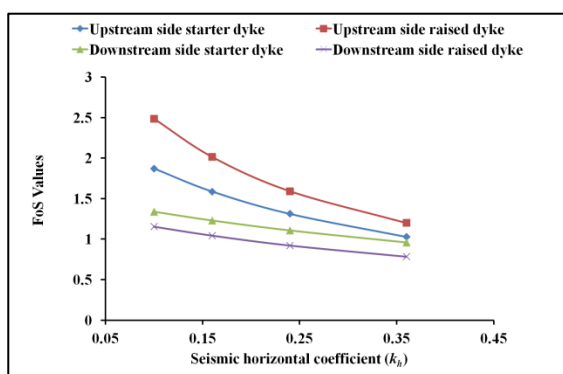


Fig. 3. Variation of FoS values with k_h in pseudostatic analysis.

It is seen that FoS value decreases with increase in horizontal seismic acceleration (k_h) for both the stages along the upstream and downstream sides of the dykes. However, the downstream side of the dyke shows failure in both the stages with increase in k_h values.

3.3 Static Analysis using FE method

The static analysis using the FE formulation makes it possible to conduct a stage-wise stability analysis starting from the construction of the starter dyke till the filling of the raised dyke with the pond ash slurry, using SIGMA/W. The initial in-situ stresses were first generated using in-situ analysis; then, the addition of the pond ash in the subsequent stages were analyzed using load/deformation method of SIGMA/W. The FoS values by FE analysis before the application of earthquake motion for all the different stages are presented below in Table 2.

Table 2: Stability values from static analysis using FE method

Stages	FoS Values	
	Upstream side	Downstream side
Stage 1: Starter dyke	1.700	1.883
Stage 2: Starter dyke + pond ash slurry	2.520	1.767
Stage 3: Raised dyke	1.492	1.670
Stage 4 : Raised dyke+ raised pond ash slurry	3.629	1.310

From the stability analysis using the FE formulation, it is observed that the ash dyke is stable in all the stages of the construction as the FoS values are well within the stable range. A typical slip surface for the upstream side of the ash dyke from static analysis using FE method is shown in Fig. 4.

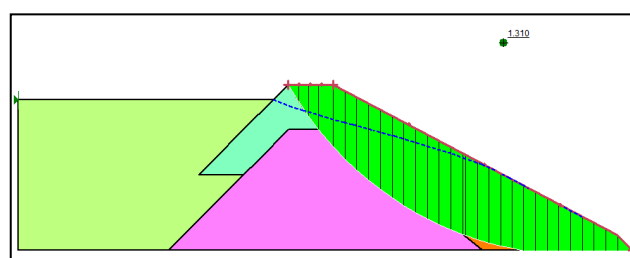


Fig. 4. Typical upstream slip surface static analysis using FE method

3.4 Dynamic Analysis

A dynamic analysis had been carried out using the Equivalent Linear model in QUAKE/W with the specified soil stiffness. In Equivalent Linear analysis, QUAKE/W generated stress is incorporated in SLOPE/W to determine the finite element based FoS values for the entire duration of earthquake. An earthquake of 10 sec duration and having peak horizontal acceleration of 0.35g had been applied in the dynamic analysis. The variation of the FoS values with

the duration of the input earthquake motion is shown for the four different stages along the upstream and downstream side of the dyke in Fig. 5 to Fig. 8.

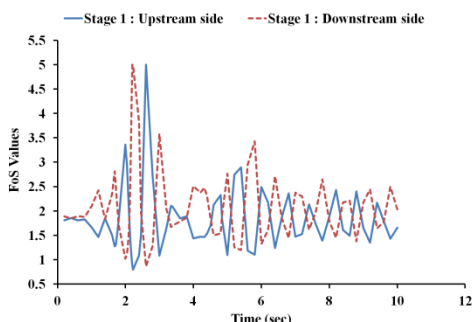


Fig. 5. Variation of FoS values with time for Stage 1

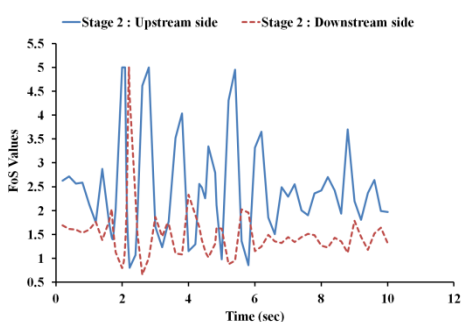


Fig. 6. Variation of FoS values with time for Stage 2

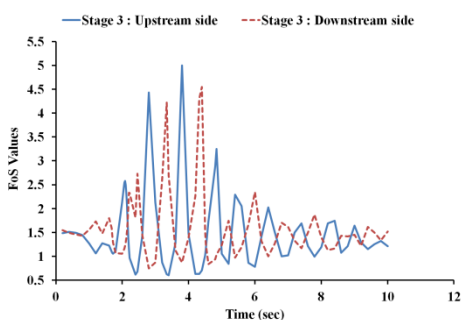


Fig. 7. Variation of FoS values with time for Stage 3

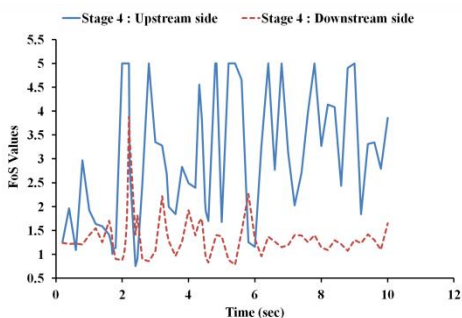


Fig. 8. Variation of FoS values with time for Stage 4

From the FoS-time plots, it is observed that the variation of factor of safety with respect to time is nearly comparable along the upstream and downstream sides for Stage 1 and Stage 3. However, a distinct variation in the FoS values along the two sides is

observed in Stage 2 and Stage 4, wherein for both the stages, higher FoS values were obtained along the upstream side of the dyke for the entire earthquake duration as compared to the downstream side. Further, from the figures, it can be concluded that in reality, the factor of safety value varies dramatically both above and below the static factor of safety. The factor of safety may even momentarily fall below 1.0, however, this does not mean the slope will necessarily totally collapse.

The variation of horizontal acceleration with time along the crest of the ash dyke is shown in Fig. 9 for all the four different stages of construction. From Fig. 9, it is evident that an amplification of the horizontal acceleration along the crest of the dyke had occurred for all the stage of construction, as the peak horizontal acceleration is more than applied peak acceleration of 0.35g as shown in Fig. 10.

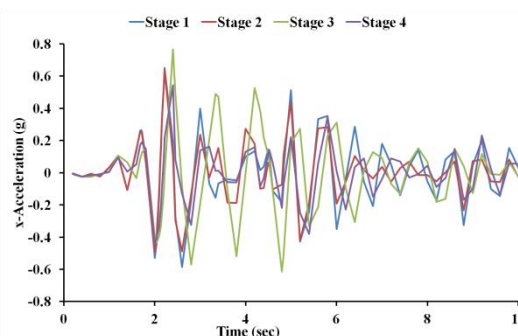


Fig. 9. Variation of horizontal acceleration with time at the crest of the dyke

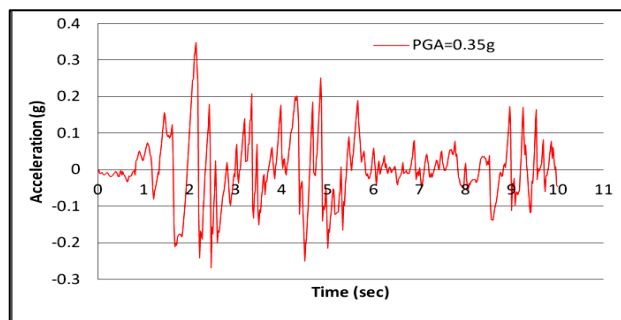


Fig. 10. Acceleration-time history of the input motion

The deformation and displacement characteristics of the ash dykes before and after the earthquake motion, along with the development of the phreatic line for two different stages of construction has been shown in Fig.11 to Fig. 14

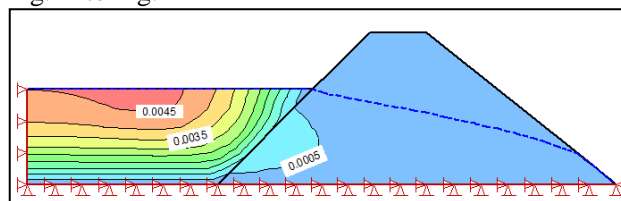


Fig.9. Displacement contours before seismic shaking for Stage 2

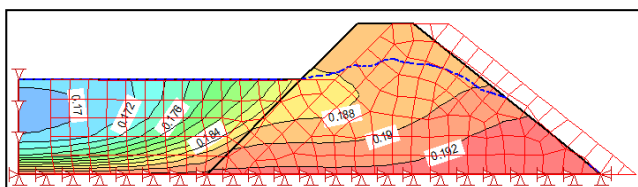


Fig. 10. Displacement contours and deformed mesh after seismic shaking for Stage 2

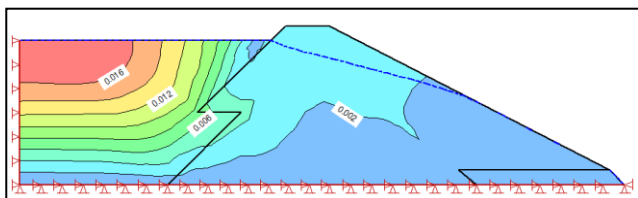


Fig. 11. Displacement contours before seismic shaking for Stage 4

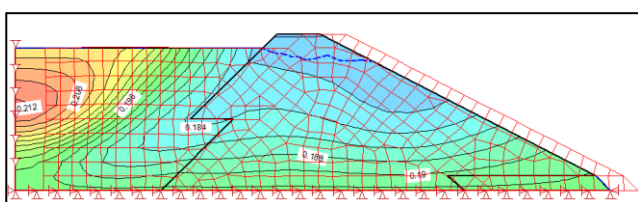


Fig. 12. Displacement contours and deformed mesh after seismic shaking for Stage 4

From the figures, it is observed that before the earthquake motion there had been small displacement with maximum value of 0.0045m for Stage 2 and 0.016m for Stage 4, indicating a rise in the value of displacement with the construction of the raising. Moreover, the level of phreatic line increases with the rise in the pond ash filling level. However, after the incorporation of the earthquake motion for the same two stages, the deformation of the ash dykes were observed. The maximum displacement values had also increased by 0.192m for Stage 2 and 0.212m for Stage 4 as compared to the static case. The rise in the phreatic line due to the generation of pore pressure during earthquake shaking can also be observed when compared to the static analysis for the same two stages.

4 CONCLUSIONS

This paper reports the stability analysis of a ash pond dyke with a single stage vertical enhancement. The single-step raising of the ash dyke was done with the same embankment material. In first stage of analysis, stability of ash dyke under static and pseudo-static condition was investigated in terms of FoS using Morgenstern-Price limit equilibrium method. In second stage of analysis, in-situ and load-deformation analysis was carried out in SIGMA/W for various stages of ash dyke raisings, and finite element based FoS was determined. In the final stage of analysis, equivalent linear dynamic analysis was conducted and QUAKE/W generated stress was incorporated in SLOPE/W for

determination of finite element based FoS values for the assigned earthquake-time history. From the analyses, it can be concluded that the ash dyke considered for this study is stable in both the static and dynamic conditions. As for the method of analysis is concerned, in static conditions, the stability values from the FE method are more realistic than the those obtained from LE method as it can capture the stress distributions and stress concentrations. In the dynamic case, the pseudo-static method provides largely conservative estimate of the stability of the ash dykes in the sense that it accounts for the peak earthquake acceleration to be acting on the ash dyke for an indefinite time. Thus, a rigorous dynamic analysis should be conducted to analyze the actual scenario of an ash dyke during the entire duration of earthquake. It can also be concluded that momentary reduction in the FoS during the earthquake might not lead to a complete collapse of the ash dyke.

In this study equivalent linear dynamic analysis had been conducted in which excess pore-pressures can be computed only at the end of the dynamic analysis. To overcome this limitation and to capture excess pore pressure during the earthquake shaking (condition more closely related to the real field), a Non-Linear effective stress analysis would be more apt.

REFERENCES

- 1) Bishop, A.W. (1955). The use of slip circle in the stability analysis of earth slopes. *Geotechnique*, 5(1), 7-17.
- 2) Janbu, N. (1957). Earth pressures and bearing capacity calculations by generalized procedure of slices. *4th International conference on Soil Mechanics and Foundation Engineering*, 2, 207-212
- 3) Morgenstern, N.R. and Price, (1965) V.E., The analysis of the stability of general slip surfaces. *Geotechnique*, 15(1), 79-93
- 4) Spencer, E. (1967). A method of analysis of the stability of embankments assuming parallel interslice forces. *Geotechnique*, 17(1), 11-26.
- 5) IS 1893 (Part 1 - 2002 R2005) *Criteria for Earthquake Resistant Design of Structures*, Bureau of Indian Standards

[Back to table of contents](#)

Optimum earthquake resistant design based on the lowest rocking response of a system to a particular earthquake excitation using MATLAB

Gitartha Kalitaⁱ⁾

i) Assistant Professor, Department of Civil Engineering, Assam Don Bosco University, Guwahati 781017, India.

ABSTRACT

Natural frequency of a system plays a significant role in contributing to the system's resistance to earthquake forces. The difference between the excitation frequency of an earthquake and the natural frequency of the system is a very important factor which decides how the structure will behave when an earthquake strikes. It is basically seen that earthquake ground motion is considered as a lateral motion in the horizontal direction. But it also has a vertical and a rotational component (Kashefi and Trifunac, 1986). It is the combined action of these components which significantly effect the rocking response of the structure (Rahman and Kalita, 2015). The natural frequency of the system is calculated and the rocking response of the system to a specific earthquake excitation is studied. Then the natural frequency of the system is further modified by making some changes in the system. The changes in the rocking response of the system with the changes in its natural frequencies are studied and a program is developed using MATLAB to select an optimum design which can give the least rocking response to an induced earthquake ground motion of a particular frequency.

Keywords: Natural frequency, Earthquake, Excitation frequency, Ground motion, Rocking response, Optimum Design

1. INTRODUCTION

In order to do the analysis a Liquid Storage Tank model is selected. The model is considered to be an Intze container is considered to be supported on 14.6 m high hollow RC shaft with reinforcement in two curtains. The top dome is 120mm thick, the top and bottom ring beam is 250mm x 300mm and 500mm x 300mm. the wall of the tank is 200mm thick. The conical dome is 250mm thick and the circular ring beam 500mm x 600mm. Grade of concrete and steel are M25 and Fe415, respectively. Site of the tank has hard soil in seismic zone IV. Density of concrete is 25 kN/m³.

2. MODEL USED IN THE STUDY

The model was inspired from the Example No. 2 of the explanatory examples section in the document of IITK-GSDMA Guidelines for Seismic Design of Liquid Storage tanks (2007).

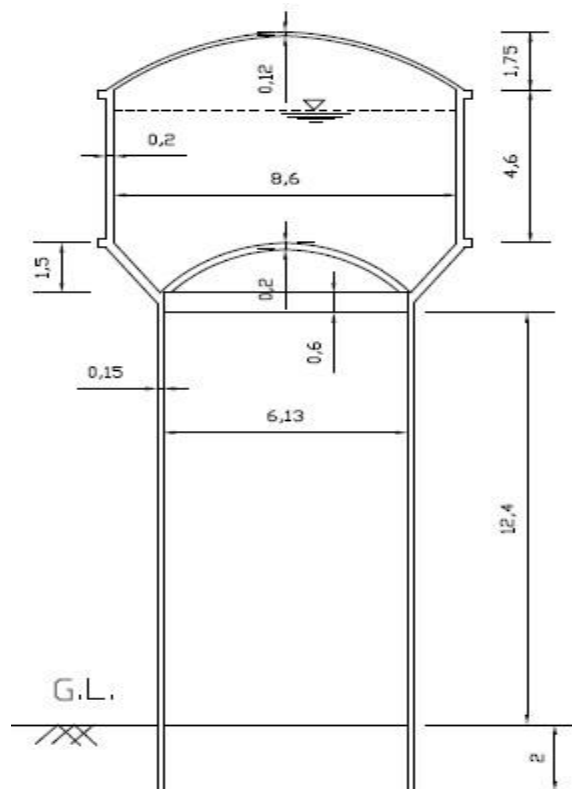


Fig. 1. Liquid Storage Tank

The thickness of the shaft = 150mm
 Weight of the shaft = 1065.37 KN
 Weight of the empty container along with one third the
 Weight of the staging = 1931 KN
 Staging Height is 15m from the footing level.
 Height of C.G. of the empty container from the footing
 level 17.88m.
 Total weight of water = 2508 KN
 Volume of water = 255.66 m³.
 Mass of water = 255658 kg.
 Internal Diameter of the tank = 8.6m.

For finding out the parameters of the spring mass model we consider an equivalent circular container of same diameter and volume. The diameter considered is equal to the diameter of the tank at the top level of liquid. The height of the equivalent circular cylinder is found out as 4.4m. The lateral stiffness of the spring staging was calculated as 3.66*10⁸ N/m. The mass moment of inertia and mass radius of gyration was calculated to be 7965932.422 kgm² and 6.281m. The real component of horizontal, vertical and rotational ground displacements corresponding to P waves are denoted by the following equations.

The equations used for horizontal displacement, vertical displacement, and the rotational displacement for P wave excitations are taken from the Report no CE 86-02 of University of Southern California, Department of Civil Engineering (Kashefi and Trifunac, 1986). In their report they used these equations for applying on a bridge model. Whereas in this study we apply these equations on a liquid storage tank model.

$$U_x = A_0 \bar{U}_{xP} \cos(\omega t - \gamma)$$

$$U_y = A_0 \bar{U}_{yP} \cos(\omega t - \gamma), \text{ and}$$

$$\Psi = A_0 \kappa_\beta \bar{\Psi}_P \cos(\omega t - \gamma - \frac{\pi}{2}) \text{ respectively.}$$

Where,

U_x = Horizontal ground motion

U_y = Vertical ground motion

Ψ = Rotation of the ground

A_0 = Amplitude of the P wave (Unit amplitude is considered in this case)

κ_β = Transverse wave number

\bar{U}_{xP} = Real component of the horizontal motion

\bar{U}_{yP} = Real component of the vertical motion

$\bar{\Psi}_P$ = Real component of the rotational motion

ω = frequency of the earthquake excitation

t = time (in seconds)

$$\gamma = \kappa_\alpha \times \text{Sin } \theta_0$$

κ_α = Longitudinal wave number

θ_0 = Angle of incidence (taken as 0.1 radians)

Velocity of P waves are taken as 8000m/sec

As a new approach, these equations were used and a program was developed in MATLAB using the formula of equation of motion. The program was developed in such a way that it would indicate the rocking displacement of the model for various earthquake excitations of different frequencies.

3. RESULTS AND CONCLUSIONS

Earthquake excitations of values 10, Hertz, 20 Hertz, 30 Hertz, 40 Hertz and 50 Hertz were applied. The corresponding rocking displacement (in radians) was observed for each of the earthquake excitations. The values that were obtained are shown in a tabular format. The values were taken for each earthquake excitation at 2 seconds, 4 seconds and 6 seconds.

For height = 14.4m, the values obtained are cited in the following table.

Table 1. Rocking (in Radians) vs Excitation Frequency

Excitation Frequency	2 seconds	4 seconds	6 seconds
10 Hertz	-0.9338	1.8115	2.4109
20 Hertz	0.9673	-0.0709	-0.8729
30 Hertz	0.6344	-0.4069	0.1386
40 Hertz	-0.6727	0.7466	0.5074
50 Hertz	-0.9925	-1.2385	-1.1429

The values obtained regarding the rocking displacement for different earthquake excitations using the program made in MATLAB shows how the increase in the earthquake intensity can give a considerable effect on the rocking of the model. We

can also observe the pattern of increase in the rocking of the model or decrease in the rocking of the model with change in values of earthquake excitations.

Now in order to do the modifications in the design using the MATLAB program we can proceed in the following manner.

We can change the height of the model and analyze for what height the rocking displacement will be within the limits we want.

For height = 10.4m, the values that are obtained are cited in the following table

Table 2. Rocking (in Radians) vs Excitation Frequency

Excitation Frequency	2 seconds	4 seconds	6 seconds
10 Hertz	-1.9357	4.2809	5.4273
20 Hertz	1.5186	0.1549	-1.7255
30 Hertz	1.3001	-1.0921	0.7767
40 Hertz	0.0336	1.0161	-0.2586
50 Hertz	-0.7547	-0.4901	-0.0912

Moreover along with the values of the rocking displacements that we obtain from the program, we can also obtain the natural frequency of the system from the program and also the stiffness of the system in different conditions with different modifications done in the structure. Looking at the different results we can make the necessary modifications in the model.

REFERENCES

- 1) Kashefi, I. and Trifunac Mihailo, D. (1986): Investigation of Earthquake Response of Simple Bridge Structures. University of Southern California, Department of Civil Engineering. Report No. CE 86-02.
- 2) Rahman, T. and Kalita, G. (2015): "Translational and Rotational Effect of Earthquake Ground Motion on a Bridge Substructure", Journal of Civil Engineering and Environmental Technology (JCEET), Volume 2, Number 4; April-June, 2015 pp 314-318.
- 3) IITK-GSDMA GUIDELINES for SEISMIC DESIGN OF LIQUID STORAGE TANKS (2007).

[Back to table of contents](#)

Seismic Response of RCC Storage Tanks in High-Risk Seismic Zones

Pratim P. Kalita⁽ⁱ⁾, Jayanta Talukdar⁽ⁱ⁾, Rimjhim Kashyap⁽ⁱⁱ⁾, Ritukesh Bharali⁽ⁱⁱⁱ⁾, Bhargob Deka^(iv), Jayanta Pathak^(v), Palash Jyoti Hazarika^(vi)

i) Project Assistant, Department of Civil Engineering, Assam Engineering College, India.

ii) Graduate Student, Department of Civil Engineering, University of Buffalo, USA

iii) Graduate Student, Department of Civil Engineering, Delft University of Technology, Netherlands

iv) Graduate Student, Department of Civil Engineering, McGill University, Canada

v) Professor, Department of Civil Engineering, Assam Engineering College, India.

vi) Professor & Head, Department of Civil Engineering, Assam Engineering College, India.

ABSTRACT

Water storage tanks and water supply network should remain functional in the post-earthquake period for effective and early disaster recovery. Around the world the life-line systems are found to be deficient against seismic forces and are reported to suffer extensive damages during major earthquakes. In this study the seismic behavior of 31 numbers of existing RCC water tanks, in operation under Guwahati Municipal Corporation (GMC), at Guwahati have been investigated to understand their seismic response and capacity for prescribed seismic forces as per the current Indian code. The analysis procedure involved assigning category to the tanks based on their capacity and geometry, condition assessment of the structural and nonstructural components through field surveys, compliance of the structural components with the current code of practice and design. The study involved equivalent static analysis, linear dynamic analysis to comprehend the effects of transient ground motion on the existing tank structures. The investigation of failure conditions were carried out by gap analysis of demand and capacity against earthquake forces prescribed, as per current code of practice. The tanks are broadly categorized into 'over-ground tanks' and 'over-head tanks' with further classifications of each category based on their dimensions. The analytical method involved equivalent static analysis as per present code of practice and then analysing the models to incorporate the earthquake response with fluid-structure interaction effects due to the dynamic response. In order to include the effect of hydrodynamic pressure in the analysis, tanks are idealized by an equivalent spring mass model, which includes the effect of tank wall – liquid interaction. The analysis procedure is formulated to analyze the existing structures with due considerations to the depreciation of strength due to aging of the structure. It has been observed during the study that the existing storage tanks, which were designed and constructed earlier as per old earthquake code require appropriate retrofitting to withstand the code level earthquake as per the new earthquake code for liquid retaining tanks.

Keywords: *Over-ground tanks, Over-head tanks, Equivalent Static Analysis, Dynamic Analysis, Fluid-Structure Interactions.*

1. INTRODUCTION

Seismic safety of liquid storage tanks and supply network is of considerable importance. Water storage tanks and water supply network should remain functional in the post earthquake period to ensure potable water supply to earthquake-affected regions and to cater to the need for fire fighting and other secondary disaster for early disaster recovery. There has been effort in the past to evaluate the dynamic response of storage reservoir against earthquake

forces (Housner, 1963; Haroun and Housner, 1984; Jain and Medhekar, 1993, 1994; Jain and Sameer, 1993; Malhotra et al., 2000; ACI, 2001;) Liquid storage tanks are mainly of two types: ground supported tanks and elevated tanks.

The work presented here involved analyzing the seismic vulnerability of 31 number of water storage tanks with capacities ranging from 20kL to 6000kL and currently servicing in a water distribution network covering almost half (Approximately 1.4×10^4

acres of land area) the city of Guwahati, from three intake points of capacities 4.5MLD, 45MLD and 22.5MLD. Among the 31 Tanks include Over ground Reservoirs (OG), Elevated Service Reservoirs (ESR) and Underground Reservoirs (UG)

2. ANALYSIS PROCEDURE

Though the importance of Water distribution system in a post Earthquake scenario is immense, a comprehensive analysis procedure to determine the seismic vulnerability of existing water storage tanks is not readily available. The damages during the Bhuj (Gujarat, India) Earthquake, 26 January 2001 (7.7 Mw) have shown that the water storage tanks, their distribution networks were deficient in design and were unable to withstand the earthquake forces. In this work , an attempt has been made to consider dynamic effect of earthquake with consideration of hydro-dynamic effect of water in various worst case scenarios.

The Analysis Procedure involves the following steps:

- STEP 1:** Assigning a category
- STEP 2:** Health assessment/ condition assessment of the structural and non structural components through field surveys.
- STEP 3:** Compliance of the structural components against the current code of practice & design. (Equivalent Static Analysis)
- STEP 4:** Dynamic analysis by numerical modeling to comprehend the effects of transient ground motion through response spectra.
- STEP 5:** Investigation of failure conditions and carry out gap analysis of capacity against Transient Ground Deformation (TGD) for earthquake as per current code of practice.

3. ASSIGNING A CATEGORY

Categories are about modeling a representation. Following categories are employed during the analysis:

- (a) **Location**
 - (i) Over ground tank
 - (ii) Under ground tank
- (b) **Geometry**
 - (i) Rectangular tank
 - (ii) Circular tank
- (c) **Ground Supported Reservoirs (Circular)**
 - (i) Reservoirs >15m diameter
 - (ii) Reservoirs <15m diameter
- (d) **Elevated Reservoir**
 - (i) Supported on RCC shafts.
 - (ii) Supported on RCC staging.

- (iii) Supported on steel staging.
- (iv) Supported on masonry pedestal.

Further, extensive categorizing strategies may be employed to arrive at a more detailed analysis procedure-starting point, scope of which may be duly investigated.

4. INTERVENTION AND FIELD SURVEYS

Health assessment of the structural and non structural components is necessary for analysis of existing structures to acquire information regarding the strength of the existing structures and make appropriate assumptions for various conditions including the depreciation of strength due to aging.

A total of four sessions of filed survey, spreading over a period of four months (approximately) in total, were conducted to assess the conditions of the structural as well as non structural components of the existing 31 numbers of water tanks and the 3 intake points. These sessions led to the preparation of a situation assessment report for each location. The major portion of the situation assessment reports consists of Detailed Visual Screening (DVS) tables devised independently to predict strength depreciation and filled out during the survey sessions. An example of the Detailed Visual Screening (DVS) table of a water tank undertaken has been shown in Figure 1.

Title: Survey by DVS of Structural Issues of Housing Reservoir 1.1 (capacity 450 KL)							
Photograph of the Reservoir Type: Over Ground (OG)	Location	Latitude - 26°11'33.8"N					
		Longitude- 91°46'15.82"E					
	Component	Issues					
		Crack	Leakage	Seepage & Moisture Ingress	Exposed Reinforcement	Spalling of Conc.	Other
	Base Plate	-	Y	Y	-	-	N
	Wall	Y	Y	Y	Y	Y	N
	Dome	Y	N	N	Y	Y	Y
Staging	-	-	-	-	-	-	
DIMENSIONS : Diameter = 13.05m Height = 3.05m Thickness (a) Base Plate=0.25m (b) Wall = 0.2m (c) Dome = 0.02m GMC Representative : Mr. Binod Sharma		REMARK ON OTHER ISSUES (i) The Base Plate Appears to be detached at some parts. (ii) The Dome is in a Alarming condition (iii) A Gap ('-') on the form means it cannot be determined					
Year Of Construction : 1993		Dates Of Visits : *-10-15,13-11-15			Evidence Pipe Network		

Fig. 1 Detailed Visual Screening Table (DVS) of Housing Reservoir (Location: Lat: 26°11'33.8", Long: 91°46'15.82")

5. EQUIVALENT STATIC ANALYSIS

The compliance of the Structural components of the existing water tanks have been done against the current draft code, IITK-GSDMA Guidelines (IITK-GSDMA, 2007) for Seismic Design of Liquid Storage Tanks. A number of important changes are

incorporated in this codal provision as compared to IS1893:1984 (BIS, 1984) which can be briefly stated as the following : analysis of ground supported tanks are included, a two-degree of freedom idealization is used for analysis for elevated tanks, bracing beam flexibility is explicitly included in the calculation of lateral stiffness of tank staging, the effect of convective hydrodynamic pressure is included, the distribution of impulsive and convective hydrodynamic pressure is represented graphically for convenience in analysis; a simplified hydrodynamic pressure distribution is also suggested for stress analysis of the tank wall and the effect of vertical ground acceleration on hydrodynamic pressure is also considered.

5.1 Spring Mass model for seismic analysis

In order to include the effect of hydrodynamic pressure in the analysis, tank can be idealized by an equivalent spring mass model, which includes the effect of tank wall – liquid interaction. The parameters of this model depend on geometry of the tank and its flexibility. The Spring mass model for Ground Supported tanks are shown in figure 2.

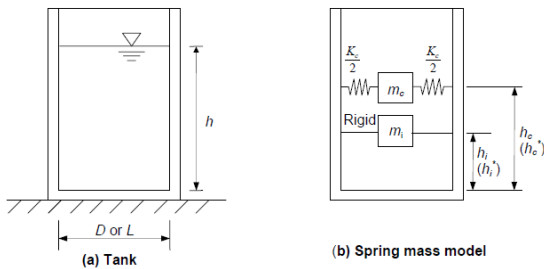


Fig.2 Spring mass model for ground supported circular and rectangular tank

The spring mass model for elevated tanks are idealized as two mass models as shown in figure 3.

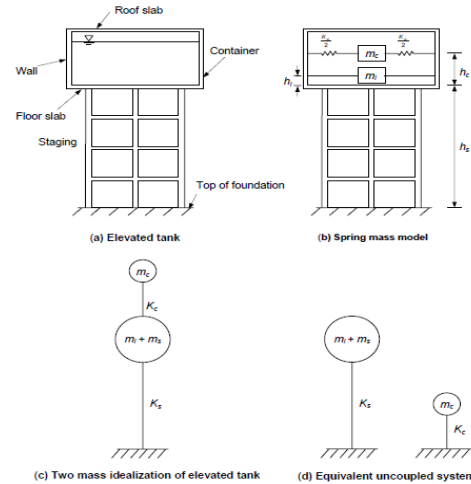


Fig.3 Spring mass model for elevated tanks - Two mass idealizations for elevated tank

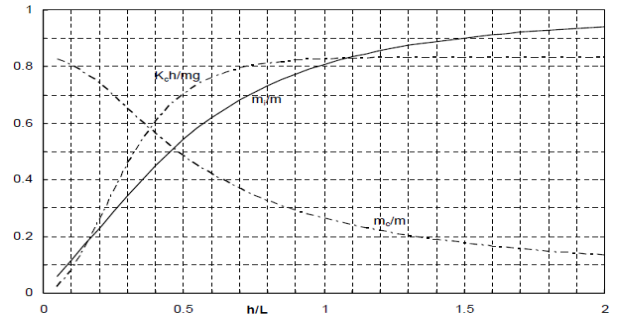
The table 1 presented below provides the parameters considered for spring mass model.

Expression for parameters of spring mass model

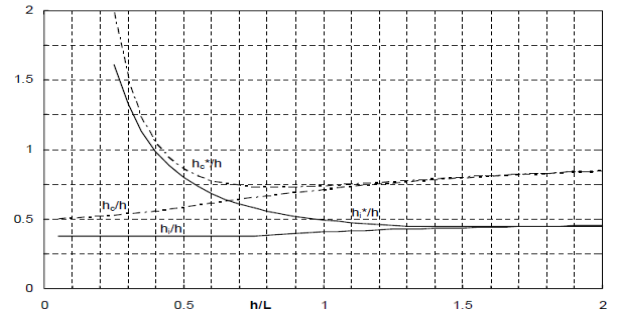
Circular tanks	Rectangular tank
$\frac{m_i}{m} = \frac{\tanh\left(\frac{0.866D}{h}\right)}{0.866D/h}$	$\frac{m_i}{m} = \frac{\tanh\left(\frac{0.866L}{h}\right)}{0.866L/h}$
$\frac{m_c}{m} = \frac{0.23 \tanh\left(\frac{3.68h}{D}\right)}{h/D}$	$\frac{m_c}{m} = \frac{0.264 \tanh\left(\frac{3.68h}{L}\right)}{h/L}$
$\frac{h_c}{h} = 1 - \frac{\text{Cosh}\left(\frac{3.68h}{D}\right) - 1.0}{3.68(h/D)\text{Sinh}\left(\frac{3.68h}{D}\right)}$	$\frac{h_c}{h} = 1 - \frac{\text{Cosh}\left(\frac{3.16h}{L}\right) - 1.0}{3.16(h/L)\text{Sinh}\left(\frac{3.16h}{L}\right)}$
$K_c = 0.836 \left(\frac{mg}{h}\right) \tanh^2\left(\frac{3.68h}{D}\right)$	$K_c = 0.833 \left(\frac{mg}{h}\right) \tanh^2\left(\frac{3.16h}{L}\right)$
$\frac{h_c^*}{h} = 1 - \frac{\text{Cosh}\left(\frac{3.68h}{D}\right) - 2.01}{3.68(h/D)\text{Sinh}\left(\frac{3.68h}{D}\right)}$	$\frac{h_c^*}{h} = 1 - \frac{\text{Cosh}\left(\frac{3.16h}{L}\right) - 2.01}{3.16(h/L)\text{Sinh}\left(\frac{3.16h}{L}\right)}$
Circular tanks	Rectangular tank
$\frac{h_i^*}{h} = \frac{0.866D}{2 \tanh\left(\frac{0.866D}{h}\right)} - 0.125,$ For $\frac{h}{D} \leq 1.33$ $= 0.45, \text{ For } h/D > 1.33$	$\frac{h_i^*}{h} = \frac{0.866L}{2 \tanh\left(\frac{0.866L}{h}\right)} - 0.125$ For $\frac{h}{L} \leq 1.33$ $= 0.45, \text{ For } h/D > 1.33$
$\frac{h_i}{h} = 0.375, \text{ for } \frac{h}{D} < 0.75$	$\frac{h_i}{h} = 0.375, \text{ for } \frac{h}{L} < 0.75$

$= 0.5 - \frac{0.09375}{\frac{h}{D}}, \text{for } \frac{h}{D} > 0.75$	$= 0.5 - \frac{0.09375}{\frac{h}{L}}, \text{for } \frac{h}{L} > 0.7$
Symbols Used	
m_i – Impulsive Mass of liquid m - Total mass of liquid in tank D - Inner diameter of Circular tank. h – Maximum Depth of liquid L - Inside length of rectangular tank parallel to the direction of seismic force. h_i - Height of impulsive mass above bottom of tank wall (without considering base pressure)	h_i^* - Height of impulsive mass above bottom of tank wall (considering base pressure) m_c – Convective mass of liquid h_c - Height of convective mass above bottom of tank wall (without considering base pressure) h_c^* - Height of convective mass above bottom of tank wall (considering base pressure) g - Acceleration due to Gravity K_c – Spring Stiffness (convective mode)

Table1 : Spring mass model parameters



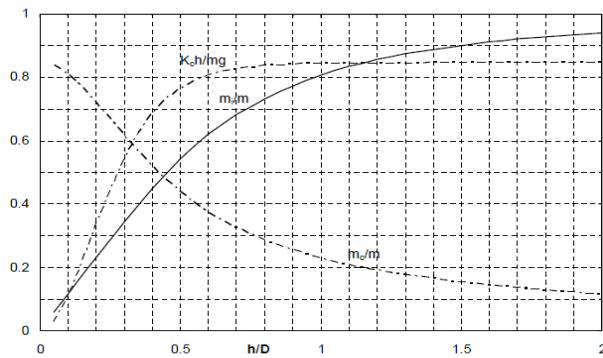
(a) Impulsive and Convective mass and Convective spring stiffness



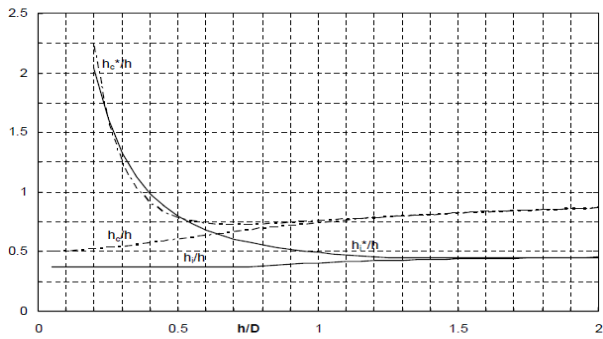
(e) Heights of impulsive and convective masses

Fig.4 Parameters of the spring mass model for rectangular tank

The spring mass model parameters can also be obtained graphically as represented in figure 4



(a) Impulsive and Convective mass and Convective spring stiffness



(b) Heights of impulsive and convective masses

Fig. Parameters of the spring mass model for circular tank

5.2 Parameters calculated for analysis from spring mass models

The various parameters calculated from the spring mass model representation are: Time period, Hydrodynamic Impulsive pressure, Hydrodynamic Convective pressure, Design Horizontal Seismic coefficient, Base Shear, Anchorage requirement, Sloshing wave height, and Vertical ground acceleration. These calculations have been carried out using macro programming in Microsoft Excel spreadsheets. A comprehensive number of excel spreadsheets for different categories of water tanks are generated and these spreadsheets may be utilized in future as general input sheets for spring mass model analysis calculators of water tanks.

6. DYNAMIC ANALYSIS

The dynamic analysis is carried out using Numerical modeling simulation to comprehend the effects of the Transient Ground Deformation (TGD). The numerical models are generated using concepts of Finite Element Modeling (FEM) using shell elements as the primary component building block, giving due consideration to the aspect ratio, joint connectivity, edge constraints and degree of freedom. The effect of strength depreciation is also duly considered in the Numerical models. The analysis procedure followed is

the Modal Response Spectrum Analysis. The Response Spectrum curve used is as per the guidelines in the draft code, IITK-GSDMA Guidelines for Seismic Design of Liquid Storage Tanks. The hydrodynamic effect of the water motion in the dynamic analysis is applied using the Impulsive and Convective pressure as per the code as shown in figure 5.

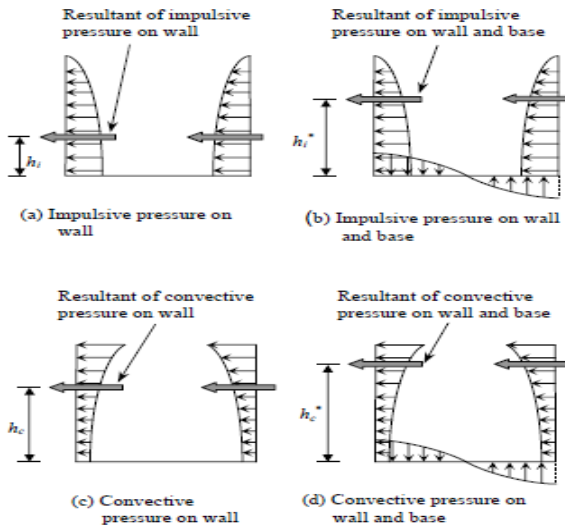


Fig.5 Qualitative description of hydrodynamic pressure distribution on tank wall and base

7. INVESTIGATION OF STRESS CONDITIONS

The parameters calculated in the Equivalent Static analysis and obtained from the Dynamic analysis are compared and scaled up appropriately to obtain the strength conditions of the existing structures based on the principles of working stress method.

7.1 Comparison of the calculated parameters

The comparison is mainly done in the Base-Shear calculation and the Time periods obtained. A total of 16 out of the 31 tanks are shown here as example, which falls in the range of categories used in the analysis within the scope of the project. The Comparison of Equivalent Static and Linear Dynamic Statistical Base Shear of Ground Supported Tanks are presented in figure 6.

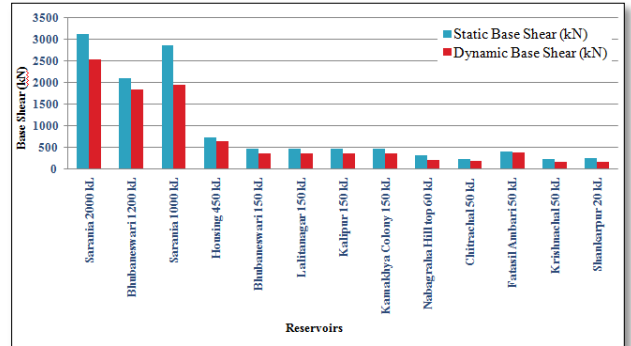


Fig. 6. Comparison of Equivalent Static and Linear Dynamic Statistical Base Shear of Ground Supported Tanks.

The Comparison of Equivalent Static and Linear Dynamic Statistical Base Shear of Elevated Tanks are presented in figure 7.

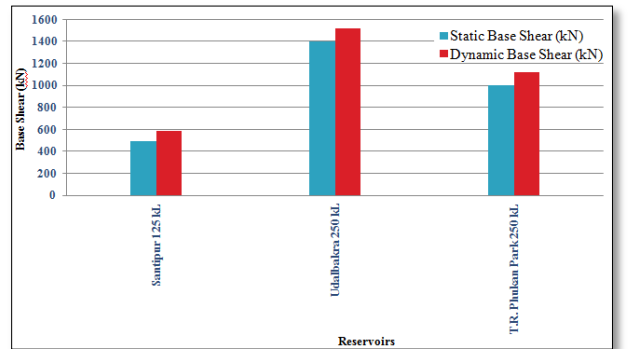


Fig. 7. Comparison of Equivalent Static and Linear Dynamic Statistical Base Shear of Elevated Tanks.

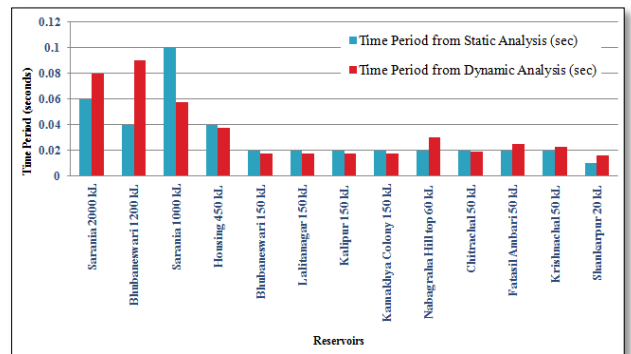


Fig.8. Comparison of Time periods in Equivalent Static and Linear Dynamic Statistical analysis of ground Supported Tanks.

The Comparison of Time periods in Equivalent Static and Linear Dynamic Statistical analysis of ground Supported Tanks are presented in figure 8.

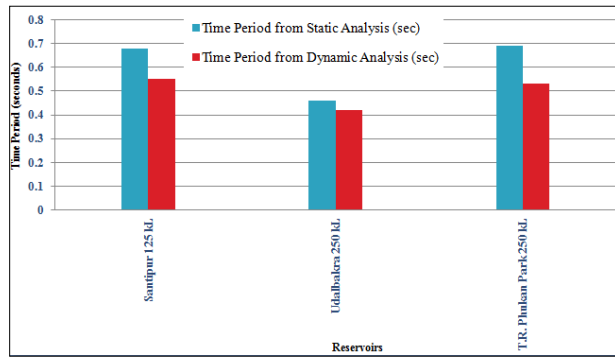


Fig.9. Comparison of Time periods in Equivalent Static and Linear Dynamic Statistical analysis of Elevated Tanks.

The Comparison of Time periods in Equivalent Static and Linear Dynamic Statistical analysis of Elevated Tanks are presented in figure 9.

7.2 Investigation of Stress conditions to predict Strength

The reservoirs are checked for Stress conditions and the resultant failure conditions, as per IS:3370 (Part 2) and IS:456 (BIS, 2000, 2009). These checks are carried out using 'stress output indicating tools', created using macro programming in Microsoft Excel spreadsheets by exporting the data from the Dynamic analysis of the generated numerical models. An extensive amount of conditional formatting is done to create these spreadsheets to check for the failure conditions of the existing tanks and predicting their available strength criteria.

8. CONCLUSION

The Elevated Service Reservoirs (ESR) supported on cylindrical shaft are inverted pendulum-type structures that resist lateral forces by the flexural strength and stiffness of the circular hollow shaft staging. The section closest to the ground is subjected to the maximum flexural demand. It was observed that the seismic performance of the existing tanks supported on cylindrical shaft are very poor with extensive flexural failure observed in shaft from the level of the first "lift" (the vertical height of shaft achieved between successive concrete pours) to several "lifts" reaching approximately up-to one-third the height of the shaft above ground level. Moreover, flexural failure is observed at the locations between the junction of storage reservoir and the shaft.

The frame-type staging is generally regarded as superior to shaft-type staging for lateral resistance because of its large redundancy and greater capacity to absorb seismic energy through inelastic actions. The RC frameworks can be designed to perform in a ductile manner under lateral loads with greater reliability and confidence, as opposed to thin shell sections of the shaft-type staging. However, the tanks supported on the frame-type system designed as per earlier code (BIS, 1984, 1985) are also found deficient at the bracing junctions near the base.

The Ground Supported tanks with diameter < 15 m have relatively better performance than those with diameter >15m where flexural cracks are observed at positions near the junction between the dome and the wall. Flexural cracks are also observed circumferentially at a positions halfway above the ground for some reservoirs with diameter > 15 m.

It has been observed during the study that the existing storage tanks, which were designed and constructed earlier as per old earthquake code (BIS, 1984, 1985) require appropriate retrofitting to withstand the code level earthquake as per the new earthquake code for liquid retaining tanks.

ACKNOWLEDGEMENT

The authors gratefully acknowledge the support received from Guwahati Municipal Corporation (GMC), Guwahati.

REFERENCES

1. ACI 350.3, 2001, "Seismic design of liquid containing concrete structures", American Concrete Institute, Farmington Hill, MI, USA.
2. Bureau of Indian Standards (BIS), 2002, IS 1893 (Part 1):2002, "Indian Standard Criteria for Earthquake Resistant Design of Structures: General Provisions and Buildings".
3. Bureau of Indian Standards (BIS), 2009, IS:3370 Part2, "Code of practice for Concrete structures for the Storage of liquids."
4. Bureau of Indian Standards (BIS), 1985, IS:11682 1985, "Criteria for Design of RCC Staging for Overhead Water Tanks",
5. Bureau of Indian Standards (BIS), 2000, IS:456 Indian Standard for Plain and Reinforced Concrete—Code of Practice. New Delhi, India.
6. Bureau of Indian Standards (BIS), 1984, IS:1893 Criteria for Earthquake Resistant Design Structures. New Delhi, India.
7. Bureau of Indian Standards (BIS), 1993, IS:13920 Ductile Detailing of Reinforced Concrete Structures Subjected to Seismic Forces— Code of Practice. New Delhi, India.
8. Draft Code, IITK GSDMA, 2007 Guidelines for seismic design of liquid storage tanks.
9. Haroun, M. A. and Housner, G. W., 1984, "Seismic design of liquid storage tanks", Journal of Technical Councils of ASCE, Vol. 107, TC1, 191-207.

[Back to table of contents](#)

10. Housner, G. W., 1963a, "Dynamic analysis of fluids in containers subjected to acceleration", Nuclear Reactors and Earthquakes, Report No. TID 7024, U. S. Atomic Energy Commission, Washington D.C.
11. Housner, G. W., 1963b, "The dynamic behavior water tanks", Bulletin of Seismological Society of America, Vol. 53, No. 2, 381-387.
12. Jain, S. K. and Medhekar, M. S., 1993, "Proposed provisions for aseismic design of liquid storage tanks: Part I – Codal provisions", Journal of Structural Engineering, Vol. 20, No. 3, 119-128.
13. Jain, S. K. and Medhekar, M. S., 1994, "Proposed provisions for aseismic design of liquid storage tanks: Part II – Commentary and examples", Journal of Structural Engineering, Vol. 20, No. 4, 167-175.
14. Jain, S. K. and S. U. Sameer, 1993. "A Review of Requirements of Indian Codes for Seismic Design of Elevated Water Tanks," Bridge & Structural Engineer. Vol. XXIII, no.1.
15. Malhotra, P. K., T. Wenk, and M. Weiland, 2000. "Simple Procedure of Seismic Analysis of Liquid Storage Tanks," Journal of Structural Engineering International. IABSE, Vol.10, no.3.

Site Response Evaluation Procedures for Earthquake Risk Management A State of the Art Review

Jyotisman Saikia ⁱ⁾, Jayanta Pathak ⁱⁱ⁾ and Diganta Goswami ⁱⁱⁱ⁾

i) Ph.D Student, Department of Civil Engineering, Assam Engineering College, Guwahati University, Guwahati-781013, India.

ii) Professor, Department of Civil Engineering, Assam Engineering College, Guwahati-781013, India.

iii) Associate Professor, Department of Civil Engineering, Assam Engineering College, Guwahati-781013, India.

ABSTRACT

It is a well established concept that ground disturbance by earthquake and intensities of damage depend on the source and path of the earthquake, and on the local site conditions. It has also been a fact that effects of local geology on ground shaking represent an important factor in earthquake risk evaluation. The seismic waves are affected by a host of factors like topography, geotechnical characteristics of surficial soil, depth of sedimentary basin and bed rock (basement) topography, basin edge conditions, vertical/inclined layering of sediments, water table, etc. During the passage of time various researchers studied the response of the site due to earthquake shaking and as such different methods of evaluating site response kept on evolving. The various site response evaluation procedures developed so far has its advantages, disadvantages and applicability under various conditions. An attempt has been made in this paper to study the various site response evaluation procedures and their applicability under various conditions with reference to various research works performed by different researchers. This review is done to find a suitable method for evaluation of site response in the Guwahati region which falls under seismic zone V, with an objective of understanding the risk in regional scale due to probable earthquake scenario in the region and to contribute for sustainable development of the growing city.

Keywords: *earthquake, site response evaluation procedure, Guwahati,*

1 INTRODUCTION

It is an established fact that ground shaking by earthquake and intensities of damage depend on the source and path of the earthquake, and on the local site conditions. It has also been long known that effects of local geology on ground shaking represent an important factor in earthquake risk evaluation. The site response parameters deciphered from geotechnical property of soil, geological setting and instrumental studies can give a good estimate of risk factor by removing both source and deep path effects assuming that these effects are same for records on bed rock and on the surface of nearby overlying soil cover. The local conditions affecting variations in seismic wave amplification are: (i) Topography, (ii) Geotechnical characteristics of surficial soil and, (iii) Depth of sedimentary basin and bed rock (basement) topography, basin edge conditions and lateral in homogeneities, vertical/inclined layering of sediments etc. Hence the response at the site during an earthquake plays a vital role in determining the vulnerability due to an earthquake in that particular area.

2 HISTORY OF SEISMIC SITE RESPONSE

The history of Seismic Site Response Analysis dates back to the mid 1950s. Li Tze (1955) studied the Earthquakes in those regions particularly from 1679 to

1780. For construction purposes the variation in seismicity in the Peking area was required and for knowing about the variation in seismicity he took into account the hydro geological conditions and the characteristics of the ground. Sieberg and Medvedev deserve special mention because they greatly extended the work into more definitive conclusions. The research work described the method of analysis with greater in depth detail which helped in forming the micro-seismic map of the Peking Area. This work came to be the first instance of the study based on seismic site response.

3 CONDITIONS FOR PERFORMING SITE RESPONSE ANALYSIS

The various conditions for performing Site Response Analysis are as follows:

- When soil conditions cannot be reasonably categorized into one of the standard site conditions.
- When empirical site factors for the site are not available.
- When special ground conditions govern the design (example:- Soil liquefaction, seismic settlement, lateral spreading, and slope stability).
- For any case where the objective is to obtain ground motions considered to be more representative of the local geologic and seismic site conditions than motions obtained from the first two approaches
- Where (nonlinear) Soil Foundation-structure

Interaction (SFSI) analysis is undertaken. (Matasovic and Hashash, 2012)

4 SOIL PROPERTIES REQUIRED FOR SITE RESPONSE ANALYSIS

The soil properties required are -

- a) Index properties such as density, Atterberg limits, and relative density of the various layers.
- b) Strength properties such as friction angle and undrained shear strength are important input properties, especially for soft soils and areas with high levels of shaking.
- c) Dynamic soil properties using cyclic triaxial, cyclic direct simple shear (DSS), and resonant column devices are by far the most common devices for defining the dynamic behavior of soils at a given site.
- d) Soil response curves in the form of normalized modulus reduction and damping curves as a function of shear strain that approximate the nonlinear hysteretic soil behavior.
- e) Hysteretic stress strain behavior of soils under symmetrical cyclic loading by (1) an equivalent shear modulus (G) that corresponds to the secant modulus through the endpoints of a hysteresis loop; and (2) equivalent viscous damping ratio (β), which is proportional to the energy loss from a single cycle of shear deformation. Both G and β are functions of shear strain amplitude (γ). (Matasovic and Hashash, 2012)

5.1. Earlier Developments

A lot of researchers evaluated various methodologies for performing site response analysis. Willis and Johnson (1959) used tape recording and analysis for one of their field trips. Willis (1960) performed spectral analyses on recordings using variable pass-band filters. In the work he studied some observations in the attenuation of seismic waves. Birtill and Whiteway (1965) studied the application of phased arrays to the analysis of seismic body waves. In the study they used Arrays of seismometers, spaced over a distance comparable to the longest apparent wavelength of the signal, to facilitate the separation and identification of seismic phases by a process of velocity filtering. Whiteway (1965) recorded and analyzed seismic body waves using linear cross arrays.

5.2 Finite Element Analysis

The finite element method (FEM) is a numerical technique for finding approximate solutions to boundary value problems for partial differential equations. It is also referred to as finite element analysis (FEA). Fem subdivides a large problem into smaller, simpler, parts, called finite elements. The simple equations that model these finite elements are

then assembled into a larger system of equations that models the entire problem. The credit for the use of finite element method goes to Idriss. Mondkar and Powell (1977) presented the theoretical and computational procedures which have been applied in the design of a general purpose computer code for static and dynamic response analysis of non-linear structures.

5.3 Microtremor Analysis-HVSR Technique

In the two last decades the micro tremor H/V spectral ratio method has been widely used for site effect studies. In this method of analysis straight forward estimate of the site effect of sediments and low-cost measurements are the main advantages of mentioned method. Micro tremor measurements rank among the most popular techniques. Using this technique, the source effect can be minimized by normalizing the horizontal spectral amplitude with the vertical spectral amplitude. In 1978 Microtremor studies were first performed. Katz and Bellon (1978) carried out Microtremor site analysis study at Beatty, Nevada. Microtremor data were collected at several sites at Beatty, Nevada, and compared to nuclear event and mathematical model ground-motion spectra. Somerville (1993) performed evaluation of seismic indices for ground and structures are done using microtremor. In the study Vulnerability indices (K-values) of ground and structures due to earthquake motions have been proposed. K-values can be calculated from microtremors measured easily everywhere and it is not impossible to estimate the vulnerabilities of all structures and ground concerned. Horike et. al. (2001) compared site response characteristics inferred from micro tremors and earthquake shear waves. Mucciarelli et. al., (2004), performed seismic site response analysis using the HVSR technique from microtremor to strong motion: empirical and statistical considerations. The HVSR technique is a widespread tool for the study of ground motion amplification. It applies to a wide range of ground motion amplitude, from microtremor to strong motion. Sometimes it becomes a mandatory choice, when there is no available outcrop for the Reference Site technique and a borehole is unfeasible. There has been a wide debate on the theoretical limitations of the methodology, especially when applied to microtremors. Del Gaudio (2008) attempted Detection of directivity in seismic site response from microtremor spectral analysis. The exact conditions for the occurrence of directional amplification remain still unclear and the implementation of investigation techniques capable to reveal the presence of such phenomena is desirable. To this purpose they tested the applicability of a method commonly used to evaluate site resonance properties (Horizontal to Vertical Noise Ratio – HVNR or Nakamura's method) as reconnaissance technique for the identification of site response directivity. Site response evolution and sediment mapping using horizontal to vertical spectral

ratios (HVSr) of ground ambient noise is done in Jammu city, NW India was done by Mundepi and Mahajan (2010). The technique of ground ambient noise (micro tremor) measurement and analysis has been successful for site characterization in many places around the world. This technique has the advantage of being a fast and easy way to estimate the effect of ground motion characteristics due to an earthquake. Single station ground ambient noise (micro tremor) measurements were carried out at 136 sites in the municipal limit of Jammu city, NW Himalaya. Basavanagowda et. al. (2012), applied Refraction Microtremor (ReMi) for seismic site characterisation. Refraction Microtremor (ReMi) survey was conducted for geotechnical site characterization based on non destructive testing method to evaluate shear wave velocity of substrata at selected locations in Bangalore city, India and to classify the site according to International Building Code 2006 (IBC 2006). The measured shear wave velocities have been used to conduct seismic site response analysis with an objective to find peak ground acceleration distribution, amplification and response spectrum at the measured sites. Mohamed et.al. (2013) estimated the near-surface site response to mitigate earthquake disasters at the October 6th city, Egypt, using HVSr and seismic techniques. The microtremor (background noises) and shallow seismic surveys (through both the seismic refraction and Multi-channel Analysis of Surface Waves (MASW)) were carried out in a specific area (The club of October 6 city and its adjacent space area). The natural periods derived from the HVSr (Horizontal to Vertical Spectral Ratio) analysis vary from 0.37 to 0.56 s. Manne (2013) performed site characterization and ground response analysis for Vijayawada urban area.

5.4 Linear Elastic Analyses, Bilinear Analysis and Equivalent Linear Analysis

Introduced by Seed and Idriss, the wave propagation through the soil deposit is solved in the frequency domain, and any given soil layer is assumed to have a constant modulus and damping throughout shaking. Equivalent-linear site response analysis uses an iterative procedure in which initial estimates of G and β ; G -equivalent shear modulus and β -equivalent viscous damping ratio, are provided for each soil layer. Using those linear, time-independent properties, linear-elastic analyses are performed and the response of the soil deposit is evaluated (Matasovic and Hashash, 2012). Idriss and Seed (1962), carried out remarkable studies of ground motions during the San Francisco earthquake. The horizontal layers are analyzed for Seismic Site Response by Idriss and Seed (1968). They used various methods of analysis which are linear elastic analyses, a bilinear analysis, and an equivalent linear analysis. Finally Seed and Idriss (1970) made remarkable strides in the advancement of seismic site

response analysis. They presented an analytical procedure for the evaluation of the seismic response of horizontal soil layers incorporating equivalent linear moduli and damping ratios varying with depth. Finn et.al. (1976) studied seismic response and liquefaction of sands. In the study an effective stress analysis has been developed for determining the dynamic response of horizontal saturated sand deposits to earthquake motions consisting of vertically propagating shear waves. The development of evolution of seismic site response study progressed further when Martin and Seed (1979) found a simplified procedure for effective stress analysis of ground response. It was found that stress reduction between a total stress analysis, where the effective confining pressure is considered to remain constant throughout the earthquake, and an effective stress analysis that accounts for both types of soil nonlinearity did not exceed about 85% under the most severe conditions. Hosseini (2010) found out the limitations of equivalent linear site response analysis considering soil nonlinearity properties. Lasley et.al. (2014) compared equivalent - linear site response analysis software. It has been shown that when using DEEPSOIL, SHAKEVT, or SHAKE91 the discretization of the profile may obscure peaks when plotting the maximum shear strain, shear stress, or acceleration with depth.

5.5 Non Linear Method of Analysis

In nonlinear site response analysis, the nonlinear behaviour of the soil during cyclic loading can be represented, which makes it possible to move away from the inherent linear approximation of the equivalent-linear analysis approach. Nonlinear analysis makes it possible to explicitly include soil strength and the effects of seismic pore water pressure generation on soil strength and stiffness. These options have significant effects on site response in areas of very high seismicity (e.g., $PGA \geq 0.4$ g) and/or when soft and/or potentially liquefiable soils are present in local soil deposits (Matasovic and Hashash, 2012). Joyner (1975) attempted a method for calculating nonlinear seismic response in two dimensions. This study came to be the first instance of nonlinear method of seismic site response analysis. Dobry et. al. (1976) analyzed behaviour of Behavior of soft clays under earthquake loading conditions. A new method is presented to compute the earthquake response of soft clay deposits. In this method, the change of properties of that soil during cyclic loading is directly incorporated into a nonlinear response calculation in, the time domain. Zienkiewicz et. al. (1978) performed Non-linear seismic response and liquefaction studies. They introduced a 'shrinkage' coupled with an elasto-plastic behaviour of the soil skeleton allows a full non-linear dynamic analysis to be conducted up to the point of structural failure for any earthquake input. Dobry (1981) like earlier researchers studied nonlinear seismic response of soft clay sites. A nonlinear stress-strain model, utilizing

Ramberg-Osgood idealization of backbone curve and allowing for its progressive degradation due to cyclic loading, is used to conduct site response studies at two soft clay sites. Niwa (1982) studied non-linear seismic response of arch dams like other researchers. The study of seismic site response progressed further when Gazetas et.al. (1983), studied Stochastic estimation of the nonlinear response of earth dams to strong earthquakes. Rassem (1992) studied the seismic site response of alluvial valleys and effects on a suspension bridge. The intent of the work has been to extend the work carried out by seismologists on the two-dimensional seismic response of alluvial valleys to include the effects of stiffness variation with depth and non-linear behaviour of soils which are mainly considered in a one-dimensional perspective. Hashash Youssef et. al. (2005) performed non-linear one-dimensional seismic ground motion propagation in the Mississippi embayment. The study describes the development of a new non-linear one-dimensional site response analysis model for vertical propagation of horizontal shear waves in deep soil deposits. Soil response is modeled using a modified hyperbolic model with extended masing criteria to represent hysteretic loading and unloading of soil. Arslan and Siyahi (2006) performed a comparative study on linear and non linear site response analysis. The study attempts to give a critical overview of the field of site response analysis. Nonlinear analysis was compared with the linear method of analysis. Rayhani (2007) studied nonlinear analysis of local site effects on seismic ground response in the bam earthquake. The effects of local site condition in the Bam 2003 earthquake was studied by establishing a 1-D ground profile at the Bam station. The seismic response of the ground surface was analysed using the finite difference code (FLAC) implementing both nonlinear and equivalent-linear methods. Moreover, Tsai and Chen (2014) found Frequency domain (FD) equivalent linear (EQL) and time domain (TD) nonlinear (NL) analyses are the most common approaches used for performing 1D seismic site response analysis.

5.6. SSR Method

The SSR is a technique where the site response is defined as the ratio of the Fourier amplitude spectrum of ground motions recorded at a soil-site to that of ground motions recorded at a rock-site record located nearby, from the same earthquake and component of motion.

6 SEISMIC SITE RESPONSE WORKS IN GUWAHATI REGION

In the Guwahati region Kumar and Krishnan (2013) Performed one dimensional equivalent-linear ground response analyses. Results are presented in terms of surface acceleration histories, strain and shear stress ratio variation, response spectrum, Fourier amplitude ratio versus frequency. The results indicate that

accelerations were amplified the most at the surface level. Kumar and Dey (2015) performed 1D ground response analysis (GRA) conducted for three typical locations at guwahati city: Amingaon, Ahomgaon and Bhangagarh. GRA for Amingaon locality was carried out using scaled strong motions pertaining to PGA 0.18g and 0.36g, scaled from the seismic ground motion recorded during the 2011 Sikkim earthquake at the IIT Guwahati campus. Ahomgaon and Bhangagarh, at Guwahati city subjected to two significantly different strong motions, Sikkim and Kobe strong motions. Soil profiles at different sites comprised of mixtures of silts, sands and clays, with a sufficiently high water table. Analyses have been conducted using equivalent linear (frequency domain) and non-linear (time domain) approaches. Moreover, seismic microzonation has also been carried out of the Guwahati city.

7 CONCLUSION

From the present study it can be found that there are various methods of performing site response analysis along with their advantages, disadvantages and its applicability under various circumstances. Hence like earlier researcher equivalent linear method of analysis was most used and can be used in our region. And as such it will reduce earthquake risk and lead to the sustainable development of the region.

8 REFERENCES

- 1) Arslan H, and Siyahi B. (2006), A comparative study on linear and nonlinear site response analysis, *Environmental Geology*, · August 2006.
- 2) Basavanagowda G.M., Govindaraju L., Chethan K. and Ramesh Babu R. (2012), Application of Refraction Microtremor (ReMi) for Seismic Site Characterisation, *Proceedings of World Conference of Earthquake Engineering*, Lisboa 2012.
- 3) Birtill J.W., Whiteway F.E. (1965), *The Application of Phased Arrays to the Analysis of Seismic Body Waves*. Published 25 November 1965. DOI: 10.1098/rsta.1965.0048.
- 4) Chiang L.T. (1955), *Earthquakes of Peking*, Institute of Geophysics and Meteorology, Academia Sinica.
- 5) Del Gaudio V., Coccia S, Wasowski J., Gallipoli M. R., and Mucciarelli M. (2008), Detection of directivity in seismic site response from microtremor spectral analysis, *Nat. Hazards Earth Syst. Sci.*, 8, 751–762.
- 6) Dobry R., Singh R.D., Doyle, E.H. and Idriss I.M. (1981), Nonlinear seismic response of soft clay sites, *American Society of Civil Engineers*, p. 1201-18.
- 7) Finn W.D.L., Byrne P.M., and Martin, G.R. (1976), Seismic Response And Liquefaction Of Sands, *Journal of Geotechnical and Geo Environmental Engineering*, Volume: 102, Issue Number: GT8, Publisher: American Society of Civil Engineers, ISSN: 1090-0241, p. 841-856.
- 8) Gazetas G., A. DebChaudhury A. and Gasparini D.A. (1982), Stochastic estimation of the nonlinear response of earth dams to strong earthquakes, *Soil Dynamics and Earthquake Engineering*, 1982, Vol 1, No 1.
- 9) Hashash Y.M.A. and Park D. (2001), Non-linear one-dimensional seismic ground motion propagation in

- the Mississippi embayment, *Engineering Geology* 62, 185-206.
- 10) Horike M., Zhao B., and Kawase H. (2001), Comparison of Site Response Characteristics Inferred from Microtremors and Earthquake Shear Waves, *Bulletin of the Seismological Society of America*, 91, 6, pp. 1526–1536.
 - 11) Idriss I.M., and Bolton Seed H. (1957), An analysis of ground motions during the 1957 San Francisco earthquake.
 - 12) Idriss, I.M. (1968), Finite element analysis for the seismic response of earth banks, Vol 94, No SM 3, Proc Paper 5929, PP 617-636, 16 FIG, 9 TAB, Serial: Journal of Soil Mechanics & Foundations Div, Files: TRIS.
 - 13) Idriss, I. M. and Seed, H. B. (1970), Seismic response of soil deposits, Vol 96, No SM2, PROC PAPER 7175, PP 631-638, 6 FIG, 12 REF.
 - 14) Katz L.J. and Bellon R.S. (1978), Microtremor site analysis study at Beatty, Nevada, By the Seismological Society of America.
 - 15) Kumar S.S. and Dey A. (2015), 1D Ground Response Analysis to Identify Liquefiable Substrata: Case Study from Guwahati City, UKIERI Workshop on Seismic Requalification of Pile Supported Structures (SRPSS), 7-9 January 2015, Guwahati.
 - 16) Kumar S.S. and Murali Krishna A. (2013), Seismic Ground Response Analysis of Some Typical Sites of Guwahati City, *International Journal of Geotechnical Earthquake Engineering*, 4(1), 83-101.
 - 17) Idriss I.M., Dobry R.M., Doyle E.M. and Singh R.D. (1976), Behavior of Soft Clays Under Earthquake Loading Conditions, Offshore Technology Conference, 3-6 May, Houston, Texas, OTC-2671-MS.
 - 18) Lasley S.J. , Green R.A. and Rodriguez-Marek A. (2014), Comparison of equivalent-linear site response analysis software, Tenth U.S. National Conference on Earthquake Engineering, Frontiers of Earthquake Engineering, July 21-25, 2014, 10NCEE Anchorage, Alaska.
 - 19) Manne A., Site characterisation and ground response analysis for Vijayawada urban, Thesis Report, Master of Science, (by Research), in Civil engineering, Earthquake Engineering Research Centre, International Institute of Information Technology Hyderabad.
 - 20) Martin, P.P. and Seed H.B. (1979), Simplified procedure for effective stress analysis of ground response, *American Society of Civil Engineers*, p. 739-758.
 - 21) Matasovic N. and Hashash Y. (2012), National Cooperative highway research Programme, Practices and Procedures for Site-Specific Evaluations of Earthquake Ground Motions, Transportation Research Board.
 - 22) Mir Mohammad Hosseini S.M., Asadolahi Pajouh M. and Mir Mohammad Hosseini F. (2010), The limitations of equivalent linear site response analysis considering soil nonlinearity properties, Fifth International Conference on Recent Advances in Geotechnical Earthquake Engineering and Soil Dynamics.
 - 23) Mucciarelli M. and Gallipoli M. R. (2004), The HVSR technique from microtremor to strong motion: empirical and statistical considerations, 13th World Conference on Earthquake Engineering, Vancouver, B.C., Canada, August 1-6, 2004, Paper No. 45.
 - 24) Mohamed A.M.E., Abdel Hafiez H.E., Taha M.A. (2013), Estimating the near-surface site response to mitigate earthquake disasters at the October 6th city, Egypt, using HVSR and seismic techniques, *NRIAG Journal of Astronomy and Geophysics* (2013) 2, 146–165.
 - 25) Mondkar D.P. and Powell G.H. (1977), Finite element analysis of non-linear static and dynamic response, *International Journal for Numerical Methods in Engineering*, Vol 11, 499-520.
 - 26) Mundepi A.K. and Mahajan A.K. (2010), Site Response Evolution and Sediment Mapping Using Horizontal to Vertical Spectral Ratios (HVSR) of Ground Ambient Noise in Jammu City, NW India, *Journal Geological Society Of India*, Vol.75, June 2010, pp.799-806.
 - 27) Niwa A. and Clough R.W. (1982), Non-linear seismic response of arch dams, *Engineering and Structural Dynamics*, Vol. 10, 267-281.
 - 28) Postma G.W. (1955), Wave propagation in a stratified medium, Shell Development Company, Houston, Texas, Publisher: Society of Exploration Geophysicists, CODEN: GPYSA7
 - 29) Raseem M.M.M. (1992), Doctorate Thesis, McMaster University.
 - 30) Rayhani M. H. T., Naggari M. H. El and Tabatabaei S.H. (2007), Nonlinear Analysis of Local Site Effects on Seismic Ground Response in the Bam Earthquake, *Geotech Geol Eng.*
 - 31) Richard E. Warrick R.E. and Oliver A.A. (1976), Analysis of seismograms from a downhole array in sediments near San Francisco Bay, By the Seismological Society of America.
 - 32) Somerville M.R., Kagami H. and McCue K.F. (1993), Seismic Amplification determined from microtremor monitoring at alluvial and rock sites in Newcastle, *Bulletin of the New Zealand national society for Earthquake Engineering*, Vol. 26, No 2.
 - 33) Tsai C.C. and Chen C.W. (2014), A comparison of site response analysis method and its impact on earthquake engineering practice, Second European Conference on Earthquake Engineering and Seismology, Istanbul, August 25-29.
 - 34) Whiteway F.E. (1965), The recording and analysis of seismic body waves using linear cross arrays, *Radio and Electronic Engineer* (Volume:29 , Issue: 1), Page(s): 33 - 45, ISSN : 0033-7722, DOI: 10.1049/ree.1965.0007, Publisher: IET.
 - 35) Willis D.E. and Johnson J.C. (1959), Some seismic results using magnetic tape recording, *Earthquake Notes*, No. 3.
 - 36) Willis D.E. (1960), Some observations on the attenuation of seismic waves, *Earthquake Notes*, September 1960, No. 31.
 - 37) Zienkiewicz O.C., Chang C.T. and Hinton E. (1978), Non-linear seismic response and liquefaction, *International Journal for Numerical and Analytical Methods in Geo Mechanics*, Vol 2, 381-404.

[Back to table of contents](#)

Site specific ground response analysis of Jorhat city

P.Bhowmickⁱ⁾ and A.Bhattacharjeeⁱⁱ⁾

i) P.G. Student, Department of Civil Engineering, Jorhat Engineering College, Jorhat, Assam-785001, India.

ii) Asstt.Professor,Department of Civil Engineering, Jorhat Engineering College, Jorhat, Assam-785007, India.

ABSTRACT

The assessment of local site effects on seismic ground motion is of great importance in geotechnical earthquake engineering. The damage at a site is greatly influenced by the response of the soil. Various parameters that are needed for seismic response analysis are soil profile and its thickness, depth to bedrock, geotechnical properties of the soil and shear wave velocity. Site response analysis can be carried out using equivalent linear and nonlinear techniques. The study area, namely, Jorhat is the second largest city of Assam. Seismically, Jorhat falls in the zone V having zone factor 0.36 [according to IS 1893 (Part I):2002] and experienced various magnitudes of earthquakes in recent past. This paper focuses on the 1D ground response analysis conducted for three locations at Jorhat city: Civil Hospital, Malow Ali, and Na-Ali using DEEPSOIL software. Soil profiles at these sites comprises of mixtures of silts, sands and clays. Three input motions, namely, Chi-Chi, Parkfield and Kobe are used for the analysis. The results are obtained in terms of acceleration time histories, stress-strain behaviour, response spectra, Fourier amplitude, PGA profile and strain profile. For present study, analyses have been conducted using non-linear (time domain) approach. Also, modulus reduction curve and damping ratio curves proposed by Vucetic and Dobry(1991) and Seed and Idriss(1991) are used to define the dynamic behaviour of clay and sandy soil respectively. Results showed that at the ground level acceleration is amplified. Again, amplification is seen to be higher for equivalent linear analysis compared to non-linear analysis. Response spectra(for 5% damping) in terms of peak spectral acceleration also varies with the soil profile of the site. Thus the study brought into light the fact that ground response is affected significantly by the type of ground motion and soil profile.

Keywords: ground response analysis, DEEPSOIL, equivalent linear analysis, non-linear analysis

1. INTRODUCTION

An earthquake is a vibration or oscillation of the earth's surface. Various parameters of the soil are involved in knowing the intensity to which the ground would amplify or de-amplify after the occurrence. In today's world, prior to the construction of any structure it becomes utmost necessary to give a look into the zone to which the area falls and design the building according to the specified criteria (so called earthquake resistant structures). The response of a structure to any ground motion mainly depends on the topography, materials, mode of construction, characteristics and duration of ground motion, and various dynamic properties of the soil.

In order to get a better design it is necessary to look into the past histories of the ground motion. Ground response analysis helps us in fulfilling this requirement. Kramer, 1996 suggested that ground response analysis can be performed by one dimensional, two dimensional and three dimensional methods. Performance by any of these methods lead to get an idea of the response spectra, the stress and strain, the Fourier amplitude and various other parameters which affect the stability of the structures.

Several investigators (Govindaraju and Bhattacharya

(2011), Ranjan(2005), Pallav et al.(2010), Nath et al.(2008),etc) have brought forward various studies on the seismic ground response analysis. Assessment of the seismic ground response of Kolkata city was carried on by Govindaraju and Bhattacharya (2011) which reflected that the amplification falls in the range 4.46-4.82 in the period 0.81s -1.17s. The spectral acceleration is in the range 0.78g - 0.95g. Seismic ground response analysis of Dehradun city was carried by Ranjan (2005) and the spectral acceleration was 0.06g - 0.37g at frequency range 1 Hz - 10Hz. At Imphal city, Pallav et al.(2010) carried out ground response analysis and reported that the Peak Ground Acceleration(PGA) lies between 0.1g - 0.16g and the amplification factor is 1.5-2.0. Analysis of Guwahati city was performed by Nath et al.(2008) and Peak Ground Acceleration(PGA) falls in the range 0.22g-1.27g with amplification factor 2-10.

North east, India is one of the most seismically active region of the world. More than 600 earthquakes of $M > 5$ have been recorded in north east in the last 100 years. As per IS 1893 (part 1) : 2002, Jorhat falls under Zone V with zone factor of 0.36 which highlights that it is a very severe zone. Among the far-source powerful earthquakes, the 1897 Shillong plateau earthquake and the 1950 Assam earthquake distinctly left its marks. So,

any construction done should be earthquake resistant. For that the study of the ground response analysis becomes important.

Mohapatra and Chowdhuri(2010) studied that the soil of Jorhat falls in class D(stiff soil) and the frequency at which the amplification is expected is 1.82 Hz-2.76Hz. The investigation at the upper 30m soil revealed shear wave velocities to range from 222m/sec to 336m/sec.

In this study a step is taken to bring to light the seismic ground response analysis of Jorhat city by selecting some specific sites. Boreholes are drilled and geological investigations provided us with the soil profile and necessary parameters which are required for performing the analysis. DEEPSOIL which is a software developed by Hashash et al.(2011) is chosen for performing the analysis. Time domain non-linear analysis is performed for all of the selected three sites and analysis is done by applying a strong ground motion at the base of the soil profile determined. Three different ground motions were selected and the results were taken for each of the sites ultimately providing us with the desired results.

2 STUDY REGION AND BOREHOLE DATA

The study area, namely, Jorhat is one of the second largest city of Assam. It is located between Brahmaputra in the north and Nagaland in the south at 26.46° N latitude and 96.16° E longitudes in central part of Brahmaputra valley. In the northern part, the topography of Jorhat district is characterized by the undulatory plains of Brahmaputra valley having an altitude range of 80m-120m above mean sea level. The southern parts of the district have low hill range having altitude from 150m-450m above mean sea level. Jorhat city is subjected to two powerful earthquakes of the past, namely, the 1897 Shillong earthquake and the Assam earthquake which occurred in 1950.

The boreholes sites are selected based on maximum population and business area of Jorhat city. The three specifically selected sites are: Civil Hospital, Malow Ali and Na-Ali. Geotechnical investigations carried out each borehole provided us with the sub-soil conditions. SPT tests were conducted at 1m interval for a depth of 15m at each borehole. It is noted that the soil profile mainly consist of clay with medium and low compressibility, silt and fine sand with silt.

At Malow Ali site, it is observed that the soil is predominantly silty up to depth of about 5m followed by sand layer upto 15m. Geotechnical investigations carried out at Na-Ali site revealed that it is a predominantly clay layer upto 15m with traces of silt. Again, the topmost soils of Civil Hospital site are found to be silty followed by a mixture of clay layer and sand layer till 15m. (Table 1).

Performing seismic ground response analysis using

DEEPSOIL software requires the knowledge of shear wave velocity and shear modulus. For this purpose, the correlations (between standard penetration test(SPT-N) and Shear wave velocity)

Table 1. Soil profile at the three considered sites

	Depth	Soil Description	SPT-N	Shear wave velocity, Vs
MALOW ALI SITE	1	SP	-	95.64
	2	ML	4	147.31
	3	ML	5	157.99
	4	ML	10	190.68
	5	ML	14	212.55
	6	SM	15	217.81
	7	SM	17	225.57
	8	SM	16	221.97
	9	SM	15	216.52
	10	SM	21	238.43
	11	SP	19	230.17
	12	SP	17	227.13
	13	SP	15	218.66
	14	SP	15	217.81
	15	SP	16	220.74
NA ALI SITE	Depth	Soil Description	SPT-N	Shear wave velocity, Vs
	1	Sc	7	170.30
	2	CL	4	151.40
	3	CL	4	148.35
	4	CL	7	146.46
	5	CL	6	168.00
	6	ML-CL	4	166.43
	7	CL	5	153.35
	8	CL	5	162.34
	9	CL	4	150.40
	10	CL	5	149.38
	11	CL	6	158.88
	12	CL	5	166.43
	13	CL	5	156.17
	14	CL	6	164.25
15	CL	5	163.17	
CIVIL HOSPITAL SITE	Depth	Soil Description	SPT-N	Shear wave velocity, Vs
	1	ML-CL	-	95.64
	2	ML-CL	4	149.90
	3	ML-CL	3	136.95
	4	SM	11	205.95
	5	ML-CL	7	178.70
	6	CI	7	178.70
	7	SM	16	231.66
	8	CH	13	217.04
	9	CH	1	97.00
	10	SM	9	193.37
	11	CL	5	160.78
	12	CL	4	149.90
	13	CI	4	149.90
	14	SM	33	290.75
15	SC	8	186.35	

provided by different authors based on different soil profiles are referred. The correlations suggested by Maheshwari et al.(2010) for all type of soil is considered for present study. The correlation suggested by Maheshwari et al.(2010) is

$$V_s = 95.64N^{0.3} \quad (1)$$

Where, V_s is the shear wave velocity in m/sec and N is the value obtained from the standard penetration test carried out at different boreholes.

3 GROUND MOTIONS

Seismically, Jorhat falls in the zone V having zone factor 0.36 (according to IS 1893(part 1):2002) it experienced various magnitudes of earthquakes in the past. In this study, three different ground motions are considered for determining the ground response analysis. Ground motion recorded during 1966 Parkfield earthquake, 1999 Chi-Chi earthquake, and 1995 Kobe earthquake having magnitude values ranging from 6.1 to 7.3 are selected for the study. Chi-Chi earthquake which occurred in 21 September, 1999 for about 40 seconds had intensity of V and PGA of 0.33g. On 17 January, 1995 Kobe earthquake occurred with an intensity of VII and PGA of 0.818g for about 20 seconds. Parkfield earthquake on the other hand occurred on 27 June, 1966 with an intensity of VI and PGA of 0.138g. The details of the earthquakes ground motion records are listed in the Table 2. It is also noted that all three earthquake have different PGA values ranging from 0.138g to 0.818g. The duration ranges from 5sec-40sec. This shows the importance of consideration of real earthquake ground motions which may be different with different frequency content and magnitudes.

Table 2. Input motion parameters for the three considered earthquakes

Parameters	Chi-Chi	Kobe	Parkfield
Date	Sept.21,1999	Jan.17,1995	June 27,1966
Magnitude	7.3	6.9	6.1
Epicentre	23.52 ⁰ N 120.45 ⁰ E	34.6 ⁰ N 135 ⁰ E	35.56 ⁰ N 120.31 ⁰ W
Depth of epicenter(km)	7	22	8.6
Duration(sec)	40	20	17
Intensity	V	VII	VI
Acceleration(g)	(0 – 0.18)	(0 – 0.6)	(0 – 0.35)
Fourier amplitude (g-sec)	(0.025 – 0.275)	(0 – 0.6)	(0 – 0.2)
PGA(g)	0.33	0.818	0.138
PSA	(0.18 – 0.5)	(0.8 – 2.64)	(0.0025 – 1.15)

The acceleration time histories of the three earthquake motions and their corresponding fourier amplitude are shown in Fig.1. It is observed from FFT that the predominant frequency of Parkfield, Chi-Chi and Kobe earthquakes are 2.34Hz, 2.23Hz and 2.60Hz respectively.

4 GROUND RESPONSE ANALYSES USING NON LINEAR ANALYSIS

Ground response analyses using non linear analysis

are carried out at all boreholes at the selected sites by applying three earthquake motions (Chi-Chi, Parkfield, Kobe). The required input parameters for this method are material type with thickness, unit weight, damping ratio, shear wave velocity and input motion data. The parameters to be defined in addition to the layer properties are:

- Reference strain
- Stress-strain curve parameter, Beta
- Stress-strain curve parameter, s
- Pressure dependent (reference strain) parameter, b
- Reference stress

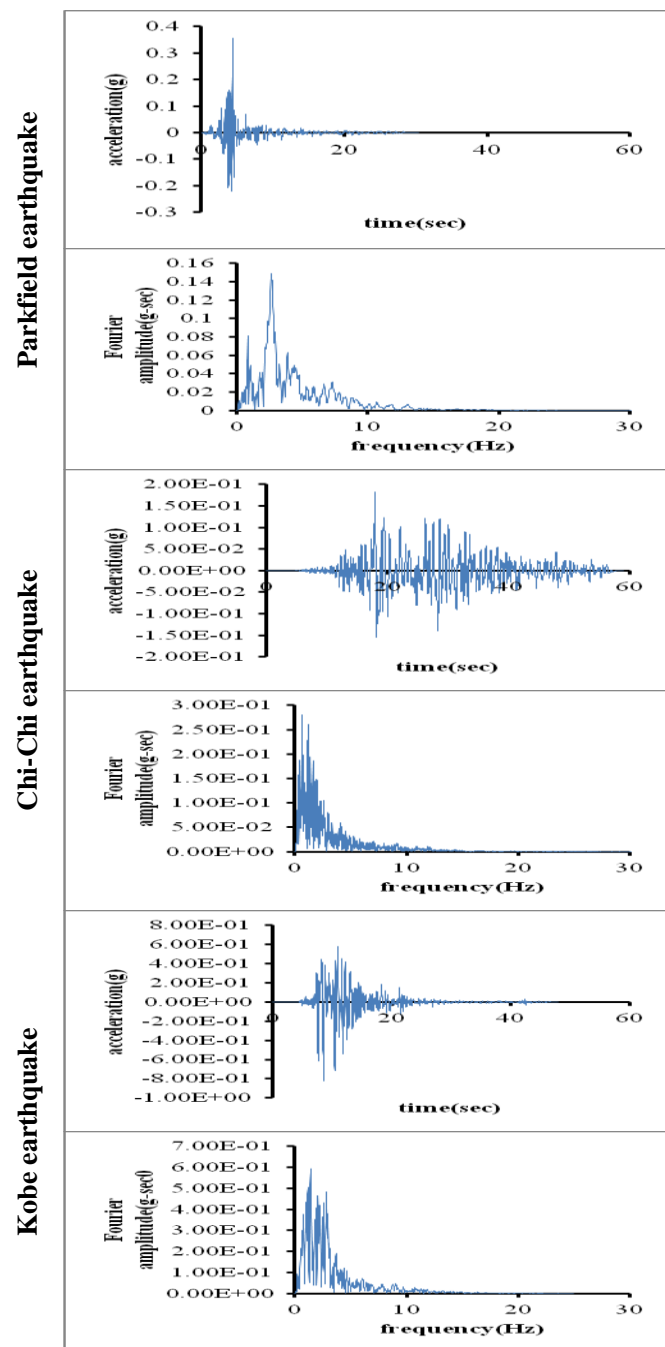


Fig. 1. Acceleration time histories and amplitude of all three earthquake ground motion.

A set of material curves are defined in DEEPSOIL for modulus reduction curves and damping ratio curves for different soils which are also been used. For present study, modulus reduction curve and damping ratio curves proposed by Vucetic and Dobry(1991) and Seed and Idriss(1991) are used to define the dynamic behaviour of clay and sandy soil respectively. The Seed and Idriss(1991) and Vucetic and Dobry(1991) curves, which are the reference curves, are shown in pink and the soil curves as blue(as shown in Fig. 2). To match the reference curves, the material constants need to be changed. The soil model incorporated in DEEPSOIL is the extended modified hyperbolic model. The parameters that control the shape of the backbone curve are β (beta), s , and ξ . The curve can be made confining pressure dependent by selecting the reference stress and the “b”-parameter. Curve fitting parameter $b = 0$ is selected to make the curve pressure independent. The small strain damping properties can also be made pressure dependent by introducing the “d” parameter. Then $d = 0$ is selected to make the curve pressure independent. Various combinations are tried to get a good match with the reference curves and the value of reference stress, reference strain, and curve fitting parameters like b , s , and d obtained from the best match curve is taken for further analysis . For nonlinear analyses, DEEPSOIL automatically check the maximum frequency of each layer.

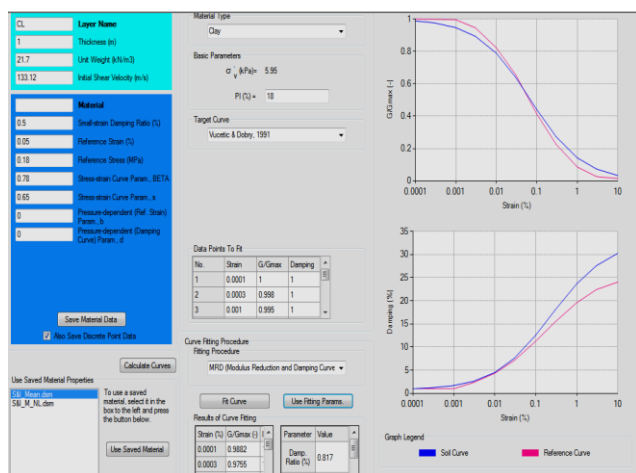


Fig. 2. Modulus reduction curve and damping ratio curves for non linear analysis(source: Deepsoil).

By considering three different locations and using Chi-Chi earthquake variation of peak ground acceleration with depth is shown in Fig.3 using non linear analysis. Figure shows non-linear variation of PGAs with depth. PGA and surface amplification exhibit the vivid effect of local site geology. Relating the PGA distribution with the soil profiles, nonlinear analysis maintain a tangent shear modulus, which changes at small time interval, governing the dynamic stress-strain characteristics.

At the three considered sites(i.e. Civil Hospital, Malow Ali, Na-Ali), PGA at bedrock level of 0.126g,

0.126g, and 0.127g was amplified to 0.185g, 0.159g, and 0.189g at surface level respectively. It can be seen that Na-Ali and Civil Hospital site which had more numbers of clay layer showed an amplification of 48% and 46% respectively but Malow Ali site on the other hand showed the least variation in the PGA values at ground level and at surface level. The percentage of amplification is found to be 26% for this site. This is because Malow Ali site consisted of predominately sand layer. Thus it can be concluded that clay layers shows higher variations compared to sand layers. Several researchers like Kumar and Dey(2015), Nath et al.(2008), Kumar and Krishna(2013),etc have also brought to light that PGA values are deamplified locally at the soft soil layer location and amplified for stiffer soils.

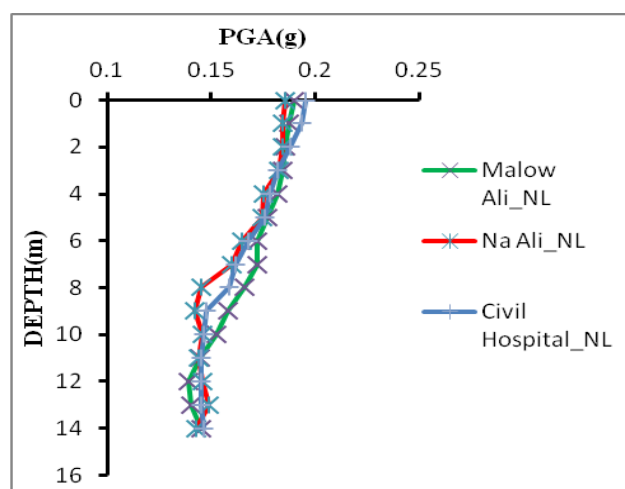


Fig. 3. Variation of PGA with depth at four different locations using Chi-Chi earthquake and non linear analysis.

For 5% damping, the response spectra in the form of peak spectral acceleration at ground level at all three sites using Chi-Chi earthquakes and non linear analysis is shown in Fig.4. The maximum spectral acceleration is found to be in the range of (0.5 – 0.6)g within time period (0-1)sec for all the three considered sites. Fig.5 shows the peak spectral acceleration at ground level for 5% damping using non-linear analysis and the three ground motions for Malow Ali site. It is seen that Chi Chi earthquake and Parkfield earthquake which have a frequency content of 2.23 Hz and 2.34 Hz respectively gives lesser values of PSA compared to Kobe earthquake which have a frequency content of 2.60 Hz. Thus the amplification is highest for Kobe earthquake because the frequency content of Kobe is highest among the three earthquake motions.

Thus, it reflects that the response spectrum at various layers of a stratified deposit can be useful for earthquake resistant design of geotechnical structures. The maximum spectral acceleration of 2.5g within time period of 0.3-0.6 sec is mentioned in IS 1893 (Part I): 2002.

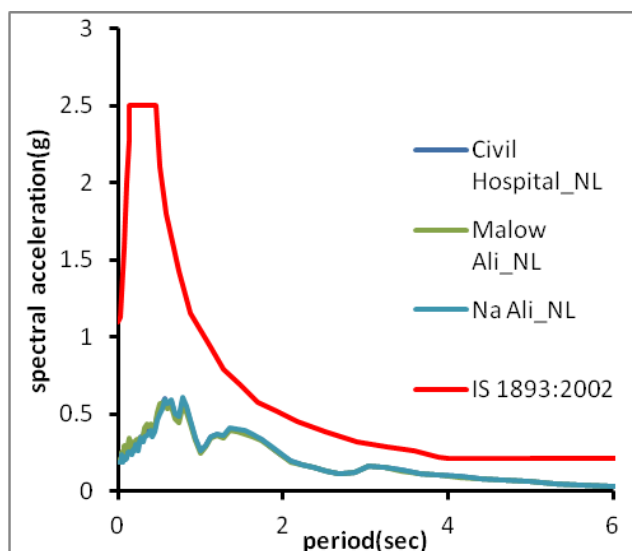


Fig. 4. Spectral acceleration (for 5% damping) at the ten considered sites using Chi-Chi earthquakes and non linear analysis method.

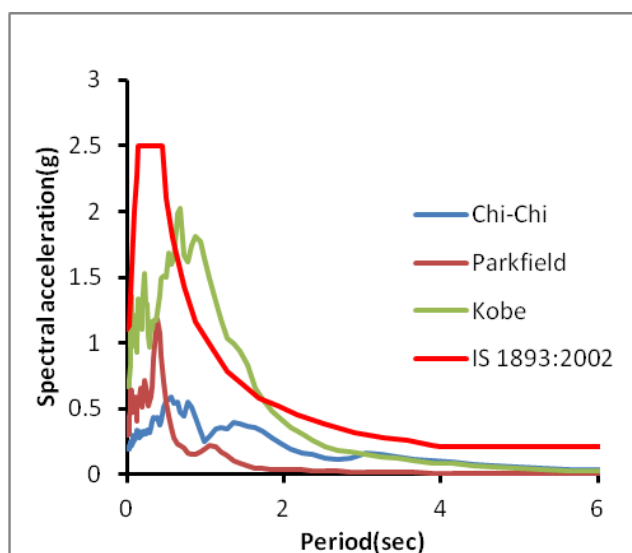


Fig. 5. Spectral acceleration (for 5% damping) at Malow Ali site using Chi-Chi, Parkfield and Kobe earthquake motions and non-linear analysis.

4 CONCLUSIONS

The following conclusions can be made from one dimensional non linear ground response analysis carried out for three different sites of Jorhat City subject to three different earthquake motions.

1. The ground response analysis is strongly influenced not only by the local site geology but also by the strong motion characteristics.
2. More amplification is observed for soil stratification with predominant clay layers.
3. The frequency content of the strong motion significantly affects the response of a multi-layered soil deposit in addition to the soil characteristics itself.

4. The time period for maximum spectral acceleration is similar to that mentioned in IS 1893 (Part I): 2002.
5. Higher amplification is observed due to higher ground acceleration experienced by the soil site and at some of the site higher amplification is observed may be due to higher shear wave velocity experience by soil column.
6. Ground motions at the surface are significantly modified in presence of local soil conditions because soil deposit act as filter to amplify or de-amplify the seismic waves because of stiffness of the soil.

REFERENCES

- 1) Govindraju, L., and Bhattacharya, S. (2011): Site-specific earthquake response study for hazard assessment in Kolkata city, India. *Journal of Natural Hazards*. Doi 10.1007/s11069-011-9940-3.
- 2) Hashash, Y.M.A., Groholski, D.R., Phillips, C.A., Park, D. and Musgrove, M. (2011): DEEPSOIL version 4.0, Tutorial and user Manual, 98.
- 3) IS.1893 (Part I):2002: Indian Standard criteria for earthquake resistant design of structures. Fifth revision, Bureau of Indian Standards, New Delhi.
- 4) Kramer, S. L. (1996): *Geotechnical earthquake engineering*, Prentice Hall.
- 5) Kumar and Krishna(2013): Seismic ground response analysis of some typical sites of Guwahati city, *International Journal of Geotechnical Earthquake engineering*, 4(1), 83-101, January-June 2013.
- 6) Kumar and Dey(2015): 1D Ground Response Analysis to Identify Liquefiable Substrata: Case Study from Guwahati City, *UKIERI Workshop on Seismic Requalification of Pile Supported Structures (SRPSS)* 7-9 January 2015, Guwahati.
- 7) Maheswari, R. U., Boominathan, A. and Dodagoudar, G. R. (2010): "Use of Surface Waves in Statistical Correlations of Shear Wave Velocity and Penetration Resistance of Chennai", *Journal of Earth Syst. Science*, 117, S2, 853-863.
- 8) Nath, S. k., Raj, A., Sharma, J., Thingbaijam, K. k. s., Kumar, A., and Nandy, D. R. et al.(2008b): Site amplification, Q_s and source parameterization in Guwahati region from seismic and geotechnical analysis. *Seismological Research Letters*, 79(4), 526-539. Doi:10.1785/gssrl.79.4.526.
- 9) Pallav, K., Raghukanth, S. T. G., and Singh, K. D.(2010): Surface level ground motion estimation for 1869 Cachar earthquake (Mw 7.5) at Imphal city, *Journal of Geophysics and Engineering*, 7, 321-331. doi:10.1088/1742-2132/7/3/010.
- 10) Rajiv, R.(2005): *Seismic response analysis of Dehradun city, India*. Unpublished M.Sc Thesis, International Institute for Geo-Information Science and Earth Observations- Enschede, Netherlands.
- 11) Seed and Idriss(1991): Moduli and Damping factors for dynamic analysis of cohesionless soils, *Journal of Geotechnical engineering*, Vol.112:Issue.11,doi: 10.1061/(ASCE)0733-9410(1991)112:11(1016).
- 12) Vucetic and Dobry(1991): Effect of soil plasticity on cyclic response, *Journal of Geotechnical engineering*, Vol.117:Issue.1,doi:10.1061/(ASCE)0733-9410(1991) 117:1(89).

Back to table of contents

Slope stability analysis with special reference to Panikhaiti hill area: A case study

Parikhit Baruahⁱ, Dr. U C Kalitaⁱⁱ

i) Assistant Professor, Department of Civil Engineering, Assam down town University, Guwahati, Assam, India.

ii) Academic Director & Head, Department of Civil Engineering, Assam down town University, Assam, India.

ABSTRACT

In this study, stability analysis of slopes of hills of Panikhaiti area of Guwahati, Kamrup Metro District of Assam is done to find out the factors of safety of these slopes. Slope failure, commonly known as landslide may occur due to various reasons like gravitational force, pore water pressure, change in overburden pressure etc. Earthquake or seismic force is also a major cause for slope failure. A slope otherwise stable may fail during an earthquake causing serious damage to life and property. In this study, for slope stability analysis Pseudo-Static method has been used. Both horizontal and vertical seismic co-efficient are considered for finding out factor of safety. Different load combinations are used to find out the minimum factor of safety. Computer programming using MATLAB software is done to find out the factors of safety for different load combinations and parameter combinations. Boreholes are done at ten different slopes to find out SPT values and collecting both disturbed and undisturbed samples to find out the soil properties. Based on the results of various field experiments and laboratory experiments done on the sample collected from the boreholes, analysis is done to find out the factor of safety. Various conclusions of this study are done based on these factors of safety and remedial measures are suggested. This method of findings out can be used in other places also and remedial measures can be suggested based on those factors of safety.

Keywords: Slope Stability, Pseudo-Static method, Seismic co-efficient, Factor of safety, SPT, MATLAB.

1. INTRODUCTION

Panikhaiti area is located in Chandrapur Tehsil in Kamrup Metro District of Assam State, India. It is located 14 KM towards East from District head quarters Guwahati. Area of this village is 304.74 hector and population is about 4000 (as per census 2011). Panikhaiti is rural area located near to Guwahati city, which will be a part of Guwahati metropolitan area by 2017 as declared by Guwahati Metropolitan Development Authority. It is basically a hilly area. State highway no – 3 passes through this area. River Brahmaputra is at north and Amachang Wildlife Sanctuary area surrounds it. Due to rapid growth of the Guwahati city and its adjacent areas like Panikhaiti has seen huge effect on environment due to manmade activities.

A study is carried out to find out factor of safety of the slopes of this region. Seismic factor or the seismic co-efficient must be considered for finding out factor of safety in this region as northeast India is in zone V from

earthquake hazard point of view i.e. highest risk zone. And also to find out maximum slope angle that can be provided in these slopes without any retaining structures or with minimum protective measures, so that, man triggered landslides can be prevented and losses of life and property due to landslide brought to minimum.

2. FIELD STUDY

Boreholes are done at ten different slopes to find out standard penetration test (SPT) values and collecting both disturbed and undisturbed samples to find out the soil properties. Classification of the soil profile is done up-to termination level of the boreholes and ground water table is also recorded. Slopes in which boreholes are done are named as slope a, slope b to slope j and respective boreholes are marked as borehole a, borehole b to borehole j. Physical measurements of the slopes such as height of the slope, slope angle and shape of the slope are also recorded during the field study.

Table: 1. Field data of the slopes

Sl. no.	Slope Identification	Height of the slope (m)	Slope angle (degree)
1	Slope A	9.23	29.93
2	Slope B	9.51	31.5
3	Slope C	9.37	22.66
4	Slope D	15.09	36.97
5	Slope E	6.77	11.36
6	Slope F	9.95	26.89
7	Slope G	13.22	30.56
8	Slope H	17.41	24.36
9	Slope I	13.18	29.93
10	Slope J	10.00	19.56

3. LABORATORY EXPERIMENTS

Different laboratory experiments are done on both disturbed and undisturbed soil samples to find out the various properties of the soil of each slope. The test are done to find out following properties – Moisture content, Specific gravity, Bulk density, Dry density, Submerged density, Saturated density, Void ratio, Porosity, Cohesion, Angle of Internal Friction, Liquid Limit, Plastic Limit and Plasticity Index. Grain size analysis is also done to find out percentage of Clay, Silt, Fine Sand, Medium Sand, Coarse Sand and Fine Gravel.

Table: 2. Results for cohesion & angle of internal friction

Slope	Cohesion (kN/sq.m)			Angle of Internal Friction		
	c max	c avg	c min	Φ max	Φ avg	Φ min
Slope A	17.7	15.7	13.7	28.0	25.6	23.0
Slope B	42.2	26.5	11.8	29.0	19.8	8.0
Slope C	40.2	34.3	25.5	18.0	13.3	10.0
Slope D	39.2	17.7	0.0	32.0	20.8	9.0
Slope E	36.3	28.4	7.8	26.0	16.5	11.0
Slope F	22.6	20.6	15.7	24.0	15.5	10.0
Slope G	19.6	19.6	19.6	27.0	27.0	27.0
Slope H	35.3	25.5	15.7	27.0	17.6	9.0
Slope I	37.3	23.5	0.0	32.0	18.8	9.0
Slope J	33.4	15.7	4.9	28.0	21.3	10.0

4. METHOD OF ANALYSIS

A slope otherwise stable may fail during an earthquake and the study area of this paper is located in the highly seismic zone (zone - V). So, it is absolutely necessary to consider a method which can accommodate seismic load for analysis of the factor of safety. Again, many methods are available in which seismic forces can be considered. For this study,

pseudo-static method (Seismic slope stability analysis by simple wedge failure theory for C- ϕ soil) is used for analysis. This is a simple method, where dynamic force of seismic activity is considered to be a static force. The shape of the sliding mass is considered to be wedge type and all the forces are considered to act through the centre of gravity of the sliding mass. Forces considered are Total stress (Weight of the sliding mass), Horizontal (both outward and inward) seismic acceleration and Vertical (both upward and downward) seismic acceleration. From these three considered loads when combinations were made, we get six load combinations. Load combinations used for analysis are denoted as I, II, III, IV, V and VI. For the different load combinations, factors of the safety are determined. So for each set of data, we will get six factor of safety value. The factors of safety are denoted as F1, F2, F3, F4, F5 and F6 From these six factors of safety value, the minimum value has to be considered as the final factor of safety for that slope. Load combinations used are – Load combination **I** = total stress & horizontal seismic acceleration (outward). Load combination **II** = total stress & horizontal seismic acceleration (inward). Load combination **III** = total stress, horizontal (outward) & vertical seismic acceleration (upward). Load combination **IV** = total stress, horizontal (outward) & vertical seismic acceleration (downward). Load combination **V** = total stress, horizontal (inward) & vertical seismic acceleration (upward). Load combination **VI** = total stress, horizontal (inward) & vertical seismic acceleration (downward).

5. PARAMETER SELECTION

In this analysis, i.e. Pseudo-static method (seismic slope stability analysis by simple wedge failure theory for c- ϕ soil) of analysis following parameters are required – cohesion, angle of internal friction, slope angle, length of sliding surface, weight of the sliding wedge and seismic co-efficient i.e. Horizontal earthquake acceleration and vertical earthquake acceleration. The parameters are selected on the basics of the following criteria.

5.1 Cohesion

From the test results of borehole data, we have different values of cohesion for different depths of the borehole. Among the values of cohesion available for different depths three values of cohesion are considered for analysis. The depth up-to which values are considered is equal to the height of the slope. If slope height is more than the depth of borehole than data available up-to maximum depth of the borehole is considered for analysis. The values of cohesion used for analysis are maximum value of cohesion (C_{max}), minimum value of cohesion (C_{min}) and average value of cohesion (C_{avg}).

5.2 Angle of internal friction

From the test results of borehole data; we have different values of angle of internal friction for different depths of the borehole. Among the values of angle of internal friction available for different depths three values of angle of internal friction are considered for analysis. The depth up-to which values are considered is equal to the height of the slope. If slope height is more than the depth of borehole than data available up-to maximum depth of the borehole is considered for analysis. The values of angle of internal friction used for analysis are maximum value of angle of internal friction (Φ_{\max}), minimum value of angle of internal friction (Φ_{\min}) and average value of angle of internal friction (Φ_{avg}).

5.3 Safe slope angle

Field slope angles are measured during the field experiments. In this study, two slope angles are considered as safe slope angle for analysis. As no actual slope failures occurred during the study. Slopes with slope angle 25 degree with horizontal surface are considered as safe slope once and again Slopes with slope angle 30 degree with horizontal surface are considered as safe slope.

5.4 Density of soil

From the test results of borehole data; we have different values of density of soil for different depths of the borehole. Again we have Bulk density, Dry density, submerged density and saturated density. Saturated density is considered as it's the maximum among the densities and slopes are more vulnerable when soil is wet. Among the values of saturated density of soil available for different depths three values of saturated density of soil are considered for analysis. The values of saturated density of soil used for analysis are maximum value of saturated density of soil (γ_{\max}), minimum value of saturated density of soil (γ_{\min}) and average value of saturated density of soil (γ_{avg}).

5.5 Length of the sliding surface & C/S area

Length of the failure surface is the wedge line which is considered or find out at site investigation. In this study, length of wedge line considering 25 degree with horizontal surface are considered as line of failure surface as no actual slope failures occurred during the study. As, these lines cannot be measured at site. Slopes with its actual dimensions are drawn using Auto-CAD software and these lines are measured. Same procedure is followed to find out the cross-sectional area of the slope. The cross-sectional areas are found out with the help of Auto-CAD drawings.

5.6 Seismic co-efficient

Selection of the pseudo-static coefficient is thus the most important aspect of pseudo-static analysis. Significant differences in approaches and resulting values clearly exist among the studies cited. Normally,

only the horizontal component of earthquake shaking is modeled because the effects of vertical forces tend to average out to near zero. But in this study, the effect of both horizontal component and vertical component of earthquake is considered. So, both horizontal co-efficient and vertical co-efficient are used for the analysis. The horizontal co-efficient is considered to be 0.15 [Seed (1979)] and vertical co-efficient is considered to be 0.075 for this study. This co-efficient are valid up-to magnitude 8.25 earthquakes and minimum factor of safety to be considered is 1.15.

5.7 Weight of the sliding wedge

Weight of the sliding wedge is calculated considering the cross-sectional area of the slope and density of soil. Though cross-sectional area of each slope is constant but three different densities considered. So, weight of the failure wedge will be different. Three weights of the failure wedge are calculated. The weights are maximum weight (W_{\max}), average weight (W_{avg}) and minimum weight (W_{\min}).

Based on the above parameters, four combinations of the parameters are considered and they are termed as Set1, Set2, Set3 and Set4. In Set1 parameters considered are maximum weight, maximum cohesion and minimum angle of internal friction. In Set2 parameters considered are average weight, average cohesion and average angle of internal friction. In Set3 parameters considered are minimum weight, minimum cohesion and maximum angle of internal friction. In Set4 parameters considered are maximum weight, minimum cohesion and minimum angle of internal friction.

MATLAB software is used to develop a programme to find out factor of safety for the given set of parameters. For each set of data it gives the six factor of safety for six different load combinations. For each slope, from four combinations of parameters we got twenty four numbers of factors of safety. Based on these factors of safety minimum one is considered.

Table: 3. Cross-sectional area and wedge failure line

Slope	C/S area for 25 degree safe slope (sq.m)	Wedge failure line for 25 degree safe slope, L (m)	C/S area for 30 degree safe slope (sq.m)	Wedge failure line for 30 degree safe slope, L (m)
A	24.496	21.840	7.156	5.750
B	24.699	22.500	6.047	19.020
C	40.914	22.170	22.808	18.740
D	147.315	35.690	98.976	30.140
E	2.711	4.990	1.912	3.680
F	8.546	23.540	0.000	22.000
G	39.398	31.280	3.356	26.440
H	222.999	41.200	160.489	34.820
I	106.406	31.220	71.276	26.400
J	41.226	23.660	22.361	16.390

Table: 4. Density of the soil for different slopes

Slope	Density (kN/cubic m)		
	γ max	γ avg	γ min
Slope A	20.1	19.6	19.1
Slope B	20.1	19.7	19.2
Slope C	20.3	20.1	19.8
Slope D	20.5	20.1	19.6
Slope E	20.2	20.1	19.8
Slope F	20.2	19.1	1.9
Slope G	21.4	21.4	21.4
Slope H	20.7	19.8	19.3
Slope I	20.5	19.6	19.1
Slope J	20.6	19.8	19.2

Table: 5. Weight of the failure wedge for safe slope angle

Slope	Weight of the failing wedge for 25 degree safe slope			Weight of the failing wedge for 30 degree safe slope		
	W max	W avg	W min	W max	W avg	W min
A	492.4	480.6	468.6	143.8	140.4	136.8
B	496.5	487.0	474.9	121.5	119.2	116.2
C	830.8	822.5	810.8	463.1	458.4	451.9
D	3020	2961	2890	2029	1989	1941
E	54.8	54.5	53.7	38.64	38.4	37.88
F	172.7	163.5	16.2	0.000	0.000	0.000
G	842.6	842.6	842.6	71.77	71.77	71.77
H	4615	4418	4309	3321	3180	3101
I	2181	2087	2035	1461	1398	1363
J	849.3	816.9	792.7	460.6	443.1	429.9

6. RESULTS

Based on various field experiments and laboratory experiments following results are obtained and they are analyzed. From the variables for each borehole and each set we get six factor of safety. For each safe slope angle we have 24 four factor of safety. Out of these 24 factors of safety, minimum one is considered. The slopes for which minimum factor of safety is found to be less than 1.15 for both 25 degree and 30 degree safe slope angle are termed as unsafe slope marked in red. In this study, four slopes are found to be unsafe slope (slope D, H, I and J). The slopes which are found to be safe for one safe angle and unsafe for other safe angle are termed as conditional slope and these slopes are marked in yellow. In this study, only one slope is found to be conditional slope (slope B). The slopes, for which minimum factor of safety is found to be more than 1.15, for both 25 degree and 30 degree safe slope angle and are termed as safe slope and are marked in green. In this study, five slopes are found to be safe slope (slope A, C, E, F and G).

Table: 6 Minimum factor of safety for each slope

Slope	Minimum factor of safety for 30 degree safe slope	Minimum factor of safety for 25 degree safe slope	Remarks
Slope A	1.370	1.460	Safe slope
Slope B	2.842	0.825	Conditional slope
Slope C	2.166	1.339	Safe slope
Slope D	0.152	0.152	Unsafe slope
Slope E	2.638	2.547	Safe slope
Slope F	NA	3.815	Safe slope
Slope G	11.396	1.729	Safe slope
Slope H	0.534	0.492	Unsafe slope
Slope I	0.195	0.195	Unsafe slope
Slope J	0.687	0.611	Unsafe slope

7. CONCLUSIONS

Following conclusions can be drawn from the result obtained-

- From this study it is found that, slopes having height more than 15 meters are unstable in this area.
- From the analysis it is found that, load combination IV [i.e. considering total stress, horizontal (outward) and vertical seismic acceleration (downward)] produces the worst factor of safety. Eight out of ten slopes shows this trend.
- From the analysis it is found that, Set 4 of parameter combination [i.e. considering maximum weight, minimum cohesion and minimum angle of internal friction] produces the least factor of safety. Eight out of ten slopes shows this trend.
- No conclusion can be drawn between slope angle and factor of safety. As no definite pattern is seen between these two parameters.
- The soil profile of the study area is found to be similar. The soil profile is clayey silt followed by compacted silty sand (weathered sandy rock).
- From the Standard Penetration Test (SPT) results it can be concluded that a soft layer is present between 4.5 meter and 6 meter from ground level. As N-value for each borehole drop at or after 4.5 meter and it shows an increasing trend after 6 meter.
- Factor of safety has to be selected wisely among the available factors of safety depending upon the importance of the

structure. As factors of safety tabled above are for the worst possible case or in the other words can be called as conservative. Otherwise design may not be economic.

REFERENCES

- Akhlaghi, T. and Neishapouri, M., (2008), "An Investigation into the Pseudo-static Analyses of the Kitayama Dam Using Fe Simulation and Observed Earthquake-Induced Deformations", Proceedings of the 14th World Conference on Earthquake Engineering, October 12-17, 2008, Beijing, China.
- Bromhead, E. N., (1997), "The Treatment of Landslides". *Journal of Proc. Instn Civ. Engrs Geotechnical Engineering*, 125, April, pp. 85-96.
- Chatterjee, D. and Krishna, A. Murali, (2014), "Seismic Stability Analyses of Two-Layered Soil Slopes", Proceedings of the North East Students Geo-Congress on Advances in Geotechnical Engineering (NES –Geocongress 2014), IIT-Guwahati.
- Chatterjee, Kaustav and Choudhury, Deepankar, (2012), "Seismic Stability Analyses of Soil Slopes using Analytical and Numerical Approaches", *ISET Golden Jubilee Symposium*, Indian Society of Earthquake Technology, IIT Roorkee, Roorkee.
- Cruden, D.M. and Varnes, D.J., (1996), "Landslide Types and Processes - Special Report", Transportation Research Board, National Academy of Sciences, 247: pp.36-75
- Guo, Mingwei et. al., (2011), "Slope Stability Analysis under Seismic Load by Vector Sum Analysis Method", *Journal of Rock Mechanics and Geotechnical Engineering*, 3 (3): pp. 282–288.
- Jibson, R.W., (2011), "Methods for Assessing the Stability of Slopes During Earthquakes—A Retrospective" *Engineering Geology*, v. 122, pp. 43-50.
- Kalita, U. C. et. al., (1989), "Geotechnical Investigation for the Failure Slopes – A Case Study", *Journal of Institute of Engineers (India)-Civil Engineering Division*. Vol-70, November, pp. 113-116.
- Kalita, U. C., (1999), "Geotechnical Investigation for a Landslide and Suggestions for Remedial Measures - A Case Study", Proceedings of the International conference S.M.G.E, Istanbul, ISBN-9058090531, pp. 443-446.
- Kandolkar, S. S. et. al., (2010), "Rational Pseudo-static Stability Analysis of Embankments", Proceedings of the Indian Geotechnical Conference – 2010, GEO trendz, December 16–18, IGS Mumbai Chapter & IIT Bombay, pp. 135-138.
- Krishnamoorthy, Agrahara, (2007), "Factor of Safety of a Slope Subjected to Seismic Load", *Electronic Journal of Geotechnical Engineering*, Volume 12E.
- Lallianthanga, R.K. and Laltanpuia, Z.D., (2013), "Landslide Hazard Zonation of Lunglei Town, Mizoram, India Using High Resolution Satellite Data", *International Journal of Advanced Remote Sensing and GIS*, Volume 2, Issue 1, pp. 148-159, Article ID Tech-111 ISSN 2320 – 0243.
- Matasovic, Neven, (1991), "Selection of Method of Seismic Slope Stability Analysis", Proceedings of the Second International Conference on Recent Advances in Geotechnical Earthquake Engineering and Soil Dynamics, St. Louis, Missouri. Paper no – 7.20.
- McCrink, Tim, (2006), "Seismic Slope Stability" Proceedings of the 100th Anniversary Earthquake Conference Commemorating the 1906 San Francisco Earthquake, Seismic Hazards Mapping Program, California Geological Survey.
- Melo, Cristiano and Sharma, Sunil, (2004), "Seismic Coefficients for Pseudostatic Slope Analysis", Proceedings of the 13th World Conference on Earthquake Engineering, Vancouver, B.C., Canada. Paper no – 369.
- Mukherjee, Siddhartha, (2013), "Seismic Slope Stability Analysis of Earth Dam: Some Modern Practices", *International Journal of Recent advances in Mechanical Engineering (IJMECH)* Vol.2, No.1, February, pp. 41-50.
- Oliphant, John et. al., (2000), "Soil Slope Stabilisation Methods", Conference proceeding GeoEng2000, Melbourne, Australia.
- Papadimitriou, Achilleas G. et al., (2012), "Methodology for Estimating Seismic Coefficients for Performance-Based Design of Earth Dams and Tall Embankments", *Soil Dynamics and Earthquake Engineering*.
- Presti, Diego Lo et al., (2010), "Pseudo-Static vs. Pseudo-Dynamic Slope Stability Analysis in Seismic Areas of the Northern Apennines (Italy)", *Rivista Italiana Di Geotecnica*, 2, Aprile – Giugno, pp. 13-29.
- Report on Sub-soil Investigation, (February, 2014), by S G Foundation, Sixmile, Guwahati, Assam at Assam down town University campus.
- Report on Sub-soil Investigation, (May, 2014), by S G Foundation, Sixmile, Guwahati, Assam at Assam down town University campus.
- Report on Sub-soil Investigation, (August, 2015), by S G Foundation, Sixmile, Guwahati, Assam at Assam down town University campus.
- Roy, E. Hunt, Geotechnical Consultant, Bricktown, New Jersey & Richard J. Deschamps, Purdue University, "Civil Engineering Handbook - Stability of Slopes", Chapter – 21, Second Edition, © 2003 by CRC Press LLC.
- Saikia, R. et. al., (2014), "Analysis and Behavior of Hill Slopes and Their Stabilization Measures", Proceedings of Indian Geotechnical conference, IGC-2014, Kakinada, India, pp. 2183-2190.
- Sarma, S.K. and Scorer, M.R., (2009), "The Effect of Vertical Accelerations on Seismic Slope Stability", Proceedings of the Conference Paper, September 2009.
- Sarmah, Pratap Chandra and Singh, Deepen, (2011), "Landslide Monitoring and Early Warning – Special Reference to NE Region of India", *Science and Culture*, Vol. 77, November-December, pp. 496-498.
- Shaw-Shong, Liew, (2005), "Soil Nailing for Slope Strengthening", Gue & Partners Sdn Bhd, Kuala Lumpur, Malaysia.
- Singh, C. D. and Singh, Joginder, (2013), "Landslides Caused Due to Ignorance - Case Studies from Northeast India", *Journal Geological Society of India*, Vol.82, July, pp. 91-94.
- Singh, Virendra Kumar, (2010), "Geotechnical Study at a Landslide Site in Northeast India", Proceedings of the 6th International Congress on Environmental Geo-technics, 2010, New Delhi, India, pp. 1249-1252.

[Back to table of contents](#)

Soil-Pile Interaction Under Dynamic Load: State-of-The-Art

Nabanita Sharmaⁱ⁾, Jayanta Pathakⁱⁱ⁾ and Diganta Goswamiⁱⁱⁱ⁾

i) Research Scholar, Department of Civil Engineering, Assam Engineering College, Gauhati University, Guwahati, Assam, India.

ii) Professor, Department of Civil Engineering, Assam Engineering College, Guwahati, Assam, India.

iii) Associate Professor, Department of Civil Engineering, Assam Engineering College, Guwahati, Assam, India.

ABSTRACT

Soil-Pile interaction is the phenomena involving the response of pile foundations caused by the flexibility of the supporting soils, as well as the response of soils caused by the presence of the pile foundations and the structures. This paper reviews the state-of-the-art of the soil-pile interaction for mid-rise buildings and the effect of dynamic load on them. Following a precise summary of the historical development in this field, the methods available for the analysis of soil-pile interaction, are elucidated. The sustainability of pile foundation under earthquake load is a concern for foundation engineers and such foundations are commonly used in the Guwahati city. A large number of mid-rise buildings are constructed in last decade, which are mostly founded on pile-foundations. It is therefore important to study the sustainability of such foundation system under earthquake load. A brief description on the interaction of soil and piled-raft foundation, which is gaining popularity in the recent years as a sustainable foundation system for buildings and other structures, is also highlighted.

Keywords: soil-pile, dynamic load, piled-raft

1 INTRODUCTION

Pile foundation is one of the most widely used deep foundations to support structures like high rise and mid-rise buildings. As per the Avenues and Mid-rise Buildings Study, Urban Marketing Collaborative, Toronto, Canada (2010), buildings with more than 12 storeys is called a high-rise building, with less than 4 storeys is a low-rise building, and having storeys between 4 and 11, are called mid-rise buildings. These buildings are subjected to static loads coming from the superstructure as well as dynamic loads mainly in the form of earthquake. During vibration, the pile interacts with surrounding soil and develops stiffness and damping of the soil-pile system (Bhowmik et al., 2013). Soil-Pile interaction refers to the complex phenomena in which the response of the soil influences the response of the pile foundation and the response of the pile influences the soil movement. As per Indian Standard Code of Practice, IS 1893-1984, the Guwahati city lies in the Seismic Zone V. The multi-storeyed buildings situated in a greater part of the city are highly vulnerable to earthquakes. Roesset (2013) stated that, the effects of the soil on the seismic response of more general structures were addressed by Sezawa and Kanai in 1935. Seismic soil structure interaction effects were addressed for the first time in the United States by Martel in 1940, where the behavior of the Hollywood Storage Building during the 1933 Long Beach earthquake was studied.

2 METHODS OF ANALYSIS

Over the last few decades, various methods have been developed for the analysis of soil-pile interaction under dynamic load. These methods are broadly grouped under three categories – Finite Element method, Experimental studies and Computer Programming.

2.1 Finite Element Method

The Finite Element Method (FEM) is a very efficient tool for numerical analysis of nonlinear dynamic response of soil-pile system (Bhowmik et al., 2013). This method is a numerical approach based on elastic continuum theory that can be used to model soil-pile interaction by considering the soil as a three-dimensional, quasi-elastic continuum (Pulikanti and Ramancharla, 2013). Kucukarslan et al. (2004) studied the inelastic analysis of pile-soil interaction, where the piles were modeled as linear finite elements and the inelastic modeling of the soil media was introduced by a rational approximation to a continuum with nonlinear interface springs along the piles and concluded that the inelastic analysis is not only capable of predicting the general trend of pile group behavior, but it is also capable of predicting the general trend of pile settlement, which is of primary importance in the design of pile foundations. Ladhane and Sawant (2010) studied the nonlinear 3D finite element analysis of pile group subjected to lateral load using Von-Mises,

Drucker-Prager and Mohr-Coulomb soil models to define plastic yielding in soil. It was found that in nonlinear analysis higher displacements occur as compared to the linear analysis at all the load levels. Luo et al. (2016) investigated the dynamic response of a seismic soil–pile–structure interaction (SSPSI) system by conducting nonlinear 3D finite element numerical simulations and found that the nonlinearity of the soil–pile interface has a great effect on the dynamic response of the system and is more suitable for simulating the real interactions between the soil and the piles. The presence of pile foundations can suppress the rocking of the structure and it will lead to decreased displacement response of soil and structure during the interaction between the soil and the piles. Finite Element method has become quite popular in analyzing soil-pile interaction and has been widely implemented in many computer programs.

2.2 Experimental Studies

Experiments prove to be a very important and efficient tool for the engineers to study the various facts. Ashour et al. (2004), assessed the behavior of a laterally loaded pile group in uniform and layered soil based on the strain wedge model approach and found that the overlap of shear zones among the piles in a group varies along the length of the pile and changes from one soil layer to another in the soil profile and, interaction among the piles grows with the increase in lateral loading. Seismic Soil-Pile Structure Interaction was studied by Malhotra (2004), where the physical processes that occur in aseismically loaded pile supported structure were categorized into far-field effects, near field effects, and inertial effects. Far-field effects consist of pore-pressure generation, ground deformation and subsequent cyclic degradation. Near field effects include strain rate effects (soil-pile slippage), cyclic degradation, and gap-slap mechanism. It is recommended that while examining SSPSI, the far-field and near-field effects should be considered along with the stress strain behavior of soils. Allotey and Naggar (2008) carried out two case studies of single piles, one in clay and one in sand, to study the effect of the type of soil on nonlinear cyclic response of piles using a recently developed beam on a nonlinear Winkler foundation (BNWF) model. It was observed that the effect of soil cave-in and recompression is to decrease pile maximum moment, move its point of occurrence closer to ground surface, and increase hysteretic energy dissipation. Maravas et al. (2008) developed a simplified discrete system in the form of a simple oscillator to analyze the dynamic behavior of structure on footings and piles on compliant ground, under harmonic excitation, and found that a structure founded on a pile generates higher radiation damping than a statically and geometrically equivalent structure resting on a spread footing. Therefore, a pile foundation acts as an elementary passive seismic protection system

offering higher amounts of damping due to wave radiation.

Chandrasekaran et al. (2010) performed static lateral load tests on 1x2, 2x2, 1x4, and 3x3 model pile groups embedded in soft clay and studied the effects of pile spacing, number of piles, embedment length, and configuration on pile-group interaction. It was found that the lateral load capacity of piles in 3x3 group at three diameter spacing is about 40% less than that of the single pile while, group interaction causes 20% increase in the maximum bending moment in piles of the groups with three diameter spacing in comparison to the single pile. Manna and Baidya (2010) carried out horizontal vibration tests on reinforced concrete single pile and group piles under varying levels of harmonic excitation acting above the center of gravity of the pile cap-loading system to study the nonlinear dynamic behavior of pile foundations. It was found that the boundary zone parameters, pile-soil separation, pile-soil-pile interaction and the embedded effect of the pile cap play a major role in the coupled dynamic response of pile foundation. The depth of fixity of piles in clay under dynamic lateral load was studied by Ayothiraman and Boominathan (2012), for which dynamic experiments were carried out on instrumented model aluminium single piles with different length to diameter ratios, embedded in clay of different constituencies to study its bending behavior under lateral loads. It was observed that the maximum bending moment due to dynamic load is magnified by about 1.5–4 times in comparison to the static load for short piles but about 9 times for long piles. Suleiman et al. (2012) measured soil-pile interaction for small diameter concrete piles embedded in loose well-graded sand subjected to lateral soil movement, by collecting experimental data to directly measure the soil-pile interaction for fully-instrumented passive pile. They found that the soil-pile interaction pressure increases on the back side of the pile for the length above the shear surface and increases on the front side of the pile. Chawhan and Quadri (2013), carried out laboratory study of a model testing of the piles embedded in sand collected from Tungabhadra River at Harihar taluk, Davangere district, Karnataka State and studied the lateral resistance of piles, variations of lateral stiffness, eccentricity and soil layer thickness ratio and the coefficient of subgrade modulus variation (N_b), the effect of the installation method, and the pile head restrained condition. It was observed that deflection, slope, shear force decreases and moments, soil reactions increase with the increase of depth of embedment of pile. Asha and Salinitha (2013) carried out an investigation to study influence of rock socket depth on seismic behavior of single end bearing pile foundations embedded in homogeneous stiff clayey soil and layered soil and found that lateral displacement under seismic load does not change beyond a rock

socket depth of 0.8D. It was also observed that when subjected to seismic load, pile groups in parallel arrangement deflected more than that in series arrangement irrespective of the group size. Chandrasekaran et al. (2013) studied the behavior of single pile on sandy soil due to both vertical and horizontal load applied directly, and found that piles supporting large load of a building undergoes minimum lateral displacement. Suleiman et al. (2014) experimentally studied the soil-structure interaction of piles which are used to stabilize failing slopes. Piles subjected to lateral soil movement are known as passive piles. It was observed that the pressure exerted on the pile by the moving soil increased as the soil movement increased, and that the soil pressure increased linearly along the pile within the moving soil. Fatahi, Hokmabadi and Samali (2014), studied the seismic performance-based design for tall buildings considering soil-pile-structure interaction by conducting a series of shaking table tests and found that presence of pile foundations change the dynamic characteristics and behavior of the superstructure which should be considered in predicting the damage level of structural and non-structural elements. Hokmabadi, Fatahi and Samali (2014) studied the effects of the seismic soil-pile-structure interaction (SSPSI) on the dynamic response of buildings with various heights by conducting a series of shaking table tests on 5-, 10-story, and 15-story model structures. It was concluded that effects of the SSPSI can change the dynamic characteristics of the soil-pile-structure system and also increase the lateral deflection. Srivastava et al. (2016) carried out physical modeling of a typical building frame resting on a pile group embedded in cohesive soil mass using complete three-dimensional finite element analysis and found that the displacement at top of frame decreases with increase in pile spacing. Also, increase in pile diameter and number of piles in a group increases the stiffness of the pile group due to which the displacement decreases.

2.3 Computer Programs

Computing has become an indispensable tool since the development of computer technology has provided powerful support for SSI analysis. The common computer programs include SHAKE, FLAC, FLUSH, DYFRA, ETABS, SASSI and so on. Use of computer to analyze soil-structure interaction has started in 1980s. Huang et al. (2004) dealt with the earthquake response of pile foundations by a three-dimensional effective stress finite element method program LIQCA. It was found that the numerical simulation can capture the fundamental aspects of the pile-soil seismic interaction, and can produce the useful results for seismic design or verification of pile foundations. Tafreshi (2010) analyzed the nonlinear soil-pile structure interaction under dynamic loads by using beam on Winkler foundation and free-field soil analysis

using DYFRA program and found that the method is a reliable method to investigate soil-pile behavior subjected to seismic loading. Maheshwari and Sarkar (2011) used the computer software MATLAB to develop finite-element code to model three-dimensional soil-pile-structure systems to study seismic behavior of soil-pile-structure interaction in liquefiable soils and found that the soil-pile-structure interaction increases the period of the structure and tend to decrease the peak response. Nisha and Divya (2013), made an attempt to evaluate the soil parameters like shear stress, angle of friction and stress behavior of clay-concrete, sand-concrete, sand-clay, concrete-geogrid, interfaces analyzed by finite element method software PLAXIS 2D. It was found that the interface stresses increased by about 11% due to the area change between the concrete, sand, clay and when different loading is given uniformly, the shear stress values are altered by about 2%. Bhowmik et al. (2013) carried out a numerical analysis of soil-pile system subjected to vertical dynamic loading, where a Finite Element model was developed using Abaqus 6.10. It was found that resonance frequency increases and resonance amplitude decreases with the increase in pile length. Khare and Chore (2013), examined the effect of soil-structure interaction on a G+3 frame resting on pile group embedded in the cohesive soil using a finite element based software program in ETABS and concluded that the effect of the soil-structure interaction in the columns placed in the leading row is less and is more in the columns placed on the right hand side. Chatterjee and Choudhury (2013) studied the effect of damping models on dynamic response of single pile using finite difference based numerical software FLAC3D. It was observed that with a change in damping models, the response of the pile foundation changes considerably. Wu et al. (2015) carried out a sensitivity analysis for the determination of vertically loaded pile-soil interface parameters in layered soil based on FLAC3D. It was concluded that the shear stiffness is related to the slope of the skin friction - pile-soil displacement curve, and the larger is stiffness, the greater is the slope. Also, the interfacial friction angle has a great influence on the skin friction. Adam et al. (2016) carried out numerical study to investigate the seismic response of mid-rise RC buildings subjected to different seismic excitations assuming full nonlinear SSI employing PLAXIS V8.2 software. It was concluded that it is essential to consider SSI effects in the seismic design of mid-rise buildings for the safety of the structure.

3 USE OF PILED RAFT FOUNDATION

Piled raft foundation is combination of pile and raft foundation that covers the entire area beneath a structure and support all wall and columns. In situations, where a raft foundation alone does not satisfy the design requirement, it may be possible to

enhance the performance of the raft by the addition of piles. The use of a limited number of piles, may improve both the ultimate load carrying capacity and the settlement performance of the raft. Rafts supported on piles are being increasingly used for multi-storeyed buildings with basements in poor soils with high water table conditions (Singh and Singh, 2013). Chaudhari and Kadam, (2013), studied the effect of piled raft design on high-rise building considering soil structure interaction using the finite element software ANSYS 11 and found that the moment carrying capacity of soil pile structure system depends on soil type, pile diameter, pile configuration and quantity of concrete. Garg et al. (2013) carried out a parametric study to observe the behavior of pile raft foundation system (PRFS) with relative stiffness of raft by modeling the PRFS in PLAXIS 3D and observed that with the increase in soil stiffness, the load transfer by pile decreases while load shared by raft increases and the overall and differential settlement reduces. Soil-foundation-structure interaction of buildings founded on Piled-Raft Foundation was evaluated through 3D-Nonlinear Finite Element Analyses using PLAXIS 3D FOUNDATION code by Ahmed et al. (2014). It was concluded that the foundation structure and soil field response is highly affected by different building structure shape and soil failure models. Also, the soil field response in layered soil is affected by presence of lesser stiff layer below the raft. Singh and Singh (2013) experimentally investigated the performance of piled raft foundation on sand and observed that the load carrying capacity increases when the load is transferred to the soil through piled-raft while the settlement per unit load is quite less. Das, Saha and Halder (2016) studied the effect of inherent variability of undrained shear strength of soil on seismic design of piled raft supported structure incorporating dynamic soil-structure-interaction. From the study, fundamental period of soil-piled-raft-structure system incorporating SSI was found to be best fitted with normal distribution function. Also, probability of failure for pile foundation embedded in very soft soil indicates a possibility of high risk of flexural as well as serviceability failure criteria for pile foundation supporting shorter/stiff period of structure under seismic loading. Badry and Satyam (2016) studied about the seismic soil structure interaction analysis for piled raft supported buildings in the recent 25th April, 2015 Nepal earthquake ($M=7.8$). The study concluded that the system response is more for the ground motion which carries, the more acceleration on the ground. Also, a higher degree of asymmetry of the superstructure increases the chances of its failure under earthquake scenario. In another work by Albusoda and Salem (2016), the effect of interaction on piled-raft system settlement subjected to earthquake excitation was studied using PLAXIS 3D. The piled raft

foundation components for this analysis are embedded pile and plate element. The settlement of a pile-raft system is influenced by the SSI, due to the effect of stresses on strain through the supporting soil.

4 CONCLUSIONS

This paper reviewed the current state-of-the-art on soil-pile interaction under earthquake load. It has been found that to have an accurate estimation of soil-pile interaction, both static and dynamic loadings need to be considered. To have a better judgment on the structural performance of mid-rise buildings, the analysis of the effects of dynamic soil-structure interaction on seismic behavior and lateral structural response of mid-rise moment resisting building frames is essential (Tabatabaiefar et al., 2013). Finite element techniques and computer programs based on Finite Element Method are found to be more effective and accurate methods for analysis of soil-pile interaction. Also, in comparison to pile foundation, piled-raft foundation is proved to be cost effective and is also found to be a problem solver for complex subsoil conditions (Patil et al., 2013).

The Guwahati city, being in seismic zone V is highly vulnerable to earthquakes. Construction of mid-rise buildings in the greater part of the city has become a matter of great concern. Therefore, seismic analysis of soil-pile behavior of pile foundations on which most of these buildings are founded is a great requisite for the sustainability of the buildings. Also, piled-raft foundation is found to be more sustainable than the conventional pile foundation system for the complicated soil conditions of the city.

REFERENCES

- 1) Adam, M. A., Kamal, O. A., El-Hoseny, Mohamed (2016), Variation Of Seismic Response Of Mid-Rise Rc Buildings Due To Soil Structure Interaction Effects, International Journal of Civil Engineering and Technology (IJCIET), Volume 7, Issue 1, Jan-Feb 2016, pp. 220-240.
- 2) Ahmed, M., Mohamed, M.H., Mallick, J. and Hasan, M.A. (2014), 3D-Analysis of Soil-Foundation-Structure Interaction in Layered Soil. Open Journal of Civil Engineering, 4, 373-385.
- 3) Albusoda, B.S, Salem, L.Kh.(2016), The Effect Of Interaction On Pile-Raft System Settlement Subjected To Earthquake Excitation, Applied Research Journal, Vol.2, Issue, 4, pp.205-214.
- 4) Allotey, N., El Naggar, M. H.(2008), A Numerical Study Into Lateral Cyclic Nonlinear Soil-Pile Response, Canadian Geotechnical Journal, Vol. 45: 1268-128.
- 5) Asha, J., Salinitha, K. (2013), Investigation On Seismic Response Of End Bearing Piles, Proceedings of Indian Geotechnical Conference, December 22-24, 2013, Roorkee.
- 6) Ashour, M., Pilling, P., Norris, G.(2004), Lateral Behavior of Pile Groups in Layered Soils, Journal of Geotechnical and Geoenvironmental Engineering, Vol. 130, No. 6, pp. 580-592.
- 7) Avenues and Mid-rise Buildings Study, Urban Marketing Collaborative, Toronto, Canada, 2010.

- 8) Ayothiraman R., Boominathan A. (2013), Depth of Fixity of Piles in Clay Under Dynamic Lateral Load, *Geotechnical and Geological Engineering An International Journal*, Springer, Vol. 31, No. 2, pp.447 – 461.
- 9) Badry, P., Satyam, N. (2016), Seismic soil structure interaction analysis for asymmetrical buildings supported on piled raft for the 2015 Nepal earthquake, *Journal of Asian Earth Sciences*.
- 10) Bhowmik, D., Baidya, D.K., Dasgupta, S.P. (2013), Numerical Analysis Of Soil-Pile System Subjected To Vertical Dynamic Loading, *Proceedings of Indian Geotechnical Conference*, December 22-24, 2013, Roorkee.
- 11) Chandrasekaran, S.S., Boominathan, A., Dodagoudar, G.R. (2010), Group Interaction Effects on Laterally Loaded Piles in Clay, *Journal Of Geotechnical And Geoenvironmental Engineering*, ASCE.
- 12) Chandrasekaran, S.S., Bhatt, M., Kumar, G.(2013), Behavior Of Piles Under The Effect Of Static Vertical And Lateral Loading In Sand, *Proceedings of Indian Geotechnical Conference*, December 22-24,2013, Roorkee.
- 13) Chatterjee, K., Choudhury, D. (2013), Effect Of Damping Models On Dynamic Response Of Single Pile, *Proceedings of Indian Geotechnical Conference*, December 22-24,2013, Roorkee.
- 14) Chaudhari, R.R., Kadam, K.N. (2013), Effect Of Piled Raft Design On High-Rise Building Considering Soil Structure Interaction, *International Journal Of Scientific & Technology Research Volume 2*, Issue 6.
- 15) Chawhan, B.S., Quadri S.S. (2013), Experimental Investigations On Laterally Loaded Piles In Multi-Layered Cohesionless Soil, *Proceedings of Indian Geotechnical Conference*, December 22-24,2013, Roorkee.
- 16) Das, B., Saha, R., Haldar, S. (2016), Effect Of In-Situ Variability Of Soil On Seismic Design Of Piled Raft Supported Structure Incorporating Dynamic Soil-Structure-Interaction, *Soil Dynamics and Earthquake Engineering*, Vol. 84, pp. 251–268.
- 17) Fatahi, B., Hokmabadi, A.S., Samali B. (2014), Seismic Performance Based Design for Tall Buildings Considering Soil-Pile-Structure Interaction, *Advances in Soil Dynamics and Foundation Engineering*.
- 18) Garg, P., Jha, J.N., Singh, H. (2013), Role Of Relative Stiffness In Piled-Raft Foundation System, *Proceedings of Indian Geotechnical Conference*, December 22-24,2013, Roorkee.
- 19) Hokmabadi, A.S., Fatahi, B., Samali B. (2014), Physical Modeling of Seismic Soil-Pile-Structure Interaction for Buildings on Soft Soils, *International Journal of Geomechanics*.
- 20) Huang, Y., Zhang, F., Yashima, A., Sawada, K., Ye, G.-L., Kubota, N. (2004), Three-Dimensional Numerical Simulation of Pile-Soil Seismic Interaction in Saturated Deposits with Liquefiable Sand and Soft Clay, *Computational Mechanics*, WCCM VI, Sept. 5-10, 2004, Beijing, China.
- 21) IS 1893-1984: Indian Standard Criteria for Earthquake Resistant Design of Structures, Reaffirmed 1998.
- 22) Khare, R.J., Chore, H.S. (2013), Interaction Of Building Frame With Pile, *International Journal of Electrical, Electronics and Computer Systems*, Volume-1, Issue -1, pp. 2347-2820.
- 23) Ladhane, K.B., Sawant, V.A. (2010), Nonlinear 3D Finite Element Analysis of Pile Group Subjected to Lateral Load, *Indian Geotechnical Conference-2010, GEOTrendz*, December 16–18, 2010, IGS Mumbai Chapter & IIT Bombay.
- 24) Luo, C., Yang, X., Zhan, C., Jin, X., Ding, Z. (2016), Nonlinear 3D finite element analysis of soil–pile–structure interaction system subjected to horizontal earthquake excitation, *Soil Dynamics and Earthquake Engineering* 84, pp. 145–156.
- 25) Maheshwari, B.K., Sarkar, R. (2011), Seismic Behavior of Soil-Pile-Structure Interaction in Liquefiable Soils: Parametric Study, *International Journal of Geomechanics*, Vol. 11, No. 4.
- 26) Malhotra, S. (2004), Soil-Pile Structure Interaction During Earthquakes, *Geotechnical Engineering for Transportation Projects*, pp. 428-440.
- 27) Manna, B., Baidya, D.K. (2010), Nonlinear Dynamic Behavior of Pile Foundations in Horizontal Vibration, *Soil Dynamics and Earthquake Engineering*, pp. 50-55.
- 28) Maravas, A., Mylonakis, G., Karabalis, D.L. (2014), Simplified discrete systems for dynamic analysis of structures on footings and piles, *Soil Dynamics and Earthquake Engineering* 61-62, pp. 29–39.
- 29) Menglin, L., Huaifeng, W., Xi, C., Yongmei, Z. (2011), Structure–soil–structure interaction: Literature review, *Soil Dynamics and Earthquake Engineering*.
- 30) Nisha, Y., Divya, P.V. (2013), Study on Soil-Structure Interface Properties, *International Journal of Research in Civil Engineering, Architecture & Design Volume 1*, Issue 1, pp. 38-44.
- 31) Patil, J.D., Vasanvala, S.A., Solanki, C.H. (2013), A Study on Piled Raft Foundation: State of Art, *International Journal of Engineering Research & Technology (IJERT)*, Vol. 2 Issue 8, ISSN: 2278-0181.
- 32) Pulikanti, S., Ramancharla, P.K. (2013), SSI Analysis of Framed Structures Supported on Pile Foundations: A Review, *Frontier in Geotechnical Engineering*, Volume 2, Issue 2, pp. 28-38.
- 33) Roesset, J.M. (2013), Soil Structure Interaction The Early Stages, *Journal of Applied Science and Engineering*, Vol. 16, No. 1, pp. 1-8.
- 34) Singh, A.K., Singh, A.N. (2013), Study Of Piled Raft Foundation, *Proceeding of Indian Geotechnical Conference*, December 22-24, 2013, Roorkee.
- 35) Srivastava, V., Chore, H.S. and Dode, P.A. (2016), Interaction of Building Frame with Pile Foundation, *Open Journal of Civil Engineering*, 6, pp. 195-202.
- 36) Suleiman et. al. (2012), Measured Soil-Pile Interaction for Small Diameter Piles Embedded in Granular Soil Subjected to Lateral Soil Movement, *GeoCongress 2012*, pp. 135-144.
- 37) Suleiman et. al. (2014), Soil-Pile Interaction for a Small Diameter Pile Embedded in Granular Soil Subjected to Passive Loading, *Journal of Geotechnical and Geoenvironmental Engineering*, 140.
- 38) Tabatabaiefar, S.H.R., Fatahi, B., Samali, B. (2013), Lateral seismic response of building frames considering dynamic soil-structure interaction effects, *Structural Engineering and Mechanics*, Vol. 45, No.3, pp. 311-321.
- 39) Tafreshi, S.N.M. (2010), Numerical Simulation of Pile-Soil-Structure Interaction under Dynamic Loading, *Deep Foundations and Geotechnical In Situ Testing, Geotechnical Special Publication No. 205*, GeoShanghai 2010 International Conference, pp. 96-103.
- 40) Wu, J.-j., Li, Y., Cheng, Q.-g., Wen, H., Liang, X. (2015), A simplified method for the determination of vertically loaded pile-soil interface parameters in layered soil based on FLAC3D, *Frontiers Of Structural And Civil Engineering*.

[Back to table of contents](#)

Site Response Studies for Sustainable Urban Planning - A Case Study of the Western Guwahati Region

Sasanka Borahⁱ⁾, Diganta Goswamiⁱⁱ⁾, Jayanta Pathakⁱⁱⁱ⁾

i) Assistant Professor, Department of Civil Engineering, Assam Engineering College, Jalukbari, Assam, India – 781 013

ii) Associate Professor, Department of Civil Engineering, Assam Engineering College, Jalukbari, Assam, India – 781 013

iii) Professor, Department of Civil Engineering, Assam Engineering College, Jalukbari, Assam, India – 781 013

* sasankaborah.ce@aec.ac.in

ABSTRACT

The entire North East Indian region is classified as under seismic zone – V by Indian Earthquake code IS-1893 (2002), the highest zone of seismic activity. The Guwahati city is located almost at the center of this region and has been the gateway and transit point for communication and transportation for all the states of the northeast. The strategic location of the city has made it a busy urban centre with high exposure with increasing vulnerability due to unplanned growth over the years. To deal with the rapid growth and related urban development issues, a Master Plan for Greater Guwahati was initially prepared in 1965, modified in 1987, and further revised to form the Comprehensive Master Plan (CMP) for Guwahati Metropolitan Area (GMA) with the perspective of the year 2025. The CMP-2025 includes an addition of 66 Sq. Km. to the existing 262 Sq. Km of area falling under GMA with a proposal to extend the city toward the western part of Guwahati city. This study presents the site amplification characteristics of the Western Guwahati region. An attempt has been made to examine the ground response as a preliminary hazard assessment for the additional GMA area of the western part of Guwahati city on the south bank of River Brahmaputra and beyond, extending up to Goalpara town, which is mostly characterized by the presence of alluvial deposits. The analysis conducted clearly indicates that the presence of soft alluvium in the region greatly influences the free-field ground motion in the low-frequency range. This study highlights the importance of the requirement of a detailed site specific site amplification study in the Western Guwahati Region for the sustainable urban development of the region, considering, the regional seismicity and the various constructional activities in the region.

Key Words: Earthquake, Site Response, Site Amplification, CMP-2025, GMA.

1 INTRODUCTION

In the evaluation of many past and recent earthquakes it has been observed that the local site conditions have a great influence on the damage distribution. The potentially severe consequences of this phenomenon were recently demonstrated in the damage patterns of the 1985 Michoacan, Mexico earthquake (Singh et al., 1988). Numerous other studies have also demonstrated the ability of surface geologic conditions to alter seismic motions (Borcherdt, 1970; Tucker and King, 1984; Aki, 1988; Field et al., 1992). Soft soil deposits significantly amplify an earthquake ground motion, which is often referred to as site effects. Site effects play a very important role in characterizing seismic ground motions because they may strongly amplify (or de-amplify) seismic motions before reaching the surface of the ground or the basement of man-made structures. The local site effects may be studied with the help of site response analysis, which helps in understanding the changes of earthquake propagation that a site might induce during an earthquake event.

2 AREA OF STUDY

The whole of northeast India falls in zone V of the seismic hazard zonation map (BIS, 2002) of India, the highest vulnerable zone in the country. This can be substantiated by the fact that devastating earthquake of Mw 8.1 in 1897 and Mw 8.6 in 1950 has occurred in this region which resulted in huge change of topography of the area.

The Guwahati city being located almost at the center of the region, acts as the gateway and transit point for communication and transportation for the seven sister states of northeastern region of India. The shifting of the capital of Assam from Shillong to Guwahati in the year 1972 increased its importance manifold. People from all over Assam and from the neighboring states have been migrating to Guwahati for job, business and education. This has resulted in rapid and unplanned growth of the city. From the early 1970's to the present time the Guwahati city has seen a drastic change in terms of building types. The city has witnessed vertical extension in the last decade with numerous multistoried residential apartment as well as office and commercial buildings built within and around the metropolitan area. To overcome the acute shortage of required space for

construction many natural water bodies have been filled up for constructions. This has made the such new constructions more vulnerable to earthquake hazard. In many cases, steep slope of the hillocks has been occupied making life and property vulnerable to co-seismic landslides and heavy rains. Keeping in view the unplanned growth of Guwahati city, a Comprehensive Master Plan-2025 (CMP-2025) has been drawn up to facilitate planned growth and decongestion of Guwahati city which encompasses an addition of 66 sq. km to the existing 262 sq. km. The proposed New Town III area (as defined in CMP-2025) is situated towards the south western part of Guwahati Metropolitan Area. It is worth mentioning that Lokapriya Gopinath Bordoloi International Airport (LGBI) is located nearby besides many residential schools, important public organizations etc. Moreover, the area under consideration has already witnessed many new housing and infrastructure projects. It has been observed that no previous study of the concerned area has been undertaken..

3 OBJECTIVE

Sustainable Urban Planning requires various aspects to be considered for effective implementation. This study attempts to showcase how site response should be inclusive for any sustainability issues, more so, if the area for which the planning is being done is seismically very active. This study considers Western Guwahati as the area of interest. an attempt has been made to give a preliminary insight to the requirements of conducting necessary site response analysis for sustainable planning with an objective of pro-active disaster mitigation of the proposed built environment.

4 DATA USED

In this study the earthquake data used were collected from PESMOS, IIT. The Bore hole data and lithological data were obtained from Central Ground Water Board (CGWB), Guwahati and Various Professional Agencies involved in subsoil investigation in the Guwahati Area. Additionally, the Bore log information has been collected from the Microzonation of Guwahati report (DST, 2008).

5 METHODOLOGY

Based on the availability of the data for analysis, three methods viz. Standard Spectral Ratio (SSR), Horizontal to Vertical Spectral Ratio (HVSR) and One Dimensional Equivalent Linear Site Response Analysis (1-DELSRA) were adopted to evaluate the site-

amplification potential in the study area. Three sites Boko, Palashbari and Guwahati –Central were considered for analysis.

5.1 Standard Spectral Ratio (SSR) Method

One of the most popular, widely accepted and used reference site method to evaluate site response is the Standard Spectral Ratio (SSR) method (Mittal et. al., 2012). The SSR is a technique where the site response is defined as the ratio of the Fourier amplitude spectrum of ground motions recorded at a soil-site to that of ground motions recorded at a rock-site record located nearby, from the same earthquake and component of motion (Borcherdt, 1970).

5.2 Horizontal to Vertical Ratio (HVSR) Method

HVSR technique (Lermo and Chavez-Garcia, 1993), a single station, non-reference site technique of analysis was applied to the recorded earthquake waves near the area of study to have an assessment of the amplification of the recorded waves.

5.3 One-Dimensional Equivalent Linear Site Response Analysis (1-DELSRA) Method

The 1-DELSRA method assumes horizontal boundaries extended to infinity and that the response of a soil deposit to earthquake excitation is predominantly caused by shear (SH) - waves propagating vertically from the bedrock below. The bedrock is also assumed to extend to infinity horizontally. In 1-DELSRA the nonlinear response of the soil is approximated by modification of the linear elastic soil properties of the soil based on the induced shear strain level due to cyclic loading.

6 RESULTS AND DISCUSSIONS

6.1 SSR Analysis

The amplification plot of the EW-component, NS-Component and VT-Component of recorded earthquake at the three sites are represented by the Fig's 1, 2, 3, 4, 5, 6, 7, 8, & 9. Significant amplification amplitude of around 10 has been observed in all the sites. Maximum amplification of around 34 can be seen in Goalpara site.

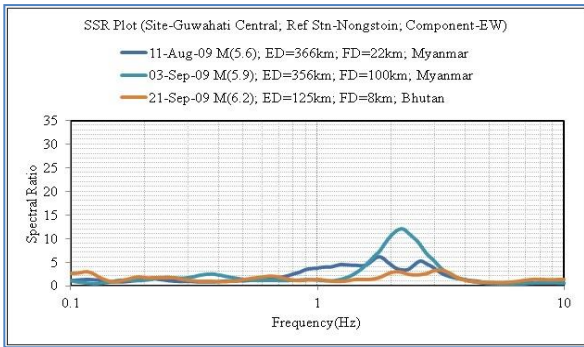


Fig-1: SSR Plot, Guwahati-Central, EW Component

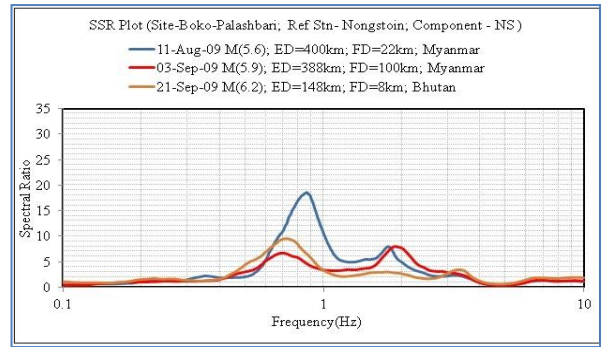


Fig-5: SSR Plot, Boko, NS Component

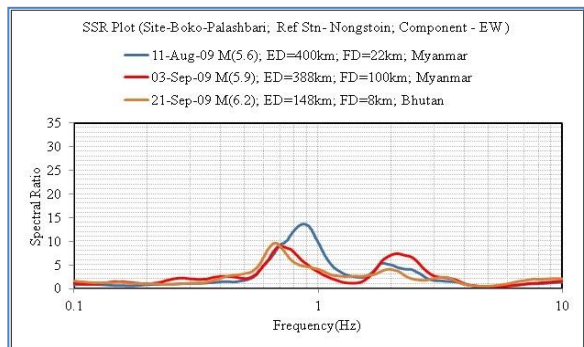


Fig-2: SSR Plot, Boko, EW Component

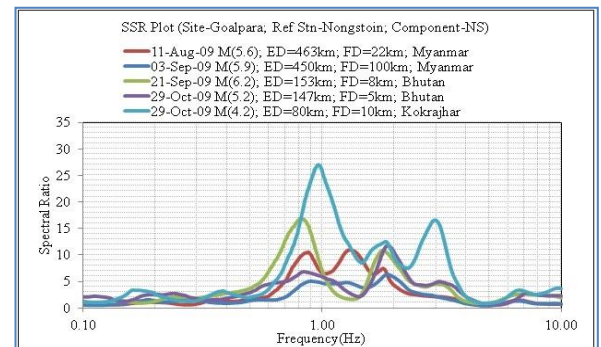


Fig-6: SSR Plot, Goalpara, NS Component

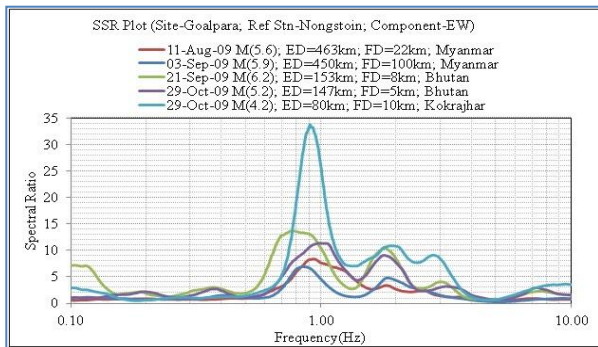


Fig-3: SSR Plot, Goalpara, EW Component

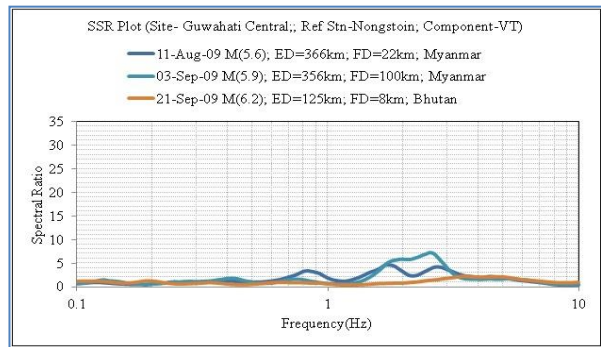


Fig-7: SSR Plot, Guwahati-Central, VT Component

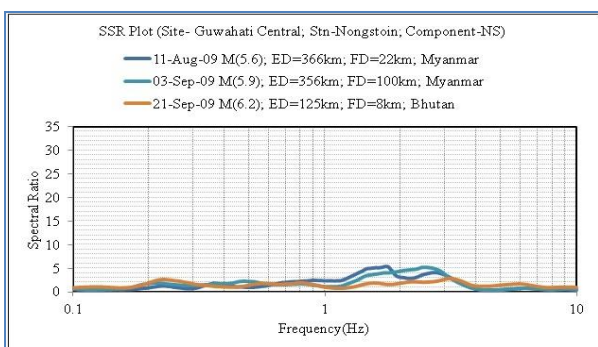


Fig-4: SSR Plot, Guwahati-Central, NS Component

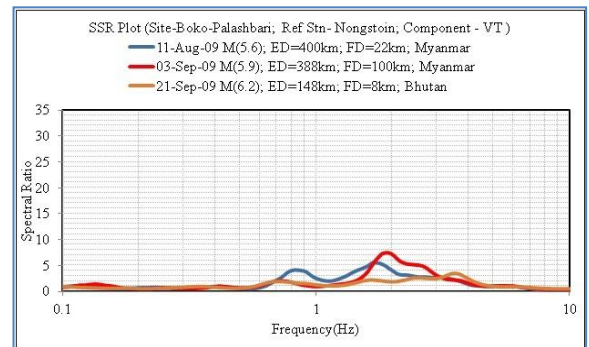


Fig-8: SSR Plot, Boko, VT Component

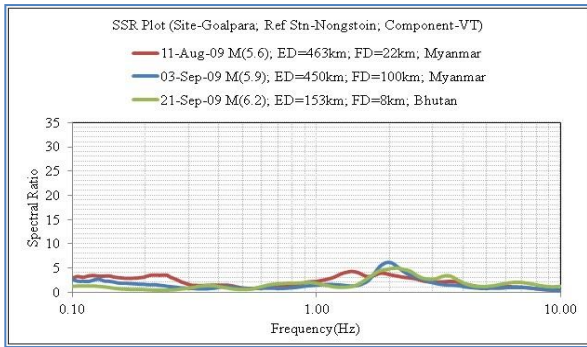


Fig-9: SSR Plot, Goalpara, VT Component

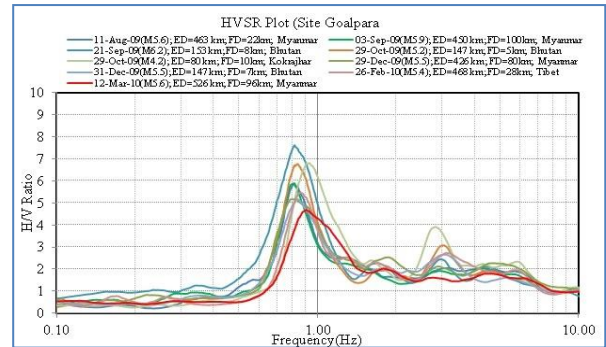


Fig. 12: HVSr Plot of Earthquake Recordings of Goalpara Station

6.2 HVSR Analysis

HVSR analysis (Lermo & Chavez-Garcia, 1993) of the earthquake waves have been conducted for the three cases. Figure 10, 11 & 12 represents the amplification obtained from the HVSR analyses. There is a general agreement among many authors (eg. Lermo and Chavez, 1993; Gitterman et. al., 1996; Seekins et. al. 1996; Fah, 1997) that predominant resonance frequency of a site can be estimated from the HVSR analysis. It was found that the predominant frequency for the site was in the range 0.5 – 2.0 Hz. Peak amplification up to around 8.0 was observed in the study area in the predominant frequency range identified.

6.3 One-Dimensional Equivalent Linear Method of Analysis

One dimensional equivalent linear site response analysis was performed by using the generalized soil of the three sites considered for the study. Amplification of seismic waves at the free field can be observed from the Figure 13, 14, & 15 which shows how the amplitude changes. It is evident from Figure 13, 14, & 15 that within the frequency range of 0.8 – 4.0 Hz, the seismic wave has amplified significantly.

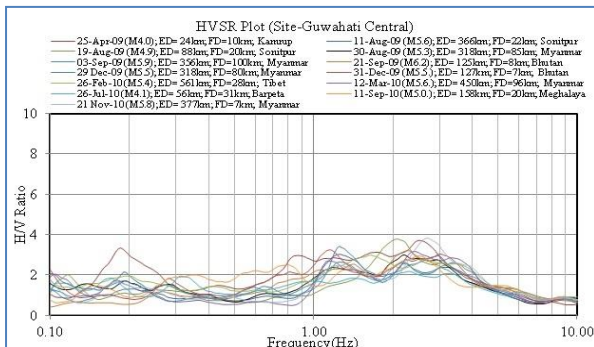


Fig. 10: HVSr Plot of Earthquake Recordings of Guwahati-Central Station

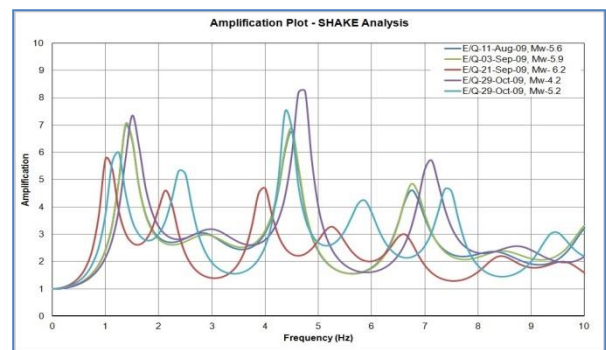


Fig. 13: Amplification Plot for Goalpara Site

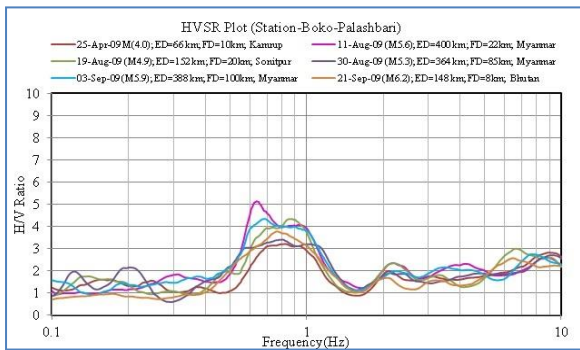


Fig. 11: HVSr Plot of Earthquake Recordings of Boko Station

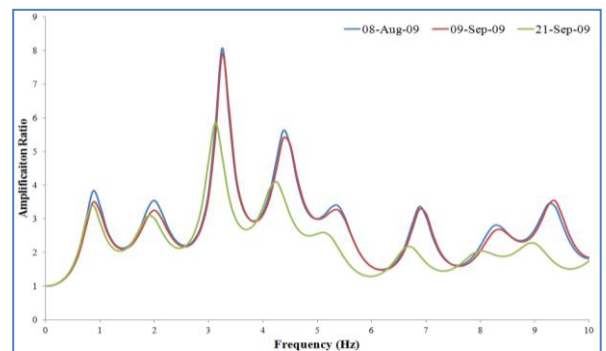


Fig. 14: Amplification Plot for Boko Site

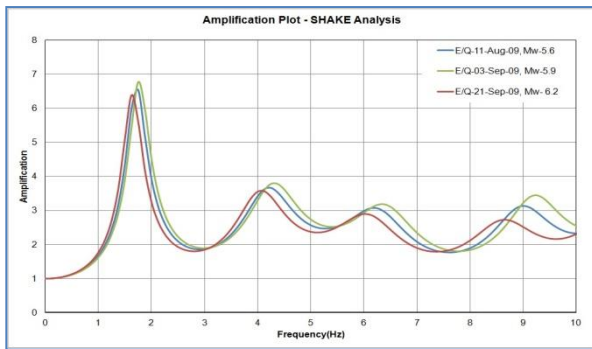


Fig. 15: Amplification Plot for Guwahati-Central Site

7 CONCLUSIONS

SSR, HVSR and 1-DELSRA analyses were carried out in this study on a test bed comprising the Western Guwahati area. The study clearly identify the possible site amplification scenario in the Western Guwahati region. Any urban planning exercise to be sustainable, it needs to be inclusive of co-seismic subsoil behaviour in addition to functional land-use planning. This study analyses, interprets and asserts how site response should be included in drawing out regional planning of land-use, especially for areas, which are seismically very active. From the study it may be concluded that, the expansion of the Guwahati metropolitan area to the western part in line of CMP-2025 requires understanding of the site amplification and other co-seismic hazard viz. liquefaction etc., for sustainable development of the built environment with appropriate risk management.

ACKNOWLEDGEMENT

The support extended by Central Ground Water Board (CGWB), Govt. of India, Guwahati, Assam is gratefully acknowledged for providing the required data, without which the study would not have been possible.

REFERENCES:

1. Aki, K. (1988), "Local site effects on strong ground motion", Earthquake Engineering and Soil Dynamics II – Recent Advances in Ground Motion Evaluation, June 27-30, Park City, Utah.
2. BIS (2002), "IS: 1893-2002: Criteria for Earthquake Resistant Design of Structure", Bureau of Indian Standards, New Delhi.
3. Borchardt, R.D. (1970), "Effects of local geology on ground motion near San Francisco Bay", Bull. Seism. Soc. Am., 60, 29-61.
4. CMP-2025, "Master Plan for Guwahati Metropolitan Area – 2025", www.gmda.co.in

5. DST (2008), "Microzonation of Guwahati City", www.amtron.in
6. Field, E.H., K.H. Jacob, and S.E. Hough (1992), "Earthquake Site Response Estimation: A weak motion case study", Bull. Seism. Soc. Am., 82, 2283-2307.
7. Fah, D. (1997), "Microzonation of the city of Basel", J. Seism., 1, 87-102.
8. Gitterman, Y., Zaslavsky, Y., Shapira, A. & Shtivelman, V. (1996), "Empirical site response evaluations: case studies in Israel", Soil Dyn. and Earthq. Eng., 15, 447-463.
9. Lermo, J. and E J. Chavez-Garcia (1993), "Site effect evaluation using spectral ratios with only one station", Bull. Seism. Soc. Am. 83, 1574-1594.
10. Mittal, H.; Kumar, A.; Ramhmachuani, R. (2012), "Indian National Strong Motion Instrumentation Network and Site Characterization of Its Stations", International Journal of Geosciences, 2012, 3, 1151-1167.
11. Seekins, L.C., Wennerberg, L., Marghereti, L. & Liu, H.-P. (1996), "Site amplification at five locations in San Francisco, California: a comparison of S waves, codas, and microtremors", Bull. seism. Soc. Am., 86, 627-635.
12. Singh, S.K., E. Mena, and R. Castro (1988), "Some aspects of source characteristics of the 19 September 1985 Michoacan earthquake and ground motion amplification in and near Mexico City from strong motion data", Bull. Seism. Soc. Am., 78, 451-477.
13. Tucker, B. E. and J. L. King (1984), "Dependence of sediment-filled valley response on input amplitude and valley properties", Bull. Seism. Soc. Am. 74, 153-165.

[Back to table of contents](#)

Recent Techniques of Seismic Liquefaction Mitigation

Bibha Das Saikia

Professor, Civil Engineering Department, RSET, Guwahati-781035

ABSTRACT

Liquefaction is one of the common phenomena of large earthquakes causing significant damages to Civil Engineering structures. Geotechnical engineers have developed different mitigation techniques, like removal and replacement of soils, pre-compression by surcharge loads, vertical sand drains, stone column, in-situ densification, vibroflotation, dynamic compaction, compaction piles, grouting, stabilization using reinforcement etc. The most recent methods are induced partial saturation (IPS), bio-cementation, bio-clogging or bio-mediated calcite precipitation of sands etc. The paper presents a brief description of the recent methods with advantages and disadvantages

Keywords: liquefaction, mitigation, partialsaturation, bio-mediated

1. INTRODUCTION

Our built environment with buildings, bridges, dams, power plants, roads, railways etc. are often affected due to ground failure caused by seismic soil liquefaction. During ground vibration pore water pressure of soil mass rises resulting in zero effective stress which causes soil to liquefy. Traditional methods like removal and replacement of soils, pre-compression by surcharge loads, vertical sand drains, stone column, in-situ densification, vibroflotation, dynamic compaction, compaction piles, grouting, stabilization using reinforcement etc. (Kramer, 2011). But these techniques are found to be expensive, cannot be implemented on sites of limited size due to disturbance of existing structures and have environmental impact. Recently some innovative practical and cost effective liquefaction mitigation techniques have been developed, such as induced partial saturation and microbial geotechnological methods which are discussed in this paper.

2. INDUCED PARTIAL SATURATION TECHNIQUE:

Good numbers of investigators (like Martin et al. in 1975, Yoshini et al. in 1989, Xia and Hue in

1991, Yang et al. in 2003, etc.), a team of researchers from North Eastern University, Boston e.g.

Yagian et al. (2007) and Eseller-Bayat et al. (2011) investigated the effect of induced partial saturation (IPS) by inducing small amount of gas or air into liquefiable soils in three directions. They are (i) laboratory study, (ii) field study and (iii) empirical model study.

2.1 Laboratory study

It is reported in stated literature that significant increase in shear strength of liquefiable soil can be achieved by reducing the degree of saturation of fully saturated sand. For this purpose, prepared partially saturated loose sand samples were tested by cyclic shear strain controlled tests (in a specially designed flexible liquefaction box). Method of electrolysis and alternatively by drainage-recharge of the pore water was used to have samples with different degree of saturation. Further shaking table tests were conducted on fully and partially saturated loose sand specimens. The test results were studied to obtain the effect of partial saturation on the generation of excess pore water pressure.

Another test series of cross-well radar technique was used in determining partial saturation in sands. Finally, the sustainability of air entrapped in the voids of the sand for long term was studied by a setup of a deep sand column. The results indicate that partial saturation can be obtained by gas generation using electrolysis or by drainage-recharge of the pore water without disturbing the void ratio of the sand specimen.

The cyclic test results indicated that the occurrence of initial liquefaction can be prevented by reducing the degree of saturation. The maximum excess pore pressure ratios varied from 0.43 to 0.72 in all the tested partially saturated samples. The changes in the degree of saturation due to generation of gases in the specimen can be detected by the cross-well radar technique. The degree of partial saturation in a column (151 cm long) was monitored for 442 days and was observed that degree of saturation increased by 1 degree from the original degree of saturation of 82.9% showing a tendency of diffusion of entrapped air out of the specimen. Therefore, the induced-partial saturation in sands can be used as a liquefaction mitigation measure.

2.2 Field study

Yegian and Alshawabkeh (2016) developed a practical and cost-effective liquefaction mitigation technique that can be applied to new sites and sites with existing structures resting on liquefiable soils. In this technique principle of Induced Partial Saturation (IPS) is used where water saturation of liquefiable sands is reduced. In the technique of induced Partial Saturation, a gas generating chemical solution is injected into the liquefiable sandy ground leading to controlled generation of oxygen gas bubbles within the pores of the sandy soils. This reduces the degree of saturation of soils. It has been remarked by research team at Northeastern University that IPS technique has broad impacts in reducing earthquake risk at any place of the world.

2.3 Empirical model:

In this model the idea of Partial saturation due to natural causes (formation of gases by decomposition of organic matter in sands) or induced is applied for

mitigation of liquefaction. Based on experimental test results on partially saturated sands using Cyclic simple shear strain tests, Eseller-Bayat et al. (2013) developed an empirical model known as RuPSS to predict the excess pore pressure ratio (r_u) in partially saturated sands under earthquake-induced shear strains. The tests were carried out in a special liquefaction box with excess pore pressure measurement. The experiments were conducted with cyclic shear strains (γ) 0.01 to 0.2%, relative densities (D_r) 20 to 67%, and degrees of saturation 40% to 90%. The test results showed that a maximum excess pore pressure ratio ($r_{u,max}$) of partially saturated sands can be obtained after application of large number of cycles of shear strain. It was observed that the excess pore pressure ratio (r_u) that partially saturated sand can achieve under a given earthquake-induced peak shear strain and the number of equivalent cycles of application can be significantly smaller than $r_{u,max}$. Therefore, the empirical model was developed in two stages. In the first stage, $r_{u,max}$ was related to degree of saturation (S , D_r) and shear strain (γ). In the second stage, a model was developed relating r_u to $r_{u,max}$, shear strain amplitude (γ), effective stress (σ'_v), and earthquake magnitude (M). The equations relating to predictive models for $r_{u,max}$ and r_u are established. Using these equations, graphical relationship of $r_{u,max}$ and r_u are provided for different ranges of soil and earthquake parameters.

In these studies, the liquefaction criterion was based on a sample reaching 5% double-amplitude (DA) axial strain under constant cyclic stresses. Therefore, a correlation was established between liquefaction resistance of partially saturated sands and an increasing number of cycles to reach 5% DA axial strain for the same cyclic stress applied.

3. BIOMEDIATED SOIL IMPROVEMENT

During the last decade bio-mediated soil improvement technique has been developed rapidly extending from laboratory study to successful field scale application (DeJongetal.2013, Chueta(2013) and DeJongetal.(2010,2013) reported that the new technique of soil improvement can be used to mitigate seismic liquefaction.

According to DeJong et al. (2010) a bio-mediated soil improvement system broadly refers to a chemical reaction network that is managed and controlled within soil through biological activity and whose byproducts alter the engineering properties of soil. An overview of these types of systems is presented schematically in Fig. 1.

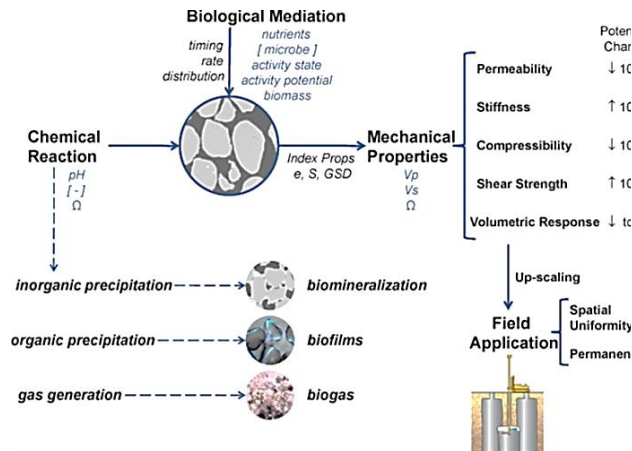


Fig.1. Overview of bio-mediated soil improvement systems. [-] = chemical concentration=resistivity, V_p =compression wave velocity, V_s = shear wave velocity.(After DeJong et al.2010)

Biological activity induces an ability to control and manage the timing, rate of reaction and spatial distribution of the chemical network reaction and hence the byproducts which improve soil properties. In the process of bio-meditations. the chemical processes of precipitation of inorganic materials, organic materials and gas generation can be termed as biomineralization, biofilm formation, and biogas generation, respectively.

Productions of magnetite, greigite, amorphous silica and calcite are known as Bio-mineralization processes. The use of microbes that control and manage the chemical processes exists in soil for millions of year .More than 10⁹ cells per gram of soil exists in the top layer of soil and the concentration cells generally decrease with depth. The lower limit of most soil improvement engineering applications, microbe concentrations of about 10⁶ cells per gram of soil can exist at 30m depth. Though microbes are very small individually, numerous microbes can be utilized for bio-mediation.

In bio-mediated soil improvement technique, the bio-mediated chemical reaction network is regulated to control the timing of the reaction with the help of additive (chemicals) into the subsurface. The microbial population in-situ is typically either stimulated (bio-stimulation) through the injection of nutrients or augmented (bio-augmentation) by the injection of additional microbes. In either case, the aim is to increase activity levels and/or concentration of the microbial activity. This enables transport and spatial distribution of the microbes and chemicals throughout the soil.

Microbial activity changes the environmental conditions gradually in the form of increasing the pH level till the environmental conditions required to initiate the chemical reaction are reached. As and when chemical reaction network is initiated ,the desired rate of production of byproduct (e.g. calcite precipitation) is controlled by the rate of microbial metabolic processes and/or the chemicals available . The soil properties improve when the byproducts are spatially located in the specific region of the soil matrix required to affect soil behavior. In the process bio-mineralization, the inorganic precipitates at particle contact surfaces do not contribute to changes in strength, stiffness, and permeability. Bio-films through organic precipitates in solution and on particle surfaces have a larger contribution to changes in permeability.

The improvement of engineering soil properties, such as permeability, stiffness, compressibility, shear strength, and volumetric behavior etc. depends on different bio-mediated treatment methods. The potential increase in shear strength of sands from bio-mediated calcite precipitation will be similar to the use of gypsum, cement, calcite in-situ precipitation system , and epoxy to improve soils strength.

3.1 Bio-mediated Calcite Precipitation

The uniform precipitation of calcite within soils can be made using biological activity where the pH value is elevated to create supersaturated conditions .In this chemical process ureolysis is used to increase the pH level .Alternative biological processes that can increase the pH level are denitrification, iron reduction, and sulfate reduction . (DeJong 2010)

3.2 Biogas generation(DeJong 2013)

Discrete gas bubbles by biological activity in the subsurface under saturated environment must be formed within a specific size range and uniformly

distributed within the pore fluid. This will significantly reduce the pore fluid compressibility.

A variety of gases e.g. carbon dioxide, hydrogen, methane and nitrogen, can be generated by microbial processes with both the organism and the oxidative/reductive environment of the pore fluid. For example, during the process of microbial respiration aerobic microbes use oxygen as the terminal electron acceptor. Typically, an organic molecule is used as the carbon and energy source. The resulting products from the reaction include water and carbon dioxide. In absence of oxygen, anaerobic respiration by methanogenic archaea occurs which results in the production of methane and often carbon dioxide. Denitrification occurs through the reduction of nitrate, producing nitrogen and carbon dioxide gas as the end product of the reaction in the environment. The reductions in the level of saturation of soil even small reduce liquefaction potential of soil.

The development of bio-mediated processes for soil improvement has several characteristics that may prove advantageous relative to industry standard soil improvement techniques. They are

- Cost reduced by use of natural materials
- Environmental impact reduction - use of natural materials that do not alter permanently subsurface conditions.
- Improvement in treatment uniformity – biological processes have potential to increase spatial uniformity.
- Optimal treatment concentration – degree of treatment can be controlled and monitored.
- Hydraulic and mechanical control –treatment process can be adjusted.
- Implementation flexibility – methods can be applied in new and old construction.

Huang & Wen (2015) suggested the use of colloidal silica grouting, bentonite suspension grouting, biocementation, air injection, bio-gas for mitigation of liquefaction.

4. CONCLUSION

1. Induced partial saturation in sand involves injection of a chemical solution that generates minute gas bubbles within the pores of initially fully saturated sand. This increases the compressibility of

the pore water and reduces or eliminates liquefaction potential. Further research is in progress for the development of a methodology for predicting liquefaction strength of partially saturated sands and for the field application.

2. Bio-mediated processes are bio mineralization, bio film formation and bio gas formation. Microbially induced calcite precipitation and bio gas formation techniques can be applied to liquefaction mitigation purpose. Further bio-geotechnical study is to be established for field applications confidently .

REFERENCES

- 1).Chu, J et al. (2013) Microbial Geotechnical engineering for disaster mitigation and coastal management, Proceeding of WCCE-ECCE-TCCE Joint Conference: Earthquake&Tsunami, www.academia.edu
- 2) DeJong, J.T. et al. (2010), Bio-mediated soil improvement of Ecological Engineering 36 pp197-210.
- 3)DeJong,T.J. et al.(2013),Biogeochemical processes and geotechnical applications:progress,opportunities and challenges ,Geotechnique 63,No.4,287-301
- 4)Eseller-Bayat et al.(2013)Liquefaction response of partially saturated sands.II: empirical model, Jof Geotech. Geoenviron. Eng.2013.1139:872-87
- 5) Eseller-Bayat et al: Prevention of liquefaction during earthquakes through Induced partial saturation in sands, www.researchgate.net
- 6) Huang,Y. & Wen Z. (2015),”Recent developments of soil improvement method for seismic liquefaction mitigation” ,J. Natural hazards, April, Vol.76,Issue 3,pp1927-1938.
- 7) Kramer,S.L(2011),Geotechnical EarthquakeEngg.Pearson
- 8) Yegian,M& Alshawabkeh,A(2016) Field Application of IPS for liquefaction Mitigation, www.nsf.gov

9) Yegian, M et al. (2007), Induced partial saturation for liquefaction mitigation : Experimental Investigation, Journal. of Geotech & Geienviron. Engg.

Back to table of contents

Comparison of Liquefaction Potential of Guwahati city by two Deterministic methods

Binu Sharmaⁱ⁾, Noorjahan Begumⁱⁱ⁾ and Kewal Aggarwalⁱⁱⁱ⁾

- i) Professor, Department of Civil Engineering, Assam Engineering College, Guwahati, Assam, India; binusharma78@gmail.com
 ii) Research Scholar, Civil Engineering Department, Assam Engineering College, Assam, India; noor2412@gmail.com
 iii) B.E. student, Civil Engineering Department, Assam Engineering College, Assam, India.

ABSTRACT

The liquefaction potential of saturated cohesionless deposits in Guwahati city, Assam, was evaluated using the deterministic approach. In the deterministic approach the liquefaction potential is evaluated by determining factor of safety against liquefaction with depth. The critical cyclic stress ratio required to cause liquefaction and the cyclic stress ratio induced by an earthquake were obtained using the modified simplified empirical procedure. This paper focuses on the determination of liquefaction potential by the modified simplified procedure that was accepted after the 1996 workshop sponsored by the National Centre for Earthquake Engineering Research (NCEER). Critical cyclic stress ratio was based on the empirical relationship between standard penetration resistance and cyclic stress ratio. The liquefaction potential was evaluated by determining factor of safety against liquefaction with depth for areas in the city. The liquefaction potential was then compared with the Idriss and Boulanger deterministic method. A soil database from 200 boreholes covering an area of 262 km² was used for the purpose. A design peak ground acceleration of 0.36 g was used since Guwahati falls in zone V according to the seismic zoning map of India. The results show that around 50 sites in Guwahati are vulnerable to liquefaction.

Keywords: liquefaction, potential, deterministic methods, comparison

1. INTRODUCTION

Guwahati is the largest city of the North Eastern part of India and serves as a gateway to all the seven North Eastern states. Seismically North Eastern region comes under the most earthquake prone zone i.e zone V as per Indian Standard code of practice. The seismic hazard level assessment of Guwahati city is of utmost importance. In an event of an earthquake, the prime concern in the field of geotechnical or soil engineering is the possibility of liquefaction of soil which may result in total structural collapse.

Over time, a methodology termed as “simplified procedure” has evolved as a standard of practice for determining liquefaction resistance of soils. According to the simplified procedure, the earthquake induced loading expressed in terms of cyclic shear stresses, is compared with the liquefaction resistance of the soil expressed in terms of cyclic shear stresses. The simplified procedure has been improved from time to time by many research workers. The development started with the pioneering work of Seed and Idriss in 1971, and gradually by Seed and Idriss (1982) and Seed et al. (1975, 1983, 1985), by Tokimatsu and Yoshimi (1983) and Yoshimi et al. (1984, 1989), by Liao and Whitman (1986), by Arango (1996). In January 1996, T. L. Youd and I. M. Idriss convened a workshop with 20 experts sponsored by the National Centre for Earthquake Engineering Research (NCEER) to update the simplified procedure and incorporate research findings from the previous decade. The findings of the workshop was reported by Youd and Idriss (1997) and by

Youd et al. (2001). This work focuses on the determination of liquefaction potential by incorporating the modifications to the simplified procedure that was recommended by the workshop for use in routine engineering practice and it is also based on the approach suggested by Idriss and Boulanger (2004).

2. EVALUATION OF LIQUEFACTION POTENTIAL

The susceptibility of a soil to liquefaction is evaluated by calculating the cyclic stress ratio (CSR) which is a measure of stress induced due to earthquake and cyclic resistance ratio (CRR) which indicate the resistance of a soil against the induced stress. The ratio of CRR to CSR is termed as the factor of safety against liquefaction. The higher the factor of safety, the more resistant the soil is to liquefaction. However, soil that has a factor of safety slightly greater than 1.0 may still liquefy during an earthquake. Generally, the minimum acceptable factor of safety is between 1.25 and 1.50 (Seed et al. 1985).

The cyclic stress ratio induced in the soil by the design earthquake may be estimated by using the following

$$(CSR)_{M=7.5, \sigma=1\sigma} = 0.65 \left(\frac{\sigma_{v2max}}{\sigma'_{v0g}} \right) \frac{r_d}{MSF K_\sigma} \quad (1)$$

where

a_{max} = peak horizontal ground surface acceleration, g = acceleration of gravity, σ_{v0} = total vertical stress, σ'_{v0} = effective vertical stress, r_d = stress reduction coefficient, MSF = magnitude scaling factor, K_σ = adjustment for confining pressure.

The stress reduction coefficient r_d as a parameter describes the ratio of cyclic stresses for a flexible soil column to the cyclic stresses for a rigid soil column. 1996 NCEER workshop recommended equation (2) for determining the mean value of r_d (T.F Blake 1996)

$$r_d = \frac{(1.000 - 0.4113z^{0.5} + 0.04052z + 0.001753z^{1.5})}{(1.000 - 0.4177z^{0.5} + 0.05729z - 0.006205z^{1.5} + 0.001210z^2)} \quad (2)$$

where z = the depth below the ground surface in m.

According to Idriss (1999), the parameter r_d could be adequately expressed as a function of depth and earthquake magnitude (M) as.

$$\left. \begin{aligned} \ln(r_d) &= \alpha(z) + \beta(z)M \\ \alpha(z) &= -1.012 - 1.126 \sin\left(\frac{z}{11.73} + 5.133\right) \\ \beta(z) &= 0.106 + 0.188 \sin\left(\frac{z}{11.28} + 5.142\right) \end{aligned} \right\} \quad (3)$$

In equation (3), z is depth in meters and M is moment magnitude. These equations are considered appropriate to a depth $z \leq 34$ m. Idriss and Boulanger (2004) adopted the recommendation of Idriss (1999) for determining the r_d values.

The liquefaction resistance (CRR) can be evaluated based on the penetration resistance denoted as $(N_1)_{60}$ which is the standard penetration test (SPT) blow count normalised to an overburden pressure of approximately 100kPa and a hammer energy ratio of 60% using SPT clean sand base curve (Seed et al.1985) which was developed for earthquake magnitude of 7.5. In the original development, Seed et al. (1985) noted an apparent increase of CRR with increased fines content. The workshop participants recommended to curve the trajectory of the clean sand base curve at low $(N_1)_{60}$ to a projected intercept of about 0.05. The clean sand base curve was approximated by using equation (4) (A.F Rauch 1998) valid for $(N_1)_{60} < 30$.

$$CRR_{7.5} = \frac{1}{34 - (N_1)_{60}} + \frac{(N_1)_{60}}{135} + \frac{50}{[10 \cdot (N_1)_{60} + 45]^2} - \frac{1}{200} \quad (4)$$

In order to obtain equivalent, clean-sand corrected N-values or $(N_1)_{60cs}$, the 1996 NCEER workshop recommended relation (5) -

$$(N_1)_{60cs} = \alpha + \beta(N_1)_{60} \quad (5)$$

Where α and β are coefficients determined using relationships 6(a) to (7c)

$$\alpha = 0 \text{ for } FC \leq 5\% \quad (6a)$$

$$\alpha = \exp\left[1.76 - \left(\frac{190}{FC^2}\right)\right] \text{ for } 5\% < FC < 35\% \quad (6b)$$

$$\alpha = 5.0 \text{ for } FC \geq 35\% \quad (6c)$$

$$\beta = 1.0 \text{ for } FC \leq 5\% \quad (7a)$$

$$\beta = \left[0.99 + \left(\frac{FC^{1.5}}{1000}\right)\right] \text{ for } 5\% < FC < 35\% \quad (7b)$$

$$\beta = 1.0 \text{ for } FC \geq 35\% \quad (7c)$$

Where $(N_1)_{60}$ is the SPT N-value corrected for field procedures and overburden stress. The normalized SPT N-values in the empirical relationships were corrected according to Youd and Idriss (1997).

Idriss and Boulanger (2004) presented a revised curve between CRR and modified SPT value based on the reexamination of the available field data. It was noted that the CRR value will increase with fines content. The equation of the revised curve can be conveniently expressed by equation (8) as follows

$$CRR = \exp\left\{\frac{(N_1)_{60cs}}{14.1} + \left(\frac{(N_1)_{60cs}}{126}\right)^2 - \left(\frac{(N_1)_{60cs}}{23.6}\right)^3 + \left(\frac{(N_1)_{60cs}}{25.4}\right)^4 - 2.8\right\} \quad (8)$$

Where $(N_1)_{60cs}$ is the clean sand corrected N-value. In order to obtain equivalent, clean-sand corrected N-values or $(N_1)_{60cs}$, Idriss and Boulanger (2004) recommended the following equation 9.

$$\left. \begin{aligned} (N_1)_{60cs} &= (N_1)_{60} + \Delta(N_1)_{60} \\ \Delta(N_1)_{60} &= \exp\left(1.63 + \frac{9.7}{FC+0.1} - \left(\frac{15.7}{FC+0.1}\right)^2\right) \end{aligned} \right\} \quad (9)$$

Where $(N_1)_{60}$ is the SPT N-value corrected for field procedures and overburden stress. $\Delta(N_1)_{60}$ is the variation of $(N_1)_{60}$ with FC (percent), FC is the fine content present in the soil in percentage.

The clean sand base curve can be adjusted for earthquake magnitudes smaller or greater than 7.5 by incorporating magnitude scaling factor (MSF) (Seed and Idriss 1982). The workshop participants suggested a range of MSF, the lower bound of which is the MSF suggested by Seed and Idriss (1982) (equation 10) and the upper bound is the MSF suggested by Andrus and Stokoe (1997) (equation 11)

$$MSF = 10^{2.24/M_W^{2.56}} \quad (10)$$

$$MSF = (M_W/7.5)^{-2.56} \quad (11)$$

The values for the MSF were subsequently re-evaluated by many research workers (Tokimatsu and Yoshimi 1983; Ambraseys 1988; Arango 1996; Idriss 1999; Seed et al. 2003). The MSF relation produced by this re-evaluation according to Idriss (1999) is given by equation (12)

$$MSF = 6.9 \exp\left(\frac{-M}{4}\right) - 0.058 \quad (12)$$

The MSF relation by Idriss (1999) is limited to a maximum value of 1.8 at small earthquake magnitudes ($M=5\frac{1}{4}$). Idriss and Boulanger (2004) reviewed various MSF relations that have been proposed for liquefaction analyses and subsequently adopted the relation by Idriss (1999). Again it is found that liquefaction resistance increases with confining stress but the rate of increase however is nonlinear. To account for the nonlinearity between CSR and effective overburden pressure, Seed et al. (1983) introduced the correction factor K_σ to extrapolate the simplified procedure to soil layers with overburden pressures >100 kPa. The value of K_σ recommended by 1996 NCEER workshop is given by the equation (13)

$$K_\sigma = \left(\frac{\sigma'_{vo}}{P_a}\right)^{(f-1)} \quad (13)$$

Where σ'_{vo} = effective vertical stress and P_a = atmospheric pressure (both are measured in the same

units), f = an exponent that is a function of sites conditions, including relative density, stress history, aging and over consolidation ratio.

The recommended K_σ values after Idriss and Boulanger (2004) is

$$K_\sigma = 1 - C_\sigma \ln\left(\frac{\sigma'_{vo}}{P_a}\right) \leq 0.3 \quad (14)$$

Where C_σ is the coefficient, P_a is normally taken as 100 kpa. Idriss and Boulanger subsequently expressed the coefficient C_σ in terms of $(N_1)_{60}$ as

$$C_\sigma = \frac{1}{18.9 - 2.55\sqrt{(N_1)_{60}}} \leq 0.3$$

With $(N_1)_{60}$ limited to a maximum value of 37.

3. SOIL STUDY OF GUWAHATI

Soils in Guwahati city mostly consists of the narrow tracts of alluvium and sediment filled low lands interspersed with Precambrian residual hills. Intensified anthropogenic activities particularly in and around the hills has led to high rate of aggradations in the low lying areas clogging the city drainage system. Alluvial soil is found in the valleys and low lying areas of the city. They are typically brown and grey coloured silty clays or clayey silts. At present most of the ancient alluvial soils are overlain by artificially transported soil and overburden material brought about by anthropogenic activities. They are visible only in excavations and borings. The hills surrounding Guwahati city are primarily composed of Porphyritic Granites and Quartzo Feldspathic Gneiss which are cross-cut by amphibolite intrusives and quartz veins. Sandy soils which are produced by weathering of porphyritic granites are found in many areas of the city. The sandy soils are rich in unsorted coarse fragments of quartz together with

associated clay and minor amounts of mica flakes. These soils are pale brown in colour and have a low degree of cohesion. Localities underlain by Quartzo-feldspathic Gneisses are covered by red coloured soils rich in clay minerals.

The input parameters required for the liquefaction potential analyses of the soil profiles at different soil sites in the city, such as groundwater depth, SPT N values, dry density, wet density and fines content (FC), are obtained from 200 SPT borehole data obtained from different sites in Guwahati city. The boreholes are spread over an area of 262 sq km. The borehole locations considered in the present study are shown in Fig. 1. The depths of boreholes are upto 30m. The SPT blow counts at some places are in the order of 2–10 indicating soft deposits of clay, whereas at many of the places it is greater than 50, showing refusal, showing dense sand.

Many building codes use average standard penetration resistance, N_{ave} , for classifying a site for purposes of incorporating local site conditions in estimation of design ground motion. The average standard penetration resistance as per provisions in International Building Code [IBC, 2003] is calculated by equation (15)

$$N_{avg} = \frac{\sum_{i=1}^n d_i}{\sum_{i=1}^n \left(\frac{d_i}{N_i}\right)} \quad (15)$$

- where d_i = thickness of each layer.
- N_i = SPT N value at i^{th} layer.
- n = total no. of layers.

The spatial distribution of average N value upto 15m depth is shown in Figure 1

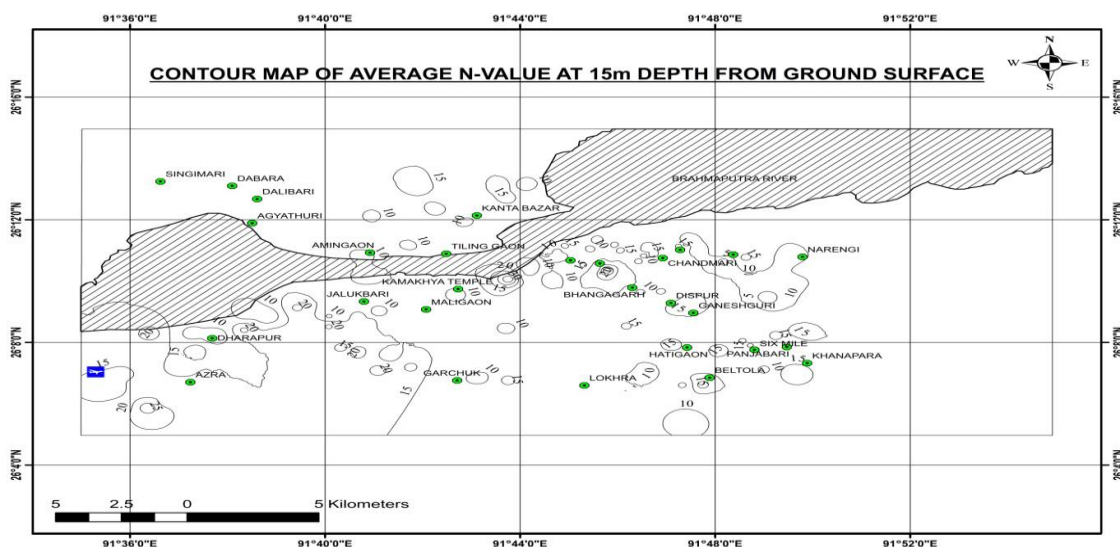


Fig.1 The spatial distribution of average N value upto 15m depth

In IBC (2000) the site classification based on N_{ave} is given. As per IBC (2000), E-type sites with low N_{ave} are susceptible to liquefaction. Out of 200 bore holes of Guwahati city 89 boreholes are classified as E type and rest of 111 boreholes belong to class D.

3.1 Results and Discussion

The first step in determining the liquefaction potential of a region is identifying the type of soils that will liquefy. According to Ishihara 1985, the hazard associated with soil liquefaction during earthquakes has been known to be encountered in deposits consisting of fine to medium sands and sands containing low plasticity. In this present study the soil layers that were identified for liquefaction analysis are fine to medium sand and silty sands that have classification of SP, SW, SC, SM, SP-SC. Inorganic silt of classification ML, ML-CL and non plastic inorganic silts were also analysed for liquefaction susceptibility. Evaluation of liquefaction potential requires peak ground acceleration (a_{max}) during earthquake. For its estimation ground motion relation are necessary where a_{max} is expressed as a function of magnitude and rupture distance. No such relation is available for N. E. India. In the absence of such a relation, the peak ground acceleration, a_{max} , for Guwahati city is taken as 0.36 g. This is according to IS 1893(2002) which puts Guwahati in Zone V, a severe seismic zone. This is for an 8.1 magnitude earthquake

occurring on a fault at an epicentral distance of 50 km from Guwahati city.

Using the procedures as laid down by the NCEER workshop (1997) and as reported in Youd and Idriss (1997), the factors of safety against liquefaction were calculated for soils identified to be susceptible to liquefaction. The factors of safety were also calculated for the same soils by the Idriss and Boulanger method (2004 also. Of the 200 sites, 48 sites in Guwahati have been found to be susceptible to liquefaction according to the Youd and Idriss (1997) method. The rest of the sites where the bore holes are located is not susceptible to liquefaction. Of the total 200 sites 49 sites are susceptible to liquefaction according to Idriss and Boulanger (2004) method.

Figure 2 shows the liquefaction potential map of Guwahati city for an earthquake magnitude of 7.5 according to Youd and Idriss (1997). In developing the map the lowest values of factor of safety, among the layers, is retained as the factor of safety for that bore hole. The maps show zones of different levels of risk of liquefaction. The map shows southern bank of river Brahmaputra with the areas of Palashbari, Azara, Jhalukbari, Pandu, Maligaon, Bharalumukh, Uzanbazar and some areas in G.S.Road, Gorchuk area and areas near Chandmari are most susceptible to liquefaction. The northern bank of the city is also susceptible to liquefaction.

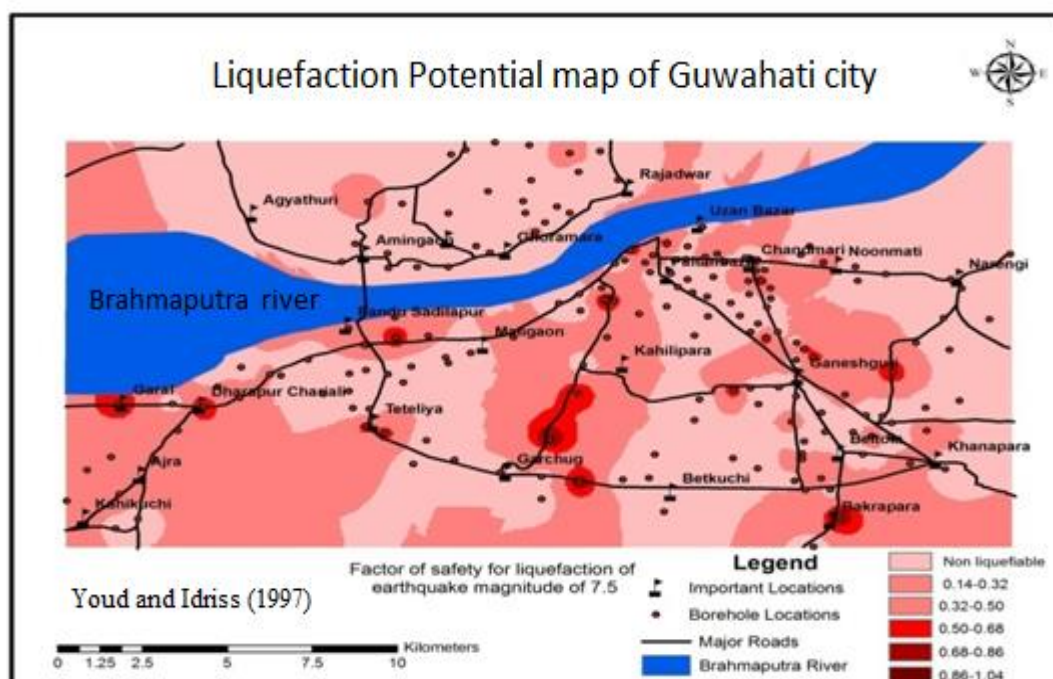


Fig.2 Liquefaction potential map of Guwahati city (M = 7.5) [Method of Youd et. al (2001)]

The factors of safety were calculated for all the bore holes having soils susceptible to liquefaction. Fig. 3 to 6

show the factors of safety with depth of four bore holes for earthquake magnitude 6, 7.5 and 8.1 according to the

Youd and Idriss (1997) method. The factors of safety were also calculated according to the Idriss and Boulanger method (2004). A comparison of factor of safety between the two methods for a 7.5 magnitude earthquake are shown from Fig 7 to 9. It is observed that the Idriss and Boulanger method under estimates the factor of safety at some depths and over estimates at some other depths. A clear picture is not visible as to which method is giving a higher value of factor of safety. The database developed by Idriss and Boulanger (2004) is regarded as an updated database.

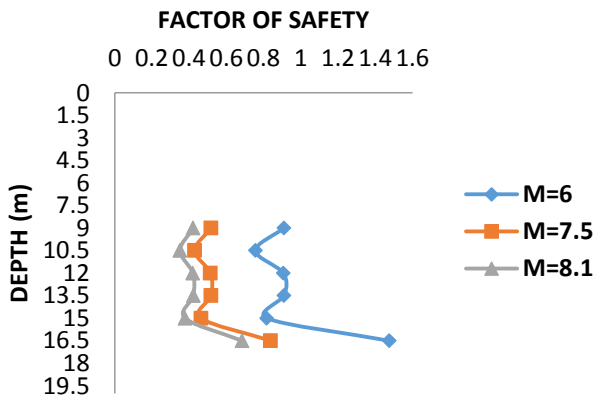


Fig.3 Factor of safety with depth for bore hole 7 according to Youd and Idriss (1997)

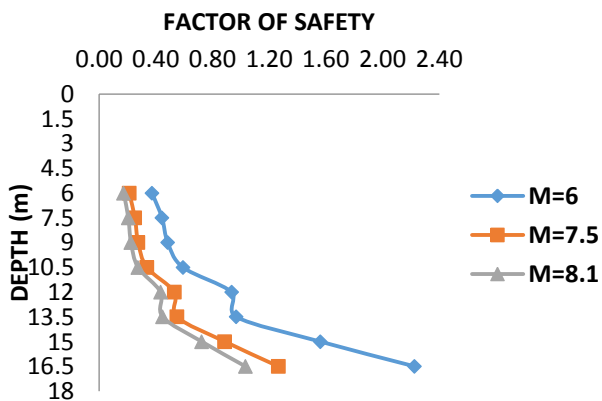


Fig.4 Factor of safety with depth for bore hole 8 according to Youd and Idriss (1997)

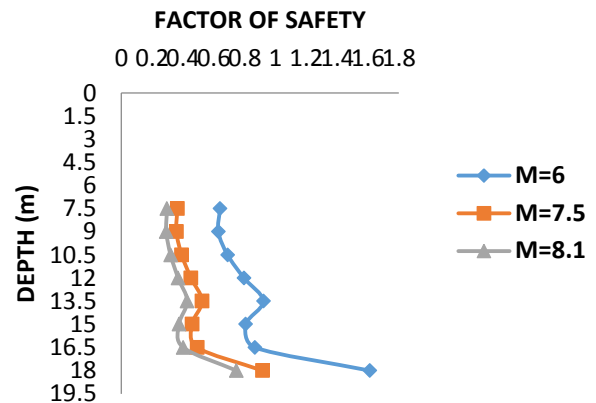


Fig.5 Factor of safety with depth for bore hole 12 according to Youd and Idriss (1997)

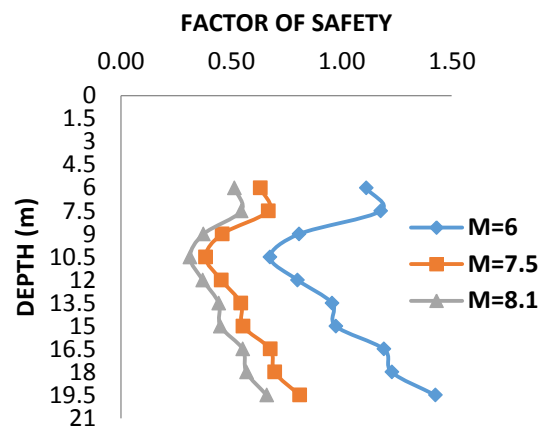


Fig.6 Factor of safety with depth for bore hole 16 according to Youd and Idriss (1997)

The findings of liquefaction potential of Guwahati city, in the present study, are not the same as reported in Ayothiraman et al. (2012). According to the authors the soil in Guwahati city is predominantly silty clay having fine content (60–100 %) out of which the silt is more than 70 %. Although the fine content is high, the city is susceptible to liquefaction, because of higher silt content soil. The present study has shown that the soils in Guwahati city is not predominantly silty clay although in a number of locations, silty clay soils were encountered. The silty clay soils were found to have classifications CL and CH and in some locations ML and ML-CL were encountered. The silts and silt-clay mixtures behave differently from sands, both with respect to development and build up of pore water pressures, and deformations under cyclic loading.

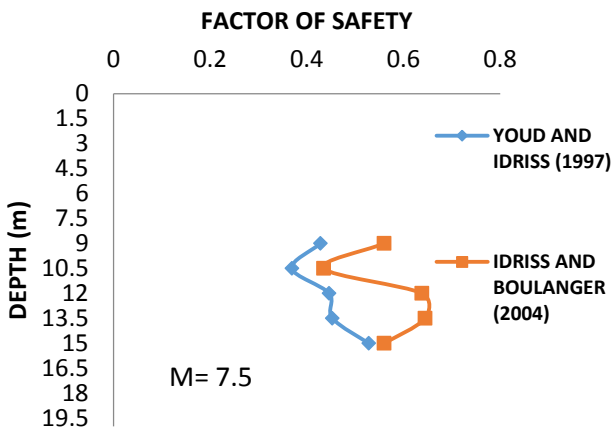


Fig.7 Comparison of Youd and Idriss (1997) and Idriss and Boulanger (2004) for bore hole 7

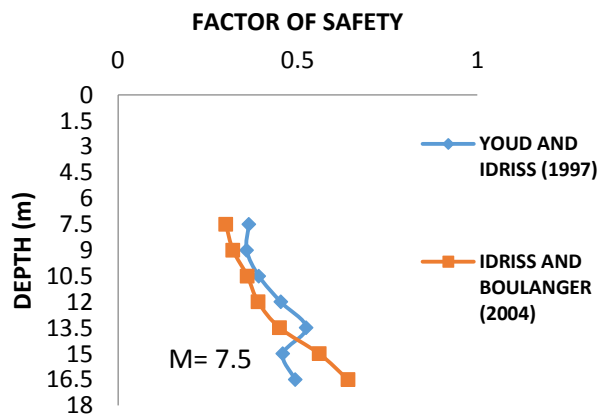


Fig.8 Comparison of Youd and Idriss (1997) and Idriss and Boulanger (2004) for bore hole 12

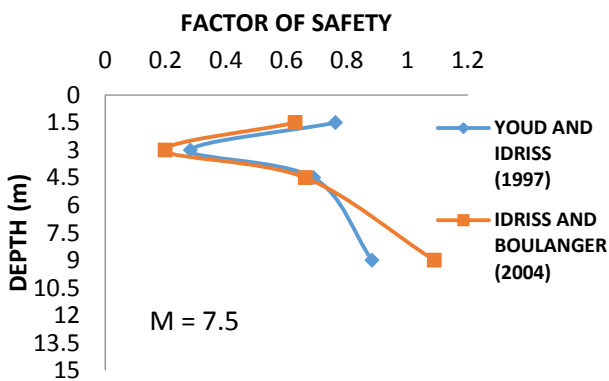


Fig. 9 Comparison of Youd and Idriss (1997) and Idriss and Boulanger (2004) for bore hole 82

4. CONCLUSIONS

In this paper the liquefaction potential of saturated cohesionless deposits in Guwahati city is evaluated using deterministic approach known as modified

simplified procedure as accepted after the 1996 workshop sponsored by the National Centre for Earthquake Engineering Research (NCEER) and the results are compared with the deterministic method put forward by Idriss and Boulanger (2004). A soil database from 200 boreholes covering an area of 262 km² was used for the computation and a design peak ground acceleration of 0.36 g was used as Guwahati falls in zone V according to the seismic zoning map of India. Amongst the 200 boreholes, application of Idriss and Boulanger (2004) method revealed that 49 sites out of 200 were susceptible to liquefaction whereas 48 out of 200 sites were found to be susceptible to liquefaction using Youd and Idriss (1997) method. The SPT blow Counts were in the order of 2-50 (refusal). A liquefaction potential map is prepared showing zones of different levels of risk of liquefaction. The map reveals that the southern bank of river Brahmaputra with the areas of Palashbari, Azara, Jhalukbari, Pandu, Maligaon, Bharalumukh, Uzanbazar and some areas in G.S.Road, Gorchuk area and areas near Chandmari are most susceptible to liquefaction. The northern bank of the city is also found to be susceptible to liquefaction.

REFERENCES

- 1) Arango I (1996): Magnitude scaling factors for soil liquefaction evaluation. Journal of GeotechEng ASCE 122(11):929–936
- 2) Idriss IM, Boulanger RW (2004): Semi-empirical procedures for evaluating liquefaction potential during earthquakes In 11th International conference on soil dynamics & earthquake engineering (ICSDEE) and the 3rd international conference on earthquake geotechnical engineering (ICEGE) January 7–9, Berkeley, California, USA, pp 32–56
- 3) Idriss IM (1999): An update to the Seed-Idriss simplified procedure for evaluating liquefaction potential. In: Proceedings, T R B workshop on new approaches to liquefaction, January. Publication No. FHWA-RD-99-165, Federal Highway Administration
- 4) Idriss IM (1999): An update to the Seed-Idriss simplified procedure for evaluating liquefaction potential. In: Proceedings, T R B workshop on new approaches to liquefaction, January. Publication No. FHWA-RD-99-165, Federal Highway Administration
- 5) Ishihara K (1985): Stability of natural deposits during earthquake. In Proceedings of the 11th international conference on soil mechanics and foundation engineering, Vol. 1, SanFrancisco, pp 321–376

- 6) IS (1893–2002) Part 1. Indian standard criteria for earthquake resistance design of structures. BIS, New Delhi
- 7) Liao SC, Whitman RV (1986): Overburden correction factors for SPT in sand. *Journal of GeotechEng ASCE* 112(3):373–377
- 8) National Center for Earthquake Engineering Research (NCEER). In: Youd TL, Idriss IM (eds) *Proceedings of the NCEER workshop on evaluation of liquefaction resistance of soils*, Technical Report NCEER-97-022, 1997
- 9) Seed, H.B, and I.M.Idriss, (1971): Simplified Procedure for evaluating soil liquefaction Potential, *Journal of the soil Mechanics and Foundation Division, ASCE, Vol.97, No.9, pp. 1249-1274.*
- 10) Seed HB, Idriss IM, Makdisi F, Banerjee N (1975): Representation of irregular stress time histories by equivalent uniform stress series in liquefaction analysis. Report No. EERC 75-29, Earthquake Engineering Research Center, University of California, Berkeley, October 1975b
- 11) Seed HB, Idriss IM (1982): Ground motions and soil liquefaction during earthquakes. *EarthqEng Res Institute, Berkeley* 134 pp
- 12) Seed HB, Idriss IM, Arango I (1983): Evaluation of liquefaction potential using field performances data, *Journal of GeotechEng ASCE* 109(3):458–483
- 13) Seed HB, Tokimatsu K, Harder LF, Chung RM (1985): Influence of SPT procedures in soil liquefaction resistance evaluations, *Journal of GeotechEng ASCE* 111(12):1425–1445
- 14) Tokimatsu K, Yoshimi Y (1983): Empirical correlation of soil liquefaction based on SPT N-value and fines content, *Soils Found JSSMFE* 23(4):56–74
- 15) Yoshimi Y, Tokimatsu K, Kaneko O, Makihara Y (1984): Undrained cyclic shear strength of a dense Nigata sand. *Soils Found JSSMFE* 24(4):131–145
- 16) Yoshimi Y, Tokimatsu K, Hosaka Y (1989): Evaluation of liquefaction resistance of clean sands based on high quality undisturbed samples. *Soils Found JGS* 29(11):93–104

[Back to table of contents](#)

Rock Slope Stabilization along the trek route to Mata Vaishno Devi Shrine - A Case Study

Gourango Singhaⁱ⁾, Lopamudra Duttaⁱⁱ⁾

i) Country Manager, Geobrugg India Pvt Ltd., JMD Megapolis, Gurgaon, Haryana 122018

ii) Technical Manager, Geobrugg India Pvt Ltd., JMD Megapolis, Gurgaon, Haryana 122018

ABSTRACT

The 11 Km long trek road to the Holy Shrine of Vaishno Devi witnesses landslides and rockfalls at various locations, the overburden slope at Adhkuwari location was posing threats of a possible landslides. On an average 20,000 visitors visits the temple every day. Therefore they decided to stabilize the 75° steep slope. As a protective measure the flexible slope stabilization system using high-tensile steel wire meshes was selected in combination with nailing along with 15 Rockfall Barriers, in order to protect the pilgrims. This widely used way to stabilize soil and rock slopes is economical and a good alternative to shotcrete solutions or massive supporting structures. Special concepts have been developed for dimensioning of flexible surface stabilization systems in steeper soil or heavily weathered loosened rock slopes, but also on jointed and layered rock in which the bodies liable to break out are determined by joint and layer planes. Stabilizations implemented in soil and rock slopes confirm that these measures are suitable for practical applications. Analyzing of the design, explanation of the installation and how the finished installation behaves will be shown. Hydro seeding was carried out to promote vegetation.

Keywords: ROVULUM, TECCO, dimensioning, flexible slope stabilization system

1. INTRODUCTION

The use of flexible slope stabilization systems have proven their suitability around the world, including Europe, Asia, North America and in colder climates, where the stabilizing facings need to be able to flex under the freeze/thaw cycle. Historically, the mesh used for these purposes is produced using mild steel wire with a tensile strength of 400–500 N/mm². The development of mesh made from high-tensile steel wire with a tensile strength of at least 1770 N/mm², offers new possibilities for the efficient and economical stabilization of slopes (Fig.1a and 1b). Sophisticated dimensioning concepts serve to dimension these kinds of slope stabilization systems against superficial instabilities by taking the statics of soil and rock into account [3].



a



b

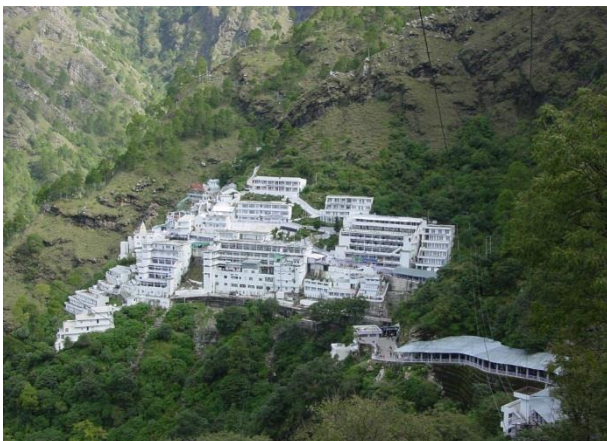
Fig. 1. High-tensile wire mesh for slope stabilization (a) and system spike plate to tension the high-tensile steel wire mesh against the slope surface (b)

2. PROJECT

Table 1. Parties involved

Client:	Mata Shri Vaishno Devi Shrine Board
Nailing and system installation:	Pioneer Foundation Engineers, Mumbai
Date of installation:	January 2014 – September 2016

There had been several cases of rockfall and landslides in the trek route of the Holy Shrine of Mata Vaishno Devi. Therefore the Shrine Board decided to actively stabilize the 75° and higher steep slope, up to a maximum height of 70 m in this section. A protective measure had to be selected to stabilize the 8050 m² of the exposed cutting against superficial instabilities, tilting as well as sliding of individual blocks and rock fall.



a



b

Fig 2. Location of the project in the Mata Vaishno Devi track route (a) and partly eroded rock slope before the installation work (b).

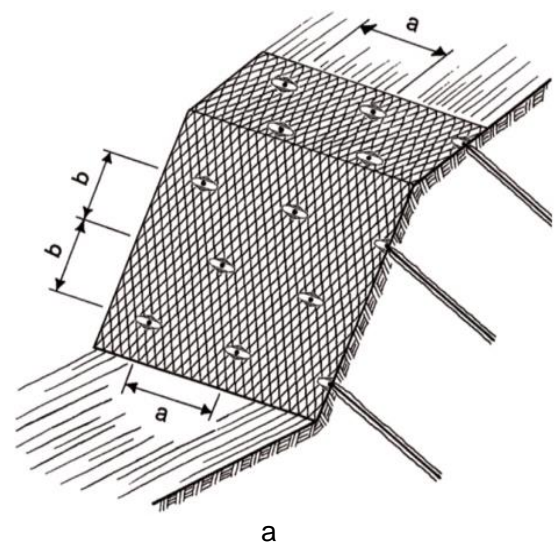
3. PROTECTION MEASURES

3.1 Slope stabilization using High Tensile Steel wire mesh

The flexible slope stabilization system consists of TECCO G65/3 high-tensile steel wire mesh and QUAROX rolled cable net, system spike plates and soil nails has been selected. The TECCO G65/3 and QUAROX wire mesh is made from 3 mm high tensile wire and uses a zinc-aluminum coating for protection against corrosion. Each diamond of the single twist of TECCO G65/3 mesh measures 83 mm x 143 mm. The high tensile steel wire used in the manufacture of the mesh has a tensile strength of 1770 N/mm², compared to mild steel which has a tensile strength of 400–500 N/mm². As a result TECCO G65/3 mesh has a tensile strength of 150 kN/m, which means substantially higher forces can be absorbed by this mesh in comparison to conventional mild steel wire mesh [1]. Aside from the higher bearing capacity, another advantage of TECCO mesh over conventional mild steel wire mesh is that it has an even load transmission and no weak zones within the mesh. This is achieved by manufacturing TECCO mesh with the same diameter high tensile wire, which forms a unified and homogenous mesh structure.

Special diamond-shaped system spike plates which match the load capacity of the mesh serve to fix the mesh to soil or rock nails. By tensioning these nails, and recessing the spike plates into the ground, the mesh is adequately tensioned to ensure it follows the surface contours.

With this slope stabilization system the rows of nails are offset to each other by half a horizontal nail distance. This limits the maximum possible break out between the individual nails to a width “a” and a length of “2 x b” (see Fig. 4a). The staggered layout is shown in Fig. 4b for this project after installation.



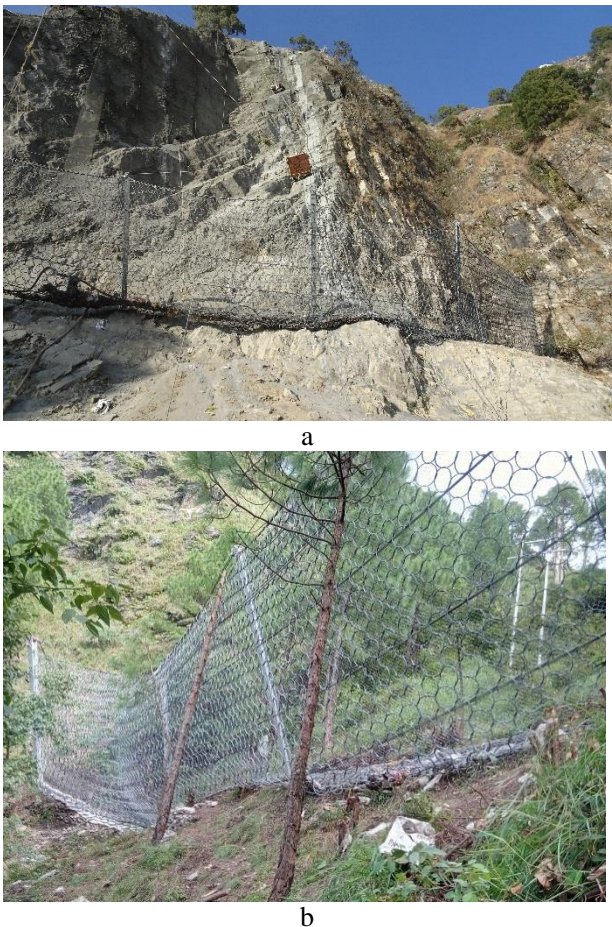
a



Fig. 4. General profile with nail arrangement (a) and staggered pattern of nail after installation – Project Vaishno Devi (b).

3.2 Rockfall protection using barriers

Based on the survey results authorities decided to apply a rockfall protection system from the RXE-Series. With its ring nets made of high-tensile steel wire the barrier design has been tested and approved to absorb impact energies of up to 8,000 KJ. A total of 15 barriers were installed in different locations with energy absorption capacity ranging from 3000 KJ – 8000 KJ



4 DIMENSIONING

4.1 Superficial slope analysis using ROVULUM

The flexible slope stabilization system was dimensioned against superficial instabilities based on the RUVOLUM concept [2]. The maximum nail spacing and the required nail length can be determined, and by utilizing the high bearing capacity of the mesh, significant cost savings can be realized by reducing the number of nails required. Conventional slope design methods are still required for deeper seated failure mechanisms.

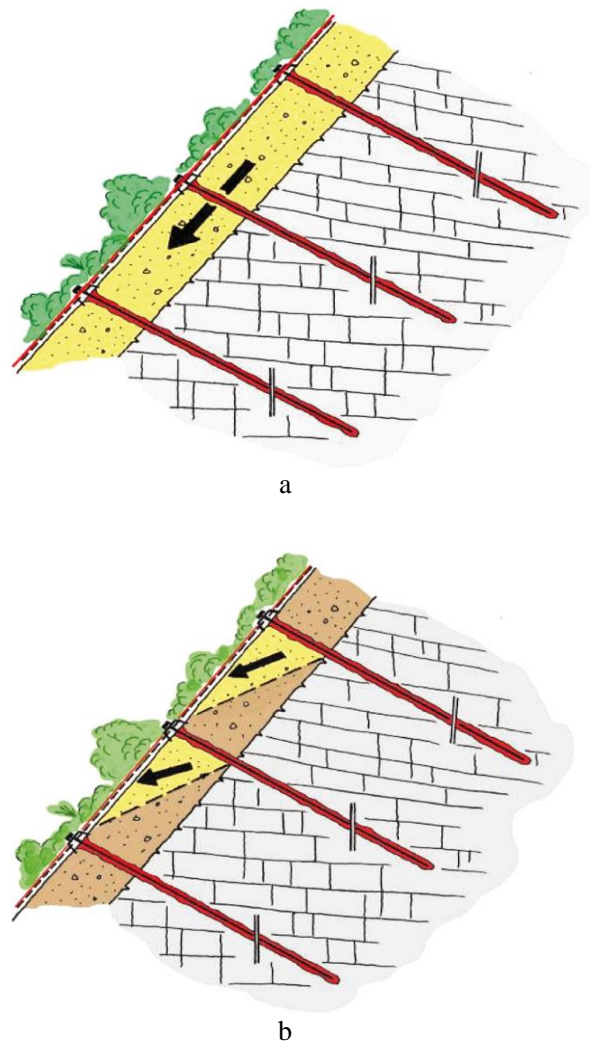


Fig. 5. The dimensioning concept is based on the investigation of superficial slope-parallel instabilities (a) and on the investigation of the local instabilities between single nails (b).

4.2 Rock fall simulation using Rockfall software

ROCKFALL is a computer program for the simulation of rockfall. It was developed by Dr. rer.

nat. R.M.Spang, Dr.-Ing. L. Weber, Dipl. Geol. N. Graf and Dr.-Ing. B. Romunde. The program is based on the laws of motion and the collision theory. The path of a single rock block or of up to 10,000 blocks, can be calculated and interpreted by the same run. At each point within a profile (especially at the positions of planned interception structures or rockfall barriers) the kinetic energies and bounce heights can be calculated. The input data are varied by a random number generator within user defined boundaries. The results are presented in class and summation histogram.

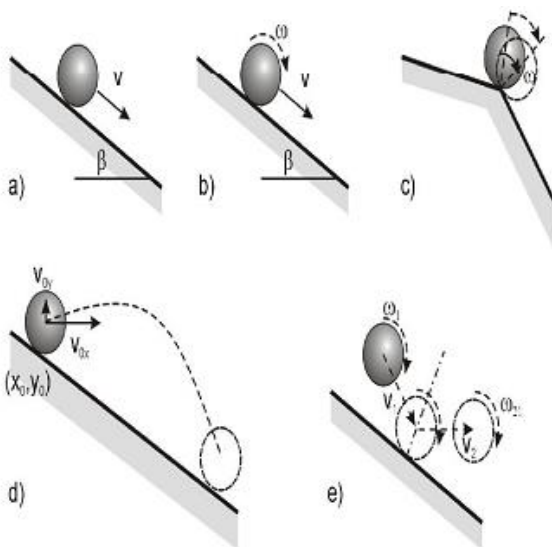
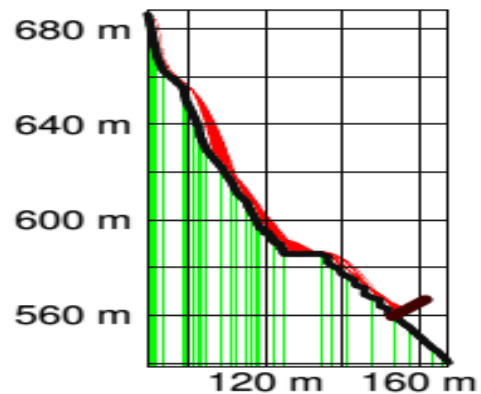
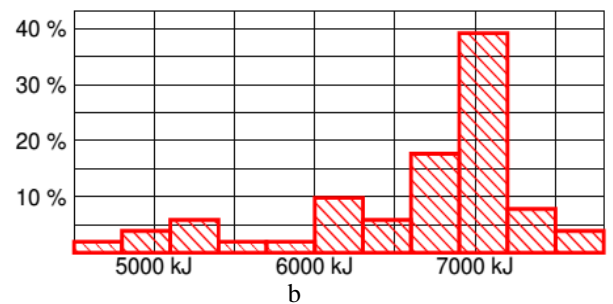


Fig 6. Kinds of motion and resulting paths, (a) sliding, (b) rolling, (c) toppling, (d) inclined throw, (e) impact on surface



a



b

Fig. 7. Rockfall simulation results; surface profile (a), Energy and bounce heights (b)

TABLE 2. PROJECT INFORMATION

Height of the slope:	60-70 m
Subsoil:	Fractured impure limestone core. The region is also formed of assorted clay, sand gravel and boulders.
Inclination of the slope:	75°
Stabilized area:	8'050 m ²
Nail type:	Gewi ø28 mm
Nail pattern:	2.2 x 2.2 – 3.0 x 3.0 m
Nail length:	L = 6-8 m
Mesh type:	High-tensile steel wire mesh TECCO G65 / 3 and QUAROX rolled cable net.
Spike plates:	System spike plate
Rock-fall barriers installed:	15 numbers of energy absorption capacities of 3000 KJ, 5000 KJ, 8000 KJ

5 INSTALLATION

Firstly, the slope was cleaned of eroded soil and smaller loose rocks. Due to the fact that there was no access to the top of the slope, the installation company decided develop an access to the steel slopes and used winch – pulley system (see Fig 7) which was hanged from the top of the slope. It was very important that the nails could be installed in deep seated spots so that the mesh could be tensioned and kept in contact with the surface.



a



b



c

Fig 8. Winch – pulley system hanged from the top of the slope (a), Materials being shifted by the winch – pulley (b), Rockfall barrier being installed at the location (c)

6 RE-VEGETATION / EROSION PROTECTION

Erosion control mats (TECMAT) can be installed underneath the mesh to aid in re-vegetation. The application of a vegetation layer can be limited by the soil or rock properties, groundwater and climate. The steeper the slope cutting, the more difficult it becomes for vegetation to grow. If re-vegetation is to be carried out, a species of plant or grass should be selected that is fast growing and suitable for the local conditions.



a



b

Fig.9 Condition of the slope in March 2015, after successful re-vegetation (a), 5000 KJ Rockfall barrier after installation (b)

7 CONCLUSION

The Slope stabilization system and Rockfall barriers can be adapted to the site specifics and static conditions in a very flexible manner. The systems can be designed and dimensioned against superficial instabilities, which is the first time flexible surface support measures can be properly designed. This approach offers the possibility to arrange the nails in a more economical way due to the capability of high tensile steel wire mesh in absorbing and transferring high loads.

When slopes stabilized with flexible high tensile steel wire mesh are combined with erosion control mats, they can regain a natural or vegetated appearance, which aesthetically is normally preferred.

8 REFERENCES

- [1] Brändlein P. (2004). LGA Nuremberg, Germany, Monitoring and supervision of laboratory testing of the TECCO slope stabilization system, Test report BPI 0400046/1.

- [2] Rügger, R.; Flum, D. (2006). *Anforderungen an flexible Böschungsstabilisierungssysteme bei der Anwendung in Boden und Fels*. Technische Akademie Esslingen, Beitrag für 4. Kolloquium „Bauen in Boden und Fels“.
- [3] Rügger, R.; Flum, D.; Haller, B. (2002). *Hochfeste Geflechte aus Stahldraht für die Oberflächensicherung in Kombination mit Vernagelungen und Verankerungen*. Technische Akademie Esslingen, Beitrag für 2. Kolloquium „Bauen in Boden und Fels“.

[Back to table of contents](#)

Comparison of methods for estimating microbial biomass in soil

Monikongkona Boruahⁱ⁾, Rojimul Hussainⁱⁱ⁾, Ankit Gargⁱⁱⁱ⁾

i) Research Trainee, Department of Civil Engineering, IIT Guwahati.

ii) MTech Student, Department of Civil Engineering, IIT Guwahati.

iii) Assistant Professor, Department of Civil Engineering, IIT Guwahati.

ABSTRACT

In the recent years, there has been an increased need for sustainable development. The use of natural fiber-reinforced soil and application of geotextiles has gained traction, with the researchers looking for alternative eco-friendly materials rather than going for exhaustible synthetic materials. Numerous studies have been done on the mechanical, hydraulic performance of such natural fiber-soil composites. However, no comprehensive study has been undertaken to measure the effect of microbial activity on such embedded reinforced natural materials. Due to the heterogeneous nature of the physicochemistry and complexity of the microbial populations, there is difficulty in their study which has led to a lack of knowledge in the interactions between various microbial communities and their role in bio-degradation. In the following review, a few of the methods of estimating soil microbial biomass have been illustrated. The work is a state of art review on the implementation of various methods in determining such microbial activity and highlights its application in geo-material degradation studies.

Keywords: sustainable development, natural fibers, reinforced soil composites, microbial activity, microbial biomass measurement

1. INTRODUCTION

Growing concern stemming from the need of sustainable development has encouraged engineers to use plant fibers for soil-reinforcement applications. The use of such bio-materials have recently gained traction due to environmental concerns, their sustainability, high elongation modulus and availability, for use in diversified industrial products including paper industry, rope and cords, and reinforcement in composite matrices (Khalil et al. 2014). The popularity of plant-fiber reinforced composites have increased because of suitable properties which are comparable to the contemporary synthetic composites. The growing interest in the automotive industry, to replace synthetic fiber with natural fiber as reinforcing material in thermoplastic composites, is an example of this (Abdullah et al. 2013). In geotechnical applications, one of the major challenges faced, while using natural fibers, is loss of mechanical strength due to environmental degradation. A major factor affecting the performance of natural fiber reinforced composites, is degradation by soil microbes. 'Microbial activity in soil' means all transformations of components of soil, which are caused by soil microorganisms (Beck, 1968). During biodegradation, the organic matter present in the fiber is converted by the micro-organisms, to generate energy and to produce new cellular metabolites, for use in their growth and other metabolic activities. In order to illustrate the intricate interrelationships and controlling mechanisms of the

input/output fluxes of nutrients and energy in the soil ecosystem, a proper and reliable estimation method of the soil microbial biomass is required. Valuable information like biomass growth, degradation time, and efficiency of C can be found out by estimation of microbial biomass C. The major objective of this paper is to provide a state-of-the-art on the different methods, used for the measurement of microbial biomass in soil. The common methods of estimating microbial biomass include enumeration techniques i.e. direct counts by microscopy (Schmidt and Paul, 1982), colony-forming units (Wollum, 1982), activity measures i.e. in situ respiration (Anderson, 1982), substrate-induced respiration (Anderson and Domsch, 1978a; Beare et al., 1990), biochemical assays (ATP analysis, Holm-Hansen and Booth, 1966) and Chloroform (CHCl₃) fumigation (Jenkinson and Powlson, 1976a). Here, a basic comparison of the following methods - Fumigation incubation method (Jenkinson and Powlson, 1976b); Fumigation extraction method (Vance et al. 1987b); Substrate induced respiration method (Anderson and Domsch 1978b); to estimate microbial biomass has been done. The work aims to provide guidelines to practicing engineers to gauge such microbial activity, to model the functional period of geotextiles and fibers derived from plant species.

2. DISCUSSION OF METHODS FOR ESTIMATING SOIL MICROBIAL BIOMASS

2.1 Chloroform fumigation incubation method

It is a commonly used method for estimating soil microbial biomass. The estimation of soil microbial biomass is important because it is an essential ecological parameter and can act as a source-sink in nutrient cycling processes and regulates many organic matter transformations (Jordan and Beare, 1991).

This method was first worked out by Jenkinson (1966), who investigated the CO₂ and ¹⁴CO₂ liberation from soil samples subjected to different treatments. The samples used, were collected from agricultural fields 1-4 years after they had been amended with tops or roots of ¹⁴C-labelled rye grass, under field conditions. He studied the liberation of labelled and unlabelled CO₂ from soil samples, subjected to irradiation, CH₃Br vapour, CHCl₃ vapour (24-hours exposure) and oven drying at 80°C. He found that all the above treatments have the common action of killing the microorganisms resulting in the flush of N and CO₂, which is caused by their degradation. Jenkinson concluded that the size of CO₂ flush should provide a measure of the original biomass of the soil sample.

The chloroform fumigation incubation method (CFIM) (Jenkinson and Powlson, 1976a) requires a post-fumigation incubation of 10 days. Jenkinson and Ladd (1981), have summarized the following assumptions that underlie the use of this method.

1. Carbon in dead organisms is more rapidly mineralized than carbon in living organisms.
2. Fumigation leads to a complete kill.
3. Death of organisms in the unfumigated soil sample is negligible compared with that in fumigated soil.
4. The only effect of soil fumigation is to kill the biomass.
5. The fraction of dead biomass carbon mineralized over a given time period does not differ across soil types.

The CFIM measures the CO₂ evolved from the decomposition of microbial cells killed by fumigation (Jenkinson, 1976).

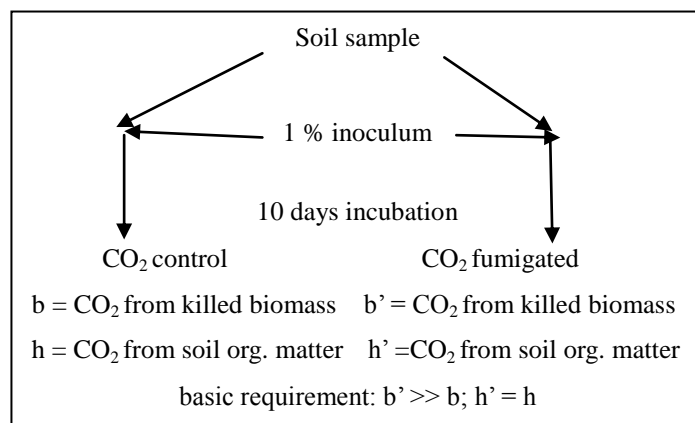
Jordan and Beare (1991) carried out a comparison between two methods (CFIM and CFEM) of estimating soil microbial biomass. During their experiments, they collected soil samples from no-tillage plots in the Horseshoe Bend experimental area (HSB) near the University of Georgia, Athens, GA. The soil samples collected have the following composition:

Table 1. Composition of soil samples.

Element	Percentage (%)
Sand	66
Silt	13
Clay	21

In this experiment performed by Jordan and Beare (1991), soil subsamples were sieved by using 2mm mesh to remove stones and roots. Two 20g portions of soil were placed in 100 ml glass beakers for each replicate analysis. One of the portions of soil was fumigated by placing the beaker in a large vacuum desiccator lined with moist paper. The other portion of soil was left unfumigated. A beaker containing 50ml of alcohol free CHCl₃ and anti-bumping granules was placed in the desiccator. The desiccator was evacuated three times until the CHCl₃ boils vigorously. The lid vent was then closed for an hour and the process was repeated. The samples were exposed to CHCl₃ for 24 hrs. The beaker containing CHCl₃ and the moist paper lining the desiccator were removed and the residual vapors were removed from the soil samples by continuous evacuation. The soil samples were brought to 30% water content by weight. Each soil sample was placed in a mason jar (air tight) with a vial containing 1 ml of 1 N NaOH. Each container was sealed and incubated at 25°C for 10 days. In addition to unfumigated controls, appropriate controls with NaOH vials but no soil were set up and maintained for 10 days at 25°C. After incubation, the NaOH in each vial was titrated using standardized 0.1N HCl. By calculating the volume of acid needed to decrease the pH of solution from 8.7 to 3.7, the amount of CO₂ evolved was estimated.

The process is illustrated in the Fig. 1



$$biomass\ C = \frac{CO_2 - C_{fumigated} - CO_2 - C_{control}}{k_c}$$

[k_c = 0.41 (22°C),
k_c = 0.45 (22°C)]

Fig. 1 Experimental procedure and calculation for the estimation of microbial biomass *C* by the CHCl₃ fumigation-incubation method (*org.organic*)

2.2 Chloroform fumigation extraction method

Jenkinson (1966), mentioned in his paper that fumigation of soils with CHCl_3 increases the amount of C extractable with 0.5 M K_2SO_4 . It was pointed out by Voroney, (1983) that there is a close correlation between the K_2SO_4 -extractable C additionally liberated by fumigation and the microbial biomass C content of soils.

The Chloroform fumigation direct extraction (CFEM) method measures the total organic carbon in extracts of CHCl_3 -fumigated and non-fumigated soils. It involves the analysis of post-fumigation extracts (0.5 M K_2SO_4) for solution concentrations of Total Organic Carbon (TOC) that avoids many of the limitations that CFIM poses (Vance et al., 1987).

Vance et al. (1987b) also proposed the following calculation to measure microbial biomass C by extraction with 0.5 M K_2SO_4 :

$$\text{Biomass C} = k_{\text{EC}} \times E_{\text{C}} \quad (1)$$

Here, E_{C} = (organic C extracted from fumigated soil) – (organic C extracted from non-fumigated soil)

Significance of 'K_c' value

The K_{c} is that portion of microbial biomass carbon mineralized to CO_2 over a prescribed incubation period. This is an important parameter that must be carefully chosen when calculating microbial biomass carbon. While Anderson and Domsch (1978a) calculated a mean value of 0.41 for k_{c} for incubations at 22°C, it was suggested to be 0.45 at 25°C by Jenkinson and Ladd (1981). It was stated that the use of any arbitrary value of K_{c} for all soils is inappropriate. It was also stated by Anderson and Domsch (1978a) that K_{c} values for bacteria and fungi do not span a very wide range. The k_{ec} value is also used in the same manner as k_{c} , to determine the microbial carbon from the C-flush (Sparling and West, 1988).

In the experiments carried out by Jordan and Beare (1990), a 20g (dry weight equivalent) moist soil sample was fumigated with chloroform for 24hrs for a complete kill of microorganisms. The samples were evacuated in the same manner as CFIM as described above. After that, the samples were extracted with 0.5 M K_2SO_4 using a 1:4 soil/solution (w/v) ratio. The mixture was shaken for 30 minutes and then filtered using no. 42 Whatman paper. The extracts may be immediately analyzed using a Total Organic Carbon (TOC) analyzer or may be frozen for later use. It was found that freezing does not affect the results.

Analysis of dissolved oxygen carbon (doc)

It involves two basic steps: decomposition of all organic carbon to CO_2 and quantitative detection of CO_2 evolved. The O.I. Model 700 combines persulphate oxidation at 100°C and an infrared gas analyzer. A precise volume, either 0.29 ml, 1 or 5 ml, was injected into a Teflon digestion vessel. An

additional 6ml was drawn to flush the sampler tube. 0.2ml phosphoric acid was injected and the existing CO_2 was purged using N_2 . The total inorganic carbon was detected. After that, usually, 1 ml of 100 mg l^{-1} sodium persulfate was injected into the digestion vessel with the CO_2 free sample. The vessel was then heated at a temperature of 100°C for at least 5 minutes. The purged CO_2 was then absorbed by a CO_2 -absorbant resin. The resin, when rapidly heated, then desorbed the CO_2 in a rapid pulse, which was carried into an infrared gas analyser (IRGA), allowing analysis in the $\mu\text{g l}^{-1}$ range.

Calculation of biomass C

The total microbial biomass carbon in soil was calculated from the amounts of CO_2 evolved or extracted from the fumigated and non-fumigated soil samples.

$$\text{Total Microbial Biomass C} = F - \text{NF}/K_{\text{C}} \text{ or } K_{\text{ec}} \quad (2)$$

Here,

F = CO_2 C evolved (CFIM) or extractable C (CFEM) from fumigated samples.

NF = CO_2 C evolved (CFIM) or extracted C (CFEM) from unfumigated samples;

K_{C} or K_{ec} = 0.45 or 0.33, the fraction of biomass C mineralized to CO_2 (CFIM) or the fraction extracted (CFEM) with K_2SO_4

2.3 Substrate induced respiration method

After investigating the contribution by fungal and bacterial biomass to total soil respiration, it was found, by Anderson and Domsch (1973) that the addition of glucose to the soil samples, resulted in a new elevated level of respiration, for a few hours (2-8 h), before the liberation of CO_2 increased due to proliferation of the soil populations. This new respiration level was called 'maximum initial response', induced by an amount of glucose, which depends on the soil sample being examined. Anderson and Domsch (1975), by adding selective inhibitors with glucose, developed a method to measure relative bacterial and fungal contributions to soil respiration. They found the fumigation-incubation method of Jenkinson and Powlson (1976b) useful in checking the maximum initial response values against the corresponding microbial biomass C content of soil samples.

Anderson and Domsch (1978b), calculated the value of regression which indicated that 40 mg biomass C respire 1 ml $\text{CO}_2 \text{ h}^{-1}$, at the stage of maximum initial response.

In their experiment, Bauer et al. (1991) checked the applicability of glucose induced respiration for the quantification of soil microbial activity. Here, 10 g of soil was dried for 24 hours at 105°C and this was carried out in duplicates. 10g soil was thoroughly mixed in a magnetic stirrer with 25 ml 0.01M CaCl_2 and the pH value of the suspension was measured after 24 hours. 20g soil was packed into a small bag (15 cm

diameter) of polyester and mounted into a screw capped 250 ml flask. 20 ml 0.05 N NaOH was placed in the flask for absorption of CO₂. The screw was closed gas tight. After a period of 24 hrs of incubation at 25°C, 25ml 1M BaCl₂ was added and the absorbed CO₂ was precipitated as BaCO₃. The remaining NaOH was titrated as with 0.05 N HCl after the addition of two/three drops of phenolphthaleine. This test was carried out four folds. A blank (without soil) was also analyzed and the result was subtracted from the mean value of the replicates. The result was expressed in mg CO₂.soil_{dried}⁻¹.24h⁻¹ (1ml 0.05N HCl represents 1.10025 mg CO₂). For the estimation of glucose induced-respiration the soil samples were supplemented with 0.4% (w/w) D(+) -glucose and were mixed thoroughly. 20 g soil samples were packed into polyester bags as described above and placed in a flask, with 10 ml of 0.05 N NaOH for the absorption of CO₂. It was sealed air tight and incubated for 4 hrs and subsequently the CO₂ produced was measured titrimetrically as in soil respiration movement described above. The result was expressed in mg CO₂.soil_{dried}⁻¹.4h⁻¹ (1 ml 0.05 N HCl represents 1.10025 mg CO₂).

3 CONCLUSION

Microbial biomass is a measure of the living component of soil organic matter. In order to understand the interrelationships and illustrate the controlling mechanisms of the input/output fluxes of nutrients and energy in the soil ecosystem, a proper and reliable estimation method of the soil microbial biomass is required.

In this paper, after reviewing three widely used methods for estimating the soil microbial biomass, it can be concluded that the Chloroform fumigation incubation method (CFIM) has been shown to consistently underestimate the results in case of low pH soils. From study, it has been observed that several assumptions and sources of error are associated with the CFIM procedure. It has been shown that, after the fumigation procedure, there is a chance of increased experimental error while the samples are incubated with a base trap for 10 days. Also, the second step which increase chances of error is titration of the samples where much care has to be taken to make sure that appropriate amount of acid is added.

Less error has been found to be associated with the Chloroform Fumigation Extraction method (CFEM), which uses TOC analyzer after fumigation, as found out from studies by Jordan and Beare (1990). If there is careful calibration and standardization of the TOC analyzer, it is seen that automated analysis of fumigation extracts can significantly reduce sample handling and consequent errors. It has been recommended to restrict the CFEM process to 'mineral' soils with a total organic carbon content of <10% (Sparling and West, 1988).

The Chloroform fumigation extraction method (CFEM), has been found to be particularly effective for low pH soils (Sparling and West, 1988; and Vance et al., 1987).

The glucose induced respiration method is based on the same principle as respiration. It was demonstrated by Anderson and Domsch that the soils differ in their initial respiratory response when supplied with the optimal concentrations of glucose. It was concluded by them, that this initial respiratory response, recorded before any growth of microorganisms occurred, could be taken as an index of the existing total microbial biomass.

Although the glucose induced respiration indicates a difference in activity, its sensitivity is found to be low. The low sensitivity of CO₂ determination, could be the reason, which will have even more influence with decreasing respiration.

REFERENCES

- 1) Anderson, J.P.E. and Domsch, K.H., (1973): Quantification of bacterial and fungal contributions to soil respiration. *Archives of Microbiology*, 93(2), pp.113-127.
- 2) Anderson, J. P. E., & Domsch, K. H. (1975): Measurement of bacterial and fungal contributions to respiration of selected agricultural and forest soils. *Canadian Journal of Microbiology*, 21(3), 314-322.
- 3) Anderson, J. P. E., & Domsch, K. H. (1978a): Mineralization of bacteria and fungi in chloroform-fumigated soils. *Soil Biology and Biochemistry*, 10(3), 207-213.
- 4) Anderson, J.P.E. and Domsch, K.H., (1978b): A physiological method for the quantitative measurement of microbial biomass in soils. *Soil biology and biochemistry*, 10(3), pp.215-221.
- 5) Anderson, J. P. (1982): Soil respiration. *Methods of soil analysis. Part 2. Chemical and microbiological properties*, (methodsofsoilan2), 831-871.
- 6) Bauer, E., Pennerstorfer, C., Holubar, P., Plas, C., & Braun, R. (1991): Microbial activity measurement in soil—a comparison of methods. *Journal of microbiological methods*, 14(2), 109-117.
- 7) Beare, M. H., Neely, C. L., Coleman, D. C., & Hargrove, W. L. (1990): A substrate-induced respiration (SIR) method for measurement of fungal and bacterial biomass on plant residues. *Soil Biology and Biochemistry*, 22(5), 585-594.
- 8) Beck, T. (1968): Mikrobiologie des Bodens.
- 9) Ellis, R.J., (2004): Artificial soil microcosms: a tool for studying microbial autecology under controlled conditions. *Journal of microbiological methods*, 56(2), pp.287-290.
- 10) Holm-Hansen, O., & Booth, C. R. (1966): The measurement of adenosine triphosphate in the ocean and its ecological significance. *Limnology and Oceanography*, 11(4), 510-519.

- 11) Jenkinson, D. S. (1966): Studies on the decomposition of plant material in soil. *Journal of Soil Science*, 17(2), 280-302.
- 12) Jenkinson, D. S., & Ladd, J. N. (1981): Microbial biomass in soil: measurement and turnover. *Soil biochemistry*.
- 13) Jenkinson, D. S., & Powlson, D. S. (1976a): The effects of biocidal treatments on metabolism in soil—I. Fumigation with chloroform. *Soil Biology and Biochemistry*, 8(3), 167-177.
- 14) Jenkinson, D. S., & Powlson, D. S. (1976b): The effects of biocidal treatments on metabolism in soil—V: a method for measuring soil biomass. *Soil biology and biochemistry*, 8(3), 209-213.
- 15) Joergensen, R.G., (1996): The fumigation-extraction method to estimate soil microbial biomass: calibration of the k EC value. *Soil Biology and Biochemistry*, 28(1), pp.25-31.
- 16) Jordan, D. and Beare, M.H., (1991): A comparison of methods for estimating soil microbial biomass carbon. *Agriculture, Ecosystems & Environment*, 34(1), pp.35-41.
- 17) Khalil, H. A., Hossain, M. S., Rosamah, E., Azli, N. A., Saddon, N., Davoudpouira, Y., ... & Dungani, R. (2015). The role of soil properties and it's interaction towards quality plant fiber: A review. *Renewable and Sustainable Energy Reviews*, 43, 1006-1015.
- 18) Meriles, J.M., Gil, S.V., Conforto, C., Figoni, G., Lovera, E., March, G.J. and Guzmán, C.A., (2009): Soil microbial communities under different soybean cropping systems: Characterization of microbial population dynamics, soil microbial activity, microbial biomass, and fatty acid profiles. *Soil and Tillage Research*, 103(2), pp.271-281.
- 19) Schmidt, E. L., & Paul, E. A. (1982): Microscopic methods for soil microorganisms. *Methods of Soil Analysis. Part 2. Chemical and Microbiological Properties*, (methodsofsoilan2), 803-814.
- 20) Sparling, G. P., & West, A. W. (1988): A direct extraction method to estimate soil microbial C: calibration in situ using microbial respiration and ¹⁴C labelled cells. *Soil Biology and Biochemistry*, 20(3), 337-343.
- 21) Vance, E.D., Brookes, P.C. and Jenkinson, D.S., (1987): An extraction method for measuring soil microbial biomass C. *Soil biology and Biochemistry*, 19(6), pp.703-707.
- 22) Voroney, R. P. (1983): Decomposition of crop residues.
- 23) Wollum, A. G. (1982): Cultural methods for soil microorganisms. *Methods of Soil Analysis. Part 2. Chemical and Microbiological Properties*, (methodsofsoilan2), 781-802.
- 24) Zaki Abdullah, M., Dan-mallam, Y., & Megat Yusoff, P. S. M. (2013). Effect of environmental degradation on mechanical properties of kenaf/polyethylene terephthalate fiber reinforced polyoxymethylene hybrid composite. *Advances in Materials Science and Engineering*, 2013.

[Back to table of contents](#)

An experimental study on the effectiveness of an optimized pendulum type tuned mass damper in reducing the response of a building structure

Dhruba J Borthakurⁱ⁾ and Dr. (Mrs) Nayanmoni Chetiaⁱⁱ⁾

i) M.E student, Jorhat Engineering College, dhrubajyoti007borthakur@gmail.com

ii) Asstt. Prof., Jorhat Engineering College, nayanmoni.chetia@gmail.com

ABSTRACT

In this paper an attempt has been made to study the reduction in different response parameters of a building frame with the introduction of an optimally designed pendulum type Tuned Mass Damper. The experiments were performed with the help of a Shake Table apparatus and a 3-storey steel frame model. A sinusoidal excitation of amplitude 1mm and frequencies ranging from 1Hz -15Hz were applied to the structure and different responses of the structure were recorded. At first the bare frame and then the frame with a central and eccentric mass of 1kg at the top storey were analysed. In the next study the same mass of 1kg was suspended with an aluminium coil from the centre of the top storey to act as a pendulum type TMD. Optimisation of the TMD was done using analytical method and the length of the suspending coil was found to be 45 mm for that 1 kg mass. The three storey structure was then introduced with the optimised Tuned Mass Damper and analysed in the Shake Table by giving the similar inputs as before. Then the comparisons were made for displacement, velocity, acceleration and drift of different stories of the frame for the above mentioned cases. Finally, the reduction of the mentioned parameters due to the incorporation of the Tuned Mass Damper system were determined and presented.

Keywords: control, response, tuned mass damper.

1. INTRODUCTION

The primary purpose of all kinds of structural systems used in the building structures is to transfer gravity loads effectively to the footing. The most common loads resulting from the effect of gravity are dead load, live load and snow load. Besides these vertical loads, buildings are also subjected to lateral loads caused by wind, blasting or earthquake. Lateral loads can develop high stresses, produce sway movement or cause vibration. Therefore, it is very important for the structure to have sufficient strength against vertical loads together with adequate stiffness to resist lateral forces.

Innovative means of enhancing structural functionality and safety against natural and manmade hazards are currently a major field of interest of various research works. Performance of a structure under lateral loads can be improved by providing the structure with different control mechanisms.

Tuned mass damper is a passive control practice in which the lateral vibration of a structure is transferred into the vibrational energy of an auxiliary mass suspended at the top storey. The mass and stiffness of the dampers are tuned in such a way that it will vibrate in a phase opposite to the building vibration.

2. EXPERIMENTAL TOOLS AND MODELS

2.1 Shake table

Shake table is an electromechanical experimental setup which would enable the study of basic issues related to vibration behaviour such as damping, dynamic response magnification, resonance, structural vibration under support motions, normal modes, vibration isolation, vibration absorption, dynamics with soft and/or weak first/intermediate stories etc. It also deals with the study of structural ductility in resisting dynamic loads, liquefaction of soils under dynamic loads, seismic wave amplification through soil layer and rocking and up throw of rigid objects under dynamic base motions. These tables have the capabilities for applying harmonic base motions and have the provision to mount the test structure at any desired angle with respect to the direction of applied base motion. The shake table consists of a connecting rod, a vibration table, linear guide ways and an eccentric cam. The cam is connected to a variable speed dc motor with the help of a gear assembly. Linear guide ways ensure that the motion of the table is linear. Fig. 1. shows an electric motor driven Shake Table.

Property specification of the electric motor driven shake table
Maximum payload = 30 kg

Sliding table dimension = 400 mm × 360 mm
 Circular mounting plate dimension = 390 mm diameter
 Motor = 1 HP variable speed dc.



Fig. 1. Electric motor driven shake table.

2.2 Experimental models

A three storey shear frame model is analyzed in the shake table without any extra mass and then with an extra mass at the central and eccentric position respectively. The model is then provided with an optimized Tuned Mass damper (Pendulum type) and analyzed in the shake table for the same harmonic excitation. Fig. 2 and 3 shows the experimental models and their properties are tabulated in Table 1.



Fig. 2. Three storey shear frame model



Fig. 3. Three storey steel frame model with optimized pendulum type TMD

Table 1. Properties of the frame

Items	Properties
Material	Mild steel
E	20000
Unit weight	7850 kg /m ³
Size of column	3 mm × 25 mm, 400 mm height
Size of slab	300 mm × 150 mm, 12 mm thick
Modal frequency of vibration	2.85hz, 8.6 hz, 12.3 hz
Weight of extra mass	1 kg
Weight of the TMD	1 kg
Length of the cable	40 mm
Dia. Of the cable	1 mm

3. THEORY

A tuned mass damper (TMD) is a device consisting of a mass, a spring and a damper that is attached to a structure in order to reduce the dynamic response of the structure. The frequency of the damper is tuned to a particular structural frequency so that when the structure is excited to that particular frequency the damper will resonate out of phase with the structural

motion. Energy is dissipated by the damper inertia force acting on the structure. The TMD concept was first applied by Frahm (Frahm, 1909) to reduce the rolling motion of ships as well as ship hull vibrations.

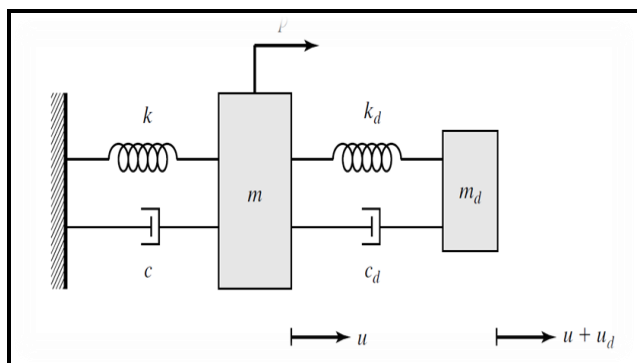


Fig. 4. Mass-spring-damper system for the TMD system

The concept of the tuned mass damper is illustrated using the two mass system shown in Fig. 4. Here, the subscript d refers to the tuned mass damper and the structure is idealized as a single degree of freedom system. [Connor J.J. (2000)]

Eq of motion for the primary mass,

$$(1 + \dot{m}) \ddot{U} + 2\xi\omega\dot{U} + \omega^2 U = P/m - \dot{m} \ddot{U}_d \quad (1)$$

Eq of motion for the tuned mass,

$$\ddot{U}_d + 2\xi_d\omega_d\dot{U}_d + \omega_d^2 U_d = -\ddot{U} \quad (2)$$

Where

- U, U_d - displacement of primary mass and damper.
- \dot{U}, \dot{U}_d - Velocity of primary mass and damper.
- \ddot{U}, \ddot{U}_d - acceleration of primary mass and damper.
- \dot{m} - mass ratio = m_d/m
- ξ, ξ_d - damping ration of the primary mass and damper
- ω, ω_d - Natural frequency of vibration of the primary mass and damper.

In case of pendulum type damper the mass is attached to the top floor by a massless spring and it oscillates like a pendulum during lateral loading. Movement of the floor excites the pendulum and the relative motion of the pendulum produces a horizontal force that opposes the floor motion. This action can be represented by an equivalent SDOF system that is attached to the floor, as indicated in Fig. 4. [Connor J.J. (2000)]

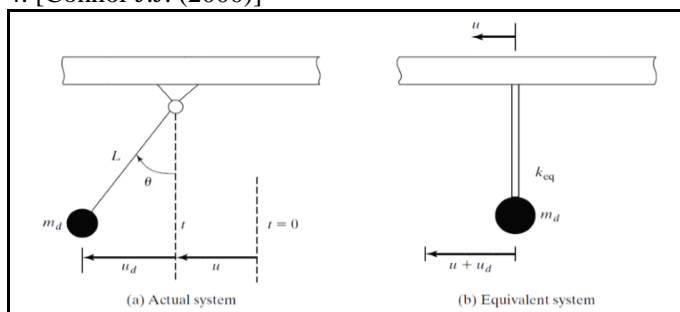


Fig. 5. A simple pendulum tuned mass damper, [Connor J.J.(2000)]

The eq of motion for the horizontal direction

$$T \sin \Theta + W_d/g (\dot{U} + \ddot{U}) = 0 \quad (3)$$

Where T is the tension in the cable and W_d is the weight of the damper. For very small value of Θ ,

$$U_d = L \sin \Theta = L\Theta \quad (4)$$

$$T \approx W \quad (5)$$

Putting these values in eq (1), we have

$$m_d \ddot{U}_d + (W_d/L) U_d = -m_d \ddot{U} \quad (6)$$

The equivalent shear spring stiffness is given by

$$K_{eq} = W_d/L \quad (7)$$

Hence the natural frequency of vibration of the pendulum

$$\omega_d^2 = K_{eq} / m_d = g/L \quad (8)$$

Natural time period of the pendulum

$$T_d = 2\pi \sqrt{L/g} \quad (9)$$

4. EXPERIMENTAL OBSERVATIONS

The three storey model is first analyzed in the shake table by introducing a harmonic excitation of $1 \sin \omega t$, ω ranging from 0 Hz to 15 Hz. Displacement, velocity and acceleration responses of the structure are recorded for each vibration.

The model is then analyzed by introducing an extra mass of 1 kg (7% of the building mass) at central and eccentric positions and by giving the same harmonic excitation. Different responses at different floor levels are then recorded.

In this case an attempt has been made to use the 1 kg weight as a tuned mass damper to reduce the response of the structure at its first mode. A pendulum type TMD is used for this purpose with a weight of 1 kg. Optimization for the TMD is done analytically and it is found that for the 1 kg weight to act optimally, the length of suspension should be 40 mm. the frame with the optimized TMD is then analyzed with the same vibrations and different responses are recorded. Reduction in different responses due to the optimized TMD are then compared and plotted.

5. OPTIMISATION OF THE TMD

Optimization of the pendulum type TMD:

Different parameters for the frame under consideration

Mass matrix, $M = \begin{bmatrix} 4.4 & 0 & 0 \\ 0 & 4.4 & 0 \\ 0 & 0 & 4 \end{bmatrix}$ kg

Stiffness matrix, $K = \begin{bmatrix} 17.1 & -8.85 & 0 \\ -8.85 & 17.7 & -8.85 \\ 0 & -8.85 & 8.85 \end{bmatrix}$ N/m

$\omega_n = \begin{bmatrix} 3.05 \\ 8.65 \\ 12.60 \end{bmatrix}$ cycl/sec = $\begin{bmatrix} 19.15 \\ 54.32 \\ 79.13 \end{bmatrix}$ rad/sec

From the eigenvalue problem, $[K - \omega^2 M] \phi = 0$ we can find out the modal mode shapes.

Mass normalized modal matrix

$\phi = \begin{bmatrix} 1.62 & -.355 & .215 \\ .290 & -.315 & -.403 \\ .350 & .04 & .143 \end{bmatrix}$

Modal mass, $m_j = \phi^T M \phi$

$m_1 = \phi_1^T M \phi_1 = 0.99$ kg

Equivalent SDOF mass parameter for mode 1 having the weight at node 3 is

$M_{1e} = m_1 \phi_{13}^2 = 0.9982 / 0.35^2 = 8.14$ kg

Therefore, mass ratio of the system,

$\bar{m} = m_d / M_{1e} = 0.12$

Based on the numerical formulae, J.J. Connor, prepared following charts between mass ratio and optimum frequency ratio. From the curve by extrapolating the values one can find the optimum frequency ratio for a mass ratio of 0.12.

The value of ξ is found out experimentally by logarithmic decrement method. A free vibration is 1st applied to the structure and then the decrease in response per cycle of vibration is measured. By using logarithmic decrement method ξ is found to be 0.057.

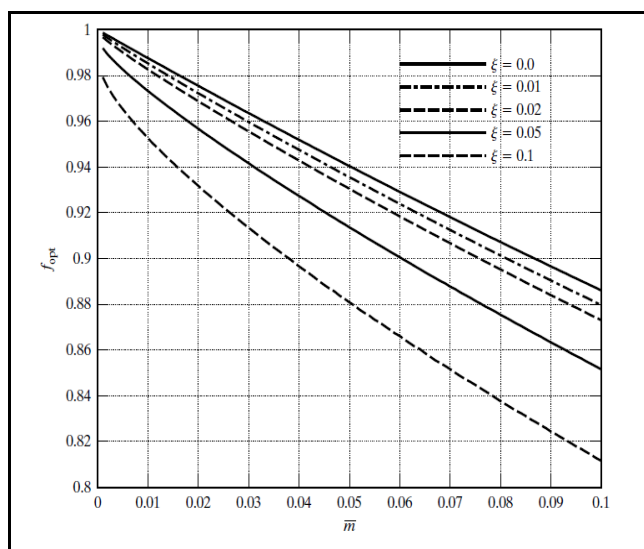


Fig. 6. Optimum tuning frequency ratio for TMD, f_{opt} , [Connor J.J. (2000)]

From the above plot we found that, $f_{opt} = 0.85$
Again, $f_{opt} = \omega_d / \omega_1$

$\omega_d = \omega_1 \times f_{opt}$
 $= 0.85 \times 19.15 = 16.27$ rad/sec

For a pendulum type damper

$\omega_d^2 = g / L$
 $L = 9.81 / 16.27^2 = 0.03705$ m = 37.05 mm

Hence for the 1kg mass to act optimally, the length of the cable should be 37 mm. For convenience a cable length of 40 mm is taken for the study.

6. RESULTS AND DISCUSSIONS

Different responses of the frame with the optimized Tuned Mass Damper are then compared with that of the frame without any TMD. The reduction in displacement, drift, velocity and acceleration responses of the top storey can be computed from the following graphs from Fig. 7 to Fig. 10.

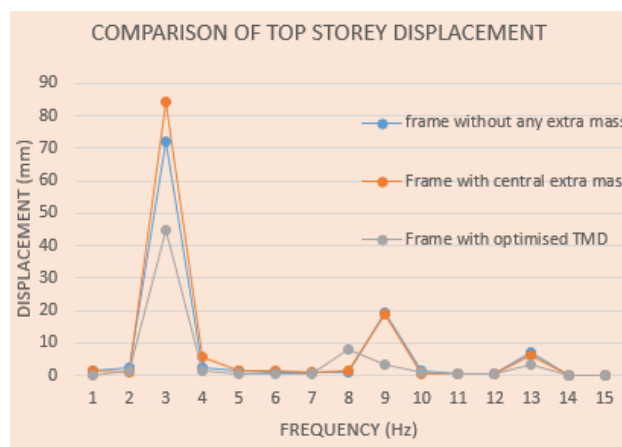


Fig. 7. Comparison of top storey displacement

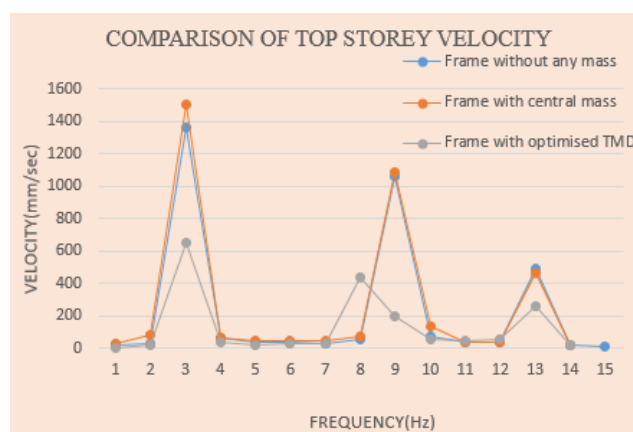


Fig. 8. Comparison of top storey velocity

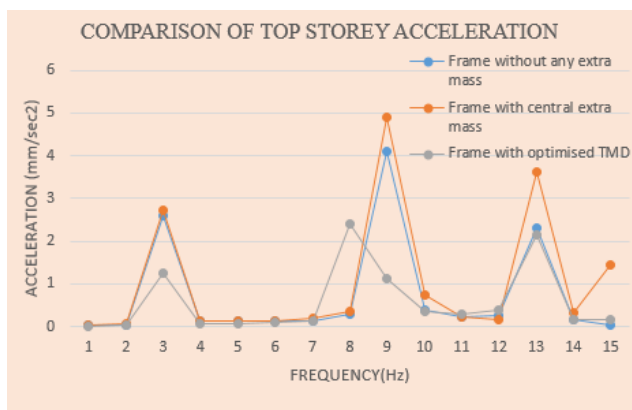


Fig. 9. Comparison of top storey acceleration

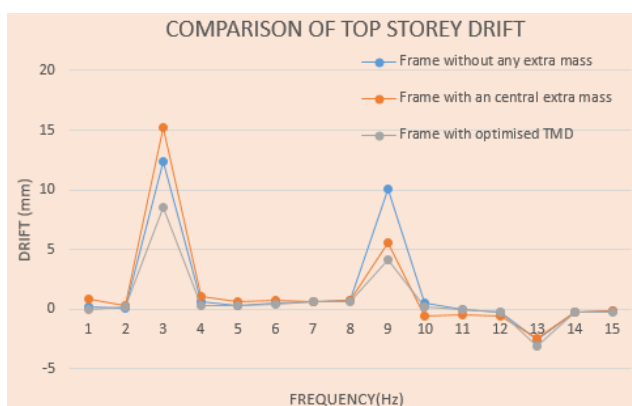


Fig. 10. Comparison of top storey drift

By placing the extra mass at an eccentric position for the frame with and without TMD, the reduction in lateral movement can be computed. Fig. 11 represents the reduction in lateral movement of the top storey of the frame (under eccentric loading) due to the incorporation of the TMD.

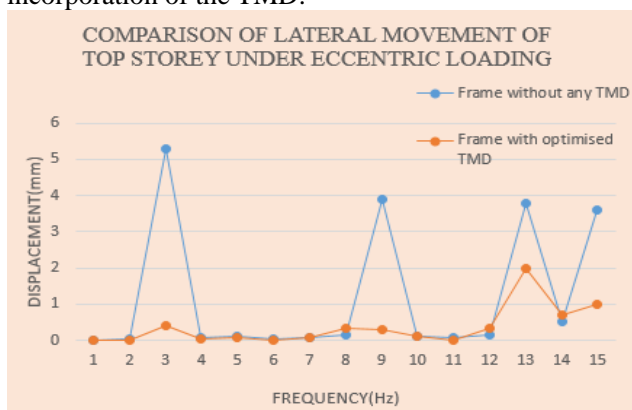


Fig. 11. Comparison of lateral movement of top storey

7. CONCLUSION

The effect of tuned mass damper in reducing different responses of a building structure was studied experimentally. A three storey shear frame model was analyzed without any damper and then with an optimized TMD. Optimization of the TMD parameters

for the model frame was done by direct method. The two frames were analyzed considering three different loading conditions as already explained. Performance of the TMD under a harmonic excitation is recorded and graphs were plotted for different parameters. From the respective plots it is observed that the introduction of an optimized pendulum TMD results in a reduction of 38% of top storey displacement, 53% of top storey velocity and 52% of top storey acceleration of the frame under the harmonic excitation. Reduction in drift was 50% of top storey drift. When the frame was eccentrically loaded the introduction of the TMD results in a reduction of 90% of the torsional vibration.

REFERENCES

1. Banerjee Susanta, "Inelastic Seismic Analysis of Reinforced Concrete Frame Building with Soft Storey", 2014; International Journal of Civil Engineering Research, Volume 5, Number 4, pp. 373-378, ISSN 2278-3652.
2. Biradar. Umesh. R and Mangalgi Shivaraj "Seismic response of reinforced concrete structure by using different bracing systems", 2013, International Journal of Research in Engineering and Technology, eISSN: 2319-1163, pISSN: 2321-7308 Cheju, Korea, August 23-25.
3. Chopra A.K., "Dynamics of Structure", 2007, PEARSON prentice Hall, pp.450-478.
4. Clough, J.W. & Penzien, J. "Dynamics of Structures", 1993 2nd Edition, McGraw-Hill.
5. Connor J.J. "Introduction to Structural Motion Control", 2000, Prentice Hall Pearson Education, Inc, pp.01-330.

[Back to table of contents](#)

Effects of Silica Fume on the Strength and Durability Properties of Concrete

Salim Barbhuiyaⁱ⁾ and Muneeb Qureshiⁱⁱ⁾

i) Lecturer, Department of Civil Engineering, Curtin University Australia.

ii) Provincial Construction Engineer, IMC Worldwide Ltd. UK.

ABSTRACT

This paper presents the effects of silica fume on compressive strength, splitting tensile strength, resistance against chloride penetration and water absorption of concrete. Results indicated that the use of silica fume in concrete increased the compressive strength of concrete. Increase in water-binder ratio reduced the compressive strength of concrete irrespective of the use of silica fume. Silica fume had no noticeable effect on the splitting tensile strength of concrete. The resistance against chloride ion penetration increased with the increase in the contents of silica fume in concrete. A reduction in water-binder ratio (from 0.35 to 0.30) increased the ability of the concrete to resist chloride ion's penetration. The introduction of silica fume in concrete reduced the water absorption capacity of concrete. A change in water-binder ratio also dramatically reduced the water absorption of concrete.

Keywords: strength; durability; silica fume; superplasticiser; sorptivity

1. INTRODUCTION

Silica fume (SF) is a by-product of the silicon and ferrosilicon industry. Until the mid 70s, nearly all the silica fume was discharged into the atmosphere. After environmental concerns necessitated the collection and landfilling of silica fume, it became economically justified to use it in various applications. Silica fume has a very high content of amorphous silicon dioxide and consists of very fine spherical particles, approximately 100 times smaller than the average cement particles. Due of its extreme fineness and high silica content, silica fume is a highly effective pozzolanic material (Siddique, 2011). The reaction mechanism of silica fume in concrete can be described basically under three roles: (i) pore-size refinement and matrix densification, (ii) reaction with free-lime, and (iii) cement paste–aggregate interfacial refinement. In concrete the characteristics of the transition zone between the aggregate particles and cement paste play a significant role in the cement-aggregate bond. The addition of silica fume reduces the thickness of the transition zone. This improves the mechanical properties and durability of concrete.

When silica fume is added to concrete, it results in a significant change in the compressive strength of the mix. This is mainly due to the aggregate-paste bond improvement and enhanced microstructure. Researchers (Wong & Razak (2005); Poon et al., 2006; Behnood & Ziari (2008)) observed that silica fume did not produce an immediate strength enhancement; instead, the blended mixes only achieved higher strength than the control from 7 days onwards. Strength loss in the early ages, which was proportional to the cement

replacement level, was probably due to the dilution effect of the pozzolan and the slow nature of pozzolanic reaction.

Gonen and Yazicioglu (2007) studied the capillary absorption of concrete by adding silica fume and fly ash in concrete mixes. The replacement levels of fly ash and silica fume were kept at 15% and 10%, respectively. The authors observed that the capillary absorption of concrete decreased with the addition of silica fume. As silica fume is very fine, pores in the bulk paste or in the interfaces between aggregate and cement paste is filled by these mineral admixtures. Hence, the capillary pores are reduced. Significant reduction in the chloride-ion diffusion in silica fume concretes was observed by other researchers (Gjrov, 1993). The main reason that could be attributed to reduced permeability is that addition of silica fume caused considerable pore refinement i.e. transformation of bigger pores into smaller one due to their pozzolanic reaction concurrent with cement hydration. By this process, the permeability of hydrated cement paste and porosity of the transition zone between cement paste and aggregate were reduced.

This paper presents the results of an investigation on the strength and durability properties of concrete containing silica fume. The strength properties studied include both the compressive and splitting tensile strength, whereas the durability properties studied include RCPT and water absorption.

2. EXPERIMENTAL PROGRAMME

2.1 Materials

Cement powder used was a General Purpose Grey Portland Cement supplied by Cockburn Cement of Western Australia. Silica fume was Rheomac SF 100 and was supplied by BASF Chemicals in Perth. Typical chemical composition of cement and silica fume are given in Table 1. The superplasticiser used was Glenium 79, a polycarboxylate-based ether hyper-plasticiser. The solids content is approximately 38%. The coarse aggregates used had a maximum size of 10mm and fine aggregates used were natural sand. The details of various mixes are given in Table 2.

Table 1: Chemical composition of cement and silica fume

Oxides (%)	OPC	Silica fume
SiO ₂	21.1	97.8
Al ₂ O ₃	4.7	-
Fe ₂ O ₃	2.8	-
CaO	63.8	-
MgO	2.0	-
SO ₃	2.5	0.3
LOI	2.1	1.4
Chloride	0.01	0.02
Na ₂ O Equivalent	0.50	0.001

Table 2: Mix proportions

MIX ID	OPC (%)	SF (%)	SP (%)	W/B	Slump (mm)
OPC100SF0-0.30	100	0	0	0.30	70
OPC90SF10-0.30	90	10	1.0	0.30	70
OPC85SF15-0.30	85	15	1.5	0.30	60
OPC100SF0-0.35	100	0	0	0.35	65
OPC90SF10-0.35	90	10	0.35	0.35	60
OPC85SF15-0.35	85	15	0.50	0.35	60

2.2 Test Methods

The compressive strength of concrete was determined in accordance to AS1012.9-1999. Splitting tensile strength test was carried out as per AS1210.10-2000. The Rapid Chloride Permeability Test (RCPT) was done according to ASTM 1202-12. This test was done to get an indication of the resistance to the penetration of chloride ions through the concrete sample. The water absorption test was carried out to evaluate the rate of absorption of the concrete samples within a time schedule in accordance with ASTM 1585-13.

3. RESULTS AND DISCUSSION

3.1 Compressive strength of concrete

Figure 1 presents the compressive strength of concrete containing silica fume at a water-binder ratio of 0.30. As can be seen, the use of silica fume increases the compressive strength of concrete with the passage of time. Whilst comparing concretes with 0% and 10% silica fume contents, marginal difference in compressive strengths can be observed. However, significant difference can be perceived in case of comparing 10% and 15% silica fume content

concrete's. It can be concluded that increase in contents of silica fume increases the compressive strength development of concrete. There is an increase of 17% in compressive strength development of concrete with 15% silica fume contents after 56 days when compared with the reference concrete and an increase of 13% when compared with concrete containing 10% silica fume.

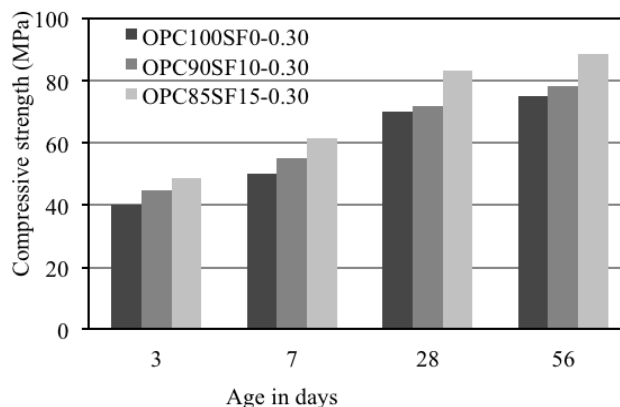


Fig. 1: Compressive strength of concrete containing silica fume at W/B= 0.30

Figure 2 shows the compressive strength of concrete containing silica fume at water-binder ratio of 0.35. It can be observed that the increase in water-binder ratio decreases the overall strength of concrete. Consequently, 0.05 increment in water-binder ratio decreased the compressive strength of concrete containing 15% silica content by 27% and for reference concrete and concrete containing 10% silica fume content, this strength reduced by 46% and 28% respectively after 56 days of casting the concretes. Though, same pattern of increase in compressive strength development was also observed when comparison is made for concrete with 15% silica fume with the reference concrete and concrete with 10% silica fume.

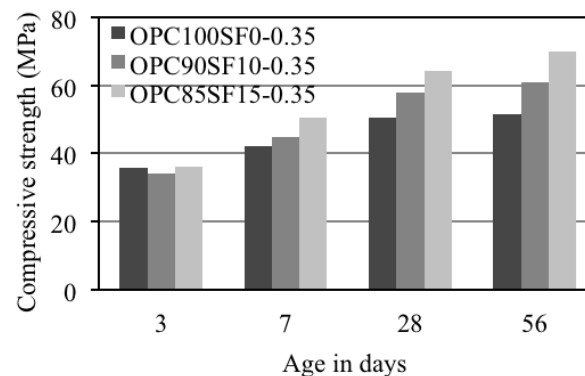


Fig. 2: Compressive strength of concrete containing silica fume at W/B= 0.35

3.2 Tensile strength of concrete

Results of splitting tensile strength of concrete with varying percentages of silica fume at water-binder ratio of 0.30 is shown in Fig. 3. No significant increase in splitting tensile strength was noticed after the use of silica fume content up to 15%. At 28 days, same strengths were observed for concrete mixes with 10% and 15% silica fume contents. Even after 56 days, splitting tensile strength of concrete with 15% silica fume was observed to be 6.45 MPa, which is 7.5% more than the reference concrete and about 4% more than the concrete with 10% silica fume contents.

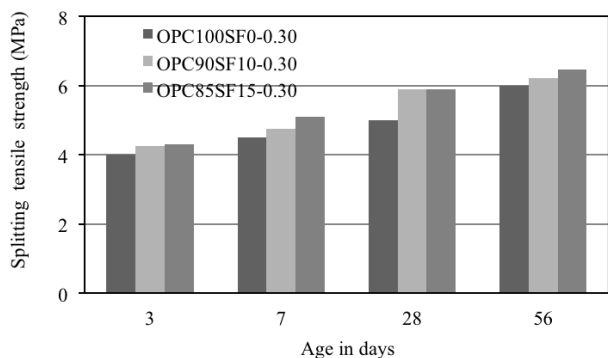


Fig. 3: Splitting tensile strength of concrete containing silica fume at W/B= 0.30

Figure 4 shows the splitting tensile strength of concrete at water-binder ratio of 0.35. It can be seen that in the beginning nearly same strengths were achieved for reference concrete, concrete with 10% and 15% silica contents. However, pronounced improvement in strengths of concrete with varying silica fume contents than reference concrete were observed after 28 days of casting. It was also observed that the difference in strengths between 10% and 15% silica fume contents become marginal after 56 days of casting the concrete. Hooton (1993) examined splitting tensile strengths of silica fume concretes up to the age of 182 days and determined that except at 28 days, splitting tensile strengths of concrete mixes containing silica fumes decreases with increase in concentration of silica fumes in the concrete mixes. Bhanja and Sengupta (2005) also reached on the conclusion that increase in the use of silica fume as a replacement in concrete mixes did not significantly increase the splitting tensile strengths of concrete, rather this became insignificant beyond 15%.

3.3 Rapid Chloride Penetration Test

Figure 5 presents the result of chloride ion penetration resistance of concrete mixes with 0%, 10% and 15% silica fume contents at two water-binder ratios (0.30 and 0.35). It can be seen that the resistance against chloride ion penetration increased with the increase in the contents of silica fume in concrete.

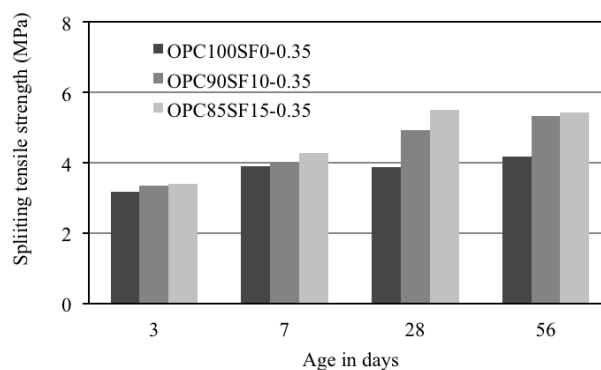


Fig. 4: Splitting tensile strength of concrete containing silica fume at W/B= 0.35

Concrete mix prepared without silica fume at a water-binder ratio 0.30 was 350% less capable of resisting chloride ion when comparison is made with concrete mix with 10% silica fume content and this competence enhances up to 830% when compared with concrete mix with 15% silica fume contents. Water-binder ratio further enhanced concrete's ability to resist chloride ion penetration. It is evident that a reduction in water-binder ratio (from 0.35 to 0.30) increased the ability of the concrete to resist chloride ion's penetration by 35% in concrete without any silica fume content. In the case of concrete mixes with 10% and 15% silica fume contents, this was up to 102% and 150% respectively. Therefore, it can be concluded that presence of silica fume in concrete increased the ability to resist chloride ion penetration. However, reduction in water-binder ratio also enhanced its aptitude to resist the penetration of chloride ions. Similar findings have been reported by Bagheri et al., (2012).

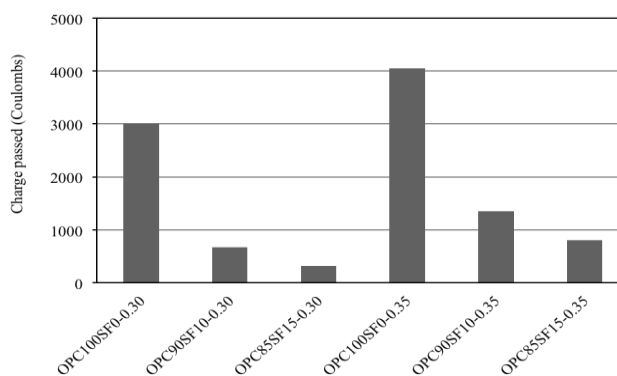


Fig. 5: Chloride penetration resistance of concrete containing silica fume

3.4 Water absorption

The rate of absorption of water (also termed as sorptivity) by concrete is shown in Fig. 6. As can be seen the introduction of silica fume in concrete reduces the water absorption capacity of concrete. At water-binder ratio of 0.30, water absorption of standard

concrete observed to be 0.03%, though it gradually reduces with increase in dosage of silica fume in the concrete. At 10% and 15% silica fume content in the concrete, water absorption capacity reduced by 17% and 40% respectively. It can also be observed that a change in water-binder ratio dramatically reduces the water absorption of concrete. When water-binder ratio was increased from 0.30 to 0.35, there was an increase of 44% in water absorption of reference concrete, 40% increase in concrete mix with 10% silica fume and 21% increase in concrete with 15% silica fume. Chahal et al., (2012) performed water absorption test at 28 days and 91 days and found drastic reduction in water-absorption of concrete mixes containing silica fume. Concrete mix with 5% silica fume had 0.30% water absorption at 28 days and this capacity further reduced to 0.10% at 91 days. This effect was most pronounced in concrete with 10% silica fume.

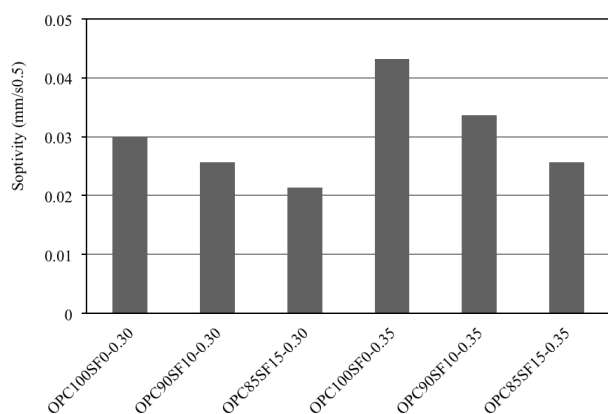


Fig. 6: Sorptivity of concrete containing silica fume

4. CONCLUSIONS

Based on this research, the following conclusions can be made:

- (i) The use of silica fume in concrete mixes increases the compressive strength of concrete. Increase in water-binder ratio reduces the compressive strength of concrete irrespective of the use of silica fume.
- (ii) Silica fume has no noticeable effect on the splitting tensile strength of concrete.
- (iii) The resistance against chloride ion penetration increases with the increase in the contents of silica fume in concrete. A reduction in water-binder ratio (from 0.35 to 0.30) increased the ability of the concrete to resist chloride ion's penetration
- (iv) The introduction of silica fume in concrete reduces the water absorption capacity of concrete. A change in water-binder ratio also dramatically reduces the water absorption of concrete.

REFERENCES:

- AS 1210.10-2000 Methods of testing concrete - Determination of indirect splitting tensile strength of concrete cylinders. Standards Australia
- AS 1012.9-1999 Methods of testing concrete - Determination of the compressive strength of concrete specimens. Standards Australia
- ASTM 1202-12 Standard Test Method for Electrical Indication of Concrete's Ability to Resist Chloride Ion Penetration
- ASTM 1585-13 Standard Test Method for Measurement of Rate of Absorption of Water by Hydraulic-Cement Concretes
- Bagheri AR, Zanganeh H, Moalemi MM. Mechanical and durability properties of ternary concretes containing silica fume and low reactivity blast furnace slag. *Cement and Concrete Composites* 2012; 34: 663–670.
- Behnood, A., Ziari, H., Effects of silica fume addition and water to cement ratio on the properties of high-strength concrete after exposure to high temperatures. *Cem. Concr. Compos.* 30(2), 106–112 (2008)
- Bhanja, S., Sengupta, B., Influence of silica fume on the tensile strength of concrete. *Cem. Concr. Res.* 35(4), 743–747 (2005)
- Chahal N, Siddique R, Rajor A. Influence of bacteria on the compressive strength, water absorption and rapid chloride permeability of concrete incorporating silica fume. *Construction and Building Materials* 2012; 37:645–651.
- Gjrov, O.E., Durability of concrete containing condensed silica fume. *ACI Special Publications SP-79*, pp. 695–708 (1993)
- Gonen, T., Yazicioglu, S., The influence of mineral admixtures on the short and long-term performance of concrete. *Build. Environ.* 42, 3080–3085 (2007)
- Hooton, R.D., Influence of silica fume replacement of cement on physical properties and resistance to sulfate attack freezing and thawing, and alkali-silica reactivity. *ACI Mater. J.* 90(2), 143–152 (1993)
- Poon, C.S., Kou, S.C., Lam, L., Compressive strength, chloride diffusivity and pore structure of high performance metakaolin and silica fume concrete. *Construct. Build. Mater.* 20(10), 858–865 (2006)
- Siddique, R., Utilization of silica fume in concrete: Review of hardened properties, *Resource, Conservation and Recycling* 2011; 55: 923–932.
- Wong, H.S., Razak, H.A., Efficiency of calcined kaolin and silica fume as cement replacement material for strength performance. *Cem. Concr. Res.* 35(4), 696–702 (2005)

[Back to table of contents](#)

Development of analytic model for determining the mechanical factor of coir fiber reinforced soil using genetic programming

Prashant Kumar Sharma ⁱ⁾, Harsha Vardhan ⁱⁱ⁾ and Ankit Garg ⁱⁱⁱ⁾

i) 3rd Year Undergraduate, IIT Guwahati, Assam 781039, India

ii) 4th Year Undergraduate, IIT Guwahati, Assam 781039, India

iii) Assistant Professor, Department of Civil Engineering, IIT Guwahati, Assam 781039, India

ABSTRACT

Coir fiber is a natural fiber extracted from the husk of coconut and used in products such as floor mats, doormats, brushes, and mattresses. Efforts are underway to use the coir in soil reinforcement. Unconfined compressive strength (UCS) of soil is the quickest way of judging the representative strength of soil used in geotechnical infrastructures. In, recent years' various analytical models have been developed to estimate UCS. However, relatively few studies to model the mechanical properties of coir-reinforced soil have been undertaken. In this study, the improvement in strength parameter of coir fiber reinforced soil has been discussed with a parameter proposed as mechanical factor, which is defined as the ratio of UCS of coir-reinforced soil to the unreinforced soil strength. The model was developed based on three experimentally obtained input parameters viz. coir content, soil density and moisture content. To find out mechanical factors, a series of laboratory tests were conducted to estimate UCS of both coir reinforced soil and unreinforced soil. Evolutionary algorithm of Genetic Programming (GP) was then used to develop model based on these measured data. The hidden non-linear relationships between mechanical factor and the three inputs were determined by sensitivity and parametric analysis of the GP model. The holistic GP model will be helpful to infield engineers to provide optimum input values for design and analysis of various geotechnical infrastructures.

Keywords: UCS, Mechanical factor, coir fiber, genetic programming

INTRODUCTION

Unconfined compressive strength (UCS) is a reliable mechanical parameter that can be used to judge the representative strength for the initial design and analysis of various geotechnical infrastructures such as subgrade soil in pavement, bearing capacity of shallow foundations and dams (Consoli et al., 1998; Maher and Ho, 2004; Cai et al., 2006; Kumar et al., 2006; Park 2009). Peak UCS is determined from the stress-strain response of the reinforced soil sample subjected to compression loading as suggested by ASTM D-2166 (2013). In recent years' researchers studied the effect of natural and synthetic fibers on strength of soil. In the past few years, researchers have propagated the use of natural and synthetic fibers for reinforcing soil and increasing its strength (Maher and Ho; 1994; Kaniraj and Gayathri, 2003; Babu et al., 2008; Chauhan et al., 2008; Ashour and Wu, 2010). UCS of reinforced soil is known to be influenced by fiber content, type of fiber as well as soil parameters such as soil moisture content and soil density (Maher and Ho, 1993; Consoli et al., 1998; Kaniraj and Havanagi, 2001; Consoli et al., 2003; Kaniraj and Gayathri, 2003; Tang et al., 2007; Babu et al., 2008; Chauhan et al., 2008). Any change in

these parameters can vary UCS which could influence the stability calculations for foundations in various geotechnical infrastructures (Tomlinson and Boorman, 2007).

In recent years, alternative approach such as soft computing methods are becoming very popular owing to its robustness to formulate models for estimation of soil properties (Ghaboussi et al., 1991; Ellis et al., 1995; Lee et al., 2003; Attoh-Okine, 2004; Dutta et al., 2015). have been developed to estimate soil strength of fiber reinforced soil but these models rarely capture the effects of soil parameters (soil moisture content; soil density) as well as fiber content (%) for a particular fiber type. The best route to understand the effects of soil parameters and fiber content is to formulate the UCS models with factor of change in strength (ratio of UCS strength of soil reinforced and UCS of unreinforced soil) due to inclusion of natural fiber as an output and soil density, soil moisture content and fiber content as input. The ratio of UCS strength of soil reinforced to UCS of unreinforced soil is termed as Mechanical Factor. Mechanical factor is the scale of increase in strength of soil on inclusion of fiber.

Present study demonstrates the use of Genetic programming (GP) to formulate the functional

relationship between mechanical factor (change in strength of coir reinforce soil) and other three parameters of soil. This model can be used to optimize the input parameters for deriving maximum advantage of soil reinforced with fibers.

Experimental study on effects of density, soil moisture and fiber content on UCS of fiber reinforced soil

Series of UCS tests were conducted to measure compressive strength of both unreinforced and reinforced soil. Tests were performed based on procedures prescribed in ASTM D-2166 (2013). Details on soil parameters, fiber selection, testing programme and procedures as well as results are provided as follows. The soil used in this study was red soil, commonly found in North Eastern part of India. Grain size distribution of the soil was determined using procedures prescribed in IS-2720-Part 4-1985. It is constituted mainly of silt (50%), sand (24%) and clay (24%) respectively. Consistency limit of the soil determined according to IS-2720-Part 5 (1985) gave liquid limit and plastic limit as 40.50% and 24.81%, respectively. The USCS classification of soil is silty sand (ASTM, D2487-11). Standard Proctor's light compaction technique was used to determine its maximum dry density (MDD) and optimum moisture content (OMC) according to procedures prescribed in Indian Standard code IS-2720 part-7 (1980). MDD and OMC were found to be 1.7 g/cc and 17% respectively. Table 1 summarizes the index and engineering properties of the soil. Coir fiber is selected as reinforced material for soil specimen. UCS tests were conducted on both unreinforced and reinforced soil-polypropylene composite at different compaction states corresponding to three soil densities (0.95 MDD, MDD and 1.05 MDD) and three moisture contents (OMC, OMC - 5% and OMC + 5%). In addition, the influence of variation in % fiber content (0.5%, 0.75% and 1% by dry weight of soil) on UCS was also investigated. The fiber percentage was restricted to 1% as the fibers tend to stick to each other while mixing thereby forming pockets of low density. For each case, tests were repeated three times (total 108 tests including unreinforced soil) to check any variability in observed UCS. All UCS tests were conducted at a constant strain rate of 1.25 mm/minute as suggested in IS-2720 part-10 (1991).

Data preparation for training of GP model

Experimental results from 81 tests are summarized in table 1. It consists of three input parameters (moisture content(%) as x_1 , density(g/cc) as x_2 , fibre content(%) as x_3) and one output (mechanical factor). Total of 81 set of data samples were obtained from the experiment as discussed in this section. Out of 81 data set we classify the data into two phase training phase and testing phase. Training phase normally consists of 80% of data set and the rest of points are called testing phase. Firstly, model is formulated on training data and tested on testing data.

In the following section, the evolutionary approach of genetic programming is discussed.

Evolutionary approach of Multi-gene Genetic Programming

The GP algorithm is related to Darwinian principle of "Survival of the fittest" (Koza 1992). In GP, genes are evolved and every gene is considered as a model. As the theory of Darwin proposed the survival of the best like this GP also provides the best possible model on the given set of data. Uniqueness of MGGP is new genes are evolved by defined combination of the old genes or models (by cross over, mutation, reproduction) and finally best model or gene can be chosen. In order, to apply GP, several steps needed to be followed in a proper sequence. Firstly, the elements of functional and terminal set are chosen based on the problem. The elements chosen in the functional set are arithmetic operators (+, -, /, ×) and non-linear functions (sin, cos, tan, exp, tanh, log). Sometime complexity of model increases as the number of functional set increases so it's better to choose what type of function to be used based upon the data to avoid complexity. The range of random constants chosen is -10 to 10. The combination of functional set, terminal set, input data forms a Gene. In this way, several genes are evolved and combined by least squares method to form a model. The number of models is represented by population size. The performance of the models in the initial population is evaluated based on the fitness function such as root mean square error (RMSE) given by

$$RMSE = \sqrt{\frac{\sum_{i=1}^N |G_i - A_i|^2}{N}} \quad (1)$$

where, N is number of training samples, A_i and G_i are actual and predicted values. If any individual of the population does not satisfy the termination criterion, then new population evolve by combining genetic operations such as selection, subtree crossover and subtree mutation are implemented on the individual. Maximum number of generations or the threshold error of the model as specified by the user is termed as termination criterion. Genetic operations, mainly crossover and mutation, form most of the individuals of the population. In this way, genetic operations on the initial population consequently form a new population. As per Koza (1992), the probabilities of crossover, mutation and reproduction is chosen at 85%, 5% and 10% respectively. The iterative process of forming new populations continues until a termination criterion is met.

RESULTS AND DISCUSSION

The parameter settings for MGGP is set based on

trial-and-error approach. The population size of 300, generations of 350, maximum number of genes at 6, functional set including elements of tanh, tan, exp, sin, plog, square, cos, addition, subtraction, times is chosen. The terminal set depends on the set of the three inputs (density, moisture and fiber content of soil). The number of runs chosen in the study is 1. Minimum training error from all runs decide the best MGGP model. In this case best MGGP model is equation 3. Correlation coefficient, mean absolute percentage error (MAPE) and RMSE are the evolutionary factor for the performance of best model and these factors are given by :

$$R^2 = \left(\frac{\sum_{i=1}^n (A_i - \bar{A}_i)(M_i - \bar{M}_i)}{\sqrt{\sum_{i=1}^n (A_i - \bar{A}_i)^2 \sum_{i=1}^n (M_i - \bar{M}_i)^2}} \right)^2 \tag{2}$$

$$MAPE(\%) = \frac{1}{n} \sum_i \left| \frac{A_i - M_i}{A_i} \right| \times 100 \tag{3}$$

where M_i and A_i are the predicted and actual values respectively, \bar{M}_i and \bar{A}_i are the average values of the predicted and actual respectively and n is the number of training samples.

The statistical fit of the model on the training and testing data is shown in Fig 1 and Fig 2. Table 1 shows the values of correlation coefficient, MAPE and RMSE. The ability of model to capture dynamics of the phenomenon with a high prediction accuracy is indicated by higher values of correlation coefficient and lower values of MAPE and RMSE.

FOS_{MGGP}=

$$-4.239 + (-4.2262) * (\exp(\text{plog}(\text{plog}(\tan(\text{plog}(x2)))) - (\tan(\text{square}(x1)))))) + (0.50184) * (x1) + (0.27621) * (\cos(\text{plog}(0.125652)) - ((x2) * (x1))) + (0.0087246) * (\tan(\tan(x3)))$$

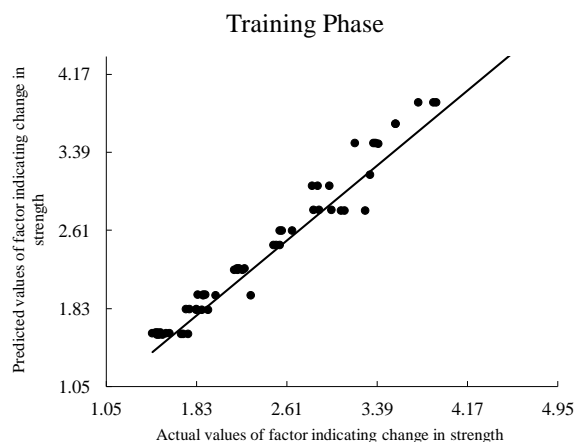


Fig 1. Fit of Predicted and actual values of factor of strength (reinforced/unreinforced strength) on training data

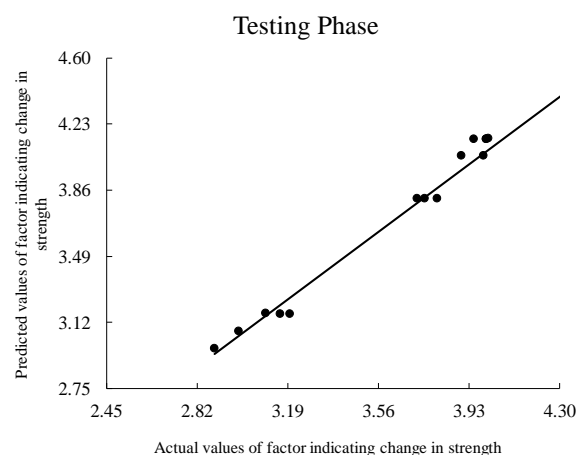


Fig. 2 Fit of Predicted and actual values of factor of strength (reinforced/unreinforced strength) on the testing data

Table 1 Error metrics for GP model

Error metrics	Training data	Testing data
R^2	0.90622	0.85862
MAPE	10.9925	8.190
RMSE	0.3302	0.3302

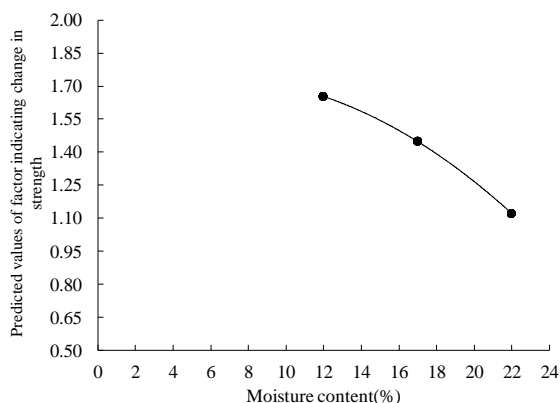


Fig 3. Variation of predicted value of mechanical factor with moisture content

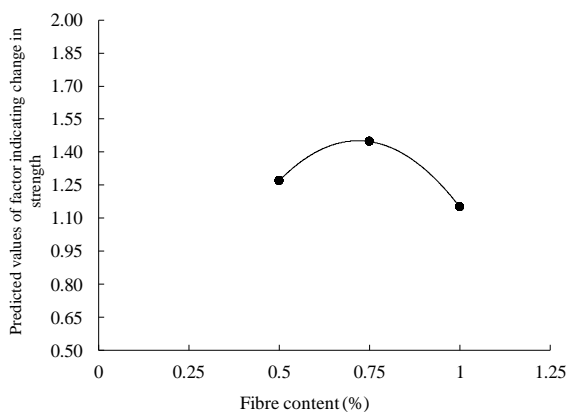


Fig 4 variation of predicted mechanical factor with fibre content

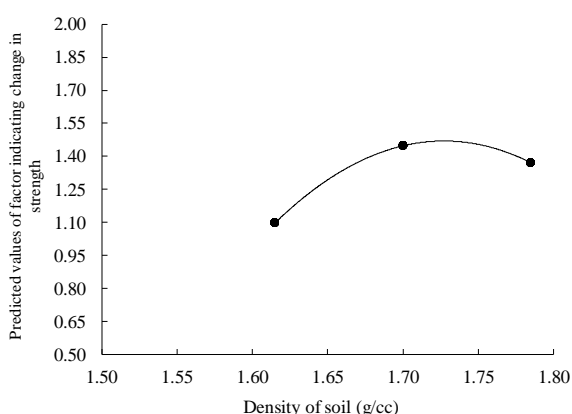


Fig 5. Variation of mechanical factor with density

Above figures shows the graphs plotted for strength factor with respect to each input. It is clear that the strength factor decreases with increase in moisture content of the soil and follows nonlinear relation with

respect to the other two inputs (density and fiber content). It is because as the moisture content increases reinforced strength rapidly as compare to unreinforced strength. For fiber content and density, there is an optimum value at which strength becomes maximum. As the fiber content increases beyond optimum value fibre-fibre interaction increases so cohesion decreases so it can be sheared easily. The behavior shown by soil for varying density only because of as the density increases particle-particle interlocking increases so its strength increases. But further increase in density does not show appreciable increase in mechanical factor. Thus parametric analysis, offers an understanding for selecting the appropriate values of inputs which maximizes the strength factor of soil reinforced with coir fiber. In this way, the GP model can be used to study the soil fiber reinforcement phenomenon effectively.

CONCLUSIONS

The new model for computing the mechanical factor (ratio of UCS of reinforced and unreinforced soil) based on the soil moisture, density and fiber content is proposed by this study. The predictions obtained from the formulated explicit model is able to satisfy the experimental data very well which can be seen in graphs. Formulated model can be used in predicting the value of mechanical factor within the input value with different values due to its higher generality of this model. This model will definitely save the money and time for the experts to predict mechanical factor. The formulated explicit GP model will be useful to determine optimum input values for achieving safe and strong bearing strata.

REFERENCE

1. ASTM D 2166 (2005). Test method for unconfined compressive strength of cohesive soil (ASTM D 2166).
2. ASTM D 2487-11 (2011). Standard Practice for Classification of Soils for Engineering Purpose (Unified Soil Classification System).
3. Attoh-Okine, N. O. (2004). Application of genetic-based neural network to lateritic soil strength modeling. *Construction and Building Materials*, 18(8), 619-623.
4. Cai, Y., Shi, B., Ng, C. W., & Tang, C. S. (2006). Effect of polypropylene fibre and lime admixture on engineering properties of clayey soil. *Engineering Geology*, 87(3), 230-240.
5. Consoli, N. C., Prietto, P. D., & Ulbrich, L. A. (1998). Influence of fiber and cement addition on behavior of sandy soil. *Journal of Geotechnical and Geoenvironmental Engineering*, 124(12), 1211-1214.
6. Crafter S.A, Njuguna S.G, Howard G.W., 1992, Wetlands of Kenya. Proceedings of the KWWG Seminar on Wetlands of Kenya, National Museums of Kenya, Nairobi, Kenya, 3-5 July 1991.
7. Dasaka, S. M., Sumesh, K. S., 2011. Effect of Coir Fiber on the Stress–Strain Behavior of a Reconstituted Fine-Grained Soil. *J Nat Fibers*,8(3), 189-204.
8. Dutta, R. K., Dutta, K., & Jeevanandham, S. (2015). Prediction of Deviator Stress of Sand Reinforced with Waste Plastic Strips Using Neural Network. *International*

- Journal of Geosynthetics and Ground Engineering, 1(2), 1-12.
9. Edinçliler, A., Cabalar, A. F., Cagatay, A., & Cevik, A. (2012). Triaxial compression behavior of sand and tire wastes using neural networks. *Neural Computing and Applications*, 21(3), 441-452.
 10. Ellis, G. W., Yao, C., Zhao, R., & Penumadu, D. (1995). Stress-strain modeling of sands using artificial neural networks. *Journal of geotechnical engineering*, 121(5), 429-435.
 11. Garg, A., and Jasmine Siu Lee Lam. "Improving environmental sustainability by formulation of generalized power consumption models using an ensemble based multi-gene genetic programming approach." *Journal of Cleaner Production* (2015), Volume 102, 1 September 2015, Pages 246–263.
 12. Garg, A., & Tai, K. (2012, June). Review of genetic programming in modeling of machining processes. In *Modelling, Identification & Control (ICMIC), 2012 Proceedings of International Conference on* (pp. 653-658). IEEE.
 13. APA Ghaboussi, J., Garrett Jr, J. H., & Wu, X. (1991). Knowledge-based modeling of material behavior with neural networks. *Journal of Engineering Mechanics*, 117(1), 132-153.
 14. Gosavi, M., Patil, K., 2004. Improvement of properties of black cotton soil subgrade through synthetic reinforcement. *J. Inst. Eng. (India), Part CV, Civil Engineering Division*, 84, 257-262.
 15. Güllü, H., Khudir, A., 2014. Effect of freeze–thaw cycles on unconfined compressive strength of fine-grained soil treated with jute fiber, steel fiber and lime. *Cold Reg. Sci. Technol*, 106, 55-65.
 16. Han, C., Wang, E., Xia, J., & Yun, S. (2015). Application of Multi-Gene Genetic Programming in Kriging Interpolation. *Journal of Geoscience and Environment Protection*, 3(05), 27.
 17. Hejazi, S. M., Sheikhzadeh, M., Abtahi, S. M., Zadhoush, A., 2012. A simple review of soil reinforcement by using natural and synthetic fibers. *Constr Build Mater*, 30, 100-116.
 18. Hengl, Tomislav, Gerard BM Heuvelink, and Alfred Stein. "A generic framework for spatial prediction of soil variables based on regression-kriging." *Geoderma* 120.1 (2004): 75-93.
 19. Hinchliffe, M., Hiden, H., McKay, B., Willis, M., Tham, M., & Barton, G. (1996). Modelling chemical process systems using a multi-gene. *Late Breaking Papers at the Genetic Programming*, 56-65.
 20. IS-2720 (Part 5), 1985, Determination of liquid and plastic limit, New Delhi: Bureau of Indian Standards publications.
 21. IS-2720 (Part10), 1991, Determination of unconfined compressive strength, New Delhi: Bureau of Indian Standards publications.
 22. IS-2720-(Part7), 1980, Determination of water content-dry density relation using light compaction. New Delhi: Bureau of Indian Standards publications.
 23. Jafari, A., Khademi, H., Finke, P. A., Van de Wauw, J., & Ayoubi, S. (2014). Spatial prediction of soil great groups by boosted regression trees using a limited point dataset in an arid region, southeastern Iran. *Geoderma*, 232, 148-163.
 24. Johari, A., Javadi, A. A., & Habibagahi, G. (2011). Modelling the mechanical behaviour of unsaturated soils using a genetic algorithm-based neural network. *Computers and Geotechnics*, 38(1), 2-13.
 25. Kaniraj, S. R., & Gayathri, V. (2004). Permeability and consolidation characteristics of compacted fly ash. *Journal of energy engineering*, 130(1), 18-43.
 26. Kanungo, D. P., Sharma, S., & Pain, A. (2014). Artificial Neural Network (ANN) and Regression Tree (CART) applications for the indirect estimation of unsaturated soil shear strength parameters. *Frontiers of earth science*, 8(3), 439-456.
 27. Khan, F. S., Azam, S., Raghunandan, M. E., Clark, R., 2014. *Compressive Strength of Compacted Clay-Sand Mixes*. *Adv. Mater. Sci. Eng.*, 2014.
 28. Khanlari, G. R., Heidari, M., Momeni, A. A., & Abdilor, Y. (2012). Prediction of shear strength parameters of soils using artificial neural networks and multivariate regression methods. *Engineering Geology*, 131, 11-18.
 29. Koza, J. R. (1992). *Genetic programming: on the programming of computers by means of natural selection* (Vol. 1). MIT press, USA.
 30. Lee, S. J., Lee, S. R., & Kim, Y. S. (2003). An approach to estimate unsaturated shear strength using artificial neural network and hyperbolic formulation. *Computers and Geotechnics*, 30(6), 489-503.
 31. Maher, M. H., & Ho, Y. C. (1994). Mechanical properties of kaolinite/fiber soil composite. *Journal of Geotechnical Engineering*, 120(8), 1381-1393.
 32. Methacanon, P., Weerawatsophon, U., Sumransin, N., Prahsarn, C., Bergado, D. T. (2010). Properties and potential application of the selected natural fibers as limited life geotextiles. *Carbohydrate Polymers*, 82(4), 1090-1096.
 33. Mirzahosseini, M., Najjar, Y. M., Alavi, A. H., & Gandomi, A. H. (2015). Next-Generation Models for Evaluation of the Flow Number of Asphalt Mixtures. *International Journal of Geomechanics*, 04015009.
 34. Mollahasani, A., Alavi, A. H., Gandomi, A. H., & Rashed, A. (2011). Nonlinear neural-based modeling of soil cohesion intercept. *KSCE Journal of Civil Engineering*, 15(5), 831-840.
 35. Patel, V. B., Patel, A. R., Patel, M. C., Madamwar, D. B., 1993. Effect of metals on anaerobic digestion of water hyacinth-cattle dung. *Appl. Biochem. Biotechnol.*, 43(1), 45-50.
 36. Patterson, D. W. (1998). *Artificial neural networks: theory and applications*. Prentice Hall PTR.
 37. Rowell, R. M., Stout, H. P., 1998. Jute and kenaf. *Handbook of fiber chemistry*, 466-502.
 38. Santoni, R. L., Tingle, J. S., Webster, S. L., 2001. Engineering properties of sand-fiber mixtures for road construction. *J Geotech Geoenviron*, 127(3), 258-268.
 39. Shoeb, F., Singh, H. J., 2000. Kinetic studies of biogas evolved from water hyacinth. *Proceedings of Agroenviron*.
 40. Tomlinson, M. J., & Boorman, R. (2001). *Foundation design and construction*. Pearson education.
 41. Vasques, G. M., S. J. O. S. Grunwald, and J. O. Sickman. "Comparison of multivariate methods for inferential modeling of soil carbon using visible/near-infrared spectra." *Geoderma* 146.1 (2008): 14-25.

[Back to table of contents](#)

Pile cap lateral resistance-statistical analysis

Dr. Utpal Kumar Nath

Assistant Professor, Department of Civil Engineering, Assam Engineering College, Guwahati-13, ukn.ce@aec.ac.in

ABSTRACT

The deep foundations consist of groups of piles coupled together by concrete pile caps. These pile caps, which are often massive and deeply buried, would be expected to provide significant resistance to lateral loads. However, practical procedures for computing the resistance of pile caps to lateral loads have not been developed, and, for this reason, cap resistance is usually ignored. Neglecting cap resistance results in estimates of pile group deflections and bending moments under load that may exceed the actual deflections and bending moments by a large amount. Advances could be realized in the design of economical pile-supported foundations and their behaviour more accurately predicted if the cap resistance can be accurately assessed.

Statistical analyses are performed on the data that are obtained from the model tests. Total 288 lateral load model tests are performed to observe this phenomenon. Two statistical modelling viz. Super Vector Machine (SVM) and M5P were done. Both these models with the experimental data were capable to predict the desired output i.e. lateral resistance of pile cap. But the difference of error of the predicted output and actual data found from the experimentation was minimum in M5P model compare to the SVM. Thus this statistical analysis indicates that the lateral pile cap resistance found from the experimentation is quite acceptable.

Keywords: statistical, pile cap, lateral-resistance, Super Vector Machine, M5P

1. INTRODUCTION

The deep foundations consist of groups of piles coupled together by concrete pile caps. These pile caps, which are often massive and deeply buried, would be expected to provide significant resistance to lateral loads. However, practical procedures for computing the resistance of pile caps to lateral loads have not been developed, and, for this reason, cap resistance is usually ignored. Neglecting cap resistance results in estimates of pile group deflections and bending moments under load that may exceed the actual deflections and bending moments by 100 % or more. Advances could be realized in the design of economical pile-supported foundation and their behaviour more accurately predicted if the cap resistance can be accurately assessed. An understanding of soil-pile-cap interactions and the mechanics of load transfer is necessary to develop a method that can be used to compute displacements, shears, and moments in pile groups. Research involving model tests, centrifuge tests, and full-scale tests has been conducted to study the lateral resistance of pile groups. However, of these studies only a few focus on the contribution of a pile cap with backfill soil to the lateral resistance. Of these limited studies, the results have shown that neglecting pile cap resistance may result in estimates of deflection and bending moment that are double the actual values (Mokwa and Duncan, 2001).

Predictive analytics is an area of statistical analysis that deals with extracting information from data and using it to predict potential trends and behaviour patterns. The core of predictive analytics relies on

capturing relationships between explanatory variables and the predicted variables from past occurrences, and exploiting it to predict future outcomes. It is important to note however that the accuracy and usability of results will depend greatly on the level of data analysis and the quality of assumptions.

The reliability of the findings from experimental study can be evaluated using statistical analysis. For a very large data sample, the regression and classification based methods perform better in all simulation scenarios, especially with homogeneous data sets, as data set found from the experimental study seems to be homogeneous.

The problem of observed data modelling is relevant to many engineering applications. In observed data modelling, a process of induction is used to build up a model of the system from which it is expected to deduce responses of the system. Thus the system able to predict probable trends and behaviour patterns. Ultimately the quantity and quality of the observations govern the performance of this empirical model.

Traditional neural network approaches have suffered difficulties with generalisation, producing models that can over fit the data. This is a consequence of the optimisation algorithms used for parameter selection and the statistical measures used to select the 'best' model. Osuna et. al. (1997) applied Super vector machines (SVM) to digital image classification for human face detection. Mukherjee et. al. (1997) and Muller et. al. (1997) used SVMs for non-linear time series predictions. Mattera and Haykin (1999) have also reported a successful application of SVMs for dynamic

reconstruction of a chaotic system.

The regression-based methods viz. Support Vector Machines (SVM) and M5P trees have been applied and compared under various simulation scenarios.

2 APPROACHES

This section describes the process that is to be followed to collect and analyze the experimental data. A classification task usually involves separating data into training and testing sets. Each instance in the training set contains one "target value" (i.e. the class labels) and several "attributes" (i.e. the features or observed variables). The goal of SVM is to produce a model (based on the training data) which predicts the target values of the test data given only the test data attributes.

Given a training set of instance-label pairs (x_i, y_i) , $i = 1, 2, \dots, l$ where $x_i \in \mathbb{R}^n$ and $y \in \{1, -1\}$, the support vector machines (SVM) (Boser et al., 1992; Cortes and Vapnik, 1995) require the solution of the following optimization problem.

$$\min_{w,b,\varepsilon} \frac{1}{2} w^T w + C \sum_{i=1}^l \varepsilon_i \quad \text{Subjected to}$$

$$y_i (w^T \phi(x_i) + b) \geq 1 - \varepsilon_i; \quad \varepsilon_i \geq 0$$

Here training vectors x_i are mapped into a higher (maybe infinite) dimensional space by the function ϕ . SVM finds a linear separating hyper-plane with the maximal margin in this higher dimensional space. $C > 0$ is the penalty parameter of the error term. Furthermore, $K(x_i, x_j) = \phi(x_i)^T \phi(x_j)$ is called the kernel function, which is a new one (Vapnik, 1995). But the basic Kernel functions are

- (1) Linear: $K(x_i, x_j) = x_i^T x_j$
- (2) Polynomial: $K(x_i, x_j) = (\gamma x_i^T x_j + \phi)^d, \gamma > 0$
- (3) RBF: $K(x_i, x_j) = \exp(-\gamma \|x_i - x_j\|^2), \gamma > 0$
- (4) Sigmoid: $K(x_i, x_j) = \tanh(\gamma x_i^T x_j + \phi)$

Here γ , ϕ and d are kernel parameters.

The general approaches of SVM are as follows.

- It has to be transformed data to the format of an SVM package.
- Conduct simple scaling on the data
- Consider the radial basis function (RBF) kernel
- Use cross-validation to find the best parameter C and γ
- Use the best parameter C and γ to train the whole training set.
- Finally test

An M5P tree is built in three stages (Wang and

Witten, 1997). These are as follows

- In the first stage a decision tree induction algorithm is used to build an initial tree.
- In the second stage of the tree construction process the tree is pruned back from each leaf.
- The last stage is called smoothing to remove any sharp discontinuities that exist between neighbouring leaves of the pruned tree.

Data available from the experimental study has to be gathered, prepare the data at the very beginning and then analyzed. In the data preparation phase select the relevant attributes from the available data, create meaningful groups within the attributes. This becomes useful for identifying those attributes that have the greatest influence on classification.

The parameter considered as input in both the approaches viz. SVMs and M5P are : (i) Number of pile in a group, (ii) Pile group spacing, (iii) Material used for piles, (iv) Length of pile, (v) Outer and inner diameter of pile and (vi) Position of pile cap which influences the lateral resistance of pile cap.

Model performance measures are essential in evaluating the predictive accuracy of the models. The predicted output i.e. pile cap lateral resistance from both SVMs and M5P after performing the steps mentioned above able to validate the consistency of the results found from the experimental study.

3 SVM AND M5P MODEL

Support Vector Machine (SVM) is a classification and regression method based on the concept of decision planes. SVM's initial introduction suffered from having to rely on quadratic programming solvers for training, a problem which has since been solved through the use of sequential minimal optimization (SMO). SVM makes use of a (nonlinear) mapping function that transforms data in input space to data in feature space in such a way as to render a problem linearly separable.

SVM is a relatively new machine learning technique originally developed by Vapnik (1998). The basic concept behind SVM is to solve a problem, i.e., classification or regression, without having to solve a more difficult problem as an intermediate step.

M5P trees are ordinary decision trees with linear regression models at the leaves that predict the value of observations that reach the leaf. The nodes of the tree represent variables and branches represent split values. Model tree induction algorithms derive from the divide-and-conquer decision tree methodology. Unlike classification trees, which choose the attribute and its splitting value for each node to maximize the information gain, model trees choose them to minimize the intra-subset variation in the class values down each branch and maximize the expected error reduction (standard deviation reduction). The fact that the tree structure divides the sample space into regions and a linear regression model is found for each of them

makes the tree somewhat interpretable.

4 ERROR MEASURES AND PERFORMANCE CRITERIA

Model performance measures are essential in evaluating the predictive accuracy of the models. The RMSE (Root Mean Squared Error) is the most commonly used and principal measure. The disadvantage of RMSE is that it tends to aggregate the effect of outliers. The MAE (Mean Absolute Error) treats errors evenly according to their magnitude. If the range of the actual property in the data set is large, relative error measures expressed as percentages can also be useful in evaluating the predictive effectiveness of the model.

RMSE and MAE will not capture this effect, but relative errors such as RRSE (Root Relative Squared Error) and RAE (Relative Absolute Error) will. The RRSE expresses the root of the total squared error normalized by the total squared error of the default predictor. In other words, this error is made relative to what it would have been if a simple predictor had been used, i.e., the average of the actual values from the training data. In the two mentioned relative error measures, the errors are normalized by the error of the simple predictor that predicts average values.

The two relative error measures try to compensate for the basic predictability or unpredictability of the dependent variable. If it lies fairly close to its average value, one can expect prediction to be good and the relative measure compensates for this. The correlation coefficient (CC) measures the statistical correlation between the actual and predicted values. The squared correlation coefficient is the goodness of fit (R^2).

4 RESULTS AND DISCUSSION

Out of total 288 input-output pairs, about 66% selected randomly, were used for training and the remaining about 34% were employed for validation. The use of SVMs requires setting of a pre user-defined parameter such as regularization parameter (C), type of kernel, kernel specific parameters such as γ etc. Determining appropriate values of these Support Vector Regression (SVR) parameters are often heuristic trial and error process. The suitable values of these parameters were obtained after a number of trials of different models used in this study.

4.1. Results from SVM

The graphical representation is shown in Figure 1 and 2.

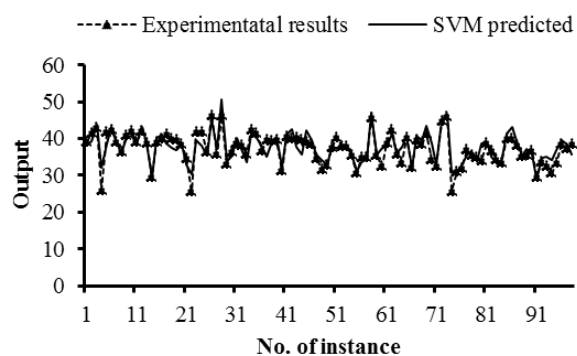


Fig. 1 Comparison of Results of Experimentation with Results Predicted by SVM

The error from the test results vs. number of instance is shown in Figure 2.

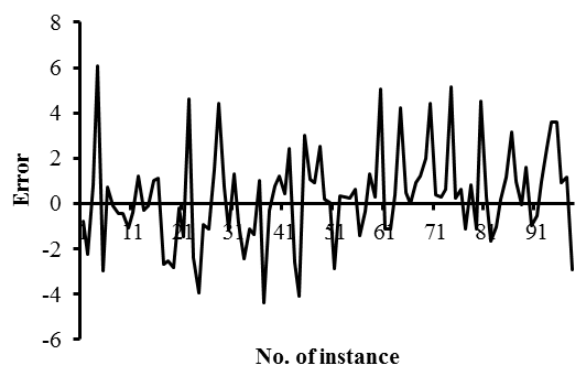


Fig. 2 Error of the Experimental Results to the Results Predicted by SVM

4.2. Results from M5P

The graphical representation is shown in Figure 3 and 4.

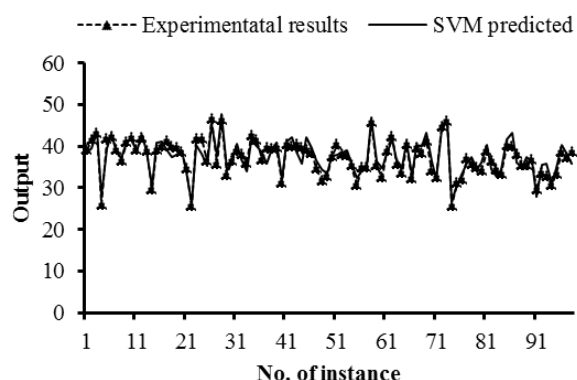


Fig. 3 Comparison of Results of Experimentation with Results Predicted by M5P

The error from the test results vs. number of instance is shown in Figure 4



Fig. 4 Error of the Experimental Results to the Results Predicted by M5P

10 CONCLUSIONS

It can be concluded that M5P algorithm is better than SVMs to study this type of problem in civil engineering field. text.

REFERENCES

- 1) Cui, D., and D. Curry. (2005): Prediction in Marketing Using the Support Vector Machine, *Marketing Science*, 24:4, 595-615.
- 2) El-Garhy, B., El-Nemr, M. and Shalaby, I. (2009): Effect of pile cap elevation below ground surface on lateral resistance of pile groups-experimental study. *International Journal Geotech. Eng.*, 3(1), 21-28.
- 3) Gandhi, S. R., and Selvam, S. (1997): Group effect on driven piles under lateral load, *Journal Geotech. Geoenviron. Eng.*, 123(8), 702-709.
- 4) McVay, M.C., Zhang, L., Han, S. and Lai, P. (2000): Experimental and numerical study of laterally loaded pile groups with pile caps at variable elevations, *Journal Transportation Research Board*, 1736/2000, 12-18.
- 5) Mokwa, R. L. (1999): Investigation of the resistance of pile caps to lateral loading. *Doctoral Thesis, Virginia Polytechnic Institute and State University, Blacksburg, Virginia.*
- 6) Mokwa, R. L., and Duncan, J. M. (1999): Investigation of the resistance of pile caps to lateral loading, *A Report of Research Performed Under Sponsorship of the VA Transportation Research Council, VTRC 99-CR.*
- 7) Mokwa, R. L., and Duncan, J. M. (2001): Experimental evaluation of lateral-load resistance of pile caps, *Journal of Geotech. Geoenviron. Eng.*, 127(2), 185-192.
- 8) Mokwa, R. L., and Duncan, J.M. (2003): Rotational Restraint of Pile Caps during Lateral Loading, *Journal of Geotech. Geoenviron. Eng.*, 129, No.9, 829-837.
- 9) Morrison, C., and Reese, L. C. (1986): A lateral-load test of full-scale pile group in sand, *GR86-1, FHWA, Washington D.C.*
- 10) Mukherjee, S. Osuna, E. and Girosi, F. (1997): Nonlinear prediction of chaotic time series using support vector machine, *International proc. IEEE Workshop on Neural Networks for Signal Processing 7, Amerlia Island, FL, 511-519.*
- 11) Muller, K.R., Smola, A. Ratsch, G., Scholkopf, B., Kohlmorgen, J. and Vapnik, V. (1997): Predicting time series with support vector machines, *Int. Conf. on Artificial Neural Networks*, 999.
- 12) Osuna, E., Freund, R. and Girosi, F. (1997): An improved training algorithm for support vector machines, *Int. Proc. of the IEEE Workshop on Neural Networks for Signal Processing VII, New York, 276-285.*
- 13) Vapnik, V. N. (1995): The Nature of Statistical Learning Theory, *Springer, New York.*
- 14) Vapnik, V. N. (1998): Statistical Learning Theory, *Wiley, New York.*
- 15) Wang, Y., and Witten, I.H. (1997): Induction of model trees for predicting continuous classes, *International Proc. of the Poster Papers of the European Conf. on Machine Learning, University of Economics, Prague.*

[Back to table of contents](#)

Prediction of pile load capacity using artificial neural network

Bhaba Jyoti Dasⁱ⁾, Dr. U. K. Nathⁱⁱ⁾

i) Lecturer, Civil Engineering Department, Scholar's Institute of Technology and Management, Guwahti-35

ii) Assistant Professor, Civil Engineering Department, Assam Engineering College, Guwahti-13

ABSTRACT

Determination of pile load capacity is very complex and uncertain. Several methods are available to determine the axial pile load capacity in compression. Only initial or full scale pile load test gives the correct approximation of pile load capacity. The other methods like static and dynamic formulae, correlation with penetration test data are prediction or estimation method only.

In this study prediction of pile load capacity is done with standard penetration resistance value with the help of artificial neural network. For prediction problem neural network has to be trained with earlier initial pile load test results, standard penetration resistance value of the site and geometry of the pile. The inputs taken in the network are average Standard Penetration resistance along pile length, Penetration Resistance value at the tip of pile, Diameter of pile, Length of pile and length to diameter ratio of pile. The output to the network will be allowable pile load capacity. Hence large number of such input-output datasets is required to train and validate the network. A total of 62 such datasets is taken for the purpose. The model has been simulated using Computers with MATLAB environment. The study is limited to bored cast-in-situ circular concrete piles only due to severity of types of piles. The results of the networks obtained in this study were compared with other empirical techniques. The results of the total pile capacity prediction demonstrated high coefficients of determination for all data records obtained from the neural network model.

Keywords: Pile Capacity, training, testing, ANN

1. INTRODUCTION

To design substructures having piles it is very important to ascertain the axial load carrying capacity of piles. The load capacity of piles in compression can be estimated by several methods like Static pile load formulae, Pile driving formulae, Pile load test and correlation with penetration test data. In-situ test such as Standard Penetration Test (SPT) provides data which represent a large mass of soil. Besides, the test is relatively simple and data are readily obtained during the site investigation. Many correlations have been developed to determine the pile load capacity on various types of soils based on Standard penetration resistance. The actual load carrying capacity can only be determined from initial pile load test on test piles. But initial pile load test is a costly and tedious procedure and not done severely. Rather routine pile load test is done on test pile to ascertain whether the test pile is able to bear a safe load.

In this study, the axial bearing capacity of bored piles as obtained from initial pile load test has been correlated with SPT data using artificial neural network (ANN). Thus this method is said to be a form of method correlation with penetration test data based on pile load test. The artificial neural network is one of the modern artificial intelligence techniques. The modeling advantage of ANNs is the ability to capture the

nonlinear and complex relationship between the bearing capacity and the factors affecting it without having to assume a prior formula of this relationship. Model complexity can be varied simply by altering the transfer functions or network structure. Traditional empirical approaches for predicting bearing capacity of piles are used by many researchers like Meyerhof (1994), H. M. Coyle and R. R. Castello (1981), Bromham and Styles (1971) and others. In the present study it is tried to predict the allowable load carrying capacity of bored cast-in-situ circular piles in as given by pile load test according to IS 2911 Part IV (1985) with the penetration test data available for that site and pile length, pile diameter and length to diameter ratio using artificial neural network. The neural network model is trained with total 62 datasets obtained from various parts of Assam. The artificial neural network model may be used as an alternative to initial pile load test for less important works or can be used to predict the allowable load capacity before initial pile load test is done for important works.

2 NEURAL NETWORK MODEL

Artificial Intelligence is an area of computer science concerned with designing intelligent computer systems that is, system that exhibit the characteristics we associate with intelligence in human behavior (Avron

Barr, Feigenbaum 1981). In general neural network is a highly interconnected network of a large number of processing element called neurons in an architecture inspired by brain. Neural network exhibits characteristics such as mapping capabilities or pattern association, generalization, robustness, fault tolerance, parallel and high speed information processing. In this study an artificial neural network model has been formed using Matlab environment.

2.1 Inputs and Outputs

The axial pile load capacity of a pile depends on several factors like angle of internal friction, cohesion, position of water table, unit weight of soil, pile length, pile diameter, pile material, method of installation and length to diameter ratio. Moreover the load capacity depends on various field test results like Cone penetration test, Standard penetration test, Pressure meter test. But construction of a NN based on all the input parameters from laboratory test, pile geometry, field test and method of installation is not possible in this study in the available time and due to unavailability of data. In this study the various input and output parameters selected are given below-

- i) Average value of corrected N-value obtained from SPT along the full length of the pile. It is denoted as N_{avg} .
- ii) Corrected N-value around the pile tip denoted as N_{tip} .
- iii) Pile length L in meter.
- iv) Pile diameter D in meter.
- v) Length to diameter ratio denoted as L/D.
- vi) The only output is the allowable pile load capacity.

2.2 Collection of database

The main challenge of the problem is the collection of suitable data. Standard penetration test should be done on the site and standard N-value should be available at regular interval of depths. Initial pile load test should be done on the site as per IS : 2911 Part IV to find the allowable load carrying capacity of the pile. Total 62 such pile load test data have been collected from different sites of Assam for training, validation and testing. Another 10 datasets has been used for independent validation for checking the accuracy of the network.

2.3 Normalization of the data

It is noticeable that in artificial neural network model input and output value ranges between -1 to +1. The input value ranges between 0 to 1 if sigmoidal, logsigmoidal or transigmoidal functions are used. But in practical cases the input and output may vary from fraction to thousands. So, to make database acceptable to the neural network, it has been used to carry out normalization process. It is conventional practice to scale the input data to values within the range [0, 1]. But to avoid the slow rate of learning near the end

points of the output range, the data are scaled into the interval [0.1,0.9]. The transformation function is shown below, which will convert original data range to come between 0.10 to 0.90, as given by Nath & Hazarika (2011).

$$X = \frac{0.8x}{(b-a)} + \frac{(0.1b-0.9a)}{(b-a)} \quad (1)$$

Where,

x = value of a variable in the original data range,

X = value of same variable in the range of 0.10 to 0.90.

a = minimum value of variable in the original range

b = maximum value of same variable in the original range.

Similarly, while calculating the error values between the observed and predicted outputs, the converted range should be back converted to lie in the original range through a back transformation function. This back-transformation is given as below-

$$x = \frac{X(b-a)}{0.8} + \frac{(0.9a-0.1b)}{0.8} \quad (2)$$

After normalization the datasets are feeded into the neural network model using Matlab, where it will be divided into training, validation and testing sets.

2.4 Determination of parameters of neural network model

To form the neural network model the first decision has to be taken regarding the type of network. A typical Multi-Layer Feed Forward Neural Network (MLFF) has three layers: the input layer, the hidden layer, and the output layer. The most popular and successful learning algorithm used to train MLFFs in areas such as pattern recognition, function fitting speech and natural language processing and system modeling is the Feed Forward Back Propagation algorithm. Standard back propagation is a gradient descent algorithm, in which the network weights are moved along the negative of the gradient of the performance function. Properly trained back propagation networks tend to give reasonable answers when presented with inputs that they have never seen. In this model also Feed Forward Back Propagation Algorithm is used. Since number of input is five hence number of neurons in the input layer is taken as five. Number of neuron in the output layer is one since allowable load carrying capacity is the only output. It should be noted that a network with one hidden layer can approximate any continuous function provided that sufficient connection weights are used (Hornik et al. 1989), consequently, one hidden layer is used in the current work. Any network that requires data compression must have a hidden layer smaller than the input layer (Swingler,1996). It should also be noted that $2I+1$ (where I is the number of input variables) hidden layer nodes is the upper limit needed to map any continuous function for a network with I number of inputs, as discussed by Caudill (1988). In this work, the optimal model geometry is obtained by utilizing a

trial-and-error approach in which the ANN models are trained using one hidden layer with 5, 6, 7, 8 and 9 hidden layer nodes. The transfer functions used in the hidden and output layers are log-sigmoidal transfer functions. The training function used is 'TRAINGDX' i.e. Gradient descent with momentum and adaptive learning rate backpropagation

The Learning rate and Momentum term is to be finalized using trial and error approach which gives the minimum mean square error. To start with learning rate is to vary between 0.1 to 0.2. Momentum coefficient has been taken as 0.5. The maximum number of epochs or iteration is taken as 1000 which is the stopping criteria. The targeted Mean Square Error is taken as 0.000.

2.5 Training the network

The network has been trained with the available 62 datasets out of which randomly selected 44 datasets are used for training and remaining 9 datasets are used for validation and 9 is used for testing. Training has been done using MATLAB 2009 with 'nntool' toolbox.

Initially random synaptic weights have been assigned automatically to the inputs and interconnected neurons. The random weights will be adjusted depending on the output and targeted output along with iterations. The mean square error (MSE) between network output and target output is used to know the performance of training. Trial and error procedure has been adopted with varying number of hidden nodes, learning rate and momentum coefficient. A total of 10 trials has been done varying the parameters and during each of the trials a neural network was formed. The suitable model is the one with smooth training, validation and testing curves with highest coefficient of correlation considering training, validation and testing.

It has been seen that almost all of the network were trained properly with good coefficient of correlation ranging from 0.97 to 0.99. It has been seen that the network with hidden neuron 7, learning rate 0.2 and momentum coefficient 0.5 has highest coefficient of correlation of 0.9915 considering training, validation and testing and is adopted for prediction.

3 INDEPENDENT TESTING OF MODEL

To know the accuracy in prediction of the model it is desirable to test the model with independent new data which were not used in training and validation. Another 10 such input-output datasets have been prepared and used for independent testing of the model. The database for independent testing has shown below.

Table 1. Database for independent testing

Sl no	N _{avg}	N _{tip}	Diameter (mm)	Length (m)	Ratio L/d	Q _a (KN)
1	10.4	12.8	400	10	25.00	186

2	22.6	23.4	400	10	25.00	383
3	6.3	7.2	400	11	27.50	162
4	10.8	10.8	400	7.5	18.75	153
5	13.3	16.4	600	13.5	22.50	389
6	15.2	16.3	500	10	20.00	353
7	19.9	20.1	500	9	18.00	375
8	33.1	36.2	450	15	33.33	1065
9	33.9	37.8	500	12	24.00	1132
10	15.2	17.8	1000	16	16.00	1167

4 RESULTS AND DISCUSSION

The neural network model for prediction of pile load capacity was used to predict allowable load carrying capacity of 10 piles. The various inputs along with actual allowable load carrying capacity, predicted load carrying capacity and the individual error in prediction is shown in table 2

Table 2. Actual and predicted load carrying capacities

Sl no	N _{av} g	N _{tip}	Diame ter (mm)	Length (m)	Q _a actual (KN)	Q _a predicted (KN)	% error in prediction
1	10.4	12.8	400	10	186	216.3	16.29
2	20.6	21.4	400	10	383	512.2	33.73
3	6.3	7.2	400	11	145	180.9	24.76
4	10.8	10.8	400	7.5	153	212.0	38.56
5	13.3	16.4	600	13.5	402	369.2	8.16
6	15.2	16.3	500	10	353	319.2	9.58
7	19.9	20.1	500	9	375	404.1	7.76
8	33.1	36.2	450	15	1065	1075.8	1.01
9	33.9	37.8	500	12	1132	1253.3	10.72
10	21.3	22.1	1000	16	1167	921.9	21.00

4.1 Comparison of the model with established method

To find the effectiveness of the model with respect to other established method to find the load carrying capacity of bored piles, the results of the network in prediction is compared with some established methods. Mayerhoff (1976) and Briaud (1985) had correlated shaft and base resistance of pile with the results of standard penetration test for driven piles in sandy soil. Since the present study includes bored cast in situ piles, hence the model can't be compared with Mayerhoff (1976) and Briaud (1985). Bromham and styles (1971) used correlation 2 for prediction of ultimate load carrying capacity for both driven and bored piles.

$$P_u = mN_p A_b + nN_{av} A_s / 50 \quad (\text{ton/ft}^2) \quad (2)$$

where,
 P_u = ultimate load carrying capacity in ton/ft²
 N_p = standard penetration resistance at pile base.

N_{av} = average N-value along pile shaft.
 A_b = cross sectional area at pile base.
 A_s = surface area of pile shaft.
 $m = 4$ for driven piles and 1.2 for bored piles.
 $n = 2$ for driven piles and 1 for bored piles.

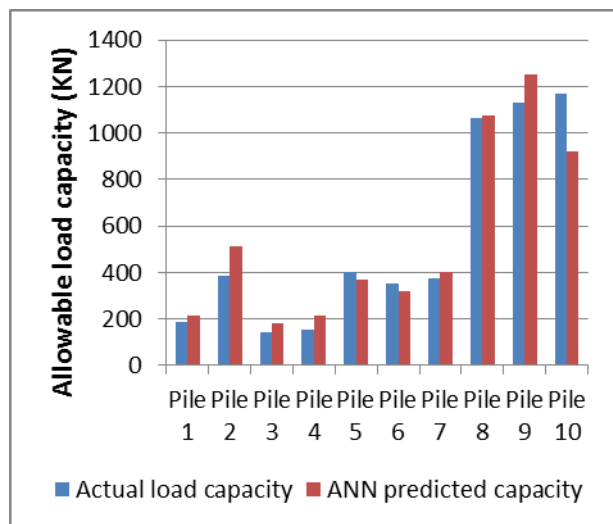


Fig. 1. Histogram showing actual and ANN predicted load capacities

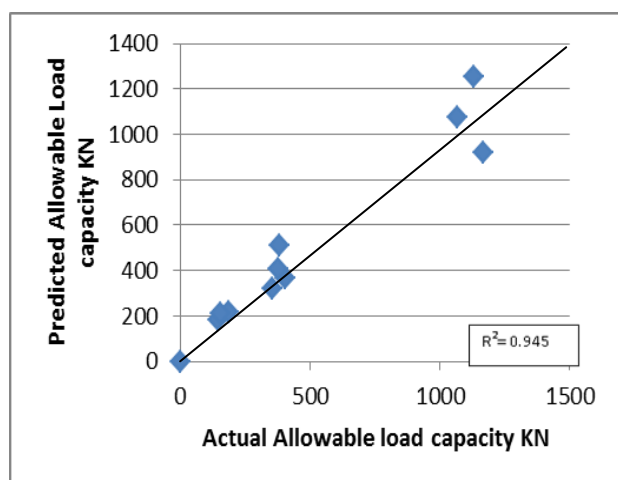


Fig. 2. Comparison of actual and ANN predicted load capacities.

Using correlation 2 the allowable load carrying capacity of the same 10 piles have been calculated and shown in table 3. A factor of safety 3 is adopted while converting the ultimate load carrying capacity to allowable load capacity. A regression line has been shown in figure 4 to show the comparison between Actual load capacity and Bromham and Style predicted capacities. The coefficient of determination of Bromham et al (1971) comes out to be 0.801.

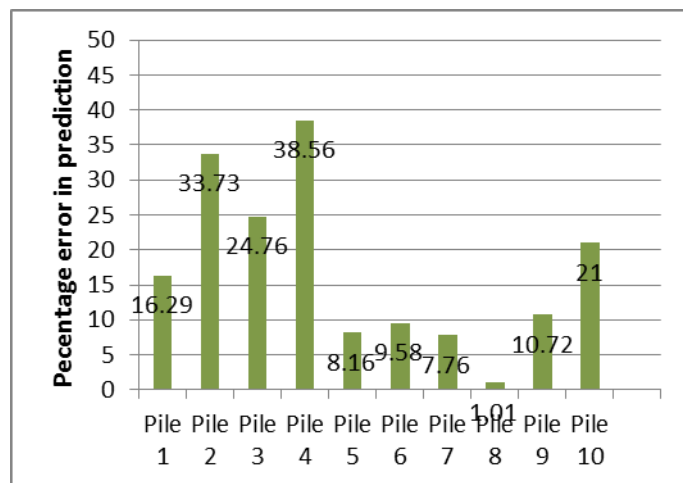


Fig. 3. Error histogram in prediction of pile load capacity by ANN

Table 3. Comparison of Actual, ANN predicted and Bromham et al predicted capacities.

SI	Q_{actual} (KN)	$Q_{a ANN}$ (KN)	$Q_{a Bromham et al}$
1	186	216.3	163.0
2	383	512.2	301.5
3	145	180.9	101.4
4	153	212.0	131.5
5	402	369.2	442.5
6	353	319.2	309.1
7	375	404.1	371.8
8	1065	1075.8	751.5
9	1132	1253.3	768.6
10	1167	921.9	1515.5

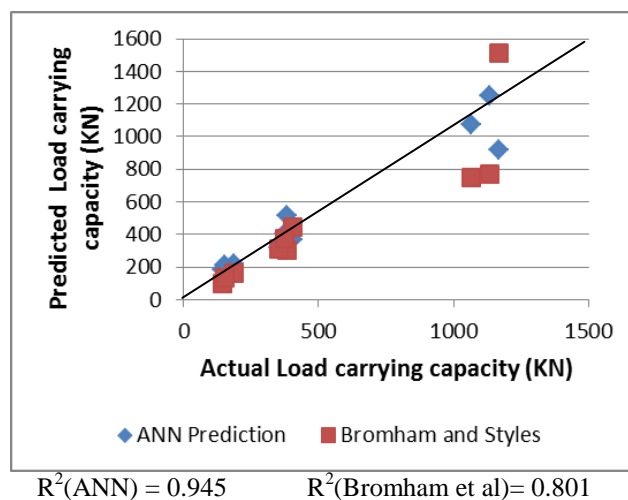


Fig. 4. Comparison of ANN model and Bromham et al. prediction

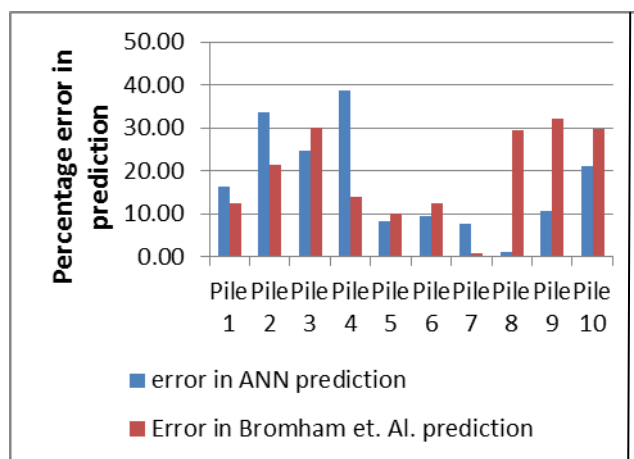


Fig. 5. Comparison of errors in prediction between ANN and Bromham et. al, (1971)

5. CONCLUSION

The artificial neural network has been formed using available 62 datasets in Matlab environment, out of which 44 datasets are used for training, 9 datasets are used for validation and only 9 dataset is used for testing. From Root Mean Square Error (RMSE) observation between target and output data it has been seen that along with number of iterations error is minimized and hence the training curves are ideal. Another 10 independent pile test data which were not used in training the network were used to check the accuracy in prediction of the model. The model is compared with the results of Bromham and Styles (1971) to know the relative performance of the model. On the basis of the experimental results and their graphical representations, the following conclusions are made-

1. It has been seen that the network has been able to predict the allowable load carrying capacity with a good coefficient of determination of 0.945.
2. The maximum and minimum error seen in prediction is 38.56 percent and 1.01 percent respectively.
3. From the observation of 10 results the average error of 17.15 percent is observed.
4. The best prediction result is obtained in pile number 8 with only 1.01 percent error in purely granular soil having high Standard penetration resistance value.
5. The ANN model is found better in predicting than traditional method of Bromham and Styles (1971) with higher coefficient of determination.
6. The limitation of the study is that only field test data is used to predict the load carrying capacity of the piles, hence may sometimes reflects high error. However, the results from SPT are only applicable for pile capacity estimation embedded in cohesionless soils which contradicts in most cases of soil profile with different layers of soils. One of the reason that SPT does not give reliable estimation of pile capacity in cohesive soils is due to ignorance of excessive pore water pressure generated during the test.

7. The beauty of artificial neural network lies in the capability of predicting values for which no mathematical correlations are available and here also it is seen that ANN is able to predict load capacity in case of C-Ø soil for which no correlations are available between standard penetration resistance and pile load capacity.

8. Exact determination of pile load capacity is very complex and depends on several inputs from laboratory as well as field data. In the present study it is seen that the model is able to predict load capacity in case of cohesive soils with some errors. The model will be able to predict with better accuracy if only data from cohesionless soil is adopted for training, testing and validation. But here a generalized model has been formed considering both cohesionless as well as C-Ø soil due to which high error in prediction in few cases has been observed.

9. It can be concluded that Artificial Neural Network is a quite handy tool in prediction if sufficient data are available for training.

6. REFERENCE

- 1) Amel, B., Nechnech A. & Verbrug Pr. (2008) :Application of Neural Networks to Predict the Ultimate Bearing Capacity in Cohesionless Soils." *J. ICCBT 2008*, E - (42) – pp519-537.
- 2) Abdelrahman, G. E. (2002): Prediction of ultimate pile load from axial load tests and penetration tests." *Lecture of soil mechanics and foundation, Cairo university, 2002.*
- 3) Anamali, E., Shkodrani, N. & Dhimitri, N. (2014): Axial Load Capacity of Cast in Place Piles from SPT and CPTU Data." *World Journal of Engineering and Technology*, 2014, 2, 100-108.
- 4) Benali, A., Nechnech, A. & Bouzid, D. A. (2013): Principal Component Analysis and Neural Networks for Predicting the Pile Capacity Using SPT." *IACSIT International Journal of Engineering and Technology*, Vol. 5, No. 1, February 2013.
- 5) Coyle, H. M. & Castello, R. R. (1981): New design correlation piles used in sand." *IEEE Trans. J. Geotech. Engrng. ASCE*, vol. 107, no. 7, pp. 965-986.
- 6) Chow, Y.K, Chan, W.T. Liu, I.F. & Lee, S.L. (1995): Predication of pile capacity from stress wave measurements: a neural network approach." *International Journal of Numerical & Analytical Methods in Geomechanics*, Vol. 19, pp. 107–126.
- 7) Das, B.M., (2011): *Principles of Foundation Engineering*, Stamford, CT, USA.
- 8) Fausett, L., (1994): *Fundamentals of Neural Networks: Architecture, Algorithms, and Applications*". Prentice-Hall, Englewood Cliffs, NJ.
- 9) Jaksa M. B. , Maier H. R. & Shahin M. A. (2008): Future Challenges for Artificial Neural Network Modelling in Geotechnical Engineering." 12th International Conference, *International Association for Computer Methods and Advances in Geomechanics*.
- 10) Kudmetha, K. K. and Dey A.,(2012): Uncertainty in Predicting Bearing capacity of Piles in sand using SPT data." *International Symposium on Engineering under Uncertainty: Safety Assessment and Management*, January. 2012.

[Back to table of contents](#)

- 11) Kiefa, M. A. (1998): General regression neural networks for driven piles in cohesionless soils," *IEEE Trans. J. Geotech. Geoenviron. Eng.*, vol. 124, no. 12, pp. 1177–1185.
- 12) Lee, I. M. & Lee, J. H. (1996): Prediction of pile bearing capacity using artificial neural networks," *IEEE Trans. Direct Science Computers and Geotechnic*, vol. 18, no. 3, pp. 189-200.
- 13) Maizir, H. and Kassim K. A., (2013): Neural Network Application in Prediction of Axial Bearing Capacity of Driven Piles." , *International MultiConference of Engineers and Computer Scientists 2013 Vol I, IMECS 2013*.
- 14) Malik, Rosely Ab & Jamil Mohamed S. (2001): The Determination of Pile Capacity Using Artificial Neural-net: An Optimization Approach." *J. Sci. & Technol. Supplement 9(1):73 – 79*.
- 15) Meyerhof, G. G. ,1976: Bearing capacity and settlement of pile foundations." *J Geotech Engg., ASCE*, 102(3), 196–228.
- 16) Momenia, E., Maizira, H., Gofara, N., Nazira R. (2013): Comparative Study on Prediction of Axial Bearing Capacity of Driven Piles in Granular Materials." *Jurnal Teknologi (Sciences & Engineering)* 61:3 (2013) 15–20.
- 17) Nath, U. K. & Hazarika, P.J. (2011): Study of Pile Cap Lateral Resistance using Artificial Neural Networks." *International Journal of Computer Applications (0975 – 8887), Volume 21– No.1*.
- 18) Punmia, B.C., Jain, A.K. & Jain, A. K. (2012): *Soil Mechanics and Foundations*. Laxmi Publications (P) Ltd., New Delhi.
- 19) Rajasekaran, S. and Pai, G.A. Vijaylakshmi (2005): *Neural networks, fuzzy logic and genetic algorithms*. PHI Private Limited, New Delhi.
- 20) Ranjan, G., Rao, A.S.R. (2012): *Basic and applied soil mechanics.*, New Age International Publisher, 2nd edition, New Delhi
- 21) Shahin, M. A.; Jaksa, M. B. & Maier, H. R. (2001): Artificial Neural Network Applications In Geotechnical Engineering." *Australian Geomechanics*, Vol. 36, No.1, pp. 49-62.
- 22) Shariatmadari, N., Eslami, A. & M. K. Fard, (2008): Bearing capacity of driven piles in sand from SPT-applied to 60 case histories," *IEEE Trans. Direct Science, Iranian Journal of Science and Technology*, Transaction B, Engineering, vol. 32, pp. 125-140.
- 23) Teh, C. I., Wong, K. S. & Goh, A. T. (1997): Prediction of pile capacity using neural networks," *IEEE Trans. Direct Science. J. Comput. Civ. Eng.*, vol. 11, no. 2, pp. 129–138.
- 24) Wardani, S.P.R., Surjandari, N.S. & Jajaputra A.A. (2013): Analysis of Ultimate Bearing Capacity of Single Pile Using the Artificial Neural Networks Approach: A Case Study." 18th International Conference on Soil Mechanics and Geotechnical Engineering, Paris 2013.

Verifications of pile load capacity using static pile load test

Ningombam Thoiba Singh

Assistant Professor, Department of Civil Engineering, Assam Don Bosco University, Azara, Guwahati -781017, India.

ABSTRACT

The static pile load test on a single pile involve uplift force, axial compression and lateral tests when applied either horizontally or perpendicular to the pile axially. These tests can be applied to the pile in groups consisting of vertical piles, batter piles or a combination of both. The observed settlements made at the top of the pile may not necessarily represent the downward movement of the pile into the ground. The possibility of local failure of the pile above the ground surface, or crushing of the ground under the test plate, should be recognized as possible factors contributing to observe settlements along with the material type and size of the test piles. The results of the test program to the foundation design and specification can often produce a substantial alteration of information and costs. Although, practically, the test results would lead to the selection of a single design load, the requirements for various types of piles and sizes, length, shape, installation methods and driving requirements could be varied over a wide range.

Keywords: pile load test, skin friction, settlement, crushing, test pile.

1. INTRODUCTION

Pile load tests are normally conducted at the construction site to verify the design load and to assess the quality of various piles. After validation and assessment, the designer confirms the design load which already obtained from the soil testing report or modified accordingly for the safer design in pile foundation. The use of pile load test result in the verification of foundation is limited to experiences and quite often neglected by the builders or agency. The variation of load bearing capacity of the pile having the same configuration is relatively narrow down by conducting various load tests to all the construction using piles. Possible increase in number of load test at the construction site, compromising the cost and time overrun is discussed. Prediction of load carrying capacity and possible settlement of the pile foundation can be extrapolated from the pile load test which is quite advantages and simple. In most of the advanced country also like Japan, USA, Canada, Australia etc. the use of the ultimate load bearing capacity from the pile load test is common practice for pile design using the empirical relations following the design codes.

Before 2010, Engg. Project India Ltd. (EPIL) started construction some buildings at the Central Agriculture University (CAU) Iroisemba, Imphal main campus. Pile load tests were initiated for every building to verify the design specifications and conducted through the Govt. College of Poly-technique, Imphal. The agency casted RCC under-reamed piles of normal diameter 400 mm and bulk diameter 750mm. The CAU is situated at the south-west corner of Lamphelpat where the place has been being known as the pat means the lake. The lake is being used for temporary water storage pond from the surface run-off during the rainy season from the surrounding catchment Imphal city area. In early 80's,

the soil obtained from the Lamphelpat was sometimes used for burning purpose during the winter as the nature of the soil is sticky expansive clay which is known as black cotton soil. The underlying soil stratum of the Lamphelpat area is found layer by layer in the form of the mattress and no good/hard soil layers are found till 50 to 60m. However, the Govt. of Manipur chosen the area as educational institution area which at presently exist like RIMS Imphal, NIT Manipur, CAU, ICMR, INDUSTRIES etc.

The problems generally facing in this area is that the septic tank or outside peripheral service drain will remain at the same level as it was because of not much weight, while the building is sinking because of its own weight heavy during heavy vehicles running near the building or earthquake. Thus, there is level difference between the septic tank/drain and inside room level at the ground floor. Because of level difference, during the rainy season, all the dirt from the Septic tank or service drain float inside the room and thus create many the unwanted situation. Therefore, it is mandatory to give full attention with research for providing a proper foundation of any buildings/projects otherwise, the buildings or the structures may found sinking and after some years the building looks like a plinth-less structure.

2. PILE DESIGN RELATIONSHIP

Normally, piles are designed based on empirical relations specified by several design codes, using SPT N-values. Single boring or more boreholes piling investigations may not be enough to apprehend the ground conditions of the whole piling site. There are different methods of estimating bearing capacity using the design codes and this situation often confused the pile designers. Therefore, conducting more number of pile load tests are the most reliable approached to

confirm the performance of the completed piles at the site. However, this approach is not performed in most of the piling projects in India, because of the conventional static pile load test and also more expenditure.

Matsumoto et al. (2016) discussed the important of conducting piles load test to verify the design factor. IS-Code 2911 (1995) for obtaining the ultimate load from the load-settlement curve whether the observed settlement is within the permissible limit or at 12mm. The necessary use of pile load test data in the prediction of pile load capacity from load settlements curve within the given criteria specified by Poulos (2012) along with two examples. Poulos (1989) concluded that the pile load tests should be accompanied by detailed site investigation to define the entire soil profile accurately. Comparison of field pile load test and FEM analysis using the ABAQUS presented by Jozefiak et. al. (2015) is discussed.

The objective of the study is to verify the load bearing capacity and settlement criteria of the pile by the method known as Initial pile load test which was used at the design center before the commencement of the piling project. After completion of piling work, routine pile load tests can be conducted to the selective piles for the confirming and safe load within the specified limiting value as given in the code.

3. TEST PILLING BEFORE PILLING WORK

Initial piled load test was conducted to confirm the design safe load by field experiment and to provide guidelines for setting up the limits of acceptance for routine tests. It is also given an idea of the suitability of the piling system following the procedures laid down in IS-2911 Part IV. The loading mechanism is the reversible reaction and the loads are continuously applied till the pile maintained the rate of displacement either 0.1 mm per 30 minutes or 0.2 mm in the first one hour or 2 hours whichever occurs first. The next load increment shall be applied on achieving the aforesaid criterion. The test load shall be carefully observed for 24 hours. Similarly, the selection of piles for the routine test is done based on the number of piles subject to the maximum of 0.5% to 2% depending on the nature of structure but maximum settlement should be within 12 mm.

The load carried by the pile is the combine effect of shaft resistance and base resistance. The behavior of the pile general follows the load settlement curve as shown in the Fig. 1 and the maximum shaft resistance is occurred from the depth 2% of pile dia. till to end of the pile length due to skin friction. The base resistance may be increased correspondingly with pile length and soil stiffness. However, in the soft clay, the base resistance is comparatively lesser than the shaft resistance. The test can be either initial or routine test and the settlement is observed for every incremental load of

10% of the estimated safe load. The ultimate load is said to be reached when the final settlement is more than 10% of the diameter or the settlement keeps on increasing at constant load.

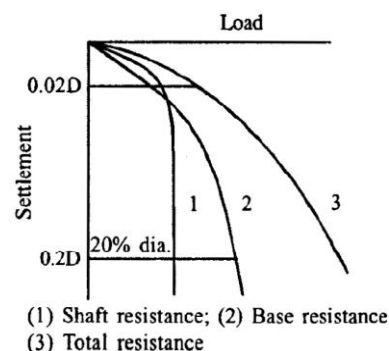


Fig. 1. Formulation of pile foundation

Recommendation as per IS-2911 (Part IV) 1995.

The recommendations are as follows:

- 2/3rd of the final load at which the total displacement attains a value of 12 mm unless otherwise required in a given case on the basis of nature and type of structure in which case, the safe load should be corresponding to the stated total displacement permissible.
- 50% of the final load at which the total displacement equals 10% of the pile diameter in case of uniform diameter piles or **7.5% of the bulb diameter in case of under reamed piles.**

4. EXPERIMENTAL WORK

The test piles were cast up to a depth of 7 m initially at various buildings like Gymkhana, Farmer Hostel, Type-II & III quarters, Guest House, PG Gents hostel, Canteen etc. as bored cast in situ under-reamed pile having normal dia. of 0.4m and bulk diameter as 0.75m. All the buildings were proposed for Ground plus two storied building. Initial pile load tests were conducted after 28 days of casting and the kentledge weight is 3 times the design load. The hydraulic load is applied till to failure. Those piles which were failed during the load test were cast again by increasing the pile length up to 12 m and 15 m and the number of bulkheads was 2 as in the case of P.G. Hostel.

Regarding the routine test, around 0.5 to 2% of the piles were selected from among the piles and tested only to the Gymkhana building. In this case, care was taken that no pile should be failed due to excessive loading.

5. RESULTS AND DISCUSSIONS

After 28 days of casting, the initial load test was conducted. Load vs settlement graph for the test is presented in Fig. 2. The design load of the pile is given

as 13.85 Ton. However, from the curve, it is predicted that the pile can carry up to 17 Ton which is safe for the building. The safe load was calculated as 2/3 of the load corresponding to 12 mm settlement from the graph i.e 25.50 Ton (approx.). Therefore, the safe load may be taken as 17 Ton. The ultimate load is also obtained from load-settlement curve as the final point of the curve if the curve is within the permissible value, Bowels (1996). Alternatively, the ultimate load can also be obtained from the load-settlement curve at the intersection of two tangents drawn at the initial point of the curve and settlement corresponding to 10% of the diameter of the pile, Tomlinson (2001).

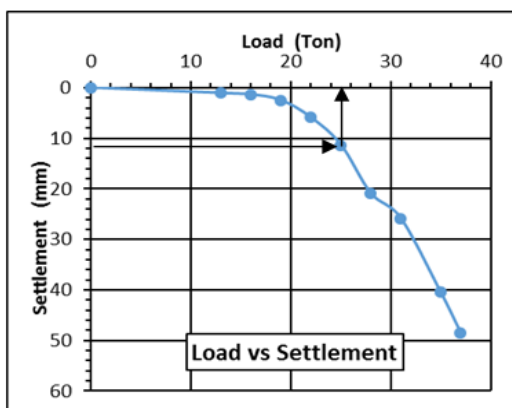


Fig. 2. Initial pile load test results of proposed building site of Gymkhana

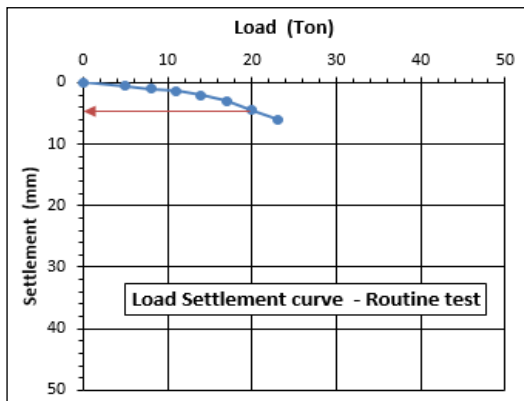


Fig. 3. Routine test result - Gymkhana

Fig. 3. shows the routine pile load test of Gymkhana building. The graph shows that all the piles are good enough and performed well as the settlement plot keeps on increasing correspondingly with the applied load i.e. no failure. The settlement corresponding to 1.5 times the working load should not exceed 12mm. i.e. 20.77 tons says 21 tons is 5 mm which is within the specified settlement of 12 mm and therefore, it is safe.

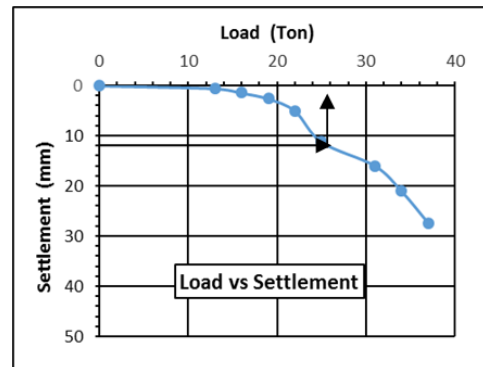


Fig. 4. Initial pile load test results of proposed building site of Farmer Hostel

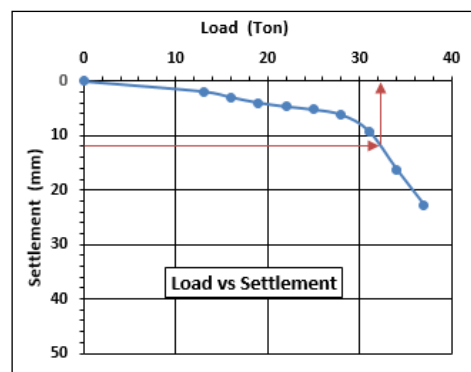


Fig. 5. Initial pile load test results of proposed building site of Type – II and III quarter

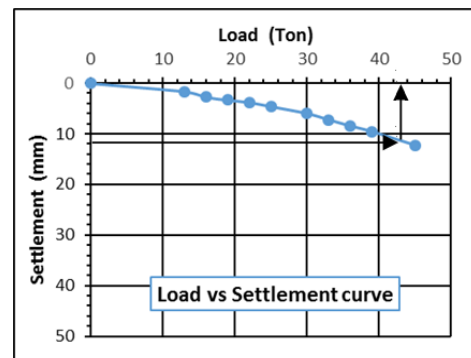


Fig. 6. Initial pile load test results of proposed building site of Guest House

Similarly, for other buildings i.e. Farmer Hostel, Type-II and III quarter, Guest House etc. initial pile load tests were conducted and the results are shown in Fig. 4 to 6 respectively. Since the buildings were proposed for G+2 storied building, the design load of 13.85 Ton (given) is same for all the buildings. The safe design load is 2/3 of the load obtained from the graph corresponding to 12mm settlement which is given in the Table-1.

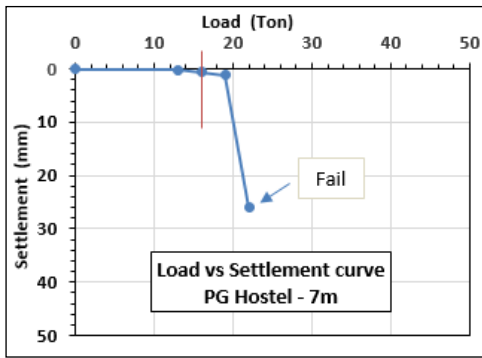


Fig. 7. Initial pile load test results of proposed building site of PG Gents hostel (1st test)

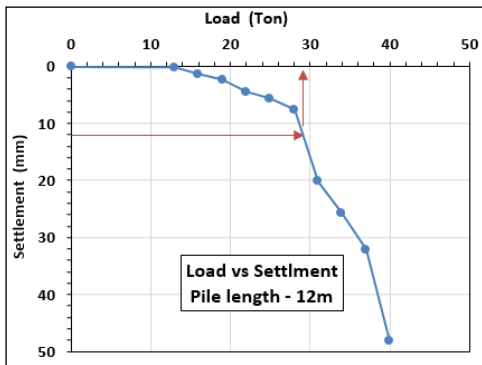


Fig. 8. Initial pile load test results of proposed building site of PG Gents Hostel (2nd test)

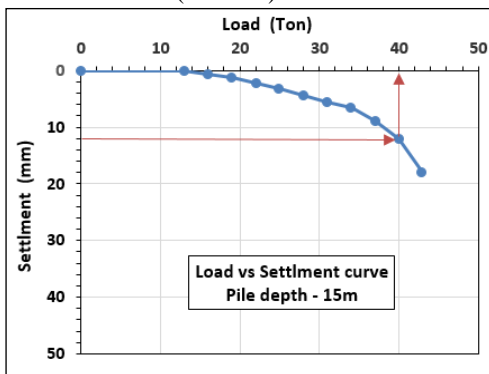


Fig. 9. Initial pile load test results of proposed building site of PG gents Hostel (3rs test)

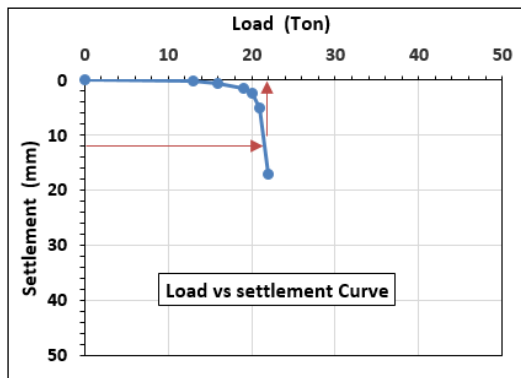


Fig. 10. Initial pile load test results of proposed building site of PG Gents hostel (1st test)

site of Canteen

In the case of P.G. Hostel, the tests were conducted 3 times because of the unsatisfied results in bearing capacity and settlement as shown in Fig. 7. and Fig. 8. The building was proposed for G+3, design load is 21 Ton. The length of the pile was subsequently increased by 12, 15m respectively. Finally, at 15m pile length, the result was found satisfactory in terms of bearing capacity and the settlement recommendation as shown in Fig. 9.

Table 1. Results of Pile load test

Name of the building	L/d.	Bulk dia. (m)	Design load (Ton)	Safe load (Ton)	Remarks
1. Gymkhana					
Initial	7/0.4	0.75	13.85	17	Fig. 2.
Routine test	7/0.4	0.75			Fig. 3.
					corresponding to 1.5*13.85 is 5mm
2. Farmer hostel	7/0.4	0.75	13.85	17	Fig. 4.
3. Type II & III quarter	7/0.4	0.75	13.85	21	Fig. 5.
4. Guest house	12/0.4	0.75	13.85	28.6	Fig. 6.
5. P.G. Hostel					
1 st test	7/0.4	0.75	21.0	7.6	Fig. 7.
2 nd test	12/0.4	0.75		19	Fig. 8.
3 rd test	15/0.4	0.75		27	Fig. 9.
6. Canteen	7/0.4	0.75	13.85	8.4	Fig. 10.

Further, it should be noted that the observed settlements made at the top of the pile may not necessarily indicate downward movement into the ground in the case of higher load test. The possibility of local failure of the pile above the ground surface, or crushing of the ground under the test plate, should be recognized as possible factors which contributing to observed settlements.

6. FEM MODELING

Finite element software, ANSYS from the IIT Guwahati was used for modeling considering the soil, piles and cap as 8-nodded brick element. The soil was modeled as Drucker-Prager having cohesion value 20 kPa, soil modulus (E_s) 2×10^4 MPa, Poisson's ratio (μ_s) 0.45 and non-linear newton Raphson's incremental methods. Whereas, the pile and cap was modeled as the elastic material (concrete) having elastic modulus (E_c) 2×10^7 MPa and Poisson's ratio (μ_c) 0.15. Because of symmetry, one fourth (1/4) of the plan was modeled i.e. 0.20×0.20 m² pile cross sectional area, $1.2 \times 1.2 \times 0.6$ m³ cap area. Regarding boundary conditions and other details are shown in Fig. 11.

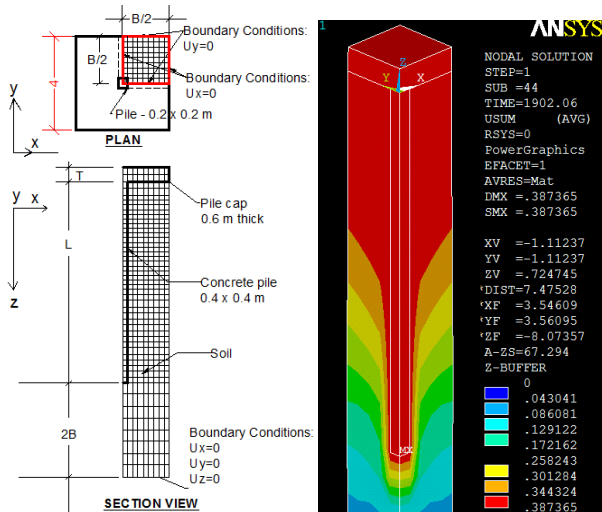


Fig. 11. FEM modeling of pile with cap and soil

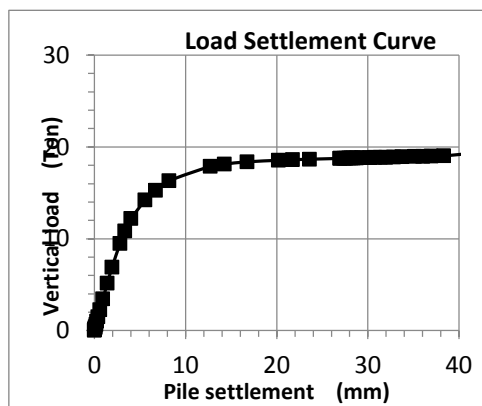


Fig. 12. Load settlement curves based on FEM analysis

After running the program, the result is plotted between the load (time steps) vs settlement and they are found to be good agreement to the field data presented in the Fig. 2 and Fig. 12.

7. CONCLUSIONS

The variation of load bearing capacity of the pile having the same configuration is relatively narrow down by conducting various load tests. Possible increase in the number of load tests at the construction site, compromising the cost and time overrun. Prediction of load carrying capacity and possible settlement of the pile foundation can be extrapolated from the pile load test which is quite advantages and simple. The use of pile load test both initial and routine pile load test result in the verification of foundations is mandatory.

At the same time proper soil investigation along with pile load tests are mandatory at the Lamphelpat area including Langol under the purview of geotechnical engineer as they fall in the same belt.

ACKNOWLEDGEMENTS

The authors would like to express sincere thanks to the authority of CAU, EPIL for allowing the opportunity to conduct this research work. Appreciations also extended to Govt. Poly-technique College for providing the data and assistance to the review of the analyses of the pile along with the verifications.

REFERENCES

- 1) Matsumoto, T. Matsuzawa, K. Kitiyodomi, P. (2016). "A role of pile load test - Pile load test as element test for design of foundation system". *Journal of Science, Technology and Practice*, 39-58.
- 2) Jozefiak, K. Zbiciak, A. Maslakowski, M. Piotrowski, T. (2015). "Numerical modelling and bearing capacity analysis of pile foundation". *XXIV R-S-P Seminar, Theoretical Foundation of Civil Engineering (24RSP) (TFoCE 2015)*, Elsevier, 356-363.
- 3) IS: 2911-Part IV (2010). "Code of Practice for Design and Construction of Pile Foundations". *Sixth Reprint*, July 2003.
- 4) Poulos, H.G. (2012). "Pile Testing & Settlement Prediction". *Geotechnical Special Publication*, March 2012, DOI :10.1061/9780784412084.0044.
- 5) Tsai, C. Zhang, Z. (2008). "Design and Load Verification of Driven Pile Foundations". *Sixth International Conference on Case Histories in Geotechnical Engineering*, Arlington, V.A, paper No. 1.59, 11-16 August, 1- 6.
- 6) Poulos, H.G. (1989). "Pile behavior- theory and application". *Geotechnique* 39, 365-415.
- 7) Susic, N. Nikovic, G.H. Dokovic, K. (2014). "Bearing capacity of piles estimate differences". *International Conference Contemporary achievements in civil Engineering*, 24-25 April, Subotica, Serbia, 259-264.
- 8) Tomlinson, M.J. (2001). "Design and Construction Practice". *7th Edition*, Prentice Hall.
- 9) Bowles. J.E. (1996). "Foundation Analysis and Design". *5th Edition*, McGraw- Hill Companies, Inc.

[Back to table of contents](#)

A study of modal behaviour of an intz type water tank under seismic loading

Pranjal Konwarⁱ⁾ Dhurba J Borthakurⁱⁱ⁾ and Dr. (Mrs) Nayanmoni Chetiaⁱⁱⁱ⁾

i) M.E student, Jorhat Engineering College, dasranjan_2222@rediffmail.com

ii) M.E student, Jorhat Engineering College, dhrubajyoti007borthakur@gmail.com

iii) Asstt. Prof., Jorhat Engineering College, nayanmoni.chetia@gmail.com

ABSTRACT

In this paper an attempt has been made to model and analyse an intz type water tank located in Zone V using SAP2000 and STAAD Pro. The objective of this paper is modal analysis of the water tank and to compare its seismic behaviour for different levels of water. Modelling was performed for four conditions namely full tank condition, half-filled condition, 1/3rd filled condition and empty condition. For modal analysis, water is defined as a solid element having standard properties. Plot between percentage volume change versus percentage change in frequency was performed. It is observed that frequency decreases with the increase in water mass. Percentage volume change versus percentage change in the amplitude of vibration shows that amplitude of vibration in a particular mode will increase with the increase in water level. By comparing the maximum displacement of the tank for different levels of water it is observed that maximum horizontal displacement of the tank in any direction will increase with the increase in water level. From the modal analysis it is seen that frequency of vibration for full tank condition is 0.90515 cycles/second and is increased by 9.88% for half-filled condition, 26.39% for 1/3rd filled condition and 38.64% for empty tank condition. Likewise the amplitude of vibration at the first mode for full tank condition is 2.04mm and is decreased by 4.62%, 36.27% and 54.08% for half tank condition, 1/3rd filled condition and empty tank condition respectively.

Keywords: Intz tank, time period, ground motion, frequency, Response Spectrum, modal analysis.

1. INTRODUCTION

Next to air, the most important requirement for human life is water. The overhead liquid storing tank is the most effectual storing competence used for domestic as well for industrial purpose. These types of tanks are built for direct distribution of water by gravity flow and are usually of smaller capacity. In case of overhead or intz type water reservoir due to the large mass concentration at the top portion in comparison to the lower staging system, they are most susceptible to failure during earthquake. For distribution purpose a considerable height is usually recommended in such type of tanks which also leads to the enhancement in seismic failure. Since it is used for storing purpose, occurrence of any crack will results in leakage making the structure unworkable. Hence in such type of water storage structure we generally adopt a greater factor of safety while designing

in gravity analysis. In this study, we are looking forward to discuss the effect of an earthquake on an intz type tank with varying heights of water level and to have a conclusion about the volume of water that can be stored during earthquake. Since the effects of vibration depend upon the volume of water present in the tank, the chance of seismic failure can be reduced by controlling the volume of stored water in the tank during earthquake. In the present study, an intz type tank of capacity 9×10^5 litre is considered which is supported by 12 numbers of columns and 3 layers of bracing system. M20 grade of concrete is considered.

1.1 Literature review

Significant research was carried out on seismic design of liquid storage tanks and a few published works on seismic response characteristics of reinforced concrete (RC) water tanks are reviewed in this section.

Algreane Gareane A. I. (2003) has done a study on the dynamic behaviour of elevated concrete water tank with alternate impulsive mass configurations. In this paper he has presented the dynamic behaviour of elevated concrete water tank by preparing six models, which were simulated to determine the effects of impulsive mass mode. Simulation of the models was carried out in three-dimensional finite element method via LUSAS FEA 14.1.

Krishna Rao M.V (2015) has done a comparative study on seismic analysis of overhead circular water tanks. The paper compares the results of seismic analysis of overhead circular water tank carried out in accordance with IS: 1893- 1984 and IS: 1893-2002 (Part-2) draft code. The analysis was carried out for elevated circular tank of 1000 Cu.m capacity, located in four seismic zones (Zone-II, Zone -III, Zone-IV, Zone-V) and on three different soil types (Hard rock, Medium soil, Soft soil). Further, three different tank-fill conditions - tank full, tank 50% full, tank empty are also considered in this study using the software SAP 2000.

Gaikwad (2006) reviewed the behaviour of elevated water tank by performing static and dynamic analysis, to compare the analysis results of elevated water tank, in order to study the effect of hydrodynamic forces on elevated water tank. He concluded that for same capacity, geometry and height with same staging system response by equivalent Static Method to Dynamic method differ considerably and this difference is increased with the increase in capacity of the tank. For this study the zone, importance factor and response reduction factors were also considered to be same. He also discussed the feasibility of these two approaches for tanks of low and high storage capacity.

2. MATERIALS AND METHODS

2.1 Material properties

The material properties used for and the shape and size of different members have been listed in table 1 and table 2 respectively.

Table 1 Material Properties

Material name	Density(N/m ³)	Elasticity(N/m ²)	Poisson's ratio
Water (solid)	9810		0.5
Concrete M20	25000	22360.68	0.2

Table 2 Member Specifications

Member name	Material	Shape	Size(mm)
Top beam	Concrete	Rectangular	400 × 360
Middle beam	Concrete	Rectangular	400 × 360
Bottom beam	Concrete	Rectangular	1200 × 600
Columns	Concrete	Circular	700(dia)
Column bracing	Concrete	Rectangular	300 × 600
Top dome	Concrete	Rectangular plates	100
Cylindrical portion	Concrete	Tapered plates	300 × 200
Inclined wall	Concrete	Rectangular plates	400
Bottom dome	Concrete	Rectangular plates	280

2.2 Response spectrum method by using staad pro

Response-spectrum analysis is useful for design decision-making because it relates structural type-selection to dynamic performance. A response spectrum function is simply a list of period versus spectral acceleration values. Lateral analysis using Staad was performed with a user defined value of $(Z/2) * (I/R)$ and calculate time periods for different modes. The program calculates S_a/g for each mode utilizing time period and damping for corresponding mode. Then the program calculates design horizontal acceleration spectrum and mode participation factors for different modes. The peak response quantities are then combined as per method CQC or SRSS or ABS or TEN.

2.3 Response Spectrum Method By Using Sap2000

Response-spectrum analysis is a linear-dynamic statistical analysis method which measures the contribution from each natural mode of vibration to indicate the likely maximum seismic response of an essentially elastic structure. Response-spectrum analysis provides insight into dynamic behaviour by measuring pseudo-spectral acceleration, velocity or displacement as a function of structural period for a given time history and level of damping. In SAP the acceleration values in the function are assumed to be normalized. The units are associated with a scale factor that multiplies the function and is specified when the response spectrum case is defined. The computation of the natural mode shapes and associated periods of vibration were done and using the structural masses and the Rayleigh analyses, the mode shapes and frequencies are automatically computed by SAP2000. SRSS directional combination option was selected.

3. LOADINGS (AT FULL CONDITION)

Live load = 1500 N/m^2

Unit weight of water = 1000 kg/m

Water pressure intensity at top ring = 0 N/m^2

Water pressure intensity at bottom ring = 5000 N/m^2

Weight of water at inclined portion = 58285 N/m^2

Weight of water at bottom dome = 25822.059 N/m^2

Similarly, loads at different points are calculated for the other three levels of water.

Schematic view of the water tank in full condition is shown below. The water level is up to the top ring beam.

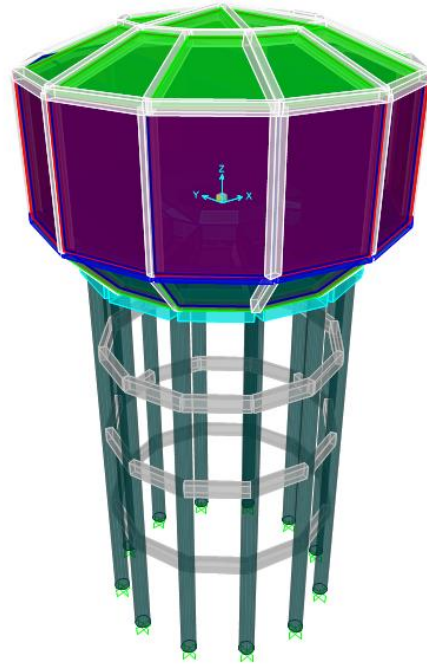


Fig.1. Tank in 100% filled condition

4. RESULTS AND DISCUSSION

Modelling analysis is done for four different loading conditions namely,

- Empty tank condition,
- Water level up to the middle ring beam referred as one third filled condition,
- Water level up to a depth of 2.5 m from top ring beam referred as half-filled condition, and
- Water level up to the top ring beam referred as full tank condition.

The frequency of vibration for different modes in the above-mentioned conditions are found out by modal analysis and the results are shown below followed by the graph between frequency of vibration versus mode no. It is seen that the frequency of vibration increases with the increase in mode number and decreases with the increase in the volume of water in the tank.

Table 3 3 Mode shapes vs. frequencies at different water level

Mode number	Empty tank condition Frequencies (cyc/sec)	One third tank condition Frequencies (cyc/sec)	Half tank condition frequencies (cyc/sec)	Full tank Condition frequencies (cyc/sec)
1	0.91754	0.8369	0.71739	0.64709
2	0.92092	0.8392	0.71859	0.65273
3	1.1486	1.0571	0.85147	0.73263
4	3.7441	3.6203	3.4405	2.162
5	3.946	3.8311	3.5411	2.4089
6	6.9608	6.9013	6.5833	3.0684
7	7.1414	7.144	6.9244	5.0429
8	7.1538	7.1617	7.1101	5.5481
9	7.4238	7.2533	7.1151	6.3043
10	7.5105	7.3414	7.1685	6.3924
11	8.3693	8.1505	7.2484	7.0534
12	9.2099	8.9117	8.6035	7.285

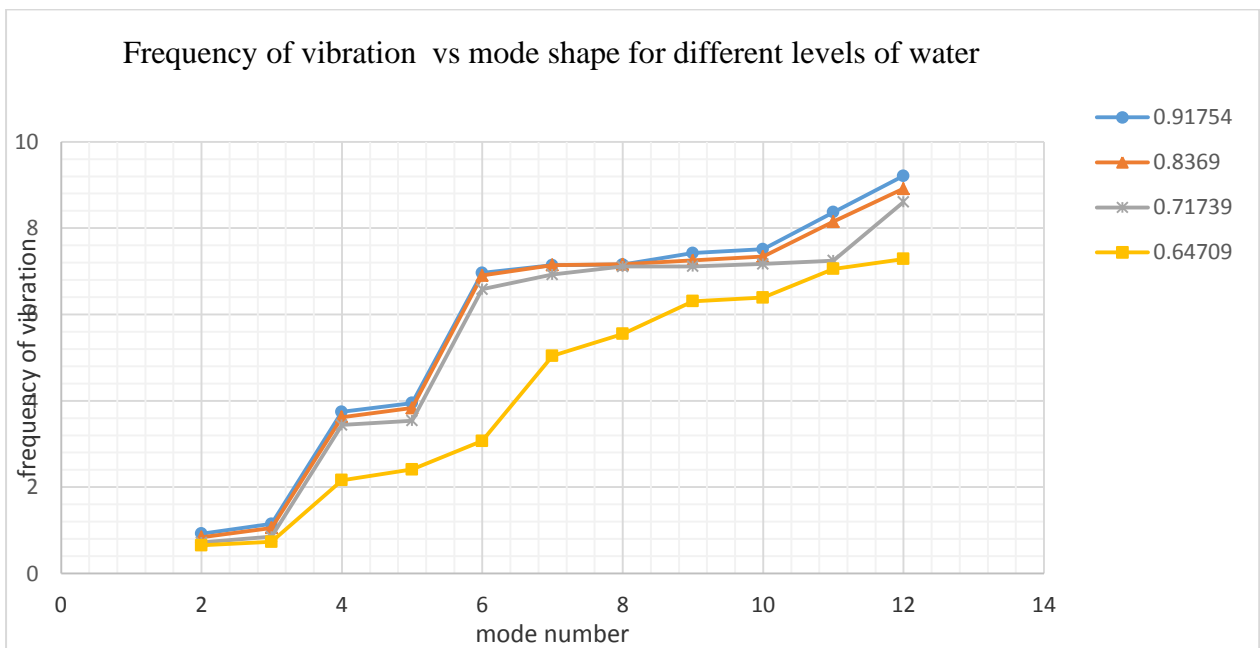


Fig . 2. Frequency of vibration vs. mode shape for different levels of water

Modal analysis results in a number of mode shapes in which the tank may vibrate and some of them are presented below.

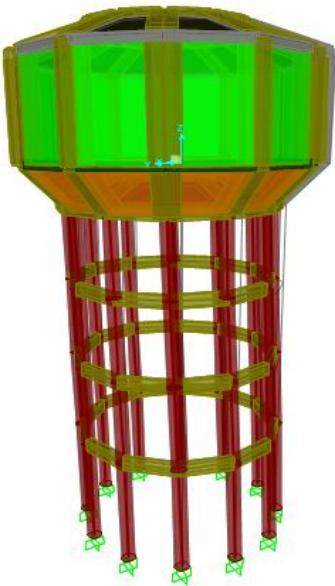


Fig. 3. Mode 1 of vibration

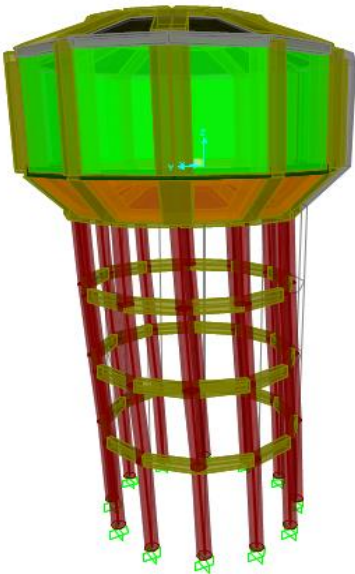


Fig. 4. Mode 2 of vibration



Fig. 5. Mode 3 of vibration



Fig. 6. Mode 4 of vibration

The change in different parameters namely frequency, amplitude of vibration and maximum deformations are studied at different levels of water in the tank .The corresponding results are presented below.

Table.4 Different seismic parameters at different levels of water

Water level	Frequency(cyc/sec)	Amplitude of vibration (mm)	Maximum deformation(mm)
Empty (0%)	0.90515	0.936747	0.0313
Upto the middle ring (13.53%)	0.82515	1.300565	0.0405
2.5 m above the middle ring beam (56.76%)	0.71739	1.9456	0.0538
Upto the top ring (full 100%)	0.65285	.04	0.0681

Based on the results graph is plotted between frequency of vibration versus percentage change in volume of water and is shown in fig 9.

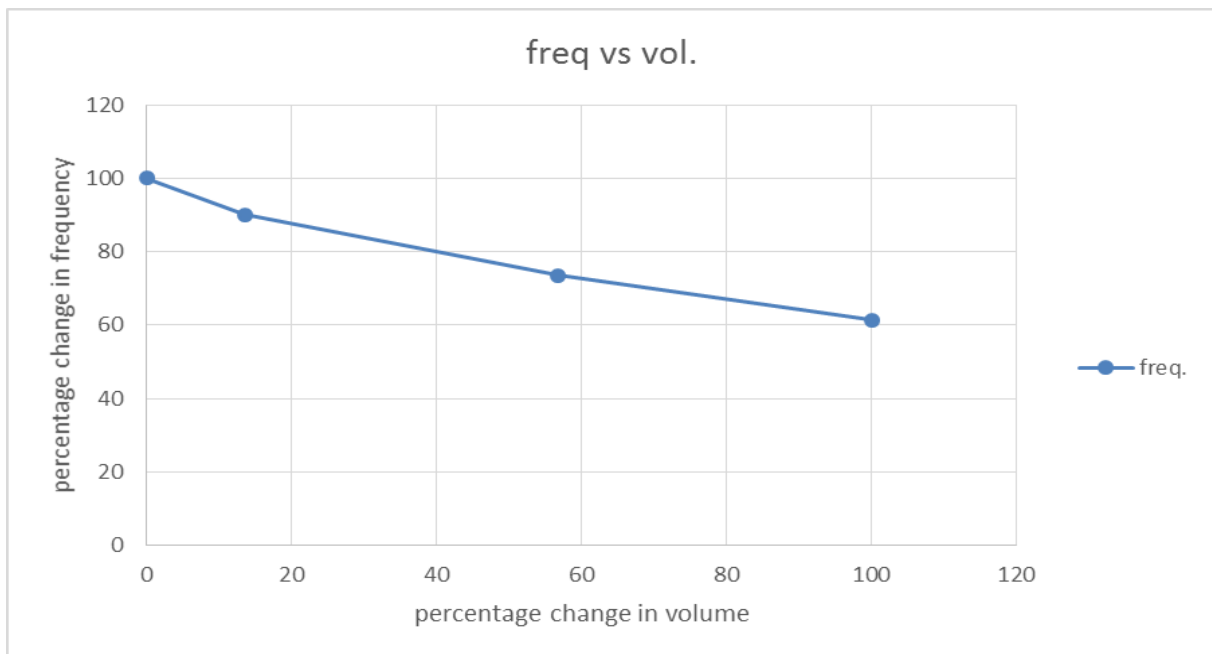


Fig. 9. Frequency vs. volume plot

Based on the results graph is plotted between amplitude of vibration at 1st mode versus percentage change in volume of water and is shown in fig 10

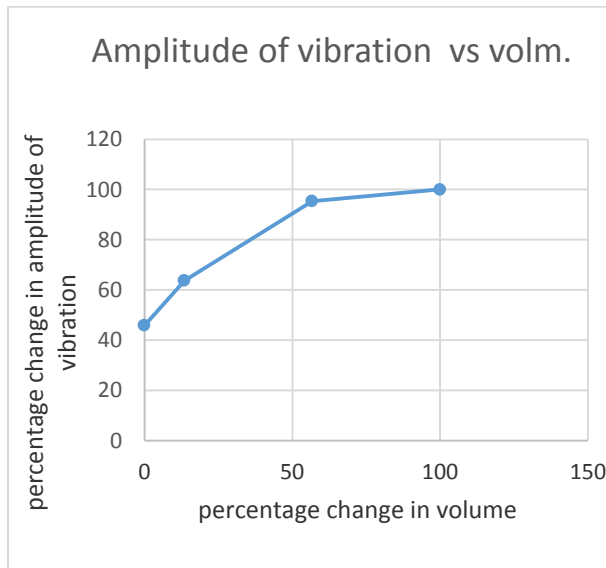


Fig. 10. Amplitude vs. volume plot

The graph is plotted between maximum deflection of the tank in a predefined earthquake versus percentage change in volume of water and is shown below

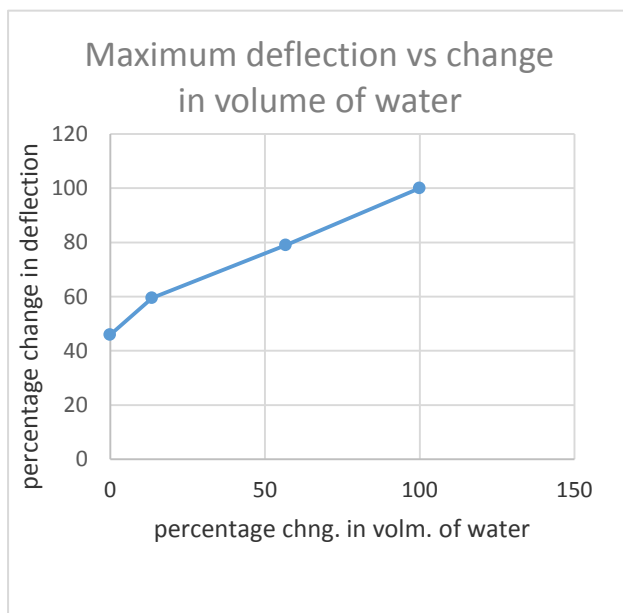


Fig. 11. Maximum deflection of the tank vs. Volume plot.

5. CONCLUSIONS

Based on the analysis results, the following conclusions can be drawn:

1. Frequency of vibration is maximum when the tank is empty and decrease by 9.88% for one-third filled condition, 26.39% for half-filled condition and 38.64% for the full condition. Hence, it indicates that the tank will vibrate with minimum frequency when it is full of water.
2. Amplitude of vibration for the first mode is maximum when the tank is full and is decreased by 4.62% for half tank condition, 36.27% for one-third filled condition and 54.08% for empty tank condition. Similarly, amplitude of vibration for following modes follows the same trend. Hence it is apparent that the tank will vibrate with maximum amplitude when it is fully filled with water.
3. Likewise, maximum displacement of the tank for a predefined response spectrum analysis is maximum when the tank is full and is decreased by 21% for half-filled condition, 40.53% for one-third filled condition and 54.1% for empty tank condition. Hence it is seen that, for a given earthquake, the deformation of the tank is minimum when the tank is empty.
4. From the above results, it is observed that a tank fully filled with water experiences maximum amplitude of vibration and maximum deformation for a given earthquake. It can be concluded that rather than keeping the tank in full condition for a long duration, it is better to release the water periodically to avoid the excessive deformation during earthquake. Moreover, it is suggested that there should be a facility for special outlet system for quick removal of water such that at the intimation of an earthquake the water level can be reduced very quickly. This will result in reduction in amplitude of vibration in any mode and also reduce the maximum deformation for any earthquake and reduce the chance of failure and cracking of RCC tank.

6. REFERENCES

1. B. Schwarz, and M. Richardson, *Experimental modal analysis*, CSI Reliability Week, Orlando, FL, 1999.
2. Chopra Anil K., *Dynamics of Structures, Theory and applications to earthquake engineering*, third edition, Pearson publications.
3. Hirde, S., Bajare, A. Hedao, M.² (2011), *Seismic performance of elevated water tanks*, International Journal of Advanced Engineering Research and Studies, 1(1), 78-87.
4. Housner G., *Dynamic pressure on accelerated fluid containers*, Bulletin of the Seismological Society of America, Vol. 147, 1957, pp. 15-35.
5. M. Haroun, and M., Tayel, *Response of tanks to vertical seismic excitation*, Earthquake Engineering and Structural Dynamic, Vol. 13, Issue 5, September/October, 1985, pp. 583-595.
6. Punmia B.C, Jain Ashok Kumar², R.C.C Designs, tenth edition, Water tanks II, pp.649 – 668.
7. R. J. Allemang, *Analytical and experimental modal analysis*, UCSDRLCN- 20-263-662, 1994, pp.166-178.

[Back to table of contents](#)

Experimental evaluation of Load-Displacement behavior of Skirted Foundation on sand

First A. Kangkan Sarmaⁱ⁾, Second B. Dr. (Mrs.) Nayanmoni Chetiaⁱⁱ⁾

i) PG Student, Department of Civil, Jorhat Engineering College, Jorhat

ii) Assistant Prof., Department of Civil, Jorhat Engineering College, Jorhat

ABSTRACT

Load test on model footings of different shapes viz, square (i.e., $L/B=1$), rectangular (i.e., $L/B=2$) and strip (i.e., $L/B=6$) were carried out to study the behaviour of the footings with and without skirts resting on sand. The model tests were conducted in a large tank of dimension $95\text{cm}\times 95\text{cm}\times 95\text{cm}$ and the footing was instrumented with dial gauges of 0.01mm least count to measure the settlement. A hydraulic jack with calibrated pressure gauge having least count of 5.0 kg was used for application of loads. The use of structural skirts with the footing improved the bearing capacity up to an improvement factor of 2.67 . Improvement is dependent upon some factors like the footings shape ratio (L/B), skirt depth ratio (D_s/B), relative density of sand (I_D), unit weight of sand (γ) etc. To establish a relationship of these factors with the ultimate bearing capacity of skirted footing, a multiple linear regression analysis was done and based on the regression analysis results a modified bearing capacity equation is proposed for skirted footings on sand by the authors.

Keywords: Bearing capacity, structural skirt, shape ratio, skirt depth ratio, strip footing, improvement factor.

1. INTRODUCTION

The shallow footings fail mainly due to the shear failure of soil below it. When the superstructural load gets transferred to the soil below the footing, it is displaced from its position due to shear failure of soil. Such failure can be duely taken care of by providing some kind of confinement around the soil below the footing. In this case, structural skirts serve as an alternative method of improving the bearing capacity and reducing the settlement of footing resting on soil. Skirts provided with foundations, form an enclosure in which soil is strictly confined and acts as a soil plug to transfer superstructural load to soil. In comparison to a surface foundation, the skirt transfers the load to a greater depth i.e., to a stronger layer of soil; thus mobilizing higher bearing capacity. Now a days shallow skirted foundations have been used in structures like oil and gas industries, replacing usual piled foundations. Also they have been used as support for large fixed substructures or as an anchorage for floating structures in offshore applications.

In this paper the methodology, test set-up and results of the experimental model study of shallow foundation of different shapes with and without skirts on sand under different relative densities subjected to central vertical loading are presented.

2 RESEARCH METHODOLOGY

2.1 Testing set-up and material

The methodology consists of performing load test

for Model Footing (MF) and Model Skirted Footing (MSF) in a test tank of dimension $95\text{cm}\times 95\text{cm}\times 95\text{cm}$ for different shape and depth of skirts. The test tank consisted of steel rigid plates welded all around and with metal braces to prevent them from lateral expansion. The test set up comprises of the loading frame, inverted hydraulic jack, pumping unit and the test tank essentially with the various footing assembly. The loading frame comprises of the reaction frame properly loaded with cement concrete cubes. A mechanically operated hydraulic jack of 100kN capacity is clamped to it. The load from hydraulic jack is transferred to the subgrade soil through footings of different shapes and sizes. Pre calibrated pressure gauge of 5kg least count is used to measure the magnitude of the applied load. The deflection dial gauges of 0.01mm least count were placed on the plates with the help of horizontal datum bars to measure settlements of plates due to loading. This datum bar arrangement is free from any connection to the loading arrangement so that any disturbance in the loading arrangement does not affect the deflection dial gauge system. The soil used in the test tank are cohesionless sand. The sand bed is prepared in the test tank in eight layers (each layer of 10cm) with pre-calibrated compacting energy to achieve the required relative densities. The plate represents Model Footing (MF) and the plate with skirt represents Model Skirted Foundation (MSF).

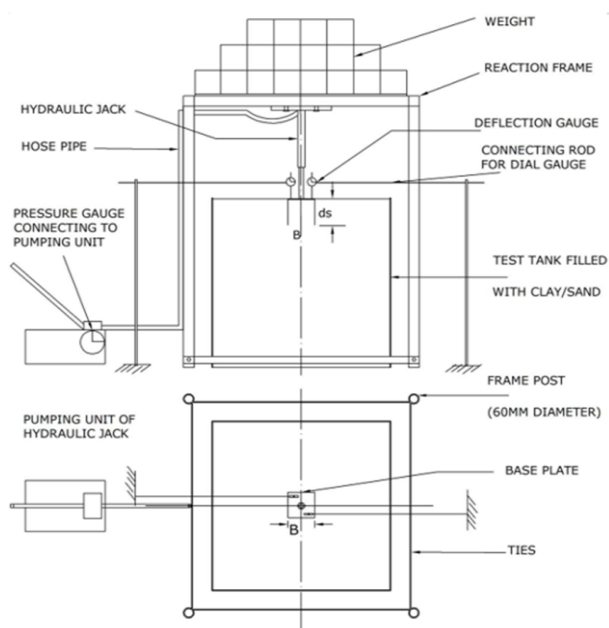


Fig.1: Schematic diagram of loading frame assembly and test tank with MSF at surface.



Fig 2: Loading frame assembly

There were basically two series of load tests. In first series load tests were conducted on MF and in the second series on MSF. The model foundations were made up of steel plate of thickness 6mm. The surfaces of plate as well as skirt were made rough before placing in the test tank. Three different sizes of steel plates 150mmx150mm, 150mmx300mm and 150mmx900mm were used as model footings to represent various shapes of square, rectangular and strip footing with $L/B=1, 2$ and 6 . Truncated wooden pyramid was used to ensure uniform distribution of the load on the model footing from the spindle of the inverted jack. The variable geometrical parameters used in the experimental programme are as follows $L/B, D_s/B$ where

D_s = Depth of the skirt
 L = Length of the plate
 B = Breadth of the plate



Fig 3 Different skirts used under plates with $L/B=1, L/B=2, L/B=6$.

2.2 Material:

The grain size distribution curve of the sand is shown in figure. From the curve the grading characteristics i.e. D_{10}, D_{30}, D_{60} were determined as 0.19, 0.23 and 0.64mm respectively. These gives uniformity coefficient, $C_u=3.36$ and coefficient of curvature, $C_c=0.44$. Thus the sand was classified as well graded sand based on unified soil classification system. The various properties of sand determined in the laboratory are listed in table 1.

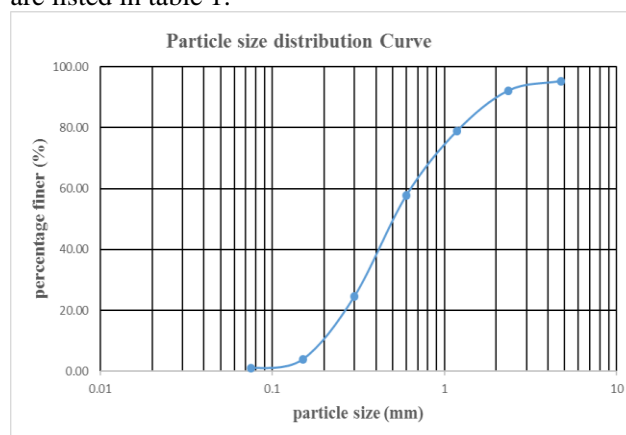


Fig. 4 Particle size distribution curve for the sand sample

Table 1 properties of sand used in the study:

Property	Test values
Specific Gravity	2.67
D_{10}	0.19
D_{30}	0.23
D_{60}	0.64
Co-efficient of uniformity, C_u	3.36
Co-efficient of curvature, C_c	0.44
Max. dry density, γ_{dmax}	16.16 kN/m ³
Min. dry density, γ_{dmin}	13.98 kN/m ³

For the preparation of the sand bed, sand raining technique was used. The height of free fall was calibrated from a number of trials. Consistency in the

placement density was checked with small aluminium cans of known volumes at different locations and at different heights. It has a hopper connected to 690mm long pipe with an inverted cone at the bottom. The sand passes through the 31 mm internal diameter pipe and disperses at bottom by a 60° inverted cone. The placement density of the sand can be varied by changing the height of free fall. To achieve lower relative density, sand is poured through a wire mesh fixed at a certain height. Four test series with relative densities 30%, 50%, 70% and 90% was done. The corresponding densities are 14.57kN/m³, 14.98kN/m³, 15.44kN/m³ and 15.89kN/m³ respectively.

2.3 Application of the Load

At first, in all cases footing was placed centrally under the spindle of the jack. The hydraulic jack is supported against the reaction frame as shown in the schematic diagram, figure 1 and figure 2. Then the jack is ejected to just touch the footing surface, at this time the reading showed in the dial gauge that were placed diagonally opposite to the footing was taken as initial reading. Then load is applied without any jerk in cumulative equal increments of 20kg for L/B=1 and 50kg for the rest. Dial gauge observations were recorded for each load increments after an interval of 5.00, 10.00, 15.00 minutes and thereafter of a 15 minutes' intervals till the rate of settlement is not more than 0.02 mm per minute. For this period, the load applied should be maintained constant. There after the next higher load is applied and the process is repeated. The testing is continued till a very high settlement is obtained.

2.4 Assumptions

- 1.The foundation is rough and rigid
- 2.No slippage occurs between footing and skirt.
- 3.The friction is considered only on the outer side of the skirt wall.
- 4.No relative movement of the soil inside the skirt takes place with respect to the skirt wall.
- 5.The load is transferred from the column to the footing and to the skirt.

Table 2. Test Details for sand

Serial No.	L/B	Relative Density (%)	D _s /B
1	1	30	0
2	1	30	0.5
3	1	30	1
4	1	50	0
5	1	50	0.5
6	1	50	1
7	1	70	0
8	1	70	0.5
9	1	70	1
10	1	90	0
11	1	90	0.5
12	1	90	1
13	2	30	0
14	2	30	0.5
15	2	30	1
16	2	50	0
17	2	50	0.5
18	2	50	1
19	2	70	0
20	2	70	0.5
21	2	70	1
22	2	90	0
23	2	90	0.5
24	2	90	1
25	6	30	0
26	6	30	0.5
27	6	30	1
28	6	50	0
29	6	50	0.5
30	6	50	1
31	6	70	0
32	6	70	0.5
33	6	70	1
34	6	90	0

3. EXPERIMENTAL RESULTS

The results of the model load tests on sand are presented and discussed here. Thirty-four numbers of load test were carried out to study the behavior of three different shape ratios of footings, viz. square (L/B=1), rectangular (L/B=2.0) and strip (L/B=6.0) on sand under different relative densities viz 30%, 50%, 70% and 90%. Pressure-Displacement characteristics have been studied for surface footing and for two skirt depths (i.e., D_s/B=0.5 and D_s/B=1) for different L/B ratios under the different relative densities.

3.1 Behaviour of surface footings without skirt

Model footing with L/B=1

Fig.5 shows the typical pressure-displacement responses for footing with L/B=1 for four different relative densities: 30%, 50%, 70%, 90%. All of the

curves show nearly the same initial slope but different failure points from which the footing displacement increases linearly with the pressure increment at a relatively high slope. The pressure at failure point i.e.; the pressure corresponding to discontinuity point at pressure-displacement curve is determined as the footing ultimate bearing capacity. From the pressure-displacement plot the ultimate bearing capacities were found as 43.6 kN/m², 61.04 kN/m², 78.48 kN/m² and 139.53 kN/m² for relative densities 30%, 50%, 70% and 90% respectively.

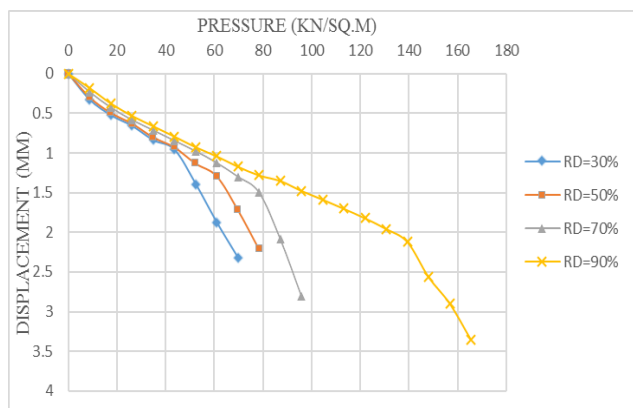


Fig.5: Pressure-Displacement curve for 15cm ×15cm surface footing without skirts.

Model footing with L/B=2

Load-displacement characteristics was studied for model footing with L/B=2. Fig.6 shows the typical pressure-displacement responses for footing with L/B=2 for different relative densities. The ultimate bearing capacities corresponding to the relative densities were found as 54.5 kN/m², 65.4 kN/m², 87.2 kN/m² and 152.6 kN/m² respectively.

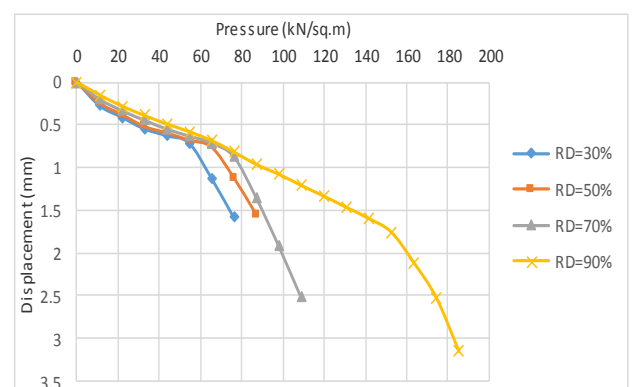


Fig.6: Pressure-Displacement curve for 15cm ×30cm surface footing without skirts

Model footing with L/B=6

Load-displacement characteristics was studied for model footing with L/B=6. Fig.7 shows the typical pressure-displacement responses for footing with L/B=6 for different relative densities. The ultimate bearing capacities corresponding to the relative

densities were found as 49.08 kN/m², 61.35kN/m², 98.16 kN/m² and 161.15 kN/m² respectively.

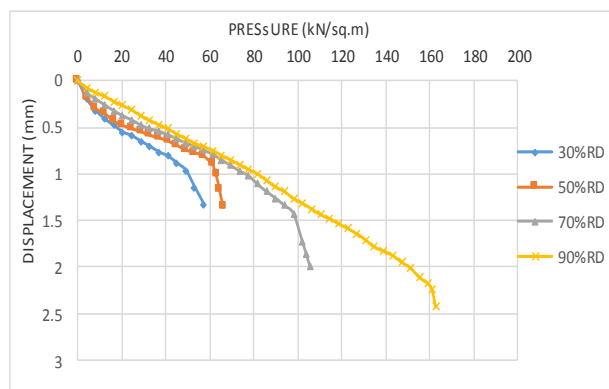


Fig.7: Pressure-Displacement curve for 15cm×90cm surface footing without skirts

3.2 Comparison of experimental and predicted values of bearing pressure

The ultimate bearing capacities ($q_{ult}(Exp.)$) obtained from the experimental load-displacement curve of the model footings (i.e.; L/B=1, L/B=2, L/B=6) for different density further compared by using angle of internal friction (ϕ) and unite weight (γ) at relative densities 30%, 50%, 70% and 90% with Terzaghi (1943), Meyerhof (1963), Hansen (1970), and Vesic (1973) bearing capacity equations.

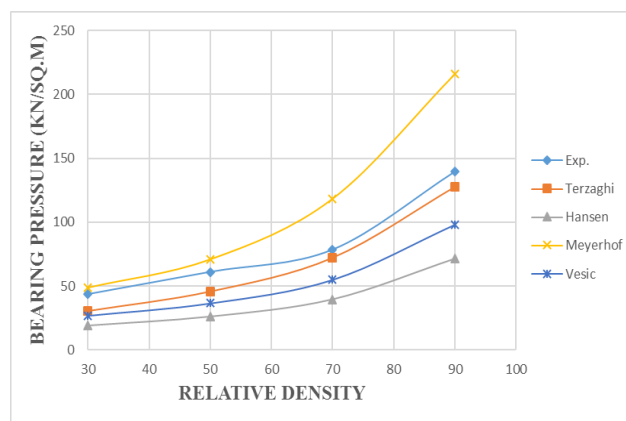


Fig.8: Bearing pressure vs Relative Density curve for 15cm×15cm (i.e.; L/B=1) Footings

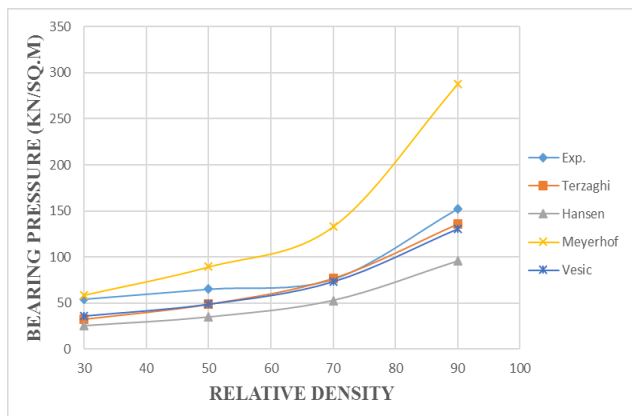


Fig.9 Bearing pressure vs Relative Density curve for 15cmx30cm (i.e. L/B=2) Footings

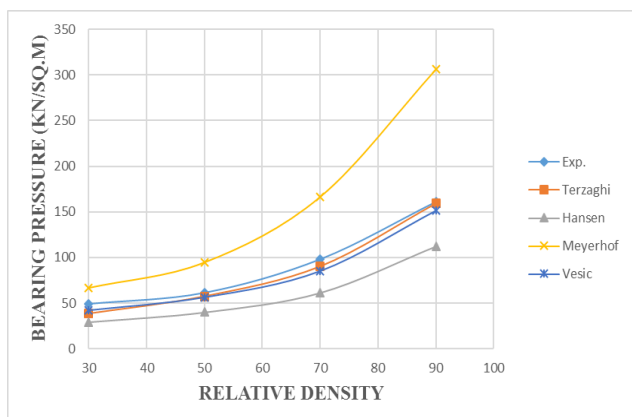


Fig.10 Bearing pressure vs Relative Density curve for 15cmx90cm (i.e. L/B=6) Footings

3.3 Behaviour of model skirted footings (MSF)

Analysis of experimental results showed that inclusion of skirts improves bearing capacity of surface footings on sand. The improvement in magnitude increases with increasing the skirt depths and relative densities.

Load –Displacement behaviour of MSF

The performance of the **square** (i.e. L/B=1), **rectangular** (i.e. L/B=2), **strip** (i.e. L/B=6) at surface with two different skirt lengths below it was studied and the respective results have been plotted in Fig.5 and 6. For model footing **L/B=1** at surface when no skirt is provided ($D_s/B=0$), ultimate bearing capacity is 43.6 kN/m², but when provided with a skirt of depth 0.075m ($D_s/B=0.5$) and 0.15m ($D_s/B=1$), ultimate bearing capacity is improved to 78.48 kN/m² and 113.36 kN/m² respectively at 30% relative density. Hence the improvement factors are 1.8 and 2.6 corresponding to $D_s/B = 0.5$ and 1.0 respectively. Similarly bearing capacity values and improvement factors for L/B=2, L/B=6 at 30%, 50%, 70% and 90% relative densities are shown in table 3

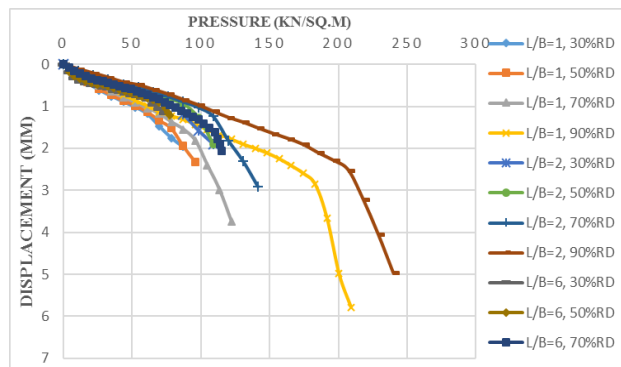


Fig.11: Pressure-Displacement behaviour for L/B=1, L/B=2 and L/B=6 Skirted footing with $D_s/B=0.5$

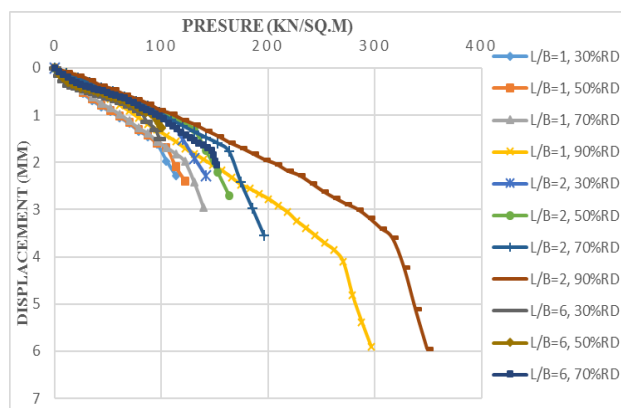


Fig.12: Pressure-Displacement behaviour for L/B=1, L/B=2 and L/B=6 Skirted footing with $D_s/B=1$

3.4 Effect of footing size (L/B) on bearing capacity

Applied bearing loads has been plotted against the size of footing (L/B) at constant skirt ratio (D_s/B) for different relative densities and is shown in figures 13 and 14. It is observed that when the L/B ratio increases the bearing loads also increases for a constant D_s/B ratio and the improvement in bearing load is higher for higher densities. The increase in bearing loads with relative density of sand may be due to the increase in angle of internal friction value of sand, which mainly occurs to additional inter locking between particles in a denser state.

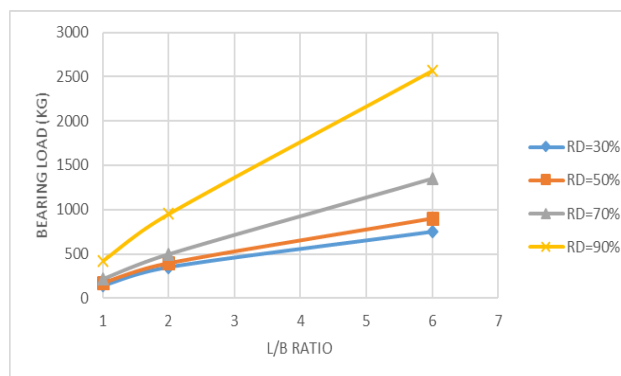


Fig.13: L/B ratio vs Bearing Load curve for $D_s/B=0.5$ under different RD

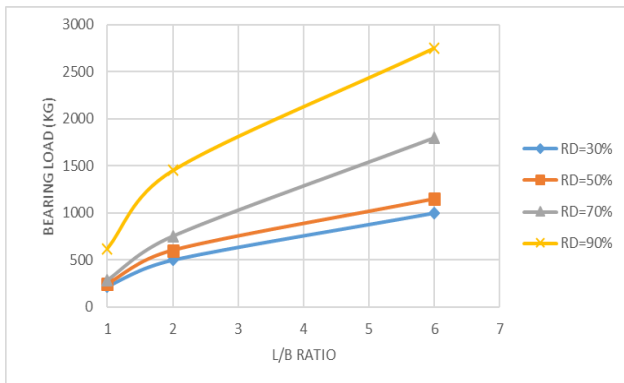


Fig.14: L/B ratio vs Bearing Load curve for $D_s/B=1$ under different RD

3.5 Effect of skirt ratios (D_s/B) on bearing capacity ratio for different shape of footings

The bearing capacity ratio (BCR) is defined as the ratio of bearing capacity of Model skirted footing to the bearing capacity of model surface footing at any relative density of sand. The variations of BCR against D_s/B ratio for different shape of footing i.e. $L/B=1$, $L/B=2$, $L/B=6$ are plotted for 30%, 50%, 70% and 90% relative densities, in fig. 15, 16 and 17 respectively.

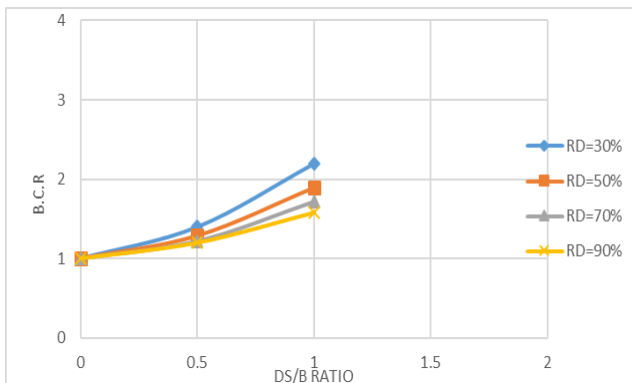


Fig.15: D_s/B ratio vs Bearing capacity ratio curve for $L/B=1$ under different RD

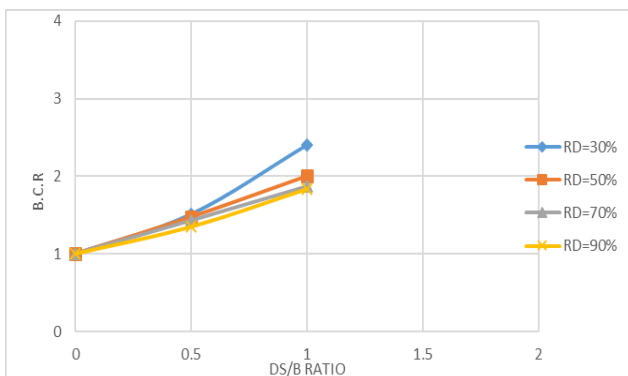


Fig.16: D_s/B ratio vs Bearing capacity ratio curve for $L/B=2$ under different RD

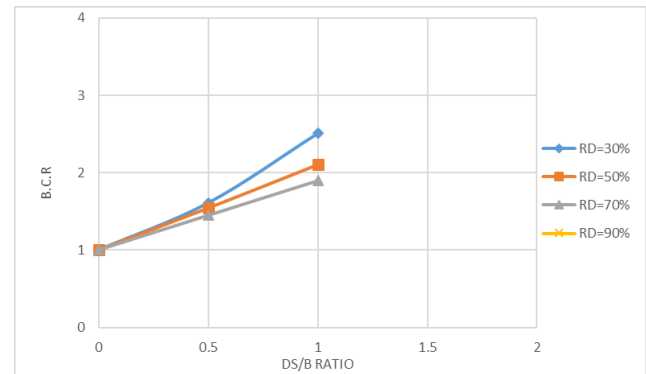


Fig.17: D_s/B ratio vs Bearing capacity ratio curve for $L/B=6$ under different RD

The BCR increases with skirt length (i.e., D_s/B) almost parabolically. However, the rate of increase in bearing capacity with skirt ratio (D_s/B) is not same for all size of footings at different relative densities. The increase in BCR with skirt ratio is higher for footings in sand with lower relative density for a particular L/B ratio. Again the increment in BCR with skirt ratio is higher for footings having lower L/B ratio with lower relative density. So it can be concluded that the improvement of bearing capacity is a function of skirt length (D_s/B), L/B ratio and also depends on the relative density of sand bed in which it is embedded.

3.6 Effect of relative density on bearing capacity ratio for different shape of footings

The bearing capacity ratio BCR is defined as the ratio of bearing capacity of skirt footing to the bearing capacity of surface footing at similar testing conditions. Figure 18 shows the variations of BCR with relative density of sand bed for $L/B=1$, 2 and 3 respectively. These curves show the decreasing of BCR with increasing the relative density of sand for all types of footings, also the BCR reduces with increasing the L/B ratio for each density and it increases with D_s/B ratio for all types of footings. Thus inclusion of Skirts showed more efficiency in enhancing bearing capacity of surface foundations resting on sand of low relative density.

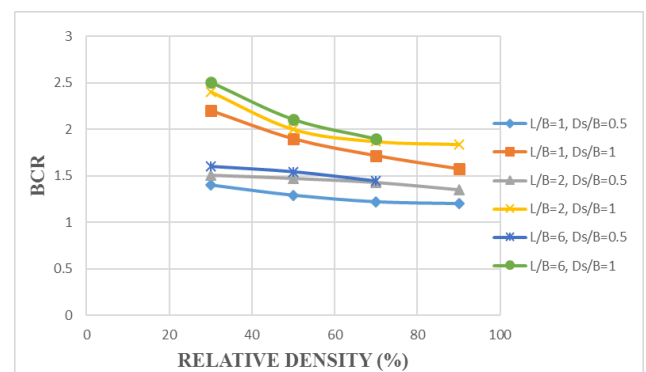


Fig.18: Relative Density Vs Bearing capacity ratio curve for $L/B=1$, $L/B=2$, $L/B=6$ under different D_s/B

From the graphs it is seen that for 15cm×15cm (L/B=1) footing at $D_s/B=1$, the BCR values are 2.6, 2.5, 2.11 and 1.90 for relative densities of 30%, 50%, 70% and 90% respectively. Similarly, the bearing capacity ratios for L/B=2 and L/B=6 are shown in table 3.

Table 3. Summary of results in terms of Bearing Capacity Improvement factors (IF) for L/B=1, L/B=2 and L/B=6

L/B	R _D (%)	D _s /B	ϕ	q _{ult} (kN/m ²)	IF
1	30	0	34.02°	43.6	1
1	30	0.5	34.02°	78.48	1.8
1	30	1	34.02°	113.36	2.6
1	50	0	35.75°	61.04	1
1	50	0.5	35.75°	104.64	1.7
1	50	1	35.75°	156.96	2.5
1	70	0	38.07°	78.48	1
1	70	0.5	38.07°	130.8	1.67
1	70	1	38.07°	165.68	2.1
1	90	0	40.85°	139.53	1
1	90	0.5	40.85°	200.56	1.44
1	90	1	40.85°	270.32	1.9
2	30	0	34.02°	54.5	1
2	30	0.5	34.02°	87.2	1.6
2	30	1	34.02°	119.9	2.2
2	50	0	35.75°	65.4	1
2	50	0.5	35.75°	98.1	1.5
2	50	1	35.75°	130.8	2
2	70	0	38.07°	87.2	1
2	70	0.5	38.07°	119.9	1.38
2	70	1	38.07°	163.5	1.88
2	90	0	40.85°	152.6	1
2	90	0.5	40.85°	207.2	1.36
2	90	1	40.85°	283.4	1.86
6	30	0	34.02°	49.08	1
6	30	0.5	34.02°	73.62	1.5
6	30	1	34.02°	98.16	2
6	50	0	35.75°	61.35	1
6	50	0.5	35.75°	85.89	1.4
6	50	1	35.75°	118.93	1.93
6	70	0	38.07°	98.16	1
6	70	0.5	38.07°	134.98	1.38
6	70	1	38.07°	159.51	1.62
6	90	0	40.85°	161.15	1

4 REGRESSION ANALYSIS

A multiple regression approach is chosen to develop a model on the basis of the experimental data, wherein the bearing pressure is taken as the dependent (response) variable, while the rest of the parameters are considered as independent (Predictor) variables. A total of 34 points were considered for analysis. The results of multiple linear regression analysis were conducted and the results are as follows.

Table 4: Goodness of fit statistics for the model skirted foundation

Regression Statistics	
Multiple R	0.97635756
R Square	0.95327409
Adjusted R Square	0.94682913
Standard Error	13.2774167
Observations	34

Table 5: Analysis of variance (ANOVA) for MSF

	df	SS	MS	F	Significance F
Regression	4	104300.2	26075.05	147.9102	7.5772E-19
Residual	29	5112.404	176.2898		
Total	33	109412.6			

Table 6. Summary of t-statistics

	Coefficients	Standard Error	t Stat	P-value
Intercept	-2092.51967	356.3957906	-5.87134	2.27E-06
Variable 1	94.09873409	7.330721805	12.83622	1.73E-13
Variable 2	67.12969497	11.55353184	5.810318	2.68E-06
Variable 3	-34.1434192	7.935896855	-4.3024	0.000175
Variable 4	-4.83928674	1.781799137	-2.71596	0.011021

The final proposed relation takes the form as,

$$q_{\text{predicted}} = -2092.51967 + 94.0987 \frac{D_s}{B} + 67.12969497 \phi - 34.1434192 I_{D\gamma} - 4.83928674 \frac{L}{B} \times \frac{D_s}{B}$$

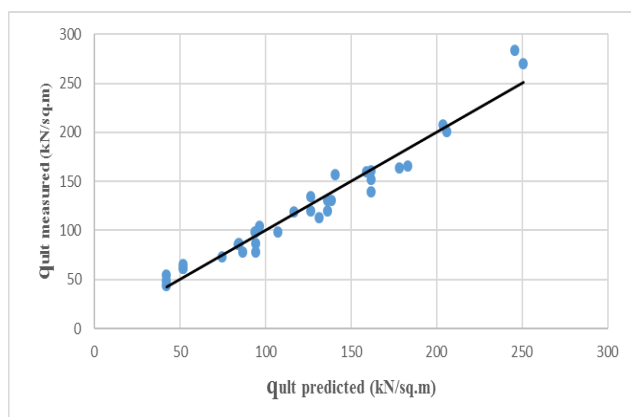


Fig.19 Comparison between observed bearing capacity and estimated bearing capacity

Conclusion:

A model load test was performed to study the behaviour of skirted foundation of different shapes bearing on cohesionless soil. The important results from this experimental investigation can be summarized as follows

1. The inclusion of structural skirt with surface footing improved the bearing capacity by a factor of up to 2.6 and the improvement in magnitude increases with increasing skirt depth.
2. Also for each type of footing, improvement in bearing capacity is higher for lower relative density. This is due to the better confinement of sand below the footing due to the skirts.
3. The structural skirts also reduce the settlement of footing.
4. Based on the experimental results on model footings, a multiple regression analysis is done to establish a relationship between the variable parameters and the ultimate bearing capacity of skirted footings. From the results of regression analysis an equation is proposed but the influence of geometric properties of footing and skirts has not been investigated. Thus further studies are required to relate this equation with actual footings.

REFERENCES

- 1) Dr. Sunil S. Pusadkar¹, Ms. Tejas Bhatkar² (2013)- "Behaviour of Raft Foundation with Vertical Skirt Using Plaxis 2d" Volume 7, Issue 6 (June 2013), PP. 20-24.
- 2) Eid, H.T. (2012) Bearing capacity and settlement of skirted shallow foundation on sand. ASCE journal.
- 3) M.Y. Al-Aghbari and Y.E-A. Mohamedzein (2004). "Bearing capacity of strip foundations with structural skirts." Geotechnical and Geological Engineering, 22(1):43-57
- 4) M. Y. AL-Aghbari (2007) - "Settlement of shallow circular foundation with structural skirts resting on sand"

5) Mahmoud M. A. and Abdrabbo F. M. (1989) Bearing capacity tests on strip footing resting on reinforced sand subgrades. Canadian Geotechnical Journal, 26, 154-159.

6) Yun, G. and Bransby, M.F. (2007) "The undrained vertical bearing of skirted foundations" Japanese geotechnical society vol. 47, NO. 3493-505.

[Back to table of contents](#)

Ductility Factor of Water hyacinth Fibre Reinforced Soil Using Evolutionary Genetic Programming Model

ShubhamTripathiⁱ⁾, Vishal Kashyapⁱⁱ⁾ and Sanadam Bordoloiⁱⁱⁱ⁾

i) B.Tech 3rd year, Department of Civil Engineering, Indian Institute of Technology Guwahati, Guwahati, Assam 781039, India.

ii) B.Tech 4th year, Department of Civil Engineering, Indian Institute of Technology Guwahati, Guwahati, Assam 781039, India.

iii) Ph.D Student, Department of Civil Engineering, Indian Institute of Technology Guwahati, Guwahati, Assam 781039, India.

ABSTRACT

Unconfined compressive strength (UCS) of soil is one of the key mechanical properties used for judging the representative strength of soil in geotechnical infrastructures. Taking stress versus strain response of a soil into account, we can find the peak strain corresponding to peak strength value of soil, for the strain hardening section of the response. Although many models exist in literature that quantifies the strength response of a fiber reinforced soil, relatively few models take soil ductility improvement in account for fiber reinforced soil. This soil ductility improvement can be studied by the development of a generalized model, based on a newly proposed ductility factor. It is represented as the ratio of peak strain of reinforced soil to the peak strain of unreinforced soil. The model takes into account three inputs such as fiber content, soil density and moisture content. Environmentally invasive weed species, water hyacinth (WH) fibers were selected in this study as fiber material. A series of UCS tests were conducted to obtain laboratory data on the soil-WH fiber composites. Evolutionary algorithm of Genetic programming (GP) was then used to formulate models based on measured laboratory UCS data. The hidden non-linear relationships between ductility factor and the three inputs were determined by sensitivity and parametric analysis of the GP model. It is believed that the holistic GP model developed will be useful for practicing engineers, to determine optimum input values for designing proper subgrade using fiber reinforced soil.

Keywords: Water Hyacinth, Ductility Factor, Genetic Programming, Unconfined Compressive Strength (UCS).

1. INTRODUCTION

Unconfined Compressive Strength (UCS) test is among the cheapest and the fastest methods of measuring shear strength. It is also the most popular method of soil shear testing and an essential parameter for the initial design and analysis of various geotechnical infrastructures like bearing capacity of soils under dams, subgrade soil in road pavements (Consoli et al., 1998; Maher and Ho, 2004; Cai et al., 2006;). As suggested by ASTM D-2166 (2005), the peak stress and peak strain can be found out by the stress strain response of reinforced soil under compression loading. Various studies suggest that soil strength characteristics increases with inclusions of relatively high tensile fibers. Water Hyacinth (WH) has been recently used as an alternative material for use in fiber reinforced soil (Bordoloi et al. 2015). Water Hyacinth is an invasive and uncontrollable weed, covers lakes and diminishes oxygen levels for aquatic species. There are various modelling methods which model the strength parameters of soil but very few of them have been used to model soil ductility. Soil ductility during loading can

be taken into account by considering a newly proposed parameter i.e. mobilized ductility factor (MDF) defined as the ratio of the peak strain of reinforced soil to the peak strain of unreinforced soil. In addition to soil being a black box, it is always better to take all the possible factors (i.e. soil ductility, fiber content, moisture content, maximum dry density) into account and model the strength parameters of the reinforced soil based on them. This model can be used to optimize the input parameters for deriving maximum advantage of soil reinforced with fibers. Thus modelling done using Genetic Programming (GP) gives the output strength very close to the obtained strength parameter using laboratory experiments. Therefore, the present study demonstrates the advanced soft computing approach of genetic programming (GP) to formulate the functional relationships between factor of change in strain (i.e. ductility factor) due to inclusion of fiber and three input parameters (i.e. soil moisture, fiber content, maximum dry density of the soil) of the soil reinforced with Water hyacinth. The performance of the model will be evaluated based on statistical metrics to

determine the best model.

2. Experimental study on effects of density, soil moisture and fiber content on UCS of fiber reinforced soil

Series of UCS tests were conducted to measure compressive strength of both unreinforced and reinforced soil. Tests were performed based on procedures prescribed in ASTM D-2166 (2005). Details on soil parameters, fiber selection, testing program and procedures as well as results are provided as follows. The soil used in this study was ML (clayey silt) as per USCS classification (ASTM, D2487-11). Procedures prescribed in IS-2720-Part4-1985 were used for determining grain size distribution of the soil. It is constituted mainly of silt (50%) followed by sand (26%) and clay (24%). Consistency limit of the soil determined according to IS-2720-Part 5 (1985) gave liquid limit and plastic limit as 40.50% and 24.81%, respectively. Standard Proctor's light compaction technique was used to determine its maximum dry density (MDD) and optimum moisture content (OMC) according to procedures prescribed in Indian Standard code IS-2720 part-7 (1980). MDD and OMC were found to be 1.72 g/cc and 16.92% respectively. UCS tests were conducted on both unreinforced and reinforced soil-WH composite at different compaction states corresponding to three soil densities (0.95 MDD, MDD and 1.05 MDD) and three moisture contents (OMC, OMC - 5% and OMC + 5%). In addition, the influence of variation in percentage fiber content (0.5%, 0.75% and 1% by dry weight of soil) on UCS was also investigated. The fiber percentage was restricted to 1% as the fibers tend to stick to each other while mixing thus forming pockets of low density. For each case, tests were repeated three times (total 108 tests including unreinforced soil) to check any variability in observed UCS. All UCS tests were conducted at a constant strain rate of 1.25 mm/minute as suggested in IS-2720 part-10 (1991).

3 DATA PREPARATION FOR TRAINING OF GP MODEL

Firstly, the training samples (80% randomly taken from measured values) and testing samples are selected. Model is formulated using training samples and tested on the testing samples. Experimental results from 81 tests are summarized in Fig. 1 and Fig. 2. Nature of the results data set collected is shown by the linear

relation obtained between actual ductility factor and the obtained ductility factor in testing and training phase as shown in figure 1 and figure 2. It comprises of inputs (soil moisture, (%), x_1) soil density (g/cc, x_2) and fiber content (% , x_3) and the output (Factor indicating change in strain due to inclusion in fibre (y)). In the following section, the evolutionary approach of genetic programming is discussed.

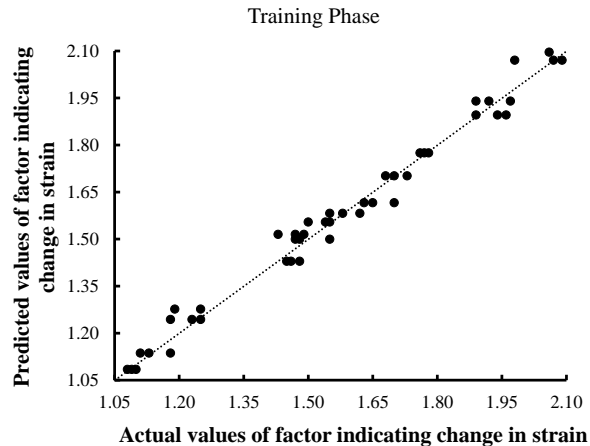


Fig. 1: Fit of Predicted and actual values of factor of strain (reinforced/unreinforced strain) on training data

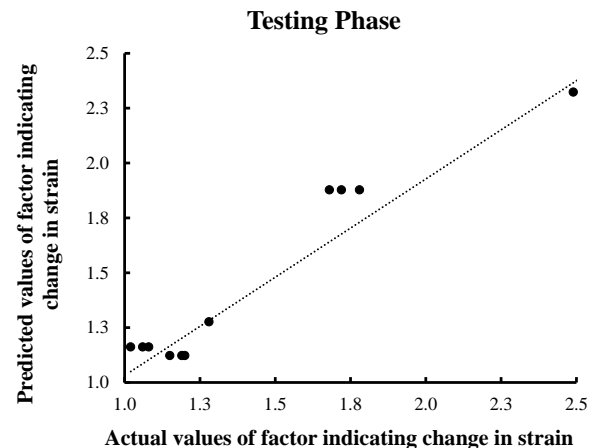


Fig. 2: Fit of Predicted and actual values of factor of strength (reinforced/unreinforced strain) on the testing data.

4 EVOLUTIONARY APPROACH OF MULTI-GENE GENETIC PROGRAMMING

Darwinian principle of "Survival of the fittest" is the idea behind Genetic Programming (G.P.) (Koza 1992). In GP, genes are evolved and every gene is considered

as a model. In MGGP, new genes are evolved by combining the old genes or models by cross over, mutation, reproduction. The step by step mechanism of MGGP is shown in Fig. 3. In order, to apply GP, several steps needed to be followed in a proper sequence. Firstly, the elements of functional and terminal set are chosen based on the problem. The functional set comprises of arithmetic operators (+, -, /, ×) and non-linear functions (sin, cos, tan, exp, tanh, log). Sometimes number of functional elements is reduced to decrease the complexity. The elements (three inputs of the soil and the range of random constants) form the terminal set. The range of random constants chosen is 0 to 0.001. These are chosen to take into account any error in the experiment/process. A gene is formed by the random combination of functional set, terminal set and data. In this way, several genes are evolved and combined by least squares method to form a model. Population size represents the number of models. The performance of the models in the initial population is evaluated based on the fitness function such as root mean square error (RMSE) given by

$$RMSE = \sqrt{\frac{\sum_{i=1}^N |G_i - A_i|^2}{N}} \text{----- (1)}$$

where, N denotes number of training samples, A_i and G_i are actual and predicted values. If any individual of the population does not satisfy the termination criterion, genetic operations such as selection, subtree crossover and subtree mutation are implemented on the individuals to evolve the new population. The program is terminated when the maximum number of generations or the threshold error of the model is reached as specified by the user. Genetic operations, mainly crossover and mutation, form most of the individuals of the population. In this way, genetic operations on the initial population consequently form a new population. As per Koza (1992), the probabilities of crossover, mutation and reproduction is chosen at 85%, 5% and 10% respectively. The iterative process of forming new populations continues until a termination criterion is met.

5 RESULTS AND DISCUSSION

The parameter settings for MGGP are set based on trial-and-error approach. The population size of 300, generations of 350, maximum number of genes at 6, functional set including elements of tanh, tan, exp, sin, plog, addition(+), subtraction(-), times(*) is chosen.

The terminal set includes the set of the three inputs (density, moisture and fiber content of soil).

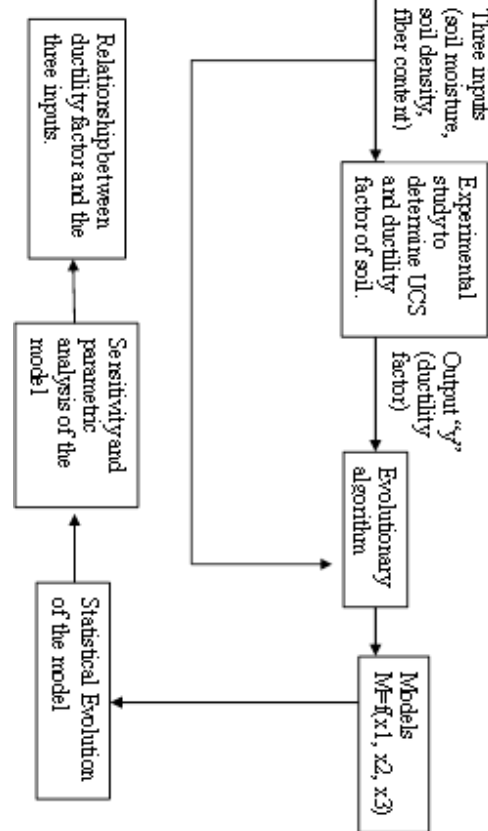


Fig.3: Procedure of modelling the strain factor of WH fiber reinforced soil by Evolutionary algorithm

The number of runs chosen in the study is 1. The best MGGP model (Equation 4) for factor indicating the ductility of the soil or ductility factor is selected based on the minimum training error from all runs.

Experimental results from 81 tests are summarized in table 1.

The performance of the best model is evaluated based on the three error metrics: correlation coefficient, mean absolute percentage error (MAPE) and RMSE given by:

$$R^2 = \frac{\sum_{i=1}^n (A_i - \bar{A}_i)(M_i - \bar{M}_i)}{\sqrt{\sum_{i=1}^n (A_i - \bar{A}_i)^2 \sum_{i=1}^n (M_i - \bar{M}_i)^2}} \text{----- (2)}$$

where M_i and A_i are the predicted and actual values respectively, \bar{M}_i and \bar{A}_i are the average values

of the predicted and actual respectively and n is the number of training samples.

$$\begin{aligned}
 FOS = & 14.8135 * \text{square}(\text{square}(\tanh(\cos(x2 - x3 - 0.000618)))) + 9.5987 * \tanh(x2 - 1.0 * x3) - \\
 & 1.3955 * \sin(\sin(x1)) * \text{square}(\cos(\text{plog}(\tan(x2 - x3)))) - \\
 & 0.1427 * \tan(\text{square}(x1 + 0.000178000001879917) + \exp(x2 - 0.00044400002917613) * (\sin(\sin(\sin(\sin(x1)))))) - \\
 & 1.0 * \tanh(\cos(\exp(x3)))) - \\
 & 0.0016405 * \tan(\text{square}(x1 + 0.000444) + \exp(x1) - 1.0 * \exp(x2) * (\tanh(\cos(\exp(x3)))) - \\
 & 1.0 * \exp(\tanh(\text{square}(x3)))) - 0.025017 * \tan(\exp(x2) - 0.000178) * \tan(x1) * (x2 - 1.0 * \tanh(\text{square}(\cos(\exp(x3)))))) - 7.2008
 \end{aligned}$$

(3)

Table 1: Error matrices for GP model

Error Matrices	Whole data	Training Data	Testing Data
RMSE	0.068225	0.037945	0.133096
R ²	0.980129	0.993126	0.944441

After finding the empirical equation for ductility factor with soil moisture (x1), soil density (x2) and fiber content (x3) as the input parameters, we can find the variation of ductility factor with soil moisture, soil density and fiber content respectively. For finding the variation of ductility factor with any one of the inputs, we can put the average value of two inputs and change the third input. By doing this we can find the variation of “y” with any of the input parameters keeping the other two input parameters constant.

Figure 4 represents the MDF variation with change in water content. The MDF increases from dry side of OMC (at 12%) till attaining the optimum moisture content (at 17%). With increase in moisture content up to 22%, the ductility factor decreases drastically. Figure 5 represents the MDF change with density. The results depict a linear decrease in MDF with increase in composite density. The fiber content change effect on MDF is shown in Fig. 6. With increase in fiber content, there is a gradual increment in MDF. This is due to more fibers mobilizing the exerted load thus resisting failure, while withstanding deformation.

CONCLUSION

This study proposes a new factor known as ductility factor and models for computing the factor (ratio of peak strain of reinforced and unreinforced soil) based on the soil moisture, density and fiber content. The error between the predicted value of Ductility factor and the actual value of the ductility factor obtained from the experiment is very less and hence the predictions obtained from the formulated explicit model are well in agreement with the experimental

data.

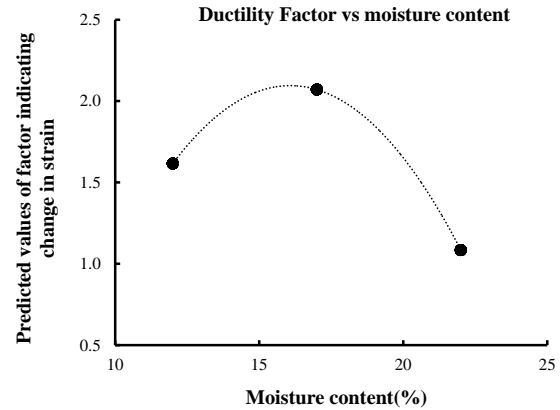


Fig.4 Variation of ductility factor with soil moisture

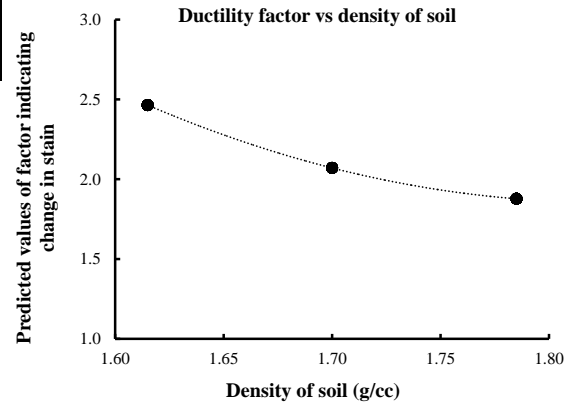


Fig. 5 Variation of Ductility factor with soil density

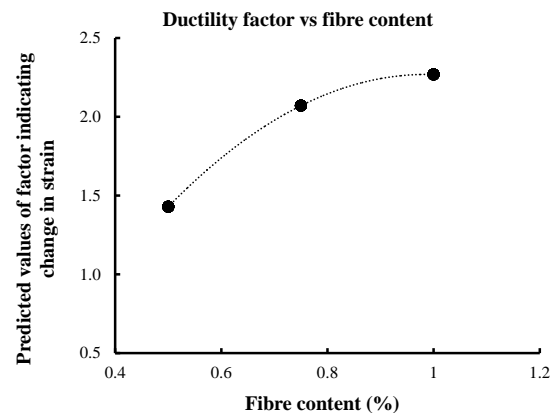


Fig. 6 Variation of ductility factor with fibre content

Variation of ductility factor with respect to the different input parameters can be useful for experts to predict the value of factor beyond the input conditions range thereby savings the necessary time and cost. The formulated explicit GP model will be useful to determine optimum input values for achieving safe and

strong bearing strata.

REFERENCES

1. ASTM D 2166 (2005). Test method for unconfined compressive strength of cohesive soil (ASTM D 2166).
2. ASTM D 2487-11 (2011). Standard Practice for Classification of Soils for Engineering Purpose (Unified Soil Classification System).
3. Bordoloi, S., Yamsani, S. K., Garg, A., Sreedeeep, S., & Borah, S. (2015). Study on the efficacy of harmful weed species *Eicchorniacrassipes* for soil reinforcement. *Ecological Engineering*, 85, 218-222.
4. Cai, Y., Shi, B., Ng, C. W., & Tang, C. S. (2006). Effect of polypropylene fibre and lime admixture on engineering properties of clayey soil. *Engineering Geology*, 87(3), 230-240.
5. Consoli, N. C., Prietto, P. D., &Ulbrich, L. A. (1998). Influence of fiber and cement addition on behavior of sandy soil. *Journal of Geotechnical and Geoenvironmental Engineering*, 124(12), 1211-1214.
6. IS-2720 (Part 4), 1985a. Methods of Test for Soils, Grain Size Analysis. Bureau of Indian Standards Publications, New Delhi
7. IS-2720 (Part 5), 1985, Determination of liquid and plastic limit, New Delhi: Bureau of Indian Standards publications.
8. IS-2720-(Part7), 1980, Determination of water content-dry density relation using light compaction. New Delhi: Bureau of Indian Standards publications.
9. IS-2720 (Part10), 1991, Determination of unconfined compressive strength, New Delhi: Bureau of Indian Standards publications.
10. Koza, J. R. (1992). Genetic programming: on the programming of computers by means of natural selection (Vol. 1). MIT press, USA.
11. Maher, M. H., & Ho, Y. C. (1994). Mechanical properties of kaolinite/fiber soil composite. *Journal of Geotechnical Engineering*, 120(8), 1381-1393.

[Back to table of contents](#)

The effect of a plant based polymeric material on the fresh and hardened states properties of cement mortar

Amrita Hazarikaⁱ⁾, Indranuj Hazarikaⁱ⁾, Nabajyoti Saikia^{ii), *}

i) Undergraduate student, Department of Civil Engineering, The Assam Kaziranga University, Jorhat 785006, Assam, India.

ii) Associate Professor, Department of Chemistry, The Assam Kaziranga University, Jorhat 785006, Assam India.

ABSTRACT

Recent researches have demonstrated that most synthetic polymeric admixtures that are used to enhance concrete properties, are toxic to human body, pose a serious threat to the sustainability of the environment, and are prohibitively expensive. These admixtures when added to concrete aggravate the already alarming rate of environmental degradation promoted by ordinary Portland cement (OPC). To address the issue, we have undertaken a study where a commonly available vegetable extract (bio-admixture) was tested for its feasibility for use as a sustainable bio-admixture in the production of cement based composite materials. Accordingly, several fresh as well as hardened state properties of cement mortar samples with and without the presence of bio-admixture were evaluated. Results indicated that the bio-admixture dramatically augmented the fresh state properties and the mechanical strength of the cement composites prepared using the same, in comparison to the reference samples prepared in the normal manner. Additionally, an improved method was developed for testing the water retention behavior of cement pastes. From our study, it can be concluded that the investigated plant based bio admixture has a potential for use as a low-cost, environmentally benign and a sustainable admixture for the production of sustainable concrete.

Keywords: Synthetic admixtures, bio-polymeric admixture, sustainable concrete, fresh-state properties, compressive strength, water retention capacity.

1. INTRODUCTION

Concrete, the mixture of cement, sand, coarse aggregate and water, is ubiquitous in the built environment. Its properties such as strength, durability, affordability and abundance of raw materials required to produce it, make it the most desirable material in the construction sector. Globally, about three tonnes of concrete are used annually per person. In addition to the regular ingredients, several other additives or admixtures are added to concrete in order to enhance its properties. However, the production of concrete as a whole, is a highly energy consuming and environmentally taxing affair.

For instance, it has been documented that the cement producing industries account for more than 4% of the global carbon dioxide release into the atmosphere (Siram and Raj, 2013). Moreover, the use of various synthetic admixtures in concrete has been proved to have contributed largely to the emission of toxic species into the atmosphere. Besides, these chemical or synthetic admixtures are patented products which are imported into developing countries and sold at exorbitant prices (Thirumalini and Sekar, 2013).

Because concrete use and production can never be halted, it is therefore vital to ensure that concrete is used in the most sustainable way (De Brito and Saikia, 2012). 'Sustainable' in a sense is the production of high performance and low carbon concrete. Considering the ills brought about by the use of synthetic

admixtures, researchers around the world have come up with a number of eco-friendly and economical biological or organic products as a substitute in preparations of various binder materials including cement mortar and concrete preparations. The term "bio admixture" is generally used to refer biopolymers and organic admixtures produced by bio-technological processes.

Organic admixtures are widely used in concrete and mortar for several decades to modify the properties of cement products (Hanehara and Yamada, 1999). Plank reported a brief overview on the various aspects of bio-polymeric admixtures (Plank, 2004). Thirumalini and Sekar (2013) published a review on the uses of herbs as admixtures in ancient lime mortars including the Indian scenario. Chandra et al (1998) used the water extract of cactus in preparation of Portland cement mortar. Izaguirre et al. (2011) studied the effect of a commercialized potato starch a biodegradable natural polymer on the properties of hardened lime. Aboudha et al. (2015) determined the suitability of blue gum extract as shrinkage reducing admixture (SRA) for concrete. Govin et al. (2015) studied the effect of guar gum derivatives on fresh state properties of Portland cement-based mortars, such as water retention, rheological behavior and the hydration delay. Otoko et al. (2014) investigated the palm liquor produced from the palm trees as a workability aid and set retarder admixture. Dwivedi et al. (2008) reported that the black gram pulse

powder could be used as low cost plasticizer in production of cement mortar and concrete.

However, compared to the other parts in the world, the amount of fruitful works done on the uses of bio-based admixtures in concrete productions in India, can be described as meager. Therefore, by considering the importance of bio admixtures in the production of modern, sustainable concrete, and its rising demand in India, much more of such systematic investigation as has been carried out elsewhere in the world, is urgently necessary to be developed. With this motivation, we have studied the suitability of a bio extract derived from a commonly available vegetable, for use as an admixture in the production of sustainable concrete. Moreover preliminary results of an improved field method for determining of water retention capacity of cement mixes are also presented.

2. MATERIALS AND METHOD

2.1 Materials

2.1.1 Plant extract

The plant extract examined for use as admixture was derived from the commonly available vegetable, okra (*Abelmoschus esculentus*). For our experiments, four different doses of the extract were prepared – 1:20, 1:30, 1:40, 1:50, and were named accordingly for reference as BA120, BA130, BA140 and BA150. For preparation of extract, the vegetable was first weighed, cut into small pieces, and then introduced in a beaker containing normal tap water in the required ratio. For example, BA120 was prepared by extracting biopolymer from 1gm vegetable using 20 ml water. Thereafter, the mix was stirred thoroughly for 5 minutes and then left to stand undisturbed for an hour. Subsequently, the colorless viscous extract was collected after an hour by sieving and transferred the contents of the beaker into a second container, followed by crushing the vegetable pieces with hand for further extraction. The extract was sieved a second time so as to ensure complete removal of any vegetable bits, since the latter could likely interfere with the results. The collected extract was finally ready for the proposed analyses, but was not stored for more than a day, to avoid its potential decay.

2.1.2 Polyvinyl alcohol

In this investigation, we compared the performance of bio polymeric extract in the cement composites with that of water soluble polymer, polyvinyl alcohol (PVA) containing mortars. To compare the performance of bio polymeric admixture, we have taken a 4% PVA solution to prepare the cement mortar samples. Accordingly, 50 g PVA sample was weighed, ground into powder, and then boiled with 1250 ml of distilled water. After continuous stirring for 5-10 minutes at a regular interval of 1 hour, the sample dissolved. Thereafter, the 4% PVA solution was kept untouched for the next 24 hours to be ready for use.

2.1.3 Cement

The cement used was Birla White Cement, produced by Ultra Tech cement company, India. It conforms to Indian Standard code IS: 8042, 1989 requirements.

2.1.4 Fine aggregate

Normal river sand was used as fine aggregate. The aggregate were graded with sieve analysis, conforming to IS 2386 – part 1 (1963). The fineness modulus was found to be 2.6.

2.1.5 Water

The water used for most operations was normal tap water available in the laboratory. However, distilled water was used for the preparation of 4% PVA.

2.2 Methodology

2.2.1 Standard consistency, water requirement and setting times

The consistency was determined by using Vicat's apparatus as per IS 4031-part 4- 1988. The test was repeated for different water and bio polymeric extract ratios. The water requirement of cement pastes were also determined by visually observing the cement pastes containing equal amounts of various types of liquid solutions. For this purpose, 50 g of cement was weighed and mixed with 100 ml of water or extract as the case may be, to check the variation in the amount of water on the consistence of the pastes.

The initial and final setting times were determined in accordance with IS.4031-part 5- 1988 using a Vicat apparatus.

2.2.2 Water retention capacity of the cement paste

Due to the unavailability of standard equipment and the associated difficulties of conducting this test by the prevalent normal methods (ASTM C1506-09 or DIN standard 18555-7 methods), we devised a unique, cost-effective and simple method for testing the water retention capacity of cement pastes. For the purpose, we incorporated the basic awareness of acid-base chemistry and the water absorbing quality of filter papers.

A handful of filter papers were first soaked in phenolphthalein solution and dried under sun. Freshly prepared cement paste made with extract or water whatever the case might be, was then immediately introduced in a mould made of inert material. Simultaneously, one of the filter papers, now dry-coated with phenolphthalein, was laid on top of a glass plate. After the mix is filled, compacted, smoothed and leveled on the top, the mould was immediately placed in the middle of the filter paper, with its open face in contact with the latter. Maximum 2 minutes should be taken to complete the whole process. Soon, a pink coloured water front appears on the filter paper due to the liberation of alkali solution from the cement paste. The circular front moved radially with increasing time span and the ultimate radius of this was used for comparing the water retaining behavior the samples containing the extract and water. The thing to note is that the operations should be done within 4-5 minutes

of mixing cement and water.

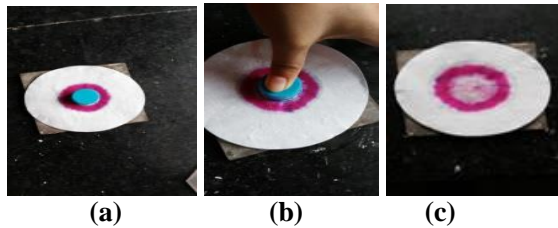


Fig. 1. Determination of water retention capacity

2.2.3 Preparation and testing of cement mortars

Apart from samples prepared by using the four different dosages of the proposed bio-admixture, reference samples were also prepared with normal tap water. For mortar, the cement to sand ratio was 1:3. The mortar cubes were cast in wooden moulds of dimensions 40mm × 40mm × 40mm. The mortar mixes were prepared by using Indian standard methods. The fresh mortar mix containing moulds were compacted on a standard vibration table as per specified in IS: 2514-1963.

A total of 48 cubes were cast i.e. 12 cubes each of reference, 4%PVA solution, B120 and BA140, according to IS: 516-1959. The mixes were filled in the moulds in three layers and then compacted in a vibrating table. The samples were then stored in laboratory environment for minimum 24 hours to harden. Adequate precautions were taken to reduce the water lost from the mortar samples. The specimens were then demoulded and cured in lime water until the respective testing ages. The 3-, 7-, 28- and 56-day compressive strengths of mortar cubes were determined using a 40kN universal testing machine.

3. RESULTS AND DISCUSSION

3.1. Water retention capacity

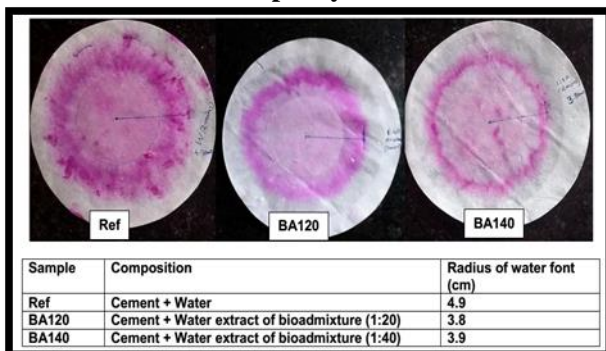


Fig. 2. Font created due to the unrestrained water movement on the filter paper after 5 minutes.

The results of typical water retention capacity determination test are presented in Fig. 2. The results have distinctly shown that the bio admixture possesses a remarkable water retention capacity. Reference pastes have produced a colored font of radius 4.9 cm and the pastes having bio-admixture have illustrated fonts of radii 3.8 cm and 3.9 cm in case of BA120 and BA140

respectively. It was also observed that higher the dose of biopolymer, higher was the water retention capacity. Thus our results confirmed that the proposed bio polymeric extract has water retention capacity which can beneficially be used in preparing sustainable concrete for specific requirements. However, higher water retention capacity of concentrated biopolymer may have some negative effect on various properties of cement composites like consistence, strength if higher doses are used (Choi et al., 2016, Kong et al., 2015).

The results also indicate the suitability of the developed method. The formation of pink coloured circular water font helps to detect the water movement quite distinctly. The principle of the test is that a basic solution when interacts with phenolphthalein indicator already present in filter paper, will give characteristic pink colour. Since the movement of colour font depends on the amount of water liberated from the paste, therefore the diameter of the circular font can directly be related with the water retention capacity of paste. The test is very simple, low cost and can be done very easily in construction sites. However, further work is necessary to relate the results with already available some other methods such as ASTM C1506-09 or DIN standard 18555-7 methods.

3.2 Effect on consistency and water requirement

Table 1. Water requirement to make cement paste

Type of Paste	Water required to make equal consistence
Ref	20
BA120	17
BA140	15

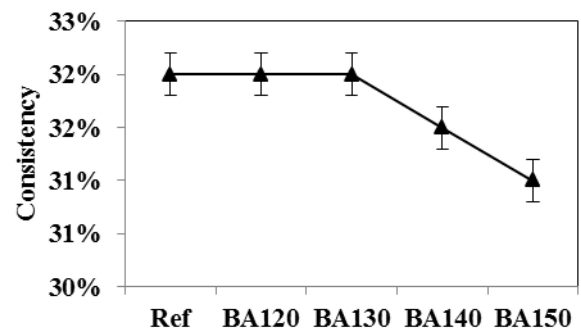


Fig. 3. Consistency of cement paste with water (Ref) and different doses of the bio-extract.

The consistency of various cement pastes are presented in Fig. 3. The cement pastes with higher doses of bio-polymeric extract (BA 120 and BA130) have showed same consistency as the reference samples. However slight decrease in consistency of resulting cement pastes due to the additions of diluted bio polymeric extracts (BA140 and BA150) indicates plasticizing effect of bio polymeric extract, which is dependent on the concentration bio-polymeric solutions. The results obtained from water requirement determination test of paste also support above

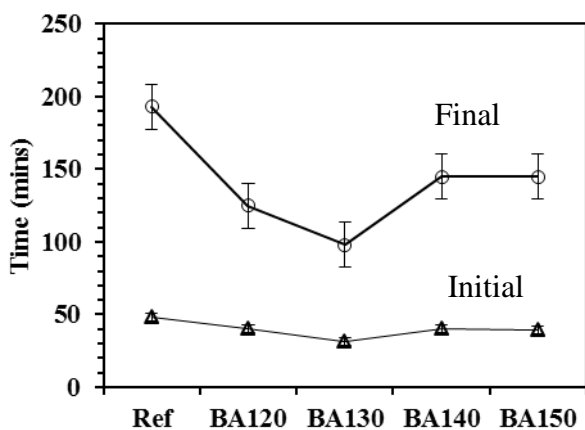
observation, i.e. the plasticizing behaviour and concentration dependence of bio polymeric extract (Table 1). At higher doses, probably, due to the higher water retention capacity of biopolymer, less amount of water is available for improving the flow behaviour (Choi et al., 2016, Kong et al., 2015).

3.3 Initial and final setting time

The initial and final setting times of various samples are presented in Fig. 4. The results indicate that the addition of bio admixture insignificantly affects the initial setting times of the cement pastes; however, at higher concentrations, bio polymeric extract additions drastically decrease the final setting time and the observed change is highest for BA130. This in turn depicts acceleration in the hydration reaction in the cement composite, brought about by the increasing addition of bio-admixture.

The results can be correlated with the solution chemistry of two different types of suspensions: the conductivity and Ca^{2+} ion concentration of cement-bio polymeric extract were quite high in comparison to the cement-water suspension (Bora, 2015). Normally Ca^{2+} ion concentrations and conductivity of polymer containing suspension are higher than that of the normal cement suspension due to the formation of protective polymeric coating on the cement particles, which stops the further hydration of cement particles in cement-polymer suspensions. Such behaviour is normally related with the delayed setting of polymeric admixture containing cement pastes (Peschard et al., 2006, Poinot et al., 2013).

However, our result is completely opposite from such results. If we correlate setting time data with the Ca^{2+} ion concentrations and conductivity data of biopolymeric-cement suspension, we can conclude that the addition of biopolymeric solution into the cement paste increases the hydration rate of cement particles, and therefore more amounts of hydration products are formed. The higher formation of such products lowers the setting time particularly at the later period of setting. Therefore, the investigated bio-polymeric extract can prove to be substantially beneficial as a quick setting admixture and can be considered for such applications.



F

ig. 4. Initial and final setting times of cement pastes.

3.4 Compressive strength behaviour

The compressive strength behaviour of various types of mortar compositions were presented in Fig. 5. The cubes having BA120, i.e. the highest dose of the biopolymer initially showed reduction in compressive strength which is similar to cubes having 4% PVA (maximum 2% of PVA is the allowable limit) solution but compressive strength recovered after 7-day curing period and at 28 days, it overcome the strength of reference mortar. The cubes having BA140 and reference cubes showed similar results up to 28th day.

Karandikar et al., (2014) also observed similar behaviour for okra extract. The 56th day or the final compressive strength results of the cubes having BA120 was in range with the reference mortar cubes but the cubes having BA140 exhibited notable amount of increase in strength compared to the reference cubes. Beyond 28th day, the strength of cubes having BA120 increased by 8.18% whereas that for BA140 increased by 10.25%. Finally, it can be concluded that the biopolymer enhanced the compressive strength of the mortar cubes as, the ones having BA140 has shown very promising results. It is known that on addition of polymer above a certain amount, the strength and hence the durability of cement composites starts declining (Knapen and Van Gemert, 2009). In case of PVA, the strength and other properties deteriorate sharply if PVA addition crosses above 2% (Knapen and Van Gemert, 2009).

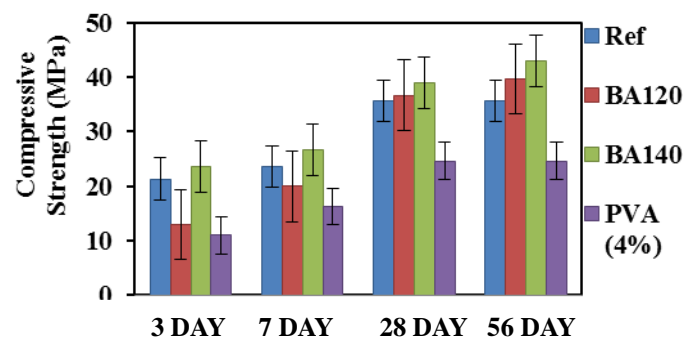


Fig. 5. Compressive strength of various mortar samples at different time periods

4. CONCLUSIONS

An investigation was undertaken to evaluate the behaviour fresh and hardened state physico-mechanical properties of a bio polymeric extract as an alternative in preparation of sustainable cement based infrastructure. Following conclusions can be taken from this investigation:

1. A method was developed and tested to evaluate the water retention capacity of cement pastes. Using the method, the movement of circular water front can be distinctly detected because of the development of colour. The diameter of circular

font can be directly related with water retention capacity of the cement paste.

2. From the water retention capacity determination test, it can be concluded that the bio-polymeric extract has found to have water retention capacity.
3. The decrease of consistency value for BA140 and BA150 solidifies the point that the bio extract has slight plasticizing ability. The plasticizing property of bio polymeric admixture can also be supported by water requirement test.
4. The decrease in the setting times indicates an accelerated hydration reaction, which is dependent on the concentration of bio polymeric extract.
5. The addition of bio-polymeric admixture also improves the compressive strength behaviour of cement mortars. The rate of increase in strength of bio polymeric mortars is normally higher than that of reference mortar samples.

5. ACKNOWLEDGEMENTS

We sincerely thank the laboratory staff members of the Concrete Laboratory, the Chemistry Laboratory, and the Workshop of The Assam Kaziranga University, Jorhat for their help.

6. REFERENCES

- 1) Siram, K.B. and K.A. Raj, (2013): Concrete+Green = Foam Concrete. *International Journal of Civil Engineering and Technology*, 4(4) 179-184.
- 2) Thirumalini, P., Sekar S. K. (2013). Review on herb used as admixture in lime mortar used in ancient structures, *Indian Journal of Applied Sciences*, 3(8): 295-298.
- 3) De Brito J., Saikia N., (2012). Recycled Aggregate in Concrete: Use of Industrial, Construction and Demolition Waste. Springer London, ISBN-10: 1447145399, ISBN-13: 978-1447145394.
- 4) Hanehara S, Yamada K., (1999). Interaction between cement and chemical admixture from the point of cement hydration, absorption behavior of admixture and paste rheology, *Cement and Concrete Research*, 29(8):1159-1165.
- 5) Plank J., (2004). Applications of biopolymers and other biotechnological products in building materials. *Applied Microbiology Biotechnology*, 66(1):1-9.
- 6) Chandra S, Aavik J., (1983). Influence of black gram (natural organic material) addition as admixture in cement mortar and concrete, *Cement and Concrete Research* 13(3): 423-430.
- 7) Izzaguirre A., Lanas J., Alvarez J.I., (2011). Effect of a biodegradable natural polymer on the properties of hardened lime-based mortars, *Materiales de Construcción*, 61(302): 257-274.
- 8) Woldemariam A. M., Oyawa W. O., Abuodha S. O., (2014). Cypress tree extract as an eco-friendly admixture in concrete. *International Journal of Civil Engineering And Technology*, 5(6): 25-36.
- 9) Govin A., Bartholin M. C., Biasotti B., Giudici M., Langella V., Grosseau P. (2015). Effect of Guar Gum Derivatives on Fresh State Properties of Portland Cement-Based Mortars. *Proceedings of the 27th Biennial National Conference of the Concrete Institute of Australia, Australia.*
- 10) Knapen, E., Van Gemert D., (2009). Water-soluble polymers for modification of cement mortars. *K.U.Leuven, Departement Burgerlijke Bouwkunde, Kasteelpark Arenberg 40, 3001 Heverlee, Belgium,*

<https://bwk.kuleuven.be/mat/publications/internationalconference/2006-knapen-watersoluble-polcon.pdf>. (Access in 7th October, 2016).

- 11) Otoko G. R., Ephraim, M.E (2014). Concrete admixture and set retarder potential of palm liquor, *European International Journal of Science and Technology* ISSN: 2304-9693, 3(2/8): 74-80.
- 12) Dwivedi V. N., Das S. S., Singh N. B., Rai S., Gajbhiye N. S., (2008). Portland cement hydration in the presence of admixtures—black gram pulse and superplasticizer, *Materials Research*, 11(4): 427–431.
- 13) Karandikar, M. V., Sarase S. B., Lele P. G., Khadaikar S. A. (2014). Use of natural bio-polymers for improved mortar and concrete properties of cement – A review. *Indian Concrete Journal*, 88(7):84-109.
- 14) Choi N. W., Kim S. H., Kim E. J., (2016). Admixture composition for a tile cement mortar and a tile cement mortar composition comprising the same, *US 9272952 B2*, Publication date: 01/03/2016.
- 15) Kong Xm., Zhang Z. L., Lu Zc., (2015). Effect of pre-soaked superabsorbent polymer on shrinkage of high-strength concrete. *Materials and Structures*, 48(9): 2741-2758.
- 16) Bora S. (2015). The effect of a biopolymeric material on the hydration of cement. M. Sc. Dissertation, Kaziranga University, India.
- 17) Peschard A., Govin A., Pourchez J., Fredon E., Bertrand L., Maximilies S., Guilhot B., (2006). Effect of polysaccharides on the hydration of cement suspension. *Journal of the European Ceramic Society*, 26(8): 1439-1445.
- 18) Poinot T., Govin A., Grosseau P., (2013). Impact of hydroxypropylguars on the early age hydration of Portland cement. *Cement and Concrete Research*, 44: 69-76.

[Back to table of contents](#)

Use of a locally available biopolymeric admixture for production of sustainable cement composites: durability behaviour of cement mortar

Indranuj Hazarikaⁱ⁾, Amrita Hazarikaⁱ⁾, Nabajyoti Saikia^{ii),*}

i) Undergraduate Student, Civil Engineering Department, The Assam Kaziranga University, Jorhat 785006, Assam, India.

ii) Department of Chemistry, The Assam Kaziranga University, Jorhat 785006, Assam India.

ABSTRACT

Sustainability in concrete industry is achieved primarily by reducing the CO₂ emission released during the construction process. This is usually acquired by using several novel techniques including addition of synthetic admixtures that enhance the properties such as strength, consistency, durability etc. of the cement based composites. But recent researches on the synthetic polymers have revealed that these chemicals are deleterious to human health. Therefore, recent researches have shifted towards the field of bio-polymeric admixture. Bio-admixtures are innocuous to health besides being organic and biodegradable. This means, they possess negligible deteriorating effect on the environment as well as human health. Researches have presented promising results for bio-admixtures. Cost effectiveness, convenience of use and availability also plays an important role in determining the bio admixture's viability. This investigation studied the influence of a locally available plant extract on the durability, porosity and internal curing of the cement composites. The experiments were conducted with available resources and equipment as per popular standards. The experiments were conducted as comparative investigations wherein the performance of the cement composites containing the bio-extract in varying dosages was compared against the ones that did not contain any extract. The results obtained from the experiments indicated the potential of the bio-admixture towards enhancing durability besides also presenting a notable decrease in porosity. This property of the bio-extract can make it a popular, environmentally benign, cost effective admixture for the production of sustainable concrete. Based on the results it can be concluded that there is a decrease of porosity when the proposed bio-admixture is used. It was also found that the deterioration of strength of samples subjected to sea water condition is distinctly less in comparison to reference, depicting higher durability under such conditions. The bio-admixture has water retention capacity and hence is tested in various curing conditions. The results showed that bio-admixture containing cube samples showed better performances than that of reference samples at different curing regimes.

Keywords: Sustainable construction, synthetic admixture, bio-polymeric admixture, durability performance, curing condition, porosity.

1. INTRODUCTION

Concrete is ubiquitous in the built environment. It is therefore essential that it is used in the most sustainable way. Sustainable in a sense is the production of high performance low carbon concrete. Concrete is comprised of three major fractions, aggregate, cement and water. It is reported that the total annual concrete production in the world is more than 10 billion tonnes. More than 0.9, 5 and 0.6 billion tonnes of Portland cement, aggregate and potable water respectively are necessary for the production of such amount of concrete. It was also found that, power and cement production sectors are the major CO₂ emitter all over the world. In 2011, production of cement accounts for 4% of total global CO₂ emission. The global emission of CO₂ in 2011 was 33.9 billion tonnes. Hence, the concepts of sustainability and sustainable development came up due to the fact that our economic imperatives, i.e. the provision for products and services, development etc. are proceeding at such a rate that undermines the planet's capacity to supply resources,

absorb wastes and to support incredibly diverse life forms on it. To provide all the facilities and benefits to the society, the development process has led to the deterioration of ecosystem, social fabric and health of all. Considering these critical phenomenon, a need was felt for the production of sustainable concrete with increasing service life and minimum maintenance, as a step to check environmental degradation (De Brito and Saikia 2012).

Sustainability in concrete production can be achieved by improving current practices, for example, improvement or innovation in concrete mix and product design approaches, improvement of the performance of concrete-based products in their service lives etc. Reducing the volume of cement in concrete by improving its mechanical strength could decrease the emissions of CO₂ around 30%. The improvement of mechanical and durability performances of concrete in their service life can indirectly reduce the CO₂ emission by increasing their service life and reducing the requirements of materials for repairing.

Now-a-days different types of sustainable concretes

and other cement based composites are produced by using various novel materials technologies (Arum and Olotuah, 2014; Adorján, 2016; Faella et al., 2016; Girskas et al., 2016). Addition of polymeric admixtures with various functionalities is one such development (Izzaguirre et al., 2011, Thong et al., 2016; Van Gemert et al., 2005, 2016; Knapen, and Van Gemert, 2006; Shen et al, 2016, 2015). Additions of polymeric admixtures into concrete can improve various mechanical and durability properties of concrete (Shen et al, 2016, 2015; Van Gemert et al., 2005, 2016). However, majority of the synthetic polymers has harmful environmental effects. Moreover use of synthetic admixture also increases the cost of a construction project manifold. Considering such limitations, now a days various types of bio-polymeric admixtures are used as alternatives to synthetic admixtures (Sathya et al., 2014; Abdulrahman and Mohammad, 2011; Chandra and Aavik, 1983; Dwivedi et al., 2008; Jonkers et al., 2016; Karandikar et al., 2014; Plank 2004; Bezerra 2016).

In this investigation, therefore, a locally available vegetable extracts is considered as an low-cost sustainable alternatives to synthetic admixture for the production of sustainable concrete. In this communication, durability performances of cement based composite materials in the presence of a vegetable extract were reported.

2. MATERIALS AND METHODS

A commercial grade white Portland cement (Birla White Cement) was used in this investigation. The bio extract was prepared by cutting the vegetable into small pieces and then transferring it into water in the solid to liquid ratio of 1:20. The mixture was first sieved using coarser sieve and then again with a finer sieve to separate the solid part. The polymeric liquid thus obtained was then used as biopolymeric admixture. The extract of lower concentration (i.e 1:40) was prepared by adding water to the extract of concentration 1:20.

The mortar mixes were prepared by mixing cement and fine aggregate of fineness modulus 2.6 in the cement to sand ratio of 1:3. In this investigation, the liquid to cement ratio (w/c) was maintained at 0.5. Mortars were casted using 40mm × 40mm × 40mm sized wooden moulds. The preparations of samples were done according to Indian standard methods. A vibrating table was used to remove the air bubbles present the freshly prepared mortar samples and then kept in laboratory conditions. Adequate precautions were taken to decrease the water loss from the mortar. The specimens were demoulded after 1 day and cured under lime water according to ASTM standard method. The mortar samples containing only water was also prepared to evaluate the behaviour of bioadmixture on the properties of cement mortar.

The water absorption capacity of 28-day cured samples was determined according to ASTM C1757-13 method. To understand the performance of mortars under sea water condition, the 28-day water cured specimens were immersed in water as well as simulated sea water solution. The 3- 7- and 21-day compressive strengths of these samples were determined by using a universal compressive strength testing machine. The effect of various humidity conditions on cement mortar samples were also evaluated using a standard method. For this purpose, the 28-day cured samples were kept in predefined environmental conditions: water immersion (normal curing), laboratory environment, outdoor environment, and oven drying at 40°C. The samples cured in various conditions are presented in Fig. 1. The 0- (before applying curing conditions), 7- and 28-day compressive strengths of the samples were then determined for evaluating the performances of the samples in various curing regime.



Fig.1. Different curing conditions applied in this investigation

3. RESULTS AND DISCUSSION

3.1. Water absorption capacity

Fig. 2 shows the water absorption capacities of various cement mortar samples. The results indicate that the addition of polymeric admixture into mortar decreases the water accessible porosity of the mortar samples. Thus, it can be concluded that the polymer containing mortars will exhibit better durability performance in aggressive environment than the normal mortar samples.

Additions of polymeric mixtures normally improve the cohesiveness of mortar mixes, which can ultimately improve the microstructure of mortar specimens. The water absorption capacity of mortar specimens was minimum for the specimens prepared by using dilute polymeric solution (i.e. 1:40 solution). This indicates that the concentrations of polymer present in water can affect the hydration behaviour of

cement. Probably 1:20 ratio is higher than the optimum amount of polymer present in water for preparing best cement mortar mixes in which optimum cohesiveness as well as the hydration of cement is observed.

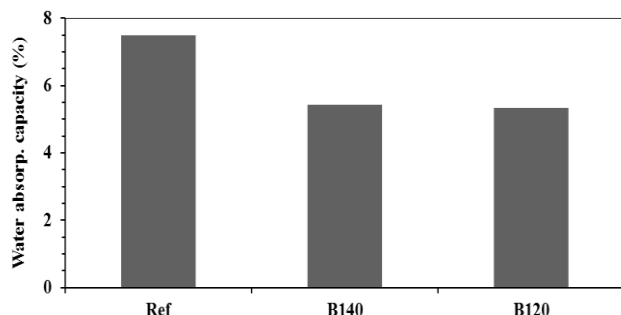


Fig. 2. Water absorption capacities of various cement mortar samples (Ref, BA120 and BA140)

Another point that needs to be considered is the formation of polymeric film, which blocks the water accessible pores in the hardened mortar sample. Since bioextract is soluble in water and therefore there is a possibility of the formation of such films in the mortar (Knäpen et al., 2016). However, at higher polymer concentrations, such films will decrease the rate of hydration reactions by blocking the reaction sites and therefore deteriorate the properties of resulting mortars e.g. mortar containing concentrated bio extract (i.e. 1:20 solution).

4.2 Behaviour in sea-water immersion test

Considering the better performance in water absorption capacity, in this investigation mortar sample containing bio extract prepared at 1:40 ratio was taken along with the reference mortar sample. Fig. 1. shows the compressive strengths of reference and polymeric extract containing mortar samples, cured for various curing periods in simulated sea water solution.

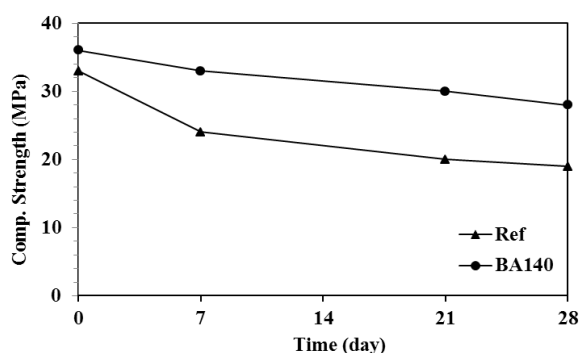


Fig. 3. Compressive strength behaviour of mortar samples after immersion in simulated sea water solution

The results indicate the better performance of polymer containing specimens than that of reference specimens. The results corroborate the findings obtained from the water absorption capacity results.

The migrations of harmful sulfate and chloride ions in cement mortar depend on the water accessible porosity of mortar samples. In case of reference, increasing water accessible porosity enhances the ingress of large amounts of harmful sulfate and chloride ions, which ultimately deteriorate the strength of the mortar samples. The improvement of water absorption capacity due to biopolymer addition into mortar samples lowers the ingress amounts of harmful ions and hence exhibit better performance. The percentage decrease in compressive strength of the sample after immersion in simulated sea water with respect to the 28-day water cured samples are presented in Fig. 4. The decrease in strength of mortar cubes after 21-day immersion is 40 % for reference mortar cubes but the same is 16% for bio polymeric cubes.

The observed improvements due to the addition of biopolymer can be related with the water absorption capacity results. The decrease in water accessible porosity due to bio polymer addition reduces the amount of harmful species that enter into the mortar and therefore increase the durability performance in sea water curing conditions. The polymeric film formed due to polymer solution addition probably acting like a seal preventing the reaction between the solution and the cement composite.

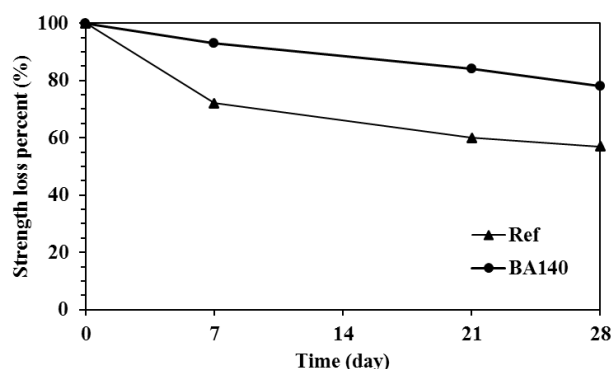


Fig. 4. Percentage decrease in compressive strength of mortar samples after immersion in sea-water.

4.3 Behaviour in various exposure conditions

The 3-day, 7-day and the 28-day compressive strengths of various mortar samples cured at various curing regimes are presented in Fig. 5. Although the compressive strengths of samples cured in laboratory and outdoor environments are respectively similar or higher than the water cured samples at all ages, yet the compressive strength of both types of mortar cubes increase with increasing curing period. In case of oven drying condition there is a decrease in strength observed for both types of samples; however the observed decrease in strength is more for reference mortar cubes. In comparison to reference mortars, the decreases in compressive strengths of bio polymeric mortars are relatively low, indicating positive effect of biopolymer on the strength development in such an

extreme conditions.

The experiment was conducted to know whether bio polymer can be used as a internal curing agent as biopolymer can retain huge amount of water from the solution. Comparing the compressive strength

behaviour of reference and bio polymeric mortar which were subjected to oven drying environment, it can be concluded that water retained by biopolymer can be used for internal curing of the mortar samples.

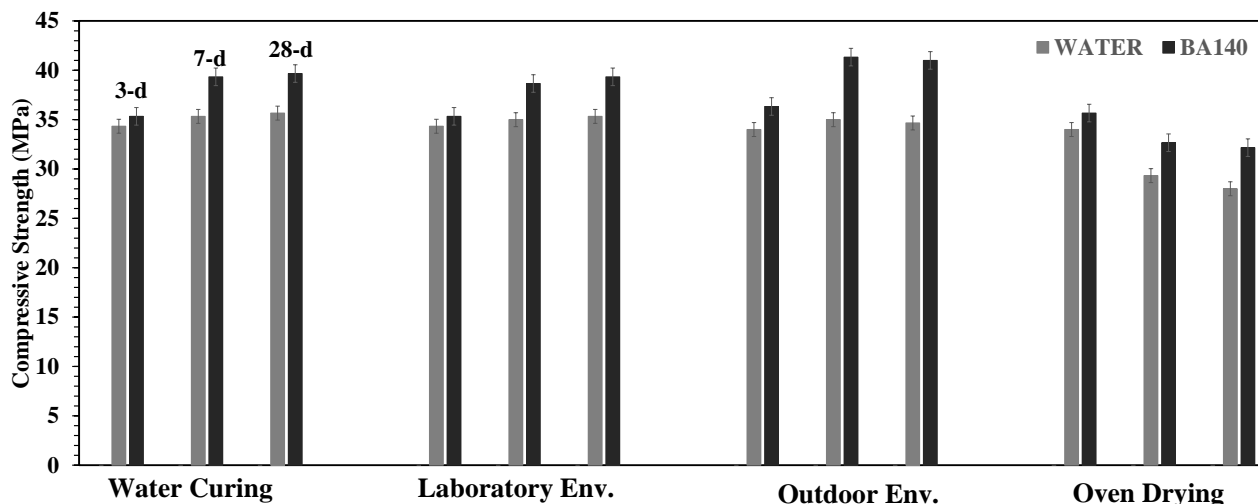


Fig. 5. Compressive strength of mortars cubes cured in different conditions.

5. CONCLUSIONS

An investigation is undertaken to evaluate a natural bio extract as a replacement of synthetic admixture in cement mortar preparation. In this investigation durability performance of the mortar samples are evaluated by evaluating water accessible porosity as well as the strength behaviour of hardened mortar samples after exposure of mortars to various environmental conditions. Following conclusions can be made from this investigation:

1. The bio polymeric extract decreases the water retention capacity of cement mortar. This indirectly indicates the lowering of water accessible porosity of the mortar cubes. The improvement of water accessible porosity is beneficial for durability performances in mortars in deleterious environment.
2. The measurement of compressive strengths of cement mortar with and without the presence of bio polymeric extract it can be concluded that the presence of bio polymeric extract improves the durability performances of cement mortar in simulated sea-water conditions.
3. The performances of the cement mortars containing bio polymeric extract are quite better than that of the reference mortars (mortars prepared by water only) in the investigated time periods. Particularly, better performances of polymeric mortar in oven dry conditions, indicates that the investigated bio polymeric extract can be considered as an internal

curing agent.

4. The durability performance can be correlated with the higher water absorption capacity of bio polymeric mortar samples.
5. The increase cohesiveness of the cement mortar due to bio polymeric extract additions and possibly formation of polymer films in the mortar samples improves pore structure of bio polymeric mortar samples, which ultimately improves the durability performance in various aggressive conditions.

6. ACKNOWLEDGEMENT

We would like to thank all the staffs of the concrete laboratory, the chemistry laboratory and the workshop of The Assam Kaziranga University, Jorhat, Assam.

7. REFERENCES

- 1) De Brito J., Saikia N., (2012). Recycled Aggregate in Concrete: Use of Industrial, Construction and Demolition Waste. Springer London, ISBN-10: 1447145399, ISBN-13: 978-1447145394.

- 2) Izzaguirre A., Lanas J., Alvarez J.I., (2011). Effect of a biodegradable natural polymer on the properties of hardened lime-based mortars, *Materiales de Construcción*, 61(302): 257-274.
- 3) Sathya A., Bhuvneshwari P., Niranjana G., Vishveswaran M., (2014). Influence of bio-admixture on mechanical properties of cement and concrete. *Asian Journal of Applied Sciences*, 7 (4): 205-214.
- 4) Arum, C., Olotuah A.O. (2006). Making of strong and durable concrete. *Emirates J. Eng. Res.*, 11: 25-31.
- 5) Woldemariam A.M., Oyawa W. O., Abuodha S. O., (2014). Cypress tree extract as an eco-friendly admixture in concrete. *International Journal Of Civil Engineering And Technology*, 5 (6): 25-36.
- 6) Adorján B., (2016). Long term durability performance and mechanical properties of high performance concretes with combined use of supplementary cementing materials, *Construction and Building Materials*, 112: 307-324.
- 7) Abdulrahman A. S., Mohammad I. (2011). Green Plant Extract as a passivation promoting Inhibitor for Reinforced Concrete. *International Journal of Engineering Science and Technology*, 3(8): 6484-6490.
- 8) Thong, C. C., Teo D.C.L., Ng C.K. (2016). Application of polyvinyl alcohol (PVA) in cement-based composite materials: A review of its engineering properties and microstructure behavior, *Construction and Building Materials*, 107: 172-180.
- 9) Chandra S, Aavik J. (1983). Influence of black gram (natural organic material) addition as admixture in cement mortar and concrete. *Cement and Concrete Research*, 13(3): 423-430.
- 10) Faella C., Lima C., Martinelli E., Pepe M., Realfonzo R., (2016). Mechanical and durability performance of sustainable structural concretes: An experimental study, *Cement and Concrete Composites*, 71: 85-96.
- 11) Van Gemert D., Czarnecki L., Łukowski P., Knapen E. (2005). Cement concrete and concrete-polymer composites: two merging worlds. A report from 11th ICPIC Congress in Berlin, 2004. *Cement and Concrete Composites*, 27(9–10): 926–933.
- 12) Van Gemert D., Knapen E., Recent Development of Concrete Polymer Composites in Belgium, *Kasteelpark Arenberg 40, 3001 Heverlee, BELGIUM*, <https://bwk.kuleuven.be/mat/publications/internationalconference/2006-vangemert-recent-polcon.pdf> (Access on 7th October, 2016).
- 13) Shen D., Wang X., Cheng C., Zhang J., Jiang G., (2016). Effect of internal curing with super absorbent polymers on autogenous shrinkage of concrete at early age, *Construction and Building Materials*, 106: 512-522.
- 14) Knapen, E., Van Gemert D., (2006). Water-soluble polymers for modification of cement mortars. *K.U.Leuven, Departement Burgerlijke Bouwkunde, Kasteelpark Arenberg 40, 3001 Heverlee, Belgium*, <https://bwk.kuleuven.be/mat/publications/internationalconference/2006-knapen-watersoluble-polcon.pdf>. (Access on 7th October, 2016).
- 15) Shen D., Wang T., Chen Y., Wang M., Jiang G. (2015). Effect of internal curing with super absorbent polymers on the relative humidity of early-age concrete, *Construction and Building Materials*, 99: 246-253.
- 16) Girskas G., Skripkiūnas G., Šahmenko G., Korjakins A. (2016). Durability of concrete containing synthetic zeolite from aluminum fluoride production waste as a supplementary cementitious material, *Construction and Building Materials*, Volume 117, 1 August 2016.
- 17) Jonkers H. M., Mors R. M., Sierra-Beltran M. G., Wiktor V., (2016). Biotech solutions for concrete repair with enhanced durability, *Biopolymers and Biotech Admixtures for Eco-Efficient Construction Materials*.
- 18) Karandikar M. V., Sarase S. B., Lele P. G., Khadaikar S. A., (2014). Use of natural bio-polymers for improved mortar and concrete properties of cement – a review. *Indian Concrete Journal*, 88(7):84-109.
- 19) Plank J. (2004). Applications of biopolymers and other biotechnological products in building materials. *Applied Microbiology Biotechnology*. 66(1):1-9.
- 20) Bezerra U.T. (2016). Biopolymers with superplasticizer properties for concrete, *Biopolymers and Biotech Admixtures for Eco-Efficient Construction Materials*.
- 21) Dwivedi V. N., Das S. S., Singh N. B., Rai S., Gajbhiye N. S., (2008). Portland cement hydration in the presence of admixtures—black gram pulse and superplasticizer, *Materials Research*, 11 (4): 427–431.

Back to table of contents

Factors influencing shear strength of sand-tyre waste mixtures

Prasanty Borahⁱ⁾, Malaya Chetiaⁱⁱ⁾ and Asuri Sridharanⁱⁱⁱ⁾

i) Former P.G. Student, Department of Civil Engineering, Assam Engineering College, Guwahati 781013, India.

ii) Assistant Professor, Department of Civil Engineering, Assam Engineering College, Guwahati 781013, India.

iii) Honorary Scientist, Indian National Science Academy, Formerly, Professor, Department of Civil Engineering, Indian Institute of Science Bangalore, Bangalore 560012, India.

ABSTRACT

Sand-tyre waste (S-T) mixtures are being used in many geotechnical applications. The reuse of tyre waste in S-T mixtures can efficiently tackle growing environmental concerns and, at the same time, provide solutions to geotechnical problems coupled with low soil shear strength. In this paper, the shear strength of dry S-T mixtures has been investigated. There are different factors that have influence on the shear strength of soil. However, there are limited studies on the effect of dry unit weight and shearing rate on the shear strength of S-T mixtures. Therefore, the present study purports to critically evaluate the effect of dry unit weight and shearing rate on the shear strength of different dry S-T mixtures. The study also investigates the influence of tyre content on the shear strength of sand to determine the optimum tyre content. Locally available sand and tyre dust waste are used in this study. Different dry S-T mixtures, in the range 0 to 40% by the weight of tyre waste, were tested using the small direct shear test at three different shearing rates and dry unit weights of the mixtures. From the test results, it has been found that the tyre content, dry unit weight and shearing rate have significant influence on the shear parameters (apparent cohesion 'c' and angle of internal friction ' ϕ ') of the S-T mixtures. At a particular tyre waste content, the shear parameters were found to increase with the increase in dry unit weight and shearing rate of the mixtures. The value of ' ϕ ' increases upto a tyre waste content of 30% and decreases further increase in the tyre waste content. The value of 'c' increases upto a tyre waste content of 40%. The optimum tyre waste content of the S-T mixtures was found to be 30%.

Keywords: sand, tyre waste, mixture, shear strength, parameters, influence

1. INTRODUCTION

Waste tyres are being generated at an increasing rate in quickly growing markets like India due to fast growth of the number of vehicles plying on their roads. If the waste tyres are stockpiled, two problems that can arise are susceptibility to ignition and suitability for breeding of insects and rats. Tyres consist of synthetic and natural rubber, sulphur and sulphur compounds, silica, phenolic resin, oil, fabric, petroleum waxes, pigments, carbon black, fatty acids, inert materials and steel wires. Rubber from worn vehicles tyres, after being shredded into smaller pieces, can often be reused in civil engineering applications.

The angle of internal friction of tyre chips ranges from 19° to 25° and the cohesion ranges from 8 kPa to 11 kPa (Humphrey et al. 1993). The angle of internal friction of the sand-tyre waste mixes is in the range 19° - 67° (Ghazavi and Sakhi 2005; Bali Reddy et al. 2016). The angle of internal friction increases with increase in tyre content and the optimum tyre content is in the range of 30-40% by weight (Ghazavi and Sakhi 2005; Bali Reddy et al. 2016). Mixtures of sand and shredded waste tyres are useful as soil reinforcement in highway fills, leachate collection systems on steep slopes, and other applications where strong and lightweight fill is needed

(Bali Reddy et al. 2016). There are different factors which influence the shear behaviour of soil, therefore, the study is to investigate the influence of dry unit weight and shearing rate on the shear strength behaviour of sand-tyre waste mixes. It must be mentioned that there are contradictory opinions regarding effects of shearing rate on the behaviour of cohesionless soils. Hence, the objective of this study is to investigate the influence of tyre waste addition on the shear behaviour of sand. It has been found from the literature that the tyre wastes used in the investigations by different researchers are in the form of tyre chips of some standard sizes. But, the tyre dust waste has been used in this work which is found to be limited in the literature. The study indicates that the apparent cohesion 'c' value of the mixtures increased upto 40% of tyre content, whereas, the angle of internal friction ' ϕ ' value increased upto 30% of tyre content and it decreased at 40% of tyre content. The shear strength parameters increased with increase in dry unit weight and shearing rate at constant shearing rate and dry unit weight respectively. The optimum tyre content of the S-T mixtures was determined.

2. EXPERIMENTAL INVESTIGATIONS

Locally available samples of sand and tyre waste are used in this study. Tyre waste used is the tyre dust which is shown in Fig. 1. The tyre wastes were grinded from truck tyres. The samples were characterized for specific gravity and grain size distribution by following the guidelines reported in the literature (IS 1980; 1985). The grain size distribution curves of the samples are shown in the Fig. 2. The sand is classified as SP as per the Unified Soil Classification System (USCS) classification (IS 1970). The specific gravity of sand is 2.62. The tyre dust size ranges from 0.075 mm to 4.75 mm. The specific gravity of tyre dust is 1.19.



Fig.1. Tyre Dust Sample.

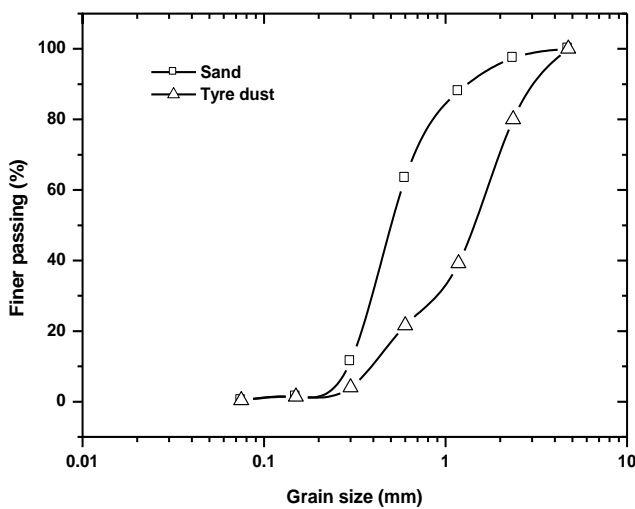


Fig.2. Particle Size Distribution of Samples Used in This Study.

The S-T mixtures were prepared manually by adding tyre waste to dry sand by weight in the range 0 to 40%. The calculated amounts were placed together and mixed thoroughly to form S-T mixtures. The mix ratio of tyre waste (%T) was evaluated by the dry weight of the tyre waste (WT) relative to that of the total mixed material (WT + WS), where, WS is the weight of sand and WT is the weight of tyre waste, as given in the following Eq. 1.

The S-T mixes weight ratios can also be converted to volume ratios using the weights of sand and tyre waste in each mixture, along with specific gravity values of

the individual materials, as shown in Eq. 2, where GS and GT are specific gravity of sand and tyre waste respectively. Figure 3 shows the relationship between weight ratios and volume ratios of tyre waste for S-T mixes at different dry unit weights.

$$\%T = \left[\frac{WT}{WT + WS} \right] \dots\dots\dots(1)$$

$$\%V = \left[\frac{\frac{WT}{GT}}{\frac{WS}{GS} + \frac{WT}{GT}} \right] \dots\dots\dots(2)$$

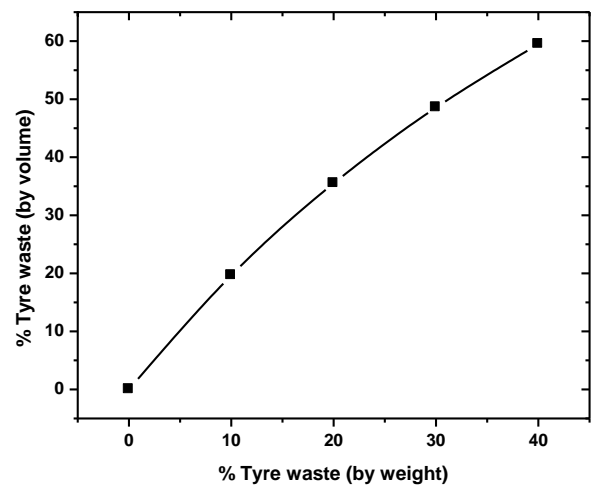


Fig. 3. Relationship between Weight Ratios and Volume Ratios of Tyre Waste for S-T Mixtures at Different Dry Unit Weights.

3. RESULTS AND DISCUSSION

Direct shear test of the samples was performed as per IS (1986) at three different dry unit weights namely 16, 18.4 and 20 kN/m³ keeping a constant shearing rate as 1.25 mm/min. It was also performed at two other shearing rates namely 0.05 and 0.25 mm/min at two dry unit weights of 16 kN/m³ and 20 kN/m³. Small direct shear test was carried out at three normal stresses i.e. 50, 100 and 150 kPa.

Based on the direct shear test results, the shear envelopes of different samples were plotted and the shear strength parameters were determined. Figure 4 shows the shear stress versus shear strain plot at dry unit weight of 20 kN/m³ and constant shearing rate of 1.25 mm/min for S-T mixtures at normal stress 150 kPa. The Fig. 4 indicates that the maximum shear stress increases with increase in tyre content. Beyond 30% of tyre content, the maximum shear stress decreases. The shear strain corresponding to maximum shear stress is more than that of sand alone which showed the

behaviour change in sand from brittle to ductile due to addition of tyre content. This finding is similar to that was observed by Bali Reddy et al. (2016) for sand-tyre chips mixtures. The curve slightly flattens beyond 30% tyre content. The Fig. 5 shows the variation of shear stress with shear strain for S-T(70:30) mixtures of different dry unit weights under normal stress of 150 kPa and shearing rate of 1.25 mm/min. The figure highlights the influence of dry unit weight on the maximum shear stress of S-T (70:30) mixtures. Similarly, the Figs. 6 and 7 show the influence of shearing rate on the maximum shear stress of S-T (70:30) mixtures. Similar observations were also obtained for other S-T mixtures.

Figure 8 shows the maximum shear stress vs. normal stress plot for S-T mixtures at dry unit weight of 20 kN/m³ and shearing rate 1.25 mm/min. The figure indicates that the maximum shear stress corresponding to normal stress is higher than that of sand alone. The slope of the trend line increases upto 30% tyre content, beyond which it decreases. The shear parameters of different S-T mixtures were obtained from this figure.

Mixtures at Normal Stress 150 kPa, Shearing Rate 1.25 mm/min and Different Dry Unit Weights.

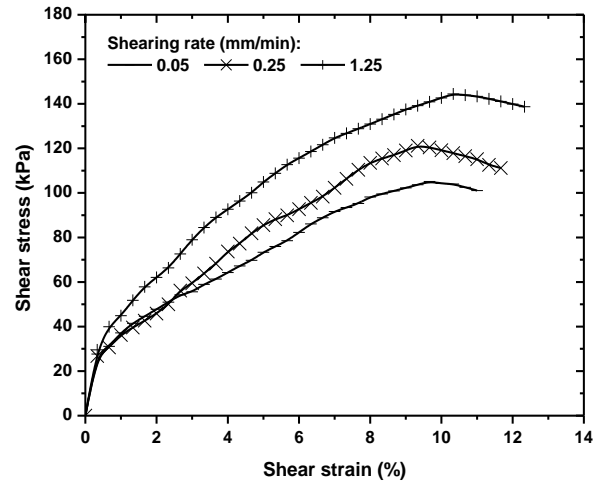


Fig. 6. Shear Stress Vs. Shear Strain Plot for S-T (70:30) Mixtures at Normal Stress 150 kPa , Dry Unit Weight of 20 kN/m³ and Different Shearing Rates.

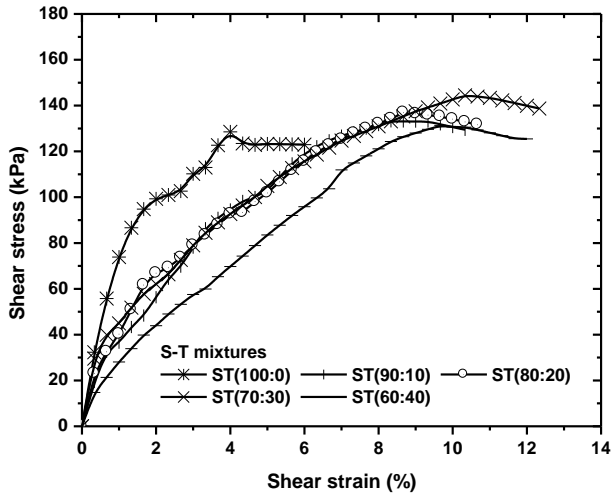


Fig. 4. Shear Stress Vs. Shear Strain Plot for S-T Mixtures at Normal Stress 150 kPa, Dry Unit Weight of 20 kN/m³ and Shearing Rate of 1.25 mm/min.

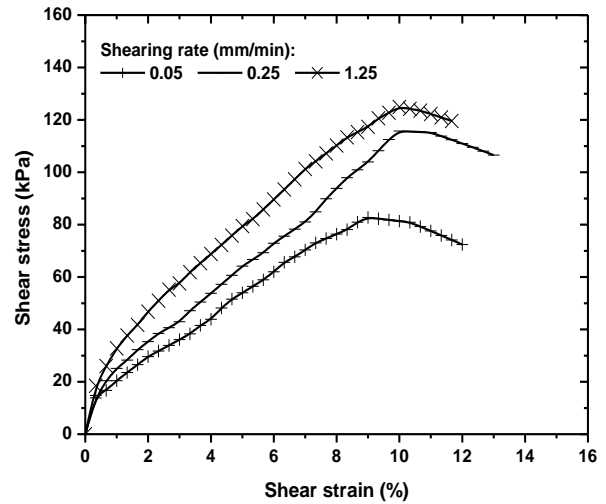


Fig. 7. Shear Stress Vs. Shear Strain Plot for S-T (70:30) Mixtures at Normal Stress 150 kPa, Dry Unit Weight of 16 kN/m³ and Different Shearing Rates.

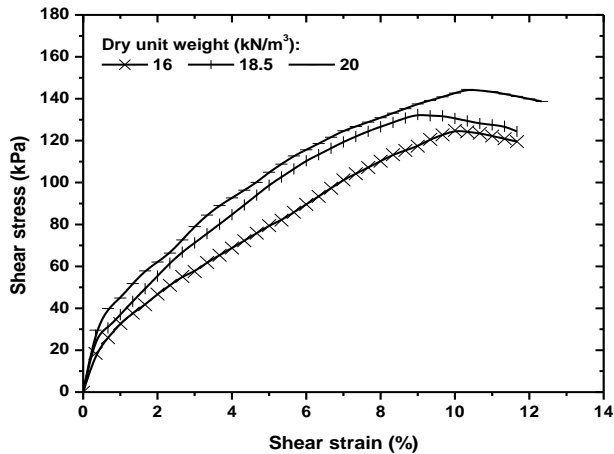


Fig. 5. Shear Stress Vs. Shear Strain Plot for S-T (70:30)

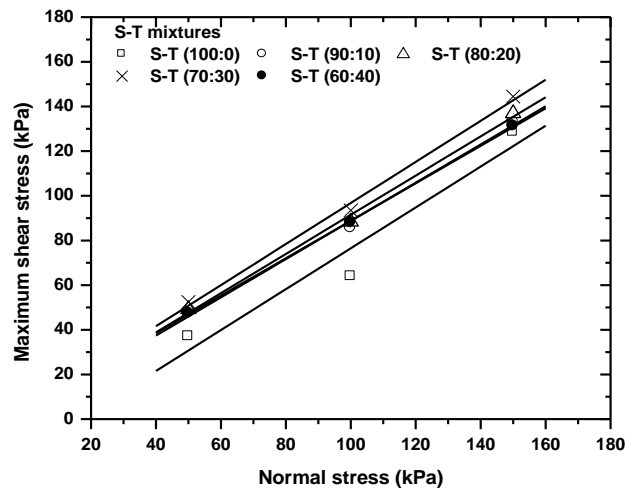


Fig. 8. Maximum Shear Stress Vs. Normal Stress Plot for S-T Mixtures at Dry Unit Weight of 20 kN/m³ and Shearing Rate of 1.25 mm/min.

The variation of ‘c’ and ‘φ’ with tyre content for S-T mixtures for different dry unit weights and shearing rate 1.25 mm is shown in the Fig. 9. From the Fig. 9, it can be said that the ‘φ’ value increases with increase in tyre content upto 30% of tyre content and decreases at 40% of tyre content for S-T mixes. At a particular tyre content, the φ value increases with increase in dry unit weight for S-T mixes. The ‘φ’ value ranges from 31 to 43° for S-T mixes. The cohesion ‘c’ increases with increase in tyre content upto 40% for all the dry unit weights of S-T mixes. The cohesion intercepts ranges from 3.2 to 13.9 kPa for S-T mixes. The increase in the shear strength parameters with tyre content is due to the interaction between T-T, S-S, and S-T. From the values of ‘φ’ and ‘c’ obtained, it was found that the change in φ value has more influence than the change in cohesion on shear strength of the mixes. The shear strength was found to be highest at 30 % of tyre content for S-T mixes. Therefore, the optimum tyre content of the mixes can be considered as 30 %. This finding is similar to that were observed by Ghazavi et al. (2011) and Bali Reddy et al. (2016) for sand-tyre chips mixtures.

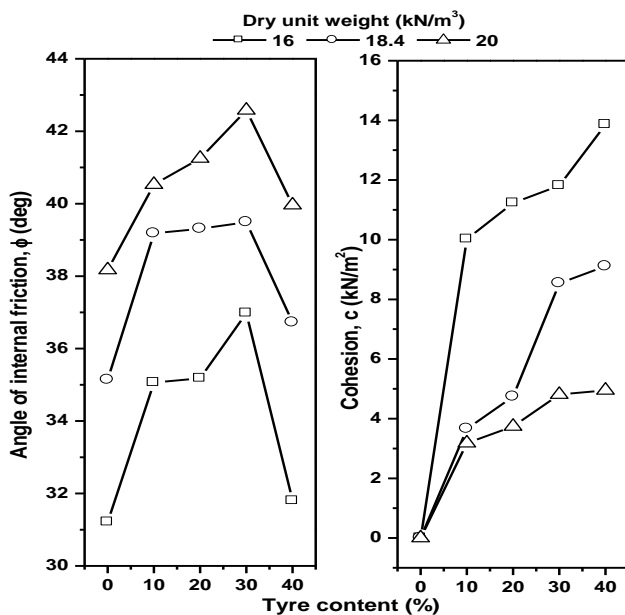


Fig. 9. Shear Strength Parameters Vs. Tyre Content Plots for S-T Mixtures at Different Dry Unit Weights and Shearing Rate of 1.25 mm/min.

Figure 10 shows the shear strength parameters versus tyre content plots of S-T mixtures at different shearing rates and constant dry unit weight of 20 kN/m³. The φ value is found to increase upto 30% tyre content at different shearing rates and constant dry unit weight for the S-T and decrease at 40% tyre content. The φ value increases with the increase in shearing rate. The

angle of internal friction of the S-T mixtures ranges from 19° to 43°.

The cohesion intercept for S-T mixtures ranges from 1.3 to 13.9 kPa. The cohesion intercept was found to increase upto 40% for S-T mixtures. Similar results were also observed in case of the mixtures when the shear tests were performed at three different shearing rates but at constant dry unit weight of 16 kN/m³. The shear parameters for these states are shown in the Fig. 11 for S-T mixtures. The optimum tyre content is found to be 30% at different shearing rates and constant dry unit weight for S-T mixtures. These results are similar to the findings of Ghazavi et al. (2011) and Bali Reddy et al. (2016) for sand-tyre chips mixtures.

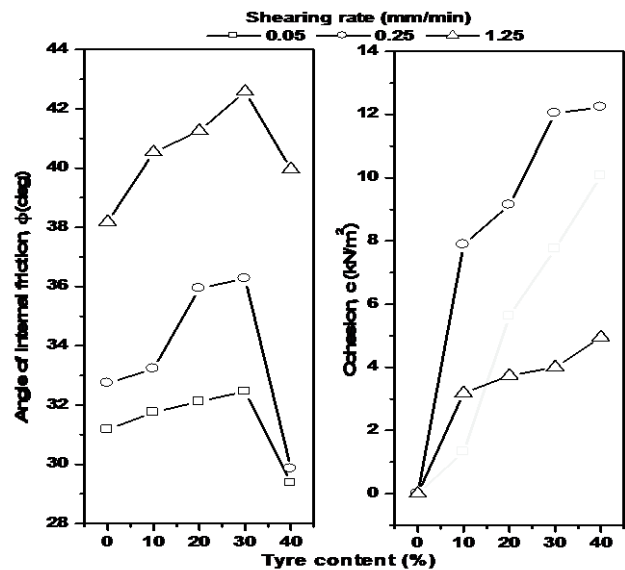


Fig. 10. Shear Strength Parameters Vs. Tyre Content Plots for S-T Mixtures at Dry Unit Weight 20 kN/m³ and Different Shearing Rates.

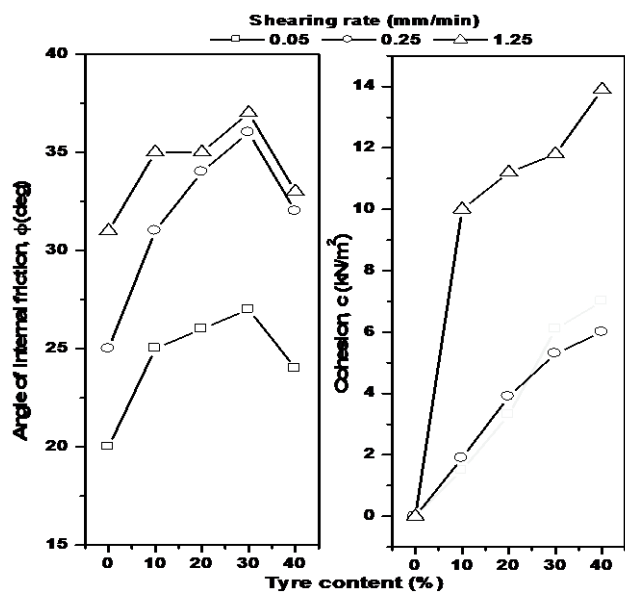


Fig. 11. Shear Strength Parameters Vs. Tyre Content Plots for S-T Mixtures at Dry Unit Weight 16 kN/m³ and Different Shearing Rates.

Apparent cohesion 'c' in the S-T mixtures may be attributed to the inter-locking effect due to the penetration of sand grains into tyre waste (Ghazavi and Sakhi 2005). This inter-locking effect becomes more significant with the increase in tyre content in the mixtures, resulting in higher apparent cohesion. At lower tyre content, the increase in ϕ value in the mixtures can be attributed to the friction mobilized between S-T, T-T, and S-S due to slight penetration of sand grains into tyre waste when shear stresses are applied (Ghazavi and Sakhi 2005). At higher tyre content, when shear stresses are applied, it is unlikely that sand grains penetrate into tyre waste and the sample tends to dilate. This dilation decreases the friction between S-T and T-T which leads to a decrease in the friction angle.

4. CONCLUSIONS

The present study investigates the influence of tyre content, unit weight and shearing rate on shear strength behaviour of dry S-T mixtures. The results of the experiments show that the shear strength of sand mixed with tyre waste is greater than pure sand. Moreover, the shear strength increases when tyre dusts are added to an optimum amount of 30%. However, the strength decreases when the tyre content increases beyond 30% because the S-T mixtures behave less like reinforced soil and more like a tyre waste mass with sand inclusions. The results also indicate that the normal stress, tyre content, dry unit weight and shearing rate are the important factors that have significant influence on the shear strength of S-T mixtures. Following conclusion are drawn from the present study.

- 1) At constant shearing rate, the angle of internal friction of the S-T mixtures increases with increase in dry unit weight upto 30% tyre content and decreases further with increase in tyre content. Cohesion intercepts are found to increase upto 40% tyre content for S-T mixtures.
- 2) At constant dry unit weight, the angle of internal friction of S-T mixtures increases with increase in shearing rate upto 30% tyre content and decrease beyond this. Cohesion intercepts are found to increase upto 40% of tyre content.
- 3) The optimum tyre content is found to be 30% for S-T mixtures at different dry unit weights and shearing rates. Therefore, the optimum mixing ratio is 70:30 (S:T).
- 4) The shear strain is found to increase with increase in tyre content in S-T mixtures and it is observed to be more compared to sand alone.

REFERENCES

- 1) Ghazavi, M. and Sakhi, M.A. (2005): Influence of optimized tire shreds on shear strength parameters of sand, *International Journal of Geomechanics*, 5(1), 58-65.
- 2) Ghazavi, M., Ghaffari, J., and Farshadfar, A. (2011): Experimental determination of waste tire chip-sand-geogrid

- interface parameters using large direct shear tests, *Proceedings of the 5th Symposium on Advances in Science and Technology*, 1-10.
- 3) Humphrey, D.N., Sandford, T.C., Cribbs, M. and Manion, W. (1993): Shear strength and compressibility of the tyre chips for use as retaining wall backfill, *Transportation Research Record No. 1422*, Lightweight Artificial and Waste Materials for Embankments over Soft Soils, Transportation Research Board, Washington, DC, United States of America, 29-35.
 - 4) IS: 1498 (1970): *Indian Standard Classification and Identification of Soils for General Engineering Purposes*, Bureau of Indian Standards, New Delhi, India.
 - 5) IS: 2720 (Part 3/section 2) (1980): *Indian Standard Method of Test of Soils: Determination of Specific Gravity, Fine, Medium and Coarse Grained Soils*, Bureau of Indian Standards, New Delhi, India.
 - 6) IS: 2720 (Part 4) (1985): *Indian Standard Method for Grain Size Analysis of Soil*, Bureau of Indian Standards, New Delhi, India.
 - 7) IS: 2720 (Part 13) (1986): (Reaffirmed in 1997), *Indian Standard Method of Test of Soils: Direct Shear Test*, Bureau of Indian Standards, New Delhi, India.
 - 8) Bali Reddy, S., Pradeep Kumar, D. and Murali Krishna, A. (2016): Evaluation of the optimum mixing ratio of a sand-tire chips mixture for geotechnical applications, *Journal of Materials in Civil Engineering, ASCE*, 28(2). DOI: 10.1061/(ASCE)MT.1943-5533.0001335.

[Back to table of contents](#)

Improvement of engineering properties of clayey soil with addition of different admixtures

P. K. Khaundⁱ⁾ and Pooja Kakatiⁱⁱ⁾

i) Professor & Head, Department of Civil Engineering, Jorhat Engineering College, Jorhat, Assam-785007, India.

ii) P.G. Student, Department of Civil Engineering, Jorhat Engineering College, Guwahati, Assam-781028, India.

ABSTRACT

For the construction of any load bearing structures, the clayey soil is not considered to be the most suitable one as it possesses low shear strength, MDD and CBR values, poor drainage and low bearing capacity etc. which makes the soil unsuitable to carry loads. This paper presents the improvement of the engineering properties of soil parameters such as CBR values, permeability, shear strength etc. due to the addition of different admixtures viz. fly ash, cement, lime and sand of various zones to high plasticity clayey soil. The variations of these soil parameters are observed with the addition of admixtures individually and also in combinations in different percentages.

Keywords: Bearing capacity, CBR, fly ash, MDD, permeability, shear parameter

1. INTRODUCTION

High plasticity clayey soil is one of the most undesirable soils, for construction of any load bearing structures. So, these soil needs to be improvised with the addition of different kinds of admixtures. In this regard, different kinds of admixtures can be added to the soil, to improve its engineering properties. Admixtures such as fly ash, cement, lime, cement kiln dust, treated tyre chips etc. can be added to the soil mass which acts as chemical stabilizers, whereas the addition of sand, aggregates, fibers, brick dust etc. acts as reinforcing agents.

In this aspect, various investigations were made by different scholars to improve the soil properties. Raymond (1961), Mateos and Davidson (1962), Gray and Lin (1972), Broms (1986), Subbarao and Ghosh (1995), Udin et al. (1997) etc. carried out different experimental study individually to investigate the compaction and stabilization of soil using different admixtures. Porbaha et al. (2000) conducted a study on two silt size fly ashes and was concluded that the shear strength increases and permeability decreases with the curing period. The research results of Show et al. (2003) with the addition of fly ash and cement on clayey soil shows that the rate of gain of shear strength decreases when fly ash is added to cement stabilized soil compared to the sample without fly ash. Tastan et al. (2011) in their research work indicates that the unconfined compressive strength of the organic soil can be increased with the addition of fly ash. Udayashankar

et al. (2012) based on their test results reported the use of fly ash up to 60% to improve the engineering properties of the soil and has found that the MDD of the soil increases up to 40% and then decreases. Similarly, CBR values increases up to 40% addition of fly ash and then decreases. Sarma et al. (2012) reported the use of fly ash up to 80% but the test results indicate that density increases up to addition of fly ash initially up to 30% and then decreases. The observation shows that with increased percentage of fly ash in soil CBR value initially increased and then it starts to decreased. Kang et al. (2014) in their study concluded that the MDD of the soil mass increases while OMC decreases with the addition of class-C fly ash and lime kiln dust on clayey soil. Also, the UCS of the admixed soil is observed to be increase with the curing period. Gupta and Sharma (2015) in their study observed that with the addition of sand and fly ash the permeability of the soil mass gets improved. But at the end of 30 days curing period the ultimate strength is observed to be more or less same. Many other researchers such as Kaniraj and Havanagi (2001), Jiang et al. (2010), Muntohar et al. (2013), Kumar and Jairaj (2014) also reported the use of fibres along with the admixtures to increase the shear strength of the soil.

In the present paper, the variation of engineering properties (MDD, CBR, shear parameters, permeability etc.) of clayey soil with the addition of admixtures such as lime, cement, fly ash and sand has been explained.

2 MATERIALS USED

Clayey soil was collected from NH-37 of the location Kakodonga and Jaysagar and the engineering properties of the virgin soil are given below in table 1. Fly ash was collected from Nagaon paper mill while the cement used is of OPC43 grade of brand Dalmia. The chemical properties of fly ash and cement are tabulated in table 2 and table 3 resp. From the chemical analysis of lime, the amount of CaO is found to be 65.25%; and the fly ash is been categorised as class-F category as CaO is less than 10%.

Table 1 Geotechnical properties of soil

Properties of soil	Values	
	Jaysagar	Kakodonga
Liquid limit (%)	62.0	65.0
Plastic limit (%)	31.34	32.15
Plasticity index (%)	30.66	32.85
Classification of soil	CH	CH
OMC (%)	24.0	25.0
MDD (gm/cc)	1.52	1.53
Soaked CBR	3.49	2.6

Table 2 Chemical properties of fly ash

Chemical composition	Values (%)
Loss of ignition	17.86
Silica	44.20
Alumina	16.99
Ferric oxide	13.68
Calcium oxide	1.88
Magnesium oxide	2.01

Table 3 Chemical properties of cement

Constituent of cement	Values (%)
Silica	20.53
Alumina	2.63
Iron	4.78
Sulphate	2.6
Calcium oxide	61.45
Magnesium Oxide	4.38
Loss on ignition	2.07

3 RESULTS AND DISCUSSION

The variation of compaction parameters with admixtures of Jaysagar sample is tabulated in table 4. The MDD of the soil increases with the increase in admixture content in the soil; while there is a continuous reduction in OMC with the addition of admixtures. This increase in MDD of the soil is due to the binding property of the admixture which binds the soil mass and hence the density of the soil gets increased. Also the finer particles of the admixtures must have occupied the space present between the sand and the soil. A similar trend is also observed for Kakodonga sample.

The trend of increase in CBR values with the addition of different admixtures in different percentages are graphically represented in fig 1 and fig 2. Rate of increase in CBR values are observed to be more in case of lime and cement compared to that of fly ash. The increase values of CBR are due to the cementing and the pozzolanic properties of the admixtures which binds the soil particles in a better way.

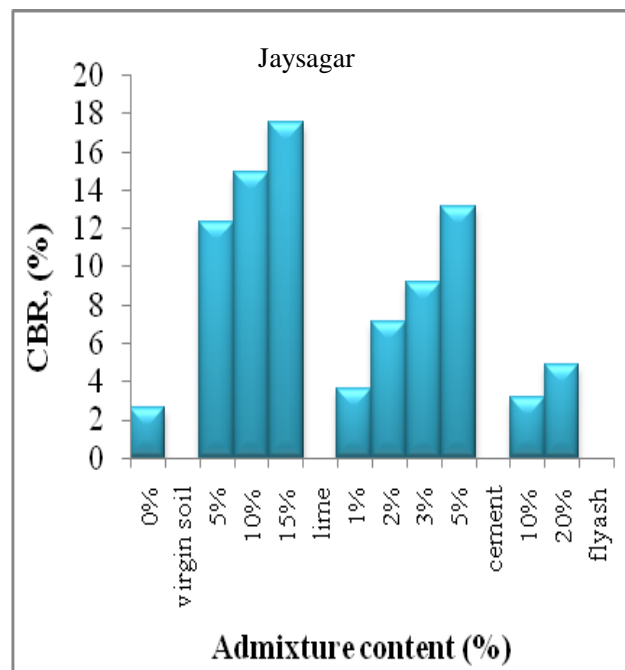


Fig. 1 Variation of CBR values with the addition of admixtures for Jaysagar sample

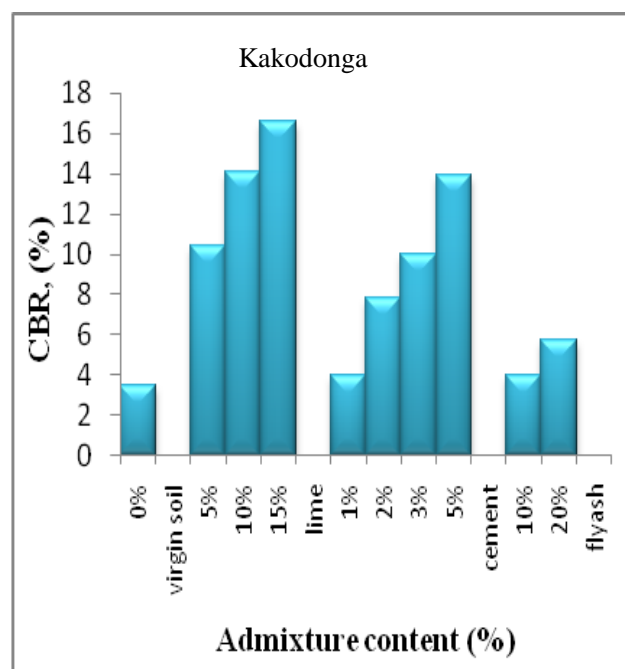


Fig. 2 Variation of CBR values with the addition of admixtures for Kakodonga sample

Table 4 Variation of compaction parameters with admixtures

Content %	Jaysagar sample										
	Lime		Cement		Flyash		Sand		Content %	Sand+Flyash	
	MDD	OMC	MDD	OMC	MDD	OMC	MDD	OMC		MDD	OMC
0	1.52	24.0	1.52	24.0	1.52	24.0	1.52	24.0	0	1.52	24.0
1	-	-	1.54	24.0	-	-	-	-	2+5	1.616	23.0
2	-	-	1.57	23.6	-	-	1.595	23.2	2+15	1.639	22.6
3	-	-	1.60	22.8	-	-	-	-	5+5	1.645	22.1
5	1.53	26.9	1.61	23.3	1.53	23.6	1.631	22.4	5+15	1.669	21.4
10	1.59	24.2	-	-	1.55	23.2	1.743	21.8	10+5	1.757	21.6
15	1.62	22.2	-	-	1.58	22.7	-	-	10+15	1.781	20.8
20	-	-	-	-	1.61	22.2	-	-	-	-	-

Tri axial test has been carried out to analyze the effect on shear parameters of soil mass with the addition of different admixtures individually and also in different combinations in different proportions. The shear parameters of the admixed soil mass are observed to be improved with the addition of the admixtures. Fig 3, fig 4, fig 5 and fig 6 show the variation of shear parameters with the addition of admixtures in combinations in different proportions. From the different tests it is clear that the combination of admixtures give better improvement compared to the individual admixtures. The angle of internal friction is observed to be increased with the increasing percentages of admixtures while the cohesive value decreases. The addition of the admixtures reduces the plastic nature of the fines due to which the angle of internal friction increases and as a result the shear strength of the soil samples gets improved.

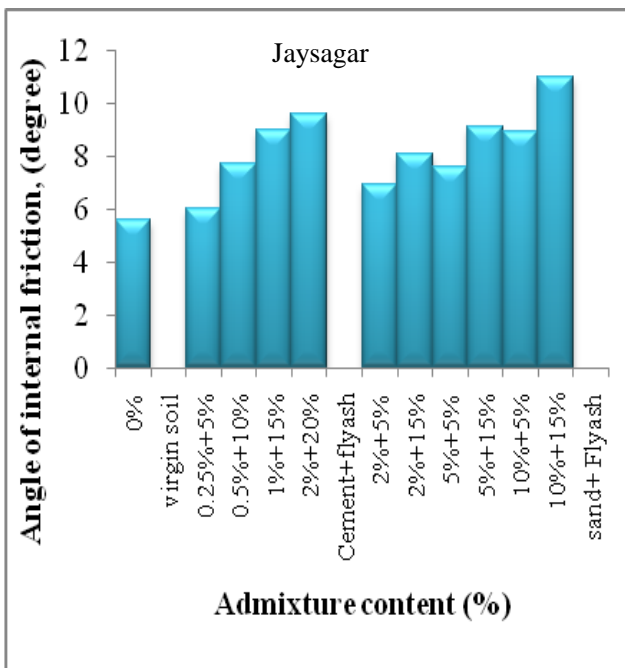


Fig. 3 Variation of angle of internal friction with admixture content for Jaysagar sample

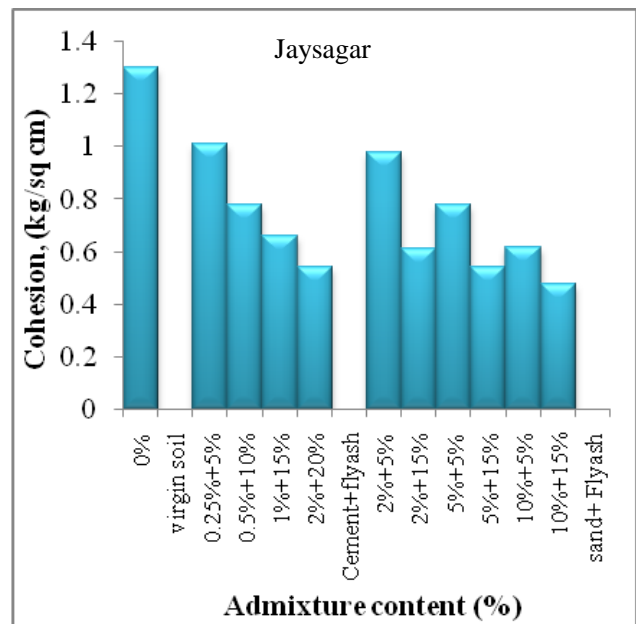


Fig. 4 Variation of cohesion with admixture content for Jaysagar sample

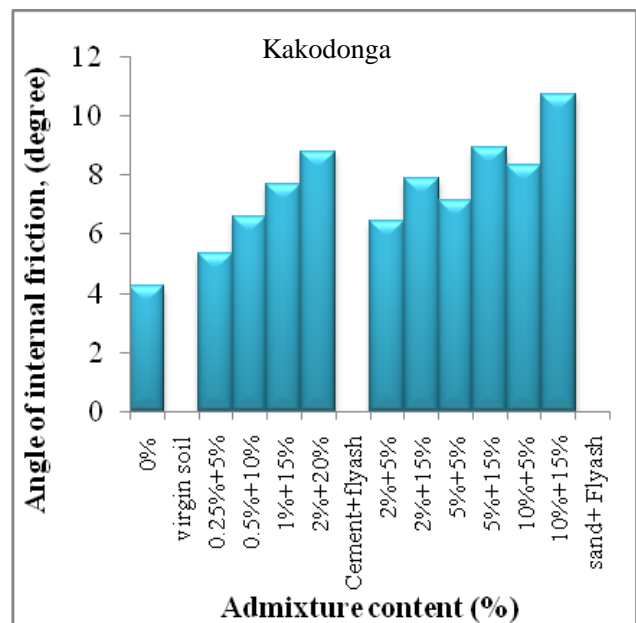


Fig. 5 Variation of angle of internal friction with admixture content for Kakodonga sample

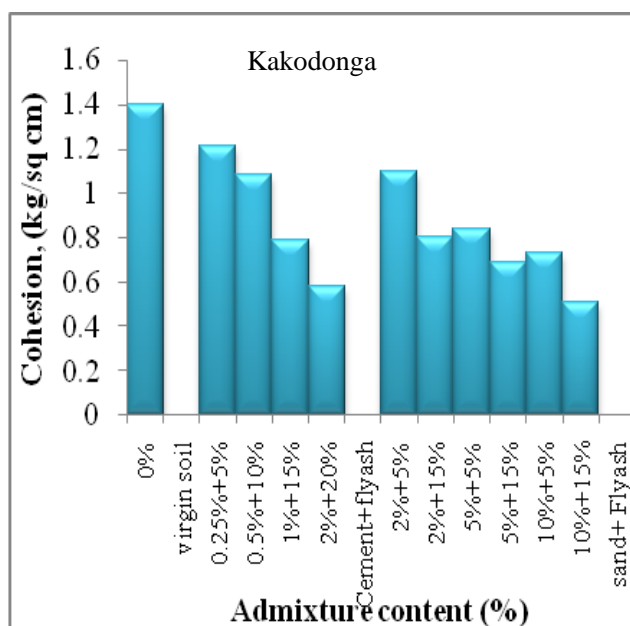


Fig. 6 Variation of cohesion with admixture content for Kakodonga sample

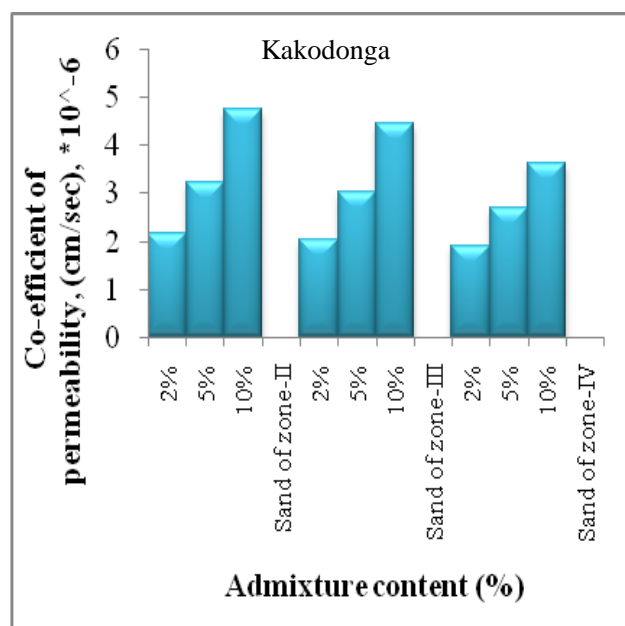


Fig. 8 Variation of permeability co-efficient values with the addition of sand for Kakodonga sample

Clayey soil possesses very low permeability co-efficient values, therefore, falling head permeability test were carried out with the virgin soil as well as with the addition of admixtures, viz. sand and fly ash. Virgin soil samples are almost impermeable. Sand of zone-II, zone-III and zone-IV are mixed with the clayey soil samples in different percentages to observe the effect on co-efficient of permeability. Sand of zone-II which possesses the coarser grain size particles has highest permeability values compared to sand of other zones. Fig 7 and fig 8 shows the permeability co-efficient values when sand is used as admixtures for both the soil samples.

Fig 9 and fig 10 represent the variation of coefficient of permeability with the addition of sand of zone-II and fly ash in as combined admixtures. From the test results it is observed that with the addition of sand permeability increases, while it decreases with the addition of fly ash. This is due to the finer particles of fly ash filled up the void spaces present in the sand admixed soil. In addition to that, due to pozzolanic reactions the gels that formed during the pozzolanic reactions might filled up the remaining void spaces and thus it resists the flow of water through the soil mass. While coarse grain size of zone-II sand of provides more pore spaces and allow permeability at higher rate values.

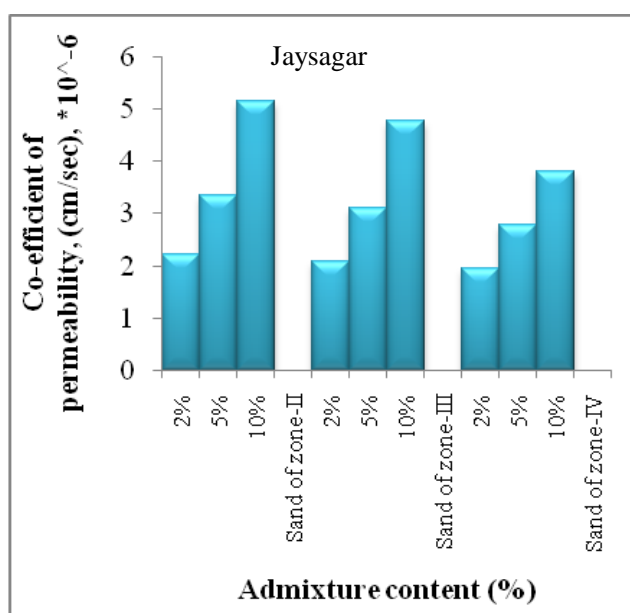


Fig. 7 Variation of permeability co-efficient values with the addition of sand for Jaysagar sample

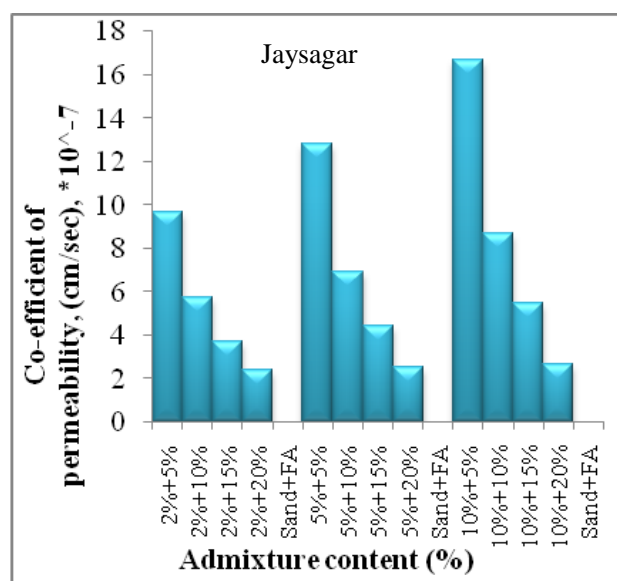


Fig. 9 Variation of permeability co-efficient values with the addition of sand and fly ash for Jaysagar sample

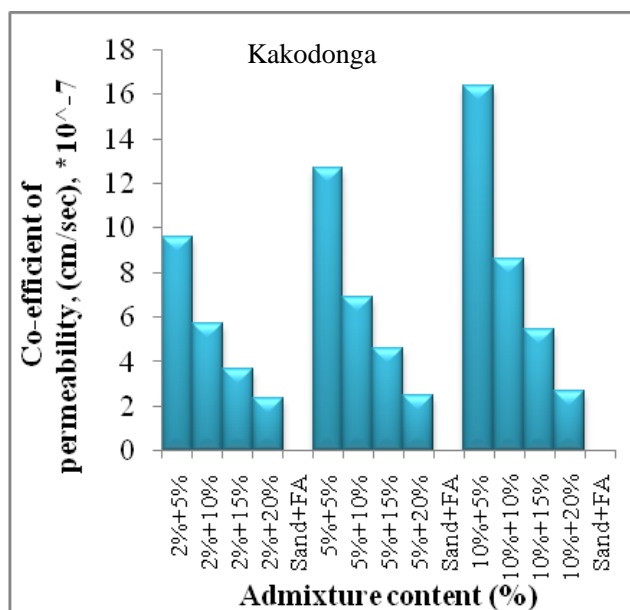


Fig. 10 Variation of permeability co-efficient values with the addition of sand and fly ash for Kakodonga sample

5 CONCLUSION

From the experimental results, it can be concluded that the engineering properties of the clayey soil can be improved with the addition of admixtures in the soil mass up to a certain extent.

The MDD and CBR values of the clayey soil improve with the addition of admixtures. The addition of cement gives better densification to the clayey soil compared to other admixtures with same percentage of addition; but considering economy, lime may be referred as one of the suitable admixture.

It has been observed that angle of internal friction of soil mass increases with the addition of different admixtures, while there is a gradual reduction in cohesion. However, with the addition of sand and fly ash in combined form gives satisfactory result compared to other admixtures.

To improve the permeability of the soil samples sand of different zones (II, III and IV) and a combination of fly ash and sand etc. are used as admixtures. From the test results it can be concluded that a significant improvement of permeability takes place with the addition of zone-II sand, while permeability reduces with the addition of fly ash along with sand.

REFERENCES

- 1) Broms, B. B. (1986): "Stabilization of soft clay with lime and cement columns in Southeast Asia", *Applied Research Project RP10/83*, Nanyang Technological Institute, Singapore.
- 2) Bushra, I. and Robinson, R. G. (2013): "Effect of Fly Ash on Cement Admixture for a Low Plasticity Marine Soil", *Advances in Civil Engineering Materials*, 2(1), 608–621, DOI: 10.1520/ACEM20120037.
- 3) Ghosh, A. and Subbarao, C. (2007): "Strength Characteristics of Class F Fly Ash Modified with Lime and Gypsum", *Journal of Geotechnical and Geoenvironmental Engineering*, ASCE, 133(7), 757-766, DOI: 10.1061/(ASCE)1090-0241(2007)133:7(757).
- 4) Gray, D. H. and Lin, Y. K. (1972): "Engineering properties of compacted fly ash", *Journal of Soil Mech. Found. Div.*, ASCE, 98(4), 361–380.
- 5) Gupta, C., Sharma, R.K. (2015): "Study of black cotton soil and local clay soil for sub grade characteristic", *50th Indian Geotechnical Conference*, Pune, Maharashtra, India.
- 6) Jiang, H., Cai, Y. and Liu, J. (2010): "Engineering Properties of Soils Reinforced by Short Discrete Polypropylene Fiber", *Journal of Materials in Civil Engineering*, ASCE, 22(12), DOI: 10.1061/(ASCE)MT.1943-5533.0000129.
- 7) Kang, X., Kang, G. C., Chang, K. T. and Ge, L. (2014): "Chemically Stabilized Soft Clays for Road-Base Construction", *Journal of Materials in Civil Engineering*, ASCE, DOI: 10.1061/(ASCE)MT.1943-5533.0001156.
- 8) Kaniraj, S. R. and Havanagi, V.G. (2001): "Behavior of cement-stabilized fiber-reinforced flyash-soil mixtures" *Journal of Geotechnical and Geoenvironmental Engineering*, ASCE, 127(7), Paper No. 20252.
- 9) Kumar, P. and Singh, S. P. (2008): "Fiber-Reinforced Fly Ash Subbases in Rural Roads", *Journal of Transportation Engineering*, ASCE, 134(4), DOI: 10.1061/(ASCE)0733-947X(2008)134:4(171).
- 10) Kumar, M. T. P. and Jairaj, (2014): "Shear Strength Parameters of BC Soil Admixed with Different Length of Coir Fiber"; *IJERT*, Vol. 3, Issue 4.
- 11) Mateos, M. and Davidson, D.T. (1962): "Lime and fly ash proportions in soil, lime and fly ash mixtures, and some aspects of soil lime stabilization.", *Highway Research Board Bulletin*, 335, 40-64.
- 12) Muntohar, A. S., Widiarti, A., Hartono, E. and Diana, W. (2013): "Engineering Properties of Silty Soil Stabilized with Lime and Rice Husk Ash and Reinforced with Waste Plastic Fibre", *Journal of Materials in Civil Engineering*, ASCE; 25(9); DOI: 10.1061/(ASCE)MT.1943-5533.0000659.
- 13) Porbaha, A., Pradhan, T. B. S. and Yamane, N. (2000): "Time Effect on Shear Strength and Permeability of Fly Ash"; *Journal of Energy Engineering*, ASCE; 126(1), Paper No. 18627.
- 14) Raymond, S. (1961): "Pulverised Fuel ash as Embankment Material", *Proceedings of the Institute of Civil Engineers*, 53, 515-536.
- 15) Show, K. Y., Tay, J. H. and Goh, A. T. C. (2003): "Reuse of Incinerator Fly Ash in Soft Soil Stabilization", *Journal of Materials in Civil Engineering*, ASCE, 15(4), 335-343, DOI: 10.1061/(ASCE)0899-1561(2003)15:4(335).
- 16) Subbarao, C. and Ghosh, A. (1995): "Multifacets of fly ash as construction material", *Proceedings of the National Conference on Civil Engineering Materials and Structures*, Osmania University, India, 48-54.
- 17) Tastan, E. O., Edil, T. B., Benson, C. H. and Aydilek, A. H. (2011): "Stabilization of Organic Soils with Fly Ash", *Journal of Geotechnical and Geoenvironmental Engineering*, ASCE, 137(9), DOI: 10.1061/(ASCE)GT.1943-5606.0000502.
- 18) Uddin, K., Balasubramaniam, A. S. and Bergado, D. T. (1997): "Engineering behavior of cement-treated Bangkok soft clay", *Geotechnical Engineering*, 28(1), 89–119.

[Back to table of contents](#)

Sustainable Developments and Challenges for Structural Engineers

First Sukumar Singh Ningthoukhongjamⁱ⁾

i) Assistant Professor, Department of Civil Engineering, Manipur Institute of Technology, Takyelpat, Imphal 795004, India.

ABSTRACT

Structural engineers play a vital role in achieving a sustainable adaptation and mitigation to ever increasing environmental challenges. Our planet has limited natural resources but developments in terms of consumption of these resources are progressing day by day. Manufacturing of main construction materials like cement and steel not only consume large amount of energy but also pollutes environment by releasing harmful gases. Structural engineers play a vital role in presenting environmentally, economically, and socially sustainable solution for this global threat. Sustainable solutions may be in the form of developing new material, recycling and reuse of existing material, efficient design methodology and promoting such solutions to practice engineers and other related persons.

Keywords: sustainable design, efficiency, recycle, reuse, economic development

1. INTRODUCTION

Sustainable development may be defined as the socio-economical development which fulfils present day requirements without posing treat to the requirement of future generation (Chaudhary and Piracha, 2013). Urbanization in terms of rapid construction of different types of industries and structures in both developed and developing countries pose a global threat in terms of high energy utilization, waste material generation, global greenhouse gases emissions, pollution and depletion of natural resources. Structural engineers have started considering this global threat as a challenge task for them and they have been working to produce a sustainable solution to mitigate this global threat. At the same time the solution must be socially, economically and environmentally acceptable one which can be termed as sustainable development and challenges to structural engineers.

Sustainable design is a good design practice which incorporates the following criteria:

- 1) It reduces consumption of construction materials.
 - 2) It enhances the status of living for people.
 - 3) It ensures better performance of economics.
 - 4) It retains natural resources for upcoming generations.
- Sustainable development study in civil engineering stream gives an idea how to perform appropriate tasks in various construction stages as demanded at site. Such activities help in maintaining ecosystem by avoiding various adverse effects brought by the various unseen unavoidable factors. In 20th century, engineering design has ignored the life cycle costs of infrastructural projects and hence the global environmental impacts due to these infrastructural projects were not discussed.

Structural engineer considers 21st century as the time to take challenges and develop sustainable solutions for the society.

Sustainable development have resulted greater interest with many developers, house owners, design professionals and contractors that they have considered it as even a sense of urgency in accomplishing the goals of sustainable design. Nowadays even the developers are also realizing that buying buildings constructed with appropriate sustainable design procedures are more advantageous than buying normal standard buildings. It has been reported that 35% or greater reduction in energy consumption has been resulted after adopting sustainable design procedure as per “The structural engineer and sustainable design” Douglas Wood & Associates, Inc. (2007). Sustainable design procedures are more efficient thereby keeping low water usage and maintenance costs, and at the same time increasing worker productivity. Such activities have resulted substantial financial improvements over the whole life span of the structures.

2 SUSTAINABLE SOLUTIONS

The sustainable solutions to this broad issue of global threat can be addressed into the following categories:

- Material - the environment impact of exploiting certain construction materials such as concrete, steel and timber; and their eco-friendly new substitute materials
- Recycling – waste products of construction materials can be reused or recycled and they

can be used while constructing new structures

- Efficiency – use of appropriate amount of materials and resources for construction of structure after adopting proper design to ensure minimum waste and maximum efficiency
- Energy – minimum consumption of energy by the structure throughout its life span
- Awareness – educating and promoting the concept of sustainable design to practice engineers and workers in construction field

2.1 Sustainable material

The trends in consumption of main construction materials like steel and concrete all over the world shows the increasing impact on environment in the field of structural design and construction as depicted in Figure 1. The primary global concern that all structural engineers should consider in particular, is the emissions of greenhouse gases due to manufacturing of structural materials. Manufacturing of Portland cement has become twice in less than 30 years, and such tremendous growth may prevail till the next century. Furthermore, each ton of cement production releases approximately one ton of CO₂ into the atmosphere and it is reported that cement industry alone contributes about 7% of entire CO₂ emissions around the globe (Chaturvedi and Ochsendorf, 2004). Iron & steel industry accounts for 27% of direct CO₂ emissions from the industry sector. 1.7 tonnes of CO₂ is emitted for every tonne of steel produced (Gervásio, 2008).

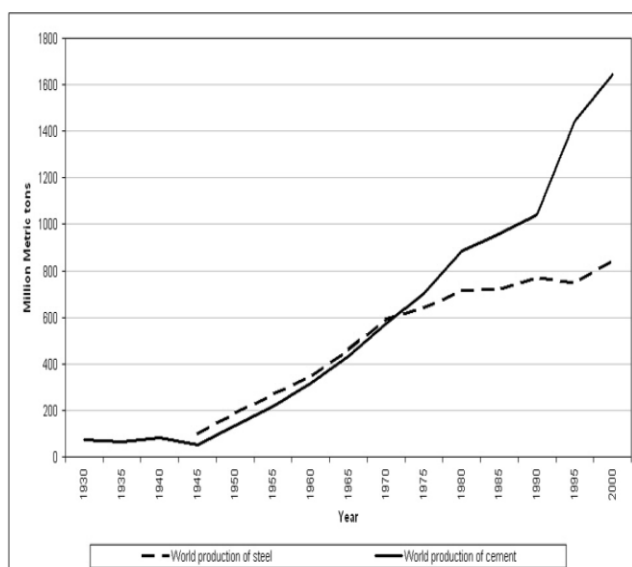


Fig. 1. World production of cement and steel (Chaturvedi and Ochsendorf, 2004)

In order to mitigate such global threat, scholars have started carrying out research work for the development of new construction materials which are sustainable in nature. These materials serve the performance requirements without damaging the condition of

environment, and at the same time also enhance the condition of the environment. "Green material" was proposed first at International Material Subject Symposium held in 1988. Then United Nations Environment and Development Conference was held in 1992, and then in 1994 sustainable product development working group of 125 was established (Ochsendorf, 2005).

Ecological building materials are considered to have the following three characteristics: (Ochsendorf, 2005)

- 1) Ecological building materials should be such it not only widen the prospect of human life but also make a broader space for humanity;
- 2) Ecological building materials should be environmental friendly thereby reducing environmental pollution under the concept of sustainable development. It ensures better socio-economic progress in coordination of human activities and external environment thereby decreasing consumption of material and energy in the manufacturing processes. This will minimize production waste and hence the quantity of waste to be recycled, and at the same time the recycled or recovered or processed waste materials should not pollute the environment;
- 3) Ecological building materials give a healthy and beautiful human life making peace and harmony with nature thereby representing a more comfortable environment in mankind.

Ecological Building Materials is a guiding principle only which is a developing concept with dynamic and uncertainty in nature. The main reason of research work on ecological building materials is to develop the necessary material having lowest environmental impact in the field of manufacturing, processing, use and reproduction, which serves the requirements of comfortable human survival and development.

2.2 Recycling of construction materials

Some existing constructions materials can be reused directly if handle properly, and also significant amounts of waste products of construction materials can be recycled and reused in appropriate way into the structural systems. For example, fly ash and blast furnace slag are waste products from the burning of coal and smelting of steel respectively. Both fly ash and slag can be used to replace some portion of cement, and the judicious use of some portion of either waste product in a concrete mix actually enhances the strength of concrete. Manufacturing of cement consumes large amount of energy and if these waste products can substitute some amount of cement then this can be another effective way of sustainable development too. The incorporation of slag and fly ash into the cement not only save the quantity of cement but also enhances the strength of the concrete giving high strength concrete mix. These days, the quantity of fly ash or slag can be added upto 25% of the total cementitious material which includes slag or fly ash

along with cement itself. Even the quantity of slag or fly ash may be added more upto 50% of the cementitious materials and as high as upto 70% in some cases.

Low strength concretes can be made from recycled materials of previously used concrete aggregates. Such materials may consist of stone, brick and waste concrete. The incorporation of such materials may greatly increase the recycled content of concrete. However, their usage is most suitable for non-structural concrete elements like pavements and other slabs-on-ground structures.

Steels used as a construction material (both reinforcing bars steel for concrete and structural steels) are 100% recyclable and they can be infinitely recycled without loss of quality. Manufacturing new steel from recycled steel reduces CO₂ emissions (in 2006, about 894 million metric tons of CO₂ were saved) (Li, and Guo, 2015). With improved design, the requirement for new steel production can be reduced as steel components can be reused without reprocessing. In construction most aluminium alloys contain high levels of recycled steel content.

2.3 Efficiency

The structural engineer has to follow the relevant design codes and their adopted standards for the designing and construction of structures within the parameters of good engineering judgment and practice. Code base design methodology mostly results into conservative design practice. Basic method of analysis and design are adopted in design codes. With the development of sophisticated structural modelling and analysis softwares, the structural engineers nowadays can perform in depth accurate analysis and design of even complicated structures efficiently giving optimum results which can be termed as sustainable design methodology. Sustainable design methodology will result into optimum quantity of construction materials as compared to conventional conservative design thereby saving unnecessary extra construction materials which are not required at all. Reduction in construction material will reduce loads on the structure and hence there will be purposeful reduction in foundation sizes. Minimum excavation of earth results minimum damage to the site and minimum energy requirement for excavating and disposal of earth as well.

Improvement of life cycle performance of the structure will minimise the total life cycle cost of the structure. Most structures are usually designed to economise the initial cost only, rather than estimating the cost of whole life time of the structure. As an example, in the case of bridge construction, usually the maintenance and demolition costs are often more than the initial cost of construction, but engineers rarely consider the costs of whole life time of the structure at the time of design. A slight increase in initial costs could have drastically reduced the whole life cycle

costs of the structure by lowering maintenance cost and at the same time making arrangement for salvage or disposal when the structures are no more in working condition. Engineered structures can become much more sustainable by reducing life cycle cost rather than the current design practices and this could help in providing valuable improved economy and as well as environmental friendly performances of structures.

Performance based design methodology is another concept to reduce life cycle cost of a building project. In performance based design method, the structures are analysed so as to assess the level of acceptable damages and accordingly the necessary degrees of functionality or occupancy of the building has been classified at the time of a major earthquake. Ultimately, this design strategy can economise the building cost in future by identifying certain amount of expected damages beforehand which the building may cause in future earthquake and thereby providing adequate structural components regardless of the provisions in the design building code.

2.4 Minimum energy consumption

Energy is required for any developmental project. Sustainable design and planning requires energy-saving technologies to reduce the environmental impact of the project. Energy consumption can be reduced only if we adopt efficient use of energy system like auto regulated lighting system based on intensity of sunlight, water-saving and other local ventilation systems, etc. Even we can introduce recycle energy system like secondary energy use, heat storage system and waste heat recovery systems as a substitute of energy supply for the running of the project. Appropriate use of durable construction materials will avoid unnecessary energy consumption due to damage and disintegration of wrongly selected degradable materials. Proper future planning of the project should be kept in mind in order to avoid fresh construction of structural parts which will require consumption of large amount of energy.

2.5 Promoting sustainable design practices

Structural engineers are struggling significant challenges to enhance the practice of sustainability concept in construction industries. Economy is the main primary challenge and new policies will have to be adopted to promote the economic incentives to those who started practicing sustainability concept in the construction industries. Currently in construction industry, engineers are rewarded on the basis of initial cost, rather than life cycle costs and this leads to higher life cycle costs of the structure with higher environmental impact. For example, the costs of infrastructural projects in government and private sectors would be dramatically reduced if they consider whole life cost of the projects in estimation of cost rather than confining to initial costs only. In order to make efficient structural whole life design, maintenance

and disposal costs should be taken into account along with initial costs. Presently in many construction industries, payment is given more when the consumption of materials is more. Such trend encourages greater material consumption whether it is required or not as per design requirements. Therefore, there is a need to develop a policy of rewarding incentives to those who use only minimum required quantity of material in construction industries.

[Back to table of contents](#)

3 CONCLUSIONS

As structural engineers, we have the responsibility to take this global threat due to ever increasing consumption of raw materials and thereby creating environmental pollution as challenge task. In order to mitigate this global issue structure engineer should offer the best possible solution to the society which we called sustainable design concept. Promoting and educating this design concept to practice engineers and other related workers is equally important to give services to the society. More concrete efforts from practitioners, researchers, and educators are sought to give more sustainable solutions to this global threat.

REFERENCES

- 1) Chaturvedi, S. and Ochsendorf, J. (2004). "Global Environmental Impacts due to Cement and Steel," *Structural Engineering International*, Zurich, IABSE, 14/3, August, pp. 198- 200.
- 2) Douglas Wood and Associates, Inc. (2007) "The structural engineer and sustainable design", 299 Alhambra circle, suite 510, Coral Gables, Florida 33134, t: (305) 461 – 3450 f: (305) 461 – 3650.
- 3) Gervásio, H. (2008). "Sustainability of Steel Structures". Institute for Sustainability and Innovation in Structural Engineering, University of Coimbra.
- 4) Li, X., and Guo, L. (2015). "Study on Civil Engineering Sustainable Development Strategy". *3rd International Conference on Management, Education, Information and Control* (pp. 405–412). Atlantis Press.
- 5) M. T. A. Chaudhary and A. Piracha, (2013). "Examining the role of structural engineers in green building ratings and sustainable development", *Australian Journal of Structural Engineering*, Vol. 14(3), pp. 217-228.
- 6) Ochsendorf, J.A. (2005). "Sustainable Engineering: The Future of Structural Design". *In Structures Congress 2005* (pp. 1–9). ASCE. doi:10.1061/40753(171)

Dynamic Analysis of RC Shear Wall in Performance Based Seismic Design of Buildings

Partha P. Debnathⁱ⁾ and S. Choudhuryⁱⁱ⁾

i) Master Scholar, Department of Civil Engineering, National Institute of Technology Silchar, India

ii) Professor, Department of Civil Engineering, National Institute of Technology Silchar, India

ABSTRACT

Frame-shear wall buildings are common for high rise multi-storied reinforced concrete (RC) buildings. When these walls are situated in advantageous positions in a building, they perform as an efficient lateral-force resisting system, and also fulfilling other functional requirements. In conventional analysis, RC shear walls are modeled as wide column, which does not always provide the realistic behavior of the wall. In this present work, buildings have been modeled and designed, and specific detailed analysis is carried out on modeling of shear walls as multi-layered shell element instead of wide-column concept. The building frame and length of shear wall design have been carried out by Unified Performance Based Design (UPBD) with takes both elastic and plastic rotation into consideration along with performance level. A few challenges in interpreting the performances of shear wall as per UPBD method were faced while using shell element. Non-linear analysis with shell element is carried out and attempts to interpret its performance in terms of stresses in different layers and hinge rotation have been carried out. This paper thus demonstrates a way of modeling shear wall as multi-layered shell element and attempts have been made to resolve issues faced in understanding wall behavior in performance based design of frame-wall buildings.

Keywords: performance based design, multi-layered shell element, performance level, plastic rotation, shear wall.

1. INTRODUCTION

Earthquake induced lateral forces on the building and the horizontal shear force resulting from it is often assigned to structural elements which referred to as shear walls. In the recent past, it has been well established that a combination of frame and shear wall building system has enhanced structural performance during the event of an earthquake like catastrophe. Therefore, proper modelling of shear-wall buildings in computational analysis is necessary so as to better understand its behavior. In conventional analysis, shear wall, is modelled as wide column, which does not always provide the realistic behaviour of a shear wall. Also, in high rise buildings, where thickness of shear wall is more, multi layered steel is common along with confined concrete.

Though there exist a lot of nonlinear analysis procedures for frame structural elements like columns and beams, non-linear analysis for shear walls needs further study to better incorporate in structural design of buildings. There are several methods to evaluate the behaviour of shear wall, like that of mid-pier element or wide column element and shell element. The non-linear behavior of shear wall is generally based on plastic hinge concept and a bilinear rotation relationship. In this present study, multi layered shell element is modelled. In this element concrete and reinforcement inside the structural element are modelled respectively with different fibers so that the cyclic behaviour of the material can be properly simulated. In the present study, non-linear analysis has been carried out for dual system buildings of height of 10 stories. The design has been done as per performance based seismic design. Design methodology of Unified Performance Based Design (UPBD) has been the tool for design. Beams and lengths and shear wall length have been decided as per UPBD method of design.

Understanding the performances in terms of stresses and rotation has been studied.

2. DESIGN PHILOSOPHY

A displacement-based design (DDBD) procedure for perimeter-enclosed frame buildings was given by Pettinga and Priestley (2005). At a later stage, a DDBD procedure initially proposed by Sullivan *et. al* (2006) for structures that comprise both frames and shear walls is presented in this method. The Multiple Degree of Freedom (MDOF) structure has to be converted into a equivalent Single Degree of Freedom (ESDOF) structure by assigning strength proportions and subsequently using moment profile in the walls to set a design displaced shape. With knowledge of the displacement profile, various equivalent SDOF properties of the structure are obtained.

Choudhury (2013) has further improved Direct Displacement Based Design of frame-wall buildings proposed by Sullivan *et. al* (2006) by combining the inter-storey drift and performance level in the theoretical treatment. The performance level of the building is related directly with the beam size. The sizes of beams are obtained as per Choudhury *et. al* (2013) and Mayengbam *et. al.*(2014).

The performance parameters of common interest are: (1) inter-storey drift and, (2) member performance level. Thus the sizes of beams and length of shear wall are to be designed as per DDBD where only the yield rotation is considered.

$$\theta_{yF} = \frac{0.5 \varepsilon_y l_b}{h_b} \quad (1)$$

Where, θ_{yF} is the frame yield rotation, ε_y is the yield strain of material, l_b is the length of beam and h_b is the beam depth.

Whereas the design angular drift of the beam, θ_d is the sum of yield rotation and plastic rotation (θ_{pb}) which may be expressed as in equation (2)

$$\theta_d = \theta_{yF} + \theta_{pb} \quad (2)$$

And hence the depth of beam may be given as:

$$h_b = \frac{0.5 \varepsilon_y l_b}{\theta_d - \theta_{pb}} \quad (3)$$

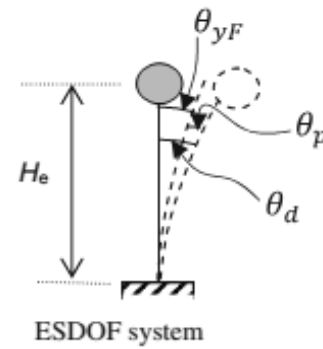


Fig. 1: Equivalent SDOF

Similarly, also for shear wall, the length (L_w) is obtained as:

$$L_w = \frac{\varepsilon_y h_{inf}}{\theta_d - \theta_{pw}} \quad (4)$$

where, h_{inf} is the height of inflection and θ_{pw} is the wall plastic rotation from FEMA 356.

After the target drift and design displacement is decided, the equivalent single degree freedom properties are determined as per Sullivan *et al.* (2006). As the design displacement and the equivalent viscous damping is produced, the time period of structure can be determined from the displacement spectra. The displacement spectra corresponding to design acceleration spectra are generated for various damping.

The Equivalent SDOF properties can be determined from:

$$\Delta_d = \frac{\sum_{i=1}^n m_i \Delta_i^2}{\sum_{i=1}^n m_i \Delta_i} \quad (5)$$

$$m_e = \frac{\sum_{i=1}^n m_i \Delta_i}{\Delta_d} \quad (6)$$

$$h_e = \frac{\sum_{i=1}^n (m_i \Delta_i h_i)}{\sum_{i=1}^n (m_i \Delta_i)} \quad (7)$$

where, Δ_d , m_e , h_e is design displacement, effective mass and effective height respectively. The equivalent viscous damping is obtained from

$$\xi_{SDoF} = \left(\frac{M_{wall} \xi_{wall} + M_{OT,frame} \xi_{frame}}{M_{wall} + M_{OT,frame}} \right) \quad (8)$$

With the effective period established, the effective stiffness K_e is determined in accordance with:

$$K_e = \frac{4\pi^2 m e}{T e^2} \quad (9)$$

This effective stiffness is then multiplied by the design displacement, Δd , to obtain the base shear, V_b as:

$$V_b = K_e \Delta d \quad (10)$$

The base shear force is distributed up the height of the structure as:

$$F_i = \frac{m_i \Delta_i}{\sum_{i=1}^n m_i \Delta_i} V_b \quad (11)$$

The design is done with expected (mean) strengths of materials. As per FEMA-356 provisions the expected strength of concrete is 1.5 times of the 28-days characteristic strength and, that for steel is 1.25 times the yield strength of rebar. The load combinations used for design are:

$$DL + LL \quad (12)$$

$$DL + LL \pm F(x) \quad (13)$$

$$DL + LL \pm F(y) \quad (14)$$

Where, DL, LL, $F(x)$, $F(y)$ correspond to dead load, live load, seismic load in x and y directions, respectively.

3. MODELLING

A typical plan of the 10-storey building model adopted is shown in Fig. 2. The buildings materials considered were M30 concrete and Fe415 grade steel with expected strength as per FEMA 356. The beam sections were designed as per UPBD method and column sections by trials. The cross sections of the columns and floor to floor height were assumed to be constant over the entire height. Columns were maintained a steel of 3% to 4% of total cross sectional area along with capacity design. The capacity design of strong-column and weak-beam was satisfied as per EC-8. Buildings were designed for Life Safety (LS) performance level and Collapse Prevention (CP). Three dimensional analytical model of the structure are shown in Fig. 3.

The inflection height of the frame–shear wall building is calculated by finding the moments carried by shear wall. The vertical distribution of wall moment is found out by subtracting the linear distribution of frame moments from the total moments. At the wall moment, there exists a contra-flexure point and the height up to

that point from the base is considered as the inflection height as shown in fig. 4.

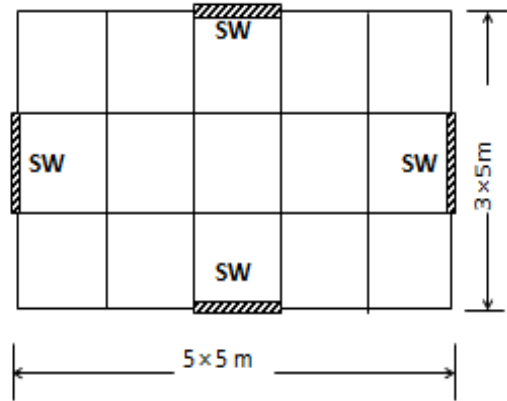


Fig. 2: Plan of the building model (SW is shear wall)

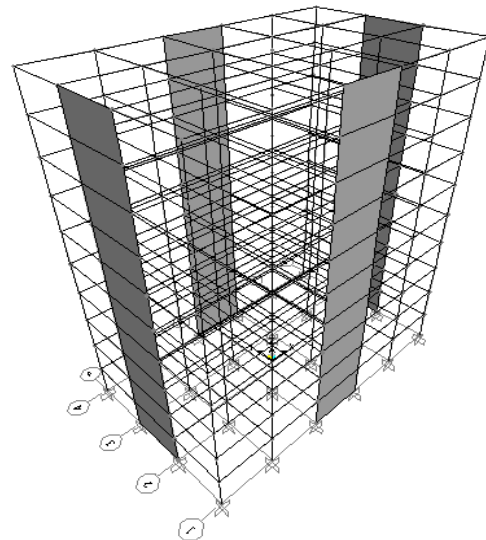


Fig. 3: 3D analytical model of 10 story building.

Here in this study, multi layered shell element is considered to model shear wall and thus understand the seismic response of these elements. In the past, Kim *et. al* (2010) had proposed a general nonlinear finite element procedure for analysis of shell structures. But analysis with respect to displacement based design needs further investigation. Although the shell element formulations include the drilling degree of freedom, analytical results show inconsistency and sensitivity of the drilling moment to mesh sizes and loading conditions. This shortcoming has significant effects on the bending moment of the in-plane beams connected to the shear wall. To resolve this problem, in engineering practice, the beam connecting to shear wall are generally modelled inside the shear wall shell elements (Fahjan *et. al*, 2010).

When these shell elements are provided in the building, intermediate link beams or rigid beams are to be provided so that proper connection and behaviour of the wall can be well established with adjoining beams and columns. The rigid elements provided are generally of highly elastic materials (≈ 10 times of modulus of elasticity of concrete). Fig. 5 shows a finite element modelling of a shell element section.

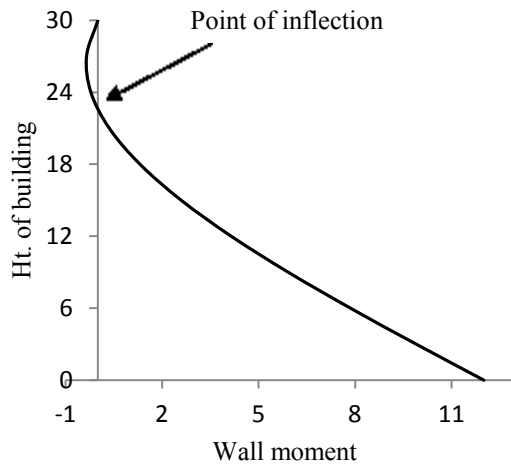


Fig.4: Height of inflection in a multi-story building.

The purpose of these rigid beams, whose dimensions are same as adjoining beams framing into wall, is to minimize the mesh sensitivity effect caused by the inadequacy of drilling degree of freedom formulations (Kubin *et al.*, 2008). By this method stable estimation of M3 moment and other internal forces for both shear-wall and connecting beams are achieved. The multi-layer shell element is based on the principles of composite material mechanics and it can simulate the coupled in-plane/out-plane bending and the coupled in-plane bending-shear nonlinear behaviours of RC shear walls (Miao *et al.*, 2006). The shell element is made up of many layers with different thickness.

Different material properties were assigned to various layers as shown in Fig. 6. This means that the reinforcement bars are smeared into one layer or more. During the finite element calculation, the axial strain and curvature of the middle layer can be obtained in one element. Then according to the assumption that plane remains plane, the strains and the curvatures of the other layers can be calculated. And then the corresponding stress will be calculated through the constitutive relations of the material assigned to the layer.

The amount of steel provided in the multi-layered shell element in two layers is according to IS 13920:1993 designed against the highest moment for the load combinations given in equations (12), (13) and (14).

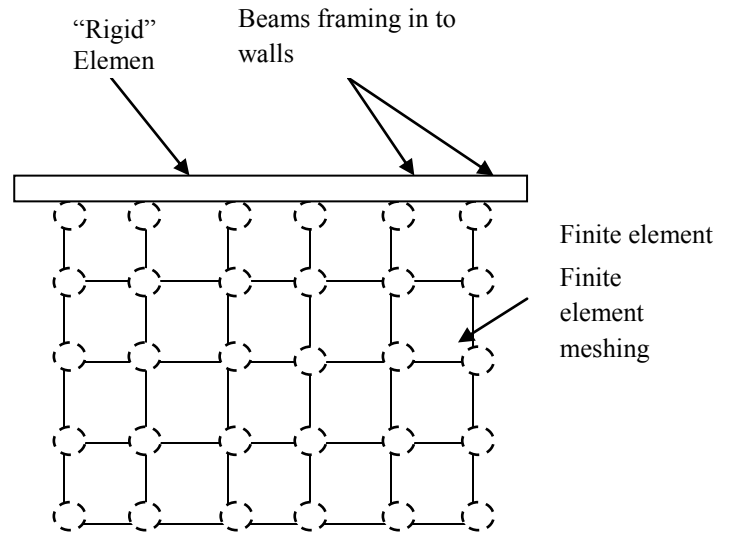


Fig. 5: Shell element provided with link beams.

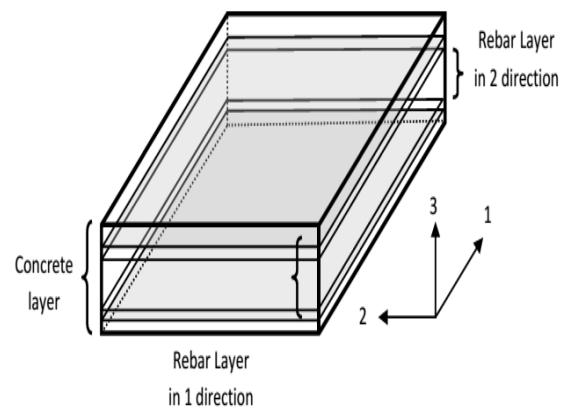


Fig. 6: Multi layered shell element in SAP2000

4. ANALYSIS AND INTERPRETATION

The building models designed with multi-layered shell element have been analyzed with Non-linear Time History Analysis (NLTHA) with ground a motion which was made compatible to EC-8 at Maximum Considered Earthquake (MCE) level. The compatible acceleration - time history data of N. Palm Spring 1986 earthquake made by using Kumar (2004) used for the analysis.

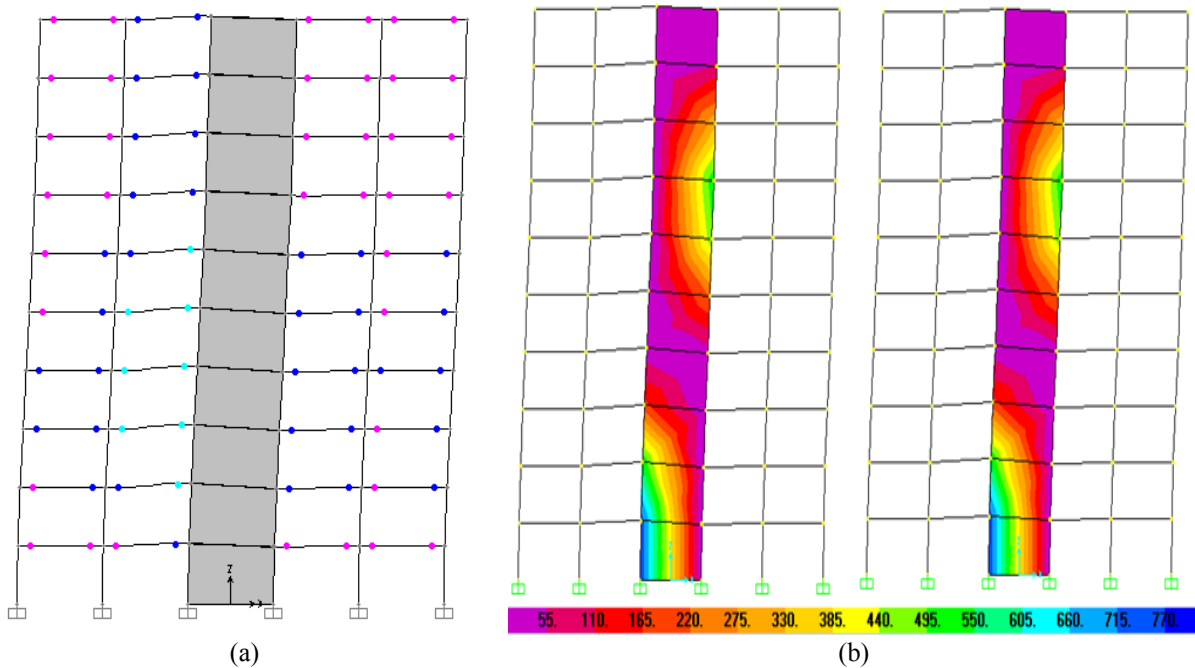


Fig. 7: (a) shows formation of plastic hinge in beams, columns and (b) shows stress diagram in steel layer.

At the end of the time history analysis performance levels were studied for the member elements in the building for each discrete time periods. The behaviour and status of the frame elements like beams and columns were studied by formation of plastic hinges in these elements.

From NLTHA various results corresponding to beam, column and shear wall performance has been attained. For performance based design, the recommendation of FEMA 356 defines the performance criteria for the flexural RC members in terms of plastic rotations. It has been observed that member performances of beam and column have attained the required performance level of Life Safety (LS), and Collapse Prevention (CP) which was identified by plastic hinge rotations as displayed in Fig. 7 (a). On the contrary, using multi layered shell element for shear wall modelling, the nonlinear behaviour can be examined by checking out the stresses in concrete and reinforcement layers. Also since, shell element is not a lumped plasticity element, it does not show any hinge formation like other elements. Separate stress diagrams are available for all the four layers in the shell element. The behaviour of the shear wall may be understood from the stress diagrams. A stress diagram in one of steel layer is presented in Fig. 7 (b).

From Figure 7 (b), it can be observed that, as the grade of steel provided was of expected strength, i.e. $415 \times 1.25 \text{ N/mm}^2$ which gives a value of nearly 518 N/mm^2 has exceeded its expected stress in the bottom storey of shear wall. So, if the yield stress value or the expected stress value is exceeded, then it is to be understood that the wall has attained plastic stage or there is a hinge formation. Also, SAP2000 software has another application of determining the total rotation in shear wall as shown in Fig. 8. This can be computed by plotting between section cut forces and generalized displacements which in turn provides the moment versus rotation graph in a hysteresis loop. From this graph the maximum rotation can be determined; however FEMA 356 plastic rotations performance levels could not be applied to understand the elastic and plastic rotations at the end of time history.

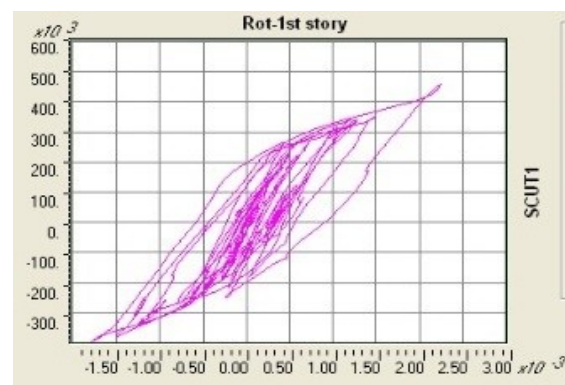


Fig. 8: Moment-rotation diagram for shell element.

5. CONCLUSIONS

This paper discusses about the interpretation of RC shear wall modelled as a double layered shell element. Shell element can be used to model confined as well as unconfined concrete in the same wall unlike modelling shear wall as a column element. The main intention of the study was to interpret nonlinear behaviour of shear walls for performance based design of buildings, which has been done by multi-layered stress diagrams and moment-rotation. The findings of the work clearly indicates that, the shell element provides a realistic behaviour of frame-shear wall system in a building, but indirect approaches to understand hinge formation in shear walls had to be identified. It is also identified that in column elements, hinge represents lumped plasticity while in non-linear layered shell it appears as localized plasticity and does not provide with a plastic hinge formation.

Thus to understand the non linearity, the two major tools available are the stress diagrams and moment-rotation diagrams, but even then the elastic rotation and plastic rotation could not be identified separately which was a specific criterion in Unified Performance Based Design (UPBD) of buildings. Thus it can be stated that, to design shear walls with shell elements, explicit elastic and plastic rotations needs to be identified to know the actual structural performance level at performance point of a push over analysis and at the end of an earthquake simulation. As such further improvement is required in modelling with multi-layered shell element for performance based seismic design of buildings.

REFERENCES

- 1) Choudhury, S. and Singh, S. (2013), "A Unified Approach to Performance-Based Design of RC Frame Buildings", *Journal of the Institution of Engineers (I)-Series-A*, Springer **94**(2):73–82.
- 2) CEN, European Prestandard ENV 1998—1-4. (May 2002).Eurocode 8- Design of Structures for Earthquake Resistance, Part 1: General Rules, Seismic Actions and Rules for Buildings. *Comité Européen de Normalisation, Brussels*. Draft No. 5, Doc CEN/TC250/SC8/N317.
- 3) Fahjan, Y. M., Kubin, J., Tan, M. T. (2010), "Non-linear Analysis Methods for Reinforced Concrete Buildings with Shear Walls" *14 European Conference on Earthquake Engineering*.
- 4) FEMA 356 (2000) "Pre-standard and Commentary on the Seismic Rehabilitation of Buildings", US Federal Emergency Management Agency.
- 5) Kim, T.H., Park, J.G., Choi, J.H. and Shin, H.M. (2010), "Nonlinear dynamic analysis of reinforced concrete shell structures", *Structural Engineering and Mechanics*, **34**(6), pp.685-702
- 6) Kubin, J., Fahjan, Y. M. and Tan, M. T., (2008), "Comparison of Practical Approaches for Modeling Shear Walls in Structural Analyses of Buildings", *The 14th World Conference on Earthquake Engineering*, Beijing.
- 7) Mayengbam, S. and Choudhury, S. (2014), "Determination of column size for displacement-based design of reinforced concrete frame buildings", *Earthquake Engineering & Structural Dynamics* **43**(8):1149–1172.
- 8) Pettinga, J. D., Priestley, M. J. N. (2005). Dynamic behaviour of reinforced concrete frames designed with direct displacement-based design. *Journal of Earthquake Engineering*. **9**(2):309–330.
- 9) Priestley, M. J. N. (2003)., *Myths and Fallacies in Earthquake Engineering, Revisited*. European School for Advanced Studies in Reduction of Seismic Risk, 9th Mallet Milne Lecture.\
- 10) Sullivan, T. J., Priestley, M. J. N., Calvi, G. M. (2006). Direct displacement-based design of frame-wall structures. *Journal of Earthquake Engineering* **10**(1):91–124.

[Back to table of contents](#)

Behaviour of multi-tiered wall: A numerical model study

Dr. Arup bhattacharjeeⁱ⁾ and Nayan Jyoti sarmaⁱⁱ⁾

i) Assistant Professor, Department of Civil Engineering, Jorhat Engineering College, Garmur, Jorhat-785007, India.

ii) P.G. Student, Department of Civil Engineering, Jorhat Engineering College, Garmur, Jorhat-785007, India.

ABSTRACT

Present study includes numerical modeling of two tiered and three tiered retaining walls with different offset distances using finite element software ANSYS®. The concrete wall facing is modeled with linear elastic properties and backfill soil is modeled using Drucker-Prager plasticity model. A quadrilateral element PLANE82 is used to simulate soil and concrete facing. Uniaxial geogrid (Tensar SR55) with non linear properties is used as the reinforcement. The two dimensional cable element LINK1 is used to simulate the geogrid. The connections between the concrete blocks are assumed to be bonded and the interface between soil and the concrete materials are assumed to be bonded in initial contact. The numerical model of reinforced soil wall is validated with physical model test conducted by Ling et al. (2000) at PWRI Japan. Using validated material properties two tiered and three tiered retaining walls are developed. The horizontal deformation of the wall, lateral stress on the wall face, vertical stress at the base of backfill and strain in geogrid layers of are being studied. Study shows numerical modeling in ANSYS® is capable of simulating the construction behavior of retaining wall. Results shows multi-tiered walls are more effective than single tiered wall. The study on multi-tiered wall provide a better understanding on the nature of tiered wall and the results obtained give a more effective design approach for tiered wall.

Keywords: retaining wall, single-tiered retaining wall, multi-tiered retaining wall, numerical modeling, geogrid, ANSYS,

1. INTRODUCTION

A multi-tiered wall system is a series of two or more stacked walls; each higher wall set back from the underlying wall. The distance between top wall facing and bottom wall facing in tiered wall is termed as offset distance. Compare to single tiered retaining wall multi-tiered retaining wall has several advantages such as sound performance, aesthetics, low cost and construction requirement etc. Guidelines regarding design of multi-tiered walls are available [AASHTO (1998); FHWA (2001); FHWA (2005); NCMA (1997)]. But these guidelines only provide design criterion for two tiered wall. Effect of other factors such as offset distance, number of tier walls more than two are not mentioned in the design process. Few researchers reported numerical study on multi-tiered reinforced soil walls [Huang, Bathurst and Hatami (2009); Leshchinsky, and Han (2004); Ling, Cardany, Sun, and Hashimoto (2000); Yoo* and Jung (2003)]. But these studies are not sufficient for the satisfactory design of multi-tiered walls in different conditions. In this research paper finite element software ANSYS® is used to simulate the response of two-tiered

and three tiered GRS walls with different offset lengths.

2. PHYSICAL MODEL DESCRIPTION OF REINFORCED SOIL WALL

Figure 1 shows geometry of concrete blocked reinforced retaining wall constructed at the Public Works Research Institute (PWRI), Ministry of Construction, in Japan [Ling, Cardany, Sun, and Hashimoto (2000)]. The wall is 6m high and 5m wide constructed in a concrete test pit with a concrete floor.

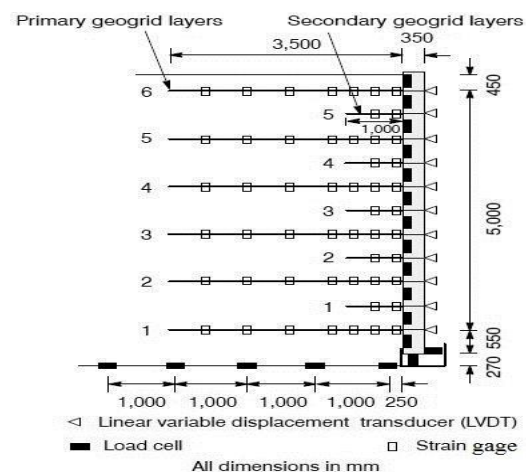


Fig. 1 PWRI wall geometry [Ling, Cardany, Sun, and Hashimoto (2000)]

For reinforcement uniaxial geogrid (Tensar SR55), manufactured from extruded high-density polyethylene (HDPE) is used. The wall consists of total six primary and five secondary geogrid layers of lengths 3.5m and 1.0m respectively. The facing wall is made of 12 blocks. Except top and bottom blocks each block is 500mm high and 350mm wide. A silty sand (mean particle diameter, $D_{50} = 0.42\text{mm}$; unit weight, $\gamma = 16.0 \text{ kN/m}^3$) are used as the backfill [Ling, Cardany, Sun, and Hashimoto (2000)].

2.1 Finite element model in ANSYS® of PWRI wall

Figure 2 shows the finite element model of 6 m high concrete block geosynthetic retaining wall developed using the program ANSYS®. The dimensions of foundation, concrete blocks, backfill and reinforcements are same as that of physical model of the wall. The foundation and concrete blocks are simulated using the Quadrilateral element PLANE82. PLANE82 is 8 noded element having two translation degrees of freedom. The concrete blocks for foundation and facing are modelled as linear elastic material. Interface between concrete-concrete are assumed to be bonded and are simulated using target element TARGE169 and contact element CONTA172. The internal friction angle between concrete- concrete is taken as 19.6° . The backfill soil is considered to be non linear and simulated using quadrilateral element PLANE82. The material model used to simulate the backfill soil is the Drucker-Prager plasticity model. Drucker-Prager plasticity model includes non linear material properties such cohesion value (6 kPa), angle of internal friction (45°) and dilatancy angle (5°). The interface between backfill soil and concrete facing are assumed to be bonded in initial contact and are simulated using target element TARGET169 and contact element CONTA172. The internal friction angle between backfill-concrete is taken as 16.5° . To simulate Geosynthetic reinforcement in reinforced soil walls two dimensional cable elements LINK1 with non-linear material properties are used. A cross sectional area of 0.001m^2 is used for the geogrids. Yield stress and tangent modulus of geogrids are $5.46 \times 10^8 \text{ kPa}$ and $2 \times 10^8 \text{ kPa}$ respectively. The material properties are tabulated in the Table 1.

Table 1. Material properties of numerical model

Materials	Backfill		Concrete	Geogrid
	Elasticity (Pa)	2×10^6	2×10^8	2×10^8
Poissons ratio	0.42	0.17	-	0.3
Density(Kg/m ³)	1631	2400	-	0.23
Cohesion (kPa)	6	-	-	-
Internal friction angle	45°	-	-	-
Dilatancy angle	5°	-	-	-
Yield stress (kPa)	-	-	-	5.46×10^8
Tangent modulus (kPa)	-	-	-	2×10^8

Table 2. Interface properties of the numerical model

Interface properties	Concrete-concrete	Soil-concret e
Friction angle	19.6°	16.5°

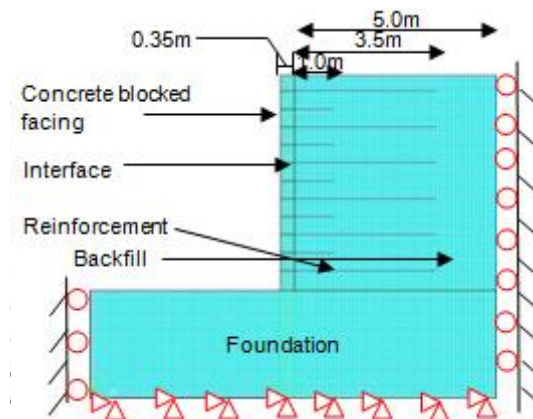


Fig. 2 Finite Element model of reinforced soil wall for 6 m high

2.2 Validation of numerical model with physical model

The results obtained after solving the numerical model of concrete blocked retaining wall is compared with that of measured value of PWRI wall. Figure 3 shows comparison between measured value and predicted values for lateral wall displacement of the wall. The maximum horizontal displacement value for the wall facing is 28.75 mm which is similar to the measured value (approximately 30 mm). Figure 4 shows the measured and predicted lateral stress distribution of the wall. Predicted lateral stress of concrete obtained after averaging all the stress values along the height of wall is same as that of measured value.

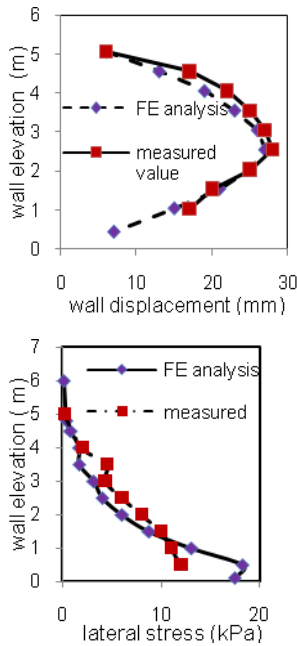


Fig. 3 (a) Numerical and measured horizontal displacement of the 6 m high wall, (b) Numerical and measured lateral stress distribution of 6 m high wall.

Thus above results shows that numerical model of retaining wall in ANSYS® produce the same characteristics as the physical model of wall.

3.0 DEVELOPMENT OF MULTI-TIERED WALL

Using the validated material properties of the 6.0m high single tiered wall six different multi-tiered wall models is designed. First a 6.0m high zero offset single tiered wall is modelled. Length of backfill is three times the height of wall i.e. 18m and geogrid lengths are 0.7 times the height of wall i.e. 4.2m. Modelling of the wall is same as PWRI wall.

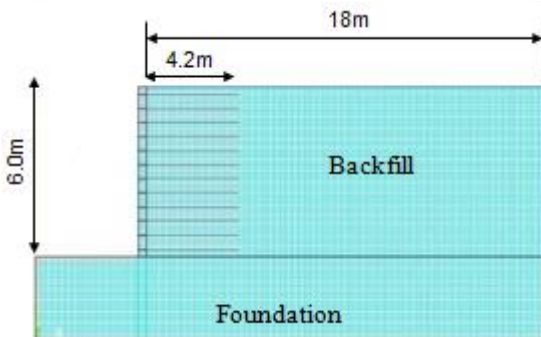


Fig. 4 Numerical model of zero offset wall

Single-tiered wall is modified to model three two-tiered walls with offset distances 0.2H, 0.4H and 0.5H (i.e. 1.2m, 2.4m and 3.0m), where H is

the overall height of wall. Heights of each tier wall in two tiered walls are 3.0m. Each tier wall has seven concrete blocks and six geogrid layers. Sizes of concrete blocks are 0.35m× 0.5m. Geogrid length is 0.7 times the overall height of wall.

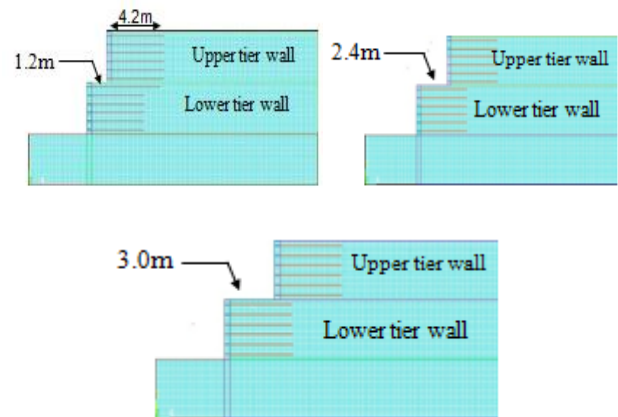


Fig. 5 Numerical model of two-tiered wall

Further, three-tiered walls with each wall height of 2.0 m having offset distances 0.2H and 0.4H are modelled, where H is the overall height of wall. Each tier wall has seven concrete blocks. Size of each concrete blocks are 0.35m×0.3m. Geogrid length is same as two-tiered wall

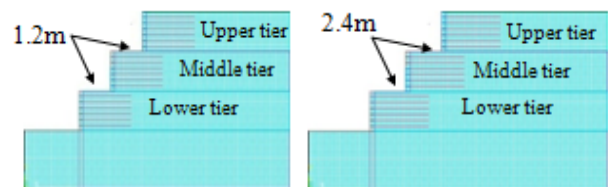


Fig. 6 Numerical model of three-tiered wall

3.1 Horizontal displacement of wall facing

For the six different tiered wall models change in horizontal wall facing displacement are studied. Figure 7 shows the comparison lateral wall displacement between zero offset wall and two tiered walls. For two tiered walls, wall displacement in upper tier is more than lower tier wall. At the top of wall displacement values is 1.4mm, 17.3mm, 12.2mm and 12.1mm respectively for wall with zero offset, 1.2 m offset, 2.0 m offset and 3.0 m offset respectively. While maximum displacements are found to be 36.3 mm, 30.6 mm, 25 mm and 24.7 mm for wall with zero offset, 1.2 m offset, 2.0 m offset and 3.0 m offset respectively. Thus by increasing the offset distances lateral wall facing displacement can be decreased.

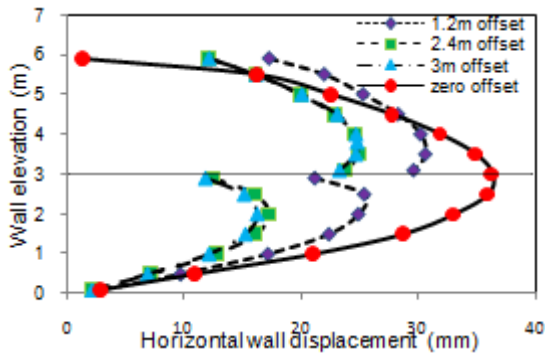


Fig. 7 Lateral wall displacement of two tiered walls

Figure 8 shows the comparison in lateral wall displacement of three tiered walls and zero offset wall. For three tiered wall all the three tier walls have different wall displacement distribution. Maximum wall displacement is at the middle tier wall. Displacement distribution in lower tier wall is comparatively less. Maximum displacements for three tiered wall with 1.2 m offset, 2.0 m offset are 26.3mm and 19.4mm respectively. At the top wall displacement 8.51mm and 3.9mm for 1.2m and 2.0m tier offset wall. Results shows for the same offset distance wall displacement value in three-tiered walls are less than two-tiered walls. Thus increasing the number of tier walls lateral displacement of wall also decreases.

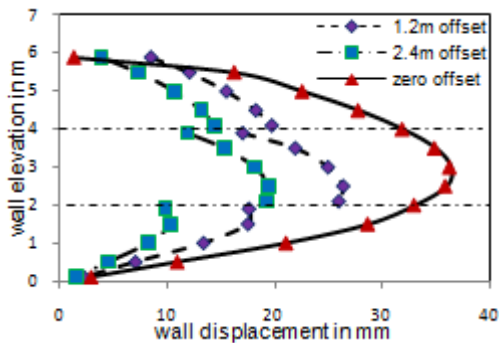


Fig. 8 Lateral wall displacement of three tiered walls

3.2 Lateral stress distribution near wall facing

Figure 9(a) shows the lateral earth pressure distribution of two-tiered walls for different offset distances. The maximum lateral stress for all the tiered walls occurs at bottom of wall and minimum occurs at the top of the wall. The maximum lateral stress values are 20 kPa, 16 kPa, and 13 kPa, 12 kPa for wall with zero offset, 1.2 m offset, and 2.4m offset and 3 m offset respectively. For tiered wall the maximum value occurs 0.5m above the bottom of wall. This is may be due to the rigid bonding between the bottom concrete blocks and foundation. Fig 7(b) shows the lateral stress distribution of three-tiered wall. In three tier wall three different stress distributions occurs. The maximum lateral stress for 1.2m and 2.4m offsets are 12.28kPa and 9.74kPa respectively. The position of the maximum stress is same as in two tiered wall. For upper tier wall 0.5m above the offset point maximum stress occurs. The values are 3.6kPa and 4.0kPa for 1.2m and 2.4m offset walls respectively. The maximum stress in middle tier wall is greater than upper tier wall. The values are 6.42kPa and 6.67kPa respectively for 1.2m and 2.4m tier offset wall. The stress distribution in each tier wall increases from top to bottom.

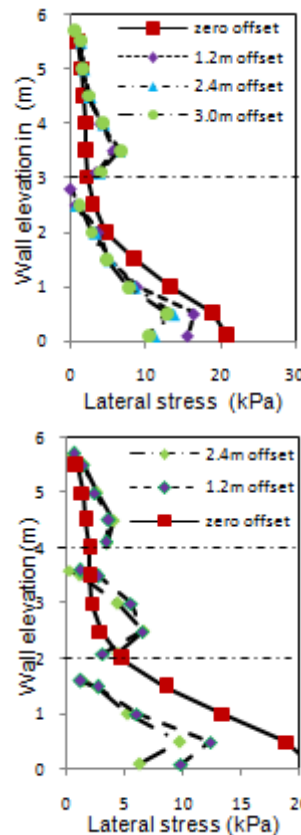


Fig. 9 (a) Lateral stress distribution of two-tiered wall, (b) lateral stress distribution of three-tiered wall

3.3 Vertical stress distribution at the base of backfill

Fig. 10 show vertical stress distribution at the base of the backfill for different tier offset walls. Near the wall facing minimum vertical stress occurs. For zero offset wall minimum stress value is 19.9kPa. For two-tiered wall with 1.2m, 2.4m and 3.0m offsets minimum vertical stress values are 16.43kPa, 12.33kPa and 12.22kPa respectively. The same stress values for three tiered walls with 1.2m and 2.4m offsets are 10.35kPa and 6.86kPa. With increase in offset distance the vertical pressure exerted by the overlaying upper tiers on the lower tier decreases as are result pressure exerted at the base near the wall facing decreases. Length of geogrids present also affected the overall stress values. As shown in figure for all the curves at a particular point vertical stress values are constant. The point at which the stress distribution of the tiered walls becomes constant depends on the length of geogrid present.

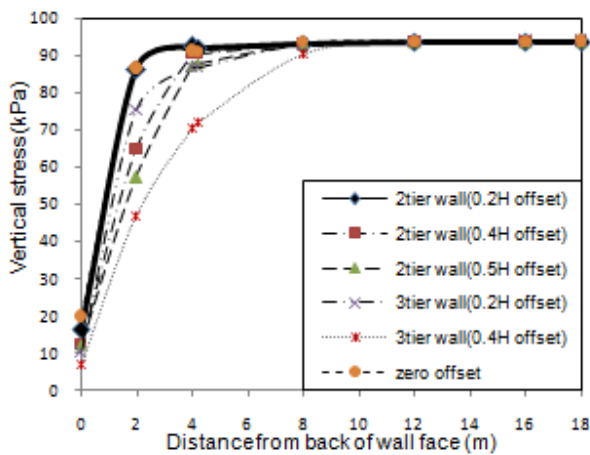


Fig. 10 Vertical stress distribution of two-tiered and three-tiered wall at the base of backfill

3.4 Strain in geogrid layers

For all the geogrid layers starting from bottom layer1 to top layer 11 axial strain distribution along the length of geogrid is observed. For zero offset wall axial strain distribution increases from bottom layer and become maximum at middle layer i.e layer 5. Beyond layer 5 strain decreases and in layer 11 minimum strain value observed. Maximum strain values are 0.19%, 0.39%, 0.43%, 0.38%, 0.25% and 0.056% for layer 1, layer 3, layer 5, layer 7, layer 9 and layer 11 respectively.

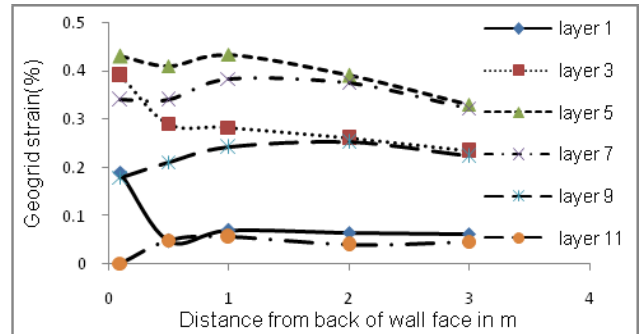


Fig. 11 Axial strain in geogrid layers of zero offset wall

Variation in strain distributions in geogrid layers of two tiered walls due to change in offset distance are also observed. Variation in lower tier wall geogrid layers are comparatively more than upper tier wall geogrid layers. Layer 1, 3, 6 are lower tier geogrid layers and layer 7,11 are upper tier geogrid layers at a height 0.25m, 1.25m, 2.75m, 3.25m and 5.25m from the base of backfill of wall. Figure 10 shows the axial strain distribution in geogrid layers of two tiered wall with 1.2m tier offset. At a distance 1.4m from the back of lower tier wall facing peak strain geogrid layers are observed. This peak strain values are 0.14%, 0.31%, 0.52%, 0.32% and 0.12% respectively for layer 1, layer 3, layer 6, layer 7 and layer 11. The sudden increase in strain in geogrid layers of lower tier wall is due to the presence of heavy concrete blocked wall on upper tier wall. Similarly peak strain in two tiered walls with 2.4m and 3.0m offset distances are observed at a distance 2.0m and 3.3m from back of lower tier wall facing.

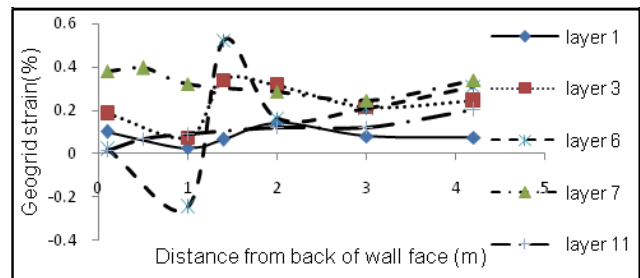


Fig. 12 Axial strain in geogrid layers of two-tiered wall with 1.2m offset distance

For three tiered wall variation in axial strain distribution mostly occur in lower tier and middle tier wall geogrid layer. Figure 11 shows the strain in geogrid layers of three tiered wall with 1.2m tier offset. Figure shows the strain distribution of layer1, 3, 6 of lower tier wall and layer 7, 9, 12 of middle tier wall. layer 1, 3, 6, 7, 9 and 12 are at a height 0.25m, 0.85m, 1.75m, 2.25m, 2.85m and 3.75m from the base of backfill of tiered wall. For lower tier wall maximum strain values are 0.18%, 0.11% and 0.27% for geogrid layer 1, 3 and 6 respectively. For middle tier wall maximum strain values are 0.29%, 0.32% and 0.22% for geogrid layer 7, 9 and 12 respectively.

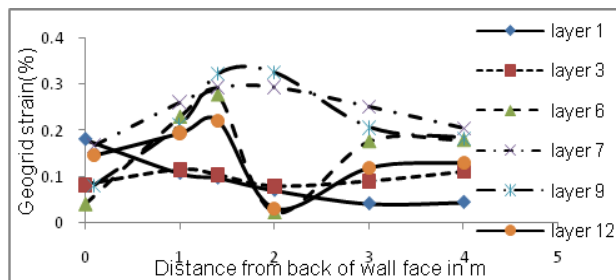


Fig. 13 Axial strain in geogrid layers of three-tiered wall with 1.2m offset distance

4.0 CONCLUSIONS

The main aim of this study on multi-tiered wall is to observe the variation in multi-tiered wall response for different offset distances using finite element software ANSYS®. Six different multi-tiered wall models with different offset distances are developed. For different tier offset variation in horizontal wall displacement, lateral stress on wall face, vertical stress at the base of backfill and strain in geogrid layers were studied. Results shows lateral displacement of wall decreases with increase in offset distance. For zero offset wall lateral displacement of wall facing is maximum. With increase in offset distance of two-tiered and three-tiered wall displacement decreases. Again compared to two tiered wall lateral wall displacement in three tiered wall is less. Thus increasing the number of tier wall further decrease in lateral displacement is observed. For multi-tiered wall each tier wall has own lateral stress distribution. Maximum lateral stress decreases with increase in number of tier wall and offset distance. But the variation in overall stress distribution along the height of wall is very less. Again results shows the vertical stress at the reinforced soil is less than the unreinforced soil. For three tiered wall length of reinforced soil is more than two tiered wall. As a result vertical stress decreases more in three-tiered wall. In the unreinforced zone stress distribution is almost same. Results also show that variations in axial strain distribution of geogrid layers are more prominent in lower tier wall. Due to surcharge effect of upper tier

wall peak strain in geogrid layers of lower tier walls are observed. Position of the peak strain depends on the offset distance. Thus reducing the surcharge effect of upper tier wall strain in lower tier wall geogrids can be reduced.

REFERENCES

- 1) AASHTO (1998): *Standard specifications for highway bridges*, American Association of State Highway and Transportation Officials, Washington, DC.
- 2) Bhattacharjee, A., Amin, M. U. (2015): Numerical Modeling of multi-tiered reinforced soil retaining walls, *50th Indian Geotechnical Conference*, 17th-19th December, Pune, Maharashtra.
- 3) FHWA (2001): Mechanically Stabilized Earth walls and Reinforced soil slopes design & construction guidelines, U.S. Department of Transportation Federal Highway Administration, *Publication No. FHWA-NHI-00-043*
- 4) FHWA (2005): Design Guidelines for Multi-Tiered MSE Walls, Center for Transportation Research The University of Texas at Austin; *Report No. 0-4485-2*
- 5) Huang, B., Bathurst, R. J. and Hatami, K. (2009): Numerical study of reinforced soil segmental walls using three different constitutive soil models, *Geotechnical and Geoenvironmental, ASCE*, 135, pp1486-1498.
- 6) Leshchinsky, D. and Han, J. (2004): Geosynthetic reinforced Multitiered walls, *Geotechnical and Geoenvironmental engineering, ASCE*, 130(12), pp 1225-1235
- 7) Ling, H.I., Cardany, C. P., Sun, L-X and Hashimoto, H. (2000): Finite element study of a Geosynthetic-reinforced soil retaining wall with concrete-block facing, *Geosynthetics International*, Vol. 7, No. 2.
- 8) NCMA (1997): *Design Manual for Segmental Retaining Walls*, National Concrete Masonry Association, Collin, J., Editor, Second Edition, Herndon, Virginia, USA.
- 9) Yoo*, C. and Jung, H., S. (2003): Measured behavior of a Geosynthetic-reinforced segmental retaining wall in a tiered configuration, *Geotextiles and Geomembranes*, 22 (2004), pp 359–376.

[Back to table of contents](#)

Synthesis and Microstructural Characterization of Geopolymer from Rice Husk Ash and Sodium Aluminate

N Shyamananda Singhⁱ⁾, Dr. Suresh Thokchomⁱⁱ⁾ and Dr. Rama Debbarmaⁱⁱⁱ⁾

i) PhD Scholar, Department of Civil Engineering, National Institute of Technology, Agartala, Tripura, India.

ii) Associate Professor, Department of Civil Engineering, Manipur Institute of Technology, Imphal, Manipur, India.

iii) Associate Professor, Department of Civil Engineering, National Institute of Technology, Agartala, Tripura, India.

ABSTRACT

In the present study, the synthesis process, composition, microstructure as well as mechanical properties of geopolymers synthesized from Rice Husk Ash (RHA) was investigated. Geopolymer from RHA with Sodium Aluminate (SA) as activator, were synthesized by varying Silicon to Aluminum (Si/Al) ratio from 1.5 up to 3.5 and maintaining Sodium to Aluminum (Na/Al) ratio of 1. The composition and microstructure were characterized by X-ray diffraction (XRD), Scanning Electron Microscopy (SEM) with Energy-dispersive X-ray (EDX). It is observed that microstructure of specimen improves with increasing Si/Al ratios till Si/Al=2. The specimen prepared with Si/Al ratio of 2 shows maximum compressive strength among all the specimens.

Keywords: Geopolymer, Rice husk Ash, X-ray diffraction, Scanning Electron Microscopy.

1. INTRODUCTION

As the process of growth and development progress, the demand for construction materials is also ever increasing and the consumption rate of Portland cement is second only to water (Malhotra 1999). The global warming which is caused by the emission of greenhouse gases, such as carbon dioxide (CO₂) contributes about 65% of global warming (Davidovits 1988). It is a known fact that one ton of Portland cement emits approximately one ton of CO₂ into the atmosphere (Davidovits 1994). It has been estimated that around 5% of the total anthropogenic CO₂ emission is due to the production of Portland cement clinker and the figure is expected to rise up to 6% by the year 2015 (Yusuf *et al* 2014). Geopolymer, as an alternative binder to the Portland cement, shows considerable promise for application in concrete industry. Any pozzolanic compound or source of silica and alumina such as fly ash (FA), ground granulated blast furnace slags (GGBFS) with strong alkali solutions such as potassium hydroxide (KOH), sodium hydroxide (NaOH) and soluble silicates (in most cases) such as sodium silicate (Na₂SiO₃) where the dissolved aluminum oxide (Al₂O₃) and silicon dioxide (SiO₂) undergoes geopolymerisation to form a three-dimensional amorphous aluminosilicate network with strength similar or higher than that of Ordinary Portland Cement (OPC) concrete (Ken *et al* 2015).

The fact that there is abundance of industrial by-products generated in various industries that was found to be suitable to use as geopolymer source materials thrive the idea of potential replacement of traditional OPC binders (Van *et al* 2002). Fly ash (FA), an industrial by-products of coal burning power plant industry, makes up of 75–80% of

global annual ash production yielded geopolymer concrete with superior mechanical and durability properties as compared to OPC concrete (Thokchom *et al* 2011, 2012a, 2012b). GGBFS, by-products of iron pig manufacture from iron ore, has also found significant use in the production of high strength geopolymer concrete (Duxson *et al* 2006, Brew *et al* 2007). The use of palm oil fuel ash (POFA), waste materials derived from the burning of empty fruit branches, palm oil shells and palm oil clinker from the palm oil industry to generate electricity as geopolymer binder, has gathered pace in recent years. POFA is widely used as geopolymer binder especially in oil palm-rich country such as Malaysia and Thailand due to its increasing amount which rendered the disposal method in the mean of landfilling not feasible (Yusuf *et al* 2007, Van *et al* 2003b). Other industrial by products, for examples rice husk ash (RHA) from the rice milling industry, red mud (RM) from the alumina refining industry, copper and hematite mine tailings from the mining industry etc (Rattanasak *et al* 2010, Provis *et al* 2008, Brew *et al* 2007, Komnitsas *et al* 2007, Van *et al* 2003a) has also find considerable interest in the fabrication of geopolymer concrete.

Traditionally, geopolymers are chemically activated by NaOH, KOH and Na₂SiO₃ solutions (Van *et al* 2002, Mustafa *et al* 2011). Sodium aluminate as source of alumina has been reported in earlier works (Provis *et al* 2008, Brew *et al* 2007). In the present work, solid silicate derived from RHA as source and sodium aluminate as a possible source of aluminum has been used for the production of geopolymer composite.

2. EXPERIMENTAL PROCEDURE

2.1 Materials and Mixing procedure

RHA for the study was source from a biomass plant in Kolkata, India. Laboratory grade (Sigma –Aldrich) sodium aluminate is used as a source for aluminum. RHA passing through 180 micron is used for the study. Blaine specific surface area is 6890 cm²/g. The chemical composition of RHA was established by X-Ray Fluorescence (XRF) and is tabulated as in Table 1.

Table 1. Chemical Composition of RHA

SiO ₂	92.19
Al ₂ O ₃	0.09
Fe ₂ O ₃	0.10
TiO ₂	0.71
CaO	0.09
MgO	0.41
K ₂ O	0.05
Na ₂ O	1.64
SO ₃	0.41
P ₂ O ₅	0.01
LOI	4.14

Sodium Aluminate solutions were prepared by distilled water and allowed to cool at room temperature. The amount of sodium aluminate added to the solution is decided by the Si/Al ratio of the geopolymer to be prepared. RHA and the sodium aluminate solution were mixed for 5 min. until a homogenous mixture is obtained. The mixture were than casted in a 50 x 50 x 50 mm cube as per ASTM C109 and oven cured at 80°C for 24 hours. After 24 hours, the samples are allowed to cool at room temperature and demolded and cured at room temperature until the testing day. The nomenclature of the sample is as shown in Table 2

Table 2. Nomenclature of RHA geopolymer sample

Nomenclature	Si/Al Ratio
SA1.5	1.5
SA2.0	2.0
SA2.5	2.5
SA3.0	3.0
SA3.5	3.5

2.2 Testing Procedure

The compressive strength were tested by FIE Make UTM 20 Ton Capacity (Model UTES -20) with rate of loading of 45 kN/min after 28 days from the date of casting. Fragments from the compressive strength test were collected for further characterization.

XRD were conducted by PANalytical with scan 2θ degree ranging from (2°-45°)with scanning step size of 0.01. The anode material used CuKα X-rays and generator

setting of 30 mA, 40 kV. SEM was performed on RHA and cured geopolymer paste samples by FEI Quanta 250 with an accelerating voltage of 15 kV and was magnified up to 3000 times. Energy dispersion X-Ray Analysis (EDAX) was also performed on all the samples as well as the source RHA. Fourier Transform Infrared Spectroscopy (FTIR-Spectrum Two, Perkin Elmer) was used for structural characterization of activated geopolymer samples.

3 RESULTS AND DISCUSSION

3.1 Compressive Strength

The compressive strength of the samples were tested after 28 days. The test were carried out in triplet samples and average values were noted. It shows a trend where the compressive strength increases as Si/Al ratio increases from 1.5 to 2 and decreased in compressive strength value for Si/Al ratio beyond 2. The maximum compressive strength is observed to be 16.96 MPa with Si/Al ratio of 2.0. The addition of sodium aluminate in the rice husk matrix increases the cross linking of the matrixes leading to the increased in the compressive strength as Si/Al ratio is increased from 1.5 to 2.0 (Rees *et al* 2004, Duxson *et al* 2007, Xu *et al* 2012). As Si/Al is increased beyond 2.0, the decrease in the mechanical strength of the geopolymer composite may be due to the extra soluble silicate which inhibits the reaction between silicate and aluminate. This lead to the non-dissolution of the silicate, leaving most of the silica unreacted and hence geopolymer has less strength (Rees *et al* 2004, Duxson *et al* 2007, Xu *et al* 2012).

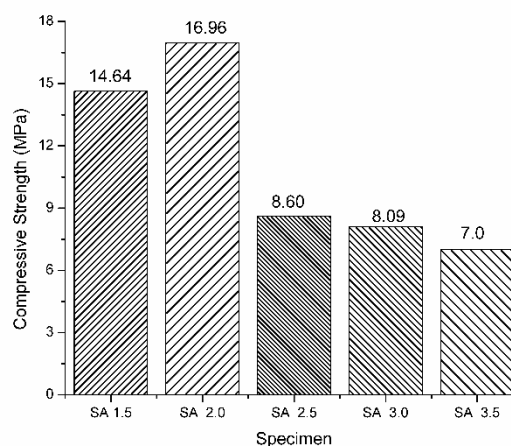


Fig 1. Compressive Strength with Si/Al Ratio.

3.2 X-ray Diffraction Analysis (XRD)

The XRD diffractograms shown in Fig.2. indicate quartz (JCPDS 05-0492), cristobalite (JCPDS 39-1425) and gibbsite (JCPDS 70-2038) as the main ingredients of original RHA samples which is consistent with the observation by earlier researchers (Rattanasak *et al*

2010). The sharp peak near 25° - 27° 2θ and 45° 2θ could be attributed to quartz. No change in the angle and peak intensity at this particular angle range is noted in the original RHA sample as well as the geopolymer samples. With the introduction of sodium aluminate into the RHA in the molar ratio from 1.5 to 3.5, new peaks were observed to have formed. The peaks around 21° - 24° 2θ and 31° - 34° 2θ could probably be arising from cristobalite (Xu *et al* 2012). The peak corresponding to cristobalite increases from raw RHA sample to Geopolymer SA2.0 and then decrease for geopolymer sample SA2.5, SA3.0 and SA3.5. It is also worthy to note that peaks around 18° 2θ rises probably from Gibbsite with the decreasing peaks intensity from Geopolymers SA2, SA2.5, SA3 and SA3.5. (Komnitsas *et al* 2007, Vanetal2003a)

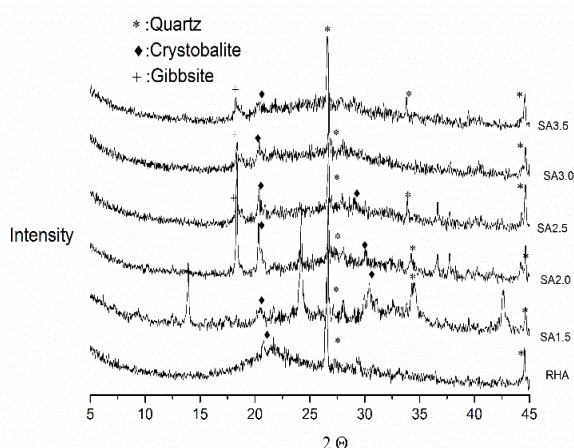


Fig 2. XRD diffractogram of RHA and Geopolymers derived from RHA

3.3 Scanning Electron Microscope with EDX

Scanning electron microscope (SEM) was used to study the microstructure of the Geopolymer. Fig. 3 shows the original RHA sample with irregular, flaky and elongated nature of the microstructures. An obvious change in the SEM micrograph as well as the EDX results are observed with the introduction of sodium aluminate to the source RHA. All the Geopolymer samples were non-homogenous with the presence of unreacted silica. Although the matrixes are dense and continuous, voids can still be observed in the geopolymer. This could be the possible explanation of the relative low compressive strength of the geopolymer paste. Among all the geopolymer, SA2.0 exhibits a denser matrixes with lesser voids which could explained the highest compressive strength among all the samples.



Fig.3 Scanning Electron Microscope of RHA

The EDX results shows Silicon (Si) as the main constituents with traces amounts of aluminum (Al), sodium (Na) and iron (Fe). It is imperative that for the formation of strong and dense matrix of geopolymer, an external source of aluminum in the form of sodium aluminate is used in the present study. It is noted that with the decrease in Si/Al ratio, the Al micrograph increases in its intensity indicating that the lack of Al in the original RHA sample is supplemented by the sodium aluminate which acts as the activator.

4 CONCLUSIONS

In the present study, RHA based geopolymer has been developed with sodium aluminate as alternative source of activator different from the traditional geopolymer where hydroxide of Sodium or Potassium and silicates has been used as activator. Geopolymer paste of reasonable compressive strength can be synthesis from RHA and sodium aluminate. The optimal Si/Al ratio observed is 2.0 from the perspective of compressive strength with value of 16.96 MPa.

XRD analysis shows that the RHA based geopolymers are X ray amorphous which is a typical characteristics of geopolymers. The main constituents are observed to be quartz, cristobalite and gibbsite. SEM results shows irregular, flaky and elongated nature of the original RHA samples. With sodium aluminate as the source of Al in the matrix, EDX results shows a mark rise in the Al graph as well the formation of dense matrix with some voids.

REFERENCES

1. Bai, J., Wild, S., Sabir, B.B. (2002) : Sorptivity and strength of air-cured and water-cured PC-PFA-MK concrete and the influence of binder composition on carbonation depth, *Cement Concrete Research*, 32, 1813.
2. Brew, D. R. M. and MacKenzie, K. J. D. (2007): Geopolymer synthesis using silica fume and sodium aluminate, *Journal of Material Science*, 42, 3990.

3. Cheng, T.W., Chiu, J.P. (2003): Fire-resistant geopolymer produced by granulated blast furnace slag, *Minerals Engineering*, 16, 205.
4. Chindaprasirt, P., Rattanasak, U., Vongvoradit, P., Jenjirapanya, S. (2012): Thermal treatment and utilization of Al-rich waste in high calcium fly ash geopolymeric materials, *International Journal of Minerals, Metallurgy and Materials*, 19(9), 872.
5. Davidovits, J. (1994): High-Alkali Cements for 21st Century Concretes. in Concrete Technology, Past, Present and Future, Proceedings of V. Mohan Malhotra Symposium, ACI SP- 144, 383.
6. Davidovits, J. (1988): Soft Mineralogy and Geopolymers, *Proceedings of the Geopolymer 88 International Conference, the Université de Technologie, Compiègne*
7. Duxson, P., Lukey, G. C. and van Deventer, J.S. J. (2006): Evolution of Gel Structure during Thermal Processing of Na-Geopolymer Gels, *Langmuir*, 22, 8750.
8. Duxson, P., Mallicoat, S.W., Lukey, G.C., Kriven, W.M., and Van Deventer, J. S. J. (2007): The effect of alkali and Si/Al ratio on the development of mechanical properties of metakaolin based geopolymers, *Colloids and Surfaces A: Physicochemical and Engineering Aspects*, 292, p. 8.
9. Fernandez-Jimenez and Palomo, A. (2005): Composition and microstructure of alkali activated fly ash binder: Effect of the activator, *Cement and Concrete Research*, 35, 1984.
10. Hua Xu, Van Deventer, J.S.J. (2002): Geopolymerisation of multiple minerals, *Minerals Engineering*, 15, 1131.
11. Ken, P. W., Ramli, M., Ban, C. C. (2015): An overview on the influence of various factors on the properties of geopolymer concrete derived from industrial by-products, *Construction and Building Materials*, 77, 370.
12. Komnitsas, K., and Zaharaki, D. (2007): Geopolymerisation: A review and prospects for the minerals industry, *Minerals Engineering*, 20, 1261.
13. Lloyd, N. A., Rangan, B. V. (2010): Geopolymer concrete : a review of development and opportunities, *Proceedings of 35th Conference on OUR WORLD IN CONCRETE & STRUCTURES*.
14. Malhotra, V. M. (1999): Making concrete 'greener' with fly ash, *ACI Concrete International*, 21, 61.
15. Mustafa A.M., Bakri, Al, Kamarudin, H. Omar, A.K, Norazian, M.N., Ruzaidi, C.M. and Rafiza, A.R. (2011): The effect of alkaline activator ratio on the compressive strength of fly ash-based Geopolymers, *Australian Journal of Basic and Applied Sciences*, 5, 1916.
16. Palomo, A., Grutzeck, M.W., Blanco, M.T. (1999): Alkali-activated fly ashes A cement for the future, *Cement and Concrete Research*, 29, 1323.
17. Provis, J. L. and van Deventer, J.S.J. (2008): One-part geopolymer mixes from geothermal silica and sodium aluminate Ailar Hajimohammadi, *Industrial and Engineering Chemical Research*, 47, 9396.
18. Rattanasak, U., Chindaprasirt, P., and Suwanvitaya, P. (2010): Development of high volume rice husk ash aluminosilicate composites, *International Journal of Minerals, Metallurgy and Materials*, 17, 654.
19. Rees, C., Lukey, G. C. and Van Deventer, J. S. J. (2004): The role of solid silicates on the formation of geopolymers derived from coal ash, *International Symposium of Research Student on Material Science and Engineering*, 1.
20. Swanepoel, J.C., Strydom, C.A. (2002): Utilisation of fly ash in a geopolymeric material, *Applied Geochemistry*, 17, 1143.
21. Thokchom, S., Ghosh, P. and Ghosh, S. (2011): Durability of Fly Ash Geopolymer Mortars in Nitric Acid—effect of Alkali (Na₂O) Content, *Journal of Civil Engineering and Management*, 17, 393.
22. Thokchom, S., Ghosh, P. and Ghosh, S. (2012a): Effect of Na₂O content on durability of geopolymer pastes in magnesium sulfate solution, *Canadian Journal of Civil Engineering*, 39(1), 34.
23. Thokchom, S., Ghosh, P. and Ghosh, S. (2012b): Effect of Si/Al ratio on the performance of fly ash geopolymer at elevated temperature, *Arabian Journal of Science and Technology*, 37, 977.
24. Van Jaarsveld, J.G.S., van Deventer, J.S.J., Lukey, and G.C. (2002): The effect of composition and temperature on the properties of fly ash- and kaolinite-based geopolymers, *Chemical Engineering Journal*, 89, 63.
25. Van Jaarsveld, J.G.S., van Deventer, J.S.J., and Lorenzen, L. (2003a): Factors Affecting the Immobilization of Metals in Geopolymerized Flyash, *Materials Letters*, 57, 1272.
26. Van Jaarsveld, J.G.S., van Deventer, J.S.J. and Lukey, G.C. (2003b): The characterisation of source materials in fly ash-based geopolymers, *Materials Letters*, 57, 1272.
27. Xu, W., Lo, Memon, T.Y., Ali, S. (2012): Microstructure and reactivity of rich husk ash, *Construction and Building Materials*, 29, 541.
28. Yusuf, M.O., Johari, M.A.M., Ahmad, Z.A and Maslehuddin, M. (2014): Strength and microstructure of alkali-activated binary blended binder containing palm oil fuel ash and ground blast-furnace slag, *Construction and Building Materials*, 52, 504.

[Back to table of contents](#)

Effect of rice husk ash(RHA) on shear parameters and California Bearing Ratio (CBR) of soil

N.Daimaryⁱ⁾ and A.Bhattacharjeeⁱⁱ⁾

i) P.G. Student, Department of Civil Engineering, Jorhat Engineering College, Jorhat, Assam-785001, India.

ii) Assistant Professor, Department of Civil Engineering, Jorhat Engineering College, Jorhat, Assam-785007, India.

ABSTRACT

The rapid population growth leads to huge production of waste materials. Rice Husk being a waste material found in abundance in rice producing countries like India causes problems of disposal, environmental problems as well as health problems. This has become a major concern to the society and so steps should be taken for the safe disposal of this waste material. On the other hand increasing cost of construction materials and admixtures (for improving soil properties) has given rise to turn up to some alternatives. Both the problems of increase in cost of construction materials as well as the problem of rice husk disposal gives rise to the idea of exploring rice husk as a stabilizer for soils. Rice Husk Ash (RHA) which is formed from burning of rice husk was used for improving the properties of soil finally reducing the cost of construction. Using RHA in engineering works will reduce the disposal problem as well as improve the soil properties. Lateritic soil samples from Guwahati and RHA from local factory of Jorhat is used in the present study. The effects of 5-30% of RHA on CBR and Shear parameters of lateritic soil were experimentally studied at different curing periods. From the present study it is seen that there is improvement in both CBR and Shear parameters of RHA treated lateritic soil. It is determined that using RHA as stabilizer leads to economical and eco friendly utilization of waste for stabilizing soil.

Keywords: Lateritic soil, RHA, CBR, Triaxial, cohesion, angle of internal friction.

1. INTRODUCTION

The present study is done focusing on two major problems of the society viz. the problem of disposal of waste materials and the problem of increasing cost of construction materials. It is well known that the existing soil condition in a project site doesn't fulfil all the design requirements for a successful project, which gives rise to the need to improve the soil in the project site. On the other hand one of the major concerns to the society is the disposal of waste materials. Rapid increase in population has caused more production of waste materials and hence more problem of disposal. Disposals of different waste materials causes environmental as well as health problems. So steps should be taken for the safe disposal of these waste materials. Also with the passage of time cost of construction materials has increased. Therefore waste material may be converted into admixtures for improvement of soil. One of the waste material which can be used to improve the soil properties is discovered to be Rice Husk Ash (RHA). RHA is obtained from burning rice husk which an agricultural waste found in rice mills. Due to its availability in abundance as a waste material it requires additional dumping space causing waste of good cultivable land and causes environmental and health problems. Lateritic soils are the most common material used for construction. In the

present study California bearing ratio (CBR) and UU triaxial shear test of lateritic soil mixed with RHA are determined to evaluate the behaviour RHA stabilized lateritic soil.

2 MATERIALS AND METHODOLOGY

2.1 Lateritic soil

Lateritic soil is generally found in warm, humid, tropical areas of the world. The geotechnical properties of these soils are quite different from those soils developed in temperate or cold regions of the world. These are reddish brown due to the presence of iron oxides and are formed on the same parent rock in the same tropical country, but under different climatic conditions have different geotechnical properties. In this tropical part of the world lateritic soils are widely used as fill materials for various construction works and are used as a road making material and they form the sub-grade of most tropical road. They are used as sub base and bases for low cost roads and these carry low to medium traffic. Laterites are nearly devoid of bases and primary silicate, but may contain large amount of quartz and kaolite. These soils are weathered under high temperatures and are formed under changing wet and dry seasons resulting in poor engineering properties such as high plasticity, poor workability, low strength,

high permeability, tendency to retain moisture and high natural moisture content. Therefore it is important to investigate its properties for design, construction and to prevent road failure. In the present study the soil that has been used as a base material is taken from the hills of Fatashil Ambari, Guwahati which is a Lateritic soil as obtained by Goswami and Singh. Chief minerals present in the parent rock to the soil are determined to be quartz, microcline, plagioclase and biotite (Goswami and Singh, 2008). Table 1 shows the mineral constituents of parent rock to the lateritic soil and the geotechnical properties of the lateritic soil collected from Guwahati are listed in Table 2. Fig 1 shows the sample of lateritic soil collected from hills of Guwahati.



Fig 1. Sample of Laterite Soil

Table 1 Mineral Constituents of Parent rock to the lateritic soil (after Goswami and Singh, 2008)

Sl. No	Mineral Constituents	% Present
1	Microcline	16.11
2	Plagioclase	24.46
3	Quartz	54.81
4	Biotite	0.36
5	Accessories	4.26

Table 2 Geotechnical properties of lateritic soil

SL NO.	PROPERTIES	VALUES
1	Specific gravity	2.65
2	Liquid Limit	44.34
3	Plastic Limit	25.63
4	Plasticity Index	18.71
5	Classification of Soil	CI
6	Optimum Moisture Content	21%
7	Un-soaked CBR (%)	3.9
8	Soaked CBR (%)	3.4
9	Triaxial Cohesion, KN/m ²	45.13
10	Triaxial Angle of Internal Friction,	15 ⁰

2.2 Rice Husk Ash

Rice husk is an agricultural waste obtained from milling of rice. It is the outer covering of the Rice grain consisting of two interlocking. This husk is used as fuel in the rice mills to generate steam for the boiling process. Rice Husk Ash (RHA) is formed by burning Rice Husk. All RHA commonly composed of silica, lime, alumina, iron oxide, magnesia. In majority of rice producing countries much of the husk produced from processing of rice is either burnt or dumped as waste.

India is a major rice producing country and about 20 million tone of RHA is produced annually. The ash is 87-97% silica, highly porous and light weight, with a very high external surface area. Its properties also varied depending on its burning temperature. RHA has a good pozzolanic property. The pozzolanic value of RHA depends on burning conditions and its color is dependent on the carbon content of the ash. It is non-plastic in nature. Its physical properties are tabulated in Table 3. However the chemical characteristics of the above mentioned RHA have not done but it is mostly comprised by SiO₂, Fe₂O₃ and Al₂O₃ as mentioned in various literatures. The silica in the ash undergoes structural transformations depending on the conditions of combustion such as time and temperature. This RHA is a great environmental threat causing damage to the land and the surrounding area in which it is dumped.

Fig 2 shows the sample of RHA obtained from local mills of Jorhat city for the present work. This was obtained from rice husks burnt as fuel in a biscuit factory. The combustion process occurred under uncontrolled condition. Specific gravity of rice husk ash is tested by pycnometer method as per IS: 2720 (Part 3)-1980 and is determined to be 2.25.



Fig 2. Samples of Rice Husk Ash

Table 3 Chemical composition of RHA (after Borgohain, 2015)

Sl. No	Components	% Present in RHA
1	Silica(SiO ₂)	73.4
2	Aluminium(Al ₂ O ₃)	5.4
3	Iron (Fe ₂ O ₃)	1.02
4	Calcium (CaO)	1.7
5	Magnesium (MgO)	1.75
6	Potassium (K ₂ O)	1.17

2.3 Methodology

Air dried soil samples passing through 19mm IS sieve are mixed with 0%, 5%, 10%, 15%, 20% and 30% RHA to determine the optimum moisture contents (OMC) and maximum dry density (MDD) as per IS 2720(Part-8) 1983. For RHA mixed up- to 20%, three samples were prepared and compacted in the CBR mould at a moisture content equal to the OMC of the respective soil and RHA mix. Immediately after compaction, one of the three samples is tested in CBR machine for un-soaked condition and then it was submerged in water for four days for soaked test at other unused face of same sample (samples tested without curing). From the three samples prepared the other two samples are kept to investigate effect of curing period for 7 and 28 days. On 7th and 28th day, samples are tested for un-soaked condition and then soaked in water for 4 days for soaked CBR as per IS: 2720, (Part-16) 1987. For all stabilized soil samples, CBR value corresponding to 2.5 mm and 5.0 mm penetration are observed in CBR testing machine. Unconsolidated undrained (UU) triaxial shear test is performed for all the combinations of RHA mix to the lateritic soil. The test is carried out in a cell on a cylindrical soil sample having a length to diameter ratio of 2. Three sets of samples are prepared at OMC obtained for a particular soil+RHA content. First set is tested immediately after preparation and other two sets are kept for 7 and 28 days of curing period. After 7 and 28 days, samples are brought out for testing. Triaxial test is carried out in advance triaxial machine where all the readings are saved automatically. Minor stresses such as 1Kg/cm², 1.5Kg/cm² and 2Kg/cm² are used during the test.

3 RESULTS AND DISCUSSION

3.1 Effects on CBR

The variation of load and penetration in un-soaked condition with varying percentage of RHA without curing and with curing period of 7 and 28 days are shown in fig 3, fig 4 and fig 5 respectively. The figure shows more variation of load with increase in percentage of RHA in soil at instant of sample preparation.

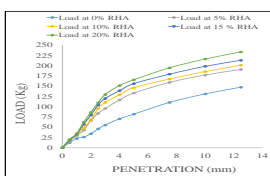


Fig 3. CBR curve for uncured soil+% RHA samples in un-soaked condition

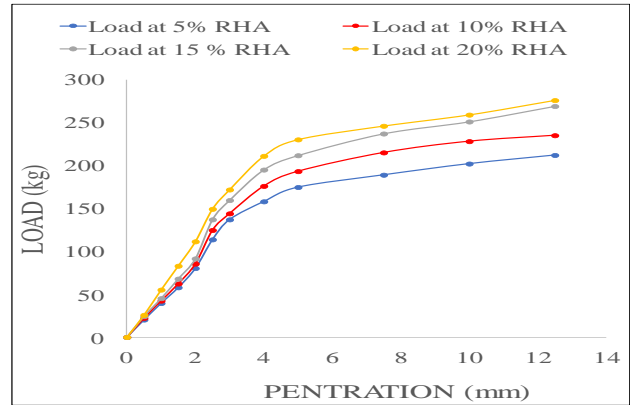


Fig 4. CBR curve for 7 days cured soil+% RHA samples in un-soaked condition.

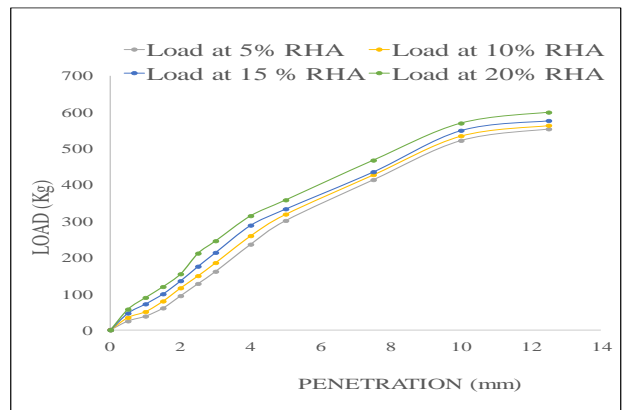


Fig 5. CBR curve for 28 days cured soil+% RHA samples in un-soaked condition

Fig 6 shows the variation of un-soaked CBR for lateritic soil+ RHA mix samples with 5%, 10%, 15% and 20% RHA after different curing period. The un-soaked CBR for lateritic soil + 5% RHA is 6.6%. An increase of 40% in un-soaked CBR is observed for addition of 5% of RHA to lateritic soil. The un-soaked CBR increases from 6.6% for soil + 5% RHA to 8.3% for soil + 20% RHA respectively. The CBR values increases with increase in percentage of RHA in lateritic soil. The variation of load for soil with increase in percentage of RHA in soil is lesser after 28 days of curing period.

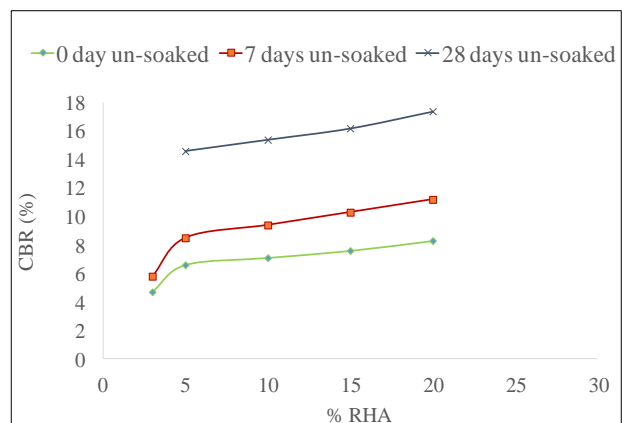


Fig 6. Variation of un-soaked CBR with varying % of RHA and curing period

Fig 7 shows the variation of load with penetration in soaked condition of uncured soil samples with varying

percentages of RHA. CBR value increased from 3.4% to 7.4% for RHA mixed to the soil up to 20%.

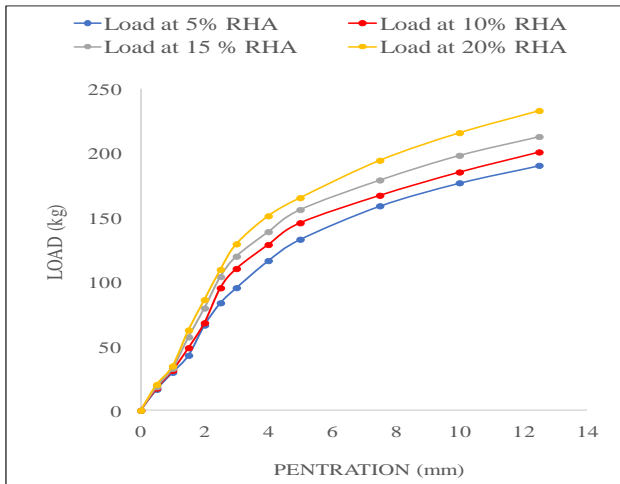


Fig 7. CBR curve for uncured soil+% RHA samples in soaked condition

Fig. 8 and fig. 9 shows the variation of load and penetration of RHA mix soil in soaked condition for a curing period of 7 and 28 days. After a curing period of 7 days and 28 days it is observed that the soaked CBR values increased up to 8.8% and 14.6% when RHA content increased to 20%. Also with the increase in curing period the soaked CBR values increased. Fig 10 shows the variation of CBR with varying percentage of RHA at different curing periods.

The increase in CBR of soil-RHA mix with time is due to more replacement of alumina by silica present in RHA. The addition of RHA with lateritic soil is acting as adhesive agent for lateritic soil in both un-soaked and soaked condition. This leads to more increase in CBR value of lateritic soil mixed with RHA. This adhesive effect increases with passage of time and more improvement of CBR value is observed with passage of time.

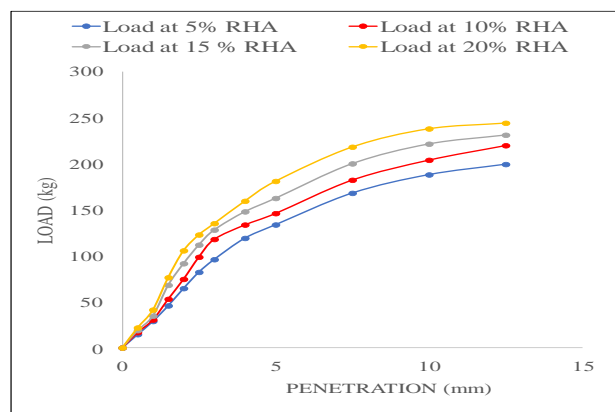


Fig 8. CBR curve for 7 days cured soil+% RHA samples soaked condition

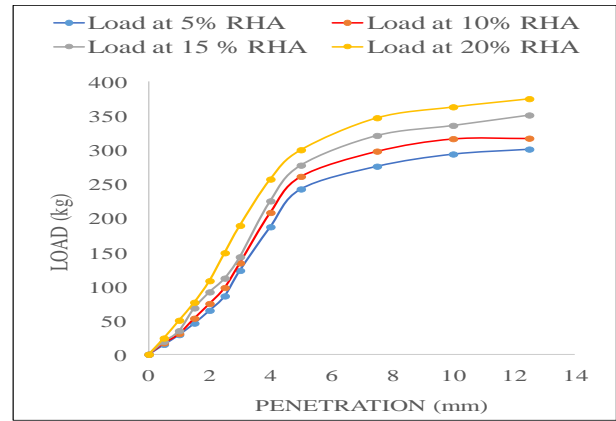


Fig 9. CBR curve for 28 days cured soil+% RHA samples in soaked condition

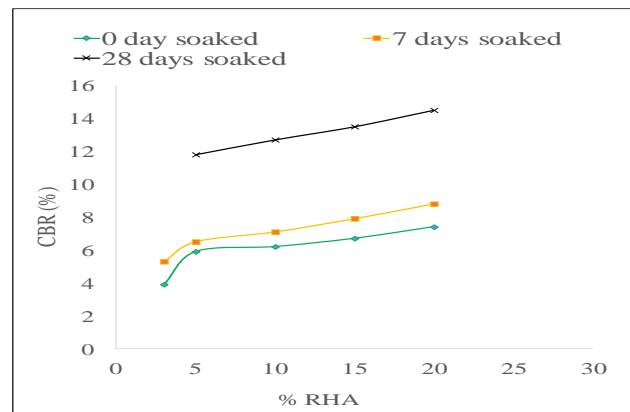


Fig 10. Variation of soaked CBR with varying % of RHA and curing period

3.2 Effects on UU triaxial shear parameters

Fig 11 shows the Mohr-Coulomb shear strength envelop of the untreated natural lateritic soil which is determined by UU triaxial test. The cohesion (C) and angle of internal friction (ϕ) are determined to be 45.12 KPa and 15° .

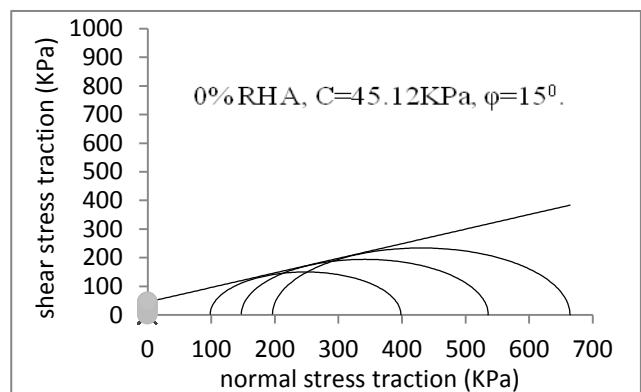


Fig 11. Shear strength parameters (C & ϕ) of Lateritic soil using UU triaxial test.

Fig 12 shows the variations of cohesion with respect to different RHA content and at different curing periods. It is observed that the cohesion of the soil increased up to 15 % RHA mixed to the lateritic soil but with further increment in RHA to the soil C decreased. It may be attributed to the coating of the soil by the rice husk ash. Percentage increase in cohesion is observed to be 25.48% while the percentage decrease in cohesion is

observed to be 37.5% without curing. On the other hand Fig 13 shows the variation of angle of internal friction, ϕ which kept increasing with increase in RHA content. For the uncured samples percentage increase in ϕ from 10 to 20 percent RHA mix is determined to be 48.32% and from 20 to 30 percent is observed to be 13.58%. The improvement of angle of internal friction (ϕ) implies that the silica content in RHA act as a binder which agglomerates the particles into a larger one and the soil changes from clay to silt. Also this indicates that the friction between the particles increases which may be due to the coating of the soil by Rice Husk, which resulted in larger particles and hence greater friction between them. By using the Mohr-Coulomb's equation, the shear strength was calculated. It was found that with increase in percentage of RHA the shear strength increased.

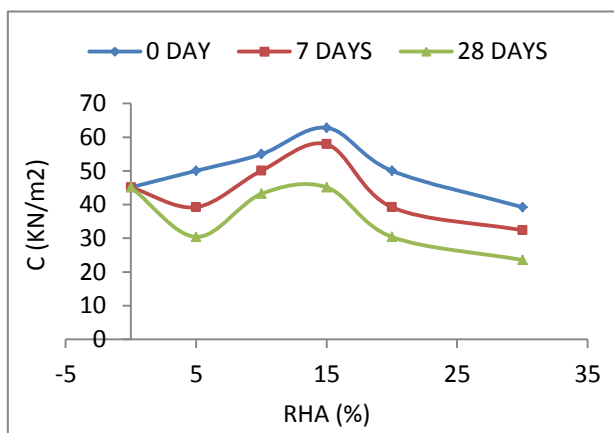


Fig 12. Variation Cohesion, C with different RHA content at different curing period

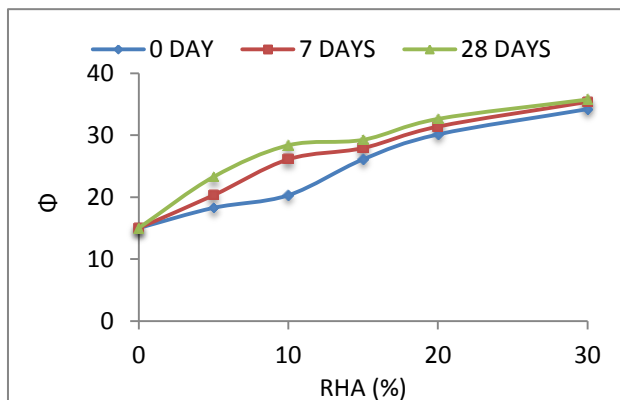


Fig 13. Variation of Angle Internal Friction, ϕ with different RHA content at different curing period.

4 CONCLUSIONS

From tests and analysis carried out in the study, the following conclusions were drawn:

- 1). Addition of RHA showed improvement in both the soaked and un-soaked CBR.
- 2). Both soaked and un-soaked CBR value increased with increase in curing period.
- 3). The UU triaxial shear test showed increase in cohesion up to 15% RHA content after which cohesion

decreased (for all days of curing) while Angle of Internal Friction kept increasing with increase in RHA content.

- 4). Both cohesion and angle of internal friction increased with increase in curing periods from 7 to 28 days.

From the results obtained it is clear that the strength of the soil improves on addition of RHA. So, it can be concluded that using RHA as a stabilizer is a suitable method for soil stabilization. RHA will not only stabilize the soil but also reduce the cost of construction as well as disposal problem of waste like RHA.

REFERENCES

- 1) Alhassan. M. (2008): *Potentials of Rice Husk Ash for soil stabilization*, Technical Report, Deptt of Civil Engg, Federal University of Technology, Minna, Niger State, Nigeria. Pp-246-250.
- 2) Borgohain, B, Daimary, N. and Bhattacharjee, A. (2016): Effects of Rice Husk Ash on Plasticity and Compaction of Lateritic Soil, *North East Students Geo-Congress On Advances in geotechnical engineering 2016*, 22 Jan 2016, NIT Agartala, 53(6), pp. 339-345.
- 3) Goswami .R.K. and Singh. B. (2008): An Analysis of causes of Urban Landslides in Residual Lateritic Soil, *6th International Conference on Case Histories in Geotechnical Engineering*, pp.1-9.
- 4) IS: 2720, (Part 11)-1993, *Methods of Test for Soils: Determination of Shear Strength Parameters of a Specimen tested in Unconsolidated Undrained Triaxial Compression without the measurement of Pore Water Pressure*, Bureau of Indian Standards, New Delhi.
- 5) IS: 2720, (Part 8)-1983, *Methods of Tests for soils: Determination of water content-dry density relation using heavy compaction*, Bureau of Indian Standards, New Delhi.
- 6) IS: 2720, (Part 16)-1987, *Indian Standards: Methods of Test for soils: Part16, Laboratory determination of CBR*, Bureau of Indian Standards, New Delhi.
- 7) Nagle, R., Jain, R. and Shinghi, A.K. (2014): Comparative study of soil, reinforced with natural waste plastic material. *International Journal of Engineering & Science Research*.4(6), 304-308.
- 8) Okafor, F. O. and Okonkwo, U. N. (2009): Effects of Rice Husk ash on some Geotechnical properties of lateritic soil, *Leonardo Electronic Journal of Practices and Technologies*, ISSN 1583-1078, Issue 15, pp. 67-74.
- 9) Rahman, Z.A., Ashari. H.H., Sahibin. A.R., Tukimat. L. and Razi. I.W.M. (2014), Effect of rice husk ash mixtures on geotechnical characteristics of treated residual soil, *American-Eurasian J. Agric. & Environ. Sci*, Vol.14 No. 12, pp. 1368-1377.
- 10) Rathan, R. R, Banupriya, S. and Dharani. R. (2016), Stabilization of soil using Rice Husk Ash. *International Journal of Computational Engineering Research (IJCER)*.06,(02), 43-50.

[Back to table of contents](#)

Optimization of roller tuned mass damper and its practical validation

Dr. (Mrs) Nayanmoni Chetiaⁱ⁾

i) Asstt. Prof., Jorhat Engineering College, nayanmoni.chetia@gmail.com

ABSTRACT

Control of deflection of flexible structures like high rise buildings, towers and skyscrapers under service load is a major topic of concern in recent days. Frequent occurrence of seismic activities and wind forces will increase the probability of lateral movement of these high rise structures. Passive, active and hybrid control devices are recently in practice to control the lateral movement of the structures. Tuned mass damper is one of the commonly used Passive control devices in which the vibrational energy of a primary structure is transferred to a secondary mass suspended at the roof level. In case of Roller TMD the mass is provided with a roller support with spring and damper system. The mass, stiffness and damping of the secondary system is so tuned that when the structure will vibrate in that particular mode, the secondary mass will move in opposite phase and thus reduces the response at the slab level. In this paper an attempt has been made to optimise the Roller Tuned Mass Damper for maximum efficiency. Optimisation is done by means of analytical method using direct approach. Performance of the optimised TMD was studied experimentally using a shake Table and shear frame model. A three storey shear frame model was first tested in the Shake table by introducing a sinusoidal excitation and responses were recorded. Optimised Roller TMD was then installed to the same frame and analysed as before under the same excitation. Comparing the results for the two cases, reduction in different responses such as displacement, velocity and acceleration due to the Roller TMD was observed.

Keywords: control, response, tuned mass damper, roller tuned mass damper

1. INTRODUCTION

The primary purpose of all kinds of structural systems used in the building structures is to transfer gravity loads effectively to the footing. The most common loads resulting from the effect of gravity are dead load, live load and snow load. Besides these vertical loads, buildings are also subjected to lateral loads caused by wind, blasting or earthquake. Lateral loads can develop high stresses, produce sway movement or cause vibration. Therefore, it is very important for the structure to have sufficient strength against vertical loads together with adequate stiffness to resist lateral forces.

Innovative means of enhancing structural functionality and safety against natural and manmade hazards are currently a major field of interest of various research works. Performance of a structure under lateral loads can be improved by providing the structure with different control mechanisms such as TMDs, base-isolation, viscous dampers etc..

Tuned mass damper is a passive control practice in which the lateral vibration of a structure is transferred into the vibrational energy of an auxiliary mass suspended at the top storey. The mass and stiffness of the dampers are tuned in such a way that it will vibrate in a

phase opposite to the building vibration. For structures where utilization of head room has constrains, the roller TMD proves to be more feasible.

2. EXPERIMENTAL TOOLS AND MODELS

2.1 Shake table

Shake table is an electromechanical experimental setup which would enable the study of basic issues related to vibration behaviour such as damping, dynamic response magnification, resonance, structural vibration under support motions, normal modes, vibration isolation, vibration absorption, dynamics with soft and/or weak first/intermediate stories etc. It also deals with the study of structural ductility in resisting dynamic loads, liquefaction of soils under dynamic loads, seismic wave amplification through soil layer and rocking and up throw of rigid objects under dynamic base motions. These tables have the capabilities for applying harmonic base motions and have the provision to mount the test structure at any desired angle with respect to the direction of applied base motion. The shake table consists of a connecting rod, a vibration table, linear guide ways and an eccentric cam. The cam is connected to a variable speed dc motor with the help of a gear assembly. Linear guide ways ensure that the motion of the table is linear. Fig. 1. shows an electric motor driven Shake Table.

Specification of the electric motor driven shake table are given herewith

Maximum payload = 30 kg

Sliding table dimension = 400 mm × 360 mm

Circular mounting plate dimension = 390 mm diameter

Motor = 1 HP variable speed dc.



Fig. 1. Electric motor driven shake table.

2.2 Experimental models

A three storey shear frame model was used for analysis (Fig 2). The shake table was first analysed without any extra mass and then with an extra mass at the central position, the same harmonic motion was then fed to the mentioned frame equipped with optimized Roller Tuned Mass damper and analyzed in the shake table. Fig. 3 shows the experimental model with roller TMD. The properties of the referred model are tabulated in Table 1.



Fig. 2. Three storey shear frame model

Three sets of accelerometers (sensors) were connected at the level of three roof slabs as shown in Fig 2 and 3 to collect the responses such as displacement, velocity and acceleration.



Fig. 3. Three storey steel frame model with optimized Roller TMD

Table 1. Properties of the frame

Items	Properties
Material	Mild steel
E	20000
Unit weight	7850 kg /m ³
Size of column	3 mm × 25 mm, 400 mm height
Size of slab	300 mm × 150 mm, 12 mm thick
Modal frequency of vibration	2.85hz, 8.6 hz, 12.3 hz
Weight of extra mass	1 kg
Weight of the TMD	975 gm
Spring constant	3.5 N/mm

3. THEORY

A tuned mass damper (TMD) is a device consisting of a mass, a spring and a damper that is attached to a structure in order to reduce the dynamic response of the structure. The frequency of the damper is tuned to a particular structural frequency so that when the structure is excited to that particular frequency the damper will resonate out of phase with the structural motion. Energy is dissipated by the damper inertia force acting on the structure. The TMD concept was first applied by Frahm (Frahm, 1909) to reduce the rolling motion of ships as well as ship hull vibrations.

In Roller TMD system, an extra mass is provided with a roller support and a pair of spring with specific spring constant is attached to the mass.

Figure 4 illustrates the typical configuration of a unidirectional translational or roller Tuned Mass Damper. The mass rests on bearings that function as rollers and allow the mass to translate laterally relative to the floor. Springs and dampers are inserted between the mass and the adjacent vertical support members, which transmit the lateral “out-of-phase” force to the floor level and then into the structural frame. [Connor J.J. (2000)]

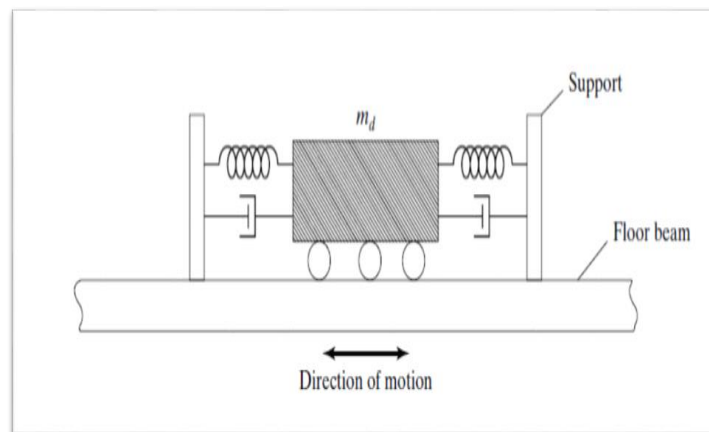


Fig. 4. Schematic diagram of a roller tuned mass damper, [Connor J.J. (2000)]⁷

Eqn of motion for the primary mass,

$$(1 + \dot{m}) \ddot{U} + 2\xi\omega\dot{U} + \omega^2 U = P/m - \dot{m} \ddot{U}_d \quad (1)$$

Eqn of motion for the tuned mass,

$$\ddot{U}_d + 2\xi_d\omega_d\dot{U}_d + \omega_d^2 U_d = -\ddot{U} \quad (2)$$

Where

U, U_d - displacement of primary mass and damper

\dot{U}, \dot{U}_d - Velocity of primary mass and damper.

\ddot{U}, \ddot{U}_d - acceleration of primary mass and damper.

\dot{m} - mass ratio = m_d/m

ξ, ξ_d - damping ratio of the primary mass and damper

ω, ω_d - natural frequency of vibration of the primary mass and damper.

After solving these equations and introducing different constants J.J. Connor has plotted following graphs for the optimized design of a TUNED MASS DAMPER.

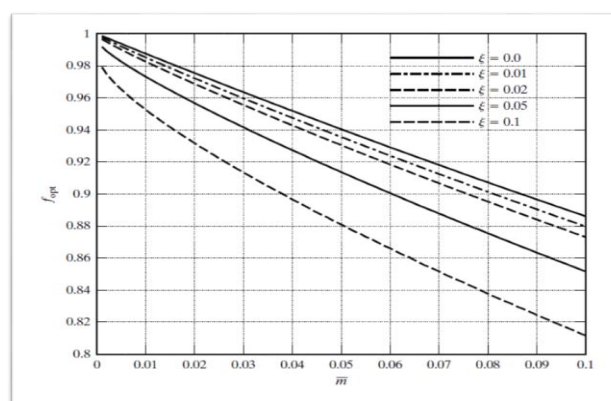


Fig. 5. Optimum tuning frequency ratio for TMD, f_{opt} , [Connor J.J.(2000)]

4. EXPERIMENTAL OBSERVATIONS

The three storey model is first analyzed in the shake table by introducing a harmonic excitation of $1 \sin \omega t$, ω ranging from 0 Hz to 15 Hz. Displacement, velocity and acceleration responses of the structure are

recorded for each vibration.

The model is analyzed by introducing a mass of 1 kg (7% of the building mass) at central positions by giving the same harmonic excitation. Different responses at different floor levels are then recorded.

In the next attempt the frame is provided with a roller TMD at the top storey and analyzed under the same input excitation. Here an extra mass is provided with roller support and spring system as shown in Fig. 3. Optimization of the Roller TMD is done analytically and the mass required is found to be 975 gm and spring constant of 3.5 N/mm for each spring. The frame with the optimized TMD is then analyzed with the same vibrations and different responses are recorded. Reduction in different responses due to the optimized TMD are then compared and plotted.

5. OPTIMISATION OF THE TMD

Optimization of the TMD for mass and stiffness is done by using direct method for MDOF system. Different steps for the optimization are given below. [Connor J.J.(2000)]

a. Determination of spring constant- For a spring with spring constant K_s , and a suspended mass m , time period of vibration.

$$T = 2 \pi \sqrt{(m/K_s)} \quad (3)$$

If two masses m_1 and m_2 are considered with the same spring than

$$K_s = 4 \pi^2 (m_2 - m_1) / (T_2^2 - T_1^2) \quad (4)$$

Three masses 100gm, 200 gm and 500gm were considered as m_1 , m_2 , m_3 and respective time periods T_1 , T_2 , T_3 are calculated by giving a free vibration.

Finally spring constant K is found to be,

$$K = (K_1 + K_2 + K_3) / 3 = 3.48 \text{ N/mm}$$

spring constant is considered as 3.5 N / mm

2. Determination of mode shape and other parameters of the structure-

Different parameters for the frame under consideration

$$\text{Mass matrix, } M = \begin{bmatrix} 4.4 & 0 & 0 \\ 0 & 4.4 & 0 \\ 0 & 0 & 4 \end{bmatrix} \text{ kg}$$

$$\text{Stiffness matrix, } K = \begin{bmatrix} 17.1 & -8.85 & 0 \\ 0 & 4.4 & -8.85 \\ 0 & 0 & 4 \end{bmatrix} \text{ N/m}$$

$$\omega_n = \begin{bmatrix} 3.05 \\ 8.65 \\ 12.60 \end{bmatrix} \text{ cycles/sec} = \begin{bmatrix} 3.05 \\ 8.65 \\ 12.60 \end{bmatrix} \text{ rad/sec}$$

From the eigenvalue problem, $[K - \omega^2 M] \phi = 0$, modal mode shapes are determined.

Mass normalized modal matrix

$$\phi = \begin{bmatrix} .162 & -.355 & .215 \\ .290 & -.315 & -.403 \\ .350 & .04 & .143 \end{bmatrix}$$

$$\text{Modal mass, } m_j^* = \phi^T M \phi \quad (5)$$

$$m_1^* = \phi_1^T M \phi_1 = .99 \text{ kg}$$

Equivalent SDOF mass parameter for mode 1 having the weight at node 3 is

$$M_{1e}^* = m_1^* \phi_{13}^2 = .9982 / .35^2 = 8.14 \text{ kg}$$

Mass ratio is defined as,

$$\dot{m} = m_d / M_{1e}^* \quad (6)$$

Therefore, mass of the damper,

$$m_d = \dot{m} \times M_{1e}^* = 8.14 \dot{m}$$

Stiffness of the TMD,

$$K_d = K_s + K_s \text{ (springs are in parallel)}$$

$$= 7 \text{ N / mm}$$

3. Determination of the TMD mass

Optimum tuning ratio,

$$f_{opt} = \omega_d / \omega_1 = \sqrt{(K_d / m_d)} \div 3.25$$

By putting the value of K_d and m_d we have,

$$f_{opt} = .291 / \sqrt{\dot{m}} \quad (7)$$

Again from the graph between \dot{m} and f_{opt} in fig. 5, the value of f_{opt} can be determined for any value of \dot{m} . By assuming an arbitrary value of mass ratio, at first f_{opt} is calculated. From the graph and putting the value of f_{opt} in eqⁿ 7, a new value of \dot{m} is obtained.. For the next iteration this new value of \dot{m} is taken and the process is repeated. After some cycles of iteration process when the value of \dot{m} is equal to that of the previous one, that will be the final \dot{m} . i.e. the value of \dot{m} which will hold good for both eqⁿ 7 and the design curve (Fig.5).

In the present study, after the iteration \dot{m} is found to be, $\dot{m} = 0.12$

Hence mass of the TMD for optimized response reduction, $m_d = 0.12 \times 8.14 = 976 \text{ gm}$.

A weight of 975 gm is applied with a roller support at the top storey with two springs of spring constant 3.5 N / mm.

6. RESULTS AND DISCUSSIONS

Different responses of the frame with the optimized Roler Tuned Mass Damper are then compared with that of the frame without any damping device. The reduction in displacement, drift, velocity and acceleration responses of the top storey are presented in graphical forms from Fig. 6 to Fig. 9.

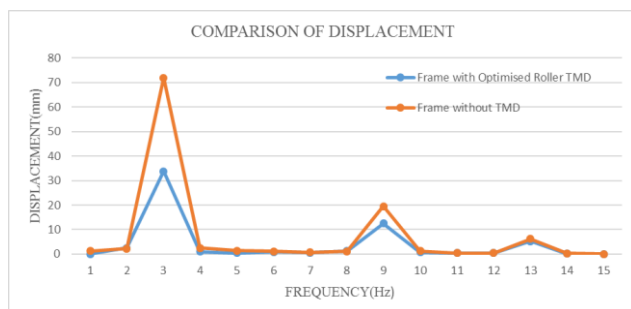


Fig. 6. Comparison of top storey displacement

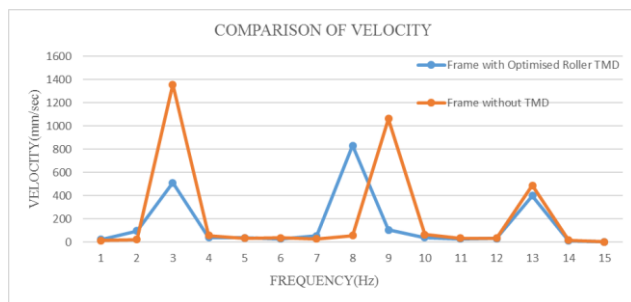


Fig. 7. Comparison of top storey velocity for the two cases.

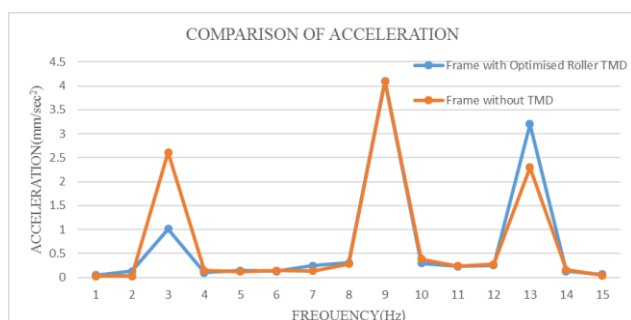


Fig. 8. Comparison of top storey acceleration

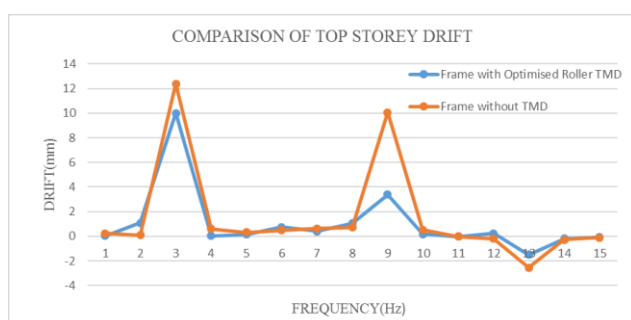


Fig. 9. Comparison of top storey drift

7. CONCLUSION

The effect of Roller Tuned Mass Damper in reducing different responses of a building structure was studied experimentally. A three storey shear frame model was analyzed without any damper and then with an optimized Roller TMD. Optimization of the TMD parameters for the model frame was done by direct method. The uncontrolled frames was analyzed

considering two different loading conditions as already explained. Performance of the Roller TMD under a harmonic excitation is recorded and graphs were plotted for different parameters. From the respective plots it is observed that the introduction of an optimized Roller TMD results in a reduction of 55% of top storey displacement, 63% of top storey velocity and 62% of top storey acceleration of the frame under the harmonic excitation. Reduction in drift was 18% of top storey drift.

The effective performance of Roller TMD in reducing structural response will encourage the possibility of changing the non-structural elements present in the top storey of high rise buildings to certain type of roller TMD. For this process to work properly, at first one has to unite the non-structural elements present in a structure to the central position of the top storey as much as possible. Method of optimization is same as illustrated in this study, only the mode shape and mass of the damper will be different for different structures. After optimization the required stiffness and damping can be imparted by bearing and roller support systems. By the application of this process, the ill effect of non-structural elements can be converted into an effective structural control technology.

REFERENCES

1. Banerjee Susanta, "Inelastic Seismic Analysis of Reinforced Concrete Frame Building with Soft Storey", 2014; International Journal of Civil Engineering Research, Volume 5, Number 4, pp. 373-378, ISSN 2278-3652.
2. Biradar. Umesh. R and Mangalgi Shivaraj "Seismic response of reinforced concrete structure by using different bracing systems", 2013, International Journal of Research in Engineering and Technology, eISSN: 2319-1163, pISSN: 2321-7308 Cheju, Korea, August 23-25.
3. Chopra A.K., "Dynamics of Structure", 2007, PEARSON prentice Hall, pp.450-478.
4. Clough, J.W. & Penzien, J. "Dynamics of Structures", 1993 2nd Edition, McGraw-Hill.
5. Connor J.J. "Introduction to Structural Motion Control", 2000, Prentice Hall Pearson Education, Inc, pp.01-330.

[Back to table of contents](#)

Application of Micropiles for Underpinning and Seismic Retrofitting of Structures

Binu Sharma

Professor, Department of Civil Engineering, Assam Engineering College, Guwahati-781013, Assam

ABSTRACT

National disasters like earthquake have urgently emphasized the need of strengthening of foundations of existing buildings. High cost of land in big cities, compel addition of new floors to existing buildings. Strengthening of foundations of existing buildings usually needs excavation and temporary support system below the foundation level which is difficult not only due to limited head room and access in congested area but also for the inherent risk of collapse of the structure during the excavation process itself. Use of micropiles may be considered as a technically viable and economically feasible solution in such situations.

Micropiles may be defined as small diameter piles (diameters less than 300mm). Therefore only a small space is needed for their construction. It is ideally suited for low headroom and limited work area conditions. Specially developed installation process eliminates noise nuisance, vibrations to surrounding soils and structures, disturbance to the production operations in individual units and disruption to the functioning of business locality. In this work, the application of micropiles for underpinning and seismic retrofitting of buildings is being investigated. This paper urgently emphasizes the need of seismic retrofitting by micropiles of vulnerable buildings in earthquake prone areas like the North Eastern Region which falls in seismic Zone V .It has been reported in literature that foundations underpinned with micropiles in Italy has already survived earthquakes of medium to high intensity.

Keywords: -

1. INTRODUCTION

Northeastern region is one of the six most seismically active region of the world. Eighteen large earthquakes with magnitude greater than 7 occurred in the Northeastern region during the last hundred years. Guwahati, the capital of Assam, is one of the largest and fastest growing city of the region. Within the span of a decade, the city has seen a considerable population growth of over 40%. This has resulted in rapid growth of the city in a most unplanned manner increasing vulnerability of human population and physical structures to the earthquakes. Survey and assessment of existing building structures for earthquake vulnerability risk has shown that many existing building structures in Guwahati are vulnerable to earthquake. This is in view of the fact that many of them were not designed in accordance with the recent seismic design procedures. As a result many of the structures constructed earlier fail to meet requirement of current codes. Again the geographic setting of the city is such that it has

restricted horizontal expansion. Vertical expansion of the city has become inevitable. Liquefaction potential hazard mapping of the city has also shown that many areas are prone to liquefaction in case of a high magnitude earthquake equal to or greater than 7. In such a situation seismic retrofitting of existing structures and liquefaction counter measures of existing structures and liquefiable ground has become inevitable.

Seismic retrofitting or liquefaction counter measures of existing structures in urban cities like Guwahati are types of work executed under restrictive execution conditions with very low headroom with other structures standing nearby and in the case of bridge foundation, the space under the bridge girders is low. Consequently, it is difficult to apply usual methods such as increasing additional piles or ground improvement technique. In such situations seismic retrofitting by micropiles proves to be the best method for reducing risk caused by earthquake. Micropiles are increasingly being used to retrofit deep foundations. This is due

to their small boring diameter which allows their construction with smaller equipments and in limited headroom conditions and it can be installed in almost any ground conditions (Mascardi, 1982). Micropiles are small diameter (100 and 250 mm) grouted drilled piles which comprises of a central steel component with an annular surround of grout that is in contact with the soil. The grout is either placed or injected under pressure (grouting pressure above 0.8 to 1Mpa). Micropiles were first introduced in Italy in 1950 and were conceived as a method to underpin old historic buildings and monuments.(Fig.1). In 1960's this technique was widely used in Europe for underpinning old sensitive structures and during mid 70's it was introduced in USA. In east Asia it gained acceptance during the 1980's and today it has become 'A micro – mini revolution worldwide.'

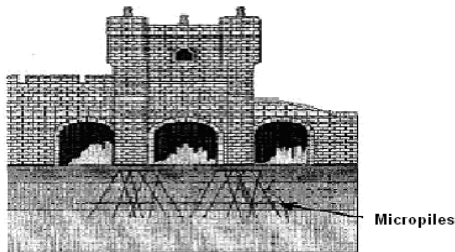


Fig.1 Underpinning of old historic buildings

2. BACKGROUND

Micropiles have been in use for more than 50 years. Originally, they were conceived as innovative solutions to aid in difficult post war reconstruction efforts. Over the past 20 years, micropile technology has expanded significantly and has evolved from the concept of low capacity micropile networks to the use of single, high capacity elements. These small elements allow engineers to solve some difficult structural support problems involving high loads and restricted access. Engineers and researchers are now giving renewed attention to micropile networks as technically and economically viable solutions to problems of slope stabilization, lateral loading and seismic retrofit.

Micropile is a very flexible pile. Due to its high slenderness ratio and its ductile steel core, it can exhibit flexible behaviour under dynamic loading and can be used for seismic retrofitting of

structures. In Italy foundation with root pile have already survived several earthquake of high intensity. In very recent years the use of micropiles for seismic retrofitting of existing foundations has been investigated by Public Work Research Institute (PWRI) Japan. Through joint research with 13 other private companies, PWRI has confirmed that micropile method for seismic retrofitting have superior execution properties under severe condition

3. BRIEF REVIEW OF LITERATURE

Micropile technology, application and seismic retrofit by micropiles are reported in literature by various research workers [Schlosser and Juran (1979), Lizzi (1983), Soliman and Munkoph (1988), O'Neill and Pierry (1989), Ting and Nithiraj (2000).

Nayak and Ketkar (1992) reported that Asia Foundation Consultancy (AFCONS) in Mumbai have underpinned eleven structures in a single complex using micropiles of 150mm diameter. Yamane, T., et al (2000) reports about efficiency of micropiles for seismic retrofitting of foundation system. Sivakumar Babu, et al (2004) reports a case history in which micropiles have been effectively used to retrofit the existing foundations in order to rehabilitate the total building foundation system. Mitrani, H. et al (2005) presents a series of centrifuge tests carried out to investigate the performance of non structural inclined micropiles as a potential liquefaction remedial measure for existing buildings. Seismic retrofitting by micropile method was described by Nishitani et. al. (2002).

4. ADVANTAGES

Micropiles have many advantages over the other methods of underpinning or soil improvement. Since micropiles are generally grouted under pressure, injection pressures nearly above 0.8 to 1.0 MPa, the shrinkage encountered between the pile and the soil is insignificant. The high pressure grouting, also creates a transitory zone between the body of the micropile and the soil, due to the penetration into the surrounding soil by the fluid part of the cement mix. This leads

to the development of a strong grout/ground bond along the micropile periphery resulting in high skin friction between the soil and the micropile. Therefore the main interaction between soil and the pile is skin friction. Due to high skin friction, load carrying capacity of micropiles is higher than the anticipated capacity based on conventional bearing capacity theory. The pressure injection of grout leads to surrounding ground improvement and together with specially designed reinforcement, the method can guarantee large bearing capacity regardless of a small diameter.

Most qualifying characteristic of micropiles as underpinning is its 'quick response' to the slightest movement of the structure. Micropiles exhibit settlement of a few mm even for load value up to crushing strength of concrete. In metropolitan cities having difficult soil problem where pile foundation is must, the engineer has to face some constraints like low headroom, congested working area and has to complete the work without causing noise nuisance and vibration to the surrounding. One of the most important advantages of the micropiles is its use in very difficult and problematic ground location and geologies and having limited headroom access. Their small boring diameter allows their construction with smaller equipments and there is little noise and vibration during execution.

The micropile method of seismic retrofitting are executed by gradually lengthening the piles by connecting short steel pipes with threaded joints. Due to this it can be executed in a location with under girder height of only 3.5m. The execution drilling machinery for micropile constructions is small which can be moved easily in a space with the width of a single vehicle lane about 3m. Moreover micropiles can be installed with a low head room of about 1.5 m. and can be driven at an angle upto about 30 to 35 degrees. The small diameter also minimizes expansion of footing width as shown in Fig. (2). Another major advantage is that micropile installation does not require detail subsoil investigation either in field or laboratory. A load test at the site may be considered sufficient. Both from investigation and construction point of view micropiles are economical and involve much savings in time.

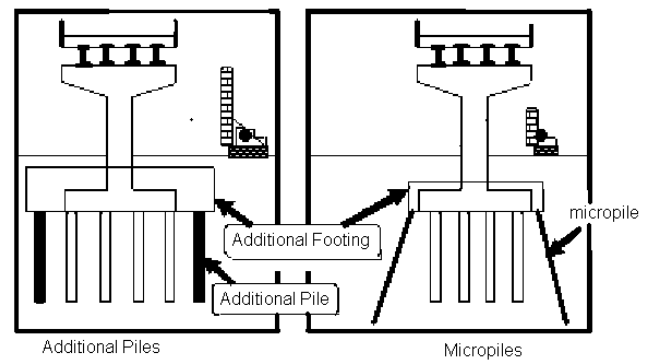


Fig.2 Retrofitting by additional piles and micropiles

Another major advantage of micropiles behaviour is positive group effect in contrast to negative group effect of conventional piles. Lizzi (1978) reported an even greater positive group effect when micropiles are arranged in the form of a network.

5. APPLICATIONS

Micropiles basically have two important applications.. One is for structural support and the other is as in situ reinforcement. As structural members it can be used for seismic retrofitting, for resisting uplift dynamic loads. Fig 3.shows a view of seismic retrofitting by micropiles and the application of micropiles in resisting uplift dynamic loads. Retrofitting by adding additional footing and micropiles is shown in Fig 2.

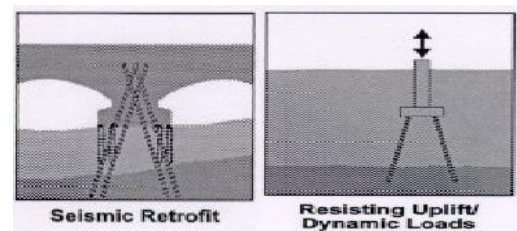


Fig.3 Micropiles as seismic retrofit and resisting uplift dynamic loads

As already mentioned it is used for strengthening of existing foundations in low headroom and congested areas as shown in fig.4 and Fig.5.

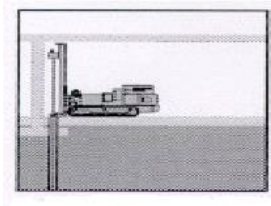


Fig.4. Underpinning of buildings in congested areas

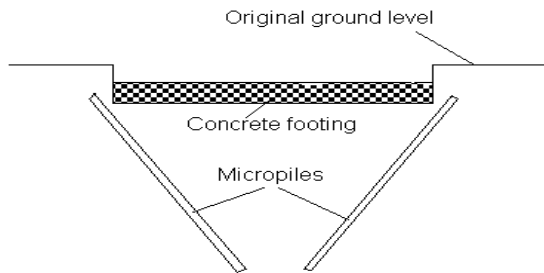


Fig.5 Strengthening of existing foundations

Micropiles are used as soil reinforcement for improvement of vertical and horizontal bearing capacity of soil. Soil is reinforced by introducing adequate nos. of micropile to obtain a composite mass providing higher bearing capacity with corresponding very small settlement (Fig.4 and 5). Reticulated root piles or reticulated micropiles are a special three dimensional network of such piles, which can be used as reinforcement, installed into the ground in several directions producing a composite soil/pile structure. Reticulated micropiles was originated by the necessity of solving a concrete problem, that is how to reinforce the soil adequately in order to allow open air excavation or tunnelling close to existing building without impairing stability of the same. Reinforcements by micropiles or reticulated micropiles also leads to liquefaction counter measures of existing structures and liquefiable ground. A distinguishing feature of micropile methods for seismic retrofitting is that the method can be applied to liquified ground (Nishitani et al 2002).

As in- situ reinforcement, it is used for slope stabilization, for arresting structural settlement, for excavation support in congested areas and as retaining structures. Fig.6 and Fig.7 show these applications.

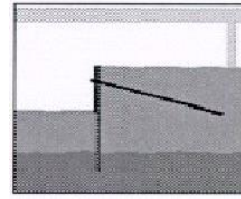


Fig6 Excavation support in congested areas

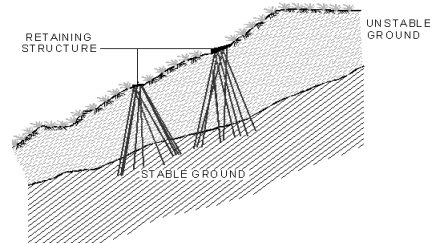


Fig7. Micropiles as slope stabilization and as retaining structures

6. MICROPILE DESIGN

When underpinned or retrofitted the total load on the structure is distributed between the old foundation and new one. Hence it is necessary to determine the total load that can be taken by the old foundation to decide the allowable bearing capacity of micropile.. The original foundation will be supporting the load until new settlement occurs and only at that moment micropile will share the load. After determining the load to be resisted by the micropile one must decide the number of micropile and capacity for each one.

The basic philosophy of micropile design differs little from that required for any other type of pile. The system must be capable of sustaining the anticipated loading conditions with the pile components operating at safe stress level and with resulting displacements falling within acceptable limits. The large cross sectional area in conventional piles results in high structural capacity and stiffness; hence the design is normally governed by the geotechnical load carrying capacity. Due to the micropiles small cross sectional area the micropile design is more frequently governed by structural and stiffness considerations. The emphasis on structural pile design is further increased by the high grout to ground bond capacities that can be attained using pressure grouting techniques.

In 1993, the Federal Highway Administration (FHWA) sponsored a desk study of the state-of-the-practice of micropiles which resulted in a document produced from this study, entitled *Drilled and Grouted Micropiles - State-of-the-Art Review* in 1997. The FHWA further sponsored the development of *Micropile Design and Construction Guidelines, Implementation Manual* containing sufficient information on micropile design, construction specifications, inspection and testing procedures. It contains the details of the design methodologies for structural foundation support and work is under progress to cover design methodologies for in situ slope stabilization.

7. SEISMIC RETROFITTING METHOD

In 1999 in order to develop a seismic retrofitting method and a liquefaction countermeasure method that are not restricted by site conditions, even directly under an existing structure, PWRI, Japan conducted joint research with the Advance Construction Technology Centre and 12 private companies for three years. As a result, three economical micropile methods with superior execution properties have been developed. The first is the High Capacity Micropile method shown in Fig. 8. It is executed by boring a hole in the ground with a boring machine, inserting deformed bars and high strength steel pipes into the ground, then pressure injecting grout into the bearing layer. This method can be executed in all kinds of ground including soft ground, gravel ground and rock. This method is a retrofitting method in the United States.

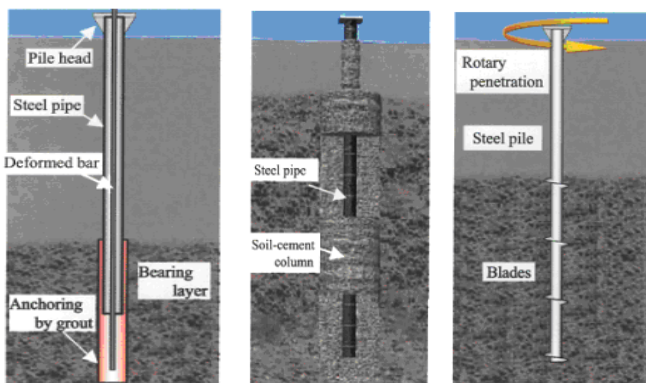


Fig.8. High Capacity Micropile, ST Micropile and Multi Helix Micropile

The second method is the ST Micropile method shown in Fig.8. It is executed by pressure injecting and agitating cement milk to improve the ground, then boring another hole in the middle of the improved ground and inserting a steel pipe, and finally pressure grouting cement milk into the gap between the steel pipe and the wall of the hole. The method does not disrupt the natural ground very much during execution because its first step is ground improvement. The third method is the Multi Helix micropile method and is executed by attaching four blades with different external diameters to the tip of a small diameter steel pipe in a tapered pattern at a fixed interval, then inserting the steel pipe directly into the ground by rotating it (Fig.8)

CONCLUSIONS

Micropile technology has proven to be effective for seismic retrofitting and underpinning of structures. This is due to their small boring diameter which allows their construction with smaller equipments and in limited headroom conditions in very congested areas. This method will be specially suitable for an unplanned congested city like Guwahati where survey and assessment of existing building structures for earthquake vulnerability risk has shown that many existing building structures in Guwahati are vulnerable to earthquake.

REFERENCES

1. B,Sivakumar et al (2004) Bearing capacity improvement using micropiles a case study. In Turner, John P and Mayne, Paul W, Eds. *Proceedings Geosupport 2004, drilled shafts, micropiling, deep mixing, remedial methods, and specialty foundation systems, proceedings of sessions of the geosupport conference: Innovation and cooperation in the geo-industry*, pages pp. 1-8, Orlando, Florida.
2. Lizzi, F. (1978): Reticulated root piles to correct landslides. *ASCE convention and Exposition*, Chicago, Illinois. October 16-20, Preprint 3370, 25 pp.
3. Ting, W.H. and Nithiraj, R. (2000) : Underpinning a Medium Rise building with Micropiles – a case history. Volume – 31, , *Geotechnical Engineering Journal of South East Asia Geotechnical Society Sponsored by Asian Institute of Technology*.
4. Mascardi, C.A. (1982), Design Criteria and Performance of Micropiles, *Symposium on Soil and Rock Improvement*

[Back to table of contents](#)

- Techniques including Geotextiles, Reinforced Earth and Modern Piling Methods.* December, Bangkok, Paper D-3.
5. Nayak, N.V. and Ketkar (1992): Consultancy and Construction capabilities in Geotechnical Engineering Investigation, 13th ICSMFE, New Delhi, 1994.
 6. Nishitani Masahiro, Umebara Takeshi, Fukui Jiro (2002). Development of Seismic retrofitting Technologies for existing foundation. [Http: // www.pwri.go.jp./> eng /Kokusai /conference/ Nishitani 021020-1-pdf-pwri japan.](http://www.pwri.go.jp/~eng/Kokusai/conference/Nishitani%201020-1-pdf-pwri-japan)
 7. O'Neil, M.W. and Pierry, R.F. (1989): Behaviour of mini-grouted piles used in foundation underpinning in Beaumont Clay, Houston, Texas, U.S.A. Proceeding of the International Conference piling and deep foundation London/15, 1 May pp.101-109.
 8. Schlosser, F. and Juran, I. (1979) : Design parameters of artificially improved soils. *ECSMFE*, Vol-5, pp. 197-225. BRIGHTON.
 9. Soliman, N. and Munkofh, G. (1988) : Foundation on drilled and grouted minipiles. A case history. *Proceeding 1st International Geotechnical seminar on deep foundations on Bored and Auger piles, GHENT/7-9 June*, pp.363-369.
 10. Ting, W.H. and Nithiraj, R. (2000) : Underpinning a Medium Rise building with Micropiles – a case history. Volume – 31, *Geotechnical Engineering Journal of South East Asia Geotechnical Society Sponsored by Asian Institute of Technology.*
 11. Yamane, T., Nakata, Y., and Otani, Y. (2000). Efficiency of micropiles for seismic retrofit of foundation system. 12th World Conference on Earthquake Engineering, Auckland, New Zealand, pp.1-8.

Performance Evaluation of Reinforced Concrete Framed Structure with Steel Bracing and Supplemental Energy Dissipation

Swanand Patil¹⁾

i) Student, Department of Earthquake Engineering, Indian Institute of Technology Roorkee, 247667, Uttarakhand, India,

ABSTRACT

In past few decades, seismic performance objectives have shifted from earthquake resistance to earthquake resilience of the structures, especially for the lifeline buildings. Features such as, negligible post-earthquake damage and replaceable damaged components, makes energy dissipating systems a valid choice for a seismically resilient building. In this study, various energy dissipation devices are applied on an eight-story moment resisting RC building model. The energy dissipating devices here include viscous type of devices. The seismic response of the building is obtained for different positioning and mechanical properties of the devices. The placement and mechanical properties of the dampers prove to be a crucial part in modelling, analyzing and designing of the structures with supplemental energy dissipation. The investigation is carried forward to the deficiently ductile RC frame. The design of fluid viscous dampers is presented in a simplified format. The effects of number, placements and damping properties of viscous dampers are discussed. The performance assessment is done on the basis of energy dissipation demand and displacement response of the modeled structures. Nonlinear dynamic analysis shows largely improved displacement response of the modeled structures.

Keywords: earthquake resilient structures, fluid viscous dampers, lifeline buildings, retrofitting of structures, supplemental energy dissipation.

1. INTRODUCTION

Earthquakes, in general, have been historically the major cause of threat to the built environment of human beings. The manmade structures are subjected to wide variety of damage patterns during an earthquake, depending upon the level of deficiency of the structure. However, the same seismic failure patterns of the structures have played a vital role in deciding the design strategy to mitigate future earthquakes better.

The capacity based design, where a measured amount of damage is allowed in predesigned structural components, is dependent upon the ductility of the structure for the seismic energy dissipation. With this approach it is perfectly possible to arrest the collapse of the structure; however the primary structural elements have to be sacrificed. This may not assure a swift post-earthquake functionality until the damaged elements are repaired or rehabilitated.

In past four decades, a gradual yet subtle shift has been observed in seismic design methodologies around the world. The objective of seismic design of structures is changing from earthquake resistance to earthquake resilience, where the structure in consideration remains essentially functional after the design earthquake. The supplemental energy dissipation and base isolation are two strategies which form a major part of these nonconventional methodologies. Both the methods aim at reducing the energy dissipation demand instead of increasing the capacity of the primary structure.

The base isolation technique consists of inclusion of a flexible layer at the foundation level of the structure, which undergoes a significant amount of displacement

during seismic activity. This reduces displacement demand on the structure and the member actions (forces and moments) reduce significantly. Analytically this can be seen as an effect of prolonged period of the base isolated structure. Base isolation system acts in series with the primary structure.

The supplemental energy dissipation aims at reducing the energy dissipation demand on the primary structural elements with the help of externally added devices. A large portion of the seismic energy which stresses, deforms the primary structural element is utilized by these said devices by means of heat transfer. Based on the working, the supplemental energy dissipation system is divided into three parts, active systems, passive systems and semi-active systems. The concentration of this paper is fluid viscous type device, which is a passive system.

The behavior of passive energy dissipation devices can be classified into following groups,

- 1) Displacement dependent or hysteretic,
- 2) Velocity dependent or viscous and
- 3) Other or a mixed behavior.

The fluid viscous damper (FVD) is a velocity dependent device. The applicability and efficiency of FVD has been a matter of research in the structural engineering community. The FVDs are successfully utilized and tested widely throughout the world.

The objective of present work is to assess the performance of FVD installed in an eight story reinforced concrete symmetric frame. The effects of mechanical properties, number of dampers on the structural response is presented. For design of the FVD a simplified design procedure based on the modal analysis of the structure is used.

2 FLUID VISCOUS DAMPERS

2.1 General

The fluid viscous damper as a general shock and vibration mitigation device is well known and one of the prominent example being its use as an automotive shock absorber. The seismic applications of FVD have started taking shape in 1988 in the form of fluid viscous wall (Arima et al., 1988).

Taylor Devices introduced a piston-cell arrangement of FVD, where the piston has orifices (Constantinou et al., 1993). Figure 1 shows general assembly of this type of FVD. The study presented in this paper is concentrated on this type of FVD.

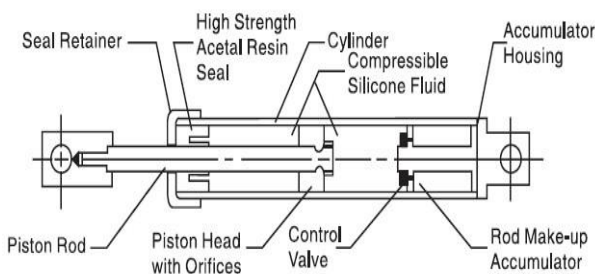


Figure 1. Assembly of fluid viscous damper

2.2 Mechanism

The seismic energy input to the FVD is essentially in the form of mechanical energy. The deformation of a thick, highly viscous fluid because of the piston converts the mechanical energy into heat energy through heat transfer. The flow of this thick fluid through orifices generates viscous drag which is proportional to the relative velocity between the two ends of the device. According to Maxwell model the FVD can be represented as,

$$F = C \operatorname{sign}(v) |v|^\alpha \quad (1)$$

Where, F is force in the damper, C is damping coefficient, v is relative velocity between two ends and

α is velocity coefficient. When $\alpha=1$, the FVD is said to be linear.

2.3 Design method

The design guidelines for the structures employed with FVDs have been provided in FEMA 450, 2003 and specifically for retrofitting of structures with FVDs in ASCE 41, 2013. Christopoulos and Filiatrault (2006) framed the today's knowledge of dissipative devices in their recent book treating also damper design procedures. However, the methods stated above utilise a trial and error procedure. The design procedure presented here has a straight approach with five steps (Silvestry et al., 2010) which are to be performed after the modal analysis of undamped structure. The design steps are as follows:

Step1. Determination of the target damping ratio of the structure on the basis of a chosen target level of structural performances

Step2. Identification of the tentative characteristics of the linear viscous dampers for preliminary design, i.e., first dimensioning of the linear damping coefficients

Step3. Development of a series of preliminary time-history analyses of the building structure equipped with viscous dampers identified in Step 2.

Step4. Identification of the characteristics of the "equivalent" nonlinear viscous damper i.e., identification of a system of manufactured viscous dampers capable of providing the structure with actions (on the structural members) comparable to those obtained in Step 3 using the linear viscous dampers identified in Step 2.

Step5. Development of a series of final time-history analyses of the building structure equipped with the viscous dampers identified in Step 4. This last step being necessary in order to verify the effectiveness of Step 4 and obtain actions both on the structural members and on the dampers to be used for the final design specifications.

The design procedure will be applied as stated for the structure under consideration in following sections.

3 CASE STUDY

3.1 Specifications

The model structure considered here is a symmetric two-bay by two-bay eight story frame. The reinforcement used is Fe415 while the concrete mix is M30. The bay length is 3m each. The story height is 3m each.

Table 1 gives the specifications regarding the structural elements used in the model.

For the design of fluid viscous damper properties as discussed in above steps, a modal analysis of the structure without dampers is carried out. The first mode characteristics are used for the design of FVD. The damping ratio of the structure is initially assumed as 5%.

Table 1. Specifications of elements

Element	Cross Section (mm)	Reinforcement (mm ²)
Beam	250*200	150.769 (T) 84.823 (C)
Ground story column	300*300	1608.500
Other than ground story column	300*300	904.779
Bracing to install FVD	75*75*4	Nil

3.2 Design of FVD for given structure

The preliminary time-history analysis is needed as we have to know the maximum story displacement. As a seismic input, El Centro, 1940 time-history record is used in this study. The analysis is done in x-direction only. The non-linear dynamic analysis gives maximum displacement of 0.2323m at roof level.

The modal analysis of the structure gives the fundamental period of structure as 2.07473 seconds. According to step 1 discussed in section 2.2, let the target displacement be 0.10m.

$$\eta = \delta_{\text{target}} / \delta_{\text{max}} \quad (2)$$

The relationship between η and target damping ratio, is used to get target damping ratio (Silvestry et al., 2010) as 55%

From simplified relation between modal damping, modal mass and fundamental frequency, the damping coefficient is worked out as 32780.74 KN.s/m. Equation (3) gives the simplified form of the used relation, where ω_1 is fundamental frequency, N is number of floors and M_{total} gives total seismic weight.

$$C_{\text{story}} = \omega_1 M_{\text{total}} (N+1) \xi \quad (3)$$

The number of dampers in each floor is four, for X-direction. This gives damping coefficient for each damper as 8200 KN.s/m. After first time-history analyses, the damper properties are kept unchanged as the results obtained were desirable.

For the numerical analysis purpose, eight different arrangements are tested. All the dampers are applied in x-direction.

Table 2. Arrangements of FVD

Number of floors damped	Number of dampers	Designation
0	0	BF
2	8	FVD-08
3	12	FVD-12
4	16	FVD-16
5	20	FVD-20
6	24	FVD-24
7	28	FVD-28
8	32	FVD-32

4 RESULTS AND DISCUSSION

4.1 Displacement response of the structures

After applying the designed FVDs in the structure, the displacement response reduces significantly. The target displacement is achieved very conservatively.

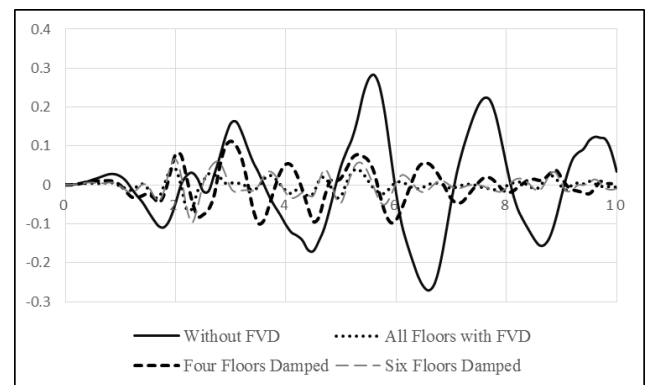


Figure 2. Displacement response

The maximum displacement of the roof node decreases with increase in number of FVDs.

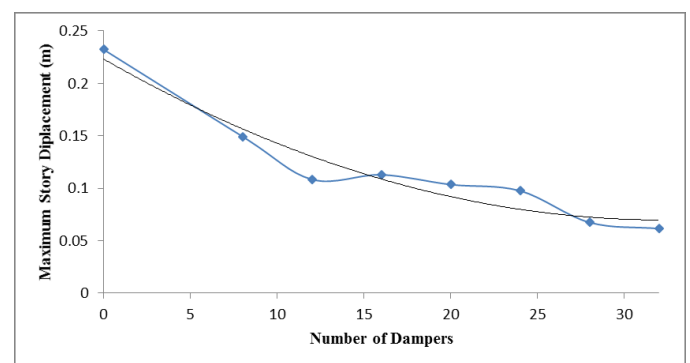


Figure 3. Maximum roof displacement

The reduction obtained is as high as 70% for 32 FVDs.

4.2 Energy dissipation response

For a linear viscous damper, the energy dissipated is proportional to the input seismic energy. From figure 4, it can be seen that a large amount of input energy is diverted to the FVDs installed, thus reducing the energy

dissipation demand on the primary structural elements. Note that the fluid viscous damper installed in a story acts in parallel with the story.

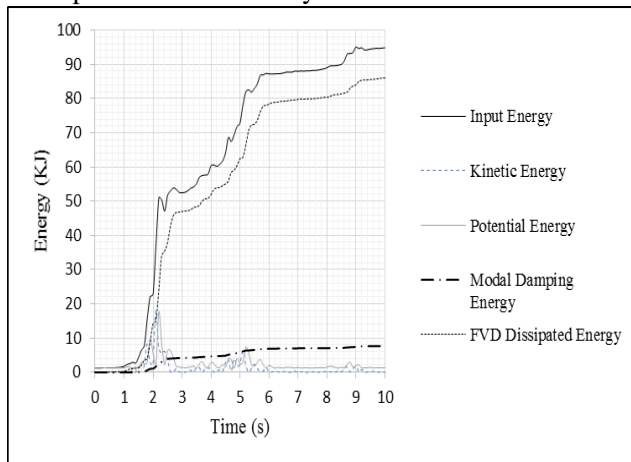


Figure 4. Energy dissipation response of FVD-32

For every arrangement from table 2, energy response is evaluated and following results were obtained. The represented energy is at 10 seconds, which is the maximum value.

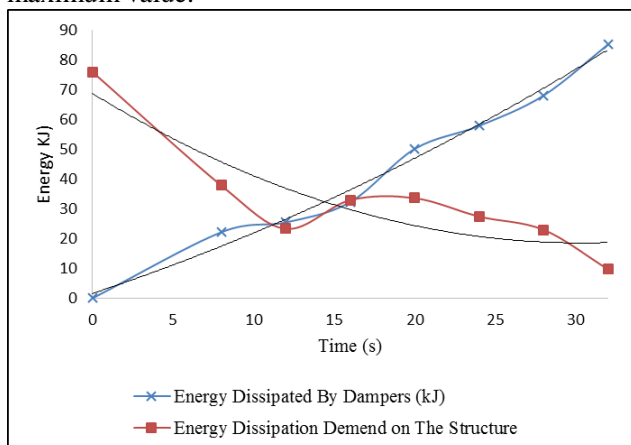


Figure 5. Effect of number of FVDs on energy dissipation demand

4.3 Response of FVD to the seismic excitation

For a linear velocity dependent damper, the force generated is out of phase with the seismic deformations. Hence the effect of damper forces are not additive to the structural forces, rather this out of phase behavior helps in increasing the efficiency if velocity dependent devices. Figure 6 shows the decrease in axial force because of FVD installation.

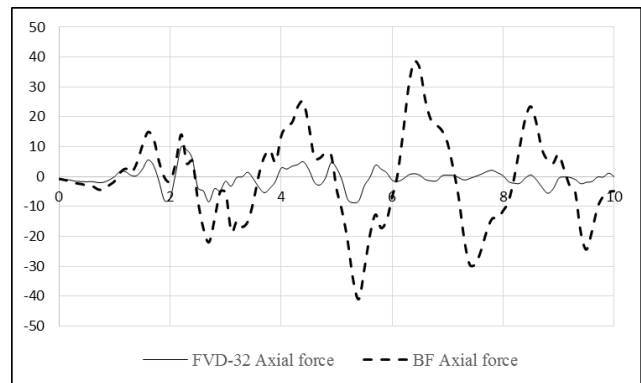


Figure 6. Axial force response history of bottom story column

For given structural arrangement, the bracing and FVD act in series. Here the stiffness of damper is taken infinite as the viscous fluid is ideally incompressible. Thus the stiffness of the system is same as the axial stiffness of bracing. This gives a steady rise in maximum damper force with increase in number of FVDs, as can be seen in figure 7.

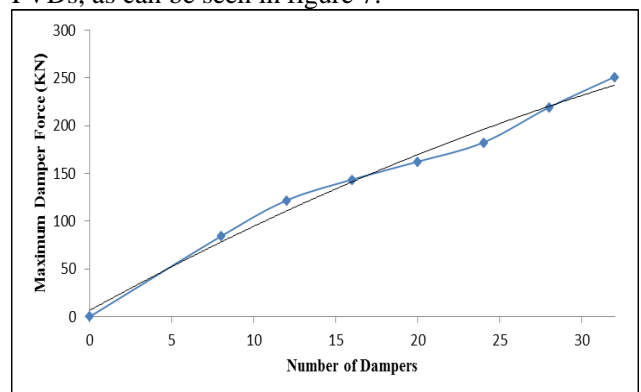


Figure 7. Maximum damper force in various arrangements

For cost optimization, damper force should be minimal. This trade-off can be achieved between velocity exponent (α), damping coefficient and damper force. Further refinements in design can reduce the costs with same target displacement.

5 CONCLUSION

The displacement based design methodology as suggested by Silvestri et al. is found valid for the studied model. Moreover, the response obtained is more on conservative side, which can be optimized with further refinements.

Due to increased damping of the order of 50%, the displacement response of the structure is effectively decreased giving ample space for fulfilling the seismic performance objectives. Also the out of phase nature of velocity dependent devices with respect to the seismic displacements reduces the forcing actions on the primary structural elements.

Because of the high amount of seismic energy dissipation by the viscous dampers, it is possible that

the primary structural members remain in linear range. This proves the applicability of the FVDs where uninterrupted post-earthquake functionality of a structure is required. Thus the fulfillment of seismic resilience objective is possible with the installation of fluid viscous dampers.

[Back to table of contents](#)

ACKNOWLEDGEMENTS

The technical consultation and personal discussions with Prof. Dr. Pankaj Agarwal (Department of Earthquake Engineering, IIT Roorkee) have played a vital role in shaping this document. I thank him for his valuable contributions.

REFERENCES

- 1) Constantinou, M. C. and Symans, M. D. "Experimental and Analytical Investigation of Seismic Response of Structures with Supplemental Fluid Viscous Dampers." Tech Rep. NCEER-92-0027, National Centre for Earthquake Engineering, Research, State Univ. of New York (SUNY) at Buffalo, N.Y.1992
- 2) FEMA 450, NEHRP, Guidelines & commentary for seismic rehabilitation of buildings, October, Washington DC. (2003)
- 3) Hwang., J. S. "Seismic Design of structures with viscous dampers", International Training Programs for Seismic Design of Building Structures hosted by National Center for Research on Earthquake Engineering sponsored by Department of International Programs, National Science Council, January 21-25, Taipei, Taiwan, 2002
- 4) Lin W.H. and Chopra A.K. (2002). Earthquake Response of Elastic SDF Systems with Non-Linear Fluid Viscous Dampers. *Earthquake Engineering and Structural Dynamics*, **31**, 1623-1642.
- 5) Miyamoto, H. K., Gilani, A. S. and Wada, S. "State of the art design of steel moment frame buildings with dampers", The 14th World conference of earthquake engineering, October 12-17, Beijing, China 2008
- 6) Soong, T. T., Dargush, G. F. Passive Energy Dissipation Systems in Structural Engineering, ISBN 0-471-968121-8, John Wiley and Sons, Inc.
- 7) Stefano Silvestri ,Giada Gasparini & Tomaso Trombetti, A Five-Step Procedure for the Dimensioning of Viscous Dampers to Be Inserted in Building Structures (2010), *Journal of Earthquake Engineering*, 14:3, 417-447, DOI: 10.1080/13632460903093891

Seismic Behaviour of Bi-Symmetric Buildings

Mayur Pisodeⁱ⁾, Yogendra Singhⁱⁱ⁾

i) M.Tech. Student, Department of Earthquake Engineering, IIT Roorkee, Roorkee -247667, India.
ii) Professor and Head, Department of Earthquake Engineering, IIT Roorkee, Roorkee -247667, India.

ABSTRACT

The draft revision of IS:1893 proposes a separation of more than 15% between the frequencies of the fundamental modes in the two directions. This is intended to avoid the swapping of energy from one translational mode to another due to coupling. This may be expected in case of bi-symmetric buildings (buildings with structural properties and periods approximately equal in the two directions). This Study explores the seismic behaviour of bi-symmetrical buildings under uniaxial and bi-axial ground motions. For this purpose, two different configurations of 8 storey buildings symmetric in plan are modelled. The first building has square columns, resulting in identical periods in the two directions, whereas the second building, with rectangular columns has a difference of 20% in periods in orthogonal directions. The numerical analysis of the seismic response of these two buildings is performed using a set of 22 ground motions from PEER NGA database and scaled as per FEMA P695 guidelines to represent the same level of intensity corresponding to the Design Basis Earthquake. The results are analyzed in terms of the displacement-time response of the buildings at roof level and corresponding maximum inter-storey drift ratios. The results show that no coupling of translational modes is observed for the considered buildings.

Keywords: Bi-symmetric buildings, Design code, Dynamic coupling, Seismic response, Multi-storey buildings

1. INTRODUCTION

Damages to structures during earthquakes continue to provoke more efforts from structural engineers towards better seismic performances. In a typical software oriented structural analysis, structural model is prepared using appropriate elements. For a framed building, modelling comprises of beam and column and a rigid diaphragm to account for the in-plane rigidity of slab at each floor. Usually in computer oriented structural analysis; three-dimensional models of buildings are used. After achieving a reasonably good structural model, next stage is to use appropriate analysis method for seismic response. IS 1893(Part D):2002, is the standard used for calculating earthquake loads on the structures. In this paper Response Spectrum Analysis is used, wherein, from the structural model of the building, natural frequencies and natural modes are obtained. Using the natural frequencies and mode shapes, static earthquake loads and response in each mode are obtained.

2. MODAL COUPLING PHENOMENON

Modal Coupling occurs when vibrational energy is swapped from one mode of vibration to another. The medium for such a coupling can be through the fundamental torsional mode, or it may be caused by

geometric coupling. In the former case, in which energy is swapped into the torsional mode and then into the translational orthogonal mode, it is sufficient that the natural frequencies of the torsional and translational modes are close. In case of geometric coupling, the necessary precondition is that the centre of torsion is offset from the geometric centre of the building.

This paper examines the coupling between the modes of the bi-symmetric building. For this purpose two 8 storey bi-symmetric buildings with symmetry in plan are modelled and designed using IS456:2000. First building consists of square columns with mass distributed uniformly on the perimeter of the building to make it torsionally flexible while the second building consists of rectangular columns. The seismic behavior of these buildings is studied under uniaxial and bi-axial ground motions from PEER NGA database.

Consider a building with 8 floors and plan as shown in Figure 1. The building is symmetric about both the axes. Beam Size of 300mm x 400 mm and column size of 350mm x 350mm for the 8th and 7th floor, 400mm x 400mm for 6th and 5th floor, 450mm x 450mm for 4th and 3rd floor, 550mm x 550mm for 2nd and 1st floor are used for design.

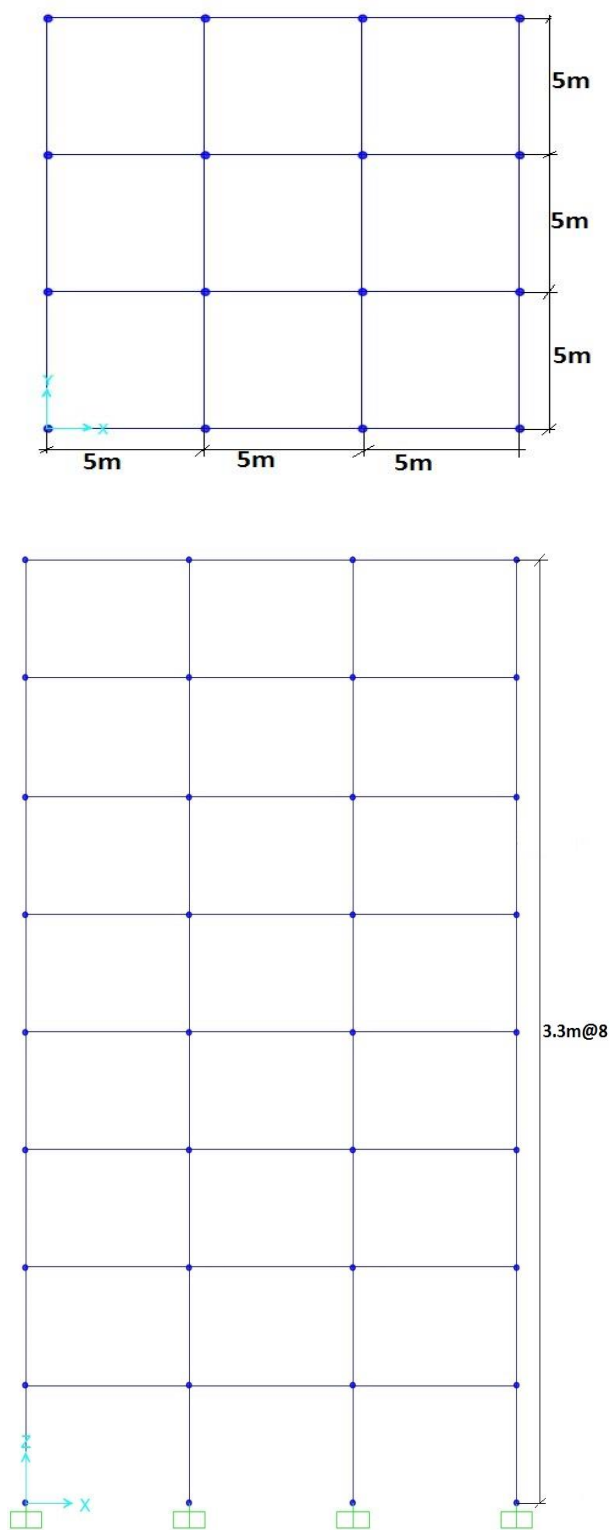


Fig. 1. Geometric details of the building

Grade of concrete used is M20 and grade of steel used is Fe415. Rigid Diaphragm for in-plane rigidity is applied at all the floor levels. Dead load of infills, slab and live load is applied on the beams. The building is analyzed using Response Spectrum Analysis. Seismic Zone V of IS 1893(Part I):2002 with hard soil is considered. The importance factor (I) is 1.0 and the

Response Reduction Factor is 5.0. The results of free vibration analysis are shown in Table 1.

Table1. Modal mass and natural periods of building with square columns

Mode No.	Period (Seconds)	Modal Mass (%)	
		M _x	M _y
1	3.18	0	0
2	3.1	0	74
3	3.1	74	0
4	1.11	0	0
5	1.05	8.8	2.3
6	1.05	2.3	8.8

From Table 1, it is seen that first mode is a torsional mode. In 2nd and 3rd mode period is same and modal mass in X and Y direction got interchanged in these two modes and hence there is no coupling whereas there is slight coupling between the two orthogonal modes in 5th and 6th mode. For the building considered above, there is symmetry in both the horizontal directions and the dynamic properties in the two orthogonal directions are similar since the columns are of square type. If rectangular columns of size 450mm x 800mm for 1st and 2nd floor, 350mm x 700mm for 3rd and 4th floor, 350mm x 650mm for 5th and 6th floor, 300mm x 500mm for 7th and 8th floor are used in the building considered above, the free vibration analysis results are shown in table 2. Also this building is designed in such a way that there is a variation of more than 15% between the periods of two orthogonal modes, same can be observed from Table 2.

Table 2. Modal mass and period of building with Rectangular columns

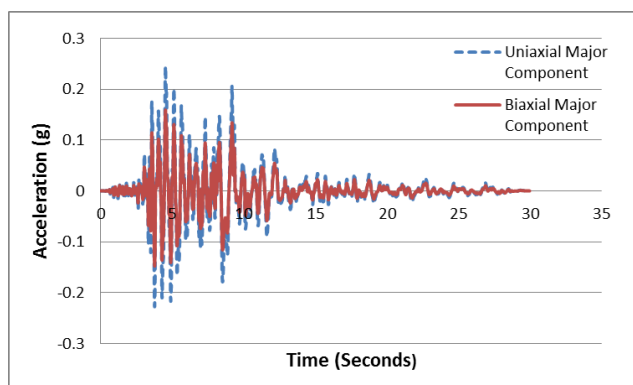
Mode No.	Period (Seconds)	Modal Mass (%)	
		M _x	M _y
1	3.26	0	75
2	2.75	73	0
3	2.49	0	0
4	1.11	0	11
5	0.85	12	0
6	0.83	0	0

From Table 2, it is seen that in 1st mode mass is excited in Y-direction only and in 2nd mode mass is excited in X-direction only and there is no coupling between the two orthogonal modes of the building.

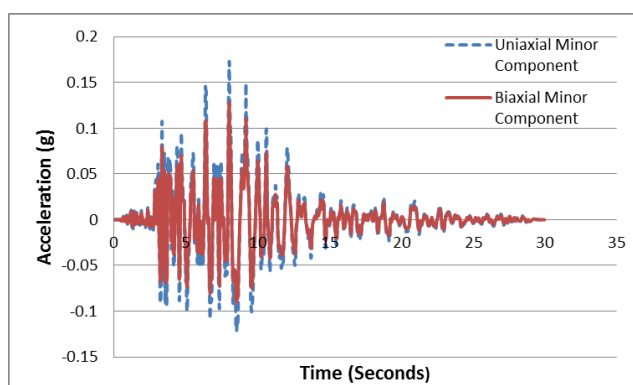
3. Dynamic Analysis

Dynamic analysis of the buildings considered above is performed using FEMAP695 guidelines. For this purpose, a set of 22 ground motions obtained from PEER NGA database are used. Individual records of the set are normalized by their respective peak ground velocities to remove unwarranted variability between

records due to inherent differences in event magnitude, distance to source, source type and site conditions. Then the ground motions are scaled to represent the same level of intensity corresponding to the Design Basis Earthquake. Scaled ground motion record of Northridge Earthquake (1994) is shown in Figure 2 for the building with square columns. In case of biaxial motion, for each pair of horizontal ground motions a square root of the sum of the squares (SRSS) of the spectral acceleration at fundamental period is taken to obtain the median of all the 22 records and this median value is then divided by the target spectral acceleration value corresponding to Design Basis Earthquake to get the scale factor. While for uniaxial motion, the spectral acceleration of individual ground motion at the fundamental period is directly divided by the target spectral acceleration value corresponding to Design Basis Earthquake to get individual scale factors. Due to this difference of scaling of records for biaxial and uniaxial motion the Peak Ground Acceleration in case of uniaxial is higher than the biaxial motion as can be seen from Figure 2 and Figure 4 for buildings with square columns and rectangular columns.



a) Major Component of ground motion

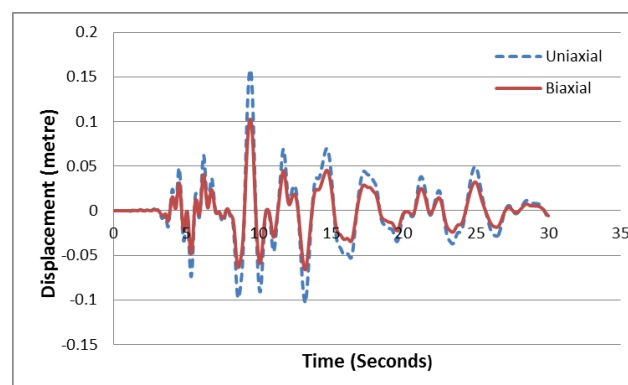


b) Minor Component of ground motion

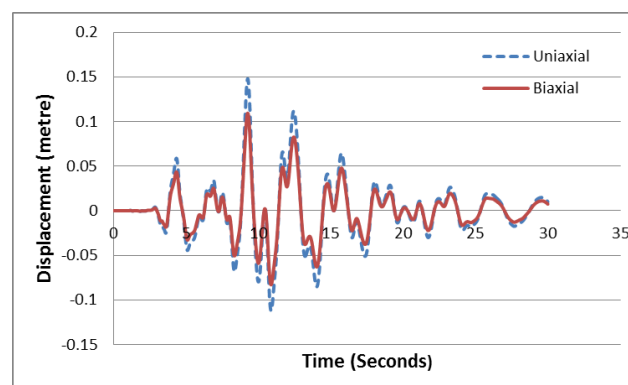
Fig. 2. Scaled Ground motion record of Northridge Earthquake (1994) for building with square columns: (a) Major component; and (b) Minor component

In uniaxial motion, the major component of ground motion is applied in Y-direction of the building and the

minor component is applied in X-direction separately whereas in Biaxial, the major and minor components are applied in Y and X-direction simultaneously for the building with square columns. In case of building with rectangular columns, the major and minor component of ground motion are applied in X-direction as well as in Y-direction for uniaxial motion since the dynamic properties are different in the two directions and hence the seismic response to these ground motions will be different in the two orthogonal directions as can be seen from Figure 5, while for biaxial motion the major and minor components are applied in X and Y-direction simultaneously. The seismic response of the buildings to these ground motions is recorded in terms of the displacement time history at roof level and the maximum inter-storey drift ratio. The displacement time history at roof level for the building with square columns subjected to uniaxial and biaxial ground motion corresponding to Northridge Earthquake is shown in Figure 3. Similar results have also been obtained for the other 21 time histories, but not shown here for brevity.



a) Displacement time history in Y- direction for major component of ground motion



b) Displacement time history in X-direction for minor component of ground motion

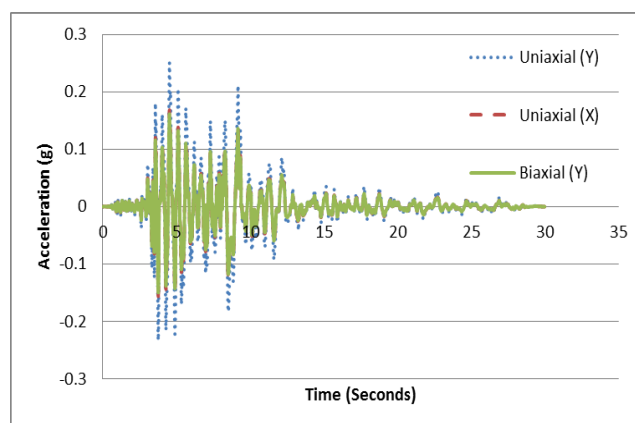
Fig.3. Displacement time history for building with square columns subjected to uniaxial and biaxial ground motion record of Northridge Earthquake (1994).

Table3. Maximum inter-storey drift ratio in percentage for building with square columns

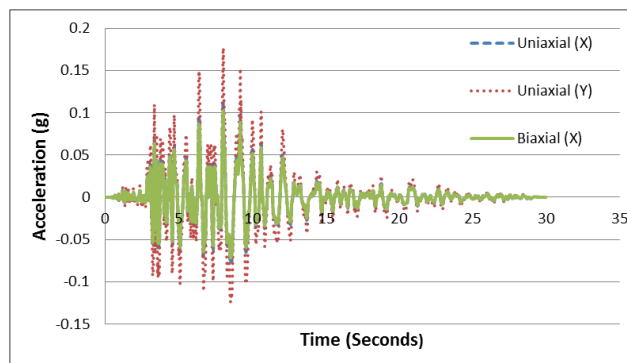
Ground Motion	Biaxial Drift Ratio (%)		Uniaxial Drift Ratio (%)	
	X	Y	X	Y
1	0.97	1.17	1.32	1.80
2	1.13	0.99	1.41	1.59
3	1.10	1.54	0.87	1.77
4	0.93	1.40	1.92	1.77
5	1.85	1.71	1.31	1.73
6	1.27	0.85	1.05	1.26
7	0.99	0.86	1.94	1.68
8	1.42	0.68	1.97	1.73
9	1.65	0.98	0.96	1.19
10	0.75	0.86	1.81	1.48
11	0.94	0.81	1.15	1.23
12	0.65	0.92	1.70	2.68
13	1.27	0.98	2.87	3.61
14	0.69	1.21	1.25	1.41
15	0.87	1.28	1.18	0.81
16	0.78	0.89	1.29	0.92
17	1.11	1.15	1.38	1.23
18	1.11	0.96	2.84	3.04
19	1.46	1.21	0.44	0.50
20	0.85	1.01	2.01	2.21
21	2.15	0.99	2.80	2.78
22	0.73	1.11	3.27	4.41
Median	1.04	0.99	1.40	1.70

From Table3, it is seen that the inter-storey drift ratio for biaxial motion is less than the drift ratio for uniaxial motion since the Peak Ground Acceleration value is less in case of biaxial ground motion as shown in Figure 2.

From Figure 4, it can be seen that the peak ground acceleration for uniaxial motion is higher than the biaxial motion for both the components of ground motion due to which the roof displacement is higher in case of uniaxial motion than the biaxial ground motion.



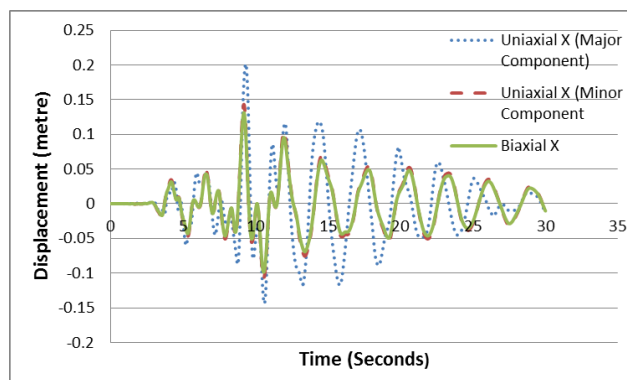
a) Major Component of ground motion



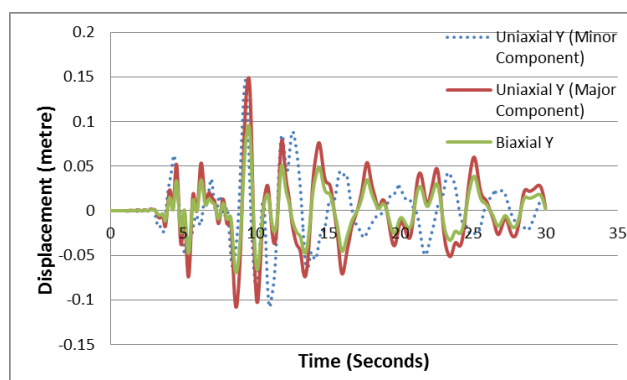
b) Minor Component of ground motion

Fig. 4. Scaled Ground motion record of Northridge Earthquake (1994) for building with rectangular columns: (a) Minor component; and (b) Major component

Figure 5 shows displacement time history for building with rectangular columns subjected to above ground motion.



a) Displacement time history for ground motion in applied in X-direction



b) Displacement time history for ground motion applied in Y-direction

Fig. 5. Displacement time history for building with rectangular columns subjected to uniaxial and biaxial

ground motion record of Northridge Earthquake (1994).

Table4. Maximum inter-storey drift ratio in percentage for building with rectangular columns

Sr. No	Biaxial Drift Ratio (%)		Uniaxial Minor Component Drift Ratio (%)		Uniaxial Major Component Drift Ratio (%)	
	Y	X	Y	X	Y	X
1	1.14	1.30	1.25	1.47	1.76	2.03
2	0.82	1.15	0.89	1.54	1.32	1.78
3	0.97	1.57	0.85	0.72	1.67	1.76
4	0.46	1.60	1.19	2.26	1.32	2.35
5	1.22	1.52	1.24	1.05	1.08	1.45
6	0.98	1.02	1.04	0.99	1.06	1.33
7	0.90	1.02	1.25	1.83	1.31	2.01
8	1.08	0.94	1.42	2.38	1.51	2.65
9	0.67	1.07	0.81	0.98	0.83	1.24
10	0.49	1.17	1.75	1.84	1.43	2.14
11	0.77	0.85	1.04	1.31	0.94	1.17
12	0.60	1.45	2.55	1.46	2.06	4.05
13	0.70	1.24	1.28	3.35	1.98	4.27
14	0.62	1.28	1.77	1.25	0.81	1.5
15	0.66	1.22	0.77	1.33	0.73	0.79
16	0.58	0.87	0.88	1.62	0.77	0.90
17	0.98	1.22	1.21	1.36	1.12	1.26
18	0.62	1.01	1.40	3.04	2.75	3.03
19	0.98	1.53	0.44	0.45	0.41	0.60
20	0.49	0.97	1.18	2.08	1.69	2.09
21	1.26	1.12	2.49	2.98	2.39	3.02
22	0.57	1.37	2.51	3.45	3.26	5.17
Median	0.74	1.19	1.23	1.51	1.32	1.89

From Table 4, it is seen that the maximum inter-storey drift ratio is lesser in case of biaxial ground motion than the uniaxial ground motion since the peak ground acceleration in case of biaxial motion is less than the peak ground acceleration in case of uniaxial motion.

4. CONCLUSION

From the dynamic analysis of the two buildings it can be observed that there is no evidence of swapping of energy between translational modes due to coupling between the two orthogonal modes of the building as the inter-storey drift ratio in case of uniaxial and biaxial ground motions, are of comparable magnitude. Also, the inter-storey drift ratio is higher in case of uniaxial ground motion than the biaxial ground motion since the Peak Ground Acceleration is higher in former case. Behaviour of the two buildings, viz. with square

columns (having identical dynamic characteristics in the two directions) and rectangular columns (having more than 15% difference in the fundamental period in the two directions) is essentially similar.

REFERENCES

- 1) Chopra A. K., Dynamics of Structures: Theory and Application to Earthquake Engineering, Prentice Hall Publication, Englewood Cliff, N.J. 1995.
- 2) FEMA P695, "Quantification of Building Seismic Performance Factors", Federal Emergency Management Agency, Washington, D.C.
- 3) IS 456(2000), "Indian Standard for Plain and Reinforced Concrete Structures", Bureau of Indian Standards(BIS), New Delhi.
- 4) IS 1893(2002), "Indian Standard for Earthquake Resistant Design of Structures", Bureau of Indian Standards(BIS), New Delhi.
- 5) PEER NGA, "Ground Motion Database", Pacific Earthquake Engineering Research Centre, University of California, Berkeley
- 6) SAP-2000 (2016), Structural Analysis Software, "Static and Dynamic Finite Element Analysis of Structures", Computers and Structures, Inc., Berkeley, USA.

[Back to table of contents](#)

Influence of sand and rock quarry dust addition on compaction properties of clay

Manash P. Baruahⁱ⁾, Malaya Chetiaⁱⁱ⁾ and Asuri Sridharanⁱⁱⁱ⁾

i) Former P.G. Student, Department of Civil Engineering, Assam Engineering College, Guwahati 781-013, India.

ii) Assistant Professor, Department of Civil Engineering, Assam Engineering College, Guwahati 781-013, India.

iii) Honorary Scientist, Indian National Science Academy, Formerly, Professor, Department of Civil Engineering, Indian Institute of Science, Bangalore 560-012, India.

ABSTRACT

Soil stabilization methods are adopted for improving the geotechnical properties of soil considered unsuitable for construction. One of the oldest methods is to add graded aggregate material to soil followed by compaction that improves the support quality of soil and is economically viable. Sand has served this purpose for decades but the vast field of application of sand leads to its shortage. Rock quarry dust, a solid waste produced during crushing operations of stones and rocks to obtain aggregates can be used in geotechnical applications in place of sand due to similarity in mineral composition and inertness in coarse grained structure. Also bulk utilization of this waste has become necessary due to its large scale production and geo environmental problems related to its disposal. The objective of this paper is to investigate the influence of sand and quarry dust addition on the compaction behavior of clay, to ensure the mass utilization of this waste for increasing support capacity of soil, replacement of sand in such applications and to determine the clay type where maximum improvement can be achieved in terms of compaction properties.

Keywords: clay, sand, rock quarry dust, mix, compaction properties, influence

1. INTRODUCTION

The scarcity of sites having good bearing capacity soil has forced the construction industry to make use of existing site condition by improving the geotechnical properties of existing unsuitable soil, which is done by adopting soil stabilization methods. Graded aggregate material addition to soil followed by compaction is one of the oldest methods of mechanical stabilization of weak soil deposits. This practice leads to increased strength, decreased plasticity, improves support capability of soil and also provides material economy. Naturally available sand has been serving this purpose for decades. But the use of sand is not only limited to geotechnical applications, it is also used in building construction, glass industry etc. The result is over exploitation of river beds and possibility of scarcity of this material in near future. Efforts have been made to find suitable substitute for it. Quarry dust is the waste product obtained during crushing operations of stones to obtain aggregates and its disposal causes many geo environmental problems. Due to comparable mineral composition to that of sand and inertness of coarse grained structure researchers have come out with the idea of utilization of quarry dust for partial or full replacement of sand in soil stabilization and other applications by bulk and effective utilization of this waste alone or with some admixtures with a motive to stabilize soil. Compaction of soil is carried out to improve soil densification. Compaction reduces volume

of air voids in the soil that leads to an increase in the shear strength and a decrease in the consolidation and the permeability characteristics of soils. The compaction parameters, maximum dry density (MDD) and optimum moisture content (OMC) are important in most of the practical situations needing densification of soil, such as embankments, highway and railway sub grades and foundation soils. Most of the earlier studies were concentrated on the effect of dust content on moisture content and dry density of soils. Soosan et al. (2005) have studied the effect of different percentages of quarry dust on compaction characteristics of three different soils and observed an increase in MDD values and decrease in OMC values with increase in dust content in the soil-dust mixes. The optimum range of quarry dust content in soil was found to be 40-60%. Sridharan et al. (2006) found similar results of increase in MDD and decrease in OMC with increase in quarry dust content in his study on variation of shear strength characteristics of soil on addition of quarry dust. Sarvade and Nayak (2014) in their investigation on behavior of lithomargic clay stabilized with quarry dust and cement obtained similar results. A significant volume of research work has been done by various researchers on the various aspects of the compaction properties of clay-quarry dust mixes. However comprehensive studies on the effect of clay type on laboratory maximum density and optimum moisture content of clay-quarry dust appeared to be very limited and are not compared with that of clay-sand mixes. It

seems important, for practical purposes, to know the clay type where bulk disposal of this waste quarry dust can be carried out with maximum improvement in compaction properties for a minimum compacting effort. The objective of this paper is to investigate the influence of sand and quarry dust addition on the compaction behavior of clay, to ensure the mass utilization of this waste for increasing support capacity of soil, replacement of sand in such applications and to determine the clay type where maximum improvement can be achieved in terms of compaction properties.

2. EXPERIMENTAL INVESTIGATIONS

Initially two clay samples, locally available clay (denoted by C) and commercially available bentonite (denoted by B), rock quarry dust (denoted by Q1) and sand (denoted by S1) samples are collected. The samples were subjected to different physical tests by following the guidelines provided by the respective Indian standard (IS) code, the results of which are presented in Table 1. According to IS soil classification system, the quarry dust and sand samples were poorly graded (SP) and clay sample was inorganic clay of medium compressibility (CI), and bentonite was inorganic clay of high compressibility (CH). Shape and mineralogical characterization of the sand and quarry dust samples were carried out from the petrographical images (BS 1994) taken with the help of electron microscope (25 \times) as shown in Fig.1, which indicate that the main mineral present in the samples was quartz. In addition to quartz significant amount of feldspar is present in quarry dust sample. Particles of quarry dust sample exhibits sub angular to angular shape whereas that of sand exhibits sub rounded to rounded shape.

Table 1. Physical properties and classification of the collected samples used in the study.

Property	Sample			
	C	B	Q1	S1
<u>Specific gravity</u>	2.61	2.67	2.71	2.65
<u>Grain size characteristics (%)</u>				
Sand (4.75-0.075 mm)	12.5	0.70	79.2	96.90
•Coarse sand (4.75-2.00 mm)	2.80	-	10.33	7.05
•Medium sand (2-0.425 mm)	5.45	-	28.67	60.7
•Fine sand (0.425-0.075 mm)	4.25	0.70	40.2	29.15
Fines (<0.075 mm)	87.5	99.30	13.6	0.60
•Silt (0.075-0.002 mm)	65.67	34.59	13.6	0.60
•Clay (<0.002 mm)	21.83	64.71	-	-
Uniformity coefficient (C_u)	-	-	8.83	3.23
Coefficient of curvature (C_c)	-	-	0.91	1.08
<u>Atterberg limits (%)</u>				
Liquid limit (w_L)	42.4	130.5	-	-
Plastic limit (w_p)	20.2	48.9	-	-
Plasticity index (I_p)	22.2	81.6	-	-
IS classification	CI	CH	SP	SP

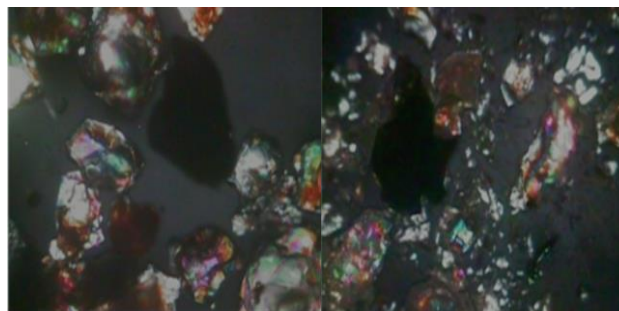


Fig. 1. Petrographic images of sand sample (left) and rock quarry dust sample (right)

In order to achieve the objectives of present study efforts have been taken to prepare a quarry dust sample Q_{S1} having grain size similar to sand sample S1.

The desired soil mixes for the study were prepared by adding quarry dust and sand samples to both clays in different proportions of dry weight of the soil mixes in dry condition. The soil mixes prepared are presented in Table 2. A soil mix prepared with nine parts of clay 'C' and one part sand 'S1' by dry weight of mix is designated as C-S1 (90:10). In similar manner other soil mixes as presented in Table 2 are designated. 8 soil mixes prepared with low compressibility clay C were kept for curing duration of 24 hours and 6 soil mixes prepared with high compressibility clay B were kept for 3 days for curing prior to light compaction test as per IS (1974) along with C and B samples.

Table 2. Designation of soil mixes prepared.

C-S mixes	C- Q_{S1} mixes	B-S1 mixes	B- Q_{S1} mixes
C-S1 (90:10)	C- Q_{S1} (90:10)	B-S1 (85:15)	B- Q_{S1} (80:15)
C-S1 (80:20)	C- Q_{S1} (80:20)	B-S1 (70:30)	B- Q_{S1} (70:30)
C-S1 (70:30)	C- Q_{S1} (70:30)	B-S1 (55:45)	B- Q_{S1} (55:45)
C-S1 (60:40)	C- Q_{S1} (60:40)		

3 RESULTS AND DISCUSSION

Figures 2 and 3 show the moisture content versus dry density plots for C-S1 and C- Q_{S1} mixes.

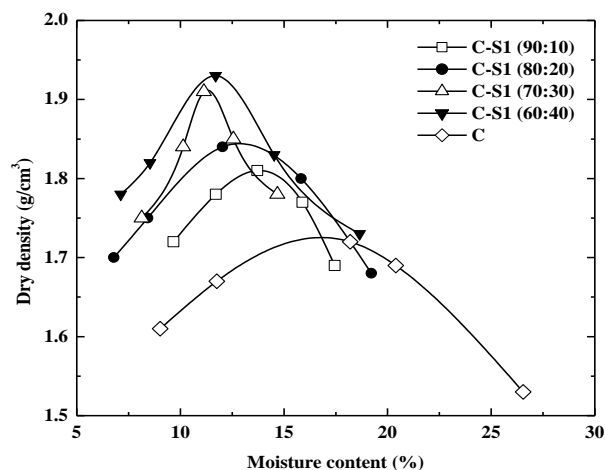


Fig. 2. Compaction curves for C and C-S1 mixes.

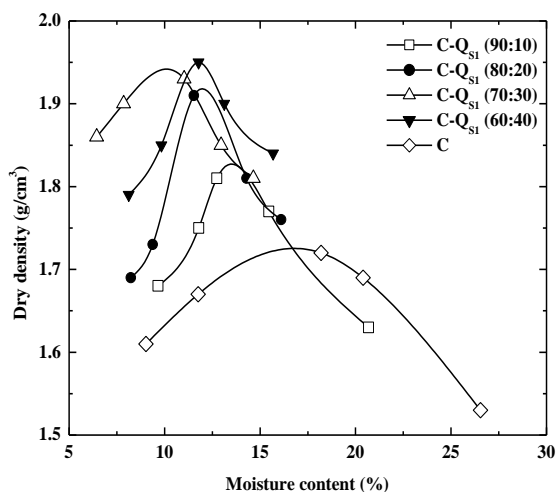


Fig. 3. Compaction curves for C and C-Q_{S1} mixes.

Compaction curves for B-S1 and B-Q_{S1} are shown in Figures 4 and 5 respectively.

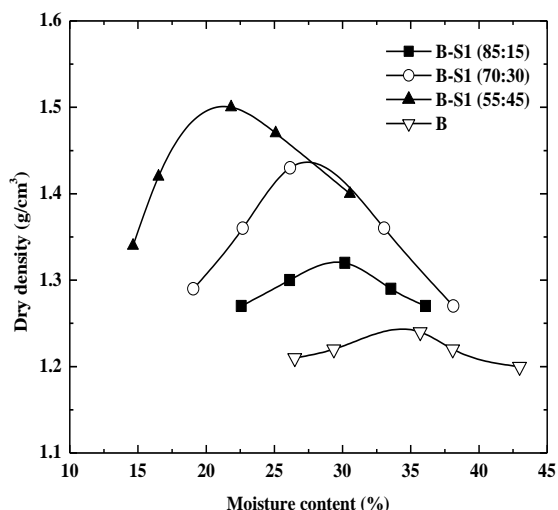


Fig. 4. Compaction curves for B and B-S1 mixes.

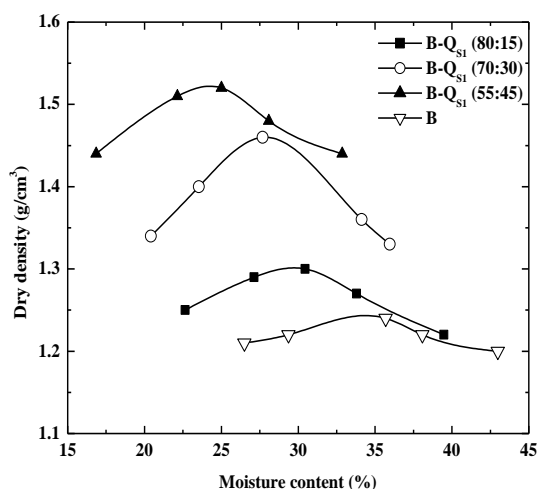


Fig. 5. Compaction curves for B and B-Q_{S1} mixes.

The compaction characteristics obtained from compaction curves of various soil mixes are presented in Table 3

Table 3. Compaction characteristics and percentage improvement in compaction characteristics of soil mixes.

Soil/Soil mix	OMC (%)	MDD (g/cm ³)	Percentage improvement in	
			OMC	MDD
C	18.2	1.73	0	0
C-S1 (90:10)	13.77	1.81	-24.34	4.62
C-S1 (80:20)	12.50	1.84	-31.32	6.36
C-S1 (70:30)	11.14	1.91	-38.79	10.40
C-S1 (60:40)	11.70	1.93	-35.71	11.56
C-Q _{S1} (90:10)	12.74	1.82	-30.00	5.20
C-Q _{S1} (80:20)	11.54	1.91	-36.59	10.40
C-Q _{S1} (70:30)	11.03	1.93	-39.40	11.56
C-Q _{S1} (60:40)	11.78	1.95	-35.27	12.72
B	35.69	1.24	0	0
B-S1 (85:15)	30.17	1.32	-15.47	6.45
B-S1 (70:30)	26.16	1.43	-26.70	15.32
B-S1 (55:45)	21.83	1.50	-38.83	20.97
B-Q _{S1} (85:15)	30.45	1.30	-14.68	4.84
B-Q _{S1} (70:30)	27.68	1.46	-22.44	17.74
B-Q _{S1} (55:45)	25.00	1.52	-29.95	22.58

3.1 MDD variation for mixes prepared with intermediate compressibility ‘C’

Figure 6 represents the variation of MDD with increasing sand and quarry dust content in C-S1 and C-Q_{S1} mixes respectively. It was observed that with increase in respective additive content in mixes MDD values are increasing. The increase can be attributed to the fact that the gradation of the mix getting well graded with incorporation of granular material which results in higher density.

Again from Fig. 6 it can be observed for each proportion of the respective mixes, C-Q_{S1} mix is showing higher values of MDD in comparison to C-S mix. The gradation of S1 and Q_{S1} being similar, variation in MDD is due to the difference in shape of the particles of these samples. Angular to subangular particles, in intermediate compressibility clay mixes, are likely to give more MDD values than that with rounded to subrounded particles, up to 40% content.

3.2 OMC variation for mixes prepared with intermediate compressibility clay ‘C’

Figure 7 represents the variation in OMC of C-S1 and C-Q_{S1} mixes with increasing sand and quarry dust content respectively. OMC values are decreasing up to quarry dust content of 30% and an increase is observed at 40% quarry dust content in the mixes. The OMC decrease with increase in sand and quarry dust content of the mixes is the result of decreasing clay fraction in the mixes. But at respective additive content of 40% in the mixes the observed increase in OMC may be due to requirement of more water with increase in amount of fines which may be due crushing of particles at higher additive content in the mixes.

The OMC values of C-Q_{S1} mix are lower than that of C-S1 mix up to 20% additive content by nearly about 1%. From 30% additive content they are almost same

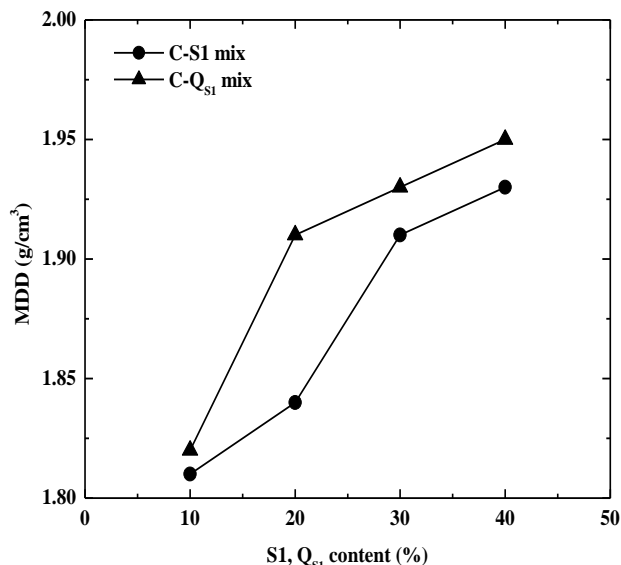


Fig. 6. MDD variation with sand and quarry dust content in intermediate compressibility clay mixes.

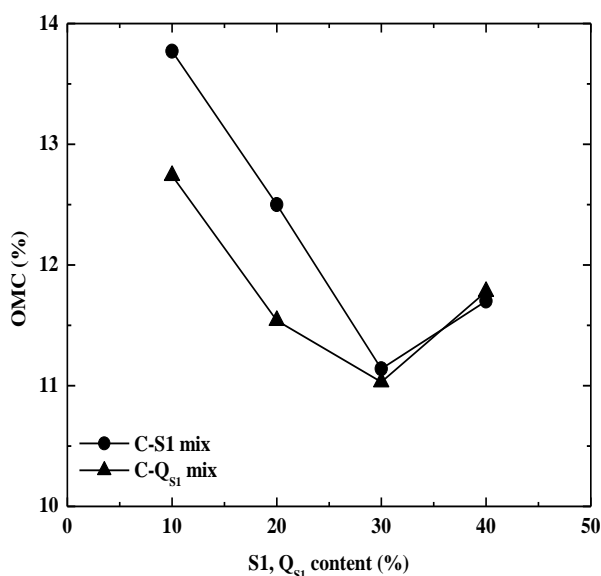


Fig. 7. OMC variation with sand and quarry dust content in intermediate compressibility clay mixes.

3.3 MDD variation for mixes prepared with high compressibility clay 'B'

The variation of MDD with increase in sand and quarry dust content for B-S1 and B-Q_{S1} mixes is presented in Fig. 8. With increasing additive content in the mixes, increase in MDD value have been observed, the reason being the addition of bigger size particles to the fines resulting in a well graded mix. Also for high compressibility clay higher MDD values are obtained with incorporation of quarry dust in comparison to that of sand at higher additive content as found in Fig. 8.

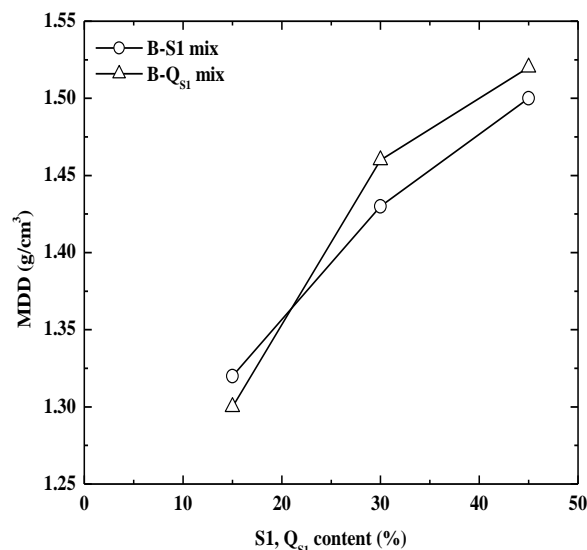


Fig. 8. MDD variation with sand and quarry dust content in high compressibility clay mixes.

3.4 OMC variation for mixes prepared with high compressibility clay 'B'

Figure 9 represents the variation in OMC with increasing S1 and Q_{S1} content in B-S1 and B-Q_{S1} mixes respectively, decrease in OMC is observed with increase in additive content in the mixes which is due to decrease in clay content. Fig. 9 reveals that the OMC requirement for high compressibility clay is more for mix prepared with quarry dusts compared to that of prepared with sand.

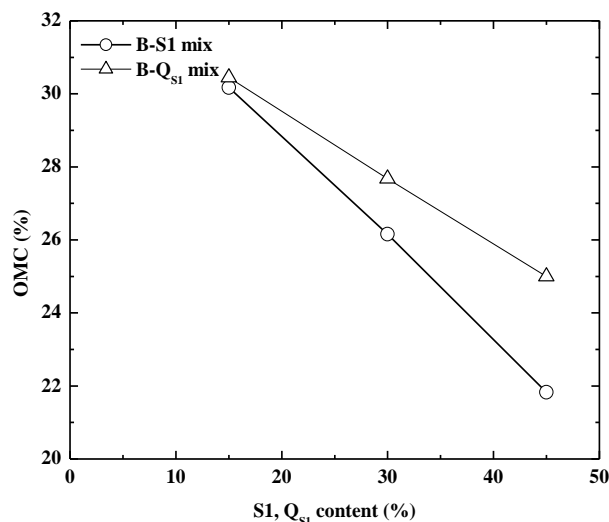


Fig. 9. OMC variation with sand and quarry dust content in intermediate compressibility clay mixes.

3.5 Influence of clay type on improvement in compaction properties

To account for the influence of clay type on compaction behavior of clay-sand and clay-quarry dust mixes, the percentage improvement of the compaction parameters to that of 100% clay samples have been

calculated. The percentage increase in MDD and percentage decrease in OMC to that of clay sample used with increasing content of sand and quarry-dust are presented in Table 3. Negative (–ve) sign represents the decrease in respective parameter.

Figure 10 compares the percentage improvement in compaction parameters of different clay-sand and clay-quarry dust mixes with increase in respective additive samples. The decrease in OMC is more in case of mixes prepared with intermediate compressibility clay in comparison to that of mixes prepared with high compressibility clay which have more water retention capacity. Maximum decrease of 38.83% in OMC is observed for B-S (55:45). Use of high amount of sand can decrease the OMC requirement of high compressibility clay. The increase in MDD percentage is more in case of mixes prepared with high compressibility clay at higher contents of sand and quarry dust than that of mixes prepared with intermediate compressibility clay. At 30% additive content in the mixes maximum increase in MDD percentage is shown by B-Q_{S1} mix. Maximum increases of 22.58% in MDD have been observed for B-Q_{S1} (55:45) mix. The result shows that bulk utilization of quarry dust can be carried out by stabilization of high compressibility clay with maximum improvement in MDD.

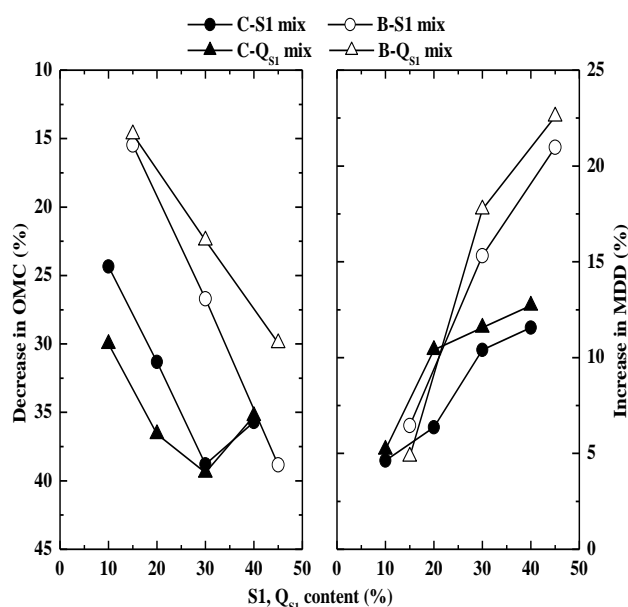


Fig. 10. Improvement in compaction characteristics of clays with increasing sand and quarry dust contents

4. CONCLUSIONS

Following conclusions can be drawn from this study:

- Increase in sand and quarry dust content in clay of intermediate compressibility increase the MDD of the mix.

- The decrease in OMC of clay of intermediate compressibility is up to a sand and quarry dust content of 30% in the respective mixes.
- For high compressibility clay mixes prepared with sand and quarry dust MDD increases and OMC decreases with increase in additive content of the mixes.
- For similar gradation of sand and quarry dust in intermediate compressibility clay, for all proportions of mix, mixes prepared with quarry dust shows higher MDD values and lower OMC values.
- Higher MDD values are obtained in case of mixes prepared with quarry dust and high compressibility clay at higher additive content and lower values of OMC are obtained for Bentonite-sand mixes for each proportion of the mix.
- Maximum improvement in terms of MDD is found for mixes prepared with quarry dust and clay B than those prepared with clay C. Similar is in case of mixes prepared with sand.
- The decrease in OMC values is more in case of mixes prepared with intermediate compressibility clay than those prepared with high compressibility clay.

REFERENCES

- 1) BS 812-104 (1994): Testing aggregates, *Method for Qualitative and Quantitative Petrographic Examination of Aggregates*, British Standards Institution.
- 2) IS 2720-III (1980): Determination of specific gravity of soils. *Indian Standard Methods of Test for Soils*, Bureau of Indian Standards, New Delhi.
- 3) IS 2720-IV (1975): Grain-size analysis, *Indian Standard Methods of Test for Soils*, Bureau of Indian Standards, New Delhi.
- 4) IS 2720-V (1985): Determination of liquid limit and plastic limit, *Indian Standard Methods of Test for Soils*, Bureau of Indian Standards, New Delhi.
- 5) IS 1498 (1970): Indian standard classification and identification of soils for general engineering purposes, *Indian Standard Methods of Test for Soils*, Bureau of Indian Standards, New Delhi.
- 6) IS 2720-VII (1974): Determination of water content-dry density relation using light compaction, *Indian Standard Methods of Test for Soils*, Bureau of Indian Standards, New Delhi.
- 7) Sarvade, P.G. and Nayak, S. (2014): Studies on utilization of quarry dust to improve the geotechnical properties of lithomargic clay, *International Journal of Advanced Structures and Geotechnical Engineering*, ISSN 2319-5347.
- 8) Soosan, T.G, Jose, B.T and Abraham B.M (2001): Use of quarry dust in embankment and highway construction, *Proceedings of Indian Geo-technical Conference, December, Indore*, pp. 274-277.
- 9) Soosan, T.G., Sridharan, A., Jose, B.T., and Abraham, B.M. (2005): Utilization of quarry dust to improve the geotechnical properties of soils in highway construction, *Geotechnical Testing Journal*, ASTM, DOI: 10.1520/GTJ11768.
- 10) Sridharan, A., Soosan, T.G, Jose, B.T., and Abraham, B.M. (2006): Shear strength studies on soil-quarry dust mixtures, *Geotechnical and Geological Engineering*, Springer, DOI: 10.1007/s10706-005-1216-9.

[Back to table of contents](#)

Hydrological modelling of Krishnai river basin

Sazidur Rahmanⁱ⁾ and B. Talukdarⁱⁱ⁾

i) M.E. (Civil) Student, Department of Civil Engineering, Assam Engineering College, Jalukbari, Guwahati-781013, Assam India

ii) Associate Professor, Department of Civil Engineering, Assam Engineering College, Jalukbari, Guwahati-781013, Assam India

ABSTRACT

A hydrological model for simulating the discharges during the flood period (May to October) is presented for the Krishnai River Basin which is situated in the North-Eastern part of India and belongs to the state of Assam and Meghalaya. The model has been developed using HEC-HMS using discharge data for the flood season of four consecutive years (2010 to 2013). The model consisted of three components/modules viz. the rainfall-runoff module, the surface runoff/direct runoff routing module (unit hydrograph method) and the channel routing module or component. Soil Conservation Services Unit Hydrograph method is used and results were compared. The rainfall data used was TRMM daily rainfall data of $0.25^{\circ} \times 0.25^{\circ}$ resolution and Thiessen Polygon method was used for average rainfall estimation. Soil parameters and Hydrological Soil Group information were extracted using HEC-GeoHMS for ArcGIS from Harmonised World Soil Database. Model parameters were calibrated against the observed discharge values of year 2010 and 2011 using the Univariate search algorithm with Nash-Sutcliffe efficiency as the objective function. Validation of the model was performed against the discharge data of the year 2012 and 2013. Overall, the model performed reasonably well for both validation and calibration having Nash Sutcliffe efficiency in the range of 0.75 to 0.85. The efficiency of the developed model could be enhanced with more accurate soil and rainfall data.

Keywords: Hydrological model, HEC-HMS, Krishnai River

1. INTRODUCTION

Natural hazards are a substantial threat to the progress and development of human communities. Floods hold a dominant position among these due to their frequent occurrence as well as their large spatial distribution with the ability to greatly damage man-made structures.

Assam, a state in the North eastern region of India, is periodically affected by floods, sometimes even with multiple floods. With the Tropical Monsoon Rainforest Climate, Assam is temperate and experiences heavy rainfall and high humidity. Every year, flooding from the Brahmaputra and other rivers deluges places in Assam. One such river which regularly creates havoc through flooding is the Krishnai River which is located in the western part of Assam originating from Garo hills in western Meghalaya. The water levels of the rivers rise because of rainfall resulting in the rivers overflowing their banks and engulfing nearby areas. Apart from houses and livestock being washed away by flood water, bridges, railway tracks and roads are also damaged by the calamity, which causes communication breakdown in many places. Fatalities are also caused by the natural disaster in many places of the State.

The objective of the study is to understand the rainfall-runoff relationship of the Krishnai River Basin which is not well understood yet but is important to plan for mitigation of subsequent flood damages. A

good understanding of the rainfall-runoff relationship is also important for predicting the prominent floods in the catchment.

Modeling of rainfall runoff has gained impetus over the years due to an increase in the effects of these hazards especially with respect to real time forecasting (Kelsch M., 2001).

Runoff which is a function of physiographic, geologic and meteorological catchment conditions, is generated by precipitation to become concentrated flow in stream channels and valleys (Rientjes, T. H. M., 2004)

The rainfall-runoff model discharge hydrograph is important in flood modeling for flood propagation in an area. The relevant characteristics derived from a hydrograph that act as tools of effecting damages include duration, lag time, time to peak discharge, peak discharge, rate of rising, flow velocity and spatial extent. These parameters are extracted from the models used. Hydrographs are useful to determine flood peaks and runoff volumes (Leenders J. K. et al., 2009)

Three important features of a hydrograph that are useful in the prediction of floods include time to peak, peak flow and total runoff/discharge. These characteristics are crucial in management of hazards as they have influence on both hazard effect and management initiatives such as to simulate flood hydrographs and peak of that area as a result of rainfall

in a catchment based on characteristics of the storm and catchment (Wang Y.C. et al., 2008)

Hydrologic model has five basic components- watershed geometry, input, governing laws, initial and boundary conditions, and output. (Pilgrim D.H., and Cordery I., 1993)

There are relatively simple modelling techniques available that have been successful in flood forecasting applications. These models can be classified according to their overlying modelling processes, their spatial and temporal scale, and their method of solution (Singh V.P., 1995)

A model process can either be lumped or distributed and developed through deterministic, stochastic, or mixed steps and the solution development of a hydrological model can be numerical, analog, or analytical in nature (Butts M.B et al., 2004)

The most common hydrologic modelling approach to accounting for ungauged small watershed prediction is the use of synthetic UH theory and stream routing procedures (Bedient P.B., and Huber W.C., 2002)

2 METHODOLOGY AND PROCEDURE

2.1 Study Area

The study area, the Krishnai river basin (Figure 1) is in the north-eastern region of India comprising seven states. The Krishnai river basin belongs to the states of Meghalaya and Assam. The physiography of the entire region is mainly divided into two divisions, namely the Meghalaya Plateau and the plains of the river Brahmaputra valley which falls into the state of Assam accounting for about 70% and 30% of the total area respectively. The geographical area of the catchment is about 1066 sq.km. The area with elevation ranging from about 600 m to 250 m above m.s.l is narrow and steep, forming deep river valleys. Major part of the sub basin is a hilly terrain with a few isolated V shaped valleys developed along the course of the river with undulating topography. The elevation of the basin decreases towards the north. The Krishnai basin enjoys an average annual rainfall of around 4000 mm. In this zone, the bulk of the rainfall occurs during the month of May to September. Significant rainfall occurs in May and October too. The remaining months are generally dry

2.2 Data Collection

Various kinds of data are required for formulation of a successful hydrological model. Data for this study was collected from various sources. Discharge data for the flood season i.e. May to October for four consecutive years (2010 to 2013) which was used for model validation and calibration was acquired from water resource department, Assam. For any hydrological model, the main source of input is rainfall. For this study, Tropical rainfall Measuring Mission (TRMM) daily rainfall data of $0.25^0 \times 0.25^0$ spatial resolution covering the entire Krishnai River basin was

used and average rainfall over the basin was determined using Thiessen Polygon Method. Harmonised World Soil Database (HWSD) was used for soil related information and for extraction of Hydrologic Soil Group (HSG) information. For Land Use Land Cover (LULC) Classification, IRS LISS-III satellite imagery of 23.5 m resolution was used and for delineation of watershed and sub-watersheds and extraction of stream network, Digital Elevation Model (DEM) of 30 m resolution was used.

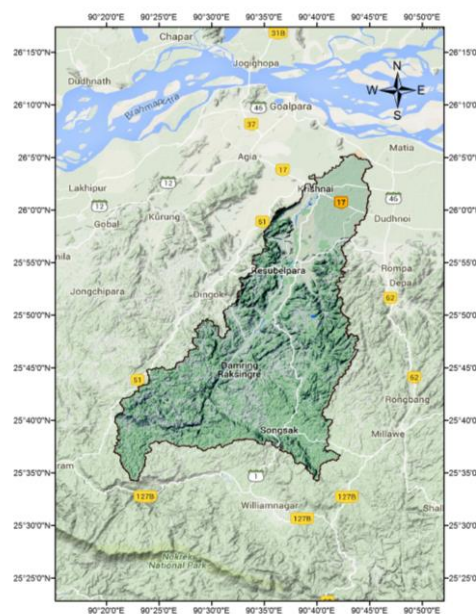


Fig. 1 Krishnai River Basin.

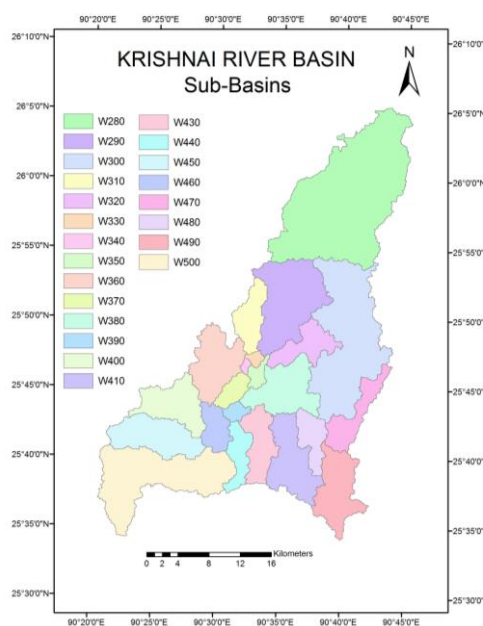


Fig.2 Sub-Basins of the Krishnai River Basin

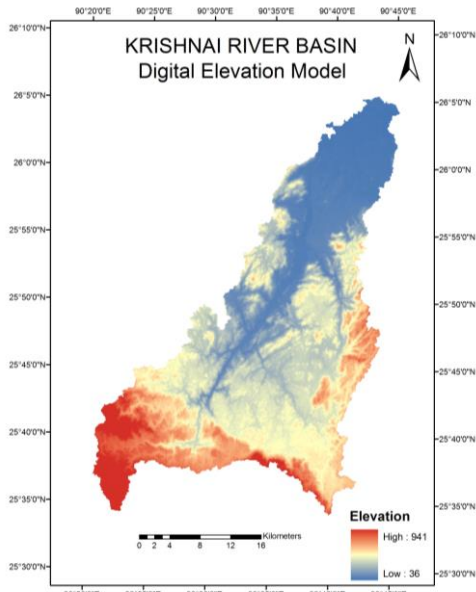


Fig. 3 Digital Elevation Model of Krishnai River Basin

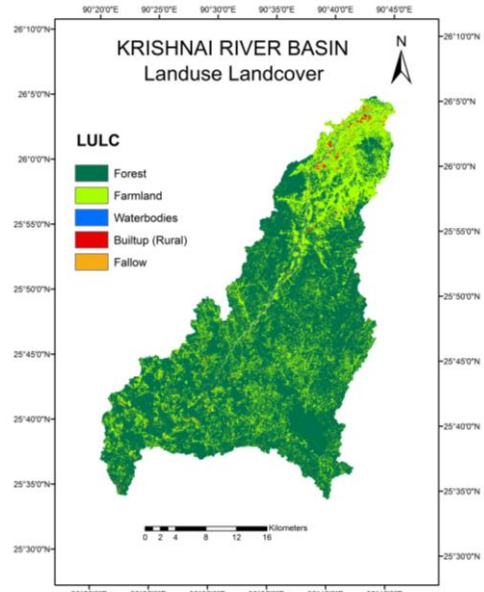


Fig. 5 Land Use Land Cover of Krishnai Basin

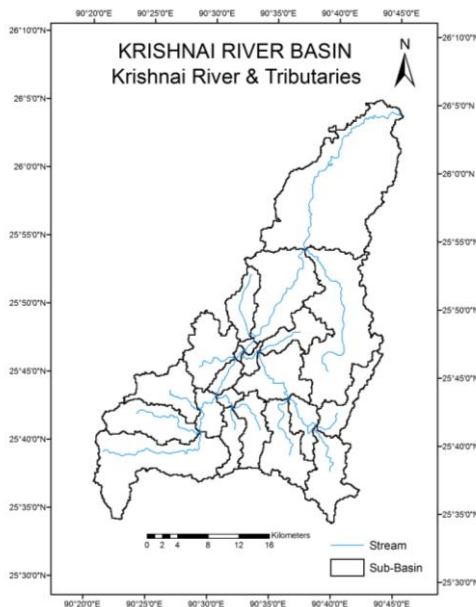


Fig. 4 Krishnai River and Its Tributaries

Figure 5 and Table 1 shows the Land Use land cover pattern of the study area:

Table 1: Land Use Land Cover in the Krishnai river basin

Cover Type	Area (sq.km)	% of extent
Forest area	777.09	32.24
Farmland	273.47	11.34
Waterbody	4.96	0.21
Built-up (rural)	3.19	0.13
Fallow land	8.13	0.34

2.3 Modeling

The hydrological model of Krishnai River Basin was developed using HEC-HMS, figure 6 shows the model set-up of HEC-HMS. The various components of rainfall-runoff generation process that are evaluated are Total Runoff Volume, Volume of Direct Runoff & Channel flow.

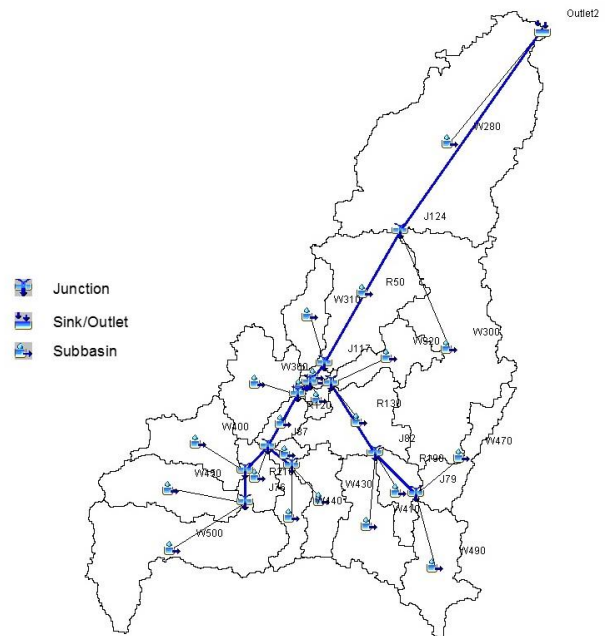


Fig. 6 HEC-HMS Model setup

Soil Conservation Services (SCS) Curve Number (CN) loss method was used for determination of total runoff volume. Curve Number is a function of Antecedent Moisture condition, Hydrologic soil group and Land Use Land cover. Curve Number for each

sub-basin was determined by creating a Curve Number Grid using the LULC Grid, the Soil Maps from HWSO containing HSG information and the Curve Number tables published by the SCS.

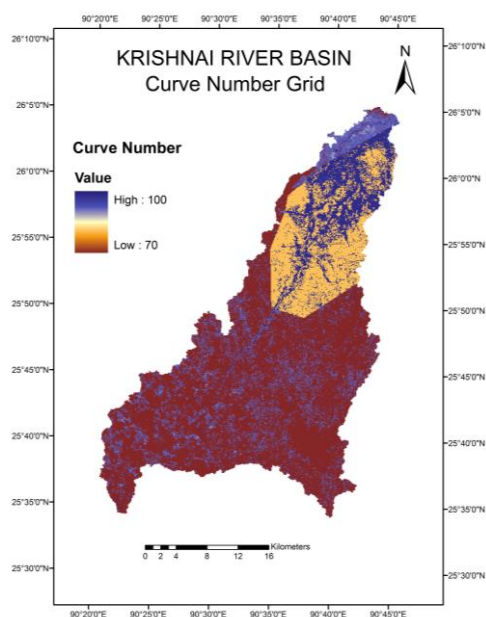


Fig. 7 Curve Number Grid for the Krishnai Basin

SCS Unit Hydrograph (UH) model was used for computation of Direct Runoff Volume. The lag time required for running this module in HEC-HMS was determined using equation (1) given by the SCS:

$$T_{lag} = \frac{(L \times 3.28 \times 10^3)^{0.8} \left(\frac{1000}{CN} - 9\right)^{0.7}}{1900 \times y^{0.5}} \quad (1)$$

Where T_{lag} = lag time in hours, L = length of the longest flow path of the sub-basin (km), CN = composite CN of the sub-basin, y = average slope of the sub-basin in percent

Following table shows the Curve Number values and Physiographic variables of the various sub-basins.

Table 2 CN and Physiographic variables of various sub-basins

Name	Basin CN	Basin Slope y (%)	Basin Lag T_{lag} (hr)	Area, A (sq.km)	Longest Flow, L (km)
W280	82.114	6.219	5.582	227.493	37.374
W290	76.968	13.575	2.432	81.808	17.648
W300	74.199	15.408	3.872	143.870	30.910
W310	73.052	16.060	2.078	27.067	13.992
W320	72.267	14.649	2.011	28.897	12.340
W330	76.081	9.357	0.789	3.431	3.314
W340	75.336	11.912	0.558	1.879	2.436

W350	72.872	13.972	1.031	7.042	5.310
W360	73.519	12.783	2.007	48.020	11.812
W370	72.767	16.590	1.212	12.606	7.206
W380	73.453	10.937	2.357	51.163	13.067
W390	72.913	15.198	0.999	6.418	5.385
W400	72.830	12.038	2.350	42.726	13.521
W410	72.311	11.206	3.197	50.950	18.660
W430	73.320	10.368	2.635	32.443	14.458
W440	72.544	8.741	2.618	20.534	12.549
W450	72.905	13.923	2.986	50.449	20.032
W460	73.373	16.953	1.377	19.951	8.753
W470	73.082	13.679	2.596	30.292	16.736
W480	71.907	8.983	2.536	22.701	11.996
W490	71.693	9.883	3.080	48.668	16.120
W500	72.797	12.884	4.215	108.424	29.254

For computation of Channel Flow, lag model of river routing was used which can be mathematically expressed as

$$O_t = I_t \text{ if } t < \text{lag time} \quad (2)$$

$$O_t = I_{t-\text{lag}} \text{ if } t > \text{lag time} \quad (3)$$

Where O_t = outflow hydrograph ordinate at time t , I_t = inflow hydrograph ordinate at time t

3 RESULTS AND DISCUSSIONS

The various data, variables and parameters were fed into the model setup in HEC-HMS and the model was run. The model output was calibrated against the observed discharges for the year 2010 and 2011. The model was then validated against the observed discharge values for the year 2012 and 2013. The model was calibrated using the Univariate search algorithm with Nash-Sutcliffe efficiency as the objective function which is given by equation 4 as follows:

$$NSE = 1 - \sum_{t=1}^T \left(\frac{q_0^t - q_m^t}{q_0^t - \bar{q}_0} \right)^2 \quad (4)$$

Where q_0 = observed flows at time t , \bar{q}_0 = mean of observed flows, q_m = modelled outflow at time t

The overall efficiency of the model in the validation stage was also assessed using Nash-Sutcliffe efficiency criterion. Overall the Hydrological Model for Krishnai River Basin performed reasonably well having average Nash Sutcliffe Efficiency of 0.76 in calibration stage and 0.81 in the validation stage. Following figures shows the comparison of output discharge with the observed discharges for the flood season of four consecutive years i.e. 2010 to 2013

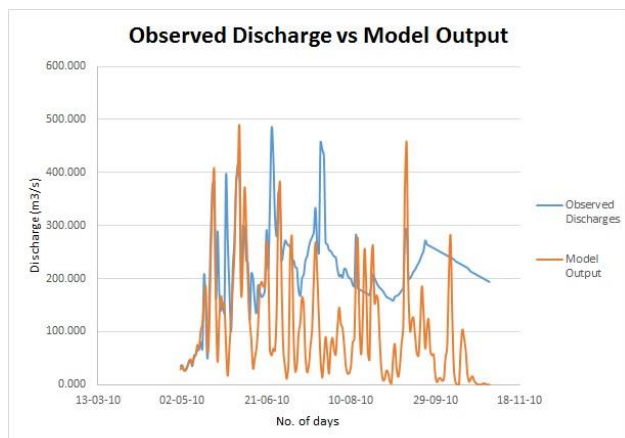


Fig. 8 Observed Discharge vs Model Ouput (2010)

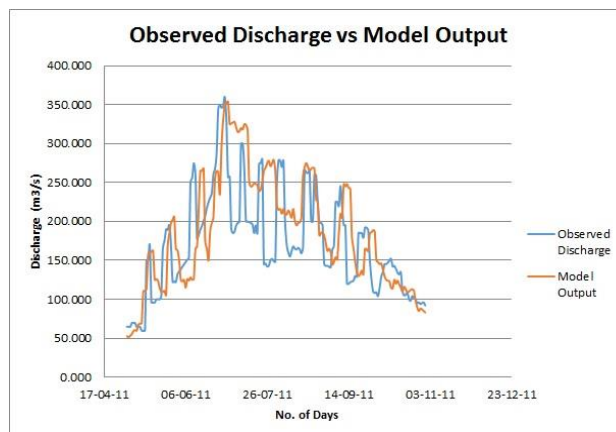


Fig. 8 Observed Discharge vs Model Ouput (2013)

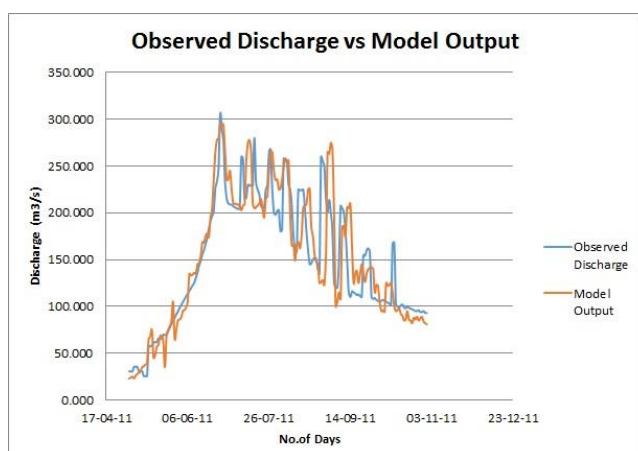


Fig. 8 Observed Discharge vs Model Ouput (2011)

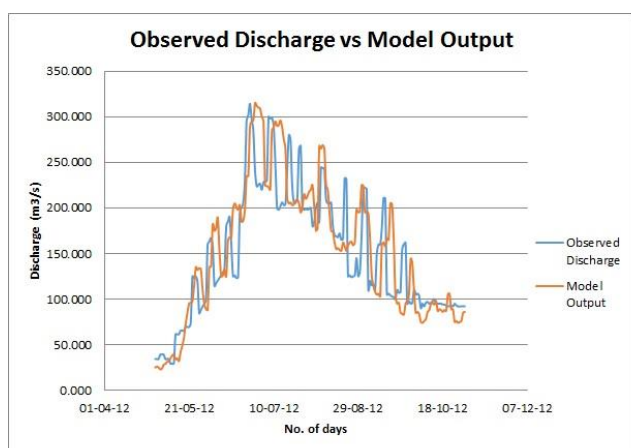


Fig. 8 Observed Discharge vs Model Ouput (2012)

4 CONCLUSIONS

The semi-distributed continuous model developed in this study for the Krishnai River Basin showed fair results for the considered time period. However, no Hydrological model is universal in nature i.e. a single model cannot present a complete accurate description of the entire process of runoff generation. Accuracy of the model depends on the number of parameters considered while developing the model, more the number of parameters more is the accuracy of the model. Furthermore realistic models can be developed considering the greater spatial and temporal variability of basin characteristics, physiography, rainfall, and soil characteristics.

5 REFERENCES

- 1) Bedient, P.B., and Huber C.W. (Eds) (2002): "Hydrology and Floodplain Analysis", 3rd Edition, New Jersey, Prince-Hall, Inc.
- 2) Butts, M.B., Payne, T. J., Kristensen M., and Madsen. H. (2004): "An Evaluation of the Impact of Model Structure on Hydrological Modelling Uncertainty For Streamflow Simulation", *Journal Of Hydrology* 298: 242-266
- 3) Kelsch, M. (Ed.) (2001): "Hydrometeorological Characteristics of Flash Floods", *Coping With Flash Floods, Environmental Security*
- 4) Leenders, J. K., Wagemeker, J., Roelevink, A., Rientjes, T. H. M. & Parodi, G. (2009): "Development of a Damage and Casualties Tool for River Floods in Northern Thailand", in Samuels (Ed.) *Flood Risk Management: Research and Practice*. London, Taylor and Francis Group.
- 5) Pilgrim, D.H., and I. Cordery. (1993): "Flood Runoff", in *Handbook of Hydrology*, Maidment D. R, (Ed), 9.1-9.42. New York: Mcgraw-Hill, Inc.
- 6) Rientjes, T. H. M. (2004): "Inverse Modelling of the Rainfall-Runoff Relation. A Multi Objective Model Calibration Approach."
- 7) Singh, V.P. (1995): "Watershed Modelling", in *Computer Models Of Watershed Hydrology*, Singh V.P. (Ed), Colorado: Water Resources Publications, 1-22
- 8) Wang, Y. C., Chen, S. T., Yu, P. S. & Yang, T. C. (2008): "Storm-Event Rainfall-Runoff Modelling Approach for Ungauged Sites in Taiwan", *Hydrological Processes*, 22: 4322-4330.

[Back to table of contents](#)

Development of Rainfall-Runoff Modelling using ArcSWAT and Artificial Neural Network in the Subansiri Basin, Assam.

Susheta Chanda¹, Triptimoni Borah²

Assam Engineering College

ABSTRACT

This study presents a comparative study on the rainfall-runoff models, by the use of a GIS-based approach (ArcSWAT) and an empirical method (Artificial Neural Network) in the Subansiri River basin. The objective of such models is to predict the long-term impacts in large basins of management and to simulate the basin scale water, to help in flood forecasting and watershed planning and management. In this proposed methodology, the first model is developed using ArcSWAT, which creates a framework for continuous time-scale modeling that integrates several years' precipitation, GIS knowledge and a hydrological model. The Subansiri watershed (35007 km²) is divided into several hydrologic response units (HRUs) that consist of homogeneous land use, topographical, and soil characteristics. In this study, the meteorological data of 1990-2010 was considered as an input and on the basis of that, comparison were made for the observed and simulated data. The second model has been formulated by using the ANN toolbox available in MATLAB, where a three-layered feed-forward back-propagation neural network was developed and validation of data was done. Both the models provided good correlation and model efficiency for simulating daily runoff. For the SWAT model, the values of R², NSE, PBIAS and RSR were computed to be 0.712, 0.673, 0.11 and 0.57 respectively. The evaluation of the results show that the ANN model performed better than SWAT model with values of 0.848, 0.845, 0.32 and 0.393 respectively. Considering the promising performance of the simple ANN model, this study suggests that the ANN approach warrants further development to explicitly address the spatial distribution of hydrologic/water quality processes within watersheds.

Keywords – Modeling, Rainfall, Runoff, Surface hydrology, ArcSWAT, Artificial Neural Network.

1. INTRODUCTION

Integrated water management can be viewed as a three or more dimensional process centered around the need for water, the policy to meet the needs, and the management to employ the policy. Integrated water management of large areas should be accomplished within a spatial unit (the watershed) through modeling and would be greatly facilitated if we have the precise amount of runoff from a catchment. Consistent stream flow estimates generated from catchments are mandatory as part of information sets that help policy makers make informed decisions on water planning and management.

There is a need for both short term and long term forecasts of stream-flow events in order to optimize the system. Hence, analytical methods and simple conceptual models are needed which simulate the relationship between the rainfall and runoff to estimate the potential water volumes in the basin. Various modeling techniques have been developed

by researchers over the time to achieve higher degrees of accuracy.

There are many physical based hydrological models available currently. Among these, SWAT is the most recent one to be used successfully for simulating runoff, sediment yield and water quality of small watersheds (MP Tripathi, RK Panda, NS Raghuvanshi, 2003; Van Liew and Garbrecht, 2003). Preceding applications of SWAT for water flow have shown encouraging comparisons with the measured counterparts in various parts of the United States (Arnold and Allen, 1996). JG Arnold, R Srinivasan, RS Muttiah, JR Williams (1998) has mentioned about the feasibility of simulating large area by the integration of hydrological models with GIS. He applied SWAT with the addition of a streamflow filter and recession methods for regional estimation of baseflow and groundwater recharge in the upper Mississippi River basin.

Usually the evaluation of the hydrological processes is done by using the conceptual models which present good results. However, conceptual models are difficult to develop and the calibration of the model parameters is subjective. In such cases, empirical models are apt alternatives which connect inputs and output by means of a mathematical function without an explicit relationship with the catchment characteristics. An artificial neural network (ANN) is an example of an empirical (black-box) model. ANN is a computing method which mimics the human brain and nervous system. Various studies of runoff-modeling (A.W. Minns and M.J. Hall, 1996; Sajikumar and Thandaveswara, 1999; MA Antar, I Ellassiouti, MN Allam, (2006), sediment discharge, reservoir precipitation, hydrologic time series modeling and sediment transport prediction. MP Tripathi, NS Raghuvanshi (2006) developed ANN models to predict both runoff and sediment yield on a daily and weekly basis, for a small watershed and reported that these ANN models based on simple input could be used for estimation of runoff and sediment yield, missing data, and testing the accuracy of other models. D Misra, T Oommen, A Agarwal, SK Mishra (2009) compared the runoff and sediment yield from an Indian watershed using the back-propagation artificial neural network modeling technique and single and multi-input linear transfer function models. They reported that the single input linear transfer function runoff and sediment yield forecasting models were more efficacious than the multi-input linear transfer function and ANN models.

2. STUDY AREA AND INPUT DATA SET

The Subansiri is one of the primary tributaries of the Brahmaputra River and it forms one of the largest sub-basins covering parts of Tibet and India. It is one of the major tributary of the river and constitutes as much as 11% of the total flow of the Brahmaputra. The Subansiri basin covers an area of 35,771 sq.km, of which 4350 sq.km falls in Assam. It is located between 26°40'N to 27°45'N and 93°15'E to 94°35'E. For this research, a part of the whole Subansiri basin, i.e. a watershed measuring 5365sq.km was taken under consideration, the outlet point being at Khabulighat (27°02'N, 94°07'E). The climatic conditions of the Lower Subansiri basin are

cool and humid. The rain stops in the area in the month of October and temperature begins to fall. In the study period of 2005-2010, the daily temperature ranges from a average maximum of 28.5°C, 39°C being the highest to an average minimum of 15°C, 5°C being the lowest. The daily mean relative humidity varies from a minimum of 26.3% in the month of April to a maximum of 97.4% in June. The period from June to September is the unpleasant part of the year, receiving heavy rainfalls as a result of which the climate becomes hot and humid. 70% of the total rainfall is confined to this period. During the monsoon period, due to heavy rain in the catchment area, the discharge in the Subansiri and its tributaries increase suddenly. The heavy rain also leads to the increase of landslide and rockslide which so often happens in the outermost hill ranges.

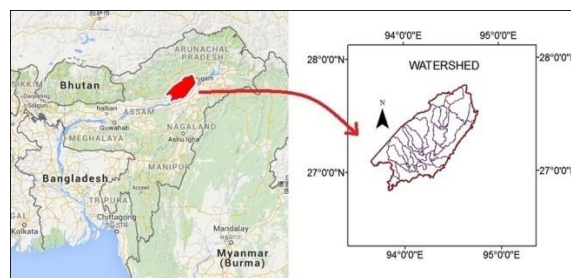


Figure 1. Location Map of the watershed area of the Subansiri Basin.

The data used in this study comprises of : daily precipitation, temperatures, relative humidity, solar radiation, and wind intensity. Also, the land use map and the soil map has been extensively used for SWAT modeling. The data has been collected partly from the Hydrology branch, Water Resources Department, Assam and also from the Global Weather Site of SWAT. A location map of the watershed is presented in Figure 1.

3. Model Description

3.1. SWAT Model

SWAT allows a number of different physical processes to be simulated in a watershed. No matter what type of problem studied with SWAT, water balance is the driving force behind everything that happens in the watershed. To accurately predict the movement of water the hydrological cycle as simulated by the model must confirm to what is

happening in the watershed. The hydrological cycle as simulated by SWAT is based on the water balance equation:

$$SW_t = SW_o + \text{sum} (R_{\text{day}} - Q_{\text{surf}} - ET_a - W_{\text{seep}} - Q_{\text{gw}}) (1)$$

SW_t = Final soil water content,

SW_o = Initial soil water content on day i ,

T = time (day),

R_{day} = Amount of precipitation on day i ,

Q_{surf} = Amount of surface runoff on day i ,

ET_a = Amount of Evapotranspiration on day i ,

W_{seep} = Amount of water entering the vadose zone from the soil profile on day i ,

Q_{gw} = Amount of return flow on day i .

In the hydrologic component, runoff is estimated separately for each sub-watershed or hydrological response unit (HRU) of the total watershed area and routed to obtain the total runoff for the watershed. Runoff volume is estimated from daily rainfall using the modified SCS-CN (Curve Number Method) and Green-Ampt methods. The model requires the input of the DEM, land use and soils as well as weather data such as daily precipitation and temperature. In the SWAT model, the watershed is partitioned into small sub-basins that are further subdivided into HRUs based on unique land cover, soil and topographic conditions. The hydrology component of the model determines a soil water balance at each time step based on daily data of precipitation, runoff, evapotranspiration, percolation, and base flow. Simulations are performed at the HRU level and summarized in each sub-watershed.

3.2. ANN Model

The ANN is an empirical method which has been used widely in simulating hydrological processes. Hecht-Nielsen proposed the following formal definition of an ANN: “A neural network is a parallel, distributed information processing structure consisting of processing elements (which can possess a local memory and can carry out localized information processing operations) interconnected via unidirectional signal channels called branches (‘fans out’) into as many collateral connections as desired; each carries the same signal – the processing element output signal. The processing element output signal can be of any mathematical type desired. The

information processing that goes in within each processing element can be defined arbitrarily with the restriction that it must be completely local; that is, it must depend only on the current values of the input signals arriving at the processing element via impinging connections and on values stored in the processing element’s local memory”.

From a mathematical point of view, ANNs can be called universal approximators, because they are often able to uncover and approximate relationships in different types of data. Even though an underlying process may be complex, an ANN can approximate it closely, provided that sufficient and appropriate data about the process is available to which the model can adapt.

ANNs are composed of neurons which are arranged in groups called layers and connected through weights. Any simple neural network structure consists of three layers: the input layer, the hidden layer and the output layer. When the input data are presented to the input layer, they pass through and are operated on by the neural network until an output is obtained at the output layer. Each neuron receives many inputs from other neurons through weighted connections. These weighted inputs are further added up and produce the argument for a transfer function such as a linear, logistic or hyperbolic tangent function which in turn produces the final output of the neuron.

4. METHODOLOGY

4.1. SWAT Model

The DEM file(90m) has been downloaded from the Shuttle Radar Topography Mission (SRTM) and has been geo-referenced to the Projection System of WGS_1984_UTM, Zone_46 N. Using the DEM, the drainage and flow pattern is obtained and the stream network is defined. The watershed is delineated according to the flow pattern, which in this case results in sub-basins. For the land use map, 7 bands(30m) of Landsat-4 imageries have been obtained from the USGS site. After supervised classification in ERDAS, they have been loaded onto the delineated area. The soil map of the area has been clipped from the soil map of India and overlapped with the delineated area. Based on soil characteristics, further classification has been done

into Hydrological Soil Groups (HSG) for SWAT interface. Soil properties such as hydrologic soil group, texture class and hydraulic conductivity are derived from the percentage content of clay, silt and sand.

4.2. ANN Model

For the present study, a three-layer feed forward back-propagation neural network with the Levenberg-Marquadt algorithm was used for learning.. The gradient-descent method was employed to modify network weights. At the beginning of the training, weights were initialized with a set of random values. The weights were systematically changed by the learning algorithm such that, for a given input, the difference between the MLP output and the actual output is small. The chosen tangent hyperbolic sigmoid transfer function may be defined as:

$$\text{tansig}(n) = \frac{2}{(1 + \exp(-2n)) - 1} \quad (2)$$

The data of January-December(2008-09) were used for validating the model. The time series of discharge were compared with the time series of rainfall, and other parameters of temperature, solar radiation, relative humidity and wind intensity. It is useful to scale the inputs and output so that they always fall within a specified range before training. In the present study, the input and output data have been scaled to make them bounded in the intervals -1 and +1, which is preferable when a tangent activation function is used in the network. The standardization function used is :

$$x_i = \frac{x_i - x_{\min}}{x_{\max} - x_{\min}} \quad (3)$$

Since the number of neurons in the hidden layer plays an important role in the model performance, 10-30 neurons were tested. As the results were observed to optimum from the use of 15 neurons, that is considered. The daily input data were used for training the multi-layer perceptron model.

5. RESULTS AND DISCUSSION

The various coefficients for calculating the model efficiency used were Coefficient of Determination(R^2), Nash-Sutcliffe Efficiency(NSE), Percent Bias(PBS) and Root Mean Squared Error-observations standard deviation ratio(RSR).

Table 1. Comparison of the performance criteria of SWAT and ANN model.

Efficiency Coeffients	SWAT Model	ANN Model
R^2	0.712	0.848
NSE(E)	0.673	0.845
PBIAS	11.185%	3.255%
RSR	0.571	0.393

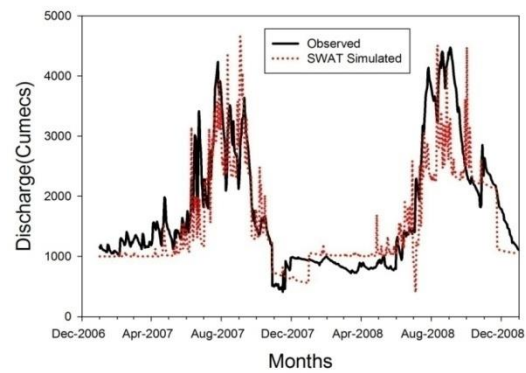


Figure 2. Comparison of Data for SWAT Model

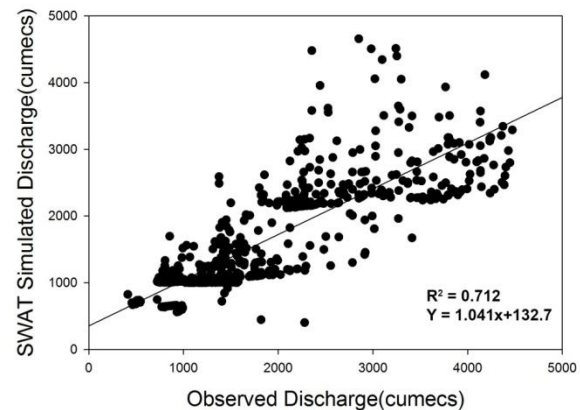


Figure 3. Regression Plot for SWAT Model

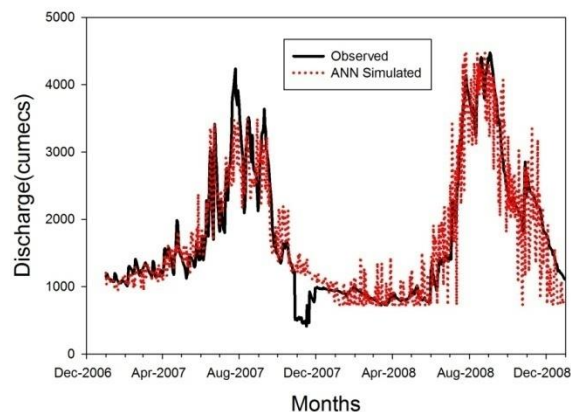


Figure 4. Comparison of Data for ANN Model

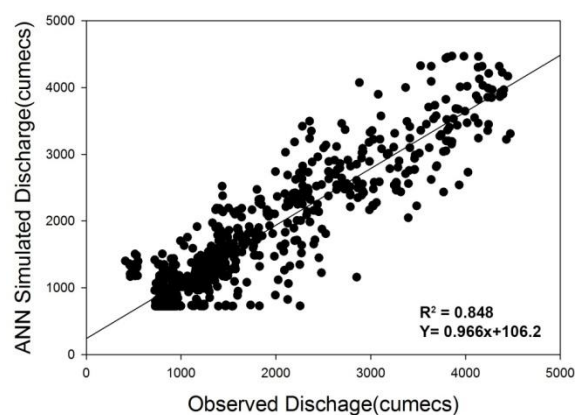


Figure 5. Regression Plot for ANN Model

6. CONCLUSION

Results suggest that SWAT adequately simulated stream flows for the non-winter and entire simulation periods. SWAT simulated daily flows were inadequate for the winter months and further, SWAT inadequately daily monthly flows for the whole duration of test period. ANN simulated flows were adequate for the entire simulation, non-winter months, and winter months. In addition, ANN stream flows were adequate for the entire simulation and non-winter months for the testing period. Also overall, results suggest that ANN simulated daily flows were closer to the observed values than SWAT simulated daily flows.

Hence, this study demonstrates that ANN is a promising modeling alternative to a traditional, process-based approach for watershed flow simulations. They have some shortcomings, such as

they do not spatially represent a watershed system and hence are incapable of predicting flows at various points along a stream network. Also, the ANN models cannot be used to predict future conditions if the land use in the watershed changes. As we have seen, it is difficult to produce a reliable model with conventional modeling approaches due to the high variance and inherent non-linear relationship of rainfall-runoff and the complexity of the hydrological process. The results of this study, however suggest that the ANN approach is sufficiently promising to warrant further development of the approach to explicitly address the spatial distribution of hydrologic and water quality processes and land use in watersheds. The ANN approach is also more efficient because it requires very few input variables and minimal resources to implement. The proposed approach can be a very efficient tool and useful alternative for the computation of rainfall-runoff relationship. The results are quite encouraging and suggest that the presented methodology may be used as a potential tool to model the rainfall runoff process of a catchment.

7. REFERENCES

- [1] Agarwal, A., Mishra, S.K., Ram, S., Singh, J.K., 2006. Simulation of runoff and sediment yield using artificial neural networks. Biosystems Engineering.
- [2] MP Tripathi, RK Panda, NS Raghuvanshi, 2003, Identification and prioritisation of critical sub-watersheds for soil conservation management using the SWAT model, Biosystems Engineering.
- [3] MW Van Liew, JD Garbrecht, Journal of Soil and Water Resources, 2003, Simulation of the impacts of flood retarding structures on streamflow for a watershed in Southwestern Oklahoma under dry, average, and wet climatic conditions.
- [4] JG Arnold, PM Allen - Estimating hydrologic budgets for three Illinois watersheds, Journal of hydrology, 1996
- [5] JG Arnold, R Srinivasan, RS Muttiah, JR Williams – 1998, Large area hydrologic modeling and assessment part I: Model development
- [6] AW Minns, MJ Hall, 1996, Artificial neural networks as rainfall-runoff models - Hydrological sciences journal.
- [7] N Sajikumar, BS Thandaveswara, 1999, A non-linear rainfall-runoff model using and artificial network – Journal of Hydrology.

[Back to table of contents](#)

Morphometric analysis and Prioritization of Kulsī Basin using Remote Sensing & GIS

Kulendu Kumar Gogoi ⁱ⁾, Er. Gulshan Tirkey ⁱⁱ⁾, Dr. Sanjay Kumar Sharma ⁱⁱⁱ⁾, Dr. C. K. Jain ^{iv)}, Dr. Mrinal Kumar Borah ^{v)}

i) Post Graduate Student (Civil), Assam Engineering College

ii) Scientist 'B' National Institute of Hydrology, Guwahati-781006

iii) Scientist 'B' National Institute of Hydrology, Guwahati-781006

iv) Scientist 'G' & Coordinator, National Institute of Hydrology, Guwahati-781006

v) Associate Professor, Civil Engineering Department, Assam Engineering College

ABSTRACT

The quantitative analysis of morphometric parameters is found to be of immense utility in watershed prioritization for soil and water conservation and natural resources management at micro level. The present study is an attempt to carry out a detailed study of linear and shape morphometric parameters in six watersheds of Kulsī Basin namely SWS 1 to SWS 6 and their prioritization for soil and water resource management. Kulsī Basin has an area of 1660.06 km² and lies between 25°30'0"N and 25°57'30"N latitude and 91°10'0"E and 91°50'0"E longitude. Sub-watersheds are delineated by Arc Map 9.3 software as per Shuttle Radar Topography Mission (SRTM) digital elevation model. Assessment of drainages and their relative parameters such as stream order, stream length, drainage frequency, drainage density, drainage texture, form factor, circulatory ratio, elongation ratio, bifurcation ratio and compactness coefficient have been calculated separately for each sub-watershed using the Remote Sensing (RS) and GIS techniques. Following Strahler's stream ordering scheme, it has been found that in Kulsī basin the total number of streams is 8242 belonging to different stream orders with the highest order of 8. The study emphasizes the prioritization of the sub-watersheds on the basis of morphometric analysis. The final score of entire six sub-watersheds was assigned as per erosion threat. The sub-watershed with the least compound parameter value was assigned as highest priority. Furthermore, the sub-watersheds have been categorized into three classes as high (2.3–2.5), medium (2.6–2.8) and low (3.0–3.3) priority on the basis of their maximum and minimum prioritized score. High priority indicates that these watersheds are susceptible to greater degree of erosion and application of soil conservation measures becomes inevitable to preserve the land from further erosion and to alleviate natural hazards.

(KEY WORDS: Morphometric analysis, Prioritization, SRTM DEM, Remote sensing & GIS)

1. Introduction

For a scientific and rational approach to different river problems and proper planning and design of water resources projects, an understanding of the morphology and behavior of the river is a pre-requisite. Morphology (of river) is a field of science which deals with the change of river plan form and cross sections due to sedimentation and erosion. In this field, dynamics of flow and sediment transport are the principal elements. The morphometric studies, therefore, play an important role in planning, designing and maintaining river engineering structures. In recent years, there has been a growing awareness about the need for taking up morphometric study of rivers in

the country, especially with particular reference to their unique problems. Morphological study provides quantitative description of the basin or sub-watershed and fluvial geometry, structural controls, geological and geomorphic aspect of a drainage basin. The quantitative analysis of morphometric parameters is of much significance in river basin evaluation, watershed prioritization, soil and water conservation, and natural resources management at micro level. It is of great significance in understanding the hydrologic scenario of an area, because a strong mutual relationship exists between morphological variables and hydrological characteristics. This modern approach of quantitative analysis of drainage basin morphology was given inputs by Horton (1945), the first pioneer in

this field. Horton's law of stream lengths suggested that a geometric relationship existed between the numbers of stream segments in successive stream orders. The law of basin areas indicated that the mean basin area of successive ordered streams formed a linear relationship when graphed. Horton's laws were subsequently modified and developed by several geomorphologists, most notably by Strahler (1952, 1957, 1958, and 1964), Schumm (1956), Morisawa (1957), Scheidegger (1965), Shreve (1967), Gregory (1968), Gregory and Walling (1966, 1973). The morphometric analysis for individual sub basins has been achieved through measurements of linear, aerial and relief aspect of the basin and slope contribution (Nag and Chakraborty, 2003).

Geographical Information system (GIS) and Remote sensing techniques using satellite images are used as a convenient tool for Morphometric analysis. Many workers have carried out morphometric analysis using these new techniques. Digital Elevation Model (DEM) by Shuttle Radar Topography Mission (SRTM) are widely used in drainage basin analysis.

2. Study Area

Kulsi basin in the state of Assam and Meghalaya, India is selected as the study area. It is a part of the Brahmaputra sub basin which spreads in the Kamrup and Goalpara district of Assam as well as west Khasi Hills and West Garo Hills district of Meghalaya. The Kulsi basin, located between latitude $25^{\circ}30'39''\text{N}$ to $25^{\circ}58'03''\text{N}$ and longitude $91^{\circ}11'52''\text{E}$ to $91^{\circ}48'09''\text{E}$ is selected for the study.

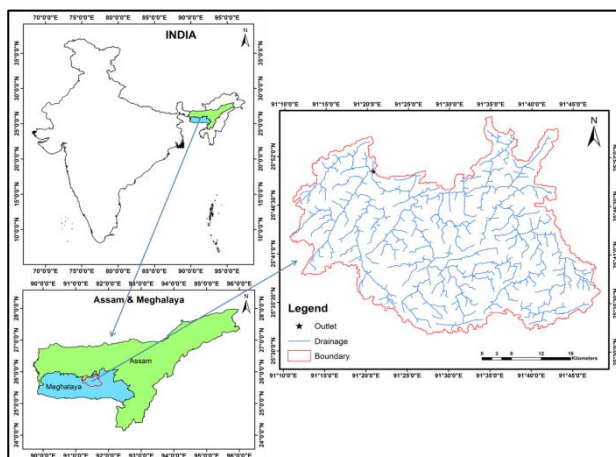


Fig. 1. Location Map of Kulsi basin

It is bounded by Bharalu and Kollong –Kopili sub-basin in the east, Krishnai –Dudhnoi sub-basin in the west, and West Khasi Hills in the south and the River Brahmaputra in the north.

The river Kulsi drains out a total area of 2806 sq. km. within the Kamrup District of Assam as well as west Khasi hills and Ri Bhoi district of Meghalaya. The Kulsi river is composed of three rivers, namely Khri, Krishniya and Umsiri, all of which originate from West Khasi Hill range and flow North and finally join the Brahmaputra. All the three rivers are joined by innumerable number of small hilly streams and rivulets till they join together and flow down as Kulsi. The total length of Kulsi from its source to outfall is about 180 km.

3. Materials and methods

The prime objective of morphometric analysis is to find out the drainage characteristic to explain the overall evaluation of the basin. Morphometric analysis comprises of a series of sequential steps. The present study is mainly concerned to evaluate morphometric characteristics of river basin at sub watershed level in order to assess the prioritization of Kulsi river basin on the basis of erodibility with geospatial techniques. To do the same DEM data (90 m resolution) is used in GIS environment. Drainage network are delineated by the Arcmap 9.3 using the DEM of SRTM. The various morphometric parameters are evaluated for the Kulsi basin and further the basin is subdivided into six sub-watersheds, and morphometric analysis are being carried out for each sub-watersheds. Computation of the basic parameters (i.e area, perimeter, stream order, stream length, stream number and elevation) of the each sub-watershed are analysed separately using the RS & GIS approach. Finally bifurcation ratio, drainage density, drainage frequency, drainage texture, form factor, circulatory ratio, elongation ratio and compactness coefficient are calculated with the help of standard formulae.

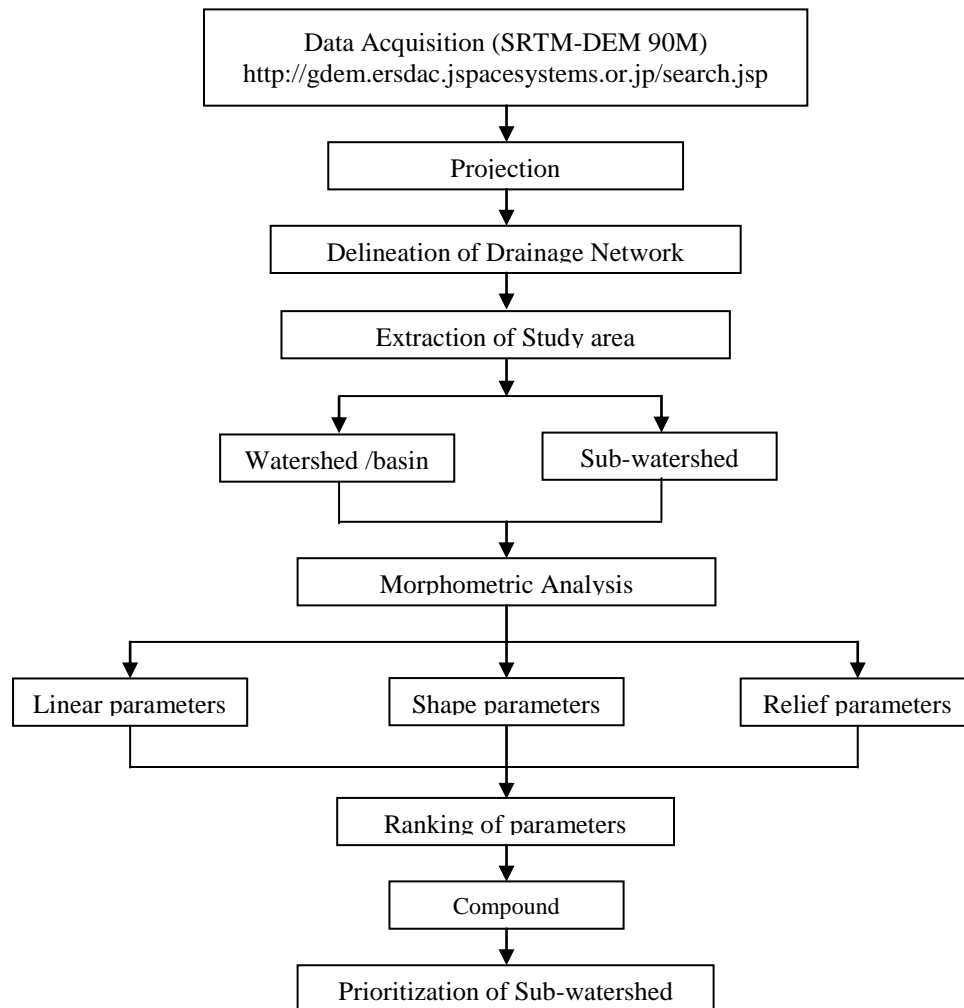


Fig. 2. Flow chart of Methodology

4. Morphometric analysis and their results

The morphometric analysis of the parameters, namely stream order, stream length, bifurcation ratio, relief ratio, drainage density, drainage frequency, form factor, circulatory and elongation ratio, area, perimeter of the basin are carried out using various mathematical formulae from the maps derived from SRTM DEM in GIS software. It is then compared with the results obtained from Toposheet for the same basin previously carried out by Scientists from National Institute of Hydrology (N. Panigrahy, B. C. Patwary).

Further more, the Kulsu basin is divided into six sub-basins and morphometric parameters are computed for each of the sub-basins.

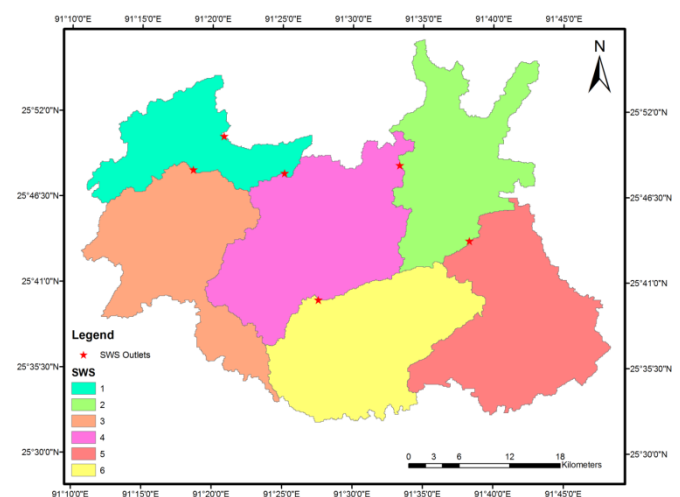


Fig. 3. Map showing six sub-watersheds of Kulsu basin

Table 1. Comparison of drainage analysis obtained from Toposheets and SRTM DEM

Toposheet			SRTM DEM		
Stream order	No. of Streams	Length of Streams (km)	Stream order	No. of Streams	Length of Streams (km)
1	6435	3322.47	1	6920	2619.86
2	1421	999.95	2	1400	1041.86
3	302	518.66	3	305	511.54
4	63	283.92	4	66	249.06
5	14	137.79	5	18	143.01
6	4	101.14	6	4	103.04
7	2	19.04	7	2	18.95
8	1	0.65	8	1	0.28
Total= 8242		Total=5383.65 km	Total= 8716	Total=4687.62 km	

4.1 Area

Basin area has been identified as the most important of all the morphometric parameters controlling catchment runoff pattern. This is because, the larger the basin, the greater the volume of rainfall it intercepts, and the higher the peak discharge that result. In the present analysis, each sub-watershed has been considered as a polygon. Areas of the different sub-watersheds were derived from GIS software as it gives area of each polygon automatically. The area of Kulsu basin was computed in the GIS software and found to be 1660.06 km². The areas of six different sub-watersheds are given in Table 4.

4.2 Perimeter

In the GIS software the Kulsu basin showed its perimeter as 403.21 km. The perimeters of six different sub-watersheds are given in Table 4.

4.3 Stream order

After analysis of the drainage map, it is found that Kulsu basin has a highest 8th order stream and drainage pattern is dendrite. The GIS analysis shows that the numbers of 1st order streams are 6920, 2nd order streams are 1400, 3rd order streams are 305, 4th order streams are 66, 5th order streams are 18, 6th order

streams are 4, 7th order streams are 2 and 8th order has 1 stream. Out of the total number of streams, first order constitutes 79.39 per cent, second order 16.06 per cent, third order 3.49 per cent, fourth order 0.75 per cent, fifth order 0.20 per cent, sixth order 0.04 per cent, seventh order 0.02 percent and eight order 0.01 percent.

4.4 Stream Length

The stream length of the various stream orders in Kulsu basin is presented in Table 1. Stream length is one of the most important hydrological features of the basin as it reveals the surface runoff characteristics. Streams of relatively smaller lengths are characteristics of areas with larger slope and finer textures. Streams with longer lengths are generally the characteristics of flatter surface with low gradients. Usually, the total length of stream segments is highest in first stream orders and decreases as the stream order increases. The number of streams of various orders in the basin was counted and their lengths measured from the mouth to the divide of the drainage basin. Stream length is a revelation of the chronological developments of the stream segments including interlude of tectonic disturbances. Total length of stream segments of different order values ranges from 2619.86 km to 0.28 km for the Kulsu basin which is presented in table 1.

Table 2. Formulae and relationships for the computations of the Morphometric parameters

Morphometric parameter	Formulae/Relationship	Reference
Stream order	Hierarchical rank	Strahler,1964
Stream length (L_u)	Length of stream	Horton,1945
Mean Stream length (L_{um})	$L_{um} = L_u/N_u$, where L_u is the total stream length of order 'u', N_u is the total number of stream segments of order 'u'	Strahler,1964
Stream length ratio (R)	$R = L_u/L_{u-1}$, where L_u is the total stream length of order 'u', L_{u-1} is the total stream length of its next lower order	Horton,1945
Bifurcation ratio (R_b)	$R_b = N_u/N_{u+1}$, where N_u is the total number of stream segment of order 'u', N_{u+1} is the number of stream segments of the next higher order	Schumn, 1956
Mean bifurcation ratio(R_{bm})	R_{bm} = average of the bifurcation ratio of all the order	Strahler,1957
Relief ratio (R_h)	$R_h = H/L_b$, where H is the total relief (relative relief) of the basin, L_b is the basin length	Schumn, 1956
Relative relief (R_r)	$R_r = H/P$, where H is the total relief (relative relief) of the basin, P is the perimeter (km) of the basin	Melton, 1957
Drainage density (D_d)	$D_d = L_u/A$, where L_u is the total stream length of order 'u' and A is the basin area in km^2	Horton,1932
Constant of channel maintenance (C_m)	$C_m = 1/D_d$, where D_d is the drainage density	Schumn, 1956
Length of overland flow (L_g)	$L_g = 1/(2 \times D_d)$, where D_d is the drainage density	Horton,1945
Ruggedness number (R_n)	$R_n = D_d \times H$, where D_d is the drainage density and H is the total relief (relative relief) of the basin	Strahler,1958
Stream/Drainage frequency (D_f)	$D_f = N_u/A$, where N_u is the total number of stream segment of order 'u' and A is the basin area in km^2	Horton,1932
Drainage texture (T)	$T = N_u/P$, where N_u is the total number of stream segment of order 'u' and P is the perimeter (km) of the basin	Horton,1945
Form factor (R_f)	$R_f = A/L_b^2$, where A is the basin area in km^2 and L_b is the basin length (km)	Horton,1932
Circulatory ratio (R_c)	$R_c = (12.57 \times A)/P^2$, where A is the area (km^2) and P is the perimeter (km) of the watershed	Miller,1953

Table 3. Morphometric parameters obtained from SRTM DEM

Sl No	Morphometric Parameters of Kulsī basin	SRTM DEM results
1	Area (A) km ²	1660.06
2	Basin Perimeter (P) km	403.21
3	Basin Length (L _b) km	88.50
4	Total no' of streams (N _u)	8716
5	Total stream Length (L _u) km	4687.62
6	Drainage Density (Dd) (km/km ²)	2.82
7	Constant of channel maintenance (C _m)	0.35
8	Total Relief (H) (km)	1.85
9	Length of overland flow (L _o) (km)	0.18
10	Drainage frequency (D _f)	5.25
11	Drainage texture (T) (Unit/km)	21.62
12	Form factor (R _f)	0.21
13	Bifurcation ratio (R _b)	3.76
14	Stream length ratio (R)	0.408
15	Elongation ratio (R _e)	0.51
16	Circulatory ratio (R _c)	0.12
17	Relief ratio (R _h)	0.02
18	Relative relief (R _r)	0.004
19	Ruggedness number (R _n)	5.22

Table 4. Sub watershed parameters of Kulsī basin

Sl No	Sub Watershed Name	Area (A) km ²	Perimeter (P) km	Max ^m Elevation m	Min ^m Elevation m	Total Relief (H) km	No of Streams (N _u)	Total Stream Length (L _u) km
1	SWS 1	169.73	122.47	868	74	0.79	949	490.72
2	SWS 2	254.49	158.60	1392	320	1.07	1417	719.64
3	SWS 3	282.02	157.59	1761	114	1.65	1422	785.35
4	SWS 4	339.29	139.10	1763	122	1.64	1801	968.37
5	SWS 5	318.26	143.51	1850	696	1.15	1655	905.89
6	SWS 6	296.26	119.08	1922	655	1.27	1479	817.66

Table 5. Order-wise Number of streams of sub-watersheds of Kulsī basin

Sl No	Sub watersheds	Number of Streams							
		Stream order	1	2	3	4	5	6	7
1	SWS 1	744	156	36	9	1	Nil	2	1
2	SWS 2	1114	231	56	13	2	1	Nil	Nil
3	SWS 3	1136	218	50	10	5	2	1	Nil
4	SWS 4	1443	285	54	12	4	2	1	Nil
5	SWS 5	1314	271	56	11	2	1	Nil	Nil
6	SWS 6	1170	239	53	12	4	1	Nil	Nil

Table 6. Order-wise Stream Lengths of sub-watersheds of Kulsi basin

Sl No	Sub watersheds	Stream Length in km							
		1	2	3	4	5	6	7	8
1	SWS 1	284.60	99.61	51.83	19.66	18.10	Nil	16.61	0.28
2	SWS 2	404.42	153.83	74.55	44	18.76	24.08	Nil	Nil
3	SWS 3	428.52	194.11	82.92	37.30	28.24	13.73	0.48	Nil
4	SWS 4	547.65	215.84	109.27	36.01	21.81	35.91	1.85	Nil
5	SWS 5	506.47	197.01	103.88	57.77	24.24	16.49	Nil	Nil
6	SWS 6	448.18	181.43	89.06	54.30	31.84	12.82	Nil	Nil

4.5 Bifurcation Ratio

Bifurcation ratio is related to the branching pattern of a drainage network and is defined as the ratio between the total numbers of stream segments of one order to that of the next higher order in a drainage basin. The sum of all the bifurcation ratios in the basin was divided by the number of bifurcation ratios to give the mean bifurcation ratio of the basin. The calculated mean bifurcation ratio for the study area is 3.76, an indication that the study area is a lowland area. This low R_b value indicates less structural disturbance in Kulsi basin. This suggests that the study area has low potentials for discharge compare to those of highland areas with bifurcation ratio of 5.0 (Strahler, 1952). Bifurcation ratios are controlled by basin physiographic factors especially basin relief and drainage density (Melton, 1957). However, in regions where the network geometry of

streams develops without pronounced lithological or structural control, bifurcation ratios between basins of different orders are stable showing little variation from one order basin to another .

Chorley had noted that lower the bifurcation ratio, the higher the risk of flooding, particularly of parts and not the entire basin. The low average bifurcation ratio of the Kulsi basin of 3.76 is an indication that parts of its segment are liable to flooding. According to Kale VS, Gupta A, bifurcation ratios ranging from 3 – 5 indicate natural drainage system characterized by homogenous rock. Table shows that mean bifurcation ratio (R_b) of the sub-watersheds values ranges from 3.51 to 4.46 for the sub-watersheds SWS 3 and SWS 5 respectively.

Table 7. Morphometric parameters for the six sub-watersheds of Kulsi basin

Morphometric parameters	SWS 1	SWS 2	SWS 3	SWS 4	SWS 5	SWS 6
Area (A) (km ²)	169.73	254.49	282.02	339.29	318.26	296.26
Perimeter (P) (km)	122.47	158.60	157.59	139.10	143.51	119.08
Basin Length (L_b) (km)	24.23	30.50	32.34	35.92	34.64	33.25
Total Relief (H) (km)	0.79	1.07	1.65	1.64	1.15	1.27
Total number of streams (N_u)	949	1417	1422	1801	1655	1479
Total stream length (L_u) (km)	490.72	719.64	785.35	968.37	905.89	817.66
Drainage density (D_d) (km/km ²)	2.89	2.83	2.78	2.85	2.85	2.76
Constant of channel maintenance (C_m)	0.35	0.35	0.36	0.35	0.35	0.36
Length of overland flow (L_o) (km)	0.17	0.18	0.18	0.18	0.18	0.18
Stream/Drainage frequency (D_f)	5.59	5.57	5.04	5.31	5.20	4.99
Drainage texture (T) (Unit/km)	7.75	8.93	9.02	12.95	11.53	12.42
Form factor (R_f)	0.29	0.27	0.27	0.26	0.27	0.27
Circulatory ratio (R_c)	0.14	0.13	0.14	0.22	0.19	0.26
Elongation ratio (R_e)	0.61	0.59	0.59	0.58	0.58	0.58
Relief ratio (R_h)	0.03	0.04	0.05	0.05	0.03	0.04
Mean Bifurcation ratio (R_b)	3.97	4.35	3.51	3.64	4.46	4.16

Relative relief (R_r)	0.01	0.01	0.01	0.01	0.01	0.01
Ruggedness number (R_n)	2.30	3.03	4.59	4.68	3.28	3.50
Compactness coefficient (C_c)	2.65	2.80	2.64	2.13	2.26	1.95
Shape Factor (B_s)	3.46	3.65	3.70	3.80	3.70	3.73

4.6 Relief Ratio

The maximum basin relief of the Kuls drainage area is 1848 m (1922 m – 47 m). The R_h normally increases with decreasing drainage area and size of sub-watersheds of a given drainage basin (Guttschalk L.C. Subodh C.P, Gopal C.D, 1964). The relief ratio of the Kuls basin is 0.02. The relief ratio of the basin is low, which is characteristics features of less resistant rocks. The lower values may indicate the presence of basement complex rocks that are exposed in the form of small ridges and mounds with lower degree of slope (Datt R, Ramanathan N.L., 1981). Low relief ratios also indicate that the recharge capabilities of the basin are low and chances of ground water potential are good (Parveen R, Kumar U, Singh V.K., 2012). The value of R_h for the study area ranges from 0.03 to 0.05 for sub-watersheds SWS (1&5) and SWS (3&4) respectively which is shown in Table 7.

4.7 Relative Relief

Melton (1957) used this term to measure the relief of watershed and is defined as H/P , where H is the total relief (relative relief) of the basin and P is the perimeter of the basin. The relative reliefs are classified into three categories viz. (i) low relative relief = 0 km – 0.1 km, (ii) moderately relative relief 0.1 km – 0.3 km and (iii) high relative relief = above 0.3 km. The value of R_r is found to be 0.01 for all the sub-watersheds which indicates low relief .

4.8 Drainage Density

Drainage densities can range from less than 5 km/km^2 when slopes are gentle, rainfall low and bedrock permeable (e.g. sandstones), to much larger values of more than 500 km/km^2 in mountainous areas where rocks are impermeable, slopes are steep and rainfall totals are high (Hugget R.J., 2003). The drainage density (D_d) of the study area is 2.82 km/km^2 . Thus, in this study, the drainage density falls less than 5 km/km^2 which indicates that the area has a gentle slope, low rainfall and permeable bedrock. Low drainage densities are often associated with widely spaced streams due to the presence of less resistant surface materials (lithologies or rock

types), or those with high infiltration capacities. Drainage basin with high D_d values indicates that a large proportion of the precipitation runs off. On the other hand, a low drainage density indicates that most rainfall infiltrates into the ground and few channels are required to carry the runoff. In general, low drainage density leads to coarse texture while high drainage density leads to fine texture (Strahler, 1952). The value of D_d ranges from 2.76 to 2.89 for sub-watersheds SWS 6 and SWS 1 respectively which is shown in Table 7.

4.9 Constant of Channel Maintenance

The value of C_m ranges from 0.35 to 0.36 for sub-watersheds SWS (1, 2, 4, 5) and SWS (3 & 6) respectively.

4.10 Length of Overland Flow

Overland flow is significantly affected by infiltration and percolation through the soil, both varying in time and space (Schmid, 1997). Generally higher value of L_o is indicative of low relief and where as low value of L_o is an indicative of high relief. Kuls basin falls under high relief area.

In this study, the length of overland flow of the Kuls basin ranges from 0.17 to 0.18 for the sub-watersheds which shows low surface runoff in the study area.

4.11 Ruggedness Number

An extremely high value of ruggedness number (R_n) is encountered, particularly when both H and D_d are large i.e. when slope is steep and long. The value of R_n ranges from 2.30 to 4.68 for sub-watersheds SWS 1 and SWS 4 respectively which is quite low in the study area.

4.12 Stream/Drainage Frequency

It mainly depends on the lithology of the basin and reflects the texture of the drainage network. The basins of the structural hills have higher stream frequency, drainage density while the basins of alluvial has minimum. The stream frequency of the

study area is 5.25 stream segments per square kilometer. The existence of less number of streams in a basin indicates matured topography, while the presence of large number of streams indicates that the stream is youthful and still undergoing erosion. The value of D_f ranges from 4.99 to 5.59 for sub-watersheds SWS 6 and SWS 1 respectively which is shown in Table 7.

4.13 Drainage Texture

Smith (1950) have classified five different drainage textures related to various drainage densities as very coarse (below 2), coarse (2 - 4), moderate (4 - 6), fine (6 - 8) and very fine (8 and above). Drainage texture depends on a number of natural factors such as climate, rainfall, vegetation, rock and soil types, infiltration capacity, relief and stage of development. Weak rocks devoid of vegetative cover produce fine texture, while rocks which are hard and with vegetative cover produce coarse texture. The value of T ranges from 7.75 to 12.95 for sub-watersheds SWS 1 and SWS 4 respectively i.e the basin comprises of fine to very fine textures.

4.14 Form Factor

Form factor is the numerical index commonly used to represent different basin shapes (Horton). The value of form factor ranges between 0.1 to 0.8. The form factor of the study area is 0.21. This shows that the basin is very elongated and thus has low peak flow of longer duration. Consequently, the flood flow of this type of basin is easier to manage than the circular basin (Onosemuode C et al). The Smaller the value of form factor, the more elongated will be the basin. The basins with high form factors (0.8), have high peak flows of shorter duration, whereas, elongated drainage basin with low form factors have lower peak flow of longer duration. The form factor (R_f) ranges from 0.26 to 0.29 for sub-watersheds SWS 4 and SWS 1 respectively.

4.15 Circulatory Ratio

The calculated R_c value for the study area is 0.12 which indicates that the drainage basin is more elongated than circular and is characterized by low

relief. The value of circularity ratio varies from 0 (in line) to 1 (in a circle). It is affected by the lithological character of the basin. The ratio is more influenced by length, frequency (D_f), and gradient of streams of various orders rather than slope conditions and drainage pattern of the basin. It is a significant ratio, which indicates the dendritic stage of a basin. Its low, medium and high values are indicative of the youth, mature and old stages of the life cycle of the tributary basins. The circulatory ratio (R_c) ranges from 0.13 to 0.26 for sub-watersheds SWS 2 and SWS 6 respectively. Sub-watershed having circular to oval shape allows quick runoff and results in a high peaked and narrow hydrograph, while elongated shape of sub-watershed allows slow disposal of water, and results in a broad and low peaked hydrograph.

4.16 Elongation Ratio

Elongation ratio determines the shape of the basin and can be classified based on these values as circular (0.9 - 1), oval (0.8 - 0.9), less elongated (0.7 - 0.8), elongated (0.5 - 0.7), more elongated (< 0.5). Regions with elongation ratios are susceptible to more erosion whereas regions with high values correspond to high infiltration capacity and low runoff. The elongation ratio of the drainage basin is 0.51 which indicates more elongation and more prone to erosion with less infiltration capacity. Circular drainage basins are more efficient in the discharge of runoff. They are at greater risk from flood hazard because they have a very short lag time and high peak flows than the elongated basins. Elongated drainage basins have low side flow for shorter duration and high main flow for longer duration and are less susceptible to flood hazard. The value of R_e ranges from 0.58 to 0.61 for sub-watersheds SWS (4, 5, 6) and SWS 1 respectively shown in Table 7.

Table 8. Assignment of ranks & Compound parameter of six sub-watersheds of Kulsī basin

Sub Watershed	Linear parameters					Shape parameters				
	Drainage density (D _d)	Drainage frequency (D _f)	Bifurcation ratio (R _b)	Drainage Texture (T)	Length of Overland flow (L _o)	Form Factor (R _f)	Shape Factor (B _s)	Compactness coefficient (C _c)	Elongation ratio (R _e)	Circulatory ratio (R _c)
SWS 1	2.89	5.59	3.97	7.75	0.17	0.29	3.46	2.65	0.61	0.14
SWS 2	2.83	5.57	4.35	8.93	0.18	0.27	3.65	2.80	0.59	0.13
SWS 3	2.78	5.04	3.51	9.02	0.18	0.27	3.70	2.64	0.59	0.14
SWS 4	2.85	5.31	3.64	12.95	0.18	0.26	3.80	2.13	0.58	0.22
SWS 5	2.85	5.20	4.46	11.53	0.18	0.27	3.70	2.26	0.58	0.19
SWS 6	2.76	4.99	4.16	12.42	0.18	0.27	3.73	1.95	0.58	0.26

Table 9. Assignment of ranks & Compound parameter of six sub-watersheds of Kulsī basin

Sub Watershed	Linear parameters					Shape parameters					Compound parameter (C _p)
	Drainage density (D _d)	Drainage frequency (D _f)	Bifurcation ratio (R _b)	Drainage Texture (T)	Length of Overland flow (L _o)	Form Factor (R _f)	Shape Factor (B _s)	Compactness coefficient (C _c)	Elongation ratio (R _e)	Circulatory ratio (R _c)	
SWS 1	1	1	4	6	2	3	1	5	3	2	2.8
SWS 2	3	2	2	5	1	2	2	6	2	1	2.6
SWS 3	4	5	6	4	1	2	3	4	2	2	3.3
SWS 4	2	3	5	1	1	1	5	2	1	4	2.5
SWS 5	2	4	1	3	1	2	3	3	1	3	2.3
SWS 6	5	6	3	2	1	2	4	1	1	5	3.0

Table 10. Classification of Sub-watersheds on basis of Erodibility

SL NO	Sub watersheds	Compound parameter (C _p)	Final Priority	Erodibility
1	SWS 1	2.8	IV	Moderate
2	SWS 2	2.6	III	Slightly High
3	SWS 3	3.3	VI	Lowest
4	SWS 4	2.5	II	High
5	SWS 5	2.3	I	Highest
6	SWS 6	3.0	V	Low

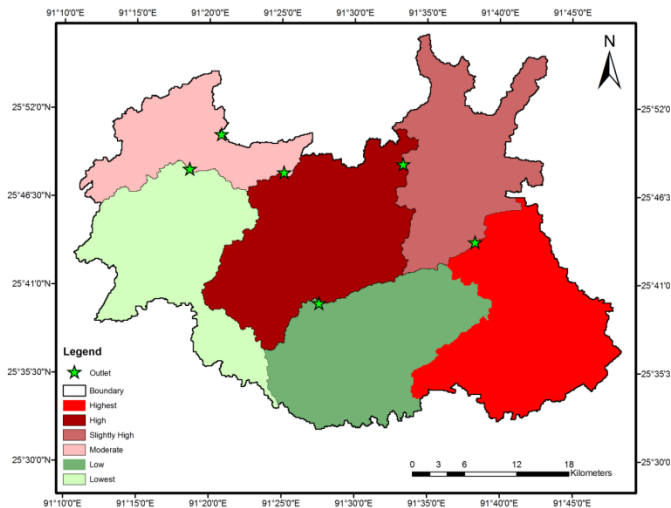


Fig. 4. Final Priority Map of sub-watersheds showing Erodibility classes

5. Prioritization of sub-watersheds

Drainage pattern of watershed refers geospatial relationship among the streams or rivers and associated with slope, soil type, rock resistance, structural and geological status of the basin. The study emphasizes the prioritization of the sub-watersheds on the basis of morphometric analysis. The final score of entire six sub-watersheds and their ranking are shown in Table 10. The maximum and minimum prioritized score of sub-watersheds is 2.3 and 3.3 respectively. High priority indicates the greater degree of erosion at specific sub-watershed. However it is necessary to improve the soil conservation measures as per priority in particular regions. In this study, linear parameters are considered as bifurcation ratio, drainage density, drainage texture, length of overland flow, drainage frequency, and the shape parameters are circularity ratio, form factor, elongation ratio and compactness coefficient. Hence the linear parameters have a direct relationship with erodability.

Prioritization of sub-watersheds, the highest value of linear parameters was assigned as rank 1, second highest value was assigned as rank 2 and so on. And the least value has been assigned as last in rank. Shape parameters such as circularity ratio, form factor, elongation ratio and compactness coefficient have an inverse relationship with erodibility (Biswas et al., 1999; Javed et al., 2009; Ratnam et al., 2005). The least value of shape parameter, has been shown more erodibility. Thus the lowest value of shape parameters was assigned as rank 1, next lower value was assigned as rank 2 and so on and the highest value was rated last

in rank. Hence, the ranking of the sub-watersheds has been determined by assigning the priority/rank. At last, the compound parameter has been calculated as averaging the all parameters in a particular sub-watershed. However the final priority has been assigned as the least rating value was assigned as highest priority, next higher value was assigned second priority and so on. Finally the highest score of compound parameter was assigned last rank (Table 6.9). The sub-watersheds has been categorized into three classes as high (2.3 – 2.5), medium (2.6 – 2.8) and low (3.0 – 3.3) priority on the basis of span of C_p value, the highest erosion prone being SWS 5 and lowest being SWS 3. In order to archive on the basis of morphometric analysis, SWS 5 & SWS 4 fall in the high priority, SWS 2 & SWS 1 fall in medium priority and SWS 6 and SWS 3 in the low priority category. In order to archive for management point of view, the conservation practices or measures are recommended as per their final priority.

6. Conclusion

An attempt has been made to carry out the quantitative morphometric analysis for Kushi basin using SRTM DEM of 90 m resolution in GIS software in absence of Toposheets.

Following are the conclusions interpreted in this study.

- The present work has illustrated morphometric analysis based on several drainage parameters, by which the watersheds have been classified as eight order basins.

- The values of form factor, circulatory ratio and elongation ratio of the study area shows that the basin is very elongated and thus has low peak flow of longer duration. Consequently, the flood flow of this type of basin is easier to manage than the circular basin.
- The low average bifurcation ratio of the Kuls basin of 3.76 is an indication that parts of its segment are liable to flooding. Bifurcation ratios ranging from 3 – 5 indicate natural drainage system characterized by homogenous rock. This low Rb value also indicates less structural disturbance in Kuls basin.
- The drainage density (D_d) of the study area is 2.82 km/km^2 . Thus, in this study, the drainage density falls less than 5 km/km^2 which indicates that the area has a gentle slope, low rainfall and permeable bedrock.
- The value of Drainage texture ranges from 7.75 to 12.95 for sub-watersheds SWS 1 and SWS 4 respectively which shows that the basin has a very fine texture.
- It is found that the SWS 5, SWS 4 and SWS 2 show higher erosion and soil loss-prone areas. Hence, suitable soil erosion control measures are required in these sub-watersheds to preserve the land from further erosion.
- The conventional methods of morphometric analysis are time consuming and error prone, so instead, GIS technique has been used for more reliable and accurate estimation of similar parameters of watersheds. However, geological field verification also agrees with the present morphological-based prioritization.
- The present study is valuable for erosion control, watershed management, land and water resources planning and future prospective related to runoff study.

REFERENCES

- 1) Biswas, S., Sudhakar, S., Desai, V., Prioritisation of subwatersheds based on morphometric analysis of drainage basin: A remote sensing and GIS approach, *Journal of the Indian society of remote sensing* **27**(1999), pp. 155-166.
- 2) Datt R, Ramanathan NL. Environmental monitoring'. Proceedings of Seminar on the Status of Environmental Studies in India, Thiruvanathapuram. 1981;284-287.
- 3) Gregory, K.J., Walling, D.E., *Drainage basin form and process: a geomorphological approach*. Edward Arnold London (1973).
- 4) Guttschalk L.C. Reservoir sedimentation. In: Chow VT (ed.), Handbook of applied hydrology, McGraw Hill, Book Company, Newyork, Sections. 1964;4-11.
- 5) Hack, J. T., 1973. Stream profile analysis and stream gradient index. U. S. Geological Survey Journal of Research, 1, pp 421-429.
- 6) Horton, R.E., Drainage-basin characteristics, *Transactions, American geophysical union* **13**(1932), pp. 350-361.
- 7) Horton, R.E., Erosional development of streams and their drainage basins; hydrophysical approach to quantitative morphology, *Geological Society of America Bulletin* **56**(1945), pp. 275-370.
- 8) Hugget RJ. Fundamentals of geomorpho-logy. London, New York, Routledge; 2003.
- 9) Javed, A., Khanday, M.Y., Ahmed, R., Prioritization of sub-watersheds based on morphometric and land use analysis using remote sensing and GIS techniques, *Journal of the Indian society of remote sensing* **37**(2009), pp. 261-274.
- 10) Melton, M.A., An analysis of the relations among elements of climate, surface properties, and geomorphology. DTIC Document (1957).
- 11) Miller, V.C., A Quantitative geomorphic study of drainage basin characteristics in the clinch mountain area virginia and tennessee. DTIC Document (1953).
- 12) Morisawa, M., Accuracy of determination of stream lengths from topographic maps, *Transactions, American Geophysical Union* **38**(1957), pp. 86-88.
- 13) N. Panigrahy, B. C. Patwary, A report on Estimation of Design Flood for Kuls Basin using GIUH Approach, National Institute of Hydrology.
- 14) Nag, S., Morphometric analysis using remote sensing techniques in the Chaka sub-basin, Purulia district, West Bengal, *Journal of the Indian society of remote sensing* **26**(1998), pp. 69-76.
- 15) Nag, S., Chakraborty, S., Influence of rock types and structures in the development of drainage network in hard rock area, *Journal of the Indian Society of Remote Sensing* **31**(2003), pp. 25-35.
- 16) Onosemuode C, Adetimirin OI, Aboderin SO. Hydrological analysis of onitsha North East drainage basin using Geoinformatic techniques. *World Applied Sciences Journal*. 2010;11(10):1297-1302.
- 17) Parveen R, Kumar U, Singh VK. Geomorphometric characterization of upper South Koel basin, Jharkhand: A remote sensing and GIS approach. *Journal of Water Resource and Protection*. 2012;4: 1042–1050.

[Back to table of contents](#)

- 18) Ratnam, K.N., Srivastava, Y., Rao, V.V., Amminedu, E., Murthy, K., Check dam positioning by prioritization of micro-watersheds using SYI model and morphometric analysis—remote sensing and GIS perspective, *Journal of the Indian society of remote sensing* **33**(2005), pp. 25-38.
- 19) Scheidegger, A.E., The algebra of stream-order numbers, *United States Geological Survey Professional Paper*(1965), pp. 187-189.
- 20) Schumm, S.A., Evolution of drainage systems and slopes in badlands at Perth Amboy, New Jersey, *Geological Society of America Bulletin* **67**(1956), pp. 597-646.
- 21) Schmid BH. Critical rainfall duration for overland flow an infiltrating plane surface. *Journal of Hydrology*. 1997;193:45-60.
- 22) Shreve, R.L., Infinite topologically random channel networks, *The Journal of Geology*(1967), pp. 178-186.
- 23) Smith, K.G. (1950). Standards for grading texture of erosional topography. *Am. J. Sci.* 248: 655-668.
- 24) Srivastava VK(1997) Study of Drainage pattern of Jharia coal field (Bihar), India using Remote Sensing Technology.*J.Indian Soc.Remote Sensing* 25(1) 41-46
- 25) Strahler, A.N., Hypsometric (area-altitude) analysis of erosional topography, *Geological Society of America Bulletin* **63**(1952), pp. 1117-1142.
- 26) Strahler, A.N., Quantitative analysis of watershed geomorphology, *Transactions of the American geophysical Union* **38**(1957), pp. 913-920.
- 27) Strahler, A.N., Dimensional analysis applied to fluvially eroded landforms, *Geological Society of America Bulletin* **69**(1958), pp. 279-300.
- 28) Strahler, A.N., 1) HANDBOOK OF APPLIED HYDROLOGY, (1964).
- 29) Subodh CP, Gopal CD. Morphometric analysis and associated land use study of a part of the Dwarkeswar watershed. *International Journal of Geomatics and Geosciences*. 2012;3(2):351–363.

Development of synthetic unit hydrographs for Kulsri river basin using Remote sensing & GIS

Ranjan Das ⁱ⁾, Dr. Sanjay Kumar Sharma ⁱⁱ⁾, Er. Gulshan Tirkey ⁱⁱⁱ⁾, Dr. C. K. Jain ^{iv)}, Dr. Mrinal Kumar Borah ^{v)}

i) Post Graduate Student (Civil), Assam Engineering College

ii) Scientist 'B' National Institute of Hydrology, Guwahati-781006

iii) Scientist 'B' National Institute of Hydrology, Guwahati-781006

iv) Scientist 'G' & Coordinator, National Institute of Hydrology, Guwahati-781006

v) Associate Professor, Civil Engineering Department, Assam Engineering College

ABSTRACT

Synthetic unit hydrograph (SUH) methods are generally used in determining watershed characteristics of un-gauged watersheds. In order to construct a unit hydrograph in areas where detailed information are not available, unit hydrograph can be synthetically generated using some relationships. The synthetic methods used were those of Snyder's, Soil Conservation Service (SCS) and Central Water Commission (CWC) method. This study presents the use of Geographic Information System (GIS) for evaluating parameters necessary for the generation of synthetic unit hydrograph of Kulsri River Basin which lies between 25°30'0"N and 25°57'30"N latitude and 91°10'0"E and 91°50'0"E longitude. Drainage network for the watershed and physiographic parameters are estimated using Shuttle Radar Topography Mission Digital Elevation Model SRTM DEM (90m x 90m). The watershed is delineated using SRTM DEM and the Longest path of the stream network including the length of centroid and watershed area and slope are generated in ArcGIS 9.3TM software. The watershed has an area of 1658.94 km² and an average slope was calculated to be 0.016m/m. The peak discharge values obtained from the methods used varied from 222.23m³/s to 254.51m³/s while the peak time ranged from 14.56 hr to 18.38 hr. The observed hydrograph of Kulsri River Basin is obtained from previous works is calculated with derived synthetic hydrographs and the best applicable method for the watershed is evaluated by graphical as well as statistical comparison. The three methods considered are useful in one way or the other, but Snyder and SCS methods have specific features utilizing major unit hydrograph characteristics and watershed parameters in generating unit hydrographs and are thus recommended in this study at River Basin scale.

KEY WORDS: Synthetic Unit hydrograph (SUH), ungauged, watershed, time of concentration, SRTM DEM, Geographic Information System.

1. INTRODUCTION

India has a great potential for agriculture and water resources utilization. The geographical area of India is 3.28 Mkm² and the annual runoff from rainfall is 167 M ha-m. However detail information regarding rainfall data and flood hydrograph are not available at certain locations. This problem has been overcome with the use of empirical equations which relate the salient hydrograph characteristics to the basin characteristics. Snyder (1938) developed the most commonly used Synthetic unit hydrograph, which was later modified by Taylor and Schwartz (1952). Mockus (1957) developed the concept of dimensionless unit hydrograph to form a basis for developing synthetic unit hydrographs. Ramirez (2000) stated that SCS dimensionless hydrograph is a Synthetic UH in which the discharge is expressed as a ratio of discharge, Q , to peak discharge, Q_p and the time by the ratio of time, t ,

to time to peak of the UH, t_p . Sule and Alabi(2013) used Synthetic Unit Hydrograph(SUH)methods to generate

unit hydrographs for the Awun River Basin in Kwara State, Nigeria. The synthetic methods used were those of Snyder's, SCS and Gray's. The three methods employed have been found useful in one way or the other, but Snyder's & SCS method have been considered distinct and more important. This study applied three methods to develop SUH for Kulsri River Basin, i.e., Snyder, SCS and CWC method the parameters of which were derived with the help of Arc GIS 9.3 software and the methods were compared with the observed ordinates of 3hr unit hydrograph derived by Scientists of National Institute of Hydrology, N.Panigrahy, B.C.Patwary and K.K.S. Bhatia (2006) both graphically and statistically and established the best method applicable for the basin under study.

2. MATERIAL AND METHODS

2.1 Study Area

The Kulsī basin is located between latitude 25°30'39"N to 25°58'03"N and longitude 91°11'52" E to 91°48'09" E . The area considered lies in the Kamrup and Goalpara distict of Assam as well as west Khasi Hills and West Garo Hills district of Meghalaya. The Kulsī river is composed of three rivers, namely Khri, Krishniya and Umsiri, all of which originate from West Khasi Hill range and flow North and finally join the Brahmaputra. The topographic map and stream networks of Kulsī Basin are derived with the help of Geographic Information System (GIS).The estimated catchment area considered in this analysis is 1698.54 km² , River length of about 104.165 km and the length along the main river channel from the outlet to a channel point nearest the watershed centroid is measured as 30.49km. Figure 1 shows location map of Kulsī River Basin and Figure 2 shows the longest flow path and stream network.

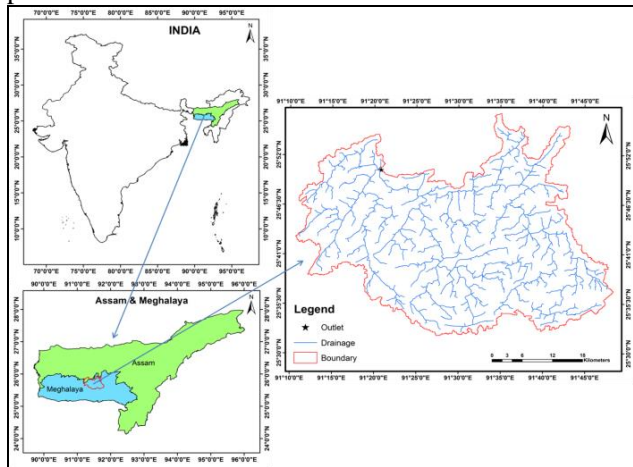


Fig.1. Location Map of Kulsī Basin

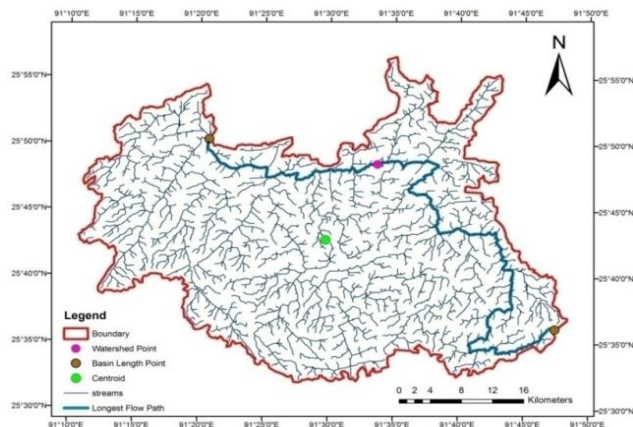
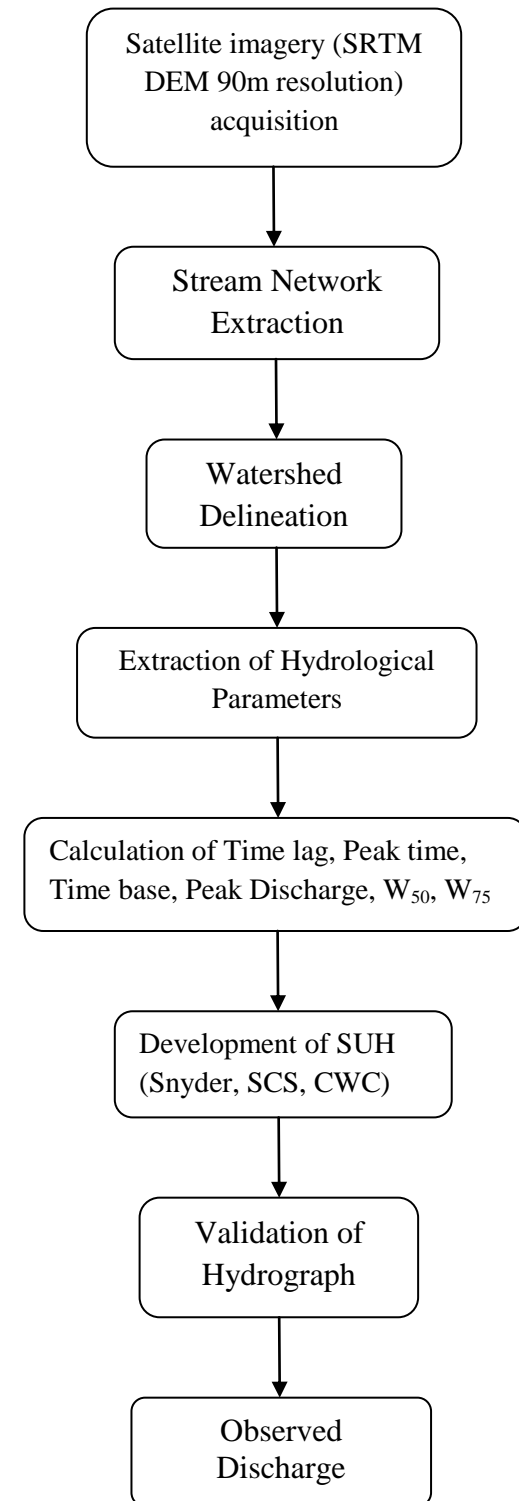


Fig.2. Longest Flow Path and Stream Network of Kulsī Basin

2.2 Flow Chart of Methodology



2.3 Development of Synthetic Unit Hydrograph

The three methods that were used in the generation of synthetic unit hydrograph for the watershed includes Snyder's, SCS, and CWC method.

2.3.1 Snyder's Method

The Snyder's method was used to compute the unit hydrograph characteristics such as lag time or basin lag, unit -hydrograph duration, peak discharge, time base or base period, and hydrograph time widths at 50 and 75% of peak flow. Determination of all these parameters allows for the development of unit hydrographs. Snyder considered the shape and area of the basin and gave the following empirical equations after analyzing a large number of hydrographs from drainage basins of areas from 25 to 25000 km².

a) Lag time or basin lag: The lag time was defined as the time from the center of mass of effective rainfall to the peak rate of flow. The basin lag is given by:

$$t_p = C_t (LL_c)^{0.3} \tag{1}$$

where t_p = the basin lag (hours), C_t = a coefficient which depends upon the basin slope and storage effects (Values of C_t varies from 1.35 to 1.65) L = length of the main stream of the catchment (km), L_c = distance from the basin outlet to a point on the stream which is nearest to the centroid of the area of the basin(km).

b) Unit- hydrograph duration: The duration of rainfall excess for Snyder's synthetic unit- hydrograph development is a function of lag time. The unit duration of the storm was given as follows:

$$t_r = t_p/5.5 \tag{2}$$

where t_r = the unit duration of the storm (hours), t_p = the basin lag (hours).

c) Peak discharge: Peak discharge is the highest volume of runoff over the basin. The peak discharge is given by the equation below:

$$Q_p = \frac{2.78 C_p A}{t_p} \tag{3}$$

The peak discharge per unit area is given by the equation below:

$$q_p = \frac{Q_p}{A} = \frac{2.78 C_p}{t_p} \tag{4}$$

where: Q_p =the peak discharge (m³/s),

C_p = the coefficient which depends upon the retention and storage characteristics of the basin (Values of C_p varies from 0.3 to 0.93).

t_p = the basin lag (hours)

A = area of the basin (km²);

d) Time base or base period: The time base of a hydrograph is the time from which the concentration curve (rising portion of a hydrograph) begins until the direct runoff component reaches zero. The base period (T_b) of the unit hydrograph is given by:

$$T_b = 72 + 3t_p(\text{hrs}) \tag{5}$$

e) Hydrograph time widths at 50 and 75% of peak flow: To assist in the sketching of unit hydrographs, the widths of unit hydrographs at 50 and 75% of the peak have been found for US catchments by the US Army Corps of Engineers. These widths (in time units) are correlated to the peak discharge intensity and are given by:

$$W_{50} = \frac{5.87}{q^{1.08}} \tag{6}$$

$$W_{75} = \frac{W_{50} - 3.4}{1.75 - q^{1.08}} \tag{7}$$

where, W_{50} = width of unit hydrograph in h at 50% peak discharge

W_{75} = width of unit hydrograph in h at 75% peak discharge

The parameters obtained by Snyder's method are shown in Table 3.

2.3.2 SCS method:

The SCS method is a method developed by the soil conservation service for constructing synthetic unit hydrographs which is basically of two types:

- i) SCS Dimensionless Unit Hydrograph and
- ii) SCS Triangular Unit Hydrograph

i) SCS Dimensionless Unit Hydrograph

Dimensionless unit hydrographs based on a study of a large number of unit hydrographs are recommended by various agencies to facilitate construction of synthetic unit hydrographs. Here the ordinate is ($\frac{Q}{Q_p}$) which is the

discharge Q expressed as a ratio to the peak discharge Q_p and the abscissa is ($\frac{t}{T_p}$), which is the time t expressed

as a ratio of the time to peak T_p . By definition, $Q/Q_p=1.0$ when $t/T_p=1.0$. The coordinates of the SCS dimensionless unit hydrograph is given in Table 1 for use in developing synthetic unit hydrograph in place of Snyder's equations.

$$S = \frac{\text{Difference in elevation along the flow path}}{\text{Maximum length of flow}} \quad (12)$$

Table 1. Coordinates of SCS Dimensionless Unit Hydrograph

t/t_p	Q/Q_p
0.0	0.000
1.0	1.000
1.50	0.660
2.00	0.320
2.60	0.130
3.00	0.074
4.00	0.018
4.50	0.009
5.00	0.004

ii) SCS Triangular Unit Hydrograph

This method requires only the determination of the time to peak and the peak discharge. The peak discharge can be expressed as follows:

$$Q_p = \frac{0.208 A}{t_p} \quad (8)$$

Where Q_p = peak discharge (m^3/s); A = drainage area (km^2); and t_p = the time to peak (hour). The time to peak is given by:

$$t_p = \frac{t_r}{2} + t_L \quad (9)$$

where: t_p = the time to peak (hour);
 t_r = the duration of rainfall (hour);
 t_L = the lag time (hour)

The lag time can be described by the equation below:

$$t_L = 0.6 t_c \quad (10)$$

where: t_c = the time of concentration (hours).
 The time of concentration can be defined as the time required, with uniform rainfall, for 100% of a tract of land to contribute to the direct runoff at the outlet. Linsley et al found that the basin lag t_p is better correlated with the catchment parameter $(LL_{ca}/\sqrt{S})^n$.

According to US practice: For small drainage basins, the time of concentration is assumed to be equal to the lag time of the peak flow. Thus $t_c = t_p$

$$t_c = C_{tl} \left(\frac{LL_{ca}}{\sqrt{S}} \right)^n \quad (11)$$

where $n=0.38$; $C_{tl}=0.50$ to 1.715

The watershed slope can be described by the expression below:

The duration of rainfall can also be expressed as:

$$t_r = 0.133 t_c \quad (13)$$

where: t_r = the duration of rainfall (hour);
 t_c = time of concentration (hour).

Parameters obtained from calculation by SCS method are shown in Table 4.

2.3.3 CWC method:

The Central Water Commission recommended some empirical equations for computing synthetic unit hydrograph for south Brahmaputra subzone. The following relationships have been derived for estimating Unit hydrograph parameters for an ungauged catchment:

Table 2. Synthetic Unit Hydrograph Empirical Equations (CWC)

SI No.	Relationship
1	$Q_p = 0.905 (A)^{0.758}$
2	$q_p = Q_p/A$
3	$t_p = 2.87/(q_p)^{0.839}$
4	$W_{50} = 2.304/(q_p)^{1.035}$
5	$W_{75} = 1.339/(q_p)^{0.978}$
6	$WR_{50} = 0.814/(q_p)^{1.018}$
7	$WR_{75} = 0.494/(q_p)^{0.966}$
8	$T_B = 2.447 (t_p)^{1.157}$
9	$T_m = t_p + t_r/2$

Table 3. SNYDER'S Parameters

T_p (h)	Q_p (m^3/s)	T_b (h)	W_{50} (h)	W_{75} (h)
18.38	254.51	122.56	44.45	25.75

Table 4. SCS Parameters

L (km)	S (m/m)	A (km^2)	t_L (h)	t_c (h)
104.165	0.016	1658.94	14.09	23.49

Table 5. CWC Parameters

T_p (h)	Q_p (m^3/s)	T_b (h)	W_{50} (h)	W_{75} (h)
-----------	-------------------	-----------	--------------	--------------

14.56	249.62	52.10	16.36	8.54
-------	--------	-------	-------	------

Table 6. Summary of unit hydrograph peak flows and times to peak for the methods employed

Method	Q_p (m^3/s)	T_p (h)
Snyder's	51	4
SCS	75	6
CWC	120	8

3. RESULTS AND DISCUSSIONS

In the present study different thematic maps for the Kushi Basin have been prepared from Raw DEM (SRTM) which are freely available on the internet. With the use of Arc GIS 9.3 different parameters are extracted which are being used in deriving Synthetic Unit Hydrograph.

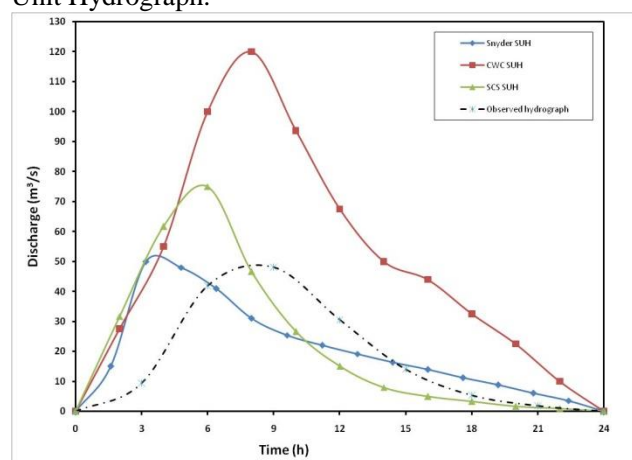


Fig. 3. Comparison of Synthetic Unit Hydrograph (SUH) with Observed Hydrograph

3.1 Statistical Analysis

A statistical analysis was adopted to establish the best possible method to be considered for the basin under study. The performance criteria that were considered for the three methods are Root Mean Square Error (RMSE), Mean Absolute Error (MAE), Coefficient of Residual Mass (CRM) and Modeling Efficiency (ME).

4. CONCLUSIONS

The results obtained so far for the ungauged basin depicts that the generation of unit hydrograph through synthetic methods were useful and effective. The methods required only the physiographic

characteristics for its calculations. The final comparison graph showed that the peak discharge value of the Snyder method and the observed exhibit similar trends. The statistical evaluation of the three methods showed that the root mean square error, mean absolute error and coefficient of residual mass of Snyder method is the lowest while the modeling efficiency of SCS method has been found to be better than the other two methods. The SCS dimensionless graph is in the intermediate position while the peak discharge of CWC method recorded the highest value. It is due to the fact that the empirical equations considered in CWC method was developed at regional scale for entire Brahmaputra. This study highlights that at sub basin scale, development of SUH techniques is more reliable than using empirical equations at regional scale. The Snyder method is considered to be most suitable for this basin, exhibiting most of the major unit hydrograph characteristics and watershed characteristics in the generation of unit hydrographs and obtaining similar peak values as that of the observed hydrograph.

REFERENCES

- 1) Arora, K.R (2004), "Irrigation, water power and water resources engineering", Standard Publishers Distributions, 1705-B, NAI SARAK, Delhi, pp.79-106.
- 2) CWC (1969), "Flood Estimation by Unit Hydrograph Method", Chapter-5, CWC Recommended Procedure.
- 3) Panigrahy N, Patwary BC, Bhatia KKS (2006), "Estimation of Design Flood for a Data Scarce Basin using GIUH Approach" Journal of Indian Water Resources Society Vol. 26 No. 3-4.
- 4) Salami A.W., Bilewu SO, Ayansola AM, Oritola SF (2009), "Evaluation of synthetic unit hydrograph methods for the development of design storm hydrographs for Rivers in South-West, Nigeria." J. Am. Sci.5 (4):23-32.
- 5) Subramanya K., (2009), "Engineering Hydrology." third edition Tata McGraw-Hill Publishing Company Limited New Delhi.
- 6) Sule B. F. and Alabi S.A. (2013), "Application of synthetic unit hydrograph methods to construct storm hydrographs." International Journal of Water Resources and Environmental Engineering Vol. 5(11),pp.639-647, DOI 10.5897/IJWREE2013.0437 ISSN 2141-6613 © 2013.

Back to table of contents

Infiltration rate of fiber reinforced soil using mini disk infiltrometer

Rojimul Hussainⁱ⁾, Vikram Agarwalⁱⁱ⁾ and Soutreya Kunduⁱⁱ⁾

i) M.Tech Student

ii) B.Tech Student

Department of Civil Engineering, IIT Guwahati, Guwahati, Assam - 781039, India.

E-mail: ⁱ⁾ rojmul.hussain@iitg.ernet.in, ⁱⁱ⁾ vikram.2015@iitg.ernet.in, ⁱⁱ⁾ soutreya.kundu@iitg.ernet.in

ABSTRACT

The infiltration rate of embankment soil is an important parameter that determines its performance against soil erosion, water drainage, and surface runoff. The use of fiber reinforced soil has gained momentum in the recent past as subgrade or in embankment applications and numerous studies have been undertaken to understand its mechanical properties. However, very few studies have accounted the infiltration of water through such fiber reinforced soil. The current study adopts an invasive species, water hyacinth (WH), as a natural fiber to reinforce soil. A series of tests have been undertaken using mini-disk infiltrometer to monitor the infiltration rate of such soil-WH fiber composite. The soil is compacted at two increment densities and the fiber percentage has been varied up to 1.00% of dry weight of the soil. The results indicate that the infiltration rate and the hydraulic conductivity of the soil amended with water hyacinth fiber increases with increasing fiber content, and decreases as the density increases compared to bare soil.

Keywords: Infiltration rate, water hyacinth, fiber reinforcement, minidisk infiltrometer.

1. INTRODUCTION

Twenty first century comes with a wave of industrialization and brings with it the challenges of sustainable development. Soil erosion and slope failure are serious impediments encountered by many countries. In the last few decades a vast range of studies have been conducted to counter the problem of soil erosion and slope failure. A major cause of soil erosion and slope failure is the low hydraulic conductivity of the soil. Higher hydraulic conductivity reduces soil erosion, enriches the ground water table by reducing surface runoff and enhances slope stability by promoting more vegetation (Horton, 1933; Damiano et al., 2010). Several studies have been done on how the mixing of different admixtures and artificial fibers such as geotextiles affect the hydraulic conductivity of the soil (Hafez, 1974; Fernandez et al., 1985; Koerner, 2012). The use of natural fibers in reinforcing soil has caught the attention of many researchers. Several studies have been done on the amendment of natural fiber such as jute, coir, water hyacinth, hemp, flax, sisal etc. in soil to reinforce and improve the strength (Hejazi et al., 2012; Fullen et al., 2007; Tang et al, 2007; Giménez et al., 2014; Faruk et al., 2012; Prabakar et al., 2002; Tang et al.,2010; Kumar et al.,2015). However, the effect of hydraulic conductivity of soil due to amendment of natural fibers has rarely been studied. The use of water hyacinth (*Eichhornia crassipes*) fiber in improvement of different soil properties are very limited. WH is not only easily available, abundant but also a cheap fiber. WH is mostly considered as an

unwanted substance because it grows in water and lowers the oxygen content of water, blocks the sunlight from entering the water bodies, thus depleting aquatic life. Nowadays, thousands of rupees are being spent for removing it. And the removed water hyacinth majorly rots as not much use of it, apart from a component of fodder, is known till date (Ding Jianqing et al., 2001). Therefore, the use of WH in soil amendment is coming into picture.

Many researchers have studied the infiltration mechanism and hydraulic conductivity of the soil using mini disk infiltrometer (MDI) (Šimůnek et al.,1998; Li et al., 2005; Holden et al.,2001). Infiltration is the process by which water present on the ground enters into the soil. A mini disk infiltrometer is an acrylic tube having two chambers namely bubble chamber and reservoir that works on the principle of suction under a certain adjustable pressure. The pressure is adjusted in the bubble chamber by means of a suction control tube dipped into water. The reservoir is filled with water, which is sucked into the soil passing through a sintered steel disk. The aim of this study is to measure the infiltration rate and hydraulic conductivity of a soil amended with water hyacinth (WH) fiber using mini disk infiltrometer (MDI).

2. MATERIAL AND METHODS

2.1 Soil composition and characteristics

The soil used in this study is collected from a site in the IIT Guwahati campus. The specific gravity of the soil was 2.67 determined as per IS-2720-Part 3-1980.

According to the provisions of IS-2720-Part 4-1985 the grain size distribution of the soil was done. The percentage of fine sand, medium sand and coarse sand was 18.85%, 6.50% and 0.11% respectively. The soil mainly consisted of silt (50.24%), and clay (24.30%). The liquid limit (40.49%) and plastic limit (24.79%) of the soil was determined with the help of IS-2720-Part 5-1985. The soil is classified as ML (ASTM D2487-11). The following table summarizes the basic engineering and physical properties of the soil.

Table 1. Engineering Properties of the soil

Sl. No.	Soil Property	Value
1	Specific Gravity	2.67
2	<u>Grain Size Distribution</u>	
	Coarse Sand (4.75mm-2mm)	0.11 (%)
	Medium Sand (2mm-0.425mm)	6.50 (%)
	Fine Sand (0.425mm-0.075mm)	18.85 (%)
	Silt (0.075mm-0.002mm)	50.24 (%)
	Clay (< 0.002mm)	24.30 (%)
3	<u>Consistency Limits</u>	
	Liquid Limit	40.49 (%)
	Plastic Limit	24.79 (%)
	Shrinkage Limit	23.31 (%)
	Plasticity Index	15.70 (%)
4	<u>Compaction Characteristics</u>	
	Optimum Moisture Content	16.00 (%)
	Maximum Dry Density	1.70 (g/cc)
5	<u>Shear Strength Parameters</u>	
	Cohesion	16.89 (kPa)
	Angle of Internal Friction	14.17 °



Fig. 1. Embankment failure at a local site inside IIT Guwahati campus.

2.2 Fiber composition and characteristics

The bio-chemical composition percentages are of great significance to determine the physical properties of a lignocellulose fiber.

Lignin is a highly cross-linked molecular complex that holds together individual cells. The lignin concentration controls the rate of decomposition of organic matter (Berg et al., 1984; Taylor et al., 1989). The standard method of TAPPIT222om-88 (TAPPI Test Methods, 1996) was followed to determine the lignin. Cellulose provides strength to the plant cell walls and thus makes them stable. It is one of the main structural components of the bio-fiber. The total cellulose content of the air-dried water hyacinth fiber was determined by Jenkins method (1930). Hemicelluloses are relatively low molecular weight polysaccharides present in plant cell walls. They remain associated with the cellulose present in the plant cell walls and are responsible for moisture absorption and biodegradation (Rowell & Stout, 2007). Goering and Van (1970) provided a method which was used to calculate the hemicellulose content from the difference between neutral detergent fiber (NDF) and acid detergent fiber (ADF). The percentage of ash present gives us an approximate estimate of the inorganic content in biological mass (McNaught and Wilkinson, 1997). The ash content was determined by the ASTM method E1755-01 (ASTM, 2007). Since the water hyacinth was air-dried, it

definitely contained some moisture. This moisture content was calculated by oven-drying the fiber at 107°C for 1 day. The moisture content of the air-dried sample was found to be 12.89 %. Table 2 shows the basic bio-chemical and physical properties of the water hyacinth fiber. Provisions of IS-2720-Part 3-1980 was followed to determine the specific gravity of the fiber; it was found to be 0.66. The average value for the breaking tensile strength of the fiber was found to be 250 N and this was determined as per the rules of IS-1670-1991.

Table 2. Properties of fiber

	Properties	Quantity
Bio-chemical Composition Of fiber	Lignin	11.14
	Cellulose	35.60
	Hemicellulose	21.18
	Ash Content	11.21
Physical properties of fiber	Specific gravity	0.66
	Thickness of fiber	0.4 mm
	Tensile Strength	245 N



Fig. 2. Overview of water hyacinth fiber

3. TEST PROCEDURE AND PREPARATION OF SAMPLE

The water hyacinth plants were extracted from the water bodies and were air dried until no significant change in moisture content was observed (Prabakar and

Sridhar, 2002). The stem of the dried plant was then separated. The water hyacinth fiber obtained was then cut into small pieces of around 2 cm length and 5-7 mm breadth (Fig. 2). After that the cut water hyacinth (WH) fiber was mixed randomly with a locally available silty clay (ML) soil till a uniform soil-WH fiber composite is obtained. Water was added in small increments in the soil fiber composite in predetermined quantities (12.00% of the dry weight of the soil) and was mixed thoroughly. Three samples were prepared for every batch of soil at different WH fiber contents (0.50%, 0.75%, 1.00% of the dry weight of the soil) and densities (0.9 MDD, 1.05 MDD) to inspect the effect of fiber variation and density variation on the hydraulic conductivity of composite respectively. The batches of soil – WH fiber composites were sealed in plastic bags then putted in the desiccator for 24 hours for moisture balance. The soil – WH fiber composite was divided into three equal parts and then each part was compacted into a steel mould of height 17.5 cm and diameter 15 cm one by one. The surface of the soil was then levelled and smoothened to place mini disk infiltrometer- MDI (Fig. 3). Water was then filled in the bubble chamber and water reservoir of the MDI and a suction rate of 2 cm was adjusted. Then the MDI was carefully placed on the smooth spot near the center of the mould and at initial time ($t=0$ seconds) the reading in the water reservoir was noted. The readings were taken after a regular time interval of 60 seconds till about 22-25 ml of water infiltrated into the soil-fiber composite.

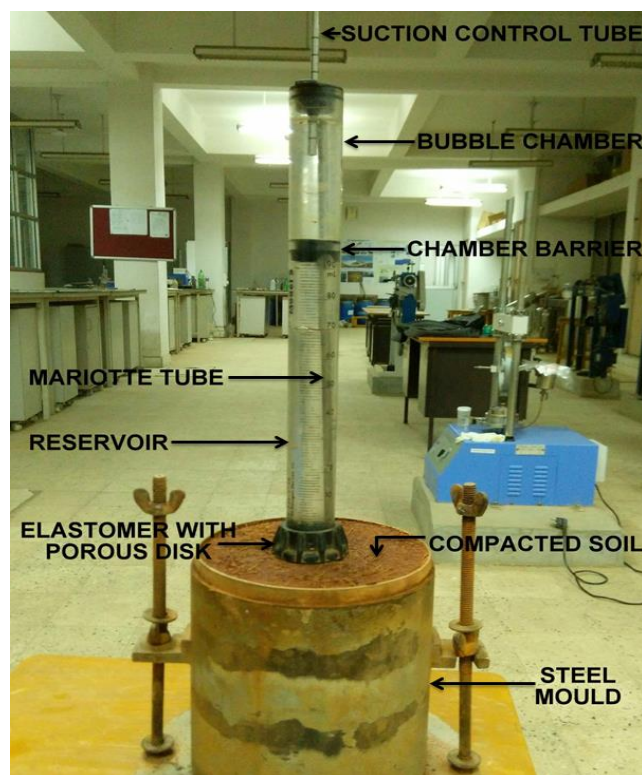


Fig. 3. Experimental setup showing infiltration process

4. RESULTS AND DISCUSSION

The data (cumulative infiltration with time) obtained from infiltration tests with mini disk infiltrometer (Fig. 4.) was analysed and the hydraulic conductivity of the soil was calculated using the spreadsheet provided by the decagon devices (instruction manual MDI, 2016). It was programed based upon the model proposed by Zhang (1997). The measured data of cumulative infiltration is best fitted with the given function:

$$I = C_1 t + C_2 \sqrt{t} \quad (1)$$

Where C_1 ($\frac{m}{s}$) is related to hydraulic conductivity and C_2 ($\frac{m}{s^{1/2}}$) is related to soil sorptivity. For the case of vertical flow, the sorptivity is negligible and our focus is mainly on hydraulic conductivity, so we have ignored the second term and targeted the first term.

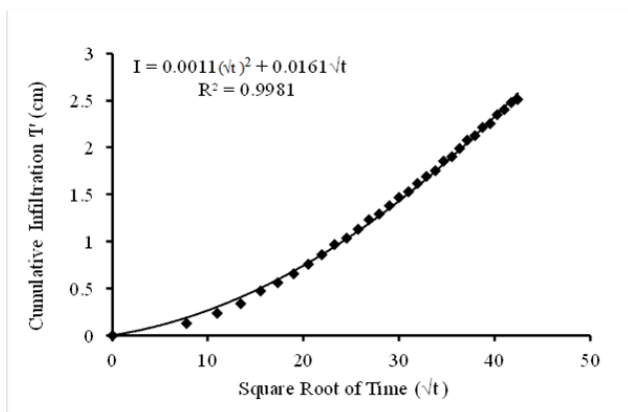


Fig. 4. Cumulative Infiltration vs square root of time plot of soil-fiber composite

The cumulative infiltration vs the square root of time plot of the soil-WH fiber composite has been shown in figure 4. The slope of the curve of the cumulative infiltration vs the square root of time is the parameter C_1 . From the figure 4 it has been observed that the cumulative infiltration of the soil-WH fiber composite increases with the decreasing rate i.e. as the time of flow of water into the soil composite increases the infiltration rate decreases. The decrease of the rate of infiltration with time is mainly because of the decrease of the moisture absorption tendency of the soil, as the flow of water continue for long time the void spaces get filled with water, the suction of the soil gets reduced and hence a decline in the tendency of moisture adsorption of the soil is observed.

The hydraulic conductivity of the soil was given by the equation.

$$k = C_1/A \quad (2)$$

Where C_1 is the slope of the cumulative infiltration

vs the square root time plot and A is a value relating the van Genuchten parameters (α , n, m).

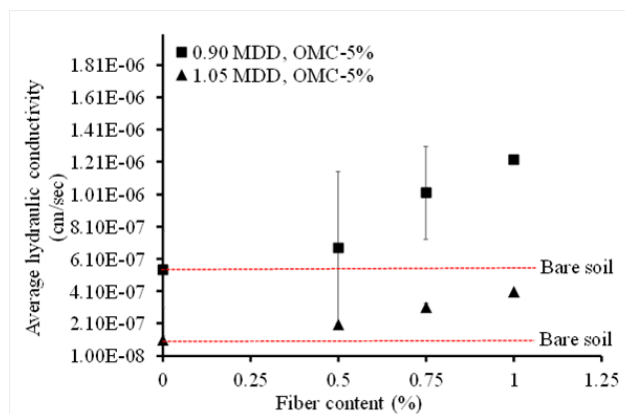


Fig. 5. Variation of average hydraulic conductivity of soil-WH fiber composite with fiber content.

The hydraulic conductivity of the soil-WH fiber composite was determined as the average hydraulic conductivity. Three test samples for each fiber content and compaction state were tested to determine the average hydraulic conductivity of the soil fiber composite. Standard deviation of these three samples were calculated to assess the deviation in each plotted point. The variation of average hydraulic conductivity with fiber content and density is shown in figure 5. From figure 5 it has been observed that with the increase of fiber content the average hydraulic conductivity of the soil-WH fiber composite increases as compare to that of bare soil. The average hydraulic conductivity increases with increasing rate upto fiber content of 0.75% and after that increases with a decreasing rate. One of the possible reasons for increase in hydraulic conductivity could be the preferential water flow through the soil-fiber interface. The standard error bar provided in each measure point indicates the variation of each point with the average value.

The average hydraulic conductivity of the soil –WH fiber composite decreases as the density of the soil fiber composite increases. The hydraulic conductivity decreases with increase in density of composite. This is mainly due to decrease in void spaces or void ratio of soil composite and higher packing of soil particles. Due to this, the water flow path of the soil fiber composite, gets blocked and hence there is a decrease in hydraulic conductivity.

5. CONCLUSIONS

One of the most important characteristics of soil is its hydraulic conductivity. The hydraulic conductivity is a property of soil related to slope stability and soil erosion, etc. Silty clay (ML) soil sample was reinforced with water hyacinth (WH) fiber and the effect of this

reinforcement on hydraulic conductivity of the soil was studied. To determine the hydraulic conductivity of the soil-WH fiber composite, infiltration test was carried out using mini disk infitrometer (MDI). The tests were conducted with two density variation (0.9MDD and 1.05MDD) and mixed with varying fiber content (0.50 %, 0.75 %, 1.00 %, by weight of dry soil). The results of the tests indicate an increase in hydraulic conductivity due to amendment of the WH fiber. Moreover, hydraulic conductivity of the soil increases on increasing the WH fiber content, whereas it decreases on increasing the density of the soil. One of the possible reason could be the preferential flow of water through the soil-fiber interface. On the other hand, increasing the soil density decreases the void spaces or void ratio of the soil, which results in blockage of flow path and consequently reduces infiltration.

REFERENCES

1. Álvarez-Mozos, J., Abad, E., Giménez, R., Campo, M. A., Goñi, M., Arive, M., Díez, J., Casalf, J., & Diego, I. (2014). Evaluation of erosion control geotextiles on steep slopes. Part 1: Effects on runoff and soil loss. *Catena*, *118*, 168-178.
2. Berg, B., Ekbohm, G., & McClaugherty, C. (1984). Lignin and holocellulose relations during long-term decomposition of some forest litters. Long-term decomposition in a Scots pine forest. IV. *Canadian Journal of Botany*, *62*(12), 2540-2550.
3. Carsel, R. F., & Parrish, R. S. (1988). Developing joint probability distributions of soil water retention characteristics. *Water Resources Research*, *24*(5), 755-769.
4. Damiano, E., & Olivares, L. (2010). The role of infiltration processes in steep slope stability of pyroclastic granular soils: laboratory and numerical investigation. *Natural hazards*, *52*(2), 329-350.
5. Faruk, O., Bledzki, A. K., Fink, H. P., & Sain, M. (2012). Biocomposites reinforced with natural fibers: 2000–2010. *Progress in polymer science*, *37*(11), 1552-1596.
6. Fernandez, F., & Quigley, R. M. (1985). Hydraulic conductivity of natural clays permeated with simple liquid hydrocarbons. *Canadian Geotechnical Journal*, *22*(2), 205-214.
7. Fullen, M. A., & Booth, C. A. (2007). Contributions of biogeotextiles to sustainable development and soil conservation in developing countries: the BORASSUS Project. *WIT Transactions on Ecology and the Environment*, *106*.
8. Ghazizade, M. J., & Safari, E. (2016). Analysis of Desiccation Crack Depth in Three Compacted Clay Liners Exposed to Annual Cycle of Atmospheric Conditions with and without a Geotextile Cover. *Journal of Geotechnical and Geoenvironmental Engineering*, 06016024.
9. Goering, H. K., & Van Soest, P. J. (1970). Forage fiber analyses (apparatus, reagents, procedures, and some applications). *USDA Agr Handb.*
10. Hafez, A. A. R. (1974). Comparative changes in soil-physical properties induced by admixtures of manures from various domestic animals. *Soil Science*, *118*(1), 53-59.
11. Hejazi, S. M., Sheikhzadeh, M., Abtahi, S. M., & Zadhoush, A. (2012). A simple review of soil reinforcement by using natural and synthetic fibers. *Construction and building materials*, *30*, 100-116.
12. Holden, J., Burt, T. P., & Cox, N. J. (2001). Macroporosity and infiltration in blanket peat: the implications of tension disk infiltrometer measurements. *Hydrological Processes*, *15*(2), 289-303.
13. Horton, R. E. (1933). The role of infiltration in the hydrologic cycle. *Eos, Transactions American Geophysical Union*, *14*(1), 446-460.
14. IS-2720 (Part 4), 1985, Methods of test for soils, Grain Size Analysis, New Delhi: Bureau of
15. IS-2720 (Part 5), 1985, Determination of liquid and plastic limit, New Delhi: Bureau of Indian
16. Jenkins, S. H. (1930). The determination of cellulose in straws. *Biochemical Journal*, *24*(5), 1428.
17. Jianqing, D., Ren, W., Weidong, F., & Guoliang, Z. (2001). Water hyacinth in China: Its distribution, problems and control status. *Biological and Integrated Control of Water Hyacinth, Eichhornia crassipes*. Canberra, Australia.
18. Koerner, R. M. (2012). *Designing with geosynthetics* (Vol. 1). Xlibris Corporation.
19. Kumar, D., Nigam, S., Nangia, A., & Tiwari, S. Improvement in CBR Values of Soil Reinforced with Jute Fiber.
20. Li, X. Y., González, A., & Solé-Benet, A. (2005). Laboratory methods for the estimation of infiltration rate of soil crusts in the Tabernas Desert badlands. *Catena*, *60*(3), 255-266.
21. Methacanon, P., Weerawatsophon, U., Sumransin, N., Prahsarn, C., & Bergado, D. T. (2010). Properties and potential application of

- the selected natural fibers as limited life geotextiles. *Carbohydrate Polymers*, 82(4), 1090-1096.
22. McNaught, A. D., & Wilkinson, A. (1997). Compendium of chemical terminology. IUPAC recommendations.
 23. Miller, C. J., & Rifai, S. (2004). Fiber reinforcement for waste containment soil liners. *Journal of Environmental Engineering*, 130(8), 891-895.
 24. Mohanty, K., Jha, M., Meikap, B. C., & Biswas, M. N. (2006). Biosorption of Cr (VI) from aqueous solutions by *Eichhornia crassipes*. *Chemical Engineering Journal*, 117(1), 71-77.
 25. Muramoto, S., & Oki, Y. (1983). Removal of some heavy metals from polluted water by water hyacinth (*Eichhornia crassipes*). *Bulletin of Environmental Contamination and Toxicology*, 30(1), 170-177.
 26. Prabakar, J., & Sridhar, R. S. (2002). Effect of random inclusion of sisal fiber on strength behaviour of soil. *Construction and Building Materials*, 16(2), 123-131.
 27. Prabakar, J., & Sridhar, R. S. (2002). Effect of random inclusion of sisal fiber on strength behaviour of soil. *Construction and Building Materials*, 16(2), 123-131.
 28. Rowell, R. M., & Stout, H. P. (2007). Jute and kenaf.
 29. Šimůnek, J., Angulo-Jaramillo, R., Schaap, M. G., Vandervaere, J. P., & Van Genuchten, M. T. (1998). Using an inverse method to estimate the hydraulic properties of crusted soils from tension-disk infiltrometer data. *Geoderma*, 86(1), 61-81.
 30. Sivakumar Babu, G. L., & Vasudevan, A. K. (2008). Seepage velocity and piping resistance of coir fiber mixed soils. *Journal of irrigation and drainage engineering*, 134(4), 485-492.
 - a. Standards publications.
 31. Tang, C. S., Shi, B., & Zhao, L. Z. (2010). Interfacial shear strength of fiber reinforced soil. *Geotextiles and Geomembranes*, 28(1), 54-62.
 32. Tang, C., Shi, B., Gao, W., Chen, F., & Cai, Y. (2007). Strength and mechanical behavior of short polypropylene fiber reinforced and cement stabilized clayey soil. *Geotextiles and Geomembranes*, 25(3), 194-202.
 33. Taylor, Barry R., Dennis Parkinson, and William FJ Parsons. "Nitrogen and lignin content as predictors of litter decay rates: a microcosm test." *Ecology* 70.1 (1989): 97-104.
 34. Zhang, R. (1997). Determination of soil sorptivity and hydraulic conductivity from the

disk infiltrometer. *Soil Science Society of America Journal*, 61(4), 1024-10

[Back to table of contents](#)

Simulation of aerobic degradation of BTEX compounds by using GMS and RT3D

Gyanashree Bora ⁱ⁾, Triptimoni Borah ⁱⁱ⁾

i) Post Graduate Student, Civil Engineering Department, Assam Engineering College, Guwahati-13

ii) Assistant Professor, Civil Engineering Department, Assam Engineering College, Guwahati-13

ABSTRACT

Groundwater is a significant water supply resource. Groundwater table decreasing in many parts of the world due to excessive overexploitation and unplanned pumping from aquifer is considered as a serious concern. One of the major environmental problems today is hydrocarbon contamination in subsurface environment. Leakage of underground storage tanks, the spills and improper disposals have been considered as major contributors in groundwater contamination. In this study, all the pollutants are considered as hydrocarbon contaminants (BTEX compounds) leaking from an underground storage tank and our main motive is to simulate the flow and transport processes of the BTEX hydrocarbons using the packages MODFLOW and MT3D available in Groundwater Modeling System (GMS). The simulation is done for a period of five years at an interval of 90 days each by using RT3D model available in GMS. The paper also presents the simulation of the aerobic degradation of the BTEX compounds in the aquifer. Oxygen is used as a natural attenuation process in this study to reduce the concentrations of the organic compounds in the contaminated groundwater.

Keywords: Hydrocarbon contamination, BTEX, MODFLOW, MT3D, RT3D, Oxygen.

1. INTRODUCTION

Volatile organic compounds mainly benzene, toluene, ethyl benzene and xylene have been considered as one of the major contributors to the deterioration of air and water quality. BTEX is an abbreviation used for four related compounds found in coal tar, crude petroleum. Once released into the environment, BTEX compounds usually evaporate quickly into the air. BTEX compounds also dissolve in water. These compounds may be found in surface and groundwater at contaminated sites or in close vicinity to natural oil, coal and gas deposits. There are different kinds of methods for monoaromatic compounds removal from groundwater, such as physical techniques (electro remediation, air sparging, carbon adsorption, filtration). Among all remediation technologies for treating monoaromatic compounds from contaminated groundwater, bioremediation appears to be an effective and environmentally sound approach. Bioremediation is the process by which

organic compounds are broken down into smaller or lesser compounds by living microbial organisms. Aerobic bioremediation takes place in the presence of oxygen and relies on the direct microbial metabolic oxidation of a contaminant. Oxygen can be added directly to the subsurface, or chemical oxidants can be applied and release oxygen as they dissolve or decompose.

Current and recent research on petroleum hydrocarbons as groundwater contaminants is extensive. This reflects the recognition of the pollution threat posed by these compounds. Fischer, A.J. et al., (1987) have described that organic compounds can be a major pollution problem in groundwater. Futagami T et al., (2008) mentioned that because of diverse industrial activities, sites contaminated with man-made chemicals are a world-wide problem. Holliger et al., (1997) described about the contaminants in the environment and its bioremediation. Cunningham JA et al., (2001) demonstrated enhancement of in

situ anaerobic biodegradation of BTEX compounds at a petroleum-contaminated aquifer.

In this study, the BTEX compounds are considered to be leaking from an underground storage tank. The degradation process of the BTEX compounds are simulated using the most advanced groundwater modeling software GMS. The flow and transport processes of the BTEX compounds in groundwater aquifer are simulated by using MODFLOW (Modular Finite Difference Flow Model) and MT3DMS (Modular Solute Transport Model) available in GMS. After the flow and transport simulation, aerobic degradation of BTEX compounds are simulated by using RT3D (Reactive Transport in Three dimensions). The concentrations distributed in the aquifer, without oxygen and with oxygen are observed at the observed well locations designated as W1, W2, W3, W4, W5, W6 and W7.

2. METHODOLOGY

2.1 Flow and Transport Equation

A transient, two-dimensional, areal groundwater flow equation for a heterogenous, anisotropic and fully saturated aquifer given by Bear in 1979 be written as-

$$\frac{\partial}{\partial x_i} \left(T_{ij} \frac{\partial h}{\partial x_j} \right) = S \frac{\partial h}{\partial x_j} + Q - W \quad (1)$$

Where, S is the storage coefficient; $T_{ij} = K_{ij}b$ is the transmissivity tensor (L^2T^{-1}); K_{ij} is the hydraulic conductivity (LT^{-1}); b is the saturated thickness of the aquifer (L); h is the hydraulic head (L); t is the time (T); Q is the pumping rate per unit area (LT^{-1}); W is the recharge flux per unit area (LT^{-1}); x_i and x_j are the Cartesian coordinates.

The two-dimensional solute transport given by Freeze and Cherry in 1979 be written as-

$$\frac{\partial (cb)}{\partial t} = \frac{\partial}{\partial x_i} \left(bD_{ij} \frac{\partial c}{\partial x_j} \right) - \frac{\partial (bcv_i)}{\partial x_i} - \frac{c'W}{n} + \frac{c'Q}{n} \quad (2)$$

Where, b is the saturated thickness of the aquifer (L); c is the concentration of the dissolved chemical species (ML^{-3}); D_{ij} is the coefficient of hydrodynamic dispersion (second order tensor) (L^2T^{-1}); c' is the concentration of the dissolved chemical in a source or sink fluid (

ML^{-3}); v_i is the seepage velocity in the direction x_i (LT^{-1}); η is the effective porosity of the aquifer (dimensionless); Q is the pumping rate per unit area (LT^{-1}); W is the recharge volume flux per unit area (LT^{-1}).

The general macroscopic equations describing the fate and transport of aqueous- and solid-phase species, respectively, in multi-dimensional saturated porous media are written as-

$$\frac{\partial C_k}{\partial t} = \frac{\partial}{\partial x_i} \left(D_{ij} \frac{\partial C_k}{\partial x_j} \right) - \frac{\partial}{\partial x_i} (v_i C_k) + \frac{q_s}{\phi} C_s + r_c \quad (3)$$

Where $k=1, 2, \dots, m$, m is the total number of aqueous-phase (mobile) species, C_k is the aqueous-phase concentration of the k^{th} species [ML^{-3}], D_{ij} is the hydrodynamic dispersion coefficient [L^2T^{-1}], v is the pore velocity [LT^{-1}], ϕ is the soil porosity, q_s is the volumetric flux of water per unit volume of aquifer representing sources and sinks [T^{-1}], C_s is the concentration of source/sink [ML^{-3}], r_c represents the rate of all reactions that occur in the aqueous phase [ML^3T^{-1}].

2.2 Overview of the Study Area

The site is a 500 m x 250 m non-uniform section of a confined aquifer with a flow gradient from left to right as shown in the There are 50 columns and 25 rows. The east and west boundaries of the aquifer are constant head boundaries and the north and south are no flow boundaries. The orange circular shapes denote the constant head. Red colour and yellow colour circular shapes denote the spill location and observation well locations as shown in Fig.1

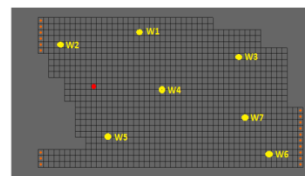


Fig.1: Study area for BTEX compounds

The aquifer has horizontal hydraulic conductivity (K_{xx}) of 50 m/day and horizontal anisotropy of 1. The effective porosity (η) of the aquifer is 0.3. The ratio of horizontal transverse dispersivity to longitudinal dispersivity is 0.3. Level of oxygen is considered as 9 mg/l. The solution scheme used for advection is Method of Characteristics (MOC). An underground storage

tank is leaking fuel hydrocarbon contaminants at 3m³/day at the location. Initially the groundwater was devoid of BTEX compounds. Later at the spill location, the observed concentration of BTEX is 1000mg/L. We will simulate a continuous spill event and compute the resulting hydrocarbon contours and oxygen contours for five years duration.

3. RESULTS AND DISCUSSIONS

3.1 Head distribution by using MODFLOW

The flow processes, which are the Head distribution in the entire aquifer, can be observed by using MODFLOW in GMS. Fig.2 shows the Head distribution in the entire aquifer when there is a steady pumping and the source is well. The rate of steady pumping rate is assumed to be Q = 3m³/d. The figure shows that the flow gradient is increasing from left and it is decreasing towards right side of the aquifer when there is a steady pumping.

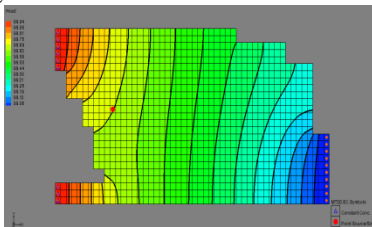


Fig. 2: Head distribution using MODFLOW

3.2 BTEX degradation by using MT3D and RT3D in absence of oxygen

After observing the head distribution by using MODFLOW, the transport process can be simulated by performing a reactive transport simulation using the RT3D model. The simulation is done for 5 years at an interval of 3months each.

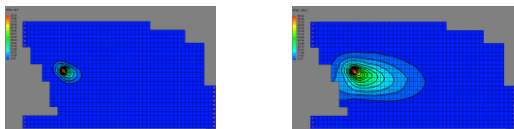


Fig.3: BTEX contour after 90 and 630 days.

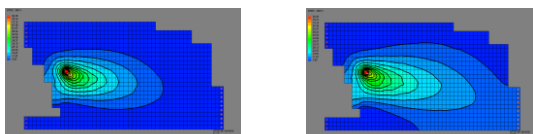


Fig.4: BTEX contour after 990 and 1800 days

Fig.3 (a,b) shows the BTEX distribution in the entire aquifer after 90 and 630 days Fig.4 (c,d) shows the distribution of the BTEX compounds in the aquifer after 990 and 1800 days.

Therefore, from the above figures it can be observed the simulation of the degradation process of BTEX compounds in a non-uniform aquifer by using MODFLOW, MT3DMS and RT3D. The simulation is done for 5 years at an interval of 3 months each. From the simulation, it can be observed that starting from 90 days to 1800 days, the BTEX compounds were entirely distributed in the aquifer. The reaction simulated used is instantaneous aerobic degradation of hydrocarbons.

3.3 Aerobic degradation of BTEX by using MT3D and RT3D in presence of oxygen

BTEX compounds mainly degrade when oxygen is added to them in subsurface environment. The principal interest when an aerobic bioremediation system is created is delivery of oxygen, which is the electron acceptor. Oxygen can be added directly to the subsurface or groundwater. The chemical oxidants can also be applied, which release oxygen as they dissolve or decompose. The end products of aerobic respiration are generally carbon dioxide and water. Aerobic degradation of BTEX compounds after 90 and 630 days are shown in Fig.5 (e,f). Fig.6 (g,h) shows the aerobic degradation of BTEX compounds after 990 and 1800 days.

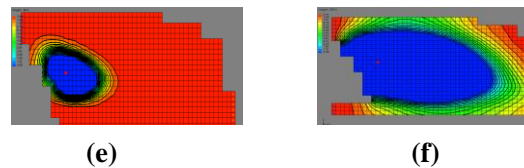


Fig.5: Aerobic degradation contour of BTEX after 90 and 630 days

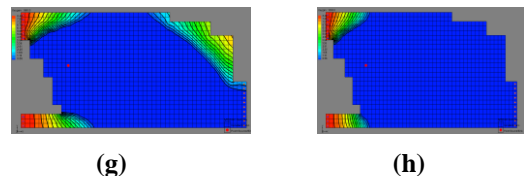


Fig.6: Aerobic degradation contour of BTEX after 990 and 1800 days

Therefore from the above figures, it can be observed that the BTEX compounds easily degrade when oxygen is added to them. This

degradation process is also known as natural attenuation of organic compounds.

3.4 Time series curves by GMS

Time series or breakthrough curves are the curves where the concentrations of the BTEX compounds are plotted with respect to time. Two time series curves are plotted as shown in Fig.7. The blue colour graph shows the distribution of the BTEX compounds in the aquifer without the presence of oxygen and the red colour graph shows the aerobic degradation of the BTEX compounds in the entire aquifer. The concentrations distributed in the entire aquifer, without oxygen and with oxygen are observed at the observed well locations. These well locations are designated as W1, W2, W3, W4, W5, W6 and W7 as shown in Fig.1.

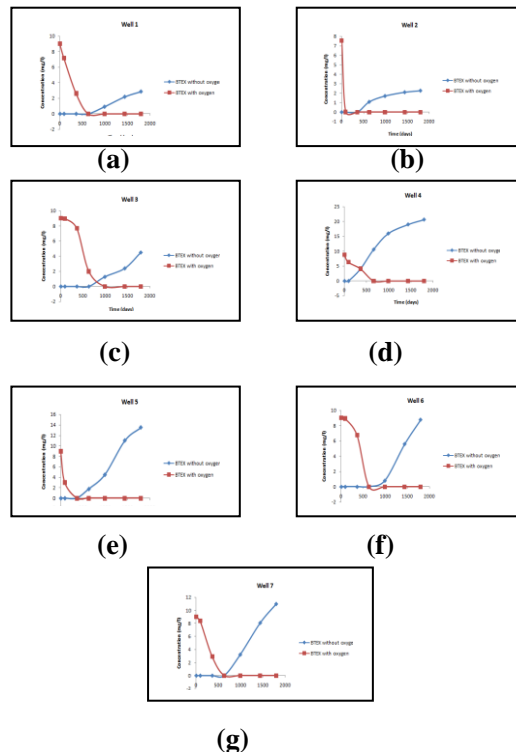


Fig.7. Time series curves for Well 1, Well 2, Well 3, Well 4, Well 5, Well 6 and Well 7

From Fig. 7(a, b, c, d, e, f, g), it can be observed that the BTEX distribution in the entire aquifer due to the spill from an underground tank gradually increases from 90 days to 1800 days. Initially the aquifer was devoid of oxygen but later when oxygen is applied to the BTEX compounds, aerobic degradation takes place. From the above

figures it can be observed the gradual diminishing of the BTEX compound as time passes from 90 to 1800 days due to the presence of oxygen and therefore, both the curves show different variations in the entire aquifer.

4. CONCLUSION

Organic compounds can be a major pollution problem in groundwater or subsurface. Their presence in water can create a hazard to the environment. BTEX is one of the most common sources of soil and groundwater contamination. BTEX are considered one of the major causes of environmental pollution because of widespread occurrences of leakage from underground petroleum storage tanks and spills at petroleum production wells, refineries, etc.

This paper summarizes the distribution of the BTEX compounds in the aquifer due to a spill from underground storage tank. The simulation is done for a period of 5 years at an interval of 3 months each by using RT3D model available in the most efficient groundwater modeling system (GMS). The paper also presents the simulation of the aerobic degradation of the BTEX compounds in the aquifer. Therefore, oxygen can be called as a natural attenuation process to reduce the concentrations of the organic compounds in a contaminated groundwater.

ACKNOWLEDGEMENT

I thank God, the almighty for his blessings without which nothing would have been possible. I would like to take the opportunity to express my sincere thanks to the entire staff of Civil Engineering Department, Assam Engineering College, Guwahati, for their kind help and cooperation to carry out this study.

REFERENCES

- 1) Bear, J.(1972), "Dynamics of Fluids in Porous Media," *Dover Publications, Inc.*, New York.
- 2) Christof Holliger, S. Gaspard, G.Glod, W.S., Fransisco Vanquez (1997), "Contaminated environments in the subsurface and bioremediation: organic contaminants," *FEMS Microbiology Reviews*, vol. 20, no. 3-4, pp. 517–523

[Back to table of contents](#)

3) Cunningham JA, Rahme H, Hopkins GD, Lebron C, Reinhard M (2001), "Enhanced in situ bioremediation of BTEX-contaminated groundwater by combined injection of nitrate and sulfate", *J. of Environ Sci Technol* April15;35(8):1663-70.

4) Datta, B.,Chakrabarti,D.,and Dhar, A.(2011), "Identification of unknown groundwater pollution sources using classical optimization with linked simulation,"*J.ofHydro-environment Research*5,25-36.

5) Fischer, A.J., E.A. Rowan and R.F. Spalding. (1987), "VOCs in Groundwater Influenced by Large Scale Withdrawals", *Ground Water* 25:407-413.

6) FutagamiT, GotoM, FurukawaK (2008), "Biochemical and genetic bases of dehalorespiration," *J. of Chem. Rec*, 8:1-12.

POTENTIAL IMPACT OF CLIMATE CHANGE ON RAINFALL INTENSITY-DURATION-FREQUENCY CURVES OF GUWAHATI CITY

Sagarika Patowary ⁱ⁾, Jayshree Hazarika ⁱⁱ⁾ and Arup K Sarma ⁱⁱⁱ⁾

i) Phd Student, Department of Civil Engineering, IIT Guwahati, Guwahati-781039, Email: sagarika.patowary@iitg.ernet.in

ii) Phd Student, Department of Civil Engineering, IIT Guwahati, Guwahati-781039, Email: jayshree@iitg.ernet.in

iii) Professor, Department of Civil Engineering, Indian Institute of Technology, Guwahati, Guwahati-781039, Email: aks@iitg.ernet.in

ABSTRACT

To reduce vulnerability of failure of hydraulic structures, a reliable rainfall intensity-duration-frequency (IDF) curve is a basic need for hydraulic design purpose. Recent experiences of having extreme rainfall events have emphasised the need of developing IDF curves considering the impact of climate change on rainfall. This paper gives a set of IDF curves of Guwahati city based on climate change impacted projection of rainfall, downscaled from Global Circulation Model (GCM). Future rainfall of Guwahati has been forecasted for the period 2006-2100 for RCP8.5, which corresponds to the highest greenhouse gas emissions pathway. The GCM model used in this study for downscaling is ESM2G. The calibrations, validation and forecasting are done with the help of Statistical Downscaling Model (SDSM). These downscaled rainfall data have been split into three time slices: 2012-2040, 2041-2070 and 2071-2100. Frequency analyses were performed by different methods for both observed (1969-2011) and downscaled daily rainfalls of every time slice. D-index test was performed to find the most suitable frequency analysis method for estimation of design daily rainfall events and these were found to be increased for all the three time slices in comparison to that calculated with respect to observed data (from 1969 to 2011). However, it is the lowest for time slice 2071-2100. IDF curves were generated with short duration rainfalls of different frequencies reduced from the design daily rainfalls by using Indian Meteorological Department (IMD) empirical reduction formula. These IDF curves show increase in intensity with increase of return period of rainfall particularly for short duration rainfall events in Guwahati city. IDF curves, thus generated under consideration of climate change impact, can provide a better preparedness to climate change adapted hydraulic design.

Keywords: Rainfall intensity-duration-frequency, ESM2G, RCP8.5, SDSM, D-Index, IMD empirical reduction formula.

1 INTRODUCTION

Increase in Greenhouse Gas (GHG) emissions induces continuous increase in atmospheric temperature due to which moisture holding capacity of air increases. According to Trenberth (2011), every 1°C rise in air temperature can lead to 7% increase in water vapour in atmosphere which in turn can produce more intense rainfall events. IPCC (2014) concludes that rainfalls will likely be more extreme in South Asia.

Many researches on climate change and hydrology with emphasis on the Indian subcontinent are already going on. It is observed that the major impacts of climate change in India would be on the hydrology, water resources and agriculture of the country (Mehrotra & Mehrotra, 1995). Considering the vast use of GCM variables for climate studies, investigation on empirical relation establishment between climatic variables and local variables are done (Wilby *et al.*, 1998(a)). Comparison of different Statistical downscaling methods using GCM output has been made (Wilby *et al.*, 1998(b)). Zhang (2005) developed a simple method for statistical downscaling of GCM output to predict soil erosion and crop production. Gosain *et al.* (2006) have developed a hydrologic modelling for various river basins in India considering climate change effect. Research suggests that studies

integrating the atmospheric and hydrological models to understand the climatic influence on hydrologic extremes are needed in the country (Mujumdar, 2008). In IIT Guwahati also, many research projects are going on related to climate change. Studies have been done on simulating the impact of climate change with the use of downscaling methods, on the rainfall characteristics and stream flow behavior of Brahmaputra as well as Barak basin. These studies have revealed that there will be significant changes in the rainfall pattern and temperature of these basins. High intensity rainfall of short duration and longer dry period will have adverse effect on flood and drought scenario of the region (Sarma *et al.*, 2012).

An Intensity-Duration-Frequency (IDF) curve is a comprehensive graphical representation of intensities of rainfall of different durations those may occur in specific frequencies. For design of various hydraulic structures a reliable intensity-duration-frequency (IDF) curve of rainfall is a basic necessity. There exist several general empirical equations of IDF relationships developed by researchers from different parts of the world (Bernard, 1932; Bell, 1969; Chen, 1983; Gert *et al.*, 1987; Yu and Cheng, 1998). In context to Indian basin also, a few general equations of IDF curves are available which are applicable to different regions of

India just only by changing the coefficients or parameters involved in the equations (Ram Babu et al., 1979; Kothyari & Garde, 1992). All these traditional IDF curves have been formed on the basis of historical or observed rainfall data which are assumed to be stationary (Srivastav et al., 2014). However, recent experiences of having extreme rainfall events have emphasised the need of developing IDF curves incorporating the future rainfall trend and variability under the impact of climate change. This will provide a better preparedness to climate change adapted hydraulic design. Recently, many researchers have regionally studied the impact of climate change on intensity of rainfall and reformed the regional IDF curves. (Mirhosseini et al. 2013, Rodriguez et al. 2013, Wang et al. 2013, Kuo et al. 2015). In India, Singh et al. (2016) has recently updated the IDF of Roorkee city considering the impact of climate change on rainfall.

Guwahati, the gateway of North East India often experiences high intense rainfall especially in monsoon period. It is located in between the Brahmaputra river and the Shillong plateau with geographic coordinates from 26° 4' 45" to 26° 13' 25" North Latitude and from 91° 34' 25" and 91° 52' 00" East Longitude. Guwahati has a humid sub tropical climate with average annual temperature 24.2°C and the average annual rainfall 1600 mm. The poor drainage system aided by haphazard urban settlement often causes urban flash flood in occurrence of short duration but intense rainfall events. Sarma and Goswami (2006) developed an intensity-duration (ID) curve for Guwahati city by using observed hourly rainfall data of 1 year period. However, for a place like Guwahati city, it is very important to generate IDF curve based on projected rainfall downscaled from Global Circulation Model (GCM). In this study, basically, future rainfall of Guwahati has been forecasted for the period 2006-2100 for the highest greenhouse gas concentration RCP8.5 and then, IDF curves are formed using those forecasted rainfalls.

2 MATERIALS AND METHODS

2.1 Projection of future rainfall

The GCM model used in this study for downscaling is ESM2G – developed by Geophysical Fluid Dynamics Laboratory (GFDL), USA under Intergovernmental Panel on Climate Change (IPCC)'s Coupled Model Intercomparison Project phase 5 (CMIP5). ESM2G is an Earth System Model, based on a coupled atmospheric and oceanic circulation model, with representations of sea ice, land and iceberg dynamics and it incorporates interactive biogeochemistry, including the carbon cycle. In ESM2G, an independently developed isopycnal model using the Generalized Ocean Layer Dynamics (GOLD) code base was used. This model has simulated datasets for historical period (up to 2005) and four future scenario

datasets for four different Representative Concentration Pathways (RCPs) (2006-2100) under CMIP5 protocol. In the present study, since our main purpose is to study the extreme events for IDF generation, hence RCP8.5 is considered for future rainfall projection; which corresponds to the highest emission of GHG. In RCP8.5, GHG emissions (measured in terms of CO₂ concentration) continue to rise throughout the 21st century. The future forecast of rainfall has been done by downscaling these climate model data till the end of 21st century. Statistical downscaling method is used here as it is found to be the most widely accepted and extensively used downscaling technique. Downscaling has been done with the help of the software Statistical Downscaling Model (SDSM), which is a hybrid of multiple linear regression (MLR) and the stochastic weather generator (SWG), developed by Wilby *et al.* (2002). Screening of predictors is the first and the most influential step of the downscaling process, as it provides the most appropriate predictors for downscaling, based on the inter-correlations among the predictors. Here, a stepwise screening of predictors is used, as proposed by Mahmood & Babel (2013), which gives the most suitable predictors for a particular region. Next, historical ESM2G datasets are used to calibrate and validate the model and dataset of ESM2G under RCP8.5 has been used for simulating the future changes in rainfall. The simulated future series for the period 2006-2100 is divided into three time slices: 2020s (2006-2040), 2050s (2041-2070) and 2080s (2071-2100).

Major disadvantage of using these climate models is the biases involved in them. Specially, in case of rainfall the magnitude of these biases fluctuate to a large extent as rainfall is an unevenly distributed parameter in temporal scale. Hence to reduce these biases, corrections need to be done before utilizing the predicted rainfall series for IDF generation. There are several bias correction methods that has been suggested for correcting rainfall simulations (Watanabe *et al.*, 2012). Here, following equation has been used for bias correction (Mahmood and Babel, 2013).

$$R_{bc} = R_{ds} \times \frac{\overline{R_{obs}}}{\overline{R_{cont}}} \quad (1)$$

where, R_{bc} is the bias corrected rainfall series, R_{ds} is the downscaled rainfall series from SDSM, $\overline{R_{obs}}$ is the mean of the observed rainfall series, $\overline{R_{cont}}$ is the mean of the downscaled series for the calibration period.

2.2 Formation of IDF curve

From the forecasted daily rainfall for the period 2012-2100 under the impact of climate change, annual maximum values of daily rainfall have been extracted. This annual maximum of daily rainfall series has been split into three parts with respect to time slices 2012-2040, 2041-2070 and 2071-2100 in order to study the variability of IDF curve with time period. To get the

design rainfalls of different return period, frequency analyses of the annual maximum rainfall series of every future time slices along with the observed one (1969-2011) have been then carried out by five different methods such as Gumbel, Pearson Type III, Log-Pearson Type III, Normal and Log-Normal method. D-index test (USWRC, 1981) was performed to find the most suitable frequency analysis method for estimation of extreme rainfall or design rainfall events. D-index (Varma, et al. 1989) is given as-

$$D\text{-index} = \frac{1}{\bar{x}} \left(\sum_{i=1}^6 \text{ABS}(x_{i,\text{observed}} - x_{i,\text{computed}}) \right) \quad (2)$$

Where, \bar{x} is the mean of the observed series, $x_{i,\text{observed}}$ ($i = 1, 2 \dots 6$) are the highest six observations in the given data and $x_{i,\text{computed}}$ ($i = 1, 2 \dots 6$) are the computed values corresponding to the return period using the probability distribution. The distribution which gives minimum D-index is considered as the best fit distribution. The suitable probability distributions for estimation of design rainfalls of the three time slices are shown in Table 1. Resulted design rainfalls of different return periods are shown in Fig. 1.

Table 1: Suitable probability distributions for estimation of design rainfalls

Rainfall of time slices	Suitable probability distribution
1969-2011 (Observed)	Log-Pearson Type III
2012-2040 (Forecasted)	Pearson Type III
2041-2070 (Forecasted)	Log-Pearson Type III
2071-2100 (Forecasted)	Gumbel

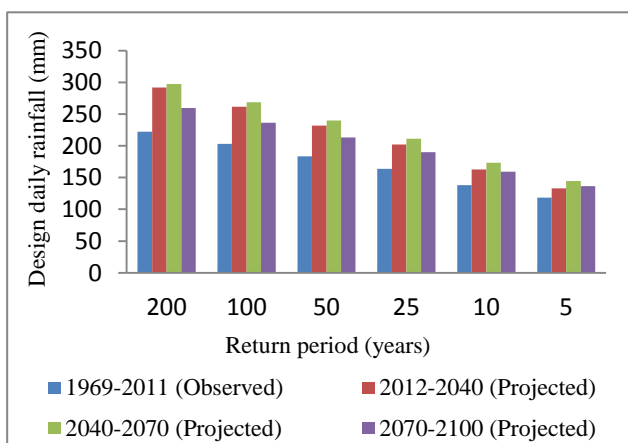


Fig.1: Design daily rainfalls of different return periods for different time slices

From Fig.1 it is observed that under the consideration of climate change impact design rainfalls of different return periods for all the three future time slices are higher in comparison to that calculated with respect to observed data (1969-2011). The projected design rainfall is found to be highest for the time slice 2041-2070 and it is to be lowest for time slice 2071-2100.

To get a short duration rainfall IDF curve, short duration rainfall data are required. Indian Meteorological Department (IMD) has given an empirical reduction formula for derivation of short duration rainfall values from daily rainfall values. This equation has been successfully applied in many studies in order to estimate short duration rainfall from daily rainfall values (Chowdhury et al., 2007; Rashid et al., 2012; Jaleel and Farawn 2013; Nyamathi and Arelt, 2013; Bhatt et al. 2014; Rasel and Islam, 2015). Here also, this IMD empirical reduction formula (Equation 3) has been used to derive short duration design rainfalls of different return periods from design daily rainfalls of corresponding return periods resulted from the frequency analysis.

$$P_t = P_{24} (t/24)^{1/3} \quad (3)$$

Where, P_t is the required rainfall depth in mm at t-hour duration, P_{24} is the daily rainfall in mm and t is the duration of rainfall in hour for which the rainfall depth is required. From the short duration rainfall data, derived, rainfall intensities of different return period has been calculated and plotted to get IDF curves of different return periods (RP) like 5, 10, 25, 50, 100 and 200 years (Shown in Fig. 2).

3 RESULTS AND DISCUSSION

In order to analyse the variation of future rainfall intensities under the impact of climate change as projected by ESM2G model under the emission scenario RCP8.5, the values of change in future rainfall intensity (in terms of percent of observed rainfall intensity) have been shown in Table 2 and graphically presented in Fig. 3. It is found that for all the future time slices, there is an increase in rainfall intensity with respect to that calculated from observed rainfall data. For a specific time slice, higher the return period (low frequency of occurrence) higher the increments in rainfall intensity relative to the observed rainfall intensity of corresponding return period. According to this climate change impact analysis, the highest intense rainfall will occur in the time slice 2041-2070, whereas relatively less intense rainfall is observed in the time slice 2071-2100. Again from Fig. 3, it is clear that variations of rainfall intensity increments with respect to return periods decrease in the order of time slices 2012-2040, 2041-2070 and 2071-2100. The ranges of rainfall intensity increments against the return period of 5 to 200 years are 12.61%-31.11%, 22.12%-33.78% and 15.30%-16.65% respectively for the time slices 2012-2040, 2041-2070 and 2071-2100.

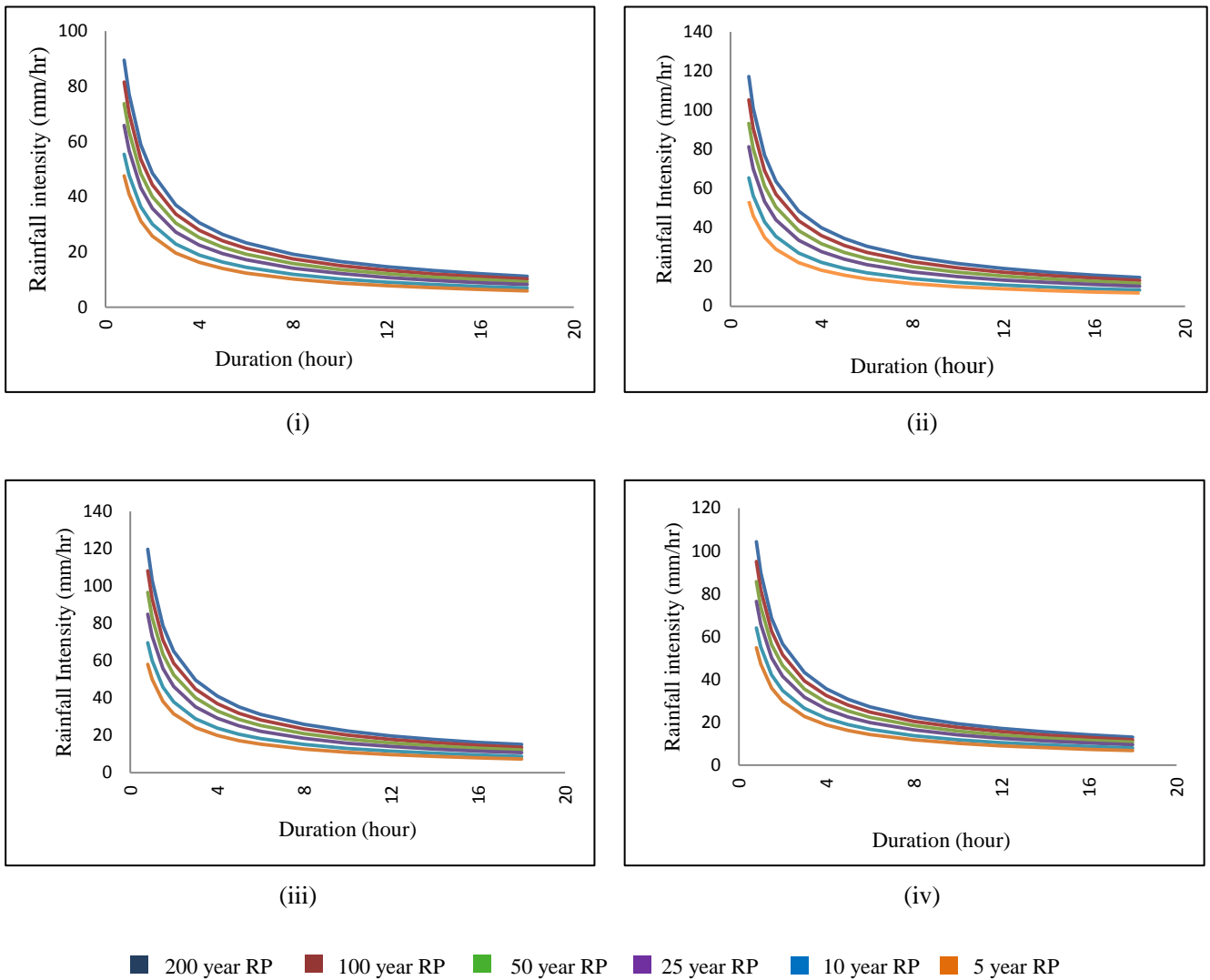


Fig. 2: IDF curves for different time slices (i) 1969-2011 (Observed) (ii) 2012-2040 (Projected) (iii) 2041-2070 (Projected) (iv) 2071-2100 (Projected)

Table 2: Change in rainfall intensity of different return periods under the impact of climate change with respect to rainfall intensity calculated from observed rainfall data. (In % of observed rainfall intensity)

Return period (years)	2012-2040	2041-2070	2071-2100
200	31.11	33.78	16.65
100	29.08	32.50	16.50
50	26.62	30.95	16.32
25	23.58	29.03	16.10
10	18.22	25.66	15.71
5	12.61	22.12	15.30

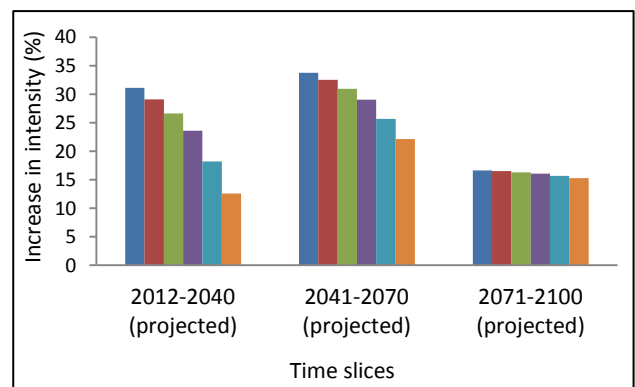


Fig. 3: Change in rainfall intensity of different return periods under the impact of climate change with respect to rainfall intensity calculated from observed rainfall data.

4 CONCLUSION

In this paper, IDF curve of Guwahati city has been developed under the consideration of future climate change scenario projected by downscaling the output of ESM2G model. The calibration, validation and forecasting of daily rainfall is done with the help of Statistical Downscaling Model (SDSM) for RCP8.5 – the highest greenhouse gas emissions pathway. Three sets of IDF curves are generated with respect to projected rainfalls of three future time slices- 2012-2040, 2041-2070 and 2071-2100. Design daily rainfalls of different return periods for every time slices were determined by using the most suitable probability distribution method among Gumbel, Pearson Type III, Log-Pearson Type III, Normal and Log-Normal methods. To derive short duration design rainfall from daily design rainfall, IMD empirical reduction formula has been used. The projected set of IDF curves are compared with the IDF curve generated with observed rainfall data of the period 1969-2011. It shows that in future the highest intense rainfall will be observed in the time slice 2041-2070. That means rainfall intensity will increase till 2070. After the year 2070, though intensity is expected to be higher in comparison to present rainfall intensity, still it is found to be lower in relative to that in period 2012-2070. Again in case of higher return periods, future rainfall intensities are projected to increase at a higher rate. This implies that the existing hydraulic structures such as storm drains, culverts etc. present in Guwahati city have to be improved or redesigned in order to cope with the projected high intense rainfall events. This statement is based on climate change projection by only one GCM model under the emission pathway RCP8.5. Some uncertainties are supposed to be associated with the projected sets of IDF curves due to inbuilt uncertainties related to GCM projections. Future work can be performed by carrying an uncertainty analysis through the use of a numbers of GCMs along with all the four RCPs. Thus, the IDF curves of Guwahati city, being developed through uncertainty analysis, can be utilized with more reliability.

REFERENCES

- Bell, F. C. (1969): Generalized rainfall-duration-frequency relationships, *Journal of Hydraulics Engineering*, ASCE, 95(1), 311-327.
- Bernard, M. M. (1932): Formulas for rainfall intensities of long duration, *Trans. ASCE*, 96, 592-624.
- Bhatt, J. V., Gandhi, H. M. and Gohil, K. V. (2014): Generation of intensity duration frequency curve using daily rainfall data for different return period, *Journal of International Academic Research for Multidisciplinary*, 2(2), 717-722.
- Chen, C. L. (1983): 'Rainfall intensity - duration - frequency formula, *Journal of Hydraulics Engineering*, ASCE, 109(12), 1603-1621.
- Chowdhury R., Alam J. B., Das P. and Alam, M. A. (2007): Short Duration Rainfall Estimation of Sylhet: IMD and USWB Method, *Journal of Indian Water Works Association*, 285-292.
- Gert, A., Wall, D. J., White, E.L. and Dunn, C.N. (1987): Regional rainfall intensity -duration-frequency curves for Pennsylvania, *Water Resources Bulletin*, 23(3), 479-486.
- Gosain, A. K., Rao, S., and Basuray, D. (2006): Climate change impact assessment on hydrology of Indian river basins, *Current Science*, 90 (3), 346-353.
- IPCC (2014): Climate Change 2014: Impacts, Adaptation, and Vulnerability, *Chapter 24* (p7).
- Jaleel, L. A. and Farawn, M. A. (2013): Developing rainfall intensity-duration frequency relationship for Basrah city, *Kufa Journal of Engineering*, 5(1), 105-112.
- Kothyari, U.C., and Garde, R. J. (1992): Rainfall intensity - duration-frequency formula for India, *Journal of Hydraulics Engineering*, ASCE, 118(2).
- Kuo, C. C., Gan, T. Y., Gizaw, M. (2015): Potential impact of climate change on intensity duration frequency curves of central Alberta, *Climatic Change*, 130(2), 115-129.
- Mahmood, R. and Babel, M. S. (2013): Evaluation of SDSM developed by annual and monthly sub-models for downscaling temperature and rainfall in the Jhelum basin, Pakistan and India, *Theoretical and Applied Climatology*, 111, 27-44.
- Mehrotra, Divya and Mehrotra, R. (1995): Climate change and hydrology with emphasis on the Indian subcontinent, *Hydrological Sciences Journal*, 40, 231-242.
- Mirhosseini, G. and Srivastava, P. (2013): The impact of climate change on rainfall Intensity–Duration–Frequency (IDF) curves in Alabama, *Reg Environ Change* 13(1), S25–S33.
- Mujumdar, P. P. (2008): Implications of climate change for sustainable water resources management in India, *Physics and Chemistry of the Earth*, 33, 354-358.
- Nyamathi, S. J. and Arelt, A. (2013): Modelling of short duration rainfall IDF equation for Bangalore city, *Research and Reviews: Journal of Engineering and Technology*, 2(3), 80-86.
- Ram Babu, Tejwani, K. K., Agrawal, M. C. and Bhusan, L. S. (1979): Rainfall intensity duration-return period equations & nomographs of India, *CSWCRTI, ICAR, Dehradun*, India.
- Rasel, M. M. and Islam, M. M. (2015): Generation of rainfall intensity-duration-frequency relationship for North-Western region in Bangladesh, *IOSR Journal of Environmental Science, Toxicology and Food Technology*, 9(9), 41-47.
- Rashid, M. M., Faruque, S. B and Alam, J. B. (2012): Modeling of Short Duration Rainfall Intensity Duration Frequency (SDR-IDF) Equation for Sylhet City in Bangladesh, *ARNP Journal of Science and Technology*, 2 (2), 92-95.
- Rodriguez, R., Navarro, X., Casas, M. C., Ribalaygua, J., Russo, B., Pouget, L. and Redano, A. (2013): Influence of climate change on IDF curves for the metropolitan area of Barcelona (Spain), *International Journal of Climatology*, 34 (3), 643–654.
- Sarma, A. K., Sarma, P. K. and Vinnarasi R. (2012): Climatic data collection from tea garden and other sources of Northeast India for climate change study, *Report submitted to Climate Change Directorate of MoWR, Govt. of India*.
- Sarma, A.K. and Goswami, P. (2006): Developing intensity duration curve with limited rainfall data, in the book '*Predictions in ungauged basins for sustainable water resources planning and management*', Jain Brothers, New Delhi, 187-194.
- Singh, R., Arya, D. S., Taxak, A. K. and Vojinovic, Z. (2016): Potential Impact of Climate Change on Rainfall Intensity-Duration-Frequency Curves in Roorkee, India, *Water Resour Manage*. (DOI 10.1007/s11269-016-1441-4).
- Srivastav, R. K., Scharong, A., and Simonovic, S. P. (2014): Equidistance quantile matching method for updating IDF curves under climate change, *Water Resour Manag*, 28(9), 2539–2562.

- 25) United States Water Resources Council. (1981): Guidelines for determining flood flow frequency, Bulletin No. 17B, Washington, DC.
- 26) Varma, C.V.J., Saxena, K.R., Rao, M.K. (1989): River behaviour management and training, Volume (1), Central Board of Irrigation and Power, New Delhi.
- 27) Wang, D., Hagen, S.C. and Alizad, K. (2013): Climate change impact and uncertainty analysis of extreme rainfall events in the Apalachicola River basin, Florida, *Journal of Hydrology*, 480, 125–135.
- 28) Watanabe, S., Kanae, S., Seto, S., Yeh, P. J. F., Hirabayashi, Y., and Oki, T. (2012): Inter-comparison of bias-correction methods for monthly temperature and rainfall simulated by multiple climate models. *Journal of Geophysical Research*, 117(D23114).
- 29) Wilby, R. L., Dawson, C. W. and Barrow, E. M. (2002): SDSM - a decision support tool for the assessment of regional climate change impacts, *Environmental Modelling and Software*, 17(2), 147 - 159.
- 30) Wilby, R. L., Hassan, H., and Hanaki, K. (1998): Statistical downscaling of hydrometeorological variables using general circulation model output, *Journal of Hydrology*, 205, 1-19.
- 31) Wilby, R. L., Wigley, T. M. L., Conway, D., Jones, P. D., Hewitson, B.C., Main, J. and Wilks, D. S. (1998): Statistical downscaling of general circulation model output: a comparison of methods, *Water Resources Research*, 34 (11), 2995-3008.
- 32) Yu, P. S. and Cheng, C. J. (1998): Incorporating uncertainty analysis into a regional IDF formula, *Hydrological Processes*, 12, 713-726.
- 33) Zhang, X. C. (2005): Spatial downscaling of global climate model output for site-specific assessment of crop production and soil erosion, *Agricultural and Forest Meteorology*, 135, 215-229.

[Back to table of contents](#)

A STUDY ON HYDROELECTRIC AND IRRIGATION POTENTIAL OF BHOGDOI RIVER, ASSAM

Mrinal Kr. Duttaⁱ⁾ and Mriganka Mazumdarⁱⁱ⁾

i) Assistant Professor, Department of Civil Engineering, Jorhat Engineering College, Jorhat - 785007, Assam, India.

ii) P.G. Student, Department of Civil Engineering, Jorhat Engineering College, Jorhat - 785007, Assam, India.

ABSTRACT

The river Bhogdoi a perennial river of length of 188.2 km originates from Assam-Nagaland border and flows through the plains of Assam and finally to the mighty Brahmaputra. Geographically, the basin lies between 26°17'17" and 26°49'22" north latitudes and 93°43'30" and 94°29'2" east longitudes and covers an area of 1179.65 km² including both plains and hills within it. The water from the river can be used for generating power or supplying water for irrigation and other purposes. Using remote sensing and geographic information system (GIS) an attempt has been made to create a thematic assessment map to locate suitable sites for dam. To describe the characteristics of catchment area various thematic layers have been derived with the help of different softwares (Arc GIS 9.3, and Global Mapper 11). A database of the catchment area is constructed to decide the locations of the proposed dams. From the three locations (site 1, 2 and 3) chosen, site 1 has been considered suitable for irrigation purposes whereas out of the sites 2 and 3 chosen for Hydropower generation, site 3 has been considered more suitable for the purpose, because of its more reservoir storage, lesser width of the channel and presence of suitable foundation material required for dam construction.

Keywords: GIS, Remote sensing, Dams sites selection, catchment area, Arcgis, Global Mapper

1. INTRODUCTION

Water is a basic resource on earth for all living beings including human beings and also for survival of plants. Importance of water is increasing due to the high population growth. As the main livelihood of people of Assam is agriculture the demand has been growing for more agricultural production to ensure food security. Thus, the need to construct dams has been growing vastly to meet the requirement of water supply, clean hydroelectric energy and irrigation. Remote sensing and GIS are widely used for delineation of terrain parameters such as slope, aspect, drainage network, watershed boundaries etc. The information about terrain surface and relief are often required for dam site selection. The derivation of topography watershed data and maps using remote sensing and GIS is fast, accurate and provide more reproducible measurement than traditional techniques compared to topographic maps. Significant effort has been devoted in recent years to derive terrain maps for engineering planning. In this study an attempt has been made to investigate the application of remote sensing and GIS techniques for suitable sites selection of the proposed dams by using remote sensing and GIS technology

The Bhogdoi river basin lies in the geographical territories of Assam and Nagaland and finally flows into the Brahmaputra as a southern sub-tributary of Brahmaputra. Due to its perennial course and presence

of active flood plains the river has an immense potential for hydroelectric and irrigation purposes. Geographically, the basin lies between 26°17'17" and 26°49'22" north lines of latitudes and 93°43'30" and 94°29'2" east lines of longitudes and covers an area of 1179.65 km² including both plains and hills within it. While travelling through Nagaland, the channel of Bhogdoi is known by different names at different places.

Remote sensing and GIS has been used to assess land use management in various resource sectors like agricultural planning, settlement surveys, environmental studies and operational planning (Li and Shen, 1973; Khoram and John, 1991; Jayakumar and Arockiasamy, 2003; Shamsudheen et al. 2005; Abushandi Eyad, 2015). Thanoon and Ahmed (2013) applied remote sensing and GIS techniques for suitable sites selection of the proposed dams in Al-Tharthar basin northern. By using capability of remote sensing and GIS technology they prepared a detailed hydrological impact analysis of the proposed dam's sites which play a vital role in analysis of any watersheds.

2. METHODOLOGY

1. For delineation of Basin Area of Bhogdoi river the survey of India toposheets Nos 83 F10, F14, J1, J2, J3, J5, J6 and J7 at 1:50000 scales of 1975 were scanned, georeferenced, mosaiced and used as resource maps. Using the various tools of Arc GIS software digitization

of mosaic maps are done to delineate basin area of the river Bhogdoi and its tributaries are demarcated. (fig 1)

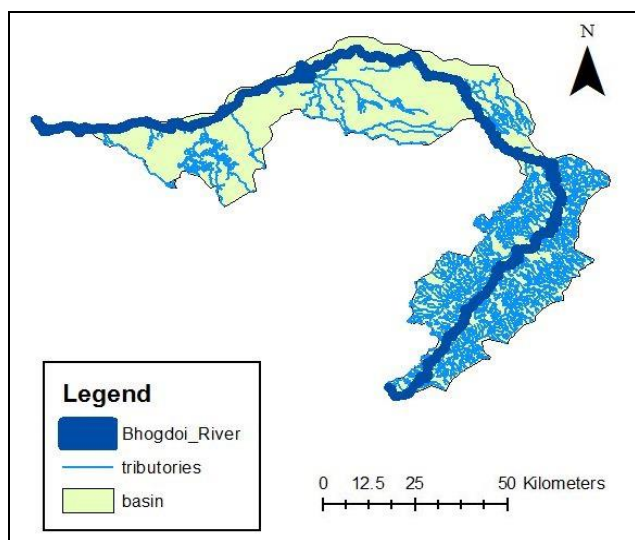


Figure 1: Digitized map of Bhogdoi river basin and its Tributaries along with its boundaries

2. To determine the land use pattern of the areas surrounding the river Bhogdoi a buffer zone of 10 kilometers around the river Bhogdoi has been marked using Arc Gis in order to assess the damage in case of any failure. Within this buffer zone various land use and land cover area such as settlement, cultivated land, forest area, teagarden etc are demarcated to measure the total area covered by each land cover. The area measured under each category will be helpful in computing the water requirement for irrigation agriculture and determining a suitable site for a dam.

3. DEM of the said area has been collected from USGS. Using the DEM and with the help of ArcGis software contour maps, aspect maps, slope maps, fill sinks map and flow direction maps are also extracted.

2. OBSERVATIONS

2.1 Basin Characteristics

A drainage basin is the area which contributes water to a particular set of channel of different orders. The Bhogdoi river basin includes the geographical territories of both Assam and Nagaland. The part of the basin within Nagaland in general is formed by low hills of 500 m above msl (mean sea level), but the southeast part of the basin has an elevation of 1300m above msl. The Bhogdoi river flows from the tertiary hills of Nagaland to the plain area of Assam and the basin comprises the floodplains of Brahmaputra on the north and the Tertiary hills of the Naga-Patkai range on the south.

From the source to summit, the total length of the channel of Bhogdoi is 188.6 km. The first 100 km of the

channel from the source is located in the hills. The length of the river channel in the plains is about 88.6 km. Finally traversing for a length of 188.6 km and draining water from an area of 1179.65 km², river Bhogdoi pours its discharge to Kakadonga.

Bhogdoi basin lies between river Janji on the east and river Kakadonga on the west. Of the total basin area of 1179.65 km², 501.34 sq km spans over the foothills of Assam-Nagaland border and 678.31 sq km area of the basin falls on the plains of Assam.

The basin is U-shaped bending towards east and its central portion is highly squeezed (Fig.1) where the width of the basin is about 3.8 km. This width gradually increases towards downstream of the river. A general westward slope of the basin in the Jorhat district compels several streams of the area to flow westward to meet Kakadonga. The central portion of the basin becomes very narrow and the width gradually increases towards north and south.

2.2 THE COURSE OF THE RIVER BHOGDOI

2.2.1 The Hilly Course

The Bhogdoi river has its source in the Mokokchung district of Nagaland and the source has an elevation of about 500 m above mean sea level. The river is totally a rain fed river. Its source is the point where 94°27'23" east meridian and 26°29'6" north parallel meet each other. Near the source the river is known as Tsujenyong Nala. The first three and half kilometer, the river flows from south to north following the steep slope of a hill ridge. Then it creates a valley between two parallel ridges. The valley has an elevation between 200 m to 300 m above msl. The channel flows nearly 25.5 km along the valley from north-east to south-west. At this point, the channel of the river crosses the 200 m contour and takes a sharp hair-pin turn. After this it starts to flow from south-west to north-east., which acts as the inter-state boundary between Assam and Nagaland.

While travelling through Nagaland, the channel of Bhogdoi is known by different names at different places. The entire hilly course of the river traverses through the terrain dotted with scattered human settlements and covered by thick vegetation cover which is now degraded due to human interference. In the hills, a large number of streams meet the channel of Bhogdoi on both right bank and left bank Some of the streams are seasonal while some others flow throughout the year.

2.2.2 The Plain Course

The river Bhogdoi enters the plains of Assam, at an

elevation of 140 m. This called as Nagajanka is six kilometres away from Mariani. In fact, Nagajanka is a hilly stream that meets Bhogdoi at that place and thus the name of the place is after the stream. Reaching the plains of Assam, the river starts flowing northward and reaches Jorhat city. At the plain course of the river passes a large number of villages and two urban centres, Mariani and Jorhat and only two major tributary streams the Kaliapani jan and Cheni jan or Ranga jan meet it. In the plain course, the western bank is wider than the eastern bank which has a maximum width of 6.5 kilometre from the river channel. In its plain course on the western bank of the channel, the Dhala jan is the major stream that meets Bhogdoi. It is formed mainly from the water of streams Saru Soikata jan and Bar Soikata jan. It flows northward and its downstream reach is known as Bar Dholi. Before meeting the channel of Bhogdoi, Bar Dholi embodies Saru Dholi which pours their joint discharge to Bhogdoi near its mouth. Few other streams like Tarajan, Rawriya jan and Tocklai jan also meet the plain course of Bhogdoi on its left bank. The part of the Bhogdoi basin in the plains shows that all the streams flow from south-east to north-west direction which signifies a general north-westward slope in the area.

3 RESULTS AND DISCUSSIONS:

A 10-km buffer zone on either side of the river has been considered for preparing land- use and land- cover map of the study area (figure 2).

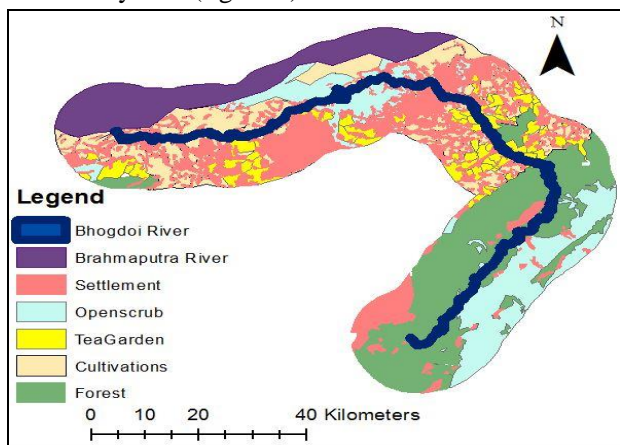


Figure 2: Land use map of the Bhogdoi basin

Out of the total land use-land cover area, 680.62 km² area is occupied by settlement, 763.20 km² area by forest, 235.71 km² by tea gardens, 448.86 km² by cultivated land, 507.96 km² area is open scrub and rest of the area is by Brahmaputra river. Thus the land- use map, help us to justify the importance of irrigation and hydroelectric project in the basin. The different categories of land use/land cover in order of abundance

can be represented as Forest (29%) >Settlement (26%) > open Scrub (19%) > Cultivated land (17%) > Tea Garden (9%). (Figure 3)

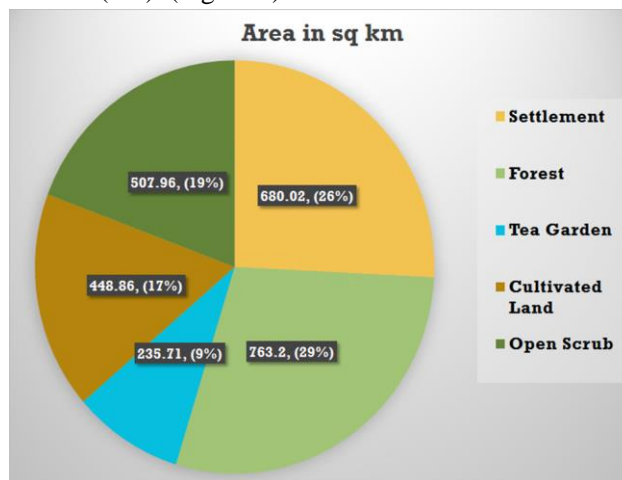


Figure 3 Area in percentage covered by different Land Use/Land Cover

Digital elevation model (Figure 3) generated from United states geological survey (USGS) data for the Bhogdoi Basin area are used as elevation reference. From the digital elevation model it has been observed that the northern parts of the basin have the lower elevations than the middle and southern parts i.e Nagaland Hills have the highest elevation. The elevation of the basin varies from 100 to 1300 m.

Slope and aspect maps of the basin (Figure 4 and 5) are generated from the DEM. Slope map shows that the basin is characterized by variable slope ranging between 0 to 51.57 degrees in certain locations. Aspect maps which is very important for determining water flow in the basin shows that the basin mostly faces north towards north

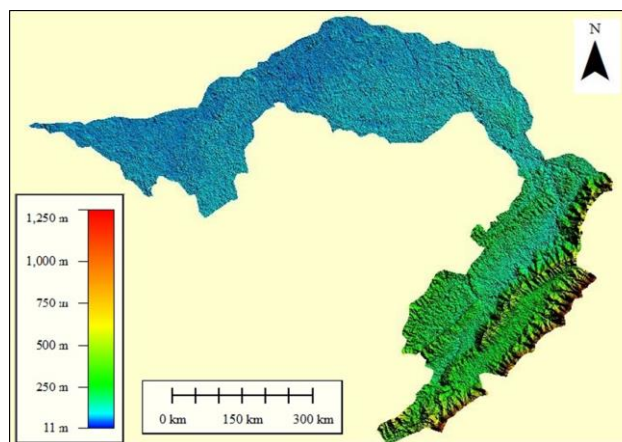


Figure 4: DEM of the Bhogdoi basin

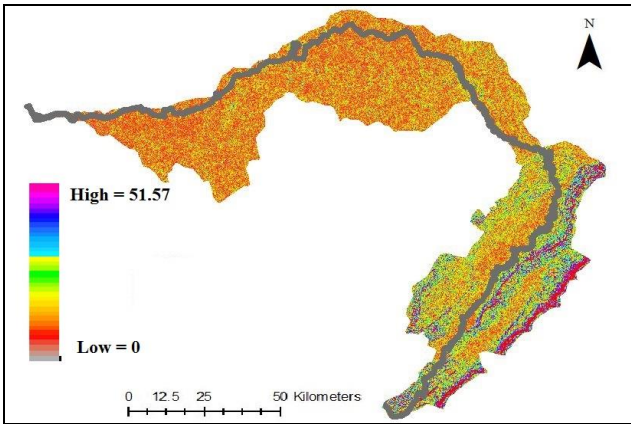


Figure 5: Slope Map of the Bhogdoi basin

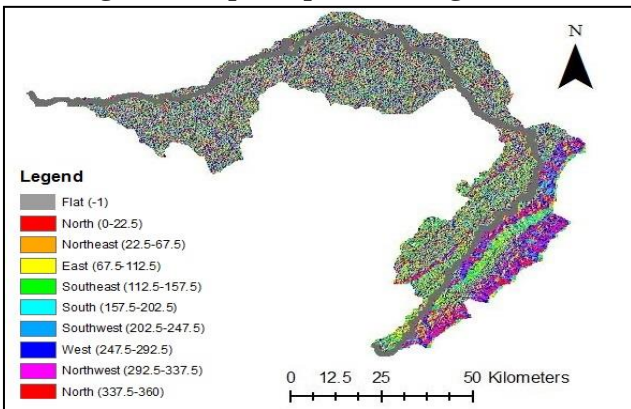


Figure 6: Aspect Map of the Bhogdoi basin

The flow directions as illustrated in figure 6 are also determined from the DEM by searching the relations between the neighboring cells with the rule that water will flow to the neighboring cell which has the highest downward slope. The drainages flow in different direction and connected together in one main stream. The drainage network is characterized by dendritic patterns.

As exhibited in figure 7 the contour map is derived from the DEM using Arc-GIS in order to observe the terrain elevation of the basin. The contour map reveals that the south eastern part of the basin has the highest elevation whereas in the northern and north western part the basin have the lowest elevation.

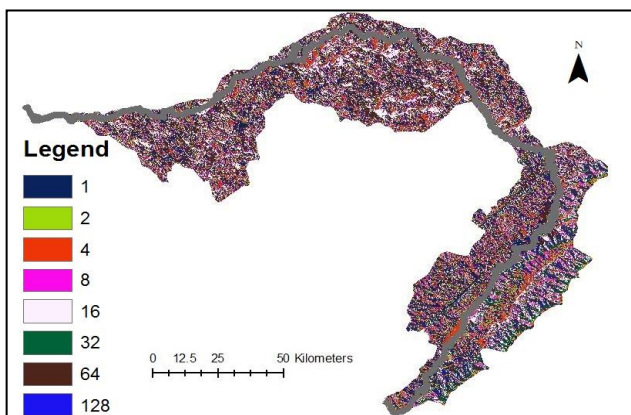


Figure 7: Flow direction map of the Bhogdoi basin

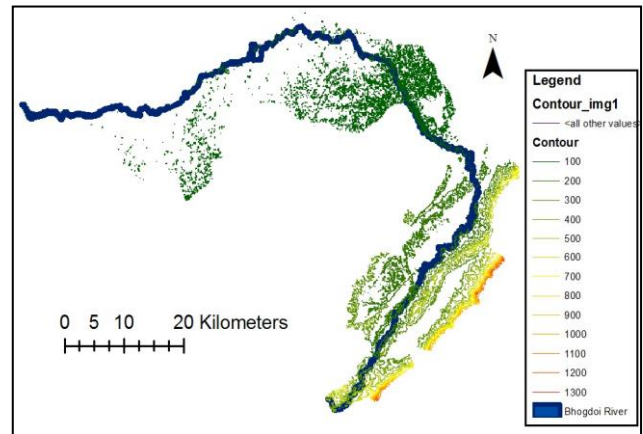


Figure 8: Contour Map of the Bhogdoi basin

After studying the various parameters of the basin, three locations were chosen in the south part of the basin. The locations of dams had been decided based on the land- use and land-cover map, geomorphology of the basin, contour map, slope map, aspect map, flow direction map and length and abutment of the dams. Site one (figure 8) was chosen at Nagajunka, site two (figure 9) was located at Aosankum Naga and site three (figure 10) was located at Disai valley reserve forest. The 1st site is considered ideal for an irrigation project whereas site 2 and 3 are ideal for generation of hydroelectricity.

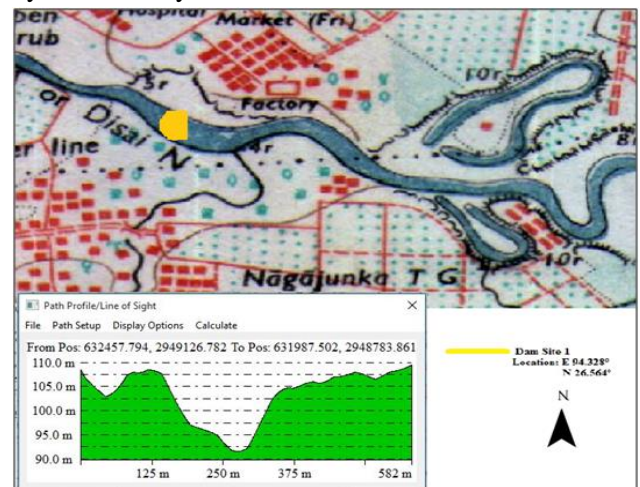


Figure 9: Site located at Nagajunka

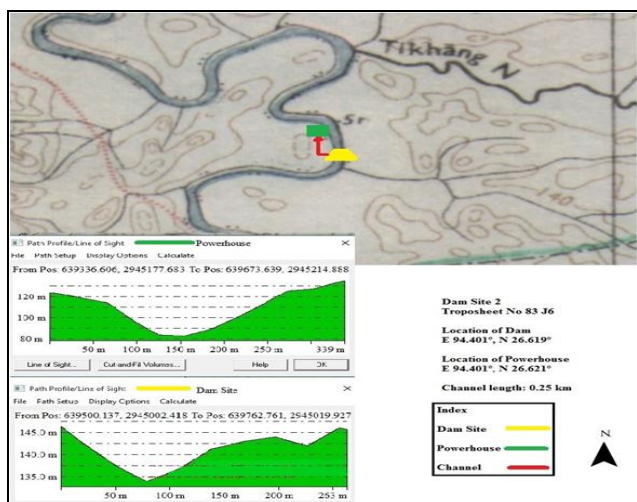


Figure 10: Site located at Aosangkum Naga

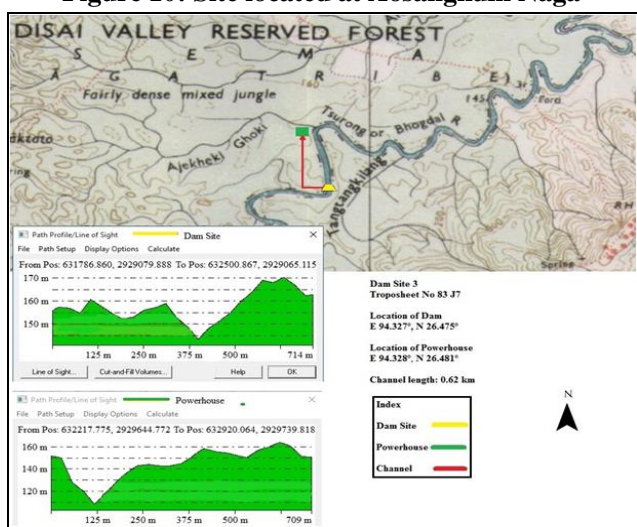


Figure 11: Site located at Disai Valley reserve Forest Using Global Mapper software and utilizing DEM data the cross sections of the three locations (shown in figure 8, 9, 10) were plotted. Cross sections plotted by Global Mapper software are utilized to find surface area, length and the height of the dams.

Table 1: Details of the 3 locations

Site	Location	Purpose	Height of Dam	Length of Channel
1	Nagajunka (E 94.328°, N 26.564°)	Irrigation	-	-
2	Aosangkum Naga (E 94.401°, N 26.619°)	Hydropower	8 m	250 m
3	Disai valley reserve forest (E 94.327°, N 26.475°)	Hydropower	9 m	620 m

4. SCOPE AND SUMMARY

By demarcating the basin area of Bhogdoi River it will be helpful in determining drainage basin of the river and find the overall area of the river basin. Also the land use and land cover will help in computing the water requirement for irrigation, agriculture and other purposes. Even during flood or failure of the dam the amount of the area and population that will be affected can be determined from the land use and land cover map. From the studies made site 3 can be considered as an ideal site for hydroelectric project. This is because its cross section width is less which can be considered ideal for constructing a dam and also the difference of elevation between the dam site and power house site is high which will further enhance in power generation. Also Site 1 is considered as ideal for constructing a dam for irrigation purpose which is at foothill of Nagaland and an area of approx. 46.42 km² of cultivated land as well as 60 km² tea garden can be irrigated from this project.

REFERENCES

- 1) Das S. J (2014) ‘Flood in the Bhogdoi Basin of Assam, India’, *The International Journal Of Engineering And Science (IJES)*, Volume 3, Issue 3, Pages 01-07, ISSN (e): 2319 – 1813 ISSN (p): 2319 – 1805
- 2) Khoram, S. and John, A.B. (1991) “A regional assessment of land use/land cover types in Sicily with Landsat data”, *International. Jour. Remote Sensing*, Volume.12(1), pp.69–78.
- 3) Thanoon Huda A.M., Ahmed Khansaa A. (2013), ‘Hydrological Information Extraction for Dams Site Selection using Remote Sensing Techniques and Geographical Information System’, College of Engineering. University of Mosul
- 4) Jayakumar, S., Arockiasamy, D I., (2003), ‘Land Use/Land Cover Mapping and Change Detection in part of Eastern Ghats of Tamil Nadu using Remote Sensing and GIS’, *Journal of the Indian Society of Remote Sensing* 31, 70-78.
- 5) Shamsudheen M., Dasog G.S. and Tejaswini N.B., (2005), ‘Land Use/Land Cover Mapping In The Coastal Area Of North Karnataka Using Remote Sensing Data’, *Journal of the Indian Society of Remote Sensing*, Vol. 33, No. 2, 2005
- 6) Website links
 - i) <https://en.wikipedia.org/wiki/Hydroelectricity>
 - ii) <https://en.wikipedia.org/wiki/Irrigation>
 - iii) http://shodhganga.inflibnet.ac.in/bitstream/10603/5500/13/13_chapter%208.pdf

Back to table of contents

Use of River Bank Filtration System for Augmentation in Drinking Water Supply at Lower Assam Region

Medalson Ronghang¹⁾, Suchandra Roy²⁾, Shatadeepa Das²⁾, NayanJyoti Konwar²⁾, Biswa Kumar Khakhlari³⁾, Nilim Kalita³⁾, Fwilao Basumatary³⁾, Evangeli Basumatary³⁾, Nomita Narzary³⁾, Pranjal Barman⁴⁾, Hemantajeet Medh⁵⁾, Kamal Kumar Brahma^{6), 7)}

¹⁾ Assistant Professor, Civil Engineering Department, Bineswar Brahma Engineering College, Kokrajhar, Assam 783370, INDIA

²⁾ Undergraduate Student, Chemical Engineering Department, Bineswar Brahma Engineering College, Kokrajhar, Assam 783370, INDIA

³⁾ Undergraduate Student, Civil Engineering Department, Central Institute of Technology, Kokrajhar, Assam 783370, INDIA

⁴⁾ Assistant Professor, Civil Engineering Department, Central Institute of Technology, Kokrajhar, Assam 783370, INDIA

⁵⁾ Assistant Professor, Chemical Engineering Department, Bineswar Brahma Engineering College, Kokrajhar, Assam 783370, INDIA

⁶⁾ Assistant Professor, Mechanical Engineering Department, Assam Engineering College, Guwahati, Assam 781014, INDIA

⁷⁾ Principal in Charge, Bineswar Brahma Engineering College, Kokrajhar, Assam 783370, INDIA

ABSTRACT

Bank filtration (BF) being a natural technique of abstracting surface water from the river or lake via sub-surface. This concept has been intensively used worldwide for augmenting water supply system for sustainability. It can be operated in various operating conditions. The energy requirements are comparatively lower than the conventional water treatment system.

Field investigations were carried out at various location of Kokrajhar district to assess the ground water quality and the aquifer characteristics. Results obtained from the analysis data suggest that major water quality parameters were within the drinking water standard of BIS 10500 (2012). The iron concentration was found to be more than permissible limit of more than 50% of the sampled water, the concentration ranged between 0.33-3.50 mg/L. The pH of water mostly lies in the range of 5.4 to 7.4, suggesting water is slightly acidic in nature. The aquifers and riverbed material collected along the bank of Gaurang River were sieved and classified as coarse silt to fine gravel. Gravel and sand were more predominant to the percent of silt. The hydraulic conductivity calculated on the basis of grain sizes distributions were in the range 5×10^{-3} to 1.4×10^{-2} m/s suggesting a good permeability of the aquifer. The maximum yield of the well that can be extracted safely was estimated to be in the range of 2000 to 7500 L/min. The mean travel time was estimated at less than a week during monsoon and for non-monsoon conditions, it was found to be more than 3 years.

This paper aims at demonstrating bank filtration method for treatment of river water naturally under wet climatic conditions for lower Brahmaputra basin represents a unique physiographic setting i.e. a powerful monsoon regime and a fragile geologic base.

Key words: Natural filtration, Hydraulic conductivity, Water quality, bank filtration

1. INTRODUCTION

River bank filtration (RBF) is considered to be an excellent water treatment technology for drinking water production in many part of the world (Grischek et al., 2003, Ray et al., 2008; Sandhu et al., 2011; Ronghang et al., 2015). As the world's growing population puts greater demands on the available supply of high quality drinking water, RBF is being increasingly used for treating waters of degraded quality (Tufenkji et al., 2002). The effectiveness of bank filtration has been recognized in Europe for more than 100 years to supply potable water to people along the Rhine, Elbe, Danube, and Seine Rivers (Eckert and Irmscher, 2006). RBF supplies 70% of drinking water to a densely populated city of Europe like Berlin (Schubert, 2002). Düsseldorf waterworks in Germany have used RBF since 1870 (Schubert, 2002), similarly the Saloppe waterworks in Dresden have also used RBF since 1875 (Grischek et al., 1994). The riverbank filtrate was pumped for public drinking water supply in the Netherlands probably in 1879 along the Rhine River at Nijmegen pumping station (Schubert, 2002). After the World War-II, when the pollution in the rivers were severe with municipal and industrial effluents, RBF and filtration of river water through sand dunes provided drinking water to many communities in Netherland (Ray et al., 2008). The process of RBF is also widely recognized in the United States (Kühn and Müller, 2000). In early 1940s, a direct connection between the alluvial aquifer and the Ohio River has been well documented. The Louisville Water Company also induced RBF as a potentially effective treatment process for removing selected water-borne contaminants and started to investigate the effectiveness for removing disinfection byproduct in the late 1970s (Hubbs, 2006). Efforts are being made in Korea to use RBF for water supply for improving the quality of short and steep slopes stream water in the urban environment (Ray et al., 2008). Other regions of the world such as Africa, Northern Asia, and South America RBF can be potentially used for water supply (Ray et al., 2008). India has many perennial rivers flowing across the length and breadth, many large cities along those rivers can easily use RBF for their water supply. The potential of RBF has developed in many cities of India along the Ganga plains (Sandhu et al., 2011). Scientific investigations have been conducted on the hydro-geological conditions, water quality, and sustainability of using bank filtration systems in the cities of Haridwar, Patna, and Varanasi along the Ganga River for providing drinking water

since 2005 (Thakur and Ojha, 2010; Dash et al. 2010). Some other sites in India are Muzaffarnagar along the Kali River in Uttar Pradesh, Nainital by Lake Nainital in Yamuna River at Palla region of Delhi, Yamuna River at Mathura and in Srinagar (Uttarakhand) along the Alaknanda River (Ronghang, 2015). RBF scheme which has been successfully implemented in India are Ahmadabad, Patna, Kharagpur, Dandeli, Haridwar, and Delhi etc. (Singh, 2008; Sprenger et al., 2008; Dash et al., 2010; Lorenzen et al., 2010; Singh et al., 2010; Sandhu et al., 2011, Kumar et al., 2012).

As a cost effective solution, many cities are experimenting with RBF to produce higher quality water from the polluted rivers (Sandhu et al., 2011). Considering the success of RBF in worldwide, the potential and limitation of RBF has been investigated for the first time in Assam at the Kokrajhar town.

2. STUDY AREA

The study area is located in the Kokrajhar district (26°13'30"-26°53'20"N Longitude and 58°52'30" E -90°33'10" E Latitude) of Bodoland Territorial Area District (BTAD) along the river Gaurang in the lower Brahmaputra valley (Figure 1).

The district in general is divided into two part (1) Northern alluvial region (between 120 – 140 m amsl) and (2) Southern swamps or flood plain of River Brahmaputra. A major portion of the district is constituted by vast alluvial area formed by Brahmaputra and its river system (CGWB 2012). The river has thick alluvial deposits (alluvium comprises thick beds of clay) with southerly slope (elevation varies from 40 to 300 m above MSL) and flat topography (CGWB 2012). Geologically it is reported that the district is occupied by older alluvium on north and Younger Alluvium of flood plain deposit towards the Brahmaputra River on southern (CGWB 2012). The climatic condition of the area is subtropical humid type, which has been characterized by dry in non-monsoon and hot and wet (heavy rainfall) in monsoon. The rivers and rivulets gets narrower and the groundwater level start depleted in dry season (winter). On the contrary, monsoon (summer) brings heavy rainfall due to which the river flows are highly turbulence and the banks of the river collapses (Das 2014). Hence, the river water gets muddy and carries suspended materials along with high loading of debris and sewage from surface runoff. Based on these factors, it has become necessary to investigate the possibility of natural filtration scheme based

on RBF system in Kokrajhar whose statistic information is given in table 1.

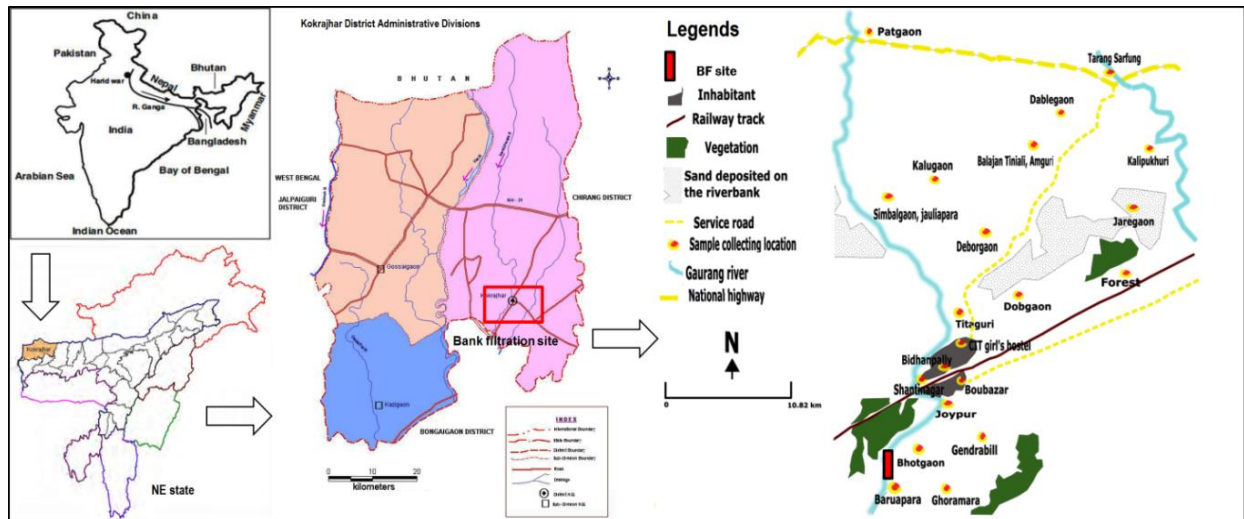


Fig. 1. Location of bank filtration site at Kokrajhar (BTAD)

Table 1. Description of the study area

Parameter	Details
Location	Patharghat, Kokrajhar town
Longitude and Latitude	26 ^o 24'37.69"N 90 ^o 15'40.89"E
Mean altitude mean sea level	75 m
Average annual Rainfall #	3100 mm
No of water supply units	Nil
Water demand per capita per day*	135
Total population of the town as (Census 2011)	32000
Average domestic water supply deficit	4.2 MLD
Distance from the available water sources (hand pump)	Less than 50 m
Projected demand for domestic and industrial use up to 2025 #	31,430 MLD
Major Ground water problems and issues#	Higher conc. of iron in some pockets

#CGWB 2012; *Adopted from Raghunath 2006

3. MATERIAL AND METHODS

Groundwater sampling campaign: The water samples were collected from different locations around the Kokrajhar sub division-I (Figure 1). The latitude and longitude of the sampling locations were measured using a GPS (Garmin) with a precision of ±0.5m. The sampling campaign was organized in March and May, 2016. The samples were collected in 500-1000 mL bottles (Figure 2a), for bacteriological analysis samples were taken in sterilized 100 mL glass bottles. The opening of the hand pump was sterilized using fire and then the water was pumped for about 2-3 minutes before collecting

the water samples (Figure 2d). Electrical conductivity (EC), total dissolved solids (TDS), and temperature were measured on-site using portable instruments whereas pH was measured using pH kits (Figure 2b&c). The collected water samples were transported to the laboratory of Public Health Engineering Department (PHED) at Kokrajhar for further testing and analysis. Sampling, storage and analyses were carried out in agreement with the procedures given in APHA Standard Methods (Eaton et al., 2005). Various parameters like hardness, chloride, iron, fluoride, arsenic, alkalinity, nitrate, manganese, turbidity and bacteriological test were analysis.



Fig.2. Sampling campaigns (a) Collecting water samples, (b) Measurement of groundwater temperature (c) Filtering of water sample for pH measurement, (d) Sterilization of hand pump before collecting water sample for bacteriological test

Aquifer Characterization: The aquifer materials were collected from different location and depth of the river bank and bed of Gaurang River on May 7, 2016 (Figure 3). Aquifer materials were carried to the geotechnical laboratory of Central Institute of Technology, Kokrajhar for grain size analysis. The samples were washed using 75 microns sieve to remove

finer, dirt and dust before oven dried at 105°C for 48 hours. The oven dried samples were weighed and transferred to the sieve shaker (Tohniwal) to obtain the grain size distribution. Hydraulic conductivity (K) of the aquifer materials were calculated using established empirical formulae adopted from Odong. (2007).

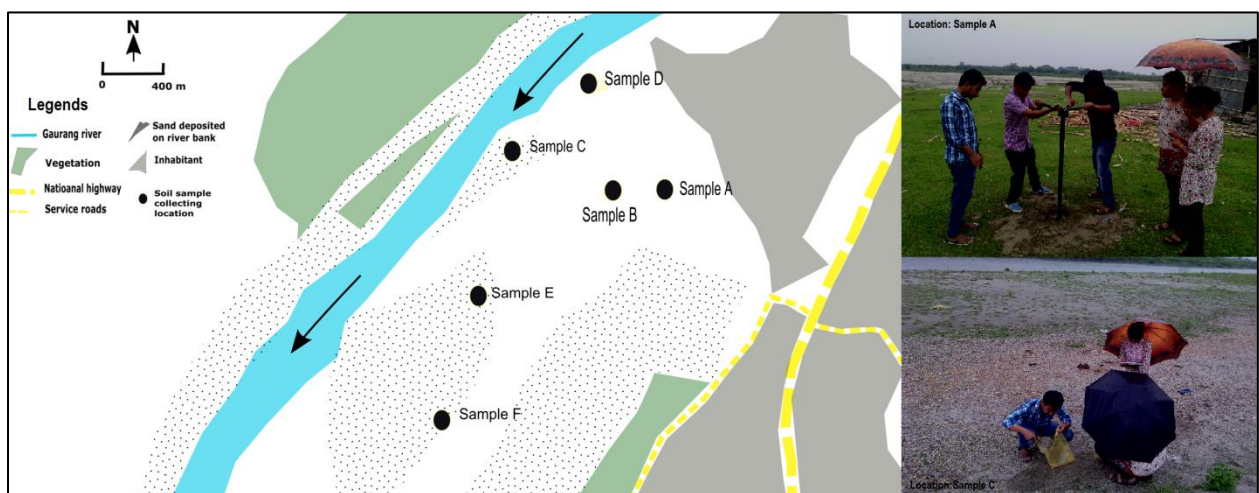


Fig.3. Location of soil sampling

Column experiment: Laboratory experiment was conducted using column packed with aquifer material of size ranging from 0.1-0.5mm. The experimental set up is shown in figure 4, container of 2L (container-2) and 20 L (container

-1) were used as a constant head and feeding tank respectively, a PVC pipe of 1m length and 2 flexible pipes of 10 mm were connected with column to pass the water. The wet sand (filter material) was filled from the top and compacted after regular interval. Precautions were taken so

that air bubbles between the gaps of sand grains were eliminated. Two polyethylene meshes were placed at both ends of the column to prevent the finer sand from flowing out. To check leakages, water from feed tank was passed overnight into the column before stabilizing the flow rate for the tracer test. The salt solution (Sodium chloride concentration 7.5 mg/L) was then poured in the container-1 (feed) and the flow rate was maintained. The salt concentration measured as electric conductivity (EC) of the feed water was

1293 μ S (EC_0). The electrical conductivity is measured from collected at the outlet (measuring cylinder) at the constant interval. The experiment was carried out at a room temperature around 26-28 $^{\circ}$ C. The break through curve was drawn after plotting fraction of the input concentration of electrical conductivity with time. The specifications of the experimental set up and characteristic of aquifer materials used are also listed in the following table 2.

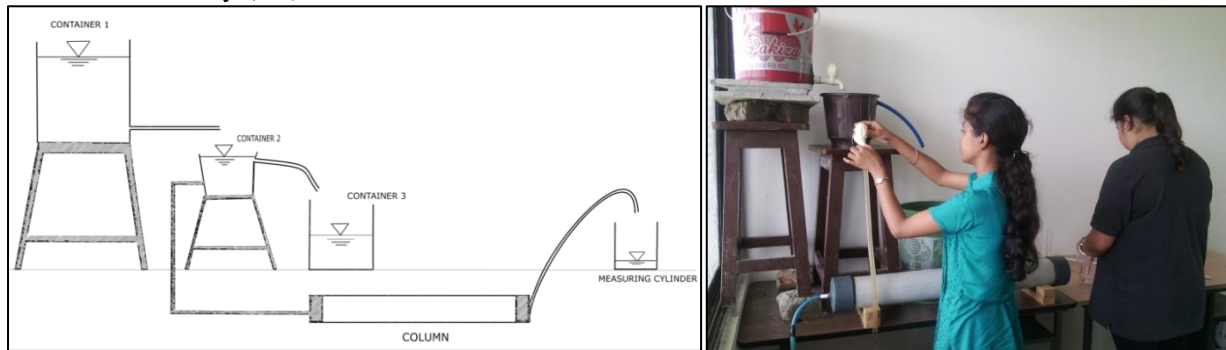


Fig.4. Photograph of the experimental set up

Table 2. Column Specifications

Parameter	
Length (cm)	91
Diameter (cm)	10
Cross-section (cm ²)	3100
Volume (cm ³)	7147
Aquifer material	
Mean grain size (mm): 0.26	Uniformity co-efficient (C_u): 2.53
Hydraulic conductivity (m/s): 9.9×10^{-3}	Porosity(%): 39.42

4. RESULTS AND DISCUSSION

Water quality: The temperature of the water samples collected from various locations was found to be in range from 24.3-27.0 $^{\circ}$ C. The pH depicts a narrow range of variation from (5.4-7.4), which indicate that the water is mostly acidic in nature (refer Figure 5a). The variation in EC and TDS was found to be (41-334) μ S/m and (22-189) mg/L respectively, which also suggest that the water has lower mineralization. This could be that the groundwater is directly recharged by the rains (refer Figure 5b). Turbidity of the water samples was found to be very low (less than 2 NTU) in most of the water samples. Only in two samples (N26 $^{\circ}$ 30'41", E90 $^{\circ}$ 21'30" and N26 $^{\circ}$ 25'55", E90 $^{\circ}$ 17'8") was observed to be 6 and 5 NTU respectively. Alkalinity and hardness of water samples ranged between 28 to 162 mg/L and 4 to 204 mg/L as calcium carbonates respectively, which is within the permissible limit (BIS: 10500-2012). The maximum alkalinity was observed in dug well-IV located at Kalipukhuri

whereas maximum hardness was found at Shantinagar, HP-I (Figure 6a & b). At some places such as Joypur (Bhatipara) and Dimalgaon (Titaguri), the hardness was observed to be less than 10 mg/L (Figure 6b). The chloride concentration in the water samples ranging from (6-82) mg/L which is much less than the permissible limit of 1000mg/L (BIS: 10500-2012). It can be inferred from the obtained data that the contamination level of water samples is not strong. At most of the places, the chloride concentration is found to be less than 30 mg/L. Only at four locations namely Shantinagar (HP-I), Bhatipara (HP-IV), Forest colony (NTPC-DAHP) and CIT girl's hostel (TW-I), the chloride concentrations are observed to be 80 mg/L. Other ionic compositions of the water samples like fluoride, arsenic and nitrate are within the desirable limit of BIS: 10500-2012 whereas iron concentrations were found to be more than 0.3 mg/L at HP-I, HP-VI, NTPC-DAHP and Dug Well-IV

This may be due to the leaching from the corroded pipe in low pH water. The concentration of manganese in water is zero at most of the places except for the eight locations (Shantinagar, Bhatipara, Simbargaon, Patgaon, Forest colony, Bidhanpally, Dobgaon and Habrubari).

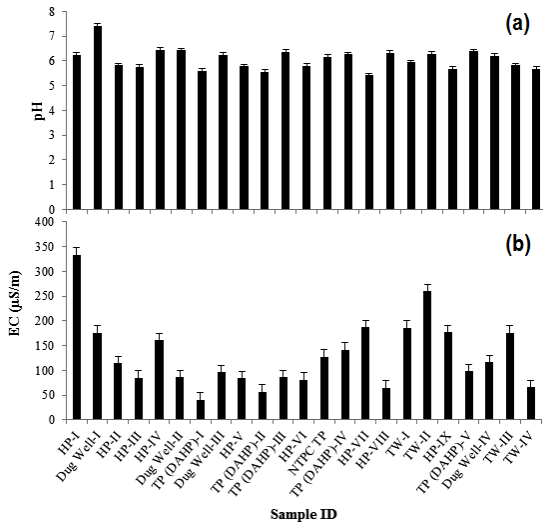


Fig.5. Variation of pH and EC of water samples

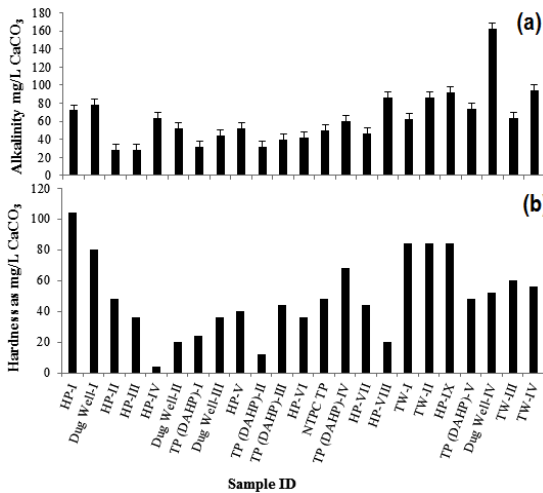


Fig.6. Variation of alkalinity and hardness in the water samples

However, this values in very low. Results obtained for arsenic concentration in the water samples inferred that arsenic is absent in most of the samples except at Titaguri, CIT girl's hostel and Kokrajhar rail gate whose concentration was 7µg/L, which is below the desirable limit of 10 µg/L.

Aquifer characteristics: The particle size distributions of the aquifer and riverbed materials were determine by plotting the grain size (mm)

against percent finer retained (p %). The grain sizes distribution help to characterize the aquifer materials were shown in figure 7.

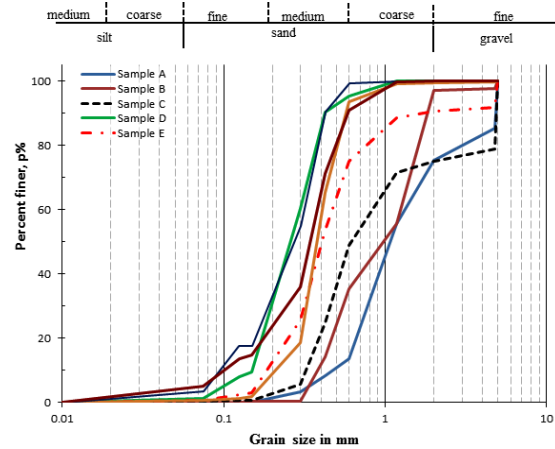


Fig.7. Sieve analysis of aquifer material

The graph suggests that the aquifer material is mostly sandy, consisting mainly of coarse to medium sand. It has been found to be homogeneous in nature with a little percentage of coarse silt and fine gravel. Some heterogeneous nature can be explained from the graph by the fact that the samples have small percentage of silt and gravel. For example, if we consider the composition of sample E, which has 10% gravel and 90% sand. The profiling of the bored log also suggests that the aquifer is unconfined. From the grain size distribution curve of the aquifer materials, characteristics like effective size (d_{10}), mean particle size (d_{50}), uniformity co-efficient (C_u), co-efficient of gradation (C_c) and porosity (η) are estimated and tabulated. Based these on estimated data, hydraulic conductivity (K) of each sample is calculated using equations adopted from Odong, 2007. For sample A, the hydraulic conductivity by Hazen equation was found to be 0.04 m/s whereas by Kozeny-Carman, Slitcher and Breyer equation's. This was found to be 0.02 m/s, 0.02 m/s and 0.04 m/s respectively (Detail tabulated in table 3). Similarly, the hydraulic conductivity of other samples were also calculated (Table 3). The hydraulic conductivity in the bank filtrate site ranges between 5×10^{-3} to 1.4×10^{-2} m/s, which is in the range of most of the bank filtration site around the globe (Ray 2008;, Dash et al., 2010; Sandhu et al., 2011; Ronghang et al., 2012; Gupta et al., 2015). From the data, it can be concluded that sample A has the highest hydraulic conductivity among all other samples. Some

samples (e.g. sample E) has lowest permeability, which indicate that sample E will retained all the finer particle whereas sample A having the highest K values cannot be used for the same as it will lead to breakthrough of finer particles. Sample B and C have the same K values and are best suited for being used as the aquifer media (Ronghang, 2015).

Table 3. Characteristic of aquifer and riverbed materials

C, Value of Co-efficient, (10 ⁻⁴) (-)				6	8.3	100	-
ID	C _u	n	d ₁₀ ² (mm ²)	Hydraulic conductivity (m/day)			
				H	KC	S	B
A	2.6	0.41	0.25	3664	1680	1303	3347
B	3.3	0.39	0.16	2157	908	708	2048
C	2.3	0.42	0.12	1867	894	691	1676
D	1.9	0.43	0.03	405	203	144	363
E	2.3	0.42	0.04	610	292	226	547
F	1.6	0.44	0.06	1026	535	411	916
G	2.9	0.40	0.01	170	75	58	158
H	3.5	0.39	0.01	163	69	54	154

Kinematic viscosity at 20° (v) m²/s=1.0×10⁻⁶ g/v (-)
)=9770916, H= Hazen, K=Kozeny-Carman, S=Slitcher, B= Breyer

The maximum safe yield of the well was estimated to be in the range of 2000 to 7500 L/min, which is similar to bank filtration well of Srinagar in India and Düsseldorf waterworks in Germany (Schubert 2002; Ronghang 2015). The estimated mean travel time was also similar to RBF of Satpuli in India (Ronghang et al., 2012; Kimothi et al., 2012).

Column experiment: The effective porosity obtained from tracer test was estimated using the equation adopted from Ronghang (2012). The t₅₀ value is estimated from the plotted curve to be 90 minutes and the effective porosity is found to be 45%, which is in accordance to the grain size analysis. 100% breakthrough of persistence and conservative pollutant like chloride may occur after 4 hrs. Thus suggesting for special attention needed to take care during high abstraction system during flood.

5. CONCLUSION

The research work conducted to assess the prospect of river bank filtration at Kokrajhar through sampling campaign to investigate the groundwater quality within the town. The ground water in most of the locations was found to be acidic. Most of the water quality parameters were

found within the desirable limit except iron. Soil samples collected from six different locations along the bank of the river to determine the aquifer characteristics suggest favorable on bank filtration system. The hydraulic conductivity was in the ranged of most existing bank filtration site around the world. An attempt has also been made to design the bank filtration scheme, inferences drawn from the designed are as follow:

- The ground water in most of the locations is acidic.
- Most of the water quality parameters were found within the desirable limit except iron.
- The hydraulic conductivity was in the ranged of most existing bank filtration site around the world.
- The maximum safe yield of a production well was estimated to be 7500 L/min

6. ACKNOWLEDGEMENTS

This research project is funded by Assam Science Technology & Environment Council (ASTEC), Guwahati under Concept Notes for Technology Generation (grant No. ASTEC/S&T/1614 (4/1)/2014-15/3767). The authors appreciate for the support and free access to the laboratories of Public Health Engineering Department, Kokrajhar Division-I and Geotechnical laboratory, CIT Kokrajhar during the testing. The Authors are also thankful to Dr. Jyotirmoy Borah of Department of Chemistry, Bineswar Brahma Engineering College, Kokrajhar for discussion of water Chemistry and Mr. Wazidur Rahman, J.E and Mr. Rino Kumar Brahma, Laboratory Assistant for Logistic support during the sampling campaign.

7. REFERENCES

- 1) CGWB (2012) Central Water Information Booklet Kokrajhar District, Assam, Ground Water Board Ground, Ministry Of Water Resources, Govt. Of India North Eastern Region Guwahati, 1-8.
- 2) Das B.K. (2014) Water quality evaluation of shallow wells in Kokrajhar Town of Assam, India, International Journal Of Environmental Sciences, 4(4) 501-506.
- 3) Dash, R. R., Prakash, E. B., Kumar, P., Mehrotra, I., Sandhu, C., & Grischek, T. (2010). River bank filtration in Haridwar, India: removal of turbidity, organics and bacteria. Hydrogeology journal, 18(4), 973-983.

- 4) Eckert, P., & Irmscher, R. (2006). Over 130 years of experience with Riverbank Filtration in Dusseldorf, Germany. *Aqua*, 55, 283-291.
- 5) Grischek, T., Dehnert, J., Neitzel, P., & Nestler, W. (1994). Groundwater/river interaction in the Elbe river basin in Saxony (No. CONF-9403190--). American Water Resources Association, Herndon, VA (United States).
- 6) Eaton, A. D., Clesceri, L. S., Rice, E. W., and Greenberg, A. E. (2005). Standard method for examination of water and wastewater. 21st edition, American Water Works Association, 949-956.
- 7) Grischek, T., Schoenheinz, D., & Ray, C. (2003). Siting and design issues for riverbank filtration schemes. In *Riverbank Filtration* (pp. 291-302). Springer Netherlands.
- 8) Gupta, A., Ronghang, M., Kumar, P., Mehrotra, I., Kumar S., Grischek, T., Sandhu, C and Knoeller, K. (2015) Nitrate Contamination of Riverbank Filtrate at Srinagar, Uttarakhand, India: A Case of Geogenic Mineralization. *Journal of hydrology* 513(3), 626-637.
- 9) Hubbs, S. A. (2006). Evaluating streambed forces impacting the capacity of riverbed filtration systems. In *Riverbank Filtration Hydrology* (pp. 21-42). Springer Netherlands.
- 10) Kimothi, P.C., Dimri, D.D., Adlakha, L.K., Kumar, S., Rawat, O.P., Patwal, P.S., Grischek, T., Sandhu, C., Ebermann, J., Ruppert, M., Dobhal, R., Ronghang. M., Kumar, P., Mehrotra, I., Uniyal, H.P. (2012) Development of Riverbank Filtration in Uttarakhand. *Journal of Indian Water Works Association*. Special Issue.
- 11) Kumar, P., Mehrotra, I., Boernick, H., Schmalz, V., Worch, E., Schmidt, W., & Grischek, T. (2012). "Riverbank filtration: an alternative to pre-chlorination." *Journal of Indian Water Works Association*, July–September issue.
- 12) Lorenzen, G., Sprenger, C., Taute, T., Pekdeger, A., Mittal, A., & Massmann, G. (2010). Assessment of the potential for bank filtration in a water-stressed megacity (Delhi, India). *Environmental Earth Sciences*, 61(7), 1419-1434.
- 13) Odong, J. (2007). Evaluation of Empirical formulae for determination of hydraulic conductivity based on grain size analysis. *Journal of American Science*, 3(3), 54-60.
- 14) Raghunath, H. M. (2006). *Hydrology: principles, analysis and design*. New Age International. New Delhi.
- 15) Ray, C. (2008). Worldwide potential of riverbank filtration. *Clean Technologies and Environmental Policy*, 10(3), 223-225.
- 16) Ronghang, M., Kumar, P., Mehrotra, I., Kimothi, P.C., Adalakra, L. K., Sandhu, C. S S., and Grischek, T. (2012) Application of riverbank filtration for year-round drinking water production in small town in the hills of Uttarakhand. *Journal of Indian Water Works Association*. 19-24, Special Issue.
- 17) Ronghang, M (2015) Efficacy of Riverbank Filtration in Hill area , PhD Thesis, Department of Civil Engineering, IIT Roorkee.
- 18) Sandhu, C., Grischek, T., Kumar, P., & Ray, C. (2011). Potential for riverbank filtration in India. *Clean Technologies and Environmental Policy*, 13(2), 295-316.
- 19) Schubert, J. (2002). Hydraulic aspects of riverbank filtration—field studies. *Journal of Hydrology*, 266(3), 145-161.
- 20) Singh, J. (2008). Horizontal collector wells for drinking water supply in Gujarat by riverbed filtration. Workshop on design and operation of riverbank filtration Schemes, 19-20 September, 2008.
- 21) Singh, P., Kumar, P., Mehrotra, I., & Grischek, T. (2010). Impact of riverbank filtration on treatment of polluted river water. *Journal of environmental management*, 91(5), 1055-1062.
- 22) Sprenger, C., Lorenzen, G., & Pekdeger, A. (2008). Occurrence and fate of microbial pathogens and organic trace compounds at riverbank filtration sites in Delhi, India. *TECHNEAU integrated project: D*, 5(6). Available: <http://www.techneau.org>; accessed: September 2012.
- 23) Thakur, A. K., & Ojha, C. S. P. (2010). Variation of turbidity during subsurface abstraction of river water: A case study. *International Journal of Sediment Research*, 25(4), 355-365.
- 24) Tufenkji, N., Ryan, J. N., & Elimelech, M. (2002). Peer reviewed: The promise of bank filtration. *Environmental science & technology*, 36(21), 422A-428A.

Back to table of contents

Investigation of hydraulic conductivity for red soil vegetated with transgenic cow pea in the absence of nutrients

Ankit Soni^{i*}, Bhushan S. Waghⁱ, Sunil K. Sihagⁱ,
Suraj Kumarⁱ, Ankit Gargⁱⁱ

i) Under graduate student, Department of Civil Engineering,
Indian Institute of Technology Guwahati, India

ii) Assistant Professor, Department of Civil Engineering,
Indian Institute of Technology Guwahati, India

ABSTRACT

Hydraulic conductivity of vegetated (rooted) soil is a key factor to assess water use efficiency. This study investigates the hydraulic conductivity of red soil vegetated with transgenic cow pea (drought resistant cow pea). Six drought resistant plants vegetated in nutrient added soil were also considered as reference. Six drought resistant cow pea plants vegetated in red soil without adding nutrients were investigated under natural boundary conditions, except controlled irrigation conditions. Hydraulic conductivity has not exhibited consistent trend over entire time period. Clear difference between hydraulic conductivity of red soil and nutrient added soil was found over the entire period. Root growth may be the reason for this difference. Except between 13th day and 19th day, higher hydraulic conductivity was found in vegetated soil under the absence of nutrients as compared to that of vegetated soil in the presence of nutrients. Lower root growth may be reason for this, by which less water repellency occurs.

Key words: hydraulic conductivity, red soil, transgenic cow pea and nutrients

1. INTRODUCTION

Hydraulic conductivity of vegetated (rooted) soil is a key factor to devise irrigation schedule and assess water use accurately (Hillel, 1972; Campbell, 1982). Extensive research has been conducted on determining hydraulic conductivity of soil vegetated with various plant species. However, hydraulic conductivity of red soil vegetated with crop species was rarely studied, under the absence of nutrients. Nutrient leaching by infiltration is a major challenge in agricultural engineering, which effects plant growth and root growth (Mengel, 1978). After leaching of nutrients, plant may need to grow in bare soil under the absence of nutrients. Hence, it is vital to investigate hydraulic conductivity of soil vegetated with crop species in the absence of nutrients to study the water retention in root zone. This investigation is highly beneficial for efficient irrigation scheduling and water use efficiency i.e., sustainable water management.

The main objective of the current work is to study the effect of absence of nutrient in vegetated soil with transgenic cow pea (crop species). The study explores the temporal variation of hydraulic conductivity in nutrient added soil and soil under the absence of nutrients.

2. MATERIAL AND METHODS

2.1 Soilproperties

The selected soil was found to inhere in CL-ML category according

to unified soil classification system (USCS) (ASTM D2487-11). The soil consists mainly silt (51 %) and sand (25 %), followed by clay (24 %) as per the grain size distribution. Atterberg limits such as liquid limit, plastic limit and shrinkage limit were found to be 40 %, 22 % and 20%. Table 1. Summarizes basic physical and engineering properties of the soil, determined under the provisions of ASTM codes (ASTM D854-06; ASTM D2487-10; ASTM D698-07 and ASTM D4318-93)

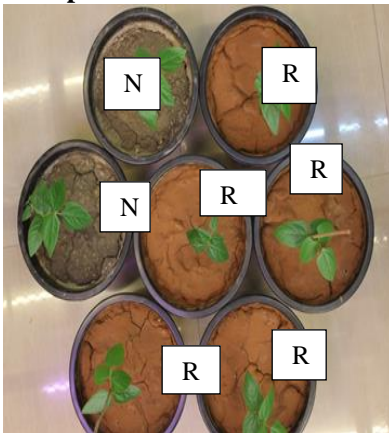
Table 1. properties pf red soil used according to ASTM D854-06; ASTM D2487-10; ASTM D698-07 and ASTM D4318-93 codes.

Index properties	Measured value or range
Maximum dry density (g/cm ³)	1.7
Optimum moisture content (by mass %)	17
Particle size distribution	
Gravel content (>2mm, %)	0
Sand content (≤2mm, %)	25
Silt (> 2µm and ≤75µm)	51
Clay content (≤ 2µm, %)	24
Specific gravity	2.69
Atterberg limits	
Plastic limit (%)	22
Liquid limit (%)	40
Plasticity index (%)	18
Shrinkage limit (%)	20
Unified soil classification system	Silty-clay (CL-ML)

2.2 Selected plant species and germination condition

Drought resistant Cowpea (*Vigna unguiculata* L.) was selected for the present study. Cowpea is well known for its adaptation to nutrient-poor soils (Ehler 1997). The mature seeds of cowpea cultivar, PusaKomal are procured from Seed Corporation of India, Delhi. These were germinated on moistened cotton in Petri dishes. After that, germinated seedlings were transplanted in the soil filled pots for conducting experiments.

2.3 Test plan



R- Transgenic cow pea vegetated in nutrient added red soil

N- Transgenic cow pea vegetated in red soil under the absence of nutrients

Fig 1. Plants in red soil and nutrient added soil

A test plan was scheduled to estimate the hydraulic conductivity

in red soil vegetated cow pea under absence of nutrients. All the experiments are conducted in natural atmospheric conditions, except irrigation. Six red soil and two nutrient mixed soil as control were placed in the greenhouse (Fig 1.). Nutrient added soil is taken to know the effect of nutrients on hydraulic conductivity. The seedlings of the plant species were germinated and transplanted to the pots. All the 8 pots were regularly irrigated at a pre-set interval. The Infiltration was measured using the minidisk infiltrometer.

2.4 Experimental setup

Relative humidity and temperature of the greenhouse were found to be $55 \pm 5\%$ and $25 \pm 2^\circ\text{C}$ respectively. The cylindrical pots of 230 mm depth and 260 mm diameter were used for experimentation. The base of the pots was perforated to allow water drainage. Pots were made of PVC plastic material. The soil was compacted up to uniform density of 1.3 g/cc (equivalent to 77 % of maximum dry density of soil) up to 185 mm from the bottom in three equal layers. Pre-set interval for irrigating all pots is 3 days. Infiltration also measured at regular interval.

2.5 Procedure for analysis of infiltration

MDI was placed on the vegetated soil to measure hydraulic conductivity as shown in Fig. 2. After placing MDI firmly, water is allowed to infiltrate into vegetated soil at the pre-set tension. Water infiltrated through the disk is measured as a function of time.



Fig 2. Infiltrometer setup in vegetated soil

Infiltration can be approximated using equation (2.1) (Zhang, 1997)

$$I = C_0 \times t + C_1 \times \sqrt{t} \quad (2.1)$$

C_0, C_1 – Fitting constants

Hydraulic conductivity can be approximated by using equation 2.2

$$k = C_0/A \quad (2.2)$$

“A”= Parameter dependent on van

Genuchten water retention curve parameters (Zhanag, 1997)

A =

$$\frac{11.65(n^{0.1}-1)\exp[2.92(n-1.9)\alpha h_0]}{(\alpha r_0)^{0.91}} \quad (2.3)$$

$$A = \frac{11.65(n^{0.1}-1)\exp[7.5(n-1.9)\alpha h_0]}{(\alpha r_0)^{0.91}} \quad (2.4)$$

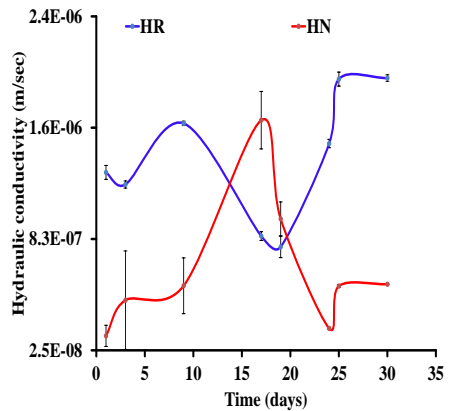
n, α = the van Genuchten parameters of vegetated soil,

r = disk radius,

h_0 = the tension applied on the disk.

n, α were adopted from Zhang (1997)

3 RESULTS AND DISCUSSIONS



HR- Hydraulic conductivity in red soil vegetated with
 HN- Hydraulic conductivity in nutrient added vegetated soil

Fig 3. Hydraulic conductivity over time.

Fig. 3 shows the hydraulic conductivity variation with time for red soil vegetated with drought resistant cow pea and nutrient soil vegetated with drought resistant cow pea. Clear difference between hydraulic conductivity of red soil and nutrient added soil was found

over the entire period. Hydraulic conductivity of nutrient added soil with vegetation is found to increase with time up to the end of 15 days. However, after 15 days it was observed to decrease up to the end of 24 days. Thereafter, sluggish increase was found. In case of red soil, hydraulic conductivity is found to decrease with time up to the end of 3 days. After 3 days, it was found to decrease up to the end of 8 days. Thereafter, hydraulic conductivity found to decrease up to the end of 19 days. After 19 days, it was observed to increase up to 26 days. Further, any change was not found. It is evident from previous studies (Dubrovsky et al. 1998) that, root growth effects the hydraulic conductivity. Root growth variation may be the reason for the difference between hydraulic conductivity of vegetated red soil and nutrient added soil. Except between 13th day and 19th day, nutrient added soil exhibited lower hydraulic conductivity as compared to that of red soil in the absence of nutrients. It is evident from previous studies that root growth may be lower in the absence of nutrients (Brouwer, 1962). Lower root growth implies lower water repellence (Wallis and Horne, 1992). This lower water repellence due to lower root growth may be reason for the higher hydraulic conductivity in the absence of nutrients.

4. FUTURE SCOPE

The obtained temporal variation of hydraulic conductivity can be adopted while devising irrigation schedule and analysing drainage.

Further studies are required to develop correlation between root growth and hydraulic conductivity in vegetated soil.

REFERENCES

- 1) ASTM D2487-11 Standard Practice for Classification of Soils for Engineering Purposes (Unified Soil Classification System). Annual book of ASTM standards
- 2) ASTM D854-14 Standard Test Methods for Specific Gravity of Soil Solids by Water Pycnometer. Annual book of ASTM standards.
- 3) ASTM D698-07 Standard Test Methods for Laboratory Compaction Characteristics of Soil Using Standard Effort (12 400 ft-lbf/ft³ (600 kN-m/m³)) Annual book of ASTM standards
- 4) ASTM D4318-93 Standard Test Methods for Liquid Limit, Plastic Limit, and Plasticity Index of Soils. Annual book of ASTM standards.
- 5) Bisdom, E. B. A., Dekker, L. W., & Schoute, J. T. (1993). Water repellency of sieve fractions from sandy soils and relationships with organic material and soil structure. *Geoderma*, 56(1-4), 105-118.
- 6) Brouwer, R., 1962. Nutritive influences on the distribution of dry matter in the plant (No. 205). [sn].
- 7) Campbell, G. S., and M. D. Campbell. "Irrigation scheduling using soil moisture measurements: theory
- 8) Dubrovsky, J.G., North, G.B. and Nobel, P.S., 1998. Root growth, developmental changes in the apex, and hydraulic conductivity for *Opuntia ficus-indica* during drought. *New Phytologist*, 138(1), pp.75-82.
- 9) Decagon Devices, Inc. 2014 operational manual: MiniDisk Infillrometer Pullman WA <http://www.decagon.com/macro>.
- 10) Ehlers, J. D., and A. E. Hall. "Cowpea (*Vigna unguiculata* L. Walp.)." *Field Crops Research* 53.1 (1997): 187-204.

- 11) Hillel, Daniel. Introduction to soil physics. Academic press, 2013.
- 12) Mengel, Konrad, and Ernest A. Kirkby. "Principles of plant nutrition." Principles of plant nutrition. (1978).
- 13) Van Genuchten, M. Th. "A closed-form equation for predicting the hydraulic conductivity of unsaturated soils." Soil science society of America journal 44.5 (1980): 892-898.
- 14) Wallis, M. G., and D. J. Horne. "Soil water repellency." Advances in soil science. Springer New York, 1992. 91-146.
- 15) Zhang, Renduo. "Determination of soil sorptivity and hydraulic conductivity from the disk infiltrometer." Soil Science Society of America Journal 61.4 (1997): 1024-1030

Back to table of contents

Performance analysis of drought resistant cowpea in red soil under the absence of nutrients

Bhushan S.Waghⁱ⁾, Ankit Soniⁱⁱ⁾, Shiv Prakashⁱⁱ⁾, Arka Dasⁱⁱⁱ⁾ and Ankit Gargⁱⁱⁱ⁾

i)Under Graduate Student, Department of Biosciences and Bioengineering, IIT Guwahati, Guwahati 781039, India.

ii)Under Graduate Student, Department of Civil Engineering, IIT Guwahati, Guwahati 781039, India.

iii)Assistant Professor, Department of Civil Engineering, IIT Guwahati, Guwahati 781039, India.

ABSTRACT

Cowpea is a widely cultivated grain Legume in Asia, Africa and South America. It is vital to investigate the performance of drought resistant cowpea under the absence of nutrients in the soil. This is because, leaching is key challenge in agriculture which implies absence of nutrients in root zone. Six drought resistant cow pea plants vegetated in soil in the absence of nutrients and other two drought resistant plants vegetated in nutrient mixed soil were investigated under natural boundary conditions, except controlled irrigation conditions. Performance has been demonstrated in terms of gravimetric water content, evapotranspiration and shoot growth. Lower gravimetric water content and higher evapotranspiration rate were found in case of plant grown under absence of nutrients as compared to plant grown in nutrient added soil. However, higher shoot growth was observed in case of plant vegetated in nutrient added soil than that of plant vegetated in red soil under the absence of nutrients. This study shows that, lower water retention may occur in the absence of nutrients. This study also reveal that, less water retention may result in lower shoot growth.

Keywords: drought resistant cowpea, red soil, evapotranspiration, gravimetric water content, shoot growth

1. INTRODUCTION

Cowpea is a widely cultivated grain Legume in Asia and South America. It provides high-quality and cheap dietary proteins for poor people (Henriet et al. 1997). Extensive research has been done

to develop transgenic cow pea (drought resistant cowpea) and its performance in nutrient mixed soil (Bakshi et al. 2012). However, performance of drought resistant cowpea in the absence of nutrients (i.e., in bare soil) was rarely studied. Leaching of nutrients due to infiltration is a major challenge in

agricultural engineering (Laird et al. 2010). After leaching of nutrients, plant may need to grow in soil under the absence of nutrients (Gordon et al. 2008). Hence, it is vital to investigate the performance of drought resistant cow pea in bare soil. This study investigates the performance of drought resistant cowpea in red soil under the absence of nutrients. This investigation is highly advantageous for sustainable water management i.e., efficient irrigation scheduling and water use efficiency. This study investigates the performance of drought resistant of nutrients.

The main objective of the present study is to study the performance of drought resistant cow pea in the red soil under the absence of nutrients. The study explores the performance in terms of gravimetric water content, evapotranspiration and shoot growth. Difference of performance in the presence and absence is demonstrated.

2. MATERIALS AND METHODS

2.1 Soil property

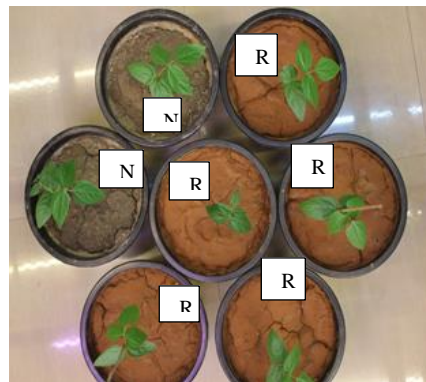
As per unified soil classification system (USCS) (ASTM D2487-11), the soil is categorised as ML. Soil composed mainly of silt (50%), clay (25%), fine sand (19%) and medium sand (6%), which is according to the grain size distribution. Liquid limit, plastic limit and shrinkage limit are 41 %, 24 % and 12 %, respectively. The properties were determined under the provisions of ASTM codes (ASTM D2487-10; ASTM D854-06; ASTM D4318-93 and ASTM D698-07).

2.2 Selected plant species

The crop species, Cowpea (*Vigna unguiculata*) is selected for the experiment. Cowpea is well known for its adaptation to nutrient-deficient soils

(Bakshi et al. 2012). The mature seeds of cowpea cultivar were procured from the Seed Corporation of India. The seeds were germinated in Petri dishes, for three days in dark. Then the germinated seedlings were transplanted to the pots to conduct experiments.

2.3 Experimental setup and test procedure



N – Nutrient added soil
R – Red soil

Fig.1 Drought resistant cowpea cultivated in nutrient added soil and red soil.

A test plan is aimed to analyze the performance of a drought-resistant cowpea in soil without nutrients, under controlled irrigation conditions. All the experiments were conducted in a Greenhouse (controlled atmospheric condition) (Fig.1). A total number of 8 pots (i.e., 6 pots filled with red soil and 2 pots with nutrient added soil) were placed in the room. The seedlings of the plant species were germinated and transplanted to the 8 pots. All the 8 pots were regularly irrigated at continuous intervals. The evaporation/evapotranspiration rate and gravimetric water content were measured frequently. The shoot length was also

measured by using scale with least count 1 mm.

The relative humidity and temperature were found at $55 \pm 5\%$ and $25 \pm 2^\circ\text{C}$ respectively. An Evaporation rate was measured by using evaporation pan. The cylindrical pots are used to conduct experiments, which were made from PVC plastic. It has a depth of 230 mm and a diameter of 260 mm, with a base which allows water drainage from the bottom. The soil is compacted in three layers to maintain a density of 1.3 g/cc (equivalent to 0.77 maximum soil dry density) up to 185 mm from the bottom. All the 8 pots were irrigated regularly at an interval of 3 days of transplantation. Gravimetric water content and Evapotranspiration rate of the 6 red soil and 2 nutrient mixed soil pots were measured by observations of change in weight.

3. RESULT AND DISCUSSION

3.1 Variation of gravimetric water content with time

As shown in Fig. 2, gravimetric water content was found to increase with time for both drought resistant cowpea cultivated in red soil as well as in nutrient mixed soil. Initially, gravimetric water content of nutrient added soil is 3% higher than that of red soil. However, by the end of 30 days gravimetric water content in nutrient added soil is 7% higher than that in red soil. This shows that, addition of nutrients increased the fine content, which further improved water retention. These variations show that, soil under the absence of nutrients retains less water as compared to soil in the presence of nutrients.

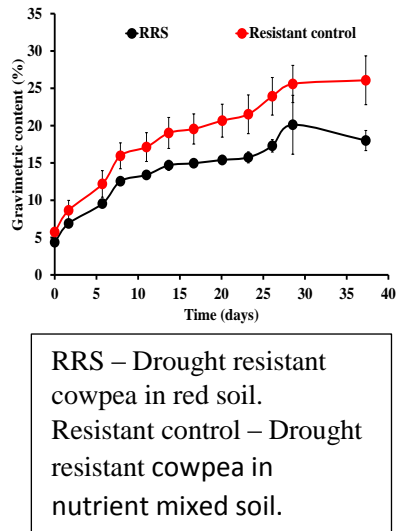
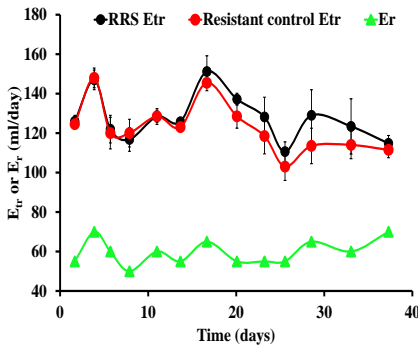


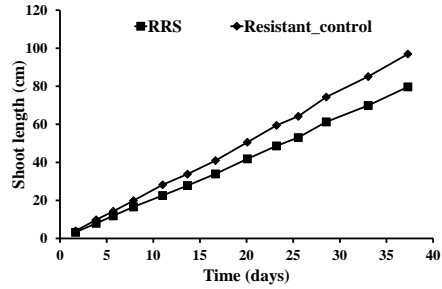
Fig. 2. Variation of gravimetric water content with respect to time.

3.2 Variation of evapotranspiration with time for both drought resistant cowpea in red soil and nutrient mixed soil

As shown in Fig. 3, evapotranspiration was found to vary between 100 to 150 ml/day for the drought resistant cowpea in nutrient mixed soil. Almost similar trend was observed for the plant in red soil. Any notable difference in evapotranspiration of drought resistant cowpea in red soil as well as nutrient mixed soil was not found up to 15 days after sowing. After 15 days, it was seen that evapotranspiration of drought resistant cowpea in red soil was higher than that in nutrient mixed soil and it continued till the end. Evapotranspiration was found to be slightly higher (i.e., difference of 2 ml/day to 5 ml/day) for plants vegetated in bare soil than those vegetated in nutrient added soil, up to 22



RRS Etr - evapotranspiration in drought resistant cowpea grown in red soil
 Resistance control Etr - evapotranspiration in drought resistant cowpea grown in nutrient mixed soil.
 Er - Evaporation



RRS – Drought resistant cowpea in red soil.
 Resistant control – Drought resistant cowpea in nutrient mixed soil.

Fig.4. Variation in the shoot length with respect to time.

of nutrients may be due to less water retention.

Fig. 3. Variation observed in evapotranspiration with respect to time.

days after sowing. After, 22 days this difference significant i.e., 4ml/ day to 12 ml/day. The reason for increase in evapotranspiration may be shoot growth due to which more root water uptake occurs.

3.3 Development of shoot with time

Shoot length was found to be increase with time in both nutrient mixed soil and red soil as shown in Fig. 4. Initially this difference is found between 1 and 3 cm. However, this difference is reached to 16 cm at the end of 34 days. Shoot growth of drought resistant cowpea in nutrient mixed soil was slightly higher than that in red soil. Shoot growth rate of cow pea plant was found 1 cm /day to 3 cm/ day higher in nutrient mixed soil. These variations show that, less shoot growth in the absence

4. SUMMARY AND CONCLUSION

Six drought resistant cow pea plants vegetated in bare soil and other two drought resistant plants vegetated in nutrient soil were studied in natural boundary conditions, except controlled irrigation conditions. Performance was demonstrated in terms of evapotranspiration, shoot growth and gravimetric water content. More evapotranspiration was found in red soil vegetated with cow pea. However shoot growth and gravimetric water content retention were found higher in nutrient added soil. The obtained performance variation due to absence of nutrients can be adopted to assess the plant growth and available water in irrigation scheduling. Further studies are required for different crop species to explore the performance in the absence of nutrients.

REFERENCES

- 1) A.S.T.M. D2487-11, 2011. Standard Practice for Classification of Soils for Engineering Purpose 251 (Unified Soil Classification System).
- 2) A.S.T.M., 2010. D2487-10. Standard Practice for Classification of Soils for Engineering Purposes (Unified Soil Classification System). Annual Book of ASTM Standards.
- 3) A.S.T.M., D4318-93, 1993. Standard Test Methods for Liquid Limit, Plastic Limit and Plasticity Index of Soils. Annual Book of ASTM Standards.
- 4) A.S.T.M.,D698-07,2007. Standard Test Methods for Laboratory Compaction Characteristics of Soil Using Standard Effort. Annual Book of ASTM Standards.
- 5) A.S.T.M.,D854-06,2007. Standard test method for specific gravity of soil solids by water pycnometer: Annual book of ASTM standards.
- 6) Bakshi, S., Roy, N.K. and Sahoo, L., 2012. Seedling preconditioning in thidiazuron enhances axillary shoot proliferation and recovery of transgenic cowpea plants. *Plant Cell, Tissue and Organ Culture (PCTOC)*, 110(1), pp.77-91.
- 7) Gordon, H., Haygarth, P.M. and Bardgett, R.D., 2008. Drying and rewetting effects on soil microbial community composition and nutrient leaching. *Soil Biology and Biochemistry*, 40(2), pp.302-311.
- 8) Henriet, J., Van Ek, G.A., Blade, S.F. and Singh, B.B., 1997. Quantitative assessment of traditional cropping systems in the Sudan savanna of northern Nigeria. I. Rapid survey of prevalent cropping systems. *Samaru Journal of Agricultural Research*, 14, pp.37-45.
- 9) Laird, D., Fleming, P., Wang, B., Horton, R. and Karlen, D., 2010. Biochar impact on nutrient leaching from a Midwestern agricultural soil. *Geoderma*,158(3), pp.436-442.

[Back to table of contents](#)

Short term river flow forecasting by Group Method of Data Handling method

Kukil Kashyapⁱ⁾, Md Altafuddinⁱⁱ⁾

i) Junior Research Fellow, Department of Civil Engineering, IIT Guwahati, Guwahati-781039, India.

ii) M.Tech Student, Department of Civil Engineering, NIT Agartala, Agartala,-799046, India.

ABSTRACT

Short term river flow forecasts helps in providing better information about future natural stream flows leading to prevention of unnecessary releases and provides opportunity to extract water during local flow peaks, thus helping in optimizing water resource system. This paper deals with the short term flow prediction of the longest ungauged river of Tripura (India), Gumti River. A spatio temporal short term flow prediction model is developed for predicting river flow in the catchment basin of ungauged Gumti River in Indian territory from Chabimura at upstream section to Sonamura at downstream section before it enters Bangladesh territory. Grid wise distributed catchment area of the Gumti River was divided into three sub-catchments from Chabimura to Sonamura. Grid wise runoff was calculated using a modified water budget equation and added to next grid according to their elevation towards the channel up to the end point of the catchment belonging to Indian Territory. River discharge at three locations namely Maharani, Udaipur and Sonamura were predicted during monsoon period using modified water budget equation and the real time primary data collected at that locations were compared with the predicted values. To minimize the difference between the predicted discharge and the real time primary data collected at three locations, weightages were used. The weightages of input parameters of the water budget equation as well as the difference of predicted and measured values were fed as inputs and outputs to GMDH respectively to obtain the best fit model equation to predict discharge values at a location for small lead times of 5-14 days for the ungauged Gumti River in Indian territory from Chabimura to Sonamura. Cumulative equivalent performance index (CEPI) calculated from RMSE, MAE, Standard deviation and Correlation, was adopted to evaluate the models performance. It was found out the highest CEPI value came out for the model from Maharani to Udaipur section. So, this model was considered to provide better prediction results for the Gumti basin and as such this technique can be used to forecast short term river flow for different meso scale river basins.

Keywords: Short term forecasting, GMDH, CEPI, Modified Water-Budget equation.

1 INTRODUCTION

Forecasting of river flows is an important component of water resources management for a variety of reasons such as helping to optimize water resources systems as well as planning for future expansion or reduction in a sustainable manner. The most common purpose of short term river flow forecasting systems is the forecasting of flood magnitudes in real time, usually for forecast lead times between 24 hours to 10 days, so as to inform authorities concerned with disaster management and aversion in the event of floods (Georgakakos and Krzysztofowicz, 2001). Highly accurate and reliable flow forecasts are particularly important in semi-arid watersheds due to the intermittent nature of river flows and frequent scarcity of water. Based on highly accurate and reliable flow forecasts, water managers in semi-arid watersheds can optimally allocate water to different sectors such as agriculture, municipalities, hydropower generation, while ensuring that environmental flows are maintained.

Various hydrologist and researchers has been studying river flow forecasting in the past few decades. There are two main techniques into which the river flow models can be grouped: Black box models and Physical based models (Shivakumar et.al., 2002). Physical model depend on parameters representing basin characteristics and contain simplified shapes of physical laws (Hsu et al.,1995). But physical models have disadvantage that they require a large amount of data i.e. large amount of parameters indicating the physical dynamics of the river basin. Stochastic hydrological black-box models that define input-output relations based on stochastic data and use mathematical and statistical concepts to link a certain input to the model output. The artificial neural network (ANN) is a nonlinear black box model which is widely accepted as a potential useful way of modeling hydrologic processes, and have been applied to a range of different areas including rainfall-runoff, water quality, sedimentation and rainfall forecasting (Abrahart et al., 2004), (Cannas et al. 2004), (Baratti et al., 2003).

Another useful tool is Ivakhnenko's group method of data handling (GMDH) (Ivakhnenko, 1970, 1989; Ivakhnenko et al., 1990). GMDH is a useful tool for processing data and identifying complex systems, especially when only a small amount of collected data is available (Farlow, 1984). The main advantage of GMDH is that it self-selects the structure of the model without using a priori information of the relationship between input and output variables. However, this method has received very little attention in the water resource literature despite important developments as long as two decades ago. There are only a few applications of GMDH to modeling of environmental and ecological systems and most of them were performed in the Soviet Union and Japan (Ikeda et al., 1976; Abdullayev et al., 1988).

In this study it is proposed to forecast short term river discharge of Gumti River, Tripura, up to next 24 hours to 10 days at particular downstream locations using the primary discharge data collected at the upstream locations by group method of data handling (GMDH) technique. The main objectives of the present study is development of a short term discharge forecasting, grid distributed model for meso scale river basin within a span of 1 to 10 days by group method of data handling (GMDH) techniques.

2 STUDY AREA

The study area selected for the present investigation is Gumti River basin in Tripura, within India. Gumti is the major river of Tripura. The basin lies in the districts of South Tripura, West Tripura and some part of Dhalai Tripura spreading from eastern to western boundary of the state. It is located between latitudes 23°19' and 23°47' N and longitudes 91°14' E and 91°58' E. The Gumti basin is surrounded by Bangladesh on its east and west. The catchment area of river Gumti is 2,492 km² within Indian Union and it has the largest basin among the rivers of Tripura. 1,921 km² lies in the hill catchment and only 571 km², which is nearly 22.9% of the total catchment, lies in the plains. The length of Gumti River is about 167.4km in Indian territory. Four locations along the Gumti River were used for primary data collection such as discharge from upstream section to downstream section namely, Chabimura (N23°33'12.48", E91°38'2.28"), Maharani (N23°31'36.72", E91°33'38.4"), Udaipur (N23°32'15.2", E91°28'30.66") and Sonamura (N23°28'20.52", E91°15'51.8") respectively. The ungauged catchment area of Gumti River from upstream location Chabimura to downstream location Sonamura is divided into 3 sub-catchments. The study area from Chabimura to Sonamura was divided into 38 grids dividing the study area into 3 sub-catchments namely: Chabimura-Maharani, Maharani-Udaipur and Udaipur-Sonamura shown in Fig 2.

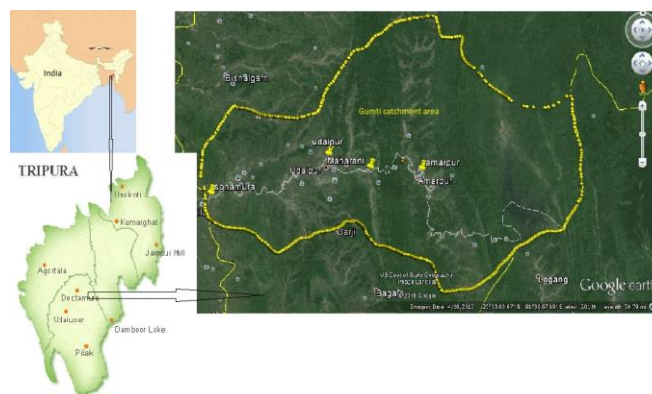


Fig. 1. Gumti river basin.

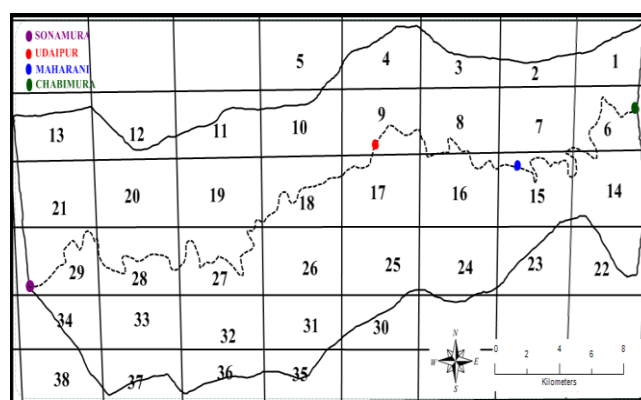


Fig. 2. Gridwise Distributed Study Area from Chabimura to Sonamura.

3 DATA COLLECTED AND MEASURED

The discharge collected at the four locations by M9 river surveyor (Sontek) is shown in table 1. The precipitation data from 2008 to 2015 were collected for the 3 rain gauge stations namely, Amarpur, Matabari and Sonamura from Tripura Agricultural Department and IMD Pune and average daily precipitation for each month for each sub-catchment was calculated by arithmetic mean method and is shown in Table 5 in Annexure. Potential Evapotranspiration (P_{et}) was calculated gridwise by Thornthwaite method and is shown in Table 6 in Annexure. Pervious land use area such as water bodies, barren land and forest cover as well as impervious land use area such as settlement areas and roads of each grid were determined by the image processing software Image J and is shown in Table 7 in Annexure.

Table 1. Discharge measured at different location by M9 River surveyor

Location	Date	Track length(m)	Discharge(m ³ /s)
Chabimura	4.8.2015	43.29	44.96
Maharani	5.8.2015	88.8	46.28
	6.8.2015	67.34	45.94
Udaipur	8.8.2015	104.98	46.7
	9.8.2015	112.67	47.215
Sonamura	15.8.2015	86.76	66.144
	21.8.2015	93.41	65.80

4 METHODOLOGY ADOPTED

The discharge of the river at a downstream section can be predicted by the summation of the surface runoff due to the past few days' rainfall from the sub-catchment along with the channel contribution calculated at the upstream section of the river. Surface runoff from each grid in a sub-catchment is calculated by the rainfall runoff relationship as shown by Equation (1) and summed up to obtain the total surface runoff from that sub-catchment which is required to forecast discharge at a downstream section of the sub-catchment from an upstream section of the sub-catchment. The rainfall runoff relationship used in this model to calculate surface runoff of each grid for a short duration of 1-10 days is a modification of water-budget equation and is as follows:

$$R = \frac{(P - P_{et}) \times IPA}{T} \quad (1)$$

$$Q = \sum R + C.C \quad (2)$$

Where

P= Total precipitation occurring in the short duration 'T' in 'm'.

P_{et}= Total potential evapotranspiration occurring in the short duration 'T' in 'm'.

IPA=Impervious area in the grid (settlement areas, roads) in 'm²'.

R= Surface runoff from the grid occurring in the short duration in 'm³/s'.

Q = discharge at a downstream section of a catchment in 'm³/s'.

$\sum R$ = Total surface runoff from all the grids of the catchment in 'm³/s'.

C.C = Channel contribution measured at the upstream river section of the catchment in 'm³/s'.

From the primary data collected in the upstream location, discharge was computed by modified water budget equation (1) and (2) at downstream location for each sub-catchment and compared with actual discharge measured in the specified downstream location on the field for that sub-catchment for a continuous duration and the difference is given in table 2.

Table 2. Actual and Measured discharge difference at each sub-catchment

Sub-Catchment	Chabimura(U/S) to Maharani(D/S) (4/8/15-6/8/15)	Maharani(U/S) to Udaipur(D/S) (6/8/15-9/8/15)	Udaipur(U/S) to Sonamura(D/S) (9/8/15-21/8/15)
Q actual (m ³ /s)	45.94 (At Maharani)	47.215 (At Udaipur)	65.8 (At Sonamura)
Q Cal (m ³ /s)	45.02451331 (At Maharani)	46.25256178 (At Udaipur)	51.63604702 (At Sonamura)
Qa-Qc (m ³ /s)	0.915	0.962	14.16
Rel. error	1.99%	2.037%	21.519%

GMDH algorithm was used to find the minimum difference between the actual discharge measured in the downstream location and the discharge computed at that location based on the conditions mentioned below for each sub-catchment and model equation was obtained which can forecast the short term runoff from Chabimura to Sonamura sub-catchment quite accurately. Discharge Q measured downstream is:

$$Q \frac{d}{s} = \frac{(W_1 \times P - W_2 \times P_{et}) \times W_3 \times IPA}{T} + W_4 \times (C.C) \quad (3)$$

Where

W1= Weightage of precipitation.

W2=Weightage of Potential evapotranspiration.

W3=Weightage of impervious area of all grids in each sub-catchment.

W4=Weightage of Channel contribution from upstream.

For each sub-catchment, GMDH models were created based on the conditions that weightages of precipitation, evapotranspiration, impervious area and channel contribution as inputs mentioned in equation (3) and difference of field measured actual discharge and calculated discharge from the sub-catchment as output.

For the three sub-catchments, 3 models were created for monsoon period, from which the model with highest Cumulative Performance Index (CEPI) was selected and best fit model equation was formed.

4.1 Group Method of Data Handling (GMDH)

Group method of data handling (GMDH) is a family of inductive algorithms for computer based mathematical modeling of multi parametric datasets that features fully automatic structural and parametric optimization of models. It establishes the input-output relationship of a complex system using a multilayered perception-type structure that is similar to a feed-forward multilayer neural network. GMDH is a useful data process for identifying complex systems, especially when only a small amount of collected data is available (Farlow, 1984). GMDH algorithms are characterized by inductive procedure that performs sorting out of gradually complicated polynomial models and selecting the best solution by means of the so called external criterion. The GMDH algorithm

generates optimal structure of the model through successive generations of partial descriptions (PDs) of data, which are described by quadratic regression polynomials most often with input variables. The basic ideas of this algorithm are as follows: .We know nothing about the system; let us generate and compare all possible input output combinations, while each element in the network implements a non-linear function of two inputs and its coefficients are determined by a regression technique. Self-selection thresholds are employed at each layer in the network to alter out those elements that are useless in predicting the correct output. Only those elements whose performance indices exceed the threshold are allowed to pass to succeeding layers, where more complex combinations are formed. The procedure is performed until a satisfactory result is reached. The GMDH model implementation was carried out in GMDH Shell software

4.2 Performance Index

Cumulative Equivalent Performance Index (CEPI) was adopted to evaluate the model’s performance. CEPI of each model was calculated from RMSE, MAE, Standard deviation and Correlation of the training and testing data.

$$CEPI = 0.4 \left(\frac{Correlation}{RMSE+MAE+Standard\ Deviation} \right)_{Training} + 0.6 \left(\frac{Correlation}{RMSE+MAE+Standard\ Deviation} \right)_{Testing} \quad (4)$$

The model with highest CEPI is selected and best fit model equation was formed to forecast the short term flow of Gumti river from Chabimura to Sonamura.

5 RESULTS AND DISCUSSIONS

The GMDH analysis for the three sub-catchments i.e. Chabimura to Maharani, Maharani to Udaipur and Udaipur to Sonamura was computed. Highest CEPI came for the non-monsoon condition in Maharani to Udaipur sub-catchment for the condition when weightages of precipitation, evapotranspiration, impervious area and channel contribution were taken as inputs and difference of field measured actual discharge and calculated discharge from the sub-catchment was taken as output as shown in Table 3.

Table 3. GMDH analysis

Model no.	1	2	3
No. of inputs	4	4	4
No. of outputs	1	1	1
Sub-catchments	Chabimura to Maharani	Maharani to Udaipur	Udaipur to Sonamura
Training Algorithm	GMDH	GMDH	GMDH
Training MAE	1.332×10 ⁻⁴	1.36×10 ⁻¹²	2.23×10 ⁻¹²
Training RMSE	1.094×10 ⁻³	1.62×10 ⁻¹²	2.80×10 ⁻¹²
Training Standard Deviation	1.0942×10 ⁻³	1.55×10 ⁻¹²	2.73×10 ⁻¹²
Training Correlation	1	1	1
Testing MAE	8.03×10 ⁻⁵	1.28×10 ⁻¹²	2.13×10 ⁻¹²
Testing RMSE	9.19×10 ⁻⁵	1.56×10 ⁻¹²	2.70×10 ⁻¹²
Testing Standard Deviation	8.03×10 ⁻⁵	1.48×10 ⁻¹²	2.61×10 ⁻¹²
Testing Correlation	1	1	1
CEPI	2.54×10 ³	2.27×10 ¹¹	1.32×10 ¹¹
Rank	3	1	2

Best fit model equation:

$$Q = 1.1574 \times 10^{-8} (0.444399P - 0.202026P_{et}) \times 0.84383 (I.A.) + 0.994326 \times (C.C) \quad (4)$$

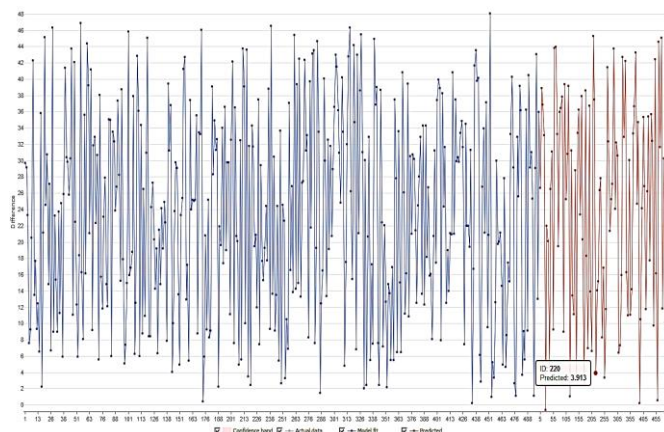


Fig. 3. Actual(blue) and Predicted(red) data of best model .

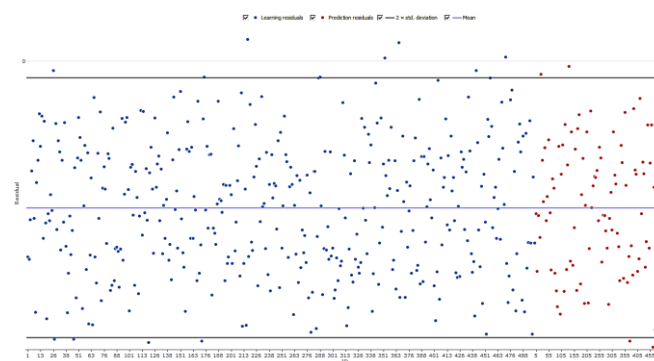


Fig. 4. Learning(blue) Vs Predicted(red) residuals.

6 MODEL VALIDATION

With the help of model equation, short term flow was forecasted for two cases from the primary data collected at the specified upstream location and compared with the actual discharge measured at downstream location and results were quite close. The two cases are shown below in table:

Table 4. Validation of model

Sl no	1	2
Date	5/8/2015-8/8/2015	9/8/2015-15/8/2015
U/S location	Maharani N23°31'36.72" E91°33'38.4"	Udaipur N23°32'15.2" E91°28'30.66"
D/S location	Udaipur N23°32'15.2" E91°28'30.66"	Sonamura N23°28'20.52" E91°15'51.8"
Q u/s	46.28	47.215
Q forecasted(d/s)	46.558	65.925
Q actual(d/s)	46.7	66.144
Qa-Qf	0.142	0.219
Rel. Error	0.304%	0.33%

6 CONCLUSION

In this study attempt has been made to implement new ideas and methods in conjunction with existing platform for a better forecasting of short term river flow in a particular region. Forecasting modeling with GMDH was done because of its usefulness in data process for identifying complex systems, especially when only a small amount of collected data is available. Accuracy of the model accepted for short term flow prediction of the study area was found quite high. Since the Gumti River is ungauged and there is lack of regular collected discharge data, predictions were made based on small amount of primary discharge data collected. A main frame structure is needed for the regular collection of the discharge data and the timely dissemination of the forecast results to the concerned bodies to enable proper utilization of the forecasting results. Such features are unavailable, which limits the reach of the output results to the concerned bodies, and also discourages the regular generation of forecasts.

REFERENCES

- 1) Abdullayev, F. A., Akhmedov, Sh. A., and Mamedov, M. I. (1988): GMDH algorithm for forecasting the optical state of the atmosphere, *Sov. J. Autom. Inf. Sci.*, 21, 58-61.
- 2) Abraham, R.J., Kneale, P.E. and See, L. (2004): *Neural Networks in Hydrology*, A.A. Balkema, Rotterdam.
- 3) Baratti, R., Cannas, B., Fanni, A., Pintus, M., Sechi, G.M., and Toreno, N. (2003): River flow forecast for reservoir management through neural networks, *NeuroComputing*, v. 55, p. 421-437.
- 4) M Cannas, B., Montisci, A., Fanni, A., See, L. and Sechi, G.M. (2004): Comparing artificial neural networks and support vector machines for modeling rainfall runoff, *World Scientific Publishing Company, Proceedings of the 6th International Conference on Hydroinformatics*.

- 5) Farlow, J. S. (1984): *Self-Organizing Methods in Modeling GMDH Type Algorithms*, Marcel Dekker, New York.
- 6) Hsu, K., Gupta, H.V. and Sorooshian, S. (1995): Artificial neural network modeling of the rainfall runoff process, *Water resources research*. 31(10). 2517-2530.
- 7) Ikeda, S., Fugishige, S., and Sawaragi, Y. (1976): Nonlinear prediction model of river flow by self-organization method, *Int. J. Syst. Sci.*, 7, 165-176.
- 8) Ivakhnenko, A.G. (1970): Heuristic self-organization in problem of engineering Ivakhnenko cybernetics, *Automatica*, 6, 207-219.
- 9) Ivakhnenko, A. G., Fateyeva, Ye N., and Ivakhnenko, N. A. (1989): Nonparametric GMDH forecasting models, Part 1. Sorting the Bayes or Wald formulas', *Sov. J. Autom. Inf. Sci.*, 22, 1, 1-8.
- 10) Ivakhnenko, A. G. (1990): Nonparametric GMDH predicting models. Part 2. Indicative systems for selective modeling, clustering, and pattern recognition, *Sov. J. Autom. Inf. Sci.*, 22, 2, 1-10.
- 11) K.P. Georgakakos and R. Krzysztofowicz. (2001): Probabilistic and Ensemble Forecasting (Editorial), *Journal of Hydrology*, 249(1), 1-4.
- 12) Shivakumar, B., Jayawardena, A.W., and Fernando, T.M.K.G. (2002): River flow forecasting: use of phase-space reconstruction and artificial neural networks approaches, *Journal of hydrology* 265 (1-4).

[Back to table of contents](#)

ANNEXURE

Table 5. Mean precipitation (mm) of the three sub-catchments

Sub-catchment	Jan	Feb	Mar	Apr	May	Jun	Jul	Aug	Sept	Oct	Nov	Dec
Chabimura to Maharani	3.05	9.44	15.63	19.4	24.33	21.81	20.57	20.6	17.4	26.61	2.45	1.8
Maharani to Udaipur	3.21	9.97	14.78	20.4	24.49	22.06	20.47	20.33	18.37	24.94	1.63	1.2
Udaipur to Sonamura	3.18	9.24	12.8	19.7	24.28	21.6	19.96	19.85	18.09	20.86	2.45	1.8

Table 6. Estimated Monthly Potential Evapotranspiration of all grids

GRID ID	PET(mm/day)											
	Jan	Feb	Mar	Apr	May	Jun	Jul	Aug	Sept	Oct	Nov	Dec
1	1.077	1.922	4.351	6.175	7.031	7.669	7.275	6.995	6.547	5.083	3.0179	1.569
2	1.077	1.922	4.351	6.174	7.03	7.668	7.273	6.994	6.547	5.083	3.0182	1.569
3	1.077	1.922	4.351	6.174	7.03	7.668	7.273	6.994	6.547	5.083	3.0182	1.569
4	1.077	1.922	4.351	6.175	7.031	7.669	7.274	6.994	6.547	5.083	3.018	1.569
5	1.077	1.922	4.351	6.175	7.031	7.669	7.274	6.994	6.547	5.083	3.018	1.569
6	1.077	1.922	4.351	6.175	7.031	7.669	7.275	6.995	6.547	5.083	3.0179	1.569
7	1.077	1.922	4.351	6.174	7.03	7.668	7.273	6.994	6.547	5.083	3.0182	1.569
8	1.077	1.922	4.351	6.174	7.03	7.668	7.273	6.994	6.547	5.083	3.0182	1.569
9	1.077	1.922	4.351	6.175	7.031	7.669	7.274	6.994	6.547	5.083	3.018	1.569
10	1.077	1.922	4.351	6.175	7.031	7.669	7.274	6.994	6.547	5.083	3.018	1.569
11	1.077	1.823	4.351	6.174	7.029	7.662	7.271	6.994	6.547	5.088	3.0186	1.569
12	1.077	1.823	4.351	6.174	7.029	7.662	7.271	6.994	6.547	5.088	3.0186	1.569
13	1.077	1.823	4.351	6.174	7.029	7.662	7.271	6.994	6.547	5.088	3.0186	1.569
14	1.077	1.922	4.351	6.175	7.031	7.669	7.275	6.995	6.547	5.083	3.0179	1.569
15	1.077	1.922	4.351	6.174	7.03	7.668	7.273	6.994	6.547	5.083	3.0182	1.569
16	1.077	1.922	4.351	6.174	7.03	7.668	7.273	6.994	6.547	5.083	3.0182	1.569
17	1.077	1.922	4.351	6.175	7.031	7.669	7.274	6.994	6.547	5.083	3.018	1.569
18	1.077	1.922	4.351	6.175	7.031	7.669	7.274	6.994	6.547	5.083	3.018	1.569
19	1.077	1.823	4.351	6.174	7.029	7.662	7.271	6.994	6.547	5.088	3.0186	1.569
20	1.077	1.823	4.351	6.174	7.029	7.662	7.271	6.994	6.547	5.088	3.0186	1.569
21	1.077	1.823	4.351	6.174	7.029	7.662	7.271	6.994	6.547	5.088	3.0186	1.569
22	1.077	1.922	4.351	6.175	7.031	7.669	7.275	6.995	6.547	5.083	3.0179	1.569
23	1.077	1.922	4.351	6.174	7.03	7.668	7.273	6.994	6.547	5.083	3.0182	1.569
24	1.077	1.922	4.351	6.174	7.03	7.668	7.273	6.994	6.547	5.083	3.0182	1.569
25	1.077	1.922	4.351	6.175	7.031	7.669	7.274	6.994	6.547	5.083	3.018	1.569
26	1.077	1.922	4.351	6.175	7.031	7.669	7.274	6.994	6.547	5.083	3.018	1.569
27	1.077	1.823	4.351	6.174	7.029	7.662	7.271	6.994	6.547	5.088	3.0186	1.569
28	1.077	1.823	4.351	6.174	7.029	7.662	7.271	6.994	6.547	5.088	3.0186	1.569
29	1.077	1.823	4.351	6.174	7.029	7.662	7.271	6.994	6.547	5.088	3.0186	1.569
30	1.077	1.922	4.351	6.175	7.031	7.669	7.274	6.994	6.547	5.083	3.018	1.569
31	1.077	1.922	4.351	6.175	7.031	7.669	7.274	6.994	6.547	5.083	3.018	1.569
32	1.077	1.823	4.351	6.174	7.029	7.662	7.271	6.994	6.547	5.088	3.0186	1.569
33	1.077	1.823	4.351	6.174	7.029	7.662	7.271	6.994	6.547	5.088	3.0186	1.569
34	1.077	1.823	4.351	6.174	7.029	7.662	7.271	6.994	6.547	5.088	3.0186	1.569
35	1.077	1.922	4.351	6.175	7.031	7.669	7.274	6.994	6.547	5.083	3.018	1.569
36	1.077	1.823	4.351	6.174	7.029	7.662	7.271	6.994	6.547	5.088	3.0186	1.569
37	1.077	1.823	4.351	6.174	7.029	7.662	7.271	6.994	6.547	5.088	3.0186	1.569
38	1.077	1.823	4.351	6.174	7.029	7.662	7.271	6.994	6.547	5.088	3.0186	1.569

Table 7. Gridwise % Land Use Area

Sub-catchment	GRID ID	Latitude and Longitude	%surface water area	%forest area	%barren land area	%settlement area
Chabimura to Maharani	1	N23°34'33"E91°37'15"	4.405	62.570	27.337	5.685
	2	N23°34'04" E91°34'14"	3.955	64.706	27.308	4.028
	6	N23°32'55" E91°37'20"	6.211	69.807	18.839	5.141
	7	N23°33'02" E91°29'16"	5.880	66.681	21.285	6.153
	14	N23°30'55" E91°37'03"	1.397	81.860	11.102	5.639
		N23°30'48" E91°28'39"				
	15		11.159	47.263	34.660	6.916
	22	N23°29'31" E91°37'28"	0.915	85.150	9.328	4.604
	23	N23°29'02" E91°28'27"	4.920	64.224	21.861	8.992
	Maharani to Udaipur	3	N23°33'51" E91°27'03"	6.007	53.275	34.122
4		N23°34'22" E91°28'30"	4.407	61.605	32.375	1.611
8		N23°32'56" E91°31'36"	10.214	39.405	41.653	8.673
9		N23°34'33" E91°37'15"	8.164	25.846	44.004	21.717
16		N23°30'55" E91°31'28"	9.934	46.732	32.541	10.772
17		N23°34'33" E91°37'15"	14.638	5.935	67.630	11.789
24		N23°28'54" E91°31'31"	3.327	71.829	22.231	2.594
25		N23°34'33" E91°37'15"	4.739	41.255	44.979	9.003
30		N23°34'33" E91°37'15"	13.339	36.947	37.126	12.564
5		N23°34'33" E91°37'15"	0.891	19.251	9.541	69.508
10		N23°32'49" E91°25'50"	1.988	52.413	25.408	20.189
11		N23°32'19" E91°22'58"	4.802	39.926	33.608	21.662
12		N23°32'11" E91°18'51"	10.925	31.949	34.966	22.158
13		N23°32'24" E91°16'41"	2.141	51.756	25.373	20.728
18		N23°34'33" E91°37'15"	9.791	17.199	51.847	21.161
19		N23°30'53" E91°22'53"	6.077	57.064	16.596	20.261
20		N23°30'49" E91°19'47"	12.534	18.542	46.454	22.468
21		N23°30'45" E91°17'02"	5.045	43.240	33.307	18.405
26		N23°29'02" E91°25'52"	5.547	32.120	41.834	20.498
27		N23°28'47" E91°22'50"	11.300	40.513	28.105	20.080
28		N23°28'52" E91°19'54"	15.711	28.322	32.098	23.867
29		N23°29'02"E91°17'16"	13.522	14.958	46.466	25.052
31		N23°29'6" E91°25'54"	7.663	19.941	51.305	21.088
32		N23°27'20" E91°22'53"	3.351	59.547	16.867	20.233
33		N23°27'26" E91°20'03"	3.352	55.738	18.800	22.108
34		N23°27'24" E91°17'40"	4.4240	44.434	30.011	21.129
35		N23°26'16" E91°25'36"	4.500	37.505	37.963	20.030
36		N23°26'12" E91°22'58"	3.257	55.664	19.937	21.140
37		N23°26'10" E91°19'52"	1.942	61.402	16.072	20.581
Udaipur to Sonamura		38	N23°26'17" E91°18'18"	1.867	50.952	27.111

Stability analysis of geobag revetment for riverbank protection

Rhitwika Barmanⁱ⁾

B. Talukdarⁱⁱ⁾

i) Guest Lecturer, Department of Civil Engineering, Assam Engineering College, Jalukbari-781013, India

ii) Associate Professor, Department of Civil Engineering, Assam Engineering College, Jalukbari-781013, India

ABSTRACT

At present in Assam, two of the major social and economical concerns caused by nature are Flood and Erosion of riverbanks. More than 7.4% of total area of the state has been already eroded since 1950. To prevent further loss of lives and properties because of this disaster, a number of ways have been engineered. One of the methods of river bank protection is bank revetment. Naturally available boulder, Cement concrete blocks and sand fill geotextile bags are commonly used revetment materials. But till now, very less study has been done for stability of geobags under submerged condition. In this study, an attempt has been made to find out whether this measure can be successfully applied as bank revetment material or not. Here, the behavior of geobags under submerged conditions has been studied experimentally. Model geobags are used in laboratory experiments to check the suitability of geobags, for different situations. The experiments are conducted with three different arrangements of geobags in two different bed slopes i.e. 1:10000 and 1:500. Failure modes and failure velocities for each case is observed in the experiments. Also the causes of geobag failure and probable remedial measures have been discussed. In theoretical analysis, stability analysis from sliding and uplift displacement criteria is done to find the theoretical safe velocities for different situations. The laboratory results are compared with the theoretical calculations and it has been found that the results from both the analysis are almost matching.

Keywords: bank erosion, geobags, failure modes, drag, lift, hydraulic stability

1. INTRODUCTION

In Assam, more than 4.27 Lakh hectares of land have been eroded away by the river Brahmaputra and its tributaries since 1950, which is 7.4% of the land area of the state. The average annual land loss is 8000 ha. Out of the myriad ways that have been engineered to save the lives and properties of people from the flood and erosion hazards, a very popular one is to use sand-filled geotextile bags (commonly called geobags) in the riverbanks. They are geosynthetic products made of polyesters, specially designed for good soil tightness and high seam efficiency. However, there is little understanding about them due to lack of scientific studies. Here, we try to determine the feasibility of using geobags both experimentally and theoretically, and also to analyze the bank erosion resistance of geobags under different circumstances. We will try to comprehend the hydrodynamic forces related to geobag failure by using a distorted scale model in a laboratory, with an artificial open channel and miniature geobags. Objectives of this study mainly concentrate on:

1. To understand the performance of a geobag revetment in submerged conditions.
2. To observe the stability of geobags under different flow parameters.
3. To explore the causes of geobag failure and look for probable remedial measures.

This work has been preceded by a few similar

studies performed by various scholars. Neil et al. (2008) conducted tests on small-scale bags to examine various aspects of design and placement, and to compare their behaviour with that of rock riprap. Multiple aspects of Sand Filled Container (SFC) stability were investigated by Recio and Oumeraci (2009). They performed laboratory experiments investigating the stability of geotextile containers arranged in a variety of configurations over a wide range of wave conditions.

Akter et al. (2009) presented the observed failure modes for a geobag structure from a series of physical model tests and they found that overtopping, sliding, puncturing, pullout/dislodgement and toe scour are the most common failure modes. They also performed laboratory experiments (Akter et al., 2013a) using both fixed bed and mobile sediment bed configurations, studying their failure modes. Also hydrodynamic forces had been modeled by using the Conveyance Estimation System software with a distorted scale model. The CES results found in the previous paper were used for preparing a mapped velocity field for a coupled DEM simulation of geobag revetment failure (Akter et al., 2013b).

Oumeraci et al. (2012) performed a study to investigate the hydraulic stability of geotextile sand container (GSC) structures for a better understanding of the processes and the parameters of GSCs, which cause

the failure.

2. METHODOLOGY AND PROCEDURE

2.1. Flume channel

The laboratory experiments were carried out in the flume channel of the hydraulics laboratory of Assam Engineering College having dimension of 20000 mm X 960 mm X 1240 mm. A mobile sediment bed of average thickness 400 mm above concrete floor of the channel has been used for the tests in which locally available sand was placed as the bed material.

2.2. Model geobags

Distorted scale model bags are used made up of the non woven geotextile material as used in the field manufactured from polypropylene or polyester, which are filled with locally available sand of characteristic grain size 0.2 to 0.25 mm, porosity 40% and C_u 1.3. The scale ratio for the experimental set up and actual size of geobags and size of model geobags used in the experiments are given in table 1 and 2 respectively.

Table 1. Scale Ratio of Model Bags.

Quantity	Dimensions	Scale Ratio
Length, Breadth	L	1:9.5
Bag volume / mass	L^3	1:857.3
Velocity	$L^{1/2}$	1:3.08
Discharge	$L^{5/2}$	1:278.17
Shear stress	$L^{3/2}$	1:29.28

Table 2. Size of geobags.

Bag Type	Bag Size	Filled L	Filled B	Filled H	Weight (kg)
Actual size	1.03 m X 0.7 m	0.9 m	0.6 m	0.15 m	126
Model size	-	95mm	65mm	15mm	0.145

The bags are partly filled with sand (1-n) and air or water (n), where n is the porosity of sand, depending on where the bag is located. The geobags are mostly placed below the waterline, i.e. the bags are nearly completely saturated with water. If ρ_b , ρ_s , ρ_w are the densities of model bags, sand and water respectively, The mass density of the bags is calculated with the equation (1), shown below.

$$\rho_b = \rho_s(1-n) + \rho_w(n) \quad (1)$$

2.3. Test section

A test section is prepared for the experiment, with a side slope of 1V:2H within the test flume as seen in figure 1. The width and height of the banks are 300mm

and 150mm respectively. A bank is constructed with river bank material immediately upstream and downstream of the test section as well as in the opposite side of the test section maintaining the same slope.



Fig 1. Laboratory model set-up

2.4. Experimental criteria

The experiments are performed for three different arrangements of geobags.

1. AM1 Jack on jack : The geobags are laid with their longer axis parallel to the flow direction in individual 'columns', with each bag being placed directly on top of another which is shown in figure 2.



Fig 2. Jack on jack bond

2. AM2 Running bond : The geobags are again laid longitudinally in a typical brick wall pattern, with the geobag joints lying in the middle of the bags in the layers directly above and below. The running bond is displayed in figure 3.



Fig 3. Running bond

3. AM3 Half-basket weave : The AM3 bond comprises of alternate layers of bags aligned with their longer and shorter axes parallel to the flow direction as shown in figure 4.



Fig 4. Half-basket weave bond

The experiments are conducted in two different bed slopes 1:10,000 and 1:500. Experiments with 1:10,000 bed slope is conducted for three different water depths A, B and C, while for 1:500 bed slope it was conducted only for water depth A. These three conditions of depth are stated below.

1. Depth A : Upto 50% of the structure height.
2. Depth B : 50% - 80% of the structure height.
3. Depth C : 80% - 100% of the structure height.

Each experiment is run for 3 hours which is sufficient for all physical processes to occur. Different failure modes in the geobag models are observed and studied. Also the theoretical analysis is carried out and results from both the analysis are compared.

3. OBSERVATIONS AND INTERPRETATIONS

3.1. Observations in the revetment

For all three arrangements in 1:10,000 bed slope same type of observations are made for different depth ranges. No change in the revetment is seen for depth A. For depth B, uplifting and sliding of the bags in the bottom layer is seen but no bag is displaced. For depth C, bags are displaced from the bottom layer but no bag is pulled out from the revetment structure. The failure modes for different arrangements and depth ranges are shown below. Failure modes for different arrangements can be seen in figure 5, 6 and 7.



Fig 5. Observation in AM1 (1:10,000 bed slope)



Fig 6. Observation in AM2 (1:10,000 bed slope)

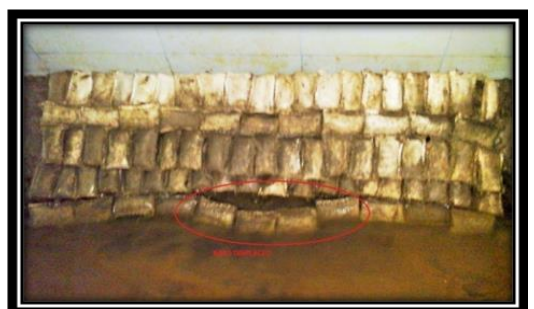


Fig 7. Observation in AM3 (1:10,000 bed slope)

The experiments in 1:500 are described for different arrangements. For AM1, sliding and displacement of bags occur as soon as the flow proceeds. For AM2, uplifting of geobags and bag displacement from the entire layer is seen. For AM3, sliding of geobags and bag displacement from bottom layer is observed. For all three arrangements mode of failure is shown in figure 8, 9 and 10.



Fig 8. Observation in AM1 (1:500 bed slope)



Fig 9. Observation in AM2 (1:500 bed slope)



Fig 10. Observation in AM3 (1:500 bed slope)

3.2. Behavior of the waterway

- In 1:10,000 bed slope, the bank with geobag is protected fully while some portion of the opposite bank is washed away.
- In 1:500 bed slope, the bank with geobag is protected but major portion of the opposite bank is washed away as seen in figure 11.
- If the revetment fails, the displaced geobags get deposited in the downstream of the channel because of which the flow is obstructed and water level rises in the upstream which suddenly fall after rising into the obstruction level giving rise to rapidly varied flow (Hydraulic jump) as shown in figure 12.



Fig 11. Erosion of opposite banks



Fig 12. Formation of hydraulic jump

3.3. Causes of failure

- In the laboratory revetment, there is a high water-pressure difference between the channel side and the geobag lee side. This introduced turbulent bursting-induced flow through the revetment voids.
- Higher stream wise velocities influenced the bag pull-out processes.
- Internal sliding, combined with other modes, characterized the failure process in almost all cases.

4. THEORETICAL ANALYSIS

The flow is associated with hydrodynamic forces, i.e. drag force, lift force, buoyancy force and the self-weight of the geobags. The drag and lift forces are calculated with the equations (2) and (3) respectively.

$$F_D = 0.5C_D\rho_w Au^2 \quad (2)$$

$$F_L = 0.5C_L\rho_w Au^2 \quad (3)$$

F_D and F_L are the drag and lift force, C_D and C_L are the drag and lift coefficients, A is the cross sectional area perpendicular to the flow and u is the velocity of flow. If the wave induced vertical forces exceed the weight of the bag, then the stability of the bag is lost from uplift displacement criteria which is expressed in equation (4).

$$F_L \leq (\rho_b - \rho_w) g V_m \quad (4)$$

Where g is the acceleration due to gravity and V_m is the volume of the bag. Again sliding occurs when wave-induced horizontal forces exceed the resisting forces. The stability criteria from sliding force is seen in equation (5).

$$F_D \leq [(\rho_b - \rho_w)gV_m - FL] \mu \quad (5)$$

Where μ is the friction factor taken as 0.53. Values of C_D and C_L is taken as 0.8 and 0.5 from the findings of Recio and Oumeraci (2009) (Ref no 6) for 1:10,000 bed slope. For 1:500 bed slope the coefficients are calculated as 3 (C_D) and 4.8 (C_L) from the equation (6), based on the findings of Wu et al. (1999).

$$C_D = 2DgS/TV^2 \quad (6)$$

D is the depth of flow, S is the bed slope, T is the height of vegetation.

Using all the equations mentioned above, theoretical safe velocities for a single geobag from uplift and sliding displacement criteria for all experimental arrangements are calculated and compared with laboratory results.

5. RESULTS AND DISCUSSIONS

Results from both experimental and theoretical analysis for 1:10,000 bed slope is shown in table 3.

Table 3. Results for 1:10,000 bed slope

Analysis	Failure modes	Model Velocity (m/s)	Prototype Velocity (m/s)
Laboratory observations	Void flow	0.2	0.62
	Sliding and uplifting	0.3	0.92
	Displacement of bags	0.4	1.23
Theoretical safe velocities	For uplift force	1.05	3.23
	For sliding force	0.72	2.21

In the laboratory tests, internal sliding of bags starts from model velocity 0.3 m/s (prototype velocity 0.92 m/s) and it advances with dragging of bags when velocity is 0.4 m/s (prototype velocity 1.23 m/s) and complete failure of the revetment has not taken place. Again safe velocities for both criteria are seen which validate the laboratory data.

For 1:500 bed slope also, the results are shown below in table 4.

Table 4. Results for 1:500 bed slope

Analysis	Failure modes	Model Velocity (m/s)	Prototype Velocity (m/s)
Laboratory observations	Void flow, internal sliding, bags pulled out	0.4	1.23
Theoretical safe velocities	For uplift force	0.43	1.23
	For sliding force	0.29	0.89

In the laboratory tests, internal sliding and pulling out of bags are seen and complete failure of the revetment takes place which is validated by theoretical safe velocities.

5. CONCLUSIONS

It is seen that uplifting and sliding are the common failure modes. There is a vast difference of failure

velocities for different bed slopes. The failure modes in the revetment structures are same for different arrangements of bags in the revetment. The two arrangements (running bond and half basket weave bond) are suitable for geobag application in field. Jack on jack bond is not useful in this purpose. The conventional geobag of size (1.03 m x 0.7 m) of 126 kg weight is applicable for 1:10,000 bed slope up to a velocity of 2.2 m/s while it is 0.9 m/s for steep slope (1:500). Therefore to resist velocity greater than that, the size and weight of a geobag should be increased.

REFERENCES

- 1) Akter, A., Wright, G., Crapper, M. and Pender, G., "Failure Mechanism in Geobag Structure", Proceedings of the 4th IASME/WSEAS International Conference on Water Resources, Hydraulics & Hydrology, pp. [25-30], 2009
- 2) Akter, A., Pender, G., Wright, G. and Crapper, M., "Performance of a Geobag Revetment I: Quasi-Physical Modelling", Journal of Hydraulic Engineering, American Society of Civil Engineers, pp. [865-876], 2013a
- 3) Akter, A., Pender, G., Wright, G. and Crapper, M., "Performance of a Geobag Revetment II: Numerical Modelling", Journal of Hydraulic Engineering, American Society of Civil Engineers, pp. [877-885], 2013b
- 4) Neill, C., Mannerström, M. and Azad, A.K., "Model Tests on Geobags for Erosion Protection", Fourth International Conference on Scour & Erosion, pp. [404-411], 2008
- 5) Recio, J. and Oumeraci, H., "Process based stability formulae for coastal structures made of geotextile sand containers." Coastal Engineering V56 , pp.[632 – 658], 2009
- 6) Recio, J., and Oumeraci, H., "Processes affecting the hydraulic stability of coastal revetments made of geotextile sand containers." Coastal Eng.,56(3), pp.[260–284], 2009
- 7) Soysa, V.A.N., Dassanayake, D.M.D.T.B. and Oumeraci, H., "Hydraulic Stability of Submerged GSC Structures", ENGINEER - The Institution of Engineers, Sri Lanka, Volume XXXXV, No. 04, pp. [31 - 40], 2012
- 8) Wu, F.C., Shen, H.W. and Chou, Y.J., "Variation of Roughness Coefficients for Unsubmerged and Submerged Vegetation", Journal of Hydraulic Engineering, pp. [934-942], 1999

[Back to table of contents](#)

A STUDY ON ARTIFICIAL FLOOD OF GUWAHATI CITY AND ITS MITIGATION

BHASKAR JYOTI HALOIⁱ⁾, ABHINAV BORAⁱⁱ⁾ & NAIRITA SARMAⁱⁱⁱ⁾

i) UG Student, Department of Civil Engineering, Assam Engineering College, Jalukbari, Guwahati, 781013-2016, India

ii) UG Student, Department of Civil Engineering, Assam Engineering College, Jalukbari, Guwahati, 781013-2016, India

iii) UG Student, Department of Civil Engineering, Assam Engineering College, Jalukbari, Guwahati, 781013-2016, India

ABSTRACT

This paper considers problems associated with the artificial flooding in Guwahati, the capital city of Assam and the Gateway of North East India and also tries to give some remedies to mitigate this problem. Two or three heavy rainfalls in a day in the city can cause severe flooding which enhances the creation of water logging and traffic congestion. Guwahati, an unplanned city where buildings, markets and many other constructions are built not only here and there but also on top of the hills by cutting earth in the hillocks. Besides, the poor flood management planning, technically lower standard drainage system, dumping of garbages in drains and blocking of natural drainages result in the failure of draining out the rain water from the heart of the city. This paper intends to show some methodologies and new technologies through which we can control or prevent the artificial flood upto a certain extent in Guwahati city. As such the methodologies like underground piping and pumping system which can easily carry the excess water from the flood affected area upto some big water bodies like river Brahmaputra instead of the normal drainage system; topmix permeable concrete which can soak or absorb upto 600 litres of water per square metre in just one minute; water boring harvesting, through which excess water can be driven into the earth's surface and implementation of some technical rules and regulations or some special Acts, play a handy role in controlling these flood problems.

Keywords: Artificial flood, Guwahati city, causes, remedies, methodologies, flood zone map.

INTRODUCTION

The city of Guwahati lies between the banks of the river Brahmaputra and the foothills of Shillong plateau. The people of Guwahati are afraid of even the slightest of rainfall because after every medium to heavy shower, occurrence of artificial flood is very common. With the rapid increase in population, the development of different construction and marketing sectors have also increased, along with the development of road construction i.e initially we had one way, gradually we developed from one to two and

now two to four and even planning of making four to eight ways. But what about the drainage system? This is a big question because if we don't maintain the development ratio between drainage development and other developments then the Guwahati city is definitely going to face some serious problems like artificial flooding, traffic congestion, inundation etc. Many natural wetlands are dumped for construction purposes,

hills are cut down, deforestation which results in the failure of accumulation of excess water of the city and as a result, the city has to face artificial flood. A thorough study is done on this topic and finally we come across a few new ideas and some new technologies which if implemented, can control or prevent the artificial flood upto a great extent in Guwahati city. The drainage system of Guwahati is not as developed as required considering the population of the city. The drainages are not wide enough and gets easily blocked by garbages and silts. So in lieu of that we can use some special underground pipe fitted with some pumps so as to carry the water without any blockage. Thus through underground piping and pumping we can carry out the excess water from flood affected areas to some near by rivers. If we are unable to carry the excess water to near by rivers then we can take an another technical method i.e water boring harvesting, through which excess water can flow down deep into the different layers of sand under the ground surface. While constructing roads, instead of the normal concrete we can use topmix permeable concrete which is two to three times costlier than ordinary concrete. But this special concrete can soak upto 600 litres of water per square metre in just 1 minute. Moreover Govt. can implement or introduce some new technological acts or laws to solve this problem.

OBJECTIVES

The main objectives of the study are -

- i) To examine the factors responsible for artificial flood in Guwahati city.
- ii) To suggest remedies through technological, social and administrative measure to mitigate the artificial flood problem.

iii) To study some of the highly flood affected areas of Guwahati and suggest some technical laws to be implemented by the Government to control this problem in those areas.

STUDY AREA

Guwahati city is located at 26.1445°N latitude and 91.7362°E longitude. Our study is going to confine within three areas, viz., (i) Anil Nagar and Nabin Nagar, (ii) Lakhimi Nagar and Sewali Path and (iii) Zoo road area. Guwahati city experiences a subtropical climate having an average annual temperature of 24.2°C and average rainfall of 1722 lit/m². This city lies at a height of 55-56 m from the mean sea level.

MATERIALS AND METHODOLOGY

Materials

- Pressure pump
- Different diameter of pipes ranging from 1 to 2 m
- Vacuum
- Soak Chamber
- Soak Chamber materials(like sand, stone, net, coal etc.)
- Topmix permeable concrete
- Underground pipe filter
- Guwahati area zone map

Methodology

The methodology adopted to study the mitigation of artificial flood in Guwahati city are illustrated below-

- **Underground piping and pumping system**

In this methodology, at first the excess rain water is soaked by the soak chamber and then by using pressure pump, the water is

pushed through the underground pipes and carry them directly into nearby river.

- **Water boring harvesting**

In the areas where excess water cannot be drained off to nearby river, we use the methodology of water boring in which the excess water flows deep into the ground surface through different layers of sand.

- **Topmix permeable concrete**

By using this methodology, we can reduce artificial flooding to a great extent as it can soak upto 600 litres of water per square metre in just 1 minute.

RESULTS AND DISCUSSION

In this paper, after thorough research of our confined areas, we mainly came across three technical methods. Generally, the methods which are implemented to mitigate the flood problem must be economical, more efficient and having fast workability with respect to time. Considering the drainage systems, it is seen that a huge amount of money is spent every year to clean the drainages which get blocked very frequently due to dumping of garbages and deposition of silts and as such their workability is reduced. At the same time the drains are not sufficiently wide enough. So instead of spending huge amount of money every year, Government can implement some technical methods which have longer durability and high efficiency as compared to the ordinary drainage systems. As such the idea of underground piping and pumping system came to our mind. In this methodology, we will use pipes of diameter in between 1 to 2 metres and after an interval of certain distance we provide some soak chambers which will behave as the inlet of the pipe and

through which excess water will enter. 60% of the soak chamber is filled by 3 different layers of materials- coal, stone and sand. On the periphery and bottom surface of the chamber, we provide some nets so that garbages, polythenes, silts cannot pass through the pipes. By using a vacuum pump, we can easily sucked up the residual garbages from the chamber. During slight rainfall, there is a provision of closing the periphery net and then 100% water will undergo the filtration process and finally enter the pipes through the bottom net. But during heavy rainfall, the periphery net will work. Then 60% of the water will go through the periphery net while 40% will go through the bottom net. In this system, we will use a pressure pump connected to the pipe which will help the water to flow through the pipe with ease and without stopping. We can implement this method in our study area (iii) Zoo road area. It carries the water through Bharalu and falls into the river Brahmaputra. Figure 1 shows a part of the Underground piping and pumping system set up designed completely by us.

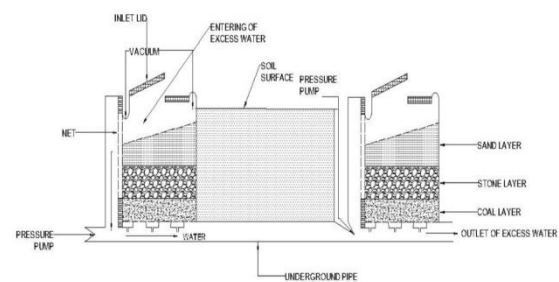


Fig. 1. Underground piping and pumping system

Now considering our second study area, i.e. (ii) Lakhiminagar and Sewali Path, the river Brahmaputra is too far away from this area. The condition of drainage system in Guwahati is very pathetic. In most of our study areas, people use drainages to dump the garbages and waste materials which results in the blockage of free

flow of water through the drains. So by using the drainage system it is not possible to carry the excess water upto the river Brahmaputra mainly because of the reason mentioned above and also the distance factor. Moreover, if we use our first technical method, i.e. underground piping and pumping system in this area, it will neither be too economical nor too efficient. Henceforth we can implement here our second technical method, i.e. the water boring harvesting system. In this methodology, we use the same soak chambers which we used in our first methodology. But instead of the pipe we just use the water boring. Boring is done upto 500-700 feet. In between this limit, we provide some filters as we find sand layer, so that excess water from the ground surface will enter through this boring and gets absorbed in these sand layers. A water boring costs Rs. 4 to 5 lakhs. Figure 2 shows how excess water can be drained out through water boring harvesting system.

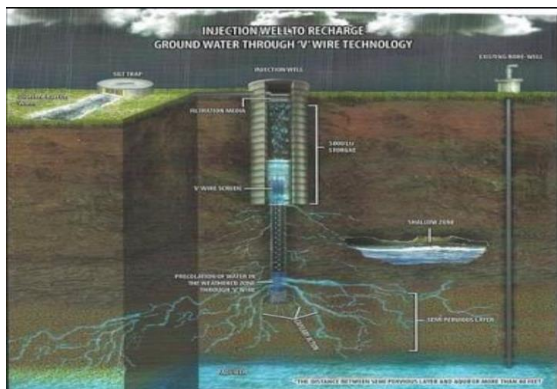


Fig. 2. Water boring harvesting system

We came across one more technical methodology i.e. the use of topmix permeable concrete. In this methodology we use a special kind of concrete called topmix permeable concrete for constructing roads instead of normal concrete roads. This concrete has a special capacity of soaking or absorbing upto 600 litres of water per square metre in just one

minute. This type of concrete is 2 to 3 times costlier than the normal concrete. This methodology should be implemented in those areas where we cannot implement our first two methodologies like flyovers, parking areas of shopping mall etc. It has some drawbacks also. The pores in this concrete gradually gets blocked by dirt and very tiny silts. Once it gets damaged, modification is not possible i.e. newly reconstruction has to be done. Otherwise it is one of the best excess rain water absorbent. Thus this concrete plays a very important role in soaking the excess water and thereby reducing the artificial flood of the city. Figure 3 shows the topmix permeable concrete road.



Fig. 3. Topmix permeable concrete

Apart from these methodologies, Government can also introduce and implement some new technical laws and acts which can reduce the impact of artificial flood in the city. For eg. if each and every houses of the particular area , instead of releasing the waste water into the drains on the side of the road, they can use the waste water harvesting system, i.e. a separate water boring of depths 100 to 200 feet in every houses. By doing so the waste water of houses will remain inside their boundary itself. It is not going to affect the drainages of the city and thereby helping the drainage system to carry the excess water more easily. Besides that, the size

of the drainage system should be planned i.e. the width of the drainages should be based on the number of population of the particular area, road condition, amount of average annual rainfall etc. Since Guwahati is a heavy rainfall area, so rain water harvesting is very necessary specially in the case of shopping malls, flats and apartments, big shopping plazas etc. By doing this, we can conserve the rain water for reuse in later period and thereby the rain water does not affect the drainage system. These above mentioned laws and acts can be implemented in our study area (i) Anil Nagar and Nabin Nagar. In this particular area we can implement our second and third methodologies as well.

CONCLUSION

The problem of artificial flood and water logging in Guwahati City is very severe, affecting the general day to day lives of the people. When excess water cannot be drained off after a heavy shower, then it affects the business, commercial and education sectors. The research presented in this paper using the methodologies which we have discussed viz., underground piping and pumping system, boring and topmix permeable concrete, can mitigate the artificial flood problem to a great extent. The study has also focused on the expenditure required for these methods and the Government can implement these methods in those particular areas within their budget.

By proper utilization of technical methods, awareness of the people of the city and specially proper implementation of some special laws and few other methods like rain water harvesting system, the people of Guwahati can see a new scenario of their very own Guwahati city.

ACKNOWLEDGEMENT

The study was carried out by all the three authors as a part of Bachelor of Engineering in the department of Civil Engineering at Assam Engineering College for the session 2014-2018. We would like to express our gratitude to Mr. Pankaj Goswami sir and the entire faculty members of civil department, Assam Engineering College. We are really overwhelmed by the help of Water Resource Department (Govt. of Assam). We extend our heartfelt gratitude to GMDA and Disaster Management Authority of Guwahati. We would also like to thank the head of the pipe industry and special thanks to plumber Prabin Das, Percept drilling company and lastly we would like to express our gratitude to all those who are connected directly or indirectly with our paper and helped in making it a successful one.

REFERENCE

- 1) Barman Plabita and Goswami Dulal C., 2009, *Flood Zone Mapping of Guwahati Municipal Corporation Area using GIS Technology*.
- 2) Baman P. , Sarma B. , Sarma A.K., *A Study on flood hazard mitigation of Guwahati city*.
- 3) Gogoi Lakhimi, December, 2013, *Degradation of Natural Resources and its Impact on Environment: a Study in Guwahati City, Assam , India*.
- 4) https://www.google.co.in/?gfe_rd=cr&ei=tHbtV7XrCcvk8AevkJXQAw#q=topmix+permeable+concrete

Back to table of contents

Improvement of Water Use Efficiency: A Case Study of Sukla Irrigation Project, Assam

Syeda Naznin Sultana ⁱ⁾, Dr. Utpal Kumar Misra ⁱⁱ⁾ and Dr. Uzzal Mani Hazarika ⁱⁱⁱ⁾

i) Student, M.E. 4th Semester, Watershed Management and Flood Control, Assam Engineering College, naznin9165@gmail.com

ii) Associate Professor, Assam Engineering College, Guwahati, Assam, utpal_misra2004@yahoo.com.

iii) Assistant Professor, NERIWALM, Tezpur, Assam, uzzal_hazarika@yahoo.com

ABSTRACT

Water is the most essential commodity for human beings to be alive and so it is very necessary to make proper use of water without wasting it. Irrigation sector is the biggest consumer of water as more than 80% of available water resources in India is being presently utilized for irrigation purposes. However, the average water use efficiency of irrigation projects in the country is assessed to be only of the order of 30 to 35%. In the north eastern region also, performance of the existing irrigation schemes (particularly, the major and medium irrigation schemes) suffer from low water use efficiency, distribution losses, poor operational maintenance and management and non-availability of water in the tail ends. The region has unique geographical, topographical, climatological settings and sociological characteristics, which are also influencing factors of low water use efficiency. Again, water demand for various purposes namely irrigation, drinking, domestic, power, industrial and other uses is increasing day by day leading to severe seasonal stress on water resources in the region. Its scarcity is more pronounced with increasing population and growing needs. In this paper the water use efficiency of the Sukla Irrigation Project is calculated as per methodology given in the guidelines for computing the Water Use Efficiency of the Irrigation Projects, CWC, February 2014. It has also been attempted to analyze the scope of improvement of the water use efficiency of the same. The water use efficiency of the project under existing condition was found to be 33.54%. The results reveal that management interventions of converting unlined canal sections into lined canal sections under practical achievable conditions can improve the conveyance efficiency (a component of water use efficiency) up to 75%. As a result, an amount of about 16 Mm³ water can be saved from which about 2673Ha additional area can be irrigated. With very good level of maintenance the conveyance efficiency can be further enhanced to 95% which will lead to saving of 53 Mm³ of water from which about 8794 Ha of additional area can be irrigated.

Keywords: Water use efficiency, conveyance efficiency, on farm application efficiency, CROPWAT.

1. INTRODUCTION

Irrigation being the main primary input for development of agriculture of any country, it has received its due priority in planning of the development programmes. But the irrigation sector particularly, has not delivered the expected benefit and has posed certain problems of techno-economic, social and environmental nature. This results in a wide gap between irrigation potential creation and utilization. This serious issue has drawn the attention of the water managers which has oriented them towards the basic objective to be achieved for better Water Use Efficiency through various intervention techniques including modernization and rehabilitation, operation and maintenance of irrigation networks, conjunctive use practices and improved on-farm development works like construction of field channels, regulatory structures, land levelling and drainage, rotational system of irrigation distribution and periodical performance evaluation of all these measures, etc.

Again, the irrigation systems due to constant use are subjected to wear and tear, due to which a number of irrigation projects in the country have been operating much below their potential and also the performance of the existing irrigation systems (particularly, the major and medium irrigation schemes) suffer from low Water Use Efficiency, distribution losses, poor operation, maintenance and management and non-availability of water in the tail ends. Thus, it becomes necessary to study the efficiency of the project from time to time so that necessary steps can be taken to improve the performance of the system for maximum production from the command area.

2 IRRIGATION EFFICIENCY

In general, Irrigation Efficiency is the ratio of the amount of water consumed by the crop to the amount of water supplied through irrigation.

The following are the various types of irrigation efficiency:

- i. Water conveyance efficiency.
- ii. Water application efficiency.
- iii. Water use efficiency.
- iv. Water storage efficiency.
- v. Water distribution efficiency and
- vi. Consumptive use efficiency.

3 WATER USE EFFICIENCY

The Central Water Commission, Ministry Of Water Resources, Government of India has provided a guideline for computing the Water Use Efficiency of irrigation projects. CWC, vide the Guideline, carries forward the standardization of the definition of the Water Use Efficiency (W_p) which is broadly divided into the following components:

1. Conveyance Efficiency W_C
2. On Farm Application Efficiency W_F

The overall Water Use Efficiency of the project is

taken as

$$W_P = W_C \times W_F$$

4 DETAILS OF SUKLA IRRIGATION PROJECT

The Sukla Irrigation Project is located in Goreswar in the Baksa district of Assam. Goreswar is a town in the Baksa district, situated in the north bank of the river Brahmaputra, surrounded by Rangia and Baihata. It has its headworks in Naokata village of Goreswar. The command area of the project falls between latitude of $91^{\circ}40'$ and $91^{\circ}51'$ and longitude $26^{\circ}20'$ and $26^{\circ}40'$. It covers around 105 villages. The source of water for the Sukla Irrigation project is the Sukla River. The Gross Command Area of the project is 22842.00 Ha, Culturable Command Area is 18083.80 Ha and the Net Irrigable Area is 17165.99 Ha. With the introduction of this irrigation project it was expected to achieve an increase of 137 % in the cultivated area of the command area.

The Sukla Irrigation Project is a diversion type irrigation project. Its headwork consists of a weir and head regulators. There are two main canals namely D1 and D2. The canal D1 has twelve minor distributaries. The canal D2 has five minor distributaries and four sub minor distributaries. In order to supply water to the fields, pipe outlets are provided in the canals each having a capacity of 1 cumec.

5 IRRIGATION POTENTIAL CREATED AND UTILISED

Although the project was designed to command a gross command area of 22,842 Ha but due to various reasons particularly damage due to floods the actual percentage utilization was quite less. The year wise potential created and potential utilized is shown in the Table 1. It is seen that a very small percentage of the irrigation potential created is being utilised by the farmers. Hence, there is an urgent need to increase the Water Use Efficiency so as to reduce the difference between the irrigation potential created and that utilised.

Table 1: Year wise irrigation potential created and irrigation potential utilized (Source: DPR of Sukla Irrigation Project).

Year	Irrigation potential created X1000 ha	Irrigation potential utilized X1000 ha	% utilization
1978-79	22.842	7.135	30
1979-80	22.842	12.5	53
1980-81	22.842	12.15	51
1981-82	22.842	14.257	60
1982-83	22.842	15.635	66
1983-84	15.635	15.635	100
1984-85	15.635	15.014	96.03
1985-86	15.635	12.702	81.24
1986-87	15.635	14.863	94.15
1987-88	15.635	14.768	94.45
1988-89	15.635	8.565	54.78
1989-90	15.635	3.573	22.8

1990-91	15.635	14.177	90.67
1991-92	15.635	14.98	98.26
1992-93	15.635	15.068	96.37
1993-94	15.724	14.603	92.87
1994-95	15.55	12.434	79.96
1995-96	12.047	10.419	86.49
1996-97	12.098	10.736	88.49
1997-98	12.116	10.052	82.96
1998-99	13.103	8.461	64.57
1999-2000	12.861	10.799	83.95
2000-01	11.976	11.694	97.65
2001-02	11.078	10.381	93.71
2002-03	4.6	3.11	67.61

inflow									
1	2	3	4	5	6	7	8	9	
D1	6.65	25000	0.004	0.344	2.290	4.356	0.655	65.50	
D2	7.49	28000	0.0052	0.298	2.233	5.251	0.701	70.11	
M1D1	0.62	5900	0.0004	0.353	0.219	0.401	0.646	64.61	
M6D1	0.68	6500	0.0005	0.393	0.267	0.412	0.606	60.65	
M9D1	0.28	2000	0.0001	0.434	0.122	0.158	0.565	56.52	
M1D2	0.74	5000	0.0005	0.469	0.347	0.393	0.531	53.06	
M3D2	0.68	3600	0.0003	0.423	0.288	0.392	0.577	57.65	
S2M3D2	0.14	1500	0.0009	0.367	0.051	0.088	0.627	62.70	
Average									61.35

The canals are unlined and hence there is huge seepage loss of the irrigation water. Also the farmers at the head and middle reaches make extensive use of the irrigation water. As a result the farmers at the tail end are not able to get benefits from the project till date because the water gets over even before reaching the tail end.

6 CONVEYANCE EFFICIENCY

The conveyance efficiency reflects the losses in the conveyance system. It mainly depends on the length of the canals, the soil type or permeability of the canal banks and the condition of the canals. While in transit through canals, losses like evaporation, deep percolation, seepage, bund breaks, overtopping of the bunds, runoff in the drain, rat holes in the canal bunds etc. eventually happen. So it is necessary to assess the losses to determine the quantity of water actually delivered to the fields in the project area. The monthly evaporation data have been collected for fourteen years from the DPR of the Sukla Irrigation project and based on that the average monthly evaporation for Kharif, Rabi and Summer season have been calculated. It was found that the average monthly evaporation for Kharif, Rabi and Summer seasons are respectively 65.31mm, 52.02mm and 75.16mm.

Water losses in the canal network have been computed by Inflow-Outflow Method: IS 9452 (Part-II) of 1980. Inflow – Outflow test was carried out in various sections of 8 canals. For the measurement of velocity, current meter conforming to IS 3910 was used. It was a cup – type magnetic water current meter. The current meter revolutions were taken at 0.6d. The depth of the various sections of the canals was measured by using a ranging rod.

On the basis of the data obtained from the Inflow-Outflow method and evaporation data the Conveyance Efficiency has been calculated and found to be 61.35% as shown in Table 2.

Table 2: Calculation of Conveyance Efficiency, W_c

Canal no.	Disc harge at head cume c	Effec tive lengt h m	Evapo- ration loss	Conve yance loss factor, m ³ /Se c per m ³ /Se c of	Total conv eyan ce loss	Deliv ery at chec k point	Ratio of 7/2	Conve yance efficie ncy Col. 8 X 100 %
-----------	---------------------------	----------------------	--------------------	---	-------------------------	---------------------------	--------------	--

7 ON FARM APPLICATION EFFICIENCY

The on farm application efficiency has two components:

- W_{F1} known as water courses/field channels efficiency which accounts for the transit losses.
- W_{F2} known as on field water application efficiency which accounts for the water loss from the field in deep percolation, leaching etc.

$$WF = W_{F1} \times W_{F2}$$

W_{F1} has been determined by the inflow-outflow method and is found to be 61.35%. For determining W_{F2} , various parameters like Reference evapotranspiration, Effective Rainfall, Percolation losses in the fields, Crop Water Requirement and Net Irrigation Requirement have been calculated for two varieties of Salipaddy.

Reference evapotranspiration is calculated using Modified Penman-Monteith method using CROPWAT-8.0 software developed by FAO as shown in Figure 1.

To account for the effect of crop characteristics on crop water requirement, crop coefficients (K_c) are required to relate ET_o with the crop evapotranspiration (ET_{crop}) or consumptive use.

Month	Avg Temp °C	Humidity %	Wind km/day	Sun hours	Rad MJ/m ² /day	ETo mm/day
January	16.7	86	60	10.8	17.7	2.10
February	19.1	73	74	11.4	21.0	2.92
March	23.0	66	96	12.0	24.8	4.24
April	26.0	68	108	12.7	28.0	5.41
May	26.9	79	98	13.3	29.9	5.84
June	28.1	84	84	13.6	30.4	6.11
July	28.7	85	69	13.4	30.0	6.13
August	28.9	85	76	12.9	28.5	5.86
September	28.2	83	72	12.3	25.8	5.17
October	26.1	83	69	11.6	22.0	4.07
November	22.4	83	57	11.0	18.4	2.91
December	18.4	86	57	10.7	16.8	2.16
Average	24.4	80	77	12.1	24.4	4.41

Fig.1: Reference Evapotranspiration, ET_o , in the command area computed using CROPWAT 8.0 software

The four stages of crop development are as follows:-

- 1st stage (nursery and initial) – Germination and initial growth
- 2nd stage (development stage) – From end of initial stage to attainment of effective full ground cover.

- iii. 3rd stage (mid stage) – From attainment of effective full ground cover to time of start of maturing.
- iv. 4th stage (late stage) – From end of mid-season stage until full maturity or harvest.

The values of K_c are fed into the CROPWAT software as shown in Fig. 2 for Salipaddy 1. The process is repeated for Salipaddy 2.

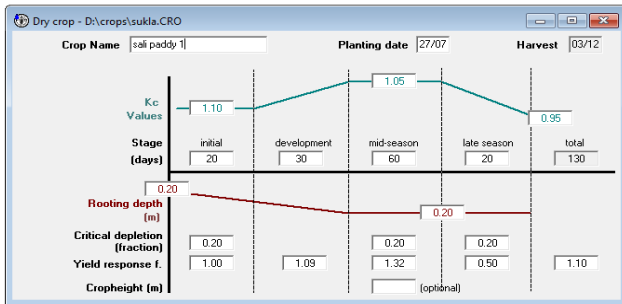


Fig. 2: Window of CROPWAT for feeding the various inputs relating to the crop Salipaddy1.

For the determination of Effective Rainfall, the rainfall data of 26 years of the command area have been collected partially from the DPR of the Sukla Irrigation Project and partially from the Water Resource Department. From these data, the average monthly rainfall has been calculated. These average monthly rainfall values have been input into the CROPWAT software. The effective rainfall is calculated using USDA Soil Conservation Service Method.

Double Ring Infiltrometer Test was performed in the fields in 5 locations to determine the percolation rate and the type of soil. From the results it was seen that the infiltration rates lie between 5 – 10 mm/hour. Therefore, the soil in the command area of the Sukla Irrigation Project is clay loam type.

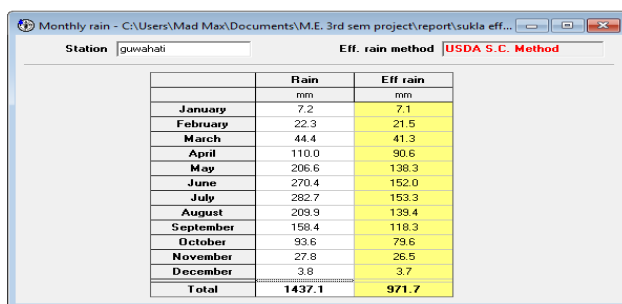


Fig. 3: Effective rainfall (mm) computed by CROPWAT 8.0 software of FAO

The amount of water required to compensate the evapotranspiration loss from the cropped field is defined as crop water requirement. With the help of the parameters like Crop Coefficient, Reference Evapotranspiration, Crop Evapotranspiration, Effective Rainfall and the soil data, the CROPWAT software calculates the Crop Water Requirement as shown in Fig. 4 for Salipaddy 1 and similarly for Salipaddy 2.

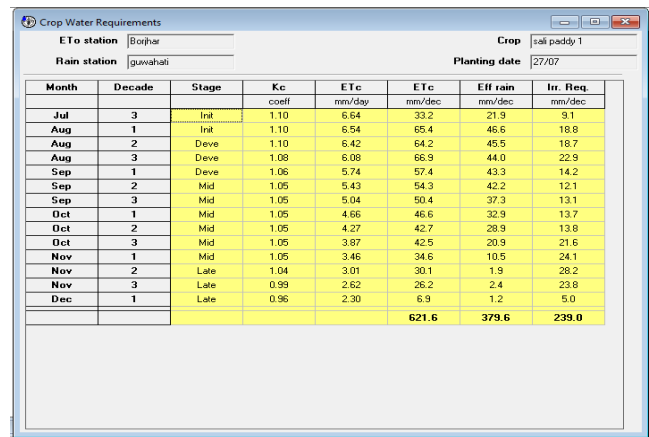


Fig. 4: Crop water requirement for Sali paddy 1.

Net Irrigation Requirement is the amount of water required to bring the soil moisture level in the effective root zone to the field capacity before applying irrigation water. For paddy crop, net irrigation requirement (NIR) is calculated as the amount of water required to meet the crop water requirement plus water required for nursery, land preparation, standing water requirement, percolation losses minus the effective rainfall.

The net irrigation requirement (NIR) has been worked out based on the “Modified Penman Method” as shown in Fig 5 and Fig 6.

$$\text{Therefore, NIR} = \frac{624.6 + 578.5}{2} = 601.55 \text{ mm}$$

$$\text{Now we know that FIR} = \frac{\text{NIR}}{\text{WF1}} = \frac{601.55}{.6135} = 980.19 \text{ mm}$$

$$\text{And WF2} = \frac{\text{FIR}}{\text{Actual supply}} = \frac{980.19}{1100.00} \times 100\% = 89.11\%$$

$$\text{Hence, On Farm Application Efficiency, } W_F = \frac{61.35}{100} \times \frac{89.11}{100} \times 100\% = 54.67\%$$

$$\text{Therefore Water Use Efficiency} = W_C \times W_F = \frac{61.35}{100} \times \frac{54.67}{100} \times 100\% = 33.54\%$$

Thus it is seen that the Water Use Efficiency is very low.

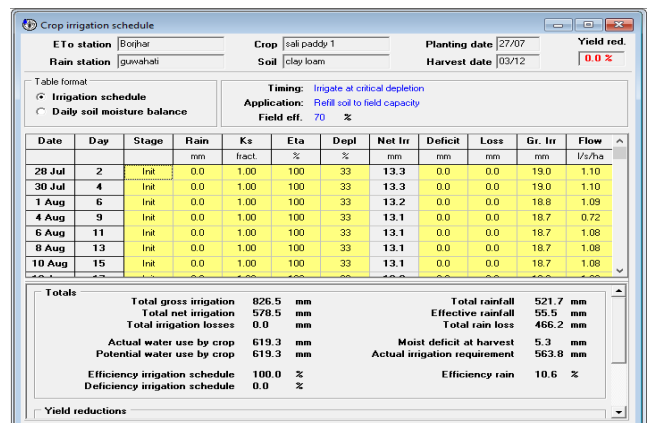


Fig. 5: Net irrigation requirement (NIR) for Sali paddy 1.

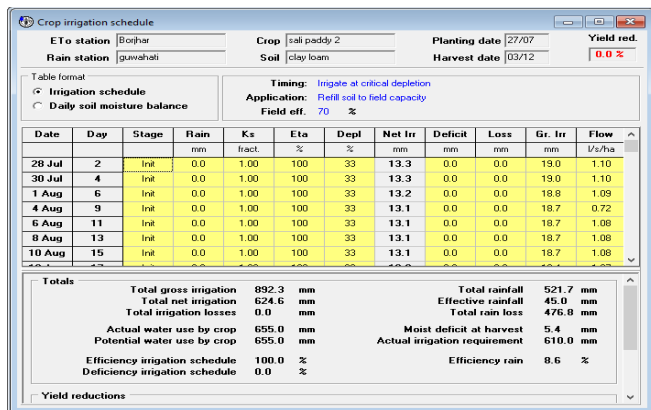


Fig. 6: Net irrigation requirement (NIR) for Sali paddy 2.

8 IMPROVEMENT OF CONVEYANCE EFFICIENCY THROUGH CANAL LINING

The conveyance efficiency of the Sukla Irrigation Project is only 61.35% which is quite low. This is mainly because the canal network is not fully lined and this causes huge seepage losses. The seepage loss in the canals accounts for major portion of water conveyance loss. Now, as per the “Guideline for computing water use efficiency (WUE) of irrigation projects” put forward by CWC, Ministry of Water Resources, Government of India, the Conveyance Efficiency can be improved and can be brought up to at least 75% for fully lined system. If the level of maintenance is very good, this value can be further improved and can be brought up to 95%. Now, if it is considered that the canal network is fully lined, then the seepage loss will reduce to a great extent. The probable water saving and predicted additional area that can be brought under irrigation after converting unlined sections of main canal and field canals into lined sections have been calculated.

As per the study carried out on eight canals, it is observed that a total volume of 16.04Mm³ can be saved if these canals are lined. With the help of this water an additional area of 2672.74 Ha can be irrigated. Apart from lining, if the maintenance level is also very good then 52.76 Mm³ of water can be saved which can irrigate an additional area of 8794.01 Ha. Thus, the tail end of the project, which at present does not receive much benefit from it, can easily be irrigated if the canals are lined.

The increase in the Conveyance Efficiency will also lead to an increase in the Water Use Efficiency.

Thus, it is seen that under practical achievable limits, the Water Use Efficiency can be increased up to 41 % by lining the whole canal network. With very good level of maintenance, it can be increased up to 51.93 %. Thus, the gap between the irrigation potential created and that utilized can be reduced to a great extent. As a result wastage of water can be avoided along with providing irrigation facilities to a larger area.

9 CONCLUSION

The irrigation sector requires better attention in order to achieve optimum water use efficiency and to reduce the gap between the irrigation potential created and irrigation potential utilized. This can be achieved through various intervention techniques including modernization and rehabilitation, operation and maintenance of irrigation networks, conjunctive use, maintenance practices, and improved on-farm development works like construction of field channels, regulatory structures, land levelling and drainage, rotational system of irrigation distribution and periodical performance evaluation of all these measures, etc.

With the introduction of the Sukla Irrigation Project it was expected to achieve an increase of about 137 percent in the cropping pattern of the region. But due to various reasons like poor management and wear and tear of the channels the increase in the cropping pattern is far less than that expected. The Conveyance Efficiency of the project based on the selected eight canals has been found to be 61.35% and the On Farm Application Efficiency is found to be 54.67%. The overall Water Use Efficiency is thus found to be 33.54%.

On the basis of the study done on the eight canals it has been observed that if these canals are lined then 16.04 Mm³ of water can be saved. Also with very good level maintenance along with providing lining, an amount of 52.76 Mm³ of water can be saved. With the help of this water, the tail end of the Sukla Irrigation Project can be easily irrigated.

REFERENCES

- 1) Dr. U. M. Hazarika, Er. R. K. Sinha, (2015): Water Use Efficiency Of Selected Irrigation Projects Of North East: Present Status And Scope Of Improvemnet, *Proceedings of the Assam Water Conference on 6th and 7th February 2015*.
- 2) P.B.Jadhav, R.T.Thokal, M.S.Mane, H.N.Bhange and S.R.Kale (2014): Conveyance Efficiency Improvement through Canal Lining and Yield Increment by Adopting Drip Irrigation in Command Area, *International Journal of Innovative Research in Science, Engineering and Technology*, 120-129.
- 3) Central Water Commission, Ministry of Water Resources, Govt. of India, (2014), Guideline for computing Water Use Efficiency for Irrigation Projects.
- 4) Smajstrla et al., (2010), Efficiencies of Florida Agricultural Irrigation System, *Institute of Food and Agricultural Science (UF/IFAS), Florida*.
- 5) Bhagirath (2007), Year 2007 Declared as Water Year, *Indian Water Resource Quarterly*.

[Back to table of contents](#)

A study of the ground water and drinking water characteristics of Jayanagar and Survey in Guwahati, Assam

A. Archita Borah ⁱ⁾, B. Khyati Manjuri Chaudhury ⁱⁱ⁾ and C. Debangana Sharmah ⁱⁱⁱ⁾

i), ii) & iii) Department of Civil Engineering, Royal School of Engineering and Technology, Gauhati University, Guwahati - 781035, India.

ABSTRACT

The following study is a comparative analysis of the ground water and drinking water of Jayanagar and Survey, two mildly populated residential localities of Guwahati. The main source of water in these two localities is ground water because of the lack of municipality water supply. Hence, the residents assure the safety of drinking water by the use of commercial water purifiers available locally. A total of 8 samples were collected, 4 from each location; out of these, 2 samples were of raw ground water and 2 were purified drinking water. 10 parameters were checked as per the protocols of Standard Methods for Examination of water and wastewater (APHA et al 1975). The study showed stark differences in water characteristics between the two locations. Ground water of survey showed a high turbidity and the pH of the same in both locations was found to be slightly less than neutral. Jayanagar registered a high alkalinity in samples, was slightly hard and showed higher Iron concentration in ground water. Fluoride concentration in the Survey sample was on the higher limits of the permissible value. No nitrate or lead was found in either location. All parameters were found to be safe as per Indian Standard Drinking Water Specification IS 10500:1991 and WHO.

Keywords: Drinking water, ground water, Jayanagar, Survey, Iron, Fluoride

1. INTRODUCTION

The gateway to the Northeast of India, Guwahati is the land of serenity and charm; flanked by the mighty Brahmaputra and picturesque hills and mountains. The city is dependent mainly on the ground water resources for meeting its water needs. Several reports suggest that nearly 69.90% of households depend on groundwater, 27% depend on piped water supply and the rest use surface water mainly from streams. It is therefore essential to ensure that all the natural sources of water are maintained in pristine conditions with no objectionable contamination.

Unfortunately, in recent years, several locations in Guwahati have reported contamination of ground water. A survey conducted by AntoDaya in 2014 showed that out of 4123 samples collected from all over the city; 21 out of 120 showed Fluoride contamination and 5 out of 120 showed Arsenic contamination. Populous localities like Panjabari and Lal Ganesh were reportedly found to record Fluoride and Arsenic contaminated waters respectively.

In Jayanagar, ground water was collected from Narmada Enclave, near N.R.L Petrol Pump, from an underground tank which stored water pumped from 380 ft below the ground. In Survey, the ground water samples were collected from an overhead tank, containing water pumped from 190ft below the ground. Drinking water samples were also collected from both locations. The purifiers used were AquaguardInfiniti

and KutchinaPurica DLX in Jayanagar and Survey respectively. Several tests were then done on both types of samples to check the quality of both ground water and drinking water. Also, a comparison was made between the waters of both the locations to see how water quality may vary between two places located so close to each other.

2 LITERATURE REVIEW

Mahanta et al. (2004) studied the potability of drinking water in 99 tea gardens of Central Assam, for a period of 5 years (1999-2003). 246 samples were checked for chemical quality and 1225 samples for bacteriological quality. Results showed that water was slightly acidic and soft to moderately hard. High Iron concentration in some samples also resulted in higher turbidity; provisions for Iron removal were recommended before use. Other parameters like total solids, total alkalinity as CaCO₃ and chloride were within acceptable limits. Only 228 samples out of 1225 (23.51%) were found satisfactory with 0-10 MPN/100 mL coliform organisms; 428 samples (34.94%) were found free from E.coli organisms.

Sharma et al. (2011) did a similar analysis on ground water quality in selected villages of Nalbari. Several regions around Nalbari had shown high levels of Fluoride, because of which this study was made to ensure that the quality of both ground water and irrigation water is not affected. 40 samples from

handpumps were collected and tested for pH, EC, TDS, Ca^{2+} , Mg^{2+} , Na^+ , K^+ , CO_3^{2-} , HCO_3^- , SO_4^{2-} , Cl^- and F^- . Results showed that the concentration order for cations was $\text{Ca}^{2+} > \text{Mg}^{2+} > \text{Na}^+ > \text{K}^+$ and for anions was $\text{HCO}_3^- > \text{Cl}^- > \text{SO}_4^{2-} > \text{F}^-$. Fluoride was found in the range of 0.02-1.56 mg/L. These samples were also checked for their suitability as irrigation water by examining parameters like Sodium Absorption Ratio, Soluble Sodium Percentage and Kelly's Ratio. All the parameters were found to be acceptable.

Gurjar et al. (2014) did an assessment of ground water in selected areas of Indore, in the month of March and April-2012. The sites were selected to cover the Indore city including residential, commercial, and industrial and agriculture area. Various parameters were studied and compared with the IS specification. Some parameters have been found undesirable in some location, Rest of the sample area has deviation within desirable and undesirable extent of tolerance.

Gajendran et al. (2013) assessed the ground water quality of Tirunelveli District in Tamil Nadu. Samples were obtained from 35 representative wells from rural areas around the district. 16 physiochemical parameters were analyzed. Results showed fantastic correlation between several parameters. TDS could be correlated with Hardness (0.847), Calcium Hardness (0.929), Chloride Hardness (0.971) and Total Hardness (0.929). No such relationships were seen between TDS and CO_3 , HCO_3 and DO.

3 MATERIALS AND METHODS

For sampling, good quality 1L plastic bottles were used. They were cleaned properly with distilled water. There were 2 types of samples that were collected – one was ground water and the other was purified drinking water. Again, for one type of sample, say ground water; one was an acidified sample and the other was non-acidified. For acidified samples, 1 or 2 drops of Nitric Acid was added to the sample after collection. The same was also done for one sample of drinking water. There were a total of 8 samples for analysis.

10 parameters were tested as per the protocols mentioned in Standard Methods for Examination of Water and Waste Water (APHA et al.1975).

The methods of analysis are discussed in Table 1 as follows:

Table 1. Parameters and their methods of analysis

Parameter	Instrument/Method	Materials
Turbidity	Digital Nephelo-Turbidimeter (Systronics 2363)	Stock Primary Standard Formazin Suspension (4000NTU) and Standards of 100 NTU and 50 NTU
pH	Digital pH meter (Labtronics) and Electrode	Standard Buffer Solutions of pH 4 and 7
Alkalinity	Titration	0.02 N H_2SO_4 , Phenolphthalein and Methyl

		Orange
Hardness	Versenate Method	As per the method
Chloride	Mohr's Method	As per the method
Fluoride	Digital Visible Spectrophotometer (Systronics 719) at 570 nm	
Sulfate	Turbidimetric Method	As per Turbidity check
Nitrate	Digital Ultra Violet Spectrophotometer (Varian 50 bio) at 220 nm and 275 nm	Stock Nitrate Solution (0.1mg/L) and intermediate Stock Nitrate Solution (0.01mg/L)
Iron and Lead	Atomic Absorption Spectroscopy (AAS) (Spectra AA,55B)	

4 RESULTS AND DISCUSSIONS

The experimental values of ground water and drinking water from Jayanagar and Survey are shown in Table 2.

Table 2. Experimental values

Parameter	Unit	Jayanagar		Beltola	
		Ground Water	Drinking Water	Ground Water	Drinking Water
Turbidity	NTU	0.4±0.2	0.1±0.1	3±0.1	0.05±0.05
pH		6.88±0.5	7.26±0.4	6.45±0.04	7.01±0.02
Alkalinity	mg/L as CaCO_3	125±1	121±1	104±4	19±1
Hardness	mg/L as CaCO_3	105±4.93	89±5	100±7.57	86±6
Chloride	mg/L	16.59±0.605	17.24±0.75	19.99±0.5	19.195±0.705
Sulfate	mg/L	1.76	3.675±0.03	2.33±0.02	3.705±0.035
Nitrate	mg/L	NIL	NIL	0.889±0.034	NIL
Fluoride	mg/L	0.67±0.0005	0.631	0.974±0.005	0.73±0.001
Iron	mg/L	0.22±0.3	0.7±0.007	0.164±0.021	0.102±0.074
Lead	mg/L	NIL	NIL	NIL	NIL

From the experimental data, it can be seen that the quality of water of Jayanagar and Survey differ from each other greatly. High turbidity was found in ground water of Survey, which on purification reduced to 0.05NTU. Both locations showed a less than neutral pH in ground water. Alkalinity was found to be high in both samples of Jayanagar. Ground water of both locations is slightly hard. Chloride, sulfate and iron levels were quite low. Fluoride concentration in Survey was closer to the upper limit at 0.974 mg/L. No nitrate or lead was found in either location.

After comparing all the parameters with IS 10500:1991 and WHO limits, quality of water is being maintained.

The figures given below draw a comparison between the ground water and drinking water of Jayanagar and Survey. As the legend suggests, the blue bar will indicate water quality of Jayanagar and the red bar, that of Survey.

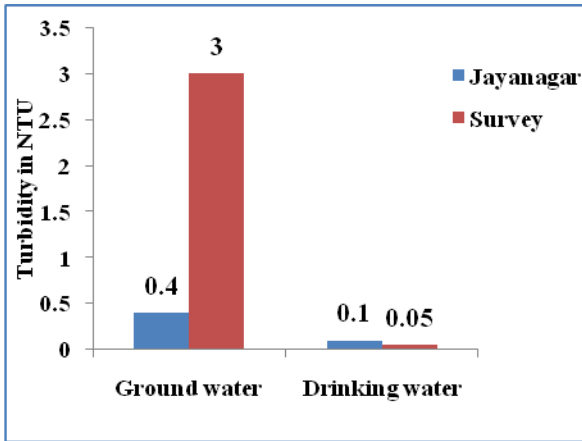


Fig 1. Turbidity (NTU) variation

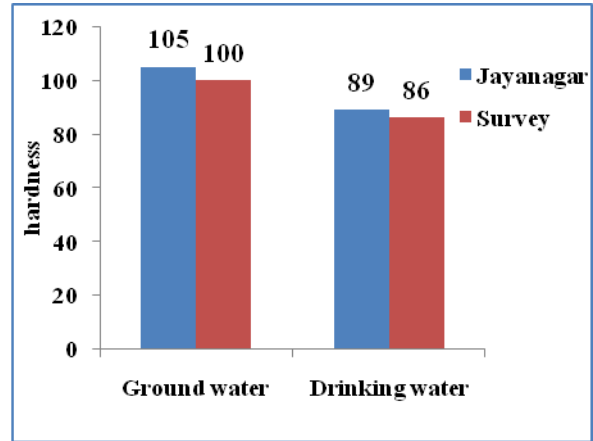


Fig 4. Hardness (mg/L as CaCO₃) variation

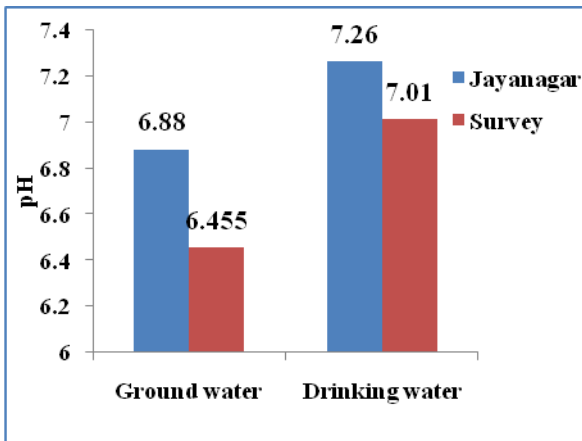


Fig 2. pH variation

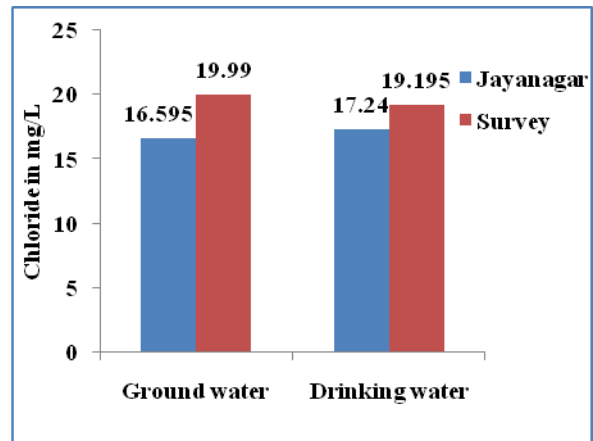


Fig 5. Chloride (mg/L) variation

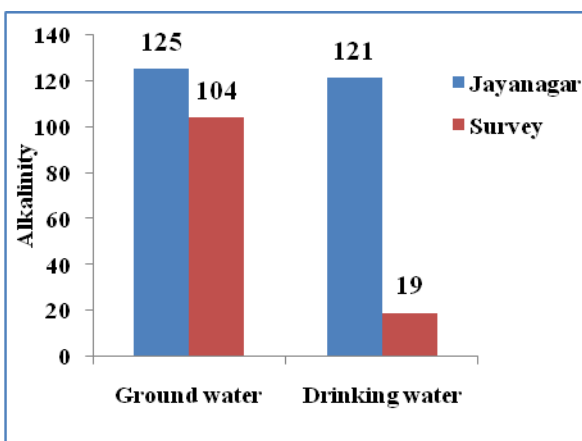


Fig 3. Alkalinity (mg/L as CaCO₃) variation

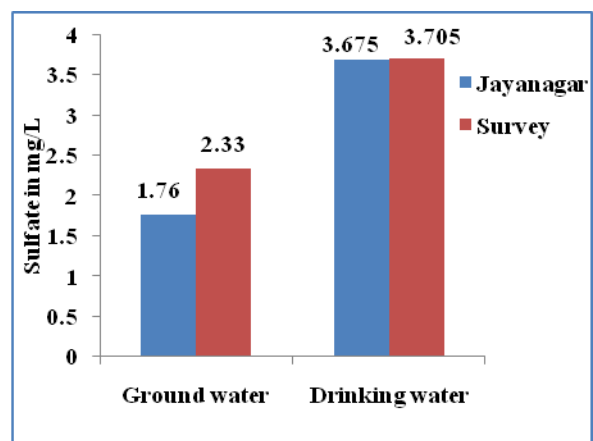


Fig 6. Sulfate (mg/L) variation

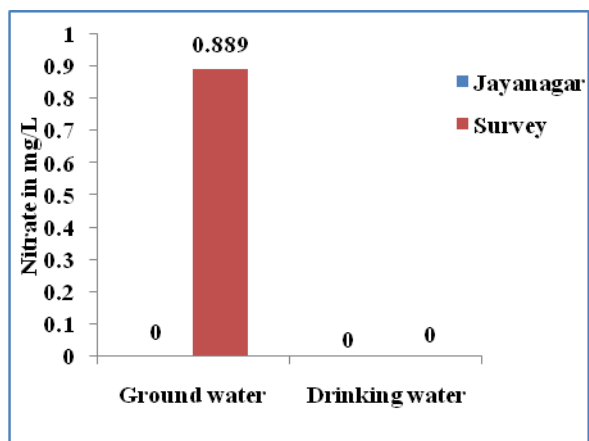


Fig 7. Nitrate (mg/L) variation

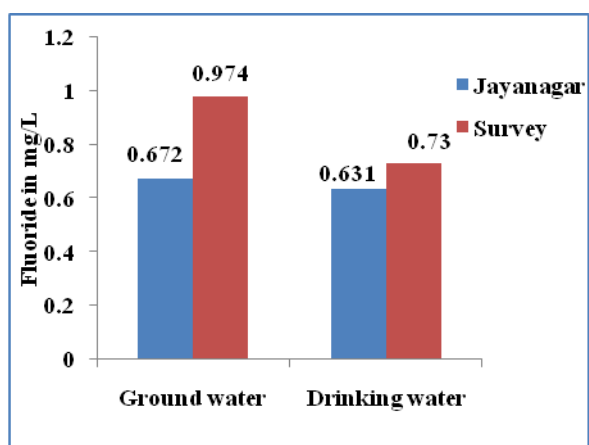


Fig 8. Fluoride (mg/L) variation

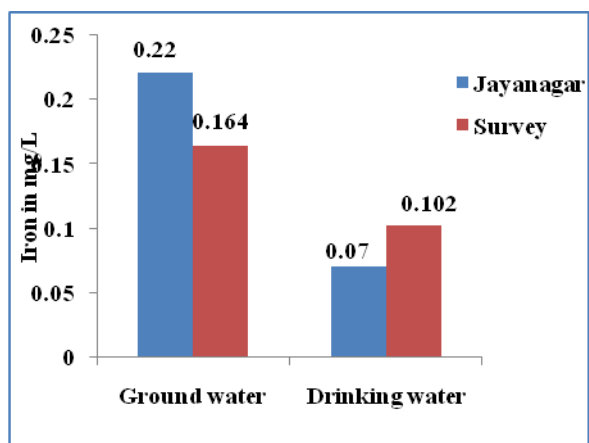


Fig 9. Iron (mg/L) variation

6 CONCLUSIONS

The ground water and drinking water quality of the two locations under study i.e Jayanagar and Survey was found to be quite good with no objectionable or alarming concentrations of any parameter. Just a slightly high concentration of Fluoride was seen in Survey, which needs some attention. This study was a small survey that took into consideration only two locations. There is a need for more surveys like this, from time to time, to ensure that the water quality of

Guwahati is being maintained at the highest possible level.

REFERENCES

- 1) Duggal K.N., Elements of Environmental Engineering, S Chand and Company Pvt Ltd.
- 2) Gajendran C., Jayapriya S., Yohannan D., Victor O., "Assessment of groundwater quality in Tirunelveli District, Tamil Nadu, India", International Journal of Environmental Sciences Volume 3, No 6, 2013, ISSN 0976 – 4402, 10.6088/ijes.2013030600009
- 3) Gurjat M., Chourney V.R., Dwivedi D., "Physico Chemical Assessment of Groundwater in Indore City", Current World Environment -An International Research Journal of Environmental Science, ISSN: 0973-4929, Online ISSN: 2320-8031, <http://dx.doi.org/10.12944/CWE.8.1.13>
- 4) Indian Standard Drinking Water Specification (First Revision) IS 10500 : 1991 (Reaffirmed 1993)
- 5) Mahanta., Das., Dutta., "Chemical and bacteriological study of drinking of drinking water in tea gardens of Central Assam", Indian Journal of Environmental Protection, Volume 24, No 9, pp. 654-660, 2004.
- 6) Sharma., Sharma., Mahanta., "Evaluation of groundwater quality with emphasis on fluoride concentration in Nalbari district, Assam, Northeast India", Volume 65, DOI 10.1007/s12665-011-1195-5, p. 2147-2159, 2011.
- 7) Standard Limits of Drinking Water as per World health Organization (WHO).

[Back to table of contents](#)

Feasibility Study of Sustainable Green Irrigation by Spiral Tube Water Wheel Pump in Assam

Dhrupad Sarmaⁱ⁾, Dr. Parimal Bakul Baruaⁱⁱ⁾, Biju Gogoiⁱⁱⁱ⁾, Khiren Kachariⁱⁱⁱ⁾,
Kailash Jyoti Saikiaⁱⁱⁱ⁾ and Prakash Miliⁱⁱⁱ⁾

i) Guest Faculty, ii) Prof. and Head, iii) B.E. Student
Mechanical Engineering Department, Jorhat Engineering College, Jorhat-785007

ABSTRACT

Sustainable irrigation at low cost and without hampering the environment is a challenge to today's engineering community. A solution to the problem seems to be a spiral tube water wheel pump, which extracts energy by a water wheel, from flowing river and then with the help of a spiral tube water pump, delivers water to the nearby paddy fields. The system is simple in construction and all the parts can be made locally. Many researchers have tested such systems in the past and reported its satisfactory operation. To verify the operational viability of spiral tube water wheel pump in Assam, in the current project a prototype pump has been designed, constructed and tested in the bank of the Bhogdoi river, near Jorhat Engineering College, Jorhat. The constructed prototype having a 3 m water wheel and 1.5 m spiral pump wheel in diameter, found to pump water 4.674 l/min at 18 ft. delivery head. At 9 ft. and 0.5 ft. delivery head, the water flow is found to be 7.5 l/min and 17.94 l/min respectively. It has been noticed that after 18 ft. delivery head, the water flow greatly reduces and practically ceases at 22 ft. During experimentation the water flow velocity of Bhogdoi river was 0.5 m/sec. From the experimentation it can be concluded that spiral tube water wheel pump is a viable solution for sustainable green irrigation in Assam.

Keywords: sustainable green irrigation, spiral tube water wheel pump, spiral tube pump design.

1. INTRODUCTION

Water is used in almost anything and everything we do in our everyday life. From household activities to industries and to irrigation, abundant water supply is essential. Human race has committed considerable amount of its resources and time to solve this problem since ancient times. Ancient example of water wheel can be found in Rome - the vertical water wheel built by Roman engineer Vitruvius (31 BC 14AD). In 31 AD the Chinese engineer Tu Shih invented a water wheel powered reciprocator for casting agricultural tools (Hansen, 2016 [5]). Initially though these designs were used for producing mechanical power, later they were also used for irrigation purpose. In this arrangement small buckets were fitted in the rim of large water wheels. When the wheel rotates these buckets collect water and as it reaches the top, spill the water over into the channels which irrigated the land further away. The height to which water can be lifted in this system is dependent on the diameter of the water wheel.

With the advent of new technologies like I.C. engine and Electric motor, new water pumping systems come to play a major role in small area irrigation. Dams placed on strategic part of a river

also have been playing a major role in huge area irrigation along with electricity generation. But due to their adverse effect on environment, a sustainable green irrigation alternative is being searched to fully or partially replace the conventional irrigation system. One major candidate for sustainable green local area irrigation seems to be Spiral Tube Water Wheel pump. In this system a rotating coil of pipe is used to pump water to a delivery height. Spiral pump was invented in 1746 by H. A. Wirtz, of Switzerland (Tailer, 1990 [2]). The main advantage of this pump is that it requires very low rpm (in the order of 5 to 20 rpm), which makes it particularly suited to be driven by a water wheel (paddle wheel). Another advantage of this system is that it can be made from locally available general construction material without needing any special machinery. A typical Spiral Tube Water Wheel pump is shown in Fig. 1.

As it can be seen in Fig.1 Spiral Water Wheel pump consists of a spiral coil of pipe. To the outer end of this pipe a scoop is attached and the inner end is connected to the hollow shaft. The volume of the scoop is kept approximately one half the volume of the outer most coil. When the pump rotates, the scoop collects water approximately one half the volume of

the outer most coil on each revolution and the remaining half volume of the outer coil is occupied by

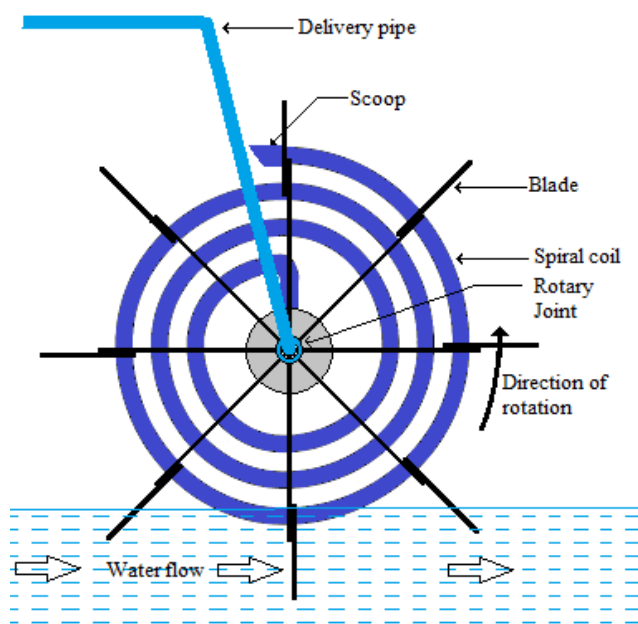


Fig. 1. A typical Spiral Tube Water Wheel pump (without support structure).

air, forming a core of water and a core of air inside the coil. Water being heavier tries to occupy the bottom portion of the coil and pushes air to the upper portion. As the coil rotates further, due to spiral shape of the coil both the water core and air core get transferred to the next inner coil. The volume left by the water core in the outermost coil is occupied by air from outside, as now the scoop is out of water. When the core of water and air get transferred to the next inner coil, due to subsequent reduction in coil volume the air core is get compressed by the water core (water being incompressible) and pressure rises. This way each subsequent coil adds up pressure and when water reaches the inner end of the coil it get discharged to the delivery pipe via hollow shaft at high pressure (Morgan, 1984 [1]).

Many researchers have tested such systems in the past and reported its satisfactory operation. **Morgan (1984)[1]** built and tested a spiral water wheel pump having wheel diameter 4 m, 16 paddles and 3 spiral coils of 50 mm diameter. The reported delivery flow of the pump is 3679 l/hr at a delivery height 8 m, while the water velocity in the canal was 1 m/s and the wheel was rotating at 3.21 rpm. It is stated that delivery head of the pump depends on number of coils in the spiral tube and is approximately equal to multiplication of the wheel diameter and number of coils. **Tailer (1990) [2]** has developed the mathematical formulations to calculate the number of coils required for a given head and presented various theoretical as well as practical aspects related to spiral coil pump. Tailer constructed a spiral water wheel pump having wheel diameter 160 feet (48.77 m) and

experimentally evaluated the effect of wheel rpm, scoop size and spiral coil pipe diameter on pump performance. It is concluded that at low rpm spiral coil pump acts as a positive displacement pump. With the increase in rpm water flow increases but after a certain rpm limit due to blow back affect water flow ceases. This phenomenon is more dominant with smaller pipe size. At high rpm, efficiency increases with increase in pipe size. The optimum scoop volume is the half volume of the outer coil. The optimized pump with spiral coil made of flexible polyethylene pipe having 1-1/4 inch (31.75 mm) inside diameter is able to pump 3,900 gallons/day (14,763 l/day) of water to a 40 feet (12.19 m) head with a peripheral speed of the wheel being 3 feet/s (0.91 m/s). **Thompson, et al. (2011) [3]** presented the design and construction of a water wheel spiral coil pump at Zambia river to provide 30 l/min of water to a distance of 30 m and at an elevation of 10 meters above the river. The pump has been reported to function up to two months without requiring any maintenance. **Yelguntar, et al. (2014) [4]** presented the working principle, functioning and design calculations of the horizontal axis type water wheel. The designed prototype could produce 35 watt power with the help of 1.10 diameter wheel having 8 blades.

From the above literature survey it is quite evident that Spiral Water Wheel pump has the potential to replace conventional water pumping systems in local area irrigation wherever there is a flowing water stream nearby.

Assam being an agricultural state having a large number of rivers, this water pumping system seems to particularly suit for fulfilling the irrigation need of our farmer. Therefore the main objective of this project work is set to study the operational feasibility of Spiral Water Wheel pump in Assam for irrigation purpose. A Spiral Water Wheel pump has been designed and constructed with the help of various data obtained from previous works on this field. The constructed pump is installed at the bank of Bhogdoi river and performance analysis have been carried out.

2. PRELIMINARY DESIGN CALCULATIONS & CONSTRUCTION DETAILS

In designing a water wheel, water velocity plays most important role. So to measure the water velocity and for the installation of the project, a field study was carried out. Proper site is selected on the Bhogdoi River where velocity of water is found highest. The depth of the water is measured by using a five feet long measuring bar at different position. The surface velocity of water was measured by measuring the time taken by a small floating object to cross a length of 1m. The velocity was found to be 0.8 m/sec during

summer i.e. during the rainy season and an average of 0.6 m/sec is considered as the average rainfall tends to change in different seasons. At the installation site average depth of the river was found to be 1.30 m.

The following assumptions are made for designing the pump:

- i. Diameter of Water wheel: 3 m
- ii. Diameter of Spiral wheel: .5 m
- iii. Pump outlet head(maximum): 6.096 m
(20 feet)
- iv. Power produced by the water wheel: 30 W

Instead of conventional single piece design, the pump has been designed having water wheel and spiral pump separately. In conventional design the spiral pump is directly attached to the water wheel. In this design the second approach has been chosen because from past experience it is seen that water velocity in Bhogdoi river changes considerably in different seasons. A single piece design may not be able to lift water in low water velocity. To accommodate this seasonal variation of water velocity the water wheel is connected to the spiral pump by a chain drive, of which gear ratio can be changed manually. The preliminary design calculations & construction details of the important components of the pump is discussed below.

2.1 Water wheel

Power developed by a water wheel is given by (Yelguntwar, et al. 2014 [4]),

$$P_w = (1/2) C_p \rho A v^3 \quad (1)$$

Where,

P_w = power developed by water wheel (30 W)

C_p = coefficient of power (0.8) [4]

ρ = density of water (1000 kg/m³)

A = area of the blade,

v = velocity of the flowing water (0.6m/s)

For the current design the power developed is assumed to be 30 W.

Thus from equation (1), area of the blade found to be,

$$A = 0.347 \text{ m}^2 \approx 0.35 \text{ m}^2$$

Now average depth of the river at the installation site is 1.3 m, but due to sedimentation the depth changes over time and the depth significantly varies over the river bed. Thus Length of the blade (l) and Width of the blade (w) is kept at 0.7 m and 0.5m respectively.

The torque developed by the water wheel significantly depends on the number of blades. But after a certain number of blades, the torque decreases due to blockage of water by the subsequent blade (Yelguntwar, et al. 2014 [4]). Therefore the number of blades should be arranged in such a way that only one blade is fully immersed at a time. Therefore the

number of blades is kept 8.

2.2 Spiral coil

Head in the nth coil (h_n) and number of coil (n) required for a given head is given by (Tailer, 1990 [2]),

$$h_n = (P_{\text{atm}} + D) \times D / (P_{\text{atm}} + H) \quad (2)$$

$$n = 6/5 \{2H / (D + h_n)\} \quad (3)$$

Where,

P_{atm} = atmospheric pressure in water column height (10.3m)

D = spiral wheel or outer coil diameter

H = pump delivery head

For, $D = 1.5$ m, $H = 6.096$ m (20 feet),

Head in the nth coil (h_n) = 1.08 m water column

Number of coil (n) = 5.67 \approx 6

The spiral coil is made from PVC Medium Duty Green Hose pipe (19 mm ID). With 6 coils the pump could only deliver water up to 3.65 m (12 foot) probably due to head losses inside the pipe, joints and in the rotary joint. To compensate these losses another three inner coils have been added in the spiral coil.

The spokes of the water wheel and the spiral wheel are made from Mild Steel (MS) square hollow bars of 25.4 mm \times 25.4 mm size. The blades and flanges are made from MS plate of 2 mm thickness.

2.3 Scoop

The scoop is made from a 101.6 mm (4 inch) hard PVC pipe section whereas the spiral coil is made from PVC hose pipe having 19 mm inner dia. To keep the volume of the scoop one half the volume of the outer coil, length of the scoop is kept at 170 mm (Tailor, 1990 [2]).

2.4 Chain drive

A chain drive has been constructed from bicycle chain sprocket system. For the construction of drive casing angular bar of size 25.4 mm (1 inch) and thickness 3 mm are used.

Table 1. Drive combinations and corresponding velocity ratios of the chain drive.

Drive Combination	Number of teeth		Velocity Ratio
	Driver Sprocket	Driven Sprocket	
1	48	17	2.82:1
2	44	17	2.58:1
3	36	21	1.71:1
4	17	17	1:1

Four drive sprockets of different sizes are attached to the water wheel shaft and four driven sprockets

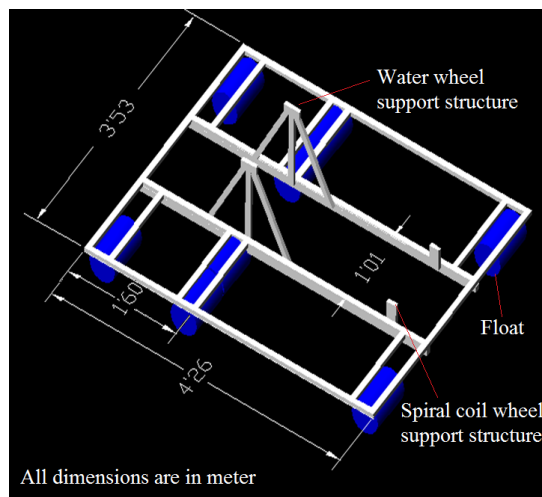
(ratchet sprockets) of different sizes are attached to the spiral pump side shaft, which provide four different velocity ratios to select from. Depending on the water velocity in the river the required velocity ratio could be engaged manually. Table 1 shows various drive combinations and corresponding velocity ratios of the chain drive.

2.5 Raft

The whole system is placed on a wooden raft, which acts as a supporting platform. Another advantage of placing the whole system on raft is that it can keep the submerged area of the blades constant irrespective of the water level in the river. Submerged area of blade greatly affects the power developed by the wheel. The total weight of the components of the Spiral Water Wheel pump and the raft is found around 300 kg. To keep the raft afloat, 8 PVC drums are used in suitable positions of the raft as a float each having a capacity of 55 liters. The wooden raft has been designed keeping in view the dimensions and relative position of the component of the pump. The dimension of the raft and position of the floats is

shown in Fig. 2. CAD drawing of the assembled raft excluding float drums and spiral coil is shown in Fig. 3.

Fig. 2. The dimension of the raft and position of the



floats

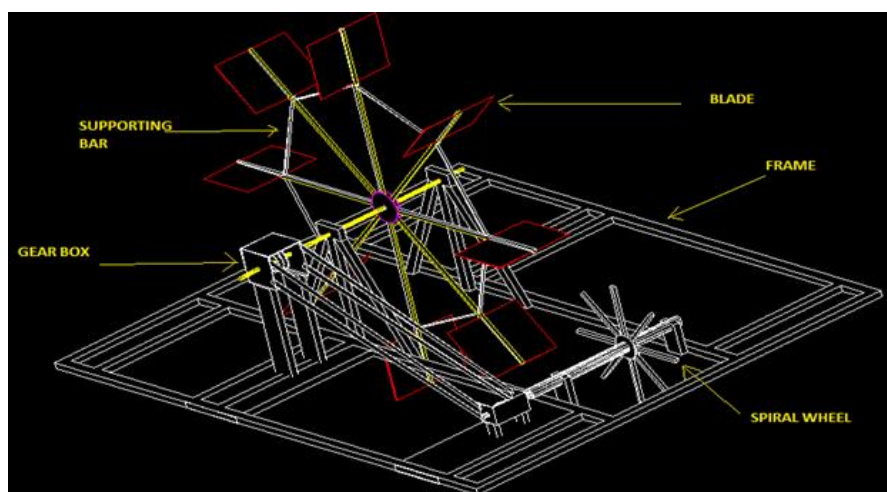


Fig. 3. CAD drawing of the assembled raft excluding float drums and spiral coil.

3. INSTALLATION & PERFORMANCE EVALUATION

The various components of the constructed pump is assembled and installed at the bank of Bhogdoi River (26.75° N, 94.25° S) near Jorhat Engineering College, Jorhat, Assam. After installation the discharge of the pump has been measured at height of 18 feet, 9 feet and 1.5 feet from water level. The static output head (the height at which water just

ceases to flow) is also found out. To measure the discharge at the aforesaid heights, time taken to fill up a 2 Liter jar at those heights has been recorded. During measurement the water flow velocity of the river is also recorded. Fig. 4 shows installation of the pump in Bhogdoi river.



Fig. 4. Installation of the pump in Bhogdoi river.

4. RESULTS & DISCUSSION

It is found that at a height of 6.70 m (22 feet) water just ceases to flow over the pipe. Thus it can be concluded that 6.70 m is the maximum possible height or static output head of the pump. It is also observed that above 5.486 m (18 feet) height water flow is negligible thus at 5.486 m (18 feet), 2.743 m (9 feet) and 0.457 m (1.5 feet) height discharge is measured. Table 2. shows the discharge rate at different head of the outlet.

Table 2. Discharge rate at different head of the outlet.

Head (m)	Jar Volume (l)	Time to fill up the jar (s)	Average Time (s)	Discharge (ml/s)	Discharge (l/min)
	2	24			
5.486	2	27	25.67	77.9	4.674
	2	26			
	2	14			
2.743	2	16	16	125	7.5
	2	18			
	2	5			
0.457	2	8	6.67	299	17.94
	2	7			

It can be seen from Table 2. discharge of the pump decreases with increase in height. This may be due to increase in pumping power required with increase in outlet height (head). Fig. 5 shows the discharge vs. outlet head graph of the pump.

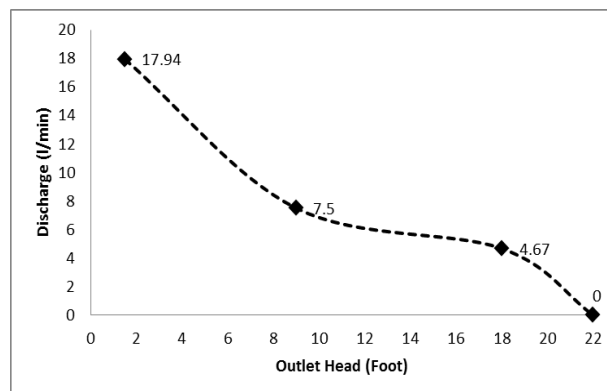


Fig. 5. Discharge vs. outlet head graph of the pump.

During the period of performance evaluation of the pump, the water flow velocity (v) of the river is measured and found to be 0.5 m/s.

Putting $v = 0.5$ m/s, $A = 0.35$ m² in Equation (1), power developed by the waterwheel,

$$P_w = 17.5 \text{ W}$$

Pump work rising Q amount of water to a height h per second is given by,

$$P_p = Q\rho gh \quad (4)$$

Where,

$$Q = \text{Discharge in m}^3/\text{s}$$

$$g = \text{Acceleration due to gravity (9.81 m/s}^2\text{)}$$

From Table 2, at height 5.486 m (h) discharge is 4.674 l/m or 0.0779×10^{-3} m³/s (Q).

From Equation (4) pump work at 5.486 m head:

$$P_p = 4.19 \text{ W}$$

Thus the efficiency of the whole system,

$$\eta = P_p / P_w \quad (5)$$

$$= 0.2394 \text{ or } 23.94 \% \text{ (at 5.486 m head)}$$

5. CONCLUSIONS

From the field testing of the pump, it can be concluded that spiral tube water wheel pump is a viable alternative for sustainable local area irrigation. During the experimentation the pump successfully delivered 4.674 l/min of water at a height of 5.486 m (18 feet) with 23.94% efficiency. The water velocity during that time was 0.5 m/s in the river. However, during the experimentation the following points are observed:

- Pump discharge decreases with the increase in delivery head and this follows until static head is reached.
- Water velocity plays a significant role in the performance of the pump.
- Few more turns of pipe are to be added (in addition to the calculated number of coils for a given head) to the spiral coil to compensate the various pressure losses.
- Loose portions of the spiral coil, may reduce

pump head and efficiency. Thus the spiral coil should be firmly attached to the spiral wheel frame.

REFERENCES

- 1) Morgan, P. (1984): A Spiral Tube Water Wheel Pump, *Blair Research Bulletin*, www. lurkertech.com Link: <http://lurkertech.com/water/pump/morgan/blair/> , accessed on: 01/09/2016.
- 2) Tailer, P. (1990): The Spiral Pump - A High Lift, Slow Turning Pump, www. lurkertech.com, Link: <http://lurkertech.com/water/pump/tailer/>, accessed on: 01/09/2016.
- 3) Thompson, P. L., Milonova, S., Reha, M., Mased, F. and Tromble, I.(2011): Coil Pump Design for a community Fountain in Zambia, *International Journal for service Learning in Engineering* ,6(1), 33-45, ISSN 1555-9033.
- 4) Yelguntwar, P., Bhange, P., Lilhare, Y. and Bahadur, A. (2014): Design, Fabrication & Testing of a Water Wheel for Power Generation in an Open Channel Flow, *International Journal of Research in Engineering & Advanced Technology*, 2(1), ISSN: 2320-8791.
- 5) Hansen, R. D., Water Wheels, www.waterhistory.org, Link: <http://www.waterhistory.org/histories/waterwheels/>, accessed on: 01/09/2016.

Back to table of contents

Precision irrigation- A tool for sustainable management of irrigation water

Arnab Sarma

Professor, Department of Civil Engineering, Royal School of Engineering and Technology
Betkuchi, Guwahati-781035, Assam, India

ABSTRACT

Of all natural resources, water is the most essential and fundamental to all vital processes. It seems abundant at first sight-almost 70% of the earth's surface is covered with water. First of all, the apparently abundant availability of water is misleading. Freshwater- the only usable kind, as far as human needs are concerned-is only a small fraction (2.5%) of the water present on our planet. Further, most of freshwater is in the form of permanent ice and snow or of groundwater which, given its life cycle of several thousand years, must be regarded as unrenewable on a human time scale. In the end only 0.30% of freshwater is renewable. Due mainly to increasing demand of fresh water with agricultural sector as the top consumer water experts over the last few decades have been trying to devise and implement systems for efficiency improvements coupled with judicious use of this scarce resources. New methods are also being planned and developed to meet fresh demands without requiring major new construction or new large-scale water transfers from one basin to the other or from one region to another. Measures are being taken world over in terms of efficiency improvements, implementation of measures for managing water demand and allocating water among stakeholders/users to reduce projected gaps and meet future needs in a sustainable manner. With world population expected to cross nine billion by the year 2050, the connections between available fresh water and food security are receiving increasing attention. This is rightly so because agriculture is by far the largest consumer of fresh water i.e. its water footprint is highest. This paper briefly discusses the various aspects of precision irrigation based on secondary research and strongly advocates further work on Precision Irrigation as part of Precision Agriculture, which is also called satellite farming or Site Specific Crop Management (SSCM). Considerable work on this approach has already been done the world over in recent times. Precision Irrigation in specific and Precision Agriculture in general, demand use of the latest technologies available to address agricultural output vis-à-vis input supply, especially water. As far as Precision Irrigation is concerned, it simply means applying water in the right place with the right amount at the right time. However, the principle to become operational requires a lot of investigation and field experimental work in terms of feasibility and applicability across a range of crops and agro-climatic regions, especially in a country like India. Moreover, the ground data gathering methods, prototype irrigation systems and its components would have to be affordable. In light of this, the next generation in irrigation planning and scheduling would be not just when and how much to irrigate but when, how much and where to irrigate. That is to say that the paradigm shift would be from 'uniform irrigation treatment' as practiced under traditional irrigation approach to 'differential irrigation treatment'.

Keywords: Precision, irrigation, demand, supply, scheduling, efficiency

INTRODUCTION

Of all natural resources, water is the most essential and fundamental to all vital processes. It seems abundant at first sight-almost 70% of the earth's surface is covered with water. However, this is misleading as freshwater is only a small fraction (2.5%) of the water present on earth. Further, most of freshwater is in the form of permanent ice and snow or groundwater with its life cycle of several thousand years. This being the case, it must be regarded as unrenewable on a human time scale. Finally, only 0.30% of freshwater is renewable. Thus, in order to understand the nature of water use issues it becomes incumbent to understand some characteristics of water supply, especially when it comes to agricultural water application and use.

About 40% of the world's population lives in areas with chronic water shortages. Fresh water for the rest too is not entirely adequate in terms of quantity and quality. Quantitative supply and quality problems are also mounting and has the potential to constrain economic growth and human well-being. Maintaining adequate levels of food and water supplies while maintaining the natural resource base and the environment for the present and future generations are two challenges that confront us. Agriculture accounts for roughly 70% of water consumption around the world, according to the United Nations World Water Development Report 2015. This calls for a balance between food production and water supply, the factors at play being growing populations, coupled with changing preferences in diets and rising demand for biofuels.

It is also estimated that about 40% of the fresh-water used for agriculture in developing countries is lost either by evaporation, spills or absorption by deeper layers of soil, beyond the reach of plants' roots (Panchard et al., 2007).

Growing pressure from other sectors (domestic, industrial, municipal, service etc) for fresh water, along with environmental demands, mean that agriculture must obtain "more crops from fewer drops" and that too with less negative impact on the environment. The shift in principle as well as practice therefore would have to be from "yield per hectare of cropped land" to "yield per drop of water used". This is a change with regard to the way we think and also a significant challenge. This on the other hand implies that water management for sustainable crop production will need to be smarter in the context of an ever growing world population, especially in countries like India and China with population of India projected to be 1600 million and that of China stabilizing at 1340 million by 2050.

THE INDIAN SCENARIO

It is evident that food consumption pattern in India over the past two decades has changed drastically owing to factors like urbanization, impact of globalization, income induced diet diversification and changing lifestyle of people from cereals to fruit, vegetables, milk, poultry, fish and meat. Although per capita consumption of food grains has declined over the years, its total demand has been projected to increase due to increase in population and demand from livestock industry. Fruit, vegetables and livestock are more water intensive compared to cereals except rice. This trend is expected to put pressure on our limited water resources. Rainfed agriculture would not be able to meet this demand and more and more areas will have to be brought under irrigation, the current scenario being 55% of area under cultivation is not covered by irrigation.

As of 2016 India accounts for about 18% of the world's population but has only 4% of fresh water resources, which is again characterized by uneven distribution. Therefore, as incomes rise and the need for water rises for reasons cited above, the pressure for efficient and sustainable use of water resources will increase manifold. A country is classified as Water Stressed and Water Scarce if per capita water availability goes below 1700 m³ and 1000 m³, respectively. With about 1544 m³ per capita water availability, India is already a water-stressed country and moving towards becoming a water scarce country should the present trend continue. The principal challenge of irrigation in India can thus be summarized as More Crop Per Drop. While the stress on limited water resources of India is rising; the scarcity is not reflected in its use as estimates point to, at least at this point of time. India uses 2-4 times more water to produce one unit of major food crops

compared to China, Brazil, USA and many other countries. This implies that if India attains water use efficiency of those countries it can save at least half of water presently used for irrigation purposes. At present, irrigation consumes about 84% of total available water followed by industrial (12%) and domestic (4%). With irrigation predicted to remain the dominant user of water for India in coming days, "more crop per drop" is inevitable. The water use efficiency must improve at the same time conserving water.

Expansion of irrigation infrastructure in India started in 1950. The total irrigation potential created from major, medium and minor irrigation schemes has increased from 22.6 Mha during pre-plan period to 113 Mha at the end of 11th Plan. This irrigation potential represents 81% of India's ultimate irrigation potential of 140 Mha. Hence, the scope for further expansion in this regard is limited. The irony however, is that there is considerable gap between the potential created and utilized for various reasons. This calls for efforts to reduce the gap mainly by increasing irrigation efficiencies (currently it is below 40%) first by plugging the existing loopholes and next by adopting smart methods (wherever possible and applicable). This is where Precision Irrigation steps in as the savior.

PRECISION IRRIGATION (PI)

As mentioned earlier, PI is a new and evolving approach. Generally, the drip system of irrigation is regarded as precise irrigation due to its ability to control water application rate and timing. The existing literature on the subject brings up a range of definitions of PI, the major being:

- Applying water in the right place with the right amount (Al-Karadsheh et al., 2002).
- Application of water to a given site in a volume and at a time needed for optimum crop production or other management objective (Camp et al., 2006)
- Irrigation management based on crop need to defined sub-areas of a field referred to as management zones (King et al., 2006).
- Precise application of water to meet specific requirements of individual plants or management units and minimize adverse environmental impact (Raine et al., 2007).

The above definitions indicate towards a common element and that is the 'differential irrigation treatment' of the field as compared to the 'uniform irrigation treatment' adopted under traditional irrigation methods. In essence, this is a high-tech sensor-based irrigation water application method with the required flexibility.

THE PREMISE

It is now accepted that improving the performance of irrigation systems to apply water uniformly over the field has reached such a stage that any further improvements will not increase the profitability of irrigated agriculture significantly. Fertility of land too has limits. The inevitable shift is to concentrate on maximization of net profit from water by applying it at the right time, quantity and place. The reasons for shifting towards the PI approach are as follows.

Internal reasons

- Fields are non-uniform and irrigation needs differ between different parts of a particular field
- The existing irrigation systems apply water at constant rates leading to some areas receiving too much water while others remain deficit.

Driving forces

- Runoff from field and leaching of nutrients and chemicals to groundwater area caused by excessive surface water application.

CHARACTERISTICS OF THE SYSTEM

Optimization of spatial and temporal components of irrigation to ensure optimal performance coupled with crop, water and solute management are the main characteristics of PI. It is not a specific technology per se, but a systems approach that is adaptive and applicable to all irrigation methods and for all crops. The system (s) is able to apply water where needed by saving water and preventing runoff and leaching.

BENEFITS OF PRECISION IRRIGATION

Field trials conducted reveal that PI can increase water application efficiency up to 80-90% compared to 40-45% in surface irrigation methods (Dukes, 2004). It can increase harvestable area and yield, save energy, decrease incidence of disease, minimize inputs (pesticides and fertilizer), reduce leaching and labour cost, improve quality, improve efficiency of water use and ensure desired return of investment.

OPERATIONALIZATION OF A PI SYSTEM

An ideal PI system would have four steps to be made operational viz. data acquisition, interpretation, control and evaluation.

Data acquisition- Data required for PI is to be generated on clear spatial and temporal scales indicating exact soil and crop conditions across the fields. Existing technology (soil-based monitoring, weather-based monitoring, plant sensing and GIS) can be used to measure the various components of the soil-crop-atmosphere continuum in real-time and can provide precise control of irrigation applications.

Interpretation- Data acquired in the previous step is interpreted and analyzed at appropriate scale and frequency. For optimizing irrigation we may use various simulation tools involving crop response.

Control- Due to variable field conditions, the PI system would have the ability to adjust irrigation at appropriate temporal and spatial scales. This can be achieved either by varying the application rate or by varying the application time. Various automatic controllers connected to sensors can be used for accurately/precisely controlling supply of irrigation water to the field.

Evaluation- As in any other irrigation, evaluation forms an integral part of PI system. This is essential to understand the performance of the system adopted in terms of its engineering, agronomic and economic indicators. The feedback received would then form the basis of improving the system.

PRECISION IRRIGATION SCHEDULING

- Scheduling under PI would involve **where, when and how much** to irrigate, the underlying objective is to maximize profit per unit of water used and minimization of energy use.
- As in standard irrigation scheduling the **where and when** to irrigate aspect may be accomplished by measuring soil moisture at specified root-zone depth, the checkbook method and also remote sensing.
- The **how much** to irrigate aspect would have to be based on crop growth stage-wise crop water requirement studies with an objective to replenish the depleted Plant Available Water within the root zone.

SYSTEMS HAVING POTENTIAL FOR PRECISION IRRIGATION

(a) Of all the irrigation systems currently in vogue, the Center Pivot and similar linear-move systems have the maximum potential to be used as precision irrigation systems firstly because of availability of a platform to mount sensors for monitoring of plant and soil conditions in real time and provide input to the decision support system. Secondly, they can be made to interact with a control system for optimal environmental benefits

(b) Drip irrigation system offers PI technology but it represents only a small share of total irrigation, the main reason being high initial investment and to some extent the problem of clogging, limiting its use to mainly high-value crops leaving other important field crops. Gravity flow drip systems appear to hold promise, especially in hilly areas of the country including the north-eastern region.

RESEARCH OPPORTUNITIES

As on date, many tools and technologies for precision irrigation systems are available the world over. However, scope for further research and development is substantial before a precision irrigation system is advocated for the irrigation community across a range of crops, soils and agro-climatic regions. The identified areas on which R & D is required to be undertaken broadly fall into the four categories viz. Integration of Technologies, Technical Feasibility, Economic Viability and Component Technologies. Additionally, for areas where paddy is grown, systematic research is required for development of locally suited PI systems for paddy cultivation. These are discussed here.

Integration of technologies

Integration of component technologies is a major issue for precision irrigation. In this regard, crop and soil sensing is needed to be integrated with appropriate crop growth simulation models so as to provide the base for the seasonal decision making model for all the major crops. The seasonal decision making model in turn is to be combined with the system for the control and optimization of the irrigation application system to make it a complete system. The system can be supplemented by data transmission unit (DTU), wireless radio frequency (RF) module and microcontroller.

Technical feasibility

The technical feasibility of PI is needed to be established both at conceptual and practical levels. Currently used simulation methods can establish the optimum spatial scales for the range of crops and application systems. At the practical level, precision irrigation systems will have to be proven and demonstrated in field trials across a range of crops, soils and agro-climatic zones.

Economic Viability

Studies indicate that there are benefits from adoption of precision irrigation (including location specific irrigation applications). However, it is obscure if the benefits outweigh the costs to warrant the adoption. More work in this regard is necessary across a range of crops, soils and irrigation systems to determine where the maximum benefit can be obtained and investment made. The idea would be to establish a benchmark in terms of either a staged or a full adoption of the system proposed.

In specific, quantifying the costs and benefits of full adoption of the PI system and the resulting agronomic benefits for a range of crops under varied conditions would be an area of high priority. It is also to be proved through sufficient field trials that the

PI system (s) can provide substantially greater benefits than simple automation and/or traditional irrigation methods to justify investment and establish economic viability under various scales of operation.

Component technologies

Needless to mention, development of improved tools/technologies will have to be an on- going process to make the PI system (s) dynamic and evolving. However, immediate needs are felt for sensing and simulation tools for incorporation into the PI system. These are:

- low- cost, spatially- distributed, non- invasive sensing of soil moisture and crop response tools;
- for center pivot and lateral move machines it would be necessary to develop such a sprinkler pattern model that would account for varying sprinkler pressure, height, sprinkler pattern overlap, wind and machine movement with a fair degree of accuracy;
- for drip systems to be used as PI it would be beneficial to develop a hydraulic diagnostic model to deliver spatially varied applications;
- advanced crop simulation models sensitive to small variations in irrigation would be useful
- short range weather radar capable of measuring spatial distribution of rainfall at a sub- field scale would be necessary.

Precision Irrigation for Paddy Cultivation

Rice is the staple food of more than half the world population, which is mostly grown under rainfed conditions and requires enormous quantity of water as compared to other field crops. Despite of water being a scarce commodity, rice production must continue to feed the population on one hand and to employ the rural agrarian population on the other. However, due to increasing demand for fresh water from other competing users water is becoming less and less available for rice. A time has come now where it has become essential for producing rice with less water. This is a formidable challenge and inevitably compels us to go for appropriate precision irrigation technology for food and water security, while maintaining water quality. Even though methods like system of rice intensification (SRI) are available, more sophistication needs to be brought in for producing rice from less water. This argument holds good for the most populous and rice producing and consuming countries like India and China, because both these nations have

already crossed the limit of water stress and are rated as water-scarce countries. In these two countries about 84% of water withdrawal takes place for agriculture, with major emphasis on flooded irrigation for rice. China however has initiated major reforms and is working hard on irrigation efficiency improvement with excellent results. More research and development is necessary by the two countries towards standardizing precision irrigation methods appropriate for growing paddy.

THE STUMBLING BLOCK

A potential stumbling block to the introduction of an effective precision irrigation system is the lack of necessary understanding of the crop production and crop and nutrient management systems. Farmers lack a knowledge-system for anticipating effects of specific irrigation practices or for retrospectively evaluating their irrigation efficiency. Difficulty also arises in identifying the interactions between the various crop inputs, the yield gains, operating constraints and costs. The crop simulation models provide the first step towards identification of optimal strategies and they form an essential part of the real-time decision support system required for precision irrigation. Soil moisture sensors are still neither easy to handle nor reliable and not adapted to all soil types. Lack of low-cost but reliable sensors to measure of crop and soil responses at required spatial scales means that precision irrigation systems will have to rely on simulation for some time to come.

CONCLUSIONS

With increasing water scarcity, there is a growing interest in improving crop water productivity in order to meet the growing global food demand with the limited freshwater resources. The challenge is thus to produce more crops with less water, thus reducing the water footprint per unit of crop produced. Precision irrigation that is intended to synchronize water application with crop water demand gives farmers the ability use irrigation water more effectively ensuring better yield per drop of water used without polluting the environment. Research confirms that precision irrigation is technologically feasible, if not yet economically advantageous. The considerations that might change this conclusion include increased awareness of need for water conservation because of increasing scarcity, drought, increased contention for short water supplies and possible future regulatory actions. The amount of water that could be conserved using precision irrigation remains a research topic. Quantitative estimates of water savings made till date shows that precision irrigation could save from 10 to 15% of the water used in conventional irrigation practice. However, it may be difficult to determine the cost

and benefits of precision irrigation at this stage. Many of the technologies used are in their infancy and the pricing of equipment and services are yet to be standardized to the level that is acceptable to farmers. This may lead to making our economic statements about a particular technology biased and erroneous. Moreover, the concept of “applying the right quantity of water at the right time and at the right place” is to a large extent influenced by intuition. The success of precision irrigation would depend on how well the knowledge needed to guide the new technologies can be found and used. To achieve success in this regard more research, prototype development, adaptive trials and technology synchronization will be required across a range of soil, crop and climatic conditions. Finally, it is not technology alone that will help reduce the blue, green and grey water footprint in crop production; equally important would be a crop production and management system that is fine-tuned with soil nutrient management practice. The other key factors would be synchronization of crop scheduling and rainfall and water harvesting and supplemental irrigation to enhance effective use of rainfall to remain cost effective.

REFERENCES

- 1) Goodwin I, O’Connell MG (2008). The future of irrigated horticulture – world and Australian perspective. *Acta Horticulturae* 792, 449–458.
- 2) Panchard J, Rao S, Prabhakar TV, Jamadagni HS, Hubaux JP (2006). COMMON-Sense net: improved water management for resource-poor farmers via sensor networks. ICTD Conference.
- 3) Arjen Y. Hoekstra, Ashok K. Chapagain (2008). Globalization of water: sharing the planet's freshwater resources, Published Online: 7 APR 2008, Online ISBN: 9780470696224
- 4) Raine SR, Meyer WS, Rassam DW, Hutson JL, Cook FJ (2007) Soil–water and solute movement under precision irrigation: knowledge gaps for managing sustainable root zones. *Irrigation Science* 26: 91–100
- 5) Camp, C. R., Sadler, E.J. and Evans, R.G. (2006) Precision water management: current realities, possibilities and trends. Srinivasan A. (ed) *Handbook of Precision Agriculture*, Food Products Press, Binghamton, NY.
- 6) Al-Karadsheh E., Sourell H., Krause R. (2002): Precision irrigation: new strategy irrigation water management. In: *Conf. Int. Research on Food Security, Natural Resource Management and Rural Development*. Deutscher Tropentag. Witzhausen, 9–11.
- 7) King B.A., Stark J.C., Wall R.W. (2006). Comparison of site-specific and conventional uniform irrigation management for potatoes. *Applied Engineering in Agriculture*, 22:677–688

[Back to table of contents](#)

Flow Characteristics around Bridge Pier

Souryadeep Chakiⁱ⁾ and Prasanna Kr. Khaundⁱⁱ⁾

i) P.G. Student, Department of Civil Engineering, Jorhat Engineering College, Jorhat, Assam-785001, India.

ii) Professor & Head, Department of Civil Engineering, Jorhat Engineering College, Jorhat, Assam-785007, India.

ABSTRACT

In this paper the experimental study on the flow characteristics such as variation of water surface profiles, velocity distributions and change in direction of flow at upstream, downstream and around the bridge pier of two different shapes (viz. Circular & Semi-Elliptical) are presented. In addition, the variation of the pressure exerted at different points on the surface of the pier has also been measured and the key points of the maximum pressure exerted on the surface of the bridge piers are traced out. From the observation of flow characteristics, the zone of possibility of occurring maximum scour are also characterised.

Keywords: Afflux, scouring, drawdown, backwater.

1. INTRODUCTION

Bridge pier acts as the principal supporting component of a bridge having more than one span over which superstructure rest. In many cases the bridge piers constricts the flow of water resulting in an increase in water level at the upstream and simultaneously a drawdown takes place around the pier as well as at the downstream. Due to the backwater effect or afflux, there is a rise in water pressure around the bridge pier which may affect the stability of the pier. Again, due to the drawdown and whirlpool created at the downstream as well as around the pier, scouring may occur on the river bed. Many researchers have studied the flow characteristics. A lots of research work has been done related to this work. Yarnell (1934), studied the obstruction of flow by bridge pier only. He carried out many lab experiments using different shapes as well as different sets of bridge pier for the prediction of backwater. Based on approximately 2600 lab experiments he suggested an empirical formula for the prediction of backwater. Charbeneau and Holley (2001), experimentally studied the flow characteristics and behaviour in sub-critical flow. They used physical pier models of different size but of the same shape i.e. circular shape for their experiments and measured the backwater created using the piers and compared the results with the backwater calculated using Yarnell's empirical formula.

In this paper an experimental study has been made on various flow parameters considering two different shapes of piers (viz. circular and semi-elliptical) in a rigid rectangular channel. The variation of different flow parameters such as water surface profile, velocity distribution across and along the flow direction, at upstream, downstream, and around the pier are expressed in a non-dimensional

form. In addition the pressure variation over the surface of the pier has also been discussed.

2. EXPERIMENTAL SETUP

The experimental works were carried out in a tilting flume in Hydraulic Engineering Laboratory of Jorhat Engineering College, Assam, India. The entire setup is divided into following arrangements

2.1 Tilting flume and pumping arrangement

The tilting flume stands for a rectangular rigid channel made o up of steel with transparent sides of effective length 5m and width of 0.30m. The flume is shown in the Fig. 1. A centrifugal pump (10hp) was used to supply water from a sump to the flume. At the tail end of the flume a sharp crested weir is provided and was calibrated to measure the rate of flow in the flume.



Fig. 1. Tilting Flume

2.2 Pier models

Pier models of two different shapes were used i.e. circular and semi-elliptical. The diameter of the circular pier is 10 cm and height of 40cm. For the semi-elliptical pier the diameter of the two semi-circles is 10cm and c/c distance of the two semi-circles is 8cm. Several pressure tubes were attached over the surface of both the pier at different elevations for measuring the pressure variations over the surface of the pier.



Fig. 2. Circular pier with pressure tubes



Fig. 3. Semi-elliptical pier with pressure tubes



Fig. 4. Circular Pier

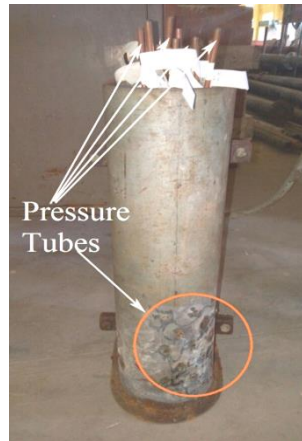


Fig. 5. Semi-elliptical pier

2.3 Manometer

A pitot tube with a U-tube manometer was used for measuring the velocity head at a particular point and for measuring the pressure variation over the surface of the pier a differential multi-manometer was used.

3 EXPERIMENTAL OBSERVATIONS AND DISCUSSION

All experimental observations were carried out separately for two pier models of different shapes as per the arrangement shown in the Fig. 6. To observe the various experimental readings in the transverse direction the various width ratios (b/B) were considered as 0.22, 0.40, 0.60 and 0.78 where, B = Bottom width of the channel and b = Width interval from the right bank. The observations were made at upstream, downstream and around the bridge pier.

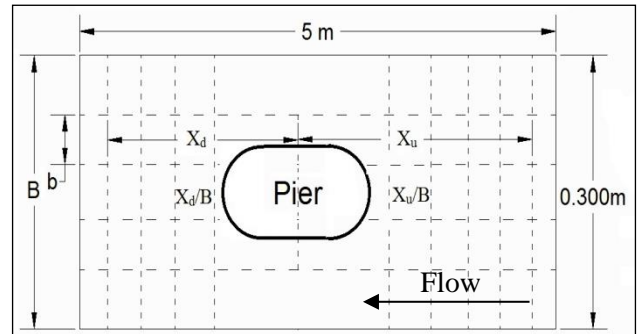


Fig. 6. Arrangement of pier model

3.1 Longitudinal water surface profile

The observations for the longitudinal water surface profile at different width ratios (b/B) = 0.22, 0.40, 0.60, 0.78 are graphically represented in the Fig 7 to Fig. 10 at different flow rates for circular pier as well as semi-elliptical pier.

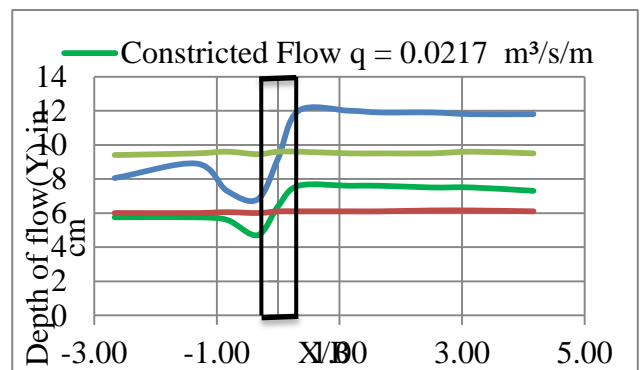


Fig. 7. Longitudinal W.S.P. at $b/B = 0.22$ (Circular Pier)

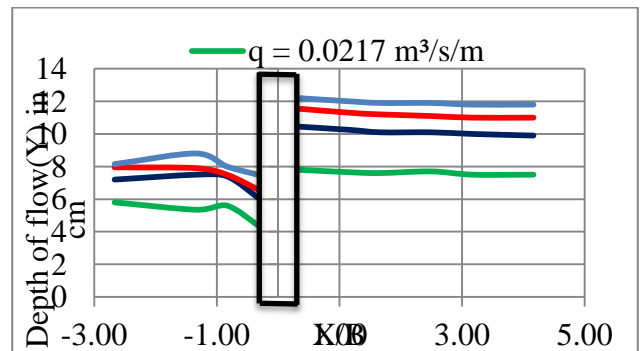


Fig. 8. Longitudinal W.S.P. at $b/B = 0.40$ (Circular pier)

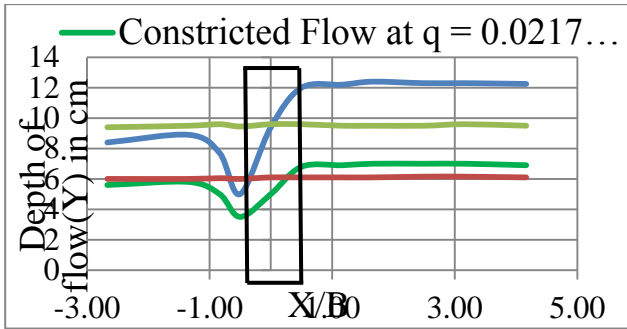


Fig. 9. Longitudinal W.S.P. at $b/B = 0.22$ (Semi-elli Pier)

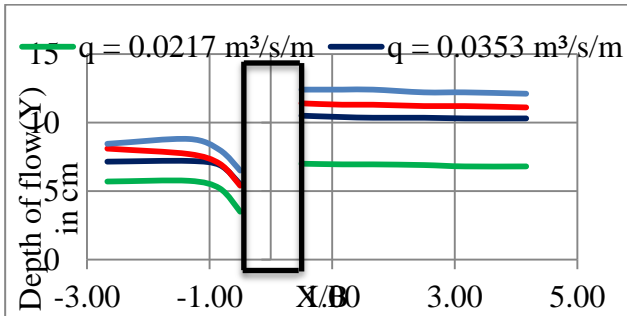


Fig. 10. Longitudinal W.S.P. at $b/B = 0.40$ (Semi-elli Pier)

The observations were made at four flow rates viz. high flow rate ($q = 0.0460 \text{ m}^3/\text{s/m}$), two intermediate flow rates ($q = 0.0353 \text{ m}^3/\text{s/m}$ and $0.0393 \text{ m}^3/\text{s/m}$) and low flow rate ($q = 0.0217 \text{ m}^3/\text{s/m}$). Fig. 7 depicts the longitudinal water surface profile observed at width ratio (b/B) = 0.22 at high flow rate and low flow rate for circular pier. The straight and curved line represents the normal and constricted water surface profile respectively. Fig. 8 represents the longitudinal water surface profile at width ratio (b/B) = 0.40. For semi-elliptical pier Fig. 9 and Fig. 10 depicts the longitudinal water surface profile at same width ratio. It was observed that for both the pier the flow patterns were almost identical. The variations of flow at the upstream were observed to be minimal at the sections away from the pier except a slight increase in depth near the nose of the pier. But at the downstream the minimum depths of flows were observed at the sections close to the pier, irrespective of the rate of flow. Beyond the section where minimum depth was observed, the depth of flow increases abruptly at downstream forming a hydraulic jump.

For both the piers the flow gets divided into two channels around the pier very close to the upstream decreasing the depth of flow with an increase in velocity. Both the flow channels meet just at the downstream of the pier creating a separation zone. The separation zone takes place upto a certain distance beyond which eddy zone develops. In the eddy zone reverse flow occurs due to which the formation of whirlpool and bed scouring may occur. Fig. 11 and Fig.12 depicts the flow condition at the upstream, downstream and around the circular pier and separation length (L_s) from the axis of the pier.

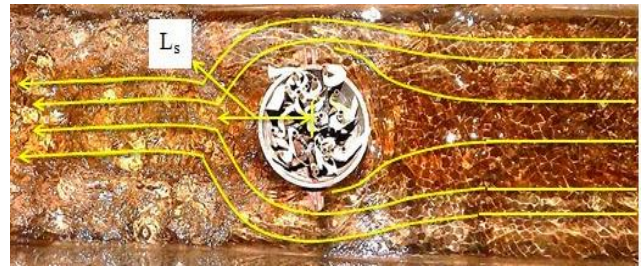


Fig. 11. Separation zone

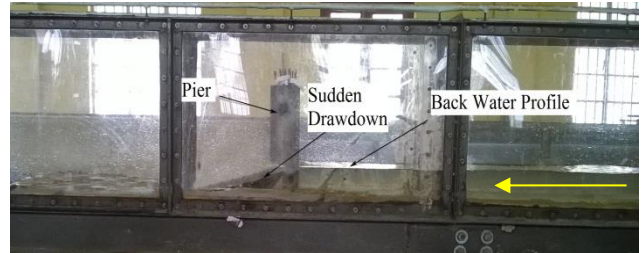


Fig. 12. Water Surface Profile

3.2 Velocity Distribution

The velocity distributions for both circular as well as semi-elliptical pier were observed at various longitudinal as well as transverse sections at the upstream and downstream.

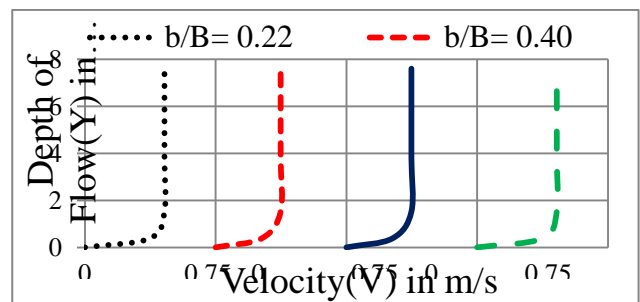


Fig. 13. Velocity distribution at $X_v/B = 1.17$ (circular pier)

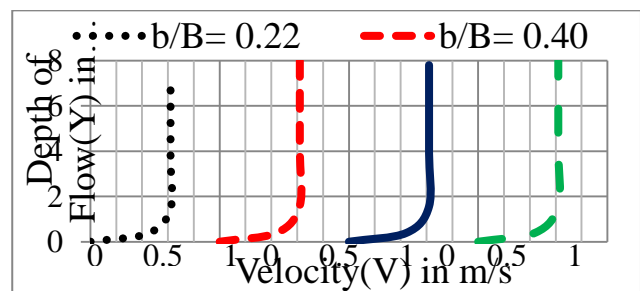


Fig. 14. Velocity distribution at $X_d/B = 0.83$ (circular pier)

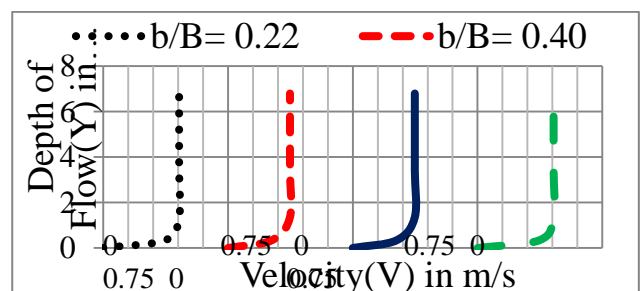


Fig. 15. Velocity distribution at $X_v/B = 1.17$

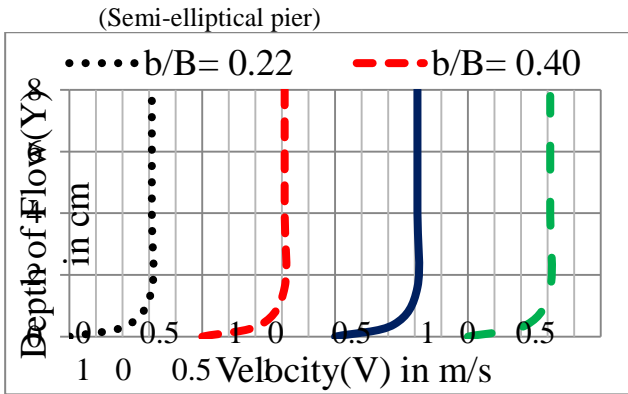


Fig. 16. Velocity distribution at $X_d/B = 0.83$ (Semi-elliptical pier)

It was observed that the variations in velocities were seemed to be quite less at the upstream irrespective of all the flow rates for both the piers. At the upstream there was a reduction in velocity of flow at the central portion, while there was a rise in velocity towards both the sides of the pier. It was observed that at the downstream the flow velocity was found to be negative in the eddy zone and it becomes positive at the further sections. The flow condition at the eddy zone is shown in the Fig. 17 and Fig. 18 for circular pier and semi-elliptical pier respectively.

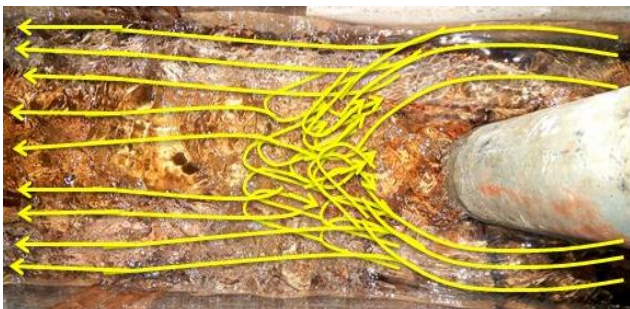


Fig. 17. Eddy zone (circular pier)

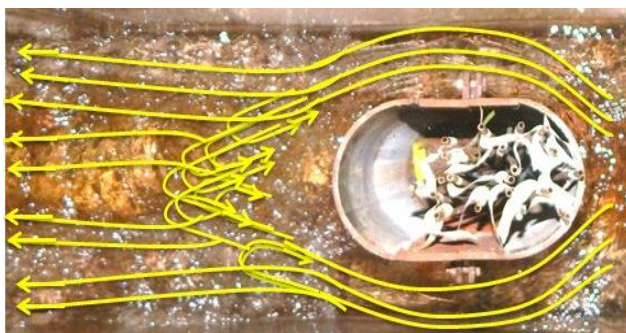


Fig. 18. Eddy zone (Semi-elliptical pier)

To verify the flow condition whether the flow is sub-critical or super-critical in nature Froude's numbers were calculated. Based on the depth of flow and velocity of flow Froude's numbers (Fr) were computed for different non-dimensional locations at the upstream (X_u/B) and downstream (X_d/B). The Froude's numbers are graphically plotted as Fr_u vs. X_u/B and Fr_d vs. X_d/B

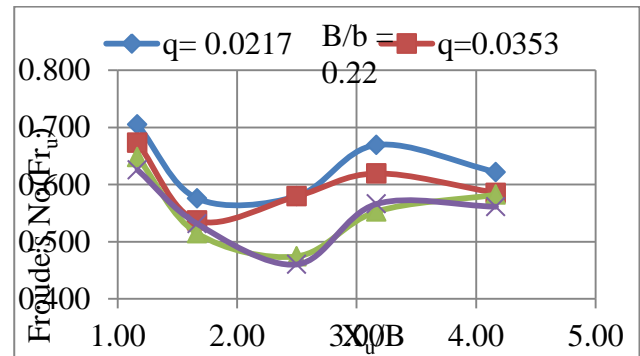


Fig. 19. Variation of Froude's Number (Fr_u) with X_u/B at width ratio (b/B) = 0.22 (Circular Pier)

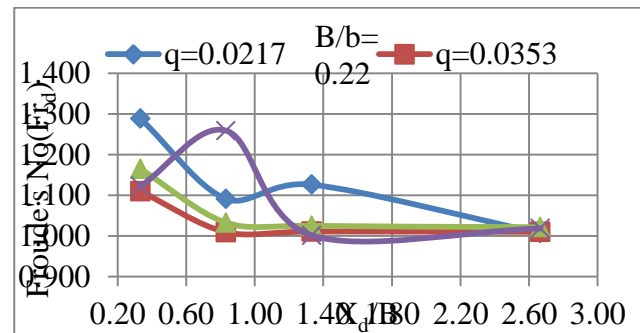


Fig. 20. Variation of Froude's Number (Fr_d) with X_d/B at width ratio (b/B) = 0.22 (Circular Pier)

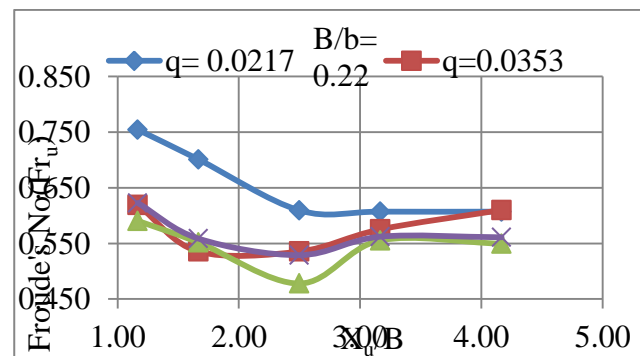


Fig. 21. Variation of Froude's Number (Fr_u) with X_u/B at width ratio (b/B) = 0.22 (Semi-elliptical Pier)

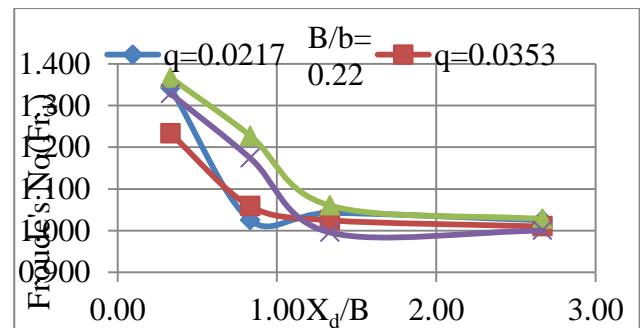


Fig. 22. Variation of Froude's Number (Fr_d) with X_d/B at width ratio (b/B) = 0.22 (Semi-elliptical Pier)

The variations of Froude's number (Fr) at the upstream and downstream at width ratio (b/B) = 0.22 is shown in the Fig. 19 to Fig. 22. It was observed that for all the sections at the upstream the Froude's number

(Fr_u) value ranges from 0.450-0.750 and at the downstream Froude's number (Fr_d) ranges from 0.9 to 1.4, irrespective of all the four flow rates. The flow condition at the upstream section remains sub-critical and at the downstream section the flow remains almost super-critical both the pier.

3.3 Pressure Variation

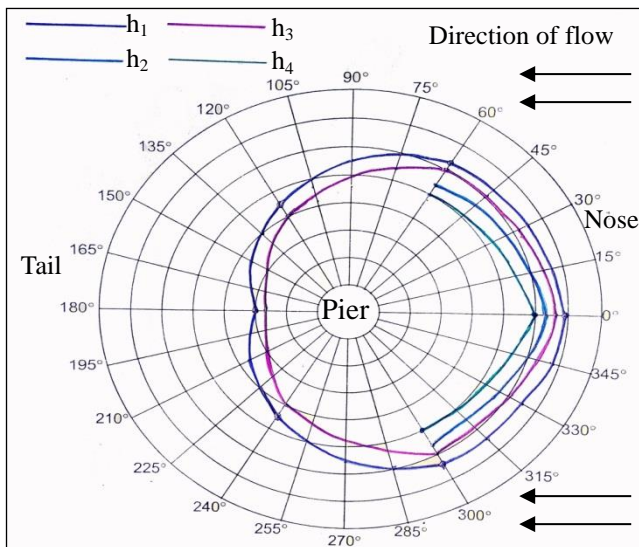


Fig. 23. Pressure variation at $q = 0.0460 \text{ m}^3/\text{m/s}$ (Circular pier)

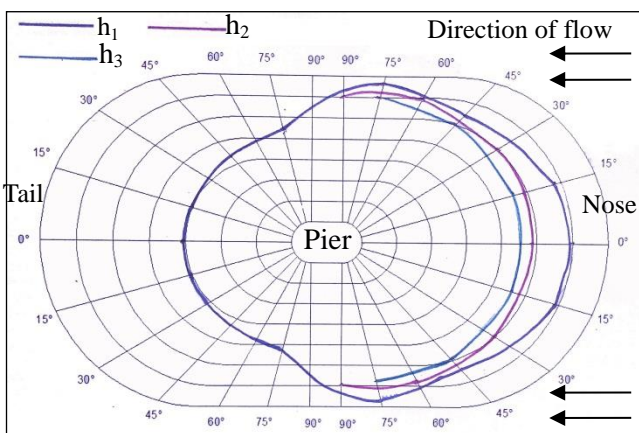


Fig. 24. Pressure variation at $q = 0.0460 \text{ m}^3/\text{m/s}$ (Semi-elliptical pier)

The variation exerted over the various points of the pier surface are measured by means of multi-manometer and graphically represented as shown in the Fig. 23 and Fig. 24. It was observed that the intensity of pressure over the surface of the pier was much more at the upstream face as compared to that of downstream face. For both circular and semi-elliptical pier the maximum pressure occurs at the nose of the pier i.e. at 0° to the direction of flow and the minimum pressure occurs at the rearmost axis of the pier. Pressure at each point over the surface gradually decreases from the bottom towards the free water surface.

4 CONCLUSION

Following conclusions are made from the present study carried out on two different shapes of pier.

- The flow at upstream of the pier is found subcritical in nature and a slight back water curve was observed irrespective of discharge and significant rise in water level takes place due to the obstruction of the pier. On the other hand the flow is found to be supercritical just at the downstream and sudden drawdown from upstream to downstream around the bridge pier.
- For both circular and semielliptical piers, the zone of supercritical flow develops up-to a certain distance behind the pier.
- At the downstream, the separation zone takes place upto a certain distance beyond which eddy zone develops for a certain distance based on the pier diameter and pier interval. There is a possibility of scouring of the river bed in the supercritical zone behind the bridge pier.
- For both circular and semi-elliptical pier the maximum pressure occurs at the nose of the pier i.e. at 0° to the direction of flow and the minimum pressure occurs at the rearmost axis of the pier. Pressure at each point over the surface gradually decreases from the bottom towards the free water surface.

REFERENCES

- 1) El-Alfy, Kassem., (2006), "Experimental study of backwater rise due to bridge piers as flow obstructions", Associate Prof., Irrigation and Hydraulics Dept., Faculty of Engineering, Mansoura University, El-Mansoura, Egypt.
- 2) Suribabu, C.R., Sabarish, R.M., Narasimhan, R., Chandhru, A.R., (2011), "Backwater rise and drag characteristics of bridge pier under sub-critical flow condition", centre for advanced research in environment, school of civil engineering, SASTRA University, Thanjavur-613-401.
- 3) Yarnell, D.L., 1934. "Bridge piers as channel obstructions." Washington, DC: US Department of Agriculture, Report 442, p. 25.
- 4) Mazumder, S.K. and Dhiman Rajni, "Computation of afflux with particular reference to widening of bridges on a roadway", I.C.T. Pvt. Ltd. A-8, Green Park, New Delhi 110 016
- 5) Randall, J. Charbeneau and Edward, R. Holley, October (2001), "Backwater effects of bridge piers in subcritical flow", Project Summary Report 1805-S, Evaluation of the Extent of Backwater Effects of Bridge Piers, Center for Transportation Research, The University of Texas At Austin.
- 6) Chow, Ven Te "Open channel hydraulics", McGraw-Hill, Inc., 1959.

[Back to table of contents](#)

AN EXPERIMENTAL STUDY OF VARIATION IN FLOW PARAMETERS DUE TO THE EFFECT OF SPUR

¹Nishimon Konwar, ²Prasanna Kumar Khaund

¹P.G. Student, ²Professor and Head of Civil Engineering Department,
Jorhat Engineering College, Assam, India.
E-mail: nishimonkonwar@rocketmail.com, prasannakhaund@yahoo.co.in,

ABSTRACT

Spur is a hydraulic structure which diverts the flow of water away from the bank. This paper is purely an experimental study which deals with the variation of flow parameters (water surface profile along longitudinal and transverse direction, velocity distribution) at upstream and downstream and around the spur/spurs. Occurrence of transverse flow, eddy formation and reverse flow etc. are also observed under different flow situations. The dimensions and channel width are all taken in a non-dimensional form. The optimum safe distance of the bank for a single spur is observed in terms of the spur length. In series arrangement of spurs, the spur interval plays an important role in observing the effect of the flow near the flood plains. Different observations are made with various spur intervals with respect to the spur length to obtain the maximum safe spur interval.

Keywords: Eddy Formation, Optimum Safe Distance, and Maximum Safe Spur Interval.

1. INTRODUCTION

Groynes or spurs are river training structures which are constructed in the transverse direction to the direction of flow of water. Spurs are usually constructed to keep the flow in the desired course away from the bank by attracting, deflecting or repelling the flow. Spurs are provided for land reclamation, navigation, and mitigation against soil erosion. Its prime objective being to divert the direction of flow of water. The secondary objective being the silting at the vicinity of the spur. In this light different investigators studied in different ways. Acheson (1968) studied that the ratio of the spur interval to the length of the spur, (L/l) to be 2 - 4 but failed to support a precise standard for the relationship between the space of the groynes and the groyne transmissivity and curvature. Fenwick (1969) classified the space of the groynes according to the purpose of their installation (for example, $L/l = 2 - 2.5$ for flow control and $L/l = 3$ for bank protection). Richardson and Simons (1974) suggested $L/l = 1.5 - 2.0$ and $L/l = 3 - 6$ along the condition of installation (for instance, 4 - 6 for a straight line or a curved groyne with a large radius and 3 - 4 for a curved groyne with a small radius) Copeland (1983) suggested to use L/l not less than 3 for bank line protection. Ahmed H. S *et.al* (2010) found out that the effective distance between the

two symmetrical Groyne(L) is 3 to 4 times of groyne length(l). In this paper for different values of (L/l), variation of flow characteristics is analyzed based on the experimental results and also able to suggest the maximum safe spur interval for bank protection.

2 EXPERIMENTAL APPARATUS AND CASE STUDY

The experiments were conducted in a tilting flume in Hydraulic Engineering Laboratory at Jorhat Engineering College in Assam, India. The flume is 0.6 m in depth, 0.3 m in width and effective length between the centers of the foundation block is 5m. The flood plains of 2.5 m long are attached at the interior edge of the flume keeping the levee side of the flood plain at the slope of 5:1 shown in fig 2. The flow velocity (m/sec) and the water depth Y (m) were measured in the longitudinal and cross sections of the channel. In the present study an impermeable groyne I have been placed at a distance of 1.4 m from the starting point of the effective length of the flume and another groyne II is placed maintaining a spur interval of $L/l=2.5$. The top width of the spur is 0.03m and bottom width 0.13m. the crest length is of 0.05m and bottom length is of 0.07m was used as shown in fig 1. The velocity of flow was

measured along the cross section with a relative width ratio of $b/B=0.36, 0.67, 1$ and 1.31 (where b = distance from the flood plain containing the spur and B = the effective width of the channel) and at a non-dimensional B/X_u and B/X_D from the centre of the groyne (where X_u and X_D are the horizontal distance at the upstream and downstream from the central axis of the groyne along the channel). Similarly, the variation of water surface profile at U/s and D/s were observed

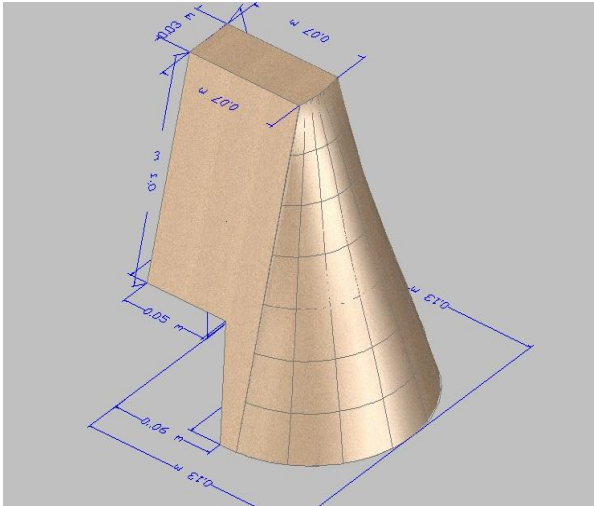


Fig 1: Perspective view of Impermeable Groyne

in various cross section for unit discharge = $0.0661 \text{ m}^3/\text{sec/m}$ (high flow) and $0.0277 \text{ m}^3/\text{sec/m}$ (low flow). The location of formation of eddies and back flow have also been observed. Observations were made on the effect of groyne at the D/s as well as in U/s is studied at various sections in transverse as well as longitudinal

directions at different depth for different discharges and the velocity of flows are measured by means of a pitot tube.

3 OBSERVATION AND DISCUSSIONS

The groynes are arranged in a relative spur interval $(L/l) = 2.5, 3, 3.5$ and 4 for different unit discharges and the observations were made accordingly at the width intervals of $b/B = 0.36, 0.67, 1$, and 1.31 along different relative distances of B/X_u and B/X_D as shown in fig 2. The longitudinal water surface profile in Fig 3 reflects that the variation of water surface profile beyond spur I the water surface ripples can be noted significantly, and the depth of flow reaching minimum beyond spur II. The water depth increases immensely at $b/B=0.36$ as it approaches the spur and the obstructed flow is diverted with high velocity towards opposite bank. The flow depth at $b/B = 0.67$ i.e. the foot of the spur is very low and gradually

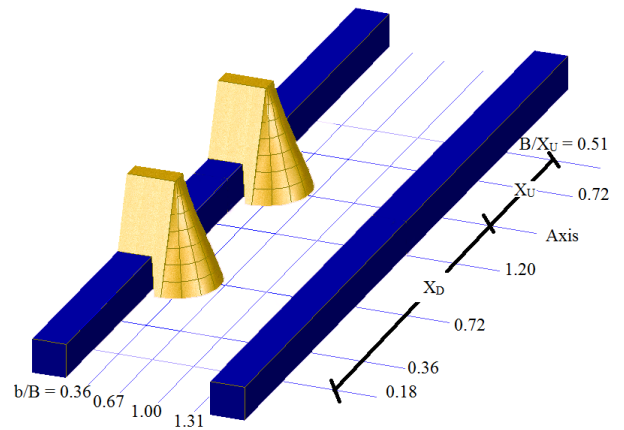


Fig 2: Schematic Diagram of the Arrangement

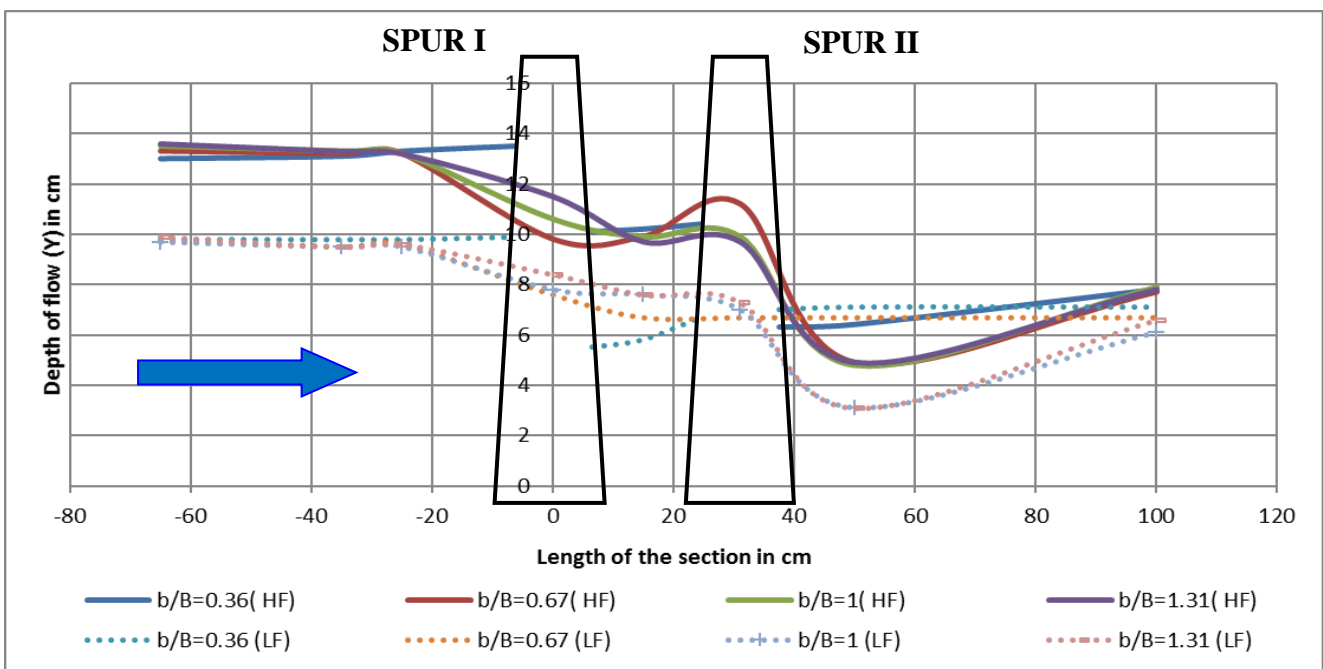


Fig 3: Longitudinal water surface profile for $L/l=2.5$

increases and after some distance it becomes equal to the normal water surface profile. Fig 4 shows the downstream section. The depth of flow at the nose of the spur I is low, so the nose has to face high velocity of flow.

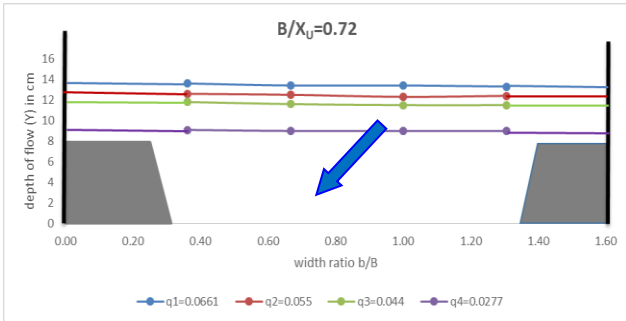


Fig 4: Relationship between depth of flow (Y) and width ratio b/B at $B/X_D=0.72$

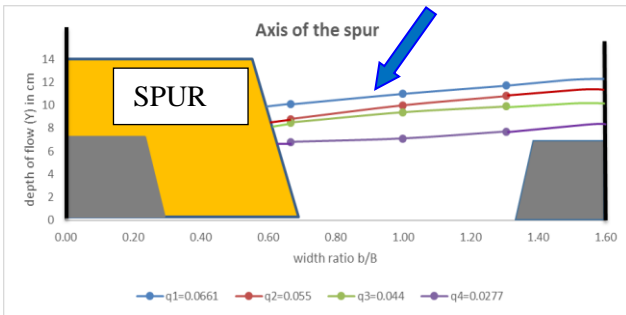


Fig 5: Relationship between depth of flow (Y) and width ratio b/B at Axis of the spur

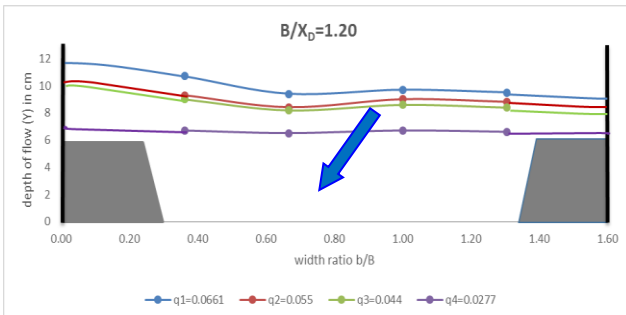


Fig 6: Relationship between depth of flow (Y) and width ratio b/B at $B/X_D=1.20$

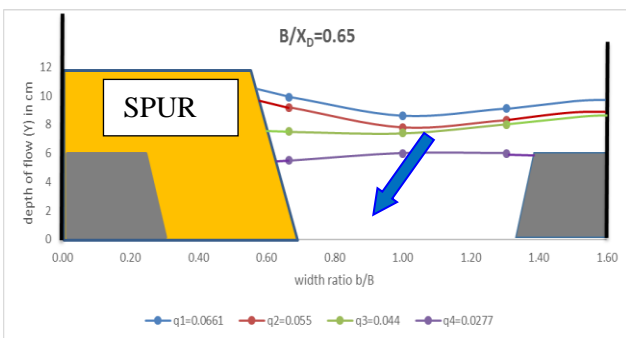


Fig 7: Relationship between depth of flow (Y) and width ratio b/B at $B/X_D=0.65$

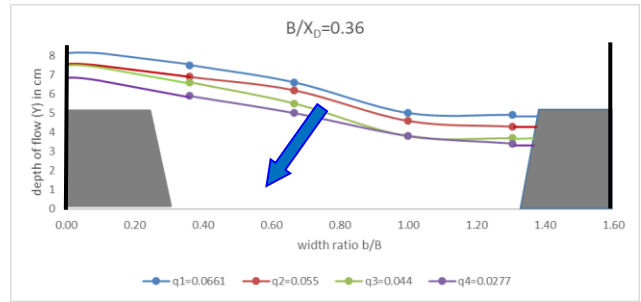


Fig 8: Relationship between depth of flow (Y) and width ratio b/B at $B/X_D=0.36$

The velocity distribution are plotted for the width ratio $b/B=0.36, 0.67, 1$ and 1.31 .for both upstream and downstream for maximum unit discharge $q_1=0.0661 \text{ m}^3/\text{s}/\text{m}$. the same sections are also plotted for different unit discharges and for different spur interval ($L/l=2.5, 3, 3.5$ and 4). From the plot it can be seen that the plot deviates from the normal plot due to the resistance offered by the air at the free surface. And due to the maximum shear-stress at the river bed the velocity becomes zero.

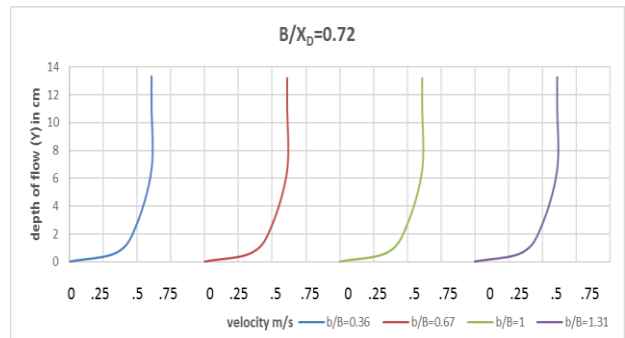


Fig 9: Relationship between depth of flow(Y) and velocity at $B/X_D=0.72$

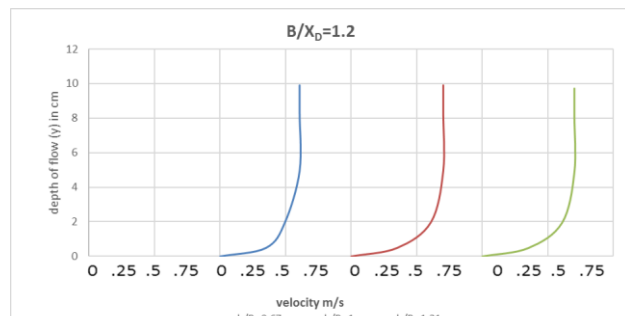


Fig 10: Relationship between depth of flow(Y) and velocity at $B/X_D=1.2$

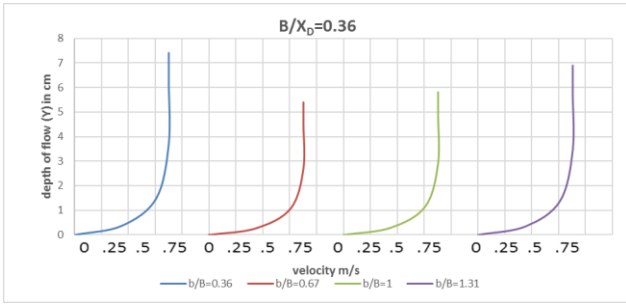


Fig 11: Relationship between depth of flow(Y) and velocity at $B/X_D=0.36$

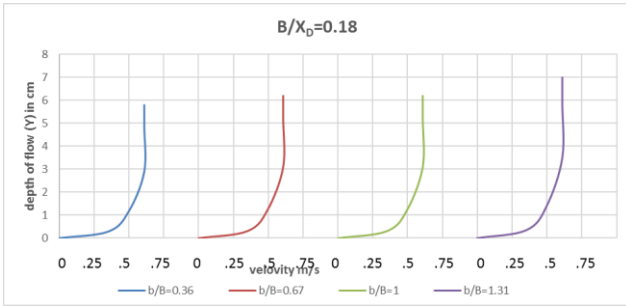


Fig 12: Relationship between depth of flow(Y) and velocity at $B/X_D=0.18$

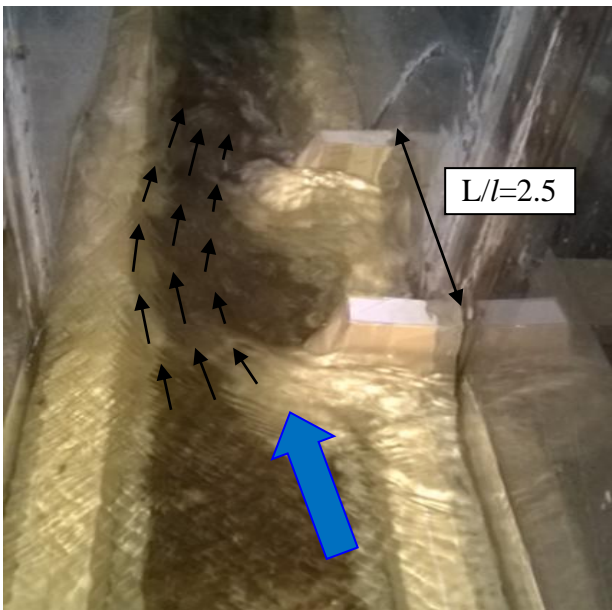


Fig 13 for spur interval $L/l=2.5$

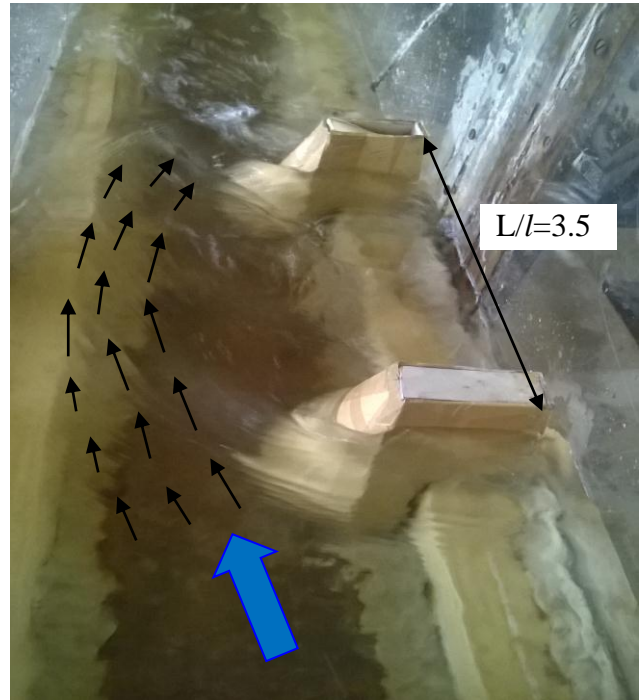


Fig 14 for spur interval $L/l=3.5$

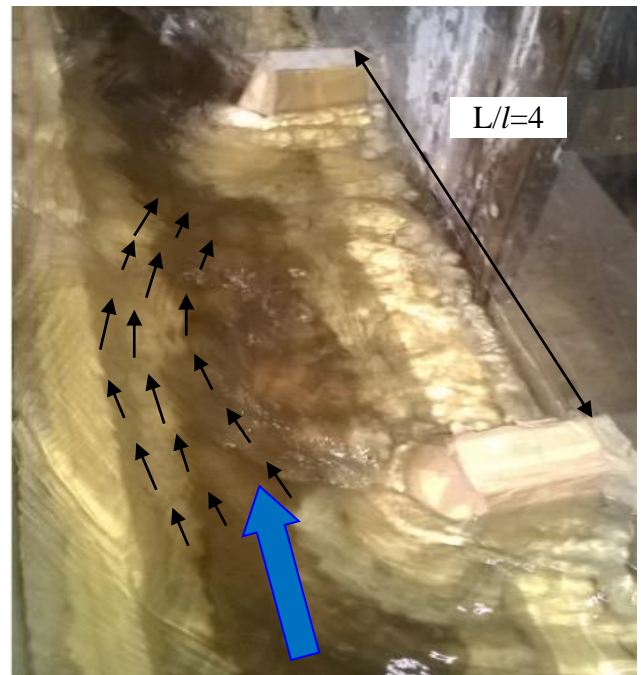


Fig 15 for spur interval $L/l=4$

CONCLUSION

Considering a double spur with varying the relative spur interval $L/l=2.5, 3, 3.5,$ and 4 and changing the unit discharges, the following conclusion can be drawn:

- i) Flow characteristics such as variation in velocity, depth of flow, direction of flow, eddy's formation mainly depend upon the non-dimensional length of the spur, i.e. $L/B,$

relative spur interval(L/l), linear discharge etc.

- ii) It has been observed that the undulation in upstream is very less irrespective of discharges except at the vicinity of the spur (upstream).
- iii) Formation of eddy's current and whirlpool formation is one of the common observation at the foot of the second spur.
- iv) The longitudinal water surface profile for all the relative spur interval (L/l) reflect that the highest depth of flow occurs at the upstream of the spur bank while the lowest depth of flow occurs at the transverse section of $B/X_D=0.36$ and from $b/B=0.67$ to $b/B=1$ in longitudinal section.
- v) Irrespective of any relative spur interval and discharges, it is observed that the depth of flow decreases from the axis of the spur towards downstream diverting the flow towards the opposite bank.
- vi) When the flow is observed by substituting a single spur, it can be seen that the flow strikes the bank downstream of the spur at a distance of 4.30 times of the spur length.
- vii) The safe relative interval between the groynes depend on the non-dimensional length of the groyne i.e. L/B ratio of the channel. Thus from this experimental observation it has been derived that the optimum safe relative interval is $L/l=3.5$. One can finally conclude the optimum safe relative interval after considering the different ratio of spur length to the width of the channel and considering silting and scouring effect.

- [3] Fenwick G. B, "State of Knowledge of Channel Stabilization in Major Alluvial River," Report No. FHWA/ RD-83/099, US Department of Transportation, Washington DC, 1969
- [4] Richardson E. V and D. B. Simons, "Spurs and Guide Banks," Open File Report, Colorado State University Engineering Research Center, Fort Collins, Colorado, 1974.

Back to table of contents

REFERENCES

- [1] Ahmed H S, Hasan Md M, Tanaka N, "analysis of flow around impermeable groyne on one side of symmetrical compound channel: an experimental study", water science and engineering, 3(1): 56-66,2010
- [2] Copeland R. R, "Bank Protection Techniques Using Spur Dikes," Miscellaneous paper HL83-1, US Army Engineer Waterways Experiment Station, 1983

Development of rubber modified asphalt as sealing material

Jyotishmoy Borah

Department of Chemistry, B.B. Engineering College, Kokrajhar-783370, India.

ABSTRACT

Waste rubber mainly from vehicles tires has been used in the different field to overcome the problem of dumping the tires in the landfills. However, approximately 1/3 of discarded tires will go for recycling and the leftover mostly goes to landfills and other waste sites. Various polymer modifiers have been disclosed and adopted for commercial use in an effort to improve the performance and extend the life of asphalt paving compositions. SBS, SBR, EPDM etc. are commonly used polymer modifiers for commercial purposes. The use of rubber modified asphalt is steadily increasing around the world in the present era. The most important application of this modified material is road construction and railway roadbeds.

In the present study, waste rubbers with different mesh size are incorporated into asphalt. Compounding and vulcanization is carried out by melt mixing method. Sulphur and phenolic curing system as well as various compatibilizers are used. Mechanical properties, morphology as well as thermal stability of the resulting rubber modified asphalt are studied. The obtained materials show an excellent mechanical and thermal stability. Among various compatibilizers, the phenolic curing system can significantly improve the young's modulus and tensile strength of the resulting material.

Keywords: asphalt, recycle, vulcanization, waste rubber, melt mixing

1. INTRODUCTION

Waste tires and other rubber products have become one of the largest and technically challenging problem in waste management (petragroup.net, 2008). It is reported that more than 1 billion tires are scrapped annually throughout the world. When disposed in dumps rubber particles take over 27 years to decompose, and tires take over 80 years to decompose naturally. Tires may trap water, and have become breeding grounds for mosquitoes and bacteria, and are excellent habitats for snakes and rodents. They present a real fire hazard, producing toxic fumes with health implications. Tires are bulky with 75% void space and are difficult to compact, it may flex back after a number of years, and break landfill covers making it unstable and costly and difficult to rehabilitate (Chamberlin, Gupta, 1986; Isayev, 2003; Johnson, Sproule, Juristovski, 1995).

As an alternative to discarding tires in dumps and landfills, present solutions to manage tire waste include the promotion of retreading rates to increase the average life of tires. Converting tire waste into Tire-derived Fuel (TDF) (Gray, 1997) by burning it is currently the most widely used method estimated at 37% of all scrap tires in US, 22% in Australia and 19% in Europe. Thermal decomposition of rubber products to recover its constituent parts was also explored, but the commercial scale of these methods was not satisfactory resolved.

Transforming tires into useful products is the most environmentally sound form of recovery. This involves shredding the tires into rubber shreds and chips and grinding it into crumbs. Crumbs are used in rubberised asphalt, or as fillers but this application is limited to low percentages and used in low-end products (Mull, Stuart, Yehia, 2002; Charania, Cano, Schnormeier, 1991). A number of methods for treating or modifying crumbs exist, which allows modified crumbs to be used at slightly higher percentages but the applications are still limited. However, approximately 1/3 of discarded tires will go for recycling and the leftover mostly goes to landfills and other waste sites (Michael, 1993). Use of recycled rubber, such as crumb rubber, can be extremely beneficial when used with asphalt. Asphalt is a visco-elastic material with desirable mechanical /rheological properties (Memon, Chollar, 1997). The unique chemistry and internal molecular association of asphalt are responsible for its mechanical properties and hence for its use as a binder in asphalt concrete pavement. Large tonnages of asphalt are used every year in constructing roads throughout the

world; thus any improvement in its properties, no matter how small, translates into considerable cost savings. Interaction of crumb rubber components with asphalt leads to a crumb rubber modified asphalt with improved rheological properties for both low and high temperatures and an improved useful temperature range (Yeh, Nien, Chen, Chen, Chen, 2005). It has been found that the quality of the asphalt after the addition of the rubber is a function of the amount of interaction between the asphalt and the crumb/ground rubber particles, which in turn is a function of the number of carboxylic sites on the surfaces of the particles. When the particles have a large number of carboxylic sites, they mix more evenly due to interaction with asphalt functional groups and the final product is much smoother; the rubber particles also stay in suspension to a much greater degree than before and hence more efficient for application than the conventional asphalt. The advantages of the rubber modified asphalt (RMA) can be summarized as (1) The toughness and ductility of RMA are usually higher than that of conventional asphalt, which makes it suitable for many applications; (2) The density of RMA is lower than the density of regular asphalt; and (3) Comparing with other recycling methods, such as using waste tires as fuel in cement plants, RMC makes a fully use of the high energy absorption feature of the rubber particles.

The use Rubber modified asphalt is steady increasing around the world in the present era. The most important application of this modified material is road construction and railway roadbeds (Giles, Clark, 1981; Burns, 1996; Zhong, Zeng, Rose, 2002; Wang, Zeng, Mullen, 2005). This material has been known to improve the rheological properties and decreased thermal cracking, potholing, deformation at low and high temperatures provide a life up to three times longer than conventional asphalt. Even though rubber modified asphalt may cost up to 100 % more than regular asphalt, the advantages may justify the added cost.

However, the major disadvantage of rubber modified asphalt is associated with the preparation process during heated storage. The used rubber such as crumb rubber and asphalt separate into two or more phases, because of the weak interaction between the rubber particle surface and the asphalt (McGennis, 1995; Bahia, 1995; Amirkhanian, 1993). Normal asphalt shows a separation of between 2 to 4 % during heated storage. Rubber modified asphalt yields a non-homogeneous blend with up to 25 % separation. This non-homogeneity reduces the reliability of the product properties. Separation

decreases the expected life of the rubber modified asphalt. Studies have shown chemically modified crumb rubber asphalt exhibits a separation range of 5 to 7 % and increase the stability of the mixture. This is due to the formation of a chemical bond instead of a physical mixture. The increased stability of the mixture and homogeneity contributes to reduce storage cost and improved life of the paved road.

2. MATERIALS

2.1. Materials selection

Two different grades of asphalts AH 50 and AH 47 were purchased from local market. The table 1 lists the basic properties of these asphalts.

Table 1. Basic properties of asphalt

Grade	Penetration 25°C(dmm)	Softening point °C	Viscosity 60°C (Poise)
AH 50	55	43	1534
AH 47	72	47	1612

Two types of rubber of different particle sizes were used to study the size effect on different properties of rubber-modified asphalt. The average size of large particles is 30 (a) and the average size of small particles is 60 mesh.

The degree of compatibility of the modified asphalt was investigated by using two different cross linkers viz sulphur and DCP, which was investigated by SEM.

2.2. Procedures

2.2.1. Sample preparation

Rubber modified asphalts was prepared by melt mixing process. Two types of rubber modified asphalt (30 mesh and 60 mesh) were prepared by slow adding (5, 10, 15 and 20 by weight of asphalt) to the asphalts (AH 50 and AH 47) at 170 ± 5 °C in a continuous (b) mode with a speed of around 1800 rpm for one and half hours. The other chemicals like Zinc Oxide, steric acid etc. were added after addition of waste rubber.

2.2.2. Molding procedure

The pre shaped sheet of the rubber-modified asphalt samples were prepared in the two rolls laboratory size open mill followed by molding at 50 °C for 7 minutes for both types of rubber modified asphalt respectively under a pressure of 4 tons in a laboratory size electrically heated two platened compression press. The sheets were kept for 7 days at ambient condition for

maturation before further studies.

2.2.2. Testing procedure

The surface morphology of rubber-modified asphalt was studied by using SEM of JEOL JSM-6700 scanning electron microscope. Thermogravimetric (TG) analysis was carried out in 209F1 (Netzsch, Germany) thermal analyzer using nitrogen flow rate of 30 mL/min and at the heat rate of 10 °C/min.

Thermogravimetric (TG) analysis was carried out in "Shimadzu TG 50" thermal analyser using nitrogen flow rate of 10 mL/min and at the heat rate of 10 °C/min. from room temperature to 700 °C.

3. RESULTS AND DISCUSSION

3.1. Morphology study

The morphology as observed from the fracture surfaces of rubber modified asphalt blend exhibit a homogenous distribution of waste rubber in the asphalt (Fig. 1) in the case DCP cured blend. However, sulphur cured blend have low homogenous distribution of rubber in the asphalt. These results indicate that waste rubber having high capability to compatibilize with asphalt in presence of DCP.

The scanning electron micrograph (SEM) images of blends also suggested that the minor phase domain size decreases on increase of the concentration of rubber particularly in the case of DCP cured blend, which indicates better mechanical properties of the blends as the dose level increases. This may be due to the uniform distribution of the blend components as well the compatibilization at the rubber/asphalt interface.

3.2. Thermal analysis

The thermal properties of both sulphur and DCP cured blend was also investigated from thermogravimetric analysis. From this this analysis it has been observed both the blends is thermally stable upto 250 °C. The initial decomposition at about 130 -150 °C may be due to the evaporation of moisture. A prominent weight loss of the blend material was observed above 300 °C. From the TG profile it can also be observed that the final residue has significantly improved.

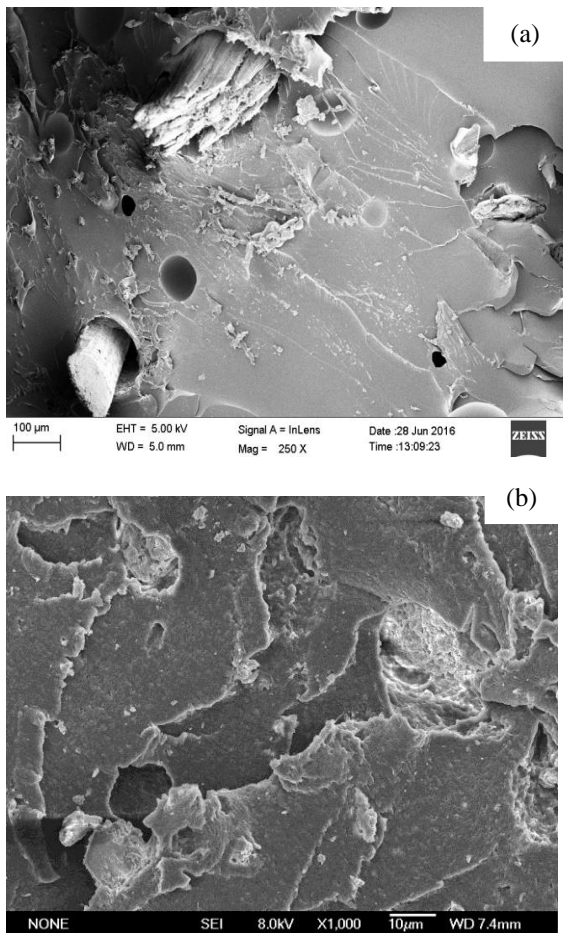


Fig. 1. SEM micrographs of blends (a) Sulphur cured rubber modified asphalt blend, (b) DCP cured rubber modified asphalt blend

4. CONCLUSIONS

In this study it is shown that 60 mesh size waste rubbers improve the different properties of the rubber asphalt blends due to the formation of homogenous blend in the binder. Again, DCP is found to provide marginally better compatibility to asphalt than sulphur cured blends.

5. REFERENCES

- Amirkhanian S.N., (1993): ASTM STP 1193, Philadelphia, PA.
- Bahia H, (1995): TRB 74th Annual Meeting, Paper no. 950792.
- Burns B., Rubber-modified asphalt paving binder, European Patent, No. EP0994161.
- Chamberlin W.P. and Gupta P.K., (1986): Use of Scrap Automobile Tire Rubber in Highway Construction, Report 85, Engineering Research and Development Bureau.
- Charania E., Cano J., and Schnormeier R, (1991): TRB 70th Annual Meeting, Paper No. 910226.
- Giles K.E. and Clark W.E., (1981): Asphalt-Rubber Interlayers on Rigid Pavements in New York State, National Seminar on Asphalt Rubber, San Antonio, Texas.

Gray T., (1997): Tire Derived Fuel: Environmental Characteristics and Performance, in Conference The Southeast Regional Scrap Tire Management, Nashville, Tennessee.

Isayev A.I., (2003): Encyclopedia of Materials: Science and Technology, Elsevier Science Ltd, Oxford.

Johnson R., Sproule J. and Juristovski A., (1995): The Full Scale Investigation of Rubberised Asphalt Concrete In British Columbia, Canadian Technical Asphalt Associate, PEI.

McGennis R.B., (1995): TRB 74th Annual Meeting, Paper no. 950368.

Memon G.M. and Chollar B.H., (1997) Thermal Characterization of Crumb Rubber Modified Asphalt, 24th NATAS Conference, San Francisco, CA.

Michael M., (1993): Identification and Application of Crumb Rubber Modified [CRM] for Asphalt Pavements. 52nd Annual meeting of the Southeastern Association of State Highway and Transportation Officials. Rouse Production.

Mull M.A., Stuart K. and Yehia A., (2002): Fracture Resistance Characterization of Chemically Modified Crumb Rubber Asphalt Pavement, J Mater Sci, 37.

Wang J.C., Zeng X. and Mullen R.L., (2005): Three-Dimensional Finite Element Simulations of Ground Vibration Generated by High-Speed Trains and Engineering Countermeasures, Journal of Vibration and Control, 11.

www.petragroup.net, date of accessed 15-03-2008.

Yeh P-H., Nien Y-H., Chen J-H., Chen W-C. and Chen J-S., (2005): Thermal and rheological properties of maleated polypropylene modified asphalt, Polym Eng Sci, 45.

Zhong X.G., Zeng X. and Rose J.G., (2002): Shear Modulus and Damping Ratio of Rubber-modified Asphalt Mixes and Unsaturated Subgrade Soils, J Mater Civil. Eng, 14.

[Back to table of contents](#)

Competition for water resource in the Brahmaputra river basin- issues of concern

Arnab Sarma

Professor, Department of Civil Engineering, Royal School of Engineering and Technology
Betkuchi, Guwahati-781035, Assam, India

ABSTRACT

The River Brahmaputra, which is essentially a transboundary river; originates in the Angsi glacier, located on the northern side of the Himalayas in Burang County of Tibet and is known as Yarlung Tsangpo. It flows for about 2,900 km across southern Tibet to break through the great Himalayas in great gorges (including the Yarlung Tsangpo Grand Canyon) and into Arunachal Pradesh, where it is known as Dihang or Siang. It flows southwest through the Assam Valley as Brahmaputra and south through Bangladesh as the Jamuna (not to be mistaken with Yamuna of India). In the vast Ganges Delta, it merges with the Padma, the popular name of the river Ganges in Bangladesh and finally the Meghna and from here it is known as Meghna before emptying into the Bay of Bengal. In the past China and India fought a war over contested territory through which the river flows and Bangladesh being at the tail end faces human security pressures in this basin that will be inevitably be magnified by upstream river practices. Despite these implications there is no bilateral or multilateral water management and water sharing accord that exists in the Brahmaputra basin. Moreover, this basin has received little scholarly attention compared with other river basins such as the Ganges, Indus, Mekong and the Amazon. Controversial dam-building activities and water diversion plans could threaten regional stability and trigger tension in the region. Thus, development, use and management of this transboundary water resource calls for an integrated approach within the conceptual framework of Integrated River Basin Management guided by transboundary water acts or any such other instrument. An attempt has therefore been made through this paper to provide greater understanding of the equities and drivers fueling water insecurity in the Brahmaputra River basin. Conclusions have been drawn and recommendations made based on desk research for various key stakeholders to consider at the sub-national, bilateral and multilateral levels to increase co-operation in the basin. The issues discussed may be of importance to policymakers, academicians, civil engineering students to discuss steps that could help manage and resolve competition of the water resources of the river Brahmaputra. This could, given the right impetus would go a long way in strengthening regional security on one hand and ensure availability of the basin's water for posterity on the other. Above all, it is strongly felt that a sustainable Brahmaputra basin ecosystem would only be possible to be maintained through this integrated approach in addition to maintaining bio-diversity of the region as a whole.

Key words: transboundary water, water sharing, stakeholders, regional security, sustainability

1. INTRODUCTION

Of all the natural resources, freshwater is our most precious natural resource. Its wise management and sharing are essential for obvious reasons. Despite this importance, globally we continue to abuse it. The world is faced with increasing water needs as population rapidly grows. Current trends show that we are not doing well in responding to the challenges. As far as Asia is concerned, India and China are in a rat race to become developed nations; implying more and more exploitation of natural resources, especially water. Against this background, transboundary water issues too often continue to be a source of major contention between the two riparian nations.

For the past few years, voices from China and India have stirred discussion about the potential for conflict and regional tension as a result of competition for water in the Brahmaputra basin. Author Brahma Chellaney's book (2011) *Water: Asia's New Battleground* raised alarm about China's dam-building efforts on the river Brahmaputra. The analysis presented in the book was to a large extent inspired by a book (2005) by Li Ling entitled "Tibet's Waters will Save China". Author Li Ling argues that water from Brahmaputra should be diverted by China for internal use in general and socio-economic development of the north-western provinces of China (that are chronically deficit of water), in specific. It is feared

that this one-sided approach and the actions planned would have far reaching consequences as far as India and Bangladesh are concerned, which are middle and lower riparian nations respectively. To quote Mark Twain “Whiskey is for drinking; water is for fighting over”. However, there are better options to avoid tension and work together towards common goals. This is possible through better allocation and management of water considering the entire Brahmaputra basin as a management unit.

2. THE BRAHMAPUTRA BASIN

The River Brahmaputra known as the Yarlung Zangbo in China has its source (s) in Tibet and flows for a length of about 2,900 km and meets the river Ganga before draining into the Bay of Bengal through Bangladesh. Brahmaputra basin is spread over an area of about 580,000 sq. km, which covers China (50.5%), India (33.6%), Bangladesh (8.1%) and Bhutan (7.8%). India receives almost one-third of its total water from the river Brahmaputra annually.

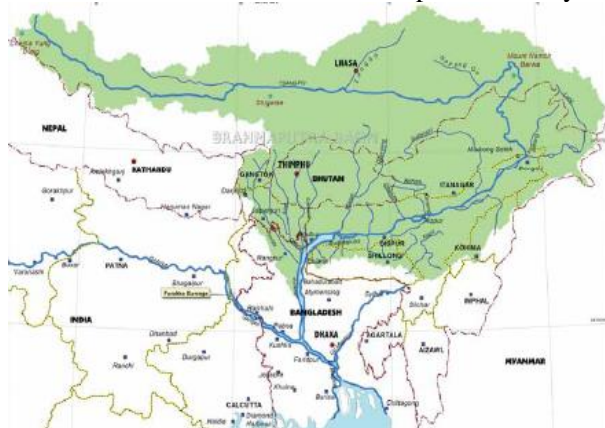


Figure-1: The Brahmaputra basin

3. POPULATION BURST, FOOD AND WATER STRESS- THE UNHOLY NEXUS

Both India and China are stressed for water coupled with skewed distribution of available water. The problem is exacerbated by depleting aquifers, climate change, rapid population and urban growth. China's current population is about 1.364 billion; marginally higher than India's population of 1.295 billion. It is projected that by 2050, India's population would be almost 1.60 billion while the population of China would fall to 1.340. Inevitably, India will experience shortage of food, water and energy. The scenarios are discussed below.

3.1 The Indian Scenario

India receives a large amount of rainfall during its monsoon season, but it lacks the ability to retain this water. Part of India's water scarcity can be attributed to poor surface water storage capacity, which is only about one-eleventh of China. China's renewable water sources are twice as large as India's, despite only having a slightly larger population. India's poor water management stems from an agriculture sector that consumes about 90% of its available water supply. Although the foreboding scenarios are conjured, climate change threatens to affect monsoon intensity and frequency. This is expected to affect Indian food security significantly. Further, rapid population growth, urban expansion and significant industrialisation will all compound India's water scarcity. By 2030, India's demand for water is expected to surpass supply by 50% of what it is today. India must enhance its water storage capacity and water use efficiency, as urbanisation is proving detrimental to India's aquifers and surface waters.

3.2 The Chinese Scenario

China is water-rich because it sources water from glacier, groundwater and surface water. At the same time it is water-poor because of uneven distribution of water creating scarcity throughout certain regions. The scenario is as follows.

- China currently holds 20% of the world's population but only 7% of fresh water resources
- China has total water reserves of 2.8 trillion cubic meters, which is 4th in the world. But per capita water reserves are only 2300 cubic meters, which is 1/4 of the world average, and comes in 121th place. China is therefore among the 13 most water-poor countries in the world.
- The agricultural sector accounts for 70% of China's water use and the coal industry uses a further 20% on which are dependent the Chinese industries at large. Both agriculture and industries are located in the arid north that receives only 20% of the country's total rainfall and snow melt, making the region very water scarce.
- Of China's more than 600 cities, more than 400 are in short supply of water and more than 200 have severe water shortages.

- About 70% of northern Chinese villages are water scarce, with per capita water availability less than one-tenth of the world average
- More than that, China's North-South distribution of water is severely skewed, given the fact that 44.3% of the population lives in the North and 59.6% of arable land is in the North. In contrast, the North has only 14.5% of China's water resources, with average per capita water reserves of 747 cubic meters (33.33% of the national average).
- This situation has been exacerbated by factors such as weak pollution controls, poor water conservation efforts and inefficient irrigation methods.
- Nearly 60% of China's groundwater is polluted. Almost 15% of water found in China's major rivers is not fit for use due to pollution and 7.4% of irrigated land is irrigated with polluted water.
- Ongoing water shortages in the north-west have already become an obstacle restricting economic and societal development. Only with large quantities of water, the north-west can improve its soil, check the expansion of deserts and finally rein in the raging dust storms.

China's food safety is threatened by pollution from rivers, farming and industrial waste. If current trends continue to 2030, China's water supply will no longer meet demand. Further, water is heavily subsidized in China, leading to an undervaluation of the resource. Consumers have little incentive to save water and industry sees it as an expendable resource, which leads to overuse and rising water pollution. The more developed China becomes, with higher disposable incomes, urban dwellings and domestic water use, as well as higher meat, vegetable and fruit consumption, the more water demand will increase. China therefore is left with no other option but to create more water infrastructure and improve upon water use efficiency at all levels.

4. STRATEGIC INTERESTS ALONG THE RIVER BRAHMAPUTRA

The Brahmaputra system makes up for 30% of India's water supply. Some experts opine that the Brahmaputra receives 70% of its flow from rainfall within India and as such there is no cause of worry if China dams Brahmaputra and diverts its water. However, the cause of worry is that this water enters

the Brahmaputra only during monsoon season. As little as a 10% change to the upstream flow could have detrimental consequences for India in terms of increased salinity. This would affect agriculture downstream and the ecosystem in general.

5. DAM BUILDING BY CHINA

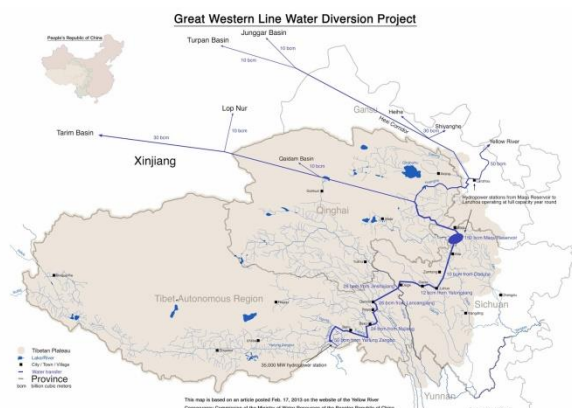
The Chinese Government announced in 2008 that it would commence building its US\$1.5 billion Zangmu hydroelectricity dam along the middle reaches of the Yarlung Zangbo that would produce 2.5 billion kilowatt hours of electricity per year. The project was perceived by India as the start of Chinese river diversion projects that would ultimately dry up the Brahmaputra. By the end of 2015, all six power-generating units of the Zangmu Dam became operational. Despite New Delhi's wariness about Beijing's intentions, China insists that it would only construct run-of-the-river dams that generate electricity and pose little danger to downstream water security. However, run-of-the-river dams too have negative impacts.

In all, China intends to build twenty (20) dams on the Brahmaputra to generate 60,000 MW of power. Eleven (11) of the twenty (20) projects on the Brahmaputra will be located between its source and the Great Bend where the Brahmaputra turns northwards, executes a huge 'U' turn and falls from an elevation of 3,500 m in Tibetan plateau to about 700 m in the undulating hills of Arunachal Pradesh in India. Dams on the straight course will generate 20,000 MW, while the balance of 40,000 MW will be generated at the Great Bend itself. Additionally, twenty (20) smaller dams are planned upon its tributaries to generate another 5,000 MW. Thus, the total generation planned is 65,000 MW.

6. WATER DIVERSION- PRESENT AND PROPOSED

Aside from generation of hydro-electric power by damming the Brahmaputra by China, there is the more disturbing move with regard to diversion of the river water to meet domestic demand, especially for irrigation. China currently faces serious water scarcity challenges. In order to address these issues, the Chinese authorities embarked upon a massive water transfer project known as the South-North Water Diversion Project (nan shui bei diao gongcheng). The project that begun in 2002 consists of three planned routes: the Eastern, the Central and the Western.

The Eastern and Central routes focus on diverting water from the southern China's river Yangtze and river Han, respectively, to the river Yellow in the north. These two routes have already been completed and they currently supply water to northern cities like Beijing and Tianjin. The proposed Western route will concentrate on diverting the headwaters of three tributaries of the river Yangtze (Tongtian, Yalong and Dadu), which are all domestic rivers on the Tibetan Plateau to the Yellow river by 2050. The completed routes are shown below.



Going by the above facts it would not be out of place to mention that the Chinese authorities would not hesitate to divert the waters of the Brahmaputra in the near future if the situation warrants.

As far as the river Brahmaputra is concerned, a number of proposals, starting from 1990 have been placed including the most recent one by Chinese experts to divert water from the upper reaches of the river Brahmaputra to the country's north-western province of Xinjiang. The water diversion route in the proposal, named the "Grand Western Canal," is slightly different from the "Western Canal" mentioned earlier. The newly proposed route is to start from the river Brahmaputra, from which China can reroute the water to Xinjiang along the Qinghai-Tibet Railway line and the Hexi Corridor (part of the Northern Silk Road located in Gansu Province). Experts warn that if China proceeds with the project, water flow will be reduced by 60%; enough to create serious consequences downstream.

Although none of these proposals has been officially endorsed, there is room to believe that China's water shortage may become so severe by 2030 (due to climate change, desertification and intensification of the hydrologic cycle) that the government will have no choice but to divert the waters of the river Brahmaputra to meet its agricultural, irrigation and industrial requirements.

7. PERCEIVED SHORTCOMINGS IN THE WATER DIVERSION PROPOSAL

This author is apprehensive of the Brahmaputra diversion proposal in light of the following issues.

- Inter-basin transfer of water is among the most expensive ways to increase water availability.
- Diversion of water from the upper reaches of Brahmaputra i.e. Tibetan Plateau may not be technically feasible due mainly to the fact that the Tibetan Plateau is geologically unstable to support a project of this scale.
- Due to the disruptive effects of such projects, plans for diversion are likely to encounter severe resistance on social and ecological grounds.

8. ILL-EFFECTS OF WATER DIVERSION

The following are some of the perceived ill-effects of water diversion projects-

- Reductions in river flows due to diversions upstream can increase the concentrations of pollutants and deposition of sediments
- It can also alter river habitat and result in changes in and loss of adjacent floodplains.
- Inter-basin water transfer changes the hydrological regime of each system and can lead to widespread introduction of alien species and can relocate entire aquatic faunas, resulting in significant problems with invasive alien species.
- Changes in hydrological regimes may also have serious consequences for the ecology of estuaries.
- Transboundary harm may also flow upstream e.g. of a dam built that prevents migratory species from swimming back upstream, where they reproduce and repopulate fisheries of biological, social and economic relevance across the border.
- It is therefore suggested that both long-term measures like afforestation and/or reforestation and short-term measures like improved water use efficiency across all sectors, shallow groundwater pumping and intra-basin water transfer may be adopted that are cost-effective, technically feasible and ecologically friendly.

9. ILL-EFFECTS OF RUN-OF-THE-RIVER (RoR) PROJECTS

The upper riparian China has been insisting that they are considering run-of-the-river projects with no “storage or diversion” that would not cause any harm to India and Bangladesh. This is not entirely correct as RUN-OF-THE-RIVER (RoR) hydro projects can do immense harm. Far from being environmentally benign, as often claimed, they are perhaps among the most destructive human interventions. “RoR” is a most misleading description: the projects involve high dams; and apart from the usual impacts of dams, there are two special features in RoR hydro projects. First, there is a break in the river between the point of diversion to the turbines and the point of return of the waters to the river. This break can be very long, upwards of 10 km, even 100 km in some cases. There would be a series of such breaks in the river in case a cascade of projects as planned by China is executed. Second, in such projects the turbines operate intermittently in accordance with the demand for electricity, which means that the waters are held back in pondage and released when the turbines need to operate, resulting in huge diurnal variations (0-400%) in a day in downstream flows. There could be a case in which the river is dry for twenty hours in the day and in the remaining four hours there is a water wall rushing down the river. No aquatic life or riparian population can cope with that order of diurnal variation. A RoR project spells death for the river.

10. WHAT INTERNATIONAL LAW SAYS

The relevant document is the UN Convention on the Law of Non-Navigational Uses of International Watercourses (1997), which is a successor to the Helsinki Rules (1968). It was ratified by the required number of countries and has come into force despite China voting against it and India abstaining. However, if the water scarcity in parts of China worsens due to reasons mentioned earlier and China considers a south-north diversion of water necessary, it is unlikely to be deterred by the UN convention.

11. CONCLUSIONS AND SUGGESTIONS

The Brahmaputra system and its unique character, economic, cultural and ecological values are under threat, due to lack of vision and mad race to exploit its potential by India and China. Lack of a framework for managing the river system as a whole has left it vulnerable to short-term, competitive exploitation. In India, massive dams are proposed on its tributaries.

As in China, these plans are being made with little concern for the wider health of the river system or the interests of the millions of people who have depended on it for thousands of years. This is not an argument against development, but a concern that wrong kind of development, pursued in competition, risks destroying vital ecosystems that we only partially understand. It is a race in which everyone risks becoming a loser. Governments, to date, have not been sincere. It is time that we stop ruthless exploitation of the river and its tributaries and start examining this system comprehensively applying principles of Ecological Engineering and not of “hydrocracy”. The following points are made.

- Execute a treaty involving Bangladesh, Bhutan, India and China and put in place a Commission similar to the Mekong Commission involving people dependent on the Brahmaputra allaying fear or else it can be a zero sum game. The way policymakers look at a river basin must change.
- Establish scientific collaboration across national boundaries, to include joint research, data sharing and expert exchange programmes.
- Carry out environmental impact assessment studies and prepare and execute environmental management plans for all the projects.
- Explore the alternatives to hydropower and promote long-term measures like afforestation and/or reforestation and short-term measures like improved water use efficiency across all sectors.
- Finally, adoption of Ecosystem Approach as enunciated by the UN Watercourses Convention would help rectify the already made mistakes and help prepare and execute better plans.

REFERENCES

1. Subramanyachary P. (2013). Water resources and sustainable development. *International Journal of Applied Research & Studies* ISSN 2278 – 9480
2. World Population Prospects: The 2015 Revision (Key Findings & Advance Tables), United Nations
3. India–China–Brahmaputra: Suggestions for an Approach (2015). *Economic & Political Weekly*, Vol-L, No. 9
4. Samaranayake N. et al (2016). *Water Resource Completion in the Brahmaputra River Basin: China, India & Bangladesh*. CNA, 3003 Washington, USA

[Back to table of contents](#)

Simulation Study of Subansiri Lower Reservoir

Dipsikha Deviⁱ⁾, Bibhash Sarmaⁱⁱ⁾

- i) Junior Research Fellow, Indian Institute of Technology Guwahati, Guwahati-781039, Assam, India
 ii) Associate Professor, Department of Civil Engineering, Assam Engineering College, Jalukbari, Guwahati-781013, Assam, India

ABSTRACT

Subansiri is the largest Trans Himalayan north bank tributary of mighty river Brahmaputra. Subansiri river flows through Dhemaji, Lakhimpur and Majuli district. Nature has bestowed upon Subansiri river basin with exuberant medley of wildlife ecosystem and natural elegance. Flora and fauna, fisheries, diversity among different ethnic groups are integral ingredients of Subansiri basin. Subansiri Lower Hydroelectric Power is the largest under construction hydropower initiative in India. It is located on the border of Assam and Arunachal Pradesh with a dam height of 116m above the river bed level. This paper elucidates the implementation of water resource system analysis for the generation of reservoir simulation model. A nonlinear optimization model clubbed with simulation model is used to determine the firm power corresponding to 90% reliability. The variation of firm power with reliability and average power are also presented.

Keywords: Subansiri , reservoir, simulation, firm power , optimization

1. INTRODUCTION

The river Subansiri is one of the largest north bank tributaries of Brahmaputra and contributes around 10% of the total flow of Brahmaputra. Due to its high perennial discharge and suitable topographic conditions several hydropower projects have been planned on different reaches of the river.

Subansiri Lower HE Project (2000MW) is the largest under construction hydropower initiative in India and is located on the border of Assam & Arunachal Pradesh. The project was initially conceived by Brahmaputra Board considering 257m high Rock Fill Dam at Gerukamukh. However it was modified as concrete dam with a height of 116m and the project was handed over to NHPC for execution. With consideration of Dam Height as 116m, NHPC carried out additional investigations so as to finalise the technical aspects of various structures of the project. Subansiri Lower HE Project comprises of dam toe power house. The project is a Run-of-the-River scheme which ensures minimum flow of 250-300 cumecs. According to NHPC the overall use pattern in downstream area is not likely to change significantly as NHPC shall operate one turbine continuously for 24 hours which will results in maintaining the natural discharge in the river during lean period. The total allocation of power from Subansiri Lower Project to home states Arunachal Pradesh and Assam are 274MW and Assam 533MW.

2 STUDY AREA

The Subansiri River originates from the western part of Mount Porom of Tibetan Himalaya. After flowing through for 190 km through Tibet, it enters India. It

continues its journey through the Himalaya of India for 200km and enters into the plains of Assam through a gorge near Gerukamukh. The Subansiri is the largest tributary of the Brahmaputra. Its total length is 520 km and it drains a basin of 37,000km². However, the major part of the basin is developed in the mountains. The river maintains an almost stable course through the mountains but the river course becomes unstable as soon as it enters the alluvial plains of Assam. . Total length of the river within Assam is 130 km which flows through the Dhemaji, Lakhimpur and Majuli districts of Assam in between 26^o50' -27^o35'N and 93^o41' -94^o23'E.

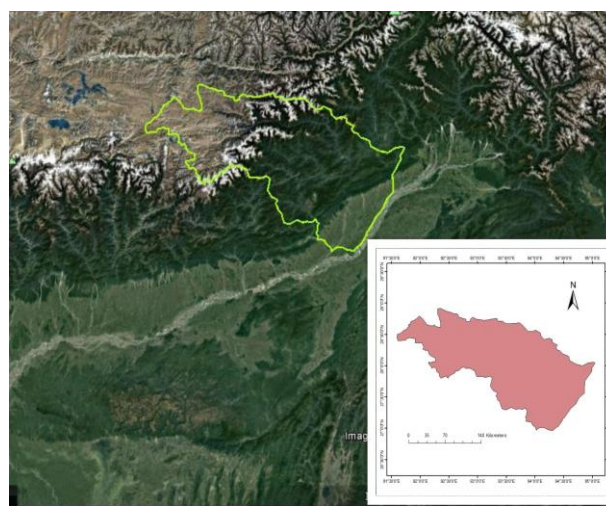


Figure1: Study Area

3 DATABASE AND METHODOLOGY

3.1 Data Used

Data collection and processing are important steps for the application of models. The various datasets that have been used for the preparation of simulation working table and formulation of optimization models are collected from NHPC, Water Resource Department, Government of Assam and Brahmaputra Board.

Table 1: Data Used

SI No.	Data Used	Source
1	Inflow data of Subansiri River	Water Resource Department
2	Elevation-Capacity-Area Relationship	NHPC
3	Maximum Water Level, 208.25m	NHPC
4	Tail Water Level, 109m	NHPC
5	Gross Storage, 1365 MCM	NHPC
6	Dead Storage, 720MCM	NHPC
7	Plant Capacity, 2000MW	NHPC
8	Efficiency, 94.07%	NHPC
9	Evaporation Data	Brahmaputra Board

The inflow data of Subansiri River are collected from Water Resource Department, Guwahati from the Khabulighat site which is around 10 km downstream of Chouldhowaghat site. The inflow data of Subansiri River are collected from Water Resource Department, Guwahati from the Khabulighat site which is around 10 km downstream of Chouldhowaghat site.

Table 2: Capacity-Area-Elevation Relationship (Source-NHPC)

Capacity(MCM)	Elevation(m)	Area(Ha)
0	94	0
13	110	250
46	120	400
93	130	550
158	140	750
245	150	1000
359	160	1300
509	170	1700
896	180	2050
923	190	2500
1198	200	3000
1532	210	3700

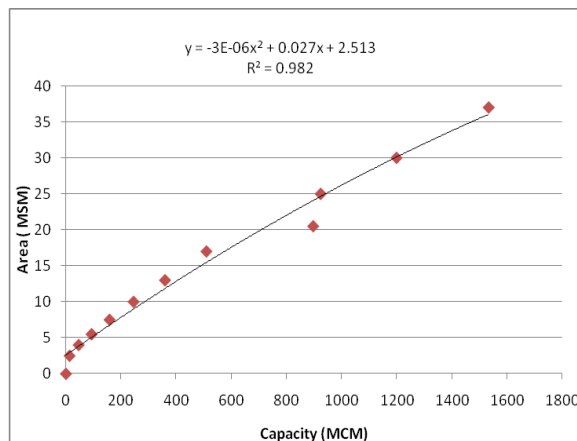


Figure 2: Area- Capacity Relationship

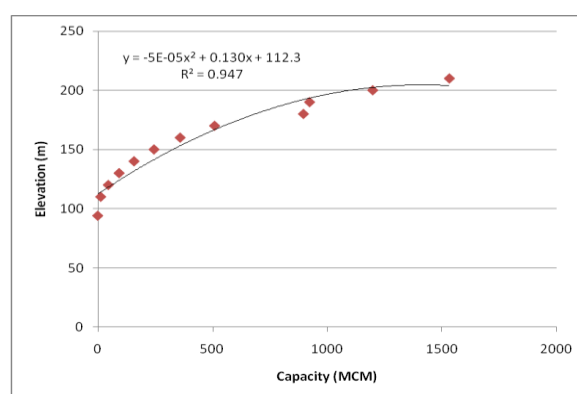


Figure 3: Elevation –Capacity Relationship

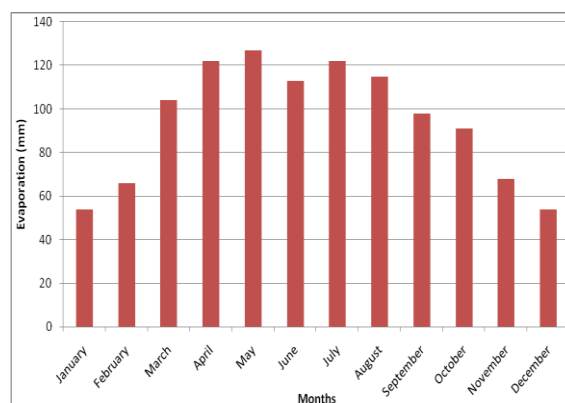


Figure 4: Evaporation Data (Source: Brahmaputra Board)

3.2 Methodology

3.2.1 The Simulation Model

Continuity Equation for a Reservoir:

$$S_t = S_{t-1} + I_t - Ev_t - O_t - Sp_t, \text{ where}$$

S_t = Final storage at the time t for the reservoir.

S_{t-1} = Initial storage at the beginning of time t for the reservoir.

I_t = Inflow to the reservoir in time t.
 E_{vt} = Evaporation from the reservoir in time t.
 O_t = Water release at time t.
 Sp_t = Water spill at time t.

Evaporation losses:

$E_{vt} = ((A_t + A_{t-1})/2 \times e_{vt})$; for all t.
 $= A_{t-1} \times e_{vt}$

Where, A_t = Surface area of reservoir in time t with respect to initial storage.

e_{vt} = Average rate of evaporation from the reservoir in time t.

Power head:

$H = El - \text{Tail water level}$

Where, El = Reservoir elevation

Active Storage:

$S_a = S_{t-1} + I_t - E_{vt} - Y_d$

where Y_d = dead storage.

S_a = Active Storage

Power Demand:

$Q_{p,t} = P_f / (9.8 \times h \times e)$

Where, $Q_{p,t}$ = Discharge required to produce firm power at time t.

P_f = Firm power

e = efficiency

Firm Power Generation:

$P_f = 9.8 \times Q_{r,t} \times h \times e$

Where, $Q_{r,t}$ = Discharge release to produce firm power at time t.

Total Release:

$Q_{tr,t} = Q_{fr,t}$

Where, $Q_{tr,t}$ = Total release, at time t.

$Q_{fr,t}$ = Water release for firm power generation, at time t.

Final storage:

$S_t = Y$; if $(S_a - Q_{tr,t} + Y_d) > Y$

$S_t = (S_a - Q_{tr,t} + Y_d)$; if $(S_a - Q_{tr,t} + Y_d) < Y$

Where, S_t = Final Storage.

Y = Reservoir Capacity

Spill:

$S_{pt} = S_t - Y$; if $S_t > Y$

$S_{pt} = 0$; if $S_t < Y$

Where, S_{pt} = Spill at time t.

Surcharge Power:

$P_{sp,t} = 9.8 \times S_{pt} \times h_1 \times e$

Where, h_1 = Power head at FRL

Actual Surcharge:

$P_{sp,t} = P_{ca} - P_{G,t}$; if $(9.8 S_{pt} h e) > P_{ca} - P_{G,t}$

Where P_{ca} = Plant Capacity

$P_{G,t}$ = Power generation at time t

Total Power:

$P_{t,g} = P_{G,t} + P_{sp,t}$

P_t = Total power generation at time t

Power reliability:

If $P_t < P_f$, then Power Reliability Index at time t $PRI_t = 0$
 and If $P_t > P_f$, then Power Reliability Index at time t $PRI_t = 1$

Firm Power Reliability = $\sum \{ PRI_t / (N+1) \} * 100\%$

3.2.2 Non Linear Programming Model

The optimization model is often used synonymously with mathematical programming, to refer to a mathematical formulation in which a formal algorithm is used to compute a set of decision variable value that minimize or maximize an objective function subject to constraints.

Objective function

Maximize, $f(z) = P_T$

Subjected to

$P_f \geq 250 \text{ MW}$

$R \geq 90\%$

Where P_T = Total firm power of the hydropower plant

P_f = Firm Power of the hydropower plant

R = Reliability of the hydropower plant

4 MODEL RESULTS AND DISCUSSIONS

4.1 Results from Simulation Working Table

4.1.1 Firm Power v/s Reliability

Firm Power is the maximum power that can be produced at any time. Thus, it corresponds to the maximum amount of water that is always available in the reservoir even during a critically dry period. Since future is uncertain that is the firm power is expressed in terms of probability. The target reliability of firm power in India is 90%.

Reliability is an important measure of an energy source's investment potential a reliable energy source is a reliable investment.

The proposed installed capacity of the project is 2000 MW with eight number of turbines, each having capacity of 250 MW. The simulation model is run for different assumed firm powers i.e, for 250 MW, 500MW, 750 MW, 1000MW, 1250 MW, 1500 MW, 1750 MW and 2000 MW. The firm power v/s reliability curve is shown in Figure 5. From the curve it is concluded that as the firm power goes on increasing the

reliability goes on decreasing.

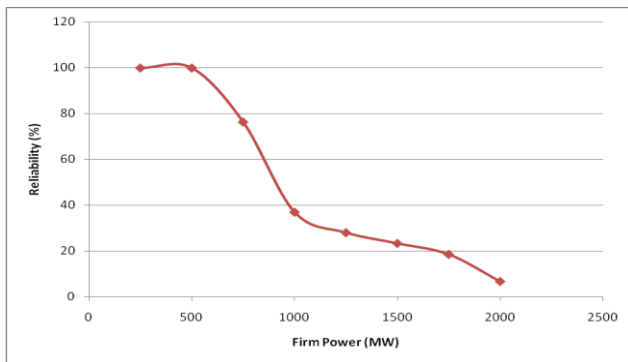


Figure 5: Firm Power v/s reliability

4.1.2 Firm Power v/s Average Power

The average power generations for different assumed firm powers are calculated using simulation. From figure it can be seen that the average power goes on decreasing as firm power increases.

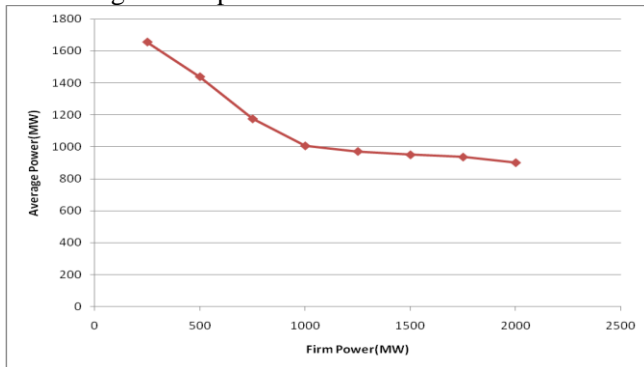


Figure 6: Firm Power v/s average power

4.1.3 VARIATION OF MONTHLY POWER AT DIFFERENT FIRM POWERS

The variation of monthly powers corresponding to different firm power is shown in figures. The maximum, minimum and average powers for different firm powers are plotted.

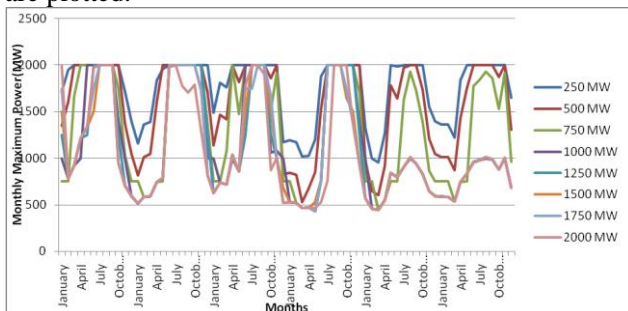


Figure 7: Monthly Maximum Power

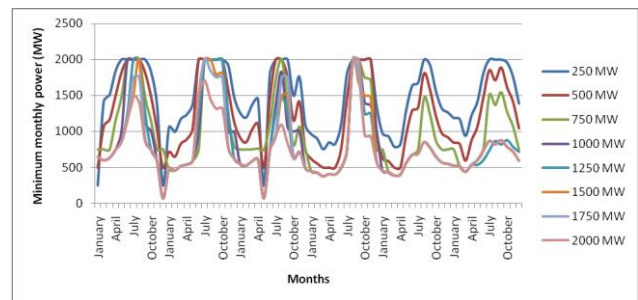


Figure 8: Monthly Minimum Power

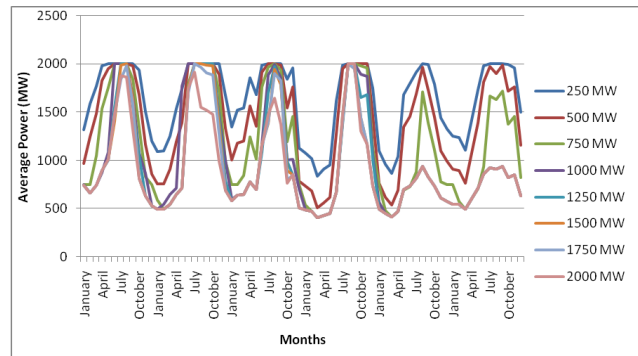


Figure 8: Monthly Average Power

Figures show the variation of monthly maximum, minimum and average powers for different firm powers. The maximum daily power for each month are taken. Figure 7 shows the maximum monthly power at different firm powers. A maximum power of 2000MW is generated in the months of June to September. As the firm power increased the monthly maximum power goes on decreasing. A similar trend can be seen for monthly minimum and monthly average power.

4.1.4 VARIATION OF MONTHLY TOTAL RELEASE AT DIFFERENT FIRM POWERS

The variations of monthly maximum, minimum and average release from the reservoir for different firm powers are shown in the figures.

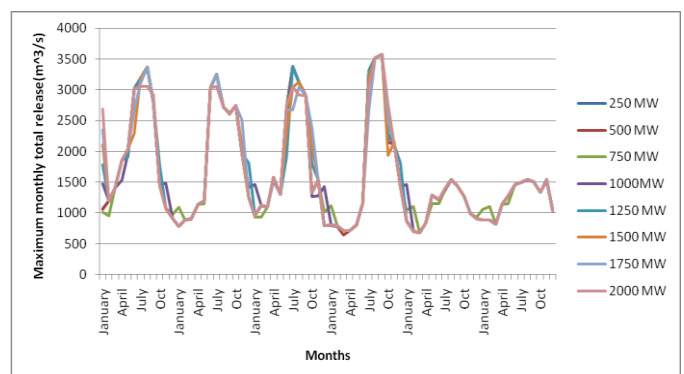


Figure 9: Maximum monthly release

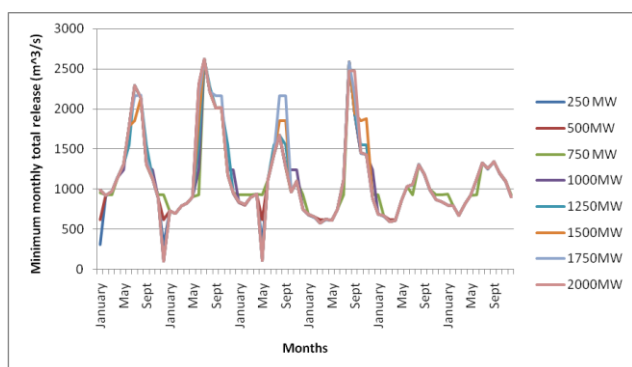


Figure 10: Minimum monthly release

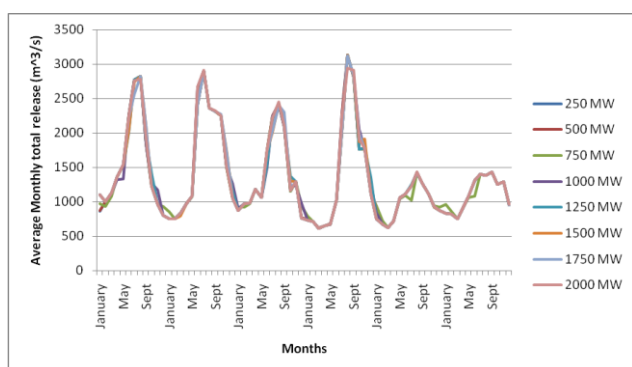


Figure 11: Average monthly release

From the above figures it is clear that for different firm powers, the release from the reservoir remains almost the same. For the generation of the above curves the monthly maximum, minimum and average release is taken. A maximum release of around 3500 m³/s occurred during the months of July to September in the year 2008. A minimum release of around 310 m³/s occurred for 250 MW firm power. An average maximum monthly release of 3130 m³/s occurred for 250 MW.

4.2 RESULTS AND DISCUSSIONS FROM OPTIMISATION MODEL

Non linear optimization model is formulated in excel solver for the generation of exact firm power attributing to 90% reliability. Concerning the firm power of 659.51 MW the monthly average power and the total release which the model generates are shown in the following figures.

Table 3: Results from optimization model

Firm Power	Reliability	Average Power
659.51	90.009	1266.6

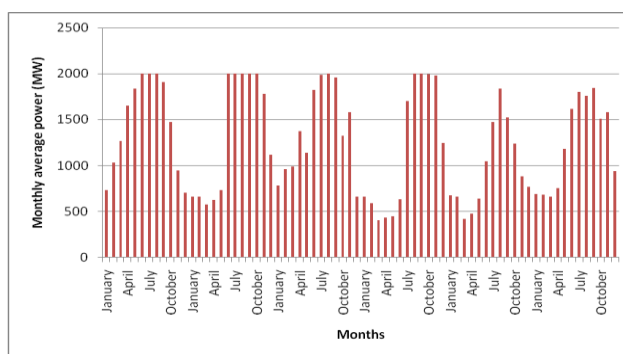


Figure 12: Monthly average power

Figure shows the bar diagram of monthly average power for different months.

CONCLUSIONS

The Subansiri Lower Hydroelectric power is the largest ongoing hydropower initiative in India of 2000MW which is situated in Assam-Arunachal border. The study is done to check the firm power for the target reliability. The simulation model is prepared to determine the variation of reliability with firm power and average power. From the reservoir simulation it is assessed that the reliability and the average power decreases as the firm power increases. A maximum power of 2000 MW is generated in the months of June, July, August and September. From the non linear optimization technique the exact firm power and the average power is found to be 659.51 MW and 1266.6 MW respectively corresponding to 90% reliability.

REFERENCES

- 1) Chaturvedi, M.C. and Srivastava, D.K. (1981). "Study of a complex water resources system with screening and simulation models" *Water Resource Res.*, 17(4), 783-794.
- 2) Loucks, D. P., Stedinger, J. R., and Haith, D. A. (1981). *Water Resources System Planning and Analysis*. Prentice Hall, Englewood Cliffs, New Jersey
- 3) Martin, Q.W. (1983). *Optimal Operation of Multiple Reservoir Systems*. *Journal of Water Resources Planning and Management*. ASCE, 109(1), 58-74, ISSN 0733-9496.
- 4) Sarma B. (2007). "An improved Multireservoir Multiyield Preliminary Screening Model" *The National Workshop on Reservoir Planning an Operation at Assam Engineering College, Guwahati, 19th Dec.2007 (27-37)*.
- 5) Sarma B., and Srivastava, D.K. (2005). "Simulation study of a river linking Project." *Proc. Of the International Conference on Hydrological Perspectives for sustainable Development (HYPESD-2005), IIT Roorkee, Feb.23-25,*

[Back to table of contents](#)

Application of simulation-optimization model in reservoir planning

Krishna Kamal Dasⁱ⁾ and Bibhash Sarmaⁱⁱ⁾

i) Ph.D Student, Department of Civil Engineering, Assam Engineering College, Guwahati

ii) Associate Professor, Department of Civil Engineering, Assam Engineering College, Guwahati

ABSTRACT

Due to increase of population, water demands for various basic and developmental purposes are increasing and at the same time this precious water is depleting day by day. So it is very much essential for the immediate development of water resources as it has a great contribution in development of human civilization. In India, the rainfall normally comes during monsoon season and also it is unevenly distributed throughout the country. So it is very important to utilize this limited water resources in a sustainable manner. Use of system analysis techniques is one of the pioneered methods in Water Resources Systems planning, design, operation and management for proper utilization of this limited water. Optimization tools are utilized to facilitate optimal decision making in the planning, design and operation of especially large scale water resources systems. This paper, aims to find the optimal solution by simulation and optimization models as a system analysis technique to study the reservoir planning and operation.

Key words: Simulation, optimization, reservoir, water resources, Non-Linear programming,

1. INTRODUCTION

System analysis techniques have been used successfully in the management and operation of complex reservoir systems. The complexities of a multipurpose reservoir system generally require release decision to be made by an optimization or simulation model. Most of the optimization models are based on some type of mathematical programming technique. In general, the available methods can be classified as follows (Yeh, 2003): linear programming, network flow, quadratic programming, dynamic programming, non-linear programming, mixed integer linear programming, interior point method and simulation. Sarma and Srivastava (2005) presented a system analysis modeling approach for planning and operation of reservoirs, involved in inter basin water transfer projects and demonstrated the approach by applying it to the Parbati-Kalisindh- Chambal water transfer link involving five reservoirs. Hydropower generation is one of the vital components of reservoir operation, especially for a large multi-purpose reservoir. Deriving optimal operational rules for such a large multi-purpose reservoir serving various purposes like irrigation, hydropower and flood control are complex, because of the large dimension of the problem and the complexity is more if the hydropower production is not an incidental. Thus optimizing the operations of a reservoir serving various purposes requires a systematic study. In a recent study, such a large multi-purpose reservoir, namely, Koyna reservoir operations

(R.Arunkumar, V.Jothiprakash, 2012) are optimized for maximizing the hydropower production subject to the condition of satisfying the irrigation demands using a non-linear programming model. The hydropower production from the reservoir is analyzed for three different dependable inflow conditions, representing wet, normal and dry years. For each dependable inflow conditions, various scenarios have been analyzed based on the constraints on the releases and the results are compared. The annual power production, combined monthly power production from all the powerhouses, end of month storage levels, evaporation losses and surplus are discussed. From different scenarios, it is observed that more hydropower can be generated for various dependable inflow conditions, if the restrictions on releases are slightly relaxed.

Aiming at the problem that traditional optimal operation of hydropower reservoir pays little attention to ecology, an optimal operation model of multi-objective hydropower reservoir with ecology consideration is established which combines the ecology and power generation (Xuewen Wu et al, 2011). The model takes the maximum annual power generation benefit, the maximum output of the minimal output stage in the year and the minimum shortage of ecological water demand as objectives, and water quantity balance of reservoir, reservoir storage, discharge flow, output and so on as constraints.

Despite the fact that most integrated use management problems are nonlinear in nature, application of nonlinear programming (NLP) has been

rather limited. This may be because of the complexity and the slow rate of convergence of the NLP algorithms, difficulty in considering stochasticity and possibility of getting a local instead of global optimal solution (Yeh, 1992)

2. LOCATION OF STUDY AREA

The Kulsi basin, a part of the Brahmaputra sub-basin is situated on the south bank of the mighty river Brahmaputra. This sub-basin spreads in the Kamrup and Goalpara District of Assam as well as west Khasi hills and west Garo hills district of Meghalaya. It is located between Latitude between 25° degree – 35° N & 26° – 07° N and Longitude 90° – 45° E and 91° – 00° E. It is bounded by Bharalu & Kallong- Kopili sub basin in the east, Krishnai- Dudhnoi sub-basin in the west, and west khasi hills in the south and the river Brahmaputra on the north.

The river Kulsi is a south bank tributary of the river Brahmaputra, The river originates from the northern slopes of the Khasi hill ranges, where in the elevation is from 1800 m to 1900 m and flows down north. It is composed of three rivers, namely Khri, Krishniya and Umsiri , all of which originate from west Khasi hill range and flows north. The river is known as Khri in the upper catchments and after being joined by two other tributaries namely Krishniya and Umsiri, within the Khasi hills in Meghalaya it flows north-west and enters Assam at Ukium and after that it flows north upto Kulsi village through the plains of Kamrup District of Assam. Finally it outflows into the Brahmaputra near Nagarbera. The river has a total catchments of 3231 sq. km. Out of which about 1666 sq. km is in Khasi hills in Meghalaya and rest is in the plains of Assam. The total length of Kulsi from its source to outfall is about 220 km. Out of which 100 km is in Meghalaya and rest 120 km is in Assam

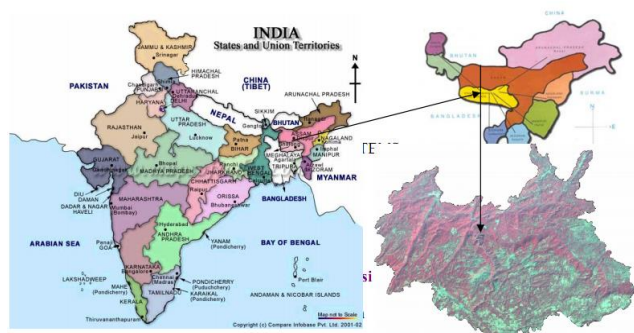


Fig 1: Location Map of Kulsi Basin

The Brahmaputra Board has proposed a reservoir in Kulsi River in Khasi Hills of Meghalaya for hydropower generation, Irrigation and flood Moderation. The Kulsi Multipurpose Project envisages construction of a dam across the river Kulsi at about 1.5

km downstream of Ukium village in Assam for hydro power, irrigation and flood moderation. Three saddles dams at Chikadonga, Mejengabari and Doledonga are proposed to be constructed for full utilization of the potential of the project. The reservoir so created will provide storage for multipurpose benefit of flood control, irrigation and power generation.

3. SALIENT FEATURES OF THE KULSI DAM PROJECT

Location of the Dam	:	Lat $25^{\circ}50'20''$ N
Project site	:	Long $91^{\circ}2'28''$ E (1.50 km D/S of Ukium village)
Name of river	:	Kulsi
Catchments area upto Dam site	:	1646.69 Sq. km
Dam site distance from NH 37	:	32 km
Average annual discharge	:	69.73 Cumec
Type of Dam	:	Rockfill dam
Gross command area	:	37908Ha
Net irrigation area	:	23882 Ha

4. METHODOLOGIES ADOPTED

This study proposes to optimize the control strategies for the Kulsi reservoir operation by applying a combination of simulation and optimization models. System analysis models used to optimize reservoir operation may be categorized as: simulation models; optimization models; and combination of simulation and optimization models. Simulation models are effective tools for studying the operation of complex physical and hydrological characteristics of a reservoir system including the experience and judgment of operators. However, since they are limited to predict the performance of a reservoir for a given operation policy, optimization models have an advantage in being able to search for the optimum policy from an infinite number of feasible operation policies that are defined through decision variables. In recent years, incorporation of an optimization technique into a simulation model to execute a certain degree of optimization has been advocated.

5. INPUT DATA

The average monthly inflows have been worked out from the 40 years of inflow data as collected and tabulated below. Table: 1 shows the average inflow in various months for preliminary planning purposes of the Kulsi Multipurpose Project.

Table: 1 Average Inflow Vs Month

Months	Average inflow (Mcm)	Months	Average inflow (Mcm)
May	47.456	November	52.303
June	94.866	December	36.534
July	150.476	January	25.571
August	132.848	February	21.564
September	117.426	March	18.805
October	93.975	April	29.767

It has been observed that the average monthly inflow for the month of July is highest as it is in the monsoon period subjected to heavy rainfall in entire North-Eastern region and it is lowest in the month of March.

Evaporation data available at the Lokapriya Gopinath Bordoloi International Airport, Borjhar, Assam, have been considered for the project as there is no evaporation data at the dam site at present.

It has been observed that the average evaporation for the month of December is highest and it is lowest in the month of September.

Gross command area of Kulsi Project has been estimated to be 37908 Ha. An area of 23882 Ha (Net Irrigable Area) is to be irrigated using the water of Kulsi reservoir.

Table: 2 Average Evaporation (mm/month) Data

Months	Average evaporation (mm/month)	Months	Average evaporation (mm/month)
Jan	157.93	Jul	68.61
Feb	158.71	Aug	52.12
Mar	147.76	Sep	39.11
Apr	146.22	Oct	67.66
May	118.62	Nov	139.01
Jun	106.20	Dec	162.30

The irrigation demands as assessed by the project authority have been considered for the purpose of the present study. The total annual irrigation demand is 171.27 Mcm. The monthly irrigation demand is highest in the month of April which is a pre-monsoon period; farmers are mostly prepared their paddy fields for sowing crop in this period. The monthly irrigation

demand is lowest in the month of February because this is mostly uncultivable season in this region.

6. MODEL FORMULATION

Ecological, irrigation and hydropower demands are considered in this model. As per the guidelines provided by National Water Development Agency, Govt. of India, 10% of the average non-monsoon flow is considered as ecological demand; and this amount should be available in the downstream river at any time. As per the National Water Policy in India, the ecological and irrigation demand are given higher priority than the hydropower demand. In Kulsi Project, irrigation and power generation are compatible, i.e., irrigation yields are also available for power generation. A combined simulation and non-linear programming model (NLP) is used. In simulation, it is assumed that in any time period if water is available, demand has to be met. The objective function of the NLP is chosen as to minimize the reservoir capacity by changing the firm power under all the constraints of conventional simulation model and also by maintaining irrigation release at minimum 75% reliability with given demand, and maintaining 90% reliability for firm power generation. Once the required reservoir capacity is obtained, only simulation model is run to assess the behavior of the project with changing scenarios and results of each run is recorded.

7. MODEL APPLICATION

The application of the model is started with the assumption that the initial storage in the reservoir is equal to 300 Mcm. Here 40 years of monthly inflow data is used and the month of "May" is considered as the start of each water year. The best fitted equations obtained from 'storage v/s elevation' and 'storage v/s area' curves, have been used in the simulation model. Initially firm power is assumed as 6 MW, reservoir capacity as 304.727 Mcm, tail water level as 51 m and plant capacity as 29 MW. From these data, by utilizing simulation and optimization model, the maximum annual hydropower, power reliability, irrigation reliability, average annual power, average annual irrigation, firm power are obtained. As per the guideline provided by National Water Development Agency, Govt. of India, 10% of the average non-monsoon flow is considered as ecological demand. With the minimum target reliability the scope to increase the irrigation supply is also obtained.

8. RESULTS

After developing the simulation model, the optimum reservoir capacity has been obtained by Non-Linear programming with Microsoft Excel Solver platform. The optimum reservoir capacity has been

obtained subject to constraints of irrigation reliability $\geq 75\%$ and power reliability $\geq 90\%$. Deterministic inflow, flow continuity, storage bounds, storage-area-elevation relationships, demand requirements, evaporation losses, spills, plant capacity constraints/relationships are incorporated in the model. The NLP gave minimum required reservoir capacity as 304.727 Mcm, fixing firm power at 90% reliability as 6.65 MW. The plant capacity assumed here is 29 MW as it is proposed by the authority. Simulation model is run to see the behaviour of the reservoir under different scenarios and summarized below.

Reservoir capacity 304.727 Mcm gives the best reliability of hydropower and irrigation. The firm power 6.65 MW gives the best reliability of hydropower and irrigation. The corresponding curve has been shown in fig.2.

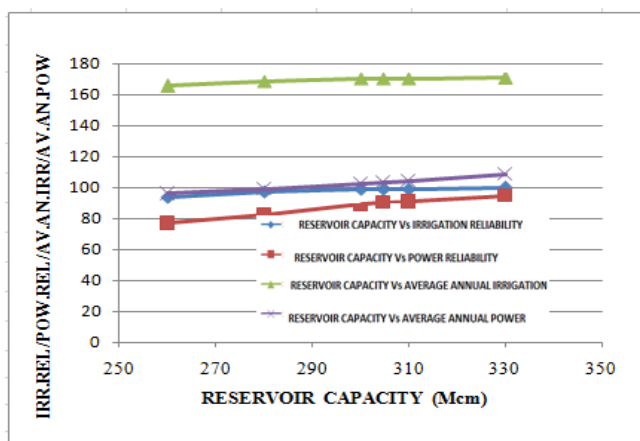


Fig 2: Reservoir capacity Vs irr. rel/pow.rel/ av.ann.irr/ av.ann.pow

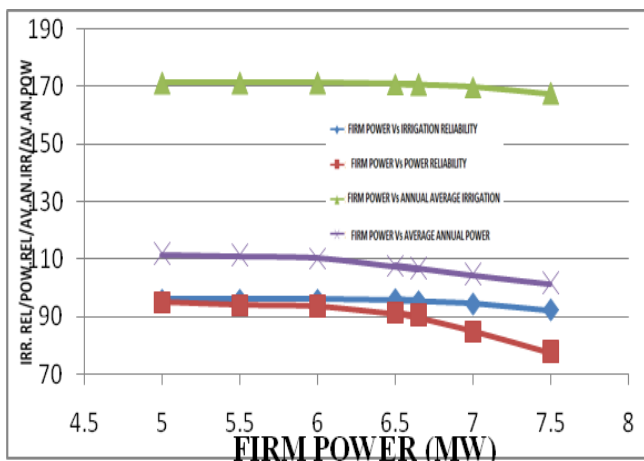


Fig 3: Firm Power Vs irr. rel/pow.rel/av.ann.irr/ av.ann.pow

The plant capacity 29 MW is fixed by the project authority. Since the turbine has a particular capacity, so the plant capacity can not increase or decrease without changing the turbine capacity. The corresponding curve has been shown in fig.3.

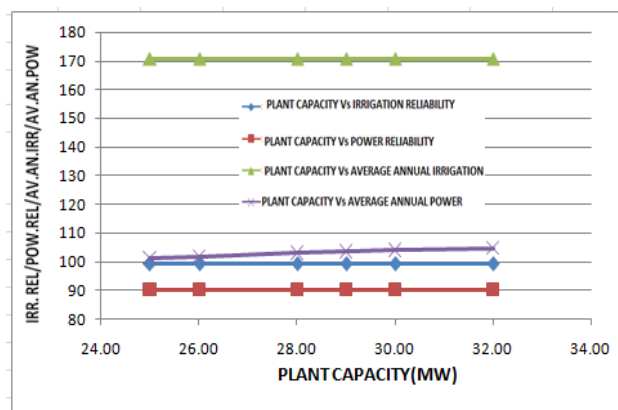


Fig 4: Plant capacity Vs irr. rel/pow.rel/av.ann.irr/ av.ann.pow

Though the given annual irrigation demand is 171.29 Mcm, the reliability of irrigation release obtained for this demand is 99.15%. This reliability is far more than the target reliability of 75%, which shows that the annual irrigation release can be increased. NLP model is run to see upto what extent of annual irrigation be increased without compromising the 90% power reliability and 75% irrigation reliability. It is observed that the annual irrigation can be increased upto 204.98 Mcm from 171.29 Mcm. To see, how these incremental increase in annual irrigation release affects the mean annual power generation, simulation model is run and results of each run is recorded. Considering reservoir capacity 304.727 Mcm and firm power 6.65 MW as constant, the annual irrigation demand is varied. Results of the iterations, where annual irrigation demand 204.98 Mcm gives the best reliability of hydropower and irrigation. Average annual irrigation demand and average annual power have been obtained corresponding to various annual irrigation demands without compromising 90% dependable firm power. It was seen that the annual irrigation demand can be increased up to 204.98 Mcm without compromising 90% dependable firm power and 75% reliable irrigation release. Average annual irrigation and average annual power at 171.29 Mcm annual irrigation demand are 170.69 Mcm and 103.48 MW, respectively; whereas, average annual irrigation and average annual power at 204.98 Mcm annual irrigation demand are 204.05 Mcm and 103.49 MW, respectively.

9. CONCLUSION

From the study, the following results have been obtained without compromising 90% dependable firm power and 75% reliability of irrigation. The optimum reservoir capacity has been found as 304.727 Mcm. The available firm power at any time is 6.65 MW. The plant capacity 29 MW is kept constant as it was fixed by the project authority. The maximum annual power 165.331

MW is found for the year 2000-2001. The average annual power and maximum monthly power are 103.49 MW and 23.2 MW respectively. The overall Power reliability and Irrigation reliability are 90.19 % and 99.15 % respectively. The Annual Irrigation Demand and Average annual irrigation are found as 204.98 Mcm and 204.05 Mcm respectively. Maximum Spill found is 573.102 Mcm in the month of July, 1984-85. The annual irrigation demand can be increased to 204.98 Mcm as against 171.29 Mcm without compromising 90% dependable power reliability and 75% irrigation reliability. The combined NLP and simulation model adopted here uses Microsoft Excel in Solver platform, and can be used by practicing engineers with ease. This simulation-optimization model may be practiced in other reservoirs also. The objective of the study was to develop a mathematical programming model: to determine maximum annual hydropower produced from the multipurpose reservoir, while meeting the irrigation and ecological demands for various specified levels of reliability.

REFERENCES

1. Sarma B, Srivastava D K (2005) "Simulation study of a river linking Project" HYPESD-2005, IIT Roorkee
2. R. Arunkumar, V. Jothiprakash (2012), "Optimal Reservoir Operation for Hydropower Generation using Non-linear Programming Model" [Journal of The Institution of Engineers \(India\): Series A](#), September 2012.
3. S. Xuewen Wu, Xianfeng Huang, Guohua Fang, Fei Kong (2011), "Optimal Operation of Multi-Objective Hydropower Reservoir with Ecology Consideration" *Journal of Water Resource and Protection*, 2011, 3, 904-911
4. Yeh W. W-G. (2003). "Reservoir management and operations models: A state of the art review." *Water Resour. Res.*, 21(12), 1797-1818.
5. Yeh WW-G. (1992), A stochastic inverse solution for transient groundwater flow: Parameter identification and reliability analysis, *Water Resour. Research.*, 28(12), 3269–3280, doi:10.1029/92WR00683. ...
6. Dr. Reddy J.R. "A Text Book of Hydrology". Laxmi Publishers, Third Edition.

Back to table of contents

Assessing applicability of Ecological Management Practices (EMPs) in hilly urban watershed management

Banasri Sarma ⁱ⁾ and Arup Kumar Sarma ⁱⁱ⁾

i) Water Quality Consultant, Public Health Engineering Department Assam, Betkuchi, Guwahati 781035, Assam, India.

ii) Professor, Civil Engineering Department, Indian Institute of Technology Guwahati, Guwahati Assam 781039, India.

ABSTRACT

Different landcovers exhibit different hydrological behaviors in terms of sediment and water yield during a storm event. Ecological Management Practices (EMPs) that are vegetative in nature can broadly be grouped into grass, creeper, forest, bushes etc. Before selecting a particular species for using as an EMP, one needs to know its implementation convenience, maintenance cost and conservation efficiency. An experimental study in a prototype scale can help in getting insight into these processes, which in turn helps in taking judicious measures for alleviating undesired impacts of unplanned residential development in hilly terrain. Therefore an experimental watershed was developed within the campus of IIT Guwahati and performances of two competitive EMPs (Grass and Golden Glory) in respect of soil conservation capabilities were assessed. Both the EMPs were found suitable for applying in hilly urban watershed of Guwahati, grass being more effective in controlling sediment yield.

Keywords: ecological management practices, urbanization, watershed management

1 INTRODUCTION

Hilly urban watersheds of Northeast India are becoming more and more vulnerable with the increasing population pressure. Haphazard developments in hilly watersheds of this region are observed to be the main culprit of massive soil erosion, landslides and extreme flash flood events in every monsoon. The Guwahati city covers an area of 383 km² (GMDA), of which a major part is occupied by hills. It has been observed that in Guwahati, though the majority of the urban developments are concentrated in the plain areas, in recent years, the built up areas are also observed to be expanding into its hilly areas with a very rapid rate. The expansion of built up areas in Guwahati city between 1972 and 2000, were about 3 times in the plains and approximately 10 times in the hills (Sarma et al., 2015). These rapid urban expansions of hilly areas are mostly haphazard and unplanned, associated with deforestation for land clearing and thus watershed degradation is continuing at an alarming rate.

Ecological Management Practices or EMPs are accepted as suitable and efficient urban watershed management practices, if adopted in a

logical and scientific manner (Sarma et al 2013). Vegetative EMPs can be used in hilly watersheds as an efficient controller of soil erosion which can broadly be grouped into grass, creeper, forest, bushes and other herbs. However, different vegetative landcovers exhibit different hydrological behaviors in terms of sediment and water yield during a storm event (Viessman and Lewis, 2008; Poff et al., 2006; Thanapakpawin et al., 2006). Again, different varieties are available within these groups which will be having varied soil conservation potential (Shino et al., 2007; Millard and Santos, 2008; Parajuli et al., 2008).

Hydrological response of different vegetation were analysed in various models and based on experimental study. Collins (2003), applying GLEAMS model in the Waiarohia catchment, predicted that grass buffer strip can reduce mean annual sediment yield by 20% that of the bare soil. Parajuli et al. (2008) applied the SWAT model to see the effectiveness of vegetative filter strips (VFS-lengths 10, 15 and 20 m) in removing sediment and fecal bacteria in the Upper Wakarusa watershed (950 km²) in northeast Kansas. The study estimated that about 73% of sediment yield can be reduced with a 10-m, 82% by a 15-m and 89% by a 20-m VFS. Gharabaghi et al. (2006) conducted a detailed

field based study with six different filter strips having combination of different species and tested their efficiency in terms of type & width of strip, and runoff flow rate and inflow sediment characteristics with artificial water supply. The study concluded that sediment removal efficiency increased from 50 to 98% as the width of the filter increased from 2.5 to 20 m. In addition, grass type and flow rate were found to be significant factors. Another field based study by Shiono et al. (2007) in Okinawa, Japan for centipede grass (*Eremochloa ophiuroides*) reported that the sediment removal efficiencies of 24% for the 0.5-m strip, 36 to 54% for the 1.5-m strip and 73% for the 3.0-m strip. The study also found that strips trapped well the sediment aggregates larger than 0.02 mm in diameter, regardless of strip length. Also, the longer strip trapped more aggregates of the 0.002–0.02-mm size class, which were dominant in the eroded sediment runoff from the plots. The strips poorly trapped aggregates smaller than 0.002 mm.

The efficiency of vegetative covers also depends on width and extent, and varies widely from place to place (Wenger, 1999). So far, no experimental study has been reported to establish suitability of different native vegetative EMPs of Northeastern part of India for application in urban watersheds. Therefore region specific experimental study is needed to analyse the applicability and efficiency of suitable EMPs. Therefore, an experimental watershed was developed within the campus of IIT Guwahati. The basic objectives of developing the experimental watershed were (i) to create a facility for studying performance of some competitive EMPs in respect of soil conservation capabilities and ease of maintenance, and (ii) to conduct experimentation on some selected competitive EMPs.

2 METHODOLOGY

To have an idea about erosion control efficiency of different EMPs, an experimental set up having facility of studying performance of 3 EMPs at a time was constructed as the experimental setup (Fig.1) in a small hilly

watershed (area=3948 m²) of IIT Guwahati campus (geographic location: 26^o11.439'N and 91^o41.452'E, elevation range: 65m to 95m, slope range: 0^o to 85^o). This experimental watershed resembled hilly area with developmental activities, where model houses were constructed to simulate the topographic conditions of a residential watershed. Three strips, each of length 4 m along the slope and of width 2 m across the slope were constructed for installing different EMPs. Varieties of grass species and other type of herbs, apparently having similar erosion control capacities, were identified. Based on convenience one indigenous common grass locally called bon in Assamese language and buffalo grass in English (Scientific name: *Paspalum conjugatum* (Poaceae) was selected for the study (Fig.2). The other selected species is an herb called Golden Glory or Wandering jew, (Scientific name: *Tradescantia zebrina* (Commelinaceae) was considered for the comparative study (Fig. 3). The reason of selecting this grass is that it is widely available and also grows easily even in undulated hilly terrain. The Golden glory is an ornamental herb having aesthetic view and thus this type of herb may be preferred for urban areas by some people. Another advantage of this species is that once grown, it requires minimal effort for maintenance and gives a good coverage within a short period.



Fig. 1. Experimental setup for performance analysis of EMPs.



Fig. 2. A close view of the grass used as EMP in the study.



Fig. 3. A close view of Golden glory used as EMP in the study.

Erosion control capabilities of these two vegetative measures were compared with that of bare land. All the strips were of equal area and similar slope condition were maintained in all the strips. Sediment traps were constructed at immediate downstream of each of these three strips. The three sediment traps were basically constructed by dividing a large chamber into three sub chambers, so that the sediment coming from these three strips can be collected separately in the three chambers and the relative efficiencies of these strips can be compared by weighing the amount of sediment that was collected in each of these three chambers. Each chamber was of 0.5 m depth, 2 m in length and 0.8 m in width.

An automatic rain gauge station (tipping bucket type) was installed near the experimental watersheds to have record of the rainfall characteristics for the study period. The rain gauge was set at a log rate of 10 min so that small duration rainfall could also be recorded. Runoff samples collected from the three chambers of the experimental setup was collected and the sediment concentration in the runoff was determined as per the guideline of ASTM (D 3977-97, method B). A known

volume of sample is then filtered through a glass fiber filter paper of 0.45 μm poresize. The filter paper was then dried and weighted, and then the sediment concentration is calculated as below:

$$S = \frac{F_w - I_w}{V} \quad (1)$$

Where,

S=sediment concentration (mg/ml)

I_w=Weight of the filter paper before filtration (mg)

F_w=Weight of the filter paper after filtration (mg)

V=Volume of sample taken (ml)

The particle size distribution of the eroded sediment from the strips was also studied by the Laser Particle Size Analyzer.

3 RESULTS AND DISCUSSION

Erosion control capability of two vegetative measures, namely, grass and Golden glory was compared with that of barren land. Grass showed a higher efficiency than Golden glory (Table 1). However, compared to barren land, Golden glory too could reduce sediment yield to a great extent. The experimental study on EMPs demonstrated that the application of EMPs can reduce soil erosion from a disturbed watershed area to a significant extent. The experimental study on two EMPs demonstrated good potential in controlling sediment yield as compared to sediment yield from barren land. Grass was observed to have potential of controlling sediment yield from 75% to 100% (average = 88%), whereas Golden glory had shown 36% to 97% efficiency (average = 64%).

Table 1: Sediment yield form the EMP strips

Date	Rainfall intensity (mm/hr)	Duration (min)	Barren (Kg)	Grass (Kg)	Golden glory (Kg)	Relative efficiency compared to barren land (%)	
						Grass	Golden Glory
2/5/2011	8.1	130	1.30	0.00	0.13	100	90
8/5/2011	9.1	30	0.51	0.18	0.31	65	38
16/5/11	5.6	150	0.07	0.01	0.02	86	71
22/5/11	29.4	210	1.17	0.01	0.04	99	97
24/5/11	2.5	30	0.01	0.00	0.00	100	80
28/5/11	38.1	130	0.14	0.01	0.03	96	80
2/6/2011	27	70	0.66	0.00	0.10	100	85
10/6/2011	3.04	140	0.58	0.00	0.04	100	93
12/6/2011	24.3	60	0.52	0.00	0.14	99	74

The particle size distributions of the sediment transported by the runoff from the barren land, Grass, Golden glory are presented in Table 2 and shown in the Fig.4, Fig 5 and Fig.6.

From these figures, it is clear that the particle size distribution is more uniformly graded in case of barren strip as compared to grass strip and the golden glory strip. This is because the surface of the bare land remains exposed to the direct impact of rain drop and surface runoff and thus because of splash erosion the soil gets detached and become finer. On the other hand with the coverage of grass or golden glory, the soil surface never gets subjected to the direct impact of rain drop. Runoff water carries some soil particles. A fraction of such eroded sediment gets detached during the process of

Table 2: Particle size distribution of sediments eroded from the EMP strips

Sample type	D10	D50	D90
Bare land	11.604 μm	72.642 μm	318.241 μm
Grass	21.071 μm	266.855 μm	734.995 μm
Golden glory	16.29 μm	237.225 μm	843.34 μm

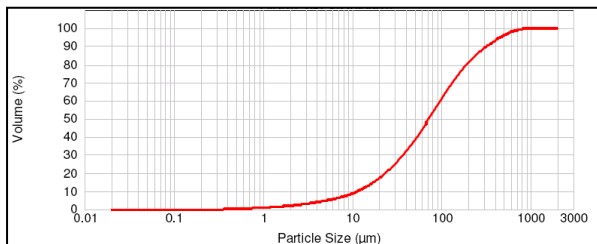


Fig.4. The particle size distribution in the sediments eroded from the barren strip

4 CONCLUSIONS

Assessing the impacts of converting forest or other natural landcovers into a residential area is essential to know the adverse consequences / impacts of unplanned residential development on the hydrological processes. An experimental study in a prototype scale can help in getting insight into these processes, which in turn helps in taking judicious measures for alleviating undesired impacts of unplanned residential development in hilly terrain. An experimental facility also helps in analyzing performance of different EMPs in respect of their soil and water conservation efficiencies. Before selecting a particular species for using as an EMP, one

needs to know its implementation convenience, maintenance cost and conservation efficiency. The study on sediment control efficiency of two competitive EMPs, Paspalum conjugatum (Poaceae) and Tradescantia zebrina (Commelinaceae) in 45° slope, showed that grass has sediment control efficiency up to 88% and Tradescantia zebrina has sediment control efficiency of 64% compared to that of bare land. Both these species were found to be convenient in terms of installation, maintenance and esthetic point of view. Therefore, grass and Golden glory can be conveniently used as sediment control measures in hilly urban areas with fair amount of

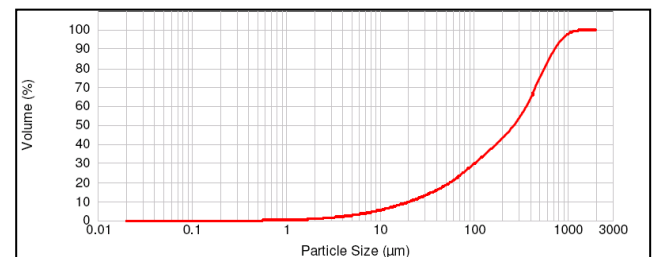


Fig.5. The particle size distribution in the sediments eroded from the grass strip

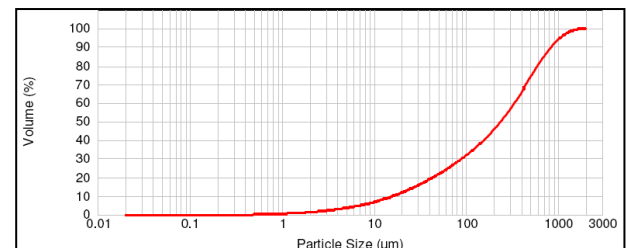


Fig.6. The particle size distribution in the sediments eroded from the Golden glory strip

needs to know its implementation convenience, maintenance cost and conservation efficiency.

The study on sediment control efficiency of two competitive EMPs, Paspalum conjugatum (Poaceae) and Tradescantia zebrina (Comelinaceae) in 45° slope, showed that grass has sediment control efficiency up to 88% and Tradescantia zebrina has sediment control efficiency of 64% compared to that of bare land. Both these species were found to be convenient in terms of installation, maintenance and esthetic point of view. Therefore, grass and Golden glory can be conveniently used as sediment control measures in hilly urban areas with fair amount of

success. Based on the study found in literature (Anbumozhi et al., 2005; Maillard et al., 2008; Parajuli et al., 2008) it is expected that the vegetative sediment controlling EMPs will also offer additional benefit of controlling nutrient loss from soil and screening of non point source pollutant generated at its upstream.

ACKNOWLEDGEMENTS

The work presented here is a part of the research work under Ministry of Urban Development (MoUD), Govt. of India sponsored project on Centre of Excellence (CoE) for “Integrated Landuse Planning and Water Resource Management”.

REFERENCES

- 1) Anbumozhi, V., Radhakrishnan, J. and Yamaji, E. (2005): Impact of riparian buffer zones on water quality and associated management considerations, *Ecological Engineering*, 24, 517–523.
- 2) ASTM (D 3977- ASTM D3977 – 97 (2007): Standard test methods for determining sediment concentration in water samples, *ASTM International Standard*, US.
- 3) Collins, R. (2003). Predicting sediment loss under proposed development in the Waiarohia catchment, *NIWA Client Report: HAM2003-063*, August 2003, NIWA Project: ARC03203, National Institute of Water & Atmospheric Research Ltd, Gate 10, Silverdale Road, Hamilton, P O Box 11115, Hamilton, New Zealand.
- 4) Gharabaghi, B., Rudra R.P. and Goel, P. K. (2006): Effectiveness of Vegetative Filter Strips in Removal of Sediments from Overland Flow, *Water quality Research Journal Canada*, 41(3), 275–282.
- 5) GMDA Building By-Laws (2006): Building By-Laws for Guwahati Metropolitan Development Authority (http://gmda.co.in/bldg_byelaws.htm as browse on 10th April 2012)
- 6) Maillard, P., and Santos, N.A. P. (2008): A spatial-statistical approach for modeling the effect of non-point source pollution on different water quality parameters in the Velhas river watershed – Brazil, *Journal of Environmental Management*, 86, 158–170.
- 7) Parajuli, P.B., Mankin, K.R. and Barnes, P.L. (2008): Applicability of targeting vegetative filter strips to abate fecal bacteria and sediment yield using SWAT, *Agricultural Water Management*, 95, 1189 – 1200.
- 8) Poff, N. L., Bledsoe, B. P. and Cuhaciyan, C. O. (2006): Hydrologic variation with land use across the contiguous United States: Geomorphic and ecological consequences for stream ecosystems, *Geomorphology*, 79, 264–285.
- 9) Sarma, B. and Sarma, A.K. and Singh, V.P. (2013): Optimal Ecological Management Practices (EMPs) for minimizing the impact of climate change and watershed degradation due to urbanization, *Water Resources Management*, 27(11), 4069-4082.
- 10) Sarma B., Sarma A.K., Mahanta C. and V.P. Singh(2015): Optimal Ecological Management Practices for Controlling Sediment and Water Yield from Hilly Urban Areas, *Journal of Hydrologic Engineering*, ASCE, 10.1061/(ASCE)HE.1943-5584.0001154 , 04015005.
- 11) Shiono, T., Yamamoto, N., Haraguchi, N. and Yoshinaga (2007): A Performance of grass strips for sediment control in Okinawa, Jarq-Japan, *Agricultural Research Quarterly*, 41(4),291-297.
- 12) Thanapakpawin, P., Richey, J. Thomas, D., Rodda S., Campbell, B. and Logsdon, M. (2007): Effects of landuse change on the hydrologic regime of the Mae Chaem river basin, NW Thailand, *Journal of Hydrology*, 334, 215–230.
- 13) Viessman, W. J. and Lewis, G. L. (2008): Introduction to Hydrology. *Prentice Hall of India*.
- 14) Wenger, S. (1999): A review of the scientific literature on riparian buffer width, extent and vegetation. Report of Office of Public Service & Outreach, Institute of Ecology University of Georgia, Revised Version March 5, 1999.

Back to table of contents

A case study on performance analysis of un-controlled intersection in Silchar, Assam

Debasish Dasⁱ⁾ Prof. Mokaddesh Ali Ahmedⁱⁱ⁾ Saikat Debⁱⁱⁱ⁾

i), iii) Ph.D Student, Department of Civil Engineering, NIT Silchar, Silchar, Assam, India.

ii) Professor, Department of Civil Engineering, NIT Silchar, Silchar, Assam, India

ABSTRACT

Mixed traffic prevails in the Indian roadways, particularly in the urban areas. In mixed traffic condition the road width is shared by all types of vehicles such as light motorized vehicles, heavy motorized vehicles and non-motorized vehicles. The rapid urbanization with economic growth results in a large volume of traffic during the peak hours in most of the Indian cities. Large traffic volume is the prime cause of traffic congestion at urban road network mainly at the intersections. Traffic congestion in urban area is a serious problem and is increasing day by day. The traffic congestion not only raises the vehicle operating cost, travel time of trip makers, but also it is the prime reason of poor performance at the intersection. In this study Silchar city has been selected as a case study area. Ambikapatti is considered for evaluation of performance. Ambikapatti is one of the major uncontrolled intersections in Silchar city. The performance of this intersection is investigated based on critical gap acceptance criteria.

Keywords: mix traffic condition, un-controlled intersection, gap acceptance, critical time, model estimation.

1. INTRODUCTION

Increasing trends of traffic in urban area is a major concern in all the cities in India. The unplanned roads, improper intersection design, narrow width of the road, lack of sight distance are the major area of concern for traffic engineers. The situation becomes more critical when different variety of vehicle sharing the same space on the roadway. The heterogeneous traffic is more diverse in nature due to lane changing and lack of lane discipline characteristics of driver's in India. The situation becomes more intense during the peak hours, when the traffic volume is increased by about 50% of the normal traffic.

2. LITERATURE REVIEW

Many research works have been done earlier. A number of literatures were tried to study to fulfill the objectives of this paper. Review for all types of intersections is discussed. Performance of uncontrolled intersections in a mixed traffic situation has always been a topic of interest among traffic engineers. Even in countries where uniform traffic conditions exist, uncontrolled intersection analysis always presents a complex scenario. This is mainly due to the unavoidable presence of critical gap in all capacity expressions. Though studies on critical gap are well documented in international literature its vastness indicates the complexities in the estimation of the procedure. One of the earlier study on gap acceptance, [1] reported that 50% of the gaps of 6.5s duration in the major road traffic stream were accepted by drivers and percentage of acceptance rose to 90 when the gap was 10s. Ashworth [2] found the effect main stream volume

on gap acceptance. Miller [8] compared nine different methods of critical gap estimation by generating 100 sets of artificial data through simulation; gaps offered were sampled from a displaced exponential distribution until one of them was accepted. The flow on main roads substantially influences the gap acceptance characteristics of drivers on the side roads [3]. The maximum likelihood method is suitable when the minor stream traffic is light and recommended the use of Siegloch's method when there is a continual queuing [10]. The critical gap for a priority movement at un-signalized intersection depends upon the amount of conflicting traffic [4]. The maximum likelihood technique also use to measure a driver's critical gap and proposed a methodology to define the gap event [11]. Highway Capacity Manual [9] provides base critical gap values for various movements of two-lane and four-lane major streets. These values adjusted for heavy vehicles, grade, two stages gap acceptance and for intersection geometry. Similar treatment is given to follow-up time also. A simplified theoretical approach also introduced for the determination of capacity at un-signalized intersections based on the method of additive conflict streams [5]. Indian Roads Congress [6] provides guidelines for design and capacity analysis of at-grade intersections in rural and urban areas. The critical gap values are given for passenger cars for various combination of vehicle maneuver, type of control, number of lanes and average running speed on major road. The concept of clearing time of a vehicle type under mixed traffic flow has been studied and found that, critical gap of U-turn vehicles obtained by conventional methods are quite low and there is a lot of variability in the critical gap values given by different

methods and concluded that methods developed under homogeneous traffic conditions do not hold good for mixed traffic conditions [7]. They proposed a method to determine critical gap which shows that value of critical gap vary with the type of maneuver and size of vehicle executing the maneuver. They also found that the entry capacity of a vehicle type is a function of conflicting traffic.

3. LOCATION OF INTERSECTION

Silchar is one of the oldest and largest cities of Nort-East India. Many commercial activities, industrial activities, educational institutes etc are situated in Silchar. The land use is not concentrated in a particular area. Keeping this fact in mind Silchar is considered as case study area. In this study, six numbers of intersections have been considered within Silchar city, Assam, India. Silchar is situated with Latitude 24.8200° N and Longitude 92.8000° E. As the selected intersections are situated in main central business district (CBD) area, these play a vital role in the transportation system. Selected area is shown in Fig 1. Location is selected on the basis of intensity of usefulness and poor traffic conditions by visual survey.



Fig. 1. Ambikapatti Intersection

4. METHODOLOGY

The study on uncontrolled intersection is based on critical gap analysis. The study methodology for the present study is indicated in Fig.2 in the form of a flowchart.

4.1. Field survey

Different field surveys, as indicated in Fig 2 are required for selected intersection to assess the performance. The survey need to be conducted and survey technique is tabulated in Table 1.

4.2. Survey methodology

A video camera is placed at a higher level of the intersection as shown in Fig 3. The data were recorded for each 15 min/ hr of our survey duration i.e. from 9:30 hours to 19:30 hours on a typical week day.

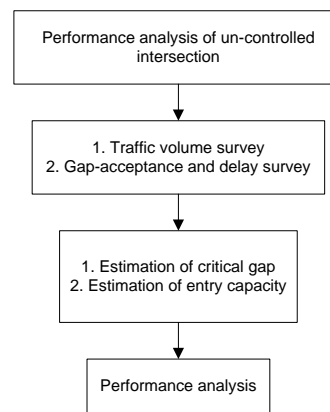


Fig 2: Methodology flow chart

Table 1: Types of surveys required for the study

SL. NO.	NAME OF INTERSECTION	TYPES OF SURVEY	SURVEY TEQNIQUE
1	Ambikapatti intersection	<ul style="list-style-type: none"> Traffic(entry volume) Turning movement Gap-acceptance Clearing time for vehicle 	Videography



Fig 3: Traffic survey, gap-acceptance time survey and clearing time survey at Ambikapatti

4.3. Data extraction

Video graphic survey is conducted to record the traffic scenario of the locations. After completing the survey we extract the video from camera via usb cable to Laptop. Then the video is played in VLC Media player in slow mode and calculate the number of arrival and departure of different type of class of vehicles. For both off-peak and peak hour the cumulative arrival rate and cumulative departure rate has been recorded.

5. INTERPRETATION

The geometric features were measured physically. Traffic survey was conducted on a typical week day from 9:30 hours to 19:30 hours. The interpreted result is shown in later sub-sections. The video graphic survey conducted at Ambikapatti intersection. Right turn of traffic from minor street maneuver has been ascertained as the most critical one from the trial survey. The video graphic survey data were analyzed. The hourly conflicting traffic volume is extracted and presented in

Table 2.

Table 2: Conflicting traffic volume at different hour of day

HOUR	NO.OFHOUR	CONFLICTING TRAFFIC VOLUME IN PCU (15MIN DATA)
09:30-10:30 HOURS	1 ST HOUR	1938
11:30-12:30 HOURS	2 ND HOUR	3000
12:30-13:30 HOURS	3 RD HOUR	1708
13:30-14:30 HOURS	4 TH HOUR	322
14:30-15:30 HOURS	5 TH HOUR	676
16:30-17:30 HOURS	6 TH HOUR	3686
18:30-19:30 HOURS	7 TH HOUR	3922

5.1. Gap-acceptance Time Data Extraction

Gap-acceptance time for each class of vehicle is extracted from recorded video. During computation gap, if made by queue of vehicles are ignored. The insignificant component consisting of bicycles, cycle rickshaws and heavy vehicles (entry restricted) were neglected in present study. The gap-acceptance time with respect to volume for “car” are presented in Table 3 as sample calculation. In the similar way the

gap-acceptance is also calculated for auto rickshaw and two-wheelers. Value outside bracket indicates time in second and within bracket no of vehicle

5.2. Clearing Time Data Extractions

The clearing time, one of crucial element involved in determine critical gap. The clearing time is the time required from extreme boundary of influence area. The clearing time as well as the numbers is extracted from the video for all three types of vehicle. The result for “car” is shown in Table 4 as a sample calculation.

Using gap-acceptance data, a new set of data is framed for different type of vehicles at various class interval of gap-acceptance time. In a similar way by clearing time and respective cumulative percentage of vehicle are calculated. The calculated data for gap-acceptance and clearing time are used to generate cumulative frequency distribution curves (Fig. 4). The computation will be different for critical time if the traffic on major road is comparatively lower. In such case the graph of clearing time is plotted by deducting the cumulative percentage of vehicle from 100. The graph is shown in Fig 5 (for car, 14:30 hours-15:30 hours).

Table 3: Gap-acceptance time and respective volume of car

Sl.No.	1 st Hour	2 nd hour	3 rd hour	4 th hour	5 th hour	6 th hour	7 th hour
1	4 (2)	2 (1)	5 (6)	8 (6)	6 (6)	2.5 (1)	2 (1)
2	6 (5)	3 (2)	6 (5)	9 (4)	7 (4)	3.5 (2)	3 (3)
3	8 (9)	4 (3)	7 (9)	10 (6)	8 (6)	4.5 (4)	4 (6)
4	10 (6)	5 (9)	8 (6)	11 (6)	9 (6)	5.5 (8)	5 (10)
5	12 (1)	6 (14)	9 (1)	12 (3)	10 (3)	6.5 (6)	6 (5)
6	-	7 (8)	-	13 (1)	11 (1)	7.5 (5)	7 (2)
7	-	8 (2)	-	-	-	8.5 (2)	9 (1)
9	-	9 (1)	-	-	-	9.5 (1)	10 (1)
10	-	-	-	-	-	-	11 (1)

Table 4: Clearing time and respective volume of car

Sl.No.	1 st Hour	2 nd hour	3 rd hour	4 th hour	5 th hour	6 th hour	7 th hour
1	2 (2)	3 (15)	3.5 (10)	10.5 (1)	7 (1)	3.5 (6)	2 (10)
2	4 (3)	6 (7)	5.5 (3)	12.5 (10)	9 (10)	7.5 (6)	4 (6)
3	8 (5)	9 (5)	7.5 (5)	14.5 (7)	11 (7)	11.5 (4)	6 (4)
4	11 (6)	12 (5)	9.5 (4)	16.5 (5)	13 (5)	15.5 (3)	8 (4)
5	14 (3)	15 (4)	11.5 (2)	18.5 (2)	15 (2)	19.5 (2)	10 (2)
6	17 (2)	18 (2)	13.5 (1)	20.5 (1)	17 (1)	23.5 (2)	12 (2)
7	20 (1)	21 (2)	15.5 (1)	-	-	27.5 (1)	14 (2)
8	23 (1)	-	17.5 (1)	-	-	31.5 (1)	16 (1)
9	-	-	-	-	-	-	18 (1)
10	-	-	-	-	-	-	-

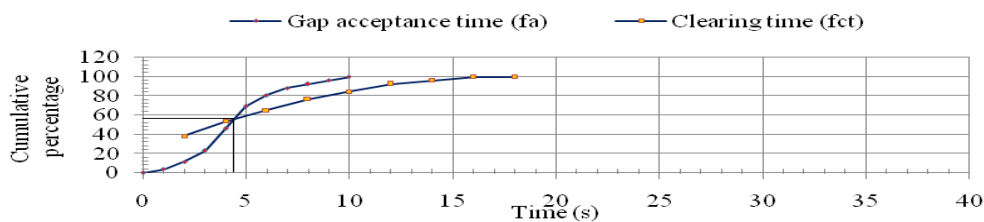


Fig 4: Cumulative frequency distribution curves for gap-acceptance time and clearing time

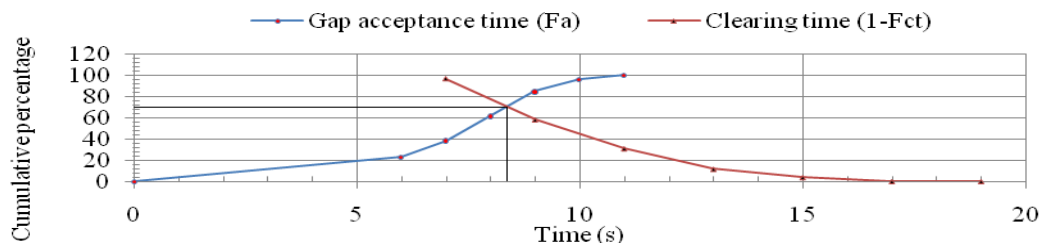


Fig 5: Cumulative frequency distribution curves for gap-acceptance time and clearing time (1-fct).

The intersecting point of two curves as shown in Fig 4 and Fig. 5 are the critical gap-acceptance time. The critical gap time and the respective volume at different hours are shown in Table 5.

Table 5: Critical gap time for different vehicles

CONFLICTING TRAFFIC VOLUME (VPH)	CRITICAL-GAP(SEC)		
	CAR	AUTO	BIKE
3922	4.72	4.39	2.98
3686	4.85	4.41	3.1
3000	5.47	4.95	3.6
1938	6.24	5.49	3.74
1708	6.5	5.83	3.92
676	8.37	6.08	4.41
322	11	7.44	5

5.3. Entry Capacity:

Entry capacity is one of the important parameter of the performance analysis of uncontrolled intersection. The mean follow-up time is used to calculate the entry capacity. The follow-up time is measured directly from the survey records. The calculated data of mean follow-up time are shown in table entry capacity are shown in Table 6.

Table 6: Mean follow-up time observed

SL NO.	VEHICLETYPE	MEANFOLLOW-UP(TIME)(SEC)
1	CAR	1.7
2	AUTO-RICKSHAW	2
3	TWO-WHEELER	1.2

The well established Blunden’s equation is used to calculate the entry capacity of each class of vehicle for a particular maneuver (right turn from minor street).

The calculated entry capacities for each type of vehicles are shown in Table 7.

Table 7: Entry capacities of vehicles for different conflicting traffic volume

CONFLICTING TRAFFIC VOLUME (VPH)	CRITICAL-GAP(SEC)		
	CAR	AUTO	BIKE
3922	27	37	209
3686	31	46	218
3000	42	60	236
1938	112	153	544
1708	141	175	613
676	514	689	1464
322	853	1010	2023

6. RESULT AND DISCUSSIONS

The primary criteria set for performance analysis for an uncontrolled intersection is the entry capacity of vehicles. The critical maneuver in Ambikapatti intersection is right turn from Minor Street. In analyzing the performance of the uncontrolled intersection critical-gap time for each type of vehicle is required to be plotted against conflicting traffic volume for that maneuver. The required data are extracted for car (from Table 3 and Table 4), auto-rickshaw and two-wheelers and the pattern of the graph is shown in Fig 6.

There are three numbers of graphs for car, auto and two wheeler showing. All the three graphs are showing declining trend.

The nature of the curve is logarithmic in nature. The equations and the R² values are shown in Table 8.

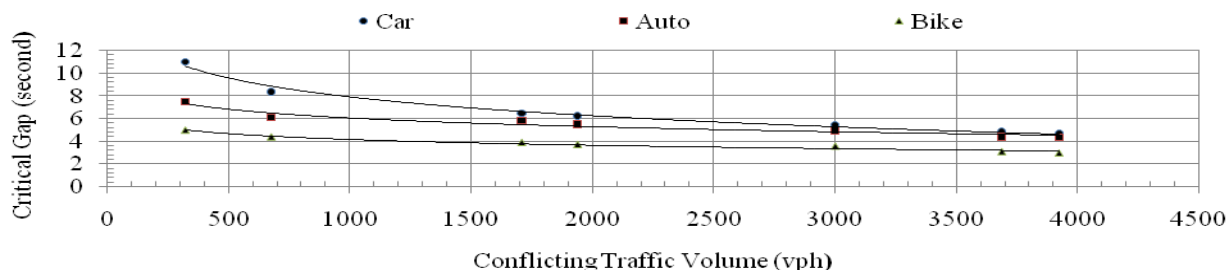


Fig 6: Variation of Critical Gap with Conflicting Traffic Volume for Each Class of Vehicles

Table 8: Curve equation and R² values for different classes of vehicles

VEHICLE TYPE	EQUATION OF CURVE	R ² VALUE
CAR	$Y = 2.38 \ln(X) + 24.41$	0.985
AUTO	$Y = 1.11 \ln(X) + 13.75$	0.939
TWOWHEELER	$Y = 0.74 \ln(X) + 9.324$	0.957

The logarithmic nature of curves suggests that the considerable reduction in critical gap time with rise of conflicting traffic volume. All the three types of vehicle follow more or less the same pattern. The functional forms of critical gaps with conflicting volumes have uniformity in all the types of vehicles. Higher R² values represent the minimum error in fitting those curves.

7. CONCLUSION

In the present study the performance of uncontrolled intersection is studied. The prime performance indicators for uncontrolled intersection are critical gap time and the conflicting traffic volume. The individual vehicle (class) entry capacity and the overall mixed entry capacity for a particular maneuver are evaluated. These capacities give us the fair idea about the performance of the intersection.

8. REFERENCES

[1] Ashworth, R., and B. D. Green.(1966), "Gap acceptance at an uncontrolled intersection." *Traffic Engineering and Control* 7.11: 676-678.

[2] Ashworth R., (1969), "The capacity of priority-type intersections with a non-uniform distribution of critical acceptance gaps", *Transportation Research*, 3, pp. 273-278.

[3] Adebisi O, Sama GN, (1989), "Influence of stopped delay on driver gap acceptance behavior", - *Journal of Transportation Engineering*, 1989 - ascelibrary.org.

[4] Brilon, W., Koenig, R. and Troutbeck, R.J., (1999). "Useful estimation procedures for critical gaps", *Transportation Research Part A: Policy and Practice*, 33(3), pp.161-186.

[5] Brilon, W. and Wu, N., 2001. "Capacity at

unsignalized intersections derived by conflict technique". *Transportation Research Record: Journal of the Transportation Research Board*, (1776), pp.82-90.

[6] Congress, I.R., 1994, "Guidelines for the Design of at grade intersections in rural and urban areas", *IRC SP*, pp.41-1994.

[7] Datta, S. and Bhuyan, P.K., 2014, "Estimation of Critical Gap for U-turn Vehicles at Median openings Under Mixed Traffic Conditions", *INROADS-An International Journal of Jaipur National University*, 3(1s), pp.133-141.

[8] Miller J.Alan, (1974), "A Note on the Analysis of Gap-Acceptance in Traffic" *Journal of the Royal Statistical Society. Series C (Applied Statistics)*, Vol. 23, No. 1 (1974), pp. 66-73, DOI: 10.2307/2347055.

[9] Manual, H.C.,2000, "Highway capacity manual (HCM)", *Washington, DC*.

[10] Troutbeck, R.J., (1992), "Estimating the critical acceptance gap from traffic movements", *Queensland University of Technology*.

[11] Tian, Z., Vandehey, M., Robinson, B.W., Kittelson, W., Kyte, M., Troutbeck, R., Brilon, W. and Wu, N., (1999). "Implementing the maximum likelihood methodology to measure a driver's critical gap", *Transportation Research Part A: Policy and Practice*, 33(3), pp.187-197.

[Back to table of contents](#)

Prediction of Shear Parameters of Soil Using Artificial Neural Network

Arunav Chakrabortyⁱ, Ankurjyoti Bhattacharyaⁱⁱ, Aditya Pratim Sarmaⁱⁱ, Lakhyajit Sarmahⁱⁱ, ArnabJyoti Dasⁱⁱ, Aminul Islamⁱⁱ

i)Assistant Professor, Civil Engineering Department, Tezpur University

ii)B.Tech Students, Civil Engineering Department, Tezpur University

ABSTRACT

The world of Civil Engineering comprises of activities which deals with the construction aspects of various projects taking place all around the world. An inevitable part of this vast world of Civil Engineering is Geotechnical Engineering where studies related to soil analogy is carried out. Any project requires a thorough study of the ground and soil conditions on which the structure is to stand. This makes it mandatory to determine the various parameters defining the strength and stability of soil. But the determination of each and every parameter would be quite cumbersome, time consuming and uneconomical. Hence the need of the hour is to establish a proper relation between two or more parameters so that experimental determination of just one or two parameters would enable us to determine others. This project deals with formulating a prediction model that predicts the values of shear parameters from Optimum Moisture Content (OMC) and Maximum Dry Density (MDD) using Artificial Neural Network (ANN). By determining the shear parameters we can help in the process of soil stabilisation and slope analysis. Thus this project can help in sustainable development of rural and urban areas.

Keywords: Optimum Moisture Content, Maximum Dry Density, Artificial Neural Network, Shear Parameters, Slope Stabilisation, Sustainable Development.

1. INTRODUCTION

Because of interest to development of urban areas in plains, many projects must be conducted on or in soils. In a world where civil infrastructures are regularly being established on a daily basis, soil study has become a must. The determination of shear parameters of soil such as cohesion (c) and internal friction angle (Φ) has become inevitable for engineering works. These parameters are an indication of the bearing capacity of the soil, stability of slopes and further give us evidence of all other minute information required for understanding the feasibility of constructing a particular structure on a soil stratum, and if found not feasible, then also we can decide the method and amount of soil strengthening to be done based on these shear parameters.

But the study of these soil parameters of the soil at and around the construction site by various tests such as direct shear test, UCS, etc. are quite cumbersome, time consuming and uneconomical, along with leading to a lot of environmental destruction. These drawbacks cease to keep our testing and construction works in agreement with the principles of 'sustainable development'. Thus, the requirement of predicting shear parameters was felt leading to researches conducted to find correlation between shear strength parameters and index properties of soil. In this paper, a study has been done to find a correlation between compaction

parameters and shear parameters both cohesive and cohesionless soils using ANN.

The 21st century has seen tremendous development in the world of computers and their application in the scientific world for various computational purposes such as the ANN. *Basma et al. (2003)* demonstrated another application of ANN by modelling time dependent swell of expansive soils. *Chang and Chao (2006)* investigated the application of back-propagation networks in debris flow prediction and it was quite evident from their results that using ANN for prediction gives values of acceptable accuracy. Furthermore, ANN was used to assess the shallow landslide susceptibility in Jabonosa River Basin by Gomez and *Kavzoglu (2008)*. *Tiryaki (2008)* also used multivariate statistics, artificial neural networks, and regression trees for predicting intactrock strength for mechanical excavations while *Moosavi et al. (2006)* applied ANN for modeling the cyclic swelling pressure of mudrock. ANN was also used by *Das and Basudhar (2008)* for prediction of residual friction angle of clays. *Kayadenal et al. (2009)* used Genetic Expression Programming (GEP) along with (ANN) and Adaptive Neuro Fuzzy (ANFIS) to predict effective angle of shearing resistance. *G.R Khanlari, M. Heidari, A.A Momeni, Y. Abdilor* too gave their contributions in prediction of shear strength parameters using artificial neural networks and multivariate regression methods.

2. MATERIALS AND METHODS

2.1 Sampling and data analysis

In order to find out the intended correlation between the above mentioned parameters, carrying out the laboratory tests on different types of soil samples was the first step. The procedures of the tests were followed as per Indian Standard Codes given in Table 1. The laboratory tests results were used to formulate the ANN prediction model using Matlab R2011a. Depending on the requirement of the project, the tests carried out were grain size distribution, Atterberg Limits, Standard Proctor test (light compaction test) and direct shear test. A total of 25 samples were collected for this research from inside and around the campus territory of Tezpur University, Napaam, Assam, India. A prediction model was formulated for predicting the shear parameters from compaction parameters using ANN.

Table 1: Tests on samples and IS codes followed

Soil test performed	IS Code followed
Soil classification	IS 1498-1970
Light compaction test	IS 2720 (Part VII)-1980
Direct shear test	IS 2720 (Part 13)-1986
Liquid limit	IS 2720 (Part V)-1985
Plastic limit	IS 2720 (Part V)-1985

2.2 Artificial Neural Network

An Artificial Neural Network (ANN) is a mathematical model based on the neural structure of the brain. It is an inter-connected group of artificial neurons, which can process information using a connectionist approach to computation. ANNs are capable of identifying and correlating patterns between input data sets and corresponding target values. In our case, the input data set comprise of the compaction parameters whereas the shear parameters are the target values. After training, ANNs can predict the outcome of new independent input data. ANN finds use in many geotechnical problems like pile capacity prediction, modelling soil behaviour, slope stability, earth-retaining structures, design of tunnels etc. The data set is divided into three distinct sets called training, testing and validation. The training set is the largest set and is used by neural network to learn patterns present in the data. The testing set is used to evaluate the generalization ability of a supposedly trained network. A final check on the performance of the trained network is made using validation set.

3. RESULTS AND DISCUSSION

The Shear parameters and Compaction parameters for 25 numbers of soil samples collected from in and around Tezpur University Campus has been shown in Table 2.

Table 2: Laboratory Test Results for different types of Soils

Sample No.	OMC (%)	MDD (kN/m ³)	C (kN/m ²)	Φ (degree)
1	14.5	18.05	44.06	23.219
2	22	16.70	24.35	27.07
3	17.2	17.07	36.44	26.197
4	22.5	15.70	16.34	32.781
5	23	16.24	17.63	23.75
6	21.1	15.87	44.61	30.79
7	21.8	17.17	9.97	31.13
8	21	16.83	14.91	21.006
9	28.14	15.40	14.04	37.38
10	16.1	17.43	48.08	16.119
11	13.5	18.47	44.14	23.66
12	14.7	17.93	40.9	21.68
13	23.2	16.26	21.9	30.23
14	21.7	16.43	27.16	27.84
15	15.1	17.78	38.82	20.32
16	16.6	17.30	35.76	19.92
17	23.5	16.23	18.78	31.07
18	22.9	16.30	24.24	29.55
19	21.3	16.48	27.04	27.23
20	14.2	18.14	43.05	23.07
21	24	16.17	12.77	32.67
22	22.8	16.31	24.84	29.37
23	24.7	16.07	6.692	34.39
24	13.8	18.32	43.86	23.53
25	24.3	16.13	9.611	33.53
26	22.2	16.38	26.84	28.49
27	20.17	16.62	30.29	25.52
28	19.82	16.66	33.97	25.24

29	17.25	17.14	36.03	24.5
30	18.63	16.85	39.24	28.6

The input parameters include Optimum Moisture Content (OMC) and Maximum Dry Density (MDD) followed by Cohesion (C) and Angle of Internal Friction (Φ) as the target value.

3.1. Artificial Neural Network (ANN)

The ANN was done in Matlab R2011a. The data set was divided into three distinct sets viz., training set, testing set and validation set. Out of 25 samples, 20 samples were used in the training of the model where 50 % of the data set was used for training and 25 % of the data set was used for both testing and validation.

After validation and testing the network is trained up using Levenberg-Marquardt back propagation till the regression coefficient R approaches to unity. An R value of 1 means a close relationship and 0 a random relationship. When the value of R of all the three sets training, validation and testing approaches close to unity, it is assumed that the prediction equation attains a close relationship and the training process is terminated. The regression plot showing the value of R for training, validation and testing for different slope stability methods is shown in figure 1.

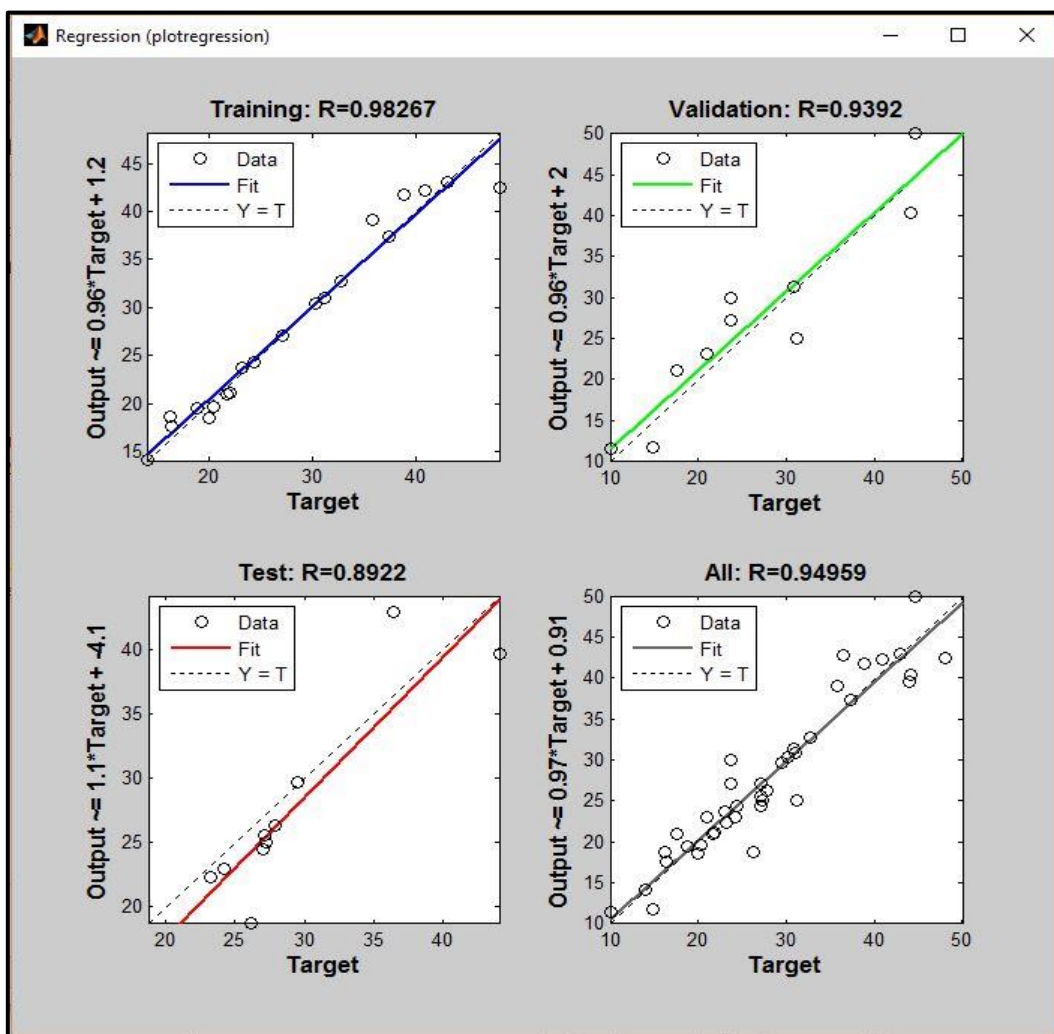


Fig 1: Regression plot for training, testing and validation set

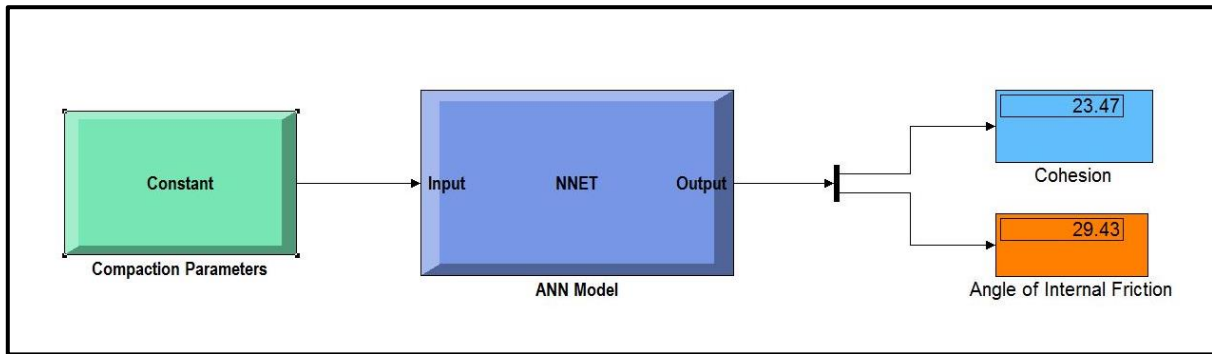


Fig 2: ANN prediction model

The prediction model obtained by ANN was validated by comparing the values of C and Φ obtained by laboratory methods for the last 5 samples. The

comparison graph of actual value and predicted value is shown in figure 3 and 4.

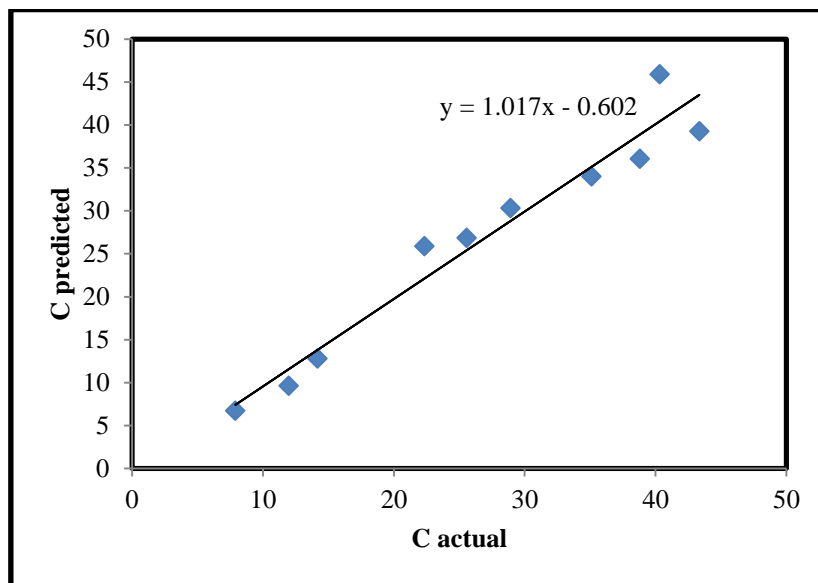


Fig 3: Graph showing predicted value and actual value for cohesion (C)

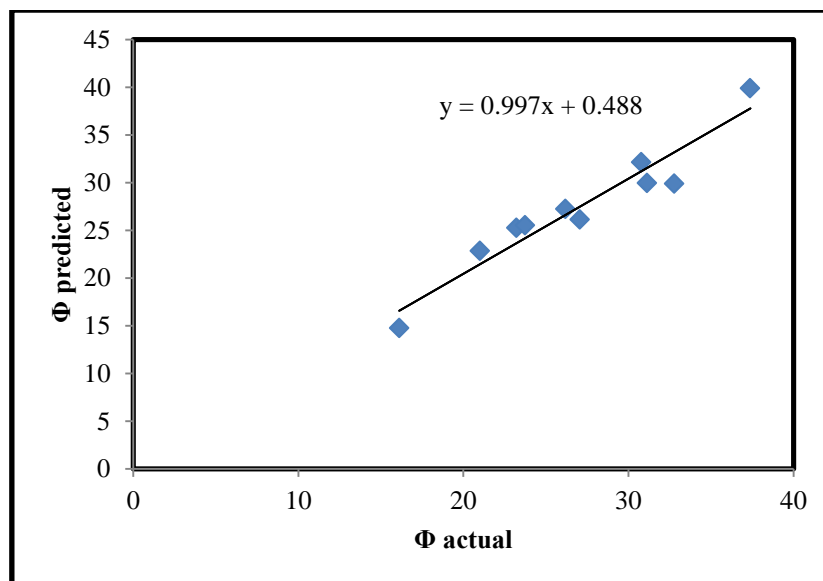


Fig 4: Graph showing predicted value and actual value for angle of internal friction (Φ)

From figure 3 and 4, it has been found that the actual values and the predicted values of cohesion and angle of internal friction using ANN bear a linear relationship. Moreover, from figure 1, it has also been found that the R value approaches very close to unity and thereby obtaining a close relationship between compaction parameters and shear parameters. Hence, ANN can be used as a tool for predicting the shear strength parameters from the compaction parameters.

4. CONCLUSION

From the graphs it can be seen that our predicted values from ANN are very close to the experimentally obtained values. This is a proper depiction of the usefulness of ANN. Not only does it save a lot of time, but also it does save a lot of cost as testing all types of samples is not very cost effective. Hence, ANN can be used as a tool for predicting the shear strength parameters from the compaction parameters.

REFERENCES

1. Baykasoglu, A., Gullu, H., Canakci, H., Ozbakir, L. (2008), Prediction of compressive and tensile strength of limestone via genetic programming. *Expert Systems with Applications* 35, pp. 111–123.
2. Bowles, J. E. (1988), *Foundation analysis and Desig*, McGraw-Hill International Edition, Singapore.
3. Canakci, H., Baykasoglu, A., Gullu, H. (2009), Prediction of compressive and tensile strength of Gaziantep basalts via neural networks and gene expression programming. *Neural Computing & Applications* 18, pp. 1031–1041.
4. Das S. K. and Basudhar P. K. (2008), Prediction of residual friction angle of clays using artificial neural network, *Engineering Geology*, 100(3-4), pp. 142-145.
5. Garson, G.D. (1991), “Interpreting neural-network connection weights.” *Artificial Intelligence Expert* 6(7), pp. 470–51.
6. Gomez H, Kavzoglu T. (2005), Assessment of shallow landslide susceptibility using artificial neural networks in Jabonosa River Basin, Venezuela, *Engineering Geology*, 78(1-2), pp. 11-27.
7. IS 1498-1970: Classification and identification of soils for general engineering purposes.
8. IS 2720 (Part VII)-1980: Methods of test for soils part vii determination of water content-dry density relation using light compaction
9. IS 2720 (Part 13)-1986: Methods of test for soils: part 13 direct shear test
10. IS 2720 (Part V)-1985: Methods of test for soils: part 5: determination of liquid and plastic limit
11. Kayadelen C, Günaydın O, Fener M, Demir A, Özvan A. (2009), Modeling of the angle of shearing resistance of soils using soft computing systems, *Expert System with Applications*, 36(9), pp. 11814-11826.
12. MacKay, D. J. C. (1992), Bayesian interpolation. *Neural Computation* 4(3), pp. 415-447.
13. Moosavi M, Yazdanpanah M. J, Doostmohammadi R. (2006), Modeling the cyclic swelling pressure of mudrock using artificial neural networks, *Engineering Geology*, 87(3-4), 178-194.
14. Tiryaki B. (2008), Predicting intact rock strength for mechanical excavation using multivariate statistics, artificial neural networks, and regression trees, *Engineering Geology*, 99(1-2), 51-60.

[Back to table of contents](#)

An Urban Heat Island magnitude study over the city of Guwahati-An integration of Remote Sensing and Ground based approach

Ajanta Goswamiⁱ⁾, Pir Mohammadⁱⁱ⁾, Ashim Sattarⁱⁱⁱ⁾, Rahul Mahanta^{iv)}, Stefania Bonafoni^{v)}

i) Assistant Professor, Department of Earth Sciences, IIT Roorkee, Uttarakhand-247667, India.

ii) Ph.D. Student, Department of Earth Sciences, IIT Roorkee, Uttarakhand-247667, India.

iii) Ph.D. Student, Department of Earth Sciences, IIT Roorkee, Uttarakhand-247667, India.

iv) Associate Professor, Department of Physics, Cotton College, Guwahati-781001, India.

v) Faculty, Department of Electronic and Information Engineering, University of Perugia, Perugia-06125, Italy.

ABSTRACT

The city of Guwahati is the prime hub for the entire north east India. It is one of the fastest growing cities of India at present day. The immigration of a huge amount of population from the surrounding states is leading to its urban extension. The major growth of the city initiated in the previous decade and is consistent and progressive throughout. A formation and growth of Urban Heat Island over the city of Guwahati is well evident. It is also understood that urbanization has led to the substantial growth of the city of Guwahati, making it the largest in north east India. This study aims the growth of UHI over the city for a period of 10 years from the year 2005 to 2015. It also depicts the effect of local meteorological parameters like temperature and precipitation acquired using automatic weather stations (AWS) and ground based stations. A temporal assessment of the LST (Land Surface Temperature) using MODIS (Moderate Resolution Imaging Spectroradiometers) data aids the growth of UHI over the city in terms of both magnitude and extent. The geospatial investigation shows a growth of UHI magnitude from 4.6°C in 2005 to 5.8°C in 2010 and also growth in its lateral extent from 62 km² to 66 km². The UHI magnitude in 2015 shows a value of 5.8 °C, the possible reason is due to cooling effect of the city as evident from the precipitation ground based data.

Keywords: Urban Heat Island (UHI), MODIS, Guwahati, LST, Gaussian fit

1. INTRODUCTION

The concept of Urban Heat Island is gaining importance with time as there is a significant increase in the urban heat generated and gradual expansion of the city limits. The phenomenon of a profound temperature difference between the urban and the surrounding area due to anthropogenic interference is called Urban Heat Island. The urban heat Island studies have been known from 1960 (Nieuwolt, 1966). Studies for UHI revealed either by the employment of ground based or remote sensing method. The ground based measurements emphasises on the point ground measurements to study the effect of UHI. On the contrary remote sensing method analyses spatial data in the thermal band to understand the temperature change (Chen, Wang & Li, 2002). Rao, 1972 introduced the application of thermal remote sensing using satellite to study urban areas. In this paper a study on the UHI pattern for the city of Guwahati for a period of 10 years using remote sensing method has been done. The thermal band is used to study the land surface temperature, also known as the skin temperature which depends on the thermal properties of the sensed material. Therefore LST has a direct correlation with the thermal inertia of the materials. For example concrete and tar would absorb and radiate more heat as

compares to vegetation and water. Various Indices like NDVI, NDWI and NDBI are indicative of UHI (Gao, 1996). Land use and land cover changes has a prominent impact on the magnitude of an area.

2 STUDY AREA AND CLIMATE

Guwahati located in north eastern part of India is a major riverine port city and among the fastest growing cities of India in the 20th century. It is situated in the south bank of river Brahmaputra in the foothills of the Shillong plateau. It lies within 26.10° N latitude and 92.49° E longitude at an altitude of 55.5 m above the mean sea level. The total geographic area of the city is 127.84 sq km. The urban area of the city is around 262 km² and has a population of about 12 lakh (Census of India, 2011). The climatic patterns of the region is characterized by humid subtropical hot climate, mild dry winters and hot humid summers. The average temperature of the city is 24.2° C. The average annual rainfall of the city is around 1722 millimeters.

3 DATA USED

In this study both remotely sensed datasets and data from ground based stations including automatic weather stations (AWS) is used for the study of urban

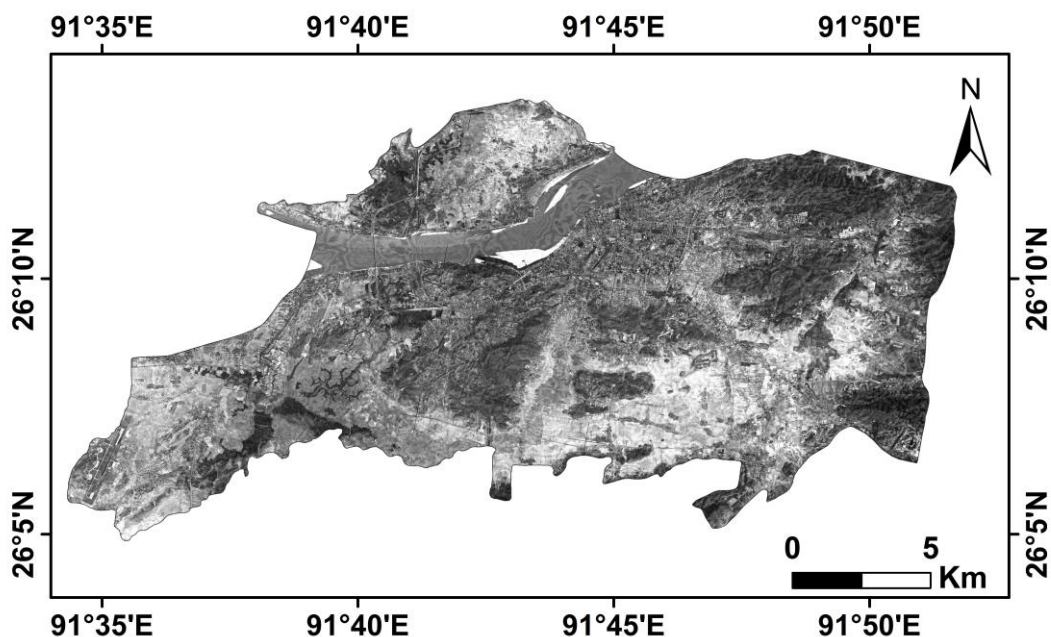


Fig 1: Location map of the study area

heat island (UHI) of the region. The MODIS (Moderate Resolution Imaging Spectroradiometers) remote sensed datasets were used to study land surface temperature (LST) of the study area. MODIS has an orbit altitude of 705 km, with a swath of 2330 km (cross track) and provide datasets for 36 different spectral bands. For the present study, MOD11A2 dataset, an eight day land surface temperature and emissivity product of MODIS with a spatial resolution of 1 km have been used. The assessment of UHI of the region from 2005 to 2015 for the Julian day 129 (May 9) is performed to understand the pattern of UHI variance over the city of Guwahati.

In addition to remotely sensed datasets, the data from automatic weather station (AWS) and ground stations for the calibration of remote sensed UHI have also been used. For this purpose, the temperature and precipitation data of the same Julian day from 2005 to 2015 has been used.

4 METHODOLOGY

4.1 Remote Sensing Approach

An area of 361 km² (19 x 19 km) covering the city of Guwahati and its surrounding rural areas is selected for the study.

The land surface temperature is a direct representation of the radiative heat from the ground surface. A remote sensing approach aids the study of such temperature studies in continuous data formats most commonly known as land surface temperature (LST). This is advantageous to that of ground based measurements as it provides continuous spatial and temporal data sets and avoid data redundancy. In the current research, analyses on day time LST extracted from MOD11A2 product, over the city of Guwahati for

9th May 2005, 2010 and 2015 have been done. A temporal assessment of LST variation over the region is performed using a Gaussian fitting algorithm for a period of 10 years.

In this study, the measurement of UHI is done using a method similar to described by Streutker (2002). The major advantage of this method is that the UHI measurement is not the absolute temperature, but the difference in simultaneous temperature between urban and rural areas. (Streutker, 2002). In this method the measurement of UHI is carried out using a least-square fit the heat island to a Gaussian Surface of the form:

$$T(x, y) = T_0 + a_1x + a_2y + \text{UHI}(x, y)$$

$$\text{UHI}(x, y) = a_0 \times \exp \left[-\frac{((x - x_0)\cos\phi + (y - y_0)\sin\phi)^2}{0.5a_x^2} - \frac{((y - y_0)\cos\phi + (x - x_0)\sin\phi)^2}{0.5a_y^2} \right]$$

where (x, y) represent the location of the a pixel, $T(x, y)$ is the LST of a pixel at (x, y) , T_0 is the mean rural surface temperature, a_1 and a_2 are the coefficients determining spatial gradient of rural temperature and $\text{UHI}(x, y)$ is the pixel based heat island intensity.

This method provide not only the rural temperature components but also the UHI magnitude representing the entire city (a_0), spatial extent (a_x and a_y), orientation (ϕ) and the central location (x_0 and y_0) of the heat island. In order to perform the fit, first all the cloud pixels were masked out from each image resulting a rural temperature image. Each rural temperature image is fit to a planar surface, determining T_0 , a_1 and a_2 . The rural temperature image is subtracted from the initial land surface temperature image giving rise to urban heat island signature. Finally, a Gaussian surface of the above form is fitted in order to determine the UHI

parameters describing the magnitude, the spatial extents, the orientation and central location of UHI (Streutker, 2002).

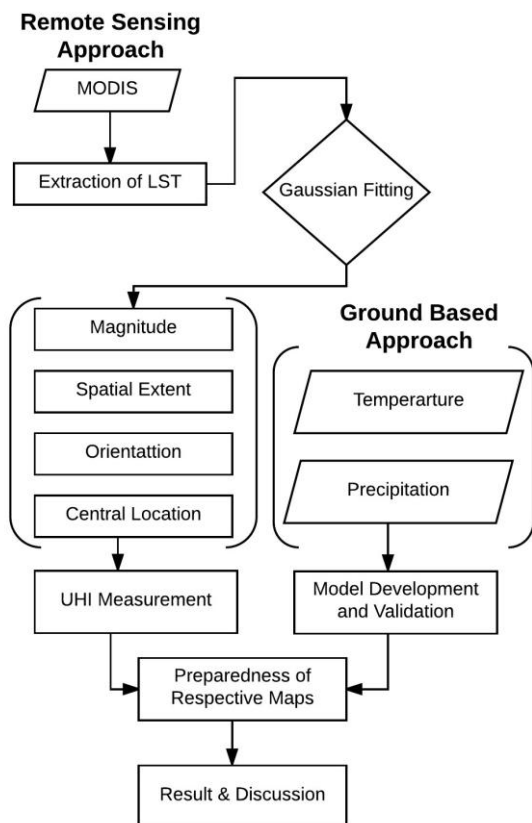


Fig 2: Flowchart showing the process of UHI estimation

4.2 Ground Based Calibration

The remote sensed data is validated using ground based station data and locally installed automated weather stations (AWS). The temperature and precipitation data is collected from station number 42410 having 26°06' latitude and 91°35' longitude at a height of 54 meter, located in the city of Guwahati. The temperature and precipitation data is collected for the month of April & May. The obtained data is correlated to satellite observations to understand the behaviour of UHI for 9th May of 2005, 2010 and 2015.

4.3 Land Use & Land Cover (LULC)

The land use land cover map for the city of Guwahati is obtained by supervised classification of pan corrected Landsat imagery of the year 2013. The results show that more than 50% of the area is covered by built up materials. This part of the land use is responsible in contributing maximum amount of radiative heat. The distribution of the LULC is shown in the form of a pie chart (Figure 3 and Figure 4).

5 RESULT AND DISCUSSION

Gaussian fit of UHI maps for the year 2005, 2010

and 2015 is shown in the Figure.5 and their respective

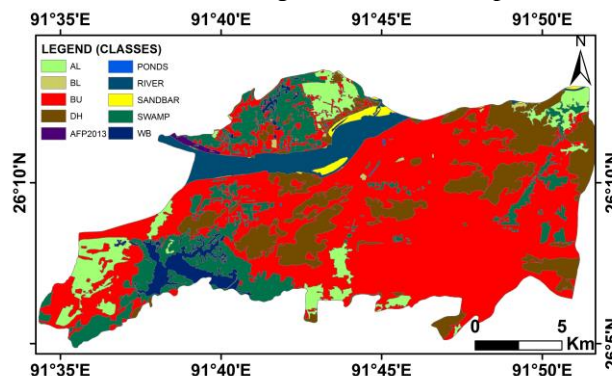


Fig 3: LULC map of Guwahati for the year 2013 (supervised classification)

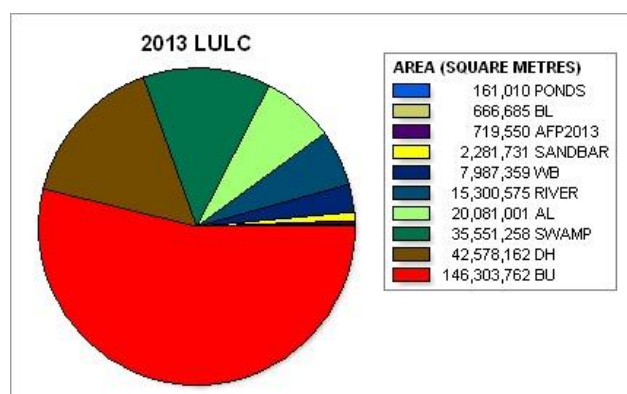


Fig 4: Pie chart showing the LULC area of Guwahati for the year 2013

Gaussian parameters were reported in Table 1. The two spatial extent parameters a_x and a_y , were used to determine the footprint area of the ellipse. The footprint area is in the form of ellipse with orientation and major and minor axes equivalent to a_x and a_y . As reported in Streutker (2003), the UHI intensity within this ellipse is maximum in the center (x_0, y_0) and decreases up to a level of $e^{-1/2}$, or 61% of its maximum value ($A_{.61\%}$). It corresponds to the inner ellipse superimposed on the maps of Fig.. The outer ellipse, instead, represents the area of the UHI for which the temperature is greater than a constant threshold of 1.0K (A_{1K}). A correlation coefficient ($corr$) was computed between the UHI image, obtained by subtracting the rural temperature surface from the $T(x, y)$ image, and the Gaussian surface used to fit the UHI image.

Table 1. Gaussian Parameters

Parameter	2005	2010	2015
a_0 (°C)	4.5758	5.7887	5.7652
x_0 (km)	1.6711	-0.783	-1.2346
y_0 (km)	1.1721	0.7574	1.2845
ϕ	17.4912	5.8242	4.9889
$A_{.61\%}$ (km ²)	20.4842	18.8393	16.9928
A_{1K} (km ²)	62.3038	66.16	59.5374
$corr$	0.736	0.8211	0.7816

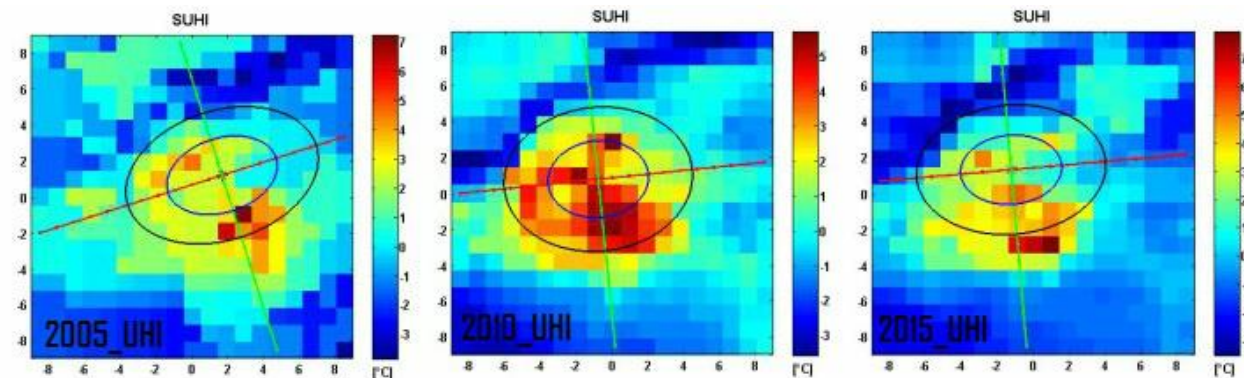


Fig 5: UHI map for the city of Guwahati for the year 2005, 2010 and 2015

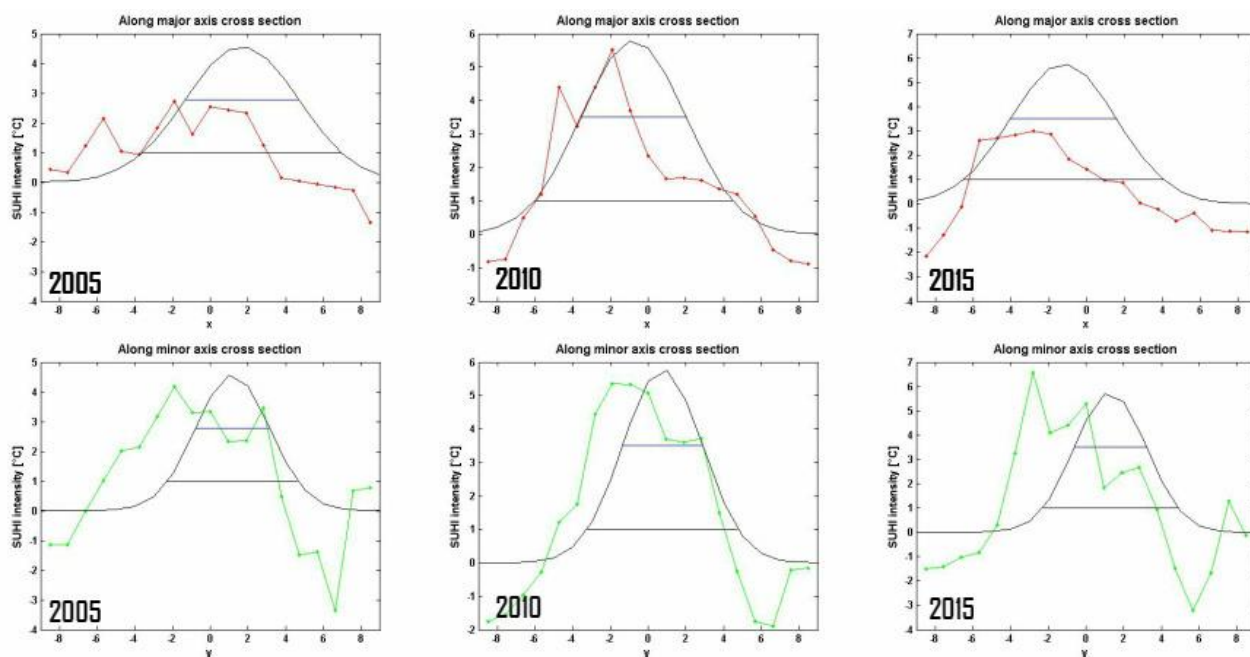


Fig 6: Vertical cross section along major and minor axis of the footprint area of the UHI images of the city of Guwahati during the year 2005, 2010 and 2015

Table 2. Ground Parameters.

Year	Mean T	Max T	Min T	PPT	Remarks
2005	81	90	74	No	Not observed before and after
2010	78.2	88.9	73	0.91G	Litter rainfall before 2 days and reaches max at this day and continue 6 days after
2015	82.1	93.2	68	No	Heavy Rainfall since 10 days but not that day

6 CONCLUSIONS

The results thus obtained using MODIS LST reveals increase in the magnitude and the extent of UHI over the city of Guwahati. The UHI magnitude has increased from 4.57 °C and 5.78 °C from 2005 to 2010. Ground station reveals little rainfall before the date of acquisition of satellite imagery on 2010 and reaches maximum

on this day and continues six days after so no significant observed on the UHI magnitude. It is observed that the magnitude have showed almost similar value in 2010 and 2015. The probable reason may be precipitation before the date of acquisition of the satellite imagery in 2015. The ground observation from weather stations show continuous previous 10 rainy days but not that day as shown in Table 2.

The geospatial investigation shows a growth of UHI

magnitude from 4.6°C in 2005 to 5.8°C in 2010 and also growth in its lateral extent from 62 km² to 66 km². The UHI magnitude in 2015 shows a value of 5.8 °C, the possible reason is due to cooling effect of the city as evident from the precipitation ground based data.

REFERENCES

- 1) Anniballe, R. and Bonafoni, S., 2015. A Stable Gaussian Fitting Procedure for the Parameterization of Remote Sensed Thermal Images. *Algorithms*, 8(2), pp.82-91.
- 2) Anniballe, R., Bonafoni, S. and Manuele P., 2014. Spatial and temporal trends of the surface and air heat island over Milan using MODIS data. *Remote Sensing of Environment*, 150, pp.163-171.
- 3) Borbora, J. and Das, A.K., 2014. Summertime urban heat island study for Guwahati City, India. *Sustainable Cities and Society*, 11, pp.61-66.
- 4) Chakraborty, S.D., Kant, Y. and Mitra, D., 2015. Assessment of land surface temperature and heat fluxes over Delhi using remote sensing data. *Journal of environmental management*, 148, pp.143-152.
- 5) Chen, X.L., Zhao, H.M., Li, P.X. and Yin, Z.Y., 2006. Remote sensing image-based analysis of the relationship between urban heat island and land use/cover changes. *Remote sensing of environment*, 104(2), pp.133-146.
- 6) Clinton, N. and Gong, P., 2013. MODIS detected surface urban heat islands and sinks: Global locations and controls. *Remote Sensing of Environment*, 134, pp.294-304.
- 7) Gao, B.C., 1996. NDWI—A normalized difference water index for remote sensing of vegetation liquid water from space. *Remote sensing of environment*, 58(3), pp.257-266.
- 8) Goswami, J., Roy, S. and Sudhakar, S., 2013. A Novel Approach in Identification of Urban Hot Spot Using Geospatial Technology: A Case Study in Kamrup Metro District of Assam. *International Journal of Geosciences*, 4(05), p.898.
- 9) Joshi, R., Raval, H., Pathak, M., Prajapati, S., Patel, A., Singh, V. and Kalubarme, M.H., 2015. Urban Heat Island Characterization and Isotherm Mapping Using Geo-Informatics Technology in Ahmedabad City, Gujarat State, India. *International Journal of Geosciences*, 6(3), p.274.
- 10) Manuele P., Bonafani S. and Biondi R., 2012. Satellite air temperature estimation for monitoring the canopy layer heat island of Milan. *Remote Sensing of Environment*, 127, pp.130–138.
- 11) Mohan, M. and Kandya, A., 2015. Impact of urbanization and land-use/land-cover change on diurnal temperature range: A case study of tropical urban airshed of India using remote sensing data. *Science of the Total Environment*, 506, pp.453-465.
- 12) Nieuwolt, S., 1966. The urban microclimate of Singapore. *Journal of Tropical geography*, 22(6), pp.30-37.
- 13) Rahman, A., Kumar, Y., Fazal, S. and Bhaskaran, S., 2011. Urbanization and quality of urban environment using remote sensing and GIS techniques in East Delhi-India. *Journal of Geographic Information System*, 3(01), p.62.
- 14) Rao, P.K., 1972. Remote sensing of urban heat islands from an environmental satellite. *Bulletin of the American meteorological society*, 53(7), p.647.
- 15) Streutker, D.R., 2002. A remote sensing study of the urban heat island of Houston, Texas. *International Journal of Remote Sensing*, 23(13), pp.2595-2608.
- 16) Streutker, D.R., 2003. Satellite-measured growth of the urban heat island of Houston, Texas. *Remote Sensing of Environment*, 85(3), pp.282-289.
- 17) Tran, H., Uchiyama, D., Ochi, S. and Yasuoka, Y., 2006. Assessment with satellite data of the urban heat island effects in Asian mega cities. *International Journal of Applied Earth Observation and Geoinformation*, 8(1), pp.34-48.
- 18) Voogt, J.A. and Oke, T.R., 2003. Thermal remote sensing of urban climates. *Remote sensing of environment*, 86(3), pp.370-384.

[Back to table of contents](#)

A remote sensing approach to study the temporal growth of the urban limits for the city of Hyderabad from 2001-2015

Pir Mohammadⁱ⁾, Ajanta Goswamiⁱⁱ⁾, Ashim Sattarⁱⁱⁱ⁾, Stefania Bonafoni^{iv)}

i) Ph.D Student, Department of Earth Sciences, IIT Roorkee, Uttarakhand-247667, India.

ii) Assistant Professor, Department of Earth Sciences, IIT Roorkee, Uttarakhand-247667, India.

iii) Ph.D Student, Department of Earth Sciences, IIT Roorkee, Uttarakhand-247667, India.

iv) Faculty, Department of Electronic and Information Engineering, University of Perugia, Perugia-06125, Italy.

ABSTRACT

The metropolitan of Hyderabad is among the top five in India with an average area of 625 km². Recent surveys of the city shows an alarming population growth rate, since the previous decade. This is causing the lateral expansion of the urban extents towards the surrounding rural area. In the current research, MODIS thermal remote sensing data is used to derive the land surface temperature (LST) over the city of Hyderabad for a period of 15 years. An urban heat island phenomenon is evident over the city with a gradual increase in its magnitude over the years from 2000 to 2015. A Gaussian fitting algorithm is performed to highlight the heat island signature with respect to the surrounding rural region. The study reveals the variability of UHI over the city for the summer season. The night time LST shows an increasing trend in the UHI magnitude for a period of 15 years. An overall increase in the urban heat island magnitude and extent is profoundly visible over the region. The city of Hyderabad shows a rate of lateral expansion 0.8km² annually from 2001 to 2005. An increase of the rate to 1.5 km² annually is evident from 2005 to 2010, the city shows a remarkable growth with a rate of 3.2km² during the last 5 years from 2010 to 2015, which is double the rate that of the previous 5 years.

Keywords: Urban growth, Gaussian fit, Heat Signature

1. INTRODUCTION

The concept of remote sensing, to highlight the heat signature of an area, in respect to the surrounding was implemented from early 1970's (Rao et al., 1972). Several statistical method have been employed to understand the change in growth of the city or urban area (Weng et al., 2004). Oke et al., 1967 have given a relation between the city size and the heat signature of the area. Remote Sensing techniques using satellite imagery has been proven to be one of the most effective tool for LULC and Urban growth studies (Mundia et al., 2005, Taubenbock et al., 2009 and Dewan et al., 2009). In this paper we emphasis a remote sensing technique which exploits thermal band of the electromagnetic spectrum to understand the growth of the city using the heat signature. It is obvious that urbanization would lead to greater expansion of the city limits and thus a greater area covered by building materials. The building materials like concrete and tar has a property of absorbing more amount of heat as compared to vegetation and water bodies (Hawes et al., 1993, Santamouris et al., 2011). In this paper we address the rate at which the city of Hyderabad in the state of Telangana is expanding over a period of 15 years. A Gaussian fitting algorithm is employed to understand the change in the heat signature as we move away from the centre of the thermal signature hotspot (a point denoting the maximum heat signature) in the area. The principle is based on the fact that heat decrease as we move away from the core of the city and eventually

minimises significantly at some point of distance which would mark roughly the city limit. Remote Sensing techniques serves well when it comes to studies in a regional and spatial inspection.

2 STUDY AREA AND CLIMATE

Hyderabad is the capital of southern state Telangana and lies within 17.38° N latitude and 78.48° E longitude. It is situated along the bank of the Musi River and has a total area of about 650 square kilometers. It lies along the hilly terrain around artificial lakes such as Hussain Sagar at an elevation of 542 meters above mean sea level. It is the fourth most populated city and sixth most populous urban agglomeration in India. Its total urban metropolitan urban population is around 11.7 million. Hyderabad is characterized by tropical wet and dry climate bordering on a hot semi-arid climate. The maximum temperature recorded exceed 40° C between April and June. The minimum temperature occur in December and January, when the lowest temperature occasionally drops to 10° C. The city receives an average annual rainfall of around 803 millimeters.

3 DATA USED

The concept of urban heat island is a spatial and continuous process and thus to monitor the changes a vast geospatial database is obligatory. The land surface

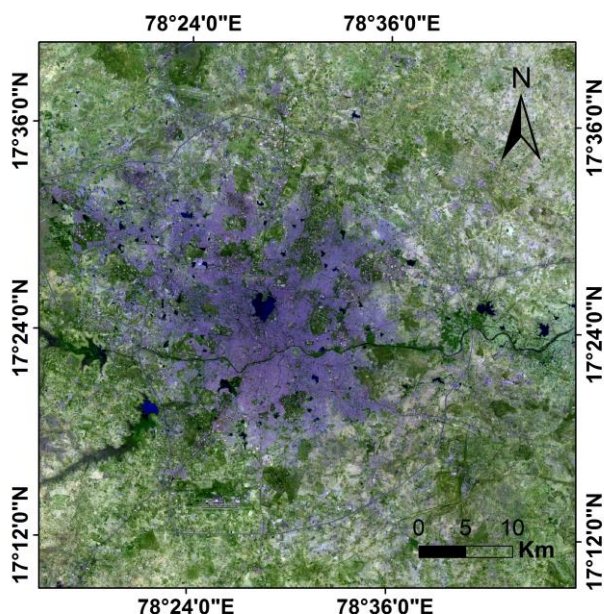


Fig 1: Location map of the study area (False colour composite of Landsat 8 comprising of band 7, 6 and 4 showing urban area in blue color)

temperature, being one of the surface data products of the MODIS (Moderate Resolution Imaging Spectrometer) on board of the Terra and Aqua spacecraft, which provides daily land surface temperature data at a resolution of 1000 m [USGS] is used in the study. MODIS has an orbit altitude of 705 km, with a swath of 2330 km (cross track) and provide datasets for 36 different spectral bands. MOD11A2 dataset, an eight day land surface temperature and emissivity product of MODIS with a spatial resolution of 1 km is used for the study. The assessment of UHI of the region from 2001 to 2015 for the summer months (April and June) is performed to understand the pattern of UHI variance over the city of Hyderabad.

4 METHODOLOGY

An area of 1600 km² (40 x40 km) covering the city of Hyderabad and its surrounding rural areas is selected for the study. The land surface temperature is a direct representation of the radiative heat from the ground surface. A remote sensing approach aids the study of such temperature studies in continuous data formats most commonly known as land surface temperature (LST). This is advantageous to that of ground based measurements as it provides continuous spatial and temporal data sets and avoid data redundancy. In the current research we analyses day time LST extracted from MOD11A2 product, over the city of Hyderabad for the summer months from 2001 to 2015.

In this study, the measurement of UHI is done using a method similar to described by Streutker (2002). The major advantage of this method is that the UHI measurement is not the absolute temperature, but the

difference in simultaneous temperature between urban and rural areas. (Streutker, 2002). In this method the measurement of UHI is carried out using a least-square fit the heat island to a Gaussian Surface of the form:

$$T(x,y) = T_0 + a_1x + a_2y + UHI(x,y)$$

$$UHI(x,y) = a_0 \times \exp \left[\frac{-((x-x_0)\cos\phi + (y-y_0)\sin\phi)^2}{0.5a_x^2} - \frac{((y-y_0)\cos\phi + (x-x_0)\sin\phi)^2}{0.5a_y^2} \right]$$

where (x,y) represent the location of the a pixel, T (x,y) is the LST of a pixel at (x,y), T₀ is the mean rural surface temperature, a₁ and a₂ are the coefficients determining spatial gradient of rural temperature and UHI (x,y) is the pixel based heat island intensity.

This method provide the spatial extent of the thermal signature (a_x and a_y), the central location (x₀ and y₀) of the heat island. In order to perform the fit, first all the cloud pixels were masked out from each image resulting a rural temperature image. Each rural temperature image is fit to a planar surface, determining T₀, a₁ and a₂. The rural temperature image is subtracted from the initial land surface temperature image giving rise to urban heat island signature. Finally, a Gaussian surface of the above form is fitted in order to determine the UHI parameters describing the magnitude, the spatial extents, the orientation and central location of UHI (Streutker, 2002).

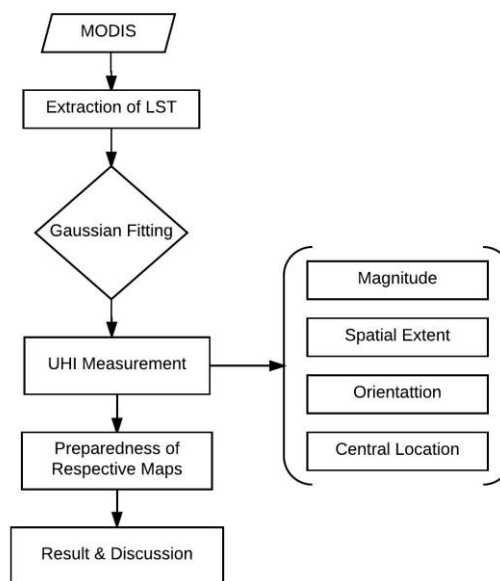


Fig. 2. Flowchart showing the process of UHI estimation.

5 LAND USE AND LAND COVER (LULC)

The land use and land cover (LULC) for the city of Hyderabad and its surrounding area is obtained from available literature. The LULC for the city of Hyderabad reveals an increase in the built up area and it can be correlated with the retrieved LST for the city. The total area under built up is reported to be 202.50 Km² in the year 2011-12 (bhuwan.nrsc.gov.in). The land use land cove temporal assessment from the year 1985 to 2005 by Roy et al., 2016 shows tremendous

increase in the built up areas in the city.

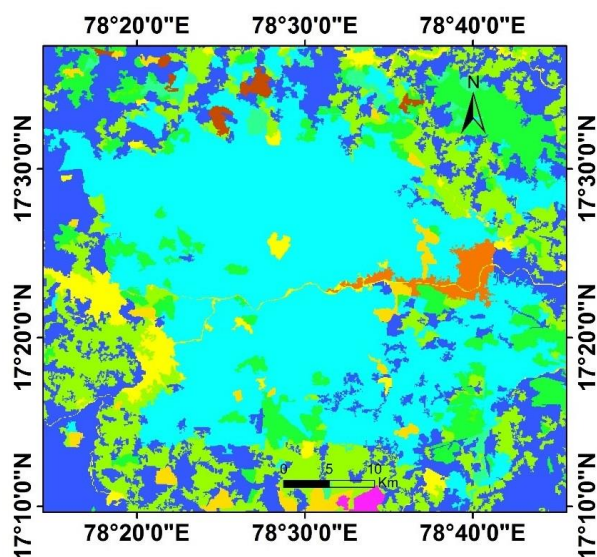


Fig 3: LULC map of Hyderabad city for the year 2005 (supervised classification) showing the build-up area in sky blue colour (Roy et al, 2016)

6 RESULTS AND DISCUSSION

Weekly land surface temperature (LST) maps were prepared for the summer months (May and June) through the year 2001, 2005, 2010 and 2015 respectively. For individual year, all the LST images are averaged providing a single image demonstrating the average LST image during the summer season in that particular year. Gaussian fir parameters are calculated from the averaged LST datasets respectively as shown in the Table 1 for the respective years. The two spatial extent parameters a_x and a_y , were used to determine the footprint area of the ellipse with orientation and major and minor axis equivalent to a_x and a_y . The intensity of UHI is maximum in the center (x_0, y_0) of the ellipse and decreases up to a level of $e^{-1/2}$, or 61% of its maximum value ($A_{61\%}$) as reported by Streutker (2003). It corresponds to the inner ellipse superimposed on the UHI maps. The outer ellipse instead, represents the area of the UHI for which the temperature is greater than a constant threshold of 1.0 K (A_{1K}).

Table 1. UHI Parameters for summer season (April-May) for the city of Hyderabad from 2001 to 2015 conditions.

Parameter	a_0 (°C)	$A_{61\%}$ (km ²)	A_{1K} (km ²)
2001	2.6266	96.6376	186.644
2005	2.6488	97.6095	191.9431
2010	2.6648	98.6372	199.6142
2015	2.7878	105.1198	215.5482

The UHI images for the year 2001, 2005, 2010 and 2015 obtained from the corresponding LST images

were shown in the Figure 4 and their respective parameters were in Table 1. Vertical cross sections of

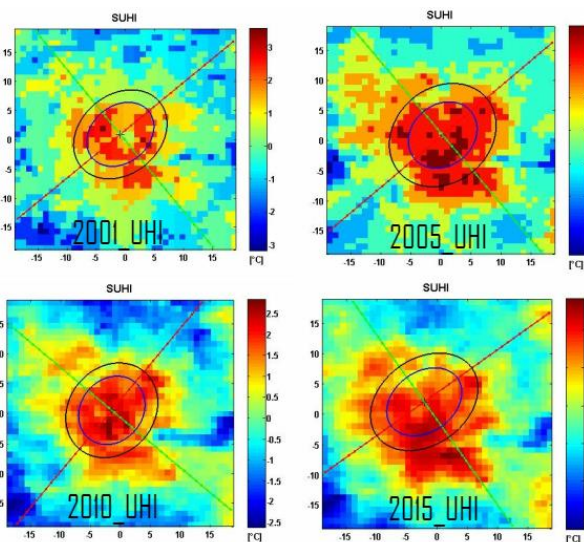


Fig 4: UHI map for the Hyderabad city during summer season from 2001 to 2015

UHI image along the major and minor axis of the footprint area the UHI map for the city is also drawn and is shown in the Figure 5 and Figure 6 respectively.

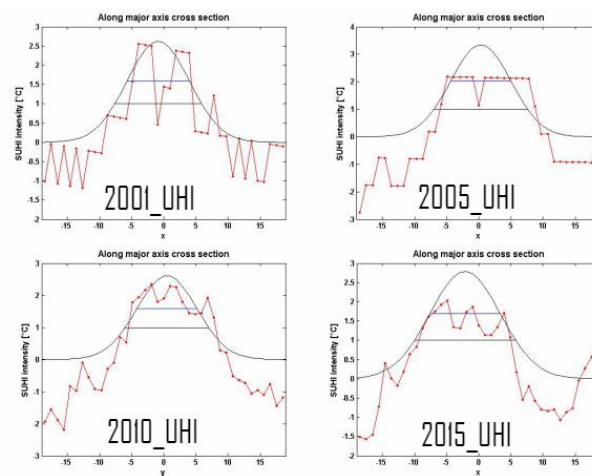


Fig 5: Vertical cross section along major axis of the footprint area of the UHI map for the city of Hyderabad during summer season from 2001 to 2015

7 CONCLUSIONS

The results clearly confirm the boosting of UHI magnitude and also the footprint area both $A_{61\%}$ and A_{1K} in the city of Hyderabad over a span of 15 years. The net increase of UHI by 0.16 °C over duration of 15 years is revealed from the analysis in the summer season. The $A_{61\%}$ area (inner ellipse) increases from 96.64 km² in 2001 to 105.12 km² in 2015 and the A_{1K} (outer ellipse) area from 186.64 km² in 2001 to 215.55 km² in 2015. The city of Hyderabad shows a rate of

lateral expansion 0.8 km^2 annually from 2001 to 2005. An increase of the rate to 1.5 km^2 annually is evident

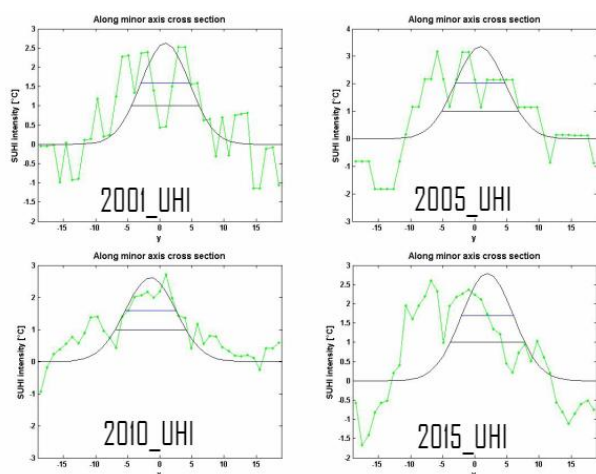


Fig 6: Vertical cross section along minor axis of the footprint area of the UHI map for the city of Hyderabad during summer season from 2001 to 2015.

from 2005 to 2010. The city shows a remarkable growth with a rate of 3.2 km^2 during the last 5 years from 2010 to 2015, which is double the rate that of the previous 5 years.

REFERENCES

- Anniballe, R. and Bonafoni, S., 2015. A Stable Gaussian Fitting Procedure for the Parameterization of Remote Sensed Thermal Images. *Algorithms*, 8(2), pp.82-91.
- Anniballe, R., Bonafoni, S. and Manuele P., 2014. Spatial and temporal trends of the surface and air heat island over Milan using MODIS data. *Remote Sensing of Environment*, 150, pp.163-171.
- Borbora, J. and Das, A.K., 2014. Summertime urban heat island study for Guwahati City, India. *Sustainable Cities and Society*, 11, pp.61-66.
- Chakraborty, S.D., Kant, Y. and Mitra, D., 2015. Assessment of land surface temperature and heat fluxes over Delhi using remote sensing data. *Journal of environmental management*, 148, pp.143-152.
- Chen, X.L., Zhao, H.M., Li, P.X. and Yin, Z.Y., 2006. Remote sensing image-based analysis of the relationship between urban heat island and land use/cover changes. *Remote sensing of environment*, 104(2), pp.133-146.
- Clinton, N. and Gong, P., 2013. MODIS detected surface urban heat islands and sinks: Global locations and controls. *Remote Sensing of Environment*, 134, pp.294-304.
- Dewan, A.M. and Yamaguchi, Y., 2009. Land use and land cover change in Greater Dhaka, Bangladesh: Using remote sensing to promote sustainable urbanization. *Applied Geography*, 29(3), pp.390-401.
- Dumka, U.C., Manchanda, R.K., Sinha, P.R., Sreenivasan, S., Moorthy, K.K. and Babu, S.S., 2013. Temporal variability and radiative impact of black carbon aerosol over tropical urban station Hyderabad. *Journal of Atmospheric and Solar-Terrestrial Physics*, 105, pp.81-90.
- Goswami, J., Roy, S. and Sudhakar, S., 2013. A Novel Approach in Identification of Urban Hot Spot Using Geospatial Technology: A Case Study in Kamrup Metro District of Assam. *International Journal of Geosciences*, 4(05), p.898.
- Hawes, D.W., Feldman, D. and Banu, D., 1993. Latent heat storage in building materials. *Energy and buildings*, 20(1), pp.77-86.
- Joshi, R., Raval, H., Pathak, M., Prajapati, S., Patel, A., Singh, V. and Kalubarme, M.H., 2015. Urban Heat Island Characterization and Isotherm Mapping Using Geo-Informatics Technology in Ahmedabad City, Gujarat State, India. *International Journal of Geosciences*, 6(3), p.274.
- Manuele P., Bonafani S. and Biondi R., 2012. Satellite air temperature estimation for monitoring the canopy layer heat island of Milan. *Remote Sensing of Environment*, 127, pp.130-138.
- Mohan, M. and Kandya, A., 2015. Impact of urbanization and land-use/land-cover change on diurnal temperature range: A case study of tropical urban airshed of India using remote sensing data. *Science of the Total Environment*, 506, pp.453-465.
- Mundia, C.N. and Aniya, M., 2005. Analysis of land use/cover changes and urban expansion of Nairobi city using remote sensing and GIS. *International Journal of Remote Sensing*, 26(13), pp.2831-2849.
- Oke, T.R., 1973. City size and the urban heat island. *Atmospheric Environment* (1967), 7(8), pp.769-779.
- Rahman, A., Kumar, Y., Fazal, S. and Bhaskaran, S., 2011. Urbanization and quality of urban environment using remote sensing and GIS techniques in East Delhi-India. *Journal of Geographic Information System*, 3(01), p.62.
- Rao, P.K., 1972. Remote sensing of urban heat islands from an environmental satellite. *Bulletin of the American meteorological society*, 53(7), p.647.
- Santamouris, M., Synnefa, A. and Karlessi, T., 2011. Using advanced cool materials in the urban built environment to mitigate heat islands and improve thermal comfort conditions. *Solar Energy*, 85(12), pp.3085-3102.
- Streutker, D.R., 2002. A remote sensing study of the urban heat island of Houston, Texas. *International Journal of Remote Sensing*, 23(13), pp.2595-2608.
- Streutker, D.R., 2003. Satellite-measured growth of the urban heat island of Houston, Texas. *Remote Sensing of Environment*, 85(3), pp.282-289.
- Taubenböck, H., Wegmann, M., Roth, A., Mehl, H. and Dech, S., 2009. Urbanization in India-Spatiotemporal analysis using remote sensing data. *Computers, Environment and Urban Systems*, 33(3), pp.179-188.
- Voogt, J.A. and Oke, T.R., 2003. Thermal remote sensing of urban climates. *Remote sensing of environment*, 86(3), pp.370-384.
- Weng, Q., Lu, D. and Schubring, J., 2004. Estimation of land surface temperature-vegetation abundance relationship for urban heat island studies. *Remote sensing of Environment*, 89(4), pp.467-483.

[Back to table of contents](#)

Source segregation of Municipal Solid Waste

Pradip Baishya¹ and Dr. Dimbendra Kumar Mahanta²

1)Assistant Professor, Department of Mechanical Engineering, Assam Engineering College, Jalukbari, Guwahati, Assam, India.

2) Professor, Department of Mechanical Engineering, Assam Engineering College, Jalukbari, Guwahati, Assam, India.

ABSTRACT

With the spiraling and sprawling growth of urban population all over the world the challenges Solid Waste Management faces today is huge. Technology available in developed countries is hard to implement in India in this sector due to funds limitation, different demographic profile of users, general education and awareness level in the community regarding waste, cost of running sophisticated waste plants, associated infrastructure required to support the system and also the extent and character of the waste to be managed. Cities in developing countries hardly spend more than 0.5% of their per capita gross national productivity (GNP) on urban waste services, which covers only about one-third of overall cost. Under these stringent budgets and complex problems to deal with, it is vital to devise ways which would strike a balance between the cost effectiveness and the quality of the waste management process. Implementation of waste management with proper segregation and supporting technologies for processing the recyclables can go a long way in minimizing the energy consumed for manufacturing. The segregation process when done efficiently produces cleaner recyclables which has a better market value and lesser energy consumption in its life cycle from generation at source to a finished product.

In this paper municipal waste collection at source using different types of waste receptacles have been experimented. A resident colony in Guwahati city was selected and 50 households were randomly selected for the study for 90 days. Two bin system and a designed segregation bin system were experimented. Data was compared using SPSS. It was found that the contamination level was low in the biodegradable and non biodegradable waste in the designed segregation bin system. It was also found that there was an improvement in the quantity of biodegradable and non biodegradable waste. Segregation at source if practiced could lead to zero waste locality with an economic viability.

Keywords: Recyclables, segregation, zero waste.

1. INTRODUCTION

Solid waste management has become one of the major issues in both urban and rural areas all over the world. With the progress of civilization, the waste generated become more complicated in nature. Cities in developing countries hardly spend more than 0.5% of their per capita gross national productivity (GNP) on urban waste services, which covers only about one-third of overall cost (World Bank, 1999). The complexities of issues surrounding the management of municipal waste in Indian cities are increasing even more day by day. An average citizen in India is far from the concept of segregation of waste and its benefits to the system. Open, uncontrolled and poorly managed land filling is commonly the practice in most

cities. Currently, most garbage collection is done by depositing everything into a single container from where they are hauled to be dumped in dumping grounds or burnt in open air. Such practices have caused serious health problem due to release of highly toxic gases and ground water contamination from pollutants and leachates (CPCB, 2000). Garbage needs to be sorted and segregated into various components and each of such components like textile materials; polythene, foodstuffs, metals and non-metallic would have to be handled separately at the disposal or recycling site. Waste management in developing countries seems to have low priority as they are more bothered about issues like hunger, health, water, employment and civil war (Chandruppa R. et.al

2012). Financial situation of most municipalities in India are not in good health. The difficulties in providing the desired level of public service in the urban centers of India are often attributed to the poor financial status of the managing municipal corporations (MoEF,2000). 80–95% of total budget of Municipal Solid Waste Management (MSWM) constitutes the process of collection and transport of waste (Sinha, 1998).

2. METHODOLOGY

Dry and wet waste required to be segregated and collected at source, is the bottle neck of the Municipal Solid Waste Management. Segregation of waste is one of the critical activities in the Solid Waste Management as it saves undue efforts on transportation and disposal of recyclable or inert wastes. Studies revealed that the characteristic of waste generated consist of more biodegradable fraction and segregation of such wastes, before they are transported to the processing /disposal site, should be carried out. A two bin system was adopted for segregation of waste into dry and wet fraction at source of generation. Normal waste disposal kitchen bins made of plastic were distributed among the residents. Information about segregation and demonstration of the segregation procedure was done at the resident colony. Table 1 below shows the details of the waste collection area.

Table 1: Details of the waste collection zone

Sl No.	Item	Quantity
1	Place/Area	Games village, Guwahati
2	No. of households	90
3	No. of bins for wet waste	90
4	No. of bins for dry waste	90

The waste was collected in two types of temporary storage bins, one for dry waste and the other for wet waste, which are collected on daily basis from door to door. After collection of waste from door to door it was segregated into biodegradable and non biodegradable. Data collection was carried out for 90 days.

2.1 Data tabulation and analysis

Structured questionnaire was administered to collect primary data at various stages of the

research. Data tabulation and analysis was performed using Statistical Package for Social Science (SPSS). Various descriptive and inferential statistical analyses were conducted for data analysis. Master data sheet was developed for database of two bin system and segregation bin system. The variable was taken as numeric with nominal scale. Data on biodegradable, non biodegradable and contaminated waste was recorded for a total of 180 days, 90 days for each bin design system. The variables were taken as numeric with a measure of metric scale in kg for the different types of waste. One way ANOVA was performed for biodegradable, non biodegradable and contaminated waste for two bin and segregation bin system.

2.2 Collection of MSW using two bin system

A two bin system was adopted for segregation of waste into dry and wet fraction at source of generation. Normal waste disposal kitchen bins made of plastic were distributed among the residents. Information about segregation and demonstration of the segregation procedure was done at the resident colony. The waste was collected in two types of temporary storage bins, one for dry waste and the other for wet waste, which are collected on daily basis from door to door. Waste was collected from 50 households for 90 days and weighted using electronic weight balance to the accuracy of two decimals. After collection of waste from door to door it was segregated into biodegradable, non biodegradable and contaminated waste.

2.3 Collection of MSW using segregation bin system

Data collection of waste composition was done from the single bin segregation system. Contamination of recyclables was found to be reduced in the single segregation unit. This was statistically proved from the data comparison of both the systems using SPSS. Data on the waste categories viz. biodegradable, non biodegradable and contaminated waste was collected by using the segregation bin.

3. RESULTS

Physical characteristics of waste at primary collection point were calculated using two bin system and segregation bin system. The data collected was analysed using SPSS for

biodegradable, non biodegradable and contaminated waste.

3.1 Two bin system

Table 2 below shows the mean values of biodegradable, non biodegradable and contaminated waste derived from the statistical analysis using SPSS.

Table 2: Mean values of type of waste using two bin system

Sl. No.	Type of waste	Mean (kg)
1.	Biodegradable	42.19
2.	Non biodegradable	5.23
3.	Contaminated	9.07

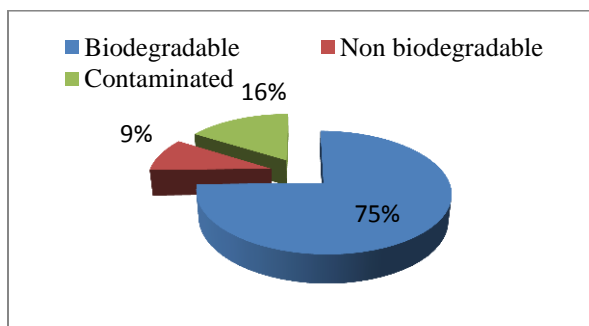


Fig. 1: Percentage of different types of waste using two bin system

It was found that there is a high level of contamination in the two bin system which exceeds the non biodegradable waste percentage as shown in fig. 1. This contamination was due to the mixing of dry waste with wet waste disposed into the dustbins. The dustbins allocated for disposing dry waste was found to be contaminated with food waste and also with contaminated polythene bags as the major components. Similarly the dustbin allocated for collecting wet waste was also found to be contaminated with polythene bags, disposable plates, cups etc.

3.2 Segregation bin system

Waste was collected using the designed segregation bin from 50 households for 90 days and the different quantities of biodegradable, non biodegradable and contaminated waste was measured. Table 3 shows the mean values of biodegradable, non biodegradable and

contaminated waste for the designed segregation bin derived from statistical analysis using SPSS.

Table 3: Mean values of type of waste using segregation bin

Sl. No.	Type of waste	Mean (kg)
1.	Biodegradable	44.05
2.	Non biodegradable	6.53
3.	Contaminated	5.42

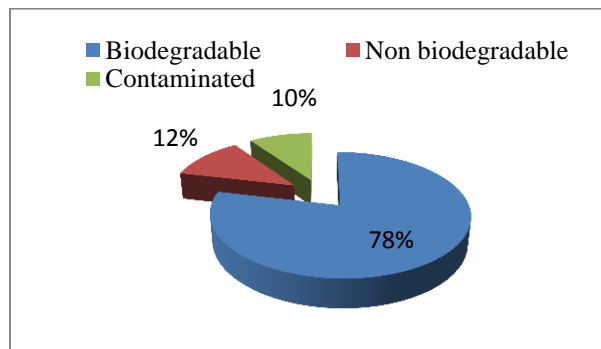


Fig. 2: Percentage of different types of waste using segregation bin system

It was found that biodegradable waste consists of the highest fraction as 78% followed by non biodegradable waste at 12% as shown in fig. 2. The contaminated waste was found to be 10% which is to be disposed into the landfill.

3.3 Comparison of two bin system and segregation bin system

On the basis of the collected data inferential statistics has been conducted to study the variance of amount of various types of waste viz. biodegradable, non biodegradable & contaminated waste with respect to two different designs of segregation bin.

Null Hypothesis:

There is no significant difference in the amount of biodegradable waste, non biodegradable waste and contaminated waste collected with two different ideas for collecting waste viz. two bin system and improvised segregation bin. One way ANOVA was conducted for a significance level of 0.05. The null hypothesis was rejected at significance level 0.048, 0.00 and 0.00 respectively.

The descriptive statistics showing the mean values of two bin system and segregation bin system for biodegradable waste is shown in table 4.

Table 4: Mean values of two bin & segregation bin for biodegradable waste

Biodegradable Waste				
	N	Mean	Minimum	Maximum
Two Bin System	90	42.19	30.52	67.73
Improvised Segregation Bin	90	44.05	31.48	70.72

Comparison of two bin system and segregation bin system in the amount of biodegradable waste collected from 50 households for 90 days taking the mean values are shown in fig. 3.

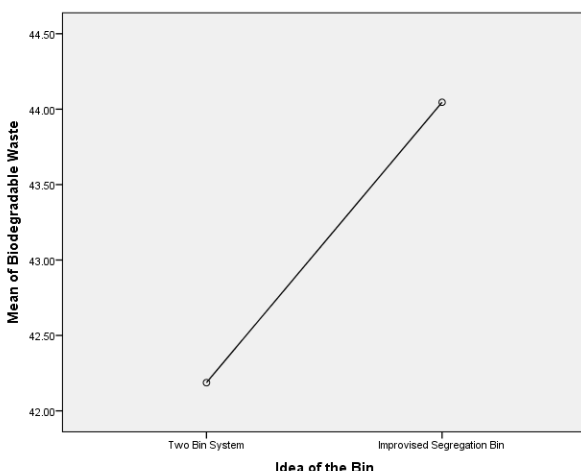


Fig. 3: Comparison between two bin system and improvised segregation bin for biodegradable waste

The descriptive statistics showing the mean values of two bin system and segregation bin system for non biodegradable waste is shown in table 5.

Table 5: Mean values of two bin & segregation bin for non biodegradable waste

Non-biodegradable Waste				
	N	Mean	Minimum	Maximum
Two Bin System	90	5.23	2.98	8.45
Improvised Segregation Bin	90	6.53	3.56	12.35

Comparison of two bin system and segregation bin system in the amount of non biodegradable waste collected from 50 households for 90 days taking the mean values are shown in fig. 4.

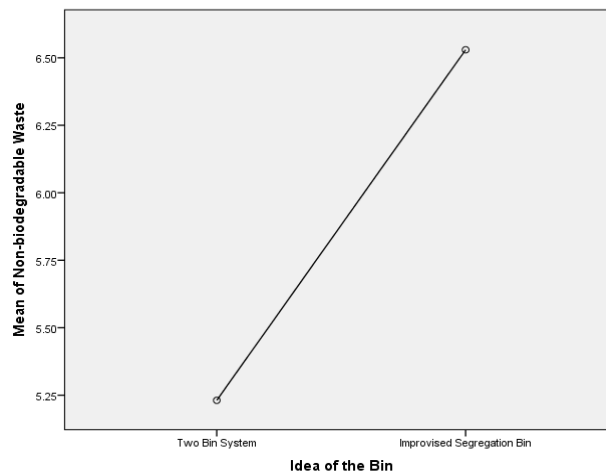


Fig. 4: Comparison between two bin system and improvised segregation bin for non biodegradable waste

The descriptive statistics showing the mean values of two bin system and segregation bin system for contaminated waste is shown in table 6.

Table 6: Mean values of two bin & segregation bin for contaminated waste

Contaminated Waste				
	N	Mean	Minimum	Maximum
Two Bin System	90	9.07	6.76	11.93
Improvised Segregation Bin	90	5.42	3.46	12.80

Comparison of two bin system and segregation bin system in the amount of contaminated waste collected from 50 households for 90 days taking the mean values are shown in fig. 5.

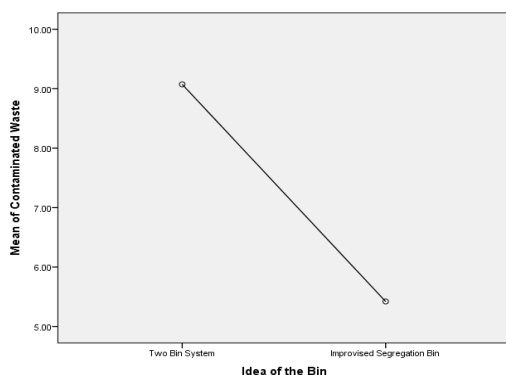


Fig. 5: Comparison between two bin system and improvised segregation bin for contaminated waste

4. DISCUSSION

The results obtained out of the segregation at source process demonstrated the importance of the process to be in the waste processing flow. Even though local authorities have financial constraints and unscientific dumping of waste is an easy practice, the segregation of waste at source will have to be given high priority. Segregation at source data stresses the urgency to integrate the process in the waste management process to minimize the impact and damages to the environment which are irreversible. It offers a feasible strategy where recycling targets could be achieved right away without major changes in the SWM chain which is a major challenge in the current scenario. It also offers a blueprint for zero waste planning of places and shows the potential to achieve them in due course of time if taken forward. The successful running of the facility and delivery of the desired outcomes brings out a feasible sketch of a model which could be replicated in for the creation of zero waste places in other cities.

5. CONCLUSION

In this paper an attempt has been made to bring out the key issues in waste disposal in the current system of management in Guwahati. Strict monitoring of the process of disposal from the point of generation to the site of disposal is needed to maintain health and safety of the citizens and the personnel involved in the process. There is

seen to be lack of awareness among the public regarding safe and environment friendly waste disposal practice. The design of a single segregation bin to be used at the source of generation has addressed the issue of responsible waste disposal and also educated the public on the environmental benefits of segregation at source. The learning curve of the sample population was seen to progress as the research evolved and progressed. The desired outcome of recyclables with minimal level of contamination was achieved in terms of segregation at source by responsible disposal of waste after several trials with different recycling proportions. The urgent need to construct sanitary landfill sites has been flagged up by this research.

The receptacle designed for segregation at source can be further developed in terms of materials and design for use in different waste situations and characteristics. Cost and portability aspects can be taken up for further development through research which would enable its use for a larger and varied audience. Research on the efficiency attribute can be carried out further to enhance the total output of recyclables.

REFERENCES

1. Chandrappa R., Das D.B. (2012). "Solid Waste Management: Principles and Practice." *Springer Science & Business Media*.
2. Management of Municipal Solid Wastes. *CPCB, 2000. Central Pollution Control Board, New Delhi, India.*
3. MoEF, Municipal Solid Wastes (Management and Handling) Rules. (2000). *New Delhi: Ministry of Environment and Forests, Government of India.*
4. Sinha C. "Open burning of municipal solid waste: state level analysis." *TERI information monitor on environmental science*, 2. New Delhi: TERI; 1998.
5. World Energy Council 2013 *World Energy Resources: Waste to Energy.*

[Back to table of contents](#)

Laboratory experimental techniques for determination of diffusion coefficients for landfill liner facilities - A review

Partha Dasⁱ⁾ and T.V. Bharatⁱⁱ⁾

i) PhD Student, Department of Civil Engineering, IIT Guwahati, email- partha.das@iitg.ernet.in

ii) Assistant Professor, Department of Civil Engineering, IIT Guwahati, email-tvb@iitg.ernet.in

ABSTRACT

The thickness of the liner is decided based on the model parameters which are the effective diffusion coefficient and retardation factor. As the clays used in liners have hydraulic conductivity as low as 10^{-9} cm/sec for which the advective flow is less significant, in such a case modelling of diffusive contaminant transport through the fine grained soil becomes critical. Laboratory diffusion testing helps in the determination of the model parameters which in turn enables the effective design of the liner facilities and assesses the migration rate of the contaminant through the barrier material. In this paper a detailed review is presented on the various laboratory measurement techniques for the estimation of the effective diffusion and retardation coefficient. The equations describing the 1D contaminant transport through compacted clay soils is presented. The analytical solutions which are utilized to determine the model parameters from the measured experimental concentration profiles based on various initial and boundary conditions for all the laboratory experimental techniques is discussed. This paper lucidly describes the underlying mechanism of contaminant transport for each laboratory methods which has been adopted by various researchers till date and also highlights the merits and demerits of using various experimental techniques.

Keywords: diffusion coefficient, retardation coefficient, analytical solutions

1 INTRODUCTION

For the design of the compacted liner facility, knowledge of the governing mechanism which involves formulation of appropriate governing differential equation is very much essential. The solution to such a differential governing equation helps in determining the concentration profile of the diffusing species with respect to space and time (Rowe *et al.*, 1988). Various literature studies have indicated that in fine-grained porous materials such as compacted clays used for landfill barriers when the hydraulic conductivity is extremely low and when coupled with low hydraulic gradients, the flux of contaminants due to diffusion will exceed that due to advection (Mike, 2004). Hence diffusion is the controlling mechanism of solute transport in many fine-grained soils (Crooks and Quigley, 1984; Quigley and Rowe, 1986; Shackelford and Daniel, 1991a, 1991b; Rowe, 1988; Kau *et al.*, 1999; Garcia *et al.*, 2001; Van Loon *et al.*, 2004).

Diffusion studies are very much essential to carry out the laboratory diffusion experiments to assess the model parameters which are the effective diffusion coefficients and the retardation coefficients. The model parameters are the essential parameters which helps in the effective and economic design of landfill liners. They govern the design of the landfill liner facility.

2 DIFFUSION THEORY

Diffusion is a process in which a solute in a solution flow due to concentration gradient that is flow from a region of high concentration to low concentration. The diffusive flux usually follows Fick's first and second law (Shackelford, 1991; Bharat, 2012). The transient state diffusive flux is derived from the Fick's second law which is given as:

$$\frac{\partial c}{\partial t} = \frac{D_e}{R_d} \frac{\partial^2 c}{\partial x^2} \quad (1)$$

where C is the concentration of the tracer in the pore water, t is the diffusing time, D_e is the apparent diffusion coefficient, n is the porosity and x is the distance from the source R_d is the retardation factor which describes the sorption potential of a soil.

3 LABORATORY EXPERIMENTAL TECHNIQUES FOR DETERMINATION OF DIFFUSION COEFFICIENTS

The various laboratory techniques to determine the model parameters which are the effective diffusion coefficient, D_e and the retardation factor R_d are the half-cell technique, in-diffusion technique, through-diffusion technique and out-diffusion technique

3.1 Half-cell method

In order to determine the diffusion coefficient of the contaminants migrating through the barrier material, half-cell method can be employed. The description of the method can be found elsewhere (Shackelford, 1991; Robin *et al.*, 1987). In this method two half cells filled with soil are taken and tagged together. In one of the half-cell the soil is contaminated and in the other half-cell the soil is uncontaminated. As such when both the half cells are connected together there will be migration of contaminants from one half-cell to the other Fig.1 With time the concentration in the tagged cell decreases as the contaminants diffuses into the untagged cell. Sand bentonite mixtures, using only bentonite and for other kind of plastic clays such a method was used initially were used to study the diffusion of strontium and chloride by half-cell technique (Gilham *et al.*, 1984, Robin *et al.*, 1987, Oscarson *et al.*, 1991; Cho *et al.*, 1993). One disadvantage of using this method is that proper contact between the cells cannot be made and as such it might end up giving erroneous results. However the diffusion testing time can be minimized.

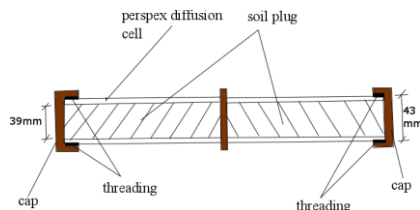


Fig. 1. Laboratory half cell (after, Robin *et al.*, 1987)

The solution to equation 1 is based upon some initial and boundary. In the finite porous medium case the concentration profile reaches to the ends of the half-cell. The initial and boundary condition for such a case is given as:

$$\begin{aligned}
 c(x \leq 0, t = 0) &= c_0 \\
 c(x > 0, t = 0) &= 0 \\
 \delta c(x = 0, t > 0) / \delta x &= 0; \quad \delta c(x = L, t > 0) / \delta x = 0
 \end{aligned}$$

Corresponding to the above initial and boundary conditions, the solution to equation 1 is given by Carslaw and Jaegar (1959) as:

$$\frac{c}{c_0} = \frac{x_0}{L} + \frac{2}{\pi} \sum_{m=1}^{\infty} \frac{\exp(-D^* m^2 \pi^2 t / R_d L^2)}{m} \cos\left(\frac{m\pi x}{L}\right) \sin\left(\frac{m\pi x_0}{L}\right) \quad (2)$$

3.2 Double reservoir or through diffusion technique

In the double reservoir the intact plug of barrier material (clay) is placed within the diffusion cell. A source and a collector reservoir is connected to the clay plug as shown in Fig. 2. The solution that is placed in the source solution may be distilled water spiked with the concerned organic species (Barone *et al.*, 1992, Rowe *et al.*, 1988; Shackelford, 1991, Shackelford *et*

al., 1989; Garcia *et al.*, 2001). And the collector solution is of pure distilled water. The initial concentration of the source solution is c_0 . After the introduction of the leachate in the source reservoir mass transport of the chemical constituents takes place by molecular diffusion due to concentration gradient (Shackelford *et al.*, 1989). This method is easy to perform and it simulates the field condition of flow through the liner however time taken can be high.

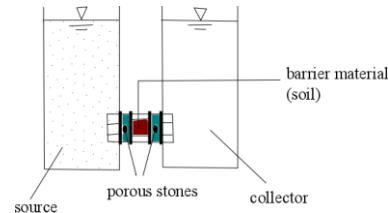


Fig. 2. Transient through diffusion set-up (after Bharat, 2013)

During the diffusion testing the source and the collector reservoir are monitored periodically to obtain the variation of the organic species concentration with time. Fitting of the theoretical variation of the species with observed experimental variation, it is possible to calculate the value of the diffusion coefficient D^* . The initial and boundary conditions of the model as depicted in Fig. 2 are:

Initial condition: $c(0 < x < L, t = 0) = 0$

Boundary condition:

$$\begin{aligned}
 c(x = 0, t) &= c_0 + \frac{nD^*}{H_s} \int_0^t \left(\frac{\delta c}{\delta x}\right)_{x=0} dt \\
 c(x = L, t) &= -\frac{nD^*}{H_c} \int_0^t \left(\frac{\delta c}{\delta x}\right)_{x=L} dt
 \end{aligned}$$

where c_0 is the initial concentration of the organic species at time $t = 0$ and H_s and H_c are the equivalent height of the source and collector reservoir respectively and L is the length of the soil plug. Using the above initial and boundary conditions the analytical solutions showing the variation of concentration in the source and collector reservoir is given elsewhere (Bharat, 2013):

$$\frac{c(x=x,t)}{c_0} = \frac{1}{2+k} + 2 \sum_{j=1}^{\infty} \frac{(\alpha j^2 + K^2) e^{-\alpha j T}}{4K\alpha j^2(k+1) - (2K - (\alpha j^2 - K^2))(\alpha j^2 - K^2)} \quad (3)$$

$$\frac{c(x=L,t)}{c_0} = \frac{1}{2+K} - 2K \sum_{j=1}^{\infty} \frac{(\alpha j^2 + K^2) e^{-\alpha j T}}{4K\alpha j^2(k+1) - (2K - (\alpha j^2 - K^2))(\alpha j^2 - K^2)} \quad (4)$$

where $K = \frac{nRdL}{Hr}$; $T = \frac{tD^*}{RL^2}$; $\tan \alpha j = \frac{2K\alpha j}{\alpha j^2 - K^2}$; αj are the roots.

Using several values of D^* and R_d , theoretical curves for the variation of concentration of organic species in the source and the collector reservoir are developed. The curves are best fitted with the curve obtained from experimental data. The best fit curve will give an indication of the D^* value of the particular organic species (Barone *et al.*, 1992).

3.3 Single reservoir or in-diffusion technique

The in-diffusion is a single reservoir technique where the diffusion cell containing the soil plug of required thickness is placed in contact with the tracer solution in the source reservoir (Barone *et al.*, 1992). The soil is saturated with standard water and compacted in molds. After the introduction of the tracer solution migration of contaminant takes place from the reservoir to the soil by molecular diffusion. In order to assess the variation of concentration in the source reservoir the tracer solution is monitored periodically by taking samples through the sampling port. After the diffusion test the cell is disassembled and the last sample is analyzed for concentration Fig. 3. The soil from the disassembled cell is taken out and the concentration profile in the soil (Shackelford and Daniel, 1991b).

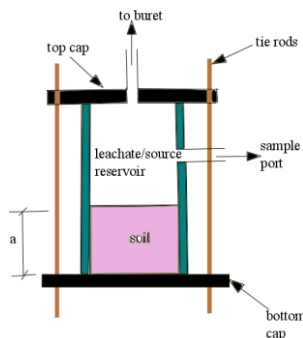


Fig. 3. Diffusion cell set up (after Shackelford and Daniel, 1991b)

Due to the transport of the contaminant by molecular diffusion there is a decrease in concentration in the source solution with time (Shackelford *et al.*, 1989). The initial and boundary conditions for such a case is as such:

$$c = 0 \text{ at } 0 \leq x \leq a, t = 0; \quad c = c_0 \text{ at } a \leq x \leq a + l, t = 0;$$

$$\frac{\delta c}{\delta x} = 0 \text{ at } x = 0, t > 0$$

where, a is the length of the diffusion cell, L = effective length of the reservoir and y is the free solute per unit of soil. The solution to equation 1 with the abovementioned initial and boundary conditions given by Crank (1975):

$$\frac{c_t}{c_0} = \frac{\alpha}{1+\alpha} + \sum_{m=1}^{\infty} \frac{2\alpha}{1+\alpha+q^2\alpha^2} \exp\left(\frac{-D^*tq^2}{R_d\alpha^2}\right) \quad (5)$$

where c_t is the solute concentration of the reservoir at any time t and q is the non-zero positive roots given by $\tan q = -\alpha q$ and $\alpha = \frac{l}{nR_d a}$

3.4 Out diffusion technique

The out diffusion technique is similar to the through diffusion technique. Unlike through diffusion technique where both the compartments (reservoirs) are filled with artificial pore water with tracer solution in the source compartment, out diffusion technique requires both the reservoirs to be filled with tracer free pore water. As the steady state condition is reached in through diffusion experiment, the tracer solution in the source reservoir is replaced by synthetic artificial water without tracer (Van loon *et al.*, 2004). The soil sample is now previously saturated with solute and the resulting concentration in the liquid is measured Fig. 4. The method is also called out-leaching technique (Sardini *et al.*, 2003). The solution from both the compartments were monitored regularly and analyzed for activity by liquid scintillation analysis. The process is repeated until all the activity is diffused out of the sample. The compartments or reservoirs used in the experiment usually has high volume for source reservoir and low volume capacity for outlet or secondary reservoir (Van Loon *et al.*, 2004). After regular intervals both the compartment solution are analyzed for activity or concentration (Tits *et al.*, 2003). The method is very time consuming and not easy to perform. The one dimensional diffusion equation given by equation 1 is solved using the initial condition taken from the through diffusion case which has a linear concentration profile that is $c(x) = c_0 \left(1 - \frac{x}{L}\right)$ and with boundary condition $c(x = 0, t) = c(x = L, t) = 0; t > 0$.

Based on these initial and boundary conditions an analytical solution is given (Jakob *et al.*, 1999):

$$c(x, t) = 2c_0 \sum_0^{\infty} \frac{1}{n\pi} e^{(-\frac{n\pi}{L})^2 \frac{D_e}{\alpha} t} \sin\left(\frac{n\pi x}{L}\right) \quad (6)$$

The values of diffusive flux at both boundaries is given as (Van Loon, 2004):

$$j(0, t) = 2c_0 \frac{D_e}{L} \sum_0^{\infty} e^{(-\frac{n\pi}{L})^2 \frac{D_e}{\alpha} t} \quad \text{at } x = 0$$

$$j(L, t) = 2c_0 \frac{D_e}{L} \sum_0^{\infty} (-1)^n e^{(-\frac{n\pi}{L})^2 \frac{D_e}{\alpha} t} \quad \text{at } x = L$$

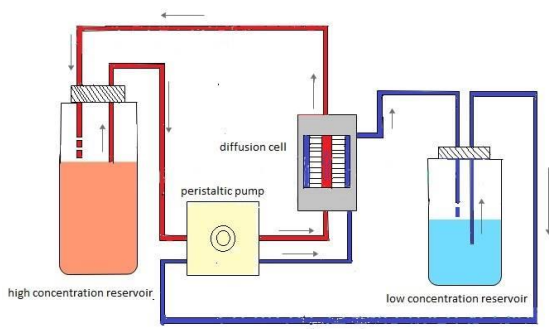


Fig. 4. Out diffusion cell set-up (after Van Loon, 2004)

4 SUMMARY

This paper describes all the four laboratory methods adopted all round the world for estimation of the model parameters which are the effective diffusion coefficient and retardation factors. The four methods are namely half-cell technique, through-diffusion technique, single reservoir technique and out-diffusion technique are described in one single paper which was not carried out earlier. This review study is conducted to provide the landfill engineers with a manual for conducting the experiments feasible as per the available resources. This study also highlights the merits and demerits of using different measurement techniques. The analytical solutions based on various boundary conditions, which utilizes the experimental data to determine the model parameters by inverse analysis are also described in this work.

REFERENCES

- 1) Barone FS, Rowe RK and Quigley RM (1992) A laboratory estimation of diffusion and adsorption coefficients for several volatile organics in a natural clayey soil. *Journal of Contaminant Hydrology* 10: 225–250.
- 2) Bharat TV, Sivapullaiah PV and Allam MM (2012) Robust solver based on modified particle swarm optimization for improved solution of diffusion transport through containment facilities. *Expert Systems with Applications* 39(12): 10812–10820.
- 3) Bharat, TV. (2013) Analytical model for 1-D contaminant diffusion through clay barriers. *Environmental Geotechnics* 1.4 (2014): 210-221
- 4) Binning PJ, Hitchcock PW and Smith DW (1999) Experimental analysis of fluoride diffusion and sorption in clays. *Journal of Contaminant Hydrology* 36: 131–15
- 5) CARSLAW, H.S., and JAEGGERJ., C. (1959). *Conduction of heat in solids*. Clarendon Press, Oxford.
- 6) Cho, W. J., D. W. Oscarson, M. N. Gray, and S. C. H. Cheung. (1993). Influence of Diffusant Concentration on Diffusion Coefficients in Clay. *Radiochim. Acta* 60: 159-163.
- 7) Crank J (1975) *The Mathematics of Diffusion*. Clarendon Press, London.
- 8) Crooks, V.E. and Quigley, R.M., (1984). Saline leachate migration through clay: A comparative laboratory and field investigation. *Can. Geotech. J.*, 21: 349-362
- 9) Garcia-Gutierrez, M., Missana, T., Mingarro, M., Samper, J., Dai, Z., Molinero, J., (2001). Solute transport properties of

compacted Ca-bentonite used in FEBEX project. *J. Contam. Hydrol.* 47, 127–137.

10) Gillham, R. W., Robin, M. J. L., Dytynyshyn, D. J., and Johnston, H. M. (1984). Diffusion of nonreactive and reactive solutes through fine-grained barrier materials. *Can. Geotech. J.*, 21(3), 541-550.

11) Jakob, A., Sarott, F.A., Spieler, P. (1999): Diffusion and sorption on hardened cement pastes - experiments and modeling results. PSI-Bericht Nr. 99-05, Paul Scherrer Institute, Villigen, Switzerland. Also published as NAGRA Technical Report NTB 99-06, Nagra, Wettingen, Switzerland.

12) Kau PMH, Binning PJ, Hitchcock PW and Smith DW (1999) Experimental analysis of fluoride diffusion and sorption in clays. *Journal of Contaminant Hydrology* 36: 131–151

13) Mike Depledge (2004) Contaminant Fluxes From Hydraulic Containment Landfills- A Review, Environment Agency Science Report SC0310/SR

14) Oscarson, DW, HB Hume and F King (1991). Sorption of Caesium in Compacted Bentonite. *Clays and Clay Minerals*

15) Quigley R. M. and Rowe, R. K. (1986). "Leachate migration through clay below a domestic waste landfill, Sarnia, Ontario, Canada: chemical interpretation and modelling philosophies." *Hazardous and industrial solid waste testing and disposal, STP 933*, D. Lorenzen, et al., (eds.), ASTM, Philadelphia, Pa., 93-103.

16) Robin, M.J.L., Gillham, R.W. and Oscarson, D.W., (1987). Diffusion of strontium and chloride in compacted clay-based materials. *J. Soil Sci. Soc. Am.*, 51:1102-1108.

17) Rowe RK, Caers CJ and Barone F (1988) Laboratory determination of diffusion and distribution coefficients of contaminants using undisturbed clayey soil. *Canadian Geotechnical Journal* 25(1): 108–118

18) Sardini P, Delay F, Hellmuth K, Porel G and Oila E (2003) Interpretation of out-diffusion experiments on crystalline rocks using random walk modeling. *Journal of Contaminant Hydrology* 61: 339–350.

19) Shackelford C, Daniel DE and Liljestrand HM (1989) Diffusion of inorganic chemical species in compacted clay soil. *Journal of Contaminant Hydrology* 4(3): 241–273.

20) Shackelford CD and Daniel DE (1991a) Diffusion in saturated soil. I. Results for compacted clay. *Journal of Geotechnical Engineering* 117(3): 485–506.

21) Shackelford CD and Daniel DE (1991b) Diffusion in saturated soil. II. Results for compacted clay. *Journal of Geotechnical Engineering* 117(3): 485–506

22) Shackelford CD (1991) Laboratory diffusion testing for waste disposal — A review. *Journal of Contaminant Hydrology* 7: 177–217.

23) Tits J, Jakob A, Wieland E and Spieler P (2003) Diffusion of tritiated water and $^{22}\text{Na}^+$ through non-degraded hardened cement pastes. *Journal of Contaminant Hydrology* 61: 45–62.

24) Van Loon, L. R., Soler, J., Müller, W. and Bradbury, M. H.: (2004), Anisotropic diffusion in layered Argillaceous Rocks: a case study with Opalinus clay. *Environ. Sci. Technol.* 38, 5721–5728.

[Back to table of contents](#)

Conceptual design for community participation in devolution of sustainable smart city system management

Bhabesh Mahanta

Executive Engineer, Irrigation Department, Chandmari, Guwahati-781003, India

ABSTRACT

Smart city building is much in vogue nowadays. Government of India has planned for about hundred smart cities to be built in coming years. There is high expectation that smart cities will provide the citizen better quality of life with the application of modern information and communication technology and by creating job opportunity by revitalizing the economy with low ecological footprint. Many smart technical definitions have been introduced by the developers but the issues of sustainability and collective actions of the citizens are not analysed from the point of human behaviour in economic environment. So concepts of citizens' engagement and building inclusive society tend to remain aloof and one can only see citizens becoming avid consumers. It follows that a set of efficient property rights held over resources enters into utility functions of the decision maker and subsequent to it right contractual laws, resource and risk allocation and types of financing is to be incorporated in smart city management. An enabling environment is the foremost precondition of much needed collective action and sustainability of any social system and to infuse producers and consumers to become 'pro-sumers'. The purpose of the present paper is to analyse how peoples' participation is viewed as important criteria for sustainable smart city management by different researchers and to explore the significance of the effect of private property rights along with their identification. This paper also attempts to identify the stakeholders of smart city and to trace their interactions such that there can be efficient contractual arrangement to attain optimality in transfer of right and risks by employing right type of PPP mode and financing structure in smart city economic transaction. Here is an attempt to map the necessity of devolution of smart city management for effective participation of citizen and behavioural change from an economic point of observation.

Keywords: property right, sustainability, collective action, smart city management, devolution, pro-sumer

1 INTRODUCTION

Currently governments of developing countries are trying to modernize their societies by building smart cities. Sustainable smart city management is a challenge for the developers. Here one of the prime necessities for the developers is to conceptualize the smart city system management as an effort to common pool resource management.

As everybody agrees resources are scarce. But nowadays due to growing population and social complexities resources are becoming increasingly scarce, polluted and politicized. As the competition over the available resources is fierce amongst different interest groups in the society, it is imperative for every nation or organization to optimize natural resources management to achieve sustainability. Moreover, the sustainability criteria should incorporate many diverse factors to include technical, financial, political, and environmental to cultural, anthropological and emotional aspects of the stakeholders. Therefore smart city designers are looking for community participation both as a means and also an end for any sustainable smart city. So, it is urgent that the policy makers develop equitable

property rights for resources and enable local communities to manage them.

The purpose of this paper is to identify frameworks for policy recommendations and research priorities towards effective efforts to devolve the management of smart city system from governments to the citizens. The paper focuses on the need of finding out essential motivating factors encompassing property rights concepts that will invoke collective action among citizens after devolution and on the need of finding out right public private partnership mode to ensure effective and sustainable smart city management.

2 THEORETICAL BACKGROUNDS

When dealing with motivation of a human we cannot ignore Maslow's theory on human motivation as he outlined it in a paper in 1943 and in a subsequent book "Motivation and Personality". In this context, it is seen that the most important human motivating factors are property right, security and incentives for the citizens to invest their time, money and calibre in any management participation. In turn, the quality of management will affect how well a system management perform and what they will

produce, such as success and sustainability. As observed by Furubotn E. G. et al (1972), “The organization per se is no longer the central focus; rather, individuals are assumed to seek their own interests and to maximize utility subject to the limits established by the existing organizational structure.” They also observed that due to property rights approach, “it becomes possible to consider the behavior of the decision maker within the firm, government bureau, or similar collective agency.” As against the traditional theory of production and exchange assumed economic behaviour as profit maximization problem, property rights theory assumes it to be an optimization problem amongst the actors and as emphasized by Furubotn et al, “Though sometimes forgotten, there should be no confusion about the fact that both trade and production involve contractual arrangements.”

Going further in the relevance of contractual agreements we can point out Contract Theory put forward by this year’s Nobel Winners in Economics Oliver Hart and Bengt Holstrom. Nobel Committee draws out implication of Laws of Contract as, “Contracts help us to be cooperative and trusting when we may otherwise be disobliging and distrusting. As employees, we have employment contracts. As borrowers, we have credit contracts. As accident-prone owners of valuable property, we have insurance contracts. ... One important reason for drawing up a contract is to regulate future actions.”

How smart city management devolution programme are structured or organized will determine what kind of property rights are given to the smart city citizens or inhabitants. On the other hand what property rights are held by the smart city dwellers will determine to what extent citizens are willing to provide collective action for smart city management? Here comes a two way interactions of interests between the stakeholders. Over all these, the quality of management will affect how well the smart city management performs and what results they produce such as success, productivity, sustainability.

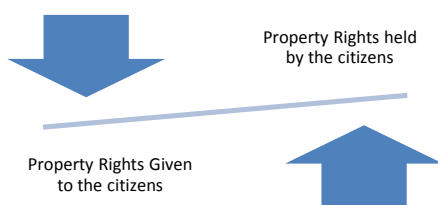


Fig. 2: Property Rights Held by and Given to Citizens

Delving into the discussion of property right, Furubotn and Pejovich (1972) and North (1990)

included both goods and services are included are included as potential objects of property or assets. Eggertson (1990) suggested three types of rights, right to use an asset, right to obtain benefit from an asset and right to alienate or sell an asset.

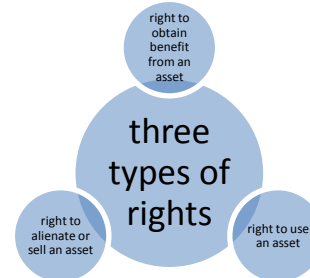


Fig. 1. Three Types of Rights

Property rights are social conceptions. But still to have force on human behaviour, they must be enforceable through sanctions (Vermillion D., 2001). Sanctions may involve modern legal codes, punishments imposed by users groups or other social pressures. Key obligations which may be attached to property rights are financing construction and maintenance of infrastructure, financing costs of service provision, and following rules regarding use or protection of the resource.

These concepts can be applied to the smart city development. Here we will consider smart city infrastructure, water, land, funds owned by a smart city organization (in public sector), its legal status and a licence or commission to provide an smart city management service to all be potential types of property, to which rights and obligations are attached.

2 SMART CITY DEVELOPMENT TREND

2.1 Current conception

Going through the evolution of the idea of smart city we can start from the fact that many countries started facing three main challenges relating to environmental issues. They are:

1. Reducing CO₂ emissions in order to mitigate climate change
2. Ensuring energy independence and security, and
3. Revitalizing economy by strengthening the competitiveness.

To tackle these, Japanese government started its reflexions about “smart cities” and “smart communities” around 2007 and 2008 (Granier et al, 2016). Japanese defines smart city projects as “a new style of city providing sustainable growth and designed to encourage healthy economic activities that reduce the burden on the environment while improving QoL (Quality of Life)”

The environmental guidelines for smart cities (Govt of Mauritius, July, 2015) notes that, “A smart city is one where capital, resources and knowledge are managed in a wise manner, with a focus on innovation, sustainability, efficiency and quality of life”. It also mentions that, “Smart city needs to forge the way towards socially inclusive communities with a low ecological footprint”.

Vanolo (2014) considers that the smart city is born out of the notions of “smart growth” and “intelligent city”. In this respect, a smart city is a city which takes advantage of Information and Communication Technology in order to ensure its growth and attractiveness. More precisely, Giffinger et al (2007) established six distinctive components, namely smart economy, smart mobility, smart governance, smart environment, smart living and smart people.

In a similar vein, and in order to clarify what they consider to be a “fuzzy concept”, Caragliu et al. (2011) “believe a city to be smart when investments in human and social capital and traditional (transport) and modern (ICT) communication infrastructure fuel sustainable economic growth and a high quality of life, with a wise management of natural resources, through participatory governance”.

Khansari et al. points out that, “the premise of a smart city is that by having the right information at the right time, citizens, service providers and city government alike will be able to make better decisions that result in increased quality of life for urban residents and the overall sustainability of the city”.

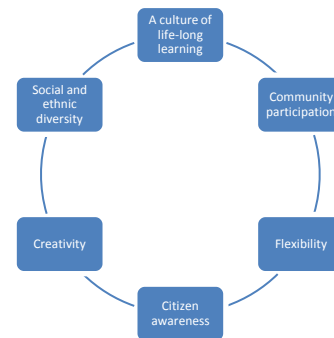
It is important to note that researchers Granier et al pointed out a difference between the idea of “smart city” and “smart community”. According to them, “Smart Communities aspire to go further the mere smart grid, since although they focus on energy issues, another of their objectives is to make “smart” not only the grid, but also industry, commerce, business and householders’ behaviours, including mobility issues”.

Japanese society benefits from strong social capital and high civic engagement and they can reap the benefits of participation and co-production. The relationship between state and society is also conceived as integrated and cooperative and is characterized by a high level of mutual trust. Ministry of Energy, Trade and Industry, Japan, indicated two innovative features of Smart Communities, namely the “participation of all stakeholders among which the citizens”, and behavioural change through “lifestyle innovation”.

The expression “smart community” is used to underscore the importance of community and citizens’ participation.

2.2 Characteristics of smart people concept

The basic concept of smart people has the following characteristics as depicted in the figure 3. (Environmental Guide, Government of Mauritius, 2015)



Each of these parameters is easy to follow but incorporation of all these in smart city design is a challenge for the developers.

Fig. 3. Characteristics of Smart People Concept

3 STAKEHOLDERS OF SMART CITY AND PARTICIPATORY GOVERNANCE

3.1 Stakeholders of smart city

In a study of people’s participation in Japanese smart cities researchers Granier et al (2016) considered four smart city stakeholders. They are: Ministry of Economy, Trade and Industry (METI); the local governments; and private actors involved in each project; as well as Smart Communities’ inhabitants.

Similarly, we can identify four smart city stakeholders in India as follows:

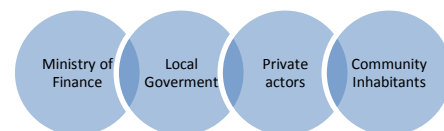


Fig. 4. Smart City Stakeholders

3.2 Participatory governance in smart city

Decades ago smart cities are supposed to be means for serving consumers’ growing demand for goods and services. Still now many people think building smart cities are technological and environmental challenge. But smart city management is an after-thought and nowadays the developers have to concentrate on their sustainability. Today there is a growing concern that smart cities are to be end in itself to be socially inclusive. Many scholars and practitioners stress that (smart) citizens play a crucial role in smart cities, not only by their appropriate

(smart) behaviour but also by their participation in (smart) governance.

Caragliu et al. (2009) highlighted the need for participatory governance, while Hollands (2008) argues that smart cities request more than cutting-edge ICT and need contributions from various stakeholders among the citizens.

However, despite the abundance of discourse about the key role of citizens in smart cities, relatively little research has been produced so far. Very little efforts have been undertaken to clarify the conceptual and real relationship between property rights, collective action and smart city management. Constructions of many projects are initiated but rules and rights, together with contract and enforcement mechanisms are not developed. As Chourabi et al (2012) put it, “addressing the topic of people and communities as part of smart cities is critical, and traditionally has been neglected”. Furthermore, they also express that “most publications frame smart city governance as a technical or managerial issue” and note a “lack of attention for the politics of technical choices” since “both sustainability and citizen participation are not analysed as issues of political struggle and debate but rather as desirables for a ‘good society’”.

Echoing these concerns, some scholars propose instead the notion of “smart community” since smart city would be “a city without politics where policies and digital services from the government are rolled out apparently without consultation and input from citizens let alone any form of democratic input or decision making”. For Mellouli et al (2014), “The concept of a smart community refers to the use of information and communication technologies by local governments and cities to better interact with their citizens, taking advantage of all available data to solve important problems”. They also add that “governments need not only to create new services to their citizens based on these technologies in order to improve their quality of life, but also to engage citizens in this new set of services”.

3.3 Participation in energy management: consumers turn to be pro-sumers

Granier et al point to a very useful feature of people’s participation.

Many smart cities intend to tackle environmental and energy challenges in introducing smart infrastructure, especially smart grids. It is seen that, energy projects often generate lively debate and face social acceptance problems. Mechanisms of public participation can be effective instruments to gain consent from citizens. Especially, co-production patterns of participation would favour citizens’ acceptance of constraints.

Granier et al observes that, introduction of smart energy technologies needs more than passive

acceptance and require active acceptance from users. Indeed, smart grids do not only promote the use of renewable energy and help to optimise energy management: they also allow for decentralized ways of production and invite citizens to take part in energy management, and to become “co-managers” (Strengers, 2013), “co-providers” [Geelen et al, 2013]; in other words, co-producers (Granier, 2016).

It is seen that while citizen engagement at the early stage would favour their active participation in energy management, depending on the projects, individuals can be considered as citizens, as mere consumers or even as obstacles. But it is also obvious that for a city to be smart from the perspective of energy management, active acceptance of citizens is needed. In Kitakyushu case of Japan (Granier et al, 2016) as in other Smart Communities, public and private stakeholders urged citizens to become “prosumers”, that is to co-produce energy production and distribution services. Smart citizenship would subsequently consist of being (co-)producer and consumer of services.

Since obtaining an active acceptance of smart energy technologies is not an easy task, stakeholders have to be very insistent with citizens. As it can be learnt from Japanese example of smart city management, public and private stakeholders have to organize a lot of meetings, even sometimes going door-to-door and strongly emphasising the “community” as it has been identified as a critical factor of citizen engagement.

3.4 Need for devolution

When we go through most definitions of smart cities, citizen engagement is a key element. But scholars have noticed that very little research has been done to focus on citizen involvement in smart cities (Benoit Granier et al, 2016). There is no doubt that a smart city is designed for utilizing the existing resources to maximise the all round benefit of the citizens in the most sustainable manner. Although preserving environmental balance is a core issue in the process of developing any smart city, the designers must focus on developing a sustainable modern community.

Devolution is the transfer of rights and obligations over resources to resource user groups (Meinzen-Dick et al, 1999). For smart city development, this normally involves transfer of rights and responsibilities for smart city management from the government to local users groups. Coordinated behaviour of the groups will generate collective action towards a common interest or purpose.

4 SMART CITY MANAGEMENT GAP AND INADEQUATE PROPERTY RIGHTS

4.1 Management gap

From the perspective on property rights and collective action, we can conclude that the usual free government assistance may create a sense of speculative dependency among end-users towards the government for the service delivery. More often government investment has served to create the impression that the project structures belong to the government and it is the responsibility of government to minimize the cost of products and service to the end-users. Such assistance practically discourages end-users from taking collective action to maintain the project.

It is now widely understood that the smart city management will also not be successful without basic devolution of some or all responsibility for management to inhabitants. For that reason, modifications must be made in the conventional analytical framework if economic model having wider applicability are to be developed. Here the usual solution is to formulate an optimization model to reach Pareto-equilibrium condition of the public and users. In this context, we should note observations made by Furubotn et al (1972), that “it is necessary to define the particular utility function that reflects the decision maker’s preferences and to determine the actual set of options (penalties and rewards) that is attainable by the decision makers. Then, according to them, the formal problem emerges as one of maximising the utility function subject to the constraint imposed by the opportunity set”.

Here, it is important to note that usually the understanding of the bureaucracy and state can be developed from consideration of individual utility maximising behaviour. As a result of this, very often, state has frequently traded inefficient property rights for revenue, and in doing so throttled economic growth (Professor North). Buchanan and Stubblebine (1962) have also noted that, “The important implication to be drawn is that full Pareto-equilibrium can never be attained via the imposition of unilaterally imposed taxes and subsidies until all marginal externalities are eliminated.”

Hence management gaps or dysfunctions can arise when property rights are inadequate to meet management requirements.

4.2 Property rights in smart city environment

The key challenge for devolution programs is to create an enabling environment. This is followed by identification of what kind of property rights should the system devolve. It is expected that in the enabling environment communities or citizen’s group will have the motivation and capacity to act collectively for an assured sustainability.

There is often a misconception that property rights are related only to physical resources. But the very definition of property right implies that its concept can be applied to smart city decision making

authority, service provision, financing in addition to common pool resource management. In broad sense, smart city system management is an integrated service delivery system and is akin to common pool resource management. Vermillion (2001) observes that organization is manifestation of “social capital”, and hence a form of group property. According to him, experience with successful management devolution indicates that rights over decision-making, service provision and financing are as important as are property rights and infrastructure use rights. Some key types of property rights which may be inherent in or devolved to citizens unit or citizens group (private actors legally registered) either fully or shared with the public sector are summarized below:

Right to determine product and services to get engaged with -- The unit has the right to select the goods and services to choose and determine potential to optimize productivity.

Infrastructure use right – The unit has the right to operate, repair, modify or eliminate structures. Without this right, the unit is unable or unwilling to invest in long-term maintenance and repair and is likely to consider the infrastructure as the property of the government.

Right to mobilize and manage finances and other resources – The unit has the power to impose service fees, establish sideline revenue activities, plan and implement budgets, require labor or other inputs from members, recruit and release staff and provide training.

Right of organizational self-determination – The unit has the right to determine its mission, scope of activities (whether single function or multiple function, including businesses), basic by-laws, rules and sanctions and method for selecting and removing officers.

Right of membership in organization – All users who are eligible for membership according to unit’s by-laws have the right to be members of the unit and receive its privileges, services and benefits--as long as they comply with its rules and obligations. This also implies the right to exclude non-members from the service provided by the unit.

Right to select and supervise service provider – Where members of the unit are unable or unwilling to directly implement the O&M service by themselves, the unit may appoint third parties (such as contractors) to implement required services. The unit has the right to set the terms of such contracts and supervise service providers.

Right to support services – Subject to government policies or agreed conditions, the unit has the right of access to support services it needs in order to function properly. This may include access to credit, banking services, agricultural extension, technical advisory services, subsidies, conflict resolution

support and other legal services, marketing assistance, training and so on.

5 STRUCTURING DEVOLUTION TO PROMOTE COLLECTIVE ACTION AND TRANSFER OF RISK

5.1 Collective action, risk transfer, value for money

In common talk, collective action denotes doing something partially or wholly as a member of a group. However, Vermillion (2001) opines that “as property rights, this action include both decision making and the behaviour invoked by it. It is collective because it represents the shared interests of a defined group of resource users.” Ostrom (1990) substantiates that there are three basic types of collective decisions and actions, such as, constitutional actions, collective choice and operational actions.

A smart city project basically includes the following characteristics and needs, (a) high complexities and uncertainties and hence the heightened need for cooperation, creative thinking, as well as technological and managerial innovations, (b) strategic impact and hence the need to optimise their overall value capture and (c) potential to develop, nurture and sustain the key performance requirements over a longer term. In this context an integrated framework is more pressing and thus arise the need for public, private partnership approach.

There are various reasons as to why governments might undertake PPPs. Grimsey et al (2005), points out that the paramount one is the objective of achieving improved value for money (VFM), or improved services for the same amount of money, as the public sector would spend to deliver a similar project. They also observed that, “There is a long history of publicly procured contracts being delayed and turning out to be more expensive than budgeted. Transferring these risks to the private sector under a PPP structure and having it bear the cost of design and construction over-runs is one way in which a PPP can potentially add value for money in a public project.”

An effective transfer of risk from the public sector to private sector is needed since it is the acceptance of risks that gives the private entity the incentive to price and produce effectively. However, for this transfer to happen, a clear property right needs to be created (Alchian, 1965).

Approaches to VFM will ensure that:

- a) Projects are awarded in a competitive manner
- b) Economic appraisal techniques, including risk assessment, be rigorously applied and that risk is allocated between the public and

private sectors so that the expected VFM is maximized.

5.2 Choosing right team

Looking for other success criterion, selecting the ‘right’ team is considered critical to the success of any project. Discussing about team selection for successful projects, Kumaraswami et al (2008) observes that, “A growing body of research supports the view that contractual parties are more willing to cooperate and to build good relationships on longer-term contracts. Focussing on short-term returns leads to neglect of, and detriment to, long-term project goals. The long-term nature of PPPs provides a good opportunity to create, develop and sustain trust and cooperation and also for the benefits to materialise.”

If we consider smart city as a system then its different organs or functional units are part of its stakeholders. These are Union Finance department, state government (elected councils) and private agents (citizens or citizen’s group coming into agreement for a defined service delivery). After designing a concessional framework and risk allocation for the participants, tendering consortia with members belonging to these stakeholders’ networks who respond to an Expression of Interest (EOI), may be assessed for their eligibility by comparing their (1) technical competence, (2) relational capacity and (3) sensitivity to key sustainability issues (Kumaraswami et al, 2008).

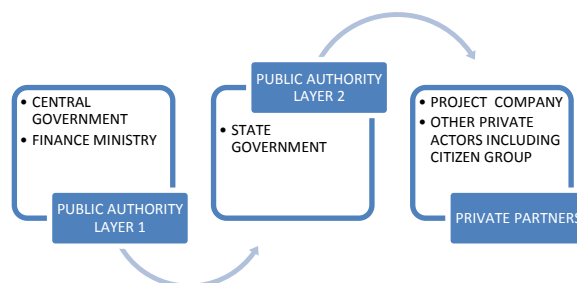


Figure 5: Public Authority and Private Partners

5.3 Choosing right type of PPP contract

There may be question whether PPP is a new form of privatization. In this context, point made by Grimsey et al (2005) is worthy to note. They expressed that, “PPPs are not privatisation because with privatisation the government no longer has a direct role in ongoing operations, whereas with a PPP the government retains ultimate responsibility. Nor do PPPs involve simply the one-off engagement of a private contractor to provide goods or services under a normal commercial arrangement. Instead, the emphasis is on long-term contracts and strict

performance regimes, such as build-operate-transfer (BOT) or design-build-finance-operate (DBFO) projects to design, construct, finance, manage and operate infrastructure under a concession, with revenues (either from government or users) according to services supplied. The private sector partner is paid for the delivery of the services to specified levels and must provide all the managerial, financial

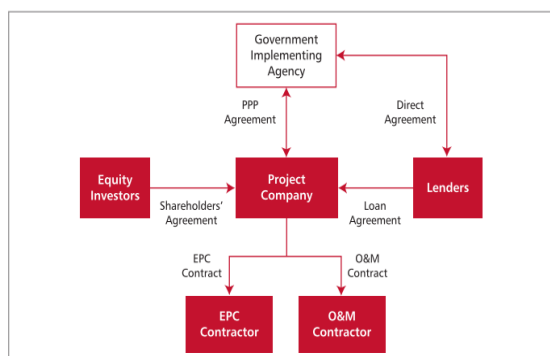


Fig. 6. Typical project structure of PPP

(Daube et al, 2008)

and technical resources needed to achieve the required standards. Importantly, the private sector must also bear the risks of achieving the service specification.”

Smart city management can employ any suitable type of PPP contract such as Build-Own-Operate (BOO), Build-Own-Transfer (BOT) Build-Rehabilitate-Operate-Transfer (BROT), Partial Privatization, Full Privatization, Rehabilitate-Operate-Transfer (ROT), Merchant Management Contract, Lease Contract, Build-Lease-Own (BLO), Build-Own-Operate-Transfer (BOOT), Rehabilitate-Lease/Rent-Transfer (RLT) (Hammami et al, 2006).

If we can practically accommodate these concepts, value for money can be thought of the best price for a given quantity and standard of output measured in terms of relative financial benefits.

6 FINANCIAL STRUCTURES FOR PPP IN SMART CITY MANAGEMENT

After selecting a right type of PPP contract, smart city management needs to be careful and precise in choosing suitable financing mode. Typical mode of financing PPP projects is almost not applicable for risk allocation in participatory management. There should be modifications in view of the practicability and the management has to search for adaptable financing ways and modes.

6.1 Typical financial structure in PPP

In general, the private party to most PPP contracts is a specific project company formed for that purpose - often called a Special Purpose Vehicle (SPV). This project company raises finance through a combination of

- Equity-provided by the project company’s shareholders, and
- Debt- provided by banks, or through
- Bonds or other financial instruments.

The financial structure is the combination of equity and debt, and contractual relationships between the equity holders and lenders.

6.2 Other modes of public finance in PPP

As noted in PPP Reference Guide, Version 2, the exclusive use of private finance is not a defining characteristic of a PPP. Governments can also finance PPP projects, either in whole or in part. However there is a disadvantage that reducing the amount of capital investment needed from the private party reduces the extent of risk transfer - weakening private sector incentives to create value for money, and making it easier for the private party to walk away if things go wrong (PPP Reference Guide by World Bank, PPIAF, ADB, IDB, Version 2, 2014).

There are several different ways in which governments can contribute to the financing structure of a PPP. They are:

- Governments may provide loan or grant finance directly to the project company, or
- Provide a government guarantee on a commercial loan. Government-owned development banks or other finance institutions can also be involved either providing finance to PPPs as part of a broader portfolio or established specifically to support the PPP program.
- Finally, governments may simply not transfer the financing function to the PPP project to the private sector, instead retaining on-going responsibility for capital expenditures.

6.3 Forfeiting model of financing

According to Daube et al, 2008, a finance structure sometimes used to reduce the cost of finance for PPPs is the forfeiting model, which can be used for ‘government-pays’ PPP projects. Under this model, once construction is completed satisfactorily, the government issues an irrevocable commitment to pay the project company a portion of the contract costs - typically sufficient to cover debt service. This can lower the project’s financing costs.

However, it means the government retains more risk under the PPP, and as debt service payments are no longer conditional on performance, the lender has less interest in ensuring project performance during operations. The forfeiting model has been widely

used in Germany for small projects - typically municipal projects - where over half of the PPPs implemented between 2002 and 2006 used this structure (PPP Reference Guide, Version 2)

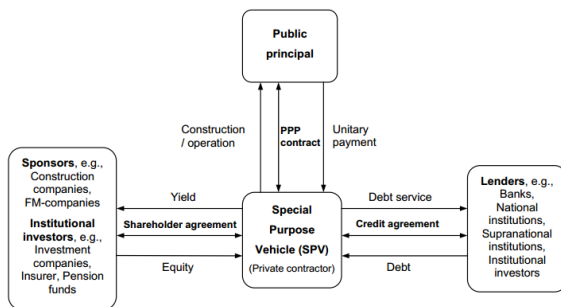


Fig. 7. Structure of Project Finance (Daube et al, 2008)

6.4 Variants of forfeiting structure

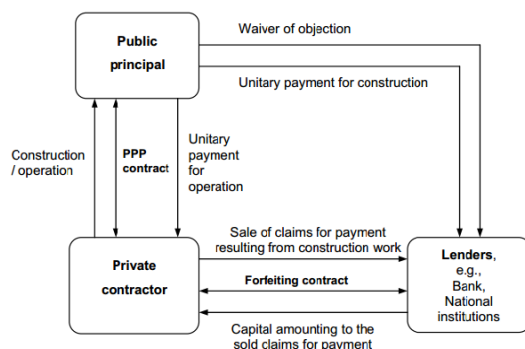


Fig.8. Structure of Forfeiting Model (Daube et al, 2008)

Cession de créance

A variant of the forfeiting model is the cession de créance (assignment of receivables) used in France. Similarly, once the infrastructure is built and operational the government may commit to making a series of payments unconditional on availability that will cover some or all of the debt service of the PPP project company (Daube et al, 2008).

'CRPAO' structure

The Government of Peru has also introduced a financing structure for PPPs that is a variant on the forfeiting model, in which these irrevocable payment commitments are issued during construction on completion of defined milestones (Daube et al, 2008).

The diagrammatic presentation of the two generally adopted financing models, project finance and forfeiting model is shown in figure 7.

10 CONCLUSIONS

A smart city is not only a set of structures and facilities built to fulfill the ever increasing demand of consumers. It is not solely a technological and environmental challenge alone. If one thinks that a smart city is simply a modern day product and citizens are its holy consumers, then smart city management will be a nightmare. A country can only be built by involvement of the citizens, so also a smart city. Citizens need to be participant, co-producers and co-managers for ensuring sustainability of a smart city project. For sustainable smart city design planners need to incorporate concepts of property right, risk transfer, value of money and selection of right kind of public private partnership mode for achieving collective action and inclusive growth.

REFERENCES

- 1) Alchian, A. (1965). SOME ECONOMICS OF PROPERTY RIGHTS. *Il Politico*, 30(4), 816-829. Retrieved from <http://www.jstor.org/stable/43206327>
- 2) Brown, H., and Ward, M. N. (2014). "A Haitian 'ecodistrict:' conceptual design for integrated, basic infrastructure for the commune of Léogâne." *Earth Perspectives*, Springer Berlin Heidelberg, 1(1), 4.
- 3) Caragliu, A., Del Bo, C., & Nijkamp, P. (2011). Smart cities in Europe. *Journal of urban technology*, 18(2), 65-82.
- 4) Chourabi, H. T. Nam, S. Walker, R. J. Gil-Garcia, S. Mellouli, K. Nahon, T. A. Prado and Scholl H. J., Understanding Smart Cities: An Integrative Framework, in: Hawaii International Conference on System Sciences, 2012, pp. 2289-2287
- 5) Daube, D., Vollrath, S., and Alfen, H. W. (2008). "A comparison of Project Finance and the Forfeiting Model as financing forms for PPP projects in Germany." *International Journal of Project Management*, 26(4), 376-387.
- 6) Douglass C. North. (2005). "Institutions, Institutional Change and Economic Performance." *Review Essay Week 6*, (February), 1-5.
- 7) Furubotn, E. G., and Pejovich, S. (1972). "Property rights and economic theory: a survey of recent literature." *Journal of Economic Literature*, 10(4), 1137-1162.
- 8) Geelen, D., A. Reinders and D. Keyson, Empowering the end-user in the smart grids: Recommendations for the design of products and services, *Energy Policy* 61 (2013), 151-161
- 9) Giffinger, R., & Pichler-Milanović, N. (2007). *Smart cities: Ranking of European medium-sized cities*. Centre of Regional Science, Vienna University of Technology.

- 10) Gramberger, M.R., “Citizens as partners: OECD handbook on information, consultation and public participation in policy-making”, OECD, 2001.
- 11) Granier, B., and Kudo, H. (2016). “How are citizens involved in smart cities? Analysing citizen participation in Japanese ‘smart Communities.’” *Information Polity*, 21(1), 61–76.
- 12) Grimsey, D., and Lewis, M. K. (2005). “Are Public Private Partnerships value for money?: Evaluating alternative approaches and comparing academic and practitioner views.” *Accounting Forum*, 29(4), 345–378.
- 13) Hammami, M., Ruhashyankiko, J., and Yehoue, E. B. (2006). “Determinants of Public-Private Partnerships in Infrastructure.” *Water*, WP, 39.
- 14) Hollands, R., (2008) “Will the real smart city please stand up? Intelligent, progressive or entrepreneurial? *City* 12(3) (2008), 303-320
- 15) Khansari, A. Mostashari and M. Mansouri, Impacting Sustainable Behaviour and Planning in Smart City, *International Journal of Sustainable Land use and Urban Planning*, 1(2) (2013), 46-61
- 16) Kumaraswamy, M. M., and Anvuur, A. M. (2008). “Selecting sustainable teams for PPP projects.” *Building and Environment*, 43(6), 999–1009.
- 17) Meinzen-Dick, R., & Knox, A. (1999, June). Collective action, property rights, and devolution of natural resource management: A conceptual framework. In *Workshop on Collective Action, Property Rights, and Devolution of Natural Resource, Puerto Azul, Philippines, June* (pp. 21-24).
- 18) Mellouli, S., Luna-Reyes, L. F., and Zhang, J. (2014). “Smart government, citizen participation and open data.” *Information Polity*, 19(1–2), 1–4.
- 19) Morales, M. C., and Harris, L. M. (2014). “Using Subjectivity and Emotion to Reconsider Participatory Natural Resource Management.” *World Development*, 64, 703–712.
- 20) PPPIRC. (2015). “PPPs in Irrigation Operator and Farmers in Irrigation PPPs Main Contractual Forms of PPPs in Irrigation Key Legal Issues Examples of PPP and Sample Agreements Further Reading Key Commercial Risks Typical Relationships Between Private Operator and Farmers.” 9–12.
- 21) Vanolo, A. (2014) “Smartmentality: the smart city as disciplinary strategy” [Urban Studies, 2014]
- 22) Vermillion, D. L. (2001). “Property Rights and Collective Action in the Devolution of Irrigation System Management.” *Collective Action, Property Rights and Devolution of*

Natural Resource Management: Exchange of Knowledge and Implications for Policy, 183–22

[Back to table of contents](#)

Sustainable interventions in Guwahati city for improving mobility, drainage and infrastructure

Rittick Hazarika

Registered Member, Council of Architecture India.

Member, Association of Architects Assam and Indian Institute of Architects, Assam Chapter, India
Proprietor, Rittick Hazarika Design Associates and Partner, Cadmetric Consulting, Guwahati, India.

ABSTRACT

This paper examines and proposes a few ideas for the sustainable development of the city of Guwahati. By definition, sustainable city will be a city which can be productive and adaptive for a long time and has the ability to reinvent and transform itself for the better as it progresses. The fast growing city of Guwahati is in need of some immediate and critical innovation in the way it tries to solve its problems regarding lack of mobility, lack of integration between various means of transport, connectivity with the proposed metro project, its lack of planned infrastructure and also its seasonal flooding problem. This document examines and proposes some ideas and solutions to some of the cities critical problems. The first is a Multi Modal Transit Interchange in Supermarket of Dispur area with a modern Greenway along the Oil pipeline land. The second is a Brahmaputra Riverfront development combining a polder/ spillway to mitigate the Bharalu flooding. The last part of the paper discussed a larger city level Redevelopment Master Plan by reconstituting available government lands in the city.

Keywords: Urban redevelopment master plan, Brahmaputra riverfront, Bharalu flood mitigation, Guwahati multi modal transit, Guwahati Greenway. Bharalu polder.

1 BACKGROUND

Guwahati is one of fastest growing cities in India and its projected growth in the coming 10 years will be equivalent to the last 30 years of its existence. As with many other cities, it also has its share of challenges regarding mobility, infrastructures and also aggravated urban flooding.

Among its key challenges is its limited road network and overall area under roads which is resulting in poor public transport options and major traffic congestions and it is rising every year.

The City is also faced with an acute flooding problem due to its Geography and unplanned drainage system.

Apart from these, the lack of planning in the growth of the City has resulted in a shortfall of open spaces, spaces for schools, hospitals and other essential features.

With this background, this paper discusses and proposes three projects and interventions which will help in transforming Guwahati into a better city.

2 CURRENT GOVERNMENT INITIATIVES

Currently the Government India is engaged in developing various Indian cities through schemes and programmes like the Smart City Plan, AMRUT, JNNURM and NERUDP etc.

The MOUD (GOI) has also advocated taking drastic and visible changes in our urban design proposals instead of small and incremental changes to improve our cities. In this regard it becomes important that Guwahati should consider some transformative urban development schemes by using these government funding programmes and improves the quality of life of its citizens and add to its sustainability.

3 PROJECT OBJECTIVES

The objective behind all the proposed interventions discussed in this paper is to highlight the applicability of these projects to address multiple problems through some innovative projects, which can be financed easily and are viable for the city authorities. These projects should also be transformative in nature and be able to effect large number of peoples with limited investment.

Another defining feature of these urban projects will be its use of sustainable technology and design to create projects that can respond to future challenges and developments in the city.

4 DISPUR SUPERMARKET INTERCHANGE AND PIPELINE GREENWAY

4.1 Concept and Rationale

An important point of confluence between North and South Guwahati is the Ganeshguri and Dispur area.

The Ganeshguri area in particular is a major mobility point and connects many different bus routes and localities of the City. It is also a hub of commercial activity with daily markets and other essential commodity shops. This area has developed organically over the years and is increasingly becoming inadequate for handling such activity and traffic.

There is now a need to create a counter magnet for such activity which is adequately linked with existing and upcoming public transport including the proposed metro corridor in G S Road.

The Supermarket area in Dispur can be designed to be one such area because of its geographical location and some advantages like the Oil pipeline corridor and proximity to some key roads.



Fig 1. Pipeline Corridor Converted to a Modern Greenway

The Oil pipeline corridor can be converted to a Greenway(Fig.1) and the other government land in the area like the old supermarket can be redeveloped with essential features to make this area a multi modal transit hub.(Fig.2)

4.2 Features and Outcomes

An elevated walkway connecting G.S.Road, Beltola Road and Hatigaon Road with the Metro corridor, thereby connecting three to four bus routes conveniently. This in turn can be linked with a modern Multi storey daily market (Fig.3) with adequate parking and public conveniences.



Fig. 2. Essential and Daily Market linked with various modes of transport.

The adjacent Oil pipeline corridor can be developed into a Greenway with only pedestrian and electric cycles that will connect areas like Six Mile with Sijubari and Lokhra etc.

These developments along with the proposed metro corridor will make this development the crucial multi modal transit hub for the future.

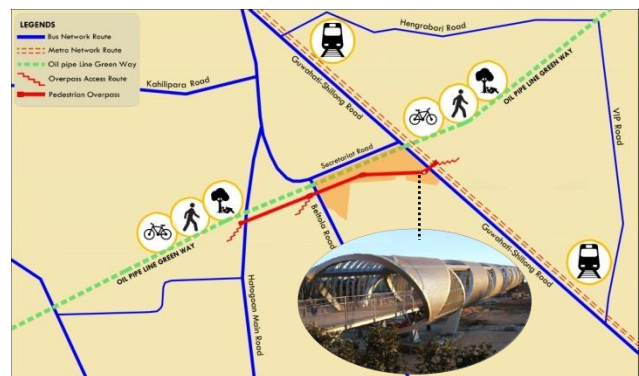


Fig. 3. Connectivity of Roads with Greenway and Pedestrian Overpass / Walkway

This can be further developed by redeveloping the existing sports facility, government quarters and other government facilities into a modern sports complex, a re-densified government housing and a modern health facility.(Fig.4)



Fig. 4. Proposed Plan of the Dispur Supermarket area.

5 BHARALU SPILLWAY AND BRAHMAPUTRA RIVERFRONT DESIGN

5.1 Concept and Rationale

The rising levels of the Brahmaputra and the increase in the storm water discharge onto Bharalu has caused regular flooding in the low lying areas of Guwahati. During the high flood season and rising Brahmaputra levels, the sluice gates of Bharalu is closed and it acts like a reservoir with limited mechanical discharge of water.(Fig.5)



Fig. 5. Bharalu Channel after heavy rainfall

Also the Brahmaputra riverfront is in need of urgent development for improving the urban life and has been a long standing public expectation. The M G Road traffic congestion also needs to be improved. Both these issues can be addressed by using the Brahmaputra riverfront imaginatively.

The Concept is for a realignment of the riverbank along the shallow area created between the two rock spurs namely, Sukleswar Ghat and Kalipur –Kamakhya Hills.(Fig.6) This shallow area is sheltered from the main Brahmaputra current because it is between two rocky outcrops .The natural sedimentation profile in this area illustrates thus feature.

This new riverbank alignment with the embankment shall create a Spillway/Polder basin for Bharalu and additional space for alignment for the MG Road which can then enable a modern riverfront development.



Fig. 6. View of proposed Riverbank alignment between two rocky outcrops.

5.2 Features and Outcomes

This engineered spillway/polder will act as a buffer reservoir between Bharalu and Brahmaputra which can mitigate flash floods arising out of excess Bharalu water during heavy rainfall.

The spillway will have arrangement for natural and mechanical discharge of water into the Brahmaputra and thereby improve the carrying capacity and discharge time of Bharalu. (Fig.7)

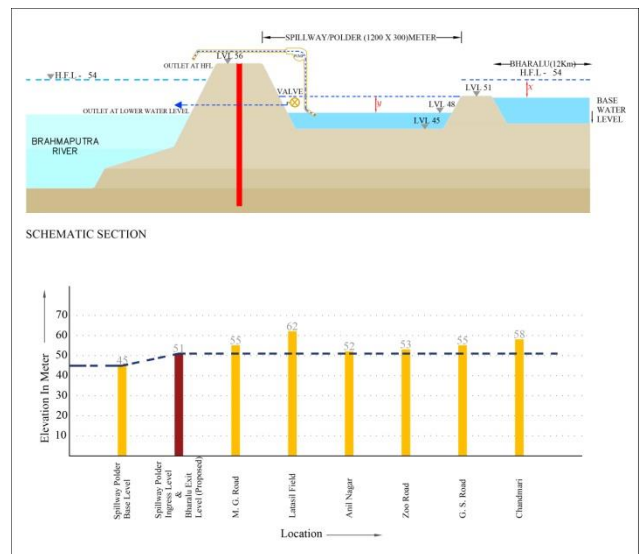


Fig. 7. Bharalu Spillway/ Polder Section and Levels. (1)

Initial calculations based on available data shows a possibility of having a 36 hour lead time before the polder is filled up completely considering a 2.0 meter rise in Bharalu water every 8 hours. (Fig.8). The performance of it can be significantly increased with the help of mechanical pumping.

The additional area created by this embankment and realignment shall be used for creating a modern Riverfront development as envisaged along with a freeway to bypass the MG Road.

X = 3.0 meter increase in Bharalu water level above 51.0 elevation
 = 3 X 12000 X 15 (Height X Length X Width)
 = 5,40,000 cu.m

Y = capacity of Polder with increase in water level for 48.0 to 51.0
 = 3 X 1200 X 300 (Height X Length X Width)
 = 10,80,000 cu.m

SUMMARY

$Y = 2X$

Assuming water level increase rate of Bharalu is 2.0Meter per 8 hour.
 Therefore, Polder Capacity \approx 36 hr without mechanical discharge.
 Real term discharge will give 36 hr lead time.

Fig. 8. Water displacement and capacity calculation.

This will decongest the MG Road and the new bypass and promenade can be exclusively designed as an iconic riverfront.(Fig.9)

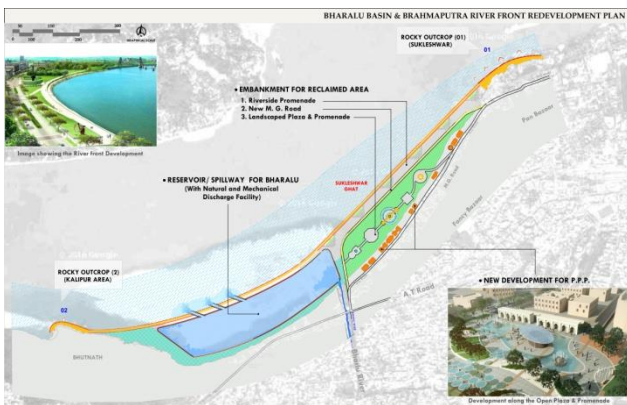


Fig. 9. Layout Plan of Proposed Riverfront with Polder.

6 RE DEVELOPMENT MASTER PLAN & LAND RECONSTITUTION OF GUWAHATI

6.1 Concept and Rationale

The unplanned nature of Guwahati means that there is paucity of land for critical urban infrastructures. It is seen that crucial infrastructure like hospitals, schools and other public facilities are either running from rented and temporary accommodation. It is also seen that most of the new schools and hospitals etc are moving away from the core city area to the outskirts.

These facilities are availed by children and the elderly and it is important that these are located within reasonable distance from residential neighbourhoods.

This crucial oversight is due the fact that the City authorities did not reserve adequate land for these activities in the past.

At the same time, the expanding city has now within its limits many government buildings and underutilised land banks through its various departments. The future

development of the city depends on how these areas are put to use.

In this context it is important that the city authorities prepare a Redevelopment Master Plan based on available and underutilised Government Land in the City. The strategy should be to consider all the available land under government use and consider them for densification, relocate, and retrofit and reuse for public purpose and also for complete change of use.

Some similar steps have already been taken up like the Shradhanjali Park and the vacated Jail land but it needs to formulate into a policy and within a comprehensive Redevelopment Master plan.(Fig.10)



Fig. 10. Land Use Plan by GMDA showing Public land and New Use Visualised. (1)

6.2 Features and Outcomes

Creation of key public facilities in critical locations like parks, schools and hospitals etc and opportunity to plan out Guwahati metro Project and its infrastructure.

Reduce traffic and increase pedestrian activity and improvement in the quality of life of the citizens.

Increase in economic activity and amalgamation of Government offices in single location.

7 CONCLUSIONS

In conclusion, this paper has attempted to remind and assert that the city of Guwahati needs urgent attention by the authorities. The very future of the city depends innovative intervention and transformative solutions for its challenges and keep the city sustainable for years to come. This paper is hence proposing these projects conceptually for further study and development to achieve the results as proposed for sustainability of a strategically located and naturally endowed city like Guwahati.

REFERENCES

- 1) Image LandSat.(2016): US Dept of State Geographer, Copyright of Google.
- 2) CES(I) Pvt Ltd. (2009): Land Use Zoning Plan 2025-Master Plan for Guwahati Metropolitan Area, GMDA

[Back to table of contents](#)

Biomedical waste management of Guwahati- a case study of Gauhati Medical College and Hospital

Rupanjan Chakraborty ⁱ⁾, Rakesh Barman ⁱⁱ⁾, Kuntal Das ⁱⁱⁱ⁾, Mrinal Roy ^{iv)}

i) U.G Student, Dept. of Civil Engineering, Assam Engineering College, Guwahati-13.

ii) U.G Student, Dept. of Civil Engineering, Assam Engineering College, Guwahati-13.

iii) U.G Student, Dept. of Civil Engineering, Assam Engineering College, Guwahati-13.

iv) Graduate Engineer, Dept. of Civil Engineering, Assam Engineering College, Guwahati-13.

ABSTRACT

The advancement in the field of science and technology has paved way for rapid augmentation in the healthcare and the medical facilities all over the world. Hospitals and other healthcare establishments have been rendering services to the society by providing healthcare facilities to the people. They also have a “duty of care” for the environment in connection to the biomedical waste they produce. The management of the biomedical waste is an important facet as delinquency of the biomedical waste management adversely affects the environment posing various kinds of health as well as environmental hazards. The biomedical waste management in India was a duty of the Municipal corporations till July 1998, when the Ministry of Forests and Environment, India promulgated Biomedical Waste (Management and Handling) Rules which shifted the onus of the biomedical waste management from the municipal corporations to the respective hospital authorities. However, the ground reality is far away from satisfactory. Keeping in view of the underlying risks emanating from the improper biomedical waste management of a hospital and its effects on environment and living beings, a study is undertaken to evaluate the biomedical waste management system of Gauhati Medical College and Hospital, one of the premier healthcare institutions of North-East India. The study includes assessment of the prevalent waste management system, practices (storage, collection, disposal) and its compliance with the standards prescribed in the Biomedical Waste Management Rules (2016). During the course of the study, it is observed that- (i) Though the hospital is equipped with latest machines and technologies to deal with the waste, the personnel involved in the waste management lack proper know-how of the potential hazards of the biomedical waste and are not properly trained. (ii) The process of collection, segregation and transportation of the wastes are not done in accordance with the standard rules. (iii) The infectious waste are properly taken care of through incinerators, autoclaves, shredders etc. The study concludes that the biomedical waste management system of the hospital is not satisfactory with the hospital lacking proper infrastructure and skilled personnel to mitigate the hazards of biomedical waste.

Keywords: Biomedical waste, segregation, incinerators, collection, disposal

1. INTRODUCTION

A hospital is a health care institution providing patient treatment with specialized staff and equipment. Hospitals and other healthcare establishments have a “duty of care” for the environment and for public health, and have particular responsibilities with respect to the waste they produce, i.e., biomedical waste (Pruss et al., 1999). The waste produced by hospitals is increasing in its amount and type due to the advances in scientific knowledge and is creating its impact on the environment (Rao SKM, Garg RK, 1994). The hospital waste, in addition to the risk for patients and personnel who handle these wastes poses a threat to public health and

environment (Singh IB, Sarma RK., 1996). The biomedical waste generated during diagnosis, treatment, and immunization processes in healthcare establishments includes wastes such as sharps, human tissue or body parts, and other infectious materials, and is often considered to be a subcategory of hospital waste (Baveja et al., 2000; Gupta and Boojh, 2006). Negligence towards biomedical waste management significantly contributes to environmental pollution, affects the health of human beings, and depletes natural and financial resources (Henry and Heinke, 1996; Oweis et al., 2005).

In India, in view of the serious situation of biomedical waste management, the Ministry of Environment and Forests, within the Government of India, formulated the Biomedical Waste (Management and Handling) Rules in July 1998, which shifted the onus of the biomedical waste management from the municipal corporations to the respective hospital authorities. This involves management of a range of activities, which are mainly engineering functions, such as collection, transportation, operation/treatment of processing systems, and disposal of waste. However, initial segregation and storage activities are the direct responsibility of nursing personnel who are engaged in the hospital. If the infectious component gets mixed with the general non-infectious waste, the entire mass becomes potentially infectious (Info Nugget, 2003). The indiscriminate and unscientific management of biomedical waste poses serious threats to human health. This also involves hazards and risks, not only for the generators and operators, but also for the general community (Sandhu and Singh, 2003). Studies on the waste management system in Indian hospitals are very few (Lakshmi, 2003; Patil and Pokhrel, 2005; Gupta et al., 2009). One of the studies on the biomedical waste management practices of a specific hospital (Balrampur) in Lucknow, India, has recommended the need for strict enforcement of legal provisions and a better environmental management system for the disposal of biomedical waste (Gupta and Boojh, 2006). The actual biomedical waste management situation in the democratic developing country like India is grim. Lakshmi (2003), in the leading national newspaper of the country, reports that even though there are Rules stipulating the method of safe disposal of Biomedical Waste (BMW), hospital waste generated by Government Hospitals is still largely being dumped in the open, waiting to be collected along with general waste.

Waste management has become one of the critical issues. It poses potential health risks and damage to the environment, which has taken a central place in the national health policy thus attracting a considerable international interest. India has a long history associated with the Biomedical waste related problems. India participated in the United Nations Conference on the Human Environment held at Stockholm in

June, 1972, where decisions were taken to take appropriate steps for the protection and improvement of human environment. Therefore, the Environment (Protection) Act 1986 (EPA) was formed under the Ministry of Environment and Forests, which is the most comprehensive Act on the Indian Statute Book relating to Environment Protection (Jaswal and Jaswal, 2000). It is general legislation for the Protection of Environment, enacted under article 253 of the Constitution, which came in force on 19th November 1986. In July 1998, the Government of India Environment (Protection) Act 1986 (Rule 29 of 1986) issued a Notification on Biomedical Waste (Management and Handling), Rules 1998, indicating the Rules for the Management and Handling of bio-medical solid waste which was further revised in 2016. The present study focuses on the review of the biomedical waste management system in Gauhati Medical College and Hospital, Guwahati (GMCH).

Gauhati Medical College and Hospital is one of the premier health care institutions in the North Eastern region of India, which provides extensive modern diagnostic facilities and specialized treatment for various diseases not only to people of Assam, but also to those coming from various other parts of North Eastern region. The hospital has all the basic specialities like General Medicine, General Surgery, Orthopaedics, Dermatology, ENT, Paediatrics and super specialities like Cardiology, Neurology, Nephrology, Neurosurgery, and Paediatric Surgery. The hospital is implanted with 2220 beds and an extra 200 beds for various emergencies.

The objective of this study was to analyse and evaluate the biomedical waste management system, including policy, practice (i.e., storage, collection, transportation and disposal), and its compliance with the standards prescribed in the Bio-Medical Waste Management Rules, 2016. In light of all of the above, this study was initiated and intended as a case study at Gauhati Medical College and Hospital (GMCH) in Guwahati, India (Fig. 1). Guwahati, one of the most picturesque and important cities of India, is a gateway to Northeast India. The city is well connected to various parts of India. Guwahati is a fast growing metropolis and with the population of 9, 62,334 (according to 2011

census) is the most populous city of Northeast India.

2. METHODOLOGY

It comprised of a series of interviews that took place with the authorities and the personnel involved in the management of bio-medical waste of Gauhati Medical College and Hospital. The information was extracted following the guidelines of Biomedical Waste (Management and Handling) Rules 2016. Regular site visits were undertaken to support and supplement the information gathered in the survey. Interviews and site visits were of paramount help in obtaining information about the management of bio-medical waste (i.e. collection, segregation, transportation storage, treatment and disposal procedures) at the hospital.

2.1 Collection

The waste (both hazardous and non-hazardous) is collected at the point of generation i.e. from the respective wards and the OPDs of the respective departments. The collection cycle occurs twice in a day once in the morning between 8am to 12 noon and once in the afternoon between 3pm to 5pm. All containers kept for the collection of hazardous waste are labelled with biohazard/cytotoxic symbols as per the Biomedical Wastes (Management and Handling) Rules 2016.

2.2 Segregation

The generated waste was segregated at the respective wards and departments using colour coded high density polyethylene bags (as mentioned in Bio Medical Waste Management Rules 2016) as shown in Table 1 and Figure 1. Though the personnel involved in the management have the knowledge of the potential hazards of the waste, but they are not properly trained.

Table 1. Segregation of bio-medical solid waste

Colour coding of polyethylene bags	Type of waste material collected
Black	Non-infectious and non-hazardous waste.
Red	Microbiological waste from pathological laboratory, items contaminated with blood and body fluids, and waste generated from disposable items other than sharps, etc.

Yellow	Human anatomical waste, microbiological waste from pathological laboratory, items contaminated with blood and body fluids, and waste generated.
Blue	Waste sharps, solid waste generated from disposable items other than the waste sharps such as tubing, catheter, IV sets, etc.



Fig. 1. Colour coded buckets in GMCH



Fig. 2. Needle Destroyer

2.3 Transportation and Storage

The hospital has pre-established routes for the transport of medical wastes, which include specific corridors, ramps and passages to transfer wastes from each ward to the storeroom in the rear side of the Hospital.

The hospital has a specially designed storage area that is properly ventilated. The waste is transported to the waste treatment facility. The Hospital has an on-site waste treatment plant which is located at the rear side of the hospital near the morgue. The waste treatment plant has three (3) numbers of Autoclaves and Shredders and one (1) incinerator. The incinerator was previously not in working condition and as a result the waste management of the hospital was assigned to a third party but recently it got fixed and now is in proper working condition. The

flowchart of the medical waste disposal at GMCH is shown in Figure 4 and Figure 5.



Fig. 3. Storage of the waste before treatment in colour coded polyethylene bags

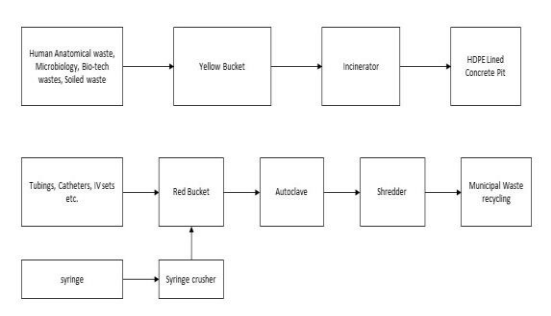


Fig. 4. Flowchart for medical waste disposal at GMCH

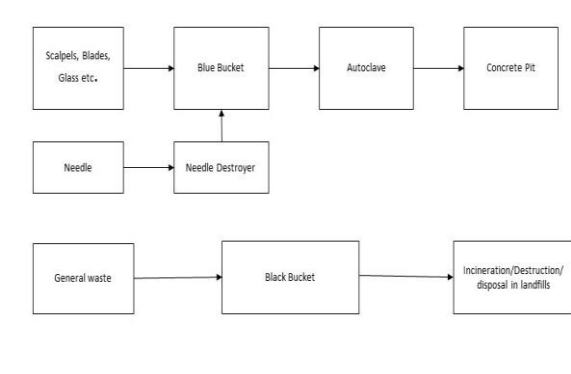


Fig. 5. Flowchart for medical waste disposal at GMCH

Though the on-site waste treatment plant at the hospital is equipped with the latest technology and infrastructure to deal with the bio-medical waste, the personnel and staff employed there, unlike their counterparts employed in collection and transportation of waste, lack proper technical knowledge of the potential hazards of the waste

and are not equipped with proper protective gears like masks, boots etc.

3. CONCLUSION

In general, the waste management system of GMCH conforms to the Biomedical waste (management and handling) Rules 2016, but the overall system is not satisfactory. There is a lack of awareness among the staff and personnel involved in the waste management system. There is scope for further improvement of the biomedical waste management of GMCH. Some suggestions are made to improve the overall system of biomedical waste management. These are as follows:

1. Periodic meetings should be conducted involving administrative and maintenance staff that are directly or indirectly involved with waste management in order to share and discuss the technical or practical difficulties and provide suggestions that may be specific to the hospital.
2. A compulsory inducting training programme should be conducted for all new staff in the hospital to familiarize them with the operating procedures practiced in the hospital.

ACKNOWLEDGEMENT

The authors express their gratitude towards the administration of Gauhati Medical College and Hospital for allowing them to conduct the survey on Bio-Medical Waste Management System. The authors also thank Dr. B.K Das (Deputy Superintendent, GMCH) and the administrative staff of the hospital for their immense support and encouragement.

REFERENCES

- 1) Baveja, G., Muralidhar, S., Aggarwal, P., 2000. Hospital Waste Management-an overview. Hospital Today 5 (9), 485–486.
- 2) Gupta, S., Boojh, R., 2006. Biomedical waste management practices at Balrampur Hospital, Lucknow, India: a case story. Waste Management and Research 24, 584–591.
- 3) Henry, G., Heinke, G., 1996. Environmental Science and Engineering. Prentice-Hall, Englewood, NJ, USA.
- 4) Info Nugget, Hospital Waste Management and Bio-degradable Waste. Government of

- India, Press Information Bureau, <http://pib.nic.in/infonug/infaug.99/i3008991.html>.
- 5) Jaswal, P.S., Jaswal, N., 2000. In Environment Law. Allahabad Law Agency, Haryana, India.
 - 6) Lakshmi, K., 2003. Norms Given by the go-by in Govt. Hospitals, The Hindu Online edition of India's National Newspaper, Monday, March 24, 2003.
 - 7) Notification: Bio-medical Waste (Management and Handling) Rules, 1998. Ministry of Environment and Forests, GOI (E), part 3(ii), New Delhi, 27.07.1998.
 - 8) Notification: Bio-medical Waste (Management and Handling) Rules, 2016. Ministry of Environment and Forests, GOI(E), part 3(ii), New Delhi, 28.03.2016
 - 9) Oweis, Rami, Al-Widyan, Mohamad, Limoon, OhoodAl, 2005. Medical waste management in Jordan: a study at the King Hussein Medical Polyclinic. Waste Management 25, 622–625.
 - 10) Patil, V.G., Pokhrel, K., 2005. Biomedical solid waste management in an Indian hospital: a case study. Waste management 25, 592–599.
 - 11) Pruss, A., Giroult, E., Rushbrook, D., 1999. Safe Management of Wastes from Health-Care Activities. World Health Organization, Geneva.
 - 12) Rao SKM, Garg RK. A study of Hospital Waste Disposal System in Service Hospital. Journal of Academy of Hospital Administration, July 1994; 6(2):27-31.
 - 13) Sandhu, T.S., Singh, N., 2003. A Hazard Going Unnoticed –Biological Waste is a Threat to the Community at Large, The Tribune, Online edition, Chandigarh, India, Monday, June 30, 2003. Notification: Bio-medical Waste (Management and Handling) Rules, 1998. Ministry of Environment and Forests, GOI (E), part 3(ii), New Delhi, 27.07.1998.
 - 14) Singh IB, Sarma RK. Hospital Waste Disposal System and Technology. Journal of Academy of Hospital Administration, July 1996;8(2):44-8

[Back to table of contents](#)

Geo-spatial Land Records Database with Bhunaksha as Sustainable Planning & Framework for Rural Development

Dibyojit Duttaⁱ⁾, D.S. Venkateshⁱⁱ⁾, Sunish Kumarⁱⁱⁱ⁾, Ms Kanika Bansal^{iv)}, Ms Seemantinee Sengupta^{v)},
D.C. Misra^{vi)}

i) Technical Director , Land Records Division, NIC HQ, New Delhi , India.

ii) Principal System Analyst , Land Records division, NIC HQ ,

iii. System Analyst, Land Records Division, NIC HQ, New Delhi , India.

iv. Scientific Assistant, Land records Division, NIC HQ , New Delhi

v) Sr. Technical Director, HoD (Land Records Division), NIC HQ, New Delhi , India.

vi). Deputy Director General, HoG(Rural Development) NIC HQ, New Delhi , India.

ABSTRACT

Land Record databases are one of the oldest and extensive database comprised of land parcel ownership details along with other land attributes viz. location, crops grown, soil type, sources of Irrigation, land use, area of land parcel, caste/tribe of owners, public, private, cultivable, non-cultivable, forest, orchard, community land, banjar, awadi, waterlogged, saline etc maintained by States with corresponding cadastral maps which can be effectively utilized as Sustainable planning and Framework for Rural development .

Government of India, under their recent flagship program DILRMP (Digital India Land Records Modernization Program) has taken up a massive exercise to modernize and update land records. Under this program, land records and cadastral parcel maps are digitized & linked using Cadastral mapping software which can be geo-referenced, over-laid on NIC/ Google/ Bhuvan / high resolution satellite data. The seeding of Adhaar Unique ID to Land Records database would further sanitise the database with only authentic land holders .

This paper is prepared to describe about Land records database, its integration with cadastral maps and then building a GIS based framework through BhuNaksha SW for development of a framework for rural development. A PoC implemented in Jind district of Haryana viz. “Pixel, Parcel and Person“ where land records, cadastral maps were digitized, seeded with Adhaar UID and the geo-referenced using BhuNaksha SW is also covered in the paper .

Keywords: Land records, Cadastral maps, Adhaar, eKYC, BhuNaksha , Pixel –parcel- persons,

1. INTRODUCTION

Land Record is one of the oldest databases maintained in the country. Sher Shah Suri (1540-1545) introduced categorization and measurement of land with crop rates and Mughal Emperor Akbar (1556-1605) introduced different methods for determining land class and land revenue. Later British modernized land administration system who started survey and settlement process in various States through establishing offices and framed several land Acts.

After independence, India adopted the land records management system from British raj with little modification. Later, in order to modernize land records management, Govt of India introduced two major schemes in the year 1988-89 i.e. Computerization of Land records(CLR) with 100% central funding and the Strengthening of Revenue Administration and Updating of Land Records(SRA&ULR) with 50:50 sharing basis with State. Later on 21.8.2008, the Cabinet approved merger of these schemes into a modified Scheme named National Land Records Modernization Program (NLRMP) which later become Digital

India Land Records Modernization Programme (DILRMP) in 2016.

2. HOW INTENSIVE IS LAND RECORDS?

Land being a State subject, the land attributes collected in Land Records database varies state to state. In a recent study conducted by NIC, it has been found that majority of States/UT capture the following attributes i.e.

Location	Village /Census code/ survey No / Land Parcel No
Owner	
Land revenue	In Rs
Crops	major & minor crops
SEASON crops	Kharif , Rabi, others
SOIL TYPES	major and minor categories
IRRIGATION SOURCES	Major, Minor, Govt, Pvt, community, cooperative, Panchayat, electrical, diesel, windmill, solar, manual etc.
LAND USE	R/Forest, S/Forest,,non agricultural uses, barren, uncultivable land , etc
AREA UNIT	Local, Metric system
OWNERSHIP	Govt, Pvt, Institution, Others
HOLDING Size	Large , Medium , Small, Marginal
Mutation	Inheritance, Succession, Will , Sale, Mortgage, Gift, Partition, Court order etc
TENANCY	Permanent , Temporary , Fixed Rent, Others
ENCROACHER TYPES	Landless Encroacher ,Illegal use , Adverse Possession etc
CASTES/ TRIBES	SC, ST , OBC ,Gen, Minorities etc
GENDER	Male , Female , Transgender, None
Transaction details	Legacy data

Details available at http://dolr.nic.in/dolr/downloads/pdfs/lrc_codes_lis_t_finaldraft300908revised.pdf

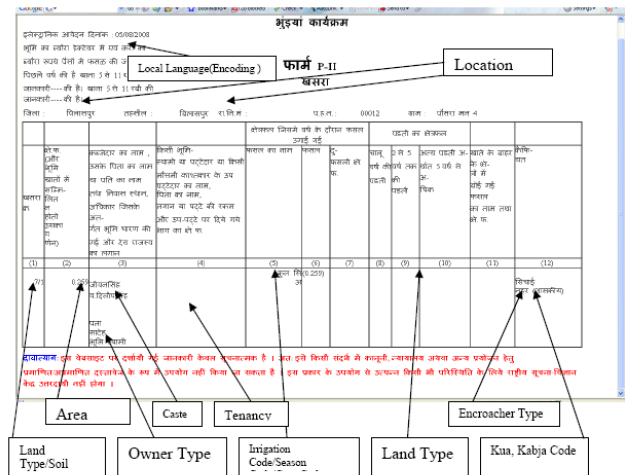


Fig 1 Details of a Khatauni(ROR) with code descriptions

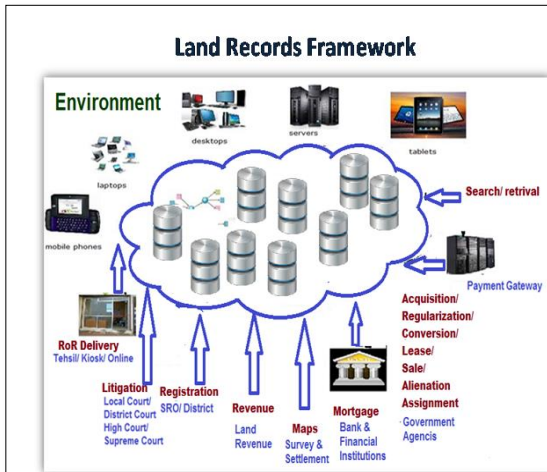
A typical land records registrar

Usually, Land records database are created and maintained at the land revenue offices at district HQ/ Sub district/ Tehsil / Circle level etc. A typical computerization of Land Record System is as follows,



3. LAND RECORDS FRAMEWORK

Several agencies are involved in the transactions of Land viz. updation of Textual records by Land Revenue dept, maps by Survey & Settlement, buying/ selling etc by Registration, litigation by Courts, Mortgage by Banks/ Financial Institutions, land acquisition/ conversion by Govt agencies etc. and the updation of land records is responsibility of all agencies. A land records Framework is as attached,



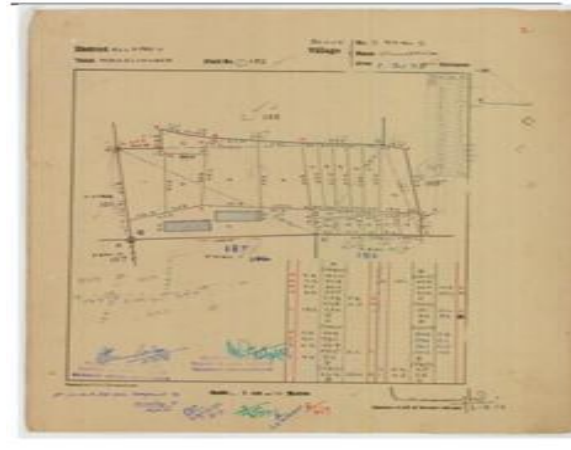
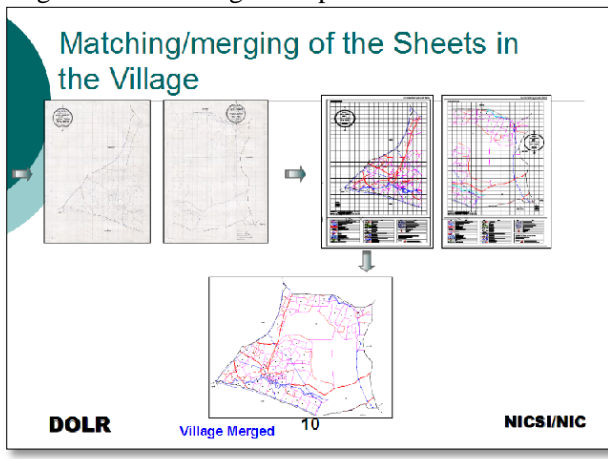
4. DIGITIZATION OF CADASTRAL MAPS

The existing cadastral maps are mostly created using chain and tapes whereas the recent ones are through latest technology i.e. ETS, DGPS, Aerial Photography, HRSI etc. In India, there are two different process of maintaining spatial data viz.

- Village Maps (North , Eastern & NE States)
- Tippan / Field Measurement Books (in Southern , Western States)

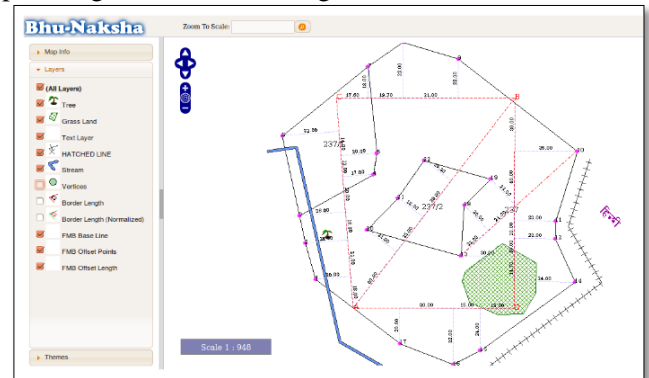


Digitization of village maps



Tippans / FMB

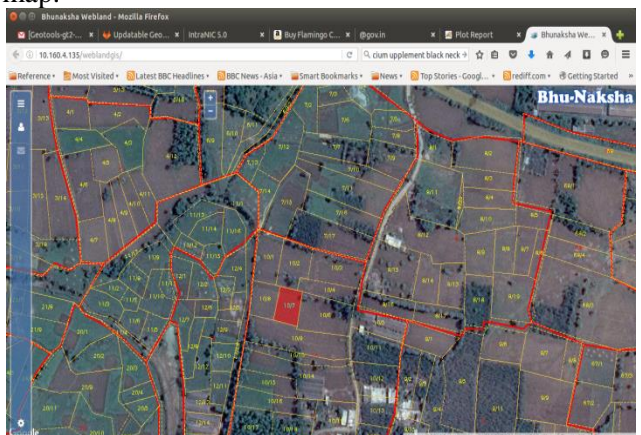
In States/UTs with ladder data as the basic records, the tippans has to be created from the ladder data and used for updation. The tippans can then be mosaic to generate village map/taluk/tehsil maps etc for planning and seamless integration.



Maps created from FMB

In States/UTs which are having the cadastral village map as the basic records, the village maps have to be digitized and these sheets need to be mosaic to make village maps.

The modern Survey/ resurvey equipments viz. ETS/ DGPS can directly generate geo-reference digitized map.



Composing Survey Data

Data extracted from ETS can be imported to BhuNaksha and processed further to build village map and other layers. BhuNaksha supports ETS data in LandXML (<http://www.landxml.org>) and comma separated value (CSV) of coordinate points. For processing survey data open Compose Survey Data module from File menu.

5. GOVERNMENT INITIATIVES

Government of India has launched National Land records Modernization Program in the year 2008 which later upgraded into Digital India Land Records Modernization programme (DILRMP) with 100% centrally sponsored scheme from 2016-17 onwards. It facilitates states/UTs to modernize management of land records, enhance transparency in the land records maintenance system, eventually moving towards guaranteed conclusive titles for immovable properties in the country. The major components of the programme are

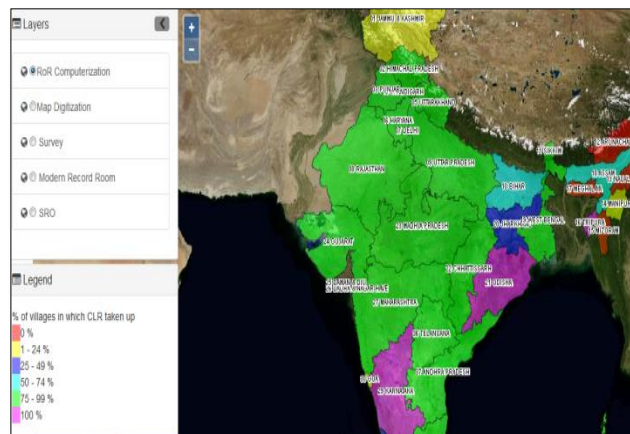
- A. Computerization of Land Records LR Application, Data Centre/ Connectivity / Modern record Rooms; Entry / Updation of RoRs/ Mutation workflow, Digitization of Cadastral Map, Integration of textual & spatial data etc.
- B. Computerization of Registration- Registration application, Documents Scanning/ Search retrieval etc
- C. Survey/Resurvey
- D. Integration of Land Records with Property Registration
- E. Development of core GIS and Cadastral Map Management
- F. Capacity Development
- G. Service Delivery.

Department of Land Resources, Government of India has been providing substantial resources/ support to various States/UTs for the effective implementation of this programme and the following milestones are expected to be achieved by the end of 2016 viz.

1. Web based LR Application,
2. Multi Tenancy Architecture
3. Aadhaar seeding
4. Unicode enabled
5. Integration of Land Records with Property registration & BhuNaksha Cadastral SW
6. Online mutation
7. e-Gov standards for interoperability

8. Security Audit
9. Deployment at State Data centre/NIC cloud
10. Porting of legacy data etc

The physical and financial progress are available in the <http://dilrmp.nic.in> with



GIS platform at <http://nlrmp.nic.in/nlrmpmap/nlrmpmap.html>

6. BHUNAKSHA CADASTRAL MAPPING SOFTWARE

BhuNaksha is a cadastral mapping software developed by NIC using Open source applications and libraries which integrates Land Records database with digitised maps. The Postgresql with PostGIS spatial module is used for storing geometry and spatial attributes of plots and other features. This SW can integrate LR database in any RDBMS format. The scanning, digitization, verification of cadastral maps are the pre-processes and input to BhuNaksha application which can take input from multiple sources i.e. Shape file, ArcInfo files, Survey Data and FMB Ladder Data etc.

The various features available in BhuNaksha are

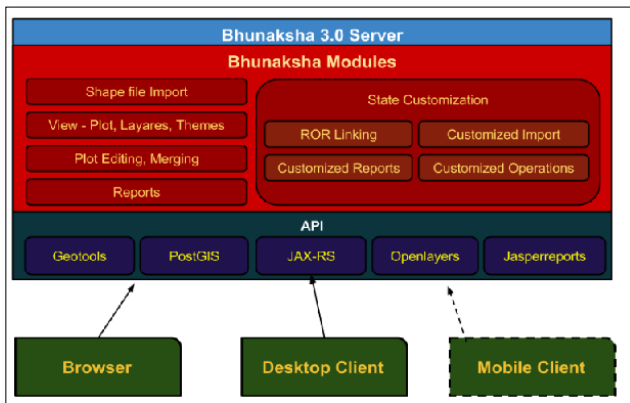
1. Web, Desktop and Mobile apps version.
2. Plugin architecture to integrate with any State's ROR/Master database.
3. Plot can be divided into multiple subdivisions in a single mutation
4. Multiple methods for creating division lines.
5. Multiple plots can be divided in a single operation for cutting road/canal etc.
6. Plot map and Village map can be displayed and printed to any scale.
7. SLD based styling of plot and layers.
8. Query based thematic maps,
9. Online Geo referencing tools for legacy maps.

10. Provide web map services and other spatial services which can be used for GIS based service delivery interfaces

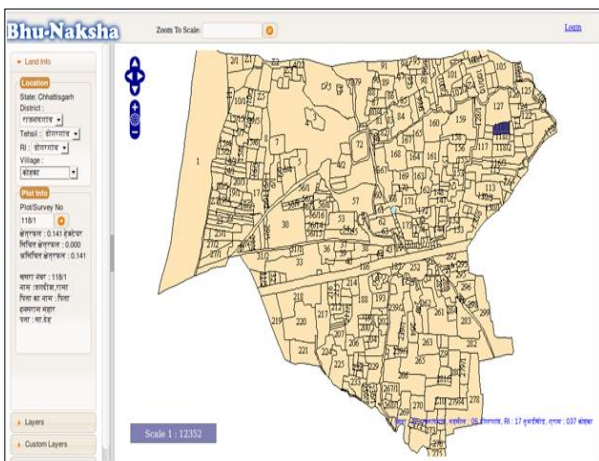
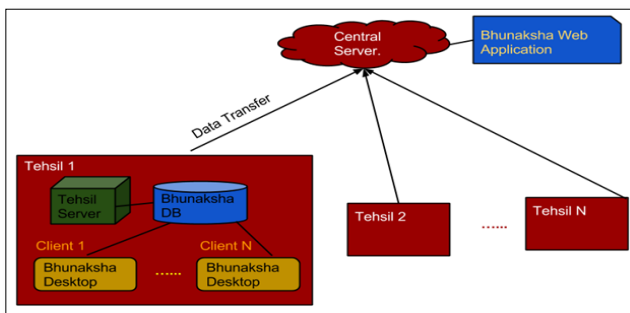
BHUNAKSHA ARCHITECTURE

Bhunaksha is designed to work in a centralized environment and distributed environment.

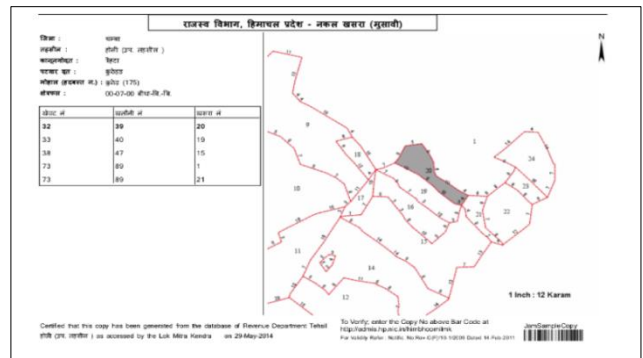
CENTRALISED ARCHITECTURE



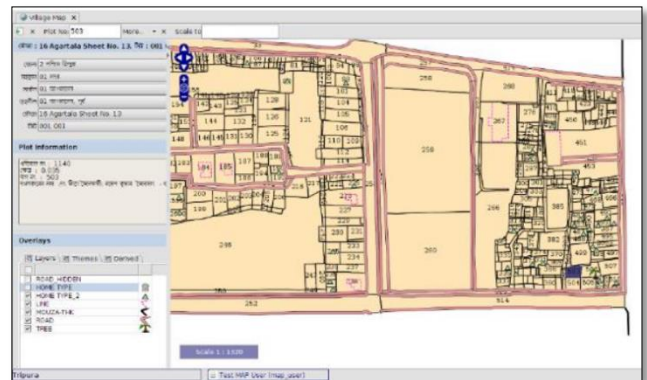
Distributed Architecture



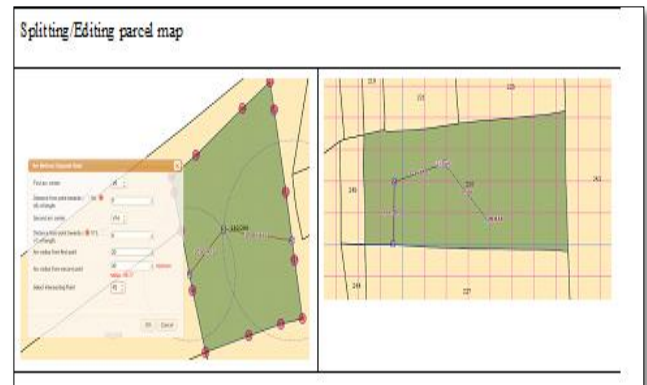
Maps are visible once shf files are ported



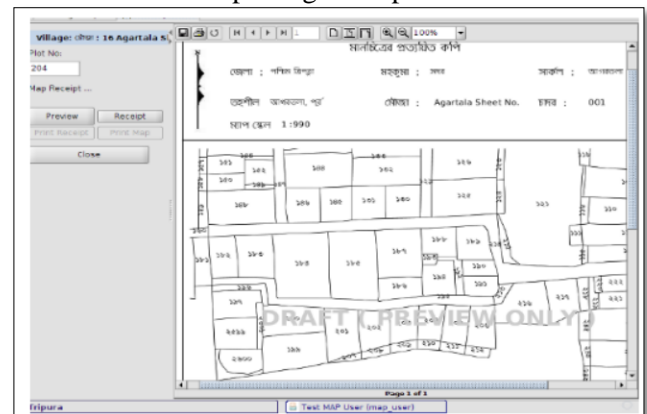
ROR with plot map



Village view maps



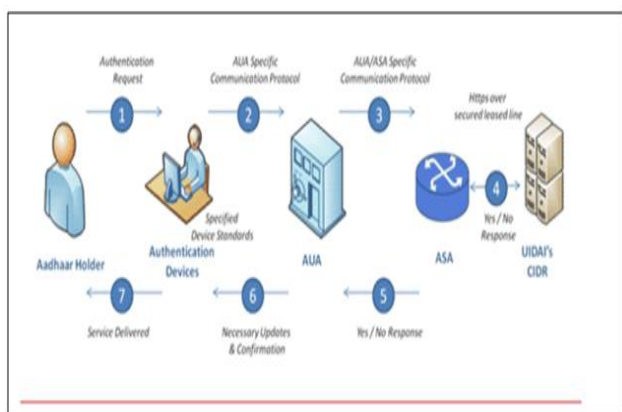
Splitting of maps



Plots Report

7. ADHAAR E-KYC AUTHENTICATION AND SEEDING

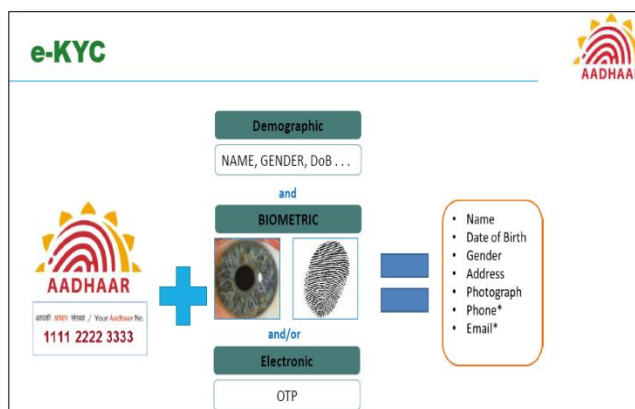
The online Authentication of a land holder's is done through UIDAI central sever using Bio-metric devices i.e. Finger print, Iris; OTP to the registered mobile or email etc. In the above e-KYC process of authentication, UIDAI provides demographic data i.e. Name, date of Birth, Gender, Address, photograph, phone & email (digitally signed & encrypted) .



The process flow of e-KYC

Features of e-KYC

- completely electronic service
- Consent based
- Eliminates Document Forgery
- Secure and compliant with the IT Act
- Non-repudiable
- Instantaneous
- Machine Readable
- Regulation friendly
-

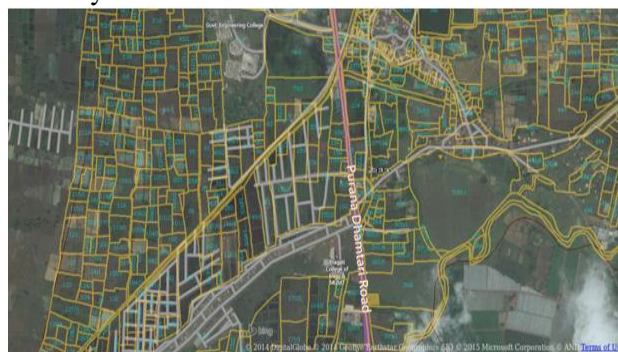


This Biometric validation can root out all bogus accounts from the system .

6. GEO-SPATIAL LAND RECORDS DATABASE WITH BHUNAKSHA AS SUSTAINABLE PLANNING & FRAMEWORK FOR RURAL DEVELOPMENT

Once land records are digitized , these are linked with BhuNaksha SW. The digitized cadastral maps are ported to BhuNaksha and linked with LR database. BhuNaksha creates geo-reference village map with the help of village boundary in layers from NIC Maps (<http://nicmaps.rsgis.nic.in/>) and other online services offered by Bing, Google, Bhuvan etc. or over-laid on high resolution satellite imagery data.

BhuNashka has provision for onscreen geo-reference of cadastral maps through correlating some known coordinates of the digitized map with the coordinates of geo-referenced maps. Identifying minimum of four such points will facilitate transforming the coordinate system to world coordinate system. Accuracy will depend on the accuracy and number of the known coordinates.



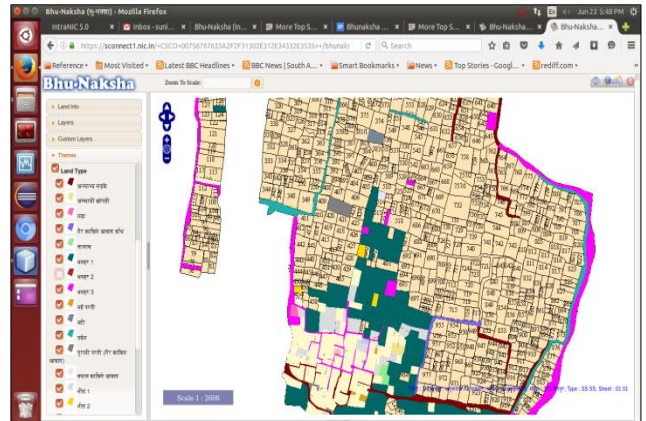
These geo-spatial Land Records with adhaar authentication will provide a sanitized, comprehensive Framework in rural areas which can be processed through BhuNaksha SW to generate a large number of thematic maps on the basis of various attributes available in the Land Records database. The online Map services can be utilized for planning and development. The policy makers, planners, land administrators, citizens can access these accurate data on land and natural resources which is the essential prerequisite to their rational use and conservation. This information is the prime requisite for making decisions related to land investment, development and management. For any disaster planning etc, the cadastral Maps can be over laid over the contour/DEM to identify the potential area inundated for various levels of water. This helps in planning the areas which needs to be evacuated

well ahead of the disaster. Similarly the buffer lying with a particular radius is also very useful.

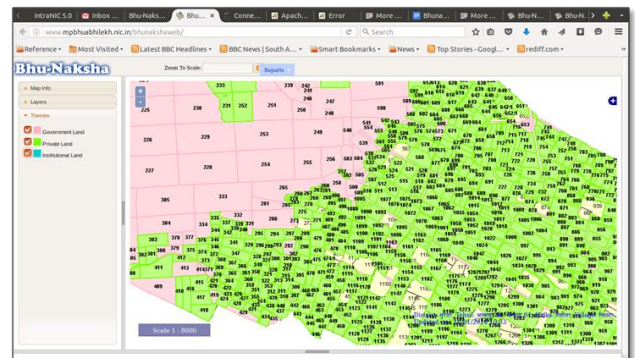
A few thematic maps generated are as follows,



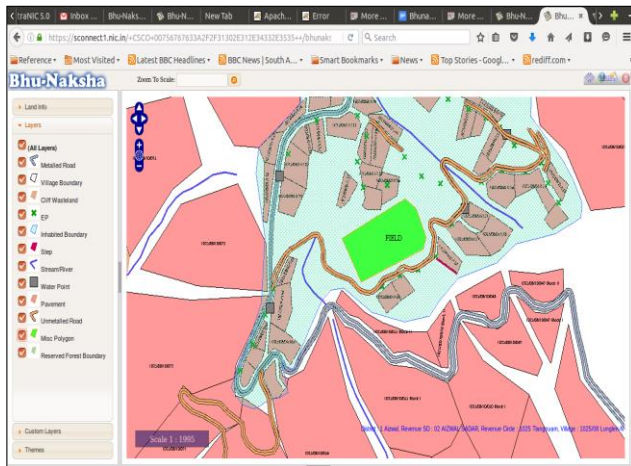
Demographic details of land holders with cadastral land boundaries



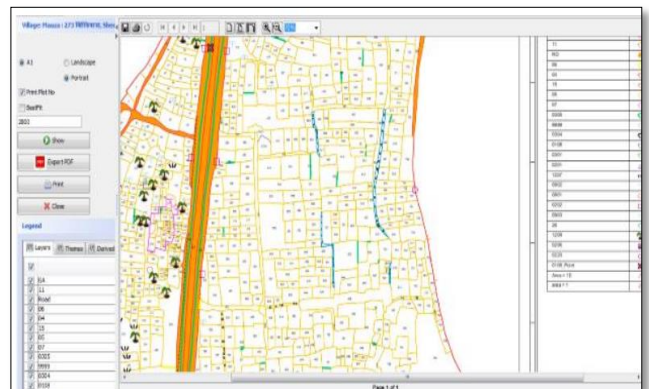
Cadastral Land Boundaries



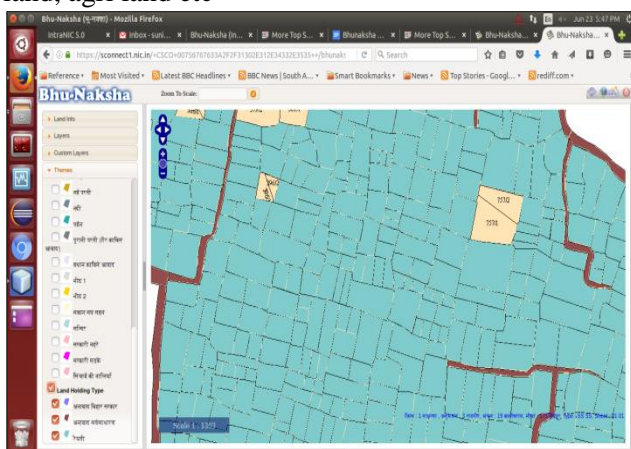
Land ownership type Govt/ Pvt/ Institutions etc.



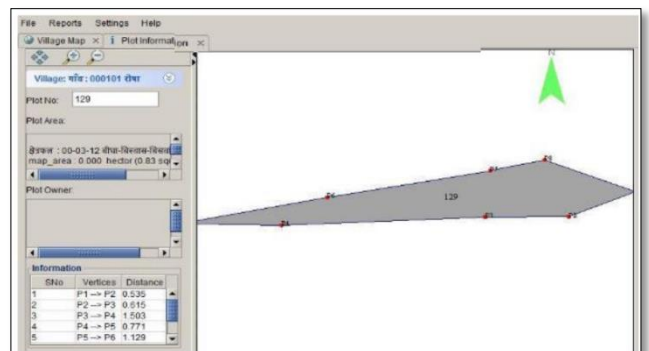
Land Type; road , river ,canal, railways, barren land, agri land etc



Village Map with selected Layers



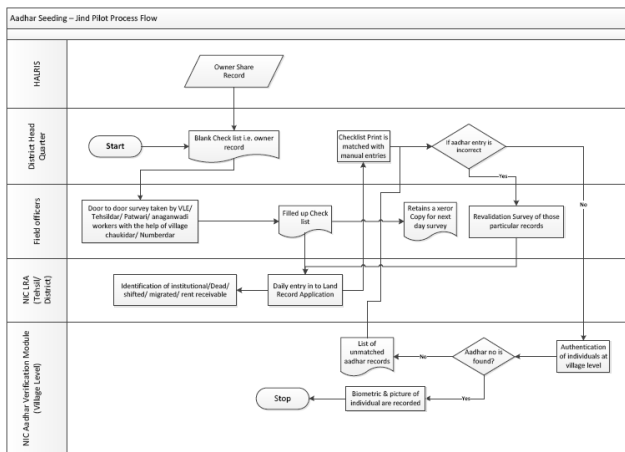
Land Holding Type



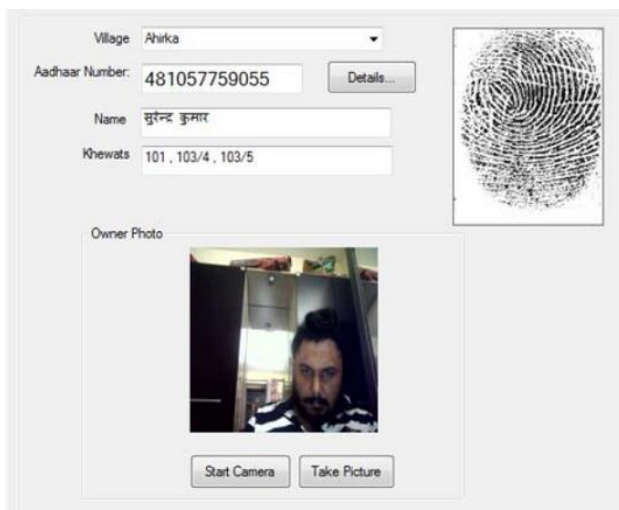
PLOTWISE INFORMATION

7. PIXEL PARCEL PERSON PROJECT AT JHIND

Jhind district, Haryana has been identified for implementation of Pixel, Parcel Person project where land records database were updated, digitized along with cadastral maps and integrated through BhUNaksha. The Adhaar authentication done through e-KYC using bio-metric devices. The Land Records application has been made web-enabled and cadastral maps are geo-reference using BhUNaksha SW. .



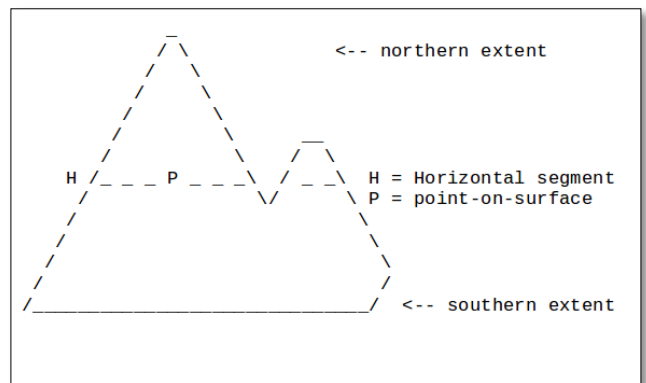
Adhaar seeding- Jhind Pilot process flow



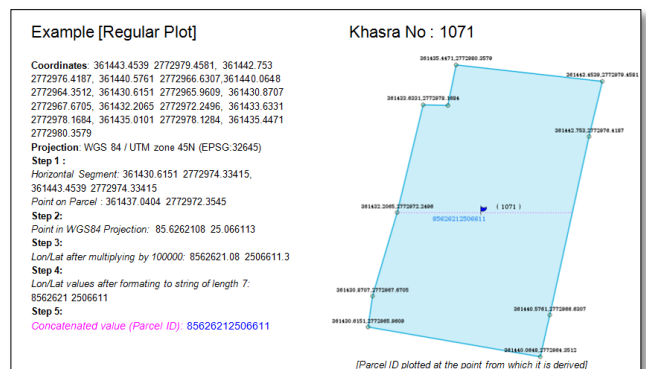
8. FUTURE

a. Unique Bhu-ID (Parcel ID)

Parcel ID can be derived from an interior coordinate of the polygon representing a land parcel. Trace an east-west ray, lying half-way between the northern and southern extents of the polygon (Horizontal Divider) and Find the longest segment of the horizontal divider that intersects the polygon



Return the point that is half-way along said segment.

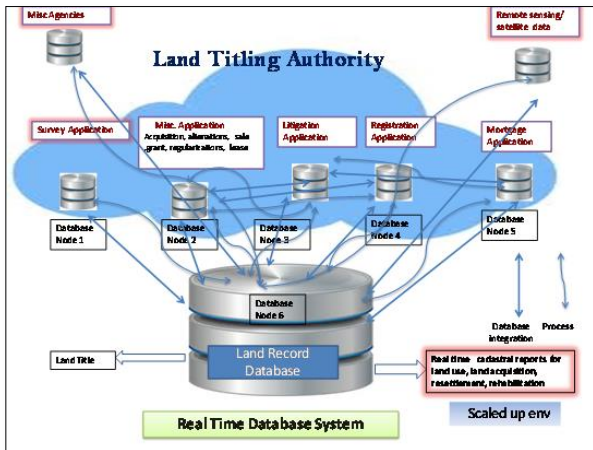


The Bhu-ID will provide one UID to each land parcel which can prevent fraudulent

b. Legal framework – Land Titling Authority

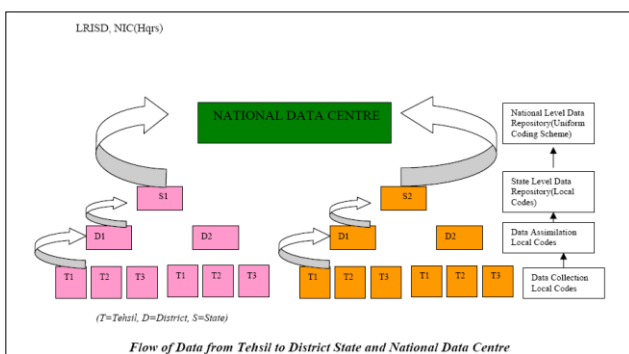
http://nlrmportal.nic.in/security_policy/Bhunaksha%20User%20Guide.pdf

[Back to table of contents](#)



The 'Land Titling Act' proposed for a single Agency viz. 'Land Titling Authority' to handle the various transactions viz. Survey, settlement, registration, land acquisition etc which will ease the integration of databases with land record database

c. National Level Data Repository



Using Uniform coding Scheme & GI cloud

The Uniform coding in IR attributes will facilitate to build National Level LR Database.

ACKNOWLEDGEMENTS

1. Rita Sinha , Former Secretary, DoLR
2. Vijay Madan, Former Secretary , DoLR

REFERENCES

- 1) DoLR website , http://dolr.nic.in/dolr/land_reforms1.asp
- 2) Study of Uniform Coding for Computerization of Land Records by NIC HQ at http://dolr.nic.in/dolr/downloads/pdfs/lrc_codes_list_finaldraft300908revised.pdf
- 3) <http://dilrmp.nic.in>
- 4) <http://nlrmportal.nic.in>
- 5) "BhuNAKsha user Guide" by NIC HQ

Effect of polypropylene fiber on strength characteristics of soil at varying compaction states

Gaurav Kr. Dasⁱ⁾, Akangsha Gogoiⁱⁱ⁾ and Himashree H. Kashyapⁱⁱⁱ⁾

i) M.Tech student, Department of Civil Engineering, Indian Institute of Technology Guwahati, Guwahati 781039, India.

ii) B.Tech student, Department of Civil Engineering, Royal School of Engineering and Technology, Guwahati, 781035, India

iii) B.Tech student, Department of Civil Engineering, Royal School of Engineering and Technology, Guwahati, 781035, India

ABSTRACT

Soil reinforcement is defined as a technique to improve the engineering characteristics of soil, such as shear strength, compressibility, and hydraulic conductivity with the inclusion of natural or synthetic additives. The main objective of this study is to explore the improvement in strength and ductility with the change in compaction state of soil. A commercially available synthetic fiber – polypropylene (PP), is used to investigate the strength characteristics of soil used in the study. The investigation is based on a series of Unconfined Compressive Strength (UCS) tests for a fiber content of 0.5% by dry weight of soil. The results of UCS tests, conducted on fiber reinforced soil, are discussed in terms of stress – strain relation, peak strength factor and compaction state. The result of this study highlights the ability of polypropylene fiber to improve the soil strength characteristics.

Keywords: Polypropylene (PP), RDFS, UCS, compaction state.

1 INTRODUCTION

Soil has been used as a construction material since time immemorial. The need for high strength materials has increased abruptly owing to construction of civil infrastructure under extreme conditions. Addition of admixtures, chemical additives and reinforcing materials are considered to increase the strength of soil. Geotextiles, geo-grids, jute textiles, fibers, etc. have been used as binding materials for reinforcing soil (Koerner, 2005). Fiber reinforced soil behaves as a composite material in which fibers of relatively high tensile strength are embedded in soil such that shear stresses in the soil, mobilize tensile resistance in the fiber, which in turn imparts greater strength to the soil. Thus, such reinforcement of soil enhances the engineering characteristics of soil, such as shear strength and compressibility (Vidal, 1969). Randomly distributed fiber-reinforced soil (RDFS) is one of the diverse reinforcing techniques, in which fibers of desired dimensions and quantity are mixed randomly in soil (Hejazi et al., 2012). Fibers can be classified in two categories, viz., synthetic and natural fibers. Synthetic fibers are preferred to natural fibers because of their higher mechanical strength. The important properties of one such fiber viz., polypropylene (PP) are its chemical resistance, low density, high melting point and moderate cost. Studies on the strength characteristics of fiber reinforced soil have been done through various methods like unconfined compressive strength test (UCS) (Maher and Ho, 1994; Santoni et al., 2001; Bordoloi et al., 2015), conventional tri – axial

test (Maher and Grey, 1990; Gosavi et al., 2004) and direct shear test (Fatani et al., 1991; Tang et al., 2007). Moreover, the effect of fiber percentage and aspect ratio has also been studied in detail (Al Refai, 1991) in the past. However, the variations in strength of fiber reinforced soil due to change in compaction states have not been addressed in detail, which is the main objective of this study. For detailed investigation, a systematic experimental study has been carried out, to address the behavior of fiber reinforced soil under varying compaction states, in terms of its compressive strength.

2 MATERIAL AND METHODS

2.1 Composition of polypropylene

The density of PP is between 0.895 and 0.92 g/cm³. The Young's modulus of PP is between 1300 and 1800 N/mm². This allows polypropylene to be used as an engineering plastic. Polypropylene has good resistance to fatigue and is not easily susceptible to variation in temperature.

2.2 Soil properties

The soil used in this study was red soil, commonly found in North Eastern part of India. Grain size distribution of the soil was determined using procedures prescribed in IS-2720-Part 4-1985. Fig. 1 depicts the grain size distribution curve of the soil used. It is constituted mainly of silt (50.27%) and clay (24.3%). Consistency limit of the soil determined according to IS-2720-Part 5 (1985) gave liquid limit and plastic limit

as 41% and 25%, respectively. The USCS classification of soil is silty clay (ASTM, D2487-11). Standard Proctor's light compaction technique was used to determine its maximum dry density (MDD) and optimum moisture content (OMC) according to procedures prescribed in Indian Standard code IS-2720 part-7 (1980). MDD and OMC were found to be 1.7 g/cc and 17%, respectively. Table 1 summarizes the index and engineering properties of the soil.

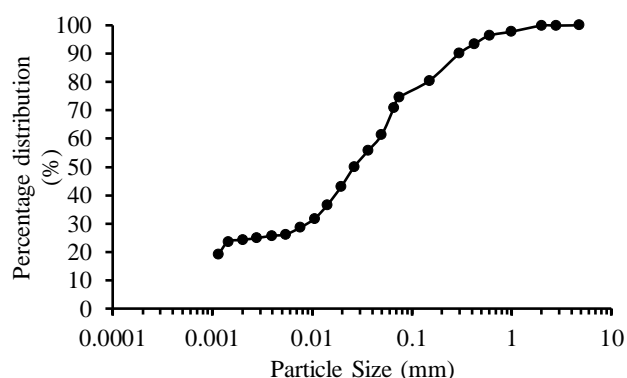


Fig. 1. Grain size distribution of soil.

Table 1. Engineering properties of soil

Sl. No.	Soil Property	Value
1	Specific Gravity	2.55
2	<u>Grain Size Distribution</u>	
	Coarse Sand (4.75mm-2mm)	0.12 (%)
	Medium Sand (2mm-0.425mm)	6.47 (%)
	Fine Sand (0.425mm-0.075mm)	18.82 (%)
	Silt (0.075mm-0.002mm)	50.27 (%)
	Clay (<0.002mm)	24.32 (%)
3	<u>Consistency Limits</u>	
	Liquid Limit	40.50 (%)
	Plastic Limit	24.81 (%)
	Shrinkage Index	23.30 (%)
	Plasticity Index	15.69 (%)
4	<u>Compaction Characteristics</u>	
	Optimum Moisture Content (OMC)	19.92 (%)
	Maximum Dry Density (MDD)	1.70 (g/cc)
5	USCS classification	ML

2.3 Experimental program and sample preparation

In order to determine the maximum dry density (MDD) and optimum moisture content (OMC), the soil is tested by proctor's light compaction technique as per IS 2720 part (14). UCS tests were conducted on both unreinforced and reinforced soil-Polypropylene (PP) composite at different compaction states corresponding to three soil densities (0.95 MDD, MDD and 1.05 MDD) and three moisture contents (OMC, OMC-5% and OMC+5%). For each case, tests were repeated three times (total 27 tests) to check any variability in observed UCS set up shown in Fig. 3). Thus, for the experiment, nine compaction states were selected

having different optimum moisture content (OMC) and maximum dry density (MDD). Randomly distributed fiber reinforced soil technique was used in conducting the test. RDFS fibers of PP are mixed randomly in soil thus making a homogeneous mass, maintaining the isotropy in strength. The percentage of fiber addition was selected at 0.5% by weight of soil. The sample dimension was kept as 38 mm × 76 mm and, based on literature, the length of fiber is set as 20mm (Maher and Ho, 1994). The thickness of fibers has been determined using digital Vernier calipers with a least count of 0.01mm. The amount of fibers to be added are weighed and dry mixed uniformly to obtain oven dried soil samples. Required amount of water is added to soil in order to meet the demands of moisture content, such that the tests could be performed at different compaction states. All UCS tests were conducted at a constant strain rate of 1.25 mm/min as suggested in IS-2720 part-10 (1991). The mixture was sealed inside a plastic bag and kept inside a desiccator for 24 h for uniform distribution of water. After that, the samples were compacted by static compaction in a specially prepared mold (Fig. 2), where compaction can be applied in opposite direction.



Fig. 2. Compaction mould

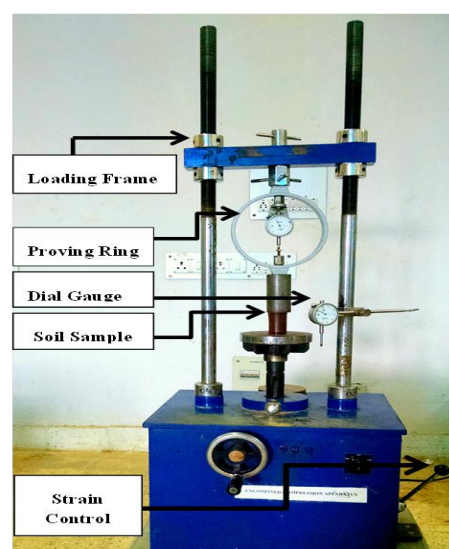


Fig.3. Overview of UCS test set up

3 RESULTS AND DISCUSSIONS

3.1 Effect of PP reinforcement on stress-strain response

Fig. 4 shows the comparison of stress–strain response between unreinforced and reinforced soil fiber composite (compacted at OMC and MDD). This figure depicts a significant increase in the peak UCS of reinforced soil. The unreinforced soil failed abruptly after attaining peak strength followed by a sharp decline of strength thereafter. However, in case of fiber reinforced soil, higher peak strength as well as post peak strength (with no abrupt failure) was observed. Thus fiber reinforced soil attains a residual strength on further straining, indicating ductile failure. This can be attributed to the fact that PP fiber has high mechanical (tensile) strength. The difference between post peak strength and peak strength is quite less for reinforced soil as compared to unreinforced soil. This indicates that the ductility behavior of the soil has also increased due to addition of PP fiber. Similar stress–strain response has been witnessed in the case of sand reinforced with polypropylene fibers (Yetimoglu and Salbas, 2003). This behavior can be attributed to readjustment of soil particles and its contact with adjoining fiber at the plane of failure. After attaining peak strength, as the strain level increases, rearrangement or rotation of particles will mobilize the tensile strength of the interlocked fibers gradually. In certain cases, shear failure was clearly observed while in other, bulging failure occurred as shown in fig. 5.

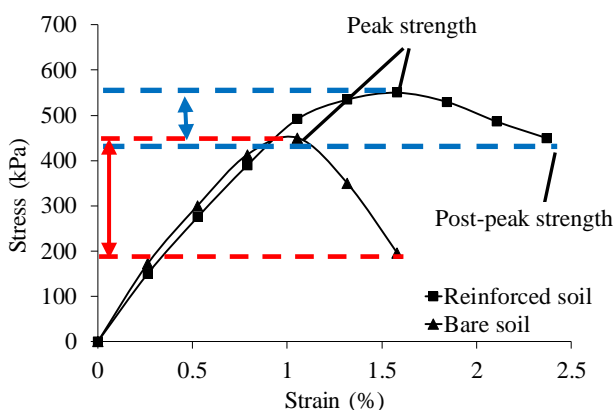


Fig.4. Stress-strain response of PP reinforced soil-fiber composite

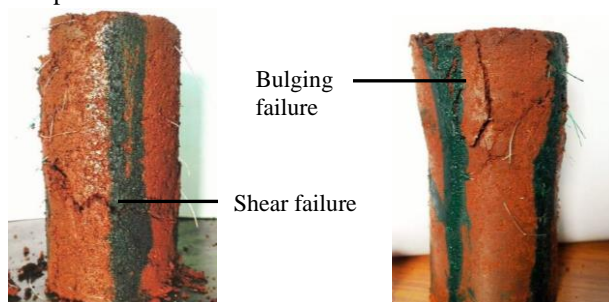


Fig. 5 Examples of shear and bulging failure observed in tests.

3.2 Comparison of peak UCS between fiber reinforced soil and unreinforced soil

Fig. 6 shows the mean UCS (from three repeated tests for each case) of soil samples (both reinforced and unreinforced) at the selected compaction states for 0.5% fiber content. The figure depicts an increase in UCS with increase in density of both fiber-reinforced and unreinforced soils. This can be attributed to higher interlocking between soil particles at a denser state. The figure further depicts that the soil samples compacted at lower moisture content exhibit higher strength as compared to that of soil with comparatively higher moisture content. This due to increase in strength associated with increase in soil suction (lower moisture content) (Khan et al., 2014). Higher moisture content allows particles to slip over one another due to which resistance to shear also decreases. Fig. 7 depicts the effect of PP fiber reinforcement on the mean UCS of unreinforced soil at different dry densities and moisture content. It can be observed that optimum compaction state (corresponding to maximum UCS) is found to be of soil compacted at 1.05 MDD and OMC-5%. Inclusion of PP fibers resulted in increase in strength for all moisture contents in comparison to unreinforced soil. The obtained range of unconfined compressive strength using PP fiber is higher than those in studies related to inclusion of natural coir fiber (Dasaka and Sumesh, 2011) and comparable to synthetic polypropylene fiber (Cai et al., 2006).

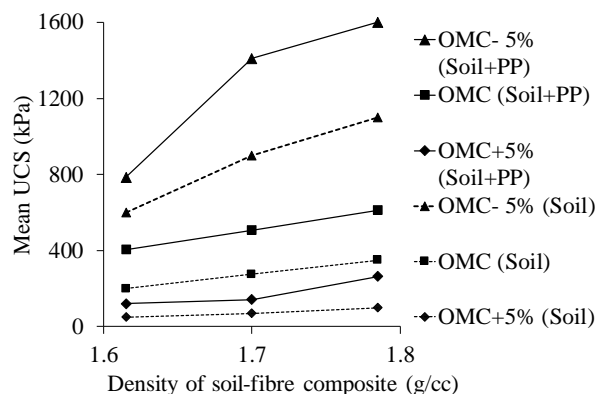


Fig.6. 0.5% PP reinforced soil-fiber composite

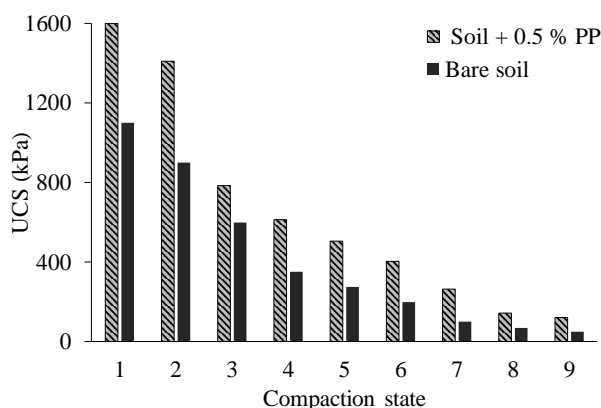


Fig.7. Bar chart comparison of tested reinforced samples

4 CONCLUSIONS

The present study explores the utility of synthetic fiber, polypropylene (PP) having high mechanical strength for its application as soil reinforcement. UCS tests were conducted to analyze unconfined compressive strength (UCS) under different soil densities and moisture content. Tests were also repeated (three in each case) to discuss any variability in observed UCS. Based on the results and discussion, following conclusions can be drawn.

- 1) The unconfined compressive strength of the unreinforced soil was observed to increase with the addition of PP fiber, attributed to its higher tensile strength.
- 2) Inclusion of PP fiber modified the brittle behavior of soil to ductile behavior of soil–fiber composite. The fiber–soil composite exhibits a low drop in post peak strength as compared to that of bare soil.
- 3) At a constant moisture content, it is observed that the unconfined compressive strength increases with increase in soil density. This effect of density is profoundly significant in case of lower moisture content of soil–fiber composite. Among the chosen compaction states carried out in this study, compaction of soil at OMC-5% and 1.05 MDD resulted in highest unconfined compressive strength.

ACKNOWLEDGEMENTS

The authors would like to thank Dr. Ankit Garg, Assistant Professor, Department of Civil Engineering, IIT Guwahati, for providing support and guidance to conduct the present study.

REFERENCES

- 1) ASTM D2487-11, 2011. Standard Practice for Classification of Soils for Engineering Purpose (Unified Soil Classification System).
- 2) Bordoloi, S., Yamsani, S. K., Garg, A., Sreedeeep, S., & Borah, S. (2015). Study on the efficacy of harmful weed species *Eichhornia crassipes* for soil reinforcement. *Ecological Engineering*, 85, 218-222.
- 3) Cai, Y., Shi, B., Ng, C.W., Tang, C.S., 2006. Effect of polypropylene fibre and lime admixture on engineering properties of clayey soil. *Eng. Geol.* 87 (3), 230–240.
- 4) Dasaka, S.M., Sumesh, K.S., 2011. Effect of coir fiber on the stress–strain behavior of a reconstituted fine-grained soil. *J. Nat. Fibers* 8 (3), 189–204.
- 5) Hejazi, S.M., Sheikhzadeh, M., Abtahi, S.M., Zadhoush, A., 2012. A simple review of soil reinforcement by using natural and synthetic fibers. *Constr. Build. Mater.* 30, 100–116.
- 6) IS-2720-(Part 3), 1980. Methods of Test for Soils. Determination of Specific Gravity. Bureau of Indian Standards Publications, New Delhi.
- 7) IS-2720 (Part 4), 1985a. Methods of Test for Soils, Grain Size Analysis. Bureau of Indian Standards Publications, New Delhi.
- 8) IS-2720 (Part 5), 1985b. Determination of Liquid and Plastic Limit. Bureau of Indian Standards Publications, New Delhi.
- 9) IS-2720-(Part7), 1980. Determination of Water Content-Dry Density Relation Using Light Compaction. Bureau of Indian Standards Publications, New Delhi.
- 10) IS-2720 (Part 10), 1991. Determination of Unconfined Compressive Strength. Bureau of Indian Standards Publications, New Delhi.
- 11) Khan, F.S., Azam, S., Raghunandan, M.E., Clark, R., 2014. Compressive strength of compacted clay–sand mixes. *Adv. Mater. Sci. Eng.* 2014.
- 12) Koerner, Robert M., 2012. Designing with geosynthetics. Vol. 1. Xlibris Corporation.
- 13) Maher, M.H., Ho, Y.C., 1994. Mechanical properties of kaolinite/fiber soil composite. *J. Geotech. Eng.* 120 (8), 1381–1393.
- 14) Santoni, R.L., Tingle, J.S., Webster, S.L., 2001. Engineering properties of sand–fiber mixtures for road construction. *J. Geotech. Geoenviron.* 127 (3), 258–268.
- 15) Vidal, H., 1969. The principle of reinforced earth. *Highw. Res. Rec.* 282.
- 16) Yetimoglu, T., Salbas, O., 2003. A study

[Back to table of contents](#)

A LABORATORY STUDY ON CBR AND PERMEABILITY PROPERTIES OF SUB-BASE MATERIALS IN A ROAD STRUCTURE USING POLYPROPYLENE FIBRE AS ADDITIVE

Tinku Kalitaⁱ⁾, Bhaskarjyoti Dasⁱⁱ⁾

i) Student, Department of Civil Engineering, Assam Engineering College, Guwahati, 781013, India.

ii) Associate Professor, Department of Civil Engineering, Assam Engineering College, Guwahati, 781013, India.

ABSTRACT

Granular Sub-Base (GSB) is placed just on top of the sub-grade and beneath the base course in a road structure, its role is to drain out the water as well as to transfer the load to sub-grade layer. The GSB material is mixed with different percentages of polypropylene fibre. Performance related tests like Maximum Dry Density (MDD) & Optimum Moisture Content (OMC), soaked California Bearing Ratio (CBR) and permeability of GSB materials were performed in the laboratory with and without fibre. Incorporation of fibre enhanced the reinforcing effect and as a result of which there was a significant improvement on the strength of the mixture. Also, the permeability characteristics of the GSB mixes are improved by the addition of polypropylene fibre. On the basis of the results, it was found that polypropylene fibre can be used as additive along with sub base material as it provide good strength to the sub-base and increases the permeability of the sub-base layer.

Keywords: Granular sub-base, Maximum Dry Density, Optimum Moisture Content, California Bearing Ratio.

1. INTRODUCTION

Aggregate is a collective term for the mineral materials such as sand, crushed stone and gravel that are used with a binding medium (such as bitumen, water, lime, Portland cement, etc.) to form compound materials (such as bituminous concrete and Portland cement concrete). Aggregate materials which are widely used in road construction and maintenance in flexible pavement layers are becoming scarce and expensive in many parts of North-Eastern region of India. This is due to uneven distribution of high quality aggregate in nature. If a high quality aggregate do exists at any particular area then that land may be kept for other uses or restrict it from mining due to public perception. Hence, construction or maintenance of roads has been hindered in certain regions both financially and logistically.

In India more than 98% roads are of flexible type, which consist of sub-grade layer, sub-base layer, base course and surface layer. The premature failure of pavement is of great concern. Stagnation of water affects adversely the performance of flexible pavements. Water enters into the pavement section through cracks, joints, infiltration. In hilly region, water infiltrates laterally through the cross-section of road.

Some of the effects of water, when trapped within the pavement structures are (a) Reduction in strength of sub-grade and base/sub-base. (b) Hydraulic pumping action due to traffic load lead to disintegration of

aggregate of pavement layer. (c) Stripping of asphalt in flexible pavement. (d) Differential swelling in expansive sub-grade soil. (e) Movement of fine particles into the base or sub-base course resulting in reduction in permeability of sub-base layer. There are two approaches to reduce water infiltration (a) pavement joint and crack should be sealed to reduce infiltration, (b) water can be removed vertically through sub-grade or laterally through the drainage layer into a system of pipe collector.

Vertical drainage is not adequate because the coefficient of permeability of compacted sub-grade is usually very low. Therefore, lateral drainage is needed to carry infiltrated water away from pavement structure i.e. through the sub-base layer. Granular sub-base (GSB) is situated above the sub-grade and serves as the foundation for the overall pavement structure. The GSB layer is divided into two parts (a) Upper GSB as drainage layer and (b) Lower GSB as filter layer to prevent intrusion of sub-grade soil into the sub-base layer and pavement.

Li et al. (1995) reported that there were notable increases in shear strength, toughness and plasticity of a cohesive soil after reinforcement with discrete polypropylene. Hoover et al. (1982) reported that the soil and fibre composite were effective in improving CBR value of sandy soil as compared to silty/clayey soil. Al-Refai (1991) studied the effect of fibre reinforcement using different types of granular soil. It

was observed that fibre- reinforcement effect seemed more profound in fine sand with sub-rounded particles than in medium grained sand with sub-angular particles. Kumar, Wallia and Bajaj (2007) observed that with the addition of 1.5% of 6mm plain fibre or 1% of 6mm crimped fibre to a mixture containing 8% lime and 15% fly-ash, increases unconfined compressive strength by about 74% as compared to that of same mixture without fibre. In most of the literatures it was found that the results obtained were for the samples which weren't categorized with respect to their physical properties. In this paper samples are segregated into strong and weak

category as per aggregate crushing value, impact value, abrasion value and water absorption value.

2 COLLECTIONS OF SAMPLE AND MATERIAL

The samples were collected from different sites of Arunachal Pradesh and Assam. The various properties of the GSB samples (SL) are given in Table 1. The polypropylene fibre with a diameter of 0.3mm was cut into 40mm length maintaining an aspect ratio of 133. (Aspect ratio is the ratio of length of fibre to the diameter of fibre).

Table 1 Physical properties of GSB material

Sl No.	Properties	Samples								
		SL 1	SL 2	SL 3	SL 4	SL 5	SL 6	SL 7	SL 8	SL 9
1	Liquid limit (W_L), %	16.64	15.89	19.1	18.21	15.72	17.52	15.54	17.37	13.47
2	Plastic limit (W_P), %	Can't be determined								
3	P.I ($W_L - W_P$), %	Non-Plastic								
4	Aggregate crushing value, %	15.57	13.21	18.54	13.24	13.12	23.61	21.42	27.42	29.13
5	Impact value, %	19.70	17.21	17.47	16.54	14.21	19.26	21.16	28.17	27.36
6	Abrasion value, %	29.51	27.26	30.12	24.21	20.01	33.13	32.11	37.11	36.21
7	Specific gravity	2.63	2.69	2.62	2.64	2.68	2.60	2.61	2.37	2.51
8	Water absorption value, %	0.42	0.34	0.46	0.32	0.22	0.82	0.78	0.79	0.73

From the properties of aggregate crushing value, impact value, abrasion value, water absorption value (Table 1) and mainly CBR value (Table 2), the sample SL1, SL2, SL3, SL4 and SL5 are regarded as relatively stronger samples and SL6, SL7, SL8, SL9 are regarded as relatively weaker samples.

3 TEST METHODOLOGY

The Standard Proctor Test were done on the untreated GSB samples and treated GSB sample with 0.5%, 1%, 1.5%, 2% polypropylene fibre, to determine the OMC and MDD of various GSB composites. The OMC obtained by the Standard Proctor Test were used in CBR sample preparation to determine the soaked CBR (curing period is 4 days) value of untreated GSB sample and fibre treated GSB samples as mentioned above. The falling head permeability tests were done on untreated and fibre treated GSB samples.

3.1 Compaction Test

The Standard Proctor Test were done as per IS

2720 (Part 7) - 1980 to determine the OMC and MDD for all the nine samples. The value of Optimum Moisture Content (OMC) and Maximum Dry Density (MDD) are given in Table 2.

3.2 California Bearing Ratio (CBR) Test

The CBR test were performed as per IS 2720 (Part 16) - 1987. Soaked CBR were done in which the untreated GSB samples and treated GSB samples with fibre were cured for four days. The CBR values of various samples are given in Table 2.

3.3 Permeability Test

Falling head permeability test were done on the untreated GSB samples and fibre treated GSB samples as per IS 2720 (Part 17) -1986.

4 RESULTS AND DISCUSSION

4.1 Compaction Test

With the addition of fibre content in the GSB

materials the value MDD decreases and OMC increases. The decrease in maximum dry density

Table 2 Engineering properties of GSB material

Sl No.	Sample ID	Properties			
		OMC, %	MDD, g/cm ³	CBR, %	Permeability, cm/sec
1	SL 1	10.50	2.010	21.46	5.226×10^{-3}
2	SL 2	10.01	2.118	22.83	4.278×10^{-3}
3	SL 3	8.20	2.011	23.44	6.261×10^{-3}
4	SL 4	8.33	2.122	27.85	3.661×10^{-3}
5	SL 5	9.58	2.113	26.54	3.842×10^{-3}
6	SL 6	10.21	1.792	15.53	9.721×10^{-3}
7	SL 7	10.40	1.821	16.40	9.221×10^{-3}
8	SL 8	11.21	1.790	15.11	9.241×10^{-3}
9	SL 9	12.21	1.699	13.21	9.524×10^{-3}

mixture per unit volume. However, with the addition of fibre on the GSB material the OMC increases. This is because addition of fibre to the GSB material increases the required amount of moisture content due to increase in surface area of the fibre, so that the composite material become workable under the load. Addition of water results in a thin lining of water around the fibre which ultimately increases the OMC of GSB composites.

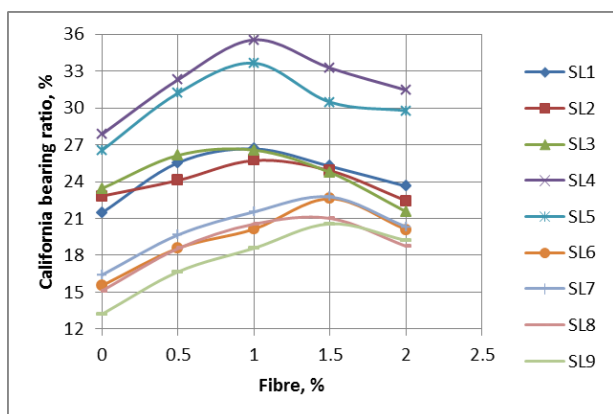


Fig. 1. Variation of California bearing ratio with different amount of fibre content.

when fibre is added to the GSB material is due to the reduction of average unit weight of solids in soil-fibre

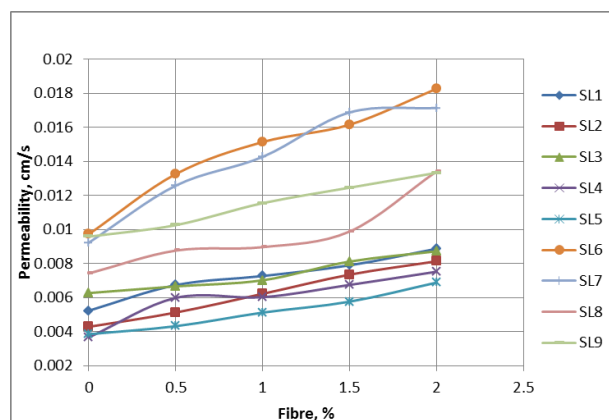


Fig. 2. Variation of permeability with different amount of fibre content.

Table 3 CBR and Permeability results of GSB samples at optimum amount of additives

Sl No	Sample ID	CBR, % (untreated)	CBR, % (treated)	Permeability, cm/sec (untreated)	Permeability, cm/sec (treated)
1	SL 1	21.46	26.67 (for 1% fibre)	5.226×10^{-3}	7.262×10^{-3} (for 1% fibre)
2	SL 2	22.83	25.72 (for 1% fibre)	4.278×10^{-3}	6.216×10^{-3} (for 1% fibre)
3	SL 3	23.44	26.57 (for 1% fibre)	6.261×10^{-3}	7.012×10^{-3} (for 1% fibre)
4	SL 4	27.85	35.54 (for 1% fibre)	3.661×10^{-3}	6.017×10^{-3} (for 1% fibre)
5	SL 5	26.54	33.65 (for 1% fibre)	3.842×10^{-3}	5.112×10^{-3} (for 1% fibre)
6	SL 6	15.53	22.61 (for 1.5% fibre)	9.721×10^{-3}	1.615×10^{-2} (for 1.5% fibre)
7	SL 7	16.40	22.76 (for 1.5% fibre)	9.221×10^{-3}	1.687×10^{-2} (for 1.5% fibre)
8	SL 8	15.11	21.01 (for 1.5% fibre)	7.417×10^{-3}	9.875×10^{-3} (for 1% fibre)
9	SL 9	13.21	20.57 (for 1.5% fibre)	9.574×10^{-3}	1.245×10^{-2} (for 1% fibre)

4.2 California Bearing Ratio

With the addition of fibre to the GSB samples, the CBR value increases up to 1% of fibre content (which is considered as optimum amount of fibre content) for SL 1, SL 2, SL 3, SL 4 and SL 5 which are relatively stronger samples and 1.5% of fibre content (which is considered as optimum amount of fibre content) for SL 6, SL 7, SL 8 and SL 9 which are relatively weaker samples, after that CBR value decreases with further addition of fibre content. The graph showing variation of California bearing ratio with the amount of fibre content is shown in Fig 1.

4.3 Permeability

Incorporation of fibre to the GSB material increases the permeability of GSB composite continuously. The graph showing variation of permeability with the amount of fibre content is shown in Fig 2.

5 CONCLUSION

From the detailed analysis of both untreated and treated GSB with polypropylene fibre, the results obtained suggests that the CBR value is maximum when 1% fibre is added to samples SL 1, SL 2, SL 3, SL 4 and SL 5 (which are considered as relatively stronger samples) and 1.5% fibre for the samples SL6, SL 7, SL 8 and SL 9 (which are considered as relatively weaker samples), and the permeability values increases continuously with the addition of fibre.

REFERENCES

- 1) Al-Refeai, T.O. (1991): ‘Behaviour of granular soil reinforced with discrete randomly oriented inclusions’, *Geotextiles and Geomembrane*, 10(4), 319-333.
- 2) Hoover, J.M., Moeller, D.T., Pitt, J.M., Smith, S.G., and Wainaina, N.W. (1982): ‘Performance of randomly oriented, fibre reinforced road-way soils’, Iowa DOT Project No. HR-211, Dept. of Transportation Engineering, Div., Iowa State Univ., 15-35.
- 3) IS: 2386 (Part 3) (1963): Determination of water absorption, Bureau of Indian Standards, New Delhi, India.
- 4) IS: 2720 (Part 4) (1985): Determination of Impact Value, Aggregate crushing value and Abrasion value, Bureau of Indian Standards, New Delhi, India.
- 5) IS: 2720 (Part 5) (1985): Determination of liquid limit and plastic limit, Bureau of Indian Standards, New Delhi, India.
- 6) IS: 2720 (Part 7) (1980): Determination of water content and dry density using light compaction, Bureau of Indian Standards, New Delhi, India.
- 7) IS: 2720 (Part 16) (1987): Laboratory Determination of CBR, Bureau of Indian Standards, New Delhi, India.
- 8) IS: 2720 (Part 17) (1986): Laboratory Determination of permeability, Bureau of Indian Standards, New Delhi, India.
- 9) Kumar, P., Chandra, S. and Vishal, R. (2006): “Comparative study of different sub-base materials” *Journal of materials in civil engineering ASCE /july/august*, 576-580.
- 10) Kumar, P. and Singh, S. P. (2008) : “Fibre-Reinforced Fly-ash Sub-base in Rural Roads” *Journal of Transportation Engineering, ASCE/ April*, 171-180.
- 11) Kumar, A., Walia, B.S. and Bajaj, A. (2008): ‘Influence of Fly ash, Lime and Polyester Fibres on compaction and strength properties of Expansive Soil’, *Journal of Materials in Civil Engineering*, 19(3), 242-248.
- 12) Li, G.X., Chen, L., Zheng, J.Q. and Jie, Y.X.,(1995): ‘Experimental study on fibre-reinforced cohesive soil’ *Shuili Xuebao/ Journal of Hydraulic Engineering*, 6, 31-36.
- 13) Mahar, M. H. and Gray, D. H. (1990): “Static response of sands reinforced with randomly distributed fibres”, *Journal of Geotechnical Engineering*, 116(11), 1661-1677.
- 14) Murahari, K. and Rao, R. M. (2013): “Effects of Polypropylene fibre on the strength properties of fly-ash based concrete”, *International Journal of Engineering Science Invention*, 2(5), 13-19.
- 15) Prasad, M., Chandak, R. and Grover, R. (2013): “A comparative study of Polypropylene fibre Reinforced Silica fume with plain Cement Concrete”, *International Journal of Engineering Research and Science and Technology*, Nov, 2(4), 127-136.

[Back to table of contents](#)

Investigation of infiltration temporal variation in different soils vegetated with drought sensitive cow pea

Shiv Prakash^{i)*}, Sunil Kumar Sihag¹⁾, Ankit Soni¹⁾, Vinay Kumar Gadiⁱⁱ⁾, Ankit Gargⁱⁱ⁾

i) Undergrad Student, Department of Civil engineering, IIT Guwahati, Kamrup, Assam, Zip-781039

ii) PhD Student, Department of Civil engineering, IIT Guwahati, Kamrup, Assam, Zip-781039

iii) Associate Professor, Department of Civil engineering, IIT Guwahati, Kamrup, Assam, Zip-781039

ABSTRACT

Infiltration in agricultural fields is fundamental for sustainable rural ecosystem. Accurate measurement of infiltration is vital to devise irrigation and to assess water use efficiency in soil vegetated with drought sensitive plants. Although previous studies found temporal variation of infiltration, comparison of infiltration in the presence and absence of nutrients was rarely studied. *Vigna unguiculata* (drought sensitive cow pea) species are considered for the present study, whose performance in drought prone area is highly dependent on infiltration. Infiltration in red soil and nutrient mixed red soil rooted with *Vigna unguiculata* is investigated in present study. The infiltration results of rooted red soil show that, trend of variation of infiltration is not consistent throughout the period of plant growth. Up to the end of 17 days, higher infiltration was found in the soil under the absence of nutrients. This may be due to higher root growth in the nutrient added soil. It is because, higher root growth induces higher preferential flow in root zone. However, after 17 days, trend of variation is found to vary frequently.

Keywords: Infiltration, Different types of soils, Rooted soil, Crop species, and Temporal variation

1. INTRODUCTION

Infiltration in agricultural fields is fundamental for sustainability of rural eco-system (Jones et al. 1994). Characterizing the response of temporal infiltration variation for different soil types, which are rooted with crop species is important for sustainability of ground water (Boller, 1997). Drought sensitive cow pea is extensively cultivated legume in Asia and Africa (Singh et al. 2002). It provides high-quality and cheap dietary proteins for poor people (Diouf, 2011). Wide research has been done on performance of drought sensitive cow pea. However, infiltration analysis was rarely done explicitly. Infiltration is a key factor for performance of plants in drought prone regions (Blum and ebercon, 1981). It is evident that, root growth effects infiltration (Meek et al. 1992) from previous studies. In these studies, temporal variation of infiltration of vegetated nutrient added soil and red soil are rarely compared.

Present study investigates infiltration characteristics of soil vegetated with drought sensitive cow pea are found. The investigation is conducted in the presence of nutrients and also in the absence of nutrients. The study explores the trend of variation of temporal variation of infiltration.

2. MATERIALS AND METHODS

2.1 Soil Property

Two types of soil were used in this experiment. One is red soil and other is nutrient-mixed agricultural soil. The nutrient-mixed soil when classified under Unified soil classification system(USCS) comes under Poorly graded sand or SP. Nutrient-mixed soil mainly consists of fine sand (51%) and medium sand (34%) followed by silt (11%) & Coarse sand (4%). Red soil is classified as low plastic silt ML. Selected red soil consists silt (50%) & clay (25%) followed by medium sand (6%) & fine sand (19%). Liquid limit, Plastic limit and shrinkage limit of red soil are 41%, 25% and 13% respectively. All of the above properties are determined under the provisions of ASTM codes (ASTM D854-06; ASTM D2487-10; ASTM D698-07 and ASTM D4318-93).

2.2 Plant species used & its germination conditions

The vegetation type selected is a crop species, Cowpea (*Vigna unguiculata*). Cowpea is an important crop widely cultivated by farmers in Sub Saharan countries and Asia, Africa and America. It is well-adapted to nutrient-deficiency in soils. It grows well even in poor soils with more than 85% sand and with less than 0.2% organic matter and low levels of phosphorus (Singh et al. 2002). Seed corporation of India provided the mature seeds of cowpea cultivar, Pusa Komal. Cotton moistened with tap water in petri dishes were used for

germination of seeds which was further kept for three days in dark, at 25°C under florescent light. After germination, seedlings were transplanted in pots for conducting experiments.

2.3 Test plan

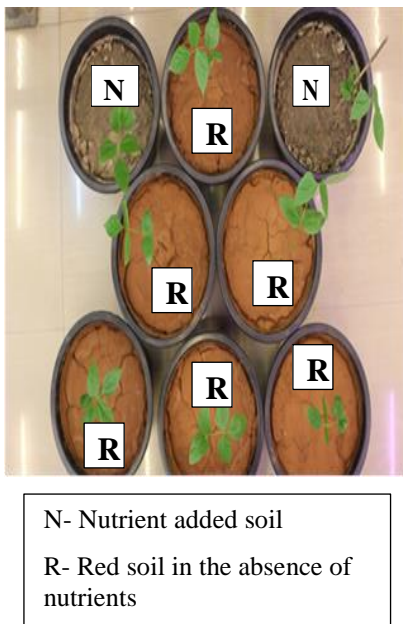


Fig. 1 Overview of vegetated soil in greenhouse

A test plan is designed to characterize the response of infiltration temporal variation for red soil & nutrient-mixed soil rooted with *Vigna unguiculata* in controlled irrigation. All the plant parameters are subjected to natural environmental conditions except irrigation. All the experiments were conducted were done in a

greenhouse (Fig. 1) where seeds were planted in pots containing two different kinds of soils. Infiltration was measured regularly with the help of mini-disk infiltrometer.

2.4 Experimental setup

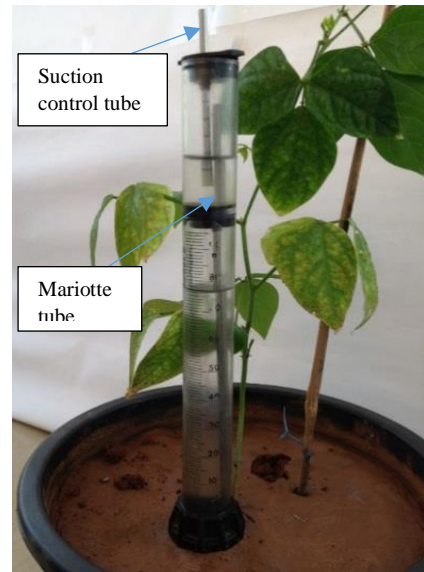


Fig. 2 Overview of mini disk infiltrometer placed in vegetated soil

The pots used to conduct experiments are cylindrical in nature with perforated base to allow water drainage from the bottom and are made of PVC plastic. Six pots of dimensions 230 mm depth and 260 mm diameter were used for each soil type. To maintain a uniform density of 1.35 g/cc or 0.74 maximum dry density, soil was compacted in three layers up to 185 mm from bottom. All the pots were irrigated regularly after every three days. The

temperature and relative humidity observed were $26\pm 4^\circ\text{C}$ and $52\pm 8\%$ respectively. Mini-disk infiltrometer (Fig. 2) is used for measuring the infiltration variation. The Infiltrometer used in this experiment has a total length of 327 mm and length of reservoir as 212 mm. Diameter of tube is 310 mm with length of suction control tube and length of mariotte tube as 102 mm and 280 mm respectively. Suction taken was 0.5 cm. Volume of water required to operate this infiltrometer is 135 ml. The variation of infiltration rate with time for red soil and nutrient-mixed soil is shown in Fig. 3.

2.5 Procedure for measuring infiltration rate

After placing mini-disk infiltrometer, water was allowed to infiltrate at the preset suction. Water that infiltrates into vegetated soil through the disc is found as a function of time. Infiltration can be found using equation 1 (Zhang, 1997a).

$$I = c_1t + c_2 \tag{1}$$

Where:

C_1, C_2 = fitting constants,
 t = time.

The near saturated hydraulic conductivity (k or k_h corresponding to suction applied on the disc (h)) defined by Zhang (1997) is given by equation (2)

$$k \text{ or } k_h = \frac{c_1}{A} \tag{2}$$

where:

A = Parameter dependent on van Genuchten SWRC parameters, suction applied on disc and radius of disc as represented by equation (3.1 and 3.2).

$$A = \frac{11.65(n^{0.1}-1)\exp[2.92(n-1.9)ah]}{(ar)^{0.91}};$$

For $n > 1.9$ (3.1)

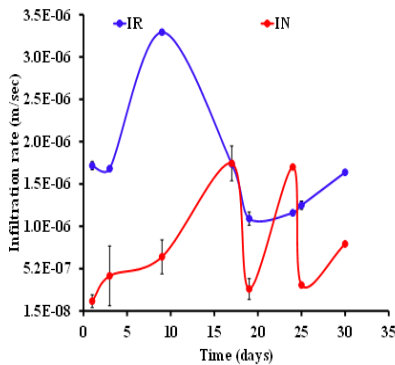
$$A = \frac{11.65(n^{0.1}-1)\exp[7.5(n-1.9)ah]}{(ar)^{0.91}};$$

For $n < 1.9$ (3.2)

where:

n, α = the van Genuchten SWRC parameters of vegetated soil adopted from Zhang (1997)
 r = radius of disc
 h = tension applied

3. RESULTS AND DISCUSSIONS



IR – Infiltration rate in vegetated soil under the absence of nutrients
 IN- Infiltration rate in vegetated nutrient added soil

Fig. 3 Temporal variation of infiltration

As shown in Fig. 3, infiltration for red soil (IR) was found to decrease with time within first three days. After that, it was found to increase up to 8 days. After 8 days, infiltration was observed to decrease up to 17 days. Again after 17 days, it was found to increase up to the end of 32 days. Any similarity of trend of variation of IR was not found with trend of variation IN. Trend of variation changes frequently in case of IR as compared to case if IN. Although root growth and root distribution occurs, any consistency of infiltration with root growth was not found. Up to 17 days, infiltration is found to be 2 to 10^2 times higher in the vegetated soil under absence of nutrients as compared to vegetated soil under the presence of soil. It is evident from

previous studies that, root growth may be higher added soil (Zhang and Forde, 1998) and roots may repel infiltration (Doer et al. 2000). These may be reasons for higher hydraulic conductivity in the absence of nutrients. The trend of hydraulic conductivity variation is found to alter frequently after 17 days. Root growth rate difference may be the reason for the dissimilar infiltrations occurred.

4. CONCLUSION

As we can see from the graph in Fig. 3, Infiltration result is not varying regularly with time and as vegetation is increasing with time which further implies that Infiltration is not only dependent on vegetation. It depends on many other factors like root length, rainfall, type of soil etc. Initially there is a considerable increase in Infiltration rate for both the soils but later it becomes irregular. As we can see from Fig. 3, the infiltration rate for both the soils are different but trend is similar and as other than soil type, all the other conditions are same which further implies that different soil give different infiltration rate but trend is similar. Further studies can be done for effect of root length on Infiltration rate.

REFERENCES

- 1)ASTM, D. "D4318-93-Liquid Limit." *Plastic Limit, and Plastic Index of Soils*.
- 2)ASTM, Standard. "D698-07,“." *Standard test method for laboratory compaction characteristics of soil using standard effort*

(12,400 ft-lb/ft³ (600 kN-m/m³)), " *Annual Book of ASTM Standards, ASTM International, West Conshohocken, PA* (2007).

3) Blum, A. and Ebercon, A., 1981. Cell membrane stability as a measure of drought and heat tolerance in wheat. *Crop Science*, 21(1), pp.43-47.

4) Boller, M., 1997. Tracking heavy metals reveals sustainability deficits of urban drainage systems. *Water Science and Technology*, 35(9), pp.77-87.

5) Designation, A. S. T. M. "D854-06, 2007." *Standard test method for specific gravity of soil solids by water pycnometer: annual book of ASTM standar*

6) Diouf, D., 2011. Recent advances in cowpea [*Vigna unguiculata* (L.) Walp.]“omics” research for genetic improvement. *African Journal of Biotechnology*, 10(15), pp.2803-2810.

Science Reviews, 51(1), pp.33-65.

7) Doerr, S. H., R. A. Shakesby, and RPDm Walsh. "Soil water repellency: its causes, characteristics and hydro-geomorphological significance." *Earth-Science Reviews* 51.1 (2000): 33-65.

8) Jones, C.G., Lawton, J.H. and Shachak, M., 1994. Organisms as ecosystem engineers. In *Ecosystem management* (pp. 130-147). Springer New York.

9) Meek, B.D., Rechel, E.R., Carter, L.M., DeTar, W.R. and Urie, A.L., 1992. Infiltration rate of a sandy loam soil: effects of traffic, tillage, and plant roots. *Soil Science Society of America Journal*, 56(3), pp.908-913.

10) Singh, B.B., 2002. Recent genetic studies in cowpea. *Challenges and Opportunities for Enhancing Sustainable Cowpea Production. International Institute of Tropical Agriculture, Ibadan, Nigeria*, pp.3-13.

11) Standard, A. S. T. M. "D2487-10." *Standard Practice for Classification of Soils for Engineering Purposes (Unified Soil Classification System), Annual Book of ASTM Standards, ASTM International, West Conshohocken, PA*(2010).

12) Zhang, H. and Forde, B.G., 1998. An Arabidopsis MAD5 box gene that controls nutrient-induced changes in root architecture. *Science*, 279(5349), pp.407-409.

13) Zhang, R., 1997. Determination of soil sorptivity and hydraulic conductivity from the disk infiltrometer. *Soil Science Society of America Journal*, 61(4), pp.1024-1030.

Back to table of contents

CESDOC 2016

**Civil Engineering for Sustainable Development
- Opportunities and Challenges**

This proceeding is published by
**Department of Civil Engineering
Assam Engineering College
Guwahati, Assam, India**